Alexander P. Demchenko

Introduction to Fluorescence Sensing

Second Edition

Springer

Alexander P. Demchenko
Laboratory of Nanobiotechnology
Palladin Institute of Biochemistry
National Academy of Sciences of Ukraine
Kiev
Ukraine

ISBN 978-3-319-20779-7 ISBN 978-3-319-20780-3 (eBook)
DOI 10.1007/978-3-319-20780-3

Library of Congress Control Number: 2015949462

Springer Cham Heidelberg New York Dordrecht London

Printed on acid-free paper

Springer International Publishing AG Switzerland is part of Springer Science+Business Media (www.springer.com)

Preface

The field of molecular sensing is immense. It is nearly the whole world of natural and synthetic compounds that have to be analyzed in a broad variety of conditions and for a broad variety of purposes. In the human body, we need to detect and quantify virtually all the genes (genomics) and the products of these genes (proteomics). In our surrounding there is a need to analyze a huge number of compounds including millions of newly synthesized products. Among them, we have to select potentially useful compounds (e.g. drugs) and discriminate those that are inefficient and harmful. No less important is to control agricultural production and food processing. There is also a practical necessity to provide control in industrial product technologies, especially in those that produce pollution. Permanent monitoring is needed to maintain safety of our environment. Protection from harmful microbes, clinical diagnostics and control of patient treatment are the key issues of modern medicine. New problems and challenges may appear with the advancement of human society in the twenty-first century. We have to be ready to meet them.

Modern society needs the solution of these problems on the highest possible scientific and technological level. The science of intermolecular interactions is traditionally a part of physical chemistry and molecular physics. Now it becomes a strongly requested background for modern sensing technologies. The most specific and efficient sensors are found in the biological world and the sensors based on biomolecular recognition (biosensors) have gotten a strong impulse for development and application. A strong move is observed for improving them by endowing new features or even by making their fully synthetic analogs. Modern electronics and optics make their own advance in providing the most efficient means for supplying the sensors the input and output signals and now become oriented at satisfying the needs of not only researchers but a broad community of users.

This book is focused on one sensing technology that is based on fluorescence. This is not only because of limited space or limited expertise of the present author. Indeed, fluorescence techniques are the most sensitive; their sensitivity reached the absolute limit of single molecules. They offer very high spatial resolution that, with overcoming the light diffraction limit, has reached molecular scale. They are also the fastest; their response develops on the scale of fluorescence lifetime and can be

as short as 10^{-8}–10^{-10} s. But their greatest advantage is versatility. Fluorescence sensing can be provided in solid, liquid and gas media and at all kinds of interfaces between these phases. It is because the fluorescence reporter and the detecting instrument are connected via light emission, fluorescence detection can be made non-invasive and equally well suited for remote industrial control and for sensing different targets within the living cells. All these features explain their high popularity.

The fascinating field of fluorescence sensing needs new brains. Therefore the book is primarily addressed to students and young scientists. Together with basic knowledge they will get an overview of different ideas in research and technology and guide to their own creative activity. Providing a link between basic sciences needed to understand sensor performance and frontier of research, where new ideas are explored and new products developed, the book will make a strong link between research and education. For the active researcher it will also be a source of useful information in nearly all areas where fluorescence sensing is used.

Thus, this book is organized with the aim to satisfy both the curious student and the busy researcher. After a short introduction, comparative analysis of basic principles used in fluorescence sensing will be made. Then we will provide a formal description of binding equilibrium and binding kinetics that are in the background of sensing technologies. After that the focus will be made on techniques of obtaining information from fluorescent reporters and on analysis of their structures and properties. The family of fluorescence reporters is broad, from small molecules to nanoparticles with composite structures. Design of various types of recognition units will be reviewed, including those selected from large libraries. The deeper understanding of basic mechanism of signal transduction in fluorescence sensing will be in our focus with a special attention to the new possibilities provided by support structures, scaffolds and integrated units that expand the range of sensor applications. Non-conventional generation and transformation of response signal will also be described. Fluorescence sensing is realized in optical instrumentation, so these devices are overviewed, including microarrays, microfluidics and flow cytometry. Detection of different targets from physical, chemical and biological worlds is discussed with presentation of many examples. We will also address the analytical means to detect different targets inside the living cells based on modern microscopy. Clinical diagnostics based on fluorescence combined with targeted drug delivery and treatment generated a new technology – theranostics. Finally, the frontiers of modern research are overviewed with the prospects for fluorescence sensing behind the horizon. Each chapter is concluded by the section ‘Sensing and Thinking’, in which after a short summary a series of questions and exercises is suggested to the reader.

After the publication of the first edition of this book, just within the last several years a tremendous progress is observed. Many new fluorophore classes were developed and the properties of many existing fluorophores were significantly improved. They include the few-atom clusters of noble metals and the nanoparticles made of pure carbon. New possibilities in improvement of the fluorescence reporters and providing them new functionalities appeared with assembling them in

nanocomposites. Microarray technologies were further developed in order to improve the capability and resolution of fluorescence detection of multiple analytes. Their nanoscale format offers an almost endless versatility and space for integrating myriad different signal transduction networks based on various fluorophores for monitoring and transferring vast amounts of data. Advanced optical instrumentation and the tools for data analysis were developed. Fluorescence sensing has gained strong positions in clinical diagnostics.

In order to follow this progress, in a new second edition a number of changes and additions have been made. Three new chapters were added. One is on fluorescent nanoparticles of different organic and inorganic origin. The other – on their multifunctional composites. A special chapter addresses the application of fluorescence in clinical diagnostics and treatment. All other chapters were revised with the addition of new information, new illustrations and new points of discussion.

In preparation of this new edition I got critical comments and advices of many colleagues. I would like to provide special thanks to Donna Arndt-Jovin, Sergey Bobrovnik, Pi-Tai Chou, Ihor Dmitruk, Ihor Dubey, Mykhaylo Dvoynenko, Dmytro Dziuba, Tom Jovin, Vasyl Pivovarenko, Oleksandr Slobodyanyuk and Olga Vasylchenko.

Enjoy your reading.

Kiev, Ukraine
April, 2015

Alexander P. Demchenko

Contents

Introduction xxv

1 Basic Principles 1
1.1 Overview of Strategies in Molecular Sensing. 1
1.1.1 Basic Definitions: Sensors and Assays, Homogeneous and Heterogeneous 2
1.1.2 Principles of Sensor Operation 7
1.1.3 Label-Free, General Approaches 8
1.1.4 Label-Free, System-Specific Approaches. 10
1.1.5 Label-Based Approaches 11
1.2 Labeling Targets in Fluorescence Assays 12
1.2.1 Arrays for DNA Hybridization 14
1.2.2 Labeling in Protein-Protein and Protein-Nucleic Acid Interactions. 14
1.2.3 Micro-array Immunosensors. 15
1.2.4 Advantages and Limitations of the Approach Based on Pool Labeling 15
1.3 Competitor Displacement Assay. 16
1.3.1 Unlabeled Sensor and Labeled Competitor in Homogeneous Assay 17
1.3.2 Labeling of Both Receptor and Competitor 19
1.3.3 Competition Involving Two Binding Sites 20
1.3.4 Advantages and Limitations of the Approach 21
1.4 Sandwich Assays 22
1.4.1 Sensing the Antigens and Antibodies. 22
1.4.2 Ultrasensitive DNA Detection Hybridization Assays. 24
1.4.3 Advantages and Limitations of the Approach 25
1.5 Catalytic Biosensors 26
1.5.1 Enzymes as Sensors 26
1.5.2 Labeling with Catalytic Amplification 27
1.5.3 Advantages and Limitations of the Approach 28

1.6 Direct Reagent-Independent Sensing 29
1.6.1 The Principle of Direct 'Mix-and-Read' Sensing. 29
1.6.2 Contact and Remote Sensors 30
1.6.3 Advantages and Limitations of the Approach 32
1.7 Sensing and Thinking: How to Make the Sensor? Comparison of Basic Principles 33
References 35

2 Theoretical Aspects 39
2.1 Parameters That Need to Be Optimized in Every Sensor 40
2.1.1 The Limit of Detection and Sensitivity. 41
2.1.2 Dynamic Range of Detectable Target Concentrations 42
2.1.3 Selectivity 43
2.2 Determination of Binding Constants 44
2.2.1 Dynamic Association-Dissociation Equilibrium 45
2.2.2 Determination of K_b by Titration 46
2.2.3 Determination of K_b by Serial Dilutions. 50
2.3 Modeling the Ligand Binding Isotherms 51
2.3.1 Receptors Free in Solution or Immobilized to a Surface . . . 51
2.3.2 Bivalent and Polyvalent Reversible Target Binding 52
2.3.3 Reversible Binding of Ligand and Competitor. 54
2.3.4 Interactions in a Small Volume. 57
2.4 Kinetics of Target Binding 58
2.5 Formats for Fluorescence Detection 60
2.5.1 Linear Response Format 61
2.5.2 Intensity-Weighted Format 62
2.6 Sensing and Thinking: How to Provide the Optimal Quantitative Measure of Target Binding?. 64
References 67

3 Fluorescence Detection Techniques 69
3.1 Fluorescence Fundamentals 70
3.1.1 The Light Emission Phenomenon. 70
3.1.2 Fluorophore Emissive Power: The Quantum Yield 73
3.1.3 Fluorescence Parameters Used in Sensing 74
3.2 Intensity-Based Sensing 75
3.2.1 Peculiarities of Fluorescence Intensity Measurements. 76
3.2.2 How to Make Use of Quenching Effects? 76
3.2.3 Quenching: Static and Dynamic 77
3.2.4 Non-linearity Effects. 78
3.2.5 Internal Calibration in Intensity Sensing 79
3.2.6 Intensity Change as a Choice for Fluorescence Sensing . . . 83
3.3 Anisotropy-Based Sensing and Polarization Assays 84
3.3.1 Background of the Method 85
3.3.2 Practical Considerations 86
3.3.3 Applications 89
3.3.4 Comparisons with Other Methods of Fluorescence Detection. 91

3.4 Lifetime-Based Fluorescence Response 92
3.4.1 Physical Background 92
3.4.2 Technique 94
3.4.3 Time-Resolved Anisotropy 95
3.4.4 Applications 95
3.4.5 Phosphorescence and Long-Lasting Luminescence 96
3.4.6 Comparison with Other Fluorescence Detection Methods 97
3.5 Excimer and Exciplex Formation 98
3.5.1 The Dyes Forming Excimers and Exciplexes 98
3.5.2 Application in Sensing Technologies 99
3.5.3 Comparison with Other Fluorescence Reporter Techniques 100
3.6 Förster Resonance Energy Transfer (FRET) 101
3.6.1 Physical Background of the Method 101
3.6.2 Homo-FRET and Hetero-FRET 104
3.6.3 FRET to Non-fluorescent Acceptor 105
3.6.4 FRET Modulated by Light 106
3.6.5 Applications of FRET Technology 106
3.6.6 Comparison with Other Detection Methods 109
3.6.7 Novel Trends in Excited-State Energy Transfer Probing . . . 110
3.7 Wavelength-Shift Sensing 111
3.7.1 The Physical Background Under the Wavelength Shifts . . . 111
3.7.2 The Measurements of Wavelength Shifts in Excitation and Emission 113
3.7.3 Wavelength-Ratiometric Measurements 115
3.7.4 Application in Sensing 116
3.7.5 Comparison with Other Fluorescence Reporting Methods . . . 117
3.8 Two-Band Wavelength-Ratiometric Sensing with a Single dye 117
3.8.1 Generation of Two-Band Ratiometric Response by Ground-State Isoforms 119
3.8.2 Excited-State Reactions Generating Two-Band Response in Emission 119
3.8.3 Excited-State Intramolecular Proton Transfer (ESIPT) 121
3.8.4 Prospects for Two-Band Ratiometric Recording 123
3.9 Sensing and Thinking: The Optimal Choice of Fluorescence Detection Technique 124
References 126

4 Molecular-Size Fluorescence Emitters 133
4.1 Fluorophores and Their Characteristics 133
4.1.1 General Properties of Fluorescent Dyes 133
4.1.2 Labeling and Sensing – Two Basic Methodologies 137
4.2 Organic Dyes as Labels and Tags 139
4.2.1 General Properties of Organic Dyes 140
4.2.2 The Most Efficient Dyes for Labeling 142

4.2.3 The Optimal FRET Pairs 148
4.2.4 Near-IR Dyes 149
4.2.5 Phosphorescent Dyes and the Dyes with Delayed Fluorescence 150
4.2.6 Combinatorial Discovery and Improvement of Fluorescent Dyes 152
4.3 The Dyes Providing Fluorescence Response 153
4.3.1 Special Requirements for Fluorescence Reporters 154
4.3.2 Fluorophores in Protic Equilibrium. pH-Reporting Dyes. . . 155
4.3.3 Hydrogen Bond Responsive Dyes 155
4.3.4 The Environment-Sensitive (Solvatochromic) Dyes 156
4.3.5 Electric Field Sensitive (Electrochromic) Dyes 160
4.3.6 Supersensitive Multicolor Ratiometric Dyes 162
4.3.7 Responsive Analogs of Amino Acids and Nucleic Acid Bases 167
4.3.8 Prospects 171
4.4 Visible Fluorescent Proteins 171
4.4.1 Green Fluorescent Protein (GFP) and Its Fluorophore. 172
4.4.2 Proteins of GFP Family 172
4.4.3 Labeling and Sensing Applications of Fluorescent Proteins 174
4.4.4 Other Proteins with Visible Fluorescence Emission. 175
4.4.5 Finding Analogs of Fluorescent Protein Fluorophores. 175
4.4.6 Prospects 176
4.5 Luminescent Metal Complexes. 176
4.5.1 Lanthanides, Their Complexes and Bioconjugates. 176
4.5.2 Photophysics of Lanthanide Chelates 178
4.5.3 Luminescence Spectra 178
4.5.4 Lanthanide Chelates as Labels and Reference Emitters 180
4.5.5 Dissociation-Enhanced Lanthanide Fluoroimmunoassay (DELFIA) 181
4.5.6 Switchable Lanthanide Chelates in Sensing 182
4.5.7 Transition Metal Complexes That Exhibit Phosphorescence. 183
4.5.8 Metal-Chelating Porphyrins 184
4.5.9 Prospects 185
4.6 Few-Atom Clusters of Noble Metals 186
4.6.1 The Cluster Structures and Their Stability 186
4.6.2 The Mechanisms of Light Absorption and Emission 187
4.6.3 Excitation and Fluorescence Emission Spectra 188
4.6.4 Silver Clusters Formed with Organic Dyes as Photosensitizing and Supporting Agents 190
4.6.5 Applications 190

4.7 Sensing and Thinking: Which Molecular Reporter to Choose for Particular Needs? 192
References 193

5 Nanoscale Fluorescence Emitters 203
5.1 Introduction to Light Emitting Nano-World 203
5.1.1 Size, Shape and Dimensions of Nanomaterials 204
5.1.2 Variations in Nanoparticles Composition, Crystallinity and Order 205
5.1.3 Interactions at Surfaces 206
5.1.4 Peculiarities of FRET with and Between Nanoparticles . . . 207
5.1.5 Concluding Remarks 208
5.2 Dye-Doped Nanoparticles and Dendrimers 209
5.2.1 Contact (Concentrational) Quenching 209
5.2.2 Organic Dyes Incorporated into Organic Polymer 210
5.2.3 Silica-Based Fluorescent Nanoparticles 212
5.2.4 Fluorescent Dendrimers 214
5.2.5 Fluorescent Nanoparticles Made of Organic Dyes and Aggregation-Induced Emission 216
5.2.6 Applications of Dye-Based Nanoparticles in Sensing 218
5.2.7 Frontiers for Future Research 219
5.3 Conjugated Polymers 220
5.3.1 Structure and Spectroscopic Properties 220
5.3.2 Fluorescence Reporting in Sensor Design 223
5.3.3 Designed Conjugated Polymer Nanoparticles 224
5.3.4 Nanocomposites Based on Conjugated Polymers 225
5.3.5 Looking Ahead 226
5.4 Fluorescent Carbon Nanostructures 227
5.4.1 Fluorescent Nanodiamonds 227
5.4.2 Graphene and Graphene Oxide Nanoparticles; Carbon Nanotubes 229
5.4.3 Carbon Dots 231
5.4.4 Origin of Fluorescence of Nanocarbon Materials 231
5.4.5 Carbon Nanoparticles as Universal Quenchers. 233
5.4.6 Applications in Fluorescence Reporting and Imaging 234
5.5 Semiconductor Quantum Dots 235
5.5.1 The Composition of Quantum Dots 236
5.5.2 The Origin of Quantum Dots Emission 237
5.5.3 The Spectroscopic Properties 237
5.5.4 Stabilization and Functionalization of Quantum Dots 240
5.5.5 Applications of Quantum Dots in Sensing 241
5.5.6 Magic-Sized Quantum Dots 244
5.5.7 Semiconductor Nanocrystals of Different Shapes and Dimensions 245

5.5.8 Porous Silicon and Silicon Nanoparticles . . . 245
5.5.9 Prospects . . . 246
5.6 Up-Converting Nanocrystals . . . 246
5.6.1 The Photophysical Mechanism . . . 247
5.6.2 The Spectroscopic Properties . . . 247
5.6.3 Present and Prospective Applications . . . 249
5.7 Sensing and Thinking: Nanoscale Emitters, What Are the Advantages? . . . 251
References . . . 253

6 Fluorescent Nanocomposites . . . 263
6.1 Fluorescence Enhancement and Quenching in Nanocomposites . . . 264
6.1.1 Assembling, Screening, Immobilization . . . 264
6.1.2 Plasmonic Enhancement . . . 265
6.1.3 Excitonic Effects . . . 266
6.1.4 Exciton-Exciton and Plasmon-Exciton Interactions in Nanocomposites . . . 267
6.2 Modulation of Emission Parameters in Multi-Fluorophore Systems . . . 269
6.2.1 Homo-FRET and Hetero-FRET . . . 269
6.2.2 General Rules for Collective Effects in FRET . . . 270
6.2.3 Light-Harvesting (Antenna) Effect . . . 271
6.2.4 Wavelength Converting . . . 273
6.2.5 Extending the Emission Lifetimes . . . 275
6.2.6 Variations of Anisotropy . . . 276
6.2.7 Modulation by Light . . . 277
6.2.8 Looking Ahead . . . 279
6.3 Optical Choice of FRET Donors and Acceptors . . . 280
6.3.1 Lanthanide Chelates and Other Metal-Chelating Luminophores . . . 281
6.3.2 Conjugated Polymers . . . 281
6.3.3 Semiconductor Quantum Dots . . . 282
6.3.4 Up-Conversion Materials . . . 282
6.3.5 Organic Dyes and Visible Fluorescent Proteins . . . 283
6.3.6 Fluorescent Carbon Nanoparticles . . . 283
6.3.7 Noble Metal Nanoparticles . . . 283
6.4 Wavelength Referencing, Multiplexing and Multicolor Coding . . . 284
6.4.1 Wavelength Referencing . . . 284
6.4.2 Multiplex Assays and Suspension Arrays . . . 286
6.4.3 Materials for Multicolor Coding . . . 287
6.4.4 Nanobeads with Quantum Dot Cores . . . 287
6.4.5 Applications of Optical Barcoding . . . 288

6.5 Combining Fluorescence with Magnetic, NMR Enhancing and Other Functionalities 289
6.5.1 Luminescent Plus Magnetic Nanocomposites 289
6.5.2 Fluorescent Plus NMR-Contrasting Nanocomposites 290
6.5.3 Nanocomposites with Multimodal Function 291
6.6 Sensing and Thinking: Achieving Multitude of Functions in Designed Nanocomposites 292
References 294

7 Recognition Units 301
7.1 Multivalency: The Principle of Molecular Recognition 301
7.1.1 The Origin of Target-Receptor Binding Selectivity 303
7.1.2 Quantitative Measure of Multivalency 303
7.1.3 Words in Conclusion 304
7.2 Recognition Units Built of Small Molecules 304
7.2.1 Crown Ethers and Cryptands 305
7.2.2 Boronic Acid Derivatives 306
7.2.3 Cyclodextrins 308
7.2.4 Calix[n]arenes 311
7.2.5 Cucurbit[n]urils 314
7.2.6 Porphyrins 315
7.2.7 Prospects 316
7.3 Antibodies and Their Recombinant Fragments 317
7.3.1 The Types of Antibodies Used in Sensing 318
7.3.2 The Assay Formats Used for Immunoassays 319
7.3.3 Prospects for Antibody Technologies 321
7.4 Ligand-Binding Proteins and Protein-Based Display Scaffolds 321
7.4.1 Engineering the Binding Sites by Mutations 322
7.4.2 Bacterial Periplasmic Binding Protein (PBP) Scaffolds 324
7.4.3 Engineering PBPs Binding Sites and Response of Environment-Sensitive Dyes 325
7.4.4 Scaffolds Based on Proteins of Lipocalin Family 326
7.4.5 Other Protein Scaffolds 327
7.4.6 Prospects 328
7.5 Designed and Randomly Synthesized Peptides 329
7.5.1 Randomly Synthesized Peptides, Why They Do Not Fold? 329
7.5.2 Template-Based Approach 330
7.5.3 The Exploration of ‘Mini-Protein’ Concept 331
7.5.4 Molecular Display Including Phage Display 331
7.5.5 Peptide Binders for Protein Targets and the Prospects of Peptide Sensor Arrays 333

7.5.6 Antimicrobial Peptides and Their Analogs. 335
7.5.7 Advantages of Peptide Technologies and Prospects for Their Development 335
7.6 Nucleic Acid Aptamers. 336
7.6.1 Selection and Production of Aptamers 336
7.6.2 Attachment of Fluorescence Reporter, Before or After Aptamer Selection? 337
7.6.3 Obtaining Fluorescence Response and Integration into Sensor Devices 339
7.6.4 Aptamer Applications. 341
7.6.5 Comparison with Other Binders: Prospects 342
7.7 Peptide Nucleic Acids. 343
7.7.1 Structure and Properties 343
7.7.2 DNA Recognition with Peptide Nucleic Acids 344
7.8 Molecularly Imprinted Polymers 345
7.8.1 The Principle of Imprinted Polymer Formation 346
7.8.2 The Coupling with Reporting Functionality. 347
7.8.3 Applications 347
7.9 Sensing and Thinking: Selecting the Tool for Optimal Target Recognition 348
References 350

8 Mechanisms of Signal Transduction 359
8.1 General Principles of Signal Transduction 359
8.1.1 Target Binding and the Release of Information-Containing Signal. 360
8.1.2 Signal Transduction with the Use of Single Emitters. 361
8.1.3 Signal Transduction with the Use of Coupled Emitters 364
8.1.4 Collective Emitters in Signal Transduction 365
8.2 Basic Signal Transduction Mechanisms: Electron, Charge and Proton Transfer 366
8.2.1 Photoinduced Electron Transfer (PET). 367
8.2.2 Intramolecular Charge Transfer (ICT) 370
8.2.3 Excited-State Proton Transfer. 376
8.2.4 Prospects. 377
8.3 Signal Transduction Via Excited-State Energy Transfer 378
8.3.1 Variation of Distance Between Individual Fluorophores . . . 378
8.3.2 Variations of Spectroscopic Parameters 379
8.3.3 FRET-Gating. 381
8.3.4 Exploration of Collective Effects in FRET. 381
8.3.5 Prospects. 383
8.4 Superenhancement and Superquenching 383
8.4.1 The Essence of Superquenching. 384
8.4.2 Realization of Superquenching. 385

8.5 Signal Transduction Via Conformational Changes 386
8.5.1 Excited-State Isomerism in the Reporter Dyes and Small Molecules 386
8.5.2 Conformational Changes in Conjugated Polymers 386
8.5.3 Conformational Changes in Peptide Sensors and Aptamers 388
8.5.4 Molecular Beacons 391
8.5.5 Proteins Exhibiting Conformational Changes 394
8.5.6 Prospects 398
8.6 Signal Transduction Via Association and Aggregation Phenomena 398
8.6.1 Association of Nanoparticles on Binding Polyvalent Target 399
8.6.2 Association-Induced FRET and Quenching 400
8.7 Smart Sensing with Logical Operations 400
8.7.1 Why Logical Operations in Fluorescence Sensing? 401
8.7.2 Logical Operations on Molecular Scale 402
8.7.3 Exploration of Basic Signal Transduction Mechanisms 403
8.7.4 Applications in Sensing and Imaging Technologies 405
8.7.5 Prospects 407
8.8 Sensing and Thinking: How to Couple the Recognition and Reporting Functionalities? 407
References 409

9 Supramolecular Structures and Interfaces Designed for Sensing 417
9.1 Self-Assembled Supramolecular Systems 418
9.1.1 Affinity Coupling 419
9.1.2 Self-Assembly 421
9.1.3 Two-Dimensional Self-Assembling of S-Layer Proteins . . . 422
9.1.4 Template-Assisted Assembly 423
9.1.5 Prospects 424
9.2 Building Blocks for Supramolecular Sensors 424
9.2.1 Graphene and Graphene Oxide 425
9.2.2 Carbon Nanotubes 427
9.2.3 Fullerenes 427
9.2.4 DNA Templates 428
9.2.5 Peptide Scaffolds 429
9.2.6 Inorganic Colloidal Scaffolds 431
9.3 Conjugation, Labeling and Cross-Linking 432
9.3.1 Nano-bio Conjugation 433
9.3.2 Techniques of Conjugation and Labeling 433
9.3.3 Co-synthetic Modifications 435
9.3.4 Chemical and Photochemical Cross-Linking 436

9.4 Supporting and Transducing Surfaces 437
9.4.1 Surfaces with Passive Role. Covalent Attachments 438
9.4.2 Self-Assembled Monolayers. 439
9.4.3 Langmuir-Blodgett Films 442
9.4.4 Layer-by-Layer Approach 443
9.4.5 Prospects. 444
9.5 Functional Lipid and Polymer Bilayers 444
9.5.1 Liposomes as Integrated Sensors 445
9.5.2 Stabilized Phospholipid Bilayers 448
9.5.3 Polymersomes. 449
9.5.4 Formation of Protein Layers Over Lipid Bilayers 450
9.5.5 Prospects. 451
9.6 Sensing and Thinking: Extending Sensing Possibilities with Smart Nano-ensembles. 451
References 453

10 Non-conventional Generation and Transformation of Response . . . 459
10.1 Chemiluminescence and Electrochemiluminescence. 460
10.1.1 Chemiluminescence. 460
10.1.2 Enhanced Chemiluminescence 462
10.1.3 Nanoparticle-Based Platforms in Chemiluminescence . . 462
10.1.4 Electrochemiluminescence 463
10.1.5 Cathodic Luminescence. 465
10.1.6 Essentials of the Techniques and Their Prospects. 466
10.2 Bioluminescence. 467
10.2.1 The Origin of Bioluminescence. 467
10.2.2 Genetic Manipulations with Luciferase. 468
10.2.3 Bioluminescence Producing Resonance Energy Transfer 469
10.2.4 Prospects 470
10.3 Radioluminescence and Cherenkov Effect 470
10.3.1 Radioluminescence 471
10.3.2 Self-Illumination by Radioactive Decay 472
10.4 Two-Photon Excitation and Stimulated Emission 474
10.4.1 Two-Photon and Multi-Photon Fluorescence 474
10.4.2 Amplified Stimulated Emission. 477
10.5 Direct Optical Generation of Electrical Response Signal. 480
10.5.1 Light-Addressable Potentiometric Sensors 480
10.5.2 The Photocells as Potential Sensors 482
10.6 Evanescent-Wave Fluorescence Sensors. 482
10.6.1 Excitation by Evanescent Field 483
10.6.2 Applications in Sensing. 484
10.7 Plasmonic Enhancement of Luminescence Emission. 485
10.7.1 Surface Plasmon Resonance and Surface Plasmon-Field Enhanced Fluorescence 486
10.7.2 Modulation of Light Emission by Plasmonic Nanoparticles. 488

10.7.3 The 'Nanoantenna' Mechanism of Fluorescence Enhancement by Local Field . . . 490
10.7.4 The Plasmonic Modulation of Emission . . . 492
10.7.5 Extended Range of Observations . . . 494
10.7.6 Applications of Metal Enhancement . . . 495
10.7.7 Microwave Acceleration of Metal-Enhanced Emission . . . 496
10.7.8 Prospects . . . 498
10.8 Sensing and Thinking: Eliminating Light Sources and Photodetectors: What Remains? . . . 498
References . . . 500

11 The Sensing Devices . . . 507
11.1 Instrumentation for Fluorescence Spectroscopy . . . 509
11.1.1 Standard Spectrofluorimeter . . . 509
11.1.2 Light Sources . . . 510
11.1.3 Light Detectors . . . 512
11.1.4 Passive Optical Elements . . . 515
11.1.5 Integrated Systems . . . 516
11.1.6 Prospects . . . 517
11.2 Optical Waveguides and Optodes . . . 518
11.2.1 Optical Fiber Sensors with Optode Tips . . . 519
11.2.2 Evanescent-Field Waveguides . . . 521
11.3 Multi-analyte Spotted Microarrays . . . 522
11.3.1 Fabrication . . . 523
11.3.2 Problems with Microarray Performance . . . 524
11.3.3 Read-Out and Data Analysis . . . 525
11.3.4 Applications of Spotted Microarrays . . . 526
11.3.5 Prospects . . . 528
11.4 Suspension Arrays and Barcoding . . . 529
11.4.1 Construction of Suspension Arrays . . . 529
11.4.2 Barcodes for Microsphere Suspension Arrays . . . 530
11.4.3 Reading the Information from Microspheres . . . 530
11.4.4 Applications . . . 532
11.4.5 Prospects . . . 533
11.5 Microfluidic Devices . . . 534
11.5.1 Fabrication and Operation of a Lab-on-a-Chip . . . 534
11.5.2 Microfluidic Devices as Microscale Reactors and Analytical Tools . . . 536
11.5.3 Fluorescence Detection in Microfluidic Devices . . . 536
11.5.4 Prospects . . . 537
11.6 Devices Incorporating the Whole Living Cells . . . 538
11.6.1 Cellular Microorganisms or Human Cultured Cell Lines? . . . 539
11.6.2 Living and Fixed Cells . . . 540
11.6.3 Single Cells in Microfluidic Devices . . . 540
11.6.4 Bacterial Cells with Genetically Incorporated Sensors . . . 542
11.6.5 The Cultured Human Cells . . . 543

11.6.6 The Whole Cell Arrays 543
11.6.7 Prospects 543
11.7 Sensing and Thinking: Optimizing Convenience, Sensitivity and Precision for Obtaining the Proper Sensor Response. 544
References 545

12 Focusing on Targets 551
12.1 Temperature, Pressure and Gas Sensing 552
12.1.1 Molecular Thermometry 552
12.1.2 Molecular Barometry. 554
12.1.3 The Sensors for Gas Phase Composition. 555
12.2 Probing the Properties of Condensed Matter 557
12.2.1 Polarity Probing in Liquids and Liquid Mixtures 557
12.2.2 Viscosity and Molecular Mobility Sensing 560
12.2.3 Probing the Ionic Liquids 562
12.2.4 The Properties of Supercritical Fluids. 563
12.2.5 The Structure and Dynamics in Polymers. 564
12.2.6 Fluorescence Probing the Interfaces 565
12.3 Detection of Small Molecules and Ions 567
12.3.1 pH Sensing. 567
12.3.2 Oxygen 568
12.3.3 Heavy Metals. 569
12.3.4 Glucose 570
12.3.5 Hydrogen Peroxide 571
12.3.6 Cholesterol. 572
12.4 Nucleic Acid Detection and Sequence Identification 572
12.4.1 Detection of Double-Stranded DNA 572
12.4.2 Distinguishing Double-Stranded and Single-Stranded DNA and RNA. 574
12.4.3 Sequence-Specific DNA Recognition 576
12.4.4 The ‘DNA Chip’ Hybridization Techniques 577
12.4.5 Sandwich Assays in DNA Hybridization 580
12.4.6 Molecular Beacon Technique 580
12.4.7 DNA Sensing Based on Conjugated Polymer 582
12.4.8 Quadruplex DNA. 583
12.4.9 Conclusive Remarks and Prospects. 583
12.5 Recognition of Protein Targets 584
12.5.1 Total Protein Content. 584
12.5.2 Specific Protein Recognition 585
12.5.3 High Throughput Protein Arrays. 586
12.6 Polysaccharides, Glycolipids and Glycoproteins 588
12.7 Detection of Harmful Microbes 589
12.7.1 Detection and Identification of Bacteria 589
12.7.2 Bacterial Spores. 590
12.7.3 Detection of Toxins 591
12.7.4 Sensors for Viruses 591

12.8 Sensing and Thinking: Adaptation of Sensor Units for Multi-scale and Hierarchical Range of Targets 592
References 593

13 Sensing Inside the Living Cells 603
13.1 Modern Fluorescence Microscopy 604
13.1.1 Epi-fluorescence Microscopy 605
13.1.2 Total Internal Reflection Fluorescence Microscopy (TIRF) 607
13.1.3 Confocal Microscopy 608
13.1.4 Programmable Array Microscope 609
13.1.5 Two-Photon and Three-Photon Microscopy 611
13.1.6 Time-Resolved and Time-Gated Imaging 612
13.1.7 Wavelength-Ratiometric Imaging 613
13.1.8 Traditional Fluorescence Microscopy: Advances and Limitations 615
13.2 Super-Resolution Microscopy. 615
13.2.1 Breaking the Diffraction Limit 616
13.2.2 Near-Field Scanning Microscopy 616
13.2.3 Stimulated Emission Depletion (STED) Microscopy . . . 618
13.2.4 Stochastic Methods in Super-Resolution Imaging (PALM, STORM, etc.) 622
13.2.5 Structured Illumination Microscopy (SIM). 625
13.2.6 Critical Comparison of the Techniques 625
13.3 Sensing and Imaging on a Single Molecule Level 626
13.3.1 Observation of Single Molecules 626
13.3.2 Considerations on the Problem of Photobleaching 628
13.3.3 Single Molecules Observed with Wide-Field Microscopic Techniques 628
13.3.4 Single-Molecular Studies in Solutions 631
13.3.5 Single-Molecular Sensors 632
13.3.6 Fluorescence Correlation Spectroscopy and Microscopy 634
13.3.7 Single Molecules Inside the Living Cells 636
13.3.8 Additional Comments 639
13.4 Site-Specific Intracellular Labeling and Genetic Encoding 639
13.4.1 Attachment of Fluorescent Reporter to Any Cellular Protein 640
13.4.2 Genetically Engineered Protein Labels 643
13.4.3 Co-synthetic Incorporation of Fluorescence Dyes 644
13.4.4 Concluding Remarks 646
13.5 Advanced Nanosensors Inside the Cells 647
13.5.1 Fluorescent Dye-Doped Nanoparticles in Cell Imaging 647
13.5.2 The Quantum Dots Applications in Imaging. 648
13.5.3 Self-Illuminating Quantum Dots 649

13.5.4 Detection of Intracellular Motions 650
13.5.5 Extending the Range of Detection Methods 651
13.6 Sensing Within the Cell Membrane 651
13.6.1 Membrane Structure and Dynamics 651
13.6.2 Lipid Asymmetry and Apoptosis. 652
13.6.3 Sensing the Membrane Potential 654
13.6.4 Membrane Receptors. 657
13.6.5 Future Directions 658
13.7 Sensing Different Targets in Cell Interior 658
13.7.1 Ion Sensing 659
13.7.2 Tracking Cellular Signaling. 662
13.7.3 Oxygen in Living Cells 663
13.7.4 Location of Metabolites and Tracking Metabolic Events 665
13.7.5 In-situ Hybridization 665
13.7.6 Looking Forward 666
13.8 Sensing and Thinking: Intellectual and Technical Means for Addressing the Systems of Great Complexity 666
References 668

14 Sensing the Whole Body and Clinical Diagnostics 677
14.1 Ex-vivo Diagnostics 678
14.1.1 Diagnosis and Treatment of Diabetes 679
14.1.2 Diagnostics with Cardiac Biomarkers 681
14.1.3 The Markers of Autoimmune Diseases 682
14.1.4 Diagnostics of Infectious Diseases 682
14.1.5 Diagnostics of Cancer 684
14.1.6 Kidney and Liver Related Diseases. 684
14.1.7 Prospects of Ex-vivo Clinical Diagnostics Technologies 685
14.2 Sensing the Whole Body. 686
14.2.1 On the Optical Properties of Human Body 686
14.2.2 Optimal Imaging Techniques. 687
14.2.3 Fluorescence Contrast Agents and Reporters 688
14.2.4 Imaging Cancer Tissues. 691
14.2.5 Monitoring the Response to Therapy 692
14.2.6 Contrasting the Blood Vessels and Lymph Nodes. 693
14.2.7 Fluorescence Image Guided Surgery. 695
14.2.8 Conclusions 697
14.3 Monitoring the Cells Inside the Living Body 697
14.3.1 The Labeling Procedure 698
14.3.2 Tracking Hematopoietic and Cancer Cells 700
14.3.3 Trafficking the Stem Cell. 700
14.3.4 Conclusions 701

14.4 Theranostics: Combining Targeting, Imaging and Therapy 702
14.4.1 Combining Different Imaging Functionalities 703
14.4.2 Combining Imaging and Targeting 704
14.4.3 Photothermal Therapy 705
14.4.4 Photodynamic Therapy 706
14.4.5 Controlled Drug Release 708
14.4.6 Gene Targeting and Release 709
14.4.7 Conclusions and Prospects 710
14.5 Sensing and Thinking: The Strategy of Controlling by Light Diagnostics and Treatment 710
References 712

15 Opening New Horizons 719
15.1 Genomics, Proteomics and Other 'Omics' 720
15.1.1 Gene Expression Analysis 721
15.1.2 The Analysis of Proteome 723
15.1.3 Addressing Interactome 727
15.1.4 Metabolomics 729
15.1.5 Outlook 729
15.2 The Sensors to Any Target and to Immense Number of Targets . . . 730
15.2.1 Combinatorial Approach on a New Level 730
15.2.2 Toxic Agents and Pollutants Inconvenient for Detection 732
15.2.3 The Problem of Coding and Two Strategies in Its Solution 733
15.2.4 Prospects 735
15.3 New Level of Clinical Diagnostics 735
15.3.1 The Need for Speed 735
15.3.2 The Whole Blood Sensing 736
15.3.3 Testing the Non-invasive Biological Fluids 737
15.3.4 Gene-Based Diagnostics 737
15.3.5 Prospects 738
15.4 Advanced Sensors in Drug Discovery 738
15.4.1 High Throughput Screening 739
15.4.2 Screening the Anti-cancer Drugs 740
15.4.3 Future Directions 740
15.5 Towards Sensors That Reproduce Human Senses 741
15.5.1 Electronic Nose 741
15.5.2 Electronic Tongue 742
15.5.3 Olfactory and Taste Cells on Chips and the Whole-Animal Sensing 743
15.5.4 Lessons Obtained for Sensing 744
15.6 Sensors Promising to Change the Society 745
15.6.1 Industrial Challenges and Safe Workplaces 745
15.6.2 Biosensor-Based Lifestyle Management 746
15.6.3 Wearable Sensors 748

15.6.4 Living in a Safe Environment and Eating Safe Products 749
15.6.5 Implantable and Digestible Miniature Sensors Are a Reality 750
15.6.6 Robotic Operations Coupled with Fluorescence Imaging 752
15.6.7 Prospects 753
15.7 Sensing and Thinking: Where Do We Stand and Where Should We Go? 754
References 755

Epilogue 761

Appendix: Glossary of Terms Used in Fluorescence/ Luminescence Sensing 765

Index 779

Introduction

The simplest common definition of a sensor is that 'a sensor is something that senses', i.e. receives information and transforms it into a form compatible with our perception, knowledge and understanding. Our body is full of sensors that respond to light, heat, taste, etc. With the development of civilization they became insufficient for orientation of personality, community or the whole society in new conditions. More and more we need objective knowledge on what is happening inside and outside of our body and what are benefits and threats to the whole society. There is a necessity to know what compounds are useful and what are harmful, how safe and healthy is our environment and to monitor them continuously. Different industrial processes including that of production of agricultural goods, food processing and storage need to be controlled as well. The human genome is a very useful piece of knowledge only when we can analyze gene expression and find its relation with individuality, age and disease. We need to know the distribution inside living cells of many compounds, including enzymes and their regulators and also substrates and products of these reactions. This information may need to be obtained throughout the whole cell life cycle including its division, differentiation, aging and apoptosis. All that can be accomplished only with the help of man-made sensors. They will be the subject of this book.

Introducing the reader to the world of science and technology in fluorescence sensing and imaging, we first introduce the definitions of chemical sensors and biosensors. Their mechanism of operation should be based on molecular recognition of the target with the involvement of some signal transduction and reporting functions. In this book we concentrate on reporting based on light emission, mostly fluorescence. Distinguishing features of fluorescence is an extremely high absolute sensitivity combined with sensitivity to energies of intermolecular interactions, ultrahigh temporal resolution and speed of response and also great spatial resolution. Together with the ability of observing optical signal at a distance, this method features unprecedented versatility.

The man-made sensors are often called *chemical sensors* and those of them that involve biology-related compounds and/or biospecific target binding – *biosensors*. According to the definition approved by IUPAC, 'a chemical sensor is a device that

transforms chemical information, ranging from the concentration of a specific sample component to total composition analysis, into an analytically useful signal'. Thus the sensor can be regarded as both a designed molecule and a miniaturized analytical device that delivers real-time and online information on the presence of specific compounds in complex samples (Thevenot et al. 1999). In a narrow sense, *the sensor is a molecule or assembled supra-molecular unit (or nanoparticle) that is able to selectively bind the target molecule (or supra-molecular structure, living cell) and provide information about this binding*. In a broader sense, it should include control and processing electronics, interconnecting networks, software and other elements needed to make the signal not only recordable but understandable.

The mechanisms operating on molecular, supra-molecular and cellular levels of acquisition of primary information on the presence and amount of target compounds, particles and cells and of reporting about that in the form of fluorescence signal will be of primary concern in this book. The relevant analytic devices will be also discussed in due course but in a much lesser extent. Our view is that the immense world of potential target compounds is incomparably larger than the variations of instrumental design based on modern electronics and optics. In principle, each member of this world needs its own sensor. It is a great challenge to create them.

Because of this broad range of potential applications (Cooper 2003a), sensing techniques are attracting an increasing interest of researchers. A number of excellent reviews have been published in the field of chemical sensors, biosensors and nanosensors. By addressing a number of publications, one can make comparative analysis of different sensing strategies: electrochemical (Warsinke et al. 2000; Palecek et al. 2002); microcantilever (Carrascosa et al. 2006); optical (Baird et al. 2002; Baird and Myszka 2001) including surface plasmon resonance (SPR) (Baird et al. 2002; Homola 2003) and microrefractometric-microreflectometric techniques (Gauglitz 2005). Regarding fluorescence sensing techniques one can find important information in the books of Lakowicz and Valeur (Lakowicz 2006; Valeur and Berberan-Santos 2012) and reviews (Lakowicz et al. 1999; de Silva et al. 2001, 1997). In some reviews, the applications in particular areas are outlined: food safety (Patel 2002), clinical applications and environment monitoring (Andreescu and Sadik 2004, 2005; Nakamura and Karube 2003), detection of biological warfare agents (Gooding 2006), pharmacology and toxicology (Cooper 2003a). Particular recognition units were highlighted, from antibodies (Luppa et al. 2001) and aptamers (O'Sullivan 2002; Tombelli et al. 2005) to functional nanoparticles (Apostolidis et al. 2004) and to whole living cells (Pancrazio et al. 1999). Sensing technologies have started to be used not only in cells but also on the level of whole human bodies (Wilson and Ammam 2007). It is difficult to get oriented in this broad and permanently increasing mass of information. Therefore, systematization of obtained results and their critical evaluation are highly needed.

The *general problem* in any sensor technology can be formulated as follows. We have the target molecule, particle or cell dispersed in a medium that may contain many similar molecules, particles or cells. We have to provide a sensor that has to be incorporated into this medium or exposed to contact with it. The presence of target should be revealed by its selective binding to the sensor. This binding should

be detected and, if necessary, quantified in target concentration. This requires some transduction mechanism that connects the binding (molecular event) and its detection by the instrument, on the scale of our vision and understanding.

The sensor and biosensor technologies used for performing this task are based on *different physical principles*. They develop in parallel, competing with and enriching each other. Some transduction principles, as those used in surface plasmon resonance (SPR) sensors, acoustic sensors, microcantilevers and microcalorimeters, can be applied to any molecular interaction because they are based on the changes in mass or in heat, which are general features of complex formation (Cooper 2003b). However, these approaches generally require sophisticated instrumentation restricting their use to research purposes. In contrast, electrochemical sensors that are based on redox reactions at electrodes (Palecek et al. 2002) are very simple since they allow direct conversion of signal on target binding into electrical signal. But they are still not always applicable because the sensing mechanism is not general enough. For instance, in biosensing they are mostly based on enzymatic activity generating a detectable product, and are therefore restricted to monitoring of substrate(s) or effector(s) of a particular enzyme. Therefore there is a need for generic sensing strategies that can be applied to the detection of any target, rely on low cost and easy-to-use instrumentation, and are suitable for on-the-spot or field analysis. In addition, as required in some applications, the response should be very fast and the spatial resolution high enough to allow obtaining microscope images of target distribution and reading from sensors assembled in microarrays containing thousands of spots. This method exists, it is fluorescence.

Thus, what distinguishes fluorescence from all other methods suggested for reporting about sensor-target interaction? Primarily it is its *ultra-high sensitivity* (Lakowicz 1999, 2006; Valeur 2002). This feature is especially needed if the analyte exists in trace amounts. High sensitivity may allow avoiding time-consuming and costly enrichment steps. Meanwhile, one has to distinguish the absolute sensitivity, which is the sensitivity of detecting the fluorescent dye (or particle) from sensitivity in response to target binding. With proper dye selection and proper experimental conditions, the absolute sensitivity may reach the limit of single molecules. This is sufficient and very attractive for many applications, particularly for those in which the dyes are used as labels and the primary response from them is not required. The other type of sensitivity is necessary to achieve for providing the necessary dynamic range of variation of the recorded fluorescence parameters in detecting the sensor-target interaction. This is a much harder task, which we will discuss in detail.

The second distinguishing feature of fluorescence is the *high speed* of response. This response can be as fast as 10^{-8}–10^{-10} s and is limited by fluorescence lifetime and the speed of photophysical or photochemical event that provides the response. Usually such high speed is not needed but sometimes it is essential. For instance, probing the rate of action potential propagation in excitable cells needs subnanosecond time resolution. The speed of sensor response commonly is not limited by fluorescence reporting. It is limited by other factors, such as the rate of target – sensor mutual diffusion and of establishment the dynamic equilibrium between bound and unbound target.

The very high spatial resolution that can be achieved with fluorescence is important. It allows detecting cellular images and operating with dense multi-analyte sensor arrays. This resolution in common microscopy is limited to about 500 nm (in visible light). The limit is due to the effect of diffraction of light when the dimensions become similar or shorter than the wavelength. Even this limit can be overcome in special conditions.

The *non-destructive* and *non-invasive* character of fluorescence sensing may be beneficial primarily for many biological and medical applications. In fluorescence sensing, the reporter dye and the detecting instrument are located at a certain distance and connected via propagation of light. This is why fluorescence detection is equally well suited to remote control of chemical reactions in industry and to sensing different targets within living cells.

But the greatest advantage of fluorescence reporting is its *versatility* coming from the basic event of the fluorescence response. It is essentially a photophysical event coupled to a molecular event of sensor-target interaction. That is why it can be achieved in any environment: in solid, liquid and gas media and at all kinds of interfaces between them. The basic mechanism of response remains always the same. It does not impose any limit on formation of any supra-molecular structures, incorporation of reporter into any nano-composite, attachment to solid support, etc. This allows not only creating smart molecular sensing devices: their attachment to the surfaces in heterogeneous assays or integration into nanoparticles endows new functional possibilities. Due to these facts, homogeneous assays in liquid media develop into nanosensor technologies in which, in addition to fluorescence, different self-assembling, magnetic and optical properties can be explored. In microfluidic devices, the detection volume can be reduced to nanoliters. Heterogeneous assays develop into multi-analyte microarrays (sensor chips), which allow simultaneous detection of several hundreds and thousands of analytes. Two-photon and confocal microscopies allow one to obtain three-dimensional images, which allow localizing target compounds in space.

In any sensing technology, the sensor should switch between two distinguishable states – free and with bound target. There are two possibilities for reporting about binding event and for providing a signal for distinguishing these states, and both of them can be realized in fluorescence sensing. First is *indirect*: to label one of these states and then to provide quantitative measure for labelling that will be connected with the quantity of bound target. This needs additional reagents and special treatments to separate bound and unbound labels and that is why we call this approach indirect. The reporter in this case should provide stable and bright fluorescence response, and additional manipulation with the sample makes this response informative. The other possibility is *direct*: the sensor reports immediately and without any treatments on the primary act of sensor-target interaction. This requires from the fluorescence reporter a different property: to change the parameters of its emission to the very act of target binding. And it is the variation of this parameter that

can be calibrated in target concentration. Both possibilities show their merits and weaknesses. And both of them allow broad possibilities for technical solutions.

The last decade has seen tremendous progress in the development of molecular binders – recognition units of molecular sensors, nanosensors and sensing devices. Each of them should exhibit high affinity to a target analyte and high level of discrimination against the species of similar structure. This can be achieved in many ways: by using complementarity in DNA and RNA sequences, by applying monoclonal antibodies and their recombinant fragments, natural protein receptors and their analogs, combinatorial peptide and polynucleotide libraries, compounds forming inclusion complexes, imprinted polymers, etc. Imagine that one succeeded to select or to design the whole range of necessary binders. In order to benefit from that and to make efficient sensors, an efficient mechanism of transduction of this effect of binding into detectable signal should be applied. The response has to be developed based on available fluorescent dyes and preferable fluorescence parameter to be recorded. Synthetic chemistry offers tremendous numbers of fluorescent organic dyes (fluorophores) plus many types of nanoparticles and nanocomposites, whereas optical detection methods are much more limited. They involve measuring only several parameters, such as fluorescence excitation and emission spectra, and also relative intensities, anisotropies (or polarizations) and lifetimes at particular wavelengths. The optimal choice among these possibilities means the optimal strategy in fluorescence sensing technology.

Particular attention should be given to the coupling of sensing elements with fluorescent reporter dyes and to the methods for producing efficient fluorescence response. Fluorescence reporter units are commonly referred to as ‘dyes’. Indeed, in most cases they are organic dyes that contain extended π-electronic systems with excitation and emission in the convenient visible range of spectrum. In addition, coordinated transition metal ions can be used since they produce luminescence emission with extended lifetimes. (In this and similar cases it should be more correct to use the term ‘luminescence sensing’ but it is still not in common use). Some semiconductor nanoparticles known as quantum dots can generate narrow-band emission and this property can also be used in sensing. The other possibility that is very attractive for intracellular studies is related to green fluorescent protein (GFP) and its analogs. In this case, the fluorescent moiety appears as a result of folding of the polypeptide chain and a reaction between proximate amino acid side groups.

One cannot predict the long-run future developments of sensor technologies. But what is sure, they are rapidly becoming a part of everyday life. Thus, for helping diabetes patients the colour-changing glucose sensor molecules are already incorporated into plastic eye contact lenses (Badugu et al. 2003) and it was reported on the development of ‘an ingestible one-use nanotechnology biosensor’ that can be swallowed like a vitamin to report in fluorescent light about the pathological changes in human tissues (Kfouri et al. 2008). So, what will happen next?

References

Andreescu S, Sadik OA (2004) Trends and challenges in biochemical sensors for clinical and environmental monitoring. Pure Appl Chem 76(4):861–878

Andreescu S, Sadik OA (2005) Advanced electrochemical sensors for cell cancer monitoring. Methods 37(1):84–93

Apostolidis A, Klimant I, Andrzejewski D, Wolfbeis OS (2004) A combinatorial approach for development of materials for optical sensing of gases. J Comb Chem 6(3):325–331

Badugu R, Lakowicz JR, Geddes CD (2003) A glucose sensing contact lens: a non-invasive technique for continuous physiological glucose monitoring. J Fluoresc 13(5):371–374

Baird CL, Myszka DG (2001) Current and emerging commercial optical biosensors. J Mol Recognit 14(5):261–268

Baird CL, Courtenay ES, Myszka DG (2002) Surface plasmon resonance characterization of drug/liposome interactions. Anal Biochem 310(1):93–99

Carrascosa LG, Moreno M, Alvarez M, Lechuga LM (2006) Nanomechanical biosensors: a new sensing tool. TrAC Trends Anal Chem 25(3):196–206

Cooper MA (2003a) Biosensor profiling of molecular interactions in pharmacology. Curr Opin Pharmacol 3(5):557–562

Cooper MA (2003b) Label-free screening of bio-molecular interactions. Anal Bioanal Chem 377(5):834–842

de Silva AP, Gunaratne HQN, Gunnaugsson T, Huxley AJM, McRoy CP, Rademacher JT, Rice TE (1997) Signaling recognition events with fluorescent sensors and switches. Chem Rev 97:1515–1566

de Silva AP, Fox DB, Moody TS, Weir SM (2001) The development of molecular fluorescent switches. Trends Biotechnol 19(1):29–34

Gauglitz G (2005) Direct optical sensors: principles and selected applications. Anal Bioanal Chem 381(1):141–155

Gooding JJ (2006) Biosensor technology for detecting biological warfare agents: recent progress and future trends. Anal Chim Acta 559(2):137–151

Homola J (2003) Present and future of surface plasmon resonance biosensors. Anal Bioanal Chem 377(3):528–539

Kfouri M, Marinov O, Quevedo P, Faramarzpour N, Shirani S, Liu LWC, Fang Q, Deen MJ (2008) Toward a miniaturized wireless fluorescence-based diagnostic Imaging system. IEEE J Sel Top Quantum Electron 14(1):226–234

Lakowicz JR (1999) Principles of fluorescence spectroscopy. Kluwer Academic, New York

Lakowicz JR (2006) Principles of fluorescence spectroscopy, 3rd edn. Springer, New York

Lakowicz JR, Gryczynski I, Gryczynski Z, Tolosa L, Dattelbaum JD, Rao G (1999) Polarization-based sensing with a self-referenced sample. Appl Spectrosc 53(9):1149–1157

Luppa PB, Sokoll LJ, Chan DW (2001) Immunosensors – principles and applications to clinical chemistry. Clin Chim Acta 314(1–2):1–26

Nakamura H, Karube I (2003) Current research activity in biosensors. Anal Bioanal Chem 377(3):446–468

O'Sullivan CK (2002) Aptasensors–the future of biosensing? Anal Bioanal Chem 372(1):44–48

Palecek E, Fojta M, Jelen F (2002) New approaches in the development of DNA sensors: hybridization and electrochemical detection of DNA and RNA at two different surfaces. Bioelectrochemistry 56(1–2):85–90

Pancrazio JJ, Whelan JP, Borkholder DA, Ma W, Stenger DA (1999) Development and application of cell-based biosensors. Ann Biomed Eng 27(6):697–711

Patel PD (2002) (Bio)sensors for measurement of analytes implicated in food safety: a review. TrAC Trends Anal Chem 21(2):96–115

Thevenot DR, Toth K, Durst RA, Wilson GS (1999) Electrochemical biosensors: recommended definitions and classification – (technical report). Pure Appl Chem 71(12):2333–2348

Tombelli S, Minunni M, Mascini M (2005) Analytical applications of aptamers. Biosens Bioelectron 20(12):2424–2434
Valeur B (2002) Molecular fluorescence. Wiley VCH, Weinheim
Valeur B, Berberan-Santos MN (2012) Molecular fluorescence: principles and applications. Wiley-VCH Verlag GmbH, Weinheim, FRG. doi: 10.1002/3527600248.fmatter_indsub
Warsinke A, Benkert A, Scheller FW (2000) Electrochemical immunoassays. Fresenius J Anal Chem 366(6–7):622–634
Wilson GS, Ammam M (2007) In vivo biosensors. FEBS J 274(21):5452–5461

Chapter 1
Basic Principles

No Interaction – No Information This principle is clearly seen in the background of all sensing technologies. In every interaction, we have at least two partners. One is, of course, the object that has to be detected, called the *target* or *analyte*. It can be a species of any size and complexity, starting from protons, small molecules and ions, up to large particles and living cells. The other partner, designed or selected for target detection, is the *sensor*.

Booming of sensor technologies is a response to a strong demand in society. As a result, almost every physical principle and technique that can detect interactions between molecules, particles and interfaces was suggested and tested for application in sensing. In this Chapter we provide a short survey of basic strategies in molecular sensing and try to determine the role of those of them that are based on fluorescence detection. Some of them are of rather general nature and others are specific for fluorescence technique.

1.1 Overview of Strategies in Molecular Sensing

The term '*sensor*' is often used in a very broad sense. In a narrow sense, however, the sensor should be a unit able to perform two important functions: (1) providing the target (analyte) binding; (2) reporting on this binding by generating an informative signal. Coupling of these functions requires a functional linker or linking mechanism that is called *transduction* (Fig. 1.1).

In order to provide information on the presence, concentration or localization of the target, the sensor-target interaction should proceed in a highly selective way, recognizing it from other objects of similar structure and properties that can be present in the probed system. The structure responsible for that is called the *recognition unit* or *receptor*. Addressing the demand of target detection, it can also be the object of any size and complexity. The target-binding properties are specific for every target. They can be realized in many different ways (antibodies, aptamers, coordina-

A.P. Demchenko, *Introduction to Fluorescence Sensing*,
DOI 10.1007/978-3-319-20780-3_1

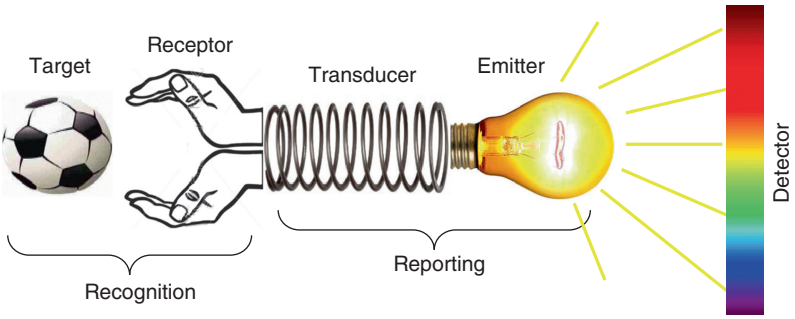

Fig. 1.1 Basic functional elements of fluorescent chemical sensor and biosensor

tion compounds, etc.). This issue is well elaborated in the literature and will be extensively discussed in Chap. 7. The target-receptor affinity interactions involve reversible multiple binding through noncovalent bonds, such as ionic bonds, hydrogen bonds, and van der Waals interactions. The product of an *affinity interaction* is a specific molecular association complex. In order for such a complex to form, the involved species should be complementary with respect to shape and provide maximal amount of attractive interactions. Optimized realization of such steric and energetic factors is called *molecular recognition*.

These interactions are 'blind' until they are detected. Therefore, the other function of the sensor is to 'visualize' them, to report about the interaction events by providing the signal that can be analyzed and counted. The structure that is responsible for generation of this signal is called a *reporter*. A variety of reporters and the mechanisms in the background of their operation will be discussed in this book with a focus on fluorescence reporting. A series of recently published books discussing different structural and functional aspects of fluorescence reporters (Demchenko 2010a, b, 2011; Valeur and Berberan-Santos 2012) may be useful for interested reader.

The transformation of the signal about the binding event into the response of a reporter is called *transduction*, and if additional elements of structure are needed for that, they got the name *transducer*. In a broader sense, the transducer is also the physical mechanism that couples the receptor and reporter functionalities, such as conformational change or electronic charge transfer. Such mechanisms will be discussed in Chap. 8.

Sensor as an analytical tool also needs a *detector*. It involves instrumentation, which is important as an interface between the micro-world of molecules and macro-world in which we live. In the micro-world the elementary events in sensing occur, and in the macro-world we have to analyze the results and make our decisions.

1.1.1 Basic Definitions: Sensors and Assays, Homogeneous and Heterogeneous

Assay is a broader term than sensor, since it may involve diverse manipulations with the tested system that may include different chemical and biochemical reactions. *Sensing* is always a more direct procedure, which is based on an interaction between the target

and a particular sensor unit and generating detectable response to this interaction. The latter can be a molecule, a particle or a solid surface in which additional reactions are not needed or can be used only for amplification of primary effect of such interaction. Both assays and sensors can operate in heterogeneous or homogeneous formats.

Experimental formats without any separation or washing steps (only "mix and measure") are called *homogeneous* whereas the formats for assays and sensors that involve multistep separation setups are referred to *heterogeneous* ones. The latter formats are those that require separation of the sensor-target complex for subsequent detection by any analytical method, including fluorescence. Most convenient way to perform that is by using a *heterogeneous system*, in which the sensor elements are immobilized on a solid support. In this case, after incubation in the tested medium the unreacted species that are present in the system can be removed prior to analysis simply by washing. If necessary, additional reagents can be added for visualization or generation of response signal (Fig. 1.2).

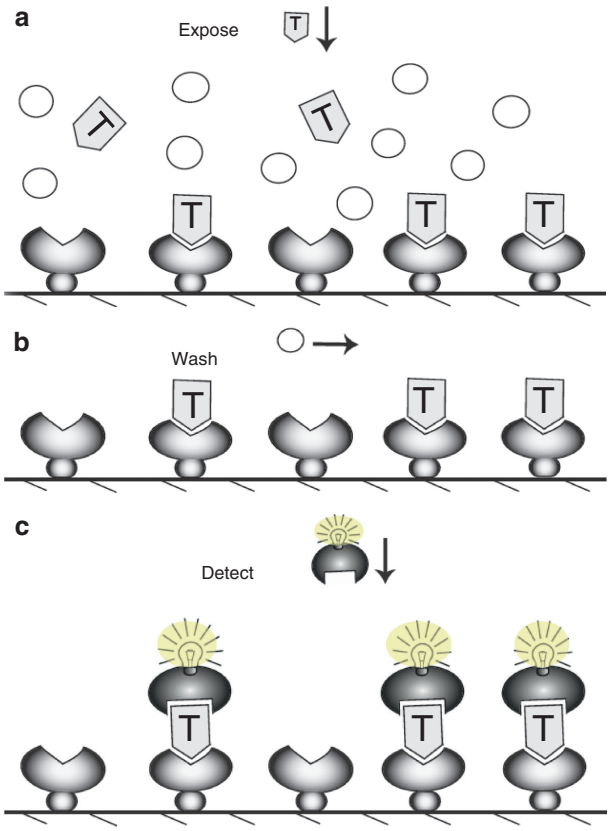

Fig. 1.2 An example of heterogeneous assay, commonly consisting of three steps. (**a**) The plate with immobilized receptor molecules is exposed to the probed sample. The targets become strongly and specifically bound, whereas contaminating compounds remain in solution. (**b**) The plate is washed. It contains only bound targets, and all unbound components of the mixture are removed. (**c**) The plate is exposed to solution of molecules or particles that are able to recognize the target and bind to it at a different site (indicator). The indicator contains fluorescent label. Here and in other illustrations below, geometrical fitting indicates specific binding (recognition)

The reader may note that in this case, after incubation in the tested medium, only the reacted species generate analytical signal, so that remaining unreacted species should be removed. The role of fluorescence reporters in this case is passive; they are used as the "*labels*", just to indicate the binding. Sensitivity of these assays can be dramatically increased by application of fluorescence nanoparticles as reporters or by appending enzyme generating chromogenic or fluorescent product.

In solution, this type of assay is also possible, but it requires separation of target-sensor complexes by chromatography, electrophoresis, etc. As we will see below, employment of this assay principle in sensor technologies allows us to achieve the broadest dynamic range of quantitative determination of the target. Because of the implied washing step, the result is less sensitive to interference of non-specifically bound components of the tested system. However, the assay is limited to high-affinity binding, since only in this case the target-sensor complexes remain intact during manipulations with the sample. All additional operations, such as separation and washing, are time-consuming, which does not allow one to obtain immediate results.

In contrast, *homogeneous assays* are those that provide the necessary signal upon target binding in the test medium without any separation or washing. Figure 1.3

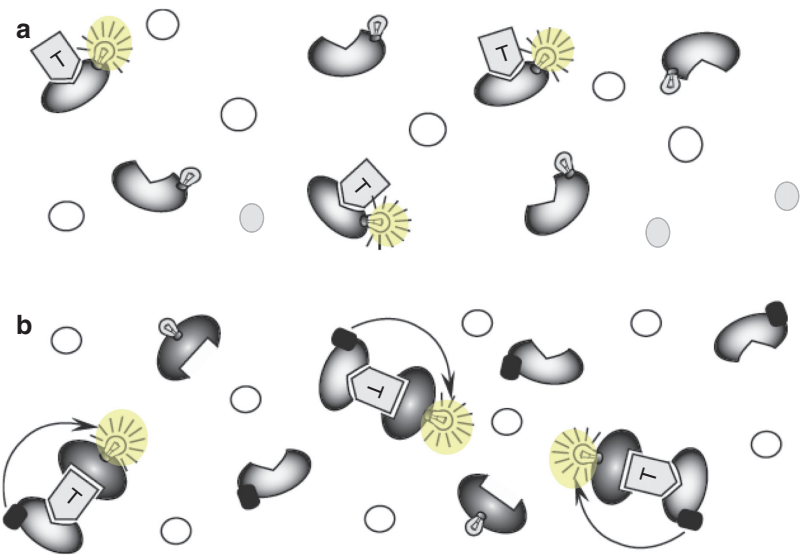

Fig. 1.3 Two examples of homogeneous assay. (**a**) Sensor molecules are composed of receptor and reporter groups and the latter change their fluorescence on target binding. (**b**) Two different sensor molecules possessing different reporters bind the target at two different binding sites. On interaction between these reporter units the fluorescence signal indicating the target binding is generated. This is possible only in the case when they bind the same target and thus appear in close proximity. In both cases, the assay may occur without the sensor immobilization and without the separation of the complex from unreacted components

illustrates different possibilities for realizing the sensor response in this format. Such tests can be provided in homogeneous test media (solutions) and conform to the definition of '*direct assays*' (Altschuh et al. 2006). Since no manipulations with the sample are needed, the sensors with this function are applicable for detecting the target distribution in the media of complex composition, including living cells. They should provide the broadest range of response by detectable changes of one or more of parameters of its emission.

A strong advantage of homogeneous assay formats is the possibility of quantitative determination of analytes in the case of their relatively low affinities, so that a dynamic concentration-dependent equilibrium is established between free and bound target. However, in this case, the *dynamic range* of the assay (the target concentration range, in which the variation of reporter signal is detected) is much narrower, usually, within two orders of magnitude (see Chap. 2).

Direct sensors are especially desirable for different practical applications due to the possibility of obtaining the results on-line. If the sensor responds directly to the target binding, then there is no need for separation, reagent addition or washing. Therefore, such sensors are also called the *reagent-independent* sensors. However, the absence of separation steps in these assays sets some major limitations to their performance. They can be very prone to interference from non-specific (non-target) binding. Moreover, the researcher is always restricted in finding the mechanism of response that is far from being universal. We will see below that there is no general simple and straightforward way to provide such direct response.

It is a matter of terminology, but some authors prefer to call heterogeneous assays as the 'assays' while homogeneous assays as the 'sensors'. This is because in homogeneous assays it is much easier to develop sensors that will not need any manipulation in the course of measurement or after it and that are applicable for continuous monitoring of target concentration. According to the International Union of Pure and Applied Chemistry (IUPAC) nomenclature recommendations, a *biosensor* (that can be extended to any type of sensor) is defined as a self-contained analytical device, which is capable of providing quantitative or semi-quantitative analytical information using a biological recognition element either integrated within or intimately associated with a physicochemical transducer (Thevenot et al. 2001). It is clearly affirmed that "*a biosensor should be clearly distinguished from a bioanalytical system which requires additional processing steps, such as the addition of reagents*". Meantime, this definition is not supported by many researchers, and different other definitions exist (Kellner et al. 2004). For instance, some authors suggest seeing among the sensors the devices, in which the response is produced in a chemical reaction with the analyte.

The distinction between 'sensors' and 'assays' is still not very strict. Moreover, the same molecules with selective target-binding function can serve in both assay and sensor techniques. Therefore, critical is the issue, how the reporter signal is provided. An example is the antibody, which is the most frequently used molecule

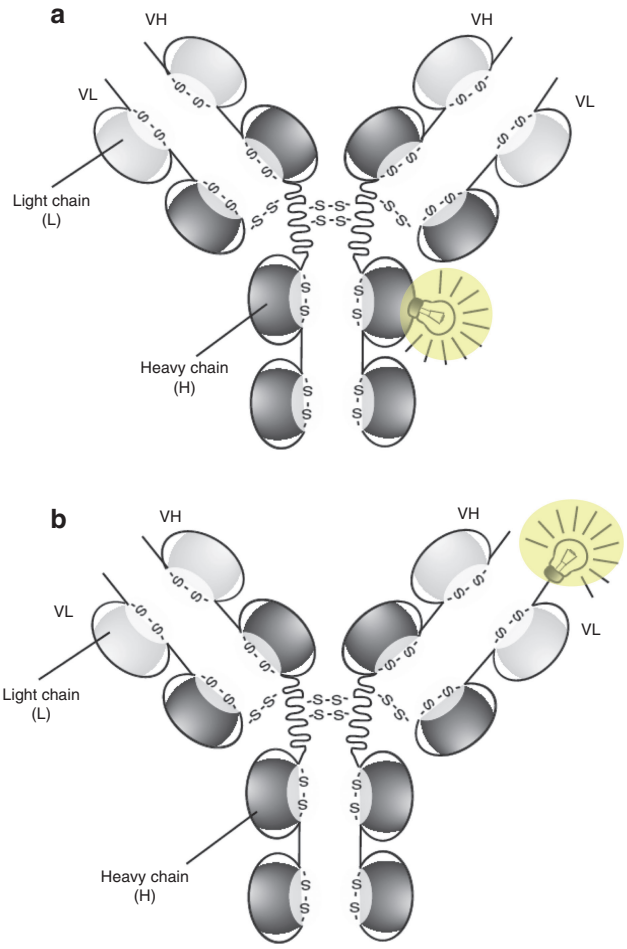

Fig. 1.4 The labeling of antibodies with fluorescence dyes for use in bioassays and biosensors. IgG antibody is shown. It is a protein molecule composed of two light (L) and two heavy (H) chains forming domains cross-linked by disulfide (–S-S-) bonds. The VL and VH domains form the target antigen binding site. The site of labeling determines the range of applications of antibodies. (**a**) The fluorescent dye is bound at the periphery of antibody molecule and serves only for the purpose of labeling. Its response is insensitive to antigen binding. (**b**) The reporter dye is located close to antigen binding site so that the interaction with antigen changes its fluorescence parameters providing the reporting signal

with the function of biological recognition (Fig. 1.4). For participating in bioassays, this molecule can be labeled at the periphery, at any site outside its target-recognition site. This is enough for providing response in heterogeneous format to immobilized target. In contrast, for its participation in sensing in homogeneous format, stringent additional requirements should be satisfied. The label should directly or indirectly sense the interaction with the target and provide the detectable reporting signal. One of the solutions to achieve that is to locate the label at the target-binding site.

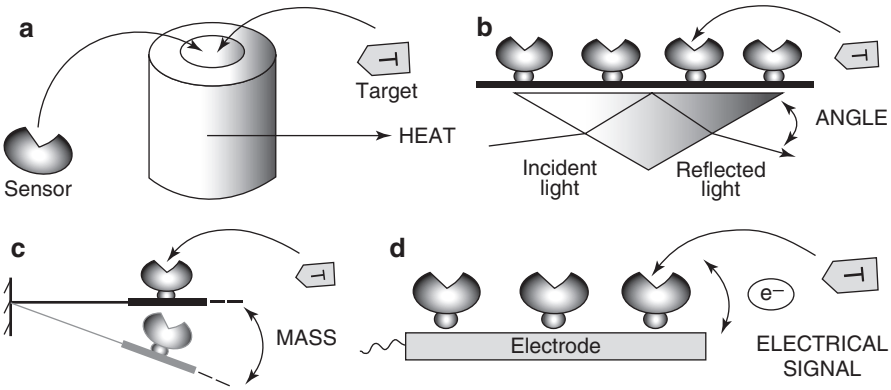

Fig. 1.5 Schematics illustrating the operation principles of sensing based on several alternative technologies. (**a**) *Calorimetry*. When target and receptor are mixed in a calorimeter, they produce heat effects. (**b**) *Surface plasmon resonance* (SPR). The layer of receptors is formed on the surface of a thin layer of gold or silver. The target binding causes the change of refractive index close to this surface that modulates the angular dependence of the reflected light beam. (**c**) *Micro-cantilever* technique. The target binding results in the mechanical signal that is detected as the change of mass. (**d**) *Electrochemistry*. The target binding usually results in electron transfer between the electroactive compound and the transducer (electrode) or in a change of the existing electrochemical signal

1.1.2 Principles of Sensor Operation

Different physical principles can be applied in sensor technologies to generate a measurable signal in response to sensor-target interaction (Fig. 1.5). The primary event of target binding by *receptor* (recognition element of the sensor) should generate some response, which is provided by a *reporter element*. These functions are different but they must be strongly coupled. The response (optical, heat, mass, etc.) is transformed into the electrical signal that can be quantitatively measured.

Every type of sensors can be classified according to three basic elements of their operation.

1. *The recognition element*. It can be as small as a group of atoms chelating a metal cation and as big as large protein molecule, DNA, membrane and even the living cell.
2. *The reporter element and the principle of reporting*. Optical (light absorption, reflection, fluorescence), electrochemical (amperometric, conductometric), mass, heat and acoustic effects can be used for this purpose.
3. *The mechanism of coupling*: electronic, conformational, through the medium (e.g. due to pH change), or by coupled chemical or electrochemical reaction.

For efficient sensor operation, some technologies need the immobilization of sensor molecules on planar surfaces or nanoparticles and some need incorporation of labels (e.g. absorbing light or producing fluorescence) serving as molecular reporters. This creates a versatility of approaches. Of great importance are the

medium conditions, in which the sensor-target binding occurs. The target recognition can occur in liquid phase or liquid–solid interface. In the former case, in order to get the response, the labeling and/or separation of target-sensor complexes may be needed. In the latter case, washing-out of unbound material may be necessary, but some methods allow avoiding this step. Using several examples, we will illustrate below the advantages and disadvantages of sensor immobilization and labeling.

1.1.3 Label-Free, General Approaches

Label-free techniques that are developed to the level of research and practical application involve those with optical detection, such as surface plasmon resonance (SPR), and also acoustic, cantilever and calorimetric biosensors.

Calorimetry (Fig. 1.5a) is an example of a general label-free approach that allows measurements in solutions without the necessity of immobilization of sensor molecules or of their labeling (Ladbury and Chowdhry 1996). This method is based on the principle of generation of heat effects that appear in the course of sensor-target binding. Since the detection is based on a general property of reaching the thermodynamic balance in the system after the formation of new target-receptor bonds, this method seems to be broadly applicable. The process of binding can be detected as a *heat effect in solution*; therefore the sensor immobilization is not needed. It should be noted, however, that this method does not possess any structural resolution. In complex mixtures, a strong binding by specific targets existing in small concentrations is not distinguishable from that of nonspecific binding at high concentrations. Thus, the advantage of measurement in label-free conditions in solutions is compromised by very restricted range of applications. However, such applications exist, for instance, in detection of explosives and other highly energetic compounds (Liu et al. 2005).

Surface plasmon resonance (SPR) is a typical example of immobilization-based but label-free technique (Fig. 1.5b). Description of an SPR principles and a review of its applications can be found in many articles (Homola 2003; Homola et al. 2005; Rich and Myszka 2006). The method is based on observing the change in refractive index close to the surface of a thin (~50 nm) metal (usually gold) film, illumination of which creates the so-called *evanescent wave* that generates optical signal. On this surface the receptor molecules or particles are immobilized. The target, when bound from a contacting solution phase, produces a detectable local increase in *refractive index*. This signal is observed as the change of the angle at which a strong decrease of intensity of reflected light occurs. Evanescent wave decreases exponentially as a function of distance from the surface of the sensor film on a scale up to 200 nm, which is convenient for the detection of large molecules. Unbound molecules and particles remain in the sample solution phase outside the detection layer and do not interfere with the measurement. This method has many attractive features. Because

of the absence of necessity of pre-treatments or after-treatments to visualize the result, it records the target binding in real time. Therefore, it has become a valuable technique not only for determining the receptor-target affinities but also for sorption–desorption kinetics of the target. Its application for simultaneous determination of multiple targets is difficult, but this problem can be overcome as it is observed in recent reports (Homola et al. 2005). Meantime, as every label-free method, SPR cannot distinguish specific and non-specific binding and therefore is not secured from false positive results.

It is interesting to note that a hybrid between fluorescence and SPR can be created. The method is called *evanescent wave fluorescence* and will be discussed in more detail in Sect. 10.6. Like SPR it can measure surface-specific binding events in real time. In this method, the excitation is by evanescent wave and response is provided by detection of fluorescence. Thus, only the species bound to the surface will be excited.

Very interesting are the developments of sensors based on the *change of mass* on target binding (Fig. 1.5c). Two techniques have been developed using this principle. One is the *acoustic* sensing. It is based on a highly sensitive detection of mass changes measured via surface acoustic wave (Lange et al. 2008). The sensor needs to be coupled to the surface of piezoelectric material, such as quartz. Its applicability for accurate detection of protein targets has been demonstrated. The second one uses a *microcantilever* (vibrating microbalance). The spring constant of this vibrating nanomechanical device is directly related to the increase of mass on target binding (Battiston et al. 2001). The latter technology needs a sensor immobilization to a specially prepared surface with special properties. The targets, interacting with the sensor, become captured on the surface and are detected.

Electrochemical sensors (Fig. 1.5d) are very popular because they use simple instrumentation and allow direct recording of target binding to immobilized receptors in the form of an electrical signal. Electrical signal can be obtained in oxidation-reduction reaction at the electrode. This can be either direct reaction with the participation of target or a coupled reaction that may involve a catalyst (Palecek 2005; Palecek and Jelen 2005). Electrochemical sensors are attractive by their simplicity, but the sensor immobilization is always needed, and in most cases the protocol involving the coupled electrochemical reaction to target binding needs to be developed.

Thus, these methods possess important obvious positive feature: *only the bound target molecules produce the response*. Therefore, if the sample contains a complex mixture of different compounds, only the target will produce the signal and no separation or washing steps will be needed. That is why these methods may allow direct kinetic measurements.

There are many possibilities to apply the *label-free approach in solutions* with the formation of high-affinity target-sensor complexes and their subsequent chromatographic separation. These complexes have to be analyzed by different analytical techniques, such as mass spectrometry, spectroscopy, enzyme inhibition or antibody binding. However, these procedures are always difficult and time-

consuming. They are limited to very strong sensor-target interactions that do not have to be disrupted by separation procedures. Finally, it should be noted that high cost of instrumentation is a characteristic feature of all general label-free and immobilization-free approaches.

1.1.4 Label-Free, System-Specific Approaches

A second group of label-free approaches is using a specific reaction. Commonly it is limited to biospecific interactions and is mainly based on the detection of *enzyme activity* (de Castro and Herrera 2003; D'Orazio 2003). Measurement of enzyme activity requires transformation of additional reagent (substrate) into reaction product, which generates the reporter signal. According to the definition presented above, these are the assays but not the sensors. Meantime, they are often recognized as '*catalytic biosensors*' in contrast to '*affinity-based sensors*' that do not use any coupled reactions.

In the case of catalytic biosensors the range of possible targets usually does not go beyond substrates or effectors of enzyme reactions, though attempts to induce artificial enzyme activity are also known. The enzyme here serves as the receptor element, and the chosen transduction principle is determined by the properties of the reaction substrate or product. In this group of sensors the generated transduction principle is often *electrochemical*, since it allows easy production of reporter signal when an enzyme is immobilized at the electrode. The first known example of such biosensor is an amperometric glucose sensor, in which the enzyme glucose oxidase was coupled with an amperometric electrode sensing P_{O2} (Palecek 2005). Fluorescence-based enzymatic sensors also exist. They will be discussed in Sect. 1.5.

Enzyme reactions can be easily observed in solutions. Nevertheless, most of the methods employing enzyme biosensors are based on *immobilized enzymes*. Immobilization solves several important problems, allowing to decrease the amount of enzyme needed for the assay, to maintain its stability and to reduce the time of enzymatic response (Amine et al. 2006). The choice of surface for enzyme immobilization is determined by the detection method, so that the surface may serve for transducing the response signal. It is not only flat but porous surfaces and also polymer gels and nanoparticles that can be used for this purpose. It should be stressed, that the advantages obtained from immobilization could be so significant that the development of immobilization protocols is justified for almost every particular case.

Finally, it should be noted that the label-free *electrochemical immunoassays* (Warsinke et al. 2000) have been described for particular antigen-antibody interaction, when the complex formation results in variations in charge density or conductivity. Since the mode of transduction is generally based on the properties of a reaction product, these sensing principles apply to the detection of particular targets (substrates or effectors) only. This severely restricts their use.

1.1.5 Label-Based Approaches

The *label-based* techniques are in principle applicable to any molecular interaction, provided that at least one of the interacting partners can be modified by attaching the label without loss of binding affinity. The disadvantage in this approach is that the labeling may affect the target binding. The label-based techniques can be used in conjunction with analytical devices, such as fiber-optic or gravimetric sensors (Luppa et al. 2001). Nevertheless, the most important advantage is that they can be used for constructing the sensors, in which the recognition element is labeled in such a way that a measurable physico-chemical property of the construct changes upon the complex formation in solution. This allows providing homogeneous assays that avoid any separation steps.

Molecular constructs can be made in such a way that they integrate both the recognition and reporter elements of a sensor, allowing target detection in a direct way. Such sensors are essentially the '*direct sensors*', since the transduction of signal generated on the step of recognition does not need any additional steps or additional interacting partners. Such molecular sensors are '*affinity-based*' because the signal is produced by the target-sensor interaction itself, in contrast to '*catalytic sensors*', in which the signal is caused by a catalytic substrate transformation. The label in most cases is a fluorescent dye or nanoparticle (*a fluorophore*), leading to a signal of fluorescence emission that is relatively easy to record. Labeling of the interacting molecules with redox compounds or enzymes has also been described (Warsinke et al. 2000). Fluorescence is often very sensitive to the changes of molecular environment and not only to target binding. If its change is coupled with molecular recognition event, this property can be also applied in sensing.

A technology based on fluorescent labeling is, in principle, of *general applicability*; it is easy-to-implement and inexpensive. In sensing applications, fluorescence detection is based on a variation in a number of fluorescence parameters upon complex formation (see Chap. 3), and the sensor operation can be made 'direct', without additional manipulations or reagent additions (Gauglitz 2005).

Versatility of this approach is also very important. Indeed, in contrast to many other methods used for the studies of macromolecular interactions and employed for construction of biosensors (electrochemical and piezoelectric sensing, SPR, etc.), the fluorescence sensors can operate as separate molecules or particles in solutions to allow homogeneous assays without any immobilization. The absence of a solid support allows the sensor molecules to move easily in solutions and to integrate spontaneously into nanoscale particles, porous materials and polymer gels, to penetrate into living cells providing a measurable response. They can also be immobilized on the surfaces of optical elements forming key parts of sensing devices. And also, they can be deposited in nanogram quantities in a mosaic way forming arrays for simultaneous detection of many analytes. Their incorporation into living cells allows non-invasive investigation of diagnostically valuable compounds using all the capabilities of fluorescence microscopy and flow cytometry. In a broader

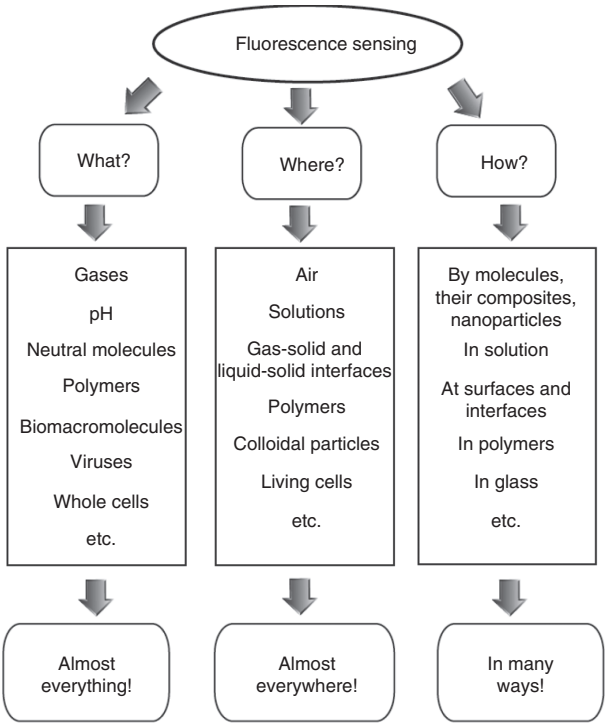

Fig. 1.6 The range of applications of fluorescence sensing technologies

sense, fluorescence allows visualization of sensor-target interactions with high spatial resolution (Fig. 1.6).

Thus, fluorescence sensing is essentially a *label-based approach* (intrinsic fluorophores, such as tryptophan in proteins, can be considered as naturally imposed labels). When comparing this approach with the label-free methods based on detection of changes of refractive index, charge or mass at the sensor surface or heat effects, one has to note the following important point. Testing often involves side effects produced by *contaminants*. These contaminants also have mass and charge; they change refractive index and produce heat effects. This results in background signal that may induce a serious complication when these techniques are used for testing realistically complex samples, such as blood serum. In contrast, specific labeling in sensing technologies always makes the response more specific leading to reduction of false positive complications in results.

1.2 Labeling Targets in Fluorescence Assays

Historically, fluorescence sensing came into play to substitute the *radioactive isotope* detection technique and to a large extent borrowed its methodology. Radioisotopes are insensitive to intermolecular interactions and all the methods based on their usage allow only their quantitative detection in the desired

locations. Their substitution by fluorescent dyes made the analysis cheaper, safer and much more sensitive. Many fluorescence technologies were developed following this line. Here the fluorescence of the dyes indicates the presence of a given target compound in the analyzed system and provides quantitative measure of this compound. Such dyes are in fact *a part of the target system* but not of the sensor system.

In this technology, the whole *pool of potential targets* has to be labeled (Fig. 1.7). Then, after reacting with the receptor, the receptor-target complexes should be isolated from the pool. If the receptor is immobilized on the surface, this can be easily done by the procedure of washing-out the unreacted target analogs. In the case when the reaction occurs in solutions, there should be a chromatographic or electrophoretic separation of a receptor-target complex (Fig. 1.8). Several examples of application of this concept are given below.

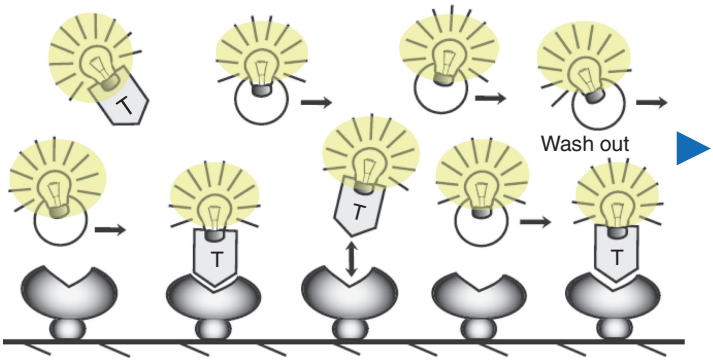

Fig. 1.7 The illustration of principle behind the initial labeling the whole pool of potential targets present in the sample. The sensors are represented by only the receptors that remain unlabeled. They bind the targets and immobilize them on the surface leaving all *labeled* contaminating compounds in solution

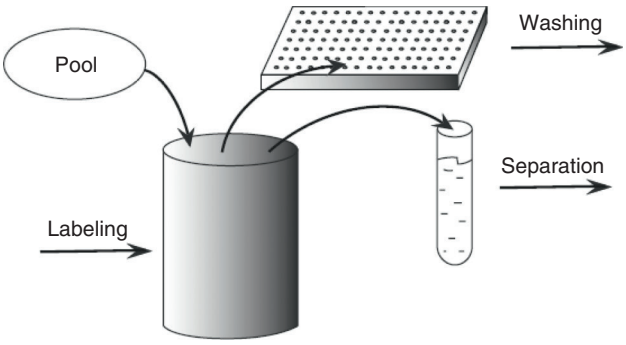

Fig. 1.8 Schematic illustration of procedures involved in sensing requiring the labeling of the whole pool of potential targets. In the case of immobilized receptors, the unbound labeled species are removed by washing, and in the case of assay in solution, a separation of complexes and unbound components is required

1.2.1 Arrays for DNA Hybridization

Presently the most popular methods of detecting specific DNA sequences are based on labeling the whole pool of these molecules in a studied system and on 'hooking-out' of target sequence by hybridizing them with unlabeled sensor sequence. The target and sensor sequences are complementary and form specific hydrogen bonds between two distinct base pairs, which are G-C and A-T in DNAs (or G-C and A-U in RNAs). Nucleic acid *hybridization* is a particular kind of affinity interaction resulting in formation of a double-strand association complex connected by these bonds (Freeman et al. 2000), as described in more detail in Sect. 12.4. Commonly, the solid-state hybridization is used, in which the sensing nucleic acid strands tethered to a solid support ('probe' strands) bind the strands of single-chain DNA or RNA molecules ('target' strands).

For identifying specific recognition between *complementary sequences*, the whole pool of poly- or oligonucleotides that may contain the 'target' strands is labeled with a fluorescent dye before application to the sensor. On the next step, the supportive plate is washed to remove unbound material and is applied to a fluorescence reader. If comparative studies are needed, the two nucleic acid pools can be labeled using different fluorescent dyes (usually a red-emitting cyanine dye Cy5 and a green-emitting dye Cy3), and applied to the same plate after mixing.

DNA or RNA *microarrays* (sometimes called microchips) are the results of miniaturization of this technology (Shoemaker and Linsley 2002; Venkatasubbarao 2004). Using hybridization on microarrays, thousands of solid-phase hybridization reactions can be performed simultaneously to determine gene expression patterns or to identify genotypes. This technique is the basis of a variety of important applications, from finding peculiarities of gene expression in disease, such as cancer, to analysis of its changes in ontogenesis and aging, detecting harmful microbes, etc.

1.2.2 Labeling in Protein-Protein and Protein-Nucleic Acid Interactions

Detection of protein targets based on microarray or any other high-throughput technology is highly needed for research and various applications. Very important is the development of '*protein function*' arrays which should consist of thousands of native proteins immobilized in a defined pattern and used for massive parallel testing of protein functions (Kodadek 2001, 2002). Such techniques are highly needed in proteomics research and also to satisfy the practical needs of pharmacology. The other type of arrays developed as '*protein detection*' devices with arrayed protein-binding agents are strongly needed for proteomics. Examples of their application could include cytokines, growth factors, apoptosis-related and other biological

systems-related arrays. They must allow detecting from dozens up to several thousands of analytes.

It has to be recognized that compared to labeling the whole pool of DNA or RNA molecules, the fluorescent labeling of a protein pool is much more difficult and much less efficient (Sect. 12.5). One may claim that covalent labeling at amino groups (N-terminal and belonging to Lys residues) is a very common procedure in protein chemistry. But the fact is that every protein in the pool will bind the dye at different sites and in different quantities, and this property is determined by its three-dimensional structure. The charged Lys residues are commonly exposed to the surface of protein molecules and their modification may hamper the binding to the receptor. This does not allow proper calibration for quantitative measurements.

Thus, labeling of protein pools has to be avoided; other methods described in this book that allow omitting this procedure could be more appropriate for protein assays.

1.2.3 Micro-array Immunosensors

Similar approach to that described above is used in antibody *micro-array* techniques (micro-array immunosensors). In a number of currently used assays, immobilized unlabeled antibodies assembled into micro-arrays are used for testing protein antigens (see Sect. 11.3). In order to record selective binding, all potential antigens in the sample have to be preliminarily labeled with fluorescent dye (MacBeath and Schreiber 2000). Thus, this approach shows the same disadvantages as the DNA and RNA hybridization assays with possibly greater errors. They can arise from nonspecific binding of analyte antigens and non-analytes present in the sample.

1.2.4 Advantages and Limitations of the Approach Based on Pool Labeling

Pool labeling is a simple, usually one-step, procedure. Nevertheless, this approach has a number of disadvantages and limitations. Some of them are technical and some derive from the fact that in such systems it is hard to achieve a true thermodynamic equilibrium between bound and unbound species. This is because of the following.

1. The correct quantitative measurement of target concentration is possible only when all target molecules (or particles) present in the system are bound to the sensor (unless separation can be made based on the spectral change induced by the binding). Therefore, measurements cannot be made in the studied system directly but only in aliquots taken from it. In order to achieve complete target

binding, the concentration of receptors should be higher than that of the targets.
2. The procedure requires a step of labeling with the dye, an incubation step for target binding and the washing step to remove unbound target analogs that contain the fluorescent label. These steps are time-consuming. Therefore, this method is not applicable for continuous monitoring the target concentration.
3. The method can be applied only to strong binders, i.e. to the cases in which the sensor-target complex can remain intact under the washing procedure. Therefore, the targets with relatively low affinities (dissociation constant K_d $10^{-5} – 10^{-7}$ M), which are of the order of magnitude in enzyme-substrate and enzyme-inhibitor complexes, cannot be analyzed reliably using this approach.
4. The label itself may influence the target recognition. There should be an independent proof that there is no modification of target affinity by the attached fluorescent label.

It is not surprising therefore, that this approach is attractive only when the tested compounds are of the same chemical nature and their labeling can be achieved quantitatively using the same general procedure. Fortunately, this is the case of many DNA and RNA hybridization assays.

The major advantages of this approach are its simplicity and the absence of limitation imposed on reporter dyes. This approach is not limited to sensing molecules. It can be extended to sensing large particles and even living cells. The label can be introduced to their pool, and specific targets can be analyzed after a separation step using electrophoresis, chromatography or flow cytometry.

1.3 Competitor Displacement Assay

Many scientists are trying to develop technologies that could avoid the introduction of fluorescence label into analyzed samples, and *competitor displacement* assay is one of these possibilities (Wu et al. 2013). In this technology, neither receptor nor target may contain a fluorescence label. Instead, an additional player in the target recognition mechanism is introduced, the fluorescent *competitor* (see Fig. 1.9). Usually a competitor is the labeled target analog that binds to the same site on the receptor as the target. After this binding, a mixture of different compounds that contains the target is applied. Due to its specific interaction (molecular recognition) with the receptor, the target displaces the competitor from the binding site. The target can be analyzed quantitatively because it is the only species that can displace the competitor. The competitor reports about its displacement by changing the parameters of its fluorescence emission. These changes can be calibrated as a function of target concentration.

There can be other configurations in competitor displacement assays (see Chap. 2). For instance, the competitor can be unlabeled and immobilized on the surface. It binds

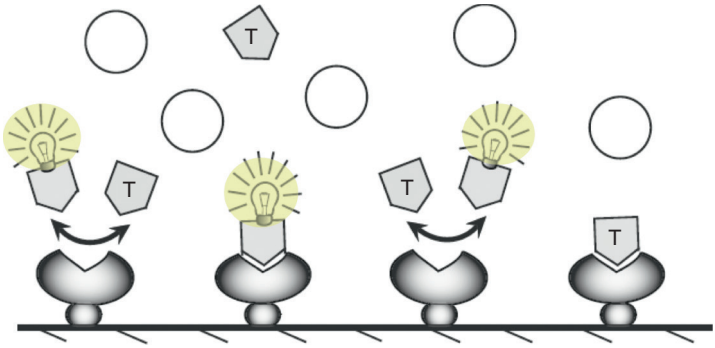

Fig. 1.9 The illustration of principle behind the competitor displacement assay. The response to target binding is obtained when the labeled competitor, competing for the binding site on the receptor, is displaced to the solution with a change in parameters of its fluorescence

the sensor molecules possessing the reporting units added to solution. When the sample that contains the target is applied, the target interacts with the sensor. The latter dissociates from the surface with the generation of a reporter signal.

1.3.1 Unlabeled Sensor and Labeled Competitor in Homogeneous Assay

Although the competitor displacement assays can be performed with *immobilized receptors*, this method allows *homogeneous assays* in solutions. In this case, there is no need to separate the receptor-target complexes from the target-free receptor molecules. It is essential that in this configuration the competitor does not interact directly with the target. It interacts with the receptor only via reversible non-covalent binding. Upon release from the complex, the competitor exhibits a change of its interactions from those existing within its complex with the receptor to those with solvent molecules (Wiskur et al. 2001). The fluorescence reporter signal in this case can be obtained by the change of different fluorescence parameters, such as intensity, polarization and lifetime (see Chap. 3). Therefore, the target is not involved in the transduction mechanism, it just substitutes the reporting competitor.

The competition assay is most convenient when the target is of relatively low molecular mass, and if it or its analog can be coupled with a fluorescent dye to produce a labeled competitor. Then the competition for a limited number of receptors can be exploited between labeled and unlabeled target molecules. In the presence of fixed amount of labeled competitor, the mole fraction bound to the receptor varies inversely with the target concentration. In this competitive format, it is necessary that some fluorescence signal should change between the two states of the competitor, its free and bound forms. The details of concentration dependences of fluorescence response in the case of competition and other formats can be found in Sect. 2.3.

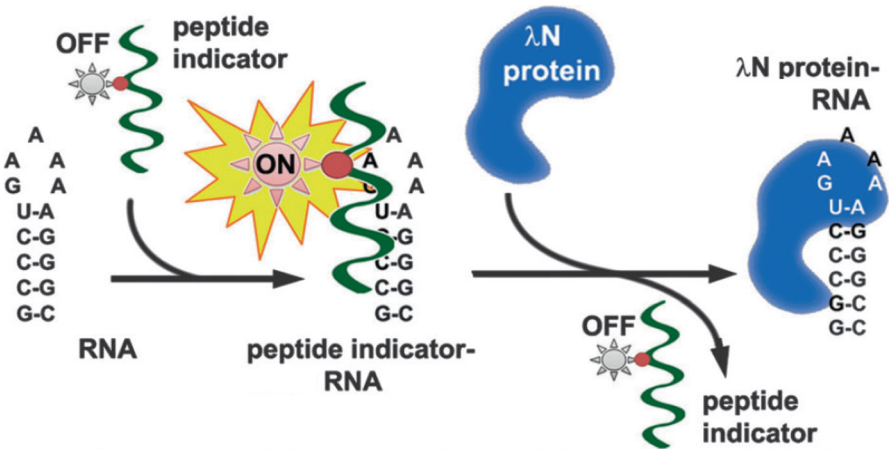

Fig. 1.10 Schematic representation of the fluorescent peptide indicator displacement assay for detecting the specific protein-RNA interaction (Jeong et al. 2013). When the labeled peptide binds with RNAs, the fluorescence intensity increases and it drops when the peptide is displaced by specific protein

As an illustration, Fig. 1.10 presents the events occurring on the sensing of RNA interaction with the RNA binding protein probed with labeled peptide competitor. The peptide recognizes target RNAs with minimal RNA binding motifs; they are readily displaced by corresponding protein that recognizes the target RNAs (Jeong et al. 2013).

As a general feature, this method requires keeping the competitor concentration on a strictly defined level; it lacks adaptability to continuous monitoring of target concentration (Piatek et al. 2004).

Many proteins can bind fluorescent dyes at their ligand-binding sites. When the ligand replaces the dye, large changes in the dye fluorescence may be observed. Based on these observations, different rather simple procedures for the determination of particular ligands can be developed. It is known, for example, that avidin and biotin forming very strong and highly specific complex can be easily quantified using the fluorescence probe 2,6-ANS (2-anilinonaphthalene-6-sulfonic acid) (Mock et al. 1988). Binding of 2,6-ANS produces dramatic increase in avidin fluorescence, and biotin, when present in the system, completely displaces it with an easily recordable fluorescence quenching.

Serum albumin has a function of binding and transporting many ligands in the blood, including different drugs. It can also bind some fluorescent dyes with high affinity at the same sites where it binds the drugs (Ercelen et al. 2005). Therefore, displacement of fluorescent ligands by the target ligands may provide a simple and efficient estimate of their concentrations in unknown media. Moreover, the tests for screening different ligands for their albumin-binding affinities can be

established. Such tests, being used for the determination of lifetimes of toxic compounds and drug in the blood circulation, may be used in toxicology and drug discovery.

A displacement assay using fluorescent *intercalator dyes* may serve as another example (Tse and Boger 2004). It can be applied for establishing DNA binding affinity and sequence selectivity for different compounds. Intercalator dyes are the dyes such as ethidium bromide or thiasole orange that can insert spontaneously between nucleic acid bases. These dyes are almost non-fluorescent in their free form in aqueous buffer. They attain strong fluorescence only in the DNA bound form, and their binding occurs only when DNA has a double-strand helical structure. Intercalation between nucleic acid bases screens them from the contacts with water that results in high-intensity emission. Application of target DNA binding compounds that disrupt the double helix destroys the binding sites for intercalator dyes with a dramatic decrease of fluorescence intensity (quenching).

Such possibility of generating the reporter signal indicates the fact that there is no absolute necessity for a competitor to be replaced by the target from the same binding site. The only requirement is that the sensor-target interaction should destroy the biding site for the competitor, which can be done in different ways.

1.3.2 Labeling of Both Receptor and Competitor

There is an alternative possibility for implementing displacement assays, which finds a broad range of applications. The receptor can be additionally labeled for providing long-range interaction with the competitor that will allow *Förster resonance energy transfer* (FRET) measurements. In this case (see Sect. 3.6), the FRET effect can be observed only in a competitor complex with a labeled receptor. When the unlabeled target replaces the competitor, the latter diffuses into the medium and the optical effect generated by energy transfer is lost. This event can report on the act of target binding.

An interesting realization of this idea is a *fluorescent immunoassay*, in which the competitor is designed by conjugation of a target compound to a fluorescently labeled protein. Bovine serum albumin can be used for that, and the whole complex can serve as a competitor in the determination of target binding to an antibody (Schobel et al. 1999). If the antibody is labeled with a FRET donor and albumin by a FRET acceptor, an enhancement of fluorescence emission of the donor can be observed at competitor displacement. This response can be analyzed in terms of target concentration. In such assays, the labeled albumin can be successfully substituted by quantum dots (see Sect. 5.5) or by other brightly fluorescent nanoparticles.

This approach can be illustrated by the operation of competitive *glucose biosensor*, the design of which was reported by many authors. Glucose-binding proteins concanavalin A (Ballerstadt et al. 2004) or apo-glucose oxidase (Chinnayelka and McShane 2004) form stable complexes with labeled dextran, so that FRET occurs between the two labels. Glucose displaces dextran in the complex, and this effect dependent on glucose concentration can be used for its determination.

In *DNA hybridization* assays, the following procedure can be applied. The sensor sequence labeled with a fluorescent dye is first hybridized with a competitor sequence labeled with a FRET acceptor (quencher). Hybridization with target DNA displaces the quencher and induces enhancement of fluorescence (Shoemaker and Linsley 2002).

Another example comes from the sensing using the *antibodies*. In the sensor targeted at determining the concentration of the explosive 2,4,6-trinitrotoluene (TNT) in aqueous environments, an antibody fragment was bound to a quantum dot, which served as a FRET donor. Trinitrotoluene analog was labeled with a dye that served as an acceptor (Goldman et al. 2003). In this case, the binding of the target TNT displaces this analog and induces enhancement of its fluorescence emission.

Interesting examples of application of competitor displacement assays can be found with *aptamer sensors* that are the oligonucleotide binders selected from large libraries (Sect. 7.6). Fluorescently labeled DNA aptamer that detects oligonucleotide sequences can form a complex with short oligonucleotide that contains a quencher. Dissociation of this complex that occurs on substitution by target on its binding brings the fluorescence enhancement (Nutiu and Li 2004). Similar strategy is used to study the ligand-RNA interactions (Zhang et al. 2010).

1.3.3 Competition Involving Two Binding Sites

An interesting approach has been applied recently in chemical *sensing of ions* (Royzen et al. 2005). Two ions are involved in this assay, Cu^{2+} as the target and Cd^{2+} as the competitor, together with two fluorescent metal chelating ligands (sensors). The latter were the dyes Calcein Blue and FluoZin-1, both of which bind the two types of ions with different affinities (Ligands 1 and 2, see Fig. 1.11). Both free ligands and their complexes with Cu^{2+} are almost non-fluorescent, whereas complexes with Cd^{2+} are strongly fluorescent with significant shifts of band maxima. In the absence of Cu^{2+} ions, the Cd^{2+} ions interact primarily with the ligand possessing higher affinity. This gives a spectrum located at shorter wavelengths. When Cu^{2+} ions are present in the system they replace Cd^{2+} ions and makes Ligand 1 non-fluorescent. Being replaced, these ions become bound to the weaker Ligand 2. This results in the appearance of strong fluorescence emission located at longer wavelengths. Thus, a convenient self-referencing two-band ratiometric recording of Cu^{2+} binding can be achieved.

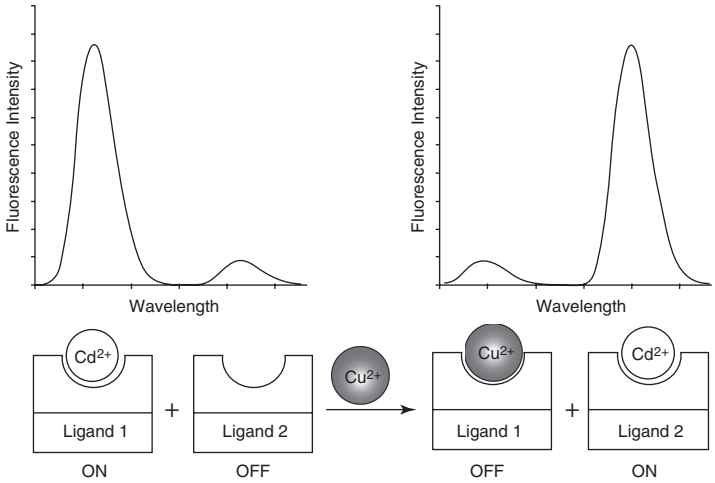

Fig. 1.11 Schematic representation of a ratiometric Cu^{2+} sensor system. In the absence of Cu^{2+}, Ligand 1 binds Cd^{2+}, which causes an enhancement of fluorescent ('ON' state). At the same time, Ligand 2 is in the uncomplexed form and is thus relatively poorly fluorescent ('OFF' state). In the presence of Cu^{2+}, Cd^{2+} is displaced from Ligand 1. Formation of [Cu(1)] complex quenches the fluorescence, therefore switching Ligand 1 'OFF' (Royzen et al. 2005)

1.3.4 Advantages and Limitations of the Approach

In principle, the approach based on competitor displacement is advantageous over techniques requiring labeling of a whole pool containing the required target. However, in practice it is difficult to implement it in many particular cases and even more difficult to make it generic. The affinity of receptor to target should be high enough to replace the competitor, but its affinity to competitor should be also high in order to withstand chromatographic separation (if the assay is performed in solution) or washing the plates (if the sensor is immobilized). Therefore, it is often not reasonable to use the attached dye only as a label; this methodology develops in a different direction, with the application of responsive dyes (see Sect. 4.3). If the dye serving as a competitor responds to dissociation from the sensor by changing its fluorescence parameters, there may be no need to apply the separation/washing steps.

Some authors distinguish between the competition and displacement assays. In displacement assays the analyte should possess a high affinity to the receptor and be totally bound substituting the labeled competitor that may be of lower affinity but present in saturating concentrations. This condition allows operating with multi-analyte sensor arrays and reading fluorescence after washing steps. In contrast, in competition assay both the target analyte and competitor may be of lower affinity, but an equilibrium condition should be established in their binding.

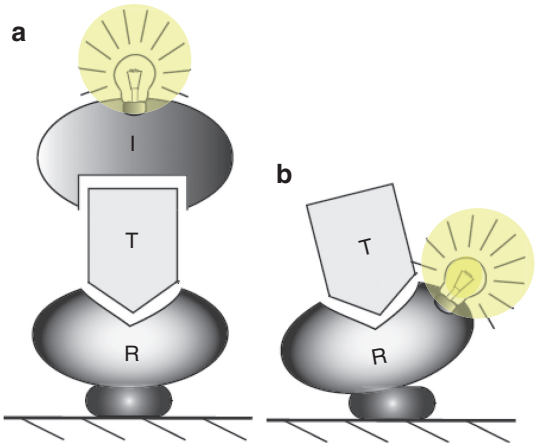

Fig. 1.12 The illustration of principles in the background of operation of 'sandwich assay' with fluorescence detection and of the sensors based on 'direct sensor' concept. (**a**) Sandwich assay. After the target (*T*) binding to immobilized receptor (*R*) and forming their complex on the surface, an indicator (*I*) that interacts with the target is introduced. The indicator is labeled, which provides labeling of the complex. (**b**) Direct sensor. Here the fluorophore labeling the receptor is the integral part of the sensor (*S*). Its response is coupled directly with the target recognition event

1.4 Sandwich Assays

The sandwich as a component of everyday food is known to everyone. It has three layers: bread at the bottom, then ham, cheese or butter in the middle and, again, bread on the top. The same is the composition of *sandwich-type fluorescence assay unit*, in which three layers are formed on target binding (Fig. 1.12a).

In a sandwich configuration the receptor molecules are at the bottom. Being attached to solid support they form a layer. In *immunosensor* techniques the receptors are *antibodies* that recognize large-size *antigens* or the antigens that recognize antibodies. The target molecules, when bound to receptor molecules are in the middle of such sandwich. Both sensors and targets are not labeled, so their complex formation does not produce any response signal. Therefore, for detecting the sensor-target interaction a third component is needed, which we will call the *indicator*. Its function is to visualize the formed complex with the aid of attached label, so it should be applied on the top. Usually it is the antibody that is specially prepared for recognizing the immobilized target at a different binding site than the receptor. In the case if the receptor-target complex is formed, the indicator has to label this complex and if not – to be removed by washing before the analysis.

1.4.1 Sensing the Antigens and Antibodies

This type of analysis is important primarily in clinical practice. *Antigens* are the viruses and bacteria as well as different strange materials that can get inside the human body or to which it can contact. *Antibodies* are the molecules forming response

to antigens. Their detection is also very important. Clinical diagnostics, response of individual to treatment, prognosis and other issues can be resolved with this analysis (see Chap. 14). In both tasks of sensing the antigens or antibodies the sandwich approaches are commonly used (Gopinath et al. 2014). This is because of strong binding between antigens and antibodies (with K_d on the level of picomoles or nanomoles). There is often the possibility to substitute the real antigen (e.g. microbe) by a molecule of a rather small size (e.g. peptide or glycolipide) that retains the antibody-binding properties. The structural elements of even smaller size, called *antigenic determinants* (epitops), are recognized by antibodies. The assay configurations for detection of antigens and antibodies are schematically presented in Fig. 1.13.

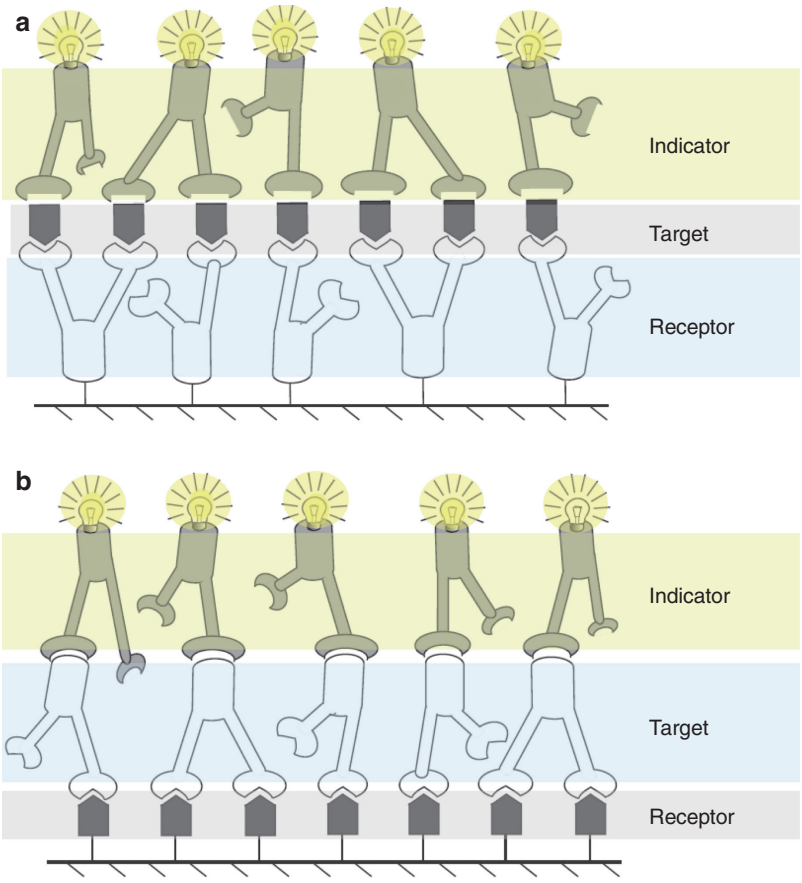

Fig. 1.13 Schematic representation of assay formats for sensing the antigens and the antibodies. (**a**) Detection of antigens. Antibodies serving as receptors are immobilized on a solid support. Each antibody (usually, bivalent) captures its respective target (called antigen) from a complex mixture. Detection is by recognizing the bound antigen by a second antibody serving as indicator that contains optical label or enzyme producing optically detectable product. (**b**) Detection of antibodies. Antigen is the receptor that is immobilized on a solid support. Antibodies specific to this antigen are the targets captured from a complex mixture (e.g. blood serum). Detection occurs by recognizing the bound antibodies by other antibodies serving as indicators. They react with the target antibodies as with their own antigens. The latter antibodies can be labelled for providing an optical signal as in the case (**a**)

The secondary antibody serving as the indicator (the *capture antibody*) can be modified in different ways for providing the most sensitive response. Because of that, the mechanism of indicator operation is rather general. In immunoassays detecting the antibodies it is simply another different antibody reacting with the target antibody. This prevents many problems. The function of indicator is universal, since it does not need to display any site-sensitivity. There is also no need in reporting function of the label. The label serves only for measuring the amount of bound indicator (Marquette and Blum 2006).

A popular version of this assay that uses the generation of colored product in enzyme reaction is called the *enzyme-linked immunosorbent assay* (ELISA). Here the indicator antibody can be fused to an enzyme, which, on addition of substrate, produces the colored (light-absorbing) reaction product during the final incubation step (Mendoza et al. 1999). Upon incubation, each such molecular complex can generate many colored molecules. Intensity of their color can be analyzed as a function of concentration of the bound target.

Application of *fluorogenic* (producing fluorescence) substrates allows increasing substantially the precision and sensitivity (Meng et al. 2005). Some enzyme-labeled fluorescence kits use phosphatase substrate that has weak blue fluorescence in solution but upon enzymatic cleavage forms a bright and highly photostable yellow-green fluorescent precipitate. The sites of binding of antibody-phosphatase complex can be detected by fluorescent precipitate deposited at the site of enzymatic activity. A very high sensitivity of these assays can be achieved, which ranges from picomoles to nanomoles in target concentrations. This is quite sufficient to satisfy many demands in clinical diagnostics. In many cases, however, the labeling without catalytic amplification can be quite sufficient for achieving this level of sensitivity, especially when ultra-bright particles such as dye-doped nanoparticles or quantum dots (see Chap. 5) are used for labeling.

1.4.2 Ultrasensitive DNA Detection Hybridization Assays

The sandwich assay format can be applied for the detection of all types of analytes that contain *two distinct molecular recognition sites*, one for binding to the receptor and the other for attaching the indicator. The DNA hybridization assays are remarkable in this respect. The recognition and detection of the single-chain DNA molecule can be provided in such a way that one part of it interacts with the receptor DNA forming a double helix. The remaining free part can interact with the indicator DNA that can carry fluorescent label. Here the most specific interaction with the formation of double helix can be realized too.

The brightest (in all aspects) application of this principle can be found in the work with brightly fluorescent dye-doped silica nanoparticles (Fig. 1.14). Their application allows detecting the DNA target molecules down to subpicomolar levels (Zhao et al. 2003).

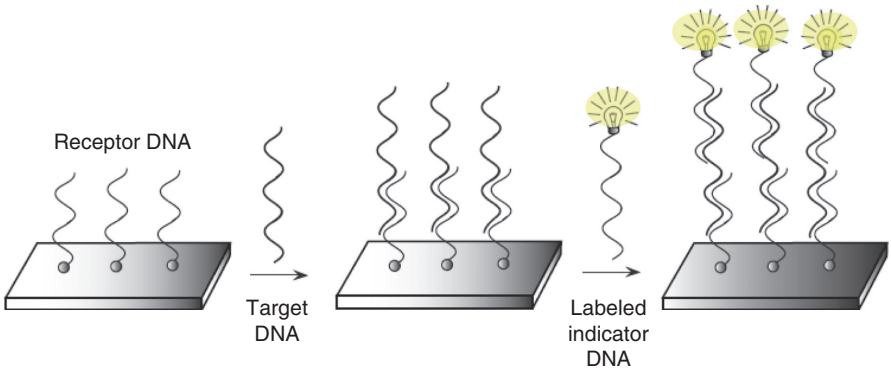

Fig. 1.14 Schematic representation of a sandwich DNA assay based on indicator DNA conjugated with dyes or nanoparticles

1.4.3 Advantages and Limitations of the Approach

The successful application of sandwich assays depends mostly on the possibility of recognizing in the target of two independent binding sites. This is because in this technology the target has to bind independently the receptor and the indicator. This limits the assay to rather large molecules (e.g. proteins) or to supramolecular structures, in which the binding to two different sites can be independent. Many small target molecules do not possess multiple structurally separate sites for binding and therefore cannot be detected by sandwich assays.

Since the indicator can be coupled with enzyme generating a light-absorbing or fluorescent product, the signal amplification can be achieved leading to a very high sensitivity of the assay. However, in all cases the response is not immediate and not direct, so that a separation of bound and unbound indicator is always needed.

The *sandwich assay* technique is well adapted to antibodies serving either as the receptors or as the targets. Regarding applications on a more general scale, their range is very limited. When used for detection of single-strand DNA, the two sites of hybridization have to be used. This technique is costly and time-consuming. In addition, it is subjective to non-specific absorption effects that increase with the number of used components, especially of proteins that can denature and provide nonspecific binding.

It can be noted that in a variety of bioassays, particularly in *enzyme-linked immunosorbent assay* (ELISA), the amplified output signal is achieved by linking (Meng et al. 2005) or by activation (Villaverde 2003) of an enzyme or ribozyme (Navani and Li 2006) producing chromogenic or fluorescent product. Being dependent on reagent addition and lengthy incubation times, these methods are limited in applications. New fluorophores with dramatically increased brightness have strong potential of substituting the enzyme amplification methods in detection techniques.

1.5 Catalytic Biosensors

Here we concentrate on fluorescence-based *catalytic biosensors*. These are the sensors, the mechanism of operation of which involves catalytic event with the generation (or consumption) of fluorescent species, and in a stringent sense they cannot be considered as 'the sensors'. The target can be detected as the modulator of this biocatalytic activity. Such modulator effect is specific for particular catalyst (enzyme, catalytic antibody, ribozyme) and can be either competitive with fluorogenic substrate or can be bound at regulatory site and provide the *allosteric modulation* of enzyme activity.

There is also a different possibility for using the species with catalytic function in sensing. Catalysis can be used for *amplification of reporting signal* produced by other sensors. The techniques based on this principle will also be considered.

Different analytical methods are based on determination of enzyme activity by monitoring the concentration of a reactant or product that is involved in the enzymatic reaction. Many of them use fluorescent substrates or products in direct or coupled reactions. These cases will not be discussed here, and the reader is addressed to a vast biochemical literature.

1.5.1 Enzymes as Sensors

It is well known that the activity of many enzymes can be modulated by binding specified molecules to the sites different from a catalytic site. Such enzymes are called *allosteric enzymes*, the sites of binding are called *allosteric sites*, and the molecules producing modulation of activity are the *allosteric effectors*. These allosteric effectors can be determined as the targets. In this case, the rate of catalytic transformation of substrate with the appearance of fluorescent products can be used as a quantitative measure of target concentration.

The binding of the effector modulates catalytic activity by coupling with a conformational change transmitted to the substrate binding site. In *allosteric sensors*, the catalytic activity of an enzyme is used not only to provide but also to amplify the response resulting from the binding of an effector. This is simply because a single binding event triggers the catalytic transformation of many substrate molecules, and in this way the reporting signal can be accumulated. This idea is illustrated in Fig. 1.15.

Thus, in such catalytic sensors the targets are analyzed as the effectors that bind to a site distinct from the active site rather than to the catalytic site and the binding signal is transmitted to a catalytic site through a conformational change, resulting in a modulation of catalytic activity (Villaverde 2003). This principle of catalytic amplification is not limited to enzyme reactions. It can be applied to organometallic and supramolecular catalysis (Zhu and Anslyn 2006).

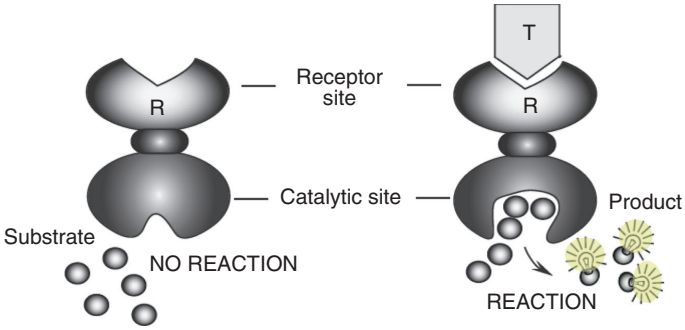

Fig. 1.15 The principle of allosteric enzyme sensors. Binding of a target at the allosteric binding site influences enzyme catalytic activity with the production of a chromogenic or fluorescent reaction product. Fluorescence of this product can serve as a measure of target binding

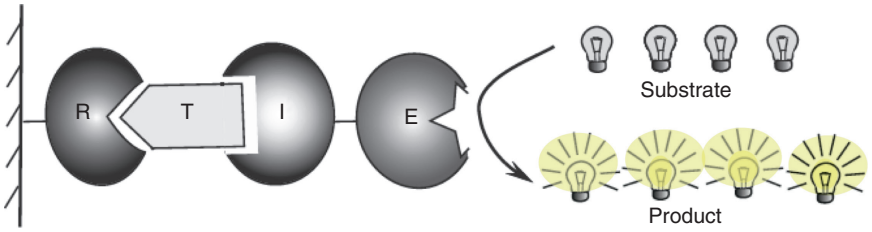

Fig. 1.16 The scheme illustrating operation of an assay using the labeled indicator with catalytic amplification. Primarily the sensor exposing the recognition unit (*R*) captures the target (*T*) that on the next step is recognized by an indicator (*I*). The indicator is fused to the enzyme (*E*). When the R – T – I complex is formed, then it can be detected by the transformation of nonfluorescent substrate (S) into fluorescent product (P) catalyzed by the enzyme

1.5.2 Labeling with Catalytic Amplification

High sensitivity of detection system is a very desirable factor that in many cases determines the strategy of sensor development. Coupling the response function with catalytic or biocatalytic transformation of reporter signal is one of the earliest ideas in the field of sensing, and it is still very actively explored. In this way, a single analyte binding event can be coupled with generation of multiple reporting molecules resulting in substantial signal amplification (Makhlynets and Korendovych 2014).

Most of these applications are related to sandwich (e.g. ELISA) techniques, where a second binder (an indicator) should carry the label, and it is the brightness of this label that determines the overall sensitivity (Sect. 1.4). Here the idea of connecting the sensing and catalysis is simple. An indicator is chemically coupled to an enzyme that, upon addition of substrate, generates colored (measured by light absorption) or fluorescent product at the site of binding. Then, if an excess of reaction substrate is provided, the *sensitivity* will depend on *incubation time* needed to generate the detectable product. Schematically this situation is depicted in Fig. 1.16.

The effect of amplification appears due to *multiple substrate transformations at a single site*. In common affinity-based sensors the sensitivity is limited by the 1:1 binding stoichiometry between the target and the sensor, which allows generation of response signal only in one reporter molecule for binding one target molecule. As a consequence, most biosensors, whatever is the transduction principle, are less sensitive than the techniques that use catalytic amplification, such as ELISA. This methodology is not focused on determination of catalytic activity or substrate concentration, although such information can be obtained. The allosteric modulation of activity in this application is also not needed. Catalyst and substrate are selected here for providing the most efficient response. Meantime, it is essential to note that the response relies on the correct assembly of the whole complex (R) – (T) – (I) – (E), which limits this methodology to heterogeneous sensor format.

As it was shown above, such limit does not exist if the catalytic transformation is provided by allosteric catalyst, and modulation of its activity is directly coupled with the target binding. Analyzing this difference, we can find analogy with the difference between sensing in sandwich assay format and direct sensing (which will be discussed in the next section). Determination of *allosteric effector* as the target resembles direct fluorescence sensing because in both cases a very efficient and specific transduction mechanism is needed. In contrast, in direct sensing the proximity effects or conformational changes in the sensor are essential for providing the response. Likewise, these changes are needed for operation of allosteric enzyme as a sensor. Here also they are requested for communicating between the target-binding site and the fluorescence reporter site. This restricts the area of application of such sensors in three respects. There should be (a) proper allosteric binding site specific for the target, (b) proper catalytic site and (c) proper allosteric coupling between the two.

It needs to be stressed again these conditions are not required if the enzyme (or catalyst, in general) functions only as the catalytic amplifier. Here enzyme is used for generating the reporter signal, and all recognition functions are played by other partners in a complex formed on target recognition. This is essentially the sandwich assay.

1.5.3 Advantages and Limitations of the Approach

The sensors with catalytic amplification possess a great reserve for increasing the sensitivity. In principle, when the enzyme reaction is triggered by target binding, the accumulation of light-absorbing or fluorescent product will continue until the reaction is stopped or substrate exhausted. However, an introduction into the sensor system of an additional player, such as enzyme, requires keeping the medium conditions (such as temperature and pH) in very narrow ranges. In addition, the catalyst and fluorogenic substrate concentrations should be set constant.

Thus, in application of catalytic biosensors there is a lot of compromise (de Castro and Herrera 2003). On one side is the simplicity of this approach and on the other side the necessity in many real cases to use an additional chromatographic separation. On one side is a high sensitivity that is achieved due to accumulation of

analyzed reaction product and on the other – a lengthy incubation step needed for this accumulation. In all the cases, manipulation with the sample, such as washing and an application of additional reagents, is needed.

Finally, catalytic amplification of reporter signal is not the only way to increase the sensor sensitivity, and other possibilities are in rapid development (Scrimin and Prins 2011). They include plasmonic enhancement (Sect. 10.7) and also antenna effects and superquenching in nanocomposites (Chap. 6).

1.6 Direct Reagent-Independent Sensing

It is known, that different parameters of fluorescence emission can be modulated in broad ranges by weak intermolecular interactions of the dyes (see Chap. 3). It must be a good idea to use this property in a straightforward and most efficient way, by making the sensor with *direct response* to sensor-target interactions (Arugula and Simonian 2014; Altschuh et al. 2006; Banala et al. 2013). In the case of success, we may get simple and universal means to provide fluorescence sensing without any limitations on the assay format.

1.6.1 The Principle of Direct 'Mix-and-Read' Sensing

On the pathway to realization of the idea of *direct sensing*, the special requirements should be imposed on the properties of fluorescent dyes. Instead of being simple labels or tags they have to attain all the features of molecular instruments reporting on particular changes in van der Waals interactions, hydrogen bonds and/or electrostatic forces. These changes should generate the reporting signal. In many cases, sophisticated transduction mechanisms have to be developed to obtain the signal on *elementary act of sensor-target binding* and transform it into the signal from fluorescence reporter (see Chap. 8).

Let us specify, what we wish to achieve. First, these new instruments should be *molecular* sensors. This means that their operation (both sensing and response) has to take place at a molecular level. If necessary, they can be easily integrated into supramolecular and macroscopic devices, although their basic operation should not require that. Therefore, they can be used for assays either in homogeneous phase (in solutions) or on their attachment to solid support. Secondly, they should be *direct* sensors. This means that they should avoid any intermediate signal-transduction factors or steps in recording the sensing event. In addition, they should be *reagent-independent* (sometimes called reagentless) sensors, so that their operation should not require the supply and consumption of additional reagents. Incorporation into sensor molecules of a fluorescent dye that changes its emission properties during the recognition event is the most promising approach for detecting the sensor – target binding. There may be many possibilities for operation with different kind of nanoparticles. They may serve as nano-size supports, as reporters or as modulators and amplifiers of the report.

The fact that no additional factors are required for the operation of direct sensors is very important. The device made of such sensors can operate in a broad range of external conditions and in any heterogeneous environment that could be a waveguide surface, a microplate or the interior of a living cell. Moreover, since this technique does not require any separation or washing steps and allows distinction between bound and unbound analyte in *thermodynamic equilibrium*, it may serve in a very broad range of target affinities (Chap. 2).

1.6.2 Contact and Remote Sensors

In the case of direct sensing, the fluorescent reporter is an integral part of the sensor (Fig. 1.12b), and its function is to provide the change of fluorescence parameters on analyte binding. This function can be introduced by covalent labeling of the recognition unit by the dye to form a molecular sensing device. Meantime, this straightforward and simple construction with efficient response function is often difficult to achieve, and there is no general methodology for that. In order to provide the transduction of the sensing event directly into fluorescence response, one has to choose between several possibilities (Fig. 1.17).

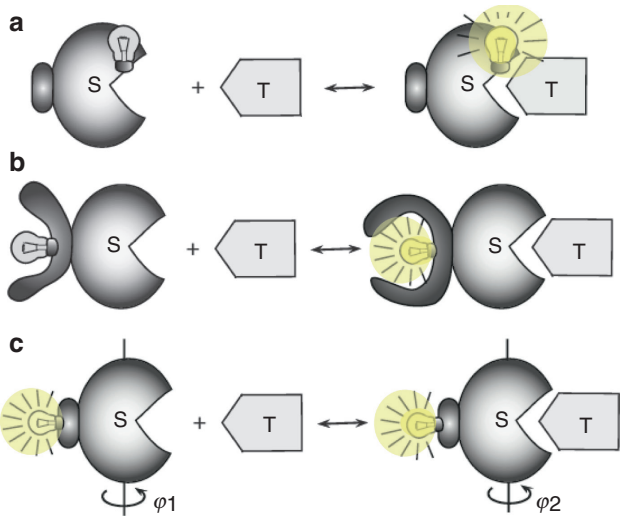

Fig. 1.17 Different possibilities for direct sensing of target (*T*) by the sensor (*S*) labeled with fluorescence reporter. (**a**) In contact sensing the reporter is involved in direct contact with the bound target. (**b**) In remote (allosteric) sensing the reporter responds to conformational change in the sensor molecule occurring on target binding, and its direct contact with the target is not needed. (**c**) In anisotropy sensing the rotational mobility of the sensor decreases on the target binding (due to increased mass of a complex), and this change is reflected as an increase of fluorescence anisotropy

(a) *Contact sensing*. Here the fluorescent reporter is involved in direct contact with the target and is a part of the recognition process. As a result of reporter-target interactions, one or more of its fluorescence parameters change. They can be scaled in target concentration. Since the reporter has to be present in sensor-target contact area, there is always a danger that it may influence the recognition of the target by producing steric and energetic barriers. Therefore, the compromise should be found between providing its strong involvement in target binding with the production of strong fluorescence response (that may also hamper the recognition) and a weaker involvement of the dye in binding that could be sometimes insufficient for providing detectable response in fluorescence. The direct contact between the target and fluorescence reporter can also be beneficial when it allows modulating the excited-state reaction occurring in the dye: electron, charge or energy transfers (see Chap. 8).

The principle of contact sensing has found optimal realization in the design of small chemical sensors detecting the ions (Valeur 2002; de Silva et al. 1997). It has also found application in sensing with peptides and proteins. Particularly, the antibody sensors were designed, in which the environment-sensitive dye is attached close to antigen binding site (Renard et al. 2002; Enander et al. 2008; Gopinath et al. 2014); the knowledge of three-dimensional structure of antibody allowed suggesting this site. This is an example of structure-based '*rational design'* approach. Meantime, the approaches using *peptide or nucleic acid libraries*, in which the dye is included into their covalent structure, may appear extremely efficient due to possibility of selection based on optimization of both sensing and reporting functions.

(b) '*Remote' sensing*. In the case of remote (e.g. allosteric) sensing, the reporting dye is located distantly from the site of analyte recognition. To provide the response, the sensor molecule should exhibit some conformational change reflected by reporter dye located at the periphery, away from the binding site. The possibilities of realizing this principle are limited to those sensor molecules, in which relatively strong global conformational changes accompany the recognition event. Nevertheless, if these changes do occur, they allow many possibilities for selecting the dye and optimizing its positioning in the sensor structure.

The changes of protein conformation on binding various ligands, including protein-protein and protein – nucleic acid interactions, are very common (Gerstein et al. 1994), up to the complete unfolding-folding (Demchenko 2001). This allows realizing many possibilities in sensor design. Recent applications of this principle include rearrangement of domains in sensing proteins and disruption of beacons, as in oligonucleotide sensors. Sensing with ligand-binding proteins (Dwyer and Hellinga 2004) often follows the principle of remote fluorescence detection. The sensing with molecular beacons and other polymers and biomolecules exhibiting conformational change deserves discussion in more detail (Sect. 8.5).

(c) A general property of the sensor should change on target binding, such as *rotational mobility* that can be observed as the change of *emission anisotropy* (Sect. 3.3).

The mechanisms coupling the binding event with signal transduction for the generation of response in emission will be discussed in different sections of this book. We will observe that the level of structural integration between the receptor and the reporter functional elements can be very different. This produces the basis for the development of many simple direct '*mix-and-read*' methods.

1.6.3 Advantages and Limitations of the Approach

A very attractive feature of direct sensors is the possibility of using nearly all possible biopolymer and mimetic systems, in which molecular recognition can be realized or simulated. This makes the background for the development of a wide range of molecular biosensor technologies, which include the use of antibodies and their fragments, ligand-binding proteins (natural and raised by selection using several scaffolds), enzymes and their chemically modified products, synthetic peptides and natural or synthetic polynucleotides. A wide variety of targets can be also analyzed, from small ions to supramolecular structures and living cells.

Still the sensitivity of direct sensors is not as high as of those indirect sensors and immunosensors that operate involving the multi-step coupled reactions and that use signal amplification, e.g. ELISA (McHugh 1994; Swartzman et al. 1999; Mendoza et al. 1999). Different methods for the dramatic increase of sensitivity have been suggested recently, and now we observe that the concept of a direct regent-free sensing offers new fascinating possibilities for the development of sensing systems.

The strong advantage of direct sensors is because they explore potentially simple *one-step binding reaction* with the response on a *time scale of measurement*. This allows continuous monitoring the analyte concentration (Galbán et al. 2012). Since this reaction allows immobilization and integration of sensor molecules into arrays, all the range of molecular, nanoscale, microscopic and macroscopic devices can be adapted to this concept. Multiple advantages make direct sensors progressive and prospective for future applications.

Another major advantage of direct sensors must be their *versatility*, which is out of competition. Direct sensors do not need the plates or any other solid supports but can use them to achieve the spatial resolution for providing simultaneous response to many targets. In direct sensing the reaction of target binding can be performed with the sensor molecules already in dilute solutions, and they can also be incorporated into nanoparticles, membrane vesicles, living cells, etc.

No less important is the advantage of *high speed of analysis* that is limited only by target diffusion in the medium (Brune et al. 1994) and by the rate of conformational changes in the sensor molecule if they occur on target binding to provide fluorescence response. This allows monitoring the process of interest on the fastest possible time scale.

With direct sensors, the range of quantitatively determined *target concentrations* can be extremely broad, which can be achieved by variation of the binding constants as described in Chap. 2. This is the result of rapid establishment of dynamic equilibrium between free and bound targets in accordance to *mass action law*. Only the bound analyte generates the fluorescence response, which allows easy determination of its *total concentration* in the volume of any size. Such sensor can be adapted for particular range of target concentrations by variation of the binding constant. Moreover, since direct sensors allow to measure target binding at equilibrium, they, in principle, can be used *many times* without regeneration and may allow *continuous monitoring*.

Thus, as an idea, the direct sensor format is always preferable. However, in practice it has to compete with other formats in terms of sensitivity and adaptability to special instrumental conditions.

1.7 Sensing and Thinking: How to Make the Sensor? Comparison of Basic Principles

The reader must be very much surprised by the fact that in such important field as chemical sensing and biosensing there is no single leading idea and dominant technology. A variety of technologies develop in parallel, and every one of them has its advocates and critics. For instance, for glucose sensing, enzymatic electrochemical techniques, light-addressable potentiometric sensors, enzyme-containing photosensitive membranes based on the microcantilever and other techniques were suggested in addition to sensing based on fluorescence detection. In this respect, fluorescence sensing develops in a very stimulating and productive environment. Its positions are very strong but not dominant, and in many application areas, the competition with other technologies is very tough.

In addition, a strong competition exists between different approaches based on fluorescence, in which fluorescence sensing of glucose can be a characteristic example. Thus, lectins, glucose-binding proteins, enzymes of glucose metabolism and boronic acid derivatives are used for glucose recognition together with response based on intensity, lifetime, spectral shifts, the resonance energy transfer and their combinations (Pickup et al. 2005a; Moschou et al. 2006). In the meantime, the diabetes patients need simple and convenient glucose monitoring *in vivo*. And the result that could fully satisfy them is still not achieved (Pickup et al. 2005b). Therefore, the competition continues.

Answering the questions listed below will help the reader to move from passive reading to thinking, analysis and creativity.

Questions and Problems

1. List all possible application areas of molecular sensors that you know. Explain what advantages appear on sensor immobilization to the surface compared to an assay in solution and how this expands or limits their application areas.

2. Explain why the potentially most general approach based on a label-free and immobilization-free principle has a rather narrow range of applications in practice.
3. What is the range of applicability of the sensing coupled with enzyme reactions? What is the difference in application between sensing based on an enzyme reaction and a ligand-binding (inhibitor-binding) allosteric sensing with the same or similar enzyme?
4. Evaluate comparatively the label-based methods using fluorescence detection. What is better to label, the receptor, the target together with the whole pool of potential targets, the capture antibody or the competitor? What range of applications is expected on application of any of these possibilities?
5. What are the application areas of indirect and direct sensors? Which are broader? In the cases if both techniques are applicable, what is preferable based on such criteria as complexity, time consumption and cost?
6. In what sense and in which conditions the techniques based on radioactive labeling (isotope tracing) and fluorescent labeling are analogous? What are the requirements for the fluorescence reporters in these applications? List the principal differences with a number of fluorescence detection techniques.
7. How does the DNA hybridization occur? How to use this process for detecting particular DNA sequence? What is the role of fluorescent labels in these assays and how in this case the fluorescence response can be technically realized?
8. Describe the problems that appear in labeling of the protein targets. Why it is better to avoid the labeling of a protein pool? Why this approach is not applicable to low-affinity targets?
9. What is the role of fluorescence reporter in competitor displacement assay? Suggest examples for proper applications of these assays. Can the sensor operate with immobilized competitor? How such sensors operate in the case of DNA intercalating dyes? What can be additionally achieved by labeling both sensor and competitor?
10. Think about an application of competitor displacement assay in complex situations, such as the case of two or more types of binding sites with different affinities.
11. Why in sandwich assays the third partner in target recognition, the indicator (e.g. capture antibody) is needed? What is gained and what is lost in its application?
12. Explain in detail the principle of operation of ELISA. How the reporting signal is generated and how the effect of amplification is achieved? Why this assay is so good with antibodies but is less practical with other binders?
13. The dyes can respond to a target binding directly, by the change of parameters of their fluorescence. Where they should be located in this case? What properties of the sensor should correspond to different locations of the reporting dye?
14. Select one protein target (let it be insulin) and explain, how you will apply all sensor strategies described above. Provide their comparative analysis in terms of speed, complexity (the number of needed manipulations), skills needed by the performers, etc.

References

Altschuh D, Oncul S, Demchenko AP (2006) Fluorescence sensing of intermolecular interactions and development of direct molecular biosensors. J Mol Recognit 19(6):459–477

Amine A, Mohammadi H, Bourais I, Palleschi G (2006) Enzyme inhibition-based biosensors for food safety and environmental monitoring. Biosens Bioelectron 21(8):1405–1423

Arugula MA, Simonian A (2014) Novel trends in affinity biosensors: current challenges and perspectives. Meas Sci Technol 25(3):032001

Ballerstadt R, Polak A, Beuhler A, Frye J (2004) In vitro long-term performance study of a near-infrared fluorescence affinity sensor for glucose monitoring. Biosens Bioelectron 19(8): 905–914

Banala S, Arts R, Aper SJ, Merkx M (2013) No washing, less waiting: engineering biomolecular reporters for single-step antibody detection in solution. Org Biomol Chem 11(44):7642–7649

Battiston FM, Ramseyer JP, Lang HP, Baller MK, Gerber C, Gimzewski JK, Meyer E, Guntherodt HJ (2001) A chemical sensor based on a microfabricated cantilever array with simultaneous resonance-frequency and bending readout. Sens Actuat B Chem 77(1–2):122–131

Brune M, Hunter JL, Corrie JET, Webb MR (1994) Direct, real-time measurement of rapid inorganic phosphate release using a novel fluorescent probe and its application to actomyosin subfragment 1 ATPase. Biochemistry 33:8262–8271

Chinnayelka S, McShane MJ (2004) Resonance energy transfer nanobiosensors based on affinity binding between apo-enzyme and its substrate. Biomacromolecules 5(5):1657–1661

D'Orazio P (2003) Biosensors in clinical chemistry. Clin Chim Acta 334(1–2):41–69

de Castro MDL, Herrera MC (2003) Enzyme inhibition-based biosensors and biosensing systems: questionable analytical devices. Biosens Bioelectron 18(2–3):279–294

de Silva AP, Gunaratne HQN, Gunnaugsson T, Huxley AJM, McRoy CP, Rademacher JT, Rice TE (1997) Signaling recognition events with fluorescent sensors and switches. Chem Rev 97: 1515–1566

Demchenko AP (2001) Recognition between flexible protein molecules: induced and assisted folding. J Mol Recognit 14(1):42–61

Demchenko AP (ed.) (2010a) Advanced Fluorescence Reporters in Chemistry and Biology I: fundamentals and molecular design. Springer Series on Fluorescence, vol. 8. Springer Berlin Heidelberg doi:10.1007/978-3-642-04702-2

Demchenko AP (ed.) (2010b) Advanced Fluorescence Reporters in Chemistry and Biology II: molecular constructions, polymers and nanoparticles. Springer Series on Fluorescence, vol. 9. Springer Berlin Heidelberg doi:10.1007/978-3-642-04701-5

Demchenko AP (ed.) (2011) Advanced Fluorescence Reporters in Chemistry and Biology III: applications in sensing and imaging. Springer Series on Fluorescence, vol. 10. Springer Berlin Heidelberg doi:10.1007/978-3-642-18035-4

Dwyer MA, Hellinga HW (2004) Periplasmic binding proteins: a versatile superfamily for protein engineering. Curr Opin Struct Biol 14(4):495–504

Enander K, Choulier L, Olsson AL, Yushchenko DA, Kanmert D, Klymchenko AS, Demchenko AP, Mely Y, Altschuh D (2008) A peptide-based, ratiometric biosensor construct for direct fluorescence detection of a protein analyte. Bioconjug Chem 19(9):1864–1870

Ercelen S, Klymchenko AS, Mely Y, Demchenko AP (2005) The binding of novel two-color fluorescence probe FA to serum albumins of different species. Int J Biol Macromol 35(5): 231–242

Freeman WM, Robertson DJ, Vrana KE (2000) Fundamentals of DNA hybridization arrays for gene expression analysis. Biotechniques 29(5):1042–+

Galbán J, Sanz-Vicente I, Ortega E, del Barrio M, de Marcos S (2012) Reagentless fluorescent biosensors based on proteins for continuous monitoring systems. Anal Bioanal Chem 402(10): 3039–3054

Gauglitz G (2005) Direct optical sensors: principles and selected applications. Anal Bioanal Chem 381(1):141–155

Gerstein M, Lesk AM, Chothia C (1994) Structural mechanisms for domain movements in proteins. Biochemistry 33(22):6739–6749
Goldman ER, Anderson GP, Lebedev N, Lingerfelt BM, Winter PT, Patterson CH, Mauro JM (2003) Analysis of aqueous 2,4,6-trinitrotoluene (TNT) using a fluorescent displacement immunoassay. Anal Bioanal Chem 375(4):471–475
Gopinath SC, Tang T-H, Citartan M, Chen Y, Lakshmipriya T (2014) Current aspects in immunosensors. Biosens Bioelectron 57:292–302
Homola J (2003) Present and future of surface plasmon resonance biosensors. Anal Bioanal Chem 377(3):528–539
Homola J, Vaisocherova H, Dostalek J, Piliarik M (2005) Multi-analyte surface plasmon resonance biosensing. Methods 37(1):26–36
Jeong HS, Choi SM, Kim HW, Park JW, Park HN, Park SM, Jang SK, Rhee YM, Kim BH (2013) Fluorescent peptide indicator displacement assay for monitoring interactions between RNA and RNA binding proteins. Mol Biosyst 9(5):948–951
Kellner R, Mermet J-M, Otto M, Valcarcei M, Widmer HM (2004) Analytical chemistry. Wiley-VCH, New York
Kodadek T (2001) Protein microarrays: prospects and problems. Chem Biol 8(2):105–115
Kodadek T (2002) Development of protein-detecting microarrays and related devices. Trends Biochem Sci 27(6):295–300
Ladbury JE, Chowdhry BZ (1996) Sensing the heat: the application of isothermal titration calorimetry to thermodynamic studies of biomolecular interactions. Chem Biol 3(10):791–801
Lange K, Rapp BE, Rapp M (2008) Surface acoustic wave biosensors: a review. Anal Bioanal Chem 391(5):1509–1519
Liu YS, Ugaz VM, Rogers WJ, Mannan MS, Saraf SR (2005) Development of an advanced nanocalorimetry system for material characterization. J Loss Prev Process Ind 18(3):139–144
Luppa PB, Sokoll LJ, Chan DW (2001) Immunosensors – principles and applications to clinical chemistry. Clin Chim Acta 314(1–2):1–26
MacBeath G, Schreiber SL (2000) Printing proteins as microarrays for high-throughput function determination. Science 289(5485):1760–1763
Makhlynets OV, Korendovych IV (2014) Design of catalytically amplified sensors for small molecules. Biomolecules 4(2):402–418
Marquette CA, Blum LJ (2006) State of the art and recent advances in immunoanalytical systems. Biosens Bioelectron 21(8):1424–1433
McHugh TM (1994) Flow microsphere immunoassay for the quantitative and simultaneous detection of multiple soluble analytes. Methods Cell Biol 42 Pt B:575–595
Mendoza LG, McQuary P, Mongan A, Gangadharan R, Brignac S, Eggers M (1999) High-throughput microarray-based enzyme-linked immunosorbent assay (ELISA). Biotechniques 27(4):778–+
Meng Y, High K, Antonello J, Washabaugh MW, Zhao QJ (2005) Enhanced sensitivity and precision in an enzyme-linked immunosorbent assay with fluorogenic substrates compared with commonly used chromogenic substrates. Anal Biochem 345(2):227–236
Mock DM, Lankford G, Horowitz P (1988) A study of the interaction of avidin with 2-anilinonaphthalene-6-sulfonic acid (2,6 Ans) as a probe of the biotin binding-site. Clin Res 36(6):A895
Moschou EA, Bachas LG, Daunert S, Deo SK (2006) Hinge-motion binding proteins: unraveling their analytical potential. Anal Chem 78(19):6692–6700
Navani NK, Li YF (2006) Nucleic acid aptamers and enzymes as sensors. Curr Opin Chem Biol 10(3):272–281
Nutiu R, Li YF (2004) Structure-switching signaling aptamers: transducing molecular recognition into fluorescence signaling. Chem Eur J 10(8):1868–1876
Palecek E (2005) Electroactivity of proteins and its possibilities in biomedicine and proteomics, chap 19. In: Palecek E, Scheller F, Wang J (eds) Electrochemistry of nucleic acids and proteins. Towards electrochemical sensors for genomics and proteomics. Elsevier, Amsterdam, pp 690–750

Palecek E, Jelen F (2005) Electrochemistry of nucleic acids. In: Palecek E, Scheller F, Wang J (eds) Electrochemistry of nucleic acids and proteins. Towards electrochemical sensors for genomics and proteomics. Elsevier, Amsterdam, pp 74–174

Piatek AM, Bomble YJ, Wiskur SL, Anslyn EV (2004) Threshold detection using indicator-displacement assays: an application in the analysis of malate in Pinot Noir grapes. J Am Chem Soc 126(19):6072–6077

Pickup JC, Hussain F, Evans ND, Rolinski OJ, Birch DJS (2005a) Fluorescence-based glucose sensors. Biosens Bioelectron 20(12):2555–2565

Pickup JC, Hussain F, Evans ND, Sachedina N (2005b) In vivo glucose monitoring: the clinical reality and the promise. Biosens Bioelectron 20(10):1897–1902

Renard M, Belkadi L, Hugo N, England P, Altschuh D, Bedouelle H (2002) Knowledge-based design of reagentless fluorescent biosensors from recombinant antibodies. J Mol Biol 318(2):429–442

Rich RL, Myszka DG (2006) Survey of the year 2005 commercial optical biosensor literature. J Mol Recognit 19(6):478–534

Royzen M, Dai ZH, Canary JW (2005) Ratiometric displacement approach to Cu(II) sensing by fluorescence. J Am Chem Soc 127(6):1612–1613

Schobel U, Egelhaaf HJ, Brecht A, Oelkrug D, Gauglitz G (1999) New-donor-acceptor pair for fluorescent immunoassays by energy transfer. Bioconjug Chem 10(6):1107–1114

Scrimin P, Prins LJ (2011) Sensing through signal amplification. Chem Soc Rev 40(9):4488–4505

Shoemaker DD, Linsley PS (2002) Recent developments in DNA microarrays. Curr Opin Microbiol 5(3):334–337

Swartzman EE, Miraglia SJ, Mellentin-Michelotti J, Evangelista L, Yuan PM (1999) A homogeneous and multiplexed immunoassay for high-throughput screening using fluorometric microvolume assay technology. Anal Biochem 271(2):143–151

Thevenot DR, Toth K, Durst RA, Wilson GS (2001) Electrochemical biosensors: recommended definitions and classification. Biosens Bioelectron 16(1–2):121–131

Tse WC, Boger DL (2004) A fluorescent intercalator displacement assay for establishing DNA binding selectivity and affinity. Acc Chem Res 37(1):61–69

Valeur B (2002) Molecular fluorescence. Wiley VCH, Weinheim

Valeur B, Berberan-Santos MN (2012) Molecular fluorescence: principles and applications. Wiley-VCH Verlag GmbH, Weinheim, FRG. doi:10.1002/3527600248.fmatter_indsub

Venkatasubbarao S (2004) Microarrays – status and prospects. Trends Biotechnol 22(12):630–637

Villaverde A (2003) Allosteric enzymes as biosensors for molecular diagnosis. FEBS Letters 554(1–2):169–172

Warsinke A, Benkert A, Scheller FW (2000) Electrochemical immunoassays. Fresenius J Anal Chem 366(6–7):622–634

Wiskur SL, Ait-Haddou H, Lavigne JJ, Anslyn EV (2001) Teaching old indicators new tricks. Acc Chem Res 34(12):963–972

Wu P, Xu C, Hou X (2013) Exploration of displacement reaction/sorption strategies in spectrometric analysis. Appl Spectrosc Rev 48(8):629–653

Zhang J, Umemoto S, Nakatani K (2010) Fluorescent indicator displacement assay for ligand – RNA interactions. J Am Chem Soc 132(11):3660–3661

Zhao X, Tapec-Dytioco R, Tan W (2003) Ultrasensitive DNA detection using highly fluorescent bioconjugated nanoparticles. J Am Chem Soc 125(38):11474–11475

Zhu L, Anslyn EV (2006) Signal amplification by allosteric catalysis. Ang Chem Int Ed 45:1190–1196

Chapter 2
Theoretical Aspects

The sensing always involves an interaction between the *target* and the system that is able to detect it (*the sensor*). The essence of sensing methodologies is *the ability to tell about the presence and quantity of target specie in a tested sample from a signal produced by its small fraction bound to the sensor*.

The amount of target binding sites (*receptors*) composing the sensors is commonly smaller by many orders of magnitude than the number of targets (*analytes*) in the tested system. For correct detection of this number, different strategies can be applied.

One of these strategies is to take out from a tested system a small aliquot of sample, expose it for strong or even irreversible binding by the sensor *receptor* and then, after calculating the number of bound targets, extrapolate this result to a whole tested system. An example of such approach is the analysis of blood or urine samples in clinical laboratories.

The other is to design the sensor in such a way that the target-receptor binding is *reversible*. Upon exposure to tested sample, only a part (often, a small number) of the target species binds to a sensor, and this binding can be sufficient to tell us about the true target concentration. In this case, the testing is not limited to size of the sample. It can be even the whole sea, to which the sensor can be immersed for continuous monitoring its pollution. In this case, we must describe and use the regularities existing between the bound and unbound species for determining their whole number, keeping in mind that only the bound species produce the sensor response signal.

The interactions on every structural level involve the *dimension of time*. The target and receptor have to approach and 'recognize' each other by many translational and rotational diffusion steps. A 'conformational adaptation' can be involved in these steps with time-dependent strengthening of these interactions with the true target and discrimination of target analogs if they are present in the system.

Thus, the target-receptor binding involves two important aspects. (a). *Thermodynamic*, describing the equilibrium between bound and unbound target. (b). *Kinetic*. The target-receptor binding needs time for their mutual diffusion and

A.P. Demchenko, *Introduction to Fluorescence Sensing*,
DOI 10.1007/978-3-319-20780-3_2

optimizing their interactions. The true equilibrium may not be reached in the course of testing, which means that the kinetic variables may influence significantly the readout signal. In this Chapter the reader finds discussion on parameters that have to be optimized in every sensor, such as selectivity, sensitivity and limit of detection. Concentrating on reversible binding, in which the mass action law is observed, the methods of determining the binding constants and modeling the ligand binding isotherms are presented. Kinetics of target binding and its influence on the results of analyte determination are discussed. Focusing on fluorescence sensing, linear and intensity-weighted formats are distinguished and analyzed.

2.1 Parameters That Need to Be Optimized in Every Sensor

In this and following sections we will see that in order to design optimal sensor we need to observe several important parameters that include not only the absolute sensitivity but also selectivity against non-specific target binding and reversibility of the binding. These parameters depend strongly on whether the sensor and target form monovalent or multivalent contacts and whether this interaction occurs in solution or in the conditions of immobilized sensor. Kinetic and equilibrium constants characterize these properties. Fluorescence response can proceed in linear and non-linear manner (Fig. 2.1).

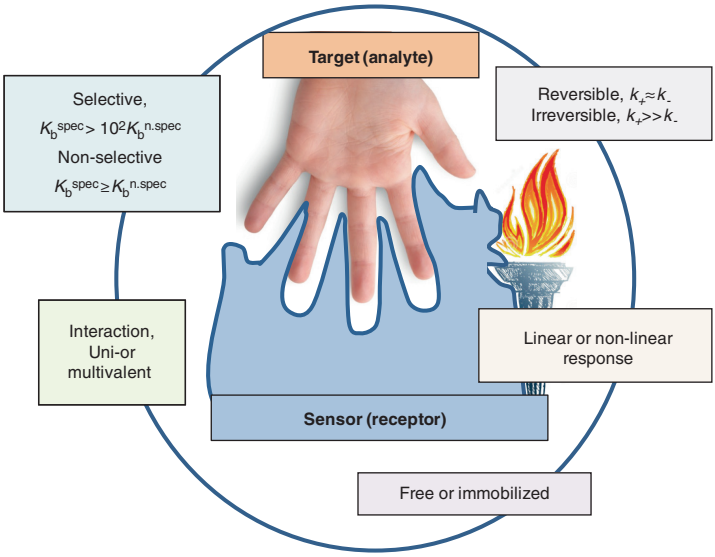

Fig. 2.1 The magnitude of parameters on which the operation of optimal sensor depends. See text for details

Table 2.1 The scale of concentrations used in molecular sensing

Notation	Concentration, mol/l	Molecules per 1 µl of solution	Examples
Molar (M)	1	~6×10^{17}	Saturated salt (NaCl, KCl) solutions
Millimolar (mM)	10^{-3}	~6×10^{14}	Normal concentration of glucose in blood (~3–6 mM)
Micromolar (µM)	10^{-6}	~6×10^{11}	Intracellular concentration of NADH
Nanomolar (nM)	10^{-9}	~6×10^{8}	Intracellular concentration of cyclic AMP
Picomolar (pM)	10^{-12}	~6×10^{5}	Single molecule in a volume ~1.7×10^{-12} l
Femtomolar (fM)	10^{-15}	~6×10^{2}	Single molecule in a volume ~1.7×10^{-9} l
Attomolar (aM)	10^{-18}	~0.6	Single molecule in a volume ~1.7×10^{-6} l (~1.7 µl)
Zeptomolar (zM)	10^{-21}	~0.0006	Single molecule in a volume ~1.7×10^{-3} l (~1.7 ml)

The concentration ranges that are needed to be analyzed in solutions are tremendous – starting from molar ones down to single molecules (Table 2.1). This puts stringent demands on many sensor parameters. Primarily it is the *absolute sensitivity*, which is the ability to detect the smallest amounts of target in the tested system. Next is the *dynamic range* of target concentrations that can be detected. The sensor developed for detecting the picomolar target concentrations may not allow to detect variations of these concentrations on millimolar levels. Very important is also the *selectivity*, which is the ability to discriminate in detection the target from its close analogs that can be also present in the tested system. These parameters are not independent, they are strongly interconnected.

2.1.1 The Limit of Detection and Sensitivity

The sensor can be characterized by the *limit of detection* (LOD). It is the lowest concentration of an analyte that the analytical process can reliably detect (Kellner et al. 2004). This concentration, C_{LOD}, has to produce a detectable signal, X_{LOD}, that is statistically distinguishable from the blank or background signal. The *sensitivity*, S, can be defined as the slope of the calibration curve (the dependence of analytical signal, X, on analyte concentration, C):

$$\mathrm{S} = \mathrm{d}X/\mathrm{d}C \approx \Delta X/\Delta C \tag{2.1}$$

The sensitivity S and the limit of detection are connected. The higher is the sensitivity, the lower is the limit of detection. It is usually accepted that C_{LOD} can be expressed as a function of S and S_{B}, which is a standard deviation of a set of blank signals obtained in serial measurements without analyte, as:

$$C_{\mathrm{LOD}} = 3S_{\mathrm{B}} / \mathrm{S} \tag{2.2}$$

The *limit of quantitation* (LOC) determines the analytical significance of the apparent analyte concentration. It is definitely above the limit of detection, and it is recommended to estimate it on the level of $10S_B/S$ (MacDougall and Crummett 1980).

The limit of detection is determined by two very different factors, the response of detection system and the target-receptor affinity. Let us consider these factors in more detail.

(a) The limit imposed by the *mechanism of detection* and the *response of detection system*. Each detection system records the meaningful signal on the background of some *noise*, which is the statistical fluctuation of the measured parameter. The noise cannot be eliminated totally, but it can be suppressed by increasing the intensity of useful signal. Thus, the limit appears as an inability to resolve the useful signal on the background of the noise level. The *signal-to-noise ratio* is an important characteristic of the sensor system. In addition, the interfering signal can appear as the background. In fluorescence sensing, this can be the signal from different fluorescent or light-scattering species that cannot be eliminated by instrumental means. If this background is variable, this may be an additional source of error.

(b) The limit imposed by *target-receptor affinity*. Imagine the case when the sensor is able to detect picomolar amounts of target, the target is present in picomolar concentrations but the sensor response is zero. This happens because the sensor responds to the amount of *bound target*, and the target-receptor affinity can be so low that no target is bound. In these cases, for shifting the target-receptor equilibrium towards binding, the affinity should be dramatically increased. This cannot always be done; therefore this limit of detection commonly exists.

2.1.2 Dynamic Range of Detectable Target Concentrations

No sensor can be operative throughout the whole concentration range from moles to single molecules. The lower limit is determined by the sensor sensitivity, and the higher limit appears due to the effects of saturation. This higher limit can also be an affinity-based, but it can also be related to the mechanism of detection.

(a) *Affinity-based limit*. Imagine that we start to apply the sensor that detects picomoles to the samples that detect nanomolar and then micromolar concentrations. The sensor will respond to increasing target concentrations up to the point, where all the sensor *receptor sites* become *saturated*. Since further increase will not cause additional binding, there will be no increased response of the sensor. This means that the sensor affinity must be strongly adapted to the required concentration range. If an extended range (covering several orders of magnitude) of target concentrations needs to be detected, a series of sensors with different affinities have to be applied to the same sample.

(b) *Saturation effects in the detection system*. These effects may exist, but in fluorescence sensing they are commonly not important (see Sect. 3.1). Particularly, they can appear at high concentrations of light-absorbing and

fluorescent species and if the light passes through the large volume (Lakowicz 2007). They can be fully ignored in miniaturized sensor systems.

For correct measurements based on reversible binding, the target concentration has to be much larger than the concentration of receptors. This is because the binding to a sensor should not change substantially its free concentration.

2.1.3 Selectivity

Selectivity is the basic characteristics of any analytical method that determines the accuracy of results. It is defined as the ability of the method to produce signals that are exclusively dependent on the analyte in the sample (Kellner et al. 2004).

In some rare cases, the target is so different from non-target species present in analyzed system that there is no competition from these species to the target binding to the sensor. In a more general case, such interference can exist, especially if the interfering species are present at much higher concentrations than the analyte. Thus, the *selectivity* can be viewed as an interplay of affinities weighted by the concentrations of the target and interfering species. In many cases, the ability of achieving the highest selectivity is vital for sensor applications. For instance, inside the living cells, the calcium ions have to be determined in the presence of much higher concentrations of magnesium ions, and the concentrations of sodium ions are much lower from that of potassium. These ion pairs have the same charge, and the difference in size is not very significant. Therefore the usefulness of the sensors that have to be applied depends strongly on the selectivity factor.

The term *specificity* is frequently used in biochemical literature. The binding is often called nonspecific, when the ligand-receptor binding isotherm (see below) does not show the effect of saturation in the studied concentration range. Mechanistically, this means that the interaction is of low affinity, so that such saturation must exist but is shifted to much higher concentrations. For describing the ability of the sensor to discriminate between true target analyte and other compounds close in properties, some authors use the term '*cross-reactivity*'. Estimation of cross-reactivity is commonly reduced to a comparison of dissociation constants between two or more species.

Specificity usually strongly correlates with the *affinity*. The stronger is the ligand-receptor binding, the more significant can be discrimination between the binding of specific and non-specific ligands (Eaton et al. 1995). This correlation is easy to understand. Specific binding involves multi-point contacts between ligand and receptor. The noncovalent interactions providing these contacts being individually weak produce collective effect increasing both affinity and specificity. The reader must not to be confused by the fact that sometimes the weaker interaction allows revealing more specific changes in target structure. Thus, the application of high-affinity probes for the detection of mismatched DNA and RNA sites shows that the increase of affinity in hybridization of complementary chains may lead to decrease in the ability of detecting single mismatches in the sequence (Demidov and Frank-Kamenetskii 2004). This is because on the background of lower affinity it is

easier to detect its variations associated with the changes of a target structure. Also interesting is the situation with polyreactive antibodies that despite their low specificity may demonstrate high affinity in ligand binding (Bobrovnik 2014).

Affinity is directly related to thermodynamic parameters characterizing the binding at equilibrium: the binding free energy ΔG and the changes of enthalpy ΔH and entropy ΔS on binding:

$$\Delta G = -RT \ln\left(K_b\right) = \Delta H - T\Delta S \tag{2.3}$$

Here R is the gas constant and T is the temperature. K_b is the *binding constant*, which is the quantitative measure of affinity that will be defined below. Both enthalpy and entropy contributions are important for target binding. ΔH reflects the bond formation energy and is responsible for heat effects. The entropy term determines the change of molecular order and therefore it depends strongly on the temperature. Though thermodynamic approach cannot allow accurate determination of affinities, it allows some estimates. For instance, in the case of involvement of electrostatic interactions the affinity will be decreased at higher electrolyte concentrations (ionic screening), and introduction into the sensor of mobile groups that loose their mobility on binding decrease the affinity by influencing the entropy term.

We observe that there are basic limitations to creation of a sensor that will be useful for target determination in all possible ranges of target concentrations and in all possible ranges of concentrations of low-specific target analogs that may compete with the assay. The regularities describing these systems and that are required for optimization the sensing will be analyzed below. Structural background of specificity as a selective multi-point binding (molecular recognition) will be discussed in Sect. 7.1.

Since these regularities are valid for any intermolecular interactions not always related to sensing, in our discussion below we will use rather general terms – the *receptor* that stands for sensor element responsible for target binding function and the *ligand* that can be the target analyte. Not only molecules can be the receptors or ligands but also the particles of different size and even the whole living cells.

2.2 Determination of Binding Constants

In the case of *reversible binding* the K_d value determines the range of target concentrations that can be detected by the sensor. There is always a limit on the lowest and highest of these concentrations. For a monovalent reversible ligand binding, the analytically useful concentration range is typically restricted to one order of magnitude below and one order above the K_d value, which is approximately the range between 10 and 90 % of a sensor fractional saturation. As it will be explained below, this statement follows directly from the *mass action law* when it is applied to interaction between two species at equilibrium. Heterogeneity of binding usually extends this range, but this may happen only

to a small extent. If the dynamic range of measured target concentrations is needed to be broader, one has to use a combination of sensors with similar specificity but of different affinities towards the target (Vallée-Bélisle et al. 2012).

2.2.1 Dynamic Association-Dissociation Equilibrium

The simplest example of receptor-ligand interactions is when a single ligand (L) interacts with single receptor (R) to form a single complex (LR) in the conditions of *dynamic equilibrium*:

$$L + R \Leftrightarrow LR \tag{2.4}$$

In the conditions of equilibrium, a rapid binding-dissociation occurs all the time but the concentrations [R], [L] and [LR] do not change over time. In this state the forward reaction of ligand binding proceeds with the same rate as the reverse reaction of its dissociation. This is why such equilibrium is called *dynamic*. It allows a simple description based on *mass action law*.

Let the kinetics of ligand binding be expressed by a rate constant k_1 and that of dissociation of the complex by rate constant k_2. Then the equilibrium can be characterized by a ratio of these constants. This can be either the *binding constant* $K_b = k_1/k_2$ or its reverse function, the *dissociation constant* $K_d = k_2/k_1$. K_b is often called also the stability or affinity constant, it is expressed in reverse molarity units (M^{-1}), whereas $K_d = 1/K_b$ is expressed in molar (M) units. Table 2.1 presents the whole scale of concentrations used in molecular sensing.

It has to be recollected that *molarity* (M) denotes the number of moles of a given substance per liter volume. The *mole* (mol), in contrast, is the unit that measures an amount of substance. One mole contains the Avogadro's number (approximately 6.022×10^{23}) of entities. The molarity dimension of K_d corresponds to the ligand molar concentration [L] at which one half of receptor binding sites are occupied. Half of the ligands in this case exists in the bound and another half in the free form. Table 2.2 provides an estimate of the typical ranges of the binding constants that can be useful for sensing.

Table 2.2 Examples of intermolecular interactions with different binding constants K_b

Type of interaction	K_b, M^{-1}	Examples
Weak	Less than 10^5	Interactions of detergents in aqueous micelles
Medium	10^5–10^7	Common enzyme-substrate and enzyme-inhibitor interactions
Strong	10^7–10^{10}	Interactions of phospholipids in biomembranes; of steroids with their cell receptors; of pharmaceutically useful drugs with their targets
Very strong	More than 10^{10}	Interactions of antibodies with highly specific antigens; of some 'suicide' enzyme inhibitors with their targets; of avidin with biotin (10^{15} M^{-1})

According to mass action law, the equilibrium concentrations of the ligand, [*L*], of receptor, [*R*] and of their complex [*LR*] are related by the binding constant K_b:

$$K_b = \frac{k_1}{k_2} = \frac{[LR]}{[L]\times[R]} \tag{2.5}$$

If the concentrations of receptor, [*R*], and ligand, [*L*], in the system are known, then with the known binding constant, Kb, one can determine the concentration of complex [*LR*]; if [*R*] and [*LR*] are known, then [*L*] can be determined because these values are connected by Eq. (2.5). Therefore if [*R*] is well determined (as it usually happens in sensing), Eq. (2.5) connects [*L*] and [*LR*]. As a result, the unknown *ligand concentration* in the studied system can be determined based on determined by sensor device the concentration of ligand-receptor complexes.

2.2.2 *Determination of* $\mathbf{K}_b$ *by Titration*

The solution of many problems in sensor technologies needs correct determination of ligand-receptor affinities. This can be done on the conditions of application of mass action law. In this case, a titration experiment allows changing gradually the concentration ratio between ligand and receptor, usually by variation of ligand concentration.

When in the system that contains a fixed amount of receptors the ligand concentration is gradually increased, the dependence of *concentration of bound ligand* on *total ligand concentration* is the curve that contains linear segment at very low ligand concentration, then declines from linearity and tends to saturation. This is because at low ligand concentrations many binding sites on receptors remain unoccupied and the equilibrium is strongly shifted towards their bound form with the ligand. With the increase of ligand concentration and of the occupancy of the binding sites, it becomes more difficult to occupy the remaining sites and the equilibrium becomes more and more shifted towards free ligand until all binding sites become occupied and all added ligand remains unbound. It can be seen that this curve tends to saturation (Fig. 2.2a). Semi-logarithmic transformations of these plots are presented in Fig. 2.2b.

The half-saturation point on this curve corresponds to *dissociation constant* K_d. Thus, K_d expressed in concentration units is a convenient characteristic of a sensor, characterizing the dynamic range of sensed concentrations. Meantime, since complete saturation is commonly not reached, such determination of K_d is not precise. The precision can be increased by taking into account all the points in *titration experiment*. This can be done by using nonlinear regression analysis or, alternatively, by transformation of the curve to a linear form, in which all the data points could be efficiently used for building a straight line. The least square method allows fitting the experimental data to a straight line in an optimal way, which allows calculation of precise values of the slope and axis intercepts that are connected with the values of K_b or K_d.

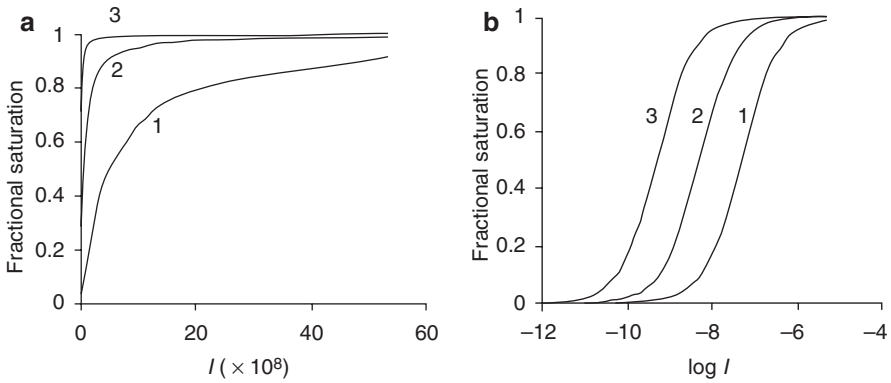

Fig. 2.2 Isotherms of ligand-receptor binding obtained by sequential addition of ligand concentrations (titration curve) in linear (**a**) and semilogarithmic (**b**) coordinates. Plots of fractional saturation f as a function of total ligand concentration l were obtained with variation of l from 1.0×10^{-11} to 6.55×10^{-7} M for the receptor concentration 1×10^{-10} M and the following K_b values: 2×10^7 M^{-1} (*1*); 2×10^8 M^{-1} (*2*); 2×10^9 M^{-1} (*3*)

Two types of linearized binding curves, associated with the names of Klotz and Scatchard are presently popular, and they will be considered below. For convenience, Eq. (2.5) can be re-written using the following notations. Let l be the total concentration of ligand, and r_0 – the total concentration of receptors. $c=[LR]$ is the concentration of the ligand-receptor complex. If every acceptor is of valence m (has m binding sites for the ligand), then mr_0 is the total concentration of receptor binding sites. Then the concentration of unbound ligand is $l-c$, and concentration of free binding sites is mr_0-c. Thus we have:

$$K_b = \frac{c}{(l-c)\times(mr_0-c)} \tag{2.6}$$

It is convenient to introduce the *fractional saturation*, f, which is the fraction of bound ligand (or of sensor binding sites that are occupied by the ligand). If l-c=f, then

$$K_b = \frac{c}{f\,(mr_0-c)} \tag{2.7}$$

The *Klotz approaches* are based on simple algebraic transformation of Eq. (2.7) into linear relationship either between the reverse concentration of bound ligand and reverse concentration of unbound ligand, or between the ratio of unbound ligand to bound, and the concentration of unbound ligand, respectively. Linear dependence of $1/c$ on $1/f$ is presented in Eq. (2.8)

$$\frac{1}{c} = \frac{1}{mr_0K_b}\times\frac{1}{f} + \frac{1}{mr_0} \tag{2.8}$$

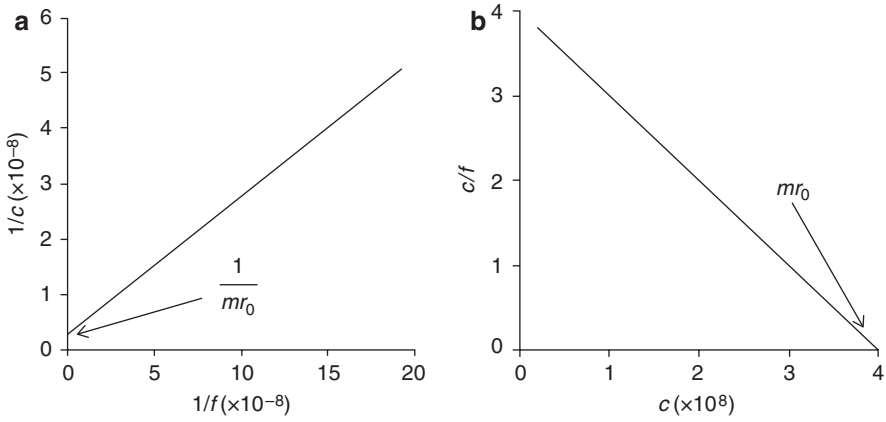

Fig. 2.3 The linearized transformations of the ligand binding isotherms. (**a**) The graph of Klotz, the dependence of $1/c$ on $1/f$. The tangent of the slope of straight line equals to $1/mr_0K_b$. (**b**) The Scatchard graph, the dependence of c/f on c. The tangent of the slope of straight line equals to K_b. The graphs are calculated for: $m=4$, $r_0=1.0\times10^{-8}$ M, $K_b=1.0\times10^8$ M^{-1}. Ligand concentration changes from $l_1=2.5\times10^{-9}$ to $l_i=2.05\times10^{-5}$ M

The graph of this dependence (the Klotz graph) is the straight line with the slope $1/mr_0K_b$ that crosses the ordinate axis at the point $1/mr_0$. Thus, with the knowledge of r_0 and using the values of $1/c$ and $1/f$ obtained in experiment one can construct the linear dependence similar to that in Fig. 2.3a and determine from its slope and from its intercept with ordinate the affinity of interaction (expressed by K_b) and the valence of receptor, m.

According to Scatchard, the linear relationship is observed between the ratio of bound to unbound ligand, c/f, and the concentration of bound ligand, c:

$$\frac{c}{f} = K_b\left(mr_0 - c\right) \tag{2.9}$$

Its graph is a declining linear function (Fig. 2.3b) with the slope equal to K_b. It crosses the ordinate axis at the point K_bmr_0 and abscissa axis at the point mr_0.

It may be noted that in many cases the experiments on determination of K_b are made with the excess of ligand (or receptor). In this case, the total concentration of the component that is in excess exceeds substantially the concentration of the formed complex, $l >> c$. This allows approximating the free concentration of this component equal to its total concentration ($f \approx l$), which avoids the necessity of its measurement. In the case of two types of binding sites with different affinities the Klotz graph may be represented by two segments, as it is depicted in Fig. 2.4.

The *Scatchard graph* is more suitable for obtaining K_b data in the case of two types of ligand binding sites of different affinities. In this case the system of four equations should be solved with four unknowns, K_{b1}, K_{b2}, m_1 and m_2. Their solution

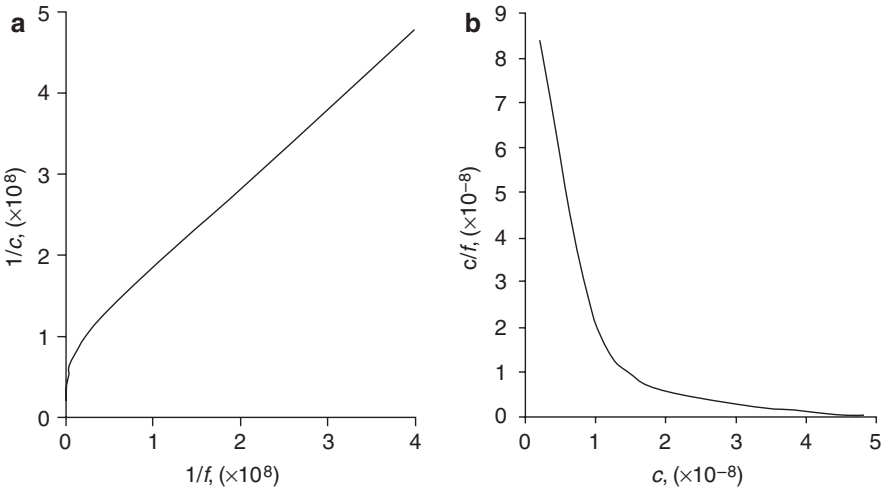

Fig. 2.4 The graphs of Klotz (**a**) and Scatchard (**b**) calculated for binding ligand by two receptors of different affinities: $m_1 = 1$, $r_{01} = 1.0 \times 10^{-8}$ M, $K_{b1} = 1.0 \times 10^{8}$ M^{-1}, $m_2 = 1$, $r_{02} = 4.0 \times 10^{-8}$ M, $K_{b1} = 1.0 \times 10^{6}$ M^{-1}. The ligand concentration l changes from 2.5×10^{-9} to 2.05×10^{-5} M. Note that the contributions of two types of binding (stronger and weaker) in these curves are different, and the Scatchard plots even allow graphical deconvolution the curve into two linear segments

is described in the literature (Klotz and Hunston 1971). When two linear segments are resolved Fig. 2.4, an approximate graphical determination of these parameters using Scatchard graph is possible.

It should be stressed that linear graphs in Klotz or Scatchard coordinates are observed only if the following conditions are satisfied:

(a) the receptor has identical binding sites for the ligand;
(b) the binding of one (or several) ligand(s) by one (or several) site(s) of the receptor does not change the affinity of its other binding sites, i.e., binding occur without cooperative (positive or negative) effect;
(c) the ligand-receptor interaction obeys the mass action law, which implies that all measurements have been done at the state of equilibrium.

Several other methods of linearization of the same binding curves can be found in the literature. They are based on the same Eq. (2.4) and contain the same information. Meantime, it has to be mentioned that, as in any linear transformations, such operations provide different statistical values to different data points along the binding curve, which may cause significant errors in extrapolated values. This issue was discussed in the literature (Klotz 1983). Non-linear approximations and direct fitting of data into Eq. (2.7) may lead to values that are more precise.

Considerations regarding the estimation of error in determined f values on precision in determining K_b can be found in ref. (Tetin and Hazlett 2000). The lowest influence of statistical error in f is introduced with the titration points when $f \approx 0.5\ K_d$.

2.2.3 Determination of K_b by Serial Dilutions

In some practical cases, the methodology based on ligand titration is inconvenient or even inapplicable, since the ligand and the receptor cannot always be obtained in purified form but their interaction can be studied in homogeneous conditions, in solutions. In these cases, an approach based on serial dilutions with the solvent of the sample that contains both receptor and ligand can be applied (Bobrovnik 2003, 2005). With the dilution, the dynamic equilibrium will be shifted to dissociated forms. This shift depends on K_b, and the determination of concentrations of bound ligand in the course of serial dilutions allows obtaining this value. It follows from Eq. (2.6) that after dilution of the system by d_i times, a new equilibrium is established and we obtain:

$$K_b = \frac{c_i}{\left(\frac{l}{d_i} - c_i\right)\left(\frac{mr_0}{d_i} - c_i\right)} \tag{2.10}$$

Thus, in principle, equilibrium constant can be obtained from re-distribution of ligand between free and bound states as a function of dilution factor d_i. In a practically convenient case when $l/d_i >> c_i$, Eq. (2.10) can be reduced to:

$$K_b = \frac{c_i}{\frac{l}{d_i}\left(\frac{mr_0}{d_i} - c_i\right)} \tag{2.11}$$

Transforming Eq. (2.11) one can obtain the dependence of c_i on d_i.

$$c_i = \frac{mr_0 l K_b}{d_i\left(d_i + lK_b\right)} \tag{2.12}$$

Several possibilities exist for linearization of $1/c_i d_i$ and $l/c_i d_i$ functions of dilution factor d_i (Bobrovnik 2005). This method has definite advantages over the titration methods discussed above. It can be successfully used when a ligand-receptor mixture already exists and obtaining a series of samples with a constant concentration of receptors and various concentrations of ligand is technically difficult or even impossible. This approach can be especially useful for studying interactions between highly-labile biological receptors and corresponding ligands as found *in vivo* (Bobrovnik 2008).

The methods discussed above are applicable with the use of common techniques measuring the changes of fluorescence intensities (see below). Meantime, in the case of very strong binding the very high dilutions are needed to achieve the

presence of ligand-dissociated form together with the bound form. With ligands immobilized on the surface and bivalent or multivalent targets (such as antibodies) in common conditions the equilibrium can be so strongly shifted that the binding becomes irreversible (Winzor 2011). Then some information can be derived from kinetics of binding/dissociation. More precise information can be obtained by applying *fluorescence correlation spectroscopy* (FCS) (see Sect. 13.3) that allows operating with very high sample dilutions. By focusing the laser beam the volume of several femtoliters can be illuminated. Based on detection of single molecules entering and leaving the illuminated volume, this method allows providing studying the binding affinities, by switching to the range of very low target and sensor concentrations (Sanchez and Gratton 2005; Tetin and Hazlett 2000).

2.3 Modeling the Ligand Binding Isotherms

The *sensor response function* (often called *sensogram*) is the function describing the correlation between the target analyte concentration and response of analytical system. Since different parameters that are used for fluorescence response (Chap. 3) are commonly proportional (or proportional with weighting, Sect. 2.5) to the amount of bound ligand (analyte), the major task here is to establish correlation between the amount (concentration) of the analyte in the tested system l and its fraction bound by the sensor (fractional saturation) f. This function is called the *ligand binding isotherm*. It has to be determined for particular sensor operation conditions. The receptor functional elements of sensors can be composed of molecules or particles distributed in a defined volume, or they can be attached to a surface.

2.3.1 Receptors Free in Solution or Immobilized to a Surface

Let us consider the case when the sensors are attached to a surface S that accommodates their receptor units with the density σ. Then the total amount of receptors on this sensor surface will be $N = \sigma \times S$. The sensors interact with the ligand (analyte) solution with concentration l in volume V and their affinity is characterized by binding constant K_b. Let l and K_b be known and our aim is to determine the part of receptors that forms the complexes with the ligand and the part that remains unoccupied.

When the solution volume is large enough ($l \times V >> N$), so that the ligand-receptor binding does not influence the ligand concentration in solution, the approximation $l \approx \text{const}$ is acceptable. Let n be the number of receptors forming a complex with ligand, then the number of free receptors is $N - n$. Then apparent concentration

of the binding sites will be N/V. Let the equilibrium condition of binding is reached, and let n receptors (out of N) bind the ligand and $N-n$ remain free. Then their apparent concentrations will be n/V and $(N-n)$/V. Applying the mass action law and providing simple transformations we get:

$$f = \frac{n}{N} = \frac{lK_b}{1+lK_b} \tag{2.13}$$

Equation (2.13) represents the *ligand binding isotherm* by the sensor, which with the account of response of the sensor system can be transformed into sensogram. The graphical forms of the function $f(l)$ in linear and logarithmic coordinates are presented in Fig. 2.2. We observe that the shape of this function does not change by any form of immobilization of receptors. It is solely determined by K_d value.

A very important consequence follows from this simple analysis. There is a *fundamental restriction on the concentration range of sensor response*. Irrespective of sensor and sample geometry this range is limited roughly to two orders of magnitude, one below and one above K_d (~0.1 K_d – ~10 K_d). Outside this range the sensor becomes insensitive, and determination of target concentration not possible.

It also follows that the presence of non-specific ligand if it is present in the same concentration as specific target ligand cannot influence significantly the determination of specific ligand if its binding is weaker by two orders of magnitude or more. Thus, the sensors operating in the conditions of equilibrium binding *can be very selective if they display higher affinity towards specific target*. And accordingly, for sensing specific targets in broad range of concentrations, one has to use a series of sensors with different affinities. For instance, this was done with mutants of maltose binding protein as saccharide receptors (Marvin et al. 1997).

2.3.2 Bivalent and Polyvalent Reversible Target Binding

A dramatically increased affinity of receptors present as *dimers* compared to monomers is explored in the design of fluorescent dyes. Thus the best fluorescent nucleic acid binders are the dimers of intercalating dyes. The intrinsic DNA binding affinity constants of typical intercalator dye ethidium bromide and its homo-dimer are reported to be 1.5×10^5 and 2×10^8 M^{-1} correspondingly (Gaugain et al. 1978). Thus, dimerization increased the affinity by three orders of magnitude. The other example is the dramatic (2,500- to 170,000-fold) increase of binding constants between the nanodevices and folate binding protein through multivalency (Hong et al. 2007).

The affinity enhancement effect produced by multivalency can be explained and to some extent predicted on a thermodynamic basis (Kitov and Bundle 2003). The effect of bivalent binding can be analyzed based on formally applied concept that

the local target (or receptor) concentration is increased on the formation of primary complex. In this case there is a difference, if the linker between binding sites is rigid or flexible (Bobrovnik 2007).

Polyvalent binding at equilibrium means establishing the dynamic equilibrium between unbound form of receptor and its bound forms with saturation of different valences m:

$$L + R_m \Leftrightarrow LR_1 + 2LR_2 + \ldots + mLR_m \tag{2.14}$$

Instead of a single K_b value, this system will be characterized by a matrix of K_{ij} values describing the equilibrium in interaction of each type of the complex with all the rest. In view of experimental data cited above, we can consider the strength of the complex expressed by K_{ij} values to increase with the ligand saturation, reaching the maximum value for mLR_m complex. This cannot be true in a general case, but we always can find the complex xLR_x, for which affinity is the highest. In order to understand better the receptor response in such complex system, we can consider the limiting cases:

(a) The sensor responds to binding of the first target with the formation of LR_1 complex. Since this complex is commonly weak, it can be formed only at very high concentrations. But at these concentrations the complex xLR_x should be formed already with all population of receptor molecules due to high affinity. Therefore, the sensor response will be seen around some efficient K_b value describing equilibrium in interactions of xLR_x complex with free ligand and all other complexes.

(b) The sensor responds only to formation of complex mLR_m, i.e. when all its valences are saturated by the ligand binding. When it is the case of a strongest complex, then we will have the situation similar to case (a) for xLR_x with the exception that intermediate complexes are not observed in response.

(c) The sensor responds in a well-resolvable manner to formation of each of these complexes. For instance, ketocyanine dye responds to formation of high-affinity hydrogen bond complexes with protic co-solvent molecules at their low concentrations and then a different change in spectra occurs on formation of such complexes of lower affinity observed at higher co-solvent concentrations (see Sect. 4.3). In this case two K_b values can be obtained in titration experiment (Pivovarenko et al. 2000). The range for determining the protic co-solvent concentrations is increased to two areas around these K_b values. The other example is the design of a sensor for extended range of pH. In fact, it is the sensor for proton binding-release to the sensor titrating groups. In the case of distinguishable or additive response of sensor groups titrating at different pH we get the sensor for extended pH range (Li et al. 2006).

Consider now in more detail the simplest but practically important case when there are two ligands in the system that bind to the same receptors with different

affinities. Let one (more specific) ligand being in concentration l_1 binds receptor with the higher binding constant K_{b1} and the other (less specific) in concentration l_2 possesses the binding constant K_{b2}. Then in the conditions of equilibrium the number of sensor receptors with the bound first ligand will be n_1, and their number with the bound second ligand – n_2. Based on the mass action law we get two equations representing this case:

$$\mathrm{K}_{b1} = \frac{\frac{n_1}{V}}{\left(\frac{N - n_1 - n_2}{V}\right)\left(l_1 - \frac{n_1}{V}\right)} = \frac{n_1 V}{\left(N - n_1 - n_2\right)\left(l_1 V - n_1\right)} \tag{2.15}$$

$$K_{b2} = \frac{\frac{n_2}{V}}{\left(\frac{N - n_1 - n_2}{V}\right)\left(l_2 - \frac{n_2}{V}\right)} = \frac{n_2 V}{\left(N - n_1 - n_2\right)\left(l_2 V - n_2\right)} \tag{2.16}$$

Attempts to finding analytical solutions for two unknowns n_1 and n_2 lead to necessity of solving complex cubic equations. Meantime, numerical solution of Eqs. (2.15) and (2.16) allows easy determination of n_1 and n_2 for known K_{b1}, K_{b2}, l_1, and l_2. Alternatively, one may find l_1 and l_2, by assigning the values of K_{b1}, K_{b2}, n_1 and n_2. Consequently, one can calculate the *ligand binding isotherm* for this particular case.

2.3.3 Reversible Binding of Ligand and Competitor

Now we consider the case of two different ligands, in which the binding of the *testing ligand* (e.g. fluorescent competitor) can provide informative signal for the binding of *target ligand*. For testing ligand, the concentration and affinity of binding are known; they can be measured in a preliminary test. This ligand can be a key player as a competitor in competition assays (Sect. 1.3). Is there any possibility of finding in such assay the target concentration in the case when its affinity is unknown? We will try to resolve this issue.

Let the unknown concentration of the target ligand be l_x, and its unknown binding constant K_{bx}. The binding constant of the testing ligand is known, it is K_{b1}. In our experiment we can add to the system any desired concentration of this ligand, l_1. These two ligands can bind with the sensor competing with each other so that the quantity of the bound testing ligand n_1 can be measured (for instance, by the response of fluorescence reporter). So, all three of its important parameters, K_{b1}, l_1 and n_1 are known. In contrast, the amount of target ligand, n_{x1}, cannot be measured directly, since it does not provide any response.

If we measure the bound testing ligand at a different concentration, l_2, then the sensor will bind a different amount of this ligand, n_2, which can also be measured. The amount of analyte ligand, n_{x2}, remains unknown. But now we are able to compose four linearly independent equations with four unknowns, l_x, K_{bx}, n_{x1} and n_{x2}. Their solutions will provide numerical values of these unknowns.

Based on the mass action law we obtain the equations describing correlations between equilibrium constants K_{b1}, or K_{bx}, and the concentrations of free ligands or of their complexes.

$$\begin{aligned} K_{b1} &= \frac{n_1 V}{\left(N - n_1 - n_{x1}\right)\left(l_1 V - n_1\right)} \\ K_{b1} &= \frac{n_2 V}{\left(N - n_2 - n_{x2}\right)\left(l_2 V - n_2\right)} \\ K_{bx} &= \frac{n_{x1} V}{\left(N - n_1 - n_{x1}\right)\left(l_1 V - n_{x1}\right)} \\ K_{bx} &= \frac{n_{x2} V}{\left(N - n_2 - n_{x2}\right)\left(l_2 V - n_{x2}\right)} \end{aligned} \tag{2.17}$$

Numerical solution of Eq. (2.17) can yield l_x, K_{bx}, n_{x1} and n_{x2}. Practical examples of these calculations will be suggested to the reader at the end of this Chapter.

When the concentrations of both these ligands are relatively high and their binding constants low, the fractional concentrations of bound ligands will be small compared to their total concentrations. So the changes of free ligand concentrations on binding can be ignored, which simplifies the analysis. We can apply two linearly independent equations based on the mass action law:

$$K_{b1} = \frac{c_1}{\left(C - c_1 - c_x\right) l_1} \tag{2.18}$$

$$K_{bx} = \frac{c_x}{\left(C - c_1 - c_x\right) l_x} \tag{2.19}$$

Here l_1 and l_{x} are the concentrations of two ligands in solution. They bind to the sensor with affinity constants K_{b1} and K_{bx}. C is the efficient concentration of receptors, which can be calculated knowing their amount, N, and solution volume V by formulae: $C = N/\mathrm{V} \times N_a$. Here N_a is the Avogadro's number and c_1 and c_{x} are the efficient concentrations of the *bound* testing and target ligands correspondingly.

After simple algebraic transformations, Eqs. (2.18) and (2.19) can be presented as:

$$c_1 = \frac{l_1 K_{b1} C}{1 + l_1 K_{b1} + l_x K_{bx}} \tag{2.20}$$

$$c_x = \frac{l_x K_{bx} C}{1 + l_1 K_{b1} + l_x K_{bx}} \tag{2.21}$$

It follows that

$$\frac{c_1}{c_x} = \frac{l_1 K_{b1}}{l_x K_{bx}} \tag{2.22}$$

The number of receptors that have bound first or second ligand will be:

$$\frac{c_1}{C} = \frac{l_1 K_{b1}}{1 + l_1 K_{b1} + l_x K_{bx}} \tag{2.23}$$

$$\frac{c_x}{C} = \frac{l_x K_{bx}}{1 + l_1 K_{b1} + l_x K_{bx}} \tag{2.24}$$

If the concentration of one of the ligands is set constant and of the other varies, then we will get the following graph of the dependence of the concentration of either ligand that is bound by the receptor (c_1 or c_x) on total target ligand concentration l_x at constant concentration of the testing ligand. This is the target ligand binding isotherm (see Fig. 2.5).

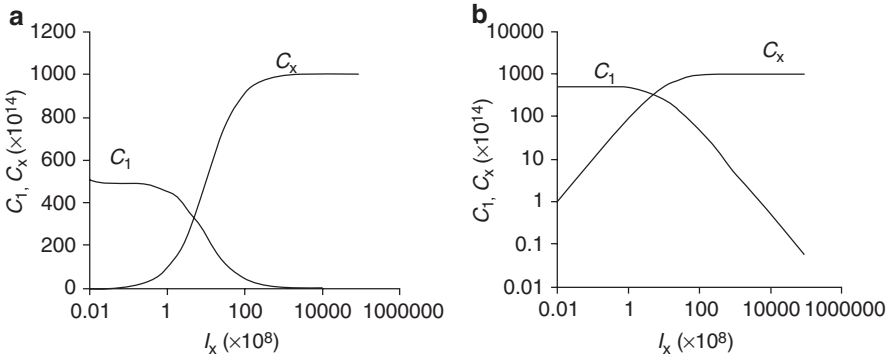

Fig. 2.5 Concentrations of the bound competitor and target ligands (c_1 and c_x) as a function of total target ligand concentration l_x at constant competitor concentration l_1 in semi-logarithmic (**a**) and double-logarithmic (**b**) coordinates. The graphs were composed for the following parameters: $N = 6.0 \times 10^9$, $K_{b1} = 1.0 \times 10^8$ M^{-1}, $K_{bx} = 1.0 \times 10^7$ M^{-1}, $l_1 = \text{const} = 1.0 \times 10^{-8}$ M, and l_x changing from 1.0×10^{-10} M to $8{,}4 \times 10^{-4}$ M

This graph shows that when the labeled competitor binds stronger than the target to the receptor, there is a range of sensor insensitivity at low target concentrations because the target cannot replace the competitor from the complex. The substitution occurs at higher concentrations, and if the competitor changes the parameters of its fluorescence in a binding-release process, this allows determining concentration of the target. When the target concentration becomes too high, all the receptor sites become occupied with the target and all the competitor released, so the sensor becomes insensitive again. Note that as in the case of sensors based on direct response to target binding, the range of target concentrations that can be detected is within the same two orders of magnitude.

2.3.4 Interactions in a Small Volume

Now we consider the case when the volume V, in which the detection is made, is so small that on binding the ligands to receptors their concentration in this volume essentially decreases (S.A. Bobrovnik, to be published). As we see below, the present tendency in sensor design is the dramatic decrease of the testing volume (Chap. 11), and this case may represent a real situation in a number of applications. Sensing inside the living cells (Chap. 13) and using the sensing devices reaching picoliter (10^{-12} *l*) detection volumes may present such cases.

As in the case discussed above, we consider the case of N receptors immobilized on planar support, whereas the tested target remains in solution. In the absence of ligand, all receptors are unoccupied, and their efficient concentration is *N*/*V*, where *V* is the sample volume. Consider the case of equimolar (1:1) reversible binding, so that at equilibrium *n* receptors are occupied; they bind *n* ligand molecules. Then the number of free receptors will be $N-n$ and their apparent concentration in solution will be $(N-n)/V$. An apparent concentration of ligand-receptor complex will be *n*/V. The free ligand concentration being initially l/V (*l* is the total amount of ligand molecules) changes on binding to receptor and becomes *l*-*n*/*V*.

The mass action law can be applied for this case in the following form:

$$K_b = \frac{\frac{n}{V}}{\left(\frac{N-n}{V}\right)\left(l-\frac{n}{V}\right)} = \frac{nV}{(N-n)(lV-n)} \tag{2.25}$$

Equation (2.23) can be rewritten as an expression for *f* as a function of *l* (*f*=*n*/*N*)

$$f = \frac{NK_b + lVK_b + V - \sqrt{(NK_b + lVK_b + V)^2 - 4NlVK_b^{\,2}}}{2K_bN} \tag{2.26}$$

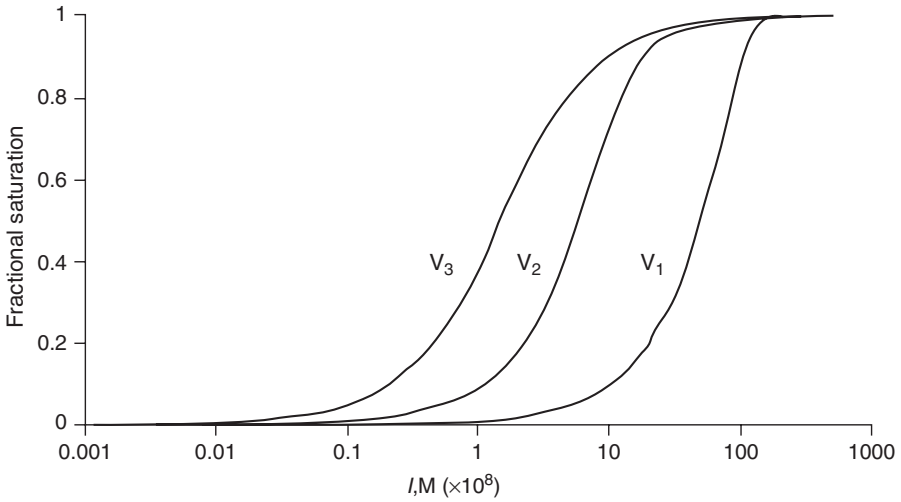

Fig. 2.6 The influence of solution volume on ligand binding isotherm (the $f(l)$ function). The graphs were composed for the following parameters: $N = 1 \times 10^{-10}$ M, $K = 1 \times 10^{8}$ M^{-1} and the solution volumes $V_1 = 0.1$ ml, $V_2 = 1$ ml and $V_3 = 10$ ml

Equation (2.26) represents the *ligand binding isotherm*. Its graph is a sigmoid dependence similar to that in Fig. 2.2. It may be interesting to analyze, how the isotherm of ligand binding will change with the decrease of detection volume. The results are presented in Fig. 2.6.

We observe that with the decrease of solution volume the ligand binding isotherm transforms significantly. It becomes narrower and shifts to higher concentrations. The origin of this effect is in ligand redistribution between its free and bound forms. When the sample volume becomes smaller, a higher ligand concentration is needed to occupy the same amount of binding sites as in a large volume. Miniaturization of sensor technologies requires accounting these effects.

2.4 Kinetics of Target Binding

The sensing commonly starts from the ligand and receptor physically separated in space, and in order to interact they first have to approach each other. It can be the motion of one partner, ligand, if the receptor is immobilized on the surface of spotted array or of both partners if the receptor molecules are free to diffuse in analyzed solution. In sensor technologies, the knowledge of ligand-receptor association-dissociation kinetics is important in several aspects. For correct applications of conditions of equilibrium binding we always need to know, when this equilibrium is established, and this determines the necessary incubation time. If the binding is

irreversible we need to wait until all the ligand is bound. Some sensing technologies allow target determination in kinetic regime.

In kinetic analysis of sensor performance the problem is *to find the amount of the ligand bound to the receptor as a function of time t* after initial application of sample containing the ligand to the sensor system. The rates of ligand binding reactions are described by differential equations that in the simplest case (1:1 stoichiometry) can be written in the form:

$$\mathrm{d}B(t)/\mathrm{d}t = k_1\left[N - B(t)\right]c_L(t) - k_2 B(t), \tag{2.27}$$

where $B(t)$ is the number of bound ligand molecules and N is the total number of receptor molecules. Here $c_L(t)$ is the local concentration of the ligand solution at the reaction surface. It is the function of $B(t)$, and this relation is the subject of modeling (Klenin et al. 2005). In general, the reaction rate as a function of time can be obtained numerically as a solution of a nonlinear integral equation, and its analytical solutions are available only for some special cases. Various sensor geometries of practical interest can be considered, but the practically important result is experimental. The output signal should reach a steady-state value as a function of time.

Depending on the receptor-target pair and on immobilization of receptors (their presence in solutions, attachment to nanoparticles or immobilization on flat or porous surface) the rate-limiting step in formation of their complexes can be different. The target-receptor mutual diffusion imposes an upper limit to the rates of all these reactions. Meantime some intermolecular interactions can be coupled with conformational isomerizations in ligand or target molecules, and their rates can be slower than the diffusion. This can be a *multistep process* of search in a conformational space.

In the case if one of interacting components (usually the receptor) is immobilized on the flat surface, the kinetics of ligand binding will become slower not only because only one component has the freedom to diffuse but also because the kinetics of ligand binding becomes time-dependent. This fact can be explained by the following. At time zero, $t=0$, all receptor binding sites are empty and every interaction with them may lead to binding. However, at $t>0$, some of the sites become occupied, and the search for smaller number of unoccupied sites slows down the process. The ligand migration along the receptor sites is usually much slower than free diffusion in solution because the desorption–sorption process at each step occurs with overcoming higher energy barriers (Sadana and Madugula 1993).

The observed strong tendency towards miniaturization of sensor systems raises new challenges. Due to a small binding area and high target concentration that is usually applied in a small volume, the kinetics of target binding depends on this concentration. For micro flow channel devices the transport equations have to be solved and diffusion processes simulated to guarantee perfect mixing.

The importance of *reaching the conditions of thermodynamic equilibrium* in target binding was discussed by many authors. They attributed the loss of reproducibility and many systematic errors in assays to the fact that these conditions were not satisfied. Both calculation and experiment show that for sensors immobilized on the surface of planar arrays the target binding occurs two to three orders of magnitude slower than on binding in solutions. Meantime most of immunosensors and DNA hybridization arrays are made by immobilization on solid surfaces, which increases the time of reaching the equilibrium to many hours and even many days (Carletti et al. 2006). Smaller decrease of the rate of binding can be achieved if the sensors are immobilized on microspheres (Sekar et al. 2005). Both array formats will be discussed in this book.

The characteristic rate of binding reaction depends on the rates of two processes: (a) the transport of analyte from the bulk compartment to the reaction area (reaction compartment) and (b) the subsequent binding process. In immunosensors the mass transport plays the major role. In contrast, in DNA arrays the process of recognition of correct sequence, in which a huge amount of target-receptor sequences hybridize simultaneously, is the most important.

Different strategies for decreasing the assay time can be applied knowing the origin of rate-limiting step: (a) decreasing the volume of tested system, (b) using inert polymers or nanoparticles in sample solutions to provide 'molecular crowding' effect, (c) the application of microwaves for local heating. Still the issue of binding kinetics remains very actual. With the knowledge of the origin of such retardation, the binding kinetics can be optimized with acceleration of target binding by several orders of magnitude (Kusnezow et al. 2003). This is especially important for microarray analysis of complex biological samples.

2.5 Formats for Fluorescence Detection

Fluorescent sensing is based on the measurement of the *amount of bound target*, and based on these data the information on the *amount of total target* in the tested system is obtained.

The detailed description of fluorescence parameters that are used in fluorescence detection techniques and the analysis of their various applications will be presented in the next Chapter. For the present discussion, we indicate that they are derived from only several types of measurements. Usually at fixed wavelengths, the intensity (in one response channel), intensity ratio (in two channels), anisotropy (or polarization) and the lifetime are recorded. The cases, in which a fluorescence parameter provides the full-scale response changing from zero to a very high value are rare. In all practically important cases, we deal with overlap of at least two signals generated by fluorescence reporters indicating the receptor sites with free and bound ligands. The simplest intensity sensing provides a *highly linear response*. The applications of anisotropy and lifetime sensing are different, they result in interesting *non-linear effects*.

2.5.1 Linear Response Format

In fluorescence sensing the dependence $f(l)$ has to be transformed into the dependence of *fluorescence response function* on ligand concentration that can be used as a calibration curve for a sensor device. Let the fluorescence signal F be proportional to the number of bound ligand molecules n (which is the same as the number of occupied receptors). Its value will be $F = \phi\, n$, where ϕ – is the proportionality factor. At saturation, when $N = n$, we have $F = F_{max}$. Since $f = n/N = F/F_{max}$ and the function $f(l)$ can be determined by calibration, the values of l in the tested system can be obtained from the *linear fluorescence response* by the sensor.

In the case if the background fluorescence and/or the fluorescence of the ligand-free sensor with the intensity $F_{\min}$ contributes to fluorescence signal, this parameter has to be accounted in determination of the ligand concentration, l. It can be presented as:

$$l = K_d \left(\frac{F - F_{min}}{F_{max} - F} \right) \tag{2.28}$$

In the design of fluorescence sensors one has first to estimate the needed range of variation of target concentrations and then try to achieve the K_d values that could allow covering this range by variation of sensor response below and above these K_d values. The formulas presented above can be of use, so that the response of measured fluorescence parameter can vary between $F_{\min}$ for free sensor and $F_{\max}$ for this sensor saturated with the target (or vice versa). If the latter values can be reached in experiment, one can obtain K_d by nonlinear fitting of the steady-state fluorescence intensity F recorded as a function of free target concentration to Eq. (2.28) (Boens et al. 2012).

A popular method in intensity sensing that allows compensating for the variation of sensor concentration is the introduction of a reference channel with a ligand-independent intensity F_{ref}. Many fluorescent dyes and nanocomposites can provide such two-channel ratiometric response (Demchenko 2010, 2014). Dividing the numerator and denominator of Eq. (2.28) by F_{ref}. we get:

$$l = K_d \left(\frac{R - R_{min}}{R_{max} - R} \right) \tag{2.29}$$

In contrast to Eq. (2.28), Eq. (2.29) contains only the intensity ratios that are independent of sensor concentration. $R = F/F_{ref}$, $R_{min} = F_{min}/F_{ref}$ and $R_{max} = F_{max}/F_{ref}$. Because of recording the ratios of intensities at different wavelengths λ such measurements are called *λ-ratiometric*. The most convenient in fluorescence detection is the application of the ratios of fluorescence intensities at two excitation or two emission wavelengths.

In sensor technologies there are the cases when the two sensor forms, ligand-free and ligand-bound, are highly emissive and they differ in positions of excitation or

emission spectra. Thus, the increase of intensity at one wavelength is coupled with its decrease at the other wavelength. The spectra of these forms are usually overlapped, and in these cases the account of such variation can be avoided if we select the wavelength for measuring the response to binding, F, at the wavelength of maximal variation of intensity and the reference intensity, F_{ref}, at the crossing point of two spectra (*isoemissive point*) where this intensity does not change. Then we can easily use Eq. (2.29).

It can be more practical to use a broader scale of intensity ratio variations by measuring the intensities at two points of its maximal change, usually at the band maxima corresponding to ligand-free and ligand-bound forms of the sensor. We can again consider the intensity at one wavelength as a 'sensor signal' and at the other wavelength as the 'reference' but we have to introduce the factor that accounts for intensity redistribution between two bands. This is the ratio of intensities of free and bound forms, F_F/F_B, at a 'reference' wavelength λ_2:

$$l = K_d \left(\frac{R - R_{min}}{R_{max} - R} \right) \left(\frac{F_F(\lambda_2)}{F_B(\lambda_2)} \right) \tag{2.30}$$

In the case of multivalent receptors these equations become more complicated, and the reader may find them in the literature (Yang et al. 2003).

If the sensing is based on the detection of changes in excitation spectra, then the F_F/F_B ratio has to be substituted by the ratio of 'brightnesses' at the reference wavelength ($\varepsilon_F\Phi_F/\varepsilon_B\Phi_B$), which is the ratio of molar absorbances, ε, multiplied by correspondent quantum yields, Φ (Lakowicz 2006).

The linear transformations of Eq. (2.30) are also possible. However, the recommended parameter estimation method is via global nonlinear fitting.

Usually in intensity sensing the linear format is observed over many orders of magnitude. There may be the cases, however, when the fluorescence reporters are connected by electronic conjugation to produce enhanced collective effect (See Chap. 8). In these cases, the response function may become complicated.

2.5.2 Intensity-Weighted Format

In Chap. 3 we will discuss the methods that are frequently applied in sensing and for which the fluorescence response function in a general case is not linear. They are the methods of *anisotropy* and *lifetime* sensing. When measured in a homogeneous population of dyes, these parameters are concentration-independent. The two states of the sensor, ligand-bound and ligand-free, may differ significantly in these parameters, and based on this difference the target concentration has to be determined. In the applications of these methods an essential non-linearity in response function appears. This is because each state (bound or unbound) displays its own polarization-resolved emission intensity and intensity decay

function. Their fractional contributions depend on the relative intensities of correspondent forms, whereas the additive law is valid only for the intensities. Therefore the parameters derived in anisotropy and lifetime sensing appear to be weighted by fractional intensities.

Fluorescence anisotropy is extremely sensitive to those intermolecular interactions, in which a small rotating unit becomes a rigidly coupled associate of a much larger size. The bound and free ligands are detected because they possess different values of anisotropy r, r_f of free and r_b of ligand-bound receptor. The measured anisotropy is obtained as being formed by contributions of these two forms weighted by fluorescence intensities of these forms:

$$r = F_f r_f + F_b r_b \tag{2.31}$$

This means that if the intensity of one of the forms is zero, such anisotropy sensor is useless since it will show anisotropy of only one of the forms. Meantime, if the test conditions are selected so that fluorescence intensity is not changed on ligand binding, $F_f = F_b$, then the fraction of bound ligand can be estimated in a simple way:

$$f = \frac{r - r_f}{r_b - r_f} \tag{2.32}$$

The account of fractional intensity factor $R = F_b/F_f$ (the ratio of intensities of bound and free forms) leads to a more complicated function:

$$f = \frac{r - r_f}{\left(r - r_f\right) + R\left(r_b - r\right)} \tag{2.33}$$

In different *polarization assays* the measured steady-state anisotropy is usually a weighted average of the low r values of free ligand and the large anisotropy of high molecular volume ligand–receptor complexes, and the fluorescence intensities as the weighting factors that can vary in both directions. The extent of nonlinearity that can appear can be illustrated in the work on fluorescein binding by antifluorescein antibody (Baker et al. 2000), in which the intensity changes on ligand binding are linear but a strong non-linearity is observed in anisotropy.

Similar situation is observed in *lifetime sensing* that will be discussed in Sect. 3.4. Fluorescence decays as a function of time (in an ideal case, exponentially), and this decay can be described by initial amplitude α and lifetime τ_F for each of the two free (with index F) and bound (with index B) forms. If both of these forms are present in emission, we observe the result of additive contributions of two decays:

$$F(t) = \alpha_F \exp\left(-t / \tau_F^{\,F}\right) + \alpha_B \exp\left(-t / \tau_F^{\,B}\right) \tag{2.34}$$

The preexponential factors α_F and α_B are related to concentrations of these forms. If for one of the forms $\alpha = 0$, there will be no sensing, since irrespective of target concentration we will observe the response of only one form, which is emissive. Meantime, if $\alpha_F = \alpha_B$, the sensor response will be determined by the ratio of $\tau_F{}^F$ and $\tau_F{}^B$ values. In a general case, the ratio of concentrations of free and occupied receptors will be determined not only by α_F and α_B values and correspondent lifetimes $\tau_F{}^F$ and $\tau_F{}^F$. They have to be weighted by correspondent brightnesses, which are the products of molar absorbances ε_F or ε_B and quantum yields Φ_F or Φ_B (Lakowicz 1999):

$$\frac{\alpha_B}{\alpha_F} = \frac{\varepsilon_B}{\varepsilon_F} \frac{\Phi_B \tau_F{}^F}{\Phi_F \tau_F{}^B} \frac{[LR]}{[L]} \tag{2.35}$$

It follows from Eq. (2.35) that the ratio of preexponential factors (α_B/α_F) represents the ratio of concentrations of ligand bound and free forms ([LR]/[L]) only if there is no change in absorbance at excitation wavelength ($\varepsilon_B = \varepsilon_F$) or of the product of quantum yield and lifetime.

Thus, the anisotropy and fluorescence decay functions change in a complex way as a function of target concentration. Species that fluoresce more intensely contribute disproportionally stronger to the measured parameters. Simultaneous measurements of intensities allow accounting this effect. It is also essential to note that neither the choice of reference signal in intensity-ratiometric measurements nor the choice of reference levels in anisotropy or lifetime sensing does not change the range of target concentrations to which the sensor can respond. In the state of equilibrium it is determined by the target-receptor affinity.

2.6 Sensing and Thinking: How to Provide the Optimal Quantitative Measure of Target Binding?

The first lesson that should be obtained from the presented above considerations is that the range of potential target concentrations is extremely large and covers in molar units 19–20 orders of magnitude. The second lesson is that no single sensor can cover such a vast range in target detection, and even no single strategy can be used for that. There may be a possibility to fit the range of sensor sensitivity by the dilution or concentration of the sample, but this cannot be done in many practical cases. In all these cases the strict limitations exist. They are determined by the target-receptor affinity.

Only in the case of *very strong binding*, the binding can be considered as *irreversible*. For determination of such targets, the concentration of receptors should be higher than the upper range of target concentrations if a small sample volume is extracted from the tested system. Then, an irreversible binding will provide the measure of target concentration. Irreversibility means that the sensor is unable to

measure the target continuously. It cannot be re-used or can be used only after regeneration. Reversible binding in these cases is also possible but at very high dilutions.

If the *affinity is lower*, then the major operation principle becomes the *reversible binding*. Thermodynamic analysis and the application of mass action law allows obtaining the optimal sensor parameters, such as affinity and concentration (or density) of receptors, for the determination of target in the desired concentration range. This range is very narrow and covers only two orders of magnitude, roughly from 0.1 K_d to 10 K_d. It can be extended by application of an array of sensors with receptors possessing different K_d values. The gradual K_d increments should cover the whole range of potential target concentrations. In order to achieve the broadest dynamic range of measurement, the receptor concentration should be lower than the expected target concentrations.

This is the first reason to use instead of a single type of receptor, an array of sensors with different receptors. The other is the *cross-reactivity* that is commonly present in real situations and that cannot be easily eliminated by better sensor design. This is the case, for instance, when the non-specific ligand when present in the concentrations much higher than the specific target, produces the same effect of binding. Designing a variety of receptors that bind to analytes with varying affinities allows providing the 'pattern recognition' (Sandanaraj et al. 2007). And the third reason for application the series of receptors derives from the fact that detecting one compound one never is able to characterize a system of even of medium complexity. The challenges that are put forward are the whole genome and whole proteome requiring analysis of many thousands of different targets.

Questions and Problems

1. Respond quickly, how many zeptomoles are in 100 picomoles? How many attomoles are in 10 nanomoles? How much should you dilute 50 μM concentration to obtain the concentration of 10 aM? 100 zM? What is the dimension of a cube filled with 1 fL of water? What volumes will you get by separating 5 pL into 100 equal portions?
2. Exercise in transferring the number of molecules (denoted as N or n) into moles. These values should be divided by solution volume, V, and then divided by Avogadro's number 6×10^{23}. For example, if the sensor is composed of 6×10^{10} receptors and it is immersed into the volume of 1 ml, then the number of moles of receptors will be $N = 6 \times 10^{10} / 10^{-3} \times 6 \times 10^{23} = 1 \times 10^{-10}$.
3. Explain why the operational range of target determination and the sensor-target affinity must be strongly correlated. Let the sensor be based on receptors with $K_d = 100$ μM. Can we measure at equilibrium the target concentrations of 1 μM? 100 μM? 100 nM?
4. The system contains the analyte displaying specific and relatively strong ($K_d = 10$ nM) binding. Its concentration varies in the range of 1–100 nM. A nonspecific ligand is also present in this system in unspecified concentrations ranging between 1 and 100 μM. Can the analyte concentration be accurately determined if for this ligand K_d is 5 μM? 100 nM?

5. What is the dynamic range of a pH sensor with a single titrating group? How to increase this range by incorporating into the sensor the groups with variable titration properties? For providing a smooth scale of pH sensitivity in the pH range 2–10, how many of these groups are needed?
6. Why weak binding is commonly associated with low selectivity? Provide the explanation based on thermodynamic considerations. Can there be a strong but low-selective binding?
7. Ca^{2+} ions are present in resting cells on the level of 100 nM, and Mg^{2+} ions on the level of 1 mM. Imagine that your sensor is based on a receptor that does not exhibit selectivity between these ions but you can vary K_d in broad ranges. Can you measure Mg^{2+} in the presence of Ca^{2+} or Ca^{2+} in the presence of Mg^{2+}? If yes, select the sensors with optimal K_d and estimate the selectivity of such measurement.
8. Analyze the practical example of calculating the occupancies of the sensor binding sites by two ligands in the case of their simultaneous presence in the tested system. Assume that for two ligands dissolved in a defined volume V we know the concentrations and the binding constants. Let $l_1 = 2 \times 10^{-8}$ M, $K_{b1} = 1 \times 10^{8}$ M^{-1}, $l_x = 5 \times 10^{-8}$ M, $K_{bx} = 3 \times 10^{-8}$ M^{-1}, the number of sensor binding sites 6×10^{12}, and the volume, V, is 1×10^{-3} l (i.e. 1 ml). Then the efficient concentration of the ligand binding sites is $6 \times 10^{12}/1 \times 10^{-3} \times 6 \times 10^{23} = 1 \times 10^{-8}$ M. From Eqs. (2.15) and (2.16) we find the number of those sites that bind first ligand: $n_1 = 4 \times 10^{-9} \times 10^{-3} \times 6 \times 10^{23} = 24 \times 10^{11}$. The number of receptors that bind second ligand will be $n_{x1} = 3.49 \times 10^{-9} \times 10^{-3} \times 6 \times 10^{23} = 20.94 \times 10^{11}$.
9. Consider the previous case in which we change the concentration of first ligand (increase it to $l_2 = 3 \times 10^{-8}$ M), whereas the concentration of the second ligand is left unchanged. Then the number of receptors that have bound first ligand will be $n_2 = 5.08 \times 10^{-9} \times 10^{-3} \times 6 \times 10^{23} = 30.54 \times 10^{11}$, and the number of receptors that bind second ligand will be $n_{x2} = 2.88 \times 10^{-9} \times 10^{-3} \times 6 \times 10^{23} = 17.28 \times 10^{11}$. The known values of n_{x1} and n_{x2}, can substituted together with the known values $l_1 = 2 \times 10^{-8}$ M, $K_{b1} = 1 \times 10^{8}$ M^{-1}, $l_2 = 3 \times 10^{-8}$ M into the system of equations (2.17). Their numerical solution yields: $l_x = 4.9997 \times 10^{-8}$ M, $K_{bx} = 3.00016 \times 10^{-8}$ M^{-1}. Thus we found the values l_x and K_{bx}, which differ very little from those values that were taken for the calculation of the number of ligand-receptor complexes, i.e. $l_x = 5 \times 10^{-8}$ M, $K_x = 3 \times 10^{-8}$ M^{-1}.
10. Compare the effects of K_b in competitive and noncompetitive assays.
11. What is the effect of the receptor total concentration on the response in competitive and noncompetitive assay?
12. What is faster, the binding to receptor in solution or the binding to the same receptor immobilized on a surface? By how much?
13. Why the kinetics of target binding to a receptor immobilized on solid surface becomes dependent on its concentration?
14. In what sensor technologies and due to what reason the response is ‘weighted’? How there appear the weighting parameters.

References

Baker GA, Pandey S, Bright FV (2000) Extending the reach of immunoassays to optically dense specimens by using two-photon excited fluorescence polarization. Anal Chem 72(22): 5748–5752

Bobrovnik SA (2003) Ligand–receptor interactions: a new method for determining the binding parameters. J Biochem Biophys Methods 55(1):71–86

Bobrovnik SA (2005) New capabilities in determining the binding parameters for ligand-receptor interaction. J Biochem Biophys Methods 65(1):30–44

Bobrovnik SA (2007) The influence of rigid or flexible linkage between two ligands on the effective affinity and avidity for reversible interactions with bivalent receptors. J Mol Recognit 20(4):253–262

Bobrovnik SA (2008) A simple and convenient approach for evaluation of the parameters of ligand–receptor interaction. Receptor blocking index and its application. J Mol Recognit 21(2):96–102

Bobrovnik SA (2014) Avidity of polyreactive immunoglobulins. Ukr Biochem J 86(6):183–189

Boens N, Leen V, Dehaen W (2012) Fluorescent indicators based on BODIPY. Chem Soc Rev 41(3):1130–1172

Carletti E, Guerra E, Alberti S (2006) The forgotten variables of DNA array hybridization. Trends Biotechnol 24(10):443–448

Demchenko AP (2010) The concept of lambda-ratiometry in fluorescence sensing and imaging. J Fluoresc 20(5):1099–1128

Demchenko AP (2014) Practical aspects of wavelength ratiometry in the studies of intermolecular interactions. J Mol Struct 1077:51–67

Demidov VV, Frank-Kamenetskii MD (2004) Two sides of the coin: affinity and specificity of nucleic acid interactions. Trends Biochem Sci 29(2):62–71

Eaton BE, Gold L, Zichi DA (1995) Let's get specific: the relationship between specificity and affinity. Chem Biol 2(10):633–638

Gaugain B, Barbet J, Capelle N, Roques BP, Le Pecq JB (1978) DNA Bifunctional intercalators. 2. Fluorescence properties and DNA binding interaction of an ethidium homodimer and an acridine ethidium heterodimer. Biochemistry 17(24):5078–5088

Hong S, Leroueil PR, Majoros IJ, Orr BG, Baker JR Jr, Banaszak Holl MM (2007) The binding avidity of a nanoparticle-based multivalent targeted drug delivery platform. Chem Biol 14(1):107–115

Kellner R, Mermet J-M, Otto M, Valcarcei M, Widmer HM (2004) Analytical chemistry. Wiley-VCH, New York

Kitov PI, Bundle DR (2003) On the nature of the multivalency effect: a thermodynamic model. J Am Chem Soc 125(52):16271–16284

Klenin KV, Kusnezow W, Langowski J (2005) Kinetics of protein binding in solid-phase immunoassays: theory. J Chem Phys 122(21):214715

Klotz IM (1983) Ligand-receptor interactions – what we can and cannot learn from binding measurements. Trends Pharmacol Sci 4(6):253–255

Klotz IM, Hunston DL (1971) Properties of graphical representations of multiple classes of binding sites. Biochemistry 10(16):3065–3069

Kusnezow W, Jacob A, Walijew A, Diehl F, Hoheisel JD (2003) Antibody microarrays: an evaluation of production parameters. Proteomics 3(3):254–264

Lakowicz JR (1999) Principles of fluorescence spectroscopy. Kluwer, New York

Lakowicz JR (2006) Principles of fluorescence spectroscopy, 3rd edn. Springer, New York

Li CY, Zhang XB, Han ZX, Akermark B, Sun L, Shen GL, Yu RQ (2006) A wide pH range optical sensing system based on a sol–gel encapsulated amino-functionalized corrole. Analyst 131(3):388–393

MacDougall D, Crummett WB (1980) Guidelines for data acquisition and data quality evaluation in environmental chemistry. Anal Chem 52(14):2242–2249

Marvin JS, Corcoran EE, Hattangadi NA, Zhang JV, Gere SA, Hellinga HW (1997) The rational design of allosteric interactions in a monomeric protein and its applications to the construction of biosensors. Proc Natl Acad Sci U S A 94(9):4366–4371

Pivovarenko VG, Klueva AV, Doroshenko AO, Demchenko AP (2000) Bands separation in fluorescence spectra of ketocyanine dyes: evidence for their complex formation with monohydric alcohols. Chem Phys Lett 325(4):389–398

Sadana A, Madugula A (1993) Binding kinetics of antigen by immobilized antibody or of antibody by immobilized antigen: influence of lateral interactions and variable rate coefficients. Biotechnol Prog 9(3):259–266

Sanchez SA, Gratton E (2005) Lipid–protein interactions revealed by two-photon microscopy and fluorescence correlation spectroscopy. Acc Chem Res 38(6):469–477

Sandanaraj BS, Demont R, Thayumanavan S (2007) Generating patterns for sensing using a single receptor scaffold. J Am Chem Soc 129(12):3506–3507

Sekar MM, Bloch W, St John PM (2005) Comparative study of sequence-dependent hybridization kinetics in solution and on microspheres. Nucleic Acids Res 33(1):366–375

Tetin SY, Hazlett TL (2000) Optical spectroscopy in studies of antibody-hapten interactions. Methods 20(3):341–361

Vallée-Bélisle A, Ricci F, Plaxco KW (2012) Engineering biosensors with extended, narrowed, or arbitrarily edited dynamic range. J Am Chem Soc 134(6):2876–2879

Winzor DJ (2011) Allowance for antibody bivalence in the characterization of interactions by ELISA. J Mol Recognit 24(2):139–148

Yang RH, Li KA, Wang KM, Zhao FL, Li N, Liu F (2003) Porphyrin assembly on beta-cyclodextrin for selective sensing and detection of a zinc ion based on the dual emission fluorescence ratio. Anal Chem 75(3):612–621

Chapter 3
Fluorescence Detection Techniques

Fluorescence is a very interesting phenomenon that is observed on interactions of light and matter. Different processes can be involved in these interactions, and fluorescence emission is one of them (Fig. 3.1).

Light can be *reflected* from the sample surface; it can pass through it exhibiting *refraction* and also be absorbed within the sample demonstrating decreased transmission due to specific *absorption* or *light scattering*. These processes changing the light intensity do not change the energies of transmitted light quanta and therefore there is no change in their recording on wavelength scale. In contrast, luminescence, and fluorescence in particular, is observed with the change in wavelength. The other its specific features are the propagation in all directions, the delay between light absorption and emission and characteristic behavior in polarization of emission. They appear because on absorption of light quantum the molecule appears in the excited state and stays there during definite *lifetime*. Light emission always competes with non-emissive processes resulting in quenching that

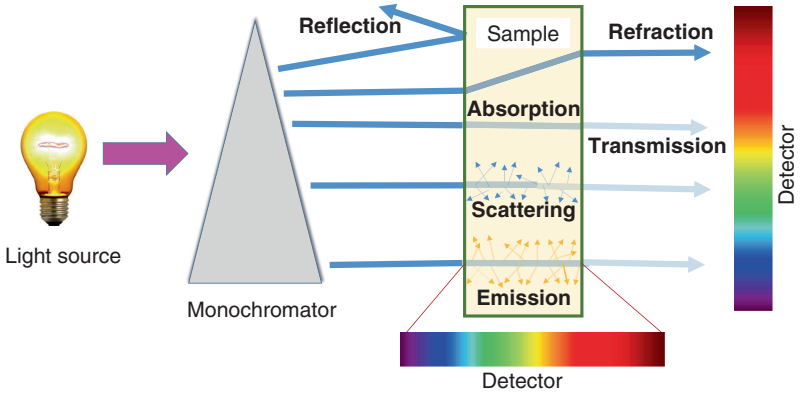

Fig. 3.1 Different phenomena observed on interaction of light and matter

A.P. Demchenko, *Introduction to Fluorescence Sensing*,
DOI 10.1007/978-3-319-20780-3_3

influences all emission parameters. During the lifetime, different processes can proceed, such as molecular rotations and electron, proton and energy transfer reactions. These processes are the sources of valuable information used in sensor technologies.

In this Chapter we concentrate on the methods of fluorescence observation. Starting from introducing the definitions and explaining fundamentals in fluorescence spectroscopy, the discussion proceeds to different methods of fluorescence that are valuable for sensing technologies. We discuss intensity-based sensing with and without intrinsic reference and the methods that do not need such reference and require the measurements of anisotropy and lifetime. The methods based on excimer and exciplex formation and Förster resonance energy transfer (FRET) involve interactions in the system of fluorescence reporters. In contrast, the sensing response based on wavelength-shifting and two-band wavelength-ratiometry relies on modulation of weak intermolecular interactions of a single fluorophore with its environment.

3.1 Fluorescence Fundamentals

Fluorescence is the phenomenon of *emission* of light quanta by a molecule or supramolecular structure (*fluorophore*) after initial electronic *excitation* in a light-absorption process. After excitation by absorbing the light quanta, a molecule resides for some time in the so-called *excited state* and its fluorescence emission can be observed usually with a lower energy (longer wavelength) than the excitation. Such change in fluorescence emission color with respect to the color of incident light was first observed by Irish scientist George Stokes and is called the Stokes shift.

The time scale of fluorescence emission depends on both the fluorophore and its interactions with local environment. Thus, for organic dyes the *fluorescence lifetime* is in picosecond (ps) to nanosecond (ns) time range, typically 10^{-8}–10^{-11} s.

Fluorescence is a part of a more general phenomenon, *luminescence*. The latter includes the emission of species excited in the course of chemical reactions (*chemiluminescence*), biochemical reactions (*bioluminescence*) or upon oxidation/reduction at electrode (*electrochemiluminescence*). Important for sensing is also the emission with long lifetime from triplet state (*phosphorescence*). Duration of these types of luminescence can be much longer than the fluorescence. For semiconductor nanocrystals it can be tens of nanoseconds (ns); for organometallic compounds and lanthanide complexes – hundreds of nanoseconds, up to milliseconds (ms).

3.1.1 The Light Emission Phenomenon

The absorption and emission of light quanta (*photons*) involves electronic transitions between quantized energy levels. This means that only the quanta of well-specified energies can be absorbed and emitted. The distribution of such electronic

transitions probabilities on their energies forms the *light absorption* and *emission spectra*. Our interest in fluorescence sensing and imaging technologies is in the usage of visible range of spectrum, from 400 to 760 nm, and of near-IR light extending to longer wavelengths.

The absorption of light quanta involves the transition from the ground *singlet state* to the excited states. This process occurs so rapidly (in femtoseconds) that electronic sub-system changes its energy without the change in atom nuclei configuration. Then different processes of relaxation proceed in the excited states, including *vibrational relaxation* (transition to the lowest in energy vibrational state) and *internal conversion* (transition to the lowest excited singlet state with the loss of energy). Then the molecule or nanoparticle has a chance to return to the ground state emitting photon in the form of fluorescence or without emission. A transition from singlet to triplet state (in which the energy is split into triplet seen in paramagnetic resonance studies) is also possible. It is called *intersystem crossing*, and from this state the *phosphorescence emission* is observed. Since the latter process involves low probable spin inversion, it proceeds on much slower time scale than fluorescence.

The proper selection of excitation and emission wavelengths is important for fluorescence sensing. Since the fluorescence spectrum is shifted with respect to excitation spectrum to longer wavelengths (the *Stokes shift*) (Fig. 3.2), the highest fluorescence intensity will be observed if the excitation is provided and emission

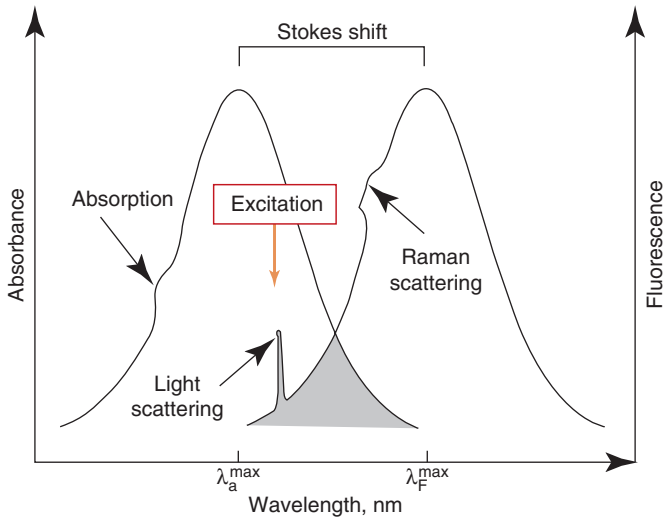

Fig. 3.2 Typical absorption and fluorescence emission spectra. Fluorescence spectrum is located at longer wavelengths with respect to the absorption spectrum. The area between absorption and emission spectrum is shadowed. The distance between their band maxima is called the Stokes shift that is usually expressed as a change in energy on a wavenumber scale ν, and $\nu\ (\mathrm{cm}^{-1}) = 10^7/\lambda\ (\mathrm{nm})$. Fluorescence excitation spectrum usually matches the absorption spectrum, and excitation wavelength is usually selected close to this band maximum. The major light-scattering band is observed at the wavelength of excitation. The Raman scattering band is shifted by a value of energy of vibrations, it is seen only if the fluorescence intensity is low

recorded at the wavelengths of the correspondent band maxima. The complicating factor is the elastic *light scattering* that occurs at the excitation wavelength and the spectral profile of which corresponds to the profile of incident light. The light-scattering complications are especially strong if the studied sample contains macromolecules or particles, the size of which is larger than the wavelength of light. Therefore, excitation and emission wavelengths should always be separated and the dyes with large Stokes shift are preferred. The *Raman scattering* bands present in any solvent are shifted with respect to the main scattering band and overlaps the fluorescence spectrum. It may produce complications in fluorescence measurements if the emission intensity is very low. In practical sense, the excitation and emission wavelengths should be selected to optimally match the radiation wavelengths provided by light source (e.g., if it is a laser) and the optimal sensitivity range of the detector.

The *Kasha's rule* states that the excess energy got in absorption and resulting in excitation to higher electronic and vibrational excited states is dissipated on a very fast scale before the emission (internal conversion), so that the emission occurs from the lowest excited state (Fig. 3.3). Practically this means that we cannot achieve generation of new fluorescence bands at shorter wavelengths if we shift the

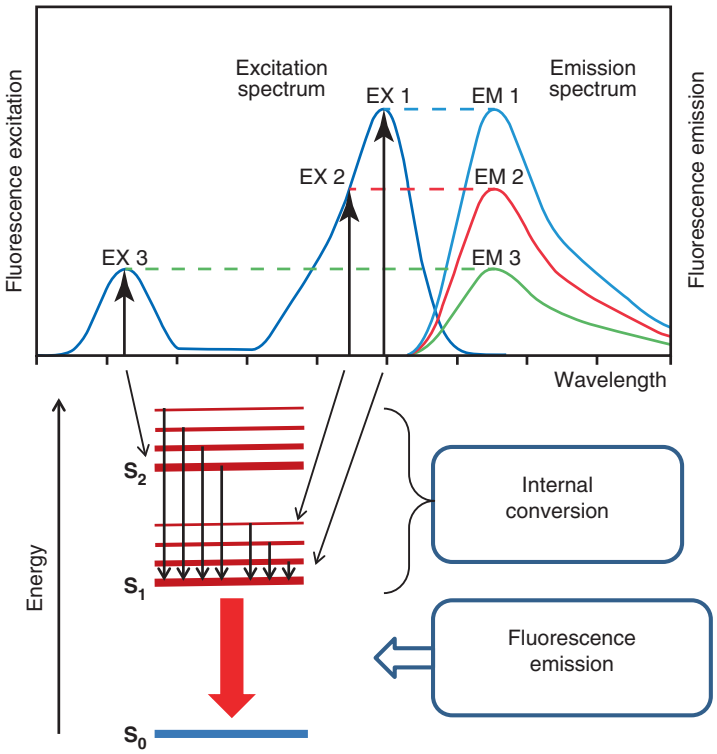

Fig. 3.3 Illustration of the Kasha's rule. The position of fluorescence emission spectrum remains unchanged whether excitation is provided at the absorption band maximum, its high-energy slope or separate band corresponding to the singlet S_2 state located at higher energies. Due to ultrafast internal conversion the fluorescence proceeds from the lowest in energy S_1 excited state to S_0 ground state

excitation to the second short-wavelength absorption band. The same rule operates also for phosphorescence, which is the emission from triplet state.

For in-depth understanding of light absorption and emission phenomena and of the laws that govern these processes the reader may address the excellent textbooks on photochemistry (Birks 1973; Turro et al. 2009) and the books with particular focus on fluorescence (Valeur and Berberan-Santos 2012; Lakowicz 2006). Here we stress characteristic features of *luminescence* (and, particularly, of *fluorescence*) that are explored actively in fluorescence probing, sensing and imaging.

- It is the wavelength-shifted emission, which allows separating optically the absorbed (and scattered) from emitted light quanta.
- It is the emission delayed in time. This allows excluding or substantially reducing not only the light scattering but also the short-living background emission.
- Many fluorophores can be excited selectively by polarized light and, depending on the conditions, emit light of variable polarization.

3.1.2 Fluorophore Emissive Power: The Quantum Yield

Fluorescence quantum yield, Φ, is defined as the ratio of the number of emitted quanta to the whole number of the quanta absorbed. In more general terms, it is the probability to emit one photon in the form of fluorescence after absorbing one photon. Fluorescence intensity at any wavelength, $F(\lambda)$, is proportional to the fluorescence quantum yield Φ. The excited state population decays as a function of time, which can be expressed by correspondent rate constants (first derivatives of concentration of excited-state species as a function of time). The quantum yield is determined by the ratio of radiative (k_r) and the sum of all non-radiative (k_{nr}) rate constants of excited-state decay:

$$\Phi = \frac{k_r}{k_r + \sum k_{nr}} = \frac{1}{1 + \sum k_{nr} / k_r} \tag{3.1}$$

In strongly fluorescent dye, the emission determined by k_r should occur much faster than all the 'dark' processes occurring with the rates Σk_{nr}.

Quantum yield of fluorescence Φ is one of the major parameters characterizing fluorescent materials (Fery-Forgues and Lavabre 1999; Crosby and Demas 1971; Rurack 2008). Being used to quantify the efficiency of the emission process, it determines the suitability of such materials for applications in chemical sensing, bioanalysis and fluorescence imaging as well as for the active components in optical devices. For accurate Φ determination, different methods were developed. One is the "absolute" method that is based on collecting the whole spatially distributed fluorescence emission or reconstructing this spatial profile. The other is a comparative method that relies on the previous knowledge the quantum yield of some standard material, for which Φ is well determined (Würth et al. 2011). The later method is the

most frequently used, since it requires only simple light absorption and fluorescence measurements with conventional instrumentation.

This method is based on one important condition, which is the perfect matching of the sample excitation band with the absorption band (*Vavilov's law*). This law derives from the fact that every absorbed light quantum over the absorption band has equal probability of emission, and this makes Φ independent of excitation wavelength λ_{ex}. This is common for organic dyes studied in solutions, but is not observed in some specific cases, namely with carbon dots.

3.1.3 Fluorescence Parameters Used in Sensing

Several parameters of fluorescence emission can be recorded and all of them can be used in sensing (Fig. 3.4). Intensity F can be measured at given wavelengths of excitation and emission (usually, band maxima). Its dependence on emission wavelength, F (λ_{em}), gives the fluorescence *emission spectrum*. If this intensity is

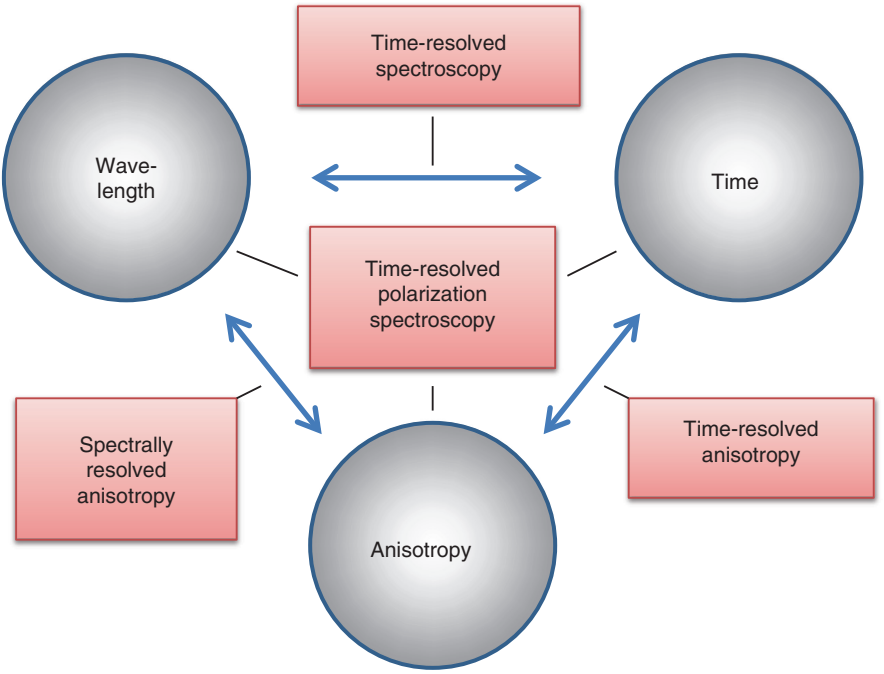

Fig. 3.4 Fluorescence parameters used in sensing. The simplest is the fluorescence intensity F measured at particular excitation (λ_{ex}) and emission (λ_{em}) wavelengths. Dependence F (λ_{ex}) gives the excitation spectrum and F (λ_{em}) the emission spectrum (wavelength domain). The rate of emission decay gives its inverse function – the fluorescence lifetime (time domain). Recording fluorescence emission at two orthogonal (perpendicular) polarizations gives emission anisotropy (anisotropy domain). Different combinations of these parameters can be realized in fluorescence techniques

measured over the range of excitation wavelengths, one can get the fluorescence *excitation spectrum F* (λ_{ex}). *Emission anisotropy*, *r* (or the similar parameter, polarization, *P*) is the function of fluorescence intensities obtained at two different polarizations, vertical and horizontal. Finally, emission can be characterized by the *fluorescence lifetime* τ_F, which is the inverse function of the rate constant of the excited state emissive depopulation, k_r. All of these parameters can be determined as a function of excitation and emission wavelengths. They can be used for reporting on sensor-target interactions, so that a variety of possibilities exist for their employment in sensor constructs.

A combination of these parameters in recording fluorescence is possible. The intensity, polarization and lifetime are usually measured with resolution in wavelength. Time-resolved (Suhling et al. 2005) and polarization-selective (Jameson and Croney 2003) measurements allow increasing efficiency in analytical applications by suppressing the background signal and increasing selectivity of response. Anisotropy with time resolution can characterize the fast rotational motions of fluorophores (Clayton et al. 2002). Meantime, as we will see in Chap. 6, the assembly of molecules and nanoparticles into nanocomposites that allows their interaction and collective photophysical events must put some corrections in interpretation of "classical" results. For instance, drop in anisotropy can occur not only because of suppression of rotations, but also due to homo-FRET that may occur without detectable spectroscopic changes. Only the observation of Red-Edge effects (Demchenko 2002) allows differentiating between these two phenomena.

Specific fluorophore design allows observation of multiple emission bands that can be due to designed combination of non-interacting fluorophore but also due to the excited-state reactions within single fluorophores or between them. This allows applying λ-ratiometry, i.e., collecting the ratio of intensities at two or more wavelengths (Demchenko 2010). This approach improves dramatically the quantitative analysis of fluorescence signal (Demchenko 2005c) and can be combined with other fluorescence detection methods.

In the following sections of this Chapter we will discuss different possibilities in using these parameters of fluorescence emission and the corresponding detection methods for design of operational fluorescence sensors.

3.2 Intensity-Based Sensing

The change from light to dark is easily observed and recorded. This change can be efficiently reproduced on molecular level with recording of response from fluorescent dyes that switch from an emissive to a dark non-emissive state. Thus, everybody knows fluorescein for its bright fluorescence emission. Fluorescence of this dye can be almost completely quenched on its binding to anti-fluorescein antibody. This provides the reader an estimate of dynamic range of intensity sensing of intermolecular interactions: from extremely bright to almost totally dark. If fluorescein is attached through a flexible linkage to another dye, tetramethylrhodamine, the opposite effect on the binding to anti-fluorescein antibody can be shown. Two

dyes make non-fluorescent stacking dimer, and the binding to antibody results in disrupting this dimer with dramatic enhancement of fluorescence by a rhodamine dye (Kapanidis and Weiss 2002). Thus, for various sensing applications, modulation of fluorescence intensity can be observed in both directions, the *quenching* and the *enhancement*, and in the broadest possible ranges.

3.2.1 Peculiarities of Fluorescence Intensity Measurements

The measurement of fluorescence intensity changes at a single wavelength (usually at the emission band maximum) is the simplest and still very sensitive method to obtain information from fluorescence reporter. In many cases, it is relatively easy to provide the coupling of this enhancement/quenching response with sensing event. The change in intensity is the reflection of changing the fundamental parameter of emission, the *fluorescence quantum yield*.

The proper selection of excitation and emission wavelengths is important for intensity sensing. Commonly, the fluorescence spectrum is shifted with respect to excitation spectrum to longer wavelengths (the *Stokes shift*) (Fig. 3.2). As it was indicated above, the highest fluorescence intensity will be observed if the excitation and emission are provided at the wavelengths of the correspondent band maxima and possible complications arising from *light scattering* are accounted.

Many dyes that can be used for providing the response to target binding can change their fluorescence emission on the variation of their weak noncovalent interaction with the local environment, and this change is mediated by non-radiative rate constants k_{nr}. A change in fluorescence intensity from very high values (that correspond to quantum yield $\Phi \sim 100\,\%$) to zero or almost zero values between the target-free and the target-bound forms can be used in the background of operation of *intensity-based sensors* exploring the quenching effects.

3.2.2 How to Make Use of Quenching Effects?

The switching between the emissive and dark states should involve some mechanism providing substantial quenching the fluorescence of reporter dye. This can be realized in different ways:

1. *The quenching can be intrinsic to the reporter molecule*, which means that the reporter dye molecule itself can switch between 'light' and 'dark' states. This is possible, but the dye molecule should be properly constructed. For instance, if the intrinsic mechanism of quenching is the *intramolecular electron transfer* (IET), then the dye should contain electron-donor and electron-acceptor fragments. There are many possibilities to make such constructions (see Sect. 8.1) and they are extensively explored, especially in ion sensing.
2. *The quenching requires intermolecular interactions*. Fluorescent dyes in their excited states may be electron-rich or electron-poor compared to the target

molecules. So on their complexation an electron-transfer quenching can be observed. An example is the detection of dopamine based on 2,7-diazapyrenium dications. In this system the quenching is observed on binding the target electron-rich dioxyarene fragment with electron-deficient excited dye molecule (Raymond et al. 2005). The same type of quenching by nucleic acid bases can be applied for their detection (Torimura et al. 2001). The quenching can also be observed on the dye interactions with heavy and transition metal ions.

Fluorescence quenching can be connected with *conformational flexibility* that may exist in some dye molecules. Should the rigidity in environment of these dyes increase, a dramatic enhancement of fluorescence can be achieved (McFarland and Finney 2001). Classical examples of this type of behavior are triarylmethane dyes, such as Crystal Violet and Malachite Green. They are non-fluorescent in liquid media but become strongly fluorescent on absorption to rigid surfaces and on binding to proteins.

3. *The quenching involves the participation of solvent*. Formation-disruption of hydrogen bonds with solvent molecules and different solvent-dependent changes of dye geometry can be observed in many organic dyes. Dramatic quenching in water (and to lesser extent in some alcohols) may occur due to formation by water molecules of the traps for solvated electrons. In addition, the solvent can influence on the dye energy states, particularly on inversion of *n* (non-fluorescent) and π (fluorescent) energy levels. According to *Kasha rule*, fluorescence occurs from the lowest excited energy state (see Fig. 3.3). If the non-emissive state becomes the lowest, then fluorescence is quenched. These and other factors can also modulate strongly the fluorescence intensity (de Silva et al. 1997). Practically for sensing applications this means that exposing or screening the fluorescence reporter from the solvent may influence dramatically the emission intensity and in this way provide the necessary response.

From this short discussion, one can derive that there exist a variety of possibilities for exploring fluorescence quenching effects. Some of them may operate together. The researcher has a lot of choice for constructing a sensor with response based on the principle of intensity sensing.

3.2.3 Quenching: Static and Dynamic

Fluorescence quenching differs not only by its intrinsic mechanism but also by the way, in which it is applied. The quencher can form the long-lasting contact with the reporter dye, so that its emission is abolished but the emission of the same closely located dyes that do not interact with the quencher may not change. Such quenching is called *static*. It decreases fluorescence intensity but not the lifetime. This is because the dyes interacting with the quencher do not emit light, and those, which do not interact, emit normally.

The other limiting case is the *dynamic quenching*. Here the effect of quenching competes on a time scale with the emission and is determined by the diffusion of a quencher in the medium and by its collisions with the excited dye. In this case, the

relative change of intensity, F_0/F, is strictly proportional to the correspondent change of fluorescence lifetime, τ_0/τ, where F_0 and τ_0 correspond to conditions without quencher. Fluorescence lifetime is the reverse function of the rate of the excited-state depopulation:

$$\tau_0 = 1/\left(k_r + \Sigma k_{nr}\right) \tag{3.2}$$

The *Stern-Volmer relationship* establishes the correlation of these changes with the quencher concentration [Q] by introducing the rate constant proportional to this concentration:

$$F_0 / F = \tau_0 / \tau = 1 + k_q \tau_0 [Q] = K_{SV} [Q] \tag{3.3}$$

Here k_q is the rate constant of quenching, which in the case of 100 % efficient quenching is equal to quencher diffusion constant (being typically in the range of 10^9–10^{10} M^{-1} s^{-1}). $K_{SV} = k_q \tau_0$ is called the Stern-Volmer quenching constant. It can be determined from the slope of the graph displaying dependence of intensity or lifetime on [Q], expressed by Eq. (3.3).

If the lifetime does not change in proportion to the change of intensity or if the quenching effect in intensity exceeds the diffusional limit, this indicates the contribution of *static quenching*. In the case if all the quenching is static, a dye bound to a quencher appears immediately (much faster than the decay) in a dark nonemissive state. The unbound fluorophores exhibit their natural lifetimes, and the slope of F_0/F vs. [Q] yields a binding constant, defined in Sect. 2.2.

The static and dynamic quenching can be distinguished also by the *temperature effects*. If the quenching is static, it decreases with the increase of temperature because of disrupting molecular complexes that produce quenching. On the contrary, the dynamic quenching increases because of increasing the quencher diffusion rate.

Both static and dynamic quenching can be used for providing the fluorescence response. In sensing technology, the target or the competitor can be used as dynamic quencher, and its concentration can be determined from Eq. (3.3). This condition could be better applied to detecting small molecules, the diffusion of which is fast. Meantime, in many cases the employment of such sensor constructs that use the static quenching produced by intramolecular or intermolecular complexation is very efficient.

3.2.4 Non-linearity Effects

When the fluorescence intensity is measured at low dye concentrations and low intensities of incident light and dye distribution in the studied system does not depend upon its concentration, this intensity should be strictly proportional to the dye concentration.

Non-linearities can appear due to several factors. They are:

(a) Those depending on *sample volume* and *geometry*. In the case of strongly absorbing (low transparent) samples, the light passing through the sample gets weaker and excites fluorescence at a lower level (primary *inner filter effect*). Also, in the cases of high fluorophore concentration, the fluorescent light emitted from illuminated volume can be *re-absorbed* in a dark volume instead of passing to detection device (secondary inner filter effect). The involvement of these factors can be diminished or even eliminated by reducing the optical path or the sample volume, by special sample geometry or introduction of correction factors (Fonin et al. 2014). This effect does not create problems at absorbances 0.05–0.1 and lower.

(b) Those depending on the *properties of the dye*. Some dyes form *non-fluorescent* dimers and aggregates and their formation is concentration-dependent. In addition, at short distances between the dye molecules the excitation can migrate between the dyes so that the dye absorbing light can transfer its energy to neighboring dyes and these non-fluorescent species may serve as the light traps. This explains why one cannot load many dye molecules (fluorescein or rhodamine derivatives) on single protein molecule (e.g., antibody); such complexes become non-fluorescent. The mechanisms of these processes will be explained in Sect. 6.1. Energy migration to nonfluorescent associates can be reduced by using the dyes with large Stokes shifts.

However, there is an efficient application of s*elf-quenching* effects. They may bring useful information in the cases when the observed phenomenon involves a strong change in the local dye concentration. For instance, the dyes trapped at high concentrations within phospholipids vesicles (liposomes) can be non-fluorescent. But when the vesicle integrity is disrupted, the dye comes out from vesicle and being diluted increases dramatically its fluorescence. Hence is the control for vesicle integrity.

(c) Those occurring at *high intensities of excitation light*. In this case, the non-linearities are explained by the fact that a large portion of molecules appears in the excited state so that the ground state becomes depopulated. Since fluorescence intensity is proportional to the ground-state concentration, the so-called *light quenching* effect appears (Lakowicz 2006) All these effects do not appear at common excitation and emission conditions and the commonly used dye concentrations but they have to be accounted for if the researcher starts working outside this range.

3.2.5 Internal Calibration in Intensity Sensing

Calibration in fluorescence sensing means the operation, as a result of which at every sensing element (molecule, nanoparticle, etc.) or at every site of the image the fluorescence signal becomes independent of any other factor except the reported

concentration of bound target (Vogt et al. 2008). The problem of calibration in intensity sensing is very important because commonly the fluorescence intensity F is measured in *relative units* that are proportional to the number of emitted quanta and have no absolute meaning if not compared with some standard measurement. When the fluorescence spectrum is recorded, the intensity at one wavelength is compared with intensities at other wavelengths; therefore, the spectrum has an information value. However, one cannot compare the fluorescence intensities of two samples measured today and 1 year after because of the difference in experimental conditions. Likewise, one cannot compare the fluorescence intensities at two neighboring spots in the sensor array, in which the amount of sensor molecules is different. Similar problem exists in cellular imaging of target distribution: the image formed of light intensities depends not only on the target distribution but also on the distribution of sensors themselves.

In the commonly used instrumentation, the fluorescence signal is obtained in *relative units* (the quanta counts or the analog signal obtained on their averaging by the detection system). In this case, the fluorescence response depends not only upon the sensor – target binding, but also upon such technical parameters as the intensity of incident light, geometry of the instrument, detector sensitivity, monochromator slit widths, etc. It is sensitive to every fluctuation in light source intensity or in sensitivity of the detector. Thus, the recorded changes of intensity always vary from instrument to instrument, and the proper reference even for compensating these instrumental effects is difficult to apply.

In common spectrofluorimeter, the measured signal can be compared with the signal coming from the reference sample. This reference could be the sensor molecules in a given concentration calibrated with the addition of given concentrations of the target. By variation of target concentration a calibration function can be obtained. It is then used for determining the target concentration from the read-out of fluorescence response from the sample. This approach is hard to realize on a microscopic level or in simultaneous analysis of different sensor-target compositions. We have to analyze why this difficulty appears with an aim to find proper solutions.

(a) It is difficult to achieve a *strictly determined concentration* (or density) of sensor molecules in analyzed volume. It is common also that both the sensing properties and their reporting abilities degrade in time due to either inactivation or photobleaching.
(b) It is difficult to provide a *separate reference* to every sensor unit in the case if there are arrays of them and each of them responds to binding of a different target.
(c) Even if this is done, it is hard to *equalize the concentrations* of sensor molecules in a sensor and in a reference element or to provide correction for their difference.

Thus, if our aim is obtaining the quantitative information about concentrations of many different targets simultaneously, we have to develop a special methodology. We have to follow the requirement that each element of the array should become

self-calibrating. This means that its response should contain not only the signal reporting on the target binding but also a different signal (or signals) that could allow providing the account or compensation of all the effects that influence the fluorescence parameter(s) besides the target binding.

In the simplest case of reversible binding with stoichiometry 1:1 the target analyte concentration [A] can be obtained from the measured fluorescence intensity F as:

$$[A] = K_d \left(\frac{F - F_{\min}}{F_{\max} - F} \right) \tag{3.4}$$

Here F_{min} is the fluorescence intensity without binding and F_{max} is the intensity if the sensor molecules are totally occupied. K_d is the dissociation constant (it was introduced in Sect. 2.2). The differences in intensities in the numerator and denominator allow compensating for the background signal and the obtained ratio can be calibrated in target concentration. However, since F, F_{min} and F_{max} are expressed in relative units, they have to be determined in the same test and in exactly the same experimental conditions. This is difficult and often not possible.

The most efficient and commonly used approach is the introduction of *reference reporter*. This additional dye can be introduced into a sensor molecule (or into support layer, the same nanoparticle, etc.) in a way that it can be excited together with the reporter dye and emit light at a different wavelength, so that it should not change its signal on target binding. This should provide an additional *independent channel of information* that could serve as a reference (Fig. 3.5). If the reference is properly selected, then one can observe two peaks in fluorescence – one from reporter with a

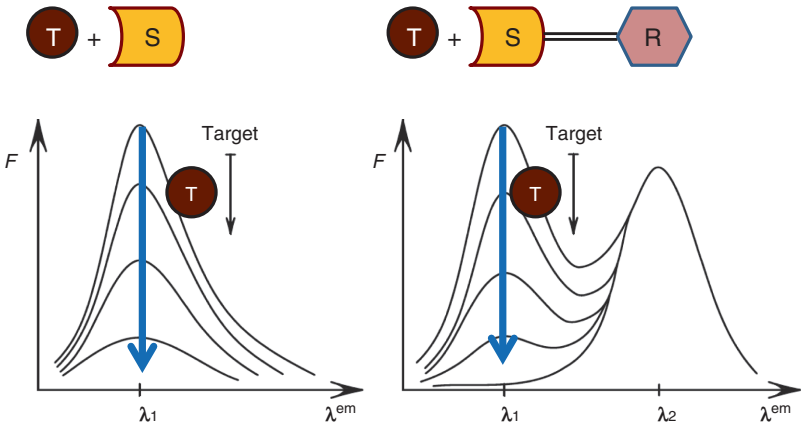

Fig. 3.5 The scheme illustrating the advantage of self-calibrated signal on sensor (S) – target (T) interaction with the aid of reference dye (R). The sensor – target interaction produces quenching of fluorescence spectra in the case of intensity sensing (*left*) and intensity sensing with the reference (*right*). The two dyes, sensing and referencing, are excited and detected simultaneously. The reference dye allows recording the ratio of two intensities detected at wavelengths λ_1 and λ_2

maximum at λ_1 and the other from the reference with a maximum at λ_2. Their intensity ratio can be calibrated in concentration of the bound target. Thus, if we divide both the numerator and denominator of Eq. (3.4) by $F_{ref}(\lambda_2)$, the intensity of the reference measured in the same conditions, we can obtain target concentration from the following equation that contains only the intensity ratios $R = F(\lambda_1)/F_{ref}(\lambda_2)$, $R_{min} = F_{min}(\lambda_1)/F_{ref}(\lambda_2)$, and $R_{max} = F_{max}(\lambda_1)/F_{ref}(\lambda_2)$:

$$[A] = K_d \left(\frac{R - R_{\min}}{R_{\max} - R} \right) \tag{3.5}$$

This approach to quantitative target assay has found many applications. As an example, it was used in the construction of double-labeled molecular biosensors based on glutamine and glucose binding proteins (Tolosa et al. 2003; Ge et al. 2004). In other research, for the design of ratiometric Cl^- sensor a molecular hybrid was synthesized that contained two covalently linked dyes (Jayaraman et al. 1999). They can be excited simultaneously but exhibit separate emission spectra. One of them is strongly quenched by Cl^- ion, while the other does not interact with Cl^- and serves as a reference for the sensor concentration. The sensor designs with the introduction of additional dyes as the references are also used in cation and pH sensing (Koronszi et al. 1998).

The intensity-responding probes are very popular in intracellular measurements of Ca^{++} ions (Minta et al. 1989). For obtaining the more accurate representation of ion concentrations, the simultaneous injection into the cell of Ca^{++}-responsive and Ca^{++}-insensitive dyes is used (Oheim et al. 1998). Of course, this is not the best solution, since the intracellular distribution of the two dyes can be different. A better possibility is to apply composite nanoparticles that incorporate two dyes, one responsive and the other insensitive to target binding. This approach has been suggested for the measurement of pH (Jiang et al. 2007), oxygen (Ge et al. 2004) and ion concentrations (Park et al. 2006) in different test media and also within the living cells.

The *separate detection of the two signals*, one from the reporter dye and the other from the reference, can be provided based not only on the difference of their fluorescence band positions, but also on the difference in anisotropy (Guo et al. 1998) or lifetime (Liebsch et al. 2001; Guo et al. 1998). The measured anisotropy or lifetime is a sum of intensity-weighted anisotropies or lifetimes of contributing species (see following Sections), so if in the presence of a reference the intensity of reporting dye changes, this change can be recorded as an anisotropy or lifetime change. This type of calibration can be used even if the reporter and the reference dyes possess strongly overlapping fluorescence spectra. The intensity calibration in the lifetime domain has an advantage in the studies in highly light scattering media.

Summarizing, we outline what is achieved and what is not achieved with the introduction of reference dye. The two dyes, responsive and non-responsive to target binding, can be excited and their fluorescence emission detected simultaneously, which compensates the instability of instrumental factors. In principle, the results should be reproducible on the instruments with a different optical arrangement, light source intensity, slit widths, etc. In addition, if the two dyes are distributed very

similarly in the illuminated volume, the two-band ratiometric signal can be calibrated in target concentration. This calibration, in some range of target concentrations, will be insensitive to the concentration of sensor (and reporter dye) molecules.

It should be remembered however that the sensor molecules can exhibit degradation, and, additionally, the dye molecules can photobleach as a function of time. These effects may provide the time-dependent and target-independent changes of the measured intensity ratios. In addition, because the reporter and reference dyes emit independently and their sensitivity to quenching (by temperature, ions, etc.) may be different, every effect of fluorescence quenching unrelated to target binding will interfere with the measured result. This can make the sensor non-reproducible in terms of obtaining precise quantitative data even in serial measurements with the same instrument. In these cases, other detection methods that will be overviewed below are preferable.

3.2.6 Intensity Change as a Choice for Fluorescence Sensing

As we observed above, in intensity sensing there are many good possibilities to choose the dye and its mechanism of response satisfying the requirements that the change of fluorescence intensity is strong, even dramatic. After choosing the proper dye and optimizing the variation of its fluorescence intensities the researcher can concentrate on other parameters that are important for operation of the sensor. There are the convenient for observation excitation and emission spectra, the high molar absorbance at the wavelength of excitation, the high quantum yield in one of the forms (bound or unbound) of the sensor and its strong change on the binding. It may be important to choose the dye with strong Stokes shift, since this will allow not only reducing the light-scattering effects but also using for detection the broad-band filters, which will increase the recorded intensity and thus the sensitivity of detection. It is also important to choose the dye with high photostability, that will not photobleach during the experiment and will provide the necessary reproducibility in serial repetitive measurements.

Concluding, we also note that the weak point of intensity sensing technique is the necessity to resolve the *problem of calibrating* the sensor element. This problem exists in all sensor applications; be it macromolecules in solutions, nanoparticles, waveguide tips or multi-sensor arrays. The light intensity depends upon the concentration of sensor molecules, excitation wavelength, optical density at this wavelength and, of course, on the emission wavelength, which still further complicates the calibration. It is difficult to obtain a linear response in fluorescence intensity operating with fiber optical waveguides. But what is really difficult or even impossible it is to calibrate or compensate the effects of light-absorption and light-scattering. This can be a serious problem, especially if the studied medium is heterogeneous, such as the colloid suspension, the solution of high-molecular-weight polymer or the suspension of living cells. If the target molecules are of large size and if they can aggregate during the measurement, this may create irresolvable problems.

When the sensor molecules are incorporated into the living cells, then an endogenous *autofluorescence* becomes also an essential problem (Billinton and Knight 2001). In addition, even if the target binding is completely reversible and both emission intensity levels without target and with the saturation by target can be easily determined, there always remains a problem of time-dependent degradation of the sensor affinity. Finally, any time-dependent processes occurring with the fluorophore, especially photobleaching, will make the sensor non-reproducible even in serial measurements with the same instrument and when all above listed conditions are kept constant or properly corrected. These difficulties justify strong efforts of the researchers to develop fluorescence dyes together with sensing and imaging methods that allow excluding or compensating these factors.

Discussing the disadvantages of sensing based on the changes of fluorescence intensity we do not have to forget its *important merits*. One such merit is the simplicity in instrumentation, in the measurement and in adjustability of this instrumentation for the use in integrated sensing devices and micro-arrays. Another merit is the highest possible absolute sensitivity, in view that in other methods based on resolution in spectra, lifetime or anisotropy there occurs the significant loss of absolute intensity. If the interfering factors such as background fluorescence and light scattering are not very important, the integral intensity over whole emission band can be collected. Thus, the sensors based on registration of ΔF changes (sometimes called *intensiometric* sensors) can be recommended for the use in qualitative or semi-quantitative detection technologies where a high sensitivity is very desirable but high precision of quantitative measurement is of secondary importance.

3.3 Anisotropy-Based Sensing and Polarization Assays

Linearly polarized light is the light that propagates with its electric field vector keeping a unique direction in space. Such light wave can excite the dyes only if they are in *definite orientation*. If these dyes are immobile on a time scale of fluorescence decay, they emit also the polarized light. However, due to rotational diffusion they may randomly change their orientation, so that being initially anisotropic, with time their orientation becomes isotropic. This leads to *depolarization* of emitted light. If the dye represents a fluorescent reporter and in the course of sensing event the size of rotating unit increases or local viscosity increases, then the rotation will slow down and we will get an increase of *fluorescence polarization* and *anisotropy*. The time window for this rotation is also important. It is given by fluorescence lifetime τ_F. When τ_F increases, our sensor will then have more time to rotate and anisotropy (or polarization) will decrease. Thus, the *rotation rate* and the *fluorescence emission rate* determine the response in anisotropy.

Recording of anisotropy requires the measurements of the *ratio of fluorescence intensities obtained at two different polarizations* of the emission light, *vertical* and *horizontal* (Guo et al. 1998; Jameson and Croney 2003). Primarily fluorescence

polarization measurements were used to study rotational mobility of labeled macromolecules, the presence of their flexible fragments, association-dissociation of protein subunits and of intermolecular interactions influencing this mobility. Later on, different *polarization assays* were developed based on the same principle: the slowing down of rotational mobility of sensor molecule on target binding, which increases the size of rotating unit. Their development led to *anisotropy-based sensor arrays*, in which small rotating sensor units are immobilized on support and target binding is detected as the decrease of its rotation rate.

3.3.1 Background of the Method

The measurement of *steady-state anisotropy*, *r*, is simple and needs two polarizers, one in excitation and the other in emission beams of the instrument (Fig. 3.6).

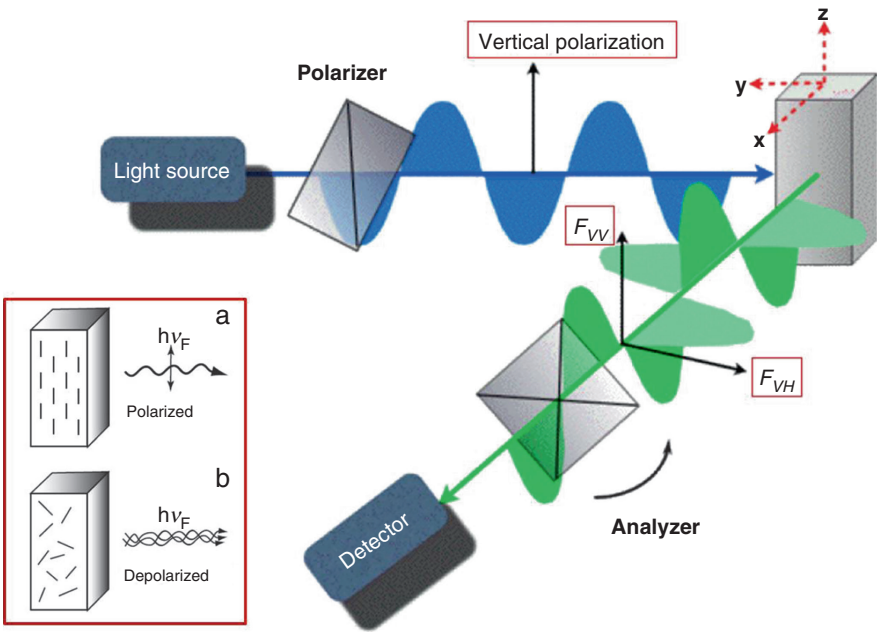

Fig. 3.6 Geometry of fluorescence anisotropy experiment and response of polarized emission to fluorophore rotation. Fluorophores in the cuvette are excited by vertically (z) polarized light causing photoselection. A polarizer in the fluorescence channel (x) can be rotated from the vertical F_{VV} to the horizontal F_{VH} position. In the insert: Connection between light depolarization and rotational mobility. Linearly polarized light is absorbed by molecules predominantly oriented a particular way, for example, parallel to the electric field vector of the incident light. If the molecules emit linearly polarized light and their orientation in during the lifetime of excited state τ_F is not changed (**a**), the total emission from volume will be polarized. If the orientation of the molecules during lifetime τ_F becomes chaotic (**b**), the total emission volume is depolarized

When the sample is excited by vertically polarized light (indexed as $_V$) and the intensity of emission is measured at vertical (F_{VV}) and horizontal (F_{VH}) polarizations, then one can obtain r from the following relation:

$$r = \frac{F_{VV} - G \times F_{VH}}{F_{VV} + G \times 2F_{VH}} = \frac{1 - G \times \left(F_{VH} / F_{VV}\right)}{1 + G \times 2\left(F_{VH} / F_{VV}\right)}, \tag{3.6}$$

where G is an instrumental factor (Jameson and Ross 2010). *Polarization P* is a similar parameter that is defined as $P = (F_{VV} - F_{VH})/(F_{VV} + F_{VH})$. Its relation to r is simple:

$$r = 2P / \left(3 - P\right) \tag{3.7}$$

It is also used for characterizing polarized emission. Though it is less convenient, it was historically the first parameter introduced, providing essentially the same information.

Equation (3.6) shows that r in fact is a *ratiometric parameter* that does not depend upon the absolute intensity of emission light because the variations of intensity influence proportionally the F_{VV} and F_{VH} values. Therefore the anisotropy, similarly to the lifetime (Sect. 3.4), is low sensitive to variation of reporter dye concentration or to its change in the course of experiment (e.g., to photobleaching). Thus, we may consider that anisotropy and polarization of emission that are derived from the intensities collected at the same wavelength at vertical (F_{VV}) and horizontal (F_{VH}) polarizations are the *intrinsic properties* of the dye molecule in particular environment.

In the simplest case when both the rotation and the fluorescence decay can be represented by single-exponential functions, the range of anisotropy variation (r) is determined by the ratio of fluorescence lifetime (τ_F) and *rotational correlation time* (τ_φ) variation. The latter describes the rotation of dye molecule or the structure to which it is rigidly attached:

$$r = \frac{r_0}{1 + \tau_F / \tau_\varphi} \tag{3.8}$$

Here r_0 is the *fundamental anisotropy*. It can be defined as the limiting anisotropy obtained in the absence of rotational motion. It is an intrinsic parameter of a fluorophore that is determined by the angle between its absorption and emission dipoles.

3.3.2 Practical Considerations

The dynamic range of anisotropy sensing is determined by the difference of this parameter observed for free sensor, which is the rapidly rotating unit and the sensor-target complex that exhibits a strongly decreased rate of rotation (Fig. 3.7).

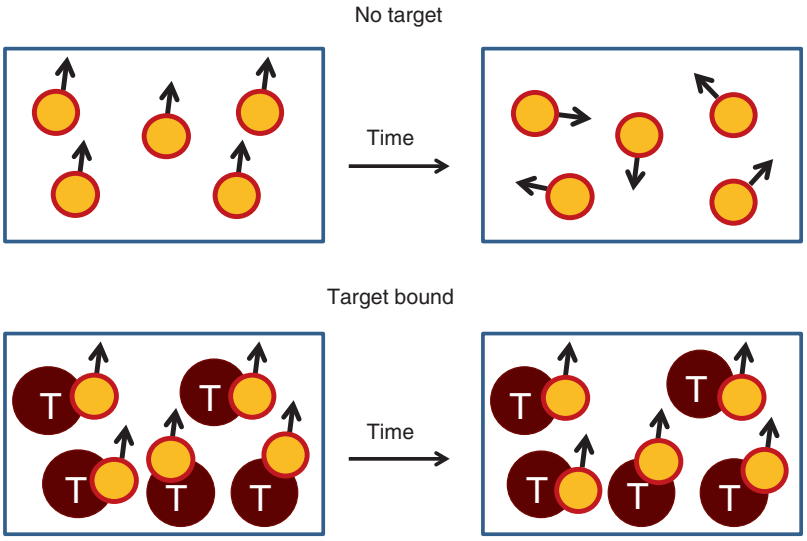

Fig. 3.7 Illustration of basic principle of fluorescence anisotropy sensing (polarization assays). Dye molecules with their absorption transition vectors (*arrows*) aligned parallel to the electric vector of linearly polarized light (along the vertical page axis) are selectively excited. Due to rapid rotational diffusion, the distribution in their orientations becomes randomized prior to emission, resulting in low fluorescence anisotropy. The binding of a large, slowly rotating target molecule or particle prevents the rotation and results in highly polarized fluorescence. The difference between the two values of anisotropy provides a direct readout of the target binding

The reporter dye should be rigidly attached to the sensor for reflecting this change of mobility.

The polarization experiment allows obtaining *two-channel information* on sensing event from a single reporter dye. The range of variation of r values in this event could extend from 0 to r_0 (which is commonly around 0.3–0.4) and it should not depend upon the instrumental factors or the dye concentration.

As follows from Eq. (3.8) and the above discussion, the variation of anisotropy can be observed in two cases, on the variation of fluorophore *rotational mobility* (the change of τ_φ) and on the variation of *emission lifetime* τ_F. At given τ_F the rate of molecular motions determines the change of r, so that in the limit of slow molecular motions ($\tau_\varphi >> \tau_F$) the r value approaches r_0, and in the limit of fast molecular motions ($\tau_\varphi << \tau_F$) r is close to 0. This determines dynamic range of the assay.

Since the change of anisotropy on target binding can be achieved by the change of two parameters, τ_φ and τ_F, it is essential that their ratio should exhibit the most significant difference between target-bound and target-free states of the sensor. This is possible, and it is highly preferable to realize the case when the change of τ_φ and τ_F occurs in opposite directions. Meanwhile it is not uncommon that the target binding resulting in increasing τ_φ due to the increase of the size of rotating unit increases also τ_F due to dye immobilization or screening from the quenching effect of water. In order to provide high sensitivity of the assay these situations need to be avoided.

Anisotropy sensing is well compatible with the methodology of *direct reagent-independent sensing* (Sect. 1.6). Attachment of the dye at the sensor-target contact areas in this case is not required, which increases the possibilities in application of this method. In competitor displacement assays (Sect. 1.3) the binding of small competitor molecule is easily detected as an increase in anisotropy. Meantime, the advantages of this method are often difficult to realize in heterogeneous assays, since for the sensor attached to the surface the rotational mobility can already be suppressed and on binding the target the anisotropy may not exhibit additional increase. Therefore, in such cases the fluorophore has to be attached to a flexible linker for maintaining its own degrees of rotational freedom relative to the sensor molecule, so that the loss of its mobility could report about the binding.

Another problem is the resolution in the response of anisotropy sensing in the case of *high molecular weight targets*. In order to achieve a good resolution in anisotropy the rotational correlation time of the labeled target should correspond to the fluorescence lifetime. Using the well-known Stokes-Einstein relation for isotropic Brownian rotational diffusion, one can estimate the rotational correlation time of solute molecule or particle (assuming its spherical shape) on the basis of molecular mass (M):

$$\varphi = \frac{\eta V}{RT} = \frac{\eta M}{RT}\left(v + h\right) \tag{3.9}$$

Here η is the viscosity of the solution, and V is the molecular volume, R is the ideal gas constant, T is the absolute temperature, v is the partial specific volume in cm^3/g, and h is the hydration (typically for proteins, 0.2 g of H_2O/g). Assuming the typical v value for a protein, temperature 20° C and the viscosity of water one can use its simplified version:

$$\tau_\varphi\left(\text{ns}\right) = 3.05 \times 10^{-4} \times M \tag{3.10}$$

It follows that for achieving the best sensing signal in assay for a protein of molecular mass 40 000 the fluorophore lifetimes should be approximately 12 ns.

From this equation, using Eq. (3.8) one can evaluate the fluorescence lifetime that will be optimal to detect the variation of anisotropy in the necessary range. The calculations based on Eq. (3.9) correlate reasonably well with experimental data. Figure 3.8 presents the graphs built on this correlation (Guo et al. 1998).

From these estimates it can be immediately seen that common organic dyes with fluorescence lifetimes of the order of 1 ns are suitable for detection in anisotropy response of only the smallest and rapidly rotating sensors (or competitors) and do not properly fit the size of even small proteins. For labeling larger molecules, such as antibodies, the luminophores with longer lifetimes are needed. They should satisfy the best sensing conditions, so that $\tau_\varphi < \tau_F$ before the binding and $\tau_\varphi > \tau_F$ after binding the target.

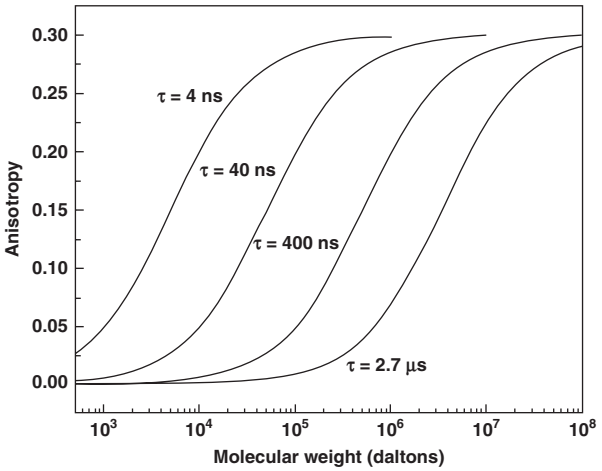

Fig. 3.8 Molecular-weight-dependent anisotropy for a protein-bound luminophore with luminescence lifetimes of 4, 40, 400, and 2700 ns. The curves are based on Eqs. 3.8 and 3.9 assuming an aqueous solution at 20 °C with a viscosity of 1 cP and $(v+h)=1.9$ (Guo et al. 1998)

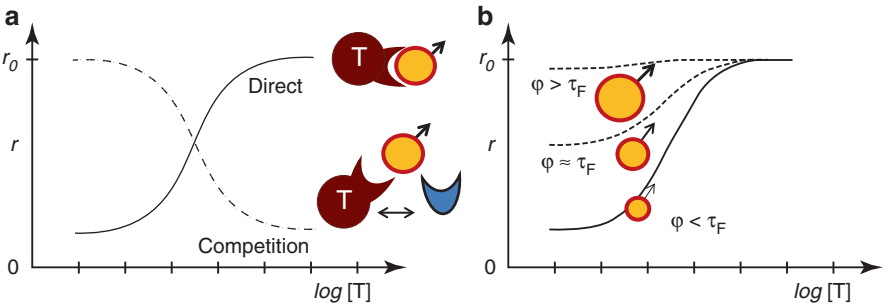

Fig. 3.9 Dependence of anisotropy sensor response on target concentration [T] in direct and competition assays (**a**) and this dependence for direct assay at different correlations between τ_φ and τ_F (**b**)

3.3.3 Applications

Like other methods of fluorescence detection, the anisotropy sensing is based on the existence of two states of the sensor, so that the switching between them depends on the concentration of bound target. In these states, the dye reporters exhibit different possibilities to emit light and to rotate. The major application of this technique in fluorescence sensing is to provide response to target binding by the change of *rotational mobility* of fluorescent reporter. If the free fluorescent sensor molecule is relatively small, it rotates rapidly and displays a low value of anisotropy. On target binding the size of this rotating unit increases producing a sharp rise in anisotropy. Due to these features, anisotropy sensing can be applied both in competitor displacement (Sect. 1.3) and direct sensing (Sect. 1.6) formats.

Figure 3.9 illustrates the change of recorded anisotropy r between 0 and r_0 values as a function of target concentration in direct assay (the target binding increases

anisotropy) and competition assay (the release of bound competitor decreases the anisotropy). This figure also shows that the target binding provides its concentration effect on correlation between τ_φ and τ_F. With the increase of size of the sensor rotating unit, increasing τ_φ, or with the increase of τ_F the response to target binding decreases and may vanish.

Variation of sensor-target concentration ratio allows determining the dissociation constants K_d, which are important for the analysis of protein-ligand interactions (Wang et al. 2013).

This method has found its most extended application in sensing techniques based on antigen-antibody recognition. The so-called "*polarization immunoassays*" are based on the measurements of steady-state anisotropy in both heterogeneous and homogeneous assay formats. In a *homogeneous* fluorescence polarization immunoassay for antigens or antibodies detection (Nielsen et al. 2000) either the antigen or the antibody can be determined in solution with the labeled fluorescent partner. On the formation of their complex the steady-state anisotropy increases due to an increase of the rotating unit size. The fluorescence polarization assay can be also used for determining the antigen-antibody affinity (Smallshaw et al. 1998).

Anisotropy measurements are also used in *competitive immunoassays* that have become common not only in research but also in routine clinical analysis. Primarily the complex of the sensor antibody with the target analog labeled with fluorescent dye is formed. Consequently, the target present in tested medium produces the change of fluorescence anisotropy by displacing the competitor from the binding site. Since the free competitor is a smaller rotating unit than its complex with the sensor, a decrease of anisotropy is detected. This procedure can be performed in solution as a *homogeneous immunoassay* as it does not require any separation steps. Similarly to other competitive assays in solutions, it cannot be extended for measuring several targets simultaneously.

An example of successful application of anisotropy detection technique in ion sensing can be the detection of Zn^{2+} picomolar to nanomolar concentrations by application of aminobenzoxadiazole dye covalently attached to genetically modified metalloprotein carbonic anhydrase (Thompson et al. 1998). The results demonstrate that using inexpensive instruments the free transition metal ions can be determined at trace levels in aqueous solution.

In *drug discovery*, the fluorescence polarization (anisotropy) technology became a routine technique because of its convenience and low price (Owicki 2000). Originally, the polarization assays were developed for the single-sample analytical measurements, but the technology was rapidly converted to high-throughput screening assays when commercial plate readers with sufficiently high sensitivity became available (Burke et al. 2003). These assays include different targets, such as kinases, phosphatases, proteases, G-protein coupled receptors, and nuclear receptors (Sportsman et al. 2003; Burke et al. 2003).

There is no limit for generalization of anisotropy sensing technique to the large-format proteomics arrays using probably the most advanced capture molecules, the nucleic acid *aptamers* (see Sect. 7.6). Aptamers can be immobilized on solid support at one point by a chain terminal and can rotate around this point of attachment with the observed decrease of anisotropy (McCauley et al. 2003). The target binding decreases the rate of their rotation.

Based on this principle a biosensor in a chip configuration that is capable of quantifying several proteins with relevance to cancer was demonstrated (McCauley et al. 2003). A rapid, homogeneous aptamer-based bioanalysis was recently reported for the sensitive detection of immunoglobulin E (IgE) in the low-nanomolar range with high specificity (Gokulrangan et al. 2005).

Summarizing, we outline three possibilities for using in sensing the fluorescence response in anisotropy (polarization):

(a) when anisotropy increases with the increase of molecular mass of rotating unit;
(b) when anisotropy increases due to increase of local viscosity producing higher friction on rotating unit;
(c) when anisotropy increases due to fluorescence lifetime decrease being coupled to any effect of dynamic quenching.

All these effects are interrelated and observed within a rather narrow range of related parameters. Nevertheless, the possibilities of this technique application are very broad.

There exist, however, the problems in application of *nanosensors*. They are twofold. First, many nanoscale emitters (e.g., quantum dots) do not exhibit detectable fundamental anisotropy. Second, the nanosecond lifetimes of fluorophores are too short to fit the microsecond rotational dynamics of nanoparticles. Therefore, the acceptable solution with anisotropy sensing is its use in competitor assays as it is shown in Fig. 3.9. For obtaining the sensing signal in anisotropy either the dye should be small enough to provide the fast rotation rate or the lifetime long enough to fit this rate scale

3.3.4 Comparisons with Other Methods of Fluorescence Detection

Anisotropy sensing allows direct response that is independent of sensor concentration and allows both direct and competitor substitution sensing. In the background of this independence is the independence of measured anisotropy (polarization) on absolute fluorescence intensity. In this respect, we have to stress the following.

(a) Two information channels in this case are derived from a single dye molecule exhibiting a single electronic transition. Thus, the two parameters, (F_{VV} and F_{VH}) are strongly coupled and proportional to the absolute intensity value.
(b) If there appear additional perturbations, such as the variations of lifetime or the appearance of additional degrees of rotational freedom, the F_{VV} and F_{VH} values change in a different manner producing a change of anisotropy that overlaps on the response obtained on target binding. In particular, any factor that causes the decrease of fluorescence lifetime (produces quenching) increases the anisotropy.

Dynamic range of the fluorescence response is determined by the "window" in anisotropy values between the readings obtained with the free sensor and the sensor with bound target (Jameson and Croney 2003); the possibility to increase this range is offered by long-lifetime luminophors (see Sect. 4.4). The scaling of *bound target concentration* is performed between these two limiting (low and high) values, and

the position of the whole scale depends on fluorescence lifetime τ_F. In the case of fluorescence quenchers presence, the whole scale will be shifted producing a systematic error. Due to this fact, the self-calibration that can be achieved in anisotropy sensing may not always be sufficient.

It should be emphasized that the weak point of this detection technique is its great *sensitivity to light-scattering effects*, especially to those that may result in non-specific aggregation of the sample during the sensing procedure. This occurs because the scattered light is always 100 % polarized, and its contribution cannot be removed in the steady-state measurements if there is a strong spectral overlap between scattered and fluorescent light. For avoiding the light-scattering artifacts, the dyes with a large Stokes shifts should be used preferably. This allows increasing the gap between excitation (and also light-scattering) and emission wavelengths.

3.4 Lifetime-Based Fluorescence Response

Fluorescence is the process that develops in time after initial electronic excitation. Its intensity decays as a function of time in subnanosecond-nanosecond time range. It is hard to imagine such short periods of time; they are outside of our everyday experience. Nevertheless, the life of molecules in these time periods is very busy. Molecules move, rotate, collide, participate in different reactions. Fluorescence emission helps us to reveal mechanisms of all these events. Duration of fluorescence emission also depends on them. If we want to make a sensor, our target should also participate in these processes.

3.4.1 Physical Background

Usually molecules emit light independently, so the decay function of their fluorescence emission is essentially concentration-independent. It is an intrinsic property of the fluorophore, of its interactions, dynamics and participation in reactions. Because the fluorescence decay is a random event, the emissions of individual quanta follow Poisson statistics. Therefore, in an ideal case of structurally identical and independent fluorescence emitters, the fluorescence decay is a *single exponential function* of time *t*:

$$F(t) = F_0 \exp(-t / \tau_F) \tag{3.11}$$

Here F_0 is the initial intensity, at time $t = 0$. The time constant τ_F is called the *excited-state* (*fluorescence*) *lifetime*, it is the reverse function of the *fluorescence decay rate*, k_F. In many real cases, the decay is not exponential, but it is often possible to characterize it by averaged lifetime, $<\tau_F>$. The necessary condition in lifetime sensing is the possibility of detecting the strong difference of $<\tau_F>$ between the target-bound and target-free forms of the sensor.

Lifetime sensing is based on two different principles:

(a) *Modulation of lifetime by dynamic quencher*. Molecular oxygen is a strong quencher of long-lifetime emission, operating by diffusional mechanism. The decrease of τ_F occurs gradually with oxygen concentration. This change obeys the Stern-Volmer relationship (Eq. 3.3), which allows determining the concentration of free oxygen. High mobility combined with potent quenching are the unique features of oxygen molecules.

(b) Shifting of the sensor to a different *discrete form with different lifetime*. The presence of distinct difference in lifetime between two forms of the sensor, free (A) and bound (B) is necessary for lifetime sensing application of this type. Belonging to the same dye, these two forms can be excited at the same wavelength. When excited, they emit light independently and therefore the observed nonexponential decay can be decomposed into two different individual decays with lifetime τ_F^A and τ_F^B:

$$F(t) = \alpha_A \exp\left(-t / \tau_F^A\right) + \alpha_B \exp\left(-t / \tau_F^B\right) \tag{3.12}$$

Important, the two forms of the sensor (target-free and target-bound) can be excited at the same wavelength and their contributions can be obtained from deconvolution of two-component decays (Lakowicz 2006).

These two principles explored in lifetime sensing are depicted in Fig. 3.10. In the first case the decay does not change its initially monoexponential character but the

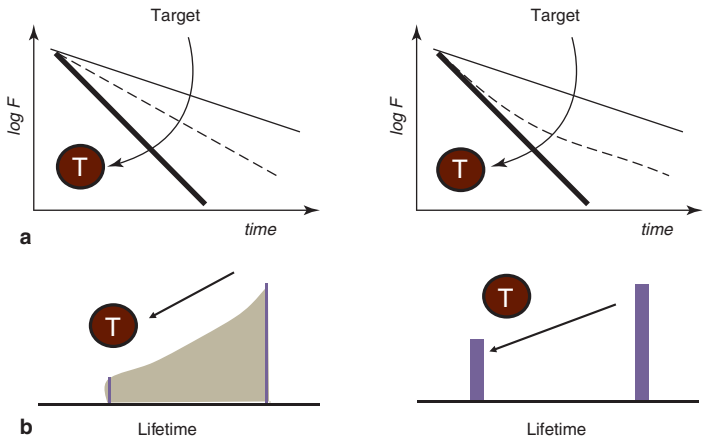

Fig. 3.10 Typical effect of target binding influence on fluorescence decay kinetics and derived lifetimes. Long fluorescence decay (large τ_F) changes to short decay (smaller τ_F) on target binding. (**a**) The fluorescence decays in logarithmic coordinates. Thin solid lines are the decays without the target, thick solid lines – with the saturation by target, the dashed line – on interaction with the target resulting in the change of lifetime between these values. (**b**) The lifetime values. In the case when the target (T) is the dynamic quencher (left) the decay becomes shorter gradually as a function of its concentration. In the case when the target binding changes the lifetime leading to its another constant value the decay is non-exponential but can be resolved into two exponential components. The relative magnitude of these components changes as the function of target concentration

gradual decrease in τ_F can be observed. This happens in dynamic quenching, so that τ_F can be plotted as a function of quencher concentration. These cases are rare and generally are not interesting, since it is hard to couple dynamic quenching with molecular recognition. The transition between two sensor forms with different lifetimes on target binding is more typical. Particularly, this can be realized detecting the lifetimes of FRET donors (see Sect. 3.6).

In relation to molecular sensing, the interest to lifetime detection techniques is due to the fact that fluorescence decay is an intrinsic characteristic of fluorophore and of its environment and *does not depend upon fluorophore concentration*. Moreover, the results are insensitive to optical parameters of the instrument, so that the attenuation of the signal in the optical path does not distort it. The light scattering produces also much lesser problems, since the scattered light decays on a very fast time scale and does not interfere with fluorescence decay observed at longer times. Most often the decays do not depend on emission wavelength (with the exception of excited-state reactions occurring on the time scale of decay), which allows to collect them from the whole spectra and achieve relatively high sensitivity.

3.4.2 Technique

Fluorescence decay functions can be obtained with the aid of special instrumentation (Berezin and Achilefu 2010). It allows recording the decay directly using the single photon counting, stroboscopic techniques or observing the demodulation and phase shift of harmonically modulated excitation light. These methods are well described in the literature (Lakowicz 2006; Valeur and Berberan-Santos 2012; Collier and McShane 2013).

In brief, in the *phase-modulation* technique the excitation light is modulated with high frequency (~100–200 MHz), and the detector records the shift in phase of modulated signal (the phase angle) and the decrease in its modulation depth in fluorescence compared to that in excitation light. The slower is fluorescence decay (the longer lifetime), the larger phase shift and the smaller modulation. In time-correlated *single-photon counting* the excitation occurs by a light source producing short pulses, and single quanta are randomly selected from every pulse to form the experimental emission decay function. The emission decay function can be also derived by mathematical transformation of the primary data obtained by phase-modulation. Thus, the methods are equivalent though their technical realization is different.

Lifetime measurements require a more complicated and expensive technique than that required for steady-state measurements, so the prospects for this method depend upon the development of simple and cheap ways for its realization. The most expensive part of this instrumentation is the light source, and the application of cheap pulsed semiconductor lasers can make this method very attractive. Until recently, these lasers were available only in the “red” spectral

region, where a very limited range of dyes was available in sensor applications. With the introduction of inexpensive blue-emitting diode lasers we expect a new increase of interest to lifetime sensing. The other extension of this methodology is the development of assays that involve the long-lifetime luminescence of rare earth ions or explore the reactions with their participation (Maliwal et al. 2001; Grichine et al. 2014).

3.4.3 Time-Resolved Anisotropy

The time-resolved detection can be combined with the measurements of anisotropy to give the *time-resolved anisotropy* $r(t)$, see Fig. 3.4. Technically this can be achieved by incorporating the polarizer and analyzer into the time-resolved fluorimeter. The time resolution allows eliminating all the light-scattering effects, to which the steady-state anisotropy is sensitive. If the two forms of a sensor, A and B, differ by anisotropy decay, then the observed decay will be composed by contributions provided by these individual forms:

$$r(t) = r_0 \left[F_A \exp\left(-t / \varphi_A\right) + F_B \exp\left(-t / \varphi_B\right) \right]. \tag{3.13}$$

Similarly to the steady-state anisotropy, $r(t)$ is an 'intensity-weighted' parameter in sensing (see Sect. 2.5). Using this method, one can sometimes yield unusual anisotropy decays that show decline to a minimum at short times and increase at long times (Lakowicz 2006).

3.4.4 Applications

Examples of application of lifetime sensing were presented for popular fluorescence probes, used for measuring cation concentration (such as Calcium Green) and pH (such as SNAFL-2 (Szmacinski and Lakowicz 1994). Remarkably, one of pH-sensitive dyes was incorporated into polymeric hydrogel, and it was shown that lifetime sensing provides reliable results in light-scattering media (Kuwana and Sevick-Muraca 2002).

The other important application is the sensing of compounds that produce decrease of τ_F in molecular collisions. An example is the chloride sensing in living cells. The mechanism of response of many cellular chloride sensors is based on collisional fluorescence quenching by Cl^- ion that decreases both the intensity and the lifetime. Using SPQ (6-methoxy-N-[3-sulfopropyl]quinolinium) chloride-sensitive probe, a comparative study of intensity-sensing and lifetime-sensing was performed and the strong advantages of lifetime sensing were demonstrated (Szmacinski and Lakowicz 1994).

In general, it is not the instrumentation that limits the lifetime-based sensing and imaging. The dyes that exist in two switchable emissive forms with different lifetimes are rare, and new efforts are needed for their synthesis and implementation. Recently reported squaraine dyes show promise for different applications including immunoassays with near-IR lifetime detection (Povrozin et al. 2009). The range of collisional quenchers as potential targets is also very limited. The dyes that gradually change their lifetimes may be of use as oxygen and viscosity sensors based on quenching effects. Variation of lifetimes of FRET donors is another possibility for implementation in sensing.

3.4.5 Phosphorescence and Long-Lasting Luminescence

Phosphorescence exhibits much longer emission lifetimes than that of fluorescence. Due to high probability for its quenching in thermal diffusion, it is commonly observed only at cryogenic temperatures. But in special conditions (incorporation of dye into a rigid matrix and removal of mobile oxygen) it can be observed also at room temperatures with lifetimes covering a very broad range 10^{-6}–10^{2} s. Rigidity of dye environment can be provided by the sol–gel or polymeric materials. The long duration of phosphorescence emission is because it involves a spin-forbidden transition from the triplet excited state to the ground state. Due to this fact, the quantum yield of phosphorescence is usually very low. Meantime there are the dyes that incorporate heavy atoms (e.g., eosin, erythrosine), so their bright phosphorescence can be observed at room temperatures. Such enhancement of phosphorescence (the Kasha heavy atom effect) was known for many years. Optical sensors with phosphorescence response are expected to feature rapid advancement with the development of new dyes of pure organic origin (Koch et al. 2014; Xu et al. 2013), incorporating heavy and transition metal atoms (Sect. 4.2) and of nano-composites hosting them.

Phosphorescence spectra are usually insensitive to environment perturbations, whereas the lifetimes may change by orders of magnitude. This makes phosphorescence very attractive for the development of sensor techniques based on decay-time measurements (Sanchez-Barragan et al. 2006). Present applications of phosphorescence lifetime sensors are addressing mostly the sensing of oxygen. Oxygen is a potent collisional quencher of phosphorescence and this effect is very strong due to long duration of this emission in comparison to oxygen diffusion rate. However, the current applications include sensing pesticides, antibiotics and CO_2 (Sanchez-Barragan et al. 2006).

Long lifetimes in the millisecond time range are characteristic also of luminescent *lanthanide* chelating complexes and phosphorescent *metal-ligand complexes* of ruthenium, rhenium and osmium ions. Long-lifetime emission was also found in porphyrins incorporating platinum or palladium atoms. The properties of these luminophores will be discussed in Sect. 4.5. Being different in the mechanisms of their emission, they share common features regarding the benefits of emission decay detection on an extended time scale. Attractive is the simplicity of time-resolved

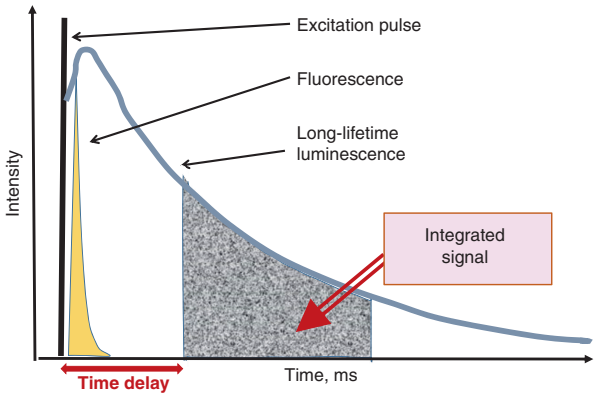

Fig. 3.11 The time-resolved measurements in the case of long-lifetime emitters. The contribution of light scattering that appears with short excitation pulse and of short-lifetime background fluorescence can be removed by collecting luminescence quanta with a time delay. In order to increase the intensity the integrated signal can be collected

detection technique compared to fluorescence. It becomes easy to discriminate the light-scattering background and contaminating fluorescence just by setting the time delay removing the 'early' channels in acquiring the data. Moreover, an integrated signal can be collected from light quanta emitted with specified time delay (Fig. 3.11).

The latter advantage makes phosphorescence and long-living luminescence sensors attractive for intracellular studies and for sensing in different heterogeneous systems, in which the background emission creates the problems. In view that all listed above types of long lifetime emission demonstrate also the strong Stokes shifts, high spectral resolution together with high temporal resolution, they feature very good prospects in sensing and imaging fields.

3.4.6 Comparison with Other Fluorescence Detection Methods

Before starting the attempts to apply lifetime sensing for detecting particular target one has to understand clearly that the cases when one of the forms of reporter fluorophore (with bound or unbound target) is quenched statically (becoming non-fluorescent) being very good for intensity measurement, cannot be analyzed with time-resolved technique. This is due to the fact that the static quenching changes the number but not the lifetimes of emitting species, so that the target binding will remain unnoticed. In contrast to static quenching, collisional quenchers produce dramatic change in lifetime. These features explain why the best results in application of lifetime sensing were obtained for determining the targets that are strong collisional quenchers of fluorescence (oxygen, chloride, sulfur dioxide, NO). Meantime, the effects of dynamic molecular collisions with the target are different from that of target binding: in these cases one can observe a gradual change of lifetime as a function of concentration of the quencher instead of intensity redistribution between two lifetimes belonging to forms with bound and unbound target.

These facts indicate the necessity of synthesizing the "lifetime-sensing" dyes, for which the response in $<\tau_F>$ to environment changes could be significant. Very beneficial for lifetime sensing must be the cases when the sensor in the unbound

form emits light with a short but well-resolved $<\tau_F>$, and on the target binding the lifetime increases substantially. This condition can be realized with careful selection of the dye and the site of its binding (Guo et al. 1998; Kuwana and Sevick-Muraca 2002). Thus, the lifetime sensing can be recommended as a more advanced substitute of intensity sensing in the cases when the local sensor concentration varies and is unable to be measured or controlled, e.g., in microscopy. It has also the advantages over intensity and anisotropy measurements in all cases where the stray and scattered light is an important problem (Guo et al. 1998; Kuwana and Sevick-Muraca 2002). It is reasonable to use this method in the cases when there are no substantial spectral changes on target binding and the wavelength-ratiometric methods cannot be applied.

3.5 Excimer and Exciplex Formation

When molecule absorbs light, its electronic properties change dramatically. It may participate in reactions that are not observable in the ground state. Particularly it can make a complex with the ground-state molecule like itself. These excited dimeric complexes are called the *excimers*. Excimer emission spectrum is very different from that of monomer; it is usually broad, shifted to longer wavelengths and it does not contain vibrational structure. Particularly this is the case of excimers of *pyrene*.

The excited-state molecule can also make complexes with molecules different in structure. Usually these unexcited partners are electron-donor molecules like amines. These complexes are called *exciplexes* (the term *exci*mer comes from excited dimer and the *exci*plex from excited complex). The formation of excimers and exciplexes is reversible: after emission they break apart into initial ground-state species and they may be formed again on excitation. There are many possibilities to use these complex formations in fluorescence sensing. Just we need to make a sensor, in which the free and target-bound forms of the sensor differ in the ability of reporter dye to form excimers and exciplexes. Then the fluorescence spectra will report on the sensing event.

3.5.1 The Dyes Forming Excimers and Exciplexes

The choice of dyes forming excimers with attractive spectroscopic properties is not large. Pyrene derivatives are chosen by many researchers due to very distinct spectra of the monomers and excimers. The structured band of monomer is observed at about 400 nm, whereas that of excimer is broad, structureless and long-wavelength shifted; it is located at 485 nm. Both forms possess the same excitation spectrum in the near-UV, which is not convenient for cellular studies due to high autofluorescence in this range. But long lifetimes (~300 ns for monomer and ~40 ns for excimer) allows easy discriminating in time-resolved experiment the background fluorescence emission (the latter usually does not extend longer than 3–5 ns).

The formation of excimers and exciplexes requires close location and proper orientation between the partners (for excimer the formation of cofacial sandwich between two heterocycles rich in π-electrons is usually needed). Since these interactions appear in the excited state and do not exist in the ground state, the complexes cannot be distinguished in excitation spectra, and both forms can be excited at the same wavelengths. If the excimer is not formed, in fluorescence spectra we observe emission of the monomer, and upon its formation there appears characteristic emission of the excimer.

3.5.2 Application in Sensing Technologies

In chemical sensing a number of molecular constructs have been suggested that employ excimer formation. The idea was to change on the target binding the *ground-state configuration* of sensor molecules in such a way that on excitation they can form excimers but only in the presence of target. Thus, for obtaining the sensor for the sodium ions a pair of dioxyanthracene molecules was included into a polyether ring. On their binding the configuration of molecule changes and the excimer emission starts to be observed (Collado et al. 2002). Similar ideas were realized in construction of sensors for other cations.

An efficient ratiometric fluorescent sensor for silver ions was suggested based on a pyrene-functionalized heterocyclic receptor. It forms an intramolecular sandwich complex via self-assembly induced by silver ion. This results in a dramatic increase in fluorescence intensity of the excimer and a dramatic decrease of monomer fluorescence (Fig. 3.12). The intensity ratio of excimer and monomer emissions

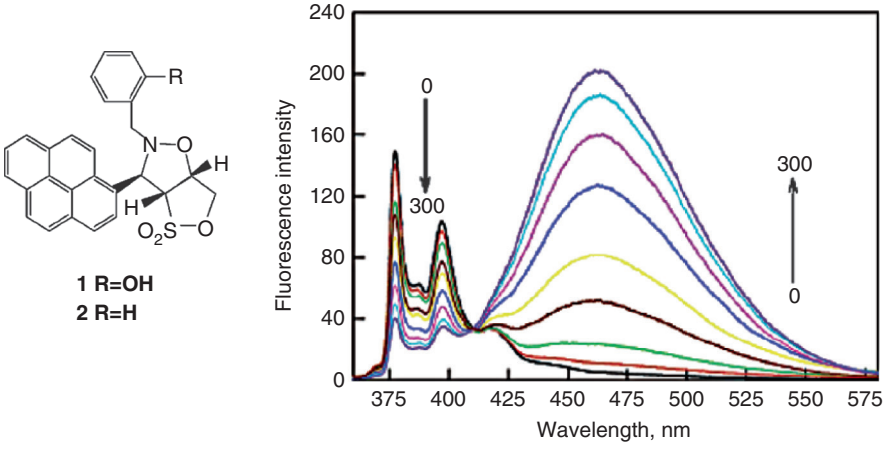

Fig. 3.12 The structure and fluorescence emission spectra of pyrene derivative (1) forming excimers in the presence of silver ions. Addition of these ions in concentrations 0, 4.0, 10, 15, 20, 40, 75, 150, 300 μM results in decrease of intensity of the normal emission with typical bands at 378 and 397 nm (excitation 344 nm) and the appearance of a red-shifted structureless maximum centered around 462 nm, typical of pyrene excimer (Yang et al. 2003)

(at 462 and 378 nm) is an ideal measure of Ag^+ ion concentrations (Yang et al. 2003). Application of molecular recognition constructs based on excimers is also popular in the sensing of neutral molecules, such as glucose (Yu and Yam 2009).

Commonly, two pyrenyl groups are attached to macromolecular sensor or they label two molecules assembled on a sensor unit, but multiple binding can be also realized (Duhamel 2012). Performance of excimer sensors has been improved on incorporation of excimer-forming reporter dyes into cyclodextrin cavity (Yamauchi et al. 1999). Excimer-forming pyrene-conjugated oligonucleotides can be used for the detection of DNA and RNA sequences (Mahara et al. 2002). Pyrene excimer probes can be applied for determination of nucleic acids in complex biological fluids (Huang et al. 2011).

Such ability to form excimers coupled with the conformational change in pyrene double-labeled flexible oligo- or polynucleotides is actively explored in DNA hybridization techniques and recognition of specific mRNA sequences (Yamana et al. 2008; Fujimoto et al. 2004). This allows quantification of these molecules in solution (Kostenko et al. 2001). Oligonucleotide conjugates bearing two pyrene residues at their 5′-phosphate terminals exhibit excimer fluorescence intensity that is highly sensitive to duplex formation: the binding to their DNA and RNA targets leads to 10-fold increase of fluorescence. It depends linearly on the concentration of target DNA and permits quantification of DNA in solution. Pyrene dimers with flexible linkers were also suggested for double-stranded DNA detection (Yang et al. 2009). A photostable pyrene derivative 1-phenylethynylpyrene that exhibits red-shifted fluorescence with excimer emission at 500–510 nm was suggested for nucleic acid labeling (Prokhorenko et al. 2009).

A prototype of double-labeled protein sensor for lipids was described (Sahoo et al. 2000). The lipid-induced helical rearrangement of apolipophorin III was sensed by the attachment of pyrene groups to two engineered Cys residues resulting in the observation of strong excimer fluorescence. The excimer band disappears upon lipid binding. This result demonstrates good prospects for the design of protein sensors with monomer-excimer λ-ratiometric response.

Aptamers (see Sect. 7.6) that use two pyrene substituents can be efficiently applied for detecting specific proteins in complex biological fluids.

Being incorporated into thermosensitive polymer, the exciplex forming pyrene groups can serve as molecular thermometers (Chandrasekharan and Kelly 2001).

3.5.3 Comparison with Other Fluorescence Reporter Techniques

Special requirements exist for the application of excimer and exciplex sensing techniques. First, the double labeling is commonly needed (with the exception if the target itself can form exciplex with the dye incorporated into sensor). Second, researcher is limited in selection of reporter dyes. Usually pyrene derivatives are used as excimer formers because of unique property of this fluorophore to form

stable excimers with fluorescence spectra and lifetimes that are very different from that of monomers. Other dyes are commonly not useful or less convenient for this application. And finally, a conformational change or self-assembly is needed in sensor molecule to couple or to remove apart the dye monomers on target binding groups (Yang et al. 2003),

If these requirements are properly addressed, the user can benefit from advantages of this technique. With the observations at two emission wavelengths one can achieve the two-channel sensor operation (λ-*ratiometry*) that will be independent of sensor concentration and allow self-calibration of fluorescence response. The recorded signal will be insensitive to instrumental factors and to the sensor (and reporter) concentration. Meantime, we have to keep in mind that the monomer and excimer (or exciplex) are independent emitters and that any non-specific influence of quenchers may be different for two forms.

3.6 Förster Resonance Energy Transfer (FRET)

Two or more dye molecules with similar excited-state energies can exchange their energies due to dipole-dipole resonance interaction between them. One molecule, serving as the *donor* of excited-state energy, can absorb and transfer it to the other molecule, the *acceptor*. The latter can be excited by this transferred energy and emit light (Clegg 1996; Selvin 2000). When there exists such communication between excited and unexcited molecules, we observe that on excitation of the donor its emission is quenched and, instead, emission of the acceptor is increased. When this coupling is absent, the emission of the donor is observed only. This approach is frequently used in sensing. Meantime, its realization usually needs labeling with two dyes serving as donor and acceptor. Only in rare lucky cases, intrinsic fluorescent group of sensor or target molecules can be used as one of the partners in FRET sensing.

The acronym FRET is frequently presented as 'Fluorescence Resonance Energy Transfer'. This is not correct since this general mechanism of energy transfer in the excited state does not necessarily involve fluorescence. It can be observed regardless of the mechanism of excitation and emission, it can be also realized as phosphorescence, bioluminescence or chemiluminescence. Therefore, according to recommendations approved by IUPAC (Braslavsky 2007) and in recognition of the first theoretical description of this mechanism by Theodor Förster, we will use the term '*Förster Resonance Energy Transfer*'.

3.6.1 Physical Background of the Method

The FRET effect depends strongly upon the *distance between donor and acceptor*. If the distance is short and one of the partners (donor) is excited, it can transfer the energy of electronic excitation to the other partner (acceptor), whereby

resulting by the latter to emit fluorescence. FRET has to be distinguished from the effect of re-absorption of the light quanta emitted by one dye by the other dye molecule: re-absorption depends on geometry of the system but FRET does not. Even at a relatively long distance (nanometers), the dyes may interact through space by dipole-dipole resonance interactions, and the resonance provided by this dipole coupling allows the energy to migrate from donor to acceptor without emission.

FRET can take place if the emission spectrum of the donor overlaps with the absorption spectrum of the acceptor (Fig. 3.13) and they are located at separation distances within ~1–10 nm from each other. It can be recognized by decrease of intensity of the

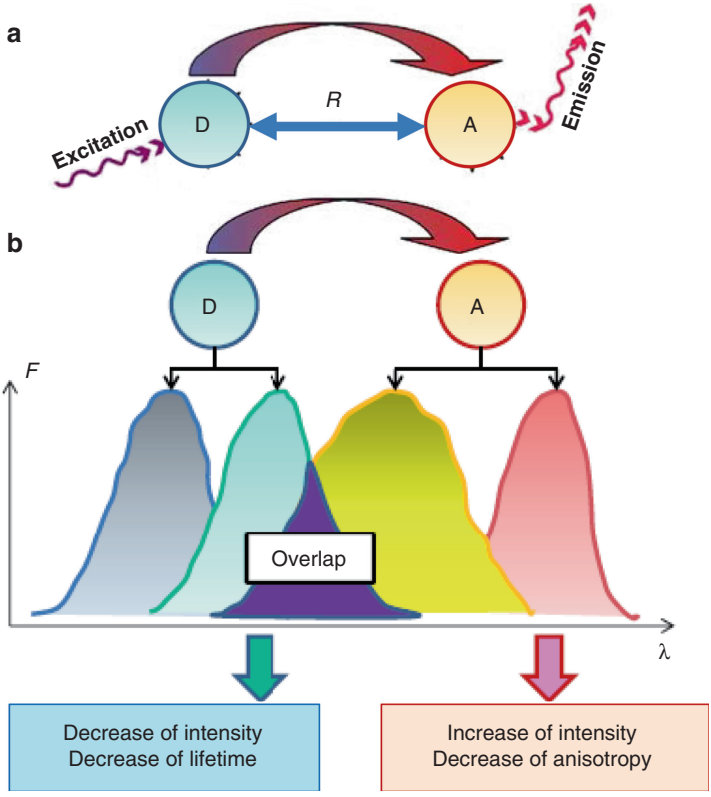

Fig. 3.13 Major factors that determine the efficiency of Förster resonance energy transfer (FRET). (**a**) The donor-acceptor distance. At their close location, the excitation of the donor results in emission of the acceptor, and if the distance is large, the donor itself will emit. This produces distance-dependent switching between two emission bands. (**b**) Absorption and fluorescence emission spectra of two FRET partners. The light-absorbing and emitting at shorter wavelengths fluorophore (donor, D) can transfer its excitation energy to another fluorophore (acceptor, A) absorbing and emitting at longer wavelengths. For efficient transfer the absorption spectrum of the acceptor should overlap the emission spectrum of the donor (*shaded area*). FRET changes the parameters of fluorescence emission

donor emission band and the correspondent increase of the acceptor emission, if the latter is not quenched. Other fluorescence parameters may change on the transfer.

The *efficiency of energy transfer E* can be defined as the number of quanta transferred from the donor to the acceptor divided by all the quanta absorbed by the donor. According to this definition, $E = 1 - F_{DA}/F_D$, where F_{DA} and F_D are the donor intensities in the presence and absence of the acceptor. Both have to be normalized to the same donor concentration. If the time-resolved measurements are used, then the knowledge of donor concentration is not required, and $E = 1 - <\tau_{DA}>/<\tau_D>$, where $<\tau_{DA}>$ and $<\tau_D>$ are the average lifetimes in the presence and absence of the acceptor (Wu and Brand 1994).

The energy transfer efficiency exhibits a very steep dependence on the distance separating two fluorophores, *R*:

$$E = R_0^{\,6} / \left(R_0^{\,6} + R^6 \right) \tag{3.14}$$

Equation (3.14) determines this steep distance function for observed intensity ratios of donor and acceptor emissions. Here R_0 is the parameter that corresponds to a distance with 50 % transfer efficiency (*the Förster radius*), expressed in Ångstroms. It is characteristic for a given donor-acceptor pair in a particular medium. It depends strongly on the quantum yield of the donor in the absence of acceptor Φ^D and on the overlap of fluorescence spectrum of the donor with absorption spectrum of the acceptor (see Fig. 3.13) expressed as normalized spectral overlap integral *J*:

$$R_0^{\,6} = 9.78 \cdot 10^3 \left(\kappa^2 n^{-4} \Phi^D J \right) \tag{3.15}$$

Here *n* is the refractive index of the medium between donor and acceptor. The spectral overlap integral *J* is a function of the fluorescence intensity of the donor, F_D, and molar absorbance of the acceptor, ε_A, as a function of wavelength, normalized against the total donor emission:

$$J = \int F_D(\lambda) \varepsilon_A(\lambda) \lambda^4 \mathrm{d}\lambda \Big/ \int F_D(\lambda) \mathrm{d}\lambda \tag{3.16}$$

In Eq. (3.16) the integration should be made over the whole spectrum. κ^2 is the orientation factor that depends on relative orientation of donor and acceptor dipoles; it can assume the values from 0 to 4. The lowest value will be if they are oriented perpendicular and the maximum value corresponds to parallel and aligned dipoles. For random orientations of donor and acceptor, $\kappa^2 = 2/3$ if they move rapidly on fluorescence time scale and $\kappa^2 = 0.475$ if they are rigidly fixed. Thus, the transfer efficiency depends on relative orientation of donor and acceptor dyes. If lifetime is long and rotations of segments containing reporter dyes are fast, then the approximation $\kappa^2 = 2/3$ is justified.

In the case of rigidly fixed donor and acceptor, the situation is less definite, and the estimation of donor-acceptor distances may lead to great errors. In designing the FRET-based sensors there are the cases when even at short distances FRET does not

occur. Such a case was described on interaction of conjugated polymer (donor) with the double-helical DNA containing dye ethidium bromide as an acceptor. Rigid structure of this complex and orthogonal orientation of transition dipole moments prevented detection of DNA hybridization by FRET (Xu et al. 2005b). Nevertheless, in practical sense, variations of both the distance and orientation may substantially increase the dynamic range of fluorescence response.

3.6.2 Homo-FRET and Hetero-FRET

In different molecular systems the same dye molecules may appear at close distances and if for them the Stokes shift is small, the same molecules may serve both as donors and acceptors and they can exchange the energies according to FRET mechanism. This case is called '*homo-FRET*'. It can be detected in rigid and highly viscous environments by the loss of fluorescence anisotropy, since orientations of donor and acceptor dipoles are generally different. High anisotropy can be retained only on excitation at the red edge of absorption band, where the homo-FRET is suppressed (the so-called *Red-Edge effect* (Demchenko 2002)). If the donor and acceptor dyes are different (the case of '*hetero-FRET*'), then the energy is transferred from the dyes with short-wavelength absorption and emission to the dyes, absorption and emission of which occurs at longer wavelengths (Demchenko 2013). This allows observing a decrease or even disappearance of fluorescence band of the donor together with an appearance and increase of the band of acceptor, generating strong λ-ratiometric signal.

The overlap integral J is the parameter that often determines the choice of donor and acceptor for particular needs. *Homo-FRET* is typical for the dyes in concentrated solutions. If it is wanted, we have to select the Stokes shift minimal (the high value of J) and if not wanted – maximal. In sensor technologies, if we need to avoid homo-FRET, we have to keep the sensor molecules spatially separated. Proper manipulation with this phenomenon may allow achieving amplification effect by combining with hetero-FRET (when donor and acceptor are different dyes), see Sect. 6.2.

The *hetero-FRET* effect is the most frequently used, and a number of donor-acceptor pairs are selected for that from organic dyes (see Sect. 4.2). By proper choice of such pairs, one can optimize the excitation and emission wavelengths and also the distance dependence of the effect. Fig. 3.14 illustrates how the dynamic range of FRET effect variation depends on donor-acceptor distance for different R_0 values. One can observe that these distances are comparable with the dimensions of many biological macromolecules and of their complexes (Clegg 1996; Selvin 2000).

The effect of FRET is not limited to organic dyes. It can be observed between large-size noble metal and semiconductor (quantum dot) nanoparticles or fluorescent proteins (Sect. 8.3). Moreover, it occurs if an acceptor is a plain conducting surface. In these cases, FRET can extend to longer distances and display $1/R^4$ func-

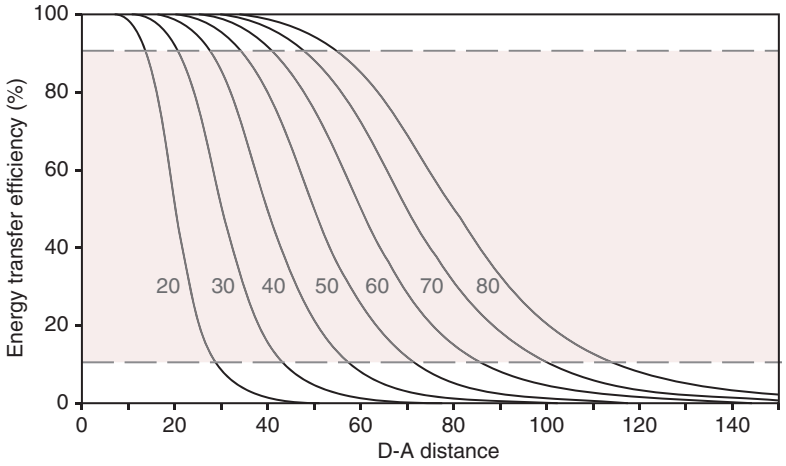

Fig. 3.14 Dependence of the dynamic range of Förster resonance energy transfer (FRET) on the donor-acceptor (D-A) distance for different R_0 values given in Ångstroms. The dotted lines delineate the regime of maximum sensitivity of response to distance variation for each D-A pair with different R_0, which is commonly between 0.7 and 1.5 R_0 (Kapanidis and Weiss 2002)

tion, thus extending the possibilities of its observation beyond the traditional distance limitations. These issues will be further discussed in Sect. 6.3.

3.6.3 FRET to Non-fluorescent Acceptor

The FRET donor should be necessarily emissive, since the transfer occurs during the lifetime of the excited state. In contrast, the FRET acceptor can be non-emissive and can provide only the quenching effect on the donor emission. Importantly, FRET to emissive acceptor can allow observing both donor and acceptor bands in two-band ratiometric emission. In contrast, if the acceptor is only a quencher, this very attractive feature is lost. Nevertheless, this situation has a different benefit. It is normally very hard to select the wavelength at which only the donor can be excited without noticeable direct excitation of the acceptor. Therefore, if the acceptor is non-emissive, its direct excitation will not influence the fluorescence spectrum and intensity.

There is one more possibility to realize FRET quenching. If the sensing event produces the shift of the acceptor absorption band, this will also influence the FRET efficiency and result in the variation of fluorescence intensity of FRET donor (Takakusa et al. 2003). There are many non-fluorescent pH indicators displaying the pH-dependent absorption spectra in the visible range with their different positions depending on ionization state. Such pH-dependent variations of absorbance can be transformed into fluorescence signal by selecting as a donor the dye with fluorescence spectrum overlapping the absorption spectrum with one form of such acceptor with no or much weaker overlap with the other form.

3.6.4 FRET Modulated by Light

In some sensing technologies and especially in cellular imaging it can be important to compare two signals or images, with and without FRET, keeping without change the composition and configuration in the system. In these cases, one can play with the light-absorption properties of FRET acceptor. The absorption spectrum disappears if this dye is selectively *photobleached*. This leads to the disappearance of FRET that allows recorded signal or image as the reference with only donor emission.

The other very elegant approach was suggested (Giordano et al. 2002) and got the name "*photochromic FRET*". The so-called *photochromic compounds* are those that change their absorbance reversibly in response to illumination at appropriate wavelengths. They can be used as FRET acceptors having the ability to undergo a reversible transformation between two different structural forms that have different absorption (and in some cases, fluorescence) spectra. Thus, they offer a possibility of reversible switching the FRET effect between "ON" and "OFF" states without any chemical intervention, just by light (Fig. 3.15).

The best compounds serving for this purpose are probably spiropyrans. These molecules exist in closed spiro forms absorbing at wavelengths shorter than 400 nm. They undergo a light-driven molecular rearrangement to an open merocyanine form with absorbance at 500–700 nm (Bahr et al. 2001). A family of such photoswitchable acceptors has been extended and includes not only small organic dyes but also conjugated polymers, fluorescent proteins, nanoparticles and their composites (Sect. 6.2).

The sensing technology benefits from these possibilities. The photo-switching quenching phenomenon provides the light-activated control of the excited states, and, consequently, control over any subsequent energy or electron-transfer processes. In imaging the living cells, the FRET switching on and off allows obtaining the necessary controls on the distribution of donor molecules and on their fluorescence parameters (Jares-Erijman and Jovin 2003). Such reversible cycles of photoconversion allow reversible transitions between two (donor and acceptor) emission colors.

The ability to undergo numerous cycles of FRET switching is extensively used in super-resolution microscopy (Sect. 13.2). This allows modulating the number of spatially resolvable emitters located in different positions in image for achieving nanoscale resolution.

3.6.5 Applications of FRET Technology

The attractive feature in application of FRET in sensing technologies is the possibility of *ratiometric* spectral observation of sensing event. However, for the detection of two-wavelength response (one emission band belonging to FRET donor, the other – to acceptor) one needs to satisfy very specific requirements, which are the

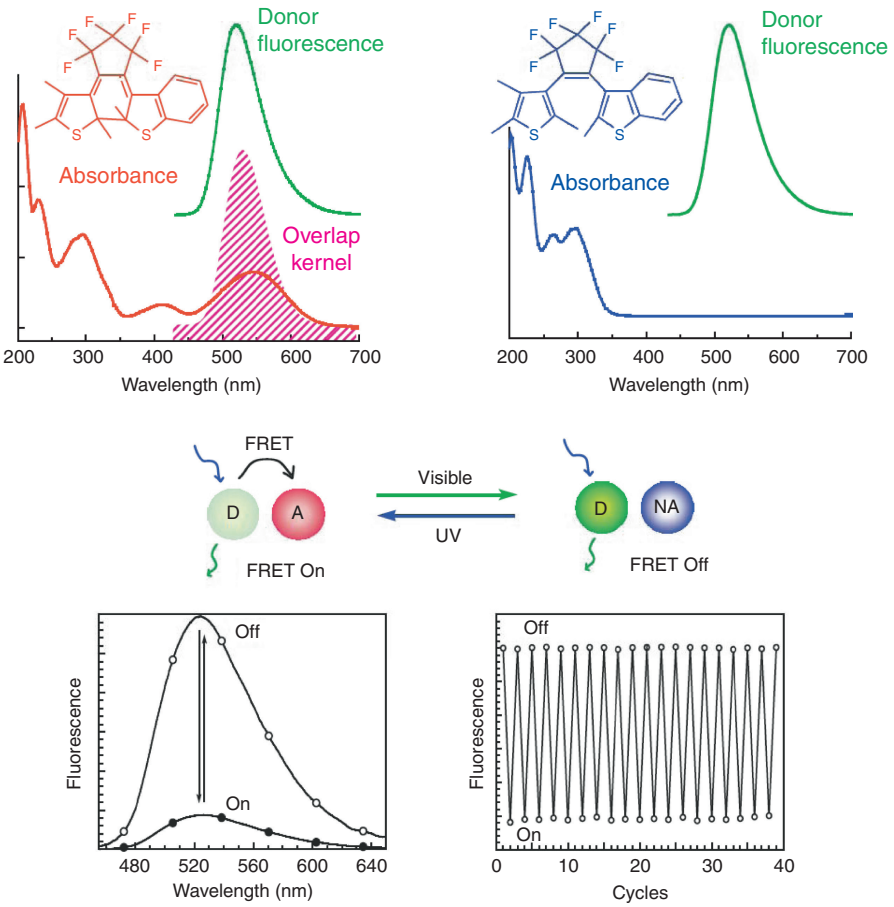

Fig. 3.15 Photochromic FRET (Jares-Erijman and Jovin 2003). The chemical structures depicted correspond to the photochromic dithienylethene in the colored closed form (*left*) and colorless open form (*right*). The absorption spectrum of the latter overlaps well with the emission spectrum of the donor; the kernel of the overlap integral (striped) corresponds to the lucifer *yellow* dye as the donor. Ultraviolet light induces the photochromic transition to the closed form (On), and visible (*green*) light reverses the process to the open form (Off)

double-labeling by different dye molecules and substantial change of wavelength-ratiometric signal during the sensing event. If the acceptor is non-fluorescent, one would record only the donor quenching with all disadvantages arising from single-wavelength intensity recording. The most straightforward application of FRET in sensing can be realized in the conditions when the distance or orientation between the donor and the acceptor changes in the sensing event.

Modulation of *donor-acceptor distance* offers a lot of possibilities (Fan et al. 2005). Since detectable switching between donor and acceptor can be achieved at separation distances up to 5–10 nm, the distance changes within this limit are explored. Such range of distances is comparable with the dimensions of many

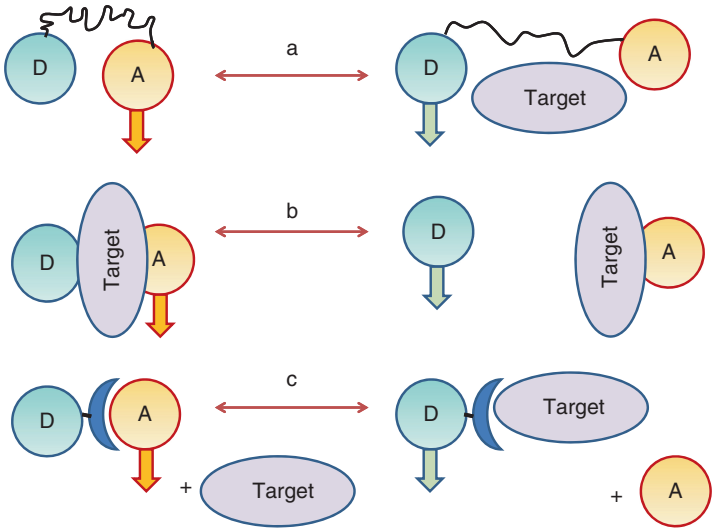

Fig. 3.16 Typical applications of FRET from excited donor (D) to fluorescent acceptor (A) in the studies of intermolecular interactions. (**a**) The changes of relative distances between molecules or their fragments (e.g., due to conformational change in one double labeled interacting partner). (**b**) The change in distance between interacting partners, each of them is labeled. (**c**) Detection of nonfluorescent target in substitution assay with labeled donor and competitor

biological macromolecules and of their complexes; therefore many constructions can be realized for coupling the response with its changes. Typical analytical experiments involving FRET pairs are depicted in Fig. 3.16. The conformational change in double labeled sensor (Petitjean and Lehn 2007), enzymatic splitting of covalent bond between two labeled units (Gershkovich and Kholodovych 1996; Takakusa et al. 2002) and substitution of labeled competitor in a complex with the labeled molecular sensor (Xu et al. 2005a) are used in these technologies. Two labels can be located in one of interacting partner indicating its conformational change, in both partners indicating their close contact and in one of the partners and the competitor.

Another possibility that is no less important is the modulation of donor-acceptor *spectral overlap integral* (Fig. 3.17). In this case, different possibilities for obtaining the sensor response are also possible (Yu and Ptaszek 2013; Kikuchi et al. 2004). The discussed above responsive photochromic and pH-sensitive dyes (as well as any dyes changing their absorption spectra as a result of change in their ground-state interactions) can be used as FRET acceptors producing the reporter signal. Additionally, the multi-step transfer can be modulated by inserting-removing the intermediates in multi-step FRET (*the FRET gating*). Such constructs and their applications will be discussed in Sect. 8.3.

Based on the response in FRET, different sensor constructs can be designed. As an example, a single-stranded dual fluorescently labeled DNA molecule that adopts a stem-loop conformation in its nonhybridized state with the close proximity of FRET donor and acceptor dyes can be constructed (the DNA hairpin, see Sect. 8.5).

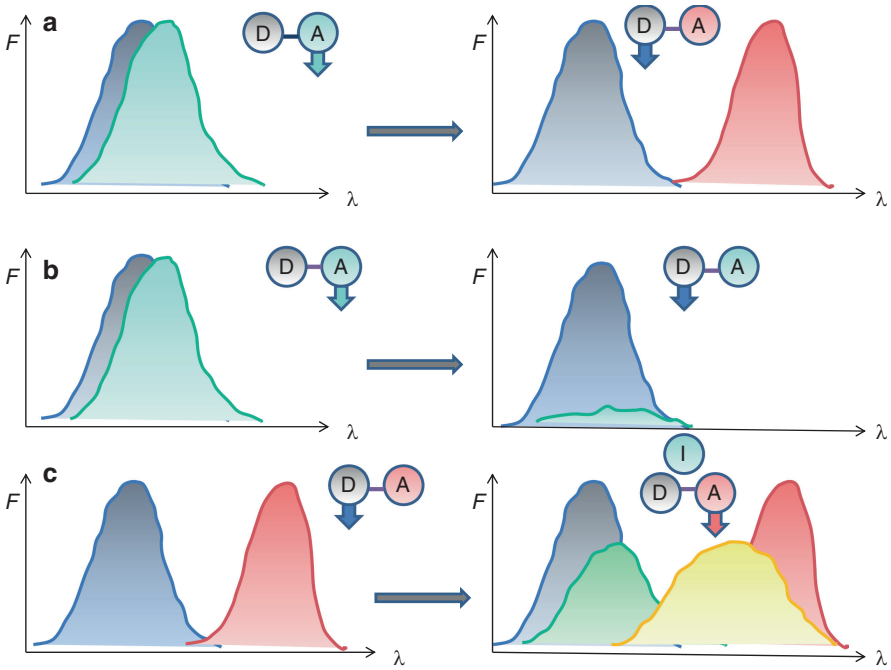

Fig. 3.17 Generation of sensor response by modulating the FRET donor-acceptor spectral overlap. (**a**) The absorption spectrum of the acceptor shifts reducing the overlap, which activates the donor emission. (**b**) The acceptor fluorophore is irreversibly or reversibly destroyed with the appearance of donor emission. (**c**) The FRET gating. The spectral overlap is initially negligible that does not allow FRET to proceed and the appearance of intermediate connecting the spectral overlaps between donor and acceptor activates FRET

It exhibits a conformational change on hybridization with an increase of dye-to-dye distance and the appearance of a new band belonging to the acceptor (Ueberfeld and Walt 2004). We can also mention the re-arrangement of subunits in the sensor protein (Adams et al. 1991) and a conformational change within the subunits. Since the distance dependence of FRET is very steep, efficient switching between the two emissions can be achieved.

3.6.6 Comparison with Other Detection Methods

FRET is increasingly popular in the studies of recognition between macromolecules and in the construction of biosensors based on this recognition. It operates with two reporter dyes (FRET donor and acceptor), which allows introducing the geometry parameter into fluorescence sensing and observing the sensing effects based on the changes in distances and orientations of the partners. Their excited-state energies modulating their spectral band positions also produce strong influence on this effect.

For better understanding the applicability of FRET technique to fluorescence sensing, one important remark should be made. While the FRET reaction allows the participating fluorophores to "talk" at sufficient distances and respond to their variations, the responses to other factors influencing the fluorescence band intensities are to a significant extent independent. For instance, the quenching of fluorescence of the donor quenches also the acceptor emission but the quenching of the acceptor emission does not influence the emission of the initially excited donor. Hence, when intermolecular interactions of fluorophores change on target binding, then one may expect a strong variation of fluorescence response unrelated to donor-acceptor distances, and this possibility has to be considered. In fact, it is used in sensor design.

3.6.7 Novel Trends in Excited-State Energy Transfer Probing

Attentive reader must note that the Förster-type energy transfer mechanism considers weak dipole-dipole interactions between donor and acceptor dyes. This allows operating with the distance, orientation and spectral overlap effects in fluorescence sensing. Limitations in choosing these parameters should be accounted by everyone who designs new fluorescence sensors based on FRET. They appear because of resonance mechanism of transfer that decays with distance and the fact that the resonant structures (donor and acceptor) must have correspondence in their excited-state energies. Although some uncertainties exist in obtaining quantitative data, we know how to exploit the critical dependences on three principal parameters: the donor-acceptor distance, the relative orientations of the respective transition dipoles, and the spectral overlap between the corresponding absorption and emission profiles. What happens if the donor and acceptor are close and interact stronger, up to overlapping their electronic orbitals?

In this case the energy is transferred due to a double electron exchange mechanism (the Dexter energy transfer) within the molecular orbitals of the donor and the acceptor. The electronic coupling leading to energy transfer requires significant orbital overlap. Therefore, close interaction between the excited donor and the acceptor ground state is necessary. This type of transfer is often called "through-bond energy transfer", in which a strong departure from the Förster-type energy transfer mechanism (FRET) is observed (Andrews et al. 2011). The Dexter-type of transfer can operate at much shorter distances; it falls off exponentially as the distance increases. Whereas the Förster-type energy transfer is able to occur over very large distances, the Dexter energy transfer dominates with much greater rates at short distances and commonly requires close contacts between the partners.

In associates of similar molecules, specific *excitonic* effects appear leading to quite characteristic spectra of J and H aggregates (See Sect. 6.1). If different dyes are coupled electronically, the requirement of spectral overlap between donor and acceptor dyes is lifted, which allows the fluorescence band shifting on a broader wavelength scale (Gong et al. 2012). Thus, instead of discussed above variations of relative distances and spectral overlaps, other mechanisms of generating the sensor response can be activated. They deserve focused study and exploration.

3.7 Wavelength-Shift Sensing

Most of the information that human brain obtains from the surrounding world is acquired by visual perception. Colored vision and characterization of visual objects in real color is an important contribution to this process. Therefore it is not surprising that in spectroscopy and in its combination with microscopy the attempts to obtain information in real color in the visible range of spectrum are in the minds of many researchers. This situation was not changed with the application of electronic photometric devices, since the spectral shift information is often easier obtained and more unambiguously interpreted than the information obtained in the studies of anisotropy and lifetimes. Therefore, the fluorescent dyes that change the color of their emission are in great demand. In many respects the application of these dyes may substitute different sensing technologies based on excimer formation and FRET, since single labeling is always easier than the labeling with two dyes.

According to the effects that are produced in original spectra, the λ-ratiometric dyes can be classified into two groups. One group combines the *wavelength-shifting* probes, in which the ratiometric effect is produced by the spectral shifts of a single band displayed in emission spectrum. Their properties and applications are overviewed in this Section. The other group of ratiometric dyes, the *two-band ratiometric*, allows achieving interplay of two emission bands intensities. Such reporters will be discussed in the next Section.

3.7.1 The Physical Background Under the Wavelength Shifts

The background of wavelength shifts in excitation or emission bands is the change of energy of correspondent electronic transitions that can be influenced by intermolecular interactions. A number of textbooks (Demchenko 1986; Lakowicz 2006; Suppan and Ghoneim 1997; Valeur and Berberan-Santos 2012) provide a detailed analysis of these mechanisms, and here we provide only their simplified description.

It has to be recollected that any molecules that are able to absorb light possess *discrete energy levels* in the *ground state* (the electronic state in which it resides at equilibrium, without excitation) and in the *excited state* (the electronic state achieved on absorption of light quanta). Molecule can absorb and emit the light quanta only of the energy that corresponds to *energy gap* between these states. This gap is inversely proportional to the wavelength position of the band maximum. In spectroscopy, the *wavenumber scale* ν (expressed in cm^{-1} units) is commonly used as an energy scale, so that $\nu\ (cm^{-1}) = 10^7/\lambda$ (nm). The spectrum recorded on a wavelength scale is in fact a reverse function of absorbed or emitted energy.

The energies of both ground and excited states are influenced by intermolecular interactions: the stronger are the interactions, the lower is the correspondent level on an energy scale. This is true for the energies of both ground and excited states. But since not only the energy but often the spatial distribution of electrons

changes dramatically on excitation, these states interact differently with surrounding molecules. If the interaction with the surrounding is stronger in the ground state, then, when this interaction increases, the difference in energy between the states increases. Then the molecule absorbs and emits light of higher energies and the spectra become shifted to higher energies, i.e., to shorter wavelengths. On the opposite, if the interaction energy is stronger in the excited state, then on increase of this interaction the spectra shift to longer wavelengths. For illustration, one may refer to classical Jablonski diagram that, for the purpose of our discussion was modified and simplified (without showing vibrational levels, high-order electronic states and intramolecular relaxations). It is presented in Fig. 3.18.

In highly fluorescent organic dyes the lowest ground-state and excited-state energy levels are formed by π-*electrons*. Commonly the π-electronic system with the inclusion of hetero-atoms becomes more *polarized* in the excited state, and becoming a stronger dipole it interacts stronger with its molecular environment. As a result, the energy gap between the ground and the excited states becomes smaller and the spectra shift to longer wavelengths.

There are possibilities to increase this effect by introducing different chemical substitutions polarizing the π-electronic system. If we attach an electron-donor group (such as dialkylamino-) on one side of molecule and an electron acceptor (such as carbonyl) on its opposite side, the charge separation in the excited state

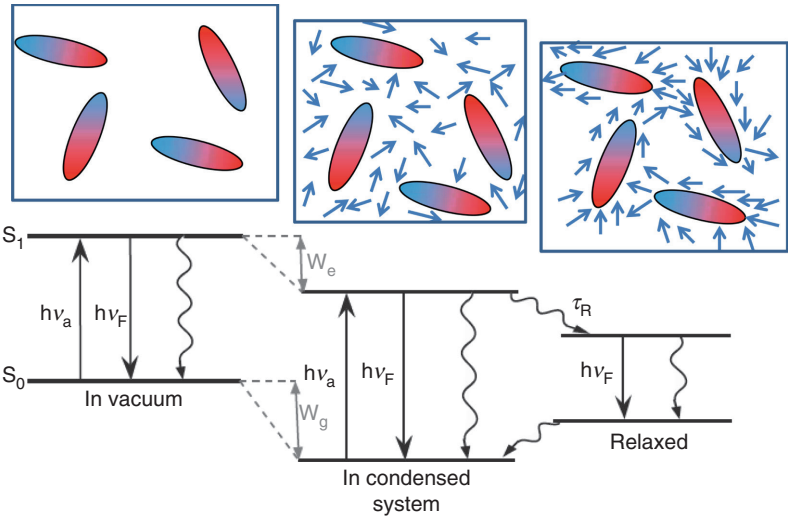

Fig. 3.18 A simplified Jablonski diagram of ground S_0 and excited S_1 energy levels and transitions between them. Vertical upward arrow shows the excitation and downward arrows show emissive (straight) and non-emissive transitions to the ground state. In condensed media, the energies of ground and excited states are decreased due to electronic interactions with the environment by arising from solute-solvent interactions solvation energies W_g and W_e correspondingly. In addition, in polar media there occurs an establishment of equilibrium in interactions of dye and surrounding dipoles (dipolar relaxation). As a result, the energy gap between S_0 and S_1 states decreases and the spectra shift to longer wavelengths

becomes greater. Molecule will become a strong electric dipole, its interactions with surrounding dipoles will become stronger and the emission spectrum will exhibit stronger shift. Such structures are often called '*push-pull structures*'. The structures of the so-called '*polarity-sensitive*' dyes follow this principle. The *higher is polarity* of the medium, the stronger is the shift of fluorescence spectra to *longer wavelengths*. Usually the dyes that exhibit the changes in emission spectra are called λ-*ratiometric* because they allow a convenient quantitative characterization of the changes in emission spectra by evaluation of intensity ratio at two selected wavelengths. The structures and properties of these dyes will be discussed in Sect. 3.8.

3.7.2 The Measurements of Wavelength Shifts in Excitation and Emission

The shift of the whole fluorescence band results in increase of intensity at one of its edges and decrease at the other. As the information channels for collecting the fluorescence intensities one can use *two selected wavelengths* at the two edges, in which the effect is the strongest (see Fig. 3.19). Commonly these are the wavelengths of the maximal slopes of the spectrum (the wavelengths of maximum and minimum of its first derivative). Then taking the intensity ratio at these points, one may benefit from two-channel ratiometric measurements. Meantime, it should be kept in mind that the intensities at the slopes of the spectra are about one half lower than at the band maxima and the presence of impurities in the sample and light-scattering effects may influence differently the intensities at these short and long-wavelength wings.

Wavelength shifts in excitation spectra are not frequently used in sensing. They are measured mostly for electrochromic dyes (e.g., aminostyryl derivatives) that are strongly sensitive to a variation of local electric fields (Sect. 4.3). Based on them, the binding of functional dyes to cell membranes and their phospholipids analogs

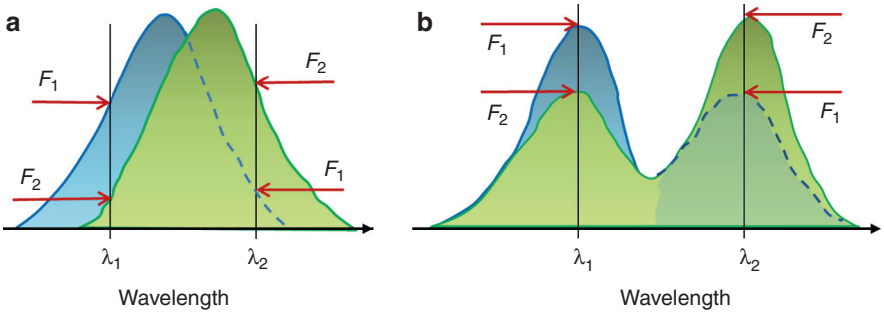

Fig. 3.19 Informative signal obtained on λ-ratiometric recording at two fixed wavelengths. (**a**). The sensor response is in the form of spectral shift (Nile Red is an example). (**b**) The response is in a decrease of intensity of one band λ_1 and in an increase at a different band λ_2. Substituted 3HCs are the examples of such behavior. The quantitative measure in this λ-ratiometry is the change in the ratio $F(\lambda_1)/F(\lambda_2)$.(Demchenko 2013)

(liposomes) allows the detection of variations in membrane potential (Gross et al. 1994). Also, the collective effects of charges that can be generated in phospholipid bilayers may be used in the development of nano-scale and whole-cell biosensors.

Wavelength-ratiometric measurements of *spectral shifts in emission* are used more frequently. Some dyes exhibit very significant (up to 100 nm and more) shifts in wavelength positions of their fluorescence spectra in response to changes in their interaction with the molecular environment (Valeur and Berberan-Santos 2012). These shifts are usually due to a combination of effects of *polarity* with the effects of intermolecular *hydrogen bonding* (Vazquez et al. 2005). The latter being stronger in the excited state may produce strong additional shifts. Thus if the dye is incorporated into the sensor molecule in such a way that its interaction with the environment changes as a result of a conformational change in the sensor or due to direct contact with the target, the event of sensing can be detected by the spectral shift. This principle is used in the design of both chemical sensors and biosensors.

It could be ideal to observe the environment-dependent spectral shifts without change or with insignificant change of integral fluorescence intensity, since this will provide the highest signal-to-noise ratio and the broadest range of variation in intensity ratios. In reality, this condition is difficult to realize because the environment-dependent quenching is the common property of these dyes. The increase of their dipole moment on excitation produces an increase in interactions in the excited state with the environment (see Fig. 3.18) and results not only in the shifts of spectra to the red but also the activation of a number of factors quenching the fluorescence (Demchenko 2005b). This is the reason why the shift to longer wavelengths is often associated with decrease of intensity (Fig. 3.20). Sometimes, this decrease is dramatic. This makes the ratiometric measurements based on wavelength shifts imprecise and subjective to systematic errors.

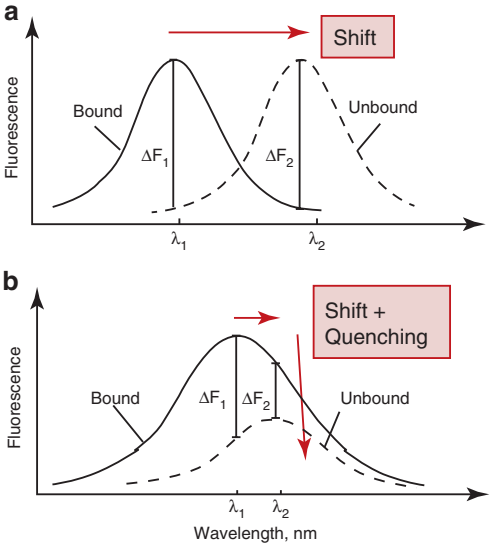

Fig. 3.20 Sensing with the wavelength-shifting fluorophores by recording the intensity ratios at two wavelengths, λ_1 and λ_2. (**a**). Ideal case, when the target-free and target-bound form (located at shorter wavelengths) of the sensor exhibit similar fluorescence intensities. (**b**). Often observed reality when in unbound form, in addition to shift, the spectrum is quenched and broadened

3.7.3 Wavelength-Ratiometric Measurements

In principle, some of the important problems observed with the intensity measurements can be avoided if the sensing response is provided by observation of substantial shift of fluorescence band on the wavelength scale. This could allow instead of measuring one parameter, $F(\lambda)$, obtaining variations of *two intensity values* at two different wavelengths, λ_1 and λ_2, and taking the *ratio of their intensities*, $F(\lambda_1)/F(\lambda_2)$. In the dynamic range of sensing, this ratio may depend on the concentration of bound target but may not depend on the concentration of the sensor molecules. Photobleaching of the fluorophore that decreases the concentration of responsive sensors will then also be without influence on the result (if, of course, the photodegradation products are non-fluorescent).

If the spectrum shifts (for instance, to the red), then the intensity at the short-wavelength slope decreases and at the long-wavelength slope increases (see Fig. 3.19), and this can allow convenient measurement of intensity ratios at two fixed wavelengths. The choice of λ_1 and λ_2 in the case of spectral shifts can be made in two different ways. One is to choose λ_1 at the point of maximal increase of intensity and λ_2 at the point of its maximal decrease. Then the dynamic range of change in $F(\lambda_1)/F(\lambda_2)$ will be the largest, and this change can be calibrated as a function of concentration of the bound target.

The other possibility is to choose λ_1 at the point at which the intensity exhibits maximal change and λ_2 at the point, in which the two spectra cross and the intensity does not change at all (*isoemissive point*). Then λ_1 can be chosen either at the blue (short-wavelength) or red (long-wavelength) slope, apart from λ_2 and in the region of maximal spectral change. Since commonly the fluorescence spectra are not symmetrical but exhibit a shallower slope at longer wavelengths, then the changes at the blue side are usually stronger and the dynamic range of response broader. However in some cases if the Stokes shift is small, the readings at shorter wavelengths can be subjected to stronger light scattering perturbation.

Formally, there is no advantage of wavelength-ratiometric sensing over two-wavelength intensity sensing with molecular reference. In both cases the ratio of two intensities at two wavelengths, λ_1 and λ_2, is obtained. The only difference is that instead of keeping a permanent value, the intensity at the second (reference) channel (at λ_2) increases or decreases in a converse manner to its change in the first channel, at λ_1. If for recording the reference signal we select the wavelength at which all the calibrated spectra cross one another (isoemissive point), then we can determine the target concentration using Eq. (3.5). In a more general case, when λ_2 is a different wavelength, (e.g., it is the maximum of the second band), then we have to include the factor that accounts for this intensity redistribution, which is the ratio of intensities of free and bound forms at λ_2:

$$[A] = K_d \left(\frac{R - R_{\min}}{R_{\max} - R} \right) \left(\frac{F_F(\lambda_2)}{F_B(\lambda_2)} \right) \tag{3.17}$$

3.7.4 Application in Sensing

In a number of studies, the fluorescence shifts were detected in response to the change in intermolecular interactions, and their ratiometric display was used in molecular sensing. As an example, a strong red shift of fluorescence spectra of Ca^{2+}-binding proteins (parvalbumin, troponin C) labeled with acrylodan was demonstrated on interaction with calcium ions (Prendergast et al. 1983). This shift was accompanied by significant decrease of intensity. It was suggested that a conformational change occurs as a result of the ion binding, and the covalently bound dye located in low-polar environment becomes exposed to the protein surface. This idea was further developed for Ca^{2+} sensing by labeling of single-Cys mutants of troponin C (Putkey et al. 1997). It was also observed that a λ-ratiometric dye attached to zinc finger responds strongly to zinc binding (Walkup and Imperiali 1996), since the binding induces formation of structured peptide conformation with the screening of fluorescence reporter from the solvent.

Some progress was also achieved in *fatty acid* and *saccharide sensing*. A significant spectral shift (by 35 nm to the red) was observed for acrylodan selectively attached to Lys residue of fatty acid binding protein upon binding fatty acids (Richieri et al. 1992). This occurs due to a displacement of the dye from hydrophobic fatty acid binding pocket. The blue shifts were observed on binding the ligand to maltose binding protein (Gilardi et al. 1994). A wavelength-shift sensor for saccharides was made based on two asymmetric diphenylpolyenes, in which dimethylamino group served as an electron donor and boronic acid group functioned both as electron acceptor and as the sensor for saccharides (Di Cesare and Lakowicz 2001). These authors achieved a blue shift and an increase of intensity on target binding and recorded a λ-ratiometric response. They also observed the decrease in fluorescence lifetime on sugar binding and claimed that the lifetime sensing may be more convenient observation in this case.

The prototype of *direct molecular immunosensor* has been described (Bright et al. 1990). For its construction the complex of human serum albumin (HSA) with anti-HSA antibody was formed and subjected to labeling by fluorescent dansyl derivative. This allowed labeling antibody outside the antigen-binding site at unspecified locations of amino groups. After removal of HSA and immobilization on solid support, the antibody becomes reactive to HSA binding demonstrating the blue shift of dansyl emission and by an increase of its intensity.

The outlined above are rather uncommon cases, in which the environment-sensitive dyes respond to target binding by fluorescence shift that is strong enough for ratiometric measurement. There are many examples when these shifts were undetected, and therefore the measurements had to be reduced to single-wavelength records of intensity. This problem is clearly seen in the work (de Lorimier et al. 2002), in which a very detailed study of 11 bacterial periplasmic binding proteins modified with 8 environmentally sensitive fluorophores were conducted. The common spectroscopic effects on the binding of target ligands were only the changes in fluorescence intensities, whereas the spectral shifts were either insignificant or even totally absent. Only in two cases, of Glu/Asp and glucose binding proteins with the bound acrylodan dye the shifts (13 and 21 nm correspondingly) were suf-

ficient for ratiometric measurements. This insensitivity can only be understood if no significant change in polarity of fluorophore environment occurs on target binding and also if the fluorophores remain highly hydrated and retain hydrogen bonds with water molecules.

3.7.5 Comparison with Other Fluorescence Reporting Methods

Ideally, the wavelength-shift detection is optimal for realizing the concept of *direct sensing*. It would be ideal to obtain response to intermolecular interactions by spectral shifts only, without the change or with insignificant change of band intensity. In reality, this condition is difficult to realize because the same interactions may result in quenching. Whereas in intensity sensing the strong change in intensity on target binding is a necessary requirement for generating the response, in wavelength-shift sensing it becomes a complicating factor.

It is difficult to predict these quenching effects and to analyze them quantitatively. They can appear due to the decrease of energy separation between locally excited and intramolecular charge transfer (ICT) states up to the level inversion, quenching by electron transfer to solvent traps, quenching via newly formed intermolecular hydrogen bonds, or increased thermal quenching due to smaller gap between ground and excited-state energies. Intramolecular flexibility in fluorophore may contribute strongly to the quenching effect (de Silva et al. 1997). These quenching effects follow quite different regularities with respect to the spectral shifts, since the two effects of shift and quenching are often not correlated.

On the increase of polarity, with the environment-sensitive dyes together with the long-wavelength shift one can commonly observe an increase of the width of the spectrum. As a result, the combination of three factors, the shift, the change of intensity and the broadening, results in a shifted component that will be strongly quenched, so that in reality one will observe the spectrum depicted in Fig. 3.20b. It will exhibit only a small shift but a strong decrease in intensity. In these cases, the application of common environment-sensitive dyes is not justified, and the fluorophores specially designed for intensity measurements are to be preferred.

3.8 Two-Band Wavelength-Ratiometric Sensing with a Single Dye

The previous section could give the reader a full impression on the advantages of operation of fluorescence reporter based on achieving the shift in fluorescence spectrum and on the difficulties associated with that. Therefore, the researchers try to develop the fluorescence reporters, in which the sensitivity to the change of intermolecular interactions could be greatly increased. Ideally, it could be using one type of dye molecules (this will eliminate double-labeling), which serves as reporter so

perfectly, that in sensing event it switches completely between two ground-state or excited-state forms (Demchenko 2014). These forms should give separate bands in excitation or emission spectra to produce a dramatic easily recordable change of color.

From basic photophysics we may derive that in order to obtain the switching *in excitation spectra* we need to operate with two or more ground-state forms of the reporter dyes and to couple the sensing event with the transitions between them. In contrast, for obtaining two switchable bands *in fluorescence emission spectra*, one ground-state form is enough (and preferable), but there should be an excited-state reaction generating new emissive species. This reaction should proceed between discrete energy states, and both the reactant and the product in this reaction should emit strong fluorescence with the shifts in energy.

These two cases are illustrated in Fig. 3.21. In the case of ground-state equilibrium the two species are the independent absorbers and emitters, so both their excitation ($h\nu_1^a$ and $h\nu_2^a$) and emission ($h\nu_1^F$ and $h\nu_2^F$) energies commonly differ. This leads to λ-ratiometric effects in both excitation and emission spectra. In the case of

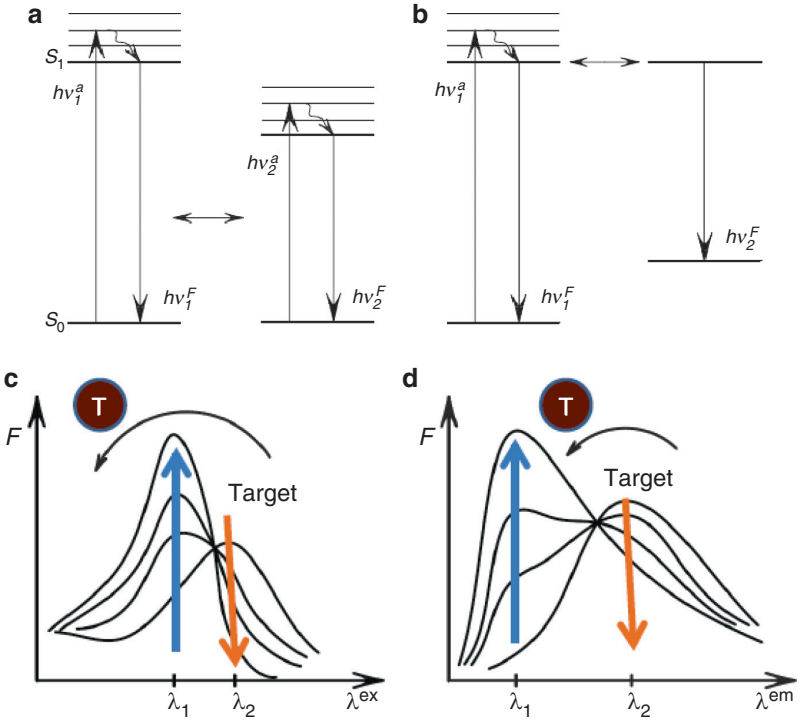

Fig. 3.21 The energy diagrams (**a**, **b**) and schematic illustration of the changes in excitation (**c**) and emission (**d**) spectra in the cases of ground-state (**a**, **c**) and excited-state (**b**, **d**) equilibrium between two emissive forms of the sensor. *Isobestic* in (**c**) and *isoemissive* in (**d**) are the crossing points in spectra, at which the intensity does not change on transition between the two forms of reporter

excited-state reaction the excitation energy $h\nu_1^a$ can be the same but the emission energies ($h\nu_1^F$ and $h\nu_2^F$) differ. The λ-ratiometric response is observed only in emission spectra. The excited state with the emission energy $h\nu_2^F$ is populated kinetically and the equilibrium may not be achieved during the lifetime τ_F.

3.8.1 Generation of Two-Band Ratiometric Response by Ground-State Isoforms

The switching of fluorescence signal can be performed between two *ground-state forms* that may be isomers, different charge-transfer forms or the forms differing in ionization of particular group. If these two forms are fluorescent, they should exhibit different excitation spectra, as it is illustrated in Fig. 3.21a, c. Though the wavelength-ratiometric recording in excitation is less convenient than in fluorescence and needs two light sources or re-tuning of a single source between two wavelengths, there are different applications of such approach in sensing, particularly when they are based on indication of pH changes or focused on sensing ions. The effects of charge can provide such a strong perturbation of the ground state that could allow switching between two forms.

The Ca^{2+}-chelating dye Fura 2 (Grynkiewicz et al. 1985) have got great popularity in cellular studies despite its near-UV excitation and low photostability. The reason is the great ratiometric effect on Ca^{2+} binding modulating the ground-state *intramolecular charge transfer* (ICT). There are also many reports on the construction of chemical sensors for other, beside calcium, ions based on ICT mechanism (de Silva et al. 1997). A new seminaphtho-fluorescein platform suggested for ion sensing (Chang et al. 2004) uses the switching between two ground-state tautomers of the dye that produce different excitation and emission spectra under the influence of the bound ion. Such effect is hard to achieve on recognition of neutral molecules.

The dyes highly polarizable in the ground state have found application in the sensing of local electric fields (Clarke et al. 1995; Callis 2010). They belong to the class of electrochromic dyes (see Sect. 4.3) that have got application in the studies of biomembrane potential.

3.8.2 Excited-State Reactions Generating Two-Band Response in Emission

When the effects of two-band switching occur in emission spectra, this offers additional advantages over that in excitation spectra. In this case, for target detection one does not have to change or re-tune the excitation light source, and ratiometric fluorescence detection can be realized even using the simplest bandpass filters. This advantage can become efficient with the use of dyes possessing strong electron-donor and electron acceptor substituents and exhibiting localized *intramolecular*

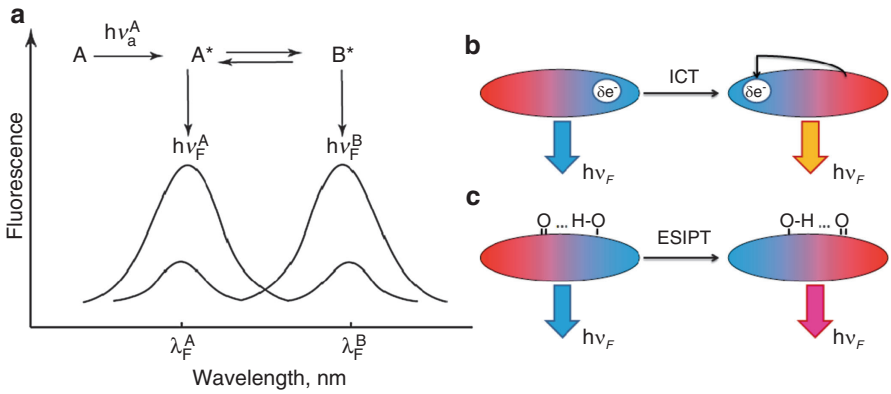

Fig. 3.22 The mechanisms of generation of new wavelength shifted fluorescence bands. (**a**) Fluorescent dye A on absorption of light quanta $h\nu_{abs}{}^{A}$ emits light quanta $h\nu_{F}{}^{A}$ from the excited state A* and also exhibits transition to another excited state B* that emits quanta of energy $h\nu_{F}{}^{B}$ at different wavelength, usually with a strong red shift. The effect of sensing switches the population of excited-state species between A* and B*, which produces the redistribution of emission intensity between A* and B* bands. (**b**) The intramolecular charge transfer (ICT). The redistribution of electron density produces the energy change of emitted quanta and observed spectral shifts. (**c**) The excited-state intramolecular proton transfer (ESIPT). The change in energy of emitted quanta occurs because of proton transfer along the intramolecular H-bond. Electronic density redistribution also takes place being coupled with proton motion. This results in commonly stronger spectral shifts

electronic charge transfer (ICT) or *excited-state intramolecular proton transfer* (ESIPT) states (Fig. 3.22).

The excited-state ICT is well described in the literature (Suppan and Ghoneim 1997). It is a basically fast and reversible transition from initially excited A* form to the product B* form. Usually in ICT the initially low-polar A* state is excited, and the reaction results in the generation of charge-transfer state that is highly polar and strongly interacting with the environment. The shift in excited-state equilibrium to the level of lower energy guides the spectroscopic effect: the stronger is the interaction with the environment of one of the excited-state forms, the stronger will be the correspondent band in fluorescence emission.

The ICT reaction can often generate the *two-band emission* in aromatic dyes possessing strong *electron-donor* and *electron acceptor* substituents (Rurack 2001; Yoshihara et al. 2003). The possibilities of functional substitutions in some of these dyes are limited, since they may alter dramatically the fluorescence properties. Thus in bianthryl (the dimer of anthracene) the two bands belonging to initially excited and ICT emissions are well separated and have a different shape with sufficiently high quantum yield. Variations of their relative intensities suggest bianthryl to be a good reporter of polarity and mobility of its environment (Demchenko and Sytnik 1991a, b) that might be used in sensing. However, this dye cannot be functionalized, since any chemical substitution changing the symmetry between two anthracene rings results in disappearance of the ability of switching between the emission bands. The other problem is the poor resolution between normal and ICT bands observed in different dyes. In some of the dyes, the ICT state stabilization in polar

media is coupled with intramolecular conformational change (twisting) leading to *Twisted Intramolecular Charge Transfer* (TICT) states with higher spectral resolution. However, significant and often unpredictable quenching effects that are often observed for separated-charge form complicate their application.

The switching between normal and ICT emissions can be in the background of efficiently operating sensors (Collado et al. 2002; Malval et al. 2003). The application of this effect in sensing will be discussed in Sect. 8.2.

3.8.3 *Excited-State Intramolecular Proton Transfer (ESIPT)*

In aromatic molecules that contain *hydrogen bond donor* and *acceptor* groups located at a close distance, proton can migrate from one group to the other giving rise to a *tautomer form* that emits fluorescence with a substantial shift of spectrum to longer wavelengths (Demchenko et al. 2013). For sensing applications the molecules exhibiting ESIPT are especially attractive because the switch between the two forms in emission can be modulated by the target. The overall ESIPT reaction is fully reversible, starting from the ground N state and returning to the same state after four-level reaction cycle (Fig. 3.23). The

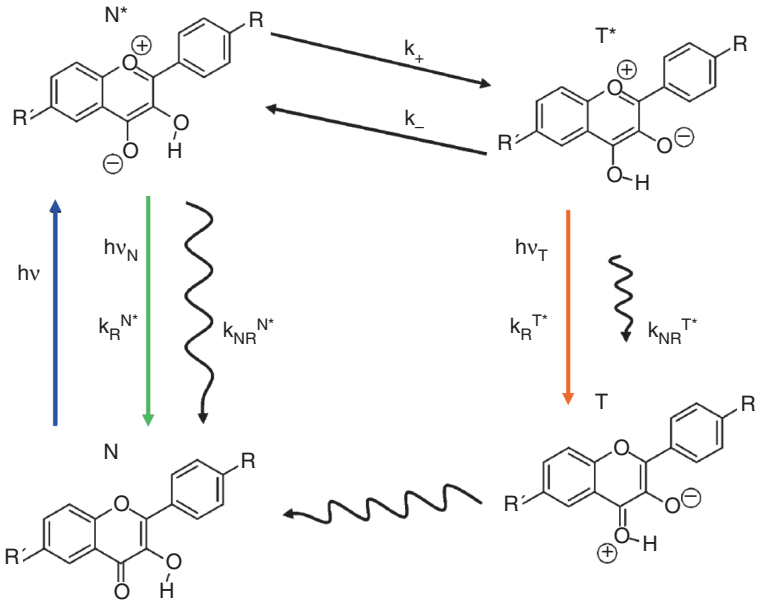

Fig. 3.23 The four-level diagram for a typical excited-state intramolecular proton transfer (ESIPT) reaction shown with correspondent rate constants. This reaction occurs between the proximate proton donor and acceptor groups connected by a hydrogen bond in the same photoexcited molecule. A number of radiative and non-radiative processes accompany this reaction. The 3-hydroxyflavone derivatives were chosen as examples. R and R' are the hydrogen atoms or their electron-donor or electron-acceptor substituents

absorption of light quantum leads to normal excited-state form (N*), which converts into the excited photoproduct, the so-called phototautomer (T*), by the translocation of proton and hence the alteration of the electronic configuration. T* is recognized by fluorescence spectrum strongly shifted to longer wavelengths. The T* relaxation (i.e., the fluorescence emission plus the decay via radiationless channels) leads to the ground-state tautomer (T) that is unstable and undergoes a fast back proton transfer with the recovery of N species, closing the reaction cycle.

Basic events in these reactions can be very fast (subpicosecond), and the needed simultaneous presence of N* and T* bands in emission could be due to two factors (Tomin et al. 2007, 2015):

(a) *Kinetic*. The equilibrium in ESIPT reaction is shifted towards the T* form but the N* and T* forms are separated by energy barrier that makes the reaction slow and comparable in rate with the emission. The barrier appears due to the presence of conformers in configurations unfavorable for the transfer. In protic environments the intermolecular hydrogen bond partners that compete with hydrogen bonds on ESIPT pathway can be involved. This slows down the ESIPT reaction, and the emission from the N* form occurs in the course of its transition to T* form.
(b) *Thermodynamic*. In this case the ESIPT reaction can remain very fast but the reverse reaction is efficient on a time scale faster than the emission. It allows establishing the equilibrium between the N* and T* forms so that the two emissions of comparable intensities can be observed.

These two cases can be recognizes by the difference in fluorescence decay functions (Shynkar et al. 2003) the effects of external collisional quenchers (Tomin et al. 2007), solvent polarity (Klymchenko and Demchenko 2003) and temperature (Oncul and Demchenko 2006) effects. The identity of long lifetimes shows that the two forms are in equilibrium. This also means that any fluorescence quenching produces identical decrease of lifetime and intensity of both forms, which allows ratiometric response to be unchanged.

Among different fluorophores exhibiting ESIPT reaction, the 3-hydroxychromone derivatives (3HCs) are unique being the only class of organic dyes that are actively explored in sensing. They exhibit ESIPT, in which the observation of two separate bands in emission can be achieved without involvement of two or more ground-state or excited-state conformers (Demchenko 2006; Demchenko et al. 2003). In 3HCs the proton-donor 3-hydroxyl and proton-acceptor 4-carbonyl are attached to a rigid skeleton and coupled by a hydrogen bond. In these dyes the emission is based on a balance between ICT and ESIPT species that occur in dynamic equilibrium. As a result, they exhibit dramatic variation of emission color as a result of ICT-ESIPT reaction (Demchenko 2006; Demchenko et al. 2003). Interplay of these two emissions can be easily observed by λ-ratiometry. By switching between them these dyes demonstrate really dramatic sensitivity of their spectra to polarity and electric fields of their environment (Demchenko and Yesylevskyy 2009; Klymchenko and

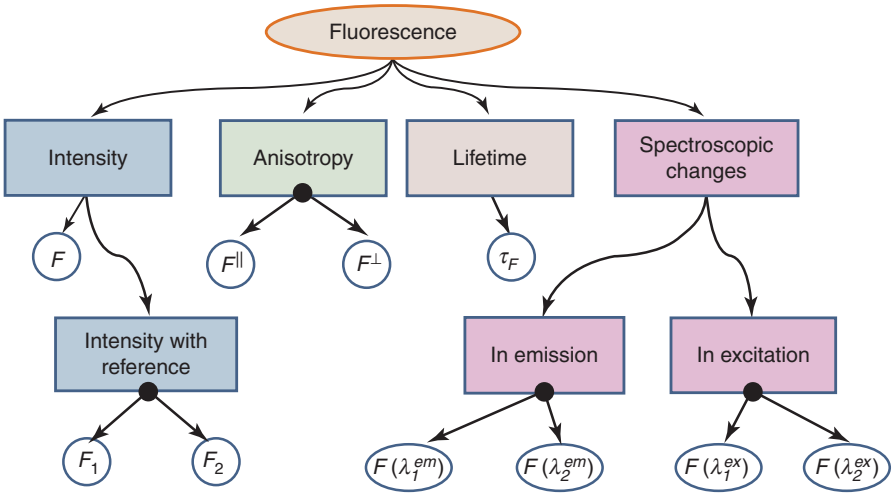

Fig. 3.24 Parameters used in fluorescence sensing and imaging. Thick arrows indicate the techniques, in which the self-referencing is provided by simultaneous recording of two parameters

Demchenko 2002) and also to intermolecular H-bonding (Shynkar et al. 2004). For more detailed information on their structures and spectroscopic properties see Sect. 4.2.

3.8.4 Prospects for Two-Band Ratiometric Recording

The two-band wavelength-ratiometric technique exhibits extreme simplicity of recording the intensity at two fluorescence band maxima combined with the possibility of obtaining strongly enhanced and internally calibrated ratiometric response (Demchenko 2010, 2014). In Fig. 3.24 the comparative analysis of different fluorescence parameters regarding possibility of internal calibration of their readout is presented. The conclusion can be made that the single-channel response allows obtaining the *internally calibrated signal* only in lifetime sensing. In anisotropy sensing the two (vertical and horizontal) polarizations provide the necessary *two channels*, and in FRET to fluorescent acceptor and in wavelength-shifting response these two channels are selected as *intensities at two wavelengths*. In two-band ratiometric sensing the ratio of intensities at two wavelengths is also obtained, but because the signal comes from a single type of the dye and the forms emitting at two wavelengths have the same lifetimes, the internally calibrated signal is resistant to any uncontrolled quenching effect.

The importance of such calibration for microarray technology and other applications has been recently indicated (Demchenko 2005a). The arguments were presented that this approach has strong advantages over other methods that allow

Table 3.1 Relevance of different fluorescence detection methods to application in direct sensing arrays

Method of detection	Number of readout channels	Insensitivity to instrumental factors	Insensitivity to sensor concentration[a]	Insensitivity to uncontrolled quenching
Intensity	1	**NO**	**NO**	**NO**
FRET	1	**NO**	**NO**	**NO**
	2	**YES**	**YES**	**NO**
Lifetime	1	**YES**	**YES**	**NO**
Wavelength shifting	2	**YES**	**YES**	**NO**
Anisotropy	2	(**YES**)	**YES**	**NO**
Two-band ratiometry[b]	2	**YES**	**YES**	**YES**

[a]In the responsive range of analyte concentrations
[b]In the case of fast reversible excited-state reaction

internal calibration – intensity sensing with the reference, anisotropy, lifetime sensing and FRET (Table 3.1).

In addition to detection and quantitative analysis in sensing, the methods based on λ-ratiometry allow providing rich multiparametric information that includes polarity, H-bonding proton-donor ability and viscosity at the site of location of applied fluorescence reporters, the pH sensing in aqueous media, the sensing of temperature and pressure. These effects depend on the properties of the surrounding medium and may be used as extremely sensitive means for characterizing these properties in the systematic application of fluorescence sensors and probes. One can detect and characterize numerous molecular events based on probe sorption–desorption to surfaces, inclusion into micelles and biomembranes, and attachment to proteins exhibiting conformational changes, self-assembly or aggregation.

3.9 Sensing and Thinking: The Optimal Choice of Fluorescence Detection Technique

The choice of fluorescence response mechanism, responsive dye and the method of observation is always a compromise in two directions. One is the compromise in choosing between the brightest dyes that are optimal for fluorescence intensity sensing and 'responsive' dyes that are needed for more complicated methods of observation based on the change in lifetime, excited-state complexes formation, band wavelength shifts or two bands fluorescence switching.

The other dilemma is between simplicity in measurements and the need for obtaining high information content of response that also depends on the selected detection technique. The choice in this respect is rather limited, but it exists.

In addition to intensity sensing, one may choose between anisotropy and lifetime measurements and use spectroscopic detection based on spectral shifts or interplay of two bands used in FRET, excimer sensing or sensing by generating the excited-state reaction.

Intensity sensing is the simplest technique, and it demonstrates many disadvantages mainly due to the absence of absolute scale and the difficulties in applying the internal calibration. Internally calibrated signal can be provided in anisotropy and lifetime sensing. In principle, this can be done in two-wavelength ratiometric recording with the application of two dyes (excimers and FRET) or a single dye exhibiting ground-state or excited-state reaction. Every one of these techniques needs proper selection of reporter dyes. Many requests therefore should be addressed to synthetic chemists and photochemists.

Questions and Problems

1. Why the wavenumber scale is more correct for presentation and analysis of spectra than the wavelength scale? Convert into wavenumbers 365 nm, 436 nm, 630 nm. Convert into wavelengths 14,820 cm^{-1}, 19,600 cm^{-1}, 24,300 cm^{-1}. Convert into wavenumbers the wavelength shift by 10 nm of fluorescence band at 400 nm and at 800 nm. Convert into wavelengths the wavenumber shift by 200 cm^{-1} at 12,500 cm^{-1} and at 24,200 cm^{-1}. Estimate in cm^{-1} the bandwidths of 50 nm for the bands located in the blue (450 nm) and red (650 nm) ranges of spectra.
2. Let the reporter dye be attached to the surface of sensor molecule and appear on sensor-target interaction at their contact interface. Count all possible effects that can be used to provide its quenching/unquenching response.
3. Explain how to introduce the reference signal into an intensity sensor to make possible its internal calibration. What output readings should then be obtained and how to calculate based on them the target concentration?
4. What are the possibilities to distinguish static and dynamic quenching? Explain the physical processes behind them.
5. How could you distinguish between two interpretations of quenching effect observed in recording the intensity on exposing your sensor to test sample? A) the target binds to the sensor producing the quenching. B) there is no target in the sample but, instead, some substance produces dynamic quenching by collisions with the sensor. How the experiments in the steady state or time-resolved studies can resolve this issue?
6. In anisotropy sensing should the free sensor or its recognition segment necessarily rotate? What rotation rate is acceptable (in comparison with the rate of fluorescence decay)? What other possibilities except providing the sensor, target or competitor rotation, can be used in anisotropy sensing?
7. What is the difference between polarization and anisotropy? Calculate the polarization values for anisotropy $r_0 = 0; 0.1; 0.2; 0.3; 0.4$.
8. Let a total quenching of fluorescence be observed on target binding, so that intensity goes down from high-level values to zero. What lifetime changes will be observed? Will the lifetime sensing in this case be efficient?

9. Explain, why the measured fluorescence anisotropy is sensitive to light scattering effects. What should be done for reducing these scattering artifacts? Explain also, why this problem may not exist in lifetime sensing.
10. Is a geometry change in a sensor molecule necessary for providing the response in excimer formation? Is this change always needed for response in FRET?
11. Let the distance between donor and acceptor on interaction with the target change from 5 to 10 Å and R_0 is 50 Å. Will this sensor be efficient?
12. Explain, what are the relative advantages and disadvantages in application of FRET with the use of fluorescent or non-fluorescent acceptor.
13. Let all the conditions for optimal FRET observation be satisfied but the donor is quenched on interaction with the target. Will this system work as efficient FRET sensor?
14. Let donor and acceptor in FRET be identical dye molecules. Can FRET be efficient between them? If yes, on what conditions? Propose the construction of sensor based on this principle.
15. Explain why and in what conditions the sensor response based on the principle of FRET between labeled sensor and labeled competitor will be more advantageous than the intensity sensing with labeling of the competitor only.
16. What is the dynamic range of λ-ratiometric response based on spectral shifts, on what factors it depends?
17. Suggest the sensor design based on a combination of λ-ratiometric response and FRET.
18. Explain the idea of signal enhancement by transforming the spectral shift into intensity ratio of two fluorescent bands.

References

Adams SR, Harootunian AT, Buechler YJ, Taylor SS, Tsien RY (1991) Fluorescence ratio imaging of cyclic AMP in single cells. Nature 349(6311):694–697

Andrews DL, Curutchet C, Scholes GD (2011) Resonance energy transfer: beyond the limits. Laser Photonics Rev 5(1):114–123

Bahr JL, Kodis G, de la Garza L, Lin S, Moore AL, Moore TA, Gust D (2001) Photoswitched singlet energy transfer in a porphyrin-spiropyran dyad. J Am Chem Soc 123(29):7124–7133

Berezin MY, Achilefu S (2010) Fluorescence lifetime measurements and biological imaging. Chem Rev 110(5):2641–2684

Billinton N, Knight AW (2001) Seeing the wood through the trees: a review of techniques for distinguishing green fluorescent protein from endogenous autofluorescence. Anal Biochem 291(2):175–197

Birks JB (1973) Organic molecular photophysics. John Wiley & Sons. New York

Braslavsky SE (2007) Glossary of terms used in Photochemistry 3(rd) Edition (IUPAC Recommendations 2006). Pure Appl Chem 79:293–465

Bright FV, Betts TA, Litwiler KS (1990) Regenerable fiber-optic-based immunosensor. Anal Chem 62:1065–1069

Burke M, O'Sullivan PJ, Soini AE, Berney H, Papkovsky DB (2003) Evaluation of the phosphorescent palladium(II)-coproporphyrin labels in separation-free hybridization assays. Anal Biochem 320(2):273–280

Callis PR (2010) Electrochromism and solvatochromism in fluorescence response of organic dyes. A nanoscopic view. In: Demchenko AP (ed) Advanced fluorescence reporters in chemistry and biology. I. Fundamentals and molecular design, vol 8, Springer series on fluorescence. Springer, Heidelberg. pp. 309–330

Chandrasekharan N, Kelly LA (2001) A dual fluorescence temperature sensor based on perylene/exciplex interconversion. J Am Chem Soc 123(40):9898–9899

Chang CJ, Javorski J, Nolan EM, Shaeng M, Lippard SJ (2004) A tautomeric zinc sensor for ratiometric fluorescence imaging: application to nitric oxide-release of intracellular zinc. Proc Natl Acad Sci U S A 101:1129–1134

Clarke RJ, Zouni A, Holzwarth JF (1995) Voltage sensitivity of the fluorescent probe RH421 in a model membrane system. Biophys J 68(4):1406–1415

Clayton AHA, Hanley QS, Arndt-Jovin DJ, Subramaniam V, Jovin TM (2002) Dynamic fluorescence anisotropy imaging microscopy in the frequency domain (rFLIM). Biophys J 83(3):1631–1649. doi:10.1016/s0006-3495(02)73932-5

Clegg RM (1996) Fluorescence resonance energy transfer. In: Wang XF, Herman B (eds) Fluorescence imaging spectroscopy and microscopy. Wiley, New York, pp 179–252

Collado D, Perez-Inestrosa E, Suau R, Desvergne JP, Bouas-Laurent H (2002) Bis(isoquinoline N-oxide) pincers as a new type of metal cation dual channel fluorosensor. Org Lett 4(5):855–858

Collier BB, McShane MJ (2013) Time-resolved measurements of luminescence. J Luminescence 144:180–190

Crosby GA, Demas JN (1971) Measurement of photoluminescence quantum yields. Review. J Phys Chem 75(8):991–1024. doi:10.1021/j100678a001

de Lorimier RM, Smith JJ, Dwyer MA, Looger LL, Sali KM, Paavola CD, Rizk SS, Sadigov S, Conrad DW, Loew L, Hellinga HW (2002) Construction of a fluorescent biosensor family. Protein Sci 11(11):2655–2675

de Silva AP, Gunaratne HQN, Gunnaugsson T, Huxley AJM, McRoy CP, Rademacher JT, Rice TE (1997) Signaling recognition events with fluorescent sensors and switches. Chem Rev 97:1515–1566

Demchenko AP (1986) Ultraviolet spectroscopy of proteins. Springer, Berlin/Heidelberg/New York

Demchenko AP (2002) The red-edge effects: 30 years of exploration. Luminescence 17(1):19–42

Demchenko AP (2005a) The future of fluorescence sensor arrays. Trends Biotechnol 23(9):456–460

Demchenko AP (2005b) Optimization of fluorescence response in the design of molecular biosensors. Anal Biochem 343(1):1–22

Demchenko AP (2005c) The problem of self-calibration of fluorescence signal in microscale sensor systems. Lab Chip 5(11):1210–1223

Demchenko AP (2006) Visualization and sensing of intermolecular interactions with two-color fluorescent probes. FEBS Letters 580(12):2951–2957

Demchenko AP (2010) The concept of lambda-ratiometry in fluorescence sensing and imaging. J Fluoresc 20(5):1099–1128

Demchenko AP (2013) Nanoparticles and nanocomposites for fluorescence sensing and imaging. Methods Appl Fluoresc 1(2):022001

Demchenko AP (2014) Practical aspects of wavelength ratiometry in the studies of intermolecular interactions. J Mol Struct 1077:51–67

Demchenko AP, Klymchenko AS, Pivovarenko VG, Ercelen S, Duportail G, Mely Y (2003) Multiparametric color-changing fluorescence probes. J Fluoresc 13(4):291–295

Demchenko AP, Sytnik AI (1991a) Site-selectivity in excited-state reactions in solutions. J Phys Chem 95:10518–10524

Demchenko AP, Sytnik AI (1991b) Solvent reorganizational red-edge effect in intramolecular electron transfer. Proc Natl Acad Sci U S A 88(20):9311–9314

Demchenko AP, Tang KC, Chou PT (2013) Excited-state proton coupled charge transfer modulated by molecular structure and media polarization. Chem Soc Rev 42(3):1379–1408. doi:10.1039/c2cs35195a

Demchenko AP, Yesylevskyy SO (2009) Nanoscopic description of biomembrane electrostatics: results of molecular dynamics simulations and fluorescence probing. Chem Phys Lipids 160(2):63–84

Di Cesare N, Lakowicz JR (2001) Wavelength-ratiometric probes for saccharides based on donor–acceptor diphenylpolyenes. J Photochem Photobiol A Chem 143:39–47

Duhamel J (2012) New insights in the study of pyrene excimer fluorescence to characterize macromolecules and their supramolecular assemblies in solution. Langmuir 28(16):6527–6538

Fan C, Plaxco KW, Heeger AJ (2005) Biosensors based on binding-modulated donor–acceptor distances. Trends Biotechnol 23(4):186–192

Fery-Forgues S, Lavabre D (1999) Are fluorescence quantum yields so tricky to measure? A demonstration using familiar stationery products. J Chem Educ 76(9):1260

Fonin AV, Sulatskaya AI, Kuznetsova IM, Turoverov KK (2014) Fluorescence of dyes in solutions with high absorbance. Inner filter effect correction. PLoS One 9(7), e103878

Fujimoto K, Shimizu H, Inouye M (2004) Unambiguous detection of target DNAs by excimer-monomer switching molecular beacons. J Org Chem 69(10):3271–3275

Ge X, Tolosa L, Govind R (2004) Dual-labeled glucose binding protein for ratiometric measurements of glucose. Anal Chem 76:1403–1410

Gershkovich AA, Kholodovych VV (1996) Fluorogenic substrates for proteases based on intramolecular fluorescence energy transfer. J Biochem Biophys Methods 33(3):135–162

Gilardi G, Zhou LQ, Hibbert L, Cass AE (1994) Engineering the maltose binding protein for reagentless fluorescence sensing. Anal Chem 66(21):3840–3847

Giordano L, Jovin TM, Irie M, Jares-Erijman EA (2002) Diheteroarylethenes as thermally stable photoswitchable acceptors in photochromic fluorescence resonance energy transfer (pcFRET). J Am Chem Soc 124(25):7481–7489

Gokulrangan G, Unruh JR, Holub DF, Ingram B, Johnson CK, Wilson GS (2005) DNA aptamer-based bioanalysis of IgE by fluorescence anisotropy. Anal Chem 77(7):1963–1970

Gong Y-J, Zhang X-B, Zhang C-C, Luo A-L, Fu T, Tan W, Shen G-L, Yu R-Q (2012) Through bond energy transfer: a convenient and universal strategy toward efficient ratiometric fluorescent probe for bioimaging applications. Anal Chem 84(24):10777–10784. doi:10.1021/ac302762d

Grichine A, Haefele A, Pascal S, Duperray A, Michel R, Andraud C, Maury O (2014) Millisecond lifetime imaging with a europium complex using a commercial confocal microscope under one or two-photon excitation. Chem Sci 5(9):3475–3485

Gross E, Bedlack RS, Loew LM (1994) Dual-wavelength ratiometric fluorescence measurement of the membrane dipole potential. Biophys J 67(1):208–216

Grynkiewicz G, Poenie M, Tsien RY (1985) A new generation of Ca2+ indicators with greatly improved fluorescence properties. J Biol Chem 260(6):3440–3450

Guo XQ, Castellano FN, Li L, Lakowicz JR (1998) Use of a long lifetime Re(I) complex in fluorescence polarization immunoassays of high-molecular weight analytes. Anal Chem 70(3):632–637

Huang J, Wu Y, Chen Y, Zhu Z, Yang X, Yang CJ, Wang K, Tan W (2011) Pyrene-excimer probes based on the hybridization chain reaction for the detection of nucleic acids in complex biological fluids. Angew Chem Int Ed 50(2):401–404

Jameson DM, Croney JC (2003) Fluorescence polarization: past, present and future. Comb Chem High Throughput Screen 6(3):167–173

Jameson DM, Ross JA (2010) Fluorescence polarization/anisotropy in diagnostics and imaging. Chem Rev 110(5):2685–2708

Jares-Erijman EA, Jovin TM (2003) FRET imaging. Nat Biotechnol 21(11):1387–1395

Jayaraman S, Biwersi J, Verkman AS (1999) Synthesis and characterization of dual-wavelength Cl–sensitive fluorescent indicators for ratio imaging. Am J Physiol 276(3 Pt 1):C747–C757

Jiang GY, Wang S, Yuan WF, Zhao Z, Duan AJ, Xu CM, Jiang L, Song YL, Zhu DB (2007) Photo- and proton-dual-responsive fluorescence switch based on a bisthienylethene-bridged naphthalimide dimer and its application in security data storage. Eur J Organic Chem 13: 2064–2067

Kapanidis AN, Weiss S (2002) Fluorescent probes and bioconjugation chemistries for single-molecule fluorescence analysis of biomolecules. J Chem Phys 117(24): 10953–10964

Kikuchi K, Takakusa H, Nagano T (2004) Recent advances in the design of small molecule-based FRET sensors for cell biology. Trends Anal Chem 23:407–415

Klymchenko AS, Demchenko AP (2002) Electrochromic modulation of excited-state intramolecular proton transfer: The new principle in design of fluorescence sensors. J Am Chem Soc 124(41):12372–12379

Klymchenko AS, Demchenko AP (2003) Multiparametric probing of intermolecular interactions with fluorescent dye exhibiting excited state intramolecular proton transfer. Phys Chem Chem Phys 5(3):461–468

Koch M, Perumal K, Blacque O, Garg JA, Saiganesh R, Kabilan S, Balasubramanian KK, Venkatesan K (2014) Metal-free triplet phosphors with high emission efficiency and high tunability. Angew Chemie Int Ed Engl 53(25):6378–6382

Koronszi I, Reichert J, Heinzmann G, Ache HJ (1998) Development of submicron optochemical potassium sensor with enhanced stability due to internal reference. Sensors Attenuators B 51: 188–195

Kostenko E, Dobrikov M, Komarova N, Pyshniy D, Vlassov V, Zenkova M (2001) 5′-bis-pyrenylated oligonucleotides display enhanced excimer fluorescence upon hybridization with DNA and RNA. Nucleosides Nucleotides Nucleic Acids 20(10–11):1859–1870

Kuwana E, Sevick-Muraca EM (2002) Fluorescence lifetime spectroscopy in multiply scattering media with dyes exhibiting multiexponential decay kinetics. Biophys J 83(2):1165–1176

Lakowicz JR (2006) Principles of fluorescence spectroscopy, 3rd edn. Springer, New York

Liebsch G, Klimant I, Krause C, Wolfbeis OS (2001) Fluorescent imaging of pH with optical sensors using time domain dual lifetime referencing. Anal Chem 73(17):4354–4363

Mahara A, Iwase R, Sakamoto T, Yamana K, Yamaoka T, Mirakami A (2002) Bispyrene-conjugated 2′-O-methyloligonucleotide as a highly specific RNA-recognition probe. Angew Chem Int Ed 41:3648–3650

Maliwal BP, Gryczynski Z, Lakowicz JR (2001) Long-wavelength long-lifetime luminophores. Anal Chem 73(17):4277–4285

Malval J-P, Lapouyade R, Leger JM, Jany C (2003) Tripodal ligand incorporating dual fluorescent ionophore: a coordinative control of photochemical electron transfer. Photochem Photobiol Sci 2:259–266

McCauley TG, Hamaguchi N, Stanton M (2003) Aptamer-based biosensor arrays for detection and quantification of biological macromolecules. Anal Biochem 319(2):244–250

McFarland SA, Finney NS (2001) Fluorescent chemosensors based on conformational restriction of a biaryl fluorophore. J Am Chem Soc 123(6):1260–1261

Minta A, Kao JP, Tsien RY (1989) Fluorescent indicators for cytosolic calcium based on rhodamine and fluorescein chromophores. J Biol Chem 264(14):8171–8178

Nielsen K, Lin M, Gall D, Jolley M (2000) Fluorescence polarization immunoassay: detection of antibody to Brucella abortus. Methods 22(1):71–76

Oheim M, Naraghi M, Muller TH, Neher E (1998) Two dye two wavelength excitation calcium imaging: results from bovine adrenal chromaffin cells. Cell Calcium 24(1):71–84

Oncul S, Demchenko AP (2006) The effects of thermal quenching on the excited-state intramolecular proton transfer reaction in 3-hydroxyflavones. Spectrochim Acta A Mol Biomol Spectrosc 65(1):179–183

Owicki JC (2000) Fluorescence polarization and anisotropy in high throughput screening: perspectives and primer. J Biomol Screen 5(5):297–306

Park HG, Song JY, Park KH, Kim MH (2006) Fluorescence-based assay formats and signal amplification strategies for DNA microarray analysis. Chem Eng Sci 61(3):954–965

Petitjean A, Lehn JM (2007) Conformational switching of the pyridine-pyrimidine-pyridine scaffold for ion-controlled FRET. Inorg Chim Acta 360(3):849–856

Povrozin YA, Kolosova OS, Obukhova OM, Tatarets AL, Sidorov VI, Terpetschnig EA, Patsenker LD (2009) Seta-633 – a NIR fluorescence lifetime label for low-molecular-weight analytes. Bioconjug Chem 20(9):1807–1812

Prendergast FG, Meyer M, Carlson GL, Iida S, Potter JD (1983) Synthesis, spectral properties, and use of 6-acryloyl-2-dimethylaminonaphthalene (Acrylodan). A thiol-selective, polarity-sensitive fluorescent probe. J Biol Chem 258:7541–7544

Prokhorenko IA, Astakhova IV, Momynaliev KT, Zatsepin TS, Korshun VA (2009) Phenylethynylpyrene excimer forming hybridization probes for fluorescence SNP detection. Methods Mol Biol 578:209–222

Putkey JA, Liu W, Lin X, Ahmed S, Zhang M, Potter JD, Kerrick WG (1997) Fluorescent probes attached to Cys 35 or Cys 84 in cardiac troponin C are differentially sensitive to Ca(2+)-dependent events in vitro and in situ. Biochemistry 36(4):970–978

Raymond FR, Ho HA, Peytavi R, Bissonnette L, Boissinot M, Picard FJ, Leclerc M, Bergeron MG (2005) Detection of target DNA using fluorescent cationic polymer and peptide nucleic acid probes on solid support. BMC Biotechnol 5

Richieri GV, Ogata RT, Kleinfeld AM (1992) A fluorescently labeled intestinal fatty acid binding protein. Interactions with fatty acids and its use in monitoring free fatty acids. J Biol Chem 267(33):23495–23501

Rurack K (2001) Flipping the light switch 'on' – the design of sensor molecules that show cation-induced fluorescence enhancement with heavy and transition metal ions. Spectrochim Acta A 57:2161–2195

Rurack K (2008) Fluorescence quantum yields: methods of determination and standards. In: Resch-Genger U (ed) Standardization and quality assurance in fluorescence measurements I, vol 5, Springer Ser Fluoresc. Springer, Berlin/Heidelberg, pp 101–145

Sahoo D, Narayanaswami V, Kay CM, Ryan RO (2000) Pyrene excimer fluorescence: a spatially sensitive probe to monitor lipid-induced helical rearrangement of apolipophorin III. Biochemistry 39(22):6594–6601

Sanchez-Barragan I, Costa-Fernandez JM, Valledor M, Campo JC, Sanz-Medel A (2006) Room-temperature phosphorescence (RTP) for optical sensing. Trends Anal Chem 25(10): 958–967

Selvin PR (2000) The renaissance of fluorescence resonance energy transfer. Nat Struct Biol 7(9):730–734

Shynkar V, Mely Y, Duportail G, Piemont E, Klymchenko AS, Demchenko AP (2003) Picosecond time-resolved fluorescence studies are consistent with reversible excited-state intramolecular proton transfer in 4′-dialkylamino-3-hydroxyflavones. J Phys Chem A 109:9522–9529

Shynkar VV, Klymchenko AS, Piemont E, Demchenko AP, Mely Y (2004) Dynamics of intermolecular hydrogen bonds in the excited states of 4′-dialkylamino-3-hydroxyflavones. On the pathway to an ideal fluorescent hydrogen bonding sensor. J Phys Chem A 108(40): 8151–8159

Smallshaw JE, Brokx S, Lee JS, Waygood EB (1998) Determination of the binding constants for three HPr-specific monoclonal antibodies and their Fab fragments. J Mol Biol 280: 765–774

Sportsman JR, Daijo J, Gaudet EA (2003) Fluorescence polarization assays in signal transduction discovery. Comb Chem High Throughput Screen 6(3):195–200

Suhling K, French PMW, Phillips D (2005) Time-resolved fluorescence microscopy. Photochem Photobiol Sci 4(1):13–22

Suppan P, Ghoneim N (1997) Solvatochromism. Royal Society of Chemistry, Cambridge, UK

Szmacinski H, Lakowicz JR (1994) Lifetime-based sensing. In: Lakowicz JR (ed) Topics in fluorescence spectroscopy, vol 4. Plenum Press, New York, pp 295–334

Takakusa H, Kikuchi K, Urano Y, Kojima H, Nagano T (2003) A novel design method of ratiometric fluorescent probes based on fluorescence resonance energy transfer switching by spectral overlap integral. Chemistry 9(7):1479–1485

Takakusa H, Kikuchi K, Urano Y, Sakamoto S, Yamaguchi K, Nagano T (2002) Design and synthesis of an enzyme-cleavable sensor molecule for phosphodiesterase activity based on fluorescence resonance energy transfer. J Am Chem Soc 124(8):1653–1657

Thompson RB, Maliwal BP, Feliccia VL, Fierke CA, McCall K (1998) Determination of picomolar concentrations of metal ions using fluorescence anisotropy: biosensing with a “reagentless” enzyme transducer. Anal Chem 70(22):4717–4723

Tolosa L, Ge X, Rao G (2003) Reagentless optical sensing of glutamine using a dual-emitting glutamine-binding protein. Anal Biochem 314(2):199–205

Tomin VI, Demchenko AP, Chou P-T (2015) Thermodynamic vs. Kinetic Control of Excited-State Proton Transfer Reactions. J Photochem Photobiol C Photochem Rev 22(1):1–18

Tomin VI, Oncul S, Smolarczyk G, Demchenko AP (2007) Dynamic quenching as a simple test for the mechanism of excited-state reaction. Chem Phys 342:126–134

Torimura M, Kurata S, Yamada K, Yokomaku T, Kamagata Y, Kanagawa T, Kurane R (2001) Fluorescence-quenching phenomenon by photoinduced electron transfer between a fluorescent dye and a nucleotide base. Anal Sci 17(1):155–160

Turro NJ, Ramamurthy V, Scaiano JC (2009) Principles of molecular photochemistry: an introduction. University Science, Sausalito

Ueberfeld J, Walt DR (2004) Reversible ratiometric probe for quantitative DNA measurements. Anal Chem 76(4):947–952

Valeur B, Berberan-Santos MN (2012) Molecular fluorescence: principles and applications. Wiley-VCH Verlag GmbH, Weinheim, FRG. doi:10.1002/3527600248.fmatter_indsub

Vazquez ME, Blanco JB, Imperiali B (2005) Photophysics and biological applications of the environment-sensitive fluorophore 6-N, N-Dimethylamino-2,3-naphthalimide. J Am Chem Soc 127(4):1300–1306

Vogt RFJ, Marti GE, Zenger V (2008) Quantitative fluorescence calibration: a tool for assessing the quality of data obtained by fluorescence measurements. In: Resch-Genger U (ed) Standardization and quality assurance in fluorescence measurements I: techniques, vol 05, Springer series on fluorescence. Springer, Heidelberg, pp 3–31

Walkup GK, Imperiali B (1996) Design and evaluation of a peptidyl fluorescent chemosensor for divalent zinc. J Am Chem Soc 118:3053–3054

Wang L, Clifford B, Graybeal L, Tolley L, McCarroll ME (2013) Detection of target proteins by fluorescence anisotropy. J Fluoresc 23(5):881–888

Wu PG, Brand L (1994) Resonance energy-transfer – methods and applications. Anal Biochem 218(1):1–13

Würth C, Grabolle M, Pauli J, Spieles M, Resch-Genger U (2011) Comparison of methods and achievable uncertainties for the relative and absolute measurement of photoluminescence quantum yields. Anal Chem 83(9):3431–3439

Xu H, Wu HP, Huang F, Song SP, Li WX, Cao Y, Fan CH (2005a) Magnetically assisted DNA assays: high selectivity using conjugated polymers for amplified fluorescent transduction. Nucleic Acids Res 33(9)

Xu J, Takai A, Kobayashi Y, Takeuchi M (2013) Phosphorescence from a pure organic fluorene derivative in solution at room temperature. Chem Commun 49(76):8447–8449

Xu QH, Wang S, Korystov D, Mikhailovsky A, Bazan GC, Moses D, Heeger AJ (2005b) The fluorescence resonance energy transfer (FRET) gate: a time-resolved study. Proc Natl Acad Sci U S A 102(3):530–535

Yamana K, Ohshita Y, Fukunaga Y, Nakamura M, Maruyama A (2008) Bis-pyrene-labeled molecular beacon: a monomer-excimer switching probe for the detection of DNA base alteration. Bioorg Med Chem 16(1):78–83

Yamauchi A, Hayashita T, Nishizawa S, Watanabe M, Teramae N (1999) Benzo-15-crown-5 fluoroionophore/cyclodextrin complex with remarkably high potassium ion sensitivity in water. J Am Chem Soc 121:2319–2320

Yang RH, Chan WH, Lee AWM, Xia PF, Zhang HK, Li KA (2003) A ratiometric fluorescent sensor for Ag-1 with high selectivity and sensitivity. J Am Chem Soc 125(10):2884–2885

Yang Y, Ji S, Zhou F, Zhao J (2009) Synthesis of novel bispyrene diamines and their application as ratiometric fluorescent probes for detection of DNA. Biosens Bioelectron 24(12):3442–3447

Yoshihara T, Galievsky VA, Druzhinin SI, Saha S, Zachariasse KA (2003) Singlet excited state dipole moments of dual fluorescent N-phenylpyrroles and 4-(dimethylamino)benzonitrile from solvatochromic and thermochromic spectral shifts. Photochem Photobiol Sci 2:342–353

Yu C, Yam VW (2009) Glucose sensing via polyanion formation and induced pyrene excimer emission. Chem Commun (Camb) 11:1347–1349

Yu Z, Ptaszek M (2013) Near-IR emissive chlorin–bacteriochlorin energy-transfer dyads with a common donor and acceptors with tunable emission wavelength. J Org Chem 78(21):10678–10691

Chapter 4
Molecular-Size Fluorescence Emitters

A variety of fluorescent and luminescent materials in the form of molecules, their complexes and nanoparticles are available for implementation as response units into sensing and imaging technologies and we discuss their general properties that are essential for these applications. Organic dyes were the first and remain to be the most popular emitters used with these purposes. Their labeling and responsive properties are overviewed. Natural fluorescent proteins and their engineered analogues incorporate organic fluorophores that are synthesized spontaneously from the polypeptide chain inside the living cells without the need of their intrusion, as the gene products. They resulted in revolutionary advancement in cell imaging and show good prospects in sensing and reporting on cellular processes. Organic heterocyclic compounds can incorporate metal ions generating long-living luminescence. Moreover, noble metal particles of a very small size exhibit unique light-absorbing and fluorescent emission properties. In this Chapter we focus on these types of fluorophores that possess subnanometer dimensions and display single type of absorption-emission cycle. The more complex nanostructures and nanocomposites will be overviewed in Chaps. 5 and 6 that follow.

4.1 Fluorophores and Their Characteristics

4.1.1 General Properties of Fluorescent Dyes

In view of tremendous diversity of structures, chemical reactivities and spectroscopic properties, one needs certain practically useful criteria for the dye selection for the purpose of sensing and imaging. They can be formulated in the form of spectroscopic parameters that have to be optimized.

A.P. Demchenko, *Introduction to Fluorescence Sensing*,
DOI 10.1007/978-3-319-20780-3_4

4.1.1.1 High Molar Absorbance, ε

It is the parameter describing the ability of molecule to absorb light at a particular wavelength. The absorbance E measured at any wavelength on spectrophotometer is proportional to the dye concentration c (in mol/l) and the light path length in a sample l (in cm). In this relation, ε plays the role of coefficient of proportionality, so that $E = \varepsilon cl$. The value of molar absorbance is obtained by purifying and drying the dye, dissolving it at low concentration and measuring E on a spectrophotometer. The broadly used term *extinction* includes absorbance and light scattering. Absorbance is a unique characteristic of a molecule under certain environmental conditions. In general, the bigger the fluorophore size, the greater is the probability that the photon will be absorbed.

The value of ε^{max} at the maximum of absorption band is the common characteristic of the light-absorbing power of the dye. The dye '*brightness*' that determines the absolute sensitivity of fluorescence detection (Wetzl et al. 2003) is the product of molar absorbance and quantum yield, Φ. The absorbance is related to optical cross-section and for organic dyes, ε^{max} varies from ca. 10^3 l mol^{-1} cm^{-1} for small dyes, such as coumarins to ca. 10^5 l mol^{-1} cm^{-1} for larger fluorophores such as cyanines and phthalocyanines (Lavis and Raines 2008). It should be selected as high as possible, but the limiting factor is the fluorophore size. Using the dyes with lower ε^{max} values is not reasonable, and much higher values are hardly achievable.

4.1.1.2 High Quantum Yield, Φ

Quantum yield of any process is the ratio of a number of quanta participating in this process to a total number of absorbed quanta. For fluorescence, it is the ratio of the number of light quanta emitted as fluorescence to the total number of quanta that were absorbed.

In addition to fluorescence, the dyes can participate in different non-emissive reactions. So, Φ is used as a measure of efficiency of fluorescence emission compared to other processes occurring during the excited-state lifetime, such as static and collisional quenching, transition to triplet state or photochemical transformations. Commonly Φ is measured by a reference method comparing in the same experimental conditions the fluorescence spectra the solutions of the studied sample and the reference (Brouwer 2011). The tabulated Φ values for the references covering the whole spectral range are available (Lakowicz 2006).

Primarily, Φ depends on the dye structure, and it is not easy to predict it based on calculations. We can only estimate the efficiency of non-emissive channels of excited-state decay, such as internal vibrations. Moreover, the quantum yield can be modulated in a most dramatic way by interactions with the dye environment. The Φ values may vary from very low numbers (in relative units) to almost 100 %. The

sensing technique, in which the change of fluorescence intensity is recorded as an effect of quenching (Sect. 3.2), is based on variations of quantum yield.

4.1.1.3 Optimal Excitation Wavelength

In order to achieve the highest brightness, one has to excite fluorescence at wavelengths close to the absorption band maximum. Since the dye brightness is estimated as the product of molar absorbance $\varepsilon(\lambda_{ex})$ (at the applied excitation wavelength) and fluorescence quantum yield Φ, it is important that the excitation wavelength, λ_{ex}, should be chosen optimally with this account.

Other factors are important for selecting the dyes with excitation band at particular wavelength, such as the availability of light sources, necessity to avoid autofluorescence background in living cell studies, etc. To avoid the cells autofluorescence, the excitation at wavelengths longer than 400–460 nm is preferable. For the diagnostic sensors implemented under the human skin one has to account that the skin has a very low transparency throughout the whole visible range due to absorption by porphyrins and skin pigments. Such absorption is dramatically reduced in the near-IR, until the vibrational overtones of water appear, so the range 650−1450 nm is optimal for this application (Pansare et al. 2012).

4.1.1.4 Optimal Emission Wavelength

The range of operational wavelengths should be selected with the account of wavelength dependence of the sensitivity of detector. If the detector is a human eye, then the emission should be in the visible range of 400–700 nm. Many spectrofluorimeters available on the market are equipped with photodetectors with the cutting edge of 750–800 nm, which is not sufficient for recording of spectra of many dyes. However, the special "red-sensitive" photomultipliers can be supplied at a special request. Different red-infrared detectors using semiconductor elements have become available in recent time.

4.1.1.5 Large Stokes Shift

This shift is between absorption and emission band maxima on the energy (wavenumber) scale. The Stokes shift reflects the loss of excitation energy in different relaxation processes before the emission and is commonly observed in the direction of low energies and long wavelengths. The strongest Stokes shifts are observed for dyes with asymmetric structure and stronger charge distribution within the fluorophore. The most popular dyes as fluorescent tags and labels, fluorescein,

rhodamines, cyanines and symmetric BODIPY derivatives, possess a rather small Stokes shift. Light scattering can be a difficult problem with such dyes enabling to provide recording of excitation and emission aside from the band maxima. Meantime, stronger separation between absorption and emission bands allows reducing the light-scattering effects and provides possibilities for more efficient collection of emitted light using broad-band filters or larger monochromator slits.

Larger Stokes shift allows reducing homo-FRET (excitation energy transfer between the same dye molecules) thus allowing to suppress the concentration-dependent depolarization and quenching (see Sect. 6.1). The high-density attachment of these dyes to macromolecules and their incorporation into nanocomposite structures is possible. In some sensing technologies the dyes possessing strong Stokes shifts behave within these high-density units as independent emitters.

4.1.1.6 Optimal Fluorescence Lifetime, τ_F

This parameter depends on the dye and cannot be longer than the radiative lifetime, which is the fundamental property of a particular dye. The lifetime also depends on the temperature and the dye immediate environment. So depending on the application it can be selected long or short by choosing the dye and its environment.

Long lifetime is easy to detect and analyze. It is usually associated with a high quantum yield (the absence or small involvement of quenching effects). However, the long lifetimes (longer than 10^{-7} s, such as that of pyrene) are quenched by oxygen diffusing in the medium, so it is sometimes difficult to control this parameter. In anisotropy sensing (polarization assays), to provide the strongest effect the lifetime should fit the time scale of molecular rotations (see Sect. 3.3). Its long values are needed to detect rotations of large molecular units.

Meantime for some applications, short τ_F is preferable. So it is in flow cytometry, in which a small number of dyes are under intensive excitation and the response may be limited by the duration of excitation-emission cycle. It must also be noted that due to a fundamental limitation, long τ_F cannot be achieved with high ε^{max}.

4.1.1.7 High Photostability

Each fluorescent dye can be degraded (photobleached) after some number of excitation-emission cycles (Eggeling et al. 1998). *Photobleaching* is a consequence of higher dye chemical reactivity in the excited states. Degradation occurs due to some photochemical reaction that often involves molecular oxygen and is coupled with the production of singlet oxygen. Fluorescein molecules can survive between 10^4 and 10^5 excitation-emission cycles before decomposing. The dyes differ strongly in their photostability, so coumarins are among the least stable and perylene,

rhodamins and cyanines are much more photostable. Commonly the dyes are distinguished as being more photostable or less photostable than fluorescein.

In sensing technologies that do not require exposure to intensive light, photostability is not a big problem. It may not be important in spectroscopic studies, in which the narrow excitation slits and fast recording of spectra are used. In flow cytometry and microplate reading, the photo-bleaching is generally not a problem because the sample remains in the laser beam for a very short period of time. Otherwise, oxygen can be removed from the system, which requires oxygen-free atmosphere or consumption of oxygen in any coupled reaction. Such possibility may not exist in fluorescence microscopy of living cells, and this often limits obtaining cellular images to a short time scale. Photostability is an important issue in single molecular studies (Sect. 13.3) and in super-resolution microscopy (Sect. 13.2), where the dye molecules are subjected to high light intensities (Ha and Tinnefeld 2012).

4.1.1.8 Optimal Solubility – Penetration – Reactivity in the Used System

Each dye has particular physical and chemical properties (polarity, charge distribution, reactivity to form covalent bonds, ability to participate in π–π stacking, hydrogen bonding and other noncovalent interactions). These properties determine the dye distribution in a heterogeneous system (e.g. on a liquid-solid interface, in cell cytoplasm or biomembrane) and determines the extent of labeling of particular macromolecules or organelles. In addition, the dye has to be chemically stable and its fluorescence should be insensitive or low sensitive to the factors like pH or temperature if this sensitivity is not wanted.

The quantum yields, lifetimes and photostabilities of organic dyes are variable in broad ranges and they can be substantially improved by encapsulating them into *macrocyclic host* molecules (Dsouza et al. 2011) such as cyclodextrins and cucurbiturils (Biedermann et al. 2012). Such macrocycle-protected dyes can be used in nanocomposite constructions being incorporated into the particles made of inorganic (Liang et al. 2010) or organic (Borisov et al. 2010) polymers (see Sect. 5.2). The most attractive are the dye-doped composites based on dendrimers, which allow maintaining the definite size and molecular order of composed structures (Bergamini et al. 2010).

4.1.2 Labeling and Sensing – Two Basic Methodologies

With regard to applications, we need to draw distinguishing line between ‘labeling’ and ‘sensing’ functions of fluorescence emitters because these functions are

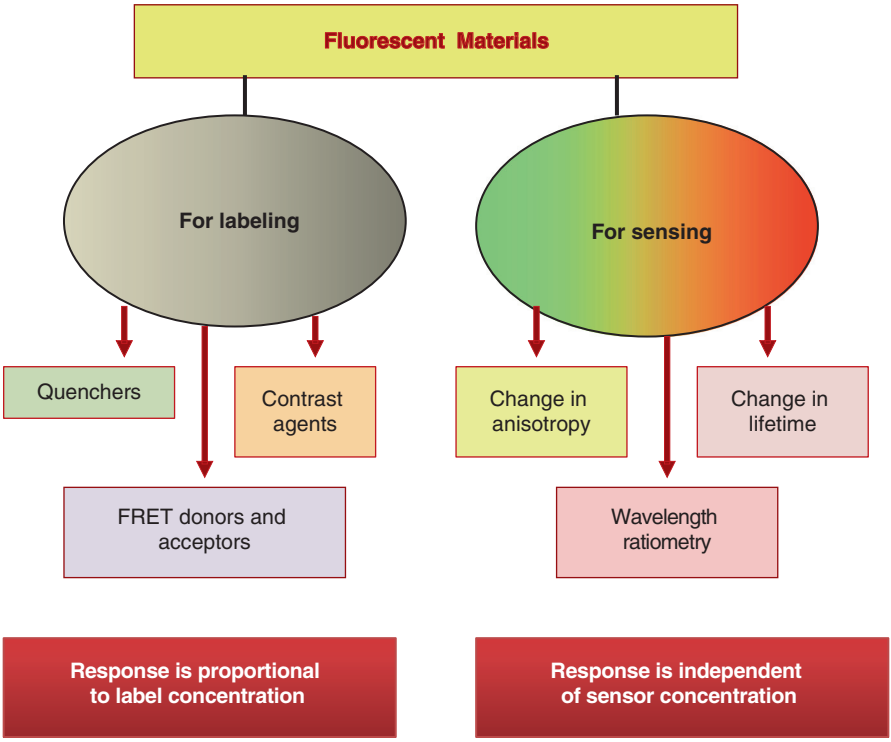

Fig. 4.1 Two trends in application of fluorescent materials in sensing and imaging. The labels should be insensitive to any parameter changing the fluorescence emission. In contrast, the fluorescence reporters participating in sensor functions should provide the changes of fluorescence parameters in response to particular stimuli in the broadest possible dynamic range

essentially different (Fig. 4.1). The role of '*labels*', '*tracers*' or '*tags*' is solely to indicate their presence in particular medium or at particular site (often achieved by their specific binding), so that their own concentration displayed as fluorescence intensity is the source of information. In the case of labeling the output signal should be proportional to fluorophore concentration. For achieving that, spatial separation between free and target-bound labeled sensor may be needed. Therefore they are used to identify and quantify the target on microarrays, microscopy images, chromatograms, electrophoregrams and other systems with spatial separation. There is a broad selection of fluorescent species for labeling. Their major parameters that have to be optimized are the brightness and photostability, together with optimal conditions for excitation and emission.

Quite a different function of fluorescent materials is their serving as '*probes*', '*sensors*' or '*reporters*'. They should respond to the changes of their molecular environment (probes) or to the target binding (sensors) by the change of parameters

of their emission and therefore they should satisfy often special and more stringent requirements. For providing informative response their fluorescence emission should be switchable and coupled with target recognition events. Here the brightness and photostability are equally important, but the optimized parameters should be those that allow their variation in the broadest possible range. Responding to sensing event they should provide the output signal independent of their own concentration and the factors intervening with sensing.

Thus, both types of dyes, for labeling and sensing are useful in fluorescence-based technologies, but in different ways. For obtaining the highest brightness and highest contrast and also for optimal protection against various quenching and bleaching effects or perturbations by the interactions with the medium one has to choose the 'labels'. Alternatively, if we wish together with the high brightness to attain the highest dynamic range of response in terms of variations of intensity, lifetime or of the wavelength of emission, we choose the 'sensors' or 'probes'. In their design we need to activate some photophysical mechanism of response (ESIPT, FRET, static or dynamic quenching, isomerizations, formation of exciplexes, etc.). This limits dramatically the choice of fluorophores that must possess desired features. In the sections that follow we will discuss different molecular-size fluorescence emitters that can perform these tasks. Nanoscale format of fluorophores offers many additional possibilities for efficient applications. They will be discussed in Chaps. 5 and 6.

4.2 Organic Dyes as Labels and Tags

Organic dyes are the most commonly used fluorophores in sensing and imaging. Their advantages are not only in easy availability and low price, but also, most importantly, in their versatility in applications. Whereas all types of fluorescence emitters can be used for labeling and can respond to external stimuli by changing the emission intensity and lifetime, organic dyes demonstrate much richer means of response, including strong changes in anisotropy and strong shifts in excitation and emission spectra. Additionally, fluorescence of organic dyes may contain chemical modifications making them reactive in certain conditions or binding analytes for their use in sensing and chemoselective bioimaging (Chan et al. 2012). Finally, the dyes can display ground-state and excited-state reactions leading to the generation of new emission bands that allow convenient and very sensitive wavelength ratiometric detection. They offer tremendous possibilities in applications due to immense variations of their structures and diversity of their spectroscopic properties (Patsenker et al. 2010a; Przhonska et al. 2010; Kim and Park 2010).

The number of fluorescent synthetic organic products is so great that a researcher can easily select the proper dye corresponding to particular need in

terms of spectroscopic properties and chemical reactivity (Dsouza et al. 2011). Within the same fluorophore family, a variety of species can be synthesized that modulate the spectroscopic properties by electron-donor and electron-acceptor substitutions (Gonçalves 2010) and the labeling with different specificity and reactivity for covalent labeling. Due to their small size and the ability of incorporation with minimal perturbation into biological structures (e.g. biomembranes, proteins or nucleic acids), organic dyes are ideally suited as both molecular labels and reporters.

In the past, the field of organic dye synthesis was strongly stimulated by the needs of color photography and dye laser technologies. These needs were diminished with the development of electronic digital photography and solid-state lasers, so that the implementation into molecular probe and sensor technologies became the major field of application of novel organic dyes. The amount of newly synthesized dyes grows exponentially, and it is not possible to describe in a small section of a book even the most important of them. Therefore, we will concentrate on their general properties that are essential for sensing applications and describe several of their classes that are frequently used. Many original publications, reviews (Lavis and Raines 2008; Wysocki and Lavis 2011; Grimm et al. 2012; Gonçalves 2008) and online resources will be of help to the researcher . In line with the classification introduced above we will discuss separately the dyes used for labeling and those used for reporting.

4.2.1 General Properties of Organic Dyes

Organic dyes, the size of which is commonly less than 1 nm, are characterized by the presence of delocalized π-electrons forming discrete energy states. Absorption of light quanta and their emission occurs as electronic transitions between these states. The wavelengths of their emission occupy the whole visible range extending to near-IR. The increase in the number of π-electrons and of electronic conjugation between their molecular fragments usually shift the fluorescence spectra to lower energies, longer wavelengths (Levitus and Ranjit 2011). Their fluorescence quantum yields can vary dramatically from almost zero to nearly 100 %. Some of the basic parameters of organic dyes are listed in Table 4.1 that may help the reader with a brief navigation of their properties and comparing them with those of other luminescent emitters discussed throughout this book.

Organic dyes offer tremendous diversity of structures, chemical reactivities and spectroscopic properties, which is the great advantage of these fluorescent materials. The weak points are their relatively low brightness and limited availability of sites for their covalent modification that often changes their properties. Their applications in cellular research are limited due to their low photostability. Some of these features can be improved by encapsulating them into polymeric or macrocyclic host

Table 4.1 The properties of organic dyes used in fluorescence sensing technologies

Parameter	Property
Size	~1 nm
Absorption spectra	Variable and often narrow, asymmetric and sometimes with vibronic structure, sensitive to intermolecular interactions
Molar absorption, ε	Variable, usually in the range 10^3–10^5 M^{-1} cm^{-1}
Emission spectra	Broad (~40–70 nm half-width) and asymmetric, position may exhibit strong sensitivity to intermolecular interactions
Stokes shifts	Variable, commonly ~10–100 nm
Excited-state lifetime, τ_F	Short, ~0.5–5 ns (with few exceptions)
Fluorescence quantum yield, Φ	Variable, strongly dependent upon the medium
Two-photonic cross-section, α	Strongly variable and uncorrelated with ε
Fundamental emission anisotropy, r^0	Variable, up to 0.3–0.4
Photostability	Variable to poor
Chemical resistance	Variable and often low
Availability of chemical modification/functionalization	Variable to high
Cell toxicity	Variable, often low. High phototoxicity may be observed in some cases

molecules (Dsouza et al. 2011), see Sect. 5.2, but at the expense of their 'molecularity'.

The great number of fluorescent organic dyes used in sensing and imaging applications reflect the fact that the ideal dyes simply do not exist, and the researcher has to compromise some properties for making other properties ideal for particular application. Therefore the first question to respond is on a ***particular role that the dye has to play in the sensing process***. It could be the labeling of a sensor, of a competitor or of a sample pool containing the target (the dye indicates its location or attachment to particular structure). These are the simplest applications, to which many dyes are well suited. If the reporting function is needed (the parameters of dye emission should be changed on interaction with the target), then additional criteria should be introduced. As it was stated above, fluorescent dyes can be classified into two broad categories: no responsive (used for labeling) and responsive (used as probes and reporters in molecular sensing). The first operate based just on their presence in particular medium or at particular site. Second, in contrast, should respond to different stimuli required in sensing and probing by the most significant change of fluorescence parameters. Ideally, this response should not depend on dye concentration.

There is a general principle. If the electronic density is delocalized over the whole fluorophore, which is characteristic of resonant or mesomeric dyes, such as fluoresceins, rhodamines, and cyanines, the spectral sensitivity to environment is small. In contrast, the dyes exhibiting polarization of electronic structures that changes on optical excitation can be potent responsive fluorescence reporters.

4.2.2 The Most Efficient Dyes for Labeling

High quantum yield of fluorescence emission in solutions can be achieved in the case of resonant or mesomeric dyes, such as fluoresceins, rhodamines, and cyanines. Their skeleton is rigid, which allows minimizing the vibrations-related energy losses and their electronic density is delocalized over the whole fluorophore. Because of the absence of strong charge asymmetry their interaction with polar environment is small and it is the reason why we observe their small Stokes shift and low spectral sensitivity to the environment.

There are several classes of dyes that conform in the best way to the criteria for optimal labels and tags. They can be efficiently used if a 'responsive' function is not needed. Those are the modified *fluorescein* and *rhodamine* derivatives, *BODIPY* and also *cyanine* dyes. Synthetic chemistry suggests many improvements in their properties. The 'classical' dyes together with their most efficient improvements are discussed below.

Figure 4.2 presents the structures of fluorescein and rhodamine 123 and the spectra of the latter, which is typical in this respect.

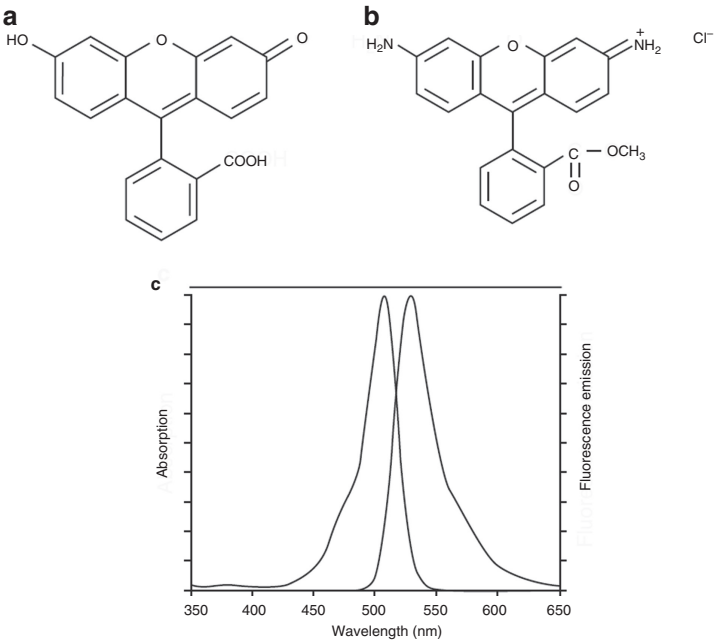

Fig. 4.2 The structures of fluorescein (**a**) and rhodamine 123 (**b**) and normalized absorption and fluorescence spectra of rhodamine 123 in methanol (**c**) (Haugland 2005)

Fluoresceins The structure of parent fluorescein dye is presented in Fig. 4.2. These dyes are widely used for labeling in the form of amine-reactive and SH-reactive derivatives (see Fig. 9.10). They possess relatively high absorbance, high fluorescence quantum yield (even in water) and high aqueous solubility. Additionally, due to the fact that their excitation band maximum matches closely the 488 nm spectral line of the most popular argon-ion laser, these dyes are very well accepted in confocal laser-scanning microscopy and flow cytometry applications. Meantime, fluorescein dyes possess many essential drawbacks. They demonstrate low photostability and also the presence of pH-sensitivity of fluorescence spectra with significant reduction of intensity below pH 7. They are subjective to strong concentration-dependent quenching that does not allow obtaining high density of labels. Photostability and pH-sensitivity of fluorescein can be finely tuned by chemical modifications. Its derivative Oregon Green behaves in a more attractive way. It is a fluorinated analogs of fluorescein that in the conditions of high degrees of labeling is quenched to a much lesser extent. It is more photostable and pH-insensitive in the physiological pH range (Haugland 1996).

Rhodamines (see Fig. 4.2) Just like fluoresceins, rhodamine dyes are considered as a popular choice of the dyes for labeling. They absorb and emit light at longer wavelengths and may be used in techniques employing them as acceptors for FRET from fluorescein dyes. Their excitation band maxima are located at about 520 nm, which is close to the green 514 nm spectral line of the argon-ion laser, making them both popular and important in the studies involving confocal microscopy and flow cytometry.

Selected as an example, rhodamine 123 is a cationic green-fluorescent dye with good solubility in water and the ability to permeate the living cells. When used in biological labeling it is sequestered by active mitochondria without cytotoxic effects. Because of its positive charge, its binding to mitochondria depends on membrane potential of this organelle. Due to small Stokes shift (see Fig. 3.2), this dye is self-quenched when accumulates in mitochondria in high concentrations and thus provides a ‘slow’ response to its membrane potential (Plasek and Sigler 1996).

New modifications of rhodamine were developed recently. Particularly important are Si-rhodamines (Koide et al. 2011) and carbo-rhodamines (Kolmakov et al. 2010). Variation of the functionality at the position 10 of rhodamine skeleton results in new near-infrared dyes with improved brightness and photostability. These dyes are particularly useful for super-resolution fluorescence microscopy.

Alexa Dyes These organic dye molecules are obtained by sulphonation of aminocoumarin, rhodamine, or carbocyanine dyes (Haugland 1996). The introduction of negatively charged sulfonic acid groups makes these molecules more water-soluble and decreases their inherent tendency to form aggregates.

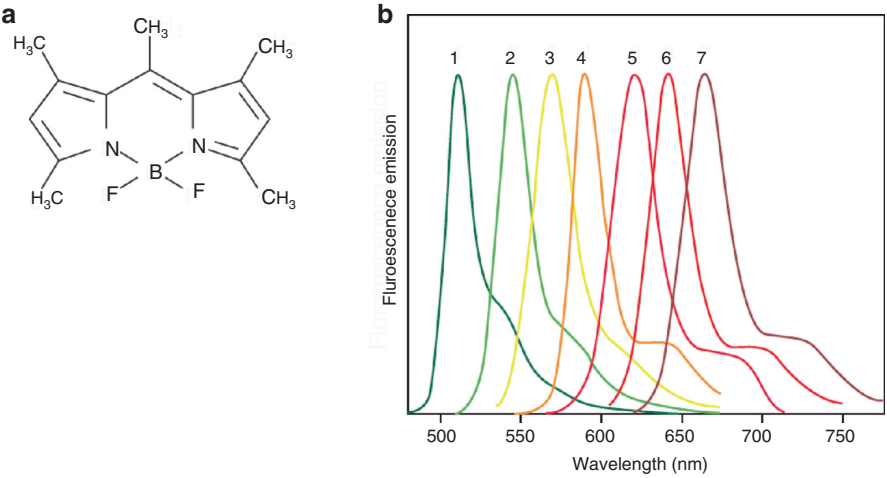

Fig. 4.3 The BODIPY (4,4-difluoro-4-bora-3a,4adiaza-s-indacene) dyes (Haugland 1996). (**a**) The structure of the parent fluorophore. (**b**) Normalized fluorescence emission spectra of (*1*) BODIPY FL, (*2*) BODIPY R6G, (*3*) BODIPY TMR, (*4*) BODIPY 581/591, (*5*) BODIPY TR, (*6*) BODIPY 630/650 and (*7*) BODIPY 650/665 dyes in methanol

This also allows performing their conjugation with biological macromolecules in the absence of organic solvents. The excitation and emission wavelength ranges of Alexa dyes cover the entire spectrum from ultraviolet to red with the retention of such properties of parent compounds as high molar absorbance. They are less subjective to self-quenching and their photostability is even higher (Panchuk-Voloshina et al. 1999).

BODIPY Dyes (Fig. 4.3) BODIPY (deriving from borondipyrromethene) are a large class of fluorescent dyes based on 4,4-difluoro-4-borata-3a-azonia-4a-aza-s-indacene skeleton The variations of their synthetic pathways and structures have been reviewed (Loudet and Burgess 2007; Ulrich et al. 2008). In contrast to many other fluorescent dyes, BODIPY molecules are uncharged. Depending on the substitution pattern these dyes can emit light in a broad wavelength range starting around 500 nm and going to the near-infrared. They are insensitive to polarity and solvent pH (Haugland 1996; Haugland 2005). They possess high molar absorbance, ε >65,000 cm^{-1} M^{-1} and quantum yield Φ approaching 100 % (even in water!). The application of these dyes is extremely versatile. They are used to produce fluorescent conjugates of proteins, nucleotides, oligonucleotides and dextrans, as well as to prepare fluorescent enzyme substrates, fatty acids, phospholipids, lipopolysaccharides, receptor ligands and polystyrene microspheres. Due to their relatively long lifetime (~4 ns and longer) they are particularly useful for fluorescence polarization-based assays.

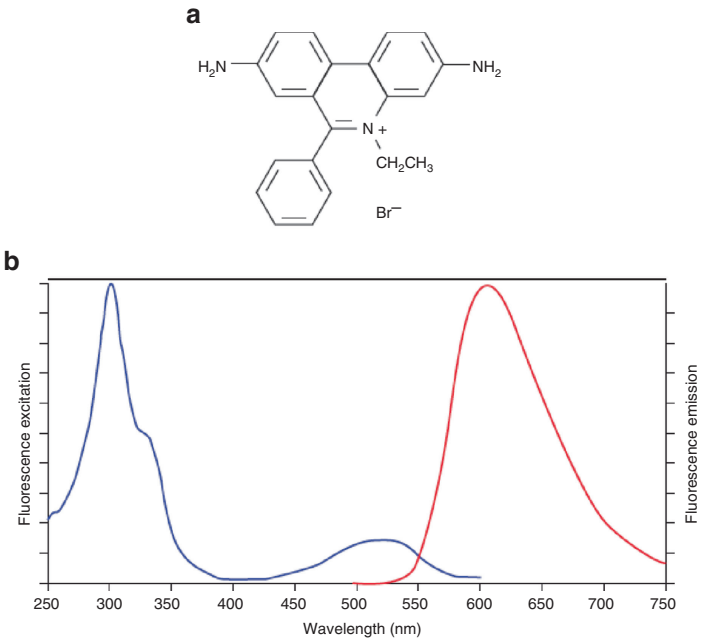

Fig. 4.4 The structure of ethidium bromide (**a**) and its absorption and fluorescence spectra on binding to double-stranded DNA (**b**)

Acrydine and Ethidium Dyes These cationic dyes are frequently used for staining double-helical DNA. They bind with a stoichiometry of one dye per 4–5 base pairs of DNA, and the binding mode is an intercalation between the nucleic acid bases with little or no sequence preference. *Intercalation* is the noncovalent inserting of molecules between the base pairs of the DNA duplex, in which the dye molecule is held stacked perpendicular to the helix axis. *Ethidium bromide* (Fig. 4.4) and its analogs exhibit approximately 30-fold enhancement of emission intensity on their binding. Screening of fluorophore moiety from the quenching effect of water is in the origin of such enhancement.

Cyanine Dyes These dyes belong to a large class of organic compounds that is in extensive use in photography and dye laser technology. A great interest to them from the side of biological labeling and sensing techniques is due to their high molar absorbance, relatively high photostability, good water solubility and usually high quantum yield (Mujumdar et al. 1993). Their common disadvantage is a small Stokes shift, short lifetime (commonly less than 1 ns) and the presence of positive charge. Their absorption and fluorescence spectra cover a broad wavelength range extending to red and near-IR.

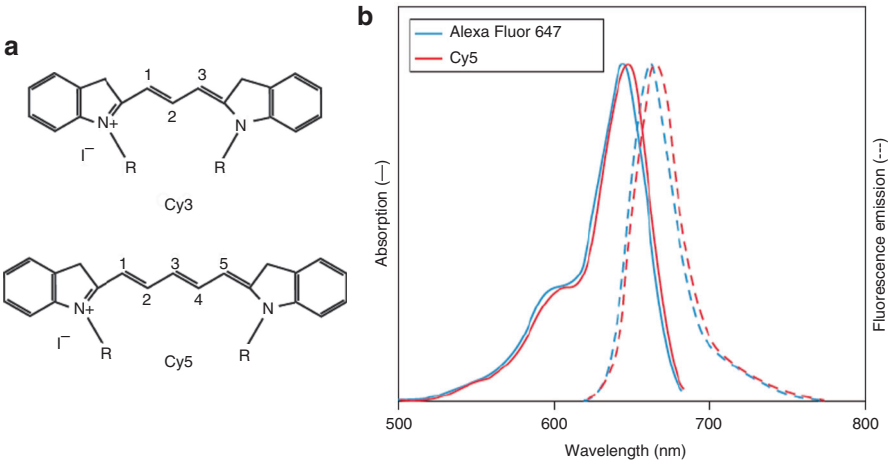

Fig. 4.5 Cyanine dyes. (**a**) The structures of Cy3 and Cy5 dyes that are popular in DNA labeling. R are the sites of substitutions that are used in covalent labeling. Usually, they are not identical. (**b**) The comparison of absorption and fluorescence spectra of Cy5 with that of Alexa Fluor 647, the product of Life Technologies. Spectra have been normalized to the same intensity for comparison purposes (Haugland 2005)

These molecules are composed of a polymethine chain with two heterocyclic units at its terminals (Fig. 4.5). The length of this chain determines the spectral range of absorption and emission: with its increase by one vinylene unit (CH=CH) the spectra shift to longer wavelengths by about 100 nm (Ishchenko et al. 1992). The shortest monomethine dyes, which include the asymmetric cyanines thiazole orange (TO), oxazole yellow (YO), or dimers of both TO and YO (TOTO, YOYO) are used for staining nucleic acids; they do not fluoresce in solution but possess intense fluorescence when are bound to them.

Polymethine Cyanines Polymethine cyanines include the frequently used dyes Cy3 and Cy5 (see Fig. 3.5) that possess increased chain length and are known for binding nucleic acids with much greater affinity. Cy3 can be maximally excited near 550 nm and emits orange light, whereas Cy5 has a narrow excitation peak at 650 nm and produces an intense signal in the far-red region of the spectrum. Their remarkable brightness is due to a high molar absorbance that can exceed 10^5 M^{-1} cm^{-1}. The extraordinary strong increase in fluorescence intensity upon binding to nucleic acids is a result of rigid fixation of their trans-conformation (Tatikolov 2012). In some of them, such increase of quantum yield can be 100-fold, from less than 1 % to nearly 100 %. Polyfluorination allows reducing their aggregation in aqueous media and enhancing their fluorescence quantum yield and photostability (Renikuntla et al. 2004). They are frequently used in DNA and RNA microarray hybridization techniques.

There are two important ways in which cyanine dyes can reversibly bind to double-strand DNA: by *intercalation* or by binding in the minor groove. As a rule, monomethine dyes act as intercalators, whereas the increase in polymethine

chain length allows their binding to the minor groove. As a rule, intercalating monomethine dyes do not exhibit specificity to DNA sequences. The longer polymethine dyes can serve as minor groove binders and display sequence specificity.

At groove binding, the cyanine dyes can interact between themselves forming aggregates. There can be face-to-face dimers called H-aggregates that possess a new absorption band shifted to shorter wavelengths with respect to the monomer band. For some cyanine dyes an end-to-end aggregation in minor groove of DNA is observed, which results in the appearance of a new very narrow absorption band shifted to longer wavelengths (Fig. 4.6). The structures producing such spectra are called *J-aggregates*.

These aggregates are useful for DNA staining in living cells using two-photon excitation (Guralchuk et al. 2007). Though the major application of J-aggregate forming dyes is in the detection of nucleic acids, they can be used in other applications, such as in measuring the membrane potentials in mitochondria (Salvioli et al. 1997). In both cases, the electrostatic effects modulate the formation of aggregates.

Dramatic change of optical properties on J-aggregation is due to very high polarizability of their π-electronic system along polymethine chain. It is a rare case when such a high polarizability is observed already in the ground state, so that it gives rise

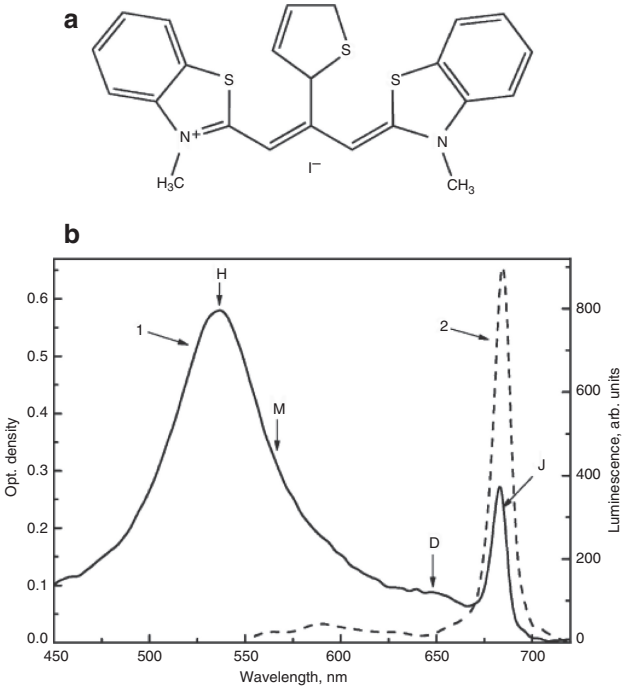

Fig. 4.6 Cyanine dye forming J-aggregates on interaction with DNA. (**a**) The structure of cyanine dye L-21. (**b**) Absorption (*1*) and fluorescence (*2*) spectra of in molecular form and in the form of J-aggregates when it binds to double-helical DNA (Reproduced with permission from (Guralchuk et al. 2007))

to extraordinary strong attraction forces between these dye molecules. In J-aggregates the appearance of narrow absorption bands that are red-shifted as compared to the monomer transition is due to the presence of *excitons* (delocalized excitations) producing the so-called 'exciton splitting' (Davydov 1971). So dramatic transformation of spectra on aggregation forms the basis for application of J-aggregates in sensing technologies (Losytskyy et al. 2002).

4.2.3 The Optimal FRET Pairs

Förster resonance energy transfer (FRET) is the excited-state reaction that requires the presence of two dyes. One (the donor) is excited initially and then it transfers its excitation energy to the other (acceptor) that may either emit or not emit light (Sect. 3.5). FRET to nonfluorescent acceptor has the advantage of the absence in necessity to account for direct excitation of the acceptor at the wavelength at which one excites the donor. Such non-fluorescent quenching dyes are denoted as *dark quenchers*. They are applied in FRET systems, where changes in donor intensity or lifetime are important and the added fluorescence of the acceptor is not necessary or desired for the experiment. One of such dark quencher dyes quenches fluorescence in a wide spectral range from visible to near-IR (Peng et al. 2009).

If acceptor is highly fluorescent, its direct excitation may contribute to the observed emission, but the two wavelengths at the emission band maxima of the donor and of the acceptor can be used for ratiometric detection. In both cases, the best FRET donors are the dyes with high molar absorbances and fluorescence quantum yields.

The needed spectroscopic matching between donor and acceptor consists in overlap of emission spectrum of the donor and absorption spectrum of the acceptor expressed as the overlap integral J (Eq. 3.16). The data on Förster distances R_0 for typical FRET pairs are presented in Table 4.2. These data are solvent-dependent and should be used only for rough estimates. Other optimal FRET pairs that fit desired

Table 4.2 Typical FRET pairs and Förster distances (compilation of literature data)

Donor	Acceptor	R_0 (nm)
Fluorescein	Tetramethylrhodamine	4.5
Dansyl	FITC	3.3–4.1
Pyrene	Coumarin	3.9
IAEDANS	Fluorescein	4.6
IAEDANS	IANBD	2.7–4.1
Carboxyfluorescein	Texas Red	4.1
Fluorescein	Fluorescein	4.4[a]
BODIPY FL	BODIPY FL	4.7[a]
AEDANS	Dabcyl	3.3[b]

Notes:
[a]Homotransfer
[b]Transfer to nonfluorescent acceptor

spectral range and allow two-band spectroscopic response can be found in different publications (Yuan et al. 2013a). Their large variety allows an almost unlimited possibility of choosing the appropriate donor and acceptor molecules.

4.2.4 Near-IR Dyes

The request for the dyes absorbing and emitting light in the *near-infrared* region comes from in vivo imaging technologies and their use as contrast agents in diagnostics of humans (Luo et al. 2011), since this is the range of relative transparency in tissues (see Sect. 13.2). Currently, there are only two near-IR fluorophores approved for this purpose by the Food and Drug Administration (FDA), indocyanine green (Fig. 4.7) and methylene blue. Both of them are small organic molecules that are non-toxic; they do not metabolize and can be rapidly excreted from the body. A range of their derivatives and the dyes belonging to other classes of organic compounds have been recently suggested (Escobedo et al. 2010). Regarding optical properties, their design and selection is clear. Extending the number of heterocycles or the conjugation length in cyanine dyes *decreases the energy gap* between ground and excited states and shifts the spectra to longer wavelengths.

Decrease of energy gap may result in strong fluorescence quenching. Maintaining rigidity of enlarged dye structures is the necessary requirement for achieving the high fluorescence quantum yield. However, other properties should be accounted.

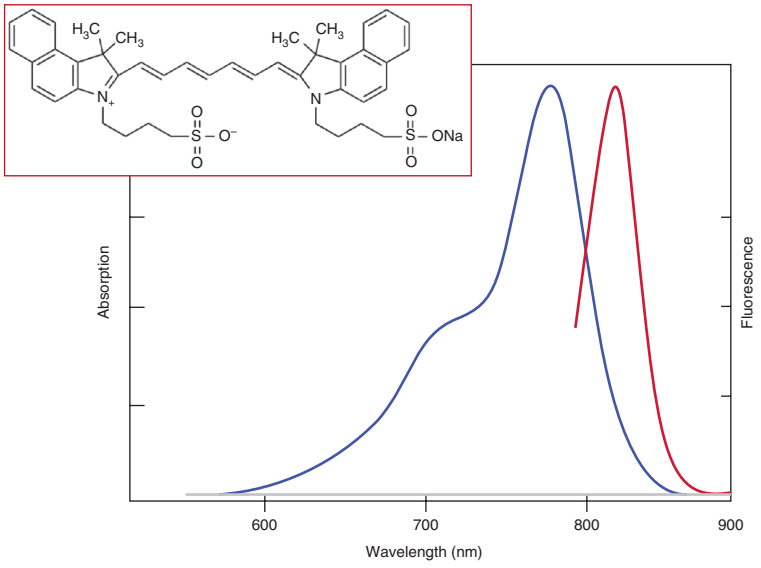

Fig. 4.7 Indocyanine green and its absorption (*blue*) and fluorescence (*red*) spectra

Among recently created and reported dyes are novel *cyanine* and *pyrrolopyrrole cyanine* derivatives. Their low water solubility and the tendency to aggregate is overcome by covalent modifications with groups that increase their polarity and also photostability (Samanta et al. 2010; Wiktorowski et al. 2014). *Porphyrins* and *phthalocyanines* and their metal complexes embody some of the most intensively studied dyes because of strong interest in their use in photodynamic cancer therapy (Sect. 14.4). A series of conjugated *porphyrin dimers* with intense absorptions ranging from 650 to 800 nm and fluorescence emission from 700 to 800 nm have been demonstrated (Kuimova et al. 2009). High biocompatibility (Samanta et al. 2010) and functionalization potential of novel dyes will allow sensing diagnostically important compounds in human tissues (Guo et al. 2014).

The *squaraines* are the dyes with an electron deficient central four-membered ring and a resonance stabilized zwitterionic structure (Patsenker et al. 2010b). The central ring is typically appended with donor moieties to afford a donor-acceptor-donor motif. The *BODIPY* (borondipyrromethane) dyes (Fig. 4.3) typically have relatively shorter wavelength emission maxima and smaller extinction coefficients as compared to the cyanines and other NIR active fluorophores, but by fusing π-excessive aromatic rings to the BODIPY core, significant increases in quantum yield, higher extinction coefficients, improvements in photostability and NIR optical activity could be achieved (Umezawa et al. 2009).

Great importance of dyes absorbing in near-IR region is manifested for *two-photon microscopy* (Sect. 13.1). Such two-photonic dyes allow near-IR excitation and emission in the visible spectral range. The most efficient of them belong to the class of cyanines (Przhonska et al. 2010). Meantime, very potent two-photonic dyes can be synthesized based on pyrene and pyridines (Niko et al. 2015) and on other constituting fragments.

4.2.5 Phosphorescent Dyes and the Dyes with Delayed Fluorescence

Phosphorescence is the emission from triplet state. It usually exhibits strong Stokes shifts, long emission lifetimes (up to milliseconds and seconds) and strong temperature-dependent quenching. Therefore in sensing techniques only those dyes are used that display strong room-temperature phosphorescence. Using phosphorescent dyes as the sensor reporters has important advantages, since a strong Stokes shift allows avoiding the background emission and light-scattering effects, whereas the long lifetimes allow additional possibility of removing fluorescent background by using time-gated detection.

The dyes that display strong room-temperature phosphorescence with the steady-state intensity comparable to that of fluorescence can be used in the λ-*ratiometric*

sensing technologies. Since phosphorescent dyes are, as a rule, also fluorescent and their phosphorescence bands are strongly shifted to longer wavelengths, the *ratio of fluorescence to phosphorescence emissions* can be achieved in a steady-state λ-ratiometric recording as a very precise, convenient and self-calibrating detection technique (Hochreiner et al. 2005). The two emissions can be also easily separated in time domain: fluorescence is a 'short-lived' and phosphorescence is a 'long-lived' emission. This difference can be used in oxygen sensing in solutions, since oxygen is a collisional quencher of long-lived emission (Sect. 12.3).

Among the dyes exhibiting room-temperature phosphorescence are the fluorescein tetra-bromo derivative *eosin* and tetra-iodo derivative *erythrosine* (Fig. 4.8). Much larger number of dyes can become phosphorescent if the dye by rigid environment is protected from quenching. They can be incorporated into porous sol-gel materials or into inorganic or organic polymer matrices, and the optimal detection technique is the emission lifetime (Sanchez-Barragan et al. 2006). The latter can exhibit variation by many orders of magnitude. The heavy atoms are used to increase

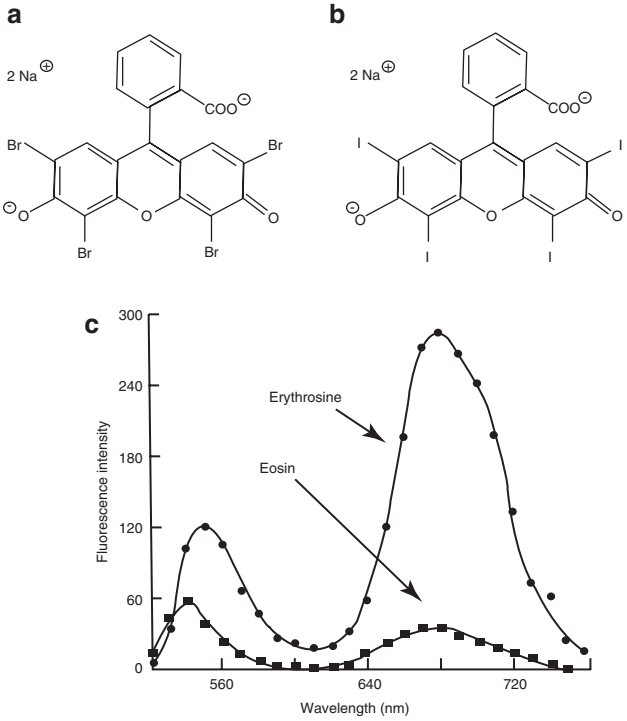

Fig. 4.8 Phosphorescent dyes eosin (**a**) and erythrosine (**b**). Presented in (**c**) are their delayed emission spectra. The long-wavelength band belongs to phosphorescence and the short-wavelength band is due to the presence of delayed fluorescence (Garland and Moore 1979)

the population of phosphorescence state by the so-called '*Kasha heavy atom effect*'. Whereas fluorescein has a fluorescence quantum yield of 0.9, for eosin it is 0.2 and for erythrosine 0.02. Phosphorescence emission increases correspondingly. It can be further increased by removing oxygen from the medium.

Phosphorescent complexes can be obtained also by incorporating the *noble metal ions* platinum, palladium and others into heterocyclic organic structures such as porphyrins (Papkovsky and O'Riordan 2005) and chelating complexes of ruthenium (Castellano et al. 1998; O'Neal et al. 2004).

Delayed fluorescence is the emission with spectral parameters as that of fluorescence and duration as that of phosphorescence (see Fig. 4.8). It can be obtained by intra- and intermolecular triplet-triplet annihilation and, in rare cases, by thermal activation. Its application in sensing and imaging technology is still limited (Benniston et al. 2007).

4.2.6 Combinatorial Discovery and Improvement of Fluorescent Dyes

Strong demand for new fluorescent dyes for different applications meets with the problem of difficulty in predicting their properties, even in simple cases. From the data analyzed in this Section we derive that for every particular application the dye parameters have to be optimized in many directions and neither empirical knowledge nor the aid of quantum mechanics calculations may be a good help for that. There are three central obstacles to the discovery of new dyes for probing and sensing based on their rational design (Finney 2006):

(a) Complexity of underlying photophysical phenomena. The excited-state processes are different from those occurring in the ground states and not so strongly related to the chemical structure. They involve multiple relaxation phenomena that are hard to predict. Because of that, fluorescence properties are hardly predictable using quantum chemical calculations.
(b) The still common one-molecule-at-a-time dye synthesis together with its purification and characterization is low productive.
(c) For the evaluation of dye properties, a labor-intensive characterization needs to be used that involves detailed spectroscopic analysis and comparison with the known standards.

The *combinatorial approaches* offer solutions to overcome these difficulties (Vendrell et al. 2012; Finney 2006). Optimization can be achieved by exploring the structural space around the known core fluorophore, keeping the line along the needed properties. This approach simplifies the synthetic challenge and generates many related compounds for comparative analysis. Then the multi-

tude of products can be evaluated in the simplest way, disregarding most of the quantitative aspects. This can be done in a high-throughput manner using fluorescence plate-readers. Any interesting hits can be then characterized in more detail. A number of *solid-phase* and *solution-phase* synthetic procedures are now well developed, and their application shows good results (Vendrell et al. 2012). Though discovery of completely new fluorophores with this approach is not addressed, this allows rapid optimization of many properties of known fluorophores together. In addition to spectroscopy, there can be the chemical reactivity or affinity to particular structures. The library design is critical in this endeavor.

4.3 The Dyes Providing Fluorescence Response

Here we concentrate on the dye properties that are required for performing fluorescence response in sensing systems (see Fig. 4.1). They should optimally correspond to detection techniques described in Chap. 3 and allow achieving the broadest dynamic range and highest sensitivity of detection. Only in sensing based on anisotropy (polarization) the role of the dye reporter can be passive to respond to rotations of large molecules or their fragments. In detection based on FRET, the response is coupled to variation of the distance between two dyes or overlap of their spectra. In all other cases, the dyes have to respond to formation/breaking of specific or nonspecific noncovalent interactions with their neighboring molecules or groups of atoms.

Among the reactions that make organic dyes so sensitive is the *intramolecular charge transfer* (ICT) that allows responding by spectral shifts to the changes in polarity of their environment. For instance, in the dye Nile Red the charge transfer occurs both in the ground and excited states, as a result of which the scale of solvent-dependent variation of both absorption and fluorescence emission spectra exceed 100 nm. Thus absorption spectrum ranges between hexane and water from 480 to 590 nm, and the variation of fluorescence spectra between these solvents reaches 130 nm, from 530 to 660 nm (Jose and Burgess 2006). The other important reaction that provides the strongest shifts of fluorescence spectra is the *excited-state intramolecular proton transfer* (ESIPT). In a series of substituted 3-hydroxychromone derivatives the dynamic balance between ICT and ESIPT states that generate switchable well-resolved emission bands can be achieved. They can be strong indicators of polarity and molecular-scale electric fields (Demchenko 2006; Demchenko et al. 2003). Formation of stable *excimers* (complexes between unexcited and excited fluorophores) is characteristic of pyrene. This reaction changes dramatically fluorescence spectrum (from 400 nm for monomer to 450 nm for excimer) and lifetime (~300 ns for monomer and ~ 40 ns for excimer) and is frequently used in

fluorescence reporting (Yang et al. 2005). The formation of excimers requires close location and proper orientation between the partners, therefore the sensing is commonly coupled with conformational changes in the sensor unit that bring the pyrene units together (Kadirvel et al. 2008).

Based on organic dyes many types of molecular sensors were developed: the pH sensors based on photo-dissociation of protons from aromatic hydroxyls (Whitaker et al. 1991), the molecular rotors that sense local viscosity (Haidekker and Theodorakis 2007), the temperature sensors based on excimer formation (Chandrasekharan and Kelly 2001), the pressure sensors based on oxygen quenching of triplet state (Hochreiner et al. 2005), the ion sensors based on switching between charge-transfer states (Grynkiewicz et al. 1985). There are several classes of dyes exhibiting electrochromism and sensitive to local electric fields (Kuhn and Fromherz 2003; Klymchenko and Demchenko 2002). Due to their small size and the ability of incorporation into biological structures (e.g. biomembranes or double stranded DNA) with minimal perturbation, the organic dyes are ideally suited as molecular sensors.

4.3.1 Special Requirements for Fluorescence Reporters

Here we analyze the special requirements for the dyes with reporter functions. They are the following:

1. *Strong variation* in one or several fluorescence parameters described in Chap. 3 that can be quantified. The response can be provided by formation of specific complexes of the dyes (e.g. with the quenchers), by formation of their dimers (e.g. excimers) or aggregates. Alternatively, they can participate in interactions that can be described by such variables as polarity, viscosity, hydrogen-bonding ability.
2. *Strong discrimination* in response to measurable parameter against the response to other parameters that influence the spectra (e.g. polarity probes should not be highly sensitive to H-bonding and the reverse). Alternatively, the possibility of multiparametric analysis of complex response may be provided (Klymchenko and Demchenko 2003).
3. *Insensitivity of response* to different interfering factors, such as impurities in the solvents, ions, temperature, pH, etc. if these factors are not the targets of assay.

Generation of reporting signal from responding dyes may involve different signal transduction mechanisms that will be described in Chap. 8, and the dye properties should be optimally selected for realizing these mechanisms. Responding to intermolecular interactions, these dyes allow realizing many possibilities: to characterize the properties (polarity, proticity, microfluidity) of the binding sites and their changes in the course of binding, to follow the binding-dissociation kinetics, to estimate the changes of molecular distances, etc.

4.3.2 Fluorophores in Protic Equilibrium. pH-Reporting Dyes

Many fluorophores conjugated with ionogenic chemical groups (phenolic hydroxyl, carboxylic and sulfonic acids) are used as fluorescent pH probes (Han and Burgess 2009). The ionization of attached groups may change dramatically the spectroscopic properties leading to the increase of fluorescence intensity or to the appearance of new bands in absorption and emission spectra. The dyes displaying these bands of high and comparable intensities can be used for λ-ratiometric sensing. Since the acidity of dissociating groups is commonly much higher in the excited than in the ground state, the pH range of sensitivity in emission spectra can be dramatically shifted to lower pH (Laws and Brand 1979; Davenport et al. 1986). This allows providing the wavelength-ratiometric recording in an extended pH range.

Presently the most extensively used dyes are the benzo[c]xanthene derivatives, such as C-SNAFL-1 (Whitaker et al. 1991; Mordon et al. 1995). The variation of their excitation spectra reflects the ground-state proton dissociation. The pH-dependent appearance of strongly red-shifted second band in emission spectra is due to deprotonation of hydroxy group in the excited state. The fact that the pH-dependent change in ionization of the dye functional groups is local and can respond to the shift in association-dissociation equilibrium of macromolecules without the change of medium pH can be efficiently used in sensing technologies.

4.3.3 Hydrogen Bond Responsive Dyes

The presence of H-bond donor and acceptor groups coupled to aromatic structures possessing π-electrons offers new possibilities for sensing based on the formation/breaking of intermolecular H-bonds. Generation of fluorescence reporting signal based on modulation of intermolecular *hydrogen bonding* could be a very important possibility for fluorescence reporting. It is known (de Silva et al. 1997) that the formation/disruption of these bonds is an important mechanism of fluorescence quenching. Enhancement of fluorescence in protic environments was also reported (Uchiyama et al. 2006) but is a rare phenomenon.

The most important issue is the possibility of λ-ratiometric detection. The intermolecular hydrogen bonds can influence the intramolecular charge-transfer (ICT) character of the excited states with the correspondent spectral shifts. These effects are usually smaller than that on protonation and occur in the same direction (Wang et al. 2002). In excitation spectra on interaction with H-bond donor at the acceptor site one can observe the shifts of spectra to longer wavelengths and on interaction with proton acceptor at the donor site – to shorter wavelengths. The fluorescence spectra on such interaction may shift strongly to longer wavelengths.

Carbonyl groups attached to π-electronic system are known as strong sensors of intermolecular H-bonding (Shynkar et al. 2004). Serving as H-bond acceptors they can be found in many organic dyes. The electron lone pairs on oxygen atoms allow

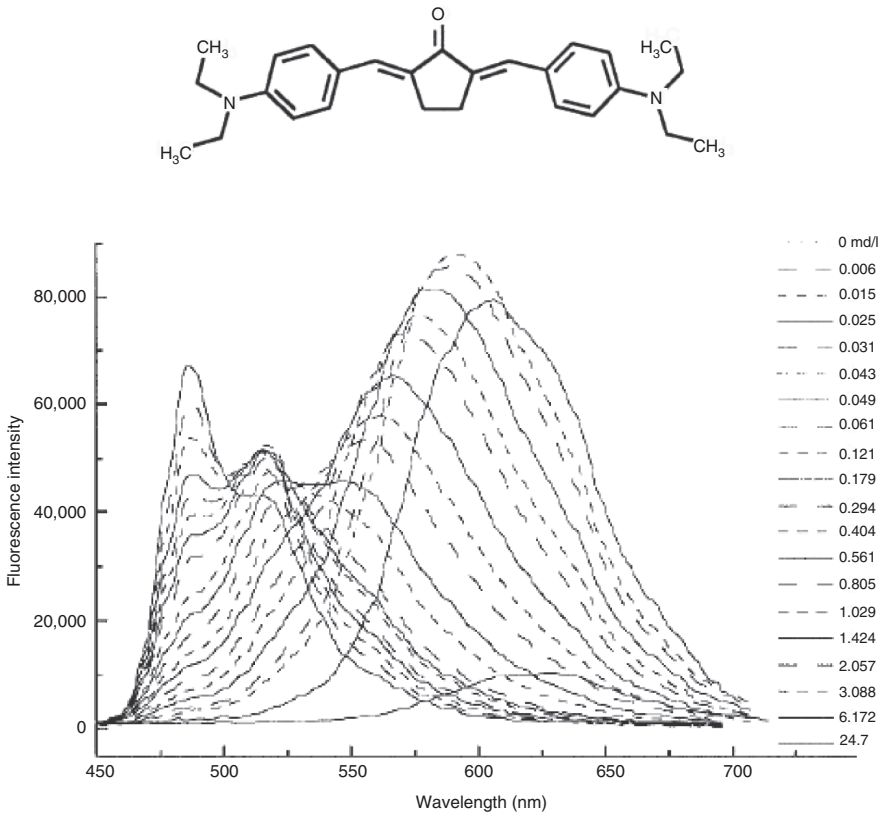

Fig. 4.9 Hydrogen bonding effects in fluorescence spectra of ketocyanine dye 2,5-bis[4-N,N-dimethylaminobenzylidene]cyclopentanone-1. The spectra are obtained in toluene (the narrow structured spectrum at shorter wavelengths) on the addition of various concentrations of methanol (Pivovarenko et al. 2000)

arrangement of two such bonds, the stronger and weaker ones. Their formation is clearly observed in fluorescence spectra (Pivovarenko et al. 2000) and can generate strong λ-ratiometric signal. As we can see in Fig. 4.9, addition of millimolar amounts of alcohol to aprotic solvent produces dramatic changes in these spectra resulting in the loss of fine vibrational structure. Higher amounts of protic molecules result in further transformation of the spectra and the spectral shifts.

4.3.4 The Environment-Sensitive (Solvatochromic) Dyes

The polarity-responsive properties are already present in amino acid *tryptophan*, which is a natural constituent of many proteins (Demchenko 1986). But small values of these effects together with inconvenient UV excitation do not allow its

extensive use in fluorescence sensing. In contrast, there are fluorophores that provide record values in solvent-dependent spectral shifts in the visible range. Like tryptophan and more than tryptophan they have to change their dipole moment on excitation that changes their interaction with surrounding molecules and results in the shifts of spectra. This concept was introduced by Gregorio Weber and the first dyes that found many applications, mostly in the studies of structure, dynamics and interactions in proteins and biomembranes, were the naphthalene sulfonate derivatives such as ANS and TNS (Fig. 4.10). A number of dye derivatives used for covalent labeling of proteins (Dansyl, Acrylodan, NBD, IAEDANS, etc. (Haugland 1996)) exhibit strong polarity-dependent shifts. They were developed for the labeling of proteins. Nowadays they are used on an extended scale, for covalent labeling to amino or SH groups of any molecular sensors (see Sect. 9.3).

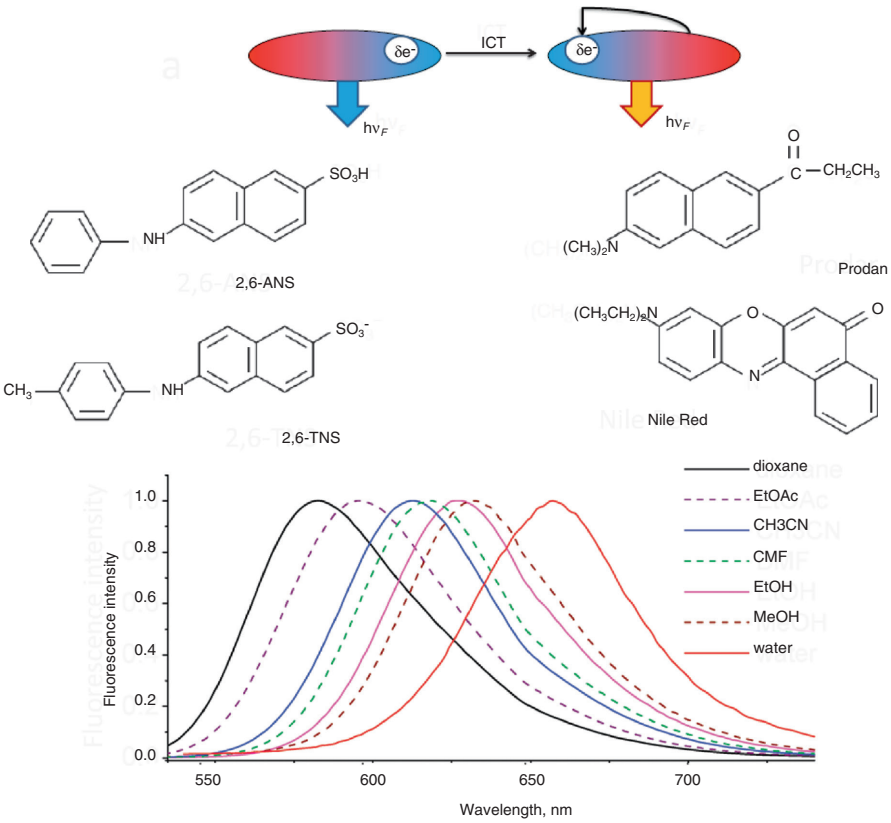

Fig. 4.10 The mechanisms of generation of spectral shifts in the case of ICT and the structures of typical environment-responsive dyes: 2,6-ANS (6-(phenylamino)-2-Naphthalenesulfonic acid); 2,6-TNS (2-(p-toluidinyl)naphthalene-6- sulfonic acid); Nile Red; Prodan (6-propionyl-2-dimethylaminonaphthalene) (**a**) and the solvent-dependent fluorescence spectra of Nile Red in indicated solvents (**b**) (Kucherak et al. 2010b)

The dyes Prodan and Nile Red (Fig. 4.10) are of latter generation demonstrating increased *solvatochromism* (the solvent-dependent shifts of spectra). The background of this effect is *intramolecular charge transfer* (ICT) between two distant groups of atoms, one serving as electron donor and the other as electron acceptor. They are integrated into π-electronic chromophore system and shift its electronic density creating strong dipoles.

Prodan is one of the most solvent-sensitive among commonly used probes operating on the principle of solvent-dependent band shift. Its absorption spectrum is observed at 350–370 nm and fluorescence spectrum ranges from 416 nm for toluene to 505 nm in methanol (Fig. 4.11). The dyes containing the H-bond proton acceptor groups, such as carbonyl group of Prodan, exhibit additional spectral shifts due to this bonding in the same direction as the increase of polarity, to longer wavelengths. In Prodan almost a half of this shift is due to hydrogen bonding (Balter et al. 1988). Water molecules are among the strong proton donors, so the sensing effect can be coupled with the change in dye hydration. The strong solvent sensitivity of this molecule is connected with disadvantages, such as dramatic fluorescence quenching in all protic media.

Recent developments resulted in obtaining Prodan analogs with superior properties. It was found that isomers of Prodan with different positioning of the donor and acceptor group in the naphthalene core exhibit much stronger

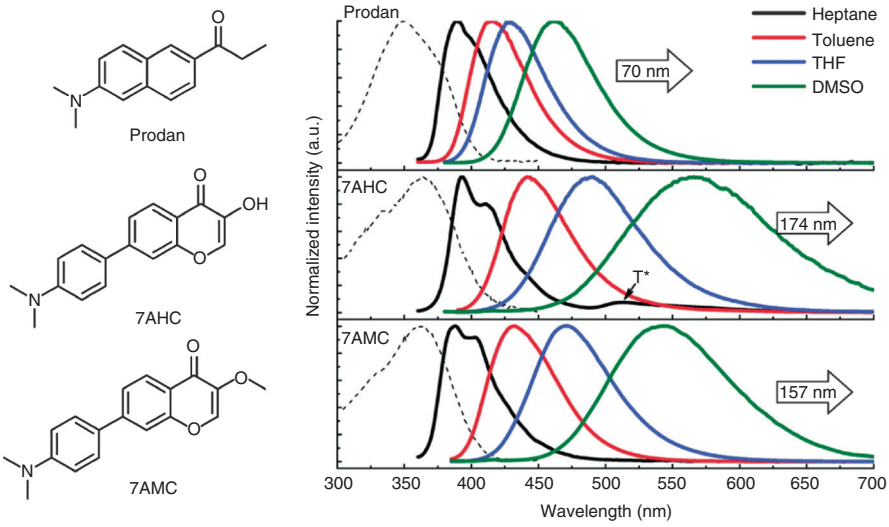

Fig 4.11 Novel strongly solvatochromic 3-hydroxychromone derivatives (Giordano et al. 2012). Absorption spectra in THF (*dashed line*) and fluorescence spectra (*solid lines*) of compounds 7AHC, 7AMC in comparison with Prodan (excitation at 370 nm). The values in arrows are the magnitudes of solvatochromic shifts in passing from heptane to DMSO

solvatochromic properties (Benedetti et al. 2012). Its naphthalene core was also substituted with aromatic hydrocarbons possessing increased electronic conjugation. Substitution by *anthracene* resulted in Anthradan, which led to the shifts of both excitation and emission spectra to the red by about 100 nm with retention of high sensitivity to polarity and hydrogen bond formation in protic environment (Lu et al. 2006). New probe on the basis of *fluorene* (Kucherak et al. 2010a) also demonstrated red-shifted absorption, twice as large of a absorption coefficient (43,000 M^{-1} cm^{-1}), and a manifold larger two-photon absorption cross section (~400 GM) compared to Prodan. Much stronger polarity-dependent shifts of spectra are due to twice as large transition dipole moment (14.0 Debye units). The strong increase of fluorescence quantum yield was also reported. Very high quantum yield in both polar and apolar solvents together with strong solvatochromy was found for Prodan analog with *pyrene* core (Niko et al. 2013). These novel derivatives with superior spectroscopic and solvatochromic properties are expected to totally substitute Prodan in molecular probing studies.

Phenoxazone dye *Nile Red*, is the typical fluorescent dye with remarkable ability of solvent-dependent spectral shifts both in absorption and fluorescence spectra. Its absorption spectrum ranges from 480 to 590 nm between hexane and water, and variation of fluorescence spectra between these solvents reaches 130 nm, from 530 to 660 nm (see Fig. 4.10). Such strong shifts occur due to generation of ICT states that are stabilized on interaction with polar media. Dramatic decrease of quantum yield of Nile Red in water is thought to be due to formation of aggregates, and the introduction of polar substituents increases not only the solubility but also the quantum yield (Jose and Burgess 2006). Derivatives of this dye have been synthesized for covalent labeling of proteins and peptides (Karpenko et al. 2014), also inside the living cells (Prifti et al. 2014), and labeling of phospholipid membranes with strong response to variations of their structures have been demonstrated (Kucherak et al. 2010b).

The design and application of solvatofluorochromic (showing solvent-dependent emission) dyes that can be used for **λ**-ratiometry (Sect. 3.7) have recently been reviewed (Benedetti et al. 2013; Vendrell et al. 2012; Boens et al. 2012).

The dyes of 3-hydroxychromone family are known to exhibit the excited-state intramolecular proton-transfer (ESIPT) reaction, which results in two-wavelength switching, as will be discussed below (Sub-section 4.3.6). Introduction of the dialkylaminophenyl group in position seven changes the orientation of the excited-state dipole moment in opposite direction and abolishes ESIPT completely. The excited ICT state demonstrates superior solvatochromic properties (~170 nm emission shift between heptane and DMSO) compared to Prodan (Fig. 4.11). Methylation of the 3-OH does not change this effect and leads to improved photostability. These probes can be efficiently used in biomembrane studies (Giordano et al. 2012).

4.3.5 *Electric Field Sensitive (Electrochromic) Dyes*

The request for sensing the *electric fields* at the distances of molecular dimensions is great. The electric field sensitive dyes can respond to electrostatic potential at interfaces, to biomembrane potential, surface potential of protein molecules or nanoparticles, etc. They can be efficiently used in those technologies, in which the sensing effect is coupled with relocation of nearby located charge. Their response is based on *electrochromism* (also known as *Stark effect*), which is the phenomenon of changing the energies of electronic transitions resulting in shifts of electronic (absorption and fluorescence) spectra under the influence of electric field (Bublitz and Boxer 1997).

The *electrochromic dye* senses the integrated electric field at the site of its location whatever this field is applied externally in a macroscopic device (e.g. inside a capacitance) or internally, on a molecular level, by a nearby charge. This allows some averaging and integration of produced field effects. The 'mesoscopic' approach considering the fluorophore as a point dipole and electric field as a vector $\vec{F}$ that averages all the fields influencing the fluorophore in the medium with efficient dielectric constant ε_{ef} can be used for the description of this effect in the simplest dipole approximation (Bublitz and Boxer 1997). The direction and magnitude of the shift, $\Delta\nu_{\mathrm{obs}}$, is proportional to the electric field vector $\vec{F}$ and the change of dipole moment associated with the spectroscopic transition $\Delta\vec{\mu}$:

$$h\Delta\nu_{obs} = -\left(1/\varepsilon_{ef}\right).\left|\Delta\vec{\mu}\right|.\left|\vec{F}\right|\cos\left(\theta\right), \tag{4.1}$$

where θ is the angle between $\Delta\vec{\mu}$ and $\vec{F}$ vectors. It follows that in order to show maximal sensitivity to electrostatic potential, the dye should exhibit substantial change of its dipole moment $\vec{\mu}$ on electronic excitation, which implies an essential redistribution of the electronic charge density. Furthermore, it should be located in low-polar environment (low ε_{ef}) and oriented parallel ($\cos\theta = 1$) or anti-parallel ($\cos\theta = -1$) to the electric field vector.

It is essential to note that electrochromism (the response to external electric field) and solvatochromism (the response to dielectric interactions with molecular environment) are based on the same physical mechanism (Liptay 1969). Practically, this means that the effects of dipoles chaotically surrounding the dye in a polar liquid (effects of polarity) are basically not distinguishable from that of dipoles arranged in organized ensemble and generating the electrostatic potential. The difference stems from stringent demands on the dye location and orientation with respect to applied field. Therefore the correlation of spectroscopic effects with the applied field strength is possible only if the dye location and orientation relative to the field are fairly known. In applications, the electrochromic effects are of value for the studies of electrostatic effects at interfaces, such as Langmuir–Blodgett films

(Tsuchida et al. 2001) and biomembranes (Demchenko and Yesylevskyy 2009; Clarke 2010).

In experiments with the charged interfaces, the high structural anisotropy and the possibility of locating the fluorophore anisotropically in different orientation to the interface, allows observing strong response based on this mechanism. The dye response that does not depend on dye orientation should be attributed to the effects of polarity and those that show such dependence should be due to electrostatic potentials.

The request of optimizing the electrochromic effect resulted in selecting the most efficient dyes. They should be the ICT dyes with the largest relocation of electronic charge. Such are the voltage-sensitive *styryl* and *naphthyl styryl* dyes. Among the best known electrochromic dyes are the 4-dialkylaminostyrylpyridinium derivatives with electron-donor and electron-acceptor substituents at the opposite ends of their rod-shaped aromatic conjugated moieties (Gross et al. 1994). They exhibit the following excited state reaction modulated by applied electric field (Fig. 4.12):

The fluorescent signal on the change of dipole moment in such dyes in response to the change of electric field is extremely fast but rather modest in magnitude.

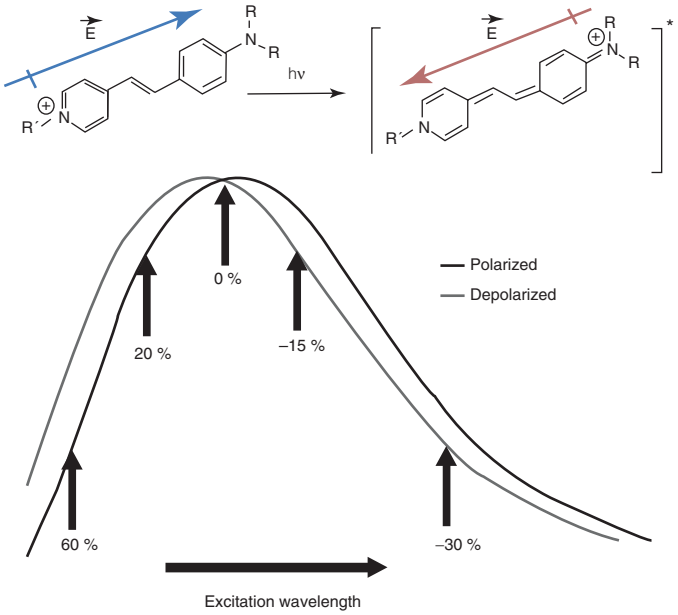

Fig. 4.12 Translocation of charge in the excited state of 4-dialkylaminostyrylpyridinium dye di-ANEPPS. The excitation spectra demonstrate the electric field induced spectral shift, and the relative change in fluorescence, $\Delta F/F$, is shown as a percentage change for different choices of detection wavelengths (Loew 2011), modified. When incorporated into cell membrane this shift indicates the difference in membrane potential between its polarized and depolarized states

These shifts are best observed in excitation spectra, where the intensities at their slopes can be recorded in ratiometric manner, whereas the shifts in fluorescence spectra are much smaller and quantitatively less reliable due to the involvement of dielectric relaxations in the excited state. Strong electrostatic effects can be observed in this way in biomembranes and their phospholipid analogs (Gross et al. 1994), in which the charged groups, adsorbed ions and oriented dipoles of lipids form very strong electric field gradients (Demchenko and Yesylevskyy 2009) that can be modulated by different factors with clear observation of response of incorporated dyes. Therefore it can be expected that electrochromic dyes will find application in sensing devices that involve charged interfaces or surfaces of nanoparticles.

Styrylpyridinium dyes are popular as electric field probes, and the descriptions of different their versions can be found in the literature (Wuskell et al. 2006; Vitha and Clarke 2007; Millard et al. 2004; Jin et al. 2006). Meantime, a critical analysis reveals that further progress requires the development of probes that do not possess a large ground-state charge asymmetry that may allow their desired location and orientation and also allow quantitative λ-ratiometric recording in fluorescence emission. Below we will see that 3-HC dyes, and particularly 4'-(dialkylamino)-3-hydroxyflavones, fit better to this requirement.

Thus, three major effects, *polarity*, *electric fields* and *hydrogen bonding* can induce strong shifts of fluorescence spectra. They can be used for probing the properties of different media (liquids, solids, their interfaces), see Sect. 12.2.

4.3.6 Supersensitive Multicolor Ratiometric Dyes

The background in operation of these dyes is the *excited-state intermolecular proton transfer* (ESIPT) coupled with the *excited-state intramolecular charge transfer* (ESICT) (Demchenko et al. 2013). This reaction allows observation of two bands in emission and switching between them as a function of small intermolecular interactions exhibited by the dye (Fig. 4.13). The designed organic dyes belonging to the family of *3-hydroxychromones* (3HCs) satisfy these requirements in the best way (Demchenko 2006; Klymchenko and Demchenko 2003; Demchenko et al. 2003). Due to rigidity of their skeleton, 3HCs (and their derivatives 3-hydroxyflavones, 3HFs) are the dyes in which the observation of two separate bands in emission is not due to the presence of two or more excited-state structural isoforms, which produce the two-band spectra in some other dyes. The second (long-wavelength) band is generated due to the ESIPT reaction proceeding along the intramolecular hydrogen bond. As shown in Fig. 3.23 for the ESIPT reaction in 3-HC derivative 4'-dialkylamino-3-hydroxyflavone, the reaction proceeds between highly dipolar and strongly interacting with the solvent N* form and the tautomer form T possessing much more symmetric charge distribution. Therefore the sensitivity of two N* and T*

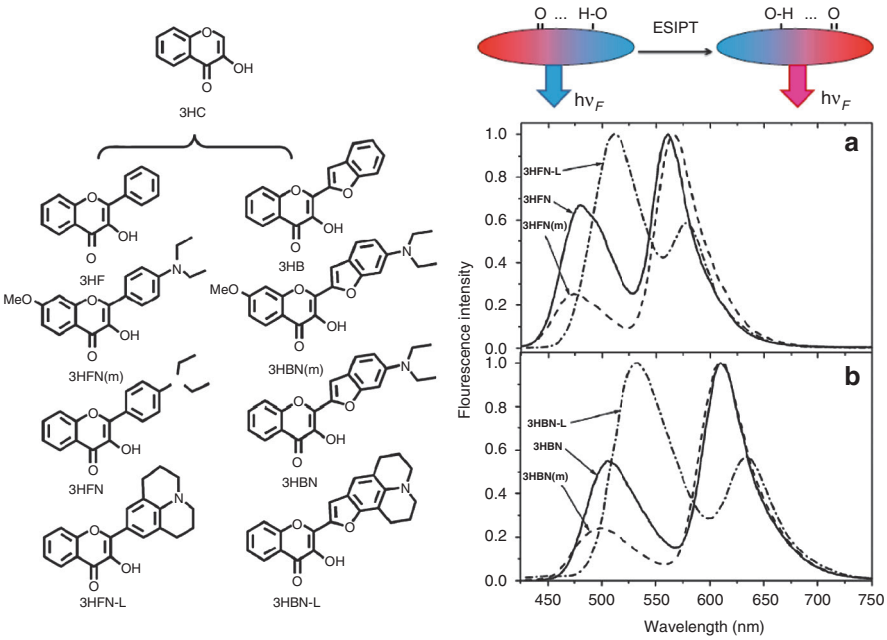

Fig. 4.13 Two series of 3-hydroxychromone dyes exhibiting dramatic variation of wavelength-ratiometric response to polarity of molecular environment (Yesylevskyy et al. 2005; Klymchenko et al. 2003b). Their two-band fluorescence spectra of flavones 3HFN, 3HFN-L and 3HFN(m) in chloroform (**a**) and benzofurylchromones 3HBN, 3HBN-L and 3HBN(m) in toluene (**b**). Excitation at 420 nm

forms to all types of intermolecular interactions is different resulting in strong variations in positions and intensities of correspondent fluorescence bands.

Structural modifications of the parent fluorophore allow variation of spectroscopic properties of these dyes in very broad ranges. In Fig. 4.13 the dyes of two series, based on 3-hydroxyflavone (left) and 2-benzofurylchromones (right) are shown being arranged in line with the increase of their excited-state dipole moments shifting the range of λ-ratiometric sensitivity to lower polarities, The choice of dyes for obtaining optimal response in particular environments can be complemented by the dyes of other series, in which naphthofuranyl (Klymchenko et al. 2001) or thiophenyl (M'Baye et al. 2007) groups are attached in position 2 of chromone heterocycle. Moreover, the compounds, in which oxygen in position 1 is substituted by a group containing nitrogen (3-hydroxy quinolones) were synthesized. They possess unique sensitivity to variation of intermolecular hydrogen bonding (Yushchenko et al. 2006).

The two-color fluorescence switching from a single dye exhibiting an excited-state reaction is very convenient for different applications (Demchenko et al. 2013). By switching between them these dyes demonstrate really dramatic sensitivity of

their spectra to polarity and electric fields of their environment (Demchenko and Yesylevskyy 2009; Klymchenko and Demchenko 2002) and also to intermolecular H-bonding (Shynkar et al. 2004), and these effects are much stronger than that observed just with spectral shifts.

From the overview presented above, we derive that organic fluorescent dyes are unique in the ability of reporting to the changes of all major types of weak noncovalent intermolecular interactions. The idea visualized schematically in Fig. 4.14 will probably be useful for the development of responsive dyes of new generations. In the state of equilibrium between the reactant and product in the excited state the difference in free energies of these states modulates fluorescence intensities of correspondent bands. If some, even weak, intermolecular interactions of reactant or product molecules change this energy balance, the stronger

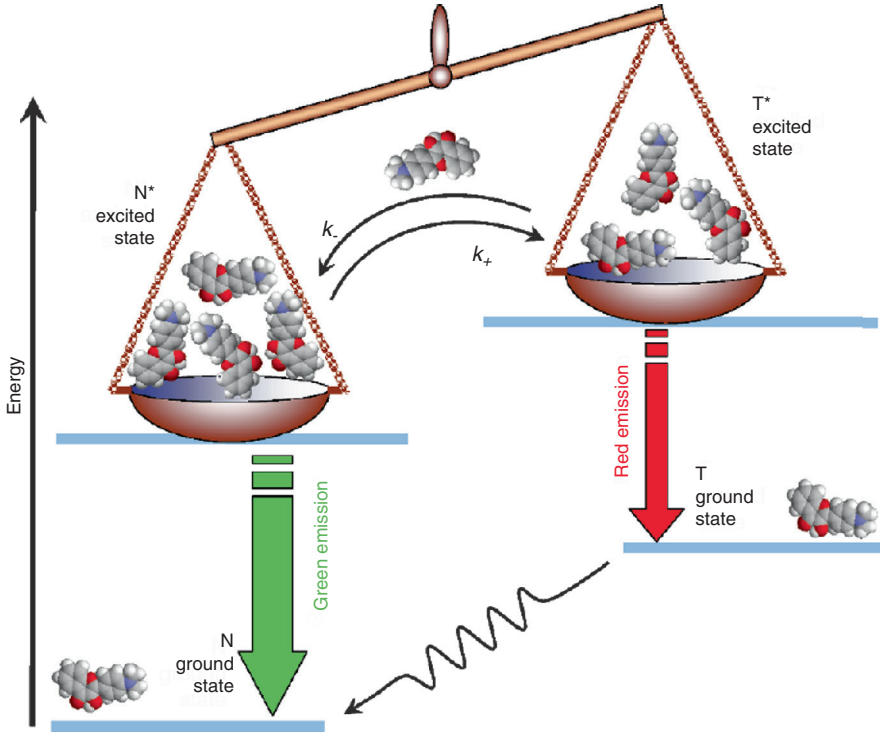

Fig. 4.14 The scheme illustrating the principle of signal amplification in two-band ratiometric fluorescence response (Demchenko 2006). The two excited species (N* and T*) are in dynamic equilibrium. For each of them the change of intermolecular interactions results in the change of energy separation between ground (N or T) and excited (N* or T*) states. The equilibrium in relative populations of two forms shifts in the direction of the form possessing lower energy, which gives higher fluorescence intensity from a more populated state. According to Boltzmann law, the difference in state populations is an exponential function of the difference in state energies. Therefore, a strongly amplified response is observed in band intensity ratios in comparison with spectral shifts

interacting state (possessing decreased energy) will become more populated, just in accordance with the Boltzmann-type statistics. With common solvatochromic dyes, in these cases we observe just the spectral shifts. However, if the two states emit fluorescence and the switching occurs between them, we achieve a strong *amplification effect in response* – a small relative change in interaction energy between two states changes dramatically the relative intensities of two emissions.

Subsequent studies have shown one more remarkable property of 3HC dyes. Observing the spectroscopic changes in *protic* environments we started to distinguish and analyze an additional H-N* band. Being characteristic for these environments only, it was attributed to intermolecular *hydrogen-bonded form* that involves 4-carbonyl group (Shynkar et al. 2004).

A new important step was the discovery of strong *electrochromism* of these dyes (Klymchenko and Demchenko 2002), which opened new dimension in their study and applications. Thus, it was shown that the positions of two emission bands and relative variations of their intensities are highly sensitive to such properties of their microenvironment as polarity, hydrogen bonding and local electric fields. In particular:

- In *polarity sensing* they exhibit an ultrasensitive two-band ratiometric response to polarity of the environment, up to complete switching between N* to T* bands in emission in a narrow range of variation of this parameter. This range can be adjusted by chemical substitutions (Klymchenko et al. 2003b) covering the range from very low (Ercelen et al. 2002) to very high (Klymchenko et al. 2004) polarities. The origin of this effect, in line with the mechanism described in Fig. 4.14, is a much stronger stabilization of the N* state in polar media, as a result of which this state becomes increasingly populated at equilibrium. The wavelength-ratiometric response is observed of such dramatic magnitude, that only the use of a number of dyes can cover the whole polarity range. The results on more detailed characterization of solvent polarity with the use of one of these dyes can be found in Sect. 12.2.
- In the *sensing of hydrogen bonding* potential of the environment (which in biomolecular structures can also be a measure of hydration), a strong response to the presence of proton donor groups is typical for these dyes. In contrast to many other carbonyl-containing fluorescent dyes, in 3HCs no formation or disruption of intramolecular H-bonds occurs in the excited state, so the probe can sense the true concentration of H-bond partners existing in the ground state (Shynkar et al. 2004). Sensitivity to hydrogen bonding can be eliminated by proper chemical substitution that provides sterical screening of this carbonyl group (Klymchenko et al. 2002b).
- In *electric field sensing* a very strong two-band ratiometric response to the magnitude and direction of the local electric field on molecular scale (the so-called *electrochromic modulation* of ESIPT reaction)was demonstrated (Klymchenko and Demchenko 2002), and this effect was applied for determination of dipole

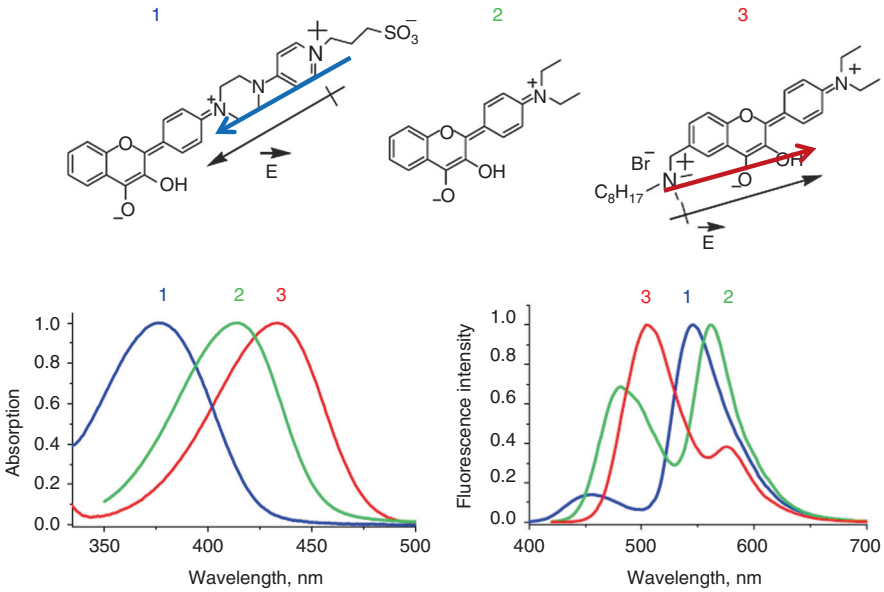

Fig. 4.15 The effect of covalently attached positively but electronically uncoupled charged groups on the absorption and fluorescence spectra of strongly dipolar 3HC dye. The two bands in fluorescence emission appear as a result of ESIPT reaction. The dye (*1*), in which the charged group is attached from the side of electron-donor dialkylamino group of dye (*2*) possesses the absorption spectrum strongly shifted to the blue. Its fluorescence spectrum possesses greatly decreased intensity of the N* band that is also shifted to the blue. The opposite effect is observed for dye (*3*), in which the positively charged group is attached through a spacer to the opposite side

potential in biomembranes (Klymchenko et al. 2003a). The origin of this response is in electrochromic (due to internal Stark effect) influence on the relative energies of the N* and T* states, as it is shown in Fig. 4.15.

By introducing different substituents, the derivatives of these dyes with the ability of vertical insertion and opposite orientations in the membrane were designed (Klymchenko et al. 2003a) . They respond to the changes in their two emission bands intensity ratio in an opposite way in accordance with their inverse orientation. Moreover, a multiparametric analysis based on band deconvolution showed that these changes are independent from the hydration parameter (M'Baye et al. 2006). In order to avoid their fast internalization and/or poor staining of plasma membranes of the living cells, a second generation of probes were introduced (Shynkar et al. 2005).

In a general sense, the sensitivity to many different types of intermolecular interactions is not an attractive feature in sensing. But in the case of 3HCs there is a possibility for deriving in the spectral response of a single fluorophore a number of spectroscopic parameters (the wavelengths of absorption and of two emission band maxima together with intensity ratios). Due to this feature we were able to develop an approach for distinguishing the effects of *polarity*, *electronic polarizability* and *hydrogen bonding* (Klymchenko and Demchenko 2003). The effects of *electric field* can be evaluated by an analysis of shifts in excitation spectra and by comparing the data obtained for 3HF probes located in different orientations to this field (Klymchenko et al. 2003a).

Thus, the molecules of the 3HC family can respond to several, the most important, types of intermolecular interactions. The common response to these interactions, the *spectral shift*, can be amplified being *transformed* into the *ratio of two band intensities*. By chemical modifications, the 3HC dyes can be supplied with a variety of functional units. They were suggested for probing biomembrane structures by locating the dyes at different orientations and depths (Klymchenko et al. 2002a). More sophisticated functional dyes sense variations of dipole potential in membranes of living cells (Shynkar et al. 2005) and are able to detect the early steps of apoptosis (Shynkar et al. 2007). Derivatives of these dyes for covalent labeling of amino and SH-groups were also obtained (Klymchenko et al. 2004), which can be used in various types of protein and peptide biosensors. Their azacrown ether derivatives exhibit dramatic spectral responses to the binding of bivalent cations (Roshal et al. 1999; 1998). Therefore these reporters can provide a link between chemical sensing and biosensing. Some of their applications will be highlighted in different sections of this book.

One can find analogy of this remarkable result – the ability to obtain from a single type of dye a record number of valuable parameters characterizing its environment and of recording them with record sensitivity –with the transition from black-and-white (intensity only) to color (multiple-channel) television. Thus, it is expected that multicolor dyes will occupy their proper position in sensing.

4.3.7 Responsive Analogs of Amino Acids and Nucleic Acid Bases

Tryptophan is the natural amino acid that is frequently used as fluorescent marker and reporter (Demchenko 1986). Its fluorescence is excited at 280–290 nm and the emission is observed with the maximum at 330–350 nm. Since in many protein molecules several Trp residues are located in their structures, for obtaining site-specific information and avoid spectral heterogeneity all Trp residues beside one target residue are typically substituted by other groups. Due to environment sensitivity of Trp fluorescence, many interesting results were obtained on protein folding and interactions. Still, because of light absorption and emission in the ultraviolet, Trp is not convenient for sensing applications. Its substitution into more efficient synthetic fluorophore can be provided by both synthetic and biosynthetic means.

Proteins possessing reactive –SH groups can be easily modified by covalent attachment of different fluorophore derivatives. An example is the labeling of oligomeric α-crystallin, the molecular chaperone and heat shock protein (Avilov et al. 2005). In this work the 3HC dye 6-bromomethyl-2-(2-furanyl)-3-hydroxychromone (BMFC) was attached covalently to a sole exposed SH-group in one of subunits of this protein. The same derivative when attached to antigenic peptide allowed detecting its specific interaction with antibody (Enander et al. 2008) and being attached to enzyme inhibitor reported on interaction with enzyme elastase (Boudier et al. 2009). The examples of such applications are demonstrated in Figs. 7.16 and 8.18.

Synthetic amino acid analogs containing fluorophore as the side group can be incorporated at desired sites of *synthetic peptides*. Based on different photophysical

mechanisms, they can provide responsive functions (Krueger and Imperiali 2013). Thus, the fluorescent λ-ratiometric analog of natural amino acid *tryptophan* (Trp) was synthesized and incorporated into the zinc finger domain of the HIV-1 nucleocapsid protein (Shvadchak et al. 2009). It retained in full the Zn^{2+} binding affinity and also the function of this protein domain. It preserved the folding, the nucleic acid binding and chaperone activity, indicating that the new amino acid can conservatively substitute Trp residues.

Due to the exceptional sensitivity of its fluorophore to hydration in highly polar environment, the new λ-ratiometric 3-hydroxychromone derivative in the form of amino acid appears as a promising tool for substituting Trp residues for site-selective investigation of peptide–nucleic acid interactions (Strizhak et al. 2012). A recent example is the use of such fluorescent L-amino acid bearing the 4'-methoxy-3-hydroxyflavone fluorophore (M3HFaa) that shows dual emission, as a result of ESIPT reaction (Fig. 4.16). By replacing the Ala30 and Trp37 residues of a HIV-1 nucleocapsid peptide, the peptide structure and functions of M3HFaa was preserved, which allowed observing strong response to the interaction of such labeled peptides with nucleic acids and lipid vesicles. It was shown that this response involves not only switching in dual emission, favoring the emission of the ESIPT product, but also increase in lifetime.

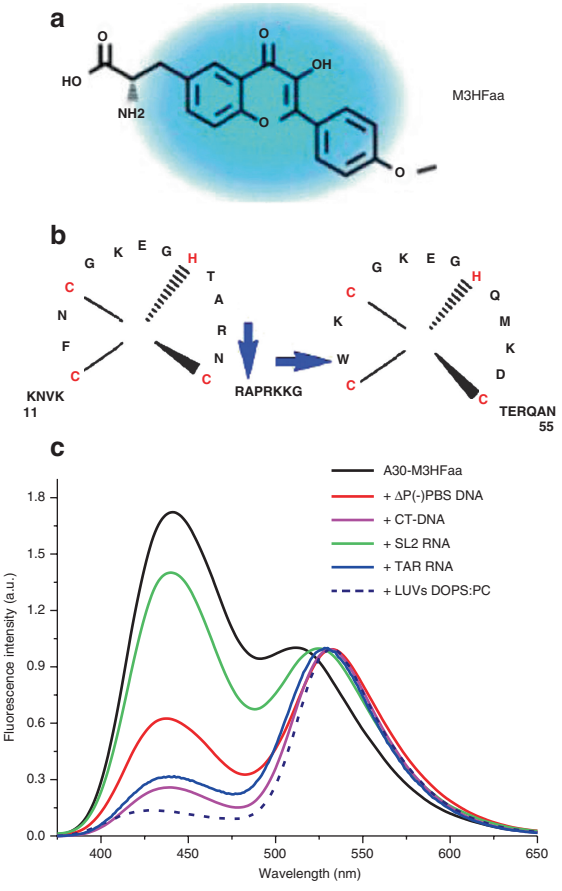

Fig. 4.16 Environment-sensitive fluorescent color-switching amino acid M3HFaa (Sholokh et al. 2014). (**a**) The structure. (**b**) Sequence of the nucleocapsid peptide NC(11-55), where the arrows show the two positions of natural amino acids (A30 and W37) replaced by M3HFaa. (**c**) Effect of different oligonucleotide sequences and phospholipid vesicles (LUVs DOPS:PC) on the normalized fluorescence spectra of the labeled NC(11-55) peptide (A30-M3HFaa). Excitation wavelength was 360 nm

The data presented in Fig. 4.16c demonstrate the two-band wavelength switching response. The characteristic fluorescence spectra reside between two limiting cases, A30- M3HFaa peptide in aqueous buffer, in which the probe is exposed to water, and when it is incorporated into phospholipid membrane, in which it is hidden in low-polar interior. On binding to SL2 RNA the probe remains exposed, and the interaction with DNA and TAR RNA demonstrates complete or partial screening in the formed complex.

The color-switching aminoacid analogs have found interesting application in the studies of interactions of peptides with biological membranes. Substitution by 3-hydroxychromone derivative of two sites in the 26 amino acid sequence of melittin, a well-studied membrane-active peptide, allowed locating these sites with respect to biomembrane based on fluorescence response to local hydration and polarity (Postupalenko et al. 2013).

Moreover, using fluorescence microscopy with a polarized light excitation, the preferential orientation of peptide parallel to the membrane surface was validated. The developed amino acid and the proposed methodology will be of interest to study other membrane peptides.

The analog of tryptophan, (*2,7-aza*)*tryptophan*, (Fig. 4.17) has been recently synthesized and suggested for probing the *hydration* of particular sites in proteins (Shen et al. 2013). This artificial amino acid can be recognized by biosynthetic

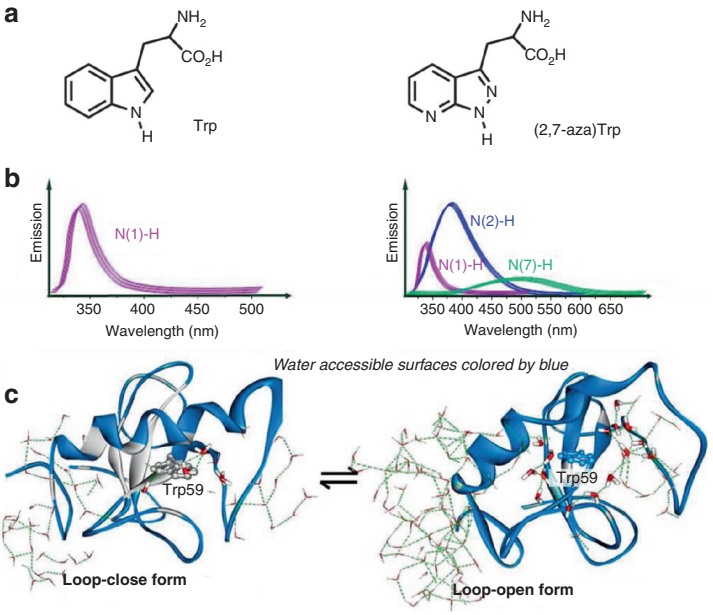

Fig. 4.17 The Trp analog (2,7-aza)Trp, its spectra and an example of its application in the studies of protein conformation (Shen et al. 2013; Chao et al. 2014). (**a**) The spectra of Trp and (2,7-aza)Trp. (**b**) The spectrum of (2,7-aza)Trp in the absence (*left*) and presence (*right*) of water. (**c**) The equilibrium between two conformations of RNase T1 detected by hydration of Trp59 site. The existence of N(2)-H isomer in the loop-open form reveals the specific hydrogen bonding between N(2)-H proton and water molecule that bridges N(2)-H and the amide oxygen of Pro60, forming a strong network. In contrast, in loop-close form the water molecules are squeezed out of this site

machine as Trp, so when added to culture media in bacteria it can replace Trp in newly synthesized proteins.

Whereas Trp emits fluorescence in the near-UV with polarity-dependent band maxima at ~330–350 nm, (2,7-aza)Trp has two additional fluorescence bands extending to the visible that appear due to water-catalyzed proton transfer reaction. In the presence of water, (2,7-aza)Trp exists in two proton-transfer forms in the ground state, the N(1)-H and N(2)-H isomers, in which the N(2)-H isomer exhibits a 380 nm emission band, and the N(1)-H isomer undergoes water catalyzed excited-state proton transfer (ESPT) reaction, giving an N(1)-H 345 nm emission band and a prominent green N(7)-H isomer 500 nm emission (see Fig. 4.17b).

Upon replacing tryptophan, (2,7-aza)Trp successfully recognizes the presence of water in its vicinity by ratiometric changes in relative intensities of these multiple emissions. Essentially, sensing hydration water in proteins occurs without disrupting their native structures (Shen et al. 2013). Using this property, it was found that RNase T1, a small protein composed of 104 amino acid residues, exhibits the structure fluctuating between the two loop-close and loop-open forms differing by exposure to water of a single residue Trp59 (Chao et al. 2014), see Fig. 4.17c.

Nitrogen-containing heterocycles which are parts of DNA and RNA, the so-called *nucleobases*, are non-fluorescent at normal conditions and cannot be used as molecular reporters. To overcome these limitations, many *emissive nucleoside analogues* have been synthesized and evaluated in the field of molecular sensing. They found applications in probing the local structure and dynamics of nucleic acids, typing single nucleotide polymorphism (SNP), investigations of DNA-proteins interactions, to name a few (Sinkeldam et al. 2010; Wilson and Kool 2006). Universal nucleoside analogues, which form stable base pairs with all natural nucleobases without discrimination, are especially important in the probing of nucleic acids (Liang et al. 2013). A nucleoside analogue incorporating a 3-hydroxychromone fluorophore as a nucleobase mimic was synthesized and incorporated into oligonucleotide chains (Dziuba et al. 2012). In comparison with existing fluorescent nucleoside analogues, this dye features exceptional environmental sensitivity switching between two well-resolved fluorescence bands. In labelling DNA, this nucleoside analogue does not alter the duplex conformation and exhibits a high fluorescence quantum yield. This probe is up to 50-fold brighter than 2-aminopurine, the fluorescent nucleoside standard. With this nucleoside, the effect of a viral chaperone protein on DNA base stacking was site-selectively monitored.

A new solvatochromic λ-ratiometric fluorophore compiled from λ-ratiometric 3-hydroxychromone and uracil fragments was also synthesized (Dziuba et al. 2014). The obtained conjugate demonstrates that its uracil and dye fragments are coupled into an electronic conjugated system, which on excitation attains strong ICT character. This provides better resolution between two emission bands.

Fluorescent nucleoside analogues with strong and informative responses to their local environment are in urgent need for DNA research, and the application of λ-ratiometric dyes offers new possibilities.

4.3.8 Prospects

It is expected that organic dyes will maintain to play the major role in designing the response units of future chemical sensors and biosensors. They offer tremendous possibilities of choice in application to sensor technologies due to their huge number, diversity of their spectroscopic properties, possibilities of variation of these properties by chemical modifications, facile methods of their synthesis and easy spectroscopic control of their properties. They can respond by the changes of all possible fluorescence parameters (positions of spectra, intensities, anisotropies and lifetimes) and allow realizing for that different basic photophysical mechanisms involving the transfers of electronic charge, proton and excited-state energy.

Computer design together with application of rapidly progressing methods of quantum chemistry calculations will aid to improvement of required properties of the dyes. It is also very attractive that the straightforward and facile synthetic routes may lead to direct chemical sensors by coupling the dyes with binders for ions and other small molecules. Their labeling of proteins and nucleic acids and also of polymers and nanoparticles becomes an easy routine procedure.

The versatility and practically unlimited possibilities for chemical modifications of organic dyes allow the researcher making the proper choice for any particular application. One has to recognize however that on a general scale, a scientifically motivated design strategy of fluorescent dyes is still lacking, and their *selection is largely empirical*. Quantum chemical calculations can predict (and with difficulty) only the excited-state energies, the charge distributions and dipole moments but not the quantum yields or lifetimes. For optimizing them, an empirical rule suggests to choose the most planar molecules without rotating segments and to select among most efficient analogs. Therefore the most efficient of presently used approaches is the selection of optimal dye within large libraries of synthetic products.

4.4 Visible Fluorescent Proteins

The green fluorescent protein (GFP), a naturally fluorescent protein derived from jellyfish *Aequorea Victoria* (Tsien 1998), and its mutants possess the absorption and emission spectra covering almost the whole visible range, starting from blue and extending into near-IR (Zimmer 2009; Tsien 2009; Stepanenko et al. 2011). They can be transferred to the living cell as genetically engineered fusion products with other proteins that can be incorporated into biological structures. This allows locating different proteins inside the cell and visualizing the structures formed by them.

In fluorescent proteins the fluorophore is formed spontaneously within the folded protein structure, the mechanisms of its formation were established and a number of modified forms were obtained (Miyawaki et al. 2005). Their fluorescent properties are similar to that of organic dyes, and some members of this family demonstrate increased photostability and high fluorescence quantum yield. On illumination with

light, some of them are amenable to long-lived transitions between various fluorescent or nonfluorescent states, resulting in processes known as photoactivation, photoconversion, or photoswitching (Bourgeois and Adam 2012).

4.4.1 Green Fluorescent Protein (GFP) and Its Fluorophore

In GFP the fluorophore formation is coupled with protein folding inside the living cell (Miyawaki et al. 2003). Upon the folding, the fluorescent group is formed spontaneously by the cyclization and oxidation of the protein's own sequence Ser–Tyr–Gly located at positions 65–67 (Fig. 4.18).

The fluorophore in GFP is essentially an '*organic dye*' located inside the barrel-like protein structure of molecular mass 28 kDa. It is located in the central helix and is surrounded by 11 β strands forming the so-called β-barrel. The position of fluorophore deeply inside the protein molecule and the absence of its contact with the solvent determine its properties (Fig. 4.19).

4.4.2 Proteins of GFP Family

Mutagenic studies gave rise to diversified and optimized variants of *fluorescent proteins*, which have never been encountered in nature (Chudakov et al. 2010). Many GFP variants have been obtained by now. They differ in protein and fluorescent group structure and allow selecting their light-absorption and fluorescence properties. Now they are available in different colors and include blue (BFP), cyan (CFP) and yellow (YFP) fluorescent proteins (Shaner et al. 2004). In recent developments, fluorescent GFP-like proteins were obtained from different sources (*Anthozoa*, *Hydrozoa* and *Copepoda* species), demonstrating the broad evolutionary and spectral diversity of this protein family (Fig. 4.20).

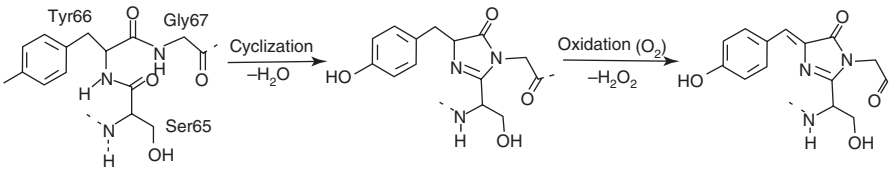

Fig. 4.18 The mechanism of intramolecular biosynthesis of GFP fluorophore. The first step is a nucleophilic attack of the amino group of Gly-67 onto the carbonyl group of Ser-64. Subsequent elimination of water results in the formation of an imidazolidinone ring. In a second step the C_α–C_β bond of Tyr-66 is oxidized to give a large delocalized π-electronic system p-hydroxybenzylidenei midazolinone

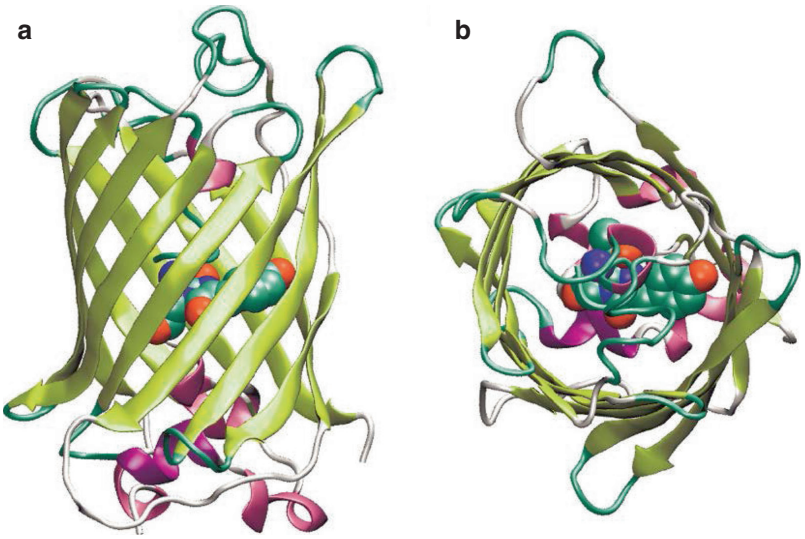

Fig. 4.19 The three-dimensional structure of green fluorescent protein from jellyfish A*equorea Victoria* in two projections. The sequence of 238 amino acid residues (26.9 kDa) is assembled into 11 β strands (shown as *yellow ribbons*) forming the so-called β-barrel. The fluorophore, located inside the beta-barrel, is shown is space-filling representation. It is formed inside this structure as a part of the central helix and is highly protected from interaction with the solvent

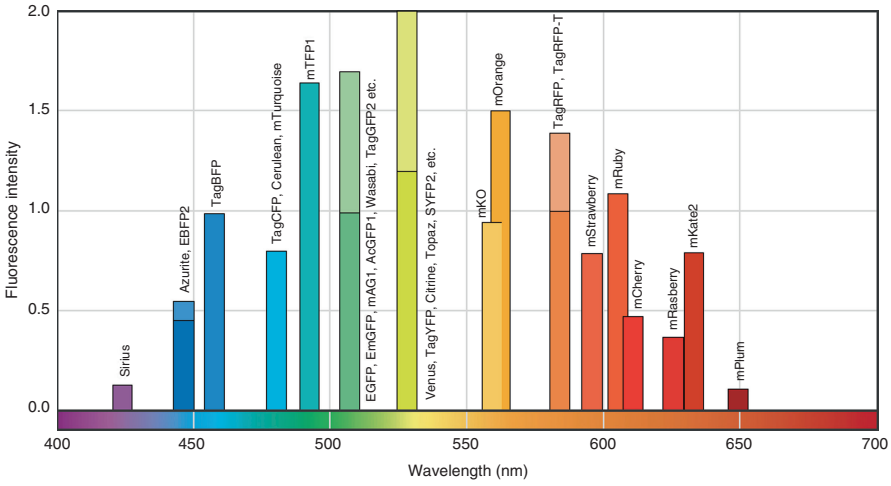

Fig. 4.20 Spectral diversity of available monomeric FPs (Chudakov et al. 2010). Columns show the positions of emission maxima and relative brightness (product of molar absorbance by fluorescence quantum yield) of representative monomers

Naturally these proteins are tetrameric, and their monomeric versions have been engineered for applications that involve fusion with other proteins. Further molecular characterization of the structure and maturation of these proteins is in progress, aimed at providing information for rational design of variants with desired fluorescence properties. It was found that the fluorescence quantum yield Φ values and brightnesses (Fig. 4.20) for these proteins are generally relatively good but depend on final structure of fluorescent group and mutations around it. Usually Φ ranges from 0.17 for BFP to 0.79 for wild-type of GFP but it is sensitive to pH, temperature, oxygen concentrations and other environment conditions (Giepmans et al. 2006).

Very promising in this respect is the red fluorescent protein from *Anthrosoa* corals (DsRed), mainly due to its strongly red-shifted fluorescence spectrum. With molar absorption coefficient 57,000 M^{-1} cm^{-1} and quantum yield 79 % it competes with GFP and shows superior properties in terms of photostability and independence of spectra on pH in the range 5.0–12.0 (Shrestha and Deo 2006). Excited in the range 558–578 nm DsRed and its mutants display fluorescence with the band maxima ranging between 583 and 605 nm. With these properties, it becomes valuable as a fluorescent tag in various cell biology applications. During the past decade many advanced red fluorescent proteins, including far-red proteins with emission wavelength larger than 620 nm have been developed (Shcherbakova et al. 2012).

4.4.3 Labeling and Sensing Applications of Fluorescent Proteins

Due to the ability to be co-expressed as *fusion proteins* with many proteins that are naturally synthesized and functioning inside the living cells, GFP and its mutant variants serve as unique tools in molecular biology and cell imaging. Presently they are the only fully genetically encoded fluorescent probes available to the researcher. The benefits of using such markers and sensors are obvious because they obviate the issues of intracellular delivering and targeting of synthetic fluorophores.

GFPs are used as tools in numerous applications. They include biological labeling to track and quantify individual or multiple protein species, probing to monitor protein–protein interactions, sensing to describe intracellular events and detecting different targets. Different applications have been realized using these proteins as FRET donors and acceptors in *fluorescence lifetime imaging microscopy* (FLIM) (Mérola et al. 2014). However, their relatively large size (~26–28 kDa) may create problems by interference with the expression and folding of fused protein partners and affecting interactions with other molecules. The GFP mutants and circularly permuted GFP variants have been used to develop fluorescent probes that sense physiological signals such as membrane potential and concentrations of free calcium (Miyawaki et al. 2005).

An important step towards the improvement of fluorescent proteins and extending the range of their applications was obtaining the species that become fluorescent

(*photoactivated*) or change the colors of emission (*photoswitchable*) upon illumination at specific wavelengths (Shcherbakova et al. 2014). Their fluorescence can be controlled within living cells by light of specific wavelengths, which is especially needed for superresolution fluorescence microscopy (see Sect. 13.2),

4.4.4 Other Proteins with Visible Fluorescence Emission

In addition to GFP and its relatives, there are other proteins that contain strongly fluorescent pigments. They can be isolated from species containing photosynthetic systems. Those are algae *phycobiliproteins* whose function is to absorb energy of light and transfer it to chlorophyll. They possess absorption maxima at 545–650 nm with the molar absorbance as large as 2.4×10^6 M^{-1} cm^{-1}. Their Stokes shift is not very large, 10–25 nm but quantum yield may reach 85 %. Such a high quantum yield is achieved because the protein matrix provides not only the location sites for a number of fluorescent pigments but also avoiding their contact that could result in self-quenching. Due to their high brightness and relatively long-wavelength emission, these proteins have found important application primarily in flow cytometry, where they can be combined with different dyes for multicolor labeling of cells. Meantime, at present it is not possible to synthesize them in fully assembled fluorescent forms inside the living cells as it is done with GFP-type proteins. This limits their application to *in vitro* testing.

Due to their high brightness and long-wavelength emission, phycobiliproteins and, in particular, *B-phycoerythrin*, are used in FRET-based immunoassays, in which they make complexes with antibodies (Petrou et al. 2002). They are also useful as acceptors in sensing technologies based on FRET. Their major disadvantage in these applications is their large molecular size (1–1.5 times the molecular mass of IgG), which results in their slow diffusion leading to long incubation time. In this application the nanoparticles are expected to be more prospective, regarding availability, stability and price.

4.4.5 Finding Analogs of Fluorescent Protein Fluorophores

Discovery and very successful applications of fluorescent proteins stimulate search of naturally formed fluorophores of peptide origin. Fluorescent proteins have shown that spontaneous reactions between amino acid residues in a peptide chain with fluorophore formation are possible. This justifies the search for simpler peptide sequences that can give rise to self-assembling and self-catalyzing reactions leading to formation of fluorescent species. The focused search within constructed ~500,000-member solid-phase combinatorial library of Trp-containing Ala-flanked peptide hexamers led to successful findings that several non-fluorescent peptides selected from the library after UV irradiation and oxidation in the air attain intensive

visible fluorescence (Juskowiak et al. 2004). A number of analogs of GFP fluorophore have been synthesized (Ivashkin et al. 2009).

The other trend in this line is mimicking the environment of GFP fluorophore analogs in order to suppress the free rotation around an aryl-alkene bond that is restricted in β-barrel protein environment. Some of the compounds synthesized along this line showed relatively bright fluorescence (Wu and Burgess 2008; Baranov et al. 2014). Of special interest was the design of fluorophores exhibiting the excited-state reactions, particularly ESIPT (Chen et al. 2007).

4.4.6 Prospects

An exciting new development in fluorescent imaging and sensing has appeared with the introduction of naturally fluorescent proteins. The interest towards these proteins is great, especially to those that can be fused with other proteins on a genetic level producing hybrids that can be synthesized inside the living cells. These hybrids can be unique intracellular markers and tags. Their applications as the sensors for small compounds (such as sugars and ions) have also been demonstrated successfully. Meantime, in this respect their application will not probably go far beyond intracellular research. The single cells with incorporated smart fluorescence proteins will become ideal whole-cell biosensors. Size reduction and also increasing the stability and brightness of their emission together with the development of sensor properties are the primary goals.

4.5 Luminescent Metal Complexes

In sensing technologies there is a strong need to overcome limitations in lifetime values and to extend the time ranges to microseconds and milliseconds. Longer lifetimes should allow observing molecular motions of large molecules and particles and using simpler instrumentation for lifetime analysis. They offer a simple way to eliminate the light-scattering effects and short-living background fluorescence, thus increasing significantly the sensitivity and precision of assays. Two types of metal complexes can achieve the long-lifetime emission – the coordination complexes of lanthanide ions and of noble metal ions of platinum group.

4.5.1 Lanthanides, Their Complexes and Bioconjugates

The *lanthanides* usually exist as trivalent cations. Strictly speaking, their emission is not a fluorescence (it does not proceed from singlet-singlet transitions)

and therefore a broader term '*luminescence*' has to be applied in this case. Only four of lanthanide ions can emit light of detectable intensity in the visible region: terbium (Tb^{+3}), europium (Eu^{+3}), samarium(Sm^{+3}) and dysprosium (Dy^{+3}), and only the first two exhibit a relatively high emission intensity (Armelao et al. 2010). This emission comes from formally forbidden transitions of *f* electrons that, being shielded from external perturbations by the filled 5 s and 5p orbits, do not interact strongly with the environment. Therefore, the emission of these ions is almost insensitive to intermolecular interactions, and because of that, there is no observed quenching on collisions with molecular oxygen (Bunzli and Piguet 2005).

The major problem with direct excitation of these ions is in their very low molar absorbance (ε ~1 M^{-1} cm^{-1}). Therefore for overcoming this drawback they are incorporated into chelating complexes formed by light-absorbing organic heterocycles that play the role of antennas (Fig. 4.21). Being primarily excited, the latter transfer the excitation energy to lanthanide ions, which become the sources of a much more efficient emission than on direct excitation. This allows increasing their molar absorbance to the values above 10,000 M^{-1} cm^{-1}, which is sufficient for many applications in fluorescence sensing.

Synthetic strategies for incorporation of lanthanide ions into molecular complexes are well developed. They use pre-organized macrocycles (such as cryptands and crowns), pre-disposed macrocycles (such as substituted cyclens), podands. Different structures formed by self-assembly process from complex heterocycles such as substituted benzimidazole pyridines (Bunzli 2006) can be also efficiently used. Modified calixarenes (see Sect. 7.2) were also suggested as ligands (Oueslati et al. 2006). This allows realizing many possibilities for modification, functionalization and incorporation into desired systems. In addition, all these complexes should be able to play their major role: to minimize the quenching induced by interatomic vibrations and protect the ion from interaction with the solvent.

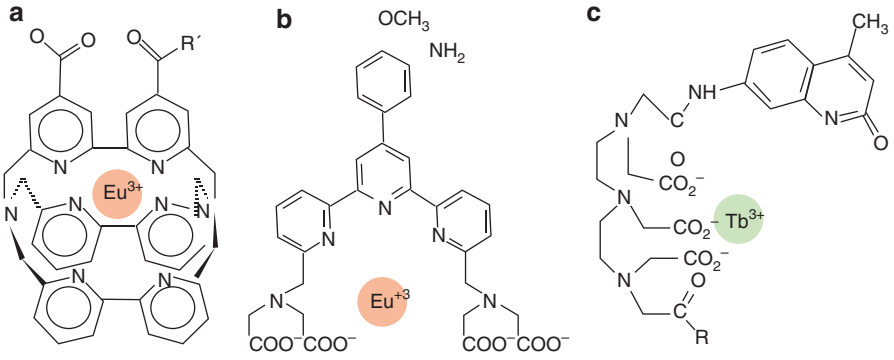

Fig. 4.21 Typical structures of chelating complexes with europium and terbium ions (Wang et al. 2006). For cryptates (**a**, *left*) and terpyridine (**b**, *center*), the chelate and antenna are logically the same entity. The complex may be composed of a chelating group and an antenna (**c**, *right*)

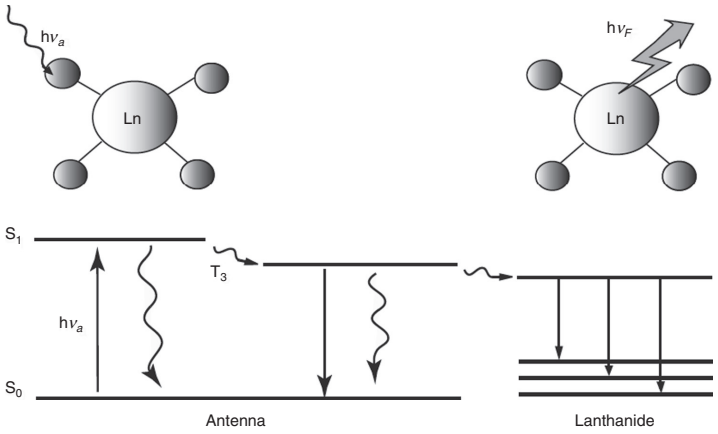

Fig. 4.22 Schematic representations of excited-state processes in lanthanide complexes. The light quanta are absorbed by aromatic ligands (*antenna*) and after conversion from singlet (S_1) to triplet (T_3) state the energy is transferred to lanthanide ion, which emits light

4.5.2 Photophysics of Lanthanide Chelates

The primary role of chelating group is to provide indirect excitation of lanthanides via antenna effect. It is realized in three steps (Bunzli and Piguet 2005). First, light is absorbed by aromatic ligands surrounding the ion, leading to its *singlet excited state*. Then a conversion occurs to their *triplet* (long-lifetime, phosphorescent) state, from which the energy is transferred to emitting lanthanide ion (Fig. 4.22). The ligand singlet excited state may also transfer its energy, but due to short lifetime of this state, such process is not efficient.

As a result, luminescence of lanthanide-chelator complexes attains *long lifetimes* (τ) that may extend from ~100 ns to milliseconds. Such property is their primarily attraction point that offers many advantages in sensing (Aoki et al. 2005). These complexes allow eliminating the background fluorescence and light-scattering by time-resolved detection, or even by technically simple time-gated detection collecting the emission after microsecond time delay (see Fig. 3.11). With τ values in the μs-ms time range the lanthanide emission can be easily distinguished from that of conventional fluorescent dyes with τ_F ~1–5 ns, and this is advantageous for multiplex sensing.

4.5.3 Luminescence Spectra

Lanthanide chelates exhibit broad *excitation spectra* (owing to their organic ligands) and several very characteristic luminescence *emission bands* of the lanthanide ions (Pandya et al. 2006). They are composed of several discrete sharply spiked bands (less than 10 nm in width). Being excited in the near-UV they exhibit very strong

Stokes shifts. Thus, for *terbium chelates* with excitation at about 340 nm, a series of emission bands is observed, starting from about 500 nm and extending to longer wavelengths giving predominantly green light emission (Fig. 4.23).

Regarding chelates of *europium ions*, multiple peaks of their emission are located in the orange-red spectral region (Fig. 4.24). Here also, the strong spectral separation between excitation and emission bands is the second, beside the long lifetime, attractive property of lanthanide ion complexes.

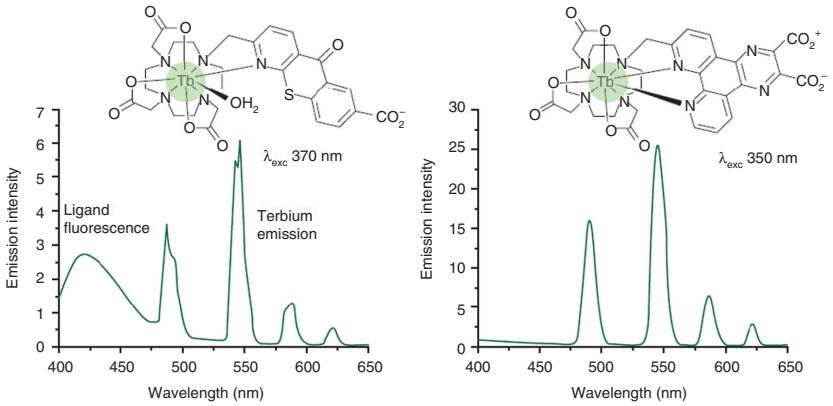

Fig. 4.23 Emission spectra for selected terbium complexes (298 K, 0.1 M NaCl), showing residual ligand fluorescence from the aza-thiaxanthone chromophore (*left*) (Pandya et al. 2006)

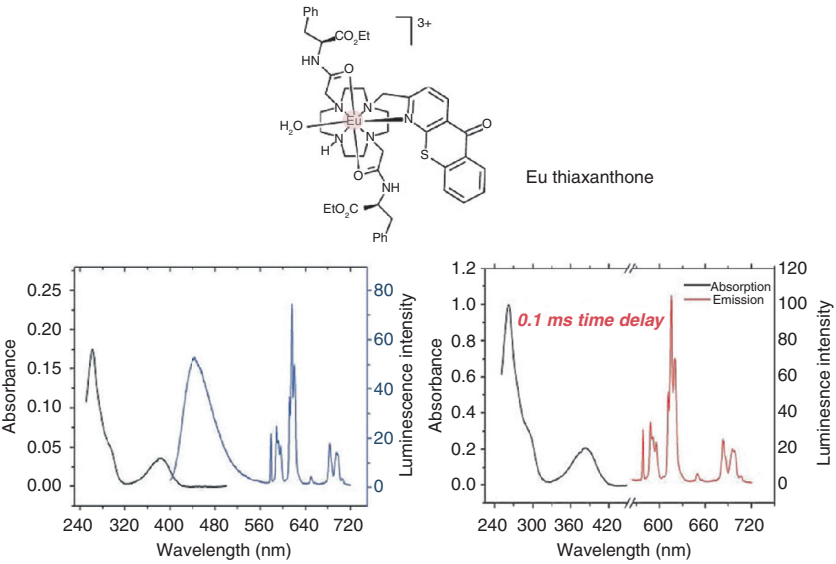

Fig. 4.24 Absorption and total emission spectra (λ_{ex} = 384 nm) for the aqua–europium complex, highlighting the short-lived ligand-based fluorescence and the long-lived europium luminescence, the latter being observed uniquely when a 100 μs time delay is used (*right*) (Pandya et al. 2006)

Table 4.3 The properties of lanthanide ion chelating complexes

Parameter	Property
Size	~1–2 nm
Absorption spectra	The broad band in the range 337–420 nm, depending on the ligand
Molar absorbance, ε	Very small (~1 M^{-1} cm^{-1}) upon direct excitation. Highly increased up to ~10,000 M^{-1} cm^{-1} in chelating complex
Emission spectra	Series of strongly separated, narrow (~10 nm half-width) bands
Tunability of emission spectra	Possible only in a very limited range (several nm)
Stokes shifts	Large, 100–200 nm
Excited-state lifetime, τ_F	Very long, up to ~1 ms, normally insensitive to oxygen quenching; sensitivity may appear due to quenching of ligand emission
Photoluminescence quantum yield, Φ	Variable, from ~0.05 to ~0.4; dramatic quenching by coordinated water
Fundamental anisotropy, r^0	Zero
Photostability	Relatively high but not ideal
Chemical stability	Often low, due to low binding energy in chelating complex. Can be increased by selecting proper ligands
Availability of chemical modification/functionalization	High, depending upon the ligand
Cell toxicity	Definitive data are absent

Luminescence *quantum yields* of lanthanide probes can be as high as 0.1–0.4, but often are much lower, ~0.05. Its severe quenching by water can be observed (Bunzli and Piguet 2005). In contrast to organic dyes (in which the quenching usually occurs due to electron transfer to traps formed in bulk water) the quenching here is due to coordinating water molecules. The latter interacting with inner coordinating sphere dissipate energy via O–H vibrations. Thus a special effort has been made for achieving the high emissive properties of these complexes in water (Charbonniere et al. 2007) by constructing the saturated co-ordination sphere around the ion. Finally, this allowed realizing different simple and sensitive bioassays (Yuan and Wang 2006). Severe quenching by water molecules is a weak point in application of these luminophores. This requires their shielding from water but also allows constructing different types of molecular sensors exploring this property (Armelao et al. 2010).

The properties of lanthanide chelating complexes are summarized in Table 4.3.

4.5.4 Lanthanide Chelates as Labels and Reference Emitters

Lanthanide coordination compounds are very efficient *labels*. This is not only because of their intrinsic properties, such as high brightness and many possibilities of their covalent and non-covalent attachments, but also because they do not exhibit *concentration quenching* and therefore can be used for loading macromolecules and nanoparticles in very high concentrations (Kokko et al. 2007).

Lanthanide complexes are ideal as the *reference dyes* in fluorescence sensors based on two-wavelength ratiometric recording (see Sect. 3.2). Their broad excitation spectra allow exciting them by the same wavelength as the reporting dyes and providing stable signal that is well separated from that of the reporter. The response of this reference should be independent of target binding and of any external perturbation and easily distinguishable from reporter signal by emission wavelength or lifetime. Low dependence of emission spectra on the temperature and on the presence of quenchers makes lanthanide chelates very attractive for this purpose.

Lanthanide probes are very important tools in cellular imaging that are beneficial with the use of lifetime imaging techniques (Heffern et al. 2013) and time-resolved immunoassays (Wang et al. 2013). In a latter case their composites with quantum dots are used as efficient FRET systems, in which they serve as excitation energy donors providing the property of long lifetime emission to the acceptor (Cywincki et al. 2014; Hildebrandt et al. 2014). For more detail about this mechanism and its applications see Sects. 6.2 and 6.3.

4.5.5 Dissociation-Enhanced Lanthanide Fluoroimmunoassay (DELFIA)

Formation-dissociation of lanthanide complexes result in dramatic (by orders of magnitude) change in their luminescence emission intensity and lifetime by on-off switching the *antenna effect*, so the idea of application of this property in sensing is straightforward. Moreover, the chelating complexes can be both strong and weak (easily dissociating), and this fact suggests very elegant ideas in applications, particularly in *immunoassays*. In DELFIA and related technologies (Hemmila and Laitala 2005) the non-luminescent lanthanide Eu^{3+} and Tb^{3+} chelates are used as labels for antibodies. The complexes are formed in such a way that metal ions are loosely bound within them and can dissociate into the medium. After performing immunoassay, in which the antibodies are bound by the antigens, the lanthanide ions dissociate from their ligands. On the next step, they are transferred to development solution, where they form new strongly emitting complexes with the high-affinity chelators that are present in this solution. These complexes can be easily detected and quantified.

This technique and its versions are very popular both in research and in clinical analysis because of high sensitivity and reproducibility. The recent comparative studies of several sensing technologies for detecting cAMP have shown that DELFIA has the highest sensitivity (Gabriel et al. 2003). It can be further enhanced dramatically by assembling the lanthanides into nanoparticles (Zhou et al. 2014). We cannot forget, meantime, that this and related techniques are the techniques based on the concept of heterogeneous assay that needs separation and reagent addition steps. Simplification of these techniques by transforming them to homogeneous format is a great challenge.

4.5.6 Switchable Lanthanide Chelates in Sensing

For producing direct sensing, one can use many possibilities to incorporate recognizing and transducing units (Fig. 4.25). Because the primary light absorption sites in lanthanide complexes are the chelating aromatic groups (sensitizers) and emission properties are determined by lanthanide ion, there are basically two application sites for inducing the changes in emission intensity and lifetime that could be used to produce sensing response (Pandya et al. 2006):

(a) *Perturbations of sensitizers*. The reporting signal can be generated by the influence on two (singlet and triplet) excited states of sensitizer groups. Photoinduced electron transfer (PET) can be used as a common mechanism of excited-state quenching, in which an electron is transferred from an electron donor moiety to an acceptor moiety. With lanthanide complexes in PET the *electron donor group* can be covalently attached to chelating heterocycle, so that coupling-decoupling of this quencher can provide the response in intensity of emission (Terai et al. 2006).

(b) *Perturbation of the lanthanide ion*. This can be provided via coupling/decoupling the sensor operation with its access to water molecules that are extremely potent quenchers (Bunzli and Piguet 2005). When these quenching water molecules are displaced, for instance, by reversible binding of anion, high emission intensity is restored with correspondent increase of lifetime. Better protection

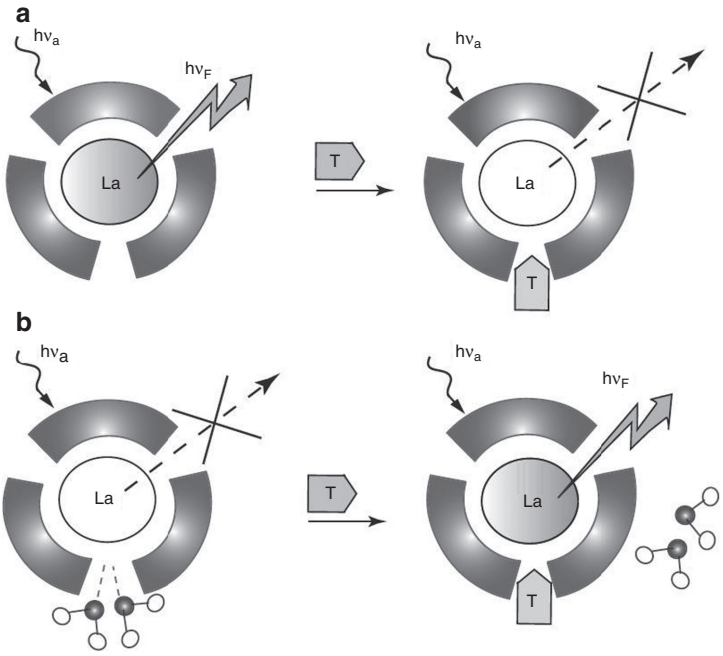

Fig. 4.25 Illustrations of the mechanisms in the background of modulation of lanthanide emission on a reversible binding of the target (*T*): (**a**) Influence on the excited-state transitions of antenna via PET mechanism. (**b**) Direct influence on luminescence by screening the access of lanthanide ion to water molecules

from interaction with water can be achieved on incorporation of the whole complex to detergent micelles and to different nanostructures, and this offers new possibilities to impose the sensor response.

Lanthanide complexes with ionizable groups incorporated into antenna may respond to the change of pH not only by variation of emission intensity but also by redistribution of intensity between emission bands. This opens the pathway for constructing the probes that are valuable for luminescent ratiometric pH imaging (Woods and Sherry 2003).

4.5.7 *Transition Metal Complexes That Exhibit Phosphorescence*

The long-living emission of transition metal complexes has a different mechanism in its background. It is due to their ability to convert to the *triplet state* and emit *phosphorescence*. This explains the fact that their emission is subjective to different quenching perturbations. Particularly, the collisions in the emissive state with oxygen molecules provide strong quenching.

The emission properties of *transition metal complexes* of ruthenium (Ru), osmium (Os) and rhenium (Re) ions with organic ligands, such as pyridine groups, are the most frequently studied and used. They exhibit the *metal-to-ligand charge transfer* (MLCT) phosphorescence (Balzani et al. 2000). The absorption and emission spectra of these complexes are broad, with strong Stokes shifts and highly polarized emission (Balzani et al. 2000). The structure of one of such complexes of Ru^{3+} with ligands, tris-(2,2'-bipyridine) chelate, $Ru(bpy)_3^{2+}$, and its absorption and emission spectra are presented in Fig. 4.26.

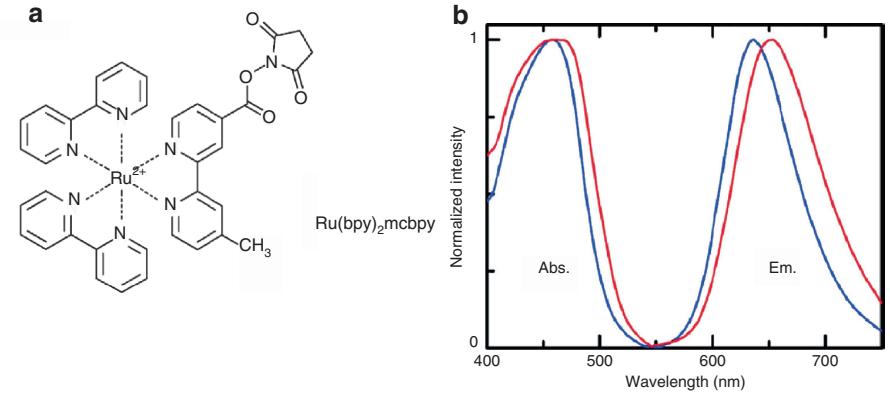

Fig. 4.26 An example of chelating complex incorporating ruthenium ions and containing a reactive group for covalent binding (Piszczek 2006). (**a**) The structure of Ru bis(2,2'-bipyridine)-4'-methyl-4-carboxybipyridine N-succinimidyl ester, $(Ru(bpy)_2mcbpy)$. (**b**) Normalized absorption and emission spectra of $(Ru(bpy)_2dcbpy)$ in aqueous buffer, pH 7.4 and when conjugated to IgG (slightly shifted to the red)

We can see that despite visual similarity in formation of ion-heterocyclic chelates, the origin of such emission is quite different from that of lanthanide complexes. Since it is the *phosphorescence* in MLCT complexes, their absorption and phosphorescence emission spectra are similar to that of typical organic dyes. The absorption spectra are broad. For Ru^{2+} complexes they are located around 470 nm with the half-width ~100 nm. Similarly broad emission spectra are observed at 610–670 nm, demonstrating a large Stokes shift.

The molar absorbances of these complexes are on the level of ~10,000–30,000 M^{-1} cm^{-1}, which is sufficient for different applications in sensing. Since phosphorescent emission occurs from the triplet state, its duration is long and can be observed on a scale of several microseconds. Remarkable, this emission is highly sensitive to temperature and concentrations of oxygen in the medium.

Long lifetime of ruthenium chelate complexes allow using them as *reference emitters* in the two-channel wavelength-ratiometric sensors based on the principle of intensity sensing with the reference (Sect. 2.1). This was done with double labeling in glucose sensor (Shav-Tal et al. 2004) and in glutamine sensor (Lakowicz et al. 1999) based on bacterial periplasmic glucose and glutamine binding proteins correspondingly, In these sensors the organic environment-sensitive dye Acrylodan was the responsive dye reacting to the target binding by quenching its emission. Ruthenium bis-(2,2′-bipyridyl)-1,10-phenanthroline-9-isothiocyanate served as a nonresponsive long-lived reference. This allowed recording the ratio of emission intensities of Acrylodan dye and ruthenium (at 515 and 610 nm) as a reporting signal, which allows increasing substantially the accuracy of sensor operation.

The other important application of metal chelate complexes is in fluorescence *anisotropy sensors* and *polarization immunoassays*. Since these complexes exhibit large fundamental anisotropy values, this allows examination of rotational dynamics on the time scale of microseconds. The problem here (as discussed in Sect. 3.3) is to develop luminescence probes with lifetimes that are comparable to rotational correlation times of the antibody, the antigen, and the bioconjugates that they form. Ruthenium or rhodium chelate complexes with lifetimes 1000-fold longer than of the common dyes allow achieving this goal.

4.5.8 Metal-Chelating Porphyrins

The porphyrins (see Fig. 7.10) are among organic heterocyclic compounds that can incorporate the transition metal ions with the formation of *phosphorescent complexes*. They possess a tetrapyrrolic structure and may contain different side substituents. These compounds can be widely found in nature forming various heme derivatives and chromophyls. Many of these structures can be now produced by chemical synthesis. Interesting for sensor applications are *metalloporphyrin*

complexes of platinum (Pt) and palladium (Pd). They display narrow and intensive absorption bands at 360–400 nm with molar absorbance $1–5 \times 10^5$ M^{-1} cm^{-1} (Soret band) and also the absorbance in 500–550 region (Q-bands). In this green part of the spectrum their absorbance is much weaker, on the level of 20,000 M^{-1} cm^{-1}. The red (600–750 nm) phosphorescence emission exhibits lifetimes in the range from 0.01 to 1 ms (Papkovsky and Ponomarev 2001). These features make these reporters useful as probes for a number of analytical applications, particularly those employing time-resolved fluorescent detection (Papkovsky and O'Riordan 2005).

A number of *analytical systems* have been developed that are based on the use of phosphorescent porphyrin probes (Papkovsky et al. 2000). Among them are the fiber-optic phosphorescence lifetime-based oxygen sensors constructed on the basis of hydrophobic platinum-porphyrins and also the biosensors for metabolites (glucose; lactate) based on detection of oxygen consumption by glucose oxidase. Water-soluble platinum- and palladium-porphyrins can also be used as labels for ultra-sensitive time-resolved phosphorescence immunoassays.

The techniques of labeling proteins and nucleic acids with porphyrins as the probes have been developed (O'Riordan et al. 2001). They can be used for labeling of oligonucleotides that are applied in hybridization assays (Burke et al. 2003). Upon hybridization with complementary sequences bearing common organic dyes, the metal chelate probes display a strong quenching due to close proximity effects, which allows establishing separation-free hybridization assays. Attractive field of application is in time-resolved luminescence microscopy (Soini et al. 2002).

4.5.9 Prospects

The most important trends in application of lanthanide chelating complexes and of charge-transfer complexes of transition metals are related with their strong *Stokes shifts* and *long luminescence lifetimes*. Both these factors strongly facilitate recording of output signal and, especially, its discrimination from background emission. More efforts are needed for their implementation in direct sensing technologies, and the first steps have already been made.

Attractive are their applications in the two-wavelength *ratiometric sensors*, in which the ion chelates serve as references or FRET donors. Moreover, due to their long lifetimes these emitters can respond to rather *slow motions* of molecules and nanoparticles, which can be the mechanism of report on binding of targets of relatively large size. In sensor operation, different *quenching* effects can be used as the mechanism of on/off switching.

The applications of metal chelates as FRET donors are the most promising. Being coupled to molecules or nanoparticles with bright but short-living fluorescence they can provide to these acceptors the property of long-lifetime emission

(this issue will be discussed in Sect. 6.3). Time-resolved detection in this case allows achieving important benefits: not only the light-scattering and background emission are suppressed, but also the short-living emission of directly excited acceptor does not contribute to detected signal.

4.6 Few-Atom Clusters of Noble Metals

Fluorescent noble metal nanoclusters have attracted a lot of attention as a new class of fluorophores. They demonstrate unique electronic structures and, subsequently, unusual physical and chemical properties. Like organic dyes, they possess *discrete electronic states*, and the electronic transitions between these states displaying strong visible fluorescence. In view of their very small size comparable with that of organic dyes, of their biocompatibility and the absence of photobleaching, these clusters represent an attractive alternative to other types of fluorescence emitters in labeling and, especially, in imaging (Yuan et al. 2013b; Choi et al. 2012).

4.6.1 The Cluster Structures and Their Stability

Up to now, significant efforts have been dedicated to the synthesis, property and application studies of *gold* and *silver* nanoclusters (Choi et al. 2012; Diez and Ras 2011). Recently, a growing number of studies on *copper* and other metal clusters have also been reported. These clusters can be obtained by chemical or photochemical reduction of ions in solutions. The application of strong chemical reductant, such as $NaBH_4$, can be substituted by treatment with UV or visible light, by electrochemical reduction or by other means. The problem is only to stabilize them by choosing appropriate scaffolds.

In the case of *silver*, reduction ($Ag^+ \rightarrow Ag^0$) is coupled directly with cluster formation. Organic scaffolds are commonly used for maintaining the cluster stability and suppressing further increase in their size. The cluster size can be of 2–3 atoms only and its strength depends on the scaffold. The clusters exhibit characteristic excitation and emission bands in the visible range of spectrum demonstrating behavior similar to that of organic dyes (Diez et al. 2012).

There is a difference in formation of gold and silver clusters. The *gold* clusters are usually larger in size incorporating several tens of atoms. To date, several atomically precise Au_n nanoclusters (e.g. Au_{20}, Au_{22}, Au_{24}, Au_{25}, Au_{38}, etc.) with thiolate ligands or stabilized by protein templates (Ghosh et al. 2014) have been synthesized, and their electronic and optical properties have been studied.

The results of recent efforts for implementation of silver clusters (Choi et al. 2012; Diez and Ras 2011) can be summarized as follows (see Table 4.4):

Table 4.4 The properties of few-atom clusters of silver

Parameter	Property
Size	<1 nm but need stabilizing template
Absorption spectra	Commonly corrupted by light-scattering. No vibronic structure observed
Molar absorbance, ε	Of the order of 10^5 M^{-1} cm^{-1}
Excitation spectra	Resolved, broad (~60 nm) and symmetric
Emission spectra	Broad (~70 nm half-width), symmetric, inhomogeneously broad
Stokes shifts	~100 nm, low sensitive to intermolecular interactions
Fluorescence quantum yield, Φ	Can be relatively high, 20–30 %
Excited-state lifetime, τ_F	Insufficiently studied. Can be between 10 and 200 ns.
Two-photonic cross-section, α	>10,000 GM
Fundamental emission anisotropy, r^0	Unexpectedly high, ~0.35
Photostability	High
Availability of chemical modifications	Depends on stabilizing template

(a) The clusters of well defined size and composition can be synthesized in both aqueous (Wu et al. 2009) and nonaqueous (Diez et al. 2012) solvents. During the reduction and cluster formation the number of clusters increases without affecting the type of emitters and the shape and position of emission spectra.
(b) Their excitation and emission spectra in the visible range of spectrum are characteristic. They may not depend on the method and duration of treatment but strongly depend on the scaffold.
(c) The excitation and emission spectra are well separated (Stokes shifts are strong).
(d) Their stability is variable and strongly depends on the support. With synthetic polymers (Diez et al. 2009), peptides and proteins (Yu et al. 2007) and DNA fragments (Vosch et al. 2007) sufficient stability for many applications has been achieved. The factors determining their stability and its dependence on scaffold are still not well understood.
(e) They exhibit a remarkable photostability.

Geometrical shapes of these clusters are not well known at present but it is clear that interaction with the support atoms is a strong determinant for their formation. This interaction determines the cluster size and stability and, finally, the parameters of fluorescence emission.

4.6.2 The Mechanisms of Light Absorption and Emission

In metallic particles with the decrease of their size smaller than the free path length of an electron (~20–30 nm for silver and gold) the electron motions become

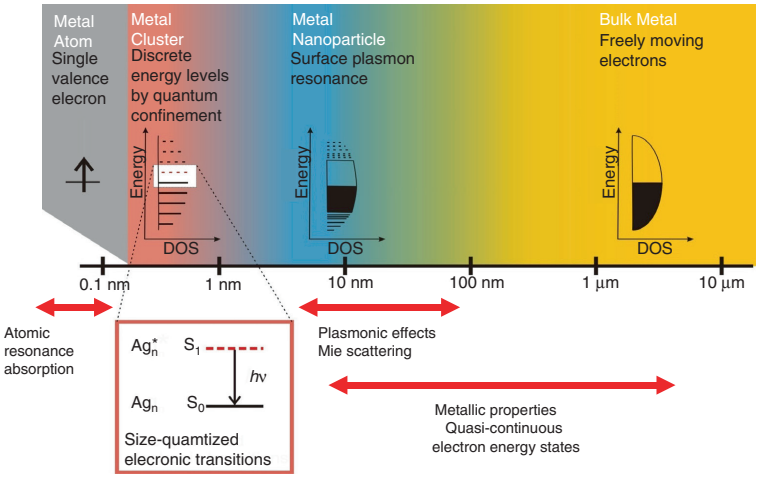

Fig. 4.27 The effect of size on metals. Whereas bulk metals and metal nanoparticles have a continuous energy profiles, the limited number of atoms in metal nanoclusters results in discrete energy levels, allowing on interaction with light the electronic transitions between these levels

restricted and the *localized plasmonic* effects are observed (Fig. 4.27). They produce strong light absorption and scattering. Due to generating strong electromagnetic fields in their surrounding, dramatic plasmonic enhancement effects are observed in the spectra of Raman scattering and also in fluorescence emission of different closely located fluorophores (see Sect. 10.7).

If we further decrease the particle size down to several atoms, plasmonic properties disappear. Being too small for forming the continuous density of states that are necessary for generating plasmons, the few-atom clusters start to behave *like molecules* (Choi et al. 2012; Diez and Ras 2011). They possess discrete electronic states and the electronic transitions between these states, bridging the gap between single atoms and nanoparticles.

4.6.3 Excitation and Fluorescence Emission Spectra

Fluorescence emission in noble metal clusters commonly possess single emission bands that may be observed in the whole visible range, extending to near-IR. The spectral positions of these bands depend on two major variables – the nature of scaffold and the cluster size. The general tendency observed for silver (Choi et al. 2012) and gold (Zheng et al. 2007) clusters is that with the increase of cluster size the excitation and emission bands shift to longer wavelengths (Fig. 4.28).

In comparison with gold clusters, the *silver clusters* are usually smaller and brighter; the positions of their spectral bands do not depend so clearly on the cluster size because of stronger dependence on supporting scaffold. Their excitation and emission spectra are usually broad, symmetric and do not possess any fine structure (Fig. 4.29). When formed on *polymeric scaffolds* they display mirror symmetry

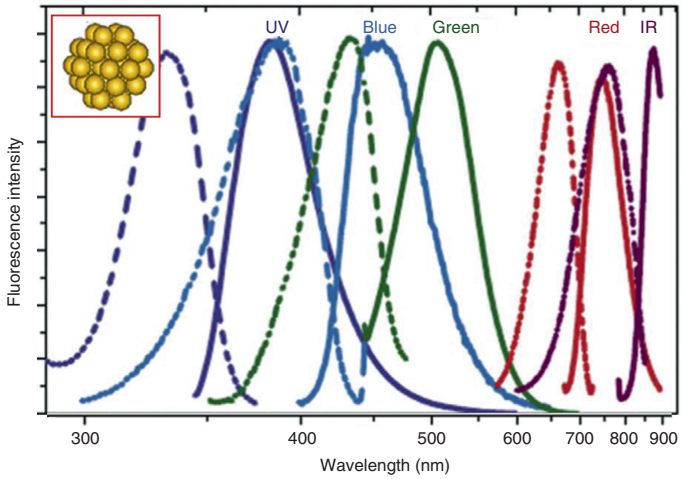

Fig. 4.28 Excitation (*dashed*) and emission (*solid*) spectra of different gold clusters. They shift to longer wavelength with increasing the cluster size in a sequence Au_5, Au_8, Au_{13}, Au_{23} and Au_{31} (Zheng et al. 2007)

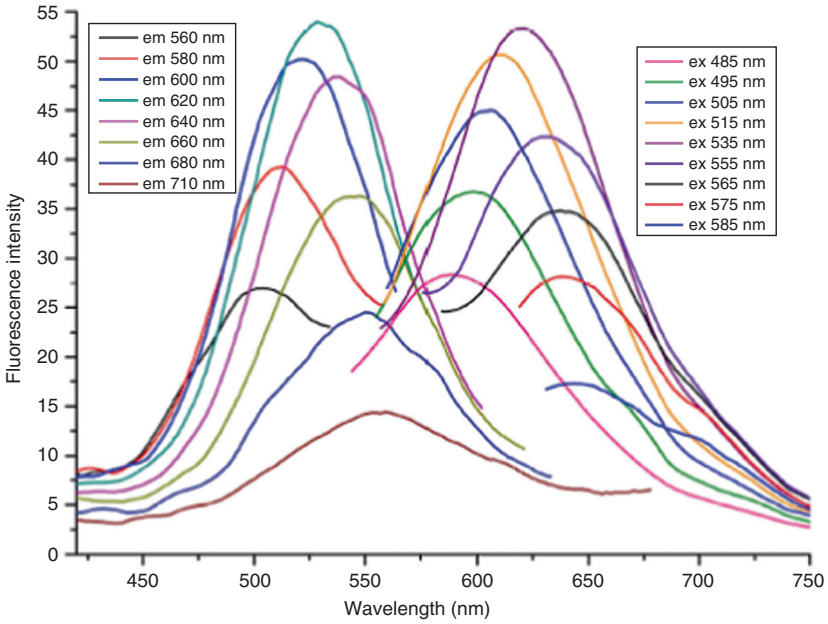

Fig. 4.29 The heterogeneities in excitation and emission spectra of clusters produced in water by photochemical reduction of silver salt on amphiphilic polystyrene-block-poly(methacrylic acid) block copolymer (Diez et al. 2013)

between excitation and emission spectra. Remarkable is their intra-band spectral heterogeneity with the retention of such symmetry (Diez et al. 2013), which can be explained by distribution in perturbing action of the scaffold and surrounding media.

Heterogeneity arising due to the presence of clusters of different sizes generates new bands, which can be observed in rare cases.

Unexpectedly high level of *anisotropy* of fluorescence emission was observed for the silver clusters made on polymer support, reaching the values $r = 0.35–0.37$ (Diez et al. 2013). This witnesses not only for the absence of rotational mobility of the clusters during fluorescence lifetime but also suggests the presence of strong excited-state dipole moment in the excited state. Since the cluster is neutral, this can be due to its strong interaction with electron donor group of the ligand (presumably, of the carbonyl group of the polymeric support) forming the *ligand-to-metal charge transfer* (LMCT) states.

4.6.4 Silver Clusters Formed with Organic Dyes as Photosensitizing and Supporting Agents

Organic dyes can serve not only as *sensitizers* in reactions of photoreduction of metal ions but also as *molecular supports* for the formed clusters. This allows obtaining novel fluorescent nanoscale materials in a simple one-step process just by UV light illumination. The results of realization of this idea are presented in Fig. 4.30. A mixed solution of silver salt with organic dye Thioflavin T after UV light treatment changes the light absorption and emission properties of Thioflavin T into novel properties of the cluster. In comparison to metal clusters formed on polymeric or DNA carriers, these fluorescent metal-dye composites are the structures very small in size and with well-defined stoichiometry. Based on mass spectrometry data it was suggested that they consist of two silver atoms and two dye molecules.

The most stable composite structures are obtained in 2-propanol, though sufficient stability can be achieved in other solvents. Their excitation and emission spectra possess the maxima at 340 and 450 nm correspondingly that are solvent-independent (Fig. 4.30b). They demonstrate dramatic Stokes shift, so that the overlap between excitation and emission bands is practically absent. It can be expected that such new fluorescent nanoscale materials will find many applications in biosensing and bioimaging technologies.

4.6.5 Applications

The water-soluble, near-IR-emitting silver clusters can be easily encapsulated into DNA molecules. They were shown to exhibit extremely bright and photostable emission on the single-molecule and bulk levels. DNA is an effective template for the preparation of fluorescent Ag clusters due to the presence of both carbonyl oxygens and doubly bonded ring nitrogens in heterocyclic bases that participate in interaction with the clusters. The affinities and fluorescence spectra of studied clusters are highly DNA-sequence-dependent owing to cytosine (C) bases that exhibit strong affinity for silver ions (Choi et al. 2012). It was noticed that, since the

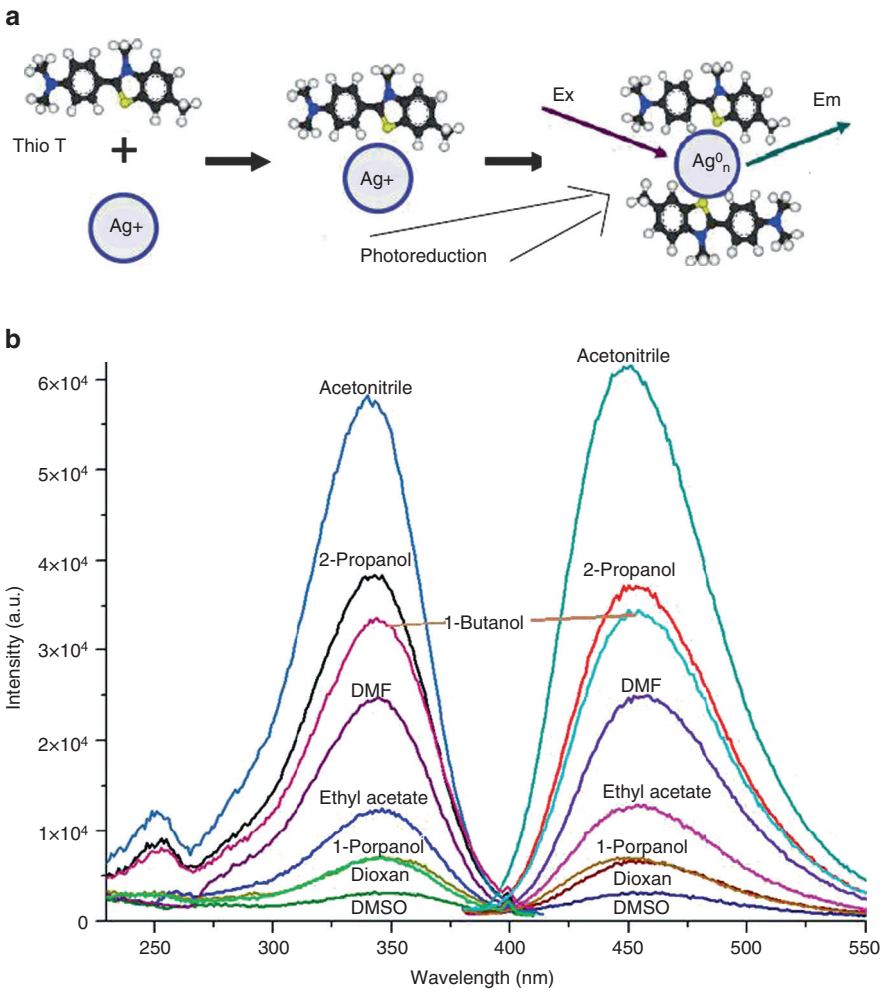

Fig. 4.30 The photosensitized reduction of Ag^+ ions and stabilization of Ag^+_n clusters by Thiophlavine T (ThioT) (**a**) and fluorescence spectra of these clusters in different solvents (**b**) (Kanyuk and Demchenko 2013)

mutations lead to a different conformation of the *dsDNA*, this hinders the formation of fluorescent silver clusters that allows the detection of single nucleotide mutations (Han and Wang 2012).

Regarding analytical applications, the easiest and most spectacular are the determinations of *mercury ions* that form strong non-emissive complexes with noble metal clusters (Yuan et al. 2012).

In conclusion, continuing developments of alternative fluorophores other than traditional organic molecules continue to expand choices for a variety of sensing and imaging applications, and noble metal clusters offer a lot of such choices. These clusters are among the strongest emitters, demonstrating high quantum yields, high

molar absorbances, nanosecond lifetimes and excellent photostabilities, still retaining small sizes of core units. Being electron dense they fit equally well for the electron microscopy imaging. Proper selection of supporting materials is the critical issue for different technologies that use them.

4.7 Sensing and Thinking: Which Molecular Reporter to Choose for Particular Needs?

Design and optimization of fluorescence reporter units remains a key determinant for the future success of sensing technologies. Presently organic dyes dominate as fluorescence reporters. Their advantage is a small size and extreme diversity of spectroscopic properties. Many synthetic procedures exist for modulating these properties and for incorporation of these dyes into different sensor constructs. Many dyes possess extremely valuable attribute to respond by the changes in parameters of their emission to the changes in intermolecular interactions with their environment and to participate directly in molecular sensing events. However, with each step of technology development, more flexibility is being required from these dyes together with increased brightness and photostability, and often traditional dyes are simply unable to meet the necessary demands.

Fluorescent proteins are unique tools for cell imaging and sensing inside the living cells. Despite tremendous success in imaging, their application in sensing is rather modest and mostly limited to proximity effects based on resonance energy transfer between two partners. These partners can be combined in one unit, providing the sensor response coupled to conformational change. Achieved recently rapid increase in their diversity and understanding their photophysical properties allow exploring these properties efficiently, especially in cell imaging. Strong efforts are still needed in this direction.

By choosing luminescent metal complexes one may get different benefits. They demonstrate series of strongly Stokes-shifted narrow emission bands and very long luminescence lifetimes. In addition to lifetime imaging, the lanthanide chelating units can be efficiently used as FRET donors even in combination with those acceptors that absorb light at the wavelengths of their own excitation, such as semiconductor quantum dots. Chemical sensing, biosensing and immunosensing technologies can efficiently use this property.

Fluorescent noble metal nanoclusters still have to find its most efficient use in sensing and, particularly, in imaging. Interesting is the possibility to generate the fluorescent image by light-induced reduction of ions inside the living cells and tissues.

Questions and Problems

1. List the most important properties of fluorescence reporter dyes. In what directions they should be optimized for application in sensor technologies described in Chap. 3?

2. The dye brightness and quantum yield are connected with measured fluorescence intensity via unknown factor of proportionality. What are the possibilities to evaluate them?
3. Working with very small amounts of dye, it is frequently needed to determine its concentration from absorbance and evaluate absorbance from concentration. Estimate the dye absorbance in concentrations 10^{-5} and 10^{-6} M. Estimate the dye concentrations for the measured absorbances 0.5 and 0.05. Assume that the dye molar absorbance is 40,000 M^{-1} cm^{-1} and the measurements are made in a cell with 1 cm path length.
4. What is photobleaching? On what physical and chemical factors does it depend and what are the possibilities to reduce it? Can it find a useful application?
5. Let the reporter dye be deposited onto the surface of sensor molecule and on sensor-target interaction let it be located at their contact interface. Specify all possible effects that could be used to provide its quenching/enhancement response.
6. Explain the mechanisms by which the fluorescence spectra may shift on the wavelength scale. Suggest several examples of application of this effect in sensing.
7. What are the basic requirements for a dye to be sensitive to polarity? To hydrogen bonding? To electric fields?
8. In view, that the optical cross-section (that determines molar absorbance) cannot be larger than the fluorophore geometrical cross-section and that the quantum yield cannot be higher than 100 %, evaluate the possibilities for improvement of presently used organic dyes.
9. How the fluorophores of GFP-type fluorescence proteins are synthesized? What is the advantage of their use in cellular studies?
10. Why lanthanide ions need to be incorporated into coordination complexes? Suggest different structures of coordination shells and possibilities to induce the sensing functionality by operating with properties of these shells.
11. Suggest the sensor design in which a conjugate between lanthanide complex and a dye-impregnated polymeric particle are used. How this sensor will work?
12. List all discussed above molecular-like emitters that can and cannot be used in polarization assays.
13. Why scaffolds are so important for efficient few-atom noble metal clusters? What are the possibilities for that?

References

Aoki S, Zulkefeli M, Shiro M, Kohsako M, Takeda K, Kimura E. 2005. A luminescence sensor of inositol 1,4,5-triphosphate and its model compound by ruthenium-templated assembly of a bis(Zn2+-cyclen) complex having a 2,2'-bipyridyl linker (cyclen = 1,4,7,10-tetraazacyclododecane). J Am Chem Soc 127:9129–39

Armelao L, Quici S, Barigelletti F, Accorsi G, Bottaro G, Cavazzini M, Tondello E (2010) Design of luminescent lanthanide complexes: from molecules to highly efficient photo-emitting materials. Coord Chem Rev 254(5–6):487–505. doi:10.1016/j.ccr.2009.07.025

Avilov SV, Bode C, Tolgyesi FG, Klymchenko AS, Fidy J, Demchenko AP (2005) Heat perturbation of bovine eye lens alpha-crystallin probed by covalently attached ratiometric fluorescent dye 4'-diethylamino-3-hydroxyflavone. Biopolymers 78(6):340–348

Balter A, Nowak W, Pawelkiewicz W, Kowalczyk A (1988) Some remarks on the interpretation of the spectral properties of prodan. Chem Physics Letters 143(6):565–570

Balzani V, Ceroni P, Gestermann S, Kauffmann C, Gorka M, Vogtle F (2000) Dendrimers as fluorescent sensors with signal amplification. Chem Commun 10:853–854

Baranov MS, Solntsev KM, Baleeva NS, Mishin AS, Lukyanov SA, Lukyanov KA, Yampolsky IV (2014) Red-shifted fluorescent aminated derivatives of conformationally locked GFP chromophore. Chem Europ J 20(41):13234–13241

Benedetti E, Kocsis LS, Brummond KM (2012) Synthesis and photophysical properties of a series of cyclopenta [b] naphthalene solvatochromic fluorophores. J Am Chem Soc 134(30): 12418–12421

Benedetti E, Veliz AB, Charpenay M, Kocsis LS, Brummond KM (2013) Attachable solvatochromic fluorophores and bioconjugation studies. Org Lett 15(11):2578–2581

Benniston AC, Harriman A, Llarena I, Sams CA (2007) Intramolecular delayed fluorescence as a tool for imaging science: synthesis and photophysical properties of a first-generation emitter. Chem Mater 19(8):1931–1938

Bergamini G, Marchi E, Ceroni P (2010) Luminescent dendrimers as ligands and sensors of metal ions. In: Demchenko AP (ed) Advanced fluorescence reporters in chemistry and biology II: molecular constructions, polymers and nanoparticles. Springer Ser Fluoresc 9:253–284

Biedermann F, Elmalem E, Ghosh I, Nau WM, Scherman OA (2012) Strongly fluorescent, switchable perylene bis(diimide) host-guest complexes with cucurbit[8]uril in water. Angew Chem Int Ed Engl. doi:10.1002/anie.201205393

Boens N, Leen V, Dehaen W (2012) Fluorescent indicators based on BODIPY. Chem Soc Rev 41(3):1130–1172

Borisov SM, Mayr T, Mistlberger G, Klimant I (2010) Dye-doped polymeric particles for sensing and imaging. In: Demchenko AP (ed) Advanced fluorescence reporters in chemistry and biology. II. Molecular constructions, polymers and nanoparticles, vol 9, Springer series on fluorescence. Springer, Heidelberg, pp 194–228

Boudier C, Klymchenko AS, Mely Y, Follenius-Wund A (2009) Local environment perturbations in alpha1-antitrypsin monitored by a ratiometric fluorescent label. Photochem Photobiol Sci 8(6):814–821. doi:10.1039/b902309g

Bourgeois D, Adam V (2012) Reversible photoswitching in fluorescent proteins: a mechanistic view. IUBMB Life 64(6):482–491. doi:10.1002/iub.1023

Brouwer AM (2011) Standards for photoluminescence quantum yield measurements in solution (IUPAC Technical Report). Pure Appl Chem 83(12):2213–2228

Bublitz GU, Boxer SG (1997) Stark spectroscopy: applications in chemistry, biology, and materials science. Annu Rev Phys Chem 48:213–242

Bunzli JCG (2006) Benefiting from the unique properties of lanthanide ions. Acc Chem Res 39(1):53–61

Bunzli J-CG, Piguet C (2005) Taking advantage of luminescent lanthanide ions. Chem Soc Rev 34(12):1048–1077

Burke TJ, Loniello KR, Beebe JA, Ervin KM (2003) Development and application of fluorescence polarization assays in drug discovery. Comb Chem High Throughput Screen 6(3):183–194

Castellano FN, Dattelbaum JD, Lakowicz JR (1998) Long-lifetime Ru(II) complexes as labeling reagents for sulfhydryl groups. Anal Biochem 255(2):165–170

Chan J, Dodani SC, Chang CJ (2012) Reaction-based small-molecule fluorescent probes for chemoselective bioimaging. Nat Chem 4(12):973–984

Chandrasekharan N, Kelly LA (2001) A dual fluorescence temperature sensor based on perylene/exciplex interconversion. J Am Chem Soc 123(40):9898–9899

Chao W-C, Shen J-Y, Lu J-F, Wang J-S, Yang H-C, Wee K, Lin L-J, Kuo Y-C, Yang C-H, Weng S-H (2014) Probing water environment of Trp59 in ribonuclease T1: insight of the structure–water network relationship. J Phys Chem B 119(6):2157–2167

Charbonniere LJ, Weibel N, Retailleau P, Ziessel R (2007) Relationship between the ligand structure and the luminescent properties of water-soluble lanthanide complexes containing bis(bipyridine) anionic arms. Chem Europ J 13(1):346–358

Chen K-Y, Cheng Y-M, Lai C-H, Hsu C-C, Ho M-L, Lee G-H, Chou P-T (2007) Ortho green fluorescence protein synthetic chromophore; Excited-state intramolecular proton transfer via a seven-membered-ring hydrogen-bonding system. J Am Chem Soc 129(15):4534–4535

Choi S, Dickson RM, Yu J (2012) Developing luminescent silver nanodots for biological applications. Chem Soc Rev 41(5):1867–1891. doi:10.1039/c1cs15226b

Chudakov DM, Matz MV, Lukyanov S, Lukyanov KA (2010) Fluorescent proteins and their applications in imaging living cells and tissues. Physiol Rev 90(3):1103–1163

Clarke RJ (2010) Electric field sensitive dyes. In: Demchenko AP (ed) Advanced fluorescence reporters in chemistry and biology I. Fundamentals and molecular design. Springer Ser Fluoresc 8:331–345

Cywincki PJ, Hammann T, HÄĽhn D, Parak WJ, Hildebrandt N, Hans-Gerd L (2014) Europium-quantum dot nanobioconjugates as luminescent probes for time-gated biosensing. J Biomed Opt 19(10):101506–101506

Davenport LD, Knutson JR, Brand L (1986) Excited-state proton transfer of equilenin and dihydro equilenin: interactions with bilayer vesicles. Biochemistry 25:1186–1195

Davydov A (1971) Theory of molecular excitons. Plenum Press, New York

de Silva AP, Gunaratne HQN, Gunnaugsson T, Huxley AJM, McRoy CP, Rademacher JT, Rice TE (1997) Signaling recognition events with fluorescent sensors and switches. Chem Rev 97:1515–1566

Demchenko AP (1986) Ultraviolet spectroscopy of proteins. Springer, Berlin/Heidelberg/New York

Demchenko AP (2006) Visualization and sensing of intermolecular interactions with two-color fluorescent probes. FEBS Letters 580(12):2951–2957

Demchenko AP, Yesylevskyy SO (2009) Nanoscopic description of biomembrane electrostatics: results of molecular dynamics simulations and fluorescence probing. Chem Phys Lipids 160(2):63–84

Demchenko AP, Klymchenko AS, Pivovarenko VG, Ercelen S, Duportail G, Mely Y (2003) Multiparametric color-changing fluorescence probes. J Fluoresc 13(4):291–295

Demchenko AP, Tang KC, Chou PT (2013) Excited-state proton coupled charge transfer modulated by molecular structure and media polarization. Chem Soc Rev 42(3):1379–1408. doi:10.1039/c2cs35195a

Diez I, Ras RH (2011) Fluorescent silver nanoclusters. Nanoscale 3(5):1963–1970. doi:10.1039/c1nr00006c

Diez I, Pusa M, Kulmala S, Jiang H, Walther A, Goldmann AS, Muller AH, Ikkala O, Ras RH (2009) Color tunability and electrochemiluminescence of silver nanoclusters. Angew Chem Int Ed Engl 48(12):2122–2125

Diez I, Kanyuk MI, Demchenko AP, Walther A, Jiang H, Ikkala O, Ras RH (2012) Blue, green and red emissive silver nanoclusters formed in organic solvents. Nanoscale 4(15):4434–4437. doi:10.1039/c2nr30642e

Diez I, Ras RH, Kanyuk MI, Demchenko AP (2013) On heterogeneity in fluorescent few-atom silver nanoclusters. Phys Chem Chem Phys 15(3):979–985. doi:10.1039/c2cp43045b

Dsouza RN, Pischel U, Nau WM (2011) Fluorescent dyes and their supramolecular host/guest complexes with macrocycles in aqueous solution. Chem Rev 111(12):7941–7980. doi:10.1021/cr200213s

Dziuba D, Postupalenko VY, Spadafora M, Klymchenko AS, Guérineau V, Mély Y, Benhida R, Burger A (2012) A universal nucleoside with strong two-band switchable fluorescence and sensitivity to the environment for investigating DNA interactions. J Am Chem Soc 134(24):10209–10213

Dziuba D, Karpenko JA, Barthes NPF, Michel BY, Klymchenko AS, Benhida R, Demchenko AP, Mély Y, Burger A (2014) Rational design of a solvatochromic fluorescent uracil analogue with dual-band ratiometric response based on 3-hydroxychromone. Chem Europ J 20:1998–2009

Eggeling C, Widengren J, Rigler R, Seidel CAM (1998) Photobleaching of fluorescent dyes under conditions used for single-molecule detection: Evidence of two-step photolysis. Anal Chem 70(13):2651–2659

Enander K, Choulier L, Olsson AL, Yushchenko DA, Kanmert D, Klymchenko AS, Demchenko AP, Mely Y, Altschuh D (2008) A peptide-based, ratiometric biosensor construct for direct fluorescence detection of a protein analyte. Bioconjug Chem 19(9):1864–1870

Ercelen S, Klymchenko AS, Demchenko AP (2002) Ultrasensitive fluorescent probe for the hydrophobic range of solvent polarities. Anal Chim Acta 464(2):273–287

Escobedo JO, Rusin O, Lim S, Strongin RM (2010) NIR dyes for bioimaging applications. Curr Opin Chem Biol 14(1):64–70

Finney NS (2006) Combinatorial discovery of fluorophores and fluorescent probes. Curr Opin Chem Biol 10(3):238–245

Gabriel D, Vernier M, Pfeifer MJ, Dasen B, Tenaillon L, Bouhelal R (2003) High throughput screening technologies for direct cyclic AMP measurement. Assay Drug Dev Technol 1(2):291–303

Garland PB, Moore CH (1979) Phosphorescence of protein-bound eosin and erythrosin. A possible probe for measurements of slow rotational mobility. Biochem J 183:561–572

Ghosh A, Hassinen J, Pulkkinen P, Tenhu H, Ras RH, Pradeep T (2014) Simple and efficient separation of atomically precise noble metal clusters. Anal Chem 86(24):12185–12190

Giepmans BNG, Adams SR, Ellisman MH, Tsien RY (2006) Review – The fluorescent toolbox for assessing protein location and function. Science 312(5771):217–224

Giordano L, Shvadchak VV, Fauerbach JA, Jares-Erijman EA, Jovin TM (2012) Highly solvatochromic 7-aryl-3-hydroxychromones. J Phys Chem Letters 3(8):1011–1016

Gonçalves MST (2008) Fluorescent labeling of biomolecules with organic probes. Chem Rev 109(1):190–212

Gonçalves MST (2010) Optimized UV/visible fluorescent markers. In: Demchenko AP (ed) Advanced fluorescence reporters in chemistry and biology I, vol 8. Springer Series on Fluorescence. Springer, Berlin/Heidelberg, pp 27–64. doi:10.1007/978-3-642-04702-2_2

Grimm JB, Heckman LM, Lavis LD (2012) The chemistry of small-molecule fluorogenic probes. Fluoresc Based Biosens: From Concepts to Applications 113:1–34

Gross E, Bedlack RS, Loew LM (1994) Dual-wavelength ratiometric fluorescence measurement of the membrane dipole potential. Biophys J 67(1):208–216

Grynkiewicz G, Poenie M, Tsien RY (1985) A new generation of Ca2+ indicators with greatly improved fluorescence properties. J Biol Chem 260(6):3440–3450

Guo Z, Park S, Yoon J, Shin I (2014) Recent progress in the development of near-infrared fluorescent probes for bioimaging applications. Chem Soc Rev 43(1):16–29

Guralchuk GY, Sorokin AV, Katrunov IK, Yefimova SL, Lebedenko AN, Malyukin YV, Yarmoluk SM (2007) Specificity of cyanine dye L-21 aggregation in solutions with nucleic acids. J Fluoresc 17(4):370–376

Ha T, Tinnefeld P (2012) Photophysics of fluorescence probes for single molecule biophysics and super-resolution imaging. Annu Rev Phys Chem 63:595

Haidekker MA, Theodorakis EA (2007) Molecular rotors–fluorescent biosensors for viscosity and flow. Org Biomol Chem 5(11):1669–1678

Han J, Burgess K (2009) Fluorescent indicators for intracellular pH. Chem Rev 110(5):2709–2728

Han B, Wang E (2012) DNA-templated fluorescent silver nanoclusters. Anal Bioanal Chem 402(1):129–138

Haugland RP (1996) Handbook of fluorescent probes and research chemicals. Molecular Probes, Eugene

Haugland RP (2005) The handbook. A guide to fluorescent probes and labeling technologies, 10th edn. Invitrogen corp, Eugene

Heffern MC, Matosziuk LM, Meade TJ (2013) Lanthanide probes for bioresponsive imaging. Chem Rev 114(8):4496–4539

Hemmila I, Laitala V (2005) Progress in lanthanides as luminescent probes. J Fluoresc 15(4):529–542

Hildebrandt N, Wegner KD, Algar WR (2014) Luminescent terbium complexes: superior Förster resonance energy transfer donors for flexible and sensitive multiplexed biosensing. Coord Chem Rev 273:125–138

Hochreiner H, Sanchez-Barragan I, Costa-Fernandez JM, Sanz-Medel A (2005) Dual emission probe for luminescence oxygen sensing: a critical comparison between intensity, lifetime and ratiometric measurements. Talanta 66(3):611–618

Ishchenko AA, Derevyanko NA, Svidro VA (1992) Effect of polymethine-chain length on fluorescence-spectra of symmetrical cyanine dyes. Opt Spektrosk 72:110–114

Ivashkin P, Yampolsky I, Lukyanov K (2009) Synthesis and properties of chromophores of fluorescent proteins. Russ J Bioorg Chem 35(6):652–669

Jin L, Millard AC, Wuskell JP, Dong X, Wu D, Clark HA, Loew LM (2006) Characterization and application of a new optical probe for membrane lipid domains. Biophys J 90(7):2563–2575. doi:10.1529/biophysj.105.072884

Jose J, Burgess K (2006) Syntheses and properties of water-soluble Nile Red derivatives. J Org Chem 71(20):7835–7839. doi:10.1021/jo061369v

Juskowiak GL, Stachel SJ, Tivitmahaisoon P, Van Vranken DL (2004) Fluorogenic peptide sequences – Transformation of short peptides into fluorophores under ambient photooxidative conditions. J Am Chem Soc 126(2):550–556

Kadirvel M, Arsic B, Freeman S, Bichenkova EV (2008) Exciplex and excimer molecular probes: detection of conformational flip in a myo-inositol chair. Org Biomol Chem 6(11):1966–1972

Kanyuk M, Demchenko A (2013) Spectroscopic studies of new fluorescent nanomaterial composed of silver atoms and organic dye. Paper presented at the nanomaterials: applications & properties (NAP-2013), 3-rd international conference Alushta, Crimea

Karpenko IA, Kreder R, Valencia C, Villa P, Mendre C, Mouillac B, Mély Y, Hibert M, Bonnet D, Klymchenko AS (2014) Red fluorescent turn-on ligands for imaging and quantifying G protein-coupled receptors in living cells. Chembiochem 15(3):359–363

Kim E, Park SB (2010) Discovery of new fluorescent dyes: targeted syn-thesis or combinatorial approach? In: Demchenko AP (ed) Advanced fluorescence reporters in chemistry and biology. I. Fundamentals and molecular design, Springer Ser Fluoresc 8:149–187

Klymchenko AS, Demchenko AP (2002) Electrochromic modulation of excited-state intramolecular proton transfer: the new principle in design of fluorescence sensors. J Am Chem Soc 124(41):12372–12379

Klymchenko AS, Demchenko AP (2003) Multiparametric probing of intermolecular interactions with fluorescent dye exhibiting excited state intramolecular proton transfer. Phys Chem Chem Phys 5(3):461–468

Klymchenko AS, Ozturk T, Pivovarenko VG, Demchenko AP (2001) Synthesis and spectroscopic properties of benzo- and naphthofuryl-3-hydroxychromones. Can J Chem Revue Canadienne De Chimie 79(4):358–363

Klymchenko AS, Duportail G, Ozturk T, Pivovarenko VG, Mely Y, Demchenko AP (2002a) Novel two-band ratiometric fluorescence probes with different location and orientation in phospholipid membranes. Chem Biol 9(11):1199–1208

Klymchenko AS, Pivovarenko VG, Ozturk T, Demchenko AP (2002b) Elimination of hydrogen bonding effect on solvatochromism of 3-hydroxyflavones. J Phys Chem A 107:4211–4216

Klymchenko AS, Duportail G, Mely Y, Demchenko AP (2003a) Ultrasensitive two-color fluorescence probes for dipole potential in phospholipid membranes. Proc Natl Acad Sci U S A 100(20):11219–11224. doi:10.1073/pnas.1934603100

Klymchenko AS, Pivovarenko VG, Ozturk T, Demchenko AP (2003b) Modulation of the solvent-dependent dual emission in 3-hydroxychromones by substituents. New J Chem 27(9): 1336–1343

Klymchenko AS, Avilov SV, Demchenko AP (2004) Resolution of Cys and Lys labeling of alpha-crystallin with site-sensitive fluorescent 3-hydroxyflavone dye. Anal Biochem 329(1):43–57

Koide Y, Urano Y, Hanaoka K, Terai T, Nagano T (2011) Evolution of group 14 rhodamines as platforms for near-infrared fluorescence probes utilizing photoinduced electron transfer. ACS Chem Biol 6(6):600–608

Kokko L, Lovgren T, Soukka T (2007) Europium(III)-chelates embedded in nanoparticles are protected from interfering compounds present in assay media. Anal Chim Acta 585(1):17–23

Kolmakov K, Belov VN, Wurm CA, Harke B, Leutenegger M, Eggeling C, Hell SW (2010) A versatile route to red-emitting Carbopyronine dyes for optical microscopy and nanoscopy. Europ J Org Chem 2010(19):3593–3610

Krueger AT, Imperiali B (2013) Fluorescent amino acids: modular building blocks for the assembly of new tools for chemical biology. Chembiochem 14(7):788–799

Kucherak OA, Didier P, Mély Y, Klymchenko AS (2010a) Fluorene analogues of Prodan with superior fluorescence brightness and solvatochromism. J Phys Chem Letters 1(3):616–620

Kucherak OA, Oncul S, Darwich Z, Yushchenko DA, Arntz Y, Didier P, Mely Y, Klymchenko AS (2010b) Switchable nile red-based probe for cholesterol and lipid order at the outer leaflet of biomembranes. J Am Chem Soc 132(13):4907–4916

Kuhn B, Fromherz P (2003) Anellated hemicyanine dyes in a neuron membrane: molecular stark effect and optical voltage recording. J Phys Chem B 107(31):7903–7913. doi:10.1021/jp0345811

Kuimova MK, Collins HA, Balaz M, Dahlstedt E, Levitt JA, Sergent N, Suhling K, Drobizhev M, Makarov NS, Rebane A (2009) Photophysical properties and intracellular imaging of water-soluble porphyrin dimers for two-photon excited photodynamic therapy. Org Biomol Chem 7(5):889–896

Lakowicz JR (2006) Principles of fluorescence spectroscopy, 3rd edn. Springer, New York

Lakowicz JR, Gryczynski I, Gryczynski Z, Tolosa L, Dattelbaum JD, Rao G (1999) Polarization-based sensing with a self-referenced sample. Appl Spectrosc 53(9):1149–1157

Lavis LD, Raines RT (2008) Bright ideas for chemical biology. ACS Chem Biol 3(3):142–155

Laws WR, Brand L (1979) Analysis of two-state excited-state reactions. The fluorescence decay of 2-naphthol. J Phys Chem 83:795

Levitus M, Ranjit S (2011) Cyanine dyes in biophysical research: the photophysics of polymethine fluorescent dyes in biomolecular environments. Q Rev Biophys 44(1):123–151

Liang S, John CL, Xu S, Chen J, Jin Y, Yuan Q, Tan W, Zhao JX (2010) Silica-based nanoparticles: design and properties. In: Demchenko AP (ed) Advanced fluorescence reporters in chemistry and biology. II. Molecular constructions, polymers and nanoparticles, Springer Ser Fluoresc 9:229–252

Liang F, Liu Y, Zhang P (2013) Universal base analogues and their applications in DNA sequencing technology. RSC Adv 3(35):14910–14928

Liptay W (1969) Electrochromism and solvatochromism. Angew Chem Internat Edit 8:177–188

Loew LM (2011) Design and use of organic voltage sensitive dyes. In: Membrane Potential Imaging in the Nervous System. Springer, New York, pp 13–23

Losytskyy MY, Yashchuk VM, Lukashov SS, Yarmoluk SM (2002) Davydov splitting in spectra of cyanine dye J-aggregates, formed on the polynucleotides. J Fluoresc 12(1):109–112

Loudet A, Burgess K (2007) BODIPY dyes and their derivatives: syntheses and spectroscopic properties. Chem Rev 107(11):4891–4932

Lu ZK, Lord SJ, Wang H, Moerner WE, Twieg RJ (2006) Long-wavelength analogue of PRODAN: Synthesis and properties of Anthradan, a fluorophore with a 2,6-donor-acceptor anthracene structure. J Org Chem 71(26):9651–9657

Luo S, Zhang E, Su Y, Cheng T, Shi C (2011) A review of NIR dyes in cancer targeting and imaging. Biomaterials 32(29):7127–7138

M'Baye G, Shynkar VV, Klymchenko AS, Mely Y, Duportail G (2006) Membrane dipole potential as measured by ratiometric 3-hydroxyflavone fluorescence probes: Accounting for hydration effects. J Fluoresc 16(1):35–42. doi:10.1007/s10895-005-0022-3

M'Baye G, Klymchenko AS, Yushchenko DA, Shvadchak VV, Ozturk T, Mely Y, Duportail G (2007) Fluorescent dyes undergoing intramolecular proton transfer with improved sensitivity to surface charge in lipid bilayers. Photochem Photobiol Sci 6(1):71–76

Mérola F, Fredj A, Betolngar DB, Ziegler C, Erard M, Pasquier H (2014) Newly engineered cyan fluorescent proteins with enhanced performances for live cell FRET imaging. Biotechnol J 9(2):180–191

Millard AC, Jin L, Wei MD, Wuskell JP, Lewis A, Loew LM (2004) Sensitivity of second harmonic generation from styryl dyes to transmembrane potential. Biophys J 86(2):1169–1176. doi:10.1016/S0006-3495(04)74191-0

Miyawaki A, Nagai T, Mizuno H (2003) Mechanisms of protein fluorophore formation and engineering. Curr Opin Chem Biol 7(5):557–562

Miyawaki A, Nagai T, Mizuno H (2005) Engineering fluorescent proteins. In: Microscopy techniques, vol 95, Advances in biochemical engineering/biotechnology. Springer, Berlin, pp 1–15

Mordon S, Devoisselle JM, Soulie S (1995) Fluorescence spectroscopy of pH in vivo using a dual-emission fluorophore (C-SNAFL-1). J Photochem Photobiol B 28(1):19–23

Mujumdar RB, Ernst LA, Mujumdar SR, Lewis CJ, Waggoner AS (1993) Cyanine dye labeling reagents – Sulfoindocyanine succinimidyl esters. Bioconjug Chem 4(2):105–111

Niko Y, Kawauchi S, Konishi GI (2013) Solvatochromic pyrene analogues of prodan exhibiting extremely high fluorescence quantum yields in apolar and polar solvents. Chem Europ J 19(30):9760–9765

Niko Y, Moritomo H, Sugihara H, Suzuki Y, Kawamata J, Konishi GI (2015) A novel pyrene-based two-photon active fluorescent dye efficiently excited and emitting in the 'tissue optical window (650–1100 nm)'. J Mater Chem B 3(2):184–190

O'Neal DP, Meledeo MA, Davis JR, Ibey BL, Gant VA, Pishko MV, Cote GL (2004) Oxygen sensor based on the fluorescence quenching of a ruthenium complex immobilized in a biocompatible poly(ethylene glycol) hydrogel. IEEE Sens J 4(6):728–734

O'Riordan TC, Soini AE, Papkovsky DB (2001) Monofunctional derivatives of coproporphyrins for phosphorescent labeling of proteins and binding assays. Anal Biochem 290(2):366–375

Oueslati I, Ferreira FAS, Carlos LD, Baleizao C, Berberan-Santos MN, de Castro B, Vicens J, Pischel U (2006) Calix 4 azacrowns as novel molecular scaffolds for the generation of visible and near-infrared lanthanide luminescence. Inorg Chem 45(6):2652–2660

Panchuk-Voloshina N, Haugland RP, Bishop-Stewart J, Bhalgat MK, Millard PJ, Mao F, Leung WY, Haugland RP (1999) Alexa dyes, a series of new fluorescent dyes that yield exceptionally bright, photostable conjugates. J Histochem Cytochem 47(9):1179–1188

Pandya S, Yu JH, Parker D (2006) Engineering emissive europium and terbium complexes for molecular imaging and sensing. Dalton Trans 23:2757–2766

Pansare VJ, Hejazi S, Faenza WJ, Prud'homme RK (2012) Review of long-wavelength optical and NIR imaging materials: contrast agents, fluorophores, and multifunctional nano carriers. Chem Mater 24(5):812–827

Papkovsky DB, O'Riordan TC (2005) Emerging applications of phosphorescent metalloporphyrins. J Fluoresc 15(4):569–584

Papkovsky DB, Ponomarev GV (2001) Spectral-luminescent study of the porphyrin-diketones and their complexes. Spectrochimica Acta Part a-Molecular and Biomolecular Spectroscopy 57(9):1897–1905

Papkovsky DB, O'Riordan T, Soini A (2000) Phosphorescent porphyrin probes in biosensors and sensitive bioassays. Biochem Soc Trans 28:74–77

Patsenker LD, Tatarets AL, Terpetschnig EA (2010) Long-wavelength probes and labels based on cyanines and squaraines. In: Demchenko AP (ed) Advanced fluorescence reporters in chemistry and biology I: fundamentals and molecular design. Springer Ser Fluoresc 8:65–104

Peng X, Chen H, Draney DR, Volcheck W, Schutz-Geschwender A, Olive DM (2009) A nonfluorescent, broad-range quencher dye for Förster resonance energy transfer assays. Anal Biochem 388(2):220–228

Petrou PS, Kakabakos SE, Christofidis I, Argitis P, Misiakos K (2002) Multi-analyte capillary immunosensor for the determination of hormones in human serum samples. Biosens Bioelectron 17(4):261–268

Piszczek G (2006) Luminescent metal-ligand complexes as probes of macromolecular interactions and biopolymer dynamics. Arch Biochem Biophys 453(1):54–62

Pivovarenko VG, Klueva AV, Doroshenko AO, Demchenko AP (2000) Bands separation in fluorescence spectra of ketocyanine dyes: evidence for their complex formation with monohydric alcohols. Chem Phys Letters 325(4):389–398

Plasek J, Sigler K (1996) Slow fluorescent indicators of membrane potential: a survey of different approaches to probe response analysis. J Photochem Photobiol B 33(2):101–124

Postupalenko VY, Zamotaiev OM, Shvadchak VV, Strizhak AV, Pivovarenko VG, Klymchenko AS, Mely Y (2013) Dual-fluorescence l-amino acid reports insertion and orientation of melittin peptide in cell membranes. Bioconjug Chem 24(12):1998–2007

Prifti E, Reymond L, Umebayashi M, Hovius R, Riezman H, Johnsson K (2014) A fluorogenic probe for SNAP-tagged plasma membrane proteins based on the solvatochromic molecule Nile Red. ACS Chem Biol 9(3):606–612

Przhonska OV, Scott Webster S, Padilha LA, Hu H, Kachkovski AD, Hagan DJ, Stryland EWV (2010) Two-photon absorption in near-IR conjugated molecules: design strategy and structure-property relations. In: Demchenko AP (ed) Advanced fluorescence reporters in chemistry and biology. I. Fundamentals and molecular design, Springer Ser Fluoresc 8:105–148

Renikuntla BR, Rose HC, Eldo J, Waggoner AS, Armitage BA (2004) Improved photostability and fluorescence properties through polyfluorination of a cyanine dye. Org Lett 6(6): 909–912

Roshal AD, Grigorovich AV, Doroshenko AO, Pivovarenko VG, Demchenko AP (1998) Flavonols and crown-flavonols as metal cation chelators. The different nature of Ba2+ and Mg2+ complexes. J Phys Chem A 102(29):5907–5914

Roshal AD, Grigorovich AV, Doroshenko AO, Pivovarenko VG, Demchenko AP (1999) Flavonols as metal-ion chelators: complex formation with Mg2+ and Ba2+ cations in the excited state. J Photochem Photobiol Chem 127(1-3):89–100

Salvioli S, Ardizzoni A, Franceschi C, Cossarizza A (1997) JC-1, but not DiOC(6)(3) or rhodamine 123, is a reliable fluorescent probe to assess Delta Psi changes in intact cells: Implications for studies on mitochondrial functionality during apoptosis. Febs Letters 411(1):77–82

Samanta A, Vendrell M, Das R, Chang Y-T (2010) Development of photostable near-infrared cyanine dyes. Chem Commun 46(39):7406–7408

Sanchez-Barragan I, Costa-Fernandez JM, Valledor M, Campo JC, Sanz-Medel A (2006) Room-temperature phosphorescence (RTP) for optical sensing. Trac-Trends Anal Chem 25(10): 958–967

Shaner NC, Campbell RE, Steinbach PA, Giepmans BNG, Palmer AE, Tsien RY (2004) Improved monomeric red, orange and yellow fluorescent proteins derived from Discosoma sp red fluorescent protein. Nat Biotechnol 22(12):1567–1572

Shav-Tal Y, Darzacq X, Shenoy SM, Fusco D, Janicki SM, Spector DL, Singer RH (2004) Dynamics of single mRNPs in nuclei of living cells. Science 304(5678):1797–1800

Shcherbakova DM, Subach OM, Verkhusha VV (2012) Red fluorescent proteins: advanced imaging applications and future design. Angew Chem Int Ed 51(43):10724–10738

Shcherbakova DM, Sengupta P, Lippincott-Schwartz J, Verkhusha VV (2014) Photocontrollable fluorescent proteins for superresolution imaging. Annu Rev Biophys 43(1):303–329

Shen J-Y, Chao W-C, Liu C, Pan H-A, Yang H-C, Chen C-L, Lan Y-K, Lin L-J, Wang J-S, Lu J-F (2013) Probing water micro-solvation in proteins by water catalysed proton-transfer tautomerism. Nat Commun 4:2611. doi:10.1038/ncomms3611

Sholokh M, Zamotaiev OM, Das R, Postupalenko VY, Richert L, Dujardin D, Zaporozhets OA, Pivovarenko VG, Klymchenko AS, Mély Y (2014) Fluorescent amino acid undergoing excited state intramolecular proton transfer for site-specific probing and imaging of peptide interactions. J Phys Chem B 119(6):2585–2595

Shrestha S, Deo SK (2006) Anthozoa red fluorescent protein in biosensing. Anal Bioanal Chem 386(3):515–524

Shvadchak VV, Klymchenko AS, de Rocquigny H, Mely Y (2009) Sensing peptide-oligonucleotide interactions by a two-color fluorescence label: application to the HIV-1 nucleocapsid protein. Nucleic Acids Research 37(3). doi:ARTN e25. DOI 10.1093/nar/gkn1083

Shynkar VV, Klymchenko AS, Piemont E, Demchenko AP, Mely Y (2004) Dynamics of intermolecular hydrogen bonds in the excited states of 4'-dialkylamino-3-hydroxyflavones. On the

pathway to an ideal fluorescent hydrogen bonding sensor. J Phys Chem A 108(40): 8151–8159
Shynkar VV, Klymchenko AS, Duportail G, Demchenko AP, Mely Y (2005) Two-color fluorescent probes for imaging the dipole potential of cell plasma membranes. Biochim Biophys Acta 1712(2):128–136
Shynkar VV, Klymchenko AS, Kunzelmann C, Duportail G, Muller CD, Demchenko AP, Freyssinet JM, Mely Y (2007) Fluorescent biomembrane probe for ratiometric detection of apoptosis. J Am Chem Soc 129(7):2187–2193
Sinkeldam RW, Greco NJ, Tor Y (2010) Fluorescent analogs of biomolecular building blocks: design, properties, and applications. Chem Rev 110(5):2579–2619
Soini AE, Seveus L, Meltola NJ, Papkovsky DB, Soini E (2002) Phosphorescent metalloporphyrins as labels in time-resolved luminescence microscopy: effect of mounting on emission intensity. Microsc Res Tech 58(2):125–131
Stepanenko OV, Shcherbakova DM, Kuznetsova IM, Turoverov KK, Verkhusha VV (2011) Modern fluorescent proteins: from chromophore formation to novel intracellular applications. Biotechniques 51(5):313–314, 316, 318 passim. doi:000113765 [pii]. 10.2144/000113765
Strizhak AV, Postupalenko VY, Shvadchak VV, Morellet N, Guittet E, Pivovarenko VG, Klymchenko AS, Mély Y (2012) Two-color fluorescent l-amino acid mimic of tryptophan for probing peptide–nucleic acid complexes. Bioconjug Chem 23(12):2434–2443
Tatikolov AS (2012) Polymethine dyes as spectral-fluorescent probes for biomacromolecules. J Photochem Photobiol C: Photochem Rev 13(1):55–90
Terai T, Kikuchi K, Iwasawa SY, Kawabe T, Hirata Y, Urano Y, Nagano T (2006) Modulation of luminescence intensity of lanthanide complexes by photoinduced electron transfer and its application to a long-lived protease probe. J Am Chem Soc 128(21):6938–6946
Tsien RY (1998) The green fluorescent protein. Annu Rev Biochem 67:509–544
Tsien RY (2009) Constructing and exploiting the fluorescent protein paintbox (Nobel Lecture). Angew Chem Int Ed Engl 48(31):5612–5626. doi:10.1002/anie.200901916
Tsuchida M, Tsujita W, Majima Y, Iwamoto M (2001) Interfacial electrostatic phenomena in phthalocyanine Langmuir-Blodgett films under photoillumination. Jap J Appl Phys 40(3R):1315
Uchiyama S, Takehira K, Yoshihara T, Tobita S, Ohwada T (2006) Environment-sensitive fluorophore emitting in protic environments. Org Lett 8(25):5869–5872
Ulrich G, Ziessel R, Harriman A (2008) The chemistry of fluorescent BODIPY dyes: versatility unsurpassed. Angew Chem Int Ed 47(7):1184–1201
Umezawa K, Matsui A, Nakamura Y, Citterio D, Suzuki K (2009) Bright, color-tunable fluorescent dyes in the Vis/NIR region: establishment of new "tailor-made" multicolor fluorophores based on borondipyrromethene. Chem Europ J 15(5):1096–1106
Vendrell M, Zhai D, Er JC, Chang Y-T (2012) Combinatorial strategies in fluorescent probe development. Chem Rev 112(8):4391–4420
Vitha MF, Clarke RJ (2007) Comparison of excitation and emission ratiometric fluorescence methods for quantifying the membrane dipole potential. Biochim Biophys Acta 1768(1):107–114. doi:10.1016/j.bbamem.2006.06.022
Vosch T, Antoku Y, Hsiang JC, Richards CI, Gonzalez JI, Dickson RM (2007) Strongly emissive individual DNA-encapsulated Ag nanoclusters as single-molecule fluorophores. Proc Natl Acad Sci U S A 104(31):12616–12621
Wang S-L, Lee T-C, Ho T-I (2002) Excited state proton transfer and steric effect on the hydrogen bonding interaction of the styrylquinoline system. J Photochem Photobiol A: Chem 151:21–26
Wang F, Tan WB, Zhang Y, Fan X, Wang M (2006) Luminescent nanomaterials for biological labelling. Nanotechnology 17:R1–R13
Wang Q, Nchimi Nono K, Syrjänpää M, Charbonnière LJ, Hovinen J, Härmä H (2013) Stable and highly fluorescent europium (III) chelates for time-resolved immunoassays. Inorg Chem 52(15):8461–8466
Wetzl B, Gruber M, Oswald B, Durkop A, Weidgans B, Probst M, Wolfbeis OS (2003) Set of fluorochromophores in the wavelength range from 450 to 700 nm and suitable for labeling proteins and amino-modified DNA. J Chromatogr B Analyt Technol Biomed Life Sci 793(1):83–92

Whitaker JE, Haugland RP, Prendergast FG (1991) Spectral and photophysical studies of benzo[c] xanthene dyes: dual emission pH sensors. Anal Biochem 194(2):330–344
Wiktorowski S, Rosazza C, Winterhalder MJ, Daltrozzo E, Zumbusch A (2014) Water-soluble pyrrolopyrrole cyanine (PPCy) NIR fluorophores. Chem Commun 50(36):4755–4758
Wilson JN, Kool ET (2006) Fluorescent DNA base replacements: reporters and sensors for biological systems. Org Biomol Chem 4(23):4265–4274
Woods M, Sherry AD (2003) Synthesis and luminescence studies of aryl substituted tetraamide complexes of europium(III): A new approach to pH responsive luminescent europium probes. Inorg Chem 42(14):4401–4408
Wu L, Burgess K (2008) Syntheses of highly fluorescent GFP-chromophore analogues. J Am Chem Soc 130(12):4089–4096
Wu Z, Lanni E, Chen W, Bier ME, Ly D, Jin R (2009) High yield, large scale synthesis of thiolate-protected Ag7 clusters. J Am Chem Soc 131(46):16672–16674
Wuskell JP, Boudreau D, Wei MD, Jin L, Engl R, Chebolu R, Bullen A, Hoffacker KD, Kerimo J, Cohen LB, Zochowski MR, Loew LM (2006) Synthesis, spectra, delivery and potentiometric responses of new styryl dyes with extended spectral ranges. J Neurosci Methods 151(2):200–215. doi:10.1016/j.jneumeth.2005.07.013
Wysocki LM, Lavis LD (2011) Advances in the chemistry of small molecule fluorescent probes. Curr Opin Chem Biol 15(6):752–759
Yang CJ, Jockusch S, Vicens M, Turro NJ, Tan W (2005) Light-switching excimer probes for rapid protein monitoring in complex biological fluids. Proc Natl Acad Sci U S A 102(48):17278–17283
Yesylevskyy SO, Klymchenko AS, Demchenko AP (2005) Semi-empirical study of two-color fluorescent dyes based on 3-hydroxychromone. J Mol Struct Theochem 755(1-3):229–239
Yu J, Patel SA, Dickson RM (2007) In vitro and intracellular production of peptide-encapsulated fluorescent silver nanoclusters. Angew Chem Int Ed Engl 46(12):2028–2030
Yuan JL, Wang GL (2006) Lanthanide-based luminescence probes and time-resolved luminescence bioassays. Trac-Trends in Anal Chem 25(5):490–500
Yuan X, Yeow TJ, Zhang Q, Lee JY, Xie J (2012) Highly luminescent Ag + nanoclusters for Hg 2+ ion detection. Nanoscale 4(6):1968–1971
Yuan L, Lin W, Zheng K, Zhu S (2013a) FRET-based small-molecule fluorescent probes: rational design and bioimaging applications. Acc Chem Res 46(7):1462–1473
Yuan X, Luo Z, Yu Y, Yao Q, Xie J (2013b) Luminescent noble metal nanoclusters as an emerging optical probe for sensor development. Chem Asian J 8:858–871
Yushchenko DA, Shvadchak VV, Bilokin MD, Klymchenko AS, Duportail G, Mely Y, Pivovarenko VG (2006) Modulation of dual fluorescence in a 3-hydroxyquinolone dye by perturbation of its intramolecular proton transfer with solvent polarity and basicity. Photochem Photobiol Sci 5(11):1038–1044
Zheng J, Nicovich PR, Dickson RM (2007) Highly fluorescent noble-metal quantum dots. Annu Rev Phys Chem 58:409–431
Zhou S, Zheng W, Chen Z, Tu D, Liu Y, Ma E, Li R, Zhu H, Huang M, Chen X (2014) Dissolution-enhanced luminescent bioassay based on inorganic lanthanide nanoparticles. Angewandte Chemie 126(46):12706–12710
Zimmer M (2009) GFP: from jellyfish to the Nobel prize and beyond. Chem Soc Rev 38(10):2823–2832. doi:10.1039/b904023d

Chapter 5
Nanoscale Fluorescence Emitters

This chapter provides comparative analysis of properties of different nanoscale materials to absorb and emit visual and near-IR light with the focus on their applications in sensing and imaging technologies. Nowadays we observe that in these applications the novel nanoscale fluorescent materials appear in strong competition with traditional organic dyes. They demonstrate diverse photophysical behavior and allow obtaining diverse information when they are incorporated into sensor composites or form the images in biological systems. Among these nanoscale emitters are the structures formed of organic dyes or by these dyes incorporated into different types of polymers with the resulting dramatically increased brightness. Collective excitonic effects appear when the aromatic units are coupled in conjugated polymers. Nanoscale structures formed of inorganic carbon in the form of nanodiamonds, graphene and graphene oxide pieces and the so-called carbon dots joined quite recently the family of fluorophores. Semiconductor quantum dots present a range of bright emitters covering whole visible and near-IR spectral range. Finally, the up-converting nanocrystals make possible visible emission with near-IR excitation. Here we overview the most important features of these nanoscale materials. The following Chap. 6 will be focused on functional nanocomposites that allow extending the useful properties of these basic components.

5.1 Introduction to Light Emitting Nano-World

Nano-world is not only the world of small dimensions. It is the world, in which different materials exhibit new and often unexpected optical properties. Inspired by a broad range of new possibilities many scientists have started exploring this new field (Liu and Tang 2010; Hötzer et al. 2012). For a short time these new materials started substituting traditionally used organic dyes in numerous practical applications in clinical diagnostics (Andreescu and Sadik 2004), monitoring the environment (Riu et al. 2006), agriculture and food safety control (Patel 2002), detection of

A.P. Demchenko, *Introduction to Fluorescence Sensing*,
DOI 10.1007/978-3-319-20780-3_5

biological warfare agents (Gooding 2006) and in different industries. Such versatility is further enriched by nano-bio interactions that allow incorporation of nanoparticles into biologically important systems, obtaining information on these systems and even modulating their properties (Amin et al. 2011; Wang 2009; Suh et al. 2009). The location of fluorescent nanoparticles can be precisely determined and monitored in the systems of high complexity, such as living cells and tissues.

5.1.1 Size, Shape and Dimensions of Nanomaterials

Molecular clusters and nanoparticles may exist of *various sizes*, from a fraction of nanometer to several hundred nanometers. Many properties of nanomaterials are size-dependent, which allows selecting them within broad range of species without any change of their chemical composition, and even of the arrangement of atoms. With the decrease of particle size there increases the ratio of surface free energy over bulk free energy. This means that the energetic, structural and, finally, optical properties of nanomaterials become dependent on interactions at their interfaces. In small nanoparticles, most of the atoms are *exposed to the surface* and participate in interactions with the surrounding. Thus, if we model a nanoparticle by a structure, in which the atoms are represented by identical balls, the minimum number of atoms to contain at least one inner-core atom is 13. The close-shell structure of 55 atoms will have 76 % of them exposed to the surface and of 147 atoms – still 63 % (Aiken Iii and Finke 1999). The interactions at interface are usually of different nature than the interactions within the particle core and this may strongly influence the electronic states and transitions of nanoparticles.

In addition to this general statement, we indicate specific effects that depend on studied materials. We observe (see below) that *excitonic effects* in semiconductor quantum dots result in strong size-dependent variation in the wavelengths of their emission. Size-dependent *plasmonic effects* of noble metal nanoparticles do not allow their strong emission, but they induce emission enhancement of other fluorophores (see Sect. 10.7). These effects appear due to confinement of their electrons to a small volume.

The size of nanostructures is usually much smaller than the wavelength of light, and this point is important for understanding a variety of photophysical and photochemical processes occurring on nanoscale. The electron and proton transfers are the short-range phenomena and if they are activated in the excited states, they proceed on a scale below 1 nm. In contrast, FRET and plasmonic enhancement of fluorescence may extend to distances of tens of nanometers. Excitation by visible light with wavelengths of several hundred nanometers does not bring nanoscale resolution in conventional microscopy but with proper design of nanoscale emitters allows estimating proximity effects on the shortest length scale.

Nanostructures can be of different *shape,* which can determine their optical properties. Nanoparticles that can be viewed as point emitters are defined as being of *zero dimension*, 0-D (Fig. 5.1). Being of spherical (or almost spherical) shape, semiconductor nanocrystals are usually considered of zero dimensionality, which

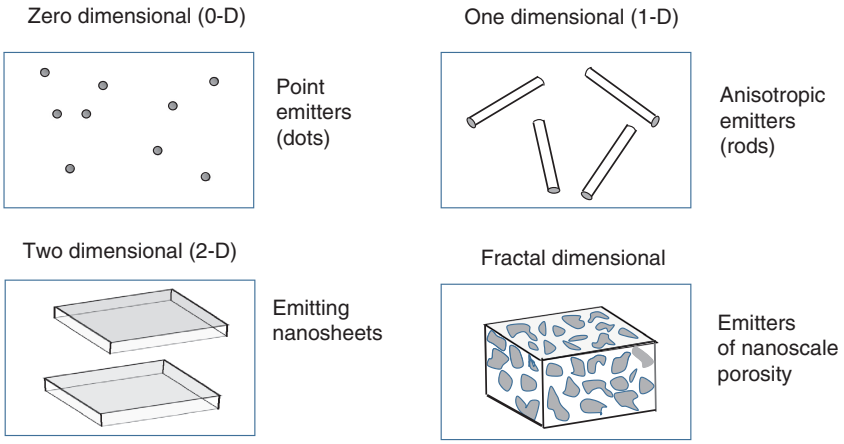

Fig. 5.1 The structures of nanoscale dimensionality

gave them the name "*quantum dots*". Similarly, other nanoscale structures without strong asymmetry are often considered as "dots" (Burda et al. 2005). The ultrathin nanowires would be the 1-D analogs of these nanomaterials (Greco et al. 2008) and can be called '*nanorods*'. The examples of 2-D nanostructures are the graphene molecular sheets of atomic thickness (Park and Ruoff 2009). In addition to size, the shape of nanoparticles may influence dramatically their optical properties. The assembled nanocomposites may contain nanoparticles or clusters of different dimensionalities (Srivastava and Kotov 2009). Precise 3D self-assembly is possible with nanocomposites (Wang et al. 2006b), as it will be seen in Chap. 6.

Nanoporous solid materials may possess optical properties similar to that of nanoparticles and a fractal dimension can be attributed to them. A bright example is porous silicon (Torres-Costa and Martín-Palma 2010), which is the material with high surface to volume ratio (as large as 500 m^2 cm^{-3}). Its emission properties are similar to that of nanocrystalline particles made of the same material, and these nanoparticles follow the same regularity as other quantum dots – the strong size-dependence of emission spectrum (Hessel et al. 2011).

5.1.2 Variations in Nanoparticles Composition, Crystallinity and Order

An intrinsic *polydispersity* in size and shape is frequently observed in nanoscale particles, which is connected with the ways of their synthesis. This is in contrast to dye molecules that are definite chemical entities (sometimes a mixture of several isomers). Quantum dots can be separated into fractions with narrow size distribution, but the number of their atoms is commonly not well determined (Alivisatos et al. 2005). The electronic effects govern the size-dependent switching from plasmonic noble metal nanoparticles to strongly fluorescent few-atom clusters (see Fig. 4.27).

Some nanomeric structures can be obtained in a way that their structural uniformity can be achieved with atomic precision. They are called the "*magic-size*" nanoparticles, the characteristic representatives of which are the fullerenes. Such ball-shaped structures of several tens of atoms can be made of different materials. For fluorescence sensing and imaging applications the most interesting are the magic-size semiconductor quantum dots, such as (CdSe)(33) and (CdSe)(34) (Kasuya et al. 2004b), the light absorption and emission properties of which are quite different from that of "conventional" nanocrystals.

Any nanoparticle will be stable only if its core is stabilized by *interactions* between the constituents (Hoang 2007, 2012). These interactions can be of different origin (covalent, ionic, van der Waals, etc.). The strength of intra-particle bonding should be sufficient to withstand variations of external conditions in the media of their functioning. That is why the micelles made of detergent molecules and also phospholipid vesicles being of nanoscale dimension are not considered as nanoparticles. Essentially, for generating the light-emitting properties, the nanoparticles should allow observing collective electronic effects resulting in formation of discrete ground and excited-state energy levels. Whereas molecules of organic dyes possess the well-specified electronic energy levels as their basic properties, in a variety of novel nano-materials the discrete energy levels appear as the sole effect of their small particle size.

Crystals are the best atomically defined structures with relatively well-understood interactions. These interactions can be of various types: ionic, metallic, covalent, van der Waals and H-bonding. What unifies crystalline structures is the presence of long-range order based on translational periodicity of a unit crystal cell. In many important cases, the process of crystallization can be stopped on a level of tens or hundreds of atoms. Being of nanoscale dimensions, even with intrinsically perfect order, these particles usually lack monodispersity but can be presented as narrow size fractions. Translating crystal order to their surfaces, they form the "sharp edges". Meantime, we always observe that nanocrystals cannot be considered as small pieces of bulk material, so that unusual forms of atomic disorder can be observed together with structural stiffening (Gilbert et al. 2004) and the deformation of crystal order is mostly typical for surface-exposed atoms (Jadzinsky et al. 2007).

In contrast, formation of nanoparticles from *soft materials* results in amorphous structures, the positions of every atom in which are not defined. They are usually less conformationally stable, but they can form smooth surfaces that maximize intrinsic interactions and minimize interactions at the surfaces. The degree of their order on atomic level is variable and many of them show micelle-like behavior. Their interface energy is lower than that in nanocrystals (Navrotsky 2003).

5.1.3 Interactions at Surfaces

For increasing the solubility of nanoparticles and their stability against decomposition or growth, their surface should often be covered with *capping agents* (Bagwe et al. 2006). Oligo(ethylene glycol) has proved to be such agent that induces the

nanoparticle solubility in polar media without specific interaction with different types of molecules of biological origin (Herrwerth et al. 2003). Polyethylene glycol coating is friendly to cells and tissues, for instance, it prevents hemolysis produced *in vivo* by silica nanoparticles (Lin and Haynes 2010). Ligand exchange resulting in formation of polar surfaces is of broad utility for hydrophobic nanoparticles that allows producing their stable suspensions in aqueous media (Wawrzynczyk et al. 2012; Dubois et al. 2007).

For all types of nanoparticles it can be observed that not only the stability but also the photophysical properties are strongly *ligand-dependent*. Core-shell structures are typical for QDs (Alivisatos et al. 2005). Such composition can resolve many problems: reducing the negative effects of sharp edges of crystal cores, increasing the solubility, allowing the incorporation of functional groups for further modifications and introducing new functionalities. Their outer layer is needed for bioconjugation. Different techniques for providing polymeric covers were developed for that (Tomczak et al. 2009). Designing nanoscale inorganic-organic interfaces is highlighted in research papers and reviews (Wang et al. 2007; Balazs et al. 2006; Tomczak et al. 2009).

Techniques of covalent attachment of organic dyes and other molecules modifying the nanoparticle surface are well developed (Hermanson 1995). Novel aspects involve application of click chemistry (Li and Binder 2011), which becomes a universal method to link reaction partners in high efficiency, solvent insensitivity and at moderate reaction conditions.

5.1.4 Peculiarities of FRET with and Between Nanoparticles

The long-range interactions leading to FRET are not limited to fluorescence and are characteristic of any emissive excited state, whatever is its origin. All these phenomena can be adequately described by *Förster-type inductive dipole resonance* mechanism. In their description we use the term ‘dye’ in its general sense, which includes organic dye molecules and different kind of molecular complexes and nanoparticles. But definitely, there are peculiarities of energy transfer with and between the particles, the size of which is comparable with the Förster radius R_0 (Eq. 3.14), since the particles of such size cannot be approximated by point dipoles and therefore evaluation of distance between them is not very definitive. Involvement of dipole orientation factor, κ^2 (Eq. 3.15), may also raze confusions.

Moreover, the *distance dependence* of energy transfer may be different from that described by $1/R^6$ function. This is because of different mechanism of this interaction. In inductive-resonance mechanism of FRET developed by Förster, the two interacting point dipoles are considered, whereas in the case of conducting particles the donor dipole interacts with a ‘Fermi gas’ of nearly free conduction electrons. Based on such modeling it was suggested that on interaction of small organic dye and large conducting metal nanoparticle the $1/R^4$ function should be observed. This suggestion was confirmed in an experiment (Yun et al. 2005), in which the gold nanoparticle was appended to the 5′ end of one DNA strand as the

energy acceptor and a fluorescein dye to the 5′ end of the complementary strand as the energy donor. Analysis of the energy transfer as a function of DNA lengths (15, 20, 30, 60 base pairs) allowed testing the distance dependence in the range 5–25 nm. The result showed conformance to $1/R^4$ function. This is one of the results showing that for signal transduction in fluorescence sensing the application of nanoparticles may allow the extension of transduction to *longer distances*, up to 15–20 nm.

An extended distance dependence of FRET *between nanoparticles* is also suggested based on quantum chemical calculations (Wong et al. 2004). The authors come to conclusion that the FRET rate at large separations exhibits several features not anticipated in the conventional theory: The actual rate shows much weaker short-range distance dependence, in this version of theory closer to $1/R^2$ in contrast to $1/R^6$ value. The Förster expression overestimates the energy transfer rate by more than two orders of magnitude at short separation (<1 nm). The distance at which the Förster rate is recovered is observed to be rather large (similar to 10 nm). Thus, the Förster expression seems to be inappropriate for condensed-phase systems where the donors and acceptors are large particles that can be closely packed, as, for example, in thin films. This and other results show that in principle, the particles possess more possibilities to manipulate with FRET effects and to optimize them than the conventional dyes (Jares-Erijman and Jovin 2003).

5.1.5 Concluding Remarks

From this short survey, one may infer that the nano-world is quite different not only from our macroscopic world but also from the world of molecules. High surface area of nanoparticles together with exposed groups able of forming different types of bonds is a good platform for conjugation of functionally important molecules including those with molecular recognition properties. Molecular recognition involves both steric and energetic control over high-affinity intermolecular interactions. It can be easily realized with nanoparticles having comparable size to common protein molecules that often serve as recognition units (Aggarwal et al. 2009). Meantime, nonspecific interactions that usually are present in the studied media may present a significant problem. Many efforts are being made for reducing nonspecific adsorption on nanoparticles covering them with polymers (Bagwe et al. 2006), peptides (Liu et al. 2010) and designed ligands (Allen et al. 2010). Special care is often needed for retaining specific activity of proteins adsorbed on the particles (Park and Hamad-Schifferli 2010). As an example it was shown that intracellular glutathione with its SH-active groups can substitute reactive sites on the surface of gold nanoparticles leading to dissociation of nanocomposites (Han et al. 2005). We have to count that biological fluids such as blood stream or cell interior possess very high concentrations of dissolved solutes (intracellular protein concentrations >300 mg/ml), so the effects of nonspecific absorption in these media must be very strong (Park and Hamad-Schifferli 2010).

5.2 Dye-Doped Nanoparticles and Dendrimers

A very high *brightness* is the desired property of every fluorescence emitter. This goal can be achieved by incorporating many dye molecules into nanostructures formed by organic or inorganic polymer. Due to large number of dye units housed in a relatively small volume of a single nanoparticle, the dye-doped nanoparticles present considerable advantages with respect to the same dyes used in molecular form. At the same excitation conditions one can obtain a fluorescence signal, which in some cases is 10^4–10^5 times stronger (Wang et al. 2006a). The benefits of such nanoparticles are clearly seen in cellular studies and in the whole-body imaging, where loading the particles with two-photonic dyes will allow achieving extreme brightness and resolution (Bertazza et al. 2006).

There may be different additional benefits for such incorporation. One, of course, is the *isolation* of the dyes from molecular contact with the test medium and thus making them insensitive to the changes of composition in this medium. Important in this respect is the possibility to avoid *degradation* of dyes in aggressive media and in living cells. The dyes in solid environments usually exhibit much higher fluorescence intensity, quantum yield and lifetime than in liquid media. This is due to stronger restriction imposed by solid matrix on rotation of dye segments, intermolecular collisions and dielectric relaxations – all the factors that quench the fluorescence (Riu et al. 2006).

The benefits are also in constructing nanocomposites (Chap. 6) and supramolecular structures (Chap. 9). Their larger surfaces may allow attachment instead of one, of several macromolecular recognition units. Attachment to their surface of various functional groups (such as avidin, biotin, antigenic peptides, ligand-binding proteins, etc.) allows their facile bioconjugation, immobilization and incorporation into various assays.

5.2.1 Contact (Concentrational) Quenching

Realization of very attractive idea to assemble many dye molecules together in a small unit meets a difficult problem. The highest density of dye molecules does not always lead to the highest brightness since the direct interactions between them or exchange of their excitation energy may lead to the so-called '*concentrational quenching*' (another names '*contact quenching*' and '*self-quenching*'). This feature was frequently observed when the protein or nucleic acid molecule is labeled by attaching an increasing number of fluorescent dyes. Then very often its fluorescence instead of linear increase passes through the maximum and falls down. For many dyes, the self-quenching is a limiting factor in the design of devices with high sensor and fluorophore density.

The explanation of this effect is illustrated in Fig. 5.2. Potentially emissive dye molecules, being located at short distances, loose the properties of independent emitters. Being excited, they start to exchange their energies in accordance to

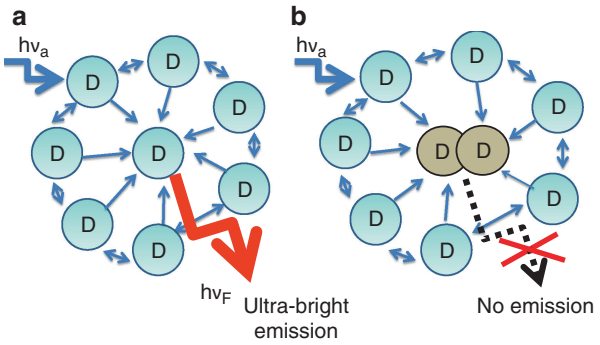

Fig. 5.2 Illustration of homo-FRET and self-quenching in dimers. (**a**) The dyes (*D*) exchange their excitation energy and are brightly emitting. (**b**) The presence of a non-fluorescent dye dimer (*DD*) acting as the trap for excitation energy results in quenching of all the dyes located at a close distance to it

homo-FRET mechanism (Sect. 3.6). Homo- FRET is realized between the same dye molecules serving as donors and acceptors to each other. Its mechanism is the same as for common hetero-FRET: it requires overlap of emission spectrum of the donor with absorption spectrum of the acceptor. So the same dye molecules can be both donors and acceptors, and, if the Stokes shift is small, the *overlap integral* (see Sect. 3.6) is small. So, they can exchange their energies even being at large distances, up to 5–7 nm (Runnels and Scarlata 1995). Normally this results in emission of one of molecules in the system (Fig. 5.2a).

With the increase of *concentration* of dye molecules and of the probability of interaction between them there may occur formation of *dimers*, then of aggregates. The interactions within these dye associates lead to static quenching of their fluorescence via electron transfer. Such traps of excitation energy accumulate the energy from other nearby located dyes but do not emit it (Fig. 5.2b). This results in *quenching* in the whole system (Lavorel 1957; Johansson and Cook 2003).

Involvement of this effect when the energy is captured by non-fluorescent species depends strongly on the properties of the dye. Fluoresceins and rhodamines exhibit high homo-FRET efficiency and also self-quenching, pyrene and perylene derivatives – high homo-FRET but little self-quenching, and luminescent metal complexes may not exhibit homo-FRET at all because of their very strong Stokes shifted emission. When the nanoparticles are composed of organic dyes or doped with these dyes such effects can be especially important.

5.2.2 *Organic Dyes Incorporated into Organic Polymer*

A convenient way to create fluorescent nanoparticles containing *high density* of organic dyes is to incorporate them into inorganic or organic polymers. The dyes can be either located inside the nanoparticles or attached to their surfaces by physical adsorption and by covalent binding to surface-exposed groups. The porous nanoparticles are the most attractive in this respect, since they exhibit the highest surface-to-volume ratio and the cavities that are suitable for efficient dye incorporation forming relatively strong multi-point contacts. The techniques for

preparing nanoparticles of organic polymer are well developed. The dyes can be incorporated into them either during or after the synthesis of polymer macromolecules (Borisov et al. 2010).

These particles can be obtained based on a variety of synthetic polymers: polystyrene, polymethyl methacrylate, polyacrylic acid, polyvinyl chloride, etc. Usually this is done by *micro-emulsion polymerization* (Landfester 2006). Micro-emulsions are the specially formulated hetero-phase systems, in which the stable nanosize droplets of one phase are dispersed in a second, continuous phase (Fig. 5.3). Each of these nanodroplets can be considered as nanoscopic individual batch reactor. Because of such confinement, a whole variety of reactions and processes resulting in both organic and inorganic nanoparticles can be performed and the size of polymerized particles controlled. Surfactants are used for stabilization of this nano-scale heterophase and an ultrasound treatment helps for dispersing these particles. With this technique, different kinds of polymerization reactions, such as radical, anionic, and enzymatic polymerization, as well as polyaddition and polycondensation, can be carried out. Microemulsion technology is highly suited for the encapsulation of various organic and inorganic, solid or liquid materials, including fluorescent dyes, into the particles.

Polystyrene latexes that form stable dispersions in water and other polar media are known and used in research for a long time. With incorporation of different dyes, they can be made highly fluorescent. The surface of the nanoparticles can be modified by amino and amidino functional groups introduced by the co-monomer and the initiator 2, 2′-azobis (2-amidinopropane) dihydrochloride. Fluorescent dye N-(2,6-diisopropylphenyl)perylene-3,4-dicarboximide was incorporated into the co-polymer nanoparticles formulated from styrene and acrylic acid or styrene and aminoethyl methacrylate hydrochloride (Holzapfel et al. 2005). The resulting latexes were stable and showed a monodisperse size distribution within the range 100–175 nm. These functionalized fluorescent particles are commonly used as markers for living cells, and the cell uptake was visualized using fluorescence microscopy.

A simple technique of *doping the nanoparticles* after their synthesis can also be applied. It involves swelling the particles in organic solvent containing the dye and

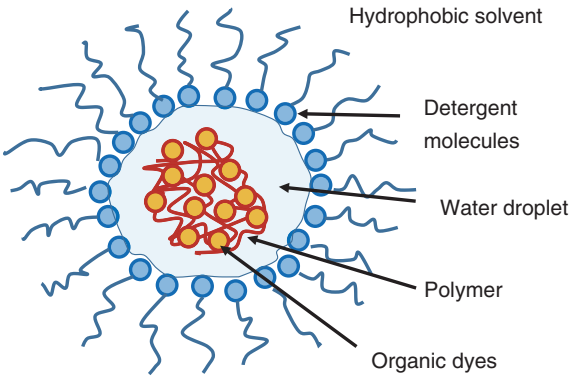

Fig. 5.3 Schematic diagram of water-in-oil micro-emulsion for synthesis of polymeric nanoparticles

then drying. Being transferred to water, these particles retain hydrophobic dyes, but the restriction exists for their use in low-polar solvents due to the possibility of washing-out the dyes. Preparation of polymer nanoparticles that form stable dispersions in nonpolar media can also be made. Several synthetic routs for that have been described in the literature, particularly, for the incorporation of pyrene (Tauer and Ahmad 2003).

Special attention in recent literature has been paid to the production of particles that contain *luminescent metal chelates*, such as Eu(III) beta-diketonates complexes. As we observed in Sect. 4.5, such complexes have a long decay time, a large Stokes shift, and very narrow emission bands in comparison with organic fluorescent dyes. Upon incorporation into polymer matrix these properties are preserved (Huhtinen et al. 2005).

The template-directed polymerization that is often called '*molecular imprinting*' (Sect. 7.8) is a very promising approach for the preparation of selective and high-affinity binding sites for different targets. In this way, the polymer nanoparticle can serve not only as a support and reporting element but also as a recognition functionality.

5.2.3 Silica-Based Fluorescent Nanoparticles

The labeled silica nanoparticles are attractive alternatives to organic polymer particles in serving the same purpose: confining, concentrating the dye molecules and making them functional. The advantage is their higher stability in organic solvents and at variations of pH (Yao et al. 2006). Compared to natural and some synthetic polymers, the silica particles are more hydrophilic and stable in biological milieu; they are not subjected to microbial attack. Their separation and fractionation is easy by sedimentation due to high density of silica (1.96 g/cm^3). Their surface modification and bioconjugation are also not very difficult: the reactive end groups can be added during the synthesis. The important for conjugation decoration of their surface with amino groups is described in detail (Liu et al. 2007). The surface of silica particles can be modified in different ways including the attachment of enzymes (Qhobosheane et al. 2001).

It is important also that silica is photophysically and optically inert. It is transparent to light in a broad optical range and it does not participate in any energy- and electron-transfer processes. Therefore, all the spectroscopic properties of the luminescent silica nanoparticles can be attributed mainly to the doping material and to its interactions.

The *sol-gel matrices* are excellent supports for immobilization of dyes and metal-chelating complexes due to their inherent mechanical and chemical stability, optical transparency and the ease of formation. Fluorescent nanoparticles composed of dye-doped silica synthesized by reverse micro-emulsion (see Fig. 5.3) allow achieving high density of dye molecules. The dye properties may improve substantially on their immobilization. The particles exhibit higher fluorescence quantum yield and stronger resistance against photobleaching. The higher polarity

than that of synthetic polymers and higher stability against the change of environment conditions together with the presence of negative charge allows efficient retention in silica matrix of fluorescent dyes, especially of those bearing positive charge.

The developed technologies allow selecting preferential location of reporter dyes – in the rigid core, at the porous periphery or at the particle surface (Ow et al. 2005). These possibilities can be realized not only with organic dye molecules but also with luminescent metal complexes (Lian et al. 2004; Qhobosheane et al. 2001). Sol-gel matrices are typically used to provide a nanoporous support matrix, in which the analyte-sensitive fluorophores are entrapped and into which smaller analyte species may diffuse and interact. The versatility of the process of producing these particles facilitates tailoring their physicochemical film properties and optimizing sensor performance.

Being highly luminescent and extremely photostable, the dye-doped silica nanoparticles have been developed for ultrasensitive bioanalysis (Yao et al. 2006). They can be used as very efficient platforms for dye assemblies with desired properties for imaging and diagnosis (Bae et al. 2012; Bonacchi et al. 2011). As a result of operation with emission color in the design of fluorescent nanoparticles, two interesting results can be cited (Fig. 5.4). In one of them a broad-range variation of fluorescence color was achieved by combining in different proportions of fluorescent dyes exhibiting FRET (Wang et al. 2006a), see Fig. 5.4a. Three dyes were chosen to have overlapping emission and excitation spectra in order to allow efficient fluorescent energy transfer to occur. By doping with different combinations of these dyes, barcode tags can be produced for multiplexed, targeted FRET under single wavelength excitation. In contrast, in Fig. 5.4b a combination of two emitters exhibiting fluorescence (FITC) and phosphorescence (tris(1,10-phenanathroline)

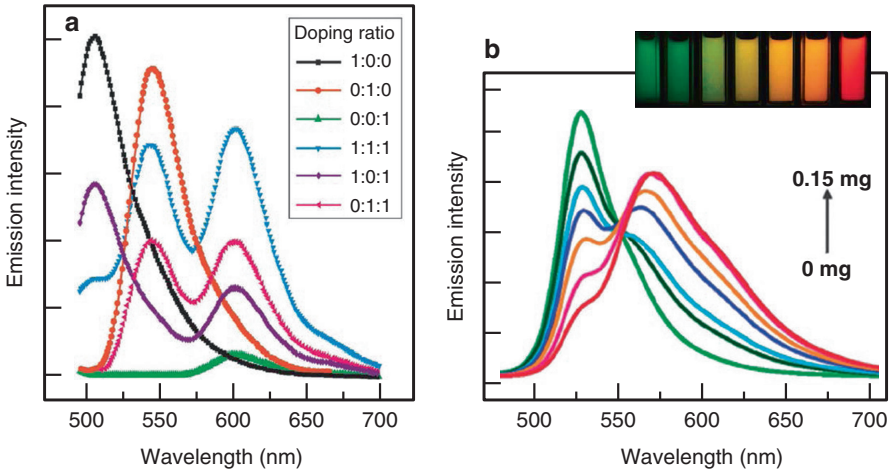

Fig. 5.4 Doping silica nanoparticles with multiple dyes. (**a**) Fluorescence spectra of particles doped with fluorescein isothiocyanate (FITC), rhodamine 6G and 6-carboxyl-X-rhodamine in different doping ratios (Wang et al. 2006a). (**b**) Emission spectra on stepwise doping with different combinations of FITC and $Ru(phen)_3^{2+}$ luminophore (Xu et al. 2010). *Insert* shows the change of emission color on the increase of $Ru(phen)_3^{2+}$ concentration from 0 to 0.15 mg

ruthenium ion) allowed excluding FRET and observing a combination of individual emissions at a single excitation wavelength 450 nm. Colors of the particles can be easily tuned by varying the doping ratios (Xu et al. 2010). Multiple doping is very prospective for various applications (Bonacchi et al. 2011), especially when such transformation of reporting signal as light harvesting, wavelength converting or extending the lifetime (Sect. 6.2) are needed.

5.2.4 Fluorescent Dendrimers

Dendrimers are currently attracting the interest of many scientists because of their unusual chemical and physical properties and the wide range of potential applications. Many possibilities for such applications exist in sensing technologies. *Dendrimers* are unique molecules of high complexity and order with precise and gradable range of dimensions within the range of several nanometers. They are highly branched spherically shaped polymeric structures that emanate from a central core (Campagna et al. 2011; Astruc et al. 2010).

Typical dendrimer contains a core monomer, from which many branches stem in all directions producing a spherical shape (Fig. 5.5). It is hard to believe that a rather simple synthetic chemistry can provide the materials of such regularity and beauty.

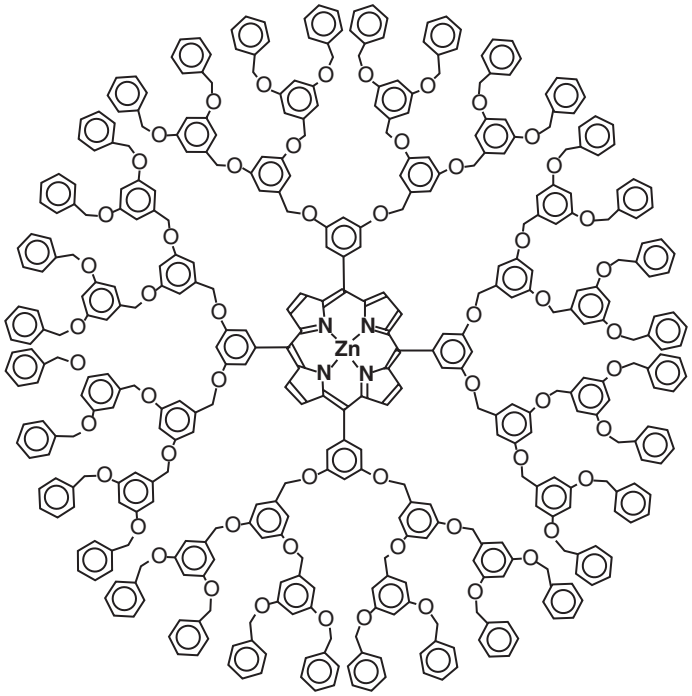

Fig. 5.5 The structure of a typical dendrimer containing porphyrin core and benzene rings forming the surface (Grayson and Frechet 2001)

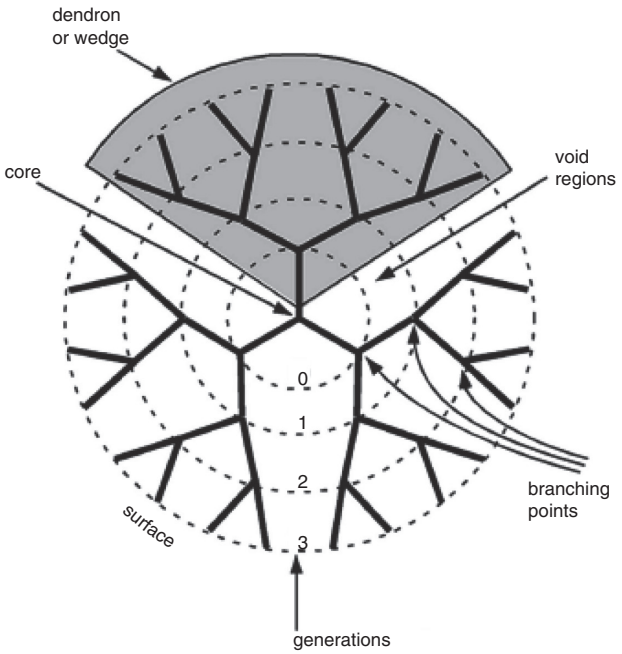

Fig. 5.6 Schematic presentation of the dendrimer structure (Bergamini et al. 2010)

General principle of arrangement of a dendrimer is illustrated in Fig. 5.6. From a topological viewpoint, dendrimers contain three different regions: core, branches, and surface. Each branch (dendron) can be further expanded by sequential branching with the addition of other layers of monomers, forming in this way the higher order dendrimer '*generations*'. Since these molecules are produced in an iterative reaction sequence, they *lack polydispersity*, so that each molecule has the same number of atoms and the same shape.

The typical and most frequently used dendrimer is the water-soluble poly(amidoamine), PAMAM, exposing amino groups on its surface (Table 5.1). Sometimes, because of different polarity of inner volume and the surface, these structures are called 'single-molecular micelles'. Their surface amino groups are exposed for covalent attachment of fluorescent dyes (Oesterling and Mullen 2007) they are the sites of covalent links in nanocomposite formations.

Table 5.1 Physical properties of PAAMAM dendrimers (Scott et al. 2005)

Generation	Number of surface groups	Number of tertiary amines	Molecular mass (Da)	Diameter (nm)
0	4	2	517	1.5
2	16	14	3256	2.9
4	64	62	14,215	4.5
6	256	254	58,048	6.7
8	1024	1022	233,383	9.7
10	4096	4094	934,720	13.5

There are other even more attractive possibilities to make the dendrimers fluorescent. First is by inserting selected chemical units in predetermined sites of the dendritic architecture. Luminescent moiety can serve as a dendrimer core, around which the branches can grow. Dendrimers formed on the basis of $Ru(bpy)_3^{2+}$ as a core exhibit the characteristic phosphorescence that can be protected from external quenchers by the dendrimer branches and sensitized by attached dyes on the periphery of dendrimer (Balzani et al. 2000).

Moreover, thanks to their flexible three-dimensional structure, the dendrimers are able of encapsulating in their *internal dynamic cavities* the ions or neutral molecules, including fluorescent dyes (Shcharbin et al. 2007; Balzani et al. 2000) and luminescent metal ions (Balzani et al. 2000; Bergamini et al. 2010). It is thus possible to construct nanocomposites, in which large number of different dyes can be located in pre-determined sites. Therefore, coupling luminescence and dendrimer chemistry can lead to interesting photophysical properties (Bergamini et al. 2010; Campagna et al. 2011), such as (1) interactions of dendritic luminescent units in the ground and/or in the excited states (possible formation of excimers and/or exciplexes), (2) quenching of dendrimer luminescence by external species, and (3) sensitization of luminescent metal ions or dyes encapsulated by the dendrimer.

The dendrimers started to find an application similar to that of organic polymers and silica. The advantage in this case is the well-defined shape and chemical organization of these structures that allows shielding the dye molecules from their direct contacts with each other, avoiding their quenching. The flexibility of dendrimeric structures is also exploited, and this allows penetration from outside into their interior of small target molecules. In addition, a broad range of functionalization is possible for the introduction of target-recognizing groups into these structures.

There is also a new type of intrinsically fluorescent dendrimers, which is even more attractive. The dendrimers can be formed of *aromatic groups with a high level of their conjugation* (Balzani et al. 2003; Astruc et al. 2010). These dendrimers resemble in many properties the conjugated polymers (Sect. 5.3) with the advantage of high level of organization of their structures. Using modern techniques it is possible to design and synthesize the dendrimers containing a variety of light absorbing and emitting groups. Even more, the effect of light harvesting (Sect. 6.2) can be easily obtained with these structures. This makes them prospective transducers and reporters in sensor technologies.

5.2.5 *Fluorescent Nanoparticles Made of Organic Dyes and Aggregation-Induced Emission*

It is textbook knowledge that chromophore aggregation generally quenches the light emission, and we discussed above the mechanisms of such quenching and the possibilities of its prevention in dye-doped nanostructures. Meantime, there are successful attempts to obtain fluorescent nanoparticles solely made of organic dyes. This is achievable by finding substituents that reduce direct interaction between aromatic groups (Yao 2010; Fery-Forgues et al. 2008). The problem in this case is

in finding the ways for self-assembly of composing units in a well-controlled manner and making the assembled structures stable in test conditions. It was shown that brightly fluorescent nanoparticles can be made of subjective to self-quenching aggregation cationic rhodamine dye by mixing this dye with hydrophobic anion tetraphenyl borate. Within these particles the fluorophores exchanged their excited-state energies and demonstrated collective blinking effect (Reisch et al. 2014).

In this regard, there are the publications describing achieving the effect opposite to aggregation-induced quenching – the *aggregation-induced emission* (Hu et al. 2014). Typically the dyes demonstrating this effect possess the propeller-like structures with flexible phenyl rings. As isolated molecules, they undergo low-frequency torsional motions and due to strong intramolecular mobility they emit very weakly in solutions. Their aggregates show strongly enhanced fluorescence mainly due to the restriction of their intramolecular rotations in the aggregate state. In contrast to the dyes forming J- or H-aggregates, the nanoparticles made of dyes with enhanced emission show only the changes in intensity but not the spectral changes. The sensors based on such intensity changes of these dyes were suggested exploring aggregation-dissociation effect (Ding et al. 2013; Zhang et al. 2014).

The studies of small propeller-like molecules were extended to polymers (Qin et al. 2012). Different polymer molecules that possess highly flexible fragments, are soluble and swell in organic solvents, are of limited solubility when they are transferred to water (Jang et al. 2006). They form nanoparticles, so that their internal structure becomes compact with immobilization of these fragments. With the increase of water content in mixed solvent, their fluorescence intensity increases dramatically (Fig. 5.7).

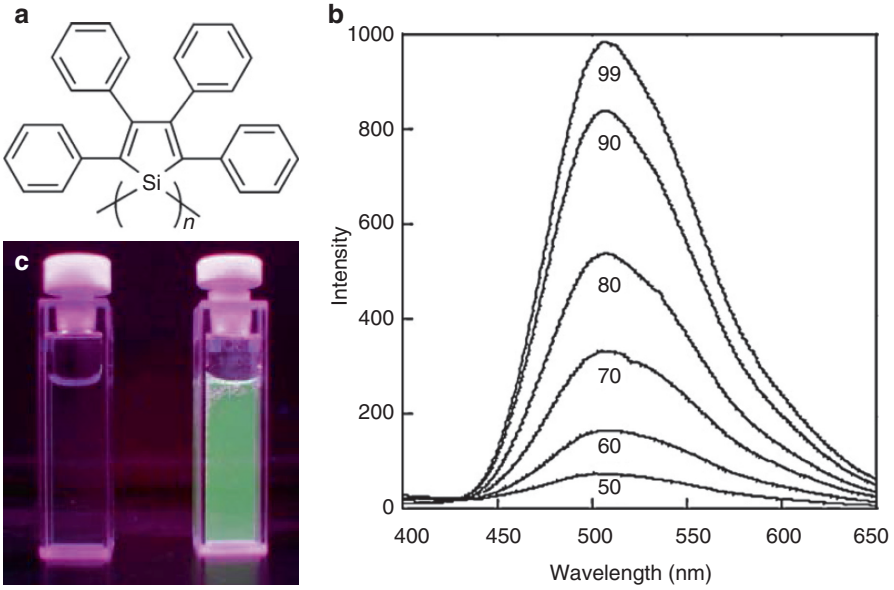

Fig. 5.7 Illustration of aggregation-induced emission (Jang et al. 2006). Fluorescence spectra of polysilole polymer (**a**) in THF/water mixtures demonstrate enhancement at increased concentrations of water (**b**). (**c**) Photograph of polysilole in THF (*left*) and in water-THF mixture (90:10 by volume)

5.2.6 *Applications of Dye-Based Nanoparticles in Sensing*

Organic polymeric and silica-based nanoparticles as well as dendrimers, with the incorporation of different dyes have found broad range of applications (Fig. 5.8). Their dramatically increased absorbance compared to individual dye molecules is their most attractive feature. They demonstrate also an increased chemical stability, photostability and protection from nonspecific interactions with quenchers in tested media. Thus, the *organic polymer* structures were suggested for application as fluorescent tags for DNA and in the cell imaging. In DNA detection (Huhtinen et al. 2004) it was easy to achieve the detection limits on the level of ~1 pg/ml for proteins and 6.1×10^4 copies of DNA. In time-resolved immunoassays, based on trapping of chelated Eu^{3+} ions polystyrene nanoparticles, the highly sensitive bioassays for prostate-specific antigens were developed (Harma et al. 2007).

The application of polymeric nanoparticles in ion sensing can be illustrated by the reported fluorescent sensor for the detection of Cu^{2+} ions in water on the nanomolar level (Meallet-Renault et al. 2004). In this application, the sensor was constructed by associating a BODIPY fluorophore and a copper chelator (cyclam) in

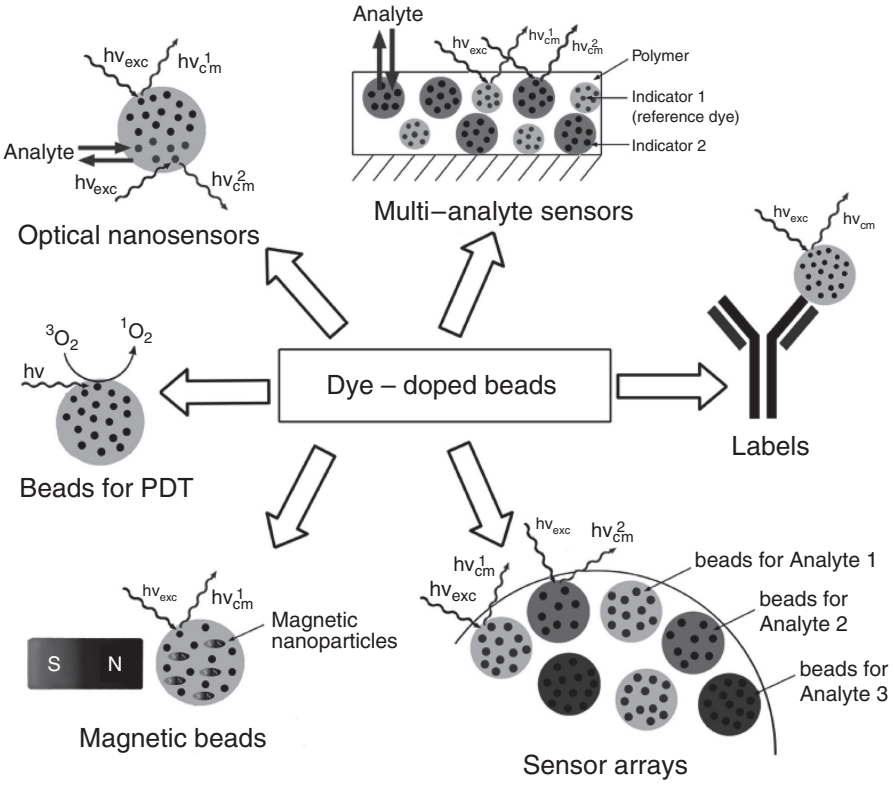

Fig. 5.8 The most common applications of dye-doped particles (Borisov et al. 2010)

ultrafine polymer nanoparticles, and the response was based on the ability of copper ion to quench the fluorescence emission.

Regarding fluorescent dye-doped *silica nanoparticles*, they are also actively used in different sensing technologies, particularly in *fluorescence immunoassays*. They offer extremely high sensitivity, especially when they are impregnated with luminescent metal chelating complexes (Wang et al. 2006a). When the luminescent silica nanoparticles were used for leukemia cell recognition, the antibody was first immobilized onto the particle through silica chemistry and the cell binding was detected by an optical microscopy imaging (Qhobosheane et al. 2001). Using these antibody-coated nanoparticles, the leukemia cells were identified easily, clearly, and with high efficiency.

The larger-size fluorescent *polymeric microspheres* are actively used in analytical assays using flow and image cytometry (Szollosi et al. 1998). In the case of detection of fluorescent labeled molecules, they can be used both as support and recognition units with the application of homogeneous assay methodology. Single-nucleotide polymorphism (SNP) genotyping directly from human genomic DNA samples is another area of their efficient applications (Rao et al. 2003).

The *dendrimers* containing high amount of fluorescent label also find application in DNA hybridization assays, improving or replacing the organic dye-based assays (Caminade et al. 2006). An immunoassay based on the composed antibody-conjugated PAMAM-dendrimer-gold quantum dot complex was also suggested (Triulzi et al. 2006). Due to the possibility of easy and efficient modification of their surface, different groups recognizing small molecules and ions can be attached to this surface. Due to their membrane permeation ability (Khandare et al. 2005), PAMAM dendrimers, especially those of higher generation, have good prospects for *in vivo* biological applications.

5.2.7 Frontiers for Future Research

Commonly fluorescence reporters are the molecules or their ensembles that use only one or several dye molecules for providing the response. In this section, we demonstrated the new and very attractive possibilities that appear on incorporation of organic dyes into and onto nanoparticles of mineral or organic origin. We could observe that, in addition to improvement of chemical stability and photostability due to full or partial protection of dye moieties from the solvent, these composite particles attain new properties. They exhibit an extremely bright emission allowing 100–10,000-fold increase over common organic dye molecules. Their large surface areas allow multi-point chemical modifications. The chemistry of dye incorporation is determined by the host particle composition and can be the same with the use of different dyes. In addition, the dyes in these nanostructures can locate in such distances and configurations that FRET between them becomes efficient but self-quenching is avoided. These features dramatically increase the sensitivity in analytical applications, and this fact has to stimulate the development of new more efficient assays.

The large and bulky size of polymer particles (10–100 nm) may limit some of the applications. In all cases when this factor is not crucial, being the brightest emitters, the dye-doped particles show the brightest prospects. Such prospect is expected in cellular studies and in the whole-body imaging, where loading the particles with two-photonic dyes will allow achieving extreme sensitivity and resolution (Bertazza et al. 2006). The technologies based on incorporation of lanthanides with long-lifetime emission have started to be explored with very promising prospects (Hötzer et al. 2012). The protection of cells from toxic effects of these dyes and protection of dyes from chemical and photochemical decomposition will appear as additional benefits. Regarding synthetic chemistry, the most rapid prospect is expected in designing the polymers with fluorescent groups linked as the side substituents in polymer chains in desired amount and strictly determined positions. Such structures may resemble folded proteins in their organization. Recent publications (Breul et al. 2013) demonstrate strong efforts to proceed in this direction.

5.3 Conjugated Polymers

The composites of dye molecules with intentionally reduced interactions between them may be considered as one extreme case. The other extreme are the conjugated polymers (Feng et al. 2010; Reppy 2010). They are polymeric molecules, in which the π-electrons of every monomeric unit are delocalized over significant part of chain sequence (Hoeben et al. 2005). Being electron-rich and with high level of π-electronic conjugation between each repeat unit, such polymeric chain is not only able to absorb and emit visible light but also to demonstrate strong collective effects in electronic excitation and emission. Due to their high molar absorbance ($\varepsilon \sim 10^6\ M^{-1}\ cm^{-1}$) these polymers are very good light harvesters in nanocomposite constructs (Achyuthan et al. 2005). Operating with substituents in the polymer chain one can modulate their solubility and their incorporation into nanocomposites.

5.3.1 Structure and Spectroscopic Properties

The *conjugated polymers* are polyunsaturated compounds with alternating single and double bonds (or aromatic units) along the polymer chain (Hoeben et al. 2005), Simple chemical structures together with many possibilities to modify them by attaching functional groups makes a number of conjugated polymers very popular. Their core elements are hydrophobic (see Fig. 5.9). Attachment of side groups allows modulating the polymer charge and hydrophobicity in broad ranges. Biosensing in water needs good polymer solubility, which is provided by introduction of charged groups. Such modification makes them the fluorescent polyelectrolytes.

The key element that determines the optical properties of conjugated polymers is their polarizable π-electronic system extended along the conjugated backbone. This

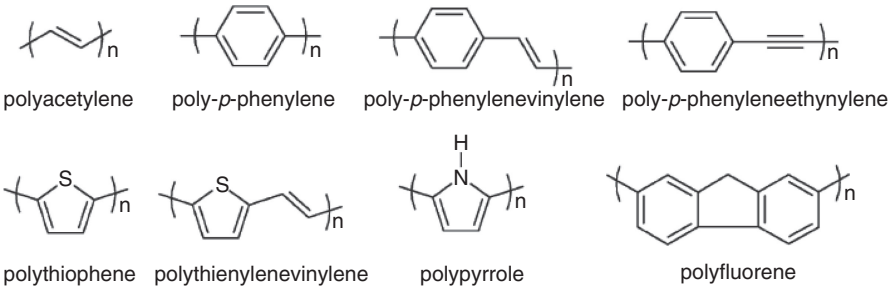

Fig. 5.9 Chemical structures of several frequently used conjugated polymers

brings these polymers the property of electronic conductance and even allows considering them as 'molecular wires'. Being electron-rich and with high level of π-electronic conjugation between each repeat unit, such polymeric chain is able to very efficiently absorb and emit visible light. Upon excitation, there appear conduction-band electrons forming together with the positively charged nuclear sites the neutral collective excitations called *excitons*.

Excitons can migrate along the polymer chain and, in densely packed aggregates, between the chains. The mechanism of this migration involves both the through-space dipolar coupling and strong mixing of electronic states. Fluorescence quenching is essentially the termination of this migration producing collective effect (Fig. 5.10). It involves not only the site of quencher location but also the whole polymer or its significant part (Thomas et al. 2007). The situation, in which a large number of otherwise brightly fluorescent monomeric units are simultaneously quenched by one quencher molecule is often referred to as '*superquenching*'

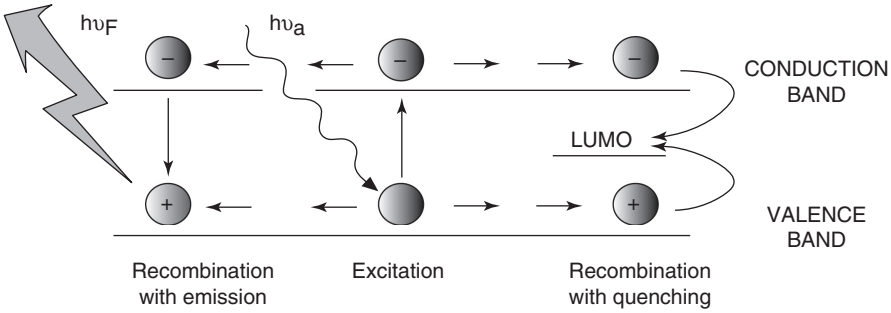

Fig. 5.10 Diagram illustrating the mechanisms of electronic excitation, exciton transport along conjugated polymer chain, fluorescence emission and quenching by electron-hole recombination. Excitation promotes electron to a high-energy conduction band with the generation of positively charged 'hole' in the ground state. Electron-hole pair generated on excitation forms the exciton that can migrate along the polymer chain with an emissive transfer to a ground state. External quencher can easily interfere into this process and induce the non-emissive recombination if its LUMO (lowest unoccupied molecular orbital) band is located lower in energy than the excited state of a polymer

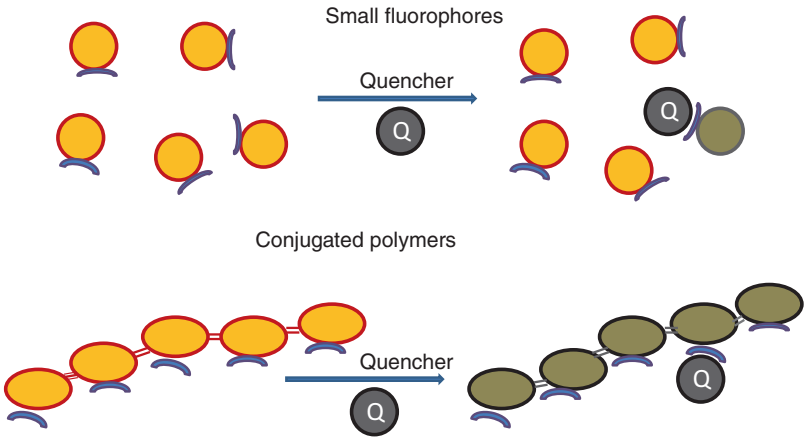

Fig. 5.11 Mechanism of superquenching in a conjugated polymer. Emitting species are *bright yellow* and quenched are *gray*. The interaction of quencher Q with a small fluorophore quenches only its emission. The same fluorophores when they are linked by conjugate polymer chain behave differently. Binding of single target molecule to a single recognition site on a chain switches off completely the fluorescence of the whole chain

(Thomas et al. 2007). Such effect appears when one element of such system binds a quencher with the result of quenching the fluorescence of the whole system, demonstrating a highly amplified response to the binding.

This effect is interesting. With the increase of chain length the fluorescence intensity becomes higher (and therefore the effect of any external quencher stronger) until certain limit is reached that is determined by the rate of *exciton migration* and its lifetime. With further increase of the chain length, the intensity does not grow and the quenching effect, if it exists, decreases. This means that *superquenching* effect stops at some particle size of polymer chain. Electron acceptors are commonly very strong fluorescence quenchers in these systems. Therefore, the presence of only one such group interacting with one element of polymer chain may quench fluorescence of the whole chain (or of its significant part if it is too long), as it is depicted in Fig. 5.11.

If a thin film is made of such polymer, one may observe a dark spot on the film, due to *exciton migration* both within and between the chains, which manifests the *superquenching*. In comparison with corresponding 'molecular excited states' that could be observed with uncoupled monomers a greater than million-fold amplification of the sensitivity to fluorescence quenching can be achieved. Such reaction is reversible if the polymer and the quencher are free to dissociate.

The emission of conjugated polymers depends on the *chain conformation*, which makes them very different from other brightly luminescent nanostructures discussed above. The changes in chain conformation from extended to bent or tilted one may change both absorption and fluorescence spectra. Planar conformation extends the chain conjugation and favors the high fluorescence quantum yield providing a broad dynamic range for realizing strong superquenching (Fig. 5.12). This property has

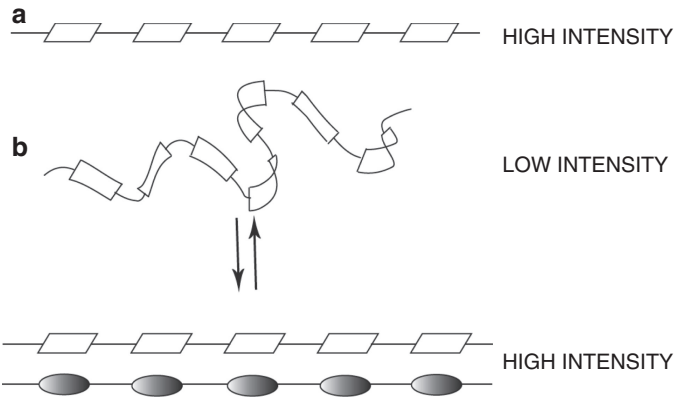

Fig. 5.12 Scheme illustrating the influence of conformation of conjugated polymer on its fluorescence. (**a**) Planar conformation. The extent of conjugation is high. Fluorescence intensity is high, so if the quenching exists it extends to significant length. The spectra may be shifted to longer wavelengths. (**b**) Non-planar conformation. The extent of conjugation is low and the emission can be to a significant extent localized. The intensity is expected to be low and the quenching effect localized. If a planar conformation is re-established in sensing event (e.g. by binding to DNA), then the high intensity can be restored

found application in homogeneous DNA assays in which extended conformation is achieved for cationic conjugated polymer on its electrostatic binding with DNA. More on these assays can be found in Sects. 8.5 and 12.4.

The change in chain conformation may produce also the shifts in emission wavelength. This is because the planar conformation favoring extended conjugation length allows achieving the strongest Stokes shift. The monomers in this conformation are more efficient excitation energy acceptors than the others and therefore they are the best emitters. Thus, when the energy is transferred to these sites, the spectrum shifts to longer wavelengths. When the planarity is destroyed as a result of conformation change, the spectra shift to shorter wavelengths.

5.3.2 Fluorescence Reporting in Sensor Design

There are many possibilities to use conjugated polymers in sensing. In all these cases, the greatly enhanced sensitivity of the polymer over the monomeric compound is due to facile energy migration along the polymer backbone that involves great number of monomeric elements. The first possibility is to combine the sensing effect with *superquenching*. The quencher could be the target itself, the competitor or a designed group in the sensor unit. In contrast to a sensor with monomeric fluorescence reporter, in which every site must be occupied for complete quenching, the polymer only needs to have a small fraction of target binding sites occupied to produce complete quenching (check Fig. 5.11). Such unique property made conjugated

polymers very popular among researchers that develop novel sensing techniques. The frequently used term '*superenhancement*' is in fact a '*super-dequenching*', since the polymer does not allow any additional enhancement over its natural emission. The strong increase in emission intensity is achieved simply by removal of quencher and allowing displaying the natural brightness.

The *aggregates* formed by non-covalent cross-linking show weak or quenched fluorescence, making them suitable fluorescent sensors for detecting signals that can influence the state of aggregation (Zhao and Schanze 2010). The other possibility that can be realized with the conjugated polymers is to modulate the *extent of conjugation*. In this case, the quencher can be present permanently. If the conjugation is high, its effect will extend over a large distance. Then the conformational change in polymer chain may reduce the conjugation, so that the quenching effect will be reduced with resulting fluorescence enhancement. Moreover, with the change in conjugation the color of fluorescence can change and this effect can be recorded in the form of ratiometric response.

There is a whole range of possibilities for introducing into the conjugated polymer structures of different functional elements. For instance, introduction of crown ester groups makes them potent ion sensors (Sect. 12.3) and of cationic groups – the DNA sensors (Sect. 12.4).

As an example of exploration of superquenching effect can be the conjugated polymer-based probes for proteases (Wosnick et al. 2005b). A set of carboxylate-functionalized poly(phenylene ethynylene) chains was synthesized, in which the carboxylic acid groups are separated from the polymer backbone by oligo(ethylene glycol) spacer units, which made the polymer water soluble. The carboxylate groups appended to each repeating unit allows covalent binding of peptides that are protease substrates. Attachment of strong fluorescence quencher dinitrophenyl group at the peptide terminal quenches the polymer emission. The presence of protease enzyme is detected by splitting the peptide leading to disconnecting the quencher and the subsequent fluorescence enhancement. If DNA or RNA being a target or when the recognition element changes its conformation, this can be detected by electrostatic binding of polycationic conjugated polymer.

5.3.3 Designed Conjugated Polymer Nanoparticles

There is a clear tendency in designing the nanoparticles made of conjugated polymers with compact structures stabilized by covalent linking or by hydrophobic interactions, *conjugated polymer dots* (Wu et al. 2010; Feng et al. 2013). The problem of water solubility and biocompatibility of conjugated polymers can be resolved by their encapsulation into organic polymer nanoparticles (Li and Liu 2014). The studies of *two-photonic* behavior of various conjugated polymers and nanoparticles have started recently with very promising results (Wu et al. 2007) showing good prospects for application in cellular studies.

Such nanoscale fluoprophores are prospective primarily for imaging and single-particle tracking. The data presented in Fig. 5.13 allows estimating their efficiency

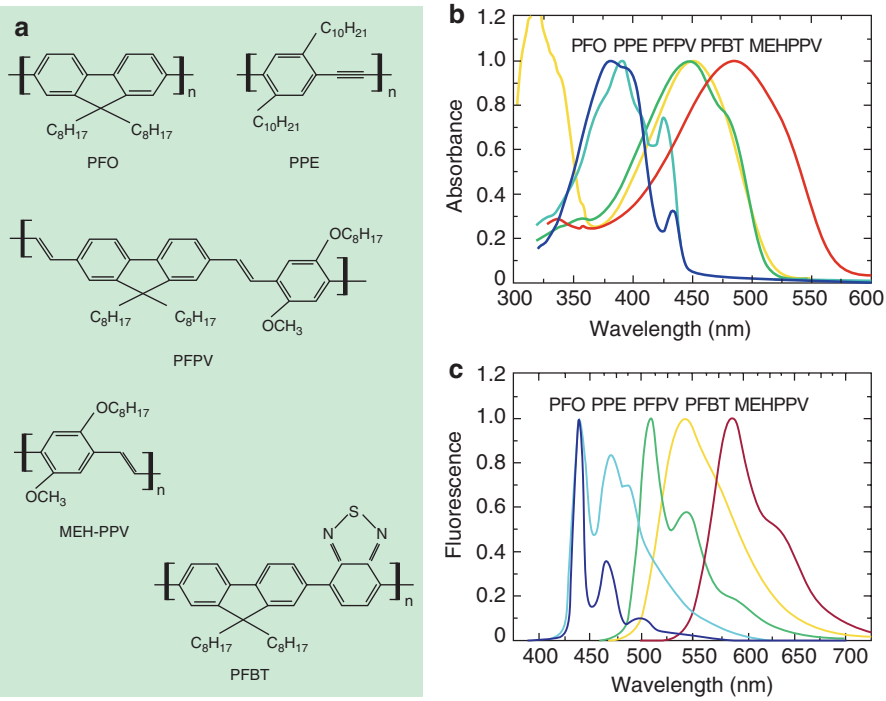

Fig. 5.13 The structures and properties of fluorescent conjugated polymer dots formed by injecting into water the THF solution of polymer (Wu et al. 2008). (**a**) Chemical composition. (**b**) Absorption spectra. (**c**) Fluorescence spectra

in comparison with other light emitters (Wu et al. 2008). Their light absorption and emission spectra are quite variable, occupying almost the whole visible range. They exhibit strongly variable quantum yields (1–40 %) and sub-picosecond lifetimes, but their benefit is very strong absorbance, by 1–2 orders of magnitude larger than of semiconductor quantum dots, which results in higher brightness under both one-photon and two-photon excitations with high photostability and the absence of blinking. The particle size does not influence the spectroscopic properties and no aggregation-induced quenching was observed.

5.3.4 Nanocomposites Based on Conjugated Polymers

Conjugated polymers allow realizing different signal transduction and reporting mechanisms being active participants in different supramolecular constructs. They endow these structures the ability to exhibit collective effect in PET and FRET quenching (see Chap. 7). A designed combination of this polymer with another partner serving as a quencher or FRET acceptor opens many interesting possibilities in sensing. One of them is a combination of conjugated polymer with *organic dye*.

The dye can be either directly attached to the polymer chain or co-incorporated into nanostructure with efficient collective effect in FRET. The latter is very efficient when it is directed from excited polyanionic conjugated polymer to a cationic cyanine dye (Tan et al. 2004).

Interesting is the possibility of combining different conjugated polymers in one unit. Their chemistry is well developed and involves the formation of not only the polymer films or latexes but also of well organized nanoparticles – *dendritic conjugated polymers* (Zhang and Feng 2007). Such encapsulation leads to new spectroscopic properties. A very small proportion of polymers that may serve as the FRET acceptors allows observing only their emission with excitation of the major component excited as the donor (Wu et al. 2006). These experiments demonstrated that fluorescence brightness of the blended polymer nanoparticles could be much higher than that of inorganic quantum dots and dye-loaded silica particles of similar dimensions. Different nano-scale support media such as silica can be used for assembly of polymer-coated particles (Wosnick et al. 2005a), in which different routes of reporter signal transduction can be activated.

An exceptional ability of *gold nanoparticles* to quench cationic conjugated polymer was demonstrated (Fan et al. 2003). During fabrication, these particles can be stabilized with citrate, so they can contain the negative charge. In the bound form, they produce the quenching effect so that one gold nanoparticle could 'superquench' several polymer chains.

A promising field of application of conjugated polymers is the sensing technology based on *thin films*, especially in gas sensing (Sect. 12.1) and development of artificial 'noses' and 'tongs' (Sect. 15.5). The proper polymer design allows avoiding the quenching in aggregates. For instance, poly(phenylene ethynylene)s with specially designed substitutions are highly emissive in aggregated forms due to formation of intermolecular excimers (Kim et al. 2005).

A series of non-aggregating carboxylate-functionalized poly(phenylene ethynylene)s have been synthesized for immobilization via electrostatic adsorption onto Eu^{3+}-polystyrene microspheres (Liao and Swager 2007). This system is shown to constitute a ratiometric system that measures fluorescence quenching with high fidelity.

5.3.5 Looking Ahead

Conjugated polymers are very interesting and prospective tools for designing fluorescence sensors. A key advantage of sensors utilizing these polymers over the devices using the elements composed of monomeric dyes is their potential to exhibit collective properties. These properties are sensitive to minor perturbations produced by occupation by the target of a very small number of binding sites. Their backbone itself can emit light and demonstrate high sensitivity to different perturbations. Due to conjugation of many fluorophores linked in chain, they provide the effect of superquenching. Its simplest application can be the introduction of external quencher

dye that allows sensing the binding of a target by coupling or decoupling of this dye with the polymer.

More complicated mechanisms of response involve the conformational change in a polymer producing a strong effect on its fluorescence. Due to these unique properties, the conjugated polymers demonstrate very promising tendency of development. Their implementation as reporters is expected to be very efficient, especially in the form of thin films and in the sensing of vapors. Their decoration with polar and charged groups increases dramatically the range of their applications, which is manifested by their successful application in DNA sensing.

5.4 Fluorescent Carbon Nanostructures

Discovery and investigation of unusual properties of nanoscale materials made of pure carbon were marked by two Nobel prizes. One was awarded for *fullerenes*, the structures in the form of hollow spheres. Later fullerenes found their use as scaffolds in designing fluorescence nanocomposites (Palma et al. 2009; Dmitruk et al. 2008) and electron-acceptor quenchers (Ito and D'Souza 2012). The other award was for *graphenes*, the two-dimensional sheets of atomic width (Huang et al. 2011) that became known as very potent fluorescence quenchers (Lu et al. 2009). The emission of their own nanoscale fragments has recently been found (Zhu et al. 2012). This property is also observed in *graphene oxides*. Meantime, there are other nanostructured materials attractive for nanosensor design. *Carbon nanotubes* exhibit emission in the near-IR, which is already used in sensing (Barone et al. 2005). Their short oxidized fragments are fluorescent in the visible range (Bottini et al. 2006).

Quite recently great interest was attracted to two new types of fluorescent carbon nanomaterials with bright and stable emission in the visible – *nanodiamonds* (NDs) (Schrand et al. 2009) and nanoparticles made of amorphous carbon – "*carbon dots*" (Baker and Baker 2010). They differ in arrangement of carbon atoms so that the mechanism of their emission must be different. Whereas the light emission from nanodiamonds occurs due to point defects in their *sp*3 hybridized carbon structures (Krueger 2008), carbon dots share many properties with other electron-rich carbon materials with *sp*2 hybridization, including the photocatalytic action (Li et al. 2010). Schematically these structures are presented in Fig. 5.14.

5.4.1 Fluorescent Nanodiamonds

The nano-sized crystals with strong potential for sensing and imaging applications are the *nanodiamonds*. On nanoscale, they represent the diamond form of carbon, which with the density of atoms of $1.76 \cdot 10^{23}$ cm^{-3} is the densest material on Earth. The *sp*3 hybridized carbon atoms are located in tetrahedron configuration at

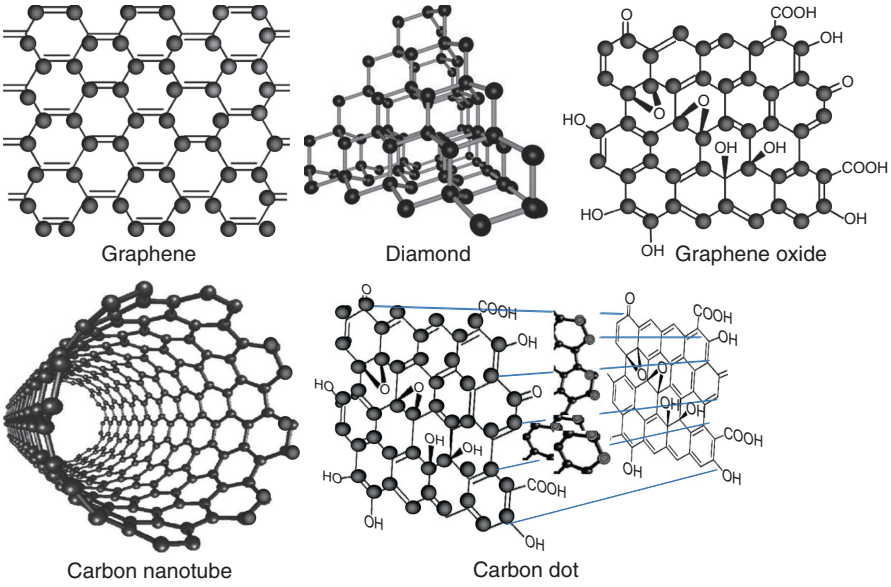

Fig. 5.14 The schematic structures of nanoscale carbon materials

distances of 1.54 Å and connected by high interaction energies of 83 kcal/mol. The nanoparticles are commonly obtained in large quantities on detonation of carbon-containing materials in the conditions of high temperatures and pressures.

Their *light emission* appears only after treatment by high-energy beams of protons or electrons that generate the so-called $(N\text{-}V)^-$ defects (Krueger 2008), see Fig. 5.15. Such centers are formed due to inclusion into their structure of atomic nitrogen on their formation (Schirhagl et al. 2014). Nanodiamonds absorb light at about 560 nm and emit at ~700 nm. Their molar absorbance is similar to that of

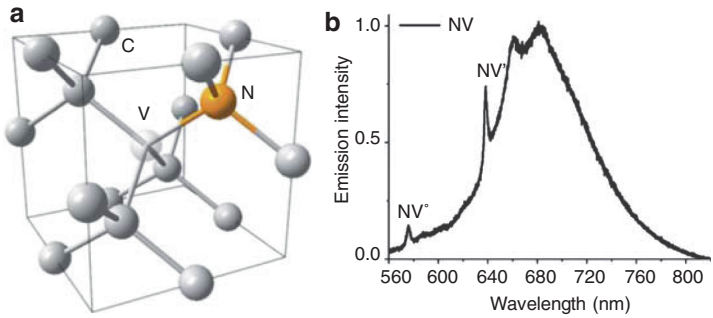

Fig. 5.15 Luminescent lattice defect in nanodiamond structure: (**a**) the structure of an N–V centre embedded in the diamond lattice; (**b**) luminescence spectrum of a diamond containing neutral $N–V^0$ and negatively charged $N–V^-$ centers. The zero phonon lines of both types are clearly distinguishable in the spectrum at 575 and 637 nm

organic dyes but quantum yield may reach almost 100 %. They exhibit relatively long lifetime, 10–20 ns (Beveratos et al. 2001).

There is no variation in absorption or emission bands between different particles, all of them demonstrate very strong Stokes shifts and relatively long lifetimes. These features determine the range of applications. In sensing and imaging, fluorescence can be excited at the same wavelength as many other emitters (e.g. organic dyes) but spectrally separated due to shorter emission wavelength of the latter. The lifetimes much longer than autofluorescence of living cells is beneficial for their microscopic studies (Kuo et al. 2013). Meantime, the efficiency in two-photonic excitation is rather poor.

Ultra-small size (4–10 nm) resulting to very high surface to volume ratio (300–400 m^2/g) and uncompensated valences on their surface result in high ability of nanodiamonds for sorption of different compounds and allows many possibilities for their functionalization. These particles are well tolerated by living cells. Being loaded with proteins, they can be used for cell labeling and targeting (Chang et al. 2013).

5.4.2 Graphene and Graphene Oxide Nanoparticles; Carbon Nanotubes

Graphene sheet is the two-dimensional elementary unit of graphite of atomic width. It can fold into balls forming fullerenes or into nanotubes that can be viewed as one-dimensional rods. In all these cases the *sp*2 hybridization of carbon atoms allows forming strong bonding with their in-plane neighbors allowing π-electrons to be delocalized over the whole structure. An extended graphene sheet with two-dimensional π-electronic network is electron conducting but unable to optical excitation and visible emission. These properties appear when the sheets are cut into small pieces and they start to resemble aromatic hydrocarbons (Yan et al. 2011). It has to be noted that the so-called graphene dots (G-dots) studied in experiment are often the nanoparticles composed of several small graphene sheets fused together forming ‘nano-graphite’. Some of the edge groups in G-dots are covalently modified with polar groups (commonly, hydroxyls and carboxyls) for induction of their solubility (Qu et al. 2012).

Graphene dots show very broad absorption bands in the UV region, around 230–280 nm, and a long tail extending into the visible range. However, their light emission spectra are puzzling. Commonly, the excitation at a very strong UV absorption band does not lead to fluorescence emission at all. In contrast, the major emission band in the visible is excited at the wavelengths 320–370 nm. It is at the far edge of absorption band, where the characteristic absorption that corresponds to this excitation band is very low (Fig. 5.16).

A variety of fluorescence colors can be observed in different preparations of G-dots with excitation at 320–400 nm. The dominant emission bands are in the *blue-green range*, and the dependence of emission spectra on excitation wavelength often demonstrates the presence of *intra-band heterogeneity* (see Fig. 5.16b). The origin of such spectral heterogeneity may result from structural variety of fluo-

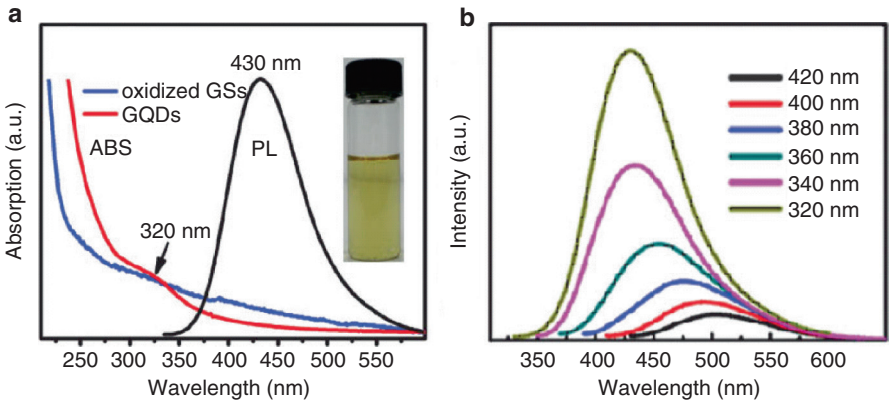

Fig. 5.16 Absorption (*ABS*, *red*) and photoluminescence (PL, at 320 nm excitation) spectra of the hydrothermally synthesized graphene dots and of their oxidized form dispersed in water (**a**) and their emission spectra at indicated excitation wavelengths (**b**) (Pan et al. 2009)

rescence emitters and of their in-particle interactions, so that their differently shifted excitation spectra form inhomogeneously broadened contour. The quantum yield of G-dots varies in broad ranges, and there is a common tendency of its increasing on passivation with organic ligands (Qu et al. 2012).

Nitrogen-doping and oxygen enrichment of the periphery of G-dot structures does not change the character of their light absorption and emission (Li et al. 2012). In all these cases fluorescence is observed only on the excitation in the near-UV-VIS (where the light absorption is very low) and remains absent or is very weak when it is excited in the range of the strongest UV light absorption.

Graphene oxides differ from graphenes by the presence of oxygen-containing groups not only at the sheet edges but also within the sheet planes (see Fig. 5.14). When graphene oxide nanoparticles (GO-dots) are synthesized through chemical processing of graphite, they contain a number of such groups, including epoxy, hydroxyl, and carboxyl. If these groups are located on the basal plane, they disrupt the extended regular conjugation, which leads to the presence of isolated *sp*2 domains (He et al. 1998). These insertions can be the sites of various chemical modifications (Qu et al. 2012).

The spectroscopic properties of GO-dots are similar to that of G-dots (Cao et al. 2012). When excited in the same 320–370 nm region they emit violet, blue or green light. Like for G-dots and their other derivatives, the far-UV excited emission is totally or almost totally quenched.

Deformation of conjugated π-electronic graphene structure in *carbon nanotubes* results in an ability for light absorption and fluorescence emission in the near-IR region (Barone et al. 2004), which can be strongly quenched in if the nanotubes are aggregated. Many studies addressing the functionalization of nanotubes noticed the appearance of strong blue-green fluorescence that was attributed to formation of graphene dots during this treatment (Minati et al. 2012).

5.4.3 Carbon Dots

Fluorescent *carbon dots* (C-dots) are versatile and less defined nanocarbon materials that share similar properties with G-dots and GO-dots that were discussed above. They attracted many researchers just because of their simple syntheses achievable by many approaches from a variety of starting organic materials (Esteves da Silva and Gonçalves 2011). On the steps of their synthesis the obtained particles may incorporate hydroxyls, carbonyls and carboxy groups that become exposed in the formed nanostructures. Importantly, the one-step synthesis allows locating on their surface in addition to carboxylic groups (which is common), the reactive amino groups, and this strongly facilitates their functionalization (Dong et al. 2012b).

The C-dots obtained from different sources and by different methods share similar *elements of structure*, such as graphene-type *sp*2 with the participation of relatively high amount of the diamond-type *sp*3 hybridization (or disorder) of carbon atoms. This suggests that the π-electronic conjugation must exist along the graphene sheets, but this conjugation may be irregular, especially in view of the presence of hydroxyl and carbonyl groups (Yang et al. 2011). Based on these data, the C-dot can be viewed as a highly defected composition of coexisting aromatic and aliphatic regions, the elementary constituents of which are graphene, graphene oxide and diamond that are assembled in proportions and with variations of surface groups that depend on the conditions of their synthesis.

Regarding *optical properties*, the absorption and emission spectra of C-dots obtained by various methods and in different labs are remarkably similar and strongly resemble that observed for other species of nanocarbon family (G-dots and GO-dots). Their fluorescence emission is concentrated in the blue and green ranges of spectra and the positions of their band maxima depend on excitation wavelength, which demonstrates structural heterogeneity (see Fig. 5.16). Carbon dots exhibit nanosecond lifetimes and high two-photonic cross-sections (Baker and Baker 2010). Their quantum yields were already reported on a relatively high level of 30–40 % (Zhai et al. 2012; Dong et al. 2012b).

5.4.4 Origin of Fluorescence of Nanocarbon Materials

The origin of fluorescence-type emission of carbon nanomaterials (G-dots, GO-dots, C-dots) is not well understood and is actively disputed. There are several reasons for that. The major one is the absence of clear analogy in behavior with any other molecular or nanoscale luminophores. Like organic dyes the carbon particles possess well resolved excitation and emission spectra, but the UV excitation that should provide the same visible emission (according to Kasha rule) in reality is quenched (Fig. 5.17). This suggests in each particle the two types of light absorbers (UV and near-UV-VIS) and one type of emitters excited in the near-UV-VIS. This fact does not support excitonic origin of electronic transitions that is present in semiconductor

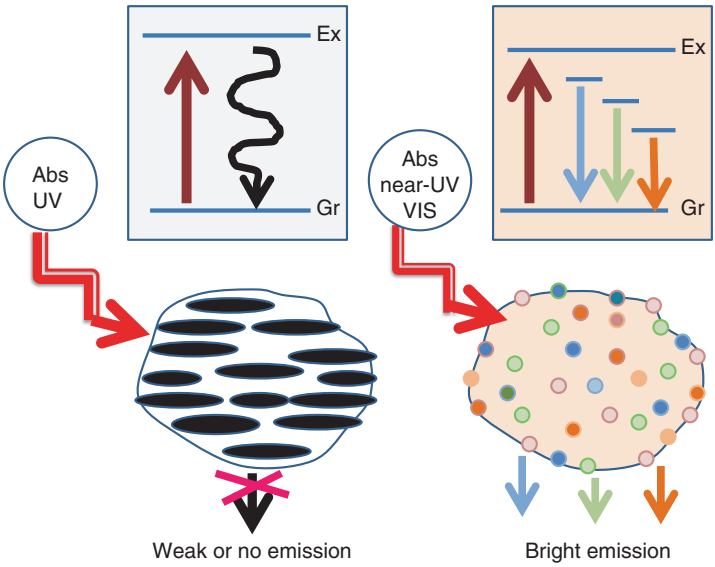

Fig. 5.17 Two types of light absorbers present in fluorescent carbon nanomaterials (Demchenko and Dekaliuk 2013). Those possessing strong absorbance in the UV demonstrate dramatic quenching (*left*). Those possessing very low absorbance in the near-UV and visible range show very bright and often multicolor emission (*right*)

nanoparticles (quantum dots). As we will see in the next Section, their excitation can be provided throughout the whole UV region, which is not our case. Another difference is the absence of strong correlation of spectral position and particle size, which in quantum dots is strictly observed due to quantum confinement effect. If, on the other hand, the carbon particles are assemblies of organic-dye-type fluorophores, why they quench so strongly emission of external fluorophores without affecting their own emission?

Different types of experiments add new mysteries. High optical anisotropy was discovered for C-dots with its strong non-exponentiality and decay on a scale of nanosecond and a strong yes-or-no quenching of emission by iodine ion (Dekaliuk et al. 2014). Analysis of intra-band heterogeneity witnesses for the absence in each particle of ensemble of fluorophores that being in close proximity should exchange energies via FRET.

So are carbon nanoparticles individual emitters? Recent experiments on a single particle level demonstrate that so it is (Ghosh et al. 2014). The studied C-dots demonstrate the ON-OFF blinking as the transitions between two states, without any intermediates. They show optical anisotropy and the behavior of single dipoles. Moreover, individually they demonstrate much narrower emission spectra and single-exponential lifetimes that are distributed within the population of particles. Concurrence with the results obtained earlier suggests that we deal with some strong collective effect mediated via particle surface.

5.4.5 *Carbon Nanoparticles as Universal Quenchers*

All carbon nanoscale materials strongly quench fluorescence of organic dyes. This suggests different applications based on sorption-desorption of labeled analytes or competitors on their surface. Such quenching effects are essentially different from that of organic quenchers because of the absence or low level of spectral selectivity and of short range of quenching effect requiring adsorption of the partner in sensor technology on the particle surface. Fullerenes, graphenes and carbon nanotubes are known as strong electron acceptors, therefore the major mechanism of quenching is the *photoinduced electron transfer* (PET) (Wróbel and Graja 2011; Zhang and Xi 2011). This explains the absence of spectral sensitivity in quenching and allows calling carbon nanomaterials the *universal quenchers*.

An example presented in Fig. 5.18 demonstrates the ability of carbon nanotubes to sense specific DNA sequences by hybridization with sensor DNA sequence labeled with fluorescent dye (Zhu et al. 2010). The latter can be adsorbed on nanotube surface, and its fluorescence is quenched. Upon hybridization, the formed

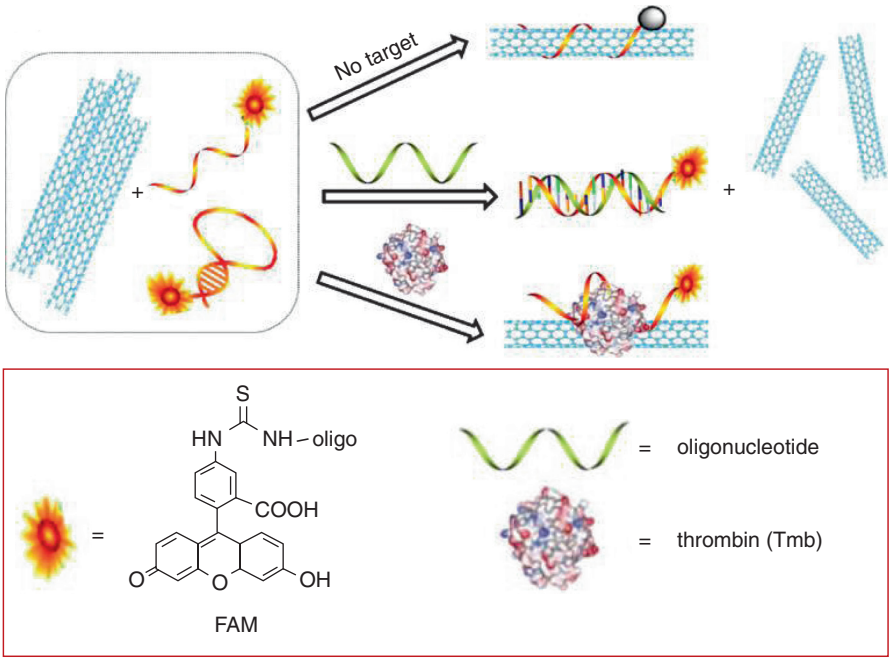

Fig. 5.18 Scheme for signaling biomolecular interactions using an assembly between carbon nanotube and dye-labeled ssDNA or thrombin-binding aptamer (Zhu et al. 2010). In the bound form fluorescence is quenched, but formation of complex with the target results in desorption of molecular sensor and its fluorescence is restored

dsDNA segment dissociates with restored fluorescence signal. In a similar way, the DNA aptamer reacting with protein target can be used. Its fluorescence is quenched when it binds to nanotube, but it is enhanced on specific interaction with the target.

Similar techniques for targeting specific nucleic acids and proteins were developed with the use of graphene particles and carbon dots. They can be extended to recognize a broad range of targets from metal ions to organic molecules, macromolecules, and even live cells. Functionalization of the surface of nanoparticles allows providing their noncovalent assembly with molecular sensors or competitors labeled with fluorescent dyes (Bartelmess et al. 2015). If the quenching ability is not desirable, surface coating with polymer or protein can provide preventive effect.

5.4.6 Applications in Fluorescence Reporting and Imaging

The most attractive range of applications of carbonic fluorophores is summarized in Table 5.2. The properties of strong absorbers of UV light, efficient quenchers of fluorescence of other emitters and their own emission abilities can be explored and efficiently combined in different sensor designs.

Carbon nanoparticles have started to be applied in different immunoassay formats, particularly in lateral flow and microarray immunoassay tests (Posthuma-Trumpie et al. 2012). It was claimed that they provide a less expensive but more sensitive and stable alternative to other commonly applied labels. Fluorescent C-dots can be used for protein staining after their separation in gel electrophoresis with the advantage of higher sensitivity over convenient staining with organic dyes (Na et al. 2013). Rapid detection of bacteria in sewage water may be achieved with fluorescent C-dots (Mandal and Parvin 2011). They are easily conjugated with bacterial cell membrane and allow counting the number of these cells.

Several examples presented below allow illustrating the use of fluorescence emission for chemical sensing in very simple constructions. It was shown that reversible binding of mercury ion results in dramatic fluorescence quenching in

Table 5.2 Basic characteristic features of fluorescent carbonic nanostructures and their applications (Demchenko and Dekaliuk 2013)

Property	Application
Very strong absorbance in the far to middle UV range	UV-selective light protection, systems for optical limiting
Strong fluorescence quenching of organic dyes and other fluorophores	Sensing response by modulation of fluorophore-quencher interaction
Strong intrinsic visible fluorescence emission	Labeling macromolecules and fluorescence imaging, photon correlation spectroscopy and single particle tracking
Quenching of intrinsic visible fluorescence	Detection of inorganic analytes (e.g. Cu and Hg ions) and biodetection
Operation as donor or acceptor in FRET	Biosensing technologies

unmodified G-dots and this effect was suggested for determining mercury in test media (Chakraborti et al. 2013). Since these ions exhibit stronger affinity to thiols, the substituting of the bound mercury ion restoring the fluorescence was applied for determining biothiols (Zhou et al. 2012b). In a similar way, extraction of bound lanthanide ion was applied for determining inorganic phosphate (Zhao et al. 2011).

More complicated detection systems can be designed. A complex of carbon dot with lysine and bovine serum albumin was used for selective determination of Cu^{2+} ions (Liu et al. 2012b). In another work these ions were determined by fluorescence quenching of C-dots decorated with polyamine polymer (Dong et al. 2012a). Of course, Cu^{2+} ions are known as the strong fluorescence quenchers operating by electron transfer mechanism, and this approach is hard to expand for detecting other analytes. Therefore, functional nanocomposites with distributed target binding, signal transduction and fluorescence emission have to be constructed.

As an example, the aptamer-functionalized C-Dots was constructed as a sensory platform for protein detection. The presence of target protein induces the aptamer-modified fluorescent C-dots to form a non-fluorescent sandwich structure with aptamer-functionalized silica nanoparticles through specific protein-aptamer interaction. This assay when realized for sensing thrombin shows high specificity (Xu et al. 2012). Another approach for the detection of thrombin in human plasma (Wang et al. 2011) is based on target-induced disruption of resonance energy transfer from upconverting phosphor to linked GO-dot. This strategy may offer a suitable approach for detection of other proteins in biological, pharmaceutical and nanomechanical applications.

Fluorescent nanocarbon materials have found many applications in cellular imaging. Being decorated with different functionalities they can enter cells, produce informative image by their distribution and report about particular interactions in the studied systems in the form of fluorescent emission (Sun et al. 2013). Here their attractive features, such as biocompatibility, excellent chemical and colloidal stability together with high brightness and resistance to photobleaching can be explored. Their weak points are the limited spectral range of their emission mostly in the ‘blue’ and ‘green’ regions, where the autofluorescence in living cells is significant.

With the advantage of low toxicity and competing in brightness with semiconductor quantum dots, the carbon nanomaterials can be successfully used for *in vivo* applications, which is witnessed by numerous results obtained on animal models (Sun et al. 2013; Liu et al. 2012a). They are attractive candidates for construction of multimodal nanocomposites possessing also the drug delivery function.

5.5 Semiconductor Quantum Dots

The term quantum dots (QDs) is commonly applied to semiconductor nanocrystals that possess unique ability of efficient absorption and emission of light in the visible range of spectra. They are emerging as a special class of fluorescent reporters with the properties and applications that are not available with traditional organic dyes or

nanocomposite structures doped with them (Sapsford et al. 2006; Costa-Fernandez et al. 2006; Grecco et al. 2004). They demonstrate very high brightness, narrow emission bands and possibility of modulating the colour of their emission just by the change of particle size within the same type of material.

Their novel features have opened new possibilities in many areas including ultrasensitive chemical analysis and cellular imaging (Jin and Hildebrandt 2012). They have started to replace traditional organic fluorophores to serve as simple fluorescent reporters in immunoassays, microarrays, fluorescent imaging applications, and other assay platforms. As a part of nanocomposites, they are in the heart of diverse technologies, from barcoding systems in suspension arrays and multiplexed identification of infectious pathogens to tracking of intracellular drug and gene delivery (Zhang and Wang 2012; Chen et al. 2012).

5.5.1 The Composition of Quantum Dots

Fluorescent quantum dots can be made of many *semiconductor materials* (CdS, CdSe, CdTe, ZnS, PbS), and their spectral properties depend on their composition. Within every type of these materials the dependence of spectral properties on particle size can be very strong (see below). These particles can be as small as 2–10 nm, corresponding to 10–50 atoms in diameter and in total 100–100,000 atoms within the QD volume. This is roughly the size of a typical globular protein. It has to be accounted, however, that for improving the brightness, solubility and functionality, additional layers are imposed on particle surface, which provides further increase in size (Sapsford et al. 2006).

Many quantum dots are the composites made of narrow dispersed highly crystalline CdSe core coated with a shell of a few atomic layers of a material with a larger band gap, such as ZnS and CdS, on top of the nanocrystal core (Fig. 5.19). Such

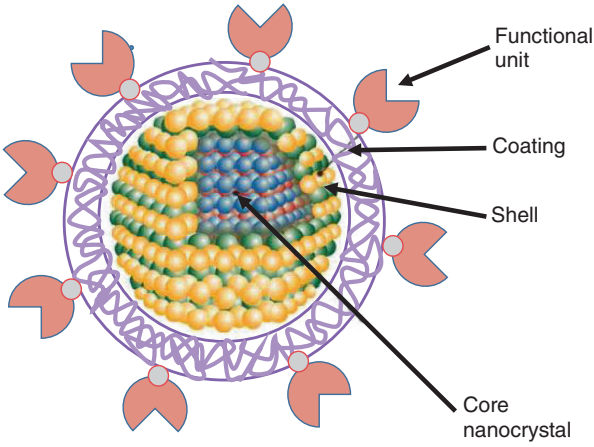

Fig. 5.19 Schematic of the overall structure of a quantum dot nanocrystal conjugate. The layers represent the distinct structural elements; they are drawn roughly to scale

constructions are beneficial because the surface defects in the crystal structure act as temporary "traps" for the electron or hole, preventing their radiative recombination and thus reducing the quantum yield. The shell also protects surface atoms from oxidation and other chemical reactions. With the proper shell design, it becomes possible to obtain photoluminescence quantum yields close to 90 % and to increase photostability by several orders of magnitude relative to conventional dyes.

5.5.2 The Origin of Quantum Dots Emission

The photophysical behavior of these nano-sized semiconductor particles is quite different from that of fluorescence emitters of organic origin. The light absorption of QDs occurs due to transition of a single electron from the valence band to the conduction band generating *localized excitons* (the bound pairs of conduction band electrons and valence band holes), so that the emission is the result of electron-hole recombination. Here the excitons are different from the Frenkel excitons observed in complexes of organic molecules and conjugated polymers by possessing high *electron affinity*. The quantized energy levels here appear because the wave function of the exciton is confined in all three spatial dimensions.

The separation between quantized ground-state and excited-state energy levels and therefore the positions of absorption and emission bands are determined by the *sizes* of QDs. The smaller they are, the fewer energy levels can be occupied by electrons and the greater is the distance between individual levels. Therefore, the decrease in particle size results in blue shifts of their emission. Such strong size dependence allows fine-tuning the QD emission wavelength in the desired range over almost the entire visible spectrum extending into near-IR.

5.5.3 The Spectroscopic Properties

The properties of semiconductor quantum dots are summarized in Table 5.3. Comparison with similar data presented for organic dyes in Table 4.1 shows that the QD features are really unique. Their *absorption spectra* are extremely broad extending from long-wavelength band far into UV region with a gradual increase of absorbance, whereas their fluorescence spectra are amazingly narrow (Fig. 5.20).

This property allows exciting fluorescence at any shorter wavelengths that are far aside from emission band and thus avoid light-scattering problems. This also suggests their efficient use as FRET donors to various acceptors with the possibility of selecting the wavelength, at which the excitation of the acceptor does not occur. Attractive is also the possibility to use for excitation the low-cost UV lamp with broad-band filter or a cheap 405 nm diode laser. With a single light source, the QDs emitting at different wavelengths throughout the entire visible range of spectrum can be excited. This allows multicolour detection of several targets.

Table 5.3 The properties of quantum dots used in sensing and imaging technologies

Parameter	Property
Size	~2–10 nm (core), much larger with cover shells
Absorption spectra	Extremely broad, extending from the first long-wavelength band continuously to the UV
Molar (particle) absorbance, ε	Very high, up to 10^7 M^{-1} cm^{-1}
Emission spectra	Narrow (~25–30 nm half-width) and symmetric, without red-side tailing
Tunability of emission spectra	Size-dependent, available in a broad range from UV to IR
Stokes shifts	Small, ~15 nm from absorption onset
Excited-state lifetime, τ_F	Usually longer than that of organic dyes, ~10–20 ns
Photoluminescence quantum yield, Φ	Variable, strongly depends on surface coating, can be ~90 %
Photostability	Excellent
Chemical resistance	Excellent
Availability of chemical modification/ functionalization	Rather poor
Cell toxicity	Disputable, insufficiently studied
Two-photonic cross-section, α	High, ~10,000 GM

The *emission spectrum* can be engineered by controlling the QD geometrical size, shape, and the strength of the confinement potential. The larger is the particle, the smaller is the energy gap between the lowest excited and the ground states and the redder (the more towards the long-wavelength end of the spectrum) is the fluorescence. Conversely, the smaller the quantum dot, the bluer (the more towards the short-wavelength end) it is (see Fig. 5.20).

Depending on the size, the core-shell CdSe-ZnS particles can change their *emission wavelength* from 480 nm (2 nm in diameter) to 660 nm (with diameter 8 nm). Correspondingly, for the redder emitting CdTe-CdSe QDs the variation of emission wavelengths is from 650 nm (4 nm diameter) to 850 nm (diameter 8 nm) (Medintz et al. 2005). The shift in emission spectra is accompanied by corresponding shift of absorption band origin, so that the relatively small Stokes shift remains approximately constant. The size-dependent fluorescence wavelength tunability allows obtaining the species with different emission colors.

Because the electronic transitions are not coupled with atomic vibrations (in contrast to organic dyes), the emission spectra of quantum dots are *symmetric* and with the width of 20–30 nm they are *narrow*, much narrower than that of organic dyes. This property together with wavelength tunability is attractive for multiple labeling and can be realized in multiplex formats.

Quantum dots exhibit *excellent brightness* due to high molar absorbance (reaching the values of several millions) and high quantum yields, typically of 20–70 %, depending on surface coating. Such brightness cannot be easily achieved with organic dyes even with their high-density coupling with synthetic polymers

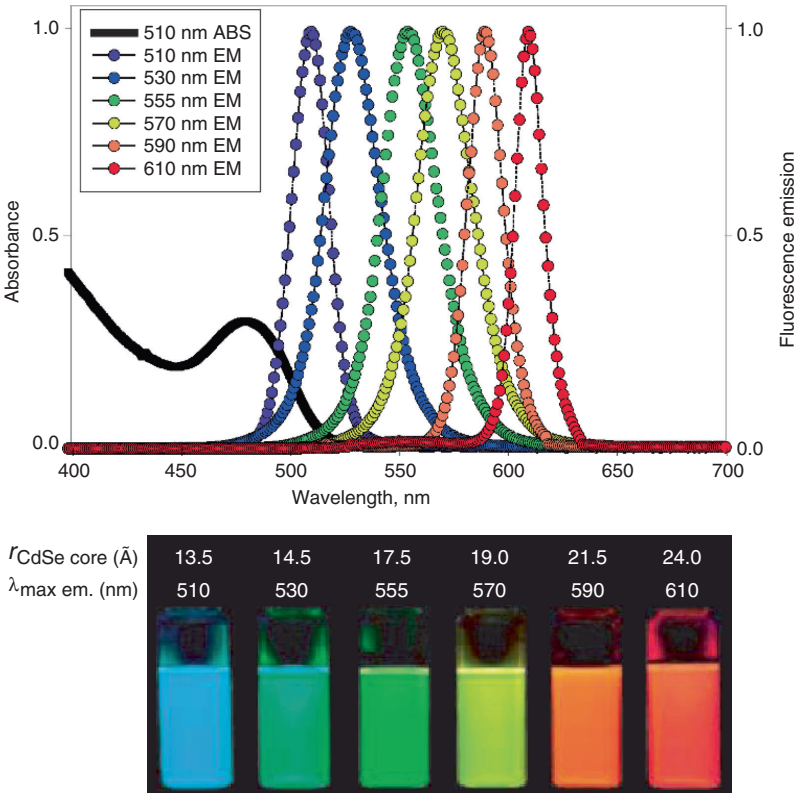

Fig. 5.20 Absorption and emission of six CdSe quantum dot dispersions differing in size (Medintz et al. 2005). The *black line* shows the absorption of the 510-nm emitting QDs. *Below*: photo demonstrating the size-tunable fluorescence properties and spectral range of the six QD dispersions possessing these spectra versus CdSe core size. All samples were excited at 365 nm with a UV source. For the 610-nm-emitting QDs, this translates into a Stokes shift of ~250 nm

and proteins or their sorption on nanoparticles. This is because of concentration-quenching effects observed in common dyes (as discussed above). In QDs these effects are absent. Excellent chemical stability and photostability are also their characteristic features.

Regarding fluorescence at *two-photon excitation*, QDs are dramatically superior to organic dyes (Rayno and Yildiz 2007), which makes them very prospective for cellular imaging or even imaging of the whole tissues using near-infrared excitation. Meantime, their cyto-toxicity is not studied in sufficient detail (Shiohara et al. 2004), it will definitely depend upon the properties of covering shells.

The negative feature of QDs is their *blinking* (the rapid switching between their emissive and non-emissive states), which reduces their applicability in single-particle imaging.

5.5.4 Stabilization and Functionalization of Quantum Dots

Naked QDs with their hydrophobic surfaces are insoluble in water and in other highly polar solvents. Their surface is not amenable for easy conjugation with functional groups needed for molecular sensing. Therefore, many efforts are being made for modifying this surface for making it friendlier to synthetic chemist (Dubois et al. 2007). There are several methods currently applied for QDs stabilization and functionalization (Sapsford et al. 2006):

(a) The use of surface *covalent modification chemistry* to generate $–NH_2$, -SH and –COOH groups on the particle surface that could be further modified to provide attachment of target recognition molecules. This method is the most commonly used for attachment of different recognition units, such as DNA or antibodies.
(b) The use of *coordination chemistry* that may allow with the exposed ZnS shell the interaction of Zn atom with polyhistidines and of sulphur atoms with thiols. For this purpose, the peptides containing His and Cys residues can be used. They can be further modified by attaching molecules with specific function.
(c) Finally, the *electrostatic interactions* with oppositely charged polymer molecules can form the surface layer around the particle. Alternatively, the amphiphilic polymers can be used, which will screen hydrophobic QD surface and expose polar groups to the solvent. A simple method for the preparation of CdSe-ZnS quantum dots that are highly fluorescent and stable in aqueous solution was reported using calix[4]arene carboxylic acids as the surface coating agents (Jin et al. 2006).

These principles are explored in various types of bioconjugation of quantum dots that are necessary for their efficient use in biosensor technologies (Fig. 5.21). They include designed biomolecules, particularly, peptides. Their use for coating the QDs can combine all these approaches since it allows realizing all types of interactions with the core particles plus using exposed reactive groups for additional functionalization (Iyer et al. 2006). Peptides have the advantage of being easily customized and can yield all necessary functions: (a) Protect the core/shell structure and maintain the original QD photophysics, (b) solubilize QDs, (c) provide a biological interface, and (d) allow the incorporation of multiple functions (Sapsford et al. 2006). A number of self-assembled QD-peptide conjugates were suggested for selective intracellular delivery (Delehanty et al. 2006).

Formation of lipid monolayer as capping functionality can also be made for intracellular imaging and intracellular detection of nucleic acids (Dubertret et al. 2002). Thus, the aim to get the QD particles coated in such a way that would allow application of common organic chemistry to make these particles functional is achievable and can be reached in different ways.

A relatively large size of quantum dots is commonly not a problem in application in different sensing technologies. Each QD particle may carry several recognition units represented by DNA or proteins (Medintz et al. 2004). They can be integrated into microfluidic cells and other integrated devices (Sapsford et al. 2004).

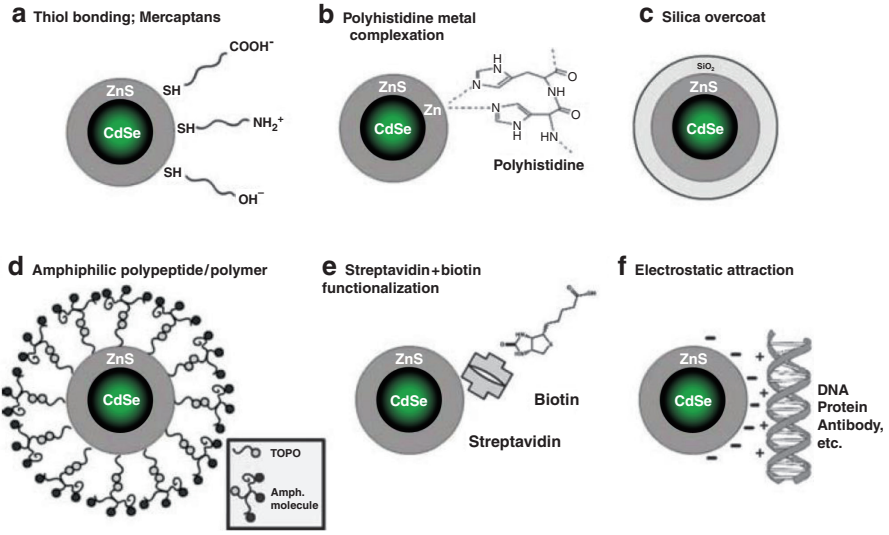

Fig. 5.21 Methods of conjugation of biomolecules to quantum dots (Goicoechea et al. 2009). (**a**) The thiol bound formation between S atoms on the QD surface and S atoms in molecules terminated with carboxylic acid, amine, or hydroxyl groups. (**b**) The formation of a complex between a Zn atom on the QD surface and polyhistidine residues by metal-affinity coordination. (**c**) The utilization of a silica overcoat which makes possible the utilization of conventional silanization techniques to functionalize the QDs. (**d**) The utilization of native TOPO ligands to functionalize the QDs using amphiphilic molecules. (**e**) The functionalization of QDs using the streptavidin-biotin affinity. (**f**) Electrostatic interactions between QDs surfaces and oppositely charged biomolecules

5.5.5 Applications of Quantum Dots in Sensing

On the first steps of their application, the QD conjugates have started to be used as simple replacements for conventional dye labels in the cases when their unique performance characteristics allow achieving better results. Their high brightness helps lowering the limit of detection when they are used as sensor reporters. The large surface areas allow simultaneous conjugation of a number of biomolecules to a single QD particle. Advantages conferred by this approach are obvious. One may achieve increased avidity for targets due to multipoint binding, the potential for obtaining cooperative binding and the possibility of simultaneous recognition of several targets. The development of *multi-colour multi-analyte assays* with a simple single-wavelength excitation based on QDs with essentially the same composition was realized. A number of "*multiplexed*" assays based on this principle were suggested for DNA and RNA hybridization (Shepard 2006; Liang et al. 2005).

Such traditional trend can be seen in technologies that involve detection by *antibodies*. The streptavidin-coated QDs can be used by their incorporation into a generic three-layer sandwich approach using (a) an antibody against a specific target, (b) a biotinylated secondary antibody, and (c) a streptavidin-coated QD labelling this

secondary antibody (Goldman et al. 2006). The same approach can be used with the ligand-binding proteins, etc. This type of application is quite similar to that of 'nonresponsive' dyes (see Sect. 4.2). The fluorescent particles play a passive role, in which their presence in the system is detected only. This cannot satisfy the researchers that try to find possibilities to make QDs directly sensitive to intermolecular interactions.

The problem here is an insignificant knowledge of QD properties that are not studied in such detail as that of organic dyes. Still little is known on the variation of different parameters of their emission in response to different kind of intermolecular interactions that can be realized in view of various possibilities of forming their surface shells. Meantime, some fragmental research in this direction shows promise. Thus, it was reported (Algar and Krull 2007) that the spectroscopic properties of CdSe/ZnS core-shell QDs change dramatically in a *pH-dependent* manner when linear thioalkyl acids of variable chain lengths are used as capping ligands. The variation of luminescence of thioalkyl acid capped QDs is a complex function of dielectric constant and electrostatic or hole-acceptor interactions with ionized ligands. These effects have to be further explored.

Sensing the target binding and the response in the change of QD emission intensity can be connected by *photoinduced electron transfer* (PET) mechanism (see Sect. 8.2), and the sensor for fatty acids was suggested as a proof-of-principle for this approach (Aryal and Benson 2006). The electron donor is a ruthenium complex, and the electron transfer occurs through fatty acid binding protein serving as recognition unit, so the binding results in quenching.

Attachment to CdSe-ZnS core-shell QDs of strongly electron-donor indolyl group resulted in dramatic *quenching* of their fluorescence (Raymo and Tomasulo 2006). Via some conformational change this effect can be coupled with the target binding by the proper recognition unit. One of the promising possibilities for inducing in this way the QD reporting function has been suggested (Yiidiz et al. 2006). It is based on the electrostatic adsorption of cationic quenchers on the surface of anionic quantum dots. The adsorbed quenchers suppress efficiently the emission of QDs due to the presence of photoinduced electron transfer. Based on this mechanism a reporting signal could be generated indicating receptor-target interactions. The QD emission is restored in the presence of target receptors able to bind the quenchers and prevent the electron transfer.

Quantum dots have started to be actively used in *sensing technologies* based on FRET to external agent that provides or mediates the sensor response acting as FRET partner adsorbed or covalently attached to semiconductor particle. Signalling may be obtained by detecting directly the luminescence from QD and/or from the conjugate (Somers et al. 2007). The approach based on QD donor and dye acceptor has found many applications: in DNA and RNA hybridization assays, in immunoassays, in the construction of biosensors based on ligand-binding proteins and enzymes.

The *donor-acceptor pairs for FRET* can be easily selected from QDs of different sizes and from the series of dyes possessing gradual variations of their fluorescence spectra, such as Alexa Fluor dyes. The choice between QDs emitting at 565, 605, and 655 nm as the energy donors and these dyes with absorbance maxima at 594,

633, 647, and 680 nm as the energy acceptors provides a lot of possibilities for selection of optimal donor-acceptor pairs (Nikiforov and Beechem 2006). This allows composing the systems for different homogeneous assays based on the formation of complexes avidin-biotin and antigen-antibody. Competitive binding assays are efficient in such systems.

Quantum dots are also prospective for applications in *immunoassays*. As the examples, the cancer cell marker protein her2 (Huang et al. 2007), diphtheria toxin and tetanus toxin have been detected successfully using QD-labeled antibodies (Hoshino et al. 2005). Usually QDs are conjugated with sensor molecules and organic dyes and are used either for the target labeling or for the labeling of target analog in a competitor displacement assay.

An example of advanced QD-based *immunosensor* could be the technique for detecting explosive 2,4,6-trinitrotoluene (TNT) in aqueous media (Goldman et al. 2005). The hybrid sensor consists of anti-TNT specific antibody fragments attached to a hydrophilic QD via metal-affinity coordination. A dye-labelled TNT analogue pre-bound at the antibody binding site quenches the QD photoluminescence via proximity-induced FRET. Analysis of the data collected at increasing the dye-labelled analogue to QD ratios provided an insight into understanding how the antibody fragments self-assemble on the QD. A soluble TNT present in the test system displaces the dye-labelled analogue, eliminating FRET and resulting in a concentration-dependent recovery of QD photoluminescence (Fig. 5.22).

Due to very high brightness, the QDs are ideal for *imaging*, and the limitation here is their relatively large size, which with the coating may reach 50–60 nm.

The peculiarities of quantum dots as the components of hybrid composite structures that dramatically improve the properties of fluorescence reporters are discussed in Sect. 6.3. Due to their very high brightness but very broad excitation band their most efficient application is as FRET donors with much lesser prospects as acceptors. However, their used as acceptors in compositions with long-lifetime donors are very beneficial in time-gated assays.

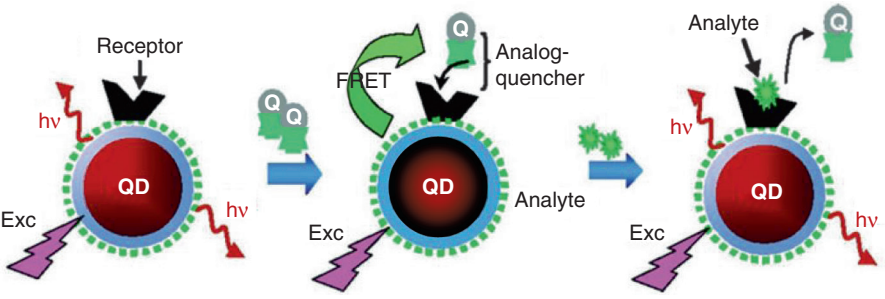

Fig. 5.22 Schematic illustration of a QD-based FRET competition assay for 2,4,6-trinitrotoluene (TNT) detection that uses attached specific antibody for TNT recognition (Goldman et al. 2005). The conjugate of TNT analogue with the quencher dye is used as the competitor. The competitor displacement removes the FRET quenching and thus produces the fluorescence response signal

5.5.6 *Magic-Sized Quantum Dots*

A special type of semiconductor nanoparticles are the particles with a specific number of atoms, the so-called *magic-sized nanoclusters*. They were identified in the mass spectra for a number of compounds, for example, $(CdSe)_{13}$, $(CdSe)_{19}$, $(CdSe)_{33}$, $(CdSe)_{34}$, $(CdSe)_{48}$. Such CdSe species were synthesized in macroscopic quantities in colloidal solutions in toluene (Kasuya et al. 2004a) and water (Park et al. 2010). Presumably, these "magic" clusters have a special structure containing strictly fixed number of atoms in the form of nested fullerene-like shells (Fig. 5.23), which explains their selective stability. Accordingly, due to the absence of broadening caused by size distribution, a structure with certain number of atoms leads to a narrow peak in the exciton absorption spectrum. In the luminescence spectra the exciton peak is also narrow, but it is always accompanied by broad long-wavelength band. The quantum yield of luminescence of synthesized to date samples is small (10 % and less), perhaps this is due to the imperfection of the surface coating of nanoparticles with surfactant.

The developed approaches for synthesis of these structures are relatively simple and highly reproducible. They can serve the basis for designing nanocomposites with two-component independent emissions. In these cases, if they are covalently fused with the dyes possessing large Stokes shifts, due to their own small Stokes shifts, there is no excited-state energy transfer between these emitters. Therefore being excited at the same wavelength, they emit independently. Such possibility was realized with 3-hydroxychromone dye (Peng et al. 2011). Combination of particles and dyes in different ratios, it became possible obtaining emission of different

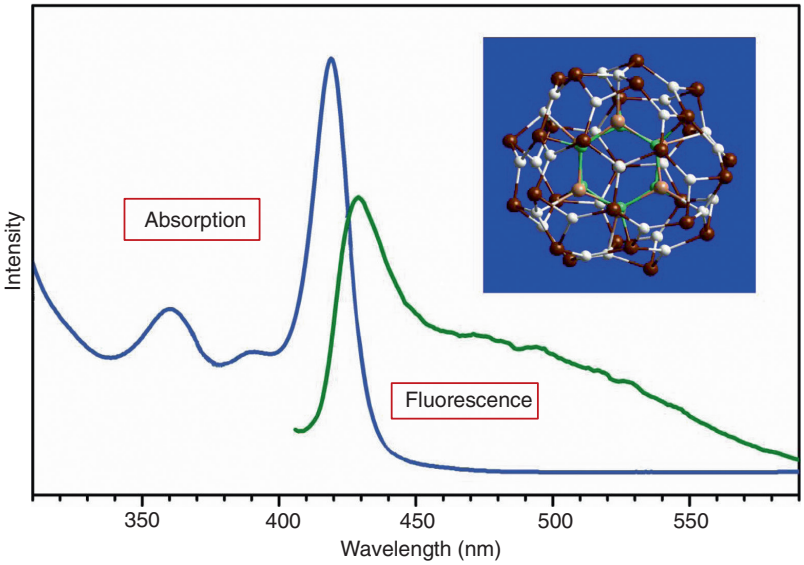

Fig. 5.23 Absorption and photoluminescence spectra of colloid solution of $(CdSe)_{34}$. The structure of nanocluster $(CdSe)_{34}$ according to the results of quantum-chemical calculations (*inset*)

colors and even white light (see Fig. 6.12). The dye retains its environment-dependent fluorescence properties in such conjugates.

5.5.7 Semiconductor Nanocrystals of Different Shapes and Dimensions

Recent studies have discovered many alternatives to classical semiconductor quantum dots with regard to shape and chemical composition. Nanostructured materials can adopt different shapes, such as nanotubes, nanorods, nanobelts, and nanowires (Huang and Choi 2007; Lim et al. 2014). Such variation of shapes opens new dimension in variations of sensor properties. It was found that nanoparticles of elongated shape, "*quantum rods*" with diameters ranging from 2 to 10 nm and with lengths ranging from 5 to 100 nm demonstrate superior properties to that of QDs, in particular, higher brightness (Fu et al. 2007).

In contrast to quantum dots, quantum rods emit *linearly polarized* fluorescence light (Lee et al. 2013) and this property can be potentially used in anisotropy (polarization) assays. Whereas QDs can allow improving the sensitivity of biological detection and imaging by at least 10- to 100-fold, quantum rods offer even superior possibilities for that. Due to their special shapes their interactions in biological media may reveal many interesting peculiarities. The antibodies labelled with quantum rods can specifically recognize the cancer markers on cellular surface.

5.5.8 Porous Silicon and Silicon Nanoparticles

Silicon, which is the basic material of microelectronics, upon photoexcitation does not demonstrate any emission. But microcrystalline silicon that is often called *porous silicon* has a bright luminescence. Such a difference is attributed to nanostructured composition of porous silicon. It possesses tiny pores that range from less than 2 nm to micrometer dimensions. Easy fabrication allows obtaining this material with high surface to volume ratio (as much as 500 m^2 cm^{-3}). Films made of porous silicon have found their own application in sensor technologies (Mizsei 2007; Zhang et al. 2007). Here we will concentrate on the properties of silicon nanocrystals, which can be presented as a new version of quantum dots. Their inertness and bio-compatibility together with high brightness has recently attracted attention of the researchers.

To date, there are only few studies on these prospective materials (Veinot 2006; Dasog et al. 2013). Physicists try to understand why photoluminescence cannot occur in infinite crystal. This is because Si, in contrast to CdS or CdSe, is an *indirect bandgap* semiconductor in which the lowest point of the conduction band and the highest point of the valence band occur at different wavevectors in reciprocal space. Hence, the optical transition is dipole-forbidden. Luminescence properties appear when the size of the structure forming elements (particle size or the size of walls of porous

silicon) are reduced to nanoscale dimensions, below Bohr exciton radius (~5 nm). Then the quantum confinement effects emerge that reduce the conduction band to discrete energy level and make electronic transition 'weakly' allowed (Buriak 2002).

Like other semiconductor QDs, the size-calibrated particles exhibit emission spectra spanning the visible range, but these spectra are much broader and exhibit stronger dependence on modifications of their surface. The commonly used in experiment small (1.2–2 nm) particles exhibit blue emission at 440–460 nm. Water-soluble derivatives of Si nanoparticles were obtained (Veinot 2006), they were used in cellular imaging.

5.5.9 Prospects

Quantum dots are now established as a new class of fluorescent labels with remarkably high brightness, resistance against photobleaching and size-dependent fluorescence emission in different colours. In comparison with the dye-doped nanoparticles they are more homogeneous in size and exhibit much narrower emission spectra. These features determine their prospect in multiplex assays. New generations of QDs have far-reaching potential for the study of intracellular processes at a single-particle level and with two-photon excitation. They offer many applications in high-resolution cellular imaging, long-term *in vivo* observation of cell trafficking, tumour targeting, and diagnostics.

Compared to fluorescent organic dyes with their many years of application, the employment of quantum dots into sensing technologies started only recently, and by trying the products that were already in use by physicists. Then the new materials better satisfying the demands appeared, and very rapid progress started to be observed (Gaponik et al. 2010). Meantime, regarding the applications in sensing these particles lack important properties observed in organic dyes. They do not exhibit photophysical effects that in organic dyes produce switching between different emissive states upon variation of their intermolecular interactions. So the general trend is the development on their basis of nanocomposites that could mediate sensor response based on electron or energy transfer that could be coupled to molecular recognition events. On the basis of these operating principles, the presence of target analytes can be transduced into detectable luminescence signals.

Fundamental research on these nanoparticles continues and it is highly probable that in near future the material nanotechnology will offer to sensor community the light-emitting reporters with the advanced properties that are very difficult to predict.

5.6 Up-Converting Nanocrystals

The up-converting materials are unique in their properties that are very attractive for various sensing and imaging applications. The physical term '*up-conversion*' means the excitation from already populated excited state to a higher energy state. An

already excited molecule can absorb additional light quantum to be raised to a higher energy level from which the emission proceeds. Thus, the up-converting materials are those, in which the emissive states are reached by two quanta: first quantum excites to long-living state, and the second quantum allows reaching the state, from which the emission occurs. Such possibilities are realized in very special type of materials – the *up-converting nanocrystals* (Mader et al. 2010; Wang et al. 2010; Haase and Schafer 2011; Gorris and Wolfbeis 2013). Except such rare earth crystalline materials, no other presently known material can exhibit such properties.

5.6.1 The Photophysical Mechanism

First, we have to draw clear distinction between the process of up-conversion and of two-photon (or multi-photon) excitation (see Sect. 10.4). The two-photon excitation process can be applied to a very broad range of fluorophores (though with different efficiency) but on a condition that the absorption of photons is simultaneous. The intermediate states do not exist, they are 'virtual'. Such excitation requires very high photon densities and is commonly realized with the application of ultrafast light pulses. In contrast, in *up-converting materials*, the 'real' long-living intermediate states should be easily populated, for which the first excited state is 'trapped' for relatively long time. Therefore the application of up-conversion effect in sensing cannot be realized with any type of dyes or nanoparticles and is limited to very special materials. Such materials are really unique.

In ceramic crystalline host matrices doped with trivalent lanthanide ions, such as Yb^{3+}, Er^{3+} and Tm^{3+}, two important properties, a *variety of electronic excited states* and *long lifetimes* of these states uniquely meet. The long-lifetime excited states can operate as metastable states excited from a ground state to be excited again with the gain of energy for reaching the emissive states (Fig. 5.24). Here the site excited to low-energy electronic state can wait until next quantum brings it to a higher excited state, from which, commonly after relaxation to lower levels, there occurs the emission of quanta of higher energies. Therefore such emission is free from restrictions imposed on two-photon excitation. It does not require very high irradiation densities and can be excited by conventional light sources.

5.6.2 The Spectroscopic Properties

Presently, the most efficient photon up-conversion is observed in inorganic crystalline $NaYF_4$ host lattices doped with Yb^{3+}, Er^{3+} and Tm^{3+}. Ytterbium is commonly used as a sensitizer because it has higher absorbance than erbium and thulium, which are used as emitting activators.

The formed nanocrystals display the ability to obtain visible emission with excitation in the near-IR (Mader et al. 2010; Wang et al. 2010; Haase and Schafer 2011). Thus, it is possible to obtain up-converted UV – visible – NIR emissions using a

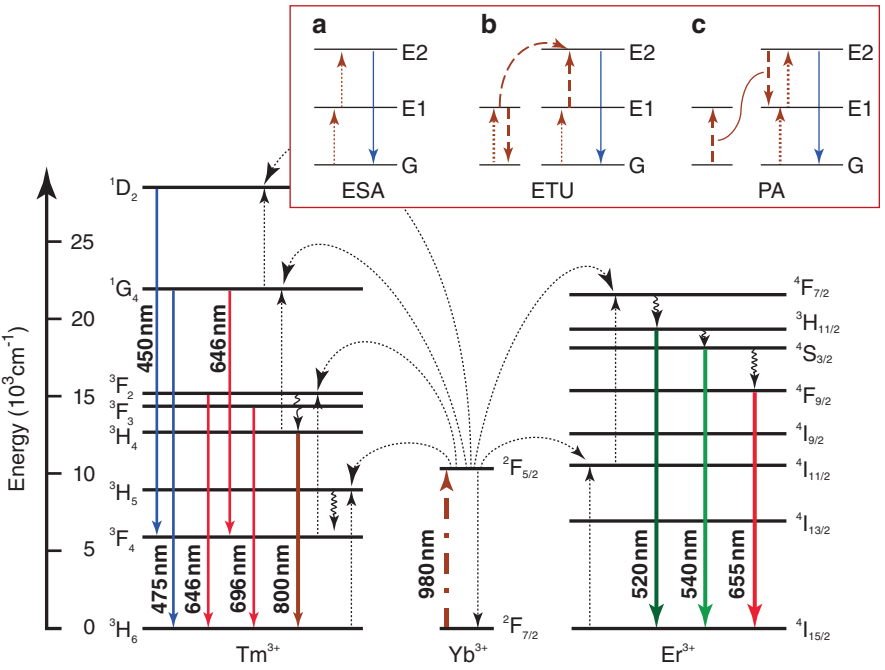

Fig. 5.24 Energy transfer and upconversion emission mechanisms in a $NaYF_4$ nanocrystal doped with Yb^{3+}, Er^{3+}, and Tm^{3+} under 980-nm excitation (Achatz et al. 2011). The *dashed-dotted*, *dotted, curly, and full arrows* refer to photon excitation, energy transfer, multi-photon relaxation, and up-conversion emission. *Insert*: Schematic representation of the three main types of processes causing up-conversion in rare earth doped materials: (**a**) excited state absorption; (**b**) energy transfer up-conversion; (**c**) photon avalanche. The *dotted lines* refer to photon excitation, *dashed lines* to non-radiative energy transfer, and *full arrows* to emissive processes, respectively

single NIR excitation source. This source can be an inexpensive commercial continuous-wave diode laser emitting at 980 nm.

One should also note that the emission of these up-converting nanocrystals is represented by a series of narrow lines that are very characteristic (Fig. 5.25). Other features include long-lifetime decays, very high chemical stability, the lack of bleaching, and the absence of blinking effects (De la Rosa et al. 2005; Mader et al. 2010).

As it is illustrated in Fig. 5.24 (see insert), three main types of operation with these particles can be realized: excited state absorption, energy transfer up-conversion and photon avalanche (Achatz et al. 2011). On absorption of two quanta, in addition to emission occurring from a single lanthanide ion, the energy can be transferred to adjacent ion. Also, on exceeding some threshold light intensity, a resonant 'avalanche' emission can be generated.

Thus, due to such two-step absorption, the excitation energies are sufficient to convert the near-IR excitation light into emission at visible wavelengths. Therefore the incorrectly called 'anti-Stokes' emission appears to be shifted dramatically (but

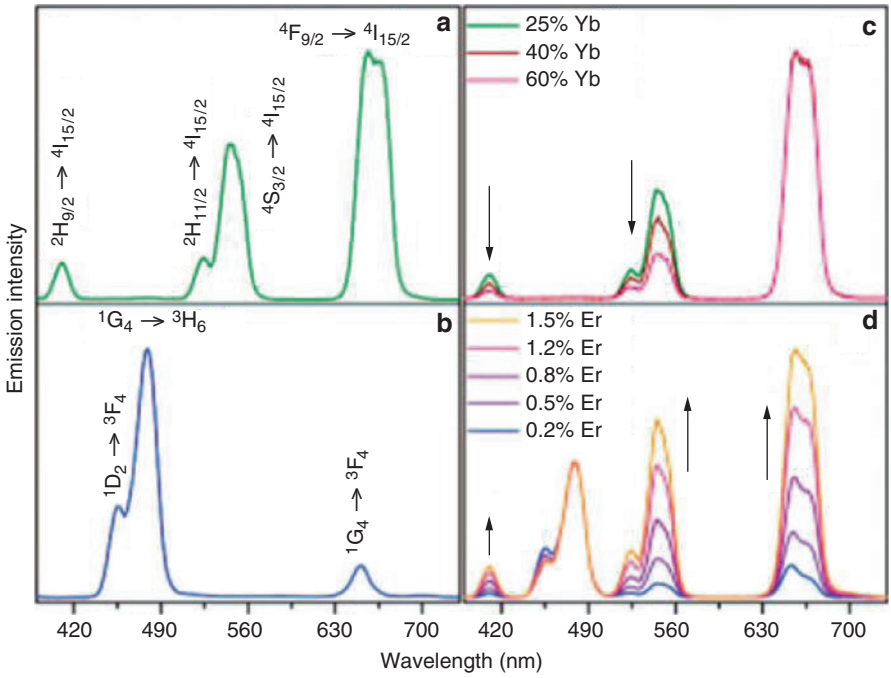

Fig. 5.25 Room temperature up-conversion emission spectra of $NaYF_4$ nanocrystals doped with (**a**) Yb/Er (18/2 mol %), (**b**) Yb/Tm (20/0.2 mol %), (**c**) Yb/Er (25–60/2 mol %), and (**d**) Yb/Tm/Er (20/0.2/0.2–1.5 mol %) particles in ethanol solutions (10 mM) (Achatz et al. 2011). The spectra in (**c**, **d**) were normalized to Er^{3+} (650-nm) and Tm^{3+} (480-nm emissions), respectively. The samples were excited at 980-nm with a 600-mW diode laser

not necessarily with doubling of energy) to shorter wavelengths with respect to excitation. For example, this emission excited at 980 nm can be measured at different wavelengths, from green to red as it is shown in Fig. 5.25.

5.6.3 Present and Prospective Applications

Unique type of luminescence emission, where the low-energy near-IR light is converted to high-energy visible emission upon sequential absorption of two or more photons is extremely attractive for various applications (Fig. 5.26).

Fascinating are the applications *in sensor technologies* of up-conversion emitters as *resonance energy transfer donors* to any molecular or nanoscale acceptors. Due to extremely sharp and narrow emission bands characteristic of luminescent lanthanide ions, no donor emission can be detected at the wavelengths of sensitized emission of the acceptor. Also, no acceptor can be excited directly because the excitation is at very low energies, in the near-IR. This means that the donor and acceptor emission channels do not overlap, which is almost impossible to achieve with organic dyes.

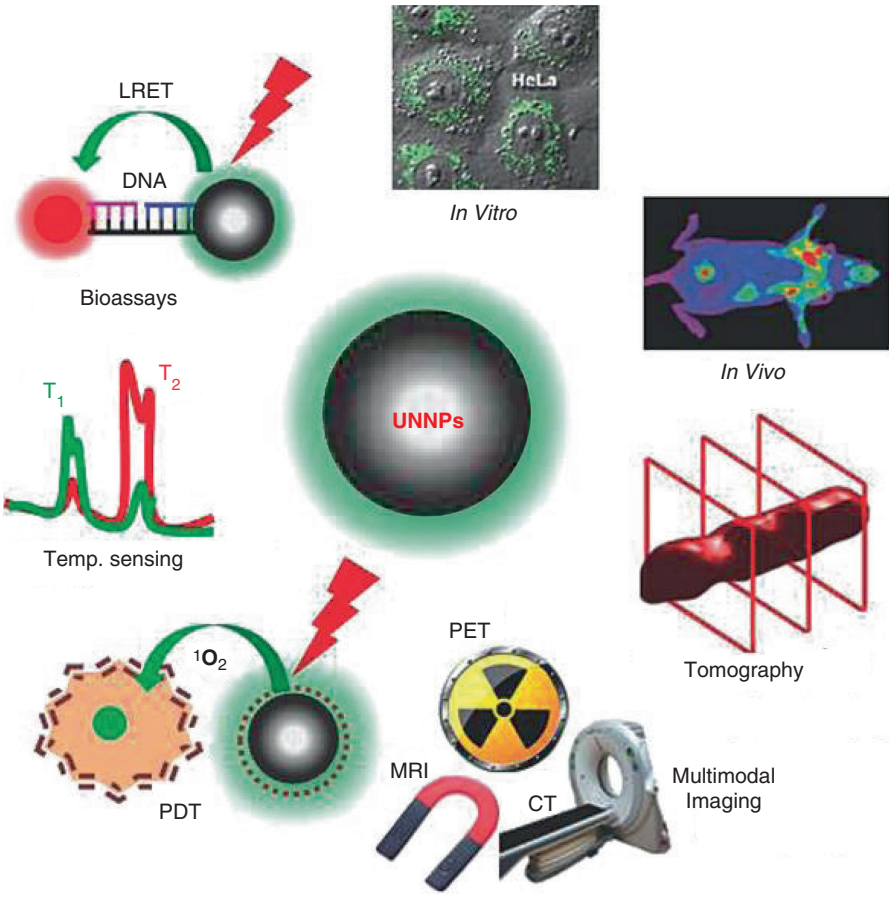

Fig. 5.26 The range of applications of up-converting nanoparticles (Xu et al. 2013)

The use of these nanoparticles as the *energy transfer acceptors* allows overcoming their weak point – a weak light absorbance of lanthanide ions. A conjugation of the nanocrystals with multiple strongly near-IR absorbing organic dyes acting as light harvesting surface ligands and providing the excitation energy to emissive sites allows to transform them into strong absorbers (Zou et al. 2012).

Manipulation with concentrations of doping ions allows *generating any color* covering the whole visible range because the narrow and multiple emission lines of up-converting nanoparticles can be adjusted individually providing the large-scale manipulation with emission color (Gorris and Wolfbeis 2013). Such designed combinations ideally suit for *color barcoding* that is needed in homogeneous multiplex assays (Sect. 6.4).

The presence of multiple emission lines together with possibility to manipulate with their relative intensities opens new possibilities in λ-ratiometric sensing. The

self-calibrating temperature sensor was developed based on this principle (Sedlmeier et al. 2012).

The fact of absence of *background emission* even in the presence of many contaminants stimulates application of sensing technique to different types of heterogeneous and biological systems. This is ideal for the analysis of strongly colored and fluorescent samples, which are often of concern in *clinical immunoassays* and in high-throughput screening (Kuningas et al. 2005). Particularly, this approach allows the sensor applications in the *whole blood*, so that blood pigments do not interfere into assays.

The straightforward application of up-converting nanoparticles is in cell and tissue *imaging* (Xu et al. 2013). With their aid, the high penetration depth of near-IR light together with the absence of light-scattering and fluorescence background allows obtaining ideal images in the visible (Chatterjee et al. 2008). This technique extends to small-animal imaging tomography (Zhou et al. 2012a). Deep penetration of near-IR light into tissues allows using the up-converting particles in new schemes of photodynamic therapy of cancer (see Sect. 14.4).

Possibility of realizing apparent advantages in sensing and imaging stimulated many efforts to obtain the up-converting nanoparticles of well-determined morphology, of small and uniform size and with shells convenient for further modifications and use in sensor technologies (Lin et al. 2012; Sedlmeier and Gorris 2015). The large size (>100 nm) of most presently available up-converting nanoparticles limits some applications. Techniques of synthesis the up-converting nanomaterials develop rapidly and is expected to meet stringent demands of researchers (Wawrzynczyk et al. 2012; Bogdan et al. 2011).

5.7 Sensing and Thinking: Nanoscale Emitters, What Are the Advantages?

The requests for new technologies in clinical diagnostics, monitoring the environment, agriculture and food safety control, detection of biological warfare agents and in different industries stimulates the appearance of many new products.

In the cases when small size of reporter unit is not important and direct response to target binding event is not requested or may be provided by the design of complex hybrid structures, the fluorescent nanoparticles have a great advantage. They can be much brighter and less susceptible to chemical damage and photodamage. These properties are achieved by different means. There could be high local concentration of dyes incorporated into silica or polymeric particles together with immobilization and protection from external quenching. There can be also plasmon effects realized in the case of metal nanoparticles and excitonic effect in the case of semiconductor quantum dots, conjugated polymers and dye J-aggregates. In the latter cases a remarkable size-dependent variation of wavelengths of their emission can be achieved. Such variation can be even broader with silver and gold nanoclusters.

Many new sensing and imaging possibilities together with the absence of fluorescent background are offered by up-converting nanoparticles.

The success in use of these materials will depend strongly not only on their fluorescence reporter properties but also on the ease with which they can be synthesized, functionalized and manipulated. Here the strategy has to be different from that commonly used with molecular emitters. Multiple groups of atoms forming the particle surface allow multiple possibilities for smart supramolecular constructions.

We have to check also the weak point of all fluorescent nanoparticles, which is a difficulty in providing a strong response of their fluorescence to external stimuli that must be explored in sensing. Regarding the changes in emission spectra induced in perturbations by intermolecular interactions, they are well behind organic dyes. General mechanism of their response is the on-off quenching with response in anisotropy and lifetime realized in rare cases. In Chap. 6 we will observe how these properties can be attained with proper modifications of these particles and formation of nanocomposites, particularly with organic dyes. In these cases the number of combinations becomes enormous.

Questions and Problems

1. What is the difference in formation of the surfaces and their properties between nanoparticles made of crystalline and soft materials?
2. In what way the FRET mechanism of excited-state energy transfer is modified on interaction with and between nanoparticles?
3. Explain the mechanism of concentrational quenching. Consider the system, which exhibits the self-quenching being composed of dyes incorporated in high density into polymeric matrix. What will be the result of introducing FRET acceptor in small concentration into this system? Draw a kinetic scheme explaining this case.
4. What is common and what is different between superquenching effect in conjugated polymer and concentrational quenching of organic dyes?
5. How to incorporate organic dye into organic polymer and into silica nanoparticle? Explain the benefits in comparison with individual dye molecules.
6. Explain the mechanism of fluorescence emission in conjugated polymer. What are the means to modulate their emission on order to generate the sensor response?
7. Can carbon nanoparticles serve as FRET energy acceptors from protein molecules? What makes them ‘universal quenchers’?
8. Explain the correlation between the size of quantum dots and the positions of their optical spectra. The size is a geometric parameter and the spectra reflect the energies of electronic transitions. Why they are connected?
9. How to make the quantum dot responsive as the detection unit in direct sensing (avoiding sandwich assays)?
10. Is it easy to achieve FRET between quantum dots of different sizes? What are the major problems? How these problems are resolved if, instead of quantum dots, another type of nanoparticles are used as FRET partners?

11. What are the general requirements for up-converting phenomenon to be observed? How they are realized in rare earth ion doped nanocrystals?
12. List the advantages and disadvantages in application of up-converting nanocrystals in sensing and imaging.

References

Achatz DE, Ali R, Wolfbeis OS (2011) Luminescent chemical sensing, biosensing, and screening using upconverting nanoparticles. In: Luminescence applied in sensor science. Springer, Berlin, pp 29–50

Achyuthan KE, Bergstedt TS, Chen L, Jones RM, Kumaraswamy S, Kushon SA, Ley KD, Lu L, McBranch D, Mukundan H, Rininsland F, Shi X, Xia W, Whitten DG (2005) Fluorescence superquenching of conjugated polyelectrolytes: applications for biosensing and drug discovery. J Mater Chem 15(27–28):2648–2656

Aggarwal P, Hall JB, McLeland CB, Dobrovolskaia MA, McNeil SE (2009) Nanoparticle interaction with plasma proteins as it relates to particle biodistribution, biocompatibility and therapeutic efficacy. Adv Drug Deliv Rev 61(6):428–437. doi:S0169-409X(09)00101-X [pii] 10.1016/j.addr.2009.03.009

Aiken Iii JD, Finke RG (1999) A review of modern transition-metal nanoclusters: their synthesis, characterization, and applications in catalysis. J Mol Catal A Chem 145(1–2):1–44. doi:10.1016/s1381-1169(99)00098-9

Algar WR, Krull UJ (2007) Luminescence and stability of aqueous thioalkyl acid capped CdSe/ZnS quantum dots correlated to ligand ionization. Chemphyschem 8(4):561–568

Alivisatos AP, Gu W, Larabell C (2005) Quantum dots as cellular probes. Annu Rev Biomed Eng 7:55–76. doi:10.1146/annurev.bioeng.7.060804.100432

Allen PM, Liu W, Chauhan VP, Lee J, Ting AY, Fukumura D, Jain RK, Bawendi MG (2010) InAs(ZnCdS) quantum dots optimized for biological imaging in the near-infrared. J Am Chem Soc 132(2):470–471. doi:10.1021/ja908250r

Amin R, Hwang S, Park SH (2011) Nanobiotechnology: an interface between nanotechnology and biotechnology. NANO: Brief Reports and Rev 6:101–111

Andreescu S, Sadik OA (2004) Trends and challenges in biochemical sensors for clinical and environmental monitoring. Pure Appl Chem 76(4):861–878

Aryal BP, Benson DE (2006) Electron donor solvent effects provide biosensing with quantum dots. J Am Chem Soc 128(50):15986–15987

Astruc D, Boisselier E, Ornelas C (2010) Dendrimers designed for functions: from physical, photophysical, and supramolecular properties to applications in sensing, catalysis, molecular electronics, photonics, and nanomedicine. Chem Rev 110(4):1857–1959

Bae SW, Tan W, Hong J-I (2012) Fluorescent dye-doped silica nanoparticles: new tools for bioapplications. Chem Commun 48(17):2270–2282

Bagwe RP, Hilliard LR, Tan W (2006) Surface modification of silica nanoparticles to reduce aggregation and nonspecific binding. Langmuir 22(9):4357–4362. doi:10.1021/la052797j

Baker SN, Baker GA (2010) Luminescent carbon nanodots: emergent nanolights. Angew Chem Int Ed 49(38):6726–6744. doi:10.1002/anie.200906623

Balazs AC, Emrick T, Russell TP (2006) Nanoparticle polymer composites: where two small worlds meet. Science 314(5802):1107–1110. doi:10.1126/science.1130557

Balzani V, Ceroni P, Gestermann S, Kauffmann C, Gorka M, Vogtle F (2000) Dendrimers as fluorescent sensors with signal amplification. Chem Commun 10:853–854

Balzani V, Credi A, Venturi M (2003) Molecular logic circuits. Chemphyschem 4(1):49–59

Barone PW, Baik S, Heller DA, Strano MS (2004) Near-infrared optical sensors based on single-walled carbon nanotubes. Nat Mater 4(1):86–92

Barone PW, Baik S, Heller DA, Strano MS (2005) Near-infrared optical sensors based on single-walled carbon nanotubes. Nat Mater 4(1):86–92. doi:nmat1276 [pii] 10.1038/nmat1276

Bartelmess J, Quinn S, Giordani S (2015) Carbon nanomaterials: multi-functional agents for biomedical fluorescence and Raman imaging. Chem Soc Rev 44(14): 4672–4698. doi: 10.1039/C4CS00306C

Bergamini G, Marchi E, Ceroni P (2010) Luminescent dendrimers as ligands and sensors of metal ions. In: Demchenko AP (ed) Advanced fluorescence reporters in chemistry and biology II: molecular constructions, polymers and nanoparticles, Springer Ser Fluoresc 9:253–284

Bertazza L, Celotti L, Fabbrini G, Loi MA, Maggini M, Mancin F, Marcuz S, Menna E, Muccini M, Tonellato U (2006) Cell penetrating silica nanoparticles doped with two-photon absorbing fluorophores. Tetrahedron 62(44):10434–10440

Beveratos A, Brouri R, Gacoin T, Poizat J-P, Grangier P (2001) Nonclassical radiation from diamond nanocrystals. Phys Rev A 64(6):061802

Bogdan N, Vetrone F, Ozin GA, Capobianco JA (2011) Synthesis of ligand-free colloidally stable water dispersible brightly luminescent lanthanide-doped upconverting nanoparticles. Nano Lett 11(2):835–840. doi:10.1021/nl1041929

Bonacchi S, Genovese D, Juris R, Montalti M, Prodi L, Rampazzo E, Zaccheroni N (2011) Luminescent silica nanoparticles: extending the frontiers of brightness. Angew Chem Int Ed 50(18):4056–4066

Borisov SM, Mayr T, Mistlberger G, Klimant I (2010) Dye-doped polymeric particles for sensing and imaging. In: Demchenko AP (ed) Advanced fluorescence reporters in chemistry and biology II: molecular constructions, polymers and nanoparticles, Springer Ser Fluoresc 9:193–228

Bottini M, Balasubramanian C, Dawson MI, Bergamaschi A, Bellucci S, Mustelin T (2006) Isolation and characterization of fluorescent nanoparticles from pristine and oxidized electric arc-produced single-walled carbon nanotubes. J Phys Chem B 110(2):831–836

Breul AM, Hager MD, Schubert US (2013) Fluorescent monomers as building blocks for dye labeled polymers: synthesis and application in energy conversion, biolabeling and sensors. Chem Soc Rev 42(12):5366–5407

Burda C, Chen XB, Narayanan R, El-Sayed MA (2005) Chemistry and properties of nanocrystals of different shapes. Chem Rev 105(4):1025–1102

Buriak JM (2002) Organometallic chemistry on silicon and germanium surfaces. Chem Rev 102(5):1271–1308

Caminade AM, Padie C, Laurent R, Maraval A, Majoral JP (2006) Uses of dendrimers for DNA microarrays. Sensors 6(8):901–914

Campagna S, Ceroni P, Puntoriero F (2011) Designing dendrimers. John Wiley & Sons, Hoboken, New Jersey

Cao L, Meziani MJ, Sahu S, Sun YP (2013) Photoluminescence properties of graphene versus other carbon nanomaterials. Acc Chem Res 46(1):171–180

Chakraborti H, Sinha S, Ghosh S, Pal SK (2013) Interfacing water soluble nanomaterials with fluorescence chemosensing: graphene quantum dot to detect Hg^{2+} in 100% aqueous solution. Mater Lett 97:78–80

Chang BM, Lin HH, Su LJ, Lin WD, Lin RJ, Tzeng YK, Lee RT, Lee YC, Yu AL, Chang HC (2013) Highly fluorescent nanodiamonds protein-functionalized for cell labeling and targeting. Adv Funct Mater 23(46):5737–5745

Chatterjee DK, Rufaihah AJ, Zhang Y (2008) Upconversion fluorescence imaging of cells and small animals using lanthanide doped nanocrystals. Biomaterials 29(7):937–943

Chen N-T, Cheng S-H, Liu C-P, Souris JS, Chen C-T, Mou C-Y, Lo L-W (2012) Recent advances in nanoparticle-based förster resonance energy transfer for biosensing, molecular imaging and drug release profiling. Int J Mol Sci 13(12):16598–16623

Costa-Fernandez JM, Pereiro R, Sanz-Medel A (2006) The use of luminescent quantum dots for optical sensing. TrAC Trends Anal Chem 25(3):207–218

Dasog M, Yang Z, Regli S, Atkins TM, Faramus A, Singh MP, Muthuswamy E, Kauzlarich SM, Tilley RD, Veinot JG (2013) Chemical insight into the origin of red and blue photoluminescence arising from freestanding silicon nanocrystals. ACS Nano 7(3):2676–2685

De la Rosa E, Salas P, Diaz-Torres LA, Martinez A, Angeles C (2005) Strong visible cooperative up-conversion emission in ZrO2:Yb3+ nanocrystals. J Nanosci Nanotechnol 5(9):1480–1486

Dekaliuk MO, Viagin O, Malyukin YV, Demchenko AP (2014) Fluorescent carbon nanomaterials: "quantum dots" or nanoclusters? Phys Chem Chem Phys 16(30):16075–16084

Delehanty JB, Medintz IL, Pons T, Brunel FM, Dawson PE, Mattoussi H (2006) Self-assembled quantum dot-peptide bioconjugates for selective intracellular delivery. Bioconjug Chem 17(4):920–927

Demchenko AP, Dekaliuk MO (2013) Novel fluorescent carbonic nanomaterials for sensing and imaging. Meth Appl Fluores 1(4):042001

Ding D, Li K, Liu B, Tang BZ (2013) Bioprobes based on AIE fluorogens. Acc Chem Res 46(11):2441–2453

Dmitruk NL, Borkovskaya OY, Mamykin SV, Naumenko DO, Berezovska NI, Dmitruk IM, Meza-Laguna V, Alvarez-Zauco E, Basiuk EV (2008) Fullerene C60-silver nanoparticles hybrid structures: optical and photoelectric characterization. J Nanosci Nanotechnol 8(11): 5958–5965

Dong Y, Wang R, Li G, Chen C, Chi Y, Chen G (2012a) Polyamine-functionalized carbon quantum dots as fluorescent probes for selective and sensitive detection of copper ions. Anal Chem 84(14):6220–6224

Dong Y, Wang R, Li H, Shao J, Chi Y, Lin X, Chen G (2012b) Polyamine-functionalized carbon quantum dots for chemical sensing. Carbon 50(8):2810–2815. doi:10.1016/j.carbon.2012.02.046

Dubertret B, Skourides P, Norris DJ, Noireaux V, Brivanlou AH, Libchaber A (2002) In vivo imaging of quantum dots encapsulated in phospholipid micelles. Science 298(5599):1759–1762

Dubois F, Mahler B, Dubertret B, Doris E, Mioskowski C (2007) A versatile strategy for quantum dot ligand exchange. J Am Chem Soc 129(3):482–483

Esteves da Silva JCG, Gonçalves HMR (2011) Analytical and bioanalytical applications of carbon dots. TrAC Trends Anal Chem 30(8):1327–1336

Fan CH, Wang S, Hong JW, Bazan GC, Plaxco KW, Heeger AJ (2003) Beyond superquenching: hyper-efficient energy transfer from conjugated polymers to gold nanoparticles. Proc Natl Acad Sci U S A 100(11):6297–6301

Feng L, Zhu C, Yuan H, Liu L, Lv F, Wang S (2013) Conjugated polymer nanoparticles: preparation, properties, functionalization and biological applications. Chem Soc Rev 42(16):6620–6633

Feng X, Liu L, Wang S, Zhu D (2010) Water-soluble fluorescent conjugated polymers and their interactions with biomacromolecules for sensitive biosensors. Chem Soc Rev 39(7):2411–2419

Fery-Forgues S, Abyan M, Lamere JF (2008) Nano- and microparticles of organic fluorescent dyes: self-organization and optical properties. Ann N Y Acad Sci 1130:272–279. doi:1130/1/272 [pii] 10.1196/annals.1430.047

Fu AH, Gu WW, Boussert B, Koski K, Gerion D, Manna L, Le Gros M, Larabell CA, Alivisatos AP (2007) Semiconductor quantum rods as single molecule fluorescent biological labels. Nano Lett 7(1):179–182

Gaponik N, Hickey SG, Dorfs D, Rogach AL, Eychmüller A (2010) Progress in the light emission of colloidal semiconductor nanocrystals. Small 6(13):1364–1378

Ghosh S, Chizhik AM, Karedla N, Dekaliuk MO, Gregor I, Schuhmann H, Seibt M, Bodensiek K, Schaap IA, Schulz O, Demchenko AP, Enderlein J, Chizhik AI (2014) The photoluminescence of carbon nanodots: dipole emission centers and electron-phonon coupling. Nano Lett 14(10):5656–5661

Gilbert B, Huang F, Zhang H, Waychunas GA, Banfield JF (2004) Nanoparticles: strained and stiff. Science 305(5684):651–654. doi:10.1126/science.1098454

Goicoechea J, Arregui FJ, Matias IR (2009) Quantum dots for sensing. In: Sensors based on nanostructured materials. Springer, New York, pp 131–181

Goldman ER, Medintz IL, Mattoussi H (2006) Luminescent quantum dots in immunoassays. Anal Bioanal Chem 384(3):560–563

Goldman ER, Medintz IL, Whitley JL, Hayhurst A, Clapp AR, Uyeda HT, Deschamps JR, Lassman ME, Mattoussi H (2005) A hybrid quantum dot-antibody fragment fluorescence resonance energy transfer-based TNT sensor. J Am Chem Soc 127(18):6744–6751

Gooding JJ (2006) Biosensor technology for detecting biological warfare agents: recent progress and future trends. Anal Chim Acta 559(2):137–151

Gorris HH, Wolfbeis OS (2013) Photon-upconverting nanoparticles for optical encoding and multiplexing of cells, biomolecules, and microspheres. Angew Chem Int Ed 52(13): 3584–3600

Grayson SM, Frechet JMJ (2001) Convergent dendrons and dendrimers: from synthesis to applications. Chem Rev 101(12):3819–3867

Grecco HE, Lidke KA, Heintzmann R, Lidke DS, Spagnuolo C, Martinez OE, Jares-Erijman EA, Jovin TM (2004) Ensemble and single particle photophysical properties (two-photon excitation, anisotropy, FRET, lifetime, spectral conversion) of commercial quantum dots in solution and in live cells. Microsc Res Tech 65(4–5):169–179

Greco P, Cavallini M, Stoliar P, Quiroga SD, Dutta S, Zacchini S, Iapalucci MC, Morandi V, Milita S, Merli PG, Biscarini F (2008) Conductive sub-micrometric wires of platinum-carbonyl clusters fabricated by soft-lithography. J Am Chem Soc 130(4):1177–1182. doi:10.1021/ja074104m

Haase M, Schafer H (2011) Upconverting nanoparticles. Angew Chem Int Ed Engl 50(26):5808–5829. doi:10.1002/anie.201005159

Han G, Chari NS, Verma A, Hong R, Martin CT, Rotello VM (2005) Controlled recovery of the transcription of nanoparticle-bound DNA by intracellular concentrations of glutathione. Bioconjug Chem 16(6):1356–1359. doi:10.1021/bc050173j

Harma H, Keranen AM, Lovgren T (2007) Synthesis and characterization of europium(III) nanoparticles for time-resolved fluoroimmunoassay of prostate-specific antigen. Nanotechnology 18(7):075604

He H, Klinowski J, Forster M, Lerf A (1998) A new structural model for graphite oxide. Chem Phys Lett 287(1):53–56

Hermanson GT (1995) Bioconjugation techniques. Academic, San Diego

Herrwerth S, Eck W, Reinhardt S, Grunze M (2003) Factors that determine the protein resistance of oligoether self-assembled monolayers –internal hydrophilicity, terminal hydrophilicity, and lateral packing density. J Am Chem Soc 125(31):9359–9366. doi:10.1021/ja034820y

Hessel CM, Reid D, Panthani MG, Rasch MR, Goodfellow BW, Wei J, Fujii H, Akhavan V, Korgel BA (2011) Synthesis of ligand-stabilized silicon nanocrystals with size-dependent photoluminescence spanning visible to near-infrared wavelengths. Chem Mater 24(2):393–401. doi:10.1021/cm2032866

Hoang VV (2007) Molecular dynamics simulation of amorphous SiO2 nanoparticles. J Phys Chem B 111(44):12649–12656. doi:10.1021/jp074237u

Hoang VV (2012) Melting of simple monatomic amorphous nanoparticles. J Phys Chem C 116(27):14728–14735. doi:10.1021/jp304211n

Hoeben FJ, Jonkheijm P, Meijer EW, Schenning AP (2005) About supramolecular assemblies of pi-conjugated systems. Chem Rev 105(4):1491–1546

Holzapfel V, Musyanovych A, Landfester K, Lorenz MR, Mailander V (2005) Preparation of fluorescent carboxyl and amino functionalized polystyrene particles by miniemulsion polymerization as markers for cells. Macromol Chem Phys 206(24):2440–2449

Hoshino A, Fujioka K, Manabe N, Yamaya S, Goto Y, Yasuhara M, Yamamoto K (2005) Simultaneous multicolor detection system of the single-molecular microbial antigen with total internal reflection fluorescence microscopy. Microbiol Immunol 49(5):461–470

Hötzer B, Medintz IL, Hildebrandt N (2012) Fluorescence in nanobiotechnology: sophisticated fluorophores for novel applications. Small 8(15):2297–2326

Hu R, Leung NL, Tang BZ (2014) AIE macromolecules: syntheses, structures and functionalities. Chem Soc Rev 43(13):4494–4562

Huang B, Wu HK, Bhaya D, Grossman A, Granier S, Kobilka BK, Zare RN (2007) Counting low-copy number proteins in a single cell. Science 315(5808):81–84

Huang X, Yin Z, Wu S, Qi X, He Q, Zhang Q, Yan Q, Boey F, Zhang H (2011) Graphene-based materials: synthesis, characterization, properties, and applications. Small 7(14):1876–1902. doi:10.1002/smll.201002009

Huang XJ, Choi YK (2007) Chemical sensors based on nanostructured materials. Sens Actuators B Chem 122(2):659–671

Huhtinen P, Kivela M, Kuronen O, Hagren V, Takalo H, Tenhu H, Lovgren T, Harma H (2005) Synthesis, characterization, and application of Eu(III), Tb(III), Sm(III), and Dy(III) lanthanide chelate nanoparticle labels. Anal Chem 77(8):2643–2648

Huhtinen P, Vaarno J, Soukka T, Lovgren T, Harma H (2004) Europium(III) nanoparticle-label-based assay for the detection of nucleic acids. Nanotechnology 15(12):1708–1715

Ito O, D'Souza F (2012) Recent advances in photoinduced electron transfer processes of fullerene-based molecular assemblies and nanocomposites. Molecules 17(5):5816–5835. doi:molecules17055816 [pii] 10.3390/molecules17055816

Iyer G, Pinaud F, Tsay J, Li JJ, Bentolila LA, Michalet X, Weiss S (2006) Peptide coated quantum dots for biological applications. IEEE Trans Nanobiosci 5(4):231–238

Jadzinsky PD, Calero G, Ackerson CJ, Bushnell DA, Kornberg RD (2007) Structure of a thiol monolayer-protected gold nanoparticle at 1.1 A resolution. Science 318(5849):430–433. doi:318/5849/430 [pii] 10.1126/science.1148624

Jang S, Kim SG, Jung D, Kwon H, Song J, Cho S, Ko YC, Sohn H (2006) Aggregation-induced emission enhancement of polysilole nanoaggregates. Bull Korean Chem Soc 27(12):1965

Jares-Erijman EA, Jovin TM (2003) FRET imaging. Nat Biotechnol 21(11):1387–1395

Jin T, Fujii F, Yamada E, Nodasaka Y, Kinjo M (2006) Control of the optical properties of quantum dots by surface coating with calix n arene carboxylic acids. J Am Chem Soc 128(29):9288–9289

Jin Z, Hildebrandt N (2012) Semiconductor quantum dots for in vitro diagnostics and cellular imaging. Trends Biotechnol 30(7):394–403. doi:S0167-7799(12)00056-X [pii] 10.1016/j.tibtech.2012.04.005

Johansson MK, Cook RM (2003) Intramolecular dimers: a new design strategy for fluorescence-quenched probes. Chemistry 9(15):3466–3471. doi:10.1002/chem.200304941

Kasuya A, Sivamohan R, Barnakov YA, Dmitruk IM, Nirasawa T, Romanyuk VR, Kumar V, Mamykin SV, Tohji K, Jeyadevan B (2004a) Ultra-stable nanoparticles of CdSe revealed from mass spectrometry. Nat Mater 3(2):99–102

Kasuya A, Sivamohan R, Barnakov YA, Dmitruk IM, Nirasawa T, Romanyuk VR, Kumar V, Mamykin SV, Tohji K, Jeyadevan B, Shinoda K, Kudo T, Terasaki O, Liu Z, Belosludov RV, Sundararajan V, Kawazoe Y (2004b) Ultra-stable nanoparticles of CdSe revealed from mass spectrometry. Nat Mater 3(2):99–102. doi:10.1038/nmat1056 nmat1056 [pii]

Khandare J, Kolhe P, Pillai O, Kannan S, Lieh-Lai M, Kannan RM (2005) Synthesis, cellular transport, and activity of polyamidoamine dendrimer-methylprednisolone conjugates. Bioconjug Chem 16(2):330–337

Kim Y, Bouffard J, Kooi SE, Swager TM (2005) Highly emissive conjugated polymer excimers. J Am Chem Soc 127(39):13726–13731

Krueger A (2008) New carbon materials: biological applications of functionalized nanodiamond materials. Chemistry 14(5):1382–1390. doi:10.1002/chem.200700987

Kuningas K, Rantanen T, Ukonaho T, Lovgren T, Soukka T (2005) Homogeneous assay technology based on upconverting phosphors. Anal Chem 77(22):7348–7355

Kuo Y, Hsu T-Y, Wu Y-C, Hsu J-H, Chang H-C (2013) Fluorescence lifetime imaging microscopy of nanodiamonds in vivo. In: Proceedings of SPIE 2013:863503–863501

Landfester K (2006) Synthesis of colloidal particles in miniemulsions. Annu Rev Mater Res 36:231–279

Lavorel J (1957) Influence of concentration on the absorption spectrum and the action spectrum of fluorescence of dye solutions. J Phys Chem 61(12):1600–1605. doi:10.1021/j150558a006

Lee J, Fujii F, Kim S, Back C, Kim S (2013) Study on the diffusions of a quantum rod using polarized fluorescence correlation spectroscopy. Proc. SPIE 8879, Nano-Bio Sensing, Imaging, and Spectroscopy, 88790R (May 20, 2013); doi:10.1117/12.2018690

Li H, He X, Kang Z, Huang H, Liu Y, Liu J, Lian S, Tsang CHA, Yang X, Lee ST (2010) Water-soluble fluorescent carbon quantum dots and photocatalyst design. Angew Chem Int Ed 49(26):4430–4434

Li K, Liu B (2014) Polymer-encapsulated organic nanoparticles for fluorescence and photoacoustic imaging. Chem Soc Rev 43(18):6570–6597

Li N, Binder WH (2011) Click-chemistry for nanoparticle-modification. J Mater Chem 21(42):16717–16734

Li Q, Zhang S, Dai L, Li L (2012) Nitrogen-doped colloidal graphene quantum dots and their size-dependent electrocatalytic activity for the oxygen reduction reaction. J Am Chem Soc 134(46):18932–18935

Lian W, Litherland SA, Badrane H, Tan WH, Wu DH, Baker HV, Gulig PA, Lim DV, Jin SG (2004) Ultrasensitive detection of biomolecules with fluorescent dye-doped nanoparticles. Anal Biochem 334(1):135–144

Liang RQ, Li W, Li Y, Tan CY, Li JX, Jin YX, Ruan KC (2005) An oligonucleotide microarray for microRNA expression analysis based on labeling RNA with quantum dot and nanogold probe. Nucleic Acids Res 33(2):e17

Liao JH, Swager TM (2007) Quantification of amplified quenching for conjugated polymer microsphere systems. Langmuir 23(1):112–115

Lim SJ, Smith A, Nie S (2014) The more exotic shapes of semiconductor nanocrystals: emerging applications in bioimaging. Curr Opin Chem Eng 4:137–143

Lin M, Zhao Y, Wang S, Liu M, Duan Z, Chen Y, Li F, Xu F, Lu T (2012) Recent advances in synthesis and surface modification of lanthanide-doped upconversion nanoparticles for biomedical applications. Biotechnol Adv 30(6):1551–1561

Lin YS, Haynes CL (2010) Impacts of mesoporous silica nanoparticle size, pore ordering, and pore integrity on hemolytic activity. J Am Chem Soc 132(13):4834–4842. doi:10.1021/ja910846q

Liu BR, Huang YW, Chiang HJ, Lee HJ (2010) Cell-penetrating peptide-functionalized quantum dots for intracellular delivery. J Nanosci Nanotechnol 10(12):7897–7905

Liu J-H, Yang S-T, Chen X-X, Wang H (2012a) Fluorescent carbon dots and nanodiamonds for biological imaging: preparation, application, pharmacokinetics and toxicity. Curr Drug Metab 13(8):1046–1056

Liu J-M, L-p L, Wang X-X, Lin S-Q, Zhang L-H, Zheng Z-Y (2012b) Highly selective and sensitive detection of Cu2+ with lysine enhancing bovine serum albumin modified-carbon dots fluorescent probe. Analyst 137(11):2637–2642

Liu S, Tang Z (2010) Nanoparticle assemblies for biological and chemical sensing. J Mater Chem 20(1):24–35

Liu S, Zhang HL, Liu TC, Liu B, Cao YC, Huang ZL, Zhao YD, Luo QM (2007) Optimization of the methods for introduction of amine groups onto the silica nanoparticle surface. J Biomed Mater Res A 80A(3):752–757

Lu C-H, Yang H-H, Zhu C-L, Chen X, Chen G-N (2009) A graphene platform for sensing biomolecules. Angew Chem Int Ed 48(26):4785–4787. doi:10.1002/anie.200901479

Mader HS, Kele P, Saleh SM, Wolfbeis OS (2010) Upconverting luminescent nanoparticles for use in bioconjugation and bioimaging. Curr Opin Chem Biol 14(5):582–596. doi:10.1016/j.cbpa.2010.08.014

Mandal TK, Parvin N (2011) Rapid detection of bacteria by carbon quantum dots. J Biomed Nanotechnol 7(6):846–848

Meallet-Renault R, Pansu R, Amigoni-Gerbier S, Larpent C (2004) Metal-chelating nanoparticles as selective fluorescent sensor for Cu2+. Chem Commun 20:2344–2345

Medintz IL, Trammell SA, Mattoussi H, Mauro JM (2004) Reversible modulation of quantum dot photoluminescence using a protein-bound photochromic fluorescence resonance energy transfer acceptor. J Am Chem Soc 126(1):30–31

Medintz IL, Uyeda HT, Goldman ER, Mattoussi H (2005) Quantum dot bioconjugates for imaging, labelling and sensing. Nat Mater 4(6):435–446

Minati L, Torrengo S, Maniglio D, Migliaresi C, Speranza G (2012) Luminescent graphene quantum dots from oxidized multi-walled carbon nanotubes. Mater Chem Phys 137(1):12–16

Mizsei J (2007) Gas sensor applications of porous Si layers. Thin Solid Films 515(23): 8310–8315
Na N, Liu T, Xu S, Zhang Y, He D, Huang L, Ouyang J (2013) Application of fluorescent carbon nanodots in fluorescence imaging of human serum proteins. J Mat Chem B 1(6):787–792
Navrotsky A (2003) Energetics of nanoparticle oxides: interplay between surface energy and polymorphism. Geochem Trans 4:34–37
Nikiforov TT, Beechem JM (2006) Development of homogeneous binding assays based on fluorescence resonance energy transfer between quantum dots and Alexa Fluor fluorophores. Anal Biochem 357(1):68–76
Oesterling I, Mullen K (2007) Multichromophoric polyphenylene dendrimers: toward brilliant light emitters with an increased number of fluorophores. J Am Chem Soc 129(15):4595–4605
Ow H, Larson DR, Srivastava M, Baird BA, Webb WW, Wiesner U (2005) Bright and stable core-shell fluorescent silica nanoparticles. Nano Lett 5(1):113–117
Palma A, Tasior M, Frimannsson DO, Vu TT, Meallet-Renault R, O'Shea DF (2009) New on-bead near-infrared fluorophores and fluorescent sensor constructs. Org Lett 11(16):3638–3641. doi:10.1021/ol901413u
Pan D, Zhang J, Li Z, Wu M (2009) Hydrothermal route for cutting graphene sheets into blue-luminescent graphene quantum dots. Adv Mater 22(6):734–738
Park S, Hamad-Schifferli K (2010) Nanoscale interfaces to biology. Curr Opin Chem Biol 14(5):616–622. doi:S1367-5931(10)00094-3 [pii] 10.1016/j.cbpa.2010.06.186
Park S, Ruoff RS (2009) Chemical methods for the production of graphenes. Nat Nanotechnol 4(4):217–224. doi:nnano.2009.58 [pii] 10.1038/nnano.2009.58
Park Y-S, Dmytruk A, Dmitruk I, Kasuya A, Okamoto Y, Kaji N, Tokeshi M, Baba Y (2010) Aqueous phase synthesized CdSe nanoparticles with well-defined numbers of constituent atoms. J Phys Chem C 114(44):18834–18840
Patel PD (2002) (Bio)sensors for measurement of analytes implicated in food safety: a review. TrAC Trends Anal Chem 21(2):96–115
Peng H-C, Kang C-C, Liang M-R, Chen C-Y, Demchenko A, Chen C-T, Chou P-T (2011) En route to white-light generation utilizing nanocomposites composed of ultrasmall CdSe nanodots and excited-state intramolecular proton transfer dyes. ACS Appl Mater Interfaces 3(5):1713–1720
Posthuma-Trumpie GA, Wichers JH, Koets M, Berendsen LB, van Amerongen A (2012) Amorphous carbon nanoparticles: a versatile label for rapid diagnostic (immuno) assays. Anal Bioanal Chem 402(2):593–600
Qhobosheane M, Santra S, Zhang P, Tan WH (2001) Biochemically functionalized silica nanoparticles. Analyst 126(8):1274–1278
Qin A, Lam JW, Tang BZ (2012) Luminogenic polymers with aggregation-induced emission characteristics. Prog Polym Sci 37(1):182–209
Qu L, Zhang Z, Zhang J, Chen N (2012) Graphene quantum dots: an emerging material for the energy-related applications and beyond. Energy Environ Sci 5(10):8869–8890
Rao KVN, Stevens PW, Hall JG, Lyamichev V, Neri BP, Kelso DM (2003) Genotyping single nucleotide polymorphisms directly from genomic DNA by invasive cleavage reaction on microspheres. Nucleic Acids Res 31(11)
Raymo FM, Tomasulo M (2006) Optical processing with photochromic switches. Chem Eur J 12(12):3186–3193
Rayno FM, Yildiz I (2007) Luminescent chemosensors based on semiconductor quantum dots. Phys Chem Chem Phys 9(17):2036–2043
Reisch A, Didier P, Richert L, Oncul S, Arntz Y, Mély Y, Klymchenko AS (2014) Collective fluorescence switching of counterion-assembled dyes in polymer nanoparticles. Nat Commun 5:4089
Reppy MA (2010) Structure, emissive properties, and reporting abilities of conjugated polymers. In: Demchenko AP (ed) Advanced fluorescence reporters in chemistry and biology II: molecular constructions, polymers and nanoparticles, Springer Ser Fluoresc 9:357–388
Riu J, Maroto A, Rius FX (2006) Nanosensors in environmental analysis. Talanta 69(2):288–301
Runnels LW, Scarlata SF (1995) Theory and application of fluorescence homotransfer to melittin oligomerization. Biophys J 69(4):1569–1583

Sapsford KE, Medintz IL, Golden JP, Deschamps JR, Uyeda HT, Mattoussi H (2004) Surface-immobilized self-assembled protein-based quantum dot nanoassemblies. Langmuir 20(18):7720–7728

Sapsford KE, Pons T, Medintz IL, Mattoussi H (2006) Biosensing with luminescent semiconductor quantum dots. Sensors 6(8):925–953

Schirhagl R, Chang K, Loretz M, Degen CL (2014) Nitrogen-vacancy centers in diamond: nanoscale sensors for physics and biology. Annu Rev Phys Chem 65:83–105

Schrand AM, Hens SAC, Shenderova OA (2009) Nanodiamond particles: properties and perspectives for bioapplications. Crit Rev Solid State Mater Sci 34(1-2):18–74. doi:10.1080/10408430902831987

Scott RW, Wilson OM, Crooks RM (2005) Synthesis, characterization, and applications of dendrimer-encapsulated nanoparticles. J Phys Chem B 109(2):692–704

Sedlmeier A, Achatz DE, Fischer LH, Gorris HH, Wolfbeis OS (2012) Photon upconverting nanoparticles for luminescent sensing of temperature. Nanoscale 4(22):7090–7096

Sedlmeier A, Gorris HH (2015) Surface modification and characterization of photon-upconverting nanoparticles for bioanalytical applications. Chem Soc Rev 44(6):1526–1560

Shcharbin D, Szwedzka M, Bryszewska M (2007) Does fluorescence of ANS reflect its binding to PAMAM dendrimer? Bioorg Chem 35(2):170–174

Shepard JRE (2006) Polychromatic microarrays: simultaneous multicolor array hybridization of eight samples. Anal Chem 78(8):2478–2486

Shiohara A, Hoshino A, Hanaki K, Suzuki K, Yamamoto K (2004) On the cyto-toxicity caused by quantum dots. Microbiol Immunol 48(9):669–675

Somers RC, Bawendi MG, Nocera DG (2007) CdSe nanocrystal based chem-/bio-sensors. Chem Soc Rev 36(4):579–591

Srivastava S, Kotov NA (2009) Nanoparticle assembly for 1D and 2D ordered structures. Soft Matter 5(6):1146–1156

Suh WH, Suh Y-H, Stucky GD (2009) Multifunctional nanosystems at the interface of physical and life sciences. Nano Today 4(1):27–36. doi:10.1016/j.nantod.2008.10.013

Sun Y-P, Luo PG, Sahu S, Yang S-T, Sonkar SK, Wang J, Wang H, LeCroy GE, Cao L (2013) Carbon 'quantum' dots for optical bioimaging. J Mater Chem B 1(16):2116–2127

Szollosi J, Damjanovich S, Matyus L (1998) Application of fluorescence resonance energy transfer in the clinical laboratory: routine and research. Cytometry 34(4):159–179

Tan CY, Alas E, Muller JG, Pinto MR, Kleiman VD, Schanze KS (2004) Amplified quenching of a conjugated polyelectrolyte by cyanine dyes. J Am Chem Soc 126(42):13685–13694

Tauer K, Ahmad H (2003) Study on the preparation and stabilization of pyrene labeled polymer particles in nonpolar media. Polym React Eng 11(3):305–318

Thomas SW 3rd, Joly GD, Swager TM (2007) Chemical sensors based on amplifying fluorescent conjugated polymers. Chem Rev 107(4):1339–1386

Tomczak N, Jańczewski D, Han M, Vancso GJ (2009) Designer polymer–quantum dot architectures. Prog Polym Sci 34(5):393–430. doi:10.1016/j.progpolymsci.2008.11.004

Torres-Costa V, Martín-Palma R (2010) Application of nanostructured porous silicon in the field of optics. A review. J Mater Sci 45(11):2823–2838. doi:10.1007/s10853-010-4251-8

Triulzi RC, Micic M, Giordani S, Serry M, Chiou WA, Leblanc RM (2006) Immunoasssay based on the antibody-conjugated PAMAM-dendrimer-gold quantum dot complex. Chem Commun 48:5068–5070

Veinot JGC (2006) Synthesis, surface functionalization, and properties of freestanding silicon nanocrystals. Chem Commun 40:4160–4168

Wang F, Banerjee D, Liu Y, Chen X, Liu X (2010) Upconversion nanoparticles in biological labeling, imaging, and therapy. Analyst 135(8):1839–1854

Wang J (2009) Biomolecule-functionalized nanowires: from nanosensors to nanocarriers. Chemphyschem 10(11):1748–1755. doi:10.1002/cphc.200900377

Wang L, Wang KM, Santra S, Zhao XJ, Hilliard LR, Smith JE, Wu JR, Tan WH (2006a) Watching silica nanoparticles glow in the biological world. Anal Chem 78(3):646–654

Wang X-L, Qin C, Wang E-B, Su Z-M, Li Y-G, Xu L (2006b) Self-assembly of nanometer-scale [Cu24I10L12]14+ cages and ball-shaped keggin clusters into a (4,12)-connected 3D framework

with photoluminescent and electrochemical properties. Angew Chem Int Ed 45(44):7411–7414. doi:10.1002/anie.200603250
Wang X, Peng Q, Li Y (2007) Interface-mediated growth of monodispersed nanostructures. Acc Chem Res 40(8):635–643. doi:10.1021/ar600007y
Wang Y, Bao L, Liu Z, Pang D-W (2011) Aptamer biosensor based on fluorescence resonance energy transfer from upconverting phosphors to carbon nanoparticles for thrombin detection in human plasma. Anal Chem 83(21):8130–8137
Wawrzynczyk D, Bednarkiewicz A, Nyk M, Cichos J, Karbowiak M, Hreniak D, Strek W, Samoc M (2012) Optimisation of ligand exchange towards stable water suspensions of crystalline NaYF4: Er3+, Yb3+ nanoluminophors. J Nanosci Nanotechnol 12(3):1886–1891. doi:10.1166/jnn.2012.5202
Wong KF, Bagchi B, Rossky PJ (2004) Distance and orientation dependence of excitation transfer rates in conjugated systems: beyond the Forster theory. J Phys Chem A 108(27):5752–5763
Wosnick JH, Liao JH, Swager TM (2005a) Layer-by-layer poly(phenylene ethynylene) films on silica microspheres for enhanced sensory amplification. Macromolecules 38(22):9287–9290
Wosnick JH, Mello CM, Swager TM (2005b) Synthesis and application of poly(phenylene ethynylene)s for bioconjugation: a conjugated polymer-based fluorogenic probe for proteases. J Am Chem Soc 127(10):3400–3405
Wróbel D, Graja A (2011) Photoinduced electron transfer processes in fullerene–organic chromophore systems. Coord Chem Rev 255(21):2555–2577
Wu C, Bull B, Szymanski C, Christensen K, McNeill J (2008) Multicolor conjugated polymer dots for biological fluorescence imaging. ACS Nano 2(11):2415–2423
Wu C, Schneider T, Zeigler M, Yu J, Schiro PG, Burnham DR, McNeill JD, Chiu DT (2010) Bioconjugation of ultrabright semiconducting polymer dots for specific cellular targeting. J Am Chem Soc 132(43):15410–15417
Wu C, Szymanski C, Cain Z, McNeill J (2007) Conjugated polymer dots for multiphoton fluorescence imaging. J Am Chem Soc 129(43):12904–12905
Wu CF, Szymanski C, McNeill J (2006) Preparation and encapsulation of highly fluorescent conjugated polymer nanoparticles. Langmuir 22(7):2956–2960
Xu B, Zhao C, Wei W, Ren J, Miyoshi D, Sugimoto N, Qu X (2012) Aptamer carbon nanodot sandwich used for fluorescent detection of protein. Analyst 137(23):5483–5486
Xu CT, Zhan Q, Liu H, Somesfalean G, Qian J, He S, Andersson-Engels S (2013) Upconverting nanoparticles for pre-clinical diffuse optical imaging, microscopy and sensing: current trends and future challenges. Laser Photonics Rev 7(5):663–697
Xu J, Liang J, Li J, Yang W (2010) Multicolor dye-doped silica nanoparticles independent of FRET. Langmuir 26(20):15722–15725
Yan X, Li B, Cui X, Wei Q, Tajima K, L-s L (2011) Independent tuning of the band gap and redox potential of graphene quantum dots. J Phys Chem Lett 2(10):1119–1124
Yang ZC, Wang M, Yong AM, Wong SY, Zhang XH, Tan H, Chang AY, Li X, Wang J (2011) Intrinsically fluorescent carbon dots with tunable emission derived from hydrothermal treatment of glucose in the presence of monopotassium phosphate. Chem Commun 47(42):11615–11617
Yao G, Wang L, Wu YR, Smith J, Xu JS, Zhao WJ, Lee EJ, Tan WH (2006) FloDots: luminescent nanoparticles. Anal Bioanal Chem 385(3):518–524
Yao H (2010) Prospects for organic dye nanoparticles. In: Demchenko AP (ed) Advanced fluorescence reporters in chemistry and biology. II. Molecular constructions, polymers and nanoparticles, vol 9, Springer series on fluorescence. Springer, Heidelberg
Yiidiz I, Tomasulo M, Raymo FM (2006) A mechanism to signal receptor-substrate interactions with luminescent quantum dots. Proc Natl Acad Sci U S A 103(31):11457–11460
Yun CS, Javier A, Jennings T, Fisher M, Hira S, Peterson S, Hopkins B, Reich NO, Strouse GF (2005) Nanometal surface energy transfer in optical rulers, breaking the FRET barrier. J Am Chem Soc 127(9):3115–3119
Zhai X, Zhang P, Liu C, Bai T, Li W, Dai L, Liu W (2012) Highly luminescent carbon nanodots by microwave-assisted pyrolysis. Chem Commun 48(64):7955–7957

Zhang JK, Zhang WL, Dong SM, Turner APF, Fan QJ, Jia SR (2007) Nano-porous light-emitting silicon chip as a potential biosensor platform. Anal Lett 40(8):1549–1555
Zhang L, Feng W (2007) Dendritic conjugated polymers. Prog Chem 19(2–3):337–349
Zhang X-F, Xi Q (2011) A graphene sheet as an efficient electron acceptor and conductor for photoinduced charge separation. Carbon 49(12):3842–3850
Zhang X, Zhang X, Tao L, Chi Z, Xu J, Wei Y (2014) Aggregation induced emission-based fluorescent nanoparticles: fabrication methodologies and biomedical applications. J Mat Chem B 2(28):4398–4414
Zhang Y, Wang T-H (2012) Quantum dot enabled molecular sensing and diagnostics. Theranostics 2(7):631
Zhao HX, Liu LQ, De Liu Z, Wang Y, Zhao XJ, Huang CZ (2011) Highly selective detection of phosphate in very complicated matrixes with an off–on fluorescent probe of europium-adjusted carbon dots. Chem Commun 47(9):2604–2606
Zhao X, Schanze KS (2010) Fluorescent ratiometric sensing of pyrophosphate via induced aggregation of a conjugated polyelectrolyte. Chem Commun 46(33):6075–6077
Zhou J, Liu Z, Li F (2012a) Upconversion nanophosphors for small-animal imaging. Chem Soc Rev 41(3):1323–1349
Zhou L, Lin Y, Huang Z, Ren J, Qu X (2012b) Carbon nanodots as fluorescence probes for rapid, sensitive, and label-free detection of Hg2+ and biothiols in complex matrices. Chem Commun 48(8):1147–1149
Zhu S, Tang S, Zhang J, Yang B (2012) Control the size and surface chemistry of graphene for the rising fluorescent materials. Chem Commun (Camb) 48(38):4527–4539. doi:10.1039/c2cc31201h
Zhu Z, Yang R, You M, Zhang X, Wu Y, Tan W (2010) Single-walled carbon nanotube as an effective quencher. Anal Bioanal Chem 396(1):73–83
Zou W, Visser C, Maduro JA, Pshenichnikov MS, Hummelen JC (2012) Broadband dye-sensitized upconversion of near-infrared light. Nat Photonics 6(8):560–564

Chapter 6
Fluorescent Nanocomposites

In previous Chapters we discussed different properties of fluorescence emitters in order to understand them and optimize them adapting for different sensing and imaging technologies. New unlimited possibilities are offered by composing the nanocomposites formed of different types of emitters. They display a variety of novel useful features and thus extend dramatically the information content of output data. Researcher can design them from different types of luminophores of molecular and nanoscale origin (Fig. 6.1), manipulating with their connection, interaction, formation of new surfaces and interfaces. Their fluorescence response can be modulated by electronic conjugation or by excited-state resonance energy transfer and coupled with other functionalities on nanoscale level.

The luminescent molecules and nanoparticles can serve as building blocks for achieving versatile functions that are not observed in separate emitters alone. These larger nanocomposites demonstrate dramatically increased brightness, the ability to

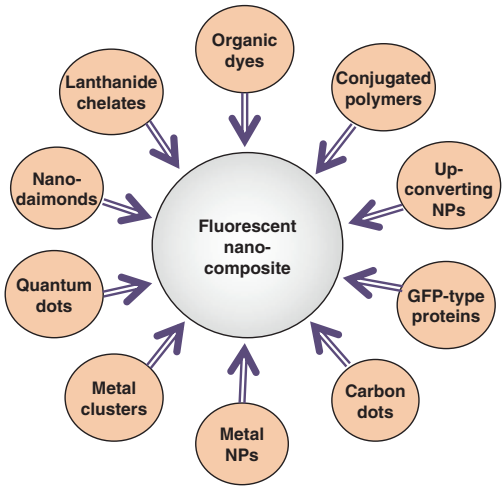

Fig. 6.1 Multitude of fluorescence reporters that can be used in design of nanocomposites

A.P. Demchenko, *Introduction to Fluorescence Sensing*,
DOI 10.1007/978-3-319-20780-3_6

concentrate emission on particular luminophores (antenna effect), shifting the emission spectrum to a desired extent (wavelength conversion), modulating emission anisotropy and lifetime. Such collective effects appear as a result of electronic conjugation and FRET. Their different combinations as FRET donors and acceptors are discussed here. New sensing technologies can be devised on this basis, which include multiplexing and multicolor coding in suspension arrays. On the level of nanocomposites fluorescence can be coupled with other functionalities, such as magnetic, NMR contrasting, etc.

6.1 Fluorescence Enhancement and Quenching in Nanocomposites

The luminescent materials presented schematically in Fig. 6.1 can be viewed as building blocks for achieving versatile functions that are not observed in separate emitters alone. In these larger nanocomposites the fluorescent intensity can be strongly enhanced (Fig. 6.2), and this can allow decreasing the *limit of detection* in analytical assays and the probe concentrations applied for imaging. The fluorophore *brightness* is defined as the product of absorbance by quantum yield of emission, and both these factors are equally important for achieving enhancement of emission intensity. We will discuss the existing possibilities for its substantial increase.

6.1.1 Assembling, Screening, Immobilization

The nanocomposites of increased brightness can be achieved by incorporating many dye molecules into nanostructures formed by organic or inorganic polymer (see Sect. 5.2). As we see in Fig. 6.2, different factors can be responsible for the

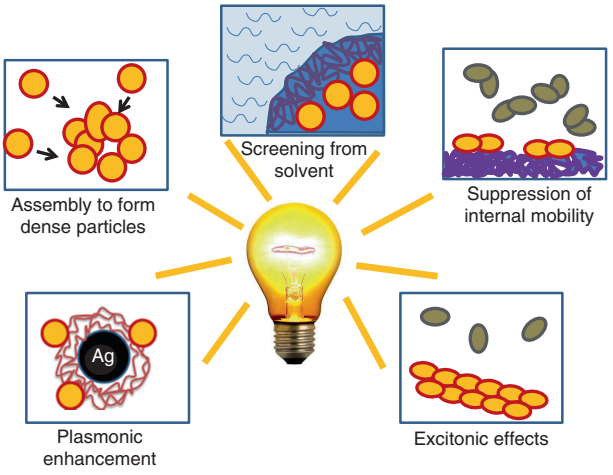

Fig. 6.2 Illustration of possibilities for enhancement of fluorescence emission upon the assembly of molecules and nanoparticles into nanocomposites. See text

enhancement of fluorescence emission on *dye assembly* into nanoparticles and nanocomposites. The most important of them is trivial. It is an increase in the absorption cross-section originated by the increase in the number of incorporated luminescent dyes (Wang et al. 2006b). Additional advantages of such incorporation could be the screening of dyes from direct molecular contact with the test medium and avoiding the dye degradation in aggressive media and also in living cells.

The results of *screening* the fluorescent dyes and luminophore moieties of nanoparticles from direct contact with polar solvents, especially water, can be dramatic. Low emission observed on dye contacting with solvent can be due to many different factors that are well described in the literature (de Silva et al. 1997). One of the most important of them is observed with the electron-rich emitters. Water molecules (and alcohols to a lesser extent) stochastically form in the bulk solvent the clusters with strong solvating power for electrons (the *electron traps*). The electron transfer from excited dye to such traps results in complete quenching (Moore et al. 1985). This effect explains very low fluorescence intensity of polarity-sensing charge transfer organic dyes. When it is removed, the dyes become shining brightly.

Many dyes possess flexible molecular structures. In solid environments they usually exhibit much higher quantum yields and lifetimes than in liquid milieu. This is due to stronger restrictions imposed by solid matrix on *rotation of dye segments*, to intermolecular collisions and to dielectric relaxations – all the factors that quench fluorescence (Riu et al. 2006). Moreover, the nanoparticles were designed that upon assembling the dyes demonstrate the *aggregation-induced emission* (Ding et al. 2013). For this purpose the dye molecules were selected that contain the internal structure elements rotating in solutions and thus possessing the pathways for non-emissive excitation decay of the excited states. Being immobilized inside the nanoparticles, they lose this mobility. Since the ultra-fast non-emissive decay associated with these motions is suppressed, the particles start to emit brightly.

Differently organized nanoparticles allow different organization of luminophores in realizing these principles. Thus, the dendrimer scaffolds allow selecting preferential location of reporter dyes – in the rigid core, at the porous periphery or at the particle surface (Ow et al. 2005). These possibilities can be realized not only with organic dye molecules but also with luminescent metal complexes (Lian et al. 2004; Qhobosheane et al. 2001). and luminescent metal ions (Balzani et al. 2000; Shcharbin et al. 2007).

6.1.2 Plasmonic Enhancement

Plasmonic enhancement can be considered as a general mechanism of increasing the brightness of different emitters. It operates on their interaction with plasmonic nanoparticles made of silver, gold and copper. The physical background of this effect and its different applications will be discussed in Sect. 10.7. Therein we will also overview the rather stringent requirements regarding the distances, orientations, spectral fitting and other factors influencing the enhancement. Here we discuss in short the enhancement effect that can be realized in nanocomposites.

Based on this effect, the composites can be constructed, in which fluorescent signal enhancement comes from the interaction between fluorophore and surface plasmon generated in metallic nanostructure. Its realization can be achieved with different configurations of composite (Stewart et al. 2008). For instance, quantum dot can be attached to metal particle covered with polymer layer (Ma et al. 2011) or the metal particles can be bound via covalently interfacing the QD surfaces (Fu et al. 2009). Efficient are also the core-shell structures, in which the dyes are located in the particle core, so that the shell is the plasmonic metal cover (Miao et al. 2010).

Gold and *silver nanoparticles* are also known as extremely potent fluorescence quenchers (Dulkeith et al. 2005). This ability can be used in combination with strong emitters such as the dyes and fluorescent nanoparticles. An immense variety of nanocomposites exhibiting plasmon-enhanced emission or efficient quenchers can be constructed. This allows achieving important goal to increase the output signal and thus to achieve lower limits of target detection in sensing and the images with highest contrast.

6.1.3 Excitonic Effects

Excitons are the mobile quasi-particles in the form of electron-hole pairs that appear in solid bodies and molecular associates upon electronic excitation. In conjugated polymers the weakly bound Frenkel-type excitons can migrate along the polymer chain and between the chains (see Sect. 5.3). It was shown that the mixing of high and low band-gap polymers in one nanoparticle can be very efficient in producing the enhancement effect. Due to exciton migration and energy transfer the composites with excellent absorbing (3.0×10^7 cm^{-1} M^{-1} at 488 nm), wavelength-converting and producing efficient deep-red emission (quantum yield = 0.56) were reported (Wu et al. 2011).

Excitons in large dye aggregates can be delocalized across many chromophores and may show coherent or incoherent energy transfer (Abramavicius et al. 2009). They can form ordered assemblies of various types, the limiting cases of which are H- and J-aggregates. Their properties can be described on dimer models (Fig. 6.3). *H-aggregates* are formed by side-by-side association, their absorption spectra are shifted to shorter wavelengths and fluorescence is almost absent. In contrast, *J-aggregates* are characterized by the appearance of new very sharp and strongly enhanced in intensity band in absorption spectrum shifted to longer wavelengths and a very bright and often sharp band in fluorescence emission (Würthner et al. 2011). Their cooperative behavior is manifested by Davydov splitting in absorption spectra. Additionally, the absorption and fluorescence bands are *narrower* because of motional and exchange narrowing that dynamically average these properties over the inhomogeneous distribution of energies.

Very efficient excitonic enhancement effects can be observed on aggregation of cyanine and squaraine dyes (see Sect. 4.2). Many of these dyes are low soluble and almost nonfluorescent in aqueous solution. Thus, a very weak emission is observed for dye CN-MBE (1-cyano-*trans*-1,2-bis-(4′-methylbiphenyl)ethylene) in solution,

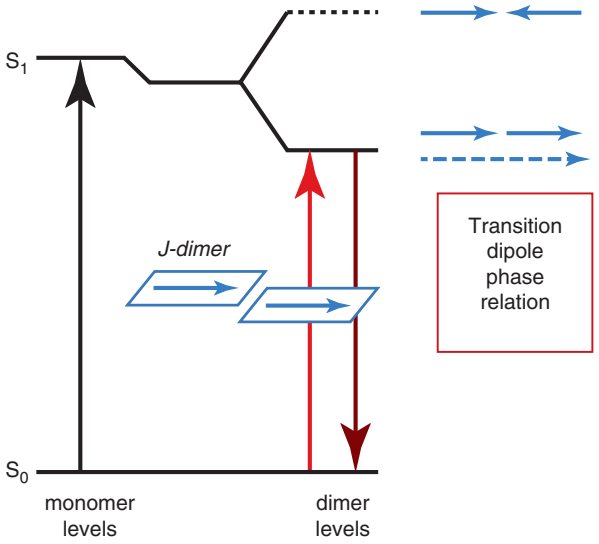

Fig. 6.3 The exciton model in spectroscopy (Kasha et al. 1965). The H-type dimers (not shown) are formed by side-to-side association and their fluorescence is quenched. In contrast, in J-type dimer the transition dipoles are in line. They exhibit a red-shift in the absorption and an increase in the transition dipole moment increasing the probability of light absorption. Their emission is bright, it takes place from the lowest energy excited electronic state (Kasha's rule) and can exhibit very narrow spectral bands

but the intensity is increased by almost 700 times in the nanoparticles (An et al. 2002) . Such strong enhancement was attributed to the synergetic effect of intramolecular planarization and J-type aggregate formation (restricted excimer formation) in nanoparticles.

Normally, the formation of dye J-aggregates needs a scaffold, and such scaffolds could be polymer nanoparticles, quantum dots (Halpert et al. 2009), macromolecules of DNA (Losytskyy et al. 2002), see Fig. 4.6, or protein molecules (Xu et al. 2010). It was shown that fluorescence intensity (at $\lambda_{em} \approx 690$ nm) of a squaraine dye increases by a factor of up to 200 upon addition of bovine serum albumin (BSA) due to formation of J-aggregates, suggesting this effect as a tool for protein detection. In the case of quantum dot – J-aggregate composites the effect of resonance energy transfer was clearly seen resulting in complete quenching of fluorescence of the donor and the appearance of very narrow and very bright fluorescence band characteristic of J-aggregate (Fig. 6.4). The J-aggregates of cyanine dyes can be also formed with the aid of plasmonic gold nanoparticles inducing their assemblies (Lim et al. 2006). Thus, a new route in designing nanocomposites that combine plasmonic and excitonic effects is opened (Saikin et al. 2013).

6.1.4 Exciton-Exciton and Plasmon-Exciton Interactions in Nanocomposites

Among different possibilities of assembling fluorescent molecules and nanoparticles into composites the combination of emitters with different background mechanisms is the most interesting but least explored. In nanocomposite presented in Fig. 6.4 the cyanine J-aggregate displaying Frenkel-type excitons and quantum dot

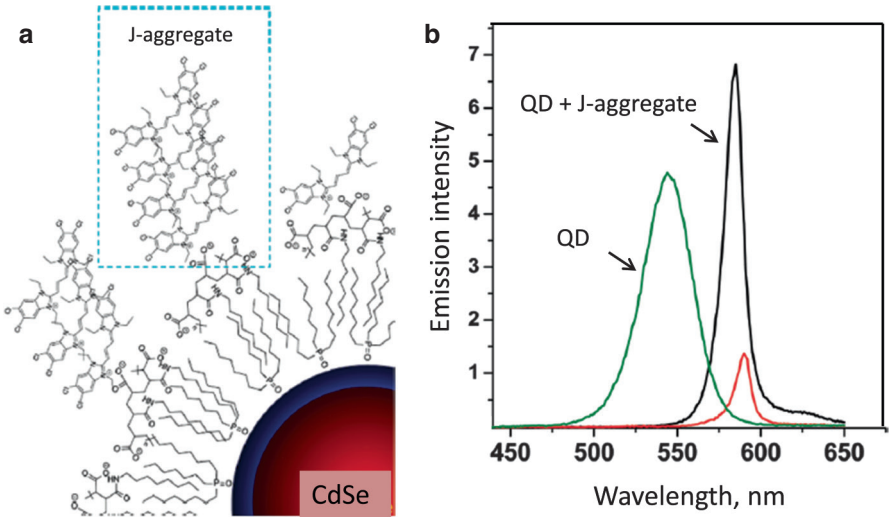

Fig. 6.4 J-aggregates as FRET acceptors (Halpert et al. 2009). (**a**) The nanocomposites construction consisting of CdSe quantum dot covered with the anionic polymer layer and assembled J-aggregate of carbocyanine dye. (**b**) Photoluminescence spectra under 375 nm excitation of the QD/carbocyanine solution before aggregation (*green curve*), and of the QD/J-aggregate constructs (*black curve*) and J-aggregates in the absence of QDs (*red curve*). The QD emission is almost completely quenched by the dye aggregates, and the emission intensity of the solution is significantly higher than for dye aggregated in the absence of QDs, with identical monomer concentrations

generating Wannier-Mott excitons interact via a layer of polymeric molecules. The interaction of species possessing different types of collective excitation can also be in direct way, extending spatially through electronic coupling between the components. For these and other exciton-generating species, interaction with metal nanoparticles may present a new interesting case of *exciton–plasmon* interactions that goes beyond plasmon enhancement.

The *size* and assembly of nanocomposites are the important parameters in nanosensor design, since in quantum dots, conjugated polymers or organic dye aggregates the exciton size is dictated instead of electron–hole interactions by the physical dimension and organization of the nanoscale system. *Energy* variables are also important, since the exciton migrates to the sites with the lowest band-gap and this must result in red-shifted emission. It was shown that mixing in a single nanoparticle of high and low band-gap polymers is very efficient, resulting in high absorbance and fluorescence quantum yield of red-shifted emission (Wu et al. 2011). Heterocomposites of conjugated polymers and quantum dots (Chan et al. 2012) demonstrated high brightness in the red and near-IR region.

Of particular interest are the systems based on *plasmon* interactions with *excitons* generated in the dye J-aggregates (Wiederrecht et al. 2004), which are known to generate very sharp bands in electronic spectra (Zheng et al. 2010). The emission

of highly mobile excitons in conjugated polymers can also be strongly enhanced on interaction with plasmonic nanoparticles, and different hybrids have been suggested that display this effect (Tang et al. 2011) that has found application in DNA sensing (Geng et al. 2011).

Concluding, we indicate that the coupling of localized excitations with collective effects in excitation (excitons and plasmons) has great potential for modulating the excitation and emission properties of hybrid nanoscale materials in the desired direction. This area is open to active research and soon we expect many interesting results and important applications.

6.2 Modulation of Emission Parameters in Multi-Fluorophore Systems

In this Section we focus on the abilities of nanocomposites to alter the fluorescence emission parameters of constituting components. Light harvesting, wavelength shifting, lifetime extension, red-edge repolarization sole or together can change fluorescence outputs in desired direction. This opens new avenues in optimizing the imaging and enhancement in sensor response.

6.2.1 Homo-FRET and Hetero-FRET

Usually in textbooks, FRET is presented as a binary event occurring between single donor and single acceptor. Meantime, when many such FRET donors and acceptors assemble in a small particle and appear within the critical distance, they lose their individuality and new collective effects appear (Demchenko 2013). One of these effects, the concentrational quenching (self-quenching) we already discussed in Sect. 5.2 in relation to nanoparticles formed by assembling organic dyes in polymeric and silica matrices or by their own self-assembly. Here we had clear example of *homo-FRET*, the excitation energy transfer between fluorophores of the same structure. Like for classical *hetero-FRET* (the transfer between different types of fluorophores), for homo-FRET the overlap between emission spectrum of the donor and absorption spectrum of the acceptor is the necessary condition (Sect. 3.6). Since in homo-FRET the donor and acceptor molecules are the same, its efficiency is determined by the Stokes shift. The smaller shift – the higher is the efficiency of transfer.

Location in close proximity of a number of dye molecules exhibiting both homo-FRET and hetero-FRET allows realizing many interesting possibilities that will be discussed below. One of them is shifting gradually the emission spectrum by proper choice of acceptor dye without altering the light absorption properties. This may be useful for *multiplex assays* (single excitation and several emissions for several sensors). Moreover, impregnation of nanoparticles with a number of different dyes serving as both donors and acceptors will make the particles efficient *wavelength converters* with emissions over the whole visible range extending to near-infrared.

The other possibility is to increase the *brightness* of the acceptor by transferring the excited-state energy from the donors. In this case, the donors may serve as '*antennas*', lighting-up the acceptor and increasing in this way the sensitivity of its response.

6.2.2 General Rules for Collective Effects in FRET

We begin this sub-section with formulation of three rules that are important for explanation of the *collective effects* in the excited-state energy transfer in a system composed of different types of light emitters participating in the energy transfer process.

1. In a system composed of structurally similar dyes located in identical environments and possessing identical absorption and emission spectra and also quantum yields and lifetimes, FRET (in this case *homo-FRET*) is just the *exchange of energies* between the dyes that is *undetected by spectroscopic or lifetime measurements*. It can only be revealed by the measurements of anisotropy and only in the case if the dyes occupy different orientations in space and their orientations do not change fast on the scale of fluorescence decay (solid or highly viscous dye environments). This rule follows from the identity of all parameters determining the FRET efficiency (Sect. 3.6) and from the kinetic scheme, in which the forward and reverse transfer rates are equal and higher than the rates of non-emissive and emissive transfers to the ground state.
2. In a system composed of structurally similar dyes possessing identical fluorescence spectra but exhibiting static quenching the effect of *quenching* will be observed *for the whole system*. The quenching efficiency will be determined by the dye with shortest lifetime τ. This follows from the kinetic scheme in which for this dye the rate of non-radiative deactivation of the excited state is comparable or faster than the rate of energy transfer. If the transfer is efficient and this dye is fully quenched, then we will observe quenching in the whole ensemble.
3. In a system composed of structurally dissimilar dyes (or similar dyes located in different environments) possessing different excitation and emission spectra *the transfer will be directional* from the dyes possessing short-wavelength to that possessing long-wavelength absorption and emission spectra (with the account of rule 2). This is because of overlap integral J for the transfer being larger if the donor emission is at shorter and acceptor absorption is at longer wavelengths than in the opposite case (see Fig. 3.13). Thus, the energy will flow from blue (short-wavelength) to red (long wavelength) emitters.

The latter case is the case of *hetero-FRET*. In the case if the transfer is efficient, the *quenching* of final acceptor quenches the whole ensemble. In a general case, the transfer and the quenching efficiencies are determined by the interplay of rate constants of all transformations of the excited states, starting from that of initially excited donor (Varnavski et al. 2002).

Based on these rules one can easily describe the effect of '*superquenching*' that can be observed in dye-doped polymeric particles, in conjugated polymers and

dendrimers (Chap. 5). Moreover, manipulating with a single trigger dye, one can provide efficient collective sensor response by switching on and off the whole ensemble of fluorescence emitters.

6.2.3 *Light-Harvesting (Antenna) Effect*

One of collective effects realized in nanoparticles is the *light harvesting* that can be observed when a large number of strong light-absorbing FRET donors, when excited, transfer their energy to a much smaller number of acceptors generating their much brighter emission (Scholes et al. 2001).

The antenna effect is illustrated in Fig. 6.5. The necessary conditions for its efficient implementation are the *high molar absorbance* of antenna dyes, *efficient energy transfer* to acceptor dye and *high quantum yield* of emission of the latter. Such system of signal transduction allows providing the response in sensor operation on several steps: energy exchange (homo-FRET) and quenching in antenna system, energy transfer to the acceptor and quenching of the acceptor emission. The possibility to manipulate with reporter properties of acceptor is retained. It may be the environment-sensitive two-band or wavelength-shifting dye or the dye forming exciplexes (Chap. 4). The acceptor spectroscopic properties should not be different from those observed on its direct excitation but can be seen on a much brighter level.

It is interesting that this principle of *light-harvesting* is used in the natural systems of photosynthesis that collect an enormous amount of solar energy by exciting the so-called antenna pigments and re-directing it to a small number of reaction centers where it is converted into redox chemical energy. So, this principle is very

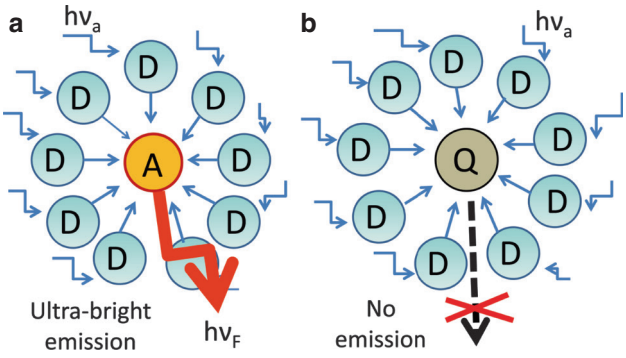

Fig. 6.5 Collective effects observed within the system of multiple fluorophores connected with efficient FRET. (**a)** Light-harvesting. Many donors (*D*) serving as antennas donate their excitation energies $h\nu_a$ to small number of acceptors (*A*) that emit light of energy $h\nu_F$ much brighter than it should be on their own excitation.(**b)** Superquenching. Instead of bright acceptor there is an acceptor with efficiently quenched emission (*Q*). Collecting the excitation light from the whole system, the quencher suppresses all its emission

general and it may be used for optimizing fluorescence (and, in general, luminescence) properties of many molecular and supramolecular systems, from dimers of organic dyes to coupled conjugated polymers (Wu et al. 2011) and complex nanocomposites (Chen et al. 2005; Frigoli et al. 2009). For instance, such 'antenna effects' are also in the background of dramatic increase of luminescence of weakly absorbing lanthanide ions when they form coordination complexes with strongly light absorbing ligands (Sect. 5.5).

With new fluorescent materials the choice of donors, acceptors, their relative concentrations, etc. can be very efficient. An example of such solution can be found in the work on blended conjugated polymer nanoparticles (Huang et al. 2007). A 90 % of conversion of blue light into green, yellow and red emissions was achieved by addition of less than 1 % of polymer emitting at these wavelengths. It was stated that because of such composition the fluorescence brightness of the blended polymer nanoparticles can be much higher than that of inorganic quantum dots and dye-loaded silica particles of similar dimensions.

It is known also that the major bottleneck in practical applications of up-converting nanoparticles (Sect. 5.6) is their low quantum yield. The light harvesting by energy transfer from the near-IR emitting cyanine dyes IR-780 serving as an antennas resulted in dramatic enhancement (by a factor of ~3300) of fluorescence intensity by the composite (Fig. 6.6). The proposed concept (Zou et al. 2012) can be extended to cover any part of the spectrum by using a set of dye molecules with overlapping absorption spectra acting as an extremely broadband antenna system connected to suitable upconverters.

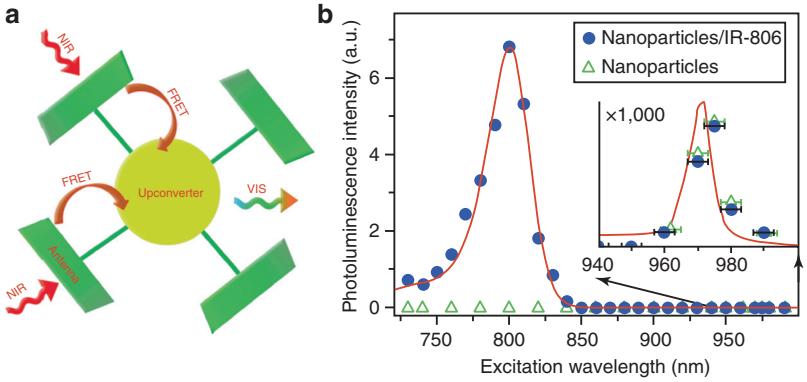

Fig. 6.6 Light harvesting excitation of up-converting nanoparticles (Zou et al. 2012). (**a**) Principal concept. Antenna dyes (*green*) absorb near-IR light and transfer it to the particle core (*yellow*), where up-conversion occurs. (**b**) Experimental up-conversion excitation spectra of b-$NaYF_4$:Yb,Er NPs/IR-806 dye (*blue circles*) and b-$NaYF_4$:Yb,Er NPs (*green triangles*), both dissolved in $CHCl_3$. The emission intensity is integrated in the 500–685 nm range upon excitation from a 2 mW CW laser. The red line shows the squared absorption spectrum. Inset: wavelength range from 940 to 1000 nm, magnified by a factor of 1000

A dramatic increase of fluorescence emission intensity of the acceptor dye due to 'focusing of antenna' compared to direct excitation some authors call an 'amplification'. It should be stressed, that in contrast to cases discussed in Sect. 6.1 there is no amplification on the level of acceptor dye, since its absorbance and quantum yield do not increase. All what happens is that via antenna it becomes excited much more frequently than on common direct excitation. This is the reason of its highly increased apparent brightness.

Photostability of acceptor dyes is important, since the increase of the frequency of the acts of photoexcitation results also in their accelerated photodegradation (Forde and Hanley 2005).

6.2.4 Wavelength Converting

Manipulating with hetero-FRET one can design the efficient '*wavelength converter*'. One can choose the primary donor with the excitation spectrum that ideally fits the used light source and the final acceptor with position of emission maximum at the desired wavelength. This wavelength can be chosen throughout all visible range, down to near-IR. The transfer, in which several different dyes provide the chain of transfer events for achieving a very significant shift in emission wavelength (as shown in Fig. 6.7), is called a '*cascade energy transfer'* (Serin et al. 2002). If the goal is in obtaining bright emission of final acceptor, it is important on this pathway to avoid the self-quenching interactions of the dyes, the 'light traps'. The 'intermediate' dyes serving as both donors and acceptors may be needed to fill the gap in the energy transfer chain. By fusing organic dyes (Ziessel and Harriman 2011) or semiconductor nanoparticles (Rogach et al. 2009), cascades with different wavelength-converting properties have been devised.

From the description of FRET effect (Sect. 3.6) one can derive that, though this process is reversible, it is always shifted towards the decrease of excitation energy resulting in the appearance of acceptor emission spectra at longer wavelengths (see Fig. 3.13). The reverse transfer is low probable, since this requires the overlap integral between long wavelength emitting donor and short wavelength absorbing acceptor. In an ensemble of fluorescence emitters, the result is in directional energy flow from short- to long-wavelength emitters (Stein et al. 2011).

Thus, by selecting the dyes with optimal spectral overlap one can excite fluorescence at short wavelength and obtain emission at much longer wavelengths. Operating with such '*wavelength converter*' (Varnavski et al. 2002) and combining several connected by FRET emitters displaying sequentially shifted excitation and emission spectra, one can shift fluorescence spectrum of the terminal acceptor over the whole visible range maintaining the short-wavelength excitation (e.g. near-UV) in the desired range. This can be achieved in cascade manner in a sequence of dyes, in which an energy acceptor of one step can serve as the donor to the dye on another step (Fig. 6.7).

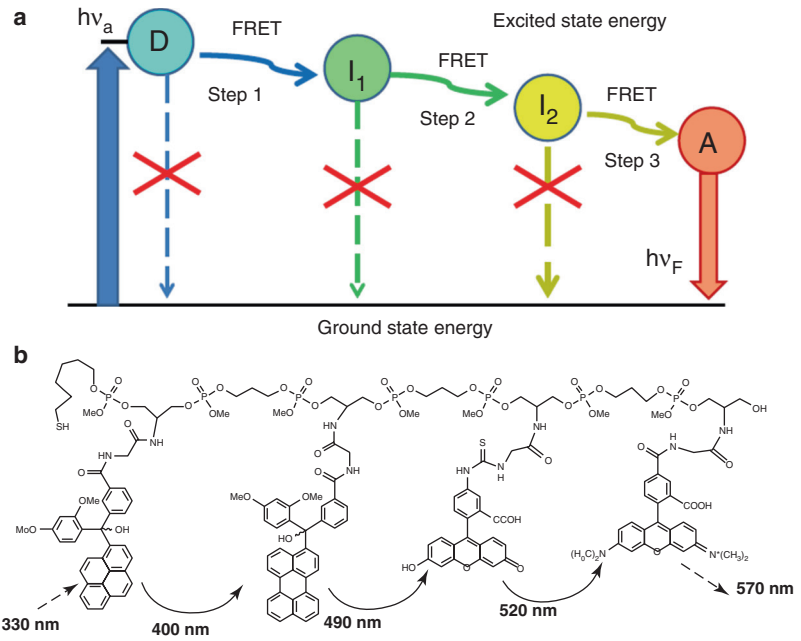

Fig. 6.7 The cascade system operating as the wavelength converter based on multi-step FRET (Demchenko 2013) (**a**). The primary donor (*D*) is excited by short-wavelength energy quanta $h\nu_a$. This energy is transferred without emission to intermediates (I_1) and (I_2) that serve as both donors and acceptors transmitting their excitation energy to final acceptor (*A*). The later emits light of very different energy $h\nu_F$. This emission though red-shifted on wavelength scale occurs with the lifetime of the donor D. (**b**) Sequential energy transfer across four chromophores tethered to a single-stranded acyclic backbone (Schwartz et al. 2010)

For such '*cascade energy transfer*' one can select the primary donor with the excitation spectrum that ideally fits the used light source and the final acceptor with the position of emission maximum at the desired wavelength optimal for the assay throughout all visible range, down to near-IR (Serin et al. 2002). A required combination of organic dyes can be easily assembled within silica nanoparticles (Wang et al. 2006a; Rampazzo et al. 2014).

Recent literature contains many examples for constructing the 'cascades' (Haustein et al. 2003). Usually they are made by covalent linking of monomer dyes, which allows strict control of their stoichiometry. Such are the pyrene-BODIPY molecular dyads and triads (Ziessel et al. 2005). Efficient energy flow was reported in a purpose-built cascade molecule bearing three distinct chromophores attached to the terminal acceptor (Harriman et al. 2008). A combinatorial approach with the selection of the best hits can be applied using the assembly of fluorescent oligonucleotide analogs (Gao et al. 2002).

Removing and adding the intermediates in a cascade FRET process and in this way modulating the emission color one can produce strong signals in λ-ratiometry

(Watrob et al. 2003). Such multi-color measurements can be efficiently applied in flow cytometry (Fábián et al. 2013).

One can combine the *light-harvesting* and *cascade-transfer* wavelength shifting. Moreover, the generation of 'superquenching' effects (Sect. 6.1) can be easily produced in cascades and under the action of light harvesters. So, if the FRET is efficient, the quenching of final acceptor quenches the whole ensemble (see Fig. 6.5b). This opens enormous possibilities in sensor design.

6.2.5 *Extending the Emission Lifetimes*

Fluorescence probing and sensing with emitters exhibiting *long lifetimes* has a great advantage by allowing the rejection of typically shorter background emission (see Fig. 3.11). This is very beneficial, particularly, for increasing the contrast in cell imaging. To address this demand, different nanocomposites were suggested, in which the long-lifetime emitter (e.g. lanthanide complex) is the *FRET donor*, and the strongly responding fluorophore (e.g. organic dye) is the *acceptor*. The fact that in cascade energy transfer the acceptor, changing the wavelength of its emission, retains the emission lifetime of the donor, τ_D, is illustrated in Fig. 6.8. In this combination the acceptor can emit light with an unnatural very long lifetime retaining its own spectroscopic response (Bunzli and Piguet 2005).

Such changes in emitter properties occur because in a donor-acceptor system connected by FRET the donor lifetime determines the lifetime of the acceptor (Hildebrandt et al. 2007). This follows from kinetic scheme of this reaction (Charbonniere et al. 2006) describing continuous energy transfer during the lifetime of the donor resulting in emission of acceptor on a much longer scale than on direct excitation. The chromophores that are not at the proper distance or do not exhibit necessary for the occurrence of FRET spectral coupling will not extend their lifetimes. This allows rejecting the background emission (Morrison 1988).

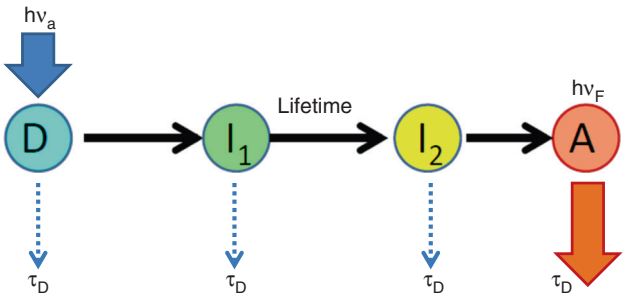

Fig. 6.8 The cascade system similar to that in Fig. 6.7, in which donor *D* has the longest lifetime. Though red-shifted on wavelength scale, this emission occurs with the unchanged lifetime τ_D of the donor and in this way the final acceptor *A* can emit light with strongly prolonged lifetime

6.2.6 *Variations of Anisotropy*

Organic dyes typically possess a high level of *optical anisotropy* detected as polarization of emission when excited by polarized light. The polarized incident light excites selectively the species in particular orientation and they emit *polarized light* (see Sect. 5.3). The necessary condition of that is the absence of rotational mobility of a fluorophore or of the particle in which it is embedded during the emission lifetime. The dyes in polymeric nanobeads can be rigidly fixed in them and their rotations are usually slow on nanosecond scale, so a high level of anisotropy can be observed.

This cannot always be so, since the other condition is the *absence of FRET*, which depolarizes the emission. In densely packed multi-fluorophore structures it is hard to avoid homo-FRET, and in its presence the anisotropy of observed emission decreases dramatically, often to zero level. This is because the orientations of donors and acceptors are usually not the same, and in the case of multiple transfers and random orientation of acceptors, the information on initial polarization is lost. In an ensemble of similar emitters the drop in anisotropy is the major indicator of the presence of homo-FRET.

This seemingly discouraging result may lead to quite positive consequences. There is a possibility of manipulating with the homo-FRET efficiency by variation of excitation wavelength within the absorption band generating the so-called Red Edge effect (Demchenko 2002; Demchenko 2008). In this way the emission anisotropy can be changed from its low values observed at the band maximum to its high values (demonstrating suppression of FRET) by *shifting the excitation* to the red (long wavelength) edge of absorption band (Fig. 6.9).

This phenomenon that was first observed by Gregorio Weber in 1970 can be explained by the effect of photoselection within an ensemble of fluorescence emitters connected by FRET (Demchenko 2002). Even if these emitters are the same molecules and exhibit homo-FRET, their local environments and interactions with these environments differ. The recorded absorption spectrum being a superposition of individual spectra is "*inhomogeneously broadened*". At the band maximum and shorter wavelengths the energy of incident light is sufficient to excite any fluorophore in the ensemble and transfer this energy to any other fluorophore, which results in low anisotropy of emission. At the 'red edge' the situation is different. The incident light selects those emitters that have the lowest excitation energy and, correspondingly, the lowest energy of emission that cannot be transferred to any other fluorophore. So the species selected at the red edge are unable to serve as FRET donors and they emit themselves highly polarized light (Demchenko 2002; Demchenko 2008).

Thus, the drop of anisotropy occurring on homo-FRET is quite different from that observed on fast rotational motions, so that 'anisotropy sensing' becomes not possible in the systems exhibiting FRET. Distinguishing the two caused of depolarization (rotations and FRET) is possible only by variation of excitation wavelength. Fluorophore rotations should not depend on the excitation energy, but in the case of homo-FRET repolarization occurs at the red edge of excitation spectrum.

This effect opens the ways of manipulating with emission anisotropy by creating or avoiding the FRET conditions. It has got interesting application in fluorescence *polarization microscopy* for detecting the interactions between the molecules within

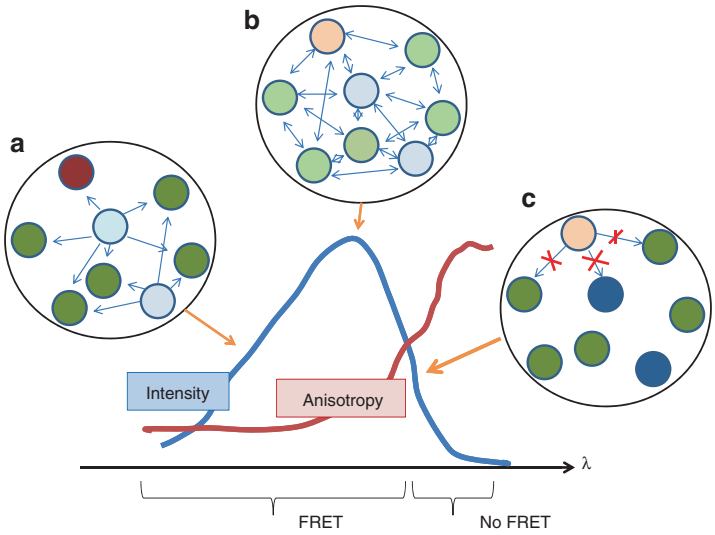

Fig. 6.9 The scheme explaining the Red-Edge effect as site-photoselection within the population of fluorescence emitters and the disappearance of FRET at the red edge of excitation spectrum that results in repolarization (Demchenko 2013). The system composed of similar molecules located within the distances of efficient homo-FRET is shown. At shorter wavelengths (case **a**) and band maximum (case **b**) the emitters exhibiting different interactions with the environment (marked with different colors) have equal probability to absorb light and transfer the excitation energy to its neighbors, which dramatically decreases the anisotropy. At long wavelength edge (case **c**) the species absorbing and emitting the low energy quanta are excited only. They do not exhibit FRET and their emission is highly polarized

the living cells (Squire et al. 2004). Homo-FRET allows single labeling in contrast to more difficult double labeling that is normally used for observing proximity effects in a hetero-FRET system.

6.2.7 Modulation by Light

Switching of emission in energy transfer cascade can be achieved by incorporation of *photochromic dyes*, whose intrinsic property to absorb and emit light is controlled by external light sources. They can also serve as key components of the systems operating by FRET mechanism (Sect. 3.6). In these composites different fluorophores (organic dyes, conjugated polymers, fluorescent proteins, quantum dots, etc.) can be used as the donors and photochromes as acceptors. Key role is played by these FRET acceptors, which can be switched reversibly between colorless *spiropyran* and colored *merocyanine* forms upon alternating irradiation with UV and visible light. In such composed *photochromic* systems, by the same excitation of the donors the emission can be switched reversibly between a fluorescent ON and a non-fluorescent OFF state (see Fig. 3.15). Since the process is reversible, the

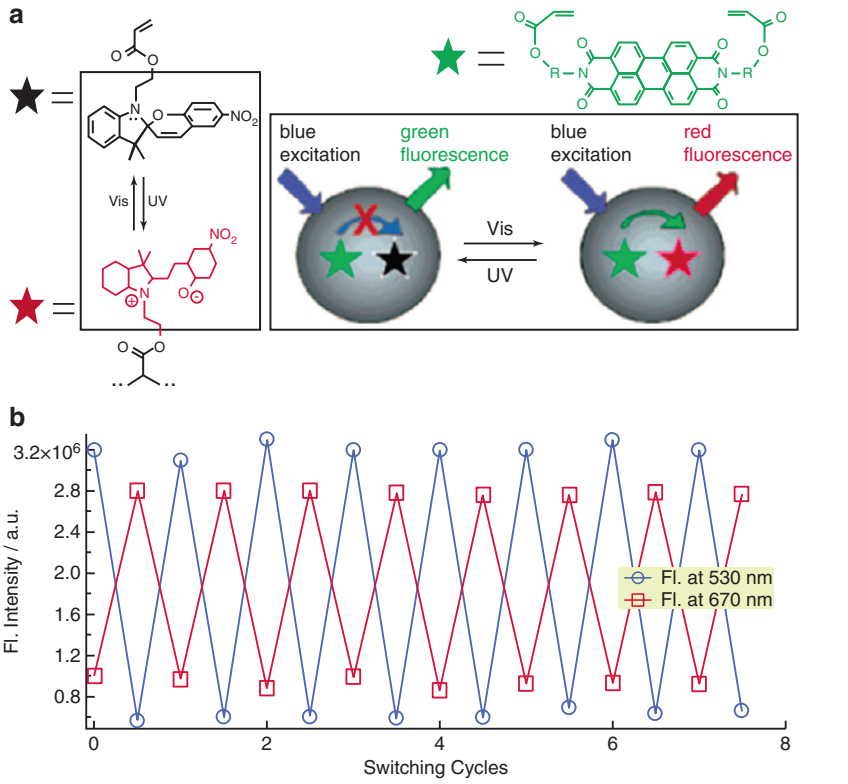

Fig. 6.10 The design principle of photoswitching nanocomposite based on polymersome stabilized by quantum dot (Díaz et al. 2013). (**a**) Lucifer Yellow dye (*marked green*) was used as the donor and diheteroarylethenes (*marked blue*) as acceptors being attached to amphiphilic polymer forming polymersomes. (**b**) Light induced switching between emissive and non-emissive forms of photochrome generates modulation in two-color fluorescence emission

fluorescent light intensities can oscillate between the FRET donor and acceptor emissions providing ON-OFF switching at each act of photoinduced transformations by light (Tian et al. 2009; Giordano et al. 2002; Jares-Erijman and Jovin 2003).

Among different photochromes, diheteroarylethenes (Fig. 6.10) present many advantages (Giordano et al. 2002) that have to be realized in nonpolar media. Therefore, for making them useful in bioimaging, the water-soluble nanoparticles with amphiphilic properties hosting them were created (Díaz et al. 2013). Lucifer Yellow dye was used as the donor and diheteroarylethenes as acceptors. Both of them were covalently bound in multiple copies to an amphiphilic polymer to create dual polarity particles in the form of polymersomes. Quantum dots were incorporated into the core of composed nanoparticle, serving as a stabilizing template. The designed architecture (Fig. 6.10) was used to increase the efficiency of the donor dye and to provide dual-color self-referenced emission at single excitation wavelength.

In photochromic composites, *quantum dots* can play a more active role being FRET donors providing excitation energy to photochrome groups coating them.

The advantage here is their large ultraviolet-visible absorption cross-section and broad range of wavelengths that can be used for excitation (Díaz et al. 2015).

There are many implications of such photochromic systems. For instance, the photochrome can be incorporated at each site of *wavelength converter* cascades described above (see Fig. 6.7), which allows switchable by light termination of change of emission color with restoration of donor emission. Moreover, the whole process may start in the near-IR by using up-converting nanoparticles (Zhang et al. 2012). Major applications of such nanocomposites are expected in fluorescence microscopy, particularly with super-resolution capability.

6.2.8 *Looking Ahead*

Concluding this section, we stress that the combination of different types of fluorophores, such as inorganic luminescent nanocrystals, organic dyes, and genetically encoded fluorescent proteins offers a promising route for the fabrication of multichromophore systems generating new properties that allow modulating the fluorescence response in very broad ranges (Table 6.1).

The collective spectroscopic effects can be both negative (e.g. formation of nonfluorescent dimers and concentrational quenching) and strongly positive (light-harvesting, wavelength-shifting, lifetime-extending and superquenching). Exploration of photo-

Table 6.1 Summary of techniques used for modulation of fluorescence response in nanocomposites

Effect achieved	Technique	Mechanism	Modulated parameter
Enhancement and modulation of intensity	Plasmonic enhancement	Interaction of different fluorescent emitters with noble metal NPs producing plasmonic effect	Quantum yield
Enhancement and modulation of intensity	Doping into polymers	Assembly of many emitters in a nanoscale volume	Molar absorbance
Enhancement and modulation of intensity	Light harvesting	Excitation of small number of emitters by energy transfer from large number of FRET donors	Molar absorbance and FRET efficiency
Shift of emission wavelength to a desired range	Wavelength conversion	Using cascade of sequential FRET reactions	Excitation and emission wavelengths
Extension of lifetime	Modulation of FRET acceptor decay	FRET from long lifetime donor to short lifetime acceptor	Fluorescence lifetime
Repolarization of fluorescence emission	Red Edge effect	Suppression of FRET on excitation at the red edge	Fluorescence anisotropy
Switching of fluorescence color	Photochromism	Reversible light-induced switching between two forms of FRET acceptor	Two-band ratiometry

physical mechanisms that govern interactions with and between fluorescence emitters allows modulating their fluorescence response in desired direction, practically at will. Excitation and emission can be set at any desired wavelength, and switching between different wavelengths can be regulated easily. The brightness can be dramatically enhanced allowing the possibility of complete quenching in the response of a sensor. The emission lifetimes can be increased by several orders of magnitude and manipulated within broad ranges. The near-IR region has started to be actively explored for excitation with convenient observation of emission in the visible.

In sensing applications the broad-scale variation of fluorescence parameters must be used with great benefit. Thus, a possibility can be realized, in which the FRET donors providing the light harvesting at the beginning of wavelength conversion cascade bring to final emitter a very strong emission intensity with its depolarization and long lifetime. The 'superquenching' and modulation by light can be activated in such systems. This opens enormous possibilities in sensor design.

6.3 Optical Choice of FRET Donors and Acceptors

With our knowledge of the properties of a variety of fluorescent materials, of their use as reporters and of new effects that appear on their assembling into nanoparticles and nanocomposites we can discuss the construction of these assembles in the most optimal way. In the discussion that follows we make an attempt to provide systematic analysis of usage of different types of fluorophores as donors or acceptors in FRET (Demchenko 2013) (Fig. 6.11).

The donors should be the most *efficient absorbers* and the *brightest emitters* and, as a favorable property, possess long lifetime and high anisotropy of emission. In

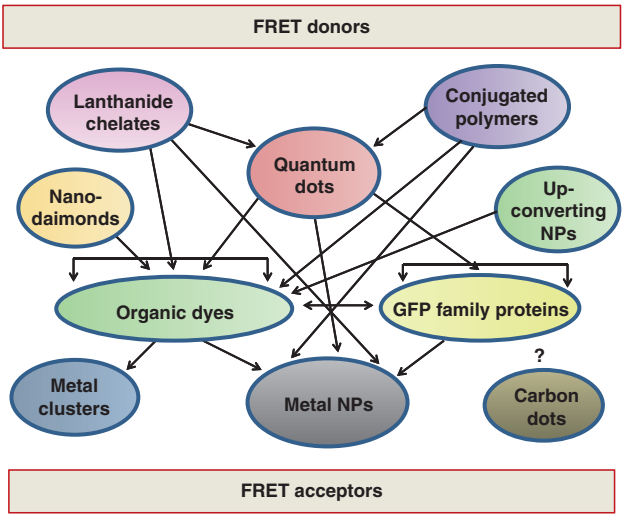

Fig. 6.11 The scheme of preferences for different fluorescent (luminescent) emitters to be the donors or acceptors in energy transfer in FRET-based nanocomposites. The arrows indicate the preferred directions of energy flow (Demchenko 2013)

contrast, the acceptors should be the most '*responsive*', changing the parameters of their emission in the broadest range. Many different types of reporters are applied as donors and acceptors in FRET because each of them has its advantages and drawbacks. Here we follow the idea to use FRET as the mechanism that could allow strengthening the strong and suppressing or eliminating the weak points in fluorescence reporting by coupling fluorescence emitters and allowing the excited-state energy transfer to occur between them.

6.3.1 Lanthanide Chelates and Other Metal-Chelating Luminophores

Short-wavelength excitations and very long lifetimes put *lanthanide chelates* to the first line of donors. Their good partner acceptors are both QDs (Charbonniere et al. 2006) and organic dyes (Selvin 2002). Combining the two optimization parameters (brightness and lifetime) one may infer that the optimal FRET donors could be the nanoparticles doped in high density with luminescent lanthanide chelates. This allows increasing the duration of transfer and enhancing in this way the FRET efficiency. Due to convenient positions of lanthanide emission bands for overlapping the absorption spectra of many organic dyes, these dyes can be used as FRET acceptors. Even more attractive as such acceptors are semiconductor quantum dots (QDs) in view of their much higher brightness. Such particles have been described in the literature (Monat et al. 2007; Casanova et al. 2006) and their efficient FRET to organic dyes (Casanova et al. 2006) and quantum dots (Charbonniere et al. 2006) were demonstrated.

There are good examples in the literature on illustration and application of this principle to *phosphorescent chelating complexes*. FRET from iridium as the donor to semiconductor QD as the acceptor resulted in increasing the lifetime from 40 to 400 ns (Anikeeva et al. 2006). Dramatic (by two or more orders of magnitude) increase of lifetimes of organic dyes can be also achieved by energy transfer from excited europium luminescent and ruthenium phosphorescent complexes.

6.3.2 Conjugated Polymers

Conjugated polymers are also in the line of optimal donors because of their very high brightness (Thomas et al. 2007; Reppy 2010), although their excitation is commonly spatially distributed over the entire polymer chain and they cannot be considered as point emitters. Their brightness is further increased reaching record values on formation of FRET complexes with organic dyes (Wu et al. 2008) and QDs (Jiang et al. 2009). Their partner organic dyes are able to transmit FRET into informative signal demonstrating modulation of their own response or displaying superquenching (Thomas et al. 2007; Pu and Liu 2009).

6.3.3 Semiconductor Quantum Dots

In addition to already mentioned advantages as *FRET donors*, such as the possibility to excite fluorescence in a very broad wavelength range, to display narrow and strongly size-dependent emission bands and high brightness (Sect. 5.5), the quantum dots possess other useful properties. They are reasonably resistant to photobleaching, and their high brightness is also observed in the conditions of two-photon excitation (Jares-Erijman and Jovin 2003).

Owing to their very broad short-wavelength excitation range and high brightness (Algar and Krull 2008; Medintz and Mattoussi 2009), the quantum dots are ideal for transferring their energy to organic dyes (Snee et al. 2006) and fluorescent proteins (Algar et al. 2010). With QDs, the excitation wavelength can be selected within broad ranges avoiding direct excitation of acceptors, and their narrow size-dependent emission spectra can be easily adjusted to acceptor absorption. They also possess the lifetimes of ~10^{-8} s, which are typically longer than that of organic dyes. Different sensors were designed based on QD-dye pairs (Suzuki et al. 2008).

The donor-acceptor pairs can be easily selected from QDs of different sizes and the series of dyes possessing also gradual shifts of their fluorescence spectra, such as Alexa dyes. FRET between quantum dots emitting at 565, 605, and 655 nm as energy donors and these dyes with absorbance maxima at 594, 633, 647, and 680 nm as energy acceptors were recently tested (Nikiforov and Beechem 2006). As a first step, the covalent conjugates between all three types of QDs and each of the Alexa labels were prepared. The FRET can be easily detected and the binding quantified in homogeneous system on formation of complexes avidin-biotin and antigen-antibody. Competitive binding assays can also be developed in such systems.

The approach based on *QD donors* and *dye acceptors* has found many applications: in DNA and RNA hybridization assays, in immunoassays, in construction of biosensors based on ligand-binding proteins and enzymes. Usually the following configuration is used: QDs are conjugated with the receptor molecules, and organic dyes are used either for target labeling or for labeling the target analogs in competitor displacement assays.

The same properties that make QDs so attractive as donors do not allow them to serve as efficient *FRET acceptors*. Particularly, their absorbance extending to UV and to part of the visible range does not allow avoiding their direct excitation. So their role as acceptors is limited to special cases, such as accepting the long-lifetime emission from lanthanide chelates (Charbonniere et al. 2006). Whereas the combination of quantum dots as FRET donors and organic dyes as acceptors is very efficient, the reverse combination, of dyes as donors and QDs as acceptors is not efficient at all! (Clapp et al. 2005a).

6.3.4 Up-Conversion Materials

The up-conversion emitters have deserved their special role primarily as FRET donors. Due to extremely sharp and narrow emission bands characteristic of luminescent lanthanide ions, and their excitation at vey low energies no donor emission

can be detected at the wavelengths of sensitized emission of the acceptor. In addition, no acceptor can be excited directly because the excitation is in the near-IR. The FRET from up-converting phosphors to QDs (Bednarkiewicz et al. 2010) and carbon nanoparticles (Wang et al. 2011) was demonstrated. The energy transfer to small-molecular dye was used for diagnostics directly in serum (Kuningas et al. 2006). An attractive sensor platform was demonstrated based on FRET quenching by graphene oxide (Liu et al. 2011). However, relatively low molar absorbance is a weak point of these prospective materials.

6.3.5 Organic Dyes and Visible Fluorescent Proteins

In the most known to date applications, *organic dye* molecules dominate as FRET acceptors from various kind of donors. This is because of their two important properties: (a) they are small molecules that allow easy and versatile conjugation with nanoparticles and (b) they may be highly responsive as reporters by changing different parameters of their emission. Their excitation via FRET increases the sensitivity of response but may not change the mechanism of this response based on its interactions and dynamics.

6.3.6 Fluorescent Carbon Nanoparticles

The spectral range available to fluorescent *nanodiamonds* is much narrower than that to organic dyes or quantum dots. Thus, with their emission maxima in the red region they can serve as the FRET donors for near-IR emitting dyes (Chen et al. 2011). The less common blue emitting nanodiamonds can transfer their energy to green emitting dye (Maitra et al. 2011).

Carbon dots and graphene or graphene oxide nanoparticles with their excitation spectra that are typically at 350–400 nm and emission spectra in the blue-green wavelength region can, in principle, serve as donors, whereas their application as acceptors is doubtful because of their strong absorption extending to shorter wavelengths (Sect. 5.4). However, because of their strong effect of contact quenching of different fluorophores, the formed constructions must be of special design.

6.3.7 Noble Metal Nanoparticles

The bottom of Fig. 6.11 is represented by metal nanoparticles that at short distances to the donors (organic dyes, QDs, etc.) can serve as FRET acceptor quenchers (Sen and Patra 2012) in addition to their known role as PET quenchers. Therefore, together with different nanocarbon structures they can serve as strong ‘universal’ (wavelength-independent) fluorescence quenchers that can be used in combination with other emitters in different sensing technologies.

Thus, we clearly observe the 'energy flow' from blue to red emitters, from long to short lifetime emitters, from emitters of higher to lower brightness, sometimes down to efficient quenchers. The strongly responsive emitters, such as organic dyes and fluorescent proteins, are requested mostly at the acceptor side. In such compositions the nanoparticles attain very useful properties that guarantee their numerous applications.

6.4 Wavelength Referencing, Multiplexing and Multicolor Coding

Now we address the problem of identifying the nanoparticles and also identifying and referencing the analytical signal produced by their fluorescence response. Providing referencing of fluorescence signal is always required in intensity sensing formats. Labeling of nano- or microparticles is needed for their identification when they are applied in fluorescence sensing in homogeneous format, together with its response to target binding. Such labeling can be achieved with the aid of series of smartly designed nanocomposites.

6.4.1 Wavelength Referencing

Being expressed in arbitrary units, the simple recording of fluorescence intensity is of limited quantitative value since it depends on fluorophore concentration, on its distribution in studied objects and also on instrumental parameters, temperature, quenchers, etc. Because of that reason, the analytical signal is difficult to scale and compare with the results obtained in different conditions of the measurement. This creates many problems in biological sensing and imaging. Introduction of a *reference* that can be excited together with the sensing fluorophore but emitting at a different wavelength (see Sect. 3.2) yields the ratiometric signal independent of these factors (Demchenko 2005, 2010). Combining two types of emitters in one nanosized unit allows making their relative concentrations well determined: one of them provides the reference signal and the other possessing different emission spectrum provides the sensor response.

One of the problems here is to exclude interactions between two or more types of fluorophores within one particle and make their emissions independent, so that the variation of reporter signal in its dynamic range should not influence the reference signal. The ideal case could be when different types of emitters are excited at the same wavelength and demonstrate very different emission spectra.

Lanthanide complexes (see Sect. 4.5) are ideal as the reference dyes in fluorescence sensors based on two-wavelength ratiometric recording (Bunzli and Piguet

2005). Their broad excitation spectra allow exciting them at the same wavelength as the reporting dyes and providing stable signal that is well separated from that of the reporter. Low dependence of emission spectra on the temperature and on the presence of quenchers make lanthanide chelates very attractive for this purpose.

Quantum dots are good solutions for designing such nanocomposites for providing the reference emission signal. Since these fluorophores demonstrate very small Stokes shifts, the problem is in responsive dyes, for which this shift should be very significant. Such two-component emission generated independently by two emitters fused in a nanocomposite can be realized by covalent attachment of ultra-small QD possessing small Stokes shift with 3-hydroxychromone dye, in which the Stokes shift is extremely large (Peng et al. 2011). There is no excited-state energy transfer between them and they emit independently. This allows the dye to exhibit its environment-dependent fluorescence properties. These components can be combined in different proportions, which allows providing the ratiometric signal by varying the range of relative intensities on a very broad level and even obtaining the composed 'white light' emission (Fig. 6.12).

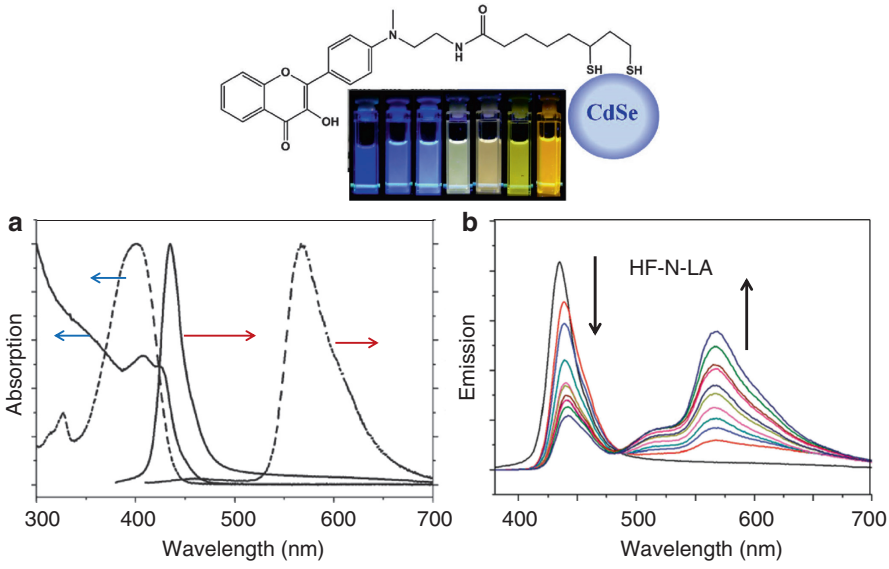

Fig. 6.12 Nanocomposites of ultra-small CdSe quantum dots and HF-N-L 3-hydroxychromone dye (Peng et al. 2011). (**a**) Absorption (*left scale*) and emission (*right scale*) spectra of CdSe quantum dots (*solid line*) and HF-N-LA molecules (*dashed line*). (**b**). Emission spectra of nanocomposites by combining different concentrations of HF-N-LA solutions with fixed amounts of QDs

6.4.2 *Multiplex Assays and Suspension Arrays*

The concept of wavelength referencing has found further development in *multiplex assays* (simultaneous analysis of many targets). In *homogeneous-type assays* there is a necessity of distinguishing several types of sensor-target interactions (and ideally, their great number). This can be realized if we are able to label every type of sensor molecule or nanoparticle with a certain '*barcode*' that could be recognizable in chromatography or flow cytometry (Lim and Zhang 2007). The dyes (and nanoparticles) emitting at different wavelengths may serve for constructing such multicolor codes (Jun et al. 2012). This allows mixing the differently encoded sensor particles and detecting the binding of specific targets to each of their diverse types. The principle of operation of such sensors is illustrated in Fig. 6.13.

The *suspension arrays* operating in solutions without any support may contain many thousand types of sensor particles. They must be different in target recognition units but display the same type of fluorescence response. To be recognized, the sensor containing the recognition unit binding particular target and reporting about that by changing its optical parameter should contain also its own unique marker. In theory, six colors at six different levels of intensity should provide nearly 40,000 unique codes (Wilson et al. 2006). In practice it is hard to achieve such values in

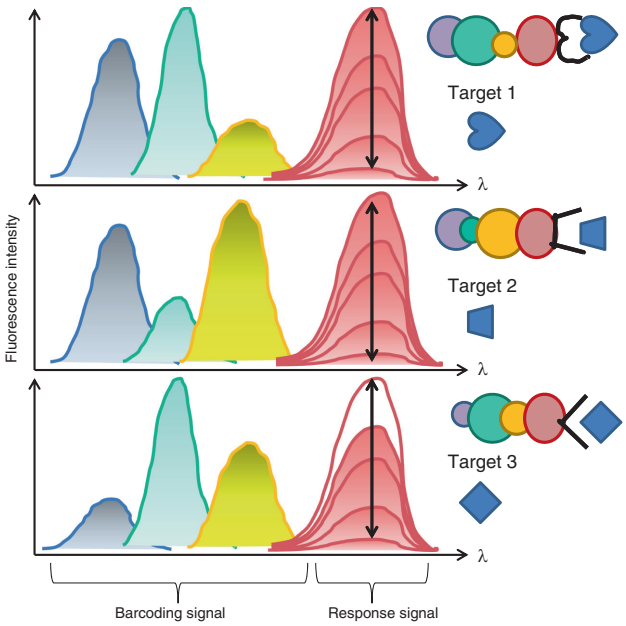

Fig. 6.13 The barcodes for fluorescence sensors (Demchenko 2013). As an example, three types of emitters (*violet*, *blue* and *yellow*) assembled in different proportions into nanocomposite make every nanocomposite recognizable by characteristic pattern of relative intensities of three bands. Fluorescence sensor included into nanocomposite can respond to the binding of its specific target (shown here as the dye changing the intensity of red light). The sensor particle interacts with particular target and its type is recognized by the barcode

view of spectral overlaps between the dyes and variability of fluorescence intensities introduced both on the steps of sensor production and reading the output signal.

6.4.3 Materials for Multicolor Coding

There are tremendous possibilities for achieving the required diversity using nanoscale composite particles with incorporated fluorescence materials. The starting conditions could be: (a) excitation of all members of such array by a single wavelength, (b) narrow emission bands of components forming the color code, and (c) chemical and photochemical stability that will not allow destroying the coding signal.

Organic dyes satisfy these requirements only partially, but their performance can be improved substantially on incorporation into nanoparticles (Jun et al. 2012). The composing dyes can emit individually forming the composite spectrum, but since a strong variation in positions of fluorescence bands is required on excitation at single wavelength, this can be realized by wavelength-converting cascade FRET (see Sect. 6.2). The dye molecules can be incorporated in different proportions into silica particles and coupled by FRET cascade reaction (Ma et al. 2007). Still, their broad adsorption and emission profiles are fundamental drawbacks reducing multiplexing capabilities.

In this respect, *quantum dots* have better prospects than organic dyes because they possess much narrower fluorescence spectra covering the whole visible range up to near-IR, they can be excited at a single wavelength and, in addition, they exhibit higher photostability (Eastman et al. 2006). Such attractive features of QDs were recognized (Medintz et al. 2005). Employing them as FRET donors and of organic dyes as acceptors allows realizing many new possibilities (Clapp et al. 2005b).

Barcodes with application of *up-converting nanoparticles* deserve special attention. They can be designed on the basis of a single host material of a-$NaYF_4$ doped with variable amounts of Yb^{3+}, Tm^{3+}, and Er^{3+} ions. This allows obtaining a broad range of color output by single wavelength excitation using a cheap diode laser at 980 nm just by variation of dopant concentrations (Wang et al. 2010). Even broader assortment of colors can be achieved when these particles are decorated with FRET-acceptor organic dyes (Gorris et al. 2011). In this way a large library of emission spectra in the visible and near-IR spectral region can be created that is particularly useful in multiplexed labeling.

Summarizing, with proper choice, variation of amount and the ratio of fluorescence emitters and by wavelength-ratiometric recording one can achieve a million-scale diversity in sensor labeling and generation of images.

6.4.4 Nanobeads with Quantum Dot Cores

For many applications the capping of QDs with small molecules such as mercaptoacetic acid is not efficient, since they can be easily degraded by hydrolysis or oxidation of the capping ligand. Therefore, the coating of silica on ZnS-CdSe dots is a

straightforward solution among many of others suggested (Gerion et al. 2001). Coating QDs with a silica layer can provide improved stability without affecting their optical properties. In addition to capping the single QDs with a silica monolayer, multiple QDs can be also encapsulated into silica nanobeads (Gao and Nie 2003).

The range of applications implying the potential of such nanobeads to incorporate QDs of different size and, therefore, different fluorescence spectrum, is tremendous. Each particle can incorporate several different QDs that may compose very specific '*color barcode*'. Such coding is needed in microsphere-based array technology (Sect. 11.4). The DNA hybridization studies demonstrate that the coding and target signals can be simultaneously read at the single-bead level, which allows to apply this technique in high throughput screening, and in medical diagnostics.

The encapsulation of quantum dots into monodisperse polystyrene latex nanobeads has also been suggested (Han et al. 2001b). The swelling method was used for tagging 1.2 μm beads with different combinations of QDs of various colors to create QD barcodes. It was demonstrated that the use of six colors and ten intensity levels can theoretically encode up to one million types of particles.

6.4.5 *Applications of Optical Barcoding*

The most efficient application of homogeneous assays employing the principle of optical barcoding was with quantum dots imbedded in polymeric structures. Fig. 6.14 illustrates applying this strategy for multiplexed DNA detection. In this work the target DNA was labeled with a fluorophore and oligonucleotide-functionalized polymeric microbeads with quantum dots designed to emit at various

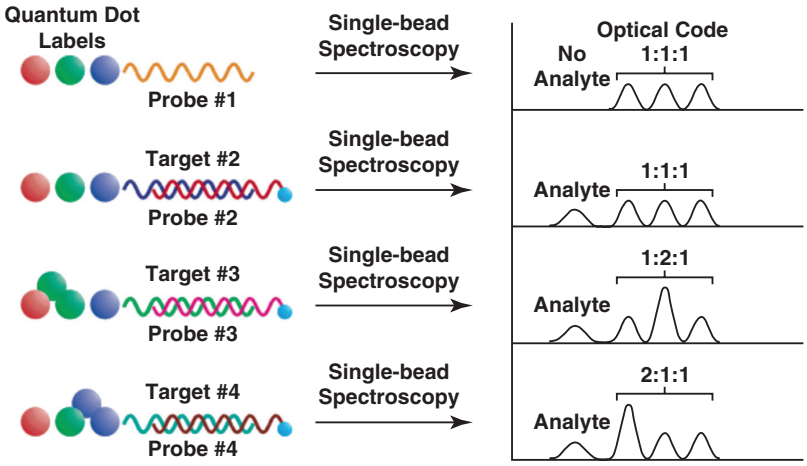

Fig. 6.14 Quantum dots can be employed for detecting multiple targets in a single assay (Han et al. 2001a). Specifically, varying the numbers and ratios of different quantum dots per target results in a unique fluorescent signal for each individual DNA target

specified wavelengths other than that of the target DNA. These particles were recognized due to different compositions of quantum dots exhibiting different fluorescence spectra. After capture of target DNA by the microbead/quantum dot assembly, single-bead spectroscopy studies revealed both the presence and the identity of the target DNA.

6.5 Combining Fluorescence with Magnetic, NMR Enhancing and Other Functionalities

Under *multifunctionality* we mean a combination of essential properties that may include the property of selective binding to a particular target (macromolecule, living cell or its organelle), of guiding to a particular target by physical means (e.g. by being magnetic), or using specificity of molecular recognition (e.g. by attached antibodies). Thus, *control on location* of the reporter and on *physical or chemical action* at the site of location (e.g. singlet oxygen generation or photothermal action) can be coupled in one nanocomposite. A request for multifunctionality becomes very important in various applications, particularly for the whole body imaging (Louie 2010) and clinical diagnostics together with treatment (Sect. 14.4).

Fluorescence is the major method for studying the living cells. It is suitable for multi-scale imaging, extending to the level of whole-body animals, but in this application it is hindered by a limited imaging depth, commonly of less than several centimeters. The multifunctional nanocomposites may incorporate fluorescence sensing and imaging with other functionalities, such as X-ray, positron and NMR tomography. The markers, contrast agents and enhancers required for these methods can be combined in multifunctional nanoscale units.

6.5.1 Luminescent Plus Magnetic Nanocomposites

When magnetic nanocrystals are of very small sizes, they can show *superparamagnetic* behavior which is very attractive for various applications. In this size range their induced magnetization is observed on a strong level only in an external magnetic field, and upon its removal any residual magnetization is lost. Therefore, they can be easily manipulated by external magnetic field, and this ‘action at a distance’ provides tremendous advantages for many applications. The range of these applications can be substantially extended by making their fluorescent composites (Lu et al. 2015). In biomedical field it includes hyperthermia, magnetic guided drug delivery, cell sorting, protein immobilization, and contrast agents in MRI.

Different magnetic nanoparticles can be coupled with fluorescent molecular and nanoscale structures to make such hybrids. As an example, bifunctional magnetic fluorescent silica nanocapsules were synthesized by employing conjugated polymers as the fluorescent emitters and *iron oxide* nanocrystals as the magnetic constituent, both of which were encapsulated inside the nanocore of a thin silica shell (Fig. 6.15) (Tan et al. 2011).

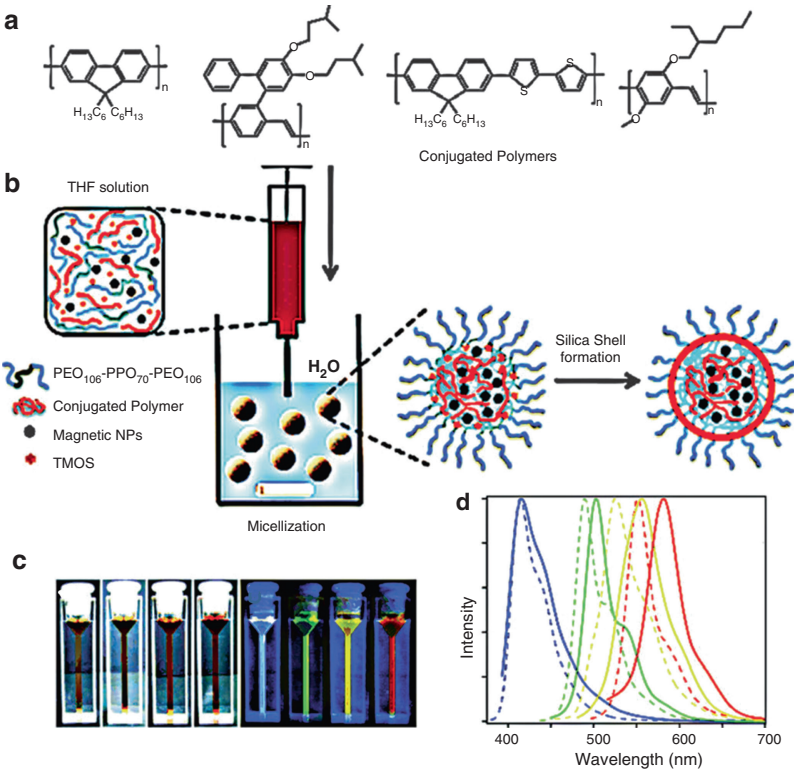

Fig. 6.15 The composites of fluorescent conjugated polymers and superparamagnetic iron oxide nanocrystals in silica nanocapsules for dual-mode cellular imaging (Tan et al. 2011). (**a**) The structures of conjugated polymers. (**b**) The formation of composites through the bioinspired silification approach. (**c**) Optical micrographs of the aqueous dispersions under white light (*left*) and UV light (*right*). (**d**) Photoluminescence spectra of the aqueous dispersions of obtained nanocomposites (*solid lines*) in comparison to respective fluorescent conjugated polymer solutions in THF (*dashed lines*)

Combining fluorescent *carbon dots* with metal nanoparticles can yield multifunctional hybrid materials that have magnetic, optical or mechanical properties. In a recent work (Wang et al. 2014) a $Ni@SiO_2$ the shell nanoreactor framework was prepared via a sol–gel process and used as an excellent magnetic model system. After that, C-dots were linked to the surface of $Ni@SiO_2$ in only one simple step. Both fluorescence and magnetism are retained in synthesized nanocomposites.

6.5.2 *Fluorescent Plus NMR-Contrasting Nanocomposites*

The main advantage of *NMR tomography* over optical imaging is the possibility of 3-dimensional imaging of deep tissues. Therefore, the advantages of dual-functional imaging nanoprobes integrating the NMR tomography with fluorescent imaging capabilities are becoming increasingly important.

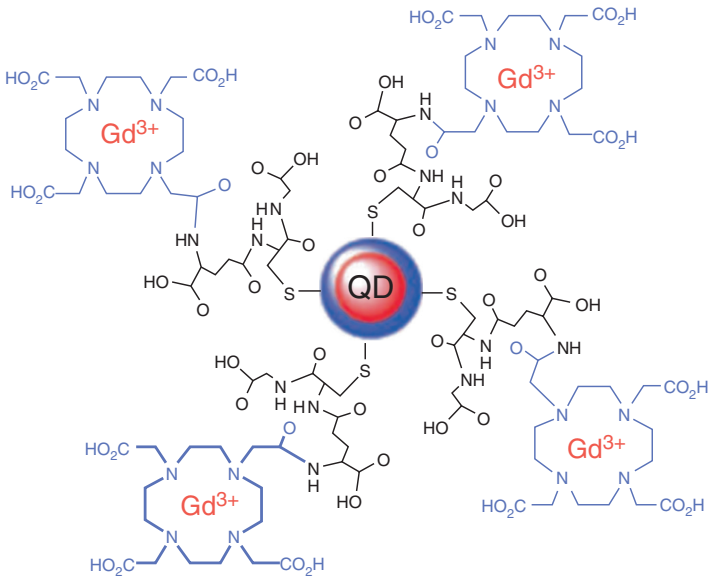

Fig. 6.16 The chelator of Gd^{3+} ions coupled to CdSeTe/CdS quantum dots (Jin et al. 2008)

Gadolinium ions (Gd^{3+}) possess seven unpaired electrons, which can efficiently alter the relaxation time of surrounding water protons and improve in this way the contrast in NMR measurements. They are extensively used for 3D NMR imaging diagnosis in routine clinical practice. Different constructions combining Gd^{3+} chelators and molecular or nanoscale fluorophores have been suggested.

One example is presented in Fig. 6.16. The composite structure assembling the near-IR-emitting CdSeTe/CdS quantum dots together with chelating groups hosting Gd^{3+} ions was constructed (Jin et al. 2008). In this design, reduced glutathione was used as a surface coating agent and then the coated surface was functionalized with Gd^{3+}-DOTA (1,4,7,10-tetraazacyclododecane-1,4,7,10-tetraacetic acid) complexes. In a similar manner, fluorescent carbon dots were loaded with Gd^{3+} ions (Bourlinos et al. 2012).

For functioning as *up-converting* fluorescent and *magnetic resonance* dual-modality imaging contrast agents, the up-converting nanocrystals were coated with paramagnetic lanthanide complex shells (Wang et al. 2013). They show excellent enhancement of both fluorescent and NMR signals in experiments *in vivo*.

6.5.3 Nanocomposites with Multimodal Function

The fact that multifunctionality imaging can circumvent the limitations of single imaging modes and provide more detailed and versatile information on the studied systems invoked a lot of activities. The functions to absorb and emit light and to respond by the changes of this emission to nanoscale and molecular events can be combined with magnetic, NMR-contrasting, electron-dense and other functions

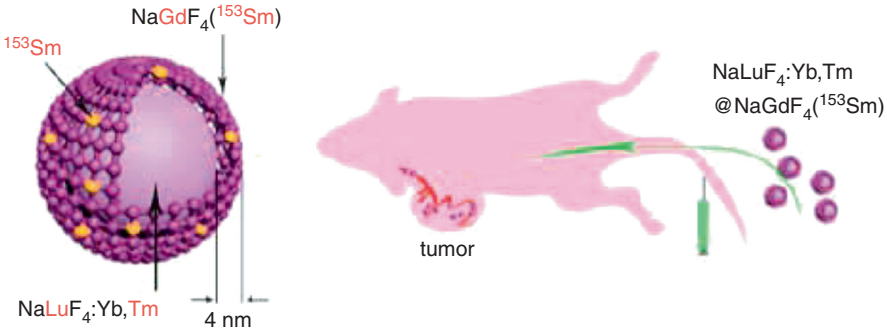

Fig. 6.17 The structure of $NaLuF_4$:Yb,Tm@$NaGdF_4$ (^{153}Sm) composite suggested as four-modal imaging probe contrasting the tumor (Sun et al. 2013)

(Cheon and Lee 2008). Three-modal and even four-modal operating nanostructures were suggested.

The most efficient in this respect are the rare earth nanocrystals. The $NaLuF_4$:Yb,Tm@$NaGdF_4$ (^{153}Sm) composite nanomaterial was confirmed to be effective and applicable for up-conversion luminescence imaging, X-ray computed tomography, magnetic resonance imaging, and single-photon emission computed tomography *in vivo* (Sun et al. 2013), see Fig. 6.17. Furthermore, these nanoparticles were applied in tumor angiogenesis analysis by combining such multimodality imaging of tumor angiogenesis.

Together with selective binding at particular sites, control of their location and detection of different analytes at this location, the novel composites are able to display the physical or chemical action at the site of location, such as drug release or photodynamic damage of cancer cells (see Sect. 14.4).

Each imaging modality has its own merits and disadvantages, and a single technique does not possess all the required capabilities for comprehensive imaging. Therefore, *multimodal imaging* methods are quickly becoming important tools for state-of-the-art biomedical research and clinical diagnostics and therapeutics.

The field of research of fluorescent nanoscale compositions develops extremely rapidly, so its new bright applications can be foreseen in the future.

6.6 Sensing and Thinking: Achieving Multitude of Functions in Designed Nanocomposites

Why we need nanocomposites? Size limit of this Chapter did not allow discussing all important cases, in which molecules and nanoparticles attain the ability to display new properties when they are combined into such smart nanoscale structures. New unique possibilities in design and application of nanocomposites appear because they are small, they can be constructed by self-assembly of components in

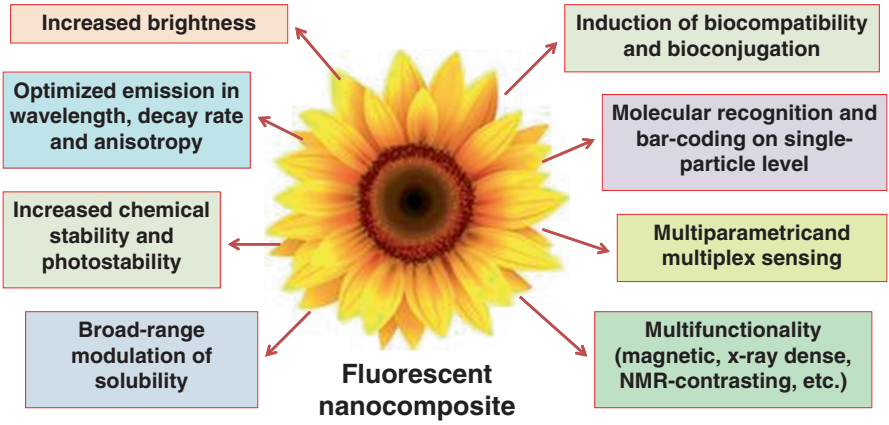

Fig. 6.18 Illustration of different functionalities that can be achieved in design of fluorescent nanomaterials from molecular and nanoparticle components. (Demchenko 2013)

solutions, they are mobile and can diffuse rapidly in solutions and penetrate into the living cells and tissues. On top of that, they are very efficient being able to display several important functions (Fig. 6.18).

On a nanoscale, there appears the possibility of obtaining organic-inorganic *hybrid materials* (e.g. up-converting nanocrystals decorated with organic dyes), which can be realized in very smart designs and attain unique features. Such nanostructures are often constructed based on a *core-shell* principle. This allows combining maximum of functionality with facile production. The core part commonly carries the supporting and reporting functions (for instance, it can be magnetic), whereas the shell is responsible for target recognition and signal transduction together with such necessary properties as solubility or adhesion to particular surface.

Among desired features that can be successfully achieved in nanocomposites is the ability of modulating their optical parameters in broad ranges and actively use in sensing and imaging all the possibilities of fluorescence detection, including wavelength-ratiometric, lifetime, anisotropy and two-photon excitation response providing the proper choice of excitation and emission parameters. Emission intensity can be enhanced manifold and the labeling can be extended to barcoding. The construction of composites from molecular and nanoscale building blocks allows achieving an unaccountable diversity in combining and enhancing the valuable properties. Such *multifunctionality* includes the ability to display a combination of several imaging possibilities *in vivo*, such as enhancement of NMR contrast.

Thus, assembly of fluorescence emitters into nanocomposites allows achieving very important functions that are not observed in separate emitters alone. Since all types of fluorescent molecules and nanoparticles can be combined in nanocomposites, the new routes are opened to perfection of fluorescence reporters by their designing on nanoscale.

Questions and Problems

1. List all discussed above possibilities for fluorescence enhancement offered by constructing nanocomposites and explain their background mechanisms.
2. What are excitons? How their effects are displayed in molecular aggregates, conjugated polymers and semiconductor nanocrystals?
3. What are J-aggregates and how their presence can be recognized in fluorescence spectra?
4. Explain the new features that are observed when the fluorophores are assembled and exhibit homo-FRET.
5. Compare the fluorescence parameters of FRET acceptor excited via energy transfer and on direct excitation. What of these parameters are different and why? Estimate the scale of their variation on direct excitation and via FRET.
6. Explain the mechanism of light harvesting. What parameters of fluorescence emission change in this process?
7. Wavelength conversion, in which direction it proceeds on the wavelength scale and why? What fluorescence parameters change in this process and what remains unchanged?
8. Explain the role of each participant in a two-step cascade energy transfer. Analyze, what will be the result of changing the fluorescence parameters of each of them.
9. What is the benefit of extending the emission lifetime? How to achieve that in nanocomposites?
10. Why anisotropy is low in the systems of fluorophores coupled by homo-FRET? What are the spectroscopic means to enhance it?
11. Explain the mechanism of modulation by exposure to light of switching the emission intensity between two colors.
12. Explain your choice of FRET donor in design of nanosensor with response of organic dye as the acceptor. Could it be quantum dot, lanthanide chelate, conjugated polymer or another dye? Explain, what are the advantages and disadvantages in all these cases.
13. In what technologies and why optical barcoding imprinted in nanoparticles becomes necessary? Do we need to activate or to suppress FRET in this application?
14. Explain the possibilities of designing nanocomposites that combine fluorescence with NMR contrasting and magnetic properties. What is the range of their applications?

References

Abramavicius D, Palmieri B, Voronine DV, Sanda F, Mukamel S (2009) Coherent multidimensional optical spectroscopy of excitons in molecular aggregates; quasiparticle versus supermolecule perspectives. Chem Rev 109(6):2350–2408

Algar WR, Krull UJ (2008) Quantum dots as donors in fluorescence resonance energy transfer for the bioanalysis of nucleic acids, proteins, and other biological molecules. Anal Bioanal Chem 391(5):1609–1618

Algar WR, Tavares AJ, Krull UJ (2010) Beyond labels: a review of the application of quantum dots as integrated components of assays, bioprobes, and biosensors utilizing optical transduction. Anal Chim Acta 673(1):1–25. doi:10.1016/j.aca.2010.05.026

An B-K, Kwon S-K, Jung S-D, Park SY (2002) Enhanced emission and its switching in fluorescent organic nanoparticles. J Am Chem Soc 124(48):14410–14415

Anikeeva PO, Madigan CF, Coe-Sullivan SA, Steckel JS, Bawendi MG, Bulovic V (2006) Photoluminescence of CdSe/ZnS core/shell quantum dots enhanced by energy transfer from a phosphorescent donor. Chem Phys Lett 424(1–3):120–125

Balzani V, Ceroni P, Gestermann S, Kauffmann C, Gorka M, Vogtle F (2000) Dendrimers as fluorescent sensors with signal amplification. Chem Commun 10:853–854

Bednarkiewicz A, Nyk M, Samoc M, Strek W (2010) Up-conversion FRET from Er3+/Yb3+:NaYF4 Nanophosphor to CdSe quantum dots. J Phys Chem C 114(41):17535–17541. doi:10.1021/jp106120d

Bourlinos AB, Bakandritsos A, Kouloumpis A, Gournis D, Krysmann M, Giannelis EP, Polakova K, Safarova K, Hola K, Zboril R (2012) Gd (III)-doped carbon dots as a dual fluorescent-MRI probe. J Mater Chem 22(44):23327–23330

Bunzli J-CG, Piguet C (2005) Taking advantage of luminescent lanthanide ions. Chem Soc Rev 34(12):1048–1077

Casanova D, Giaume D, Gacoin T, Boilot JP, Alexandrou A (2006) Single lanthanide-doped oxide nanoparticles as donors in fluorescence resonance energy transfer experiments. J Phys Chem B 110(39):19264–19270

Chan Y-H, Ye F, Gallina ME, Zhang X, Jin Y, Wu I-C, Chiu DT (2012) Hybrid semiconducting polymer dot–quantum dot with narrow-band emission, near-infrared fluorescence, and high brightness. J Am Chem Soc 134(17):7309–7312

Charbonniere LJ, Hildebrandt N, Ziessel RF, Loehmannsroeben HG (2006) Lanthanides to quantum dots resonance energy transfer in time-resolved fluoro-immunoassays and luminescence microscopy. J Am Chem Soc 128(39):12800–12809

Chen CH, Liu KY, Sudhakar S, Lim TS, Fann W, Hsu CP, Luh TY (2005) Efficient light harvesting and energy transfer in organic-inorganic hybrid multichromophoric materials. J Phys Chem B 109(38):17887–17891

Chen Y-Y, Shu H, Kuo Y, Tzeng Y-K, Chang H-C (2011) Measuring Förster resonance energy transfer between fluorescent nanodiamonds and near-infrared dyes by acceptor photobleaching. Diamond Relat Mater 20(5–6):803–807. doi:10.1016/j.diamond.2011.03.039

Cheon J, Lee JH (2008) Synergistically integrated nanoparticles as multimodal probes for nanobiotechnology. Acc Chem Res 41(12):1630–1640. doi:10.1021/ar800045c

Clapp AR, Medintz IL, Fisher BR, Anderson GP, Mattoussi H (2005a) Can luminescent quantum dots be efficient energy acceptors with organic dye donors? J Am Chem Soc 127(4):1242–1250

Clapp AR, Medintz IL, Uyeda HT, Fisher BR, Goldman ER, Bawendi MG, Mattoussi H (2005b) Quantum dot-based multiplexed fluorescence resonance energy transfer. J Am Chem Soc 127(51):18212–18221

de Silva AP, Gunaratne HQN, Gunnaugsson T, Huxley AJM, McRoy CP, Rademacher JT, Rice TE (1997) Signaling recognition events with fluorescent sensors and switches. Chem Rev 97:1515–1566

Demchenko AP (2002) The red-edge effects: 30 years of exploration. Luminescence 17(1):19–42

Demchenko AP (2005) The problem of self-calibration of fluorescence signal in microscale sensor systems. Lab Chip 5(11):1210–1223

Demchenko AP (2008) Site-selective red-edge effects. Chapter 4. Methods Enzymol 450:59–78

Demchenko AP (2010) The concept of lambda-ratiometry in fluorescence sensing and imaging. J Fluoresc 20(5):1099–1128

Demchenko AP (2013) Nanoparticles and nanocomposites for fluorescence sensing and imaging. Methods Appl Fluoresc 1(2):022001

Díaz SA, Giordano L, Azcárate JC, Jovin TM, Jares-Erijman EA (2013) Quantum dots as templates for self-assembly of photoswitchable polymers: small, dual-color nanoparticles capable of facile photomodulation. J Am Chem Soc 135(8):3208–3217

Díaz SA, Gillanders F, Jares-Erijman EA, Jovin TM (2015) Photoswitchable semiconductor nanocrystals with self-regulating photochromic Förster resonance energy transfer acceptors. Nat Commun 6:6036. doi:10.1038/ncomms7036

Ding D, Li K, Liu B, Tang BZ (2013) Bioprobes based on AIE fluorogens. Acc Chem Res 46(11): 2441–2453

Dulkeith E, Ringler M, Klar T, Feldmann J, Munoz Javier A, Parak W (2005) Gold nanoparticles quench fluorescence by phase induced radiative rate suppression. Nano Lett 5(4): 585–589

Eastman PS, Ruan WM, Doctolero M, Nuttall R, De Feo G, Park JS, Chu JSF, Cooke P, Gray JW, Li S, Chen FQF (2006) Qdot nanobarcodes for multiplexed gene expression analysis. Nano Lett 6(5):1059–1064

Fábián Á, Horváth G, Vámosi G, Vereb G, Szöllősi J (2013) TripleFRET measurements in flow cytometry. Cytometry Part A 83(4):375–385

Forde TS, Hanley QS (2005) Following FRET through five energy transfer steps: spectroscopic photobleaching, recovery of spectra, and a sequential mechanism of FRET. Photochem Photobiol Sci 4(8):609–616

Frigoli M, Ouadahi K, Larpent C (2009) A cascade FRET-mediated ratiometric sensor for Cu2+ ions based on dual fluorescent ligand-coated polymer nanoparticles. Chemistry 15(33): 8319–8330

Fu Y, Zhang J, Lakowicz JR (2009) Silver-enhanced fluorescence emission of single quantum dot nanocomposites. Chem Commun 3:313–315

Gao XH, Nie SM (2003) Doping mesoporous materials with multicolor quantum dots. J Phys Chem B 107(42):11575–11578

Gao J, Strassler C, Tahmassebi D, Kool ET (2002) Libraries of composite polyfluors built from fluorescent deoxyribosides. J Am Chem Soc 124(39):11590–11591

Geng J, Liang J, Wang Y, Gurzadyan GG, Liu B (2011) Metal-enhanced fluorescence of conjugated polyelectrolytes with self-assembled silver nanoparticle platforms. J Phys Chem B 115(13):3281–3288

Gerion D, Pinaud F, Williams SC, Parak WJ, Zanchet D, Weiss S, Alivisatos AP (2001) Synthesis and properties of biocompatible water-soluble silica-coated CdSe/ZnS semiconductor quantum dots. J Phys Chem B 105(37):8861–8871

Giordano L, Jovin TM, Irie M, Jares-Erijman EA (2002) Diheteroarylethenes as thermally stable photoswitchable acceptors in photochromic fluorescence resonance energy transfer (pcFRET). J Am Chem Soc 124(25):7481–7489

Gorris HH, Ali R, Saleh SM, Wolfbeis OS (2011) Tuning the dual emission of photon-upconverting nanoparticles for ratiometric multiplexed encoding. Adv Mater 23(14):1652–1655

Halpert JE, Tischler JR, Nair G, Walker BJ, Liu W, Bulovic V, Bawendi MG (2009) Electrostatic formation of quantum dot/J-aggregate FRET pairs in solution. J Phys Chem C 113(23): 9986–9992

Han M, Gao X, Su JZ, Nie S (2001) Quantum-dot-tagged microbeads for multiplexed optical coding of biomolecules. Nat Biotechnol 19(7):631–635

Harriman A, Mallon L, Ziessel R (2008) Energy flow in a purpose-built cascade molecule bearing three distinct chromophores attached to the terminal acceptor. Chemistry 14(36): 11461–11473

Haustein E, Jahnz M, Schwille P (2003) Triple FRET: a tool for studying long-range molecular interactions. Chemphyschem 4(7):745–748

Hildebrandt N, Charbonniere LJ, Lohmannsroben HG (2007) Time-resolved analysis of a highly sensitive forster resonance energy transfer immunoassay using terbium complexes as donors and quantum dots as acceptors. J Biomed Biotechnol 2007:79169

Huang B, Wu HK, Bhaya D, Grossman A, Granier S, Kobilka BK, Zare RN (2007) Counting low-copy number proteins in a single cell. Science 315(5808):81–84

Jares-Erijman EA, Jovin TM (2003) FRET imaging. Nat Biotechnol 21(11):1387–1395

Jiang G, Susha AS, Lutich AA, Stefani FD, Feldmann J, Rogach AL (2009) Cascaded FRET in conjugated polymer/quantum dot/dye-labeled DNA complexes for DNA hybridization detection. ACS Nano 3(12):4127–4131. doi:10.1021/nn901324y

Jin T, Yoshioka Y, Fujii F, Komai Y, Seki J, Seiyama A (2008) Gd 3+-functionalized near-infrared quantum dots for in vivo dual modal (fluorescence/magnetic resonance) imaging. Chem Commun 44:5764–5766

Jun BH, Kang H, Lee YS, Jeong DH (2012) Fluorescence-based multiplex protein detection using optically encoded microbeads. Molecules 17(3):2474–2490, doi:molecules17032474 [pii] 10.3390/molecules17032474

Kasha M, Rawls H, Ashraf El-Bayoumi M (1965) The exciton model in molecular spectroscopy. Pure Appl Chem 11(3–4):371–392

Kuningas K, Ukonaho T, Pakkila H, Rantanen T, Rosenberg J, Lovgren T, Soukka T (2006) Upconversion fluorescence resonance energy transfer in a homogeneous immunoassay for estradiol. Anal Chem 78(13):4690–4696

Lian W, Litherland SA, Badrane H, Tan WH, Wu DH, Baker HV, Gulig PA, Lim DV, Jin SG (2004) Ultrasensitive detection of biomolecules with fluorescent dye-doped nanoparticles. Anal Biochem 334(1):135–144

Lim CT, Zhang Y (2007) Bead-based microfluidic immunoassays: the next generation. Biosens Bioelectron 22(7):1197–1204

Lim I-IS, Goroleski F, Mott D, Kariuki N, Ip W, Luo J, Zhong C-J (2006) Adsorption of cyanine dyes on gold nanoparticles and formation of J-aggregates in the nanoparticle assembly. J Phys Chem B 110(13):6673–6682

Liu C, Wang Z, Jia H, Li Z (2011) Efficient fluorescence resonance energy transfer between upconversion nanophosphors and graphene oxide: a highly sensitive biosensing platform. Chem Commun 47(16):4661–4663

Losytskyy MY, Yashchuk VM, Lukashov SS, Yarmoluk SM (2002) Davydov splitting in spectra of cyanine dye J-aggregates, formed on the polynucleotides. J Fluoresc 12(1):109–112

Louie A (2010) Multimodality imaging probes: design and challenges. Chem Rev 110(5): 3146–3195

Lu Y, He B, Shen J, Li J, Yang W, Yin M (2015) Multifunctional magnetic and fluorescent core–shell nanoparticles for bioimaging. Nanoscale 7:1606–1609

Ma Q, Wang XY, Li YB, Shi YH, Su XG (2007) Multicolor quantum dot-encoded microspheres for the detection of biomolecules. Talanta 72(4):1446–1452

Ma X, Fletcher K, Kipp T, Grzelczak MP, Wang Z, Guerrero-Martínez A, Pastoriza-Santos I, Kornowski A, Liz-Marzán LM, Mews A (2011) Photoluminescence of individual Au/CdSe nanocrystal complexes with variable interparticle distances. J Phys Chem Lett 2(19): 2466–2471

Maitra U, Jain A, George SJ, Rao CNR (2011) Tunable fluorescence in chromophore-functionalized nanodiamond induced by energy transfer. Nanoscale 3(8):3192–3197

Medintz IL, Mattoussi H (2009) Quantum dot-based resonance energy transfer and its growing application in biology. Phys Chem Chem Phys 11(1):17–45

Medintz IL, Uyeda HT, Goldman ER, Mattoussi H (2005) Quantum dot bioconjugates for imaging, labelling and sensing. Nat Mater 4(6):435–446

Miao X, Brener I, Luk TS (2010) Nanocomposite plasmonic fluorescence emitters with core/shell configurations. J Opt Soc Am B 27(8):1561–1570

Monat C, Grillet C, Domachuk R, Smith C, Magi E, Moss DJ, Nguyen HC, Tomljenovic-Hanic S, Cronin-Golomb M, Eggleton BJ, Freeman D, Madden S, Luther-Davies B, Mutzenich S, Rosengarten G, Mitchell A (2007) Frontiers in microphotonics: tunability and all-optical control. Laser Phys Lett 4(3):177–186

Moore R, Lee J, Robinson GW (1985) Hydration dynamics of electrons from a fluorescent probe molecule. J Phys Chem 89(17):3648–3654

Morrison LE (1988) Time-resolved detection of energy transfer: theory and application to immunoassays. Anal Biochem 174(1):101–120

Nikiforov TT, Beechem JM (2006) Development of homogeneous binding assays based on fluorescence resonance energy transfer between quantum dots and Alexa Fluor fluorophores. Anal Biochem 357(1):68–76

Ow H, Larson DR, Srivastava M, Baird BA, Webb WW, Wiesner U (2005) Bright and stable core-shell fluorescent silica nanoparticles. Nano Lett 5(1):113–117

Peng H-C, Kang C-C, Liang M-R, Chen C-Y, Demchenko A, Chen C-T, Chou P-T (2011) En route to white-light generation utilizing nanocomposites composed of ultrasmall CdSe nanodots and excited-state intramolecular proton transfer dyes. ACS Appl Mater Interfaces 3(5):1713–1720

Pu KY, Liu B (2009) Optimizing the cationic conjugated polymer-sensitized fluorescent signal of dye labeled oligonucleotide for biosensor applications. Biosens Bioelectron 24(5):1067–1073
Qhobosheane M, Santra S, Zhang P, Tan WH (2001) Biochemically functionalized silica nanoparticles. Analyst 126(8):1274–1278
Rampazzo E, Bonacchi S, Genovese D, Juris R, Montalti M, Paterlini V, Zaccheroni N, Dumas-Verdes C, Clavier G, Méallet-Renault R (2014) Pluronic-Silica (PluS) Nanoparticles Doped with Multiple Dyes Featuring Complete Energy Transfer. J Phys Chem C 118(17):9261–9267
Reppy MA (2010) Structure, emissive properties, and reporting abilities of conjugated polymers. In: Demchenko AP (ed) Advanced fluorescence reporters in chemistry and biology II: molecular constructions, polymers and nanoparticles, Springer Ser Fluoresc 9:357–388
Riu J, Maroto A, Rius FX (2006) Nanosensors in environmental analysis. Talanta 69(2):288–301
Rogach AL, Klar TA, Lupton JM, Meijerink A, Feldmann J (2009) Energy transfer with semiconductor nanocrystals. J Mater Chem 19(9):1208–1221
Saikin SK, Eisfeld A, Valleau S, Aspuru-Guzik A (2013) Photonics meets excitonics: natural and artificial molecular aggregates. Nanophotonics 2(1):21–38
Scholes GD, Jordanides XJ, Fleming GR (2001) Adapting the Förster theory of energy transfer for modeling dynamics in aggregated molecular assemblies. J Phys Chem B 105(8):1640–1651
Schwartz E, Le Gac S, Cornelissen JJ, Nolte RJ, Rowan AE (2010) Macromolecular multichromophoric scaffolding. Chem Soc Rev 39(5):1576–1599
Selvin PR (2002) Principles and biophysical applications of lanthanide-based probes. Annu Rev Biophys Biomol Struct 31:275–302
Sen T, Patra A (2012) Recent advances in energy transfer processes in gold-nanoparticle-based assemblies. J Phys Chem C. doi:10.1021/jp302615d
Serin JM, Brousmiche DW, Frechet JMJ (2002) Cascade energy transfer in a conformationally mobile multichromophoric dendrimer. Chem Commun 22:2605–2607
Shcharbin D, Szwedzka M, Bryszewska M (2007) Does fluorescence of ANS reflect its binding to PAMAM dendrimer? Bioorg Chem 35(2):170–174
Snee PT, Somers RC, Nair G, Zimmer JP, Bawendi MG, Nocera DG (2006) A ratiometric CdSe/ZnS nanocrystal pH sensor. J Am Chem Soc 128(41):13320–13321
Squire A, Verveer PJ, Rocks O, Bastiaens PI (2004) Red-edge anisotropy microscopy enables dynamic imaging of homo-FRET between green fluorescent proteins in cells. J Struct Biol 147(1):62–69
Stein IH, Steinhauer C, Tinnefeld P (2011) Single-molecule four-color FRET visualizes energy-transfer paths on DNA origami. J Am Chem Soc 133(12):4193–4195
Stewart ME, Anderton CR, Thompson LB, Maria J, Gray SK, Rogers JA, Nuzzo RG (2008) Nanostructured plasmonic sensors. Chem Rev 108(2):494–521
Sun Y, Zhu X, Peng J, Li F (2013) Core–shell lanthanide upconversion nanophosphors as four-modal probes for tumor angiogenesis imaging. ACS Nano 7(12):11290–11300
Suzuki M, Husimi Y, Komatsu H, Suzuki K, Douglas KT (2008) Quantum dot FRET biosensors that respond to pH, to proteolytic or nucleolytic cleavage, to DNA synthesis, or to a multiplexing combination. J Am Chem Soc 130(17):5720–5725
Tan H, Wang M, Yang CT, Pant S, Bhakoo KK, Wong SY, Chen ZK, Li X, Wang J (2011) Silica nanocapsules of fluorescent conjugated polymers and superparamagnetic nanocrystals for dual-mode cellular imaging. Chemistry 17(24):6696–6706
Tang F, Ma N, Wang X, He F, Li L (2011) Hybrid conjugated polymer-Ag@ PNIPAM fluorescent nanoparticles with metal-enhanced fluorescence. J Mater Chem 21(42):16943–16948
Thomas SW 3rd, Joly GD, Swager TM (2007) Chemical sensors based on amplifying fluorescent conjugated polymers. Chem Rev 107(4):1339–1386
Tian Z, Wu W, Li AD (2009) Photoswitchable fluorescent nanoparticles: preparation, properties and applications. Chemphyschem 10(15):2577–2591
Varnavski OP, Ostrowski JC, Sukhomlinova L, Twieg RJ, Bazan GC, Goodson T (2002) Coherent effects in energy transport in model dendritic structures investigated by ultrafast fluorescence anisotropy spectroscopy. J Am Chem Soc 124(8):1736–1743

Wang F, Tan WB, Zhang Y, Fan X, Wang M (2006a) Luminescent nanomaterials for biological labelling. Nanotechnology 17:R1–R13

Wang L, Wang KM, Santra S, Zhao XJ, Hilliard LR, Smith JE, Wu JR, Tan WH (2006b) Watching silica nanoparticles glow in the biological world. Anal Chem 78(3):646–654

Wang F, Banerjee D, Liu Y, Chen X, Liu X (2010) Upconversion nanoparticles in biological labeling, imaging, and therapy. Analyst 135(8):1839–1854

Wang Y, Bao L, Liu Z, Pang DW (2011) Aptamer biosensor based on fluorescence resonance energy transfer from upconverting phosphors to carbon nanoparticles for thrombin detection in human plasma. Anal Chem 83(21):8130–8137. doi:10.1021/ac201631b

Wang Y, Ji L, Zhang B, Yin P, Qiu Y, Song D, Zhou J, Li Q (2013) Upconverting rare-earth nanoparticles with a paramagnetic lanthanide complex shell for upconversion fluorescent and magnetic resonance dual-modality imaging. Nanotechnology 24(17):175101

Wang D, Guo Y, Liu W, Qin W (2014) Preparation and photoluminescent properties of magnetic Ni@ SiO 2–CDs fluorescent nanocomposites. RSC Adv 4(15):7435–7439

Watrob HM, Pan C-P, Barkley MD (2003) Two-step FRET as a structural tool. J Am Chem Soc 125(24):7336–7343

Wiederrecht GP, Wurtz GA, Hranisavljevic J (2004) Coherent coupling of molecular excitons to electronic polarizations of noble metal nanoparticles. Nano Lett 4(11):2121–2125

Wilson R, Cossins AR, Spiller DG (2006) Encoded microcarriers for high-throughput multiplexed detection. Angew Chem Int Ed Engl 45(37):6104–6117

Wu C, Zheng Y, Szymanski C, McNeill J (2008) Energy transfer in a nanoscale multichromophoric system: fluorescent dye-doped conjugated polymer nanoparticles. J Phys Chem C Nanomater Interfaces 112(6):1772–1781. doi:10.1021/jp074149+

Wu C, Hansen SJ, Hou Q, Yu J, Zeigler M, Jin Y, Burnham DR, McNeill JD, Olson JM, Chiu DT (2011) Design of highly emissive polymer dot bioconjugates for in vivo tumor targeting. Angew Chem Int Ed 50(15):3430–3434

Würthner F, Kaiser TE, Saha-Möller CR (2011) J-aggregates: from serendipitous discovery to supramolecular engineering of functional dye materials. Angew Chem Int Ed 50(15):3376–3410. doi:10.1002/anie.201002307

Xu Y, Li Z, Malkovskiy A, Sun S, Pang Y (2010) Aggregation control of squaraines and their use as near-infrared fluorescent sensors for protein. J Phys Chem B 114(25):8574–8580

Zhang BF, Frigoli M, Angiuli F, Vetrone F, Capobianco JA (2012) Photoswitching of bis-spiropyran using near-infrared excited upconverting nanoparticles. Chem Commun 48(58):7244–7246

Zheng YB, Juluri BK, Lin Jensen L, Ahmed D, Lu M, Jensen L, Huang TJ (2010) Dynamic tuning of plasmon–exciton coupling in arrays of nanodisk–J-aggregate complexes. Adv Mater 22(32):3603–3607

Ziessel R, Harriman A (2011) Artificial light-harvesting antennae: electronic energy transfer by way of molecular funnels. Chem Commun 47(2):611–631

Ziessel R, Goze C, Ulrich G, Cesario M, Retailleau P, Harriman A, Rostron JP (2005) Intramolecular energy transfer in pyrene-BODIPY molecular dyads and triads. Chemistry 11(24):7366–7378

Zou W, Visser C, Maduro JA, Pshenichnikov MS, Hummelen JC (2012) Broadband dye-sensitized upconversion of near-infrared light. Nat Photonics 6(8):560–564

Chapter 7
Recognition Units

The heart of any chemosensor or biosensor is its recognition unit (*binder* or *receptor*). It is constructed for providing selective target binding from a mixture of different and sometimes closely related compounds, materials or living cells. The high specificity and affinity of this unit is achieved by its appropriate structures allowing multi-point non-covalent interactions with the target. Such highly selective binding is called *molecular recognition*.

Recognition units are the key functional units of molecular sensors that are responsible for selective target binding in the proper range of its concentrations. Multi-point non-covalent interactions with the target with desired affinity allow providing selective target binding from a mixture of different and sometimes closely related compounds. In this Chapter we discuss different binding units and the principles of their design, construction and performance. They range from small coordination compounds targeting small molecules and ions to macromolecules such as enzyme substrates, proteins, nucleic acids, macromolecular assemblies or even the living cells. Their immense number requires a great variety of means for specific detection. All of these *receptors* or *recognition units* must be transformed into sensors by coupling a fluorescent dye or nano-particle for responding to the presence of the target without affecting the binding affinity. Therefore our goal is to achieve optimal binding and efficient labeling of the binder but still to maintain the target binding properties intact while adding the reporter function.

7.1 Multivalency: The Principle of Molecular Recognition

The term *molecular recognition* is used to indicate noncovalent specific interactions between molecules of chemical or biological origin. Such interactions could be hydrogen bonding, metal coordination forces, van der Waals interactions, π-π stacking, etc. (Bishop et al. 2009). For providing stable intermolecular complex formation, each of these forces is not strong enough to compete with solute-solvent

A.P. Demchenko, *Introduction to Fluorescence Sensing*,
DOI 10.1007/978-3-319-20780-3_7

interactions, compensate entropy loss or to withstand thermal fluctuations. Multiplicity of these interactions allows providing sufficient stability of formed intermolecular assemblies.

Specificity is achieved by optimal spatial location of atoms and their groups participating in these interactions, and this determines highly selective complexation of interacting partners. It can be defined as the ability to discriminate between molecular recognition from other low-affinity binding.

Multivalency is a key principle in realizing molecular recognition for achieving strong, specific, yet reversible interactions. Being applicable to both biological (Mammen et al. 1998; Meyer and Knapp 2014) and synthetic (Badjic et al. 2005) systems, it states that molecular recognition can be realized only on formation of multiple, interconnected supramolecular binding modules. The difference between monovalency and multivalency is illustrated in Fig. 7.1. Individually weak

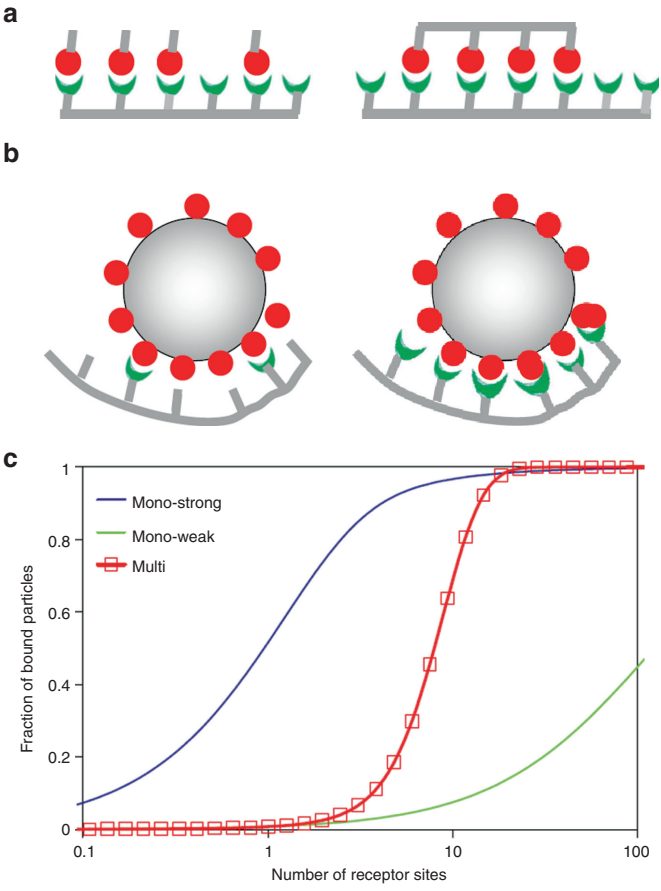

Fig. 7.1 Illustration of multivalency. (**a**) Single-valency (*left*) and multivalency (*right*) binding. (**b**) Interaction of functional nanoparticles with receptors on cell surface. *Left* – small number of receptors. *Right* – large number of receptors and their maximal saturation. (**c**) The effect of supersensitivity (Martinez-Veracoechea and Frenkel 2011). Direct comparison between monovalent and multivalent binding in a model of interacting nanoparticles with cell surface shows that the fraction of bound particles varies sharply (in a highly nonlinear way) with the receptor concentration

interactions produce cumulative effect, so that multi-point binding between interacting structures produces generalized effect that differs from that obtained by summation of individual interactions. This principle is the guideline for design and selection of recognition units in fluorescence sensing, since sensing requires the target binding in complex multi-component systems with components existing in different concentrations and possessing different binding affinities.

7.1.1 The Origin of Target-Receptor Binding Selectivity

It was frequently observed that the binding between two multivalent (i.e. having more than one binding site) entities involving n ($n > 1$) binding events occurs with an affinity higher than the sum of n individual monovalent interactions (Mammen et al. 1998). The classical example is the lectin binding with saccharides (Fasting et al. 2012). In the case of monosaccharide molecule, as a result of combination of noncovalent interactions such as hydrogen bonds, hydrophobic interactions and van der Waals interactions, the binding constants K are typically in the range of 10^3–10^4 M^{-1}, so the binding is relatively weak and low specific compared to that in other biological recognition events. It becomes much stronger in oligosaccharides, K up to 10^6 M^{-1}, as a result of spatial extension of the binding sites, and upon association of lectin molecules it can increase further, to 10^9 M^{-1}. The formation of lectin tetramer is a prototypical illustration of the multivalency generated by self-assembly leading to defined arrays of functional groups and binding patterns (Chmielewski et al. 2014).

Essentially, the effects of multiplicity appears when two or more structurally linked sites on one of the partners (receptor) interacts with two or more linked sites of the other partner (ligand). If one of the partners is monovalent and binds to several sites of the second partner, then no multivalency effects will be observed. This effect can be seen without *cooperativity* (the influence of binding at one site on the binding affinity of other sites). Cooperativity can be rigorously defined for consecutive monovalent interactions at a multivalent platform (Mulder et al. 2004). In general, it does not require multivalency (for instance, binding of oxygen to hemoglobin is cooperative but not multivalent). However, the positive cooperativity, if present, may enhance the effect.

The contribution of different factors to the origin of multiplicity is not easy to evaluate since they reside on the changes of both interaction energy and entropy. The entropy effects of binding at the first site can be complemented by that on mutual steric adaptation and conformational changes in both interacting partners. The effect will depend substantially on whether the interacting sites are connected by rigid or flexible linkers.

7.1.2 Quantitative Measure of Multivalency

To characterize a multivalent binding effect, one can use an enhancement factor b (Mammen et al. 1998), introduced as the ratio of the binding constant for the multivalent binding (K_{multi}) of a multivalent ligand to a multivalent receptor with the

binding constant for the monovalent binding (K_{mono}) of a monovalent ligand to a multivalent receptor, $b=(K_{multi})/(K_{mono})$. An advantage of this enhancement factor is that it can be used even if the multiplicity of effective binding interactions is unknown.

In contrast to univalently interacting molecules and particles, the multivalent nano-particles that can bind to a larger number of ligands simultaneously, display regimes of "*super selectivity*" where the fraction of bound particles varies sharply with the receptor concentration (Martinez-Veracoechea and Frenkel 2011). Numerical simulations were made showing that multivalent nano-particles can be designed in such a way that they approach the "on-off" binding behavior when these particles interact with receptors located on the surface. Unexpectedly, it was found that weak bonds are more selective than strong ones. Such sharp discrimination between surfaces with high and low receptor coverage should be accounted in the design of sensor technologies. It was derived that the super selectivity is due to the fact that the number of distinct ligand-receptor binding arrangements increases in a highly nonlinear manner (Fig. 7.1).

7.1.3 Words in Conclusion

Constellation of weak intermolecular interactions and their optimal arrangement allow achieving high affinity and selectivity even with relatively small molecules as receptors. Multivalency is the means for not only providing fine modulation of these interactions but also for achieving their *reversibility*. Reversibility in target-receptor binding is very important for different sensing technologies. It has to be clearly understood, that the sensor detects the *bound* target, whereas the information is always needed on the *total* concentration of target present in the system, both bound and unbound. When the equilibrium between bound and unbound target is established, its distribution between these forms can be achieved based on mass action law. Thus, the detection range of any two-state responsive sensor is limited to two orders of magnitude, below and above *dissociation constant* K_d (Chap. 2). This puts additional requirement on sensor *affinity*, which should fit to this rather narrow range of required target concentrations. Too strong binding is often as useless as too weak binding. Very important also is the *selectivity* of binding – the ability to discriminate from other species that may be close in structure and properties. Both affinity and selectivity can be modulated by substituents in the discussed below small-molecular binders.

7.2 Recognition Units Built of Small Molecules

The possibilities of organic chemistry to synthesize new molecules with increasing complexity and with more and more specialized functional behavior are tremendous. Organic molecules are able to specifically bind small molecules such as ions, monosaccharides, amino acids and short peptides, but such binding needs special

design. Whereas small heterocycles (crown ethers, cryptands) are ideal for recognizing ions, boronic acid derivatives are strong saccharide binders and the macrocyclic cavity formers, such as cyclodextrins, calix[n]arenes and cucurbit[n] urils, are able to recognize particular motives at the interfaces and even on the surfaces of protein molecules.

Already with these small binders we observe the operation of *principle of multivalency*: the space-filling binding with saturation of all possible weak intermolecular interactions is observed. With cycled rigid structures, multivalency attains new features. One is the *macrocyclic effect*. The stability in a complex of cyclic molecules with their guests is usually enhanced over a linear multivalent counterpart because the interaction sites are prefixed into a preferred conformation and there is less configurational entropy for macrocyclic receptors to lose on binding. The other is *chelate effect*, so that formation of first in many noncovalent bonds stabilizing the structure increases dramatically the formation of other bonds just due to increase of local concentration. Thus, both reduction of flexibility and complementarity in dimension, topology and saturation with noncovalent bonds – all of that matters for the creation of highly stable and selective molecular recognition events.

7.2.1 Crown Ethers and Cryptands

Crown ethers are cyclic chemical compounds that contain a ring composed of several ether groups. Together with nitrogen containing *azacrowns* they can be strong binders of different small molecules, particularly ions. *Cryptands* are the advanced derivatives of crown ethers that possess three-dimensional spatial structures and higher association constants compared with crown ethers. The introduction of the additional arms makes cryptand-based host–guest systems responsive to more stimuli, which is crucial for the construction of adaptive or smart materials (Zhang et al. 2014). Both crown ethers and cryptands can be fused with organic dyes. In this case the dyes, incorporating the target-binding groups, attain new properties. The binding provides a perturbation of the dye electronic structure and such perturbation may change dramatically when the target binds, generating a strong spectroscopic response. The targets in these cases are of small size: the metal ions, such as Ca^{2+}, or small neutral compounds such as glucose.

The literature contains a great number of dyes and their modifications with incorporation of recognition units (de Silva et al. 1997; Lakowicz 2006; Valeur 2002). Some of them will be discussed in Sect. 12.3 on the detection of small-molecular targets. Organic dyes and conjugated polymers allow combining efficiently in one molecule of recognition and reporting properties. Several examples are given below (Fig. 7.2).

Various mechanisms of signal transduction and response can be employed here. They include modulation of reactions, in which the electrons participate in the excited states – the photoinduced electron, charge and energy transfers (PET, ICT and FRET reactions correspondingly). The first two of these reactions can exhibit influences by the neighboring charges by electrostatic interactions and therefore

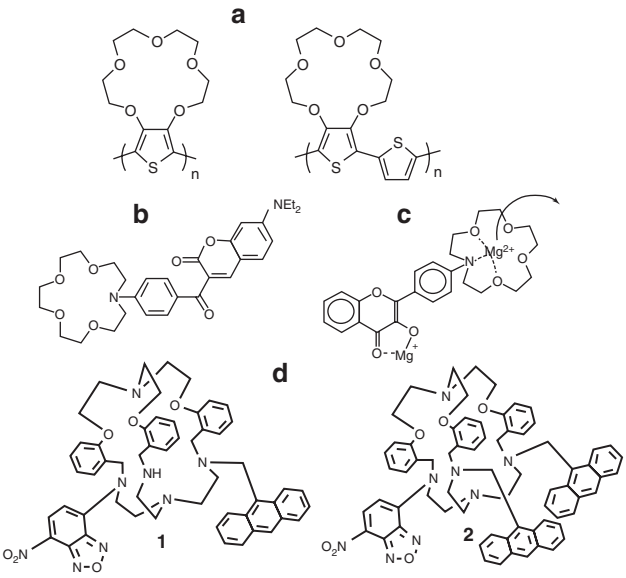

Fig. 7.2 Examples of fluorescent organic molecules that can bind and detect ions. (**a**) Conjugated polymer with incorporated crown ether groups. The ions when are bound to some of crown ether groups produce fluorescence quenching of the whole chain (McQuade et al. 2000). (**b**) The dye containing azacrown ether group and two carbonyls that provide selective binding of Pb^{2+} ions with fluorescence enhancement response (Chen and Huang 2002). (**c**) Azacrown ether derivative of 3-hydroxyflavone has two centers of binding bivalent cations, Ma^{2+} and Ba^{2+}. The ions bound at azacrown site are ejected upon excitation. This leads to different effects of binding in excitation and emission spectra (Roshal et al. 1999). (**d**) A laterally nonsymmetric azacryptand derivatized with one 7-nitrobenz-2-oxa-1,3-diazole (*1*) and one/two anthracenes (*2*). These compounds give a large enhancement on binding of Cu^{2+}, Ag^{+}, and proton. The enhancement is observed in the diazole moiety even when the anthracene fluorophore is excited because of substantial fluorescence resonance energy transfer from anthracene to the diazole moiety (Sadhu et al. 2007)

these effects are the most applicable for detection of charged compounds and ions. Modulation of FRET can be used due to the change of overlap integral on target binding and conformational change leading to the change in electronic conjugation between fragments of the dye molecule. The mechanisms of these reactions will be discussed in Chap. 8.

7.2.2 Boronic Acid Derivatives

Boronic acids and their derivatives are valuable as molecular recognition units due to their distinguished features to recognize diol motifs through boronic ester formation (Wu et al. 2013; Nishiyabu et al. 2012). They can reversibly interact with 1,2-diols or 1,3-diols in aqueous solution to form 5- or 6-membered ring cyclic esters (Fig. 7.3). This reaction results in formation of covalent bonds, but still it is

Fig. 7.3 Interaction of boronic acid with diols

reversible. Since it occurs in aqueous media at neutral pH values, it has become very attractive as the basis for an important sensing scheme in biologically relevant conditions for saccharides, including glucose.

Borinic acid derivatives show good examples of multivalency. Binding of diols is already bivalent. In order to increase affinity to multi-hydroxylic compounds, a number of dimeric derivatives of boronic acid were synthesized (Fig. 7.4). They became ideal for highly selective binding of saccharides interacting with their linked arrays of hydroxy groups.

The major focus in application of boronic acids is in glucose sensing, since glucose level is one of the major indices in clinical diagnostics. Other saccharides and glycans on cell surface provide an ideal structural framework for binding to boronic acids. As this interaction is covalent, it allows efficient labeling of the cell surface (Yang et al. 2004). Being potent substitutes of *lectins* they are of diagnostic significance. Incorporation of several boronic acid groups into a covalent framework or non-covalent assembly of boronic acid are the two general methods used to create such recognition parts of smart sensors. Being able to generate multivalent saccharide-binding architectures, they resemble lectin oligomers (see Fig. 7.4).

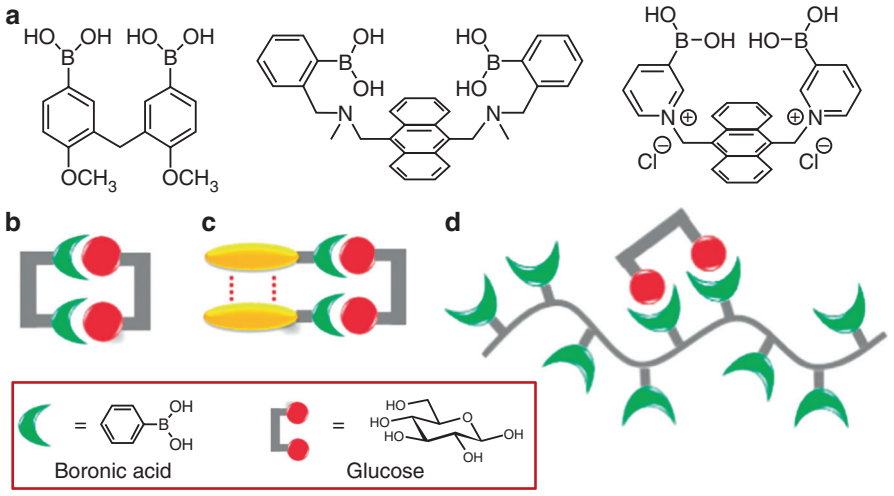

Fig. 7.4 The strategies in applications of boronic acid derivatives for selective saccharide sensing via multivalent boronic acid–saccharide interactions (Wu et al. 2013). (**a**) Typical synthetic diboronic acids that form 1:1 cyclic boronate esters with glucose. (**b**) Cartoon representation of diboronic acid binding to glucose; (**c**) aggregation of simple boronic acids via noncovalent interactions allowing multivalent glucose binding; (**d**) boronic acid-containing polymers or nanomaterials that bind glucose with two of pendant boronic acid moieties

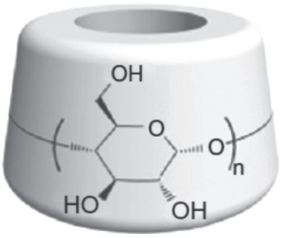

	α-CD	β-CD	γ-CD
Number of glucose units	6	7	8
Molecular weight	972.86	1135.01	1297.15
Water solubility (g/L)	145	18.5	232
Internal diameter	4.7–5.2	6.0–6.4	7.5–8.3
Depth	6.7	7.0	7.0

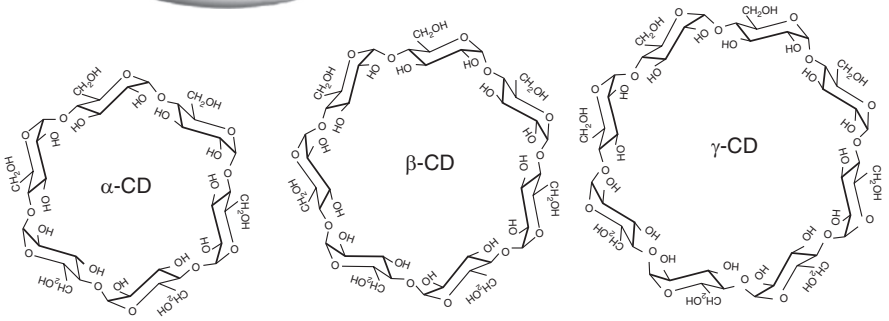

Fig. 7.5 Schematic drawing (*above*) and the chemical structures (*below*) of α, β and γ cyclodextrins (From (Wenz et al. 2006) and (Szejtli 1998))

7.2.3 Cyclodextrins

Cyclodextrins make up a family of *cyclic oligosaccharides* containing six (α-cyclodextrin), seven (β-cyclodextrin) and eight (γ-cyclodextrin) α-D-glucose subunits in a ring, creating a conical shape (Fig. 7.5).

The primary hydroxyl groups are directed to the narrow side, and the secondary ones are located on the wide side of the torus. With hydroxyl groups facing the outer space, these molecules are highly soluble in water, whereas the inner space can accommodate different low-polar molecules, such as cholesterol. Their binding affinity is determined by the cavity size. It increases from α-cyclodextrin (α-CD) to β-cyclodextrin (β-CD) and to γ-cyclodextrin (γ-CD), see Table 7.1.

Inclusion complexes are known as the entities comprising two or more molecules, in which one of them, serving as the '*host*' includes a '*guest*' molecule only by physical forces, i.e. without covalent bonding. Cyclodextrins are typical 'host' molecules that can include a great variety of molecules that have the size

Table 7.1 Minimum internal diameters d_{min}, cross-sectional areas A_{min} and inner volume V of cyclodextrins

Cyclodextrin	d_{min} (Å)	A_{min} (Å^2)	V (Å^3)
α-CD	4.4	15	174
β-CD	5.8	26	262
γ-CD	7.4	43	427

conforming to the size of cavity (Szejtli 1998). Thus, α-cyclodextrin can form inclusion complex with one, β-cyclodextrin – with two and γ-cyclodextrin – with three pyrene molecules. Cyclodextrins can be produced in large quantities from starch by simple and cheap enzymatic conversion, which adds its popularity as a carrier of drugs, in cosmetic industry and, of course, in sensing technologies (Szejtli 1998).

The presence of a number of exposed hydroxyl groups (18 in α-cyclodextrin, 21 in β-cyclodextrin and 24 in γ-cyclodextrin) allows a practically unlimited number of *chemical modifications*, and many of them can modify the selectivity in formation of inclusion complexes with different molecular guests. The most popular are methylated and hydroxyalkylated derivatives that increase affinity to low-polar guests. Dimeric and oligomeric forms of cyclodextrins can be easily obtained. They may show increased affinity to large molecules, even to proteins, incorporating their segments. It was observed that such covalently linked dimeric structures could even disrupt the interactions between protein subunits in multimeric proteins by competition for exposed low-polar residues and thereby inhibit protein aggregation.

Cyclodextrins have received much attention as the very *specific binders* in molecular and supramolecular studies, for providing nano-scale media for chemical reactions (Oshovsky et al. 2007), even for modelling biomolecular catalysis (Breslow and Dong 1998). It was demonstrated that with proper modification, the sensing with cyclodextrins can be enantioselective, so that clear discrimination between D- or L-amino acids can be achieved (Pagliari et al. 2004).

Many organic dyes form *inclusion complexes* with cyclodextrins (Al-Hassan and Khanfer 1998). Decrease of polarity, dehydration effects and immobilization effects were detected in fluorescence response of these dyes. Comparative studies on binding of different neutral, anionic and cationic dyes (Balabai et al. 1998) demonstrated that the binding is mainly hydrophobic and is only insignificantly affected by the charge of guest molecule. In all studied cases the tight complexes are formed. This is manifested by a decrease of anisotropy decay, which detects rotation of the whole complex. Meantime, ultrafast dynamics of guest molecules exists, and it was characterized by time-resolved methods (Douhal 2004).

Inclusion into cyclodextrin cavity changes the photophysical and spectroscopic properties of organic dye molecules. Thus, for solvatochromic dye Nile Red a remarkable decrease of non-radiative decay of ICT state was observed on inclusion into β-cyclodextrin cavity (Hazra et al. 2004). The influence on protonation equilibrium (Mohanty et al. 2006) and excited-state proton transfer from pyranine to acetate in gamma-cyclodextrin and hydroxypropyl gamma-cyclodextrin (Mondal et al. 2006) was also reported. Different excited-state reactions, such as ESIPT (Organero et al. 2007), are also affected by binding in nanocavity.

The *fluorescence reporting* signal can be generated in a simple but efficient way by displacement by the target molecule of the dye bound in cyclodextrin cavity. If the dye is not attached covalently to cyclodextrin host, we will get competitor displacement assay (as explained in Chap. 1). If the dye is covalently bound by a flexible link, we can get the direct sensor. The target binding properties can be modulated by chemical substitutions.

An increase of selectivity and affinity of cyclodextrin to its target is achieved when the sensor is made '*bivalent*' so that the linker connects two cyclodextrin molecules (Yang et al. 2003b). Possessing two beta-cyclodextrin cavities in close vicinity and a functional linker with good structural variety in a single molecule, these bridged bis(beta-cyclodextrin)s can significantly enhance the original binding ability and molecular selectivity. In this case the possibility of multipoint interaction with the target increases and recognition of molecules as large as proteins can be achieved by binding the dimer at two exposed sites.

It was shown that biquinolino-modified beta-cyclodextrin dimers and their metal complexes may serve as efficient fluorescent sensors for the molecular recognition of steroids (Liu et al. 2004). The length of the linker between two monomers is an important variable that can significantly modify steroid binding (Fig. 7.6).

It was shown that a γ-cyclodextrin dimer exhibits strong molecular recognition ability for bile acids and endocrine disruptors (Makabe et al. 2002). Attached pyrene moieties allow detecting the binding as the ratio of their monomer and excimer fluorescence intensities. It was indicated that pyrene residues participate in guest binding and serve as hydrophobic cups for the cavities.

Conjugation with peptides expands the possibilities of cyclodextrins for detecting steroid molecules (Hossain et al. 2003). Double labelling with FRET detection can be a method of choice in fluorescence reporting. Construction of more sophisticated conjugates with proteins was also reported, particularly, for sensing maltose based on *E. coli* maltose binding protein (MBP) (Medintz et al. 2003).

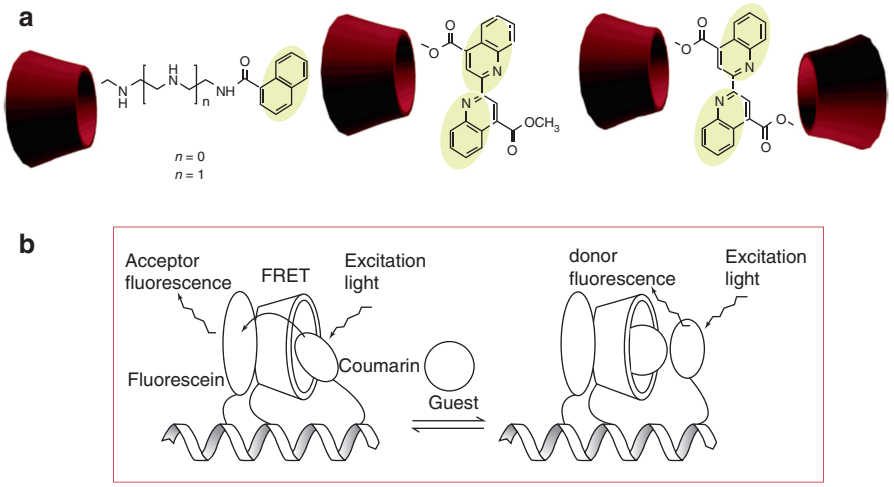

Fig. 7.6 Examples of cyclodextrin conjugates with fluorescence dyes. (**a**) From *left* to *right*: quinoline dye attached through the spacer (n = 1–2); biquinoline dye attached to a monomer; biquinoline dye forming a link between two cyclodextrin molecules (Liu et al. 2004). (**b**) Illustration of application of cyclodextrins in FRET-based sensing (Ogoshi and Harada 2008). Cyclodextrin plus two dyes (donor and acceptor in FRET) are assembled on a peptide scaffold. The target molecule (guest) substituting the dye located within the cavity and disrupting FRET generates fluorescence output

7.2.4 Calix[n]arenes

Calix[n]arenes are a class of polycyclic compounds that can allow (by proper chemical substitutions) achieving high-affinity binding of many small molecules. Calix[n]arenes are cyclic oligomers composed of n = 4–6 phenyl groups connected by methylene bridges that are obtained by phenol-formaldehyde condensation. They exist in a 'cup-like' shape with a defined upper and lower rim and a central annulus. Their rigid conformation of skeleton forming a cavity together with some flexibility of side groups (allowing their flip-flop) enables them to act as host molecules for different small molecules and ions. Their basic structure resembling a vase (calix = vase) together with modifications with short peptides in its upper rim is presented in Fig. 7.7. This beautiful structure resembles a basket of flowers.

Based on calixarene scaffold, a broad variety of structures can be realized by *modifications* of both upper (Sliwa and Deska 2011) and lower (Joseph and Rao 2011) rims. Examples of such derivatives are presented in Fig. 7.8. By functionally modifying these sites it is possible to prepare various derivatives with differing selectivity for various guest molecules. Mostly they are small molecules and ions, but with proper modifications they can target the structural elements of large molecules, such as proteins. At these sites fluorescent labelling can be achieved.

Calix[4]arene structure allows many possibilities for targeting *proteins*. Their upper rim displays four positions that can be used for covalent attachments. Moreover, the nature and symmetry of such recognition elements may be varied to

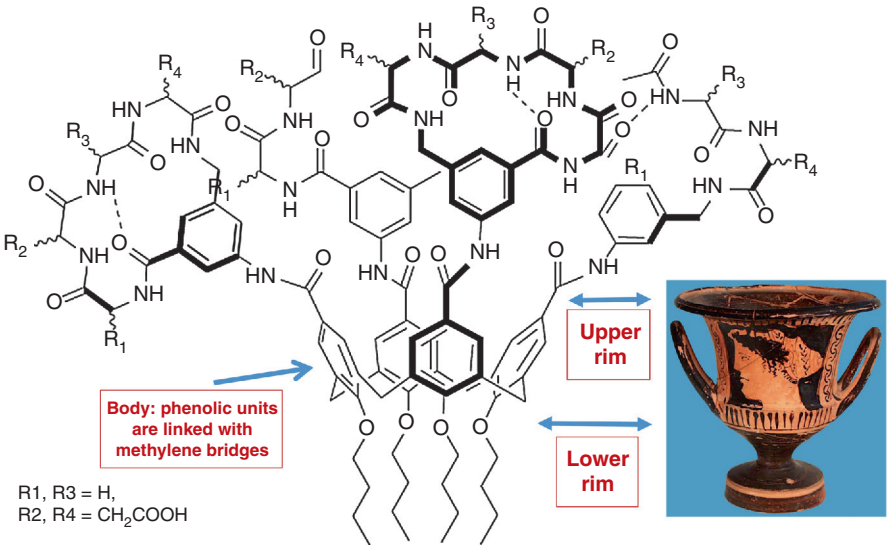

Fig. 7.7 Calix[4]arene derivatives that mimic the properties of antibodies to recognize protein targets. R_1-R_2-R_3-R_4 could be H, CH_2COOH; $(CH_2)_4NH_2$ (Peczuh and Hamilton 2000). This arrangement provides the recognition pattern of negative and positive charges

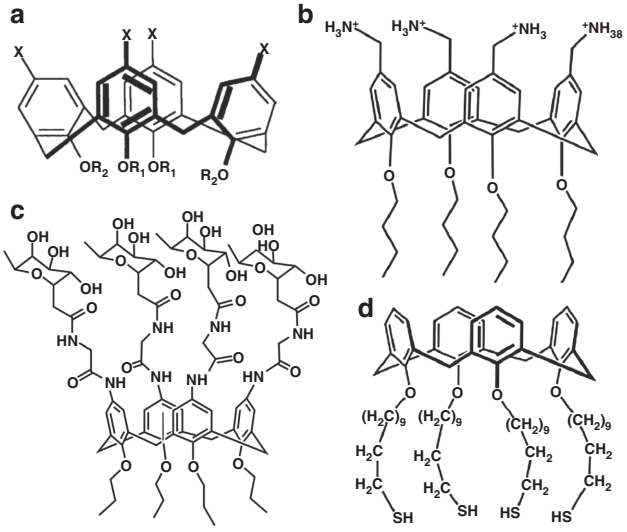

Fig. 7.8 Parent calix[4]arene in a cone conformation. (**a**) The sites of substitutions with covalent attachment of recognition units and fluorescent dyes in the upper rim are marked *X*. In the lower rim, the substitution sites are denoted as R_1 and R_2. (**b**) Calix[4]arenes with amino groups at the upper rim. They can be used for convenient chemical modifications. (**c**) and (**d**) Typical calix[4] arenes with substitutions at the upper and lower rims correspondingly

selectively target the highly irregular surfaces, comprised of charged, polar and hydrophobic sites.

A series of synthetic receptors was prepared, in which four peptide loop domains are attached to a central calix[4]arene scaffold (Peczuh and Hamilton 2000). Each peptide loop is based on a cyclic hexapeptide, in which two residues have been replaced by a 3-aminomethyl benzoate dipeptide mimetic, which also contains a 5-amino substituent for anchoring the peptide to the scaffold. Through the attachment of various peptide loops, the authors made a series of calix[4]arenes expressing negatively and positively charged regions as well as hydrophobic regions and thus achieved binding to complementary regions of several proteins. They demonstrated the binding to platelet-derived growth factor (PDGF) and inhibition of its interaction with its cell surface receptor PDGFR. A similar structure interacts specifically with cytochrome c (see Fig. 7.7).

Fluorescence reporting on the binding of different targets to calix[4]arene structures is commonly introduced in two ways.

(a) Using the property of these molecules to bind different dyes at the site within the cavity, where there occurs the binding of many targets. Then the binding of target molecule can displace the fluorescent dye. When the dye dissociates, it changes its fluorescence. The chelating properties of calix[4]arenes towards different dyes were reported by many researchers (Kubinyi et al. 2005). In all these cases, formation of the complex leads to dramatic fluorescence quenching, and this

result suggests a convenient possibility for transforming the receptors into efficient sensors. This suggests using calix[4]arene derivatives in *competitor substitution* assays. Ample possibilities for modulating the target affinities by covalent modifications and a broad choice of responsive dyes with different affinities promise easy development of simple and efficient assays for many targets.

(b) *Covalent conjugation* of calix[4]arene side groups with fluorescent dyes (Nanduri et al. 2006). In this case, several mechanisms of fluorescence response can be realized. One can be easily applied in ion sensing and is based on induction/perturbation of photoinduced intramolecular charge transfer (ICT). The tert-butylcalix[4]arene was synthesized either with one appended fluorophore and three ester groups or with four appended fluorescent reporters (Leray et al. 2001). The dyes were 6-acyl-2-methoxynaphthalene derivatives, which contained an electron-donating substituent (methoxy group) conjugated to an electron-withdrawing substituent (carbonyl group). This is a typical arrangement for fluorescent reporters operating on the basis of ICT principle (Sect. 8.2).

It was shown, that such molecules respond to binding the ions not only by expected red shifts of the absorption and emission spectra but also by a drastic enhancement of the fluorescence quantum yield Φ. Thus, the compound with one substituent was synthesized, for which Φ increases from 0.001 to 0.68 on binding the Ca^{2+} ions. In the case of four substitutions, the emission was strongly depolarized due to the energy transfer (homo-FRET). Regarding the complex-forming ability, a high selectivity for Na^+ over K^+, Li^+, Ca^{2+} and Mg^{2+} was observed. This selectivity (Na^+/other cations) expressed as the ratio of the stability constants was found to be more than 400. This result certifies the abilities of calixarenes as useful building platforms in the design of complex systems, in which not only ICT but also other excited-state phenomena (electron, and proton transfer, excimer formation and resonance energy transfer) are controlled by ions. The applications mainly concern ion sensing with high selectivity (Valeur and Leray 2007).

The sensors based on calixarene platform with covalent attachment of reporter dye can be very efficient. A variety of environment-sensitive dyes were used for attachment, particularly, to an upper rim of their structures. In one of the recent studies, such modification was made with cyanine dyes (Kachkovskiy et al. 2006), which opens the pathway for extending the sensing techniques to a near-IR range.

In a number of reports the dye was constructed as a part of recognition mechanism, and the changes in its interactions with environment induced by target binding produced the necessary reporter signal. *Enantioselective* (distinguishing stereoisomers) molecular sensing of aromatic amines was achieved using their quenching on interaction with the chiral host tetra-(S)-di-2-naphthylprolinol calix[4]arene (Jennings and Diamond 2001).

In addition to the role of recognition elements of small molecular sensors, calix[4]arenes play an important role in construction of fluorescent *functional nanocomposites*. They are used for coating quantum dots (Jin et al. 2006), which allows achieving their bright emission and high stability in aqueous solutions. A fluorescent conjugated polymer poly(phenylene ethynylene) containing

calix[4]arene-based recognition units displays a sensitivity to be quenched by the N-methylquinolinium ion. This effect is over three times larger than that seen in a control polymer lacking calix[4]arenes (Wosnick and Swager 2004).

Very attractive is the ability of calix[4]arenes to host rare earth cations. These ions are highly luminescent only in the ligand-bound forms (Sect. 4.5), and calix[4]arenes may serve as such ligands. The water soluble calix[4]arene derivatives can form luminescent complexes with europium(III) and terbium(III) ions (Yang et al. 2003a, b). This transforms the whole complex into luminophore with long-duration emission that allows many new possibilities for sensor developments.

7.2.5 *Cucurbit[n]urils*

Cucurbit[n]urils are the macrocycles, which like cyclodextrins and calixarenes, exist in different sizes (n = 5–8, 10). They are composed of a different number of glycoluril units joined by pairs of methylene bridges (Fig. 7.9). They are obtained by acid-catalyzed condensation of glycoluril with formaldehyde under carefully controlled conditions. The size of the inner cavity ranges from 68 to 691 $Å^3$ (for n between 5 and 10) allowing different guest molecules of largely variable sizes to be included within the cavity with remarkable selectivity. Similarly to cyclodextrins and calixarenes, cucurbiturils have a nonpolar inner cavity which is prone to bind organic residues or guests by hydrophobic interactions (Nau et al. 2011). Meantime, there is a remarkable difference from calixarenes, and not only in high rigidity of their structures. In calixarenes the inner surface is polarizable due to the presence of phenyl groups and in cucurbiturils the cavity is extremely non-polarizable.

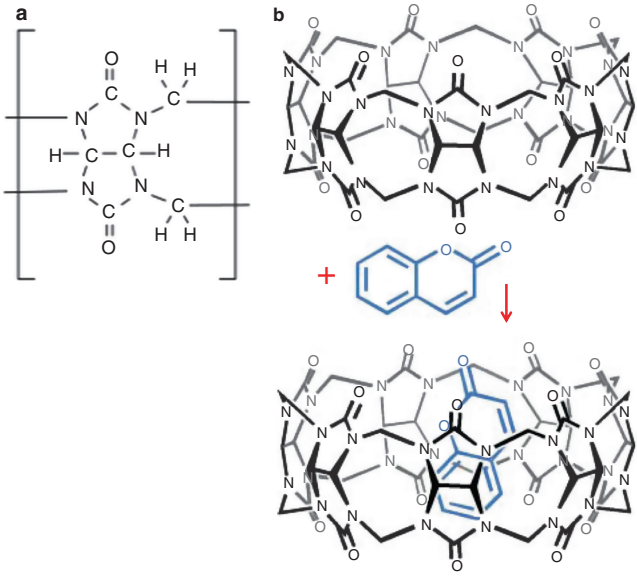

Fig. 7.9 The structure of cucurbiturils (Wang et al. 2009). These molecules are composed of a different number of glycoluril units joined by pairs of methylene bridges (**a**). The interaction of curbit[7]uril with coumarin dye (**b**). The 1:1 host – guest complex is formed by dye inclusion into the host cavity

This class of macrocycles display a relatively low water-solubility and strong complexation with many fluorescent dyes (Dsouza et al. 2011). Their host/guest complexes are much stronger than that of cyclodextrins, with binding constants typically ranging from 10^4 M^{-1} to much higher values. Cucurbiturils are known as cation receptors due to their two identical carbonyl rim portals.

7.2.6 Porphyrins

Porphyrin molecule is a heterocyclic macrocycle derived from four pyrrole-like subunits interconnected by means of α carbon atoms via methine bridges (=CH-). This macrocycle is planar and with high electronic conjugation, it contains 26 π-electrons. Many substitutions can be made at the periphery of porphyrin ring (Fig. 7.10) and they determine the binding ability to different targets.

Porphyrins can combine *sensing and reporting properties*, since they possess their own light-absorption and fluorescence spectra. Their fluorescence depends on the presence of coordinated metal cation in the center of their structure. In most cases, the emission spectra of free base porphyrins and of porphyrins with coordinated cation (metalloporphyrins) are different from each other. Since the free and bound forms can be easily distinguished, this suggests the possibility of making sensors for these ions (Purrello et al. 1999). It is hard to do that with natural porphyrins, in which the fluorescence intensity of free base in water is very low and the selectivity of binding is not sufficient to discriminate between different ions in their mixture. Hopefully, porphyrins scaffold allows for many functional substitutions and complexations that are able to improve, if necessary, their binding properties.

Such improvements can be achieved upon *complex formation with cyclodextrins*. These complexes can be particularly useful for determination of zinc ion. The zinc binding changes the fluorescence spectrum of porphyrin (Fig. 7.11), that allows ratiometric recording of zinc concentration (Yang et al. 2003b). Upon binding the zinc ion the fluorescence emission of tetraphenyl porphyrin at 656 nm band decreases while that at 606 nm increases, which allows a wavelength-ratiometric detection.

The binding of synthetic porphyrins to proteins that contain heme group in their native form can be very strong. After enhancing the hydrophobicity of the porphyrin core and by increasing the number of peripheral carboxylic acids from 8 to 16, the

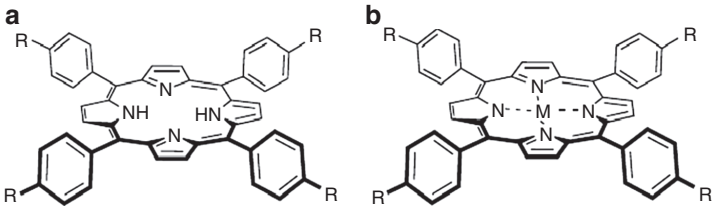

Fig. 7.10 The core structure of synthetic porphyrins. (**a**) Metal-free form. (**b**) Metal-coordinated form. '*R*' marks the positions of various substitutions. They can be selected for high-affinity binding to proteins

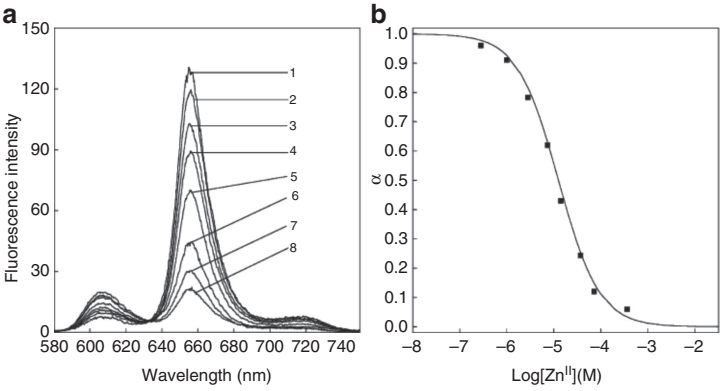

Fig. 7.11 Ratiometric detection of zinc by fluorescence response in porphyrins-cyclodextrin complex (Yang et al. 2003b). (**a**) Effects of zinc ion concentration on the fluorescence emission spectra (spectra 1–8 correspond to the increasing zinc concentrations from 0 to 7.2×10^5 M). (**b**) Relative fluorescence ratio, α, as a function of $\log[Zn^{2+}]$ at pH 8.0

binding to cytochrome *c* with sub-nanomolar dissociation constant was achieved (Ozaki et al. 2006). With $K_d = 0.67 \pm 0.34$ nM this is probably one of the most potent synthetic protein receptors ever designed. The use of porphyrin derivatives as very strong binders was also demonstrated for other proteins. The strategies for protein surface recognition that offer a new use for porphyrins as molecular scaffolds are discussed in the literature (Tsou et al. 2004).

A novel protein-detecting array based on porphyrins containing peripheral amino acids acting as protein surface receptors was reported (Zhou et al. 2006). The *array of porphyrin receptors* showed a unique pattern of fluorescence change upon interaction with certain protein samples. Both metal and nonmetal-containing proteins and mixtures of proteins provide distinct patterns, allowing their unambiguous identification.

7.2.7 Prospects

Recognition units discussed in this Section are designed for specific binding of three classes of molecules: ions, small molecules and proteins. Organic heterocyclic compounds are better suited for detection of ions, because the ions can be easily coordinated into heterocycles and because the ion binding can be electronically coupled with the dye response. Well-developed surface of cyclodextrins, calixarenes and cucurbiturils allows, in addition to specific ion binding, to provide the selective binding of small neutral molecules. Porphyrins can suggest the response in their own emission. Regarding the sensing of small hydrophobic molecules, such as steroids, cyclodextrins are the most attractive. This is because cyclodextrin cavities fit to their sizes, the binding can be selective and involve target penetration into the cavity and forming strong inclusion complexes. We observe also that in the present

conditions, when compared to great progress in nucleic acid recognition, the protein recognition is not sufficiently well developed, these compounds can offer themselves as promising protein binders. Much like the antibodies, such binders should recognize particular patterns on protein molecular surfaces – the 'hot spots'.

Of importance is the fact that the quantum yields, lifetimes and photostabilities of organic dyes can be substantially improved by encapsulating them into macrocyclic host molecules (Dsouza et al. 2011), such as cyclodextrins and cucurbiturils (Biedermann et al. 2012). Such macrocycle-protected dyes can be used in nanocomposite constructions.

7.3 Antibodies and Their Recombinant Fragments

Antibodies (Abs) are the powerful recognition tools used in many sensing technologies. They can be developed to bind target compounds (*antigens*) of any size, starting from steroids, oligosaccharides and oligopeptides. Usually in sensing applications, the antibodies of immunoglobulin G (IgG) type are used. They are globular glycoproteins with molecular mass of 150,000–160,000 Da formed of two light (L) chains and two heavy (H) chains joined to form a Y-shaped molecule. This molecule is composed of β-structured domains stabilized by disulfide bonds (see Fig. 7.12). Their *antigen* (Ag) *binding sites* are formed of six loops contributed by two different so-called variable domains (called VL and VH). Because antibodies contain two VL-VH pairs, they are bivalent: they can react with two antigenic binding sites simultaneously. Specificity to any target is determined by the amino acid composition of these domains. Variability of this composition is responsible for the diversity of the antibody repertoire.

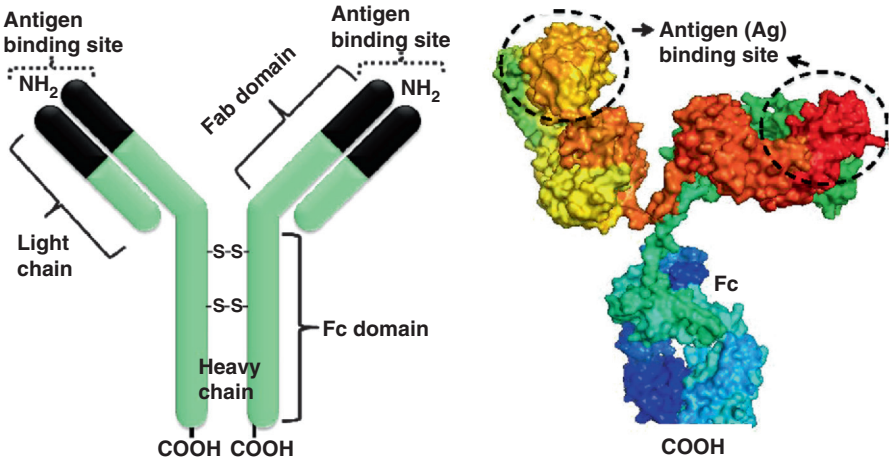

Fig. 7.12 Structure of an antibody (Gopinath et al. 2014): (**a**) diagrammatic representation of an Ab with different regions displayed; (**b**) three-dimensional view of an Ab (PDB code: 1IGT). *Circles* indicate the region of interaction between the antibody and the antigen

Antibodies are used extensively as diagnostic tools in a wide array of different analyses (Gopinath et al. 2014). Because of their unique diversity, they provide a never ending source of molecules with unlimited possibilities for target detection. Antibodies are very efficient in detecting proteins. They recognize regions of the protein surface called *antigenic determinants* or *epitopes*. The contact area between protein and bound antibody is relatively large (600–950 $Å^2$). The contact surfaces exhibit a high level of steric and physico-chemical complementarity.

7.3.1 The Types of Antibodies Used in Sensing

Several types of antibodies and antibody fragments can be used in sensing technologies (Goodchild et al. 2006). *Polyclonal antibodies* are purified from sera of immunized animals. The serum contains antibodies with varying specificities and affinities. For obtaining high affinity antibodies specific for a given target, purification and fractionation steps are needed.

Structurally homogeneous *monoclonal antibodies* are produced by hybridoma cell line clones. Here the problem of achieving high affinity and selectivity is solved by exposing the animals (usually rabbits or mice) to antigens. Then the Ab-producing cells that are raised in their bodies in response to that treatment are selected. Individual Ab-producing animal cells are known to synthesize antibodies of uniform structure, so when they are fused with myeloma cells that are capable of continuous propagation, they synthesize identical antibody molecules. These hybrids can be grown for months and years. Their cultivation is already a part of industry allowing large-scale antibody production.

Recombinant antibody fragments are attractive for sensing technologies because they allow to decrease the size of sensor molecule and also to include substitutions in their primary structures that can facilitate their attachment to surfaces or carriers (including nanoparticles). Groups that can be used for coupling of fluorescence reporters (particularly, –SH groups) can also be introduced. Whereas antibodies specific for most compounds can be obtained relatively rapidly from the serum of immunized laboratory animals, their site-specific labeling requires the production of recombinant antibody fragments by molecular biology techniques, a time-consuming and technically demanding procedure. Libraries of binding fragments have been created. This allows the *in vitro* selection of a recombinant protein specific for a given target by phage-display and other library screening techniques (Benhar 2007) without the need for animal immunization.

The most widely used recombinant antibody fragments contain the VL and VH domains linked by a peptide chain (scFv). Antibody fragments with desired binding specificity can be selected from libraries constructed from repertoires of antibody V genes, bypassing hybridoma technology and even immunization. The V gene repertoires are harvested from populations of lymphocytes, or are assembled *in vitro*. They are cloned for display the fragment on the surface of filamentous bacteriophage. Phages that carry scFvs with desired specificity are selected from the repertoire by panning on antigen; soluble antibody fragments are expressed from

infected bacteria; and the affinity of binding of selected antibodies is improved by mutation. The process mimics immune selection, and antibody fragments with many different binding specificities have been isolated from the same phage repertoire. The probability of identifying a high affinity binder increases with library size (Hust and Dubel 2004), which for phage-displayed libraries ranges between 10^7 and 10^{10} clones (Azzazy and Highsmith 2002).

Thus, human antibody fragments have been isolated with specificities against both foreign and self antigens, carbohydrates, secreted and cell surface proteins, viral coat proteins, and intracellular antigens from the lumen of the endoplasmic reticulum and the nucleus. Such antibodies have potential as reagents for research and in therapy (Jespers et al. 2004).

Heavy-chain fragments, "domain antibodies". Antibody fragments made of heavy chains only have become available recently. Occurring naturally in 'heavy chain' antibodies from camels and now produced in fully humanized form, domain antibodies (dAbs) are the smallest known antigen-binding fragments of antibodies, ranging from 11 to 15 kDa. When they are expressed in microbial cell culture, they show favorable biophysical properties including solubility and temperature stability. They are well suited for selection and affinity maturation by *in vitro* selection systems such as phage display. dAbs are the monomers and, owing to their small size and inherent stability, they can be formatted into larger molecules to create drugs with prolonged serum half-lives or other pharmacological activities. They bind to targets with high affinity and specificity (Muyldermans 2001).

7.3.2 The Assay Formats Used for Immunoassays

The term '*immunosensor*' has been applied to various direct or indirect detection assays involving antibodies (immunoassays). Outstanding recognition properties of antibodies allowed realize these assays in several formats.

Sandwich immunoassays (Fig. 1.13) are the most popular and convenient types of assays that are based on heterogeneous assay principle. Immobilization of receptor molecules (antibodies or their *antigens*) on solid support, application of the sample and washing steps are required before target detection. The antigen-antibody complex is routinely detected using a secondary antibody specific for the antigen or for the constant domain of antibodies. In *enzyme-linked immunosorbent assay* (ELISA), the secondary antibody is coupled to an enzyme, allowing to achieve high detection sensitivity due to enzymatic amplification.

Fluorescence polarization immunoassays. Detection in the change of polarization (or anisotropy) of fluorescence emission (see Sect. 3.3) is one of the most frequently used procedures in sensing with antibodies and is the basis of many commercially available test systems. Rotations of antibodies themselves occur on a time scale of 100 ns or longer, so they are too slow to be detected by common dyes with nanosecond decay. Therefore, this method is mostly used for detection of relatively small molecules. If the target molecules are not fluorescent, then a competitive assay format (see Sect. 1.3) is applied. The target molecules compete for the Ab

binding sites with target analogs coupled with fluorescent dyes. The test is based on the interplay in response of free analog exhibiting low polarization and of that immobilized on binding to antibody for which polarization of emission is high. The testing can be made when the antibody is free in solution, but it can be also immobilized on solid support.

Time-resolved immunoassays. These assays and sensors usually use labeled antibodies or antigen analogs (for competitive assays) with chelating complexes of europium(III) or terbium(III) ions possessing lifetimes typically from 0.01 to 1 s. As it was pointed out in Sect. 3.4, this allows increasing dramatically the sensitivity, suppressing background emission and avoiding the problems with light-scattering.

FRET immunoassays. They are commonly performed when the antibody is labeled with FRET donor and the target or competitor is the FRET acceptor (quencher).

It may be often attractive to construct a *direct sensor* by obtaining the response signal from primary interaction of antibody and target antigen in a way that avoids double labeling as in FRET or complicated instrumentation as in polarization or time-resolved immunoassays. But this is not easy in view that the antigen binding is not associated with large conformational changes, so the signal transduction via conformational change (Sect. 8.5) for providing the reporter signal may not be efficient. Therefore, a contact sensing using environmentally sensitive covalently attached reporters located in proximity to the antigen-binding site must be used (see Fig. 1.12b). This can be achieved by introducing at the desired Ab location a reactive group, such as –SH groups of Cys residues, for coupling the reporter dye, which can be done by recombinant techniques.

The difficulty lies in the choice of a coupling site. In order to find the best solution for this problem the scientists follow two general strategies.

(a) The reporter dye should be located at the *periphery of the binding site*. It should not interfere with the interaction between the receptor and the target, but its micro-environment should change in response to Ab-target complex formation (Renard et al. 2002).
(b) The reporter group should be located *within the binding site* in such way that it becomes one of the key participants in antigen binding (Jespers et al. 2004). In a latter case, the reporter molecule can be chemically linked to a hypervariable loop of an antibody repertoire displayed on phage, and this repertoire can be selected for antigen binding. The fluorescence of the probe has to respond quantitatively to antigen binding. Recently, the prototypes of "quenchbodies" have been suggested (Ueda and Dong 2014). They work on the principle of fluorescence quenching of attached dye and its antigen-dependent release.

Because of lack of sufficient data, it is too early to provide comparative analysis of these two strategies. In experiments when the dye was coupled to an antibody fragment (single chain variable fragment, scFv), 17 sites were selected for the coupling of responsive dye (Renard et al. 2002). Being located at the periphery of binding site, only few of them provided fluorescence response to the presence of antigen (lysozyme). A much stronger response as a substantial decrease of fluorescence intensity was observed by applying the second strategy (Jespers et al.

2004). Thus, the possibility for designing semi-synthetic antibody-based sensors with fully integrated reporter dyes exists and it should be explored in future research.

7.3.3 Prospects for Antibody Technologies

Analyzing the application of antibodies as recognition elements of sensors we obtained very important lessons taught us by Nature. Generation and synthesis in living body of these high-affinity binders occurs via selection-amplification steps starting from genetically available potentially innumerous library. The random mutation-selection principle can be applied *in vitro* for creation of libraries of engineered antibodies and their fragments. This allows producing the recognition units to non-immunogenic or toxic molecules. Despite significant technical difficulties, academic and commercial laboratories have now developed large (more than 10^{10} variants) phage display antibody libraries, from which diverse sub-nanomolar affinity antibody clones can be isolated. The description of one such library yielding over 1000 distinct antibodies against a given antigen can be found in the literature (Edwards et al. 2003).

Possessing the tools for selection and amplified synthesis of optimal binders, one can solve the problem of coupling the binding with fluorescence reporting. Despite several promising attempts, direct sensors with the properly attached environment-sensitive dyes still did not find their proper application (Ueda and Dong 2014). With solution of this problem, antibodies will be able to establish themselves as preferred recognition units in all biosensor technologies, including highly needed microarrays for detection of carbohydrates and proteins, probably on a proteome scale. A great potential for the development in cellular research is expected from presently almost unexplored possibility of fusing antibodies to different marker proteins (Casadei et al. 1990) and to GTP-type fluorescent proteins (Zeytun et al. 2003). Obtaining such molecular hybrids may allow combining two important functions – targeted binding at particular sites and sensing different analytes at these sites.

7.4 Ligand-Binding Proteins and Protein-Based Display Scaffolds

Now we address a broad class of proteins possessing important functions of binding and transport of different substances along their metabolic routes. Their structures are very diverse. Many protein-protein complexes with multivalent interactions can be found in protein database (Meyer and Knapp 2014). Some of them are almost ready biosensors, and only the fluorescence response units are needed for incorporation into them. Some others can be used as the scaffolds for generation of sensors with new functions. An increased understanding of structure and function of natural ligand-binding proteins together with the advances in protein engineering has also triggered the exploration of various alternative protein architectures.

With these tools, valuable protein-binding molecular scaffolds have been obtained. They represent promising alternatives to antibodies for biotechnological and, potentially, clinical applications (Binz and Pluckthun 2005). Regarding sensor applications, their strong competition with antibodies is expected in the nearest future.

7.4.1 Engineering the Binding Sites by Mutations

There are several techniques that can be efficiently applied for generation of new proteins with desired ligand-binding properties. The most efficient of them start from well-known and almost-optimal protein structures that can be taken as scaffolds. Then sequential steps of random mutations and product selection are taken. Mutations are induced in specific regions of protein structure, usually at the ligand-binding pockets. The frequently applied procedure involves display the mutated proteins on the surface of filamentous bacteriophage, the virus that can infect only the bacteria (Uchiyama et al. 2005). Mutations can be induced by standard molecular biology procedures. The phage display technique allows for *in vitro* mutagenesis-selection. The multiple steps of growth phage-infected bacteria are used to amplify the promising binders and to provide their further selection. This process is often described as '*in vitro* evolution'. It can be especially good for finding the affinity binders for relatively small molecules of metabolites and drugs.

These modern methods of molecular biology allow creating huge combinatorial libraries containing millions of structurally diverse species. Usually these libraries are so constructed that they consist of underlying constant scaffold and randomized variable regions that differ from each other. Why then not to synthesize the library of binding proteins *de novo*, since there are all necessary means for that? The reason is that fully synthetic proteins usually do not fold to compact native-like structures and, if they fold, they possess insufficiently low stability. Therefore it is reasonable to follow the practical trend – to select the structure of a known protein as scaffold and to provide targeted or random mutations only at particular sites (Glasner et al. 2007).

The scaffold is usually based on the most rigid elements of protein structure formed by α-helices and β-sheets (Fig. 7.13). According to (Hosse et al. 2006), scaffold proteins can be assigned to one of three groups based on architecture of their backbone:

1. scaffolds consisting of α-helices (images **a**–**d**);
2. small scaffolds with few secondary structures or an irregular architecture of α-helices and β -sheets (image **e**), and
3. predominantly β -sheet scaffolds, representing the majority of proteins used for library display (images **f**–**i**).

The scaffolds differ in the presence or the absence of stabilizing disulfide bonds linking spatially separated strands of the protein, a distinction that has consequences for the choice of expression system (Hosse et al. 2006). Various reactive groups extending to the surface can be selected for inducing or modifying particular

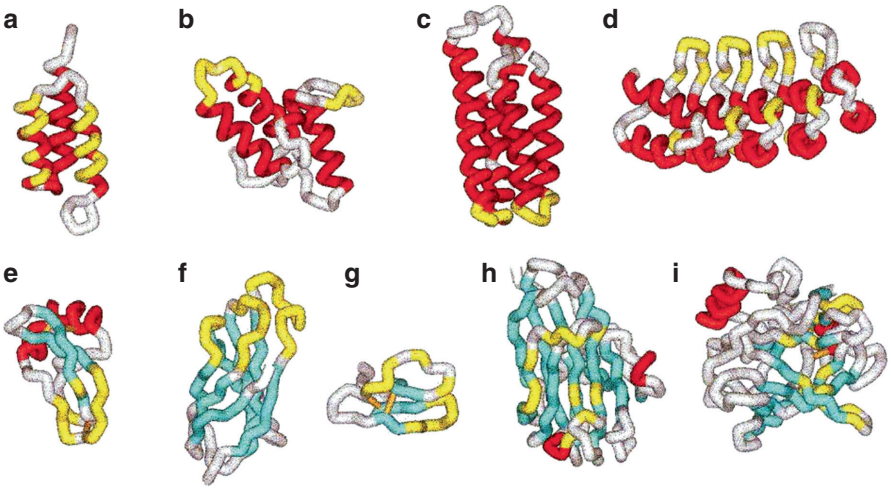

Fig. 7.13 Representative protein display scaffolds that can be selected for grafting the functional recognition units and library construction of specific molecular recognition binders (Hosse et al. 2006). Scaffold proteins in **a**–**d** consist of α-coils, the small kunitz domain inhibitor (in **e**) shows an irregular α-coil and β-sheet architecture, whereas **f**–**i** show scaffolds predominantly consisting of β-sheet frameworks. α-Helices are depicted in *red*; β-sheets, in *blue*; disulfide bonds, in *orange*; and positions subjected to random or restricted substitutions, in *yellow*. The PDB IDs used to generate this figure are given in parentheses: (**a**) Affibody: Z-domain of protein A (1Q2N), (**b**) immunity protein: ImmE7 (1CEI), (**c**) cytochrome b562 (1M6T), (**d**) repeat-motif protein: ankyrin repeat protein (1SVX), (**e**) kunitz-domain inhibitor: Alzheimer's amyloid b-protein precursor inhibitor (1AAP), (**f**) 10th fibronectin type III domain (1FNA), (**g**) knottin: cellulose binding domain from cellobiohydrolase Cel7A (1CBH), (**h**) carbohydrate binding module CBM4-2 (1 K45); and (**i**) anticalin FluA: bilin-binding protein (1T0V) with cavity randomization for fluorescein binding

function, e.g. targeting particular ligand or providing the fluorescence reporter signal. Because of this enormous variety achieved by either rational or combinatorial protein engineering, it is possible to isolate library members binding strongly and specifically virtually to any target.

The scaffold principle was in fact borrowed from Nature. Nature implemented it in construction of *antibodies* (see Sect. 7.3 above). The bodies of these molecules are well-defined and highly homologous, except the so-called variable domains. The latter contain six hypervariable loops each, and it is their variability that is responsible for a population of about 10^8 antibodies of different specificity circulating normally in human body. Therefore popular among researchers are the β-sandwich and β-barrel scaffolds that resemble the antigen-binding variable domains of antibodies (Binz et al. 2005; Binz and Pluckthun 2005).

In contrast, the *ligand-binding proteins* are very conservative by themselves, and for modulation of their binding properties genetic manipulations are required from the researcher. Protein engineering allows insertion of structural elements such as folds or loops and, even more, manipulation with whole domains. Thus, proteins with new ligand-binding functions can be engineered through a combinatorial process called random domain insertion (Guntas and Ostermeier 2004). The gene coding domain of

one protein can be randomly inserted into the gene sequence of another protein, and this hybrid can show novel not only ligand-binding but also allosteric properties.

Design of sensor molecules by *random mutations* at particular sites has shown its efficiency when applied to proteins with natural binding and transport functions. The results can be compared and even coupled with those obtained by site-directed mutagenesis – amino acid substitutions at pre-defined positions. The latter is the common way of inserting Cys residues that are often needed for labeling with fluorescence reporter dyes that are reactive with –SH groups. Design of such molecular constructs could take lots of skills, especially working with mutant proteins, in which the protein scaffold is stabilized by disulfide bonds. Co-synthetic incorporation of fluorescent amino acid analogs into antibody fragments is an interesting alternative (Hamada et al. 2005). Combination of designed and random-selected protein structures opens far-fetched prospects.

7.4.2 Bacterial Periplasmic Binding Protein (PBP) Scaffolds

In line with their function, transport proteins are commonly highly specific towards their ligands, allowing applications for sensing these ligands as the targets. The *periplasmic binding proteins* (PBPs) of bacteria are the leaders in this sensing strategy. These structurally diverse transport proteins demonstrate high affinity in binding their specific ligands, such as maltose, glucose, glutamine, histidine, phosphate, etc. High-resolution crystallographic structures of the ligand-free and ligand-bound forms showed that PBPs are formed of two domains linked by a hinge and that a hinge-bending motion occurs upon ligand binding (Quiocho and Ledvina 1996). The diversity of biological function, ligand binding, conformational changes and structural adaptability of these proteins have been exploited to engineer biosensors, allosteric control elements, biologically active receptors and enzymes using a combination of techniques, including computational design. PBPs and their ligands have been used as models systems to develop fluorescent sensors based on various transduction principles (Dwyer and Hellinga 2004).

Since the ligand binding site and the fluorescence reporter group may be located in spatially distant areas, these proteins seems appropriate for designing sensors with new ligand binding specificities but sharing similar reporting functions (de Lorimier et al. 2002; Marvin and Hellinga 2001b). Computational methods for redesigning ligand binding specificities of proteins develop actively (Looger et al. 2003). Based on computational findings the mutant binding proteins can be constructed by protein engineering methods. With an environmentally sensitive fluorophore inserted in the hinge between the two domains, they demonstrate experimentally specific response to the bound targets.

Maltose binding protein of *E. coli* is so far the most efficiently used protein of this family (Medintz and Deschamps 2006). It allows combining two important biosensor properties: specificity of recognition and conformational change. The protein molecule of ~3×4×6.5 nm in dimension consists of two domains of almost equal size. In open form the binding pocket is exposed to the solvent. Upon binding maltose,

this pocket closes by rotation of domains by ~35° and lateral twist by ~8° relative to each other. This brings amino- and carboxy-termini closer by ~0.7 nm. Intra-domain conformation also exhibits some changes (see Fig. 8.16). This allows exploring both contact and remote response to target binding (Dwyer and Hellinga 2004).

7.4.3 Engineering PBPs Binding Sites and Response of Environment-Sensitive Dyes

There were many successful attempts to transform PBPs into sensors by binding the environmentally sensitive dyes (Fonin et al. 2014; Pickup et al. 2013; Khan and Pickup 2013). Initially, in the maltose binding protein a position close to the cleft, where the ligand binds, but not involved in binding itself, was visually selected (Gilardi et al. 1994). It was shown that on binding of maltose the fluorescence intensity of acrylodan and IANBD dyes increased dramatically. These changes were accompanied by blue shifts of emission spectra. They can be explained by re-location of the dye from highly polar and exposed to solvent water environment to an environment that is low-polar and screened from the contact with water.

Similar effect was observed in *phosphate binding protein* that was suggested as a sensor for inorganic phosphate (P_i) (Brune et al. 1994). Upon P_i binding the fluorescence spectrum of this label shifts to the blue and undergoes a 5.2-fold increase of emission intensity. The response is very fast, on the time scale of 50 ms.

The possibility to locate the environment-sensitive fluorescence reporter in a position *remote from the ligand binding site* was thoroughly exploited. Such locations that show the largest structural differences in the ligand-free and ligand-bound forms were identified by comparing inter-atomic distances in the two forms (Marvin et al. 1997). Spatial separation of the binding site and reporter groups allows their intrinsic properties to be manipulated independently. In the cited research, three different dyes were coupled at six positions, yielding 18 different constructs. Three out of the 18 constructs showed a larger than two-fold increase in fluorescence intensity. Provided allosteric linkage is maintained, the ligand binding can therefore be altered without affecting fluorescence reporting. To demonstrate applicability to biosensor technology, the authors introduced a series of point mutations in the maltose-binding site that lower the affinity of the protein for its ligand. These mutant proteins were combined in a composite biosensor capable of measuring substrate concentration within 5 % accuracy over a concentration range spanning five orders of magnitude.

A successful attempt to modulate the *binding affinity* of maltose binding protein that does not involve the binding site was demonstrated. This can be done by introducing mutations located at some distance from the ligand binding pocket that sterically affect the equilibrium between an open, apo-state and a closed, ligand-bound state (Marvin and Hellinga 2001b). The possibility to radically change the specificity of this protein was demonstrated by converting it into a zinc sensor using a targeted design approach (Marvin and Hellinga 2001a). In this new molecular sensor, zinc binding is detected in the form of fluorescence signal by use of an

engineered conformational coupling mechanism linking ligand binding to reporter group response.

Glucose binding protein was also the subject of extensive studies. The 'non-allosteric' and 'allosteric' locations of amino acid residues were selected based on the known protein structures in the open and closed forms. These sites were substituted with cysteins for attachment of environment-sensitive acrylodan and NBD dyes. Allosterically located dyes behaved efficiently, demonstrating several-fold change of fluorescence signal intensity (Marvin and Hellinga 1998). Strong changes in fluorescence intensity of 'allosterically' located acrylodan dye were also observed in glutamate binding protein (Tolosa et al. 2003).

In an extended study, De Lorimier et al. (2002) have conjugated different environmentally sensitive fluorophores at various positions in 11 members of the PBP family. They selected positions that either directly contact with the ligand, are located near the ligand-binding site, or are located away from the binding site, in a region that changes conformation on ligand binding. Approximately a quarter of the 320 conjugates gave a satisfactory sensor response. Binding affinities were mostly affected in the group of constructs where the fluorophores directly contacted the ligand. Wavelength shifts together with the changes of intensity were observed for the environment sensitive dyes, such as acrylodan and NBD. Meantime, for some of labeled PBPs these changes were very little or even undetected, showing that the dye response is strongly position-dependent.

7.4.4 Scaffolds Based on Proteins of Lipocalin Family

Another class of protein ligand binders, the '*anticalins*', are the artificial products constructed by introducing structural diversity into the binding site of lipocalins, a family of small monomeric ligand-transporting proteins (Weiss and Lowman 2000). Lipocalins are the molecules of 160–180 amino acid residues that are involved in storage of hydrophobic and/or chemically sensitive organic compounds (Flower et al. 2000). They consist of β-barrel formed of eight anti-parallel strands, which is the central folding unit forming a conical cavity. The cavity is relatively deep and largely nonpolar. The entrance to this cavity is formed by four loops that can be randomly mutated for generating of molecular pockets with a diversity of shapes and providing the binding sites to different ligands (Fig. 7.14).

The first anticalins were derived from insect origin. They allowed obtaining sensors for small molecules such as steroids (Korndorfer et al. 2003). In addition to low molecular weight compounds, they can be targeted towards proteins. This was shown for a member of the lipocalin family of human origin, apolipoprotein D. Its function is to transport arachidonic acid and progesterone in various body fluids. After randomization of 24 amino acids located within the loop region, a mutant was selected that started to bind hemoglobin (Vogt and Skerra 2004).

Anticalins as binders, offer some advantages over traditional antibodies (Richter et al. 2014). They are especially important in molecular recognition between

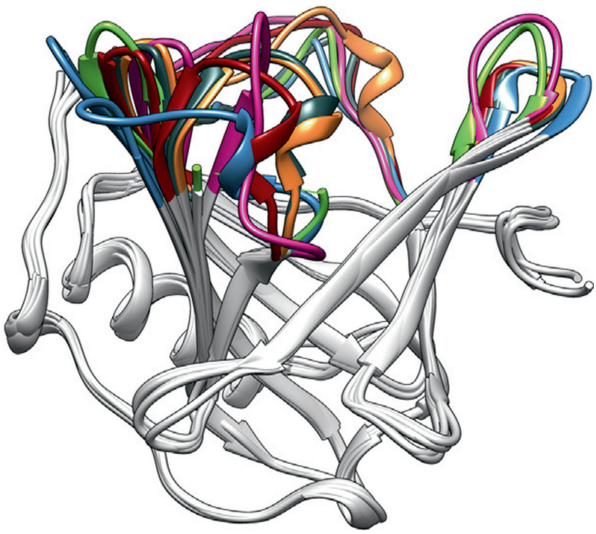

Fig. 7.14 Anticalins. Like immunoglobulins they comprise a structurally conserved framework (*grey*) supporting a set of hypervariable loops (*colored*) that account for target recognition

receptors and small molecule ligands (Weiss and Lowman 2000). Still, as molecular sensors, their application presently does not go beyond the cases, where the ligands are fluorescent, such as retinol. The proper large-scale applications in fluorescence sensing technologies are still in prospect. These technologies should be adapted to small size of these proteins, to the rather rigid conformation of their binding sites and to the absence of global conformational changes upon ligand binding.

7.4.5 Other Protein Scaffolds

In addition to scaffolds based on fragments of antibodies, periplasmic ligand-binding proteins and lipocalins, other protein scaffolds were suggested to create the libraries of different binding proteins (Boersma and Plückthun 2011; Skerra 2007). They were developed with different purposes and focused on mostly pharmaceutical applications. But some of them may be attractive as potential sensors. It can be observed that if the scaffold is based on the protein that binds small ligands, then it is easier to achieve specific binding of such ligands. In other cases, the scaffolds are better adapted to large ligands such as proteins (Hosse et al. 2006). If the three-dimensional structure of a target and a scaffold are known, the mutation sites can be assigned based on computational design (Wiederstein and Sippl 2005). A variety of protein scaffolds can be analyzed *in silico* by generation of computer images and the results of this analysis fit the experimental data satisfactorily.

Among the prospective sensors are the '*affibodies*'. Derived from bacterial cell surface receptors, they represent an engineered version (Z domain) of one of the five stable three-α-helix bundle domains from antibody-binding region of staphylococcal protein A (Renberg et al. 2005; Eklund et al. 2002). They are small (6 kDa and

58 residues only), highly soluble, do not contain S-S bonds and can be fused on a genetic level with other proteins (Ronnmark et al. 2003). Their small size and the ability of spontaneous folding allowed providing their complete chemical synthesis and assembly on automated peptide synthesizer. Moreover, during this synthetic process the fluorescent dyes and reactive groups for attaching protein to the surface can be incorporated in the desired positions (Engfeldt et al. 2005). Also, a biotin moiety can be introduced in the same way. This allows providing not only the reporting function but also the binding to a required site. The affibodies have found application in constructing protein microarrays (Renberg et al. 2007), but the presently suggested technologies still rely on target labeling or on sandwich format. Meantime, being labeled with fluorescent dyes (Miao et al. 2010) or attached to nanoparticles (Pu et al. 2011), affibodies found application for tumor imaging.

Thus we observe that the concept of *'minimal' protein scaffolds* together with the idea of artificial target recognition sites led to many successful developments. Members of several protein families represent promising model systems in this respect. Other examples of 'minimal' protein scaffolds include mutated forms of *cytochrome* b_{562}, *ankyrin repeat domains*, *leucine-rich repeat proteins*, insect *defensin* A, *protease inhibitors* and *scorpion toxins* (Binz and Pluckthun 2005; Hosse et al. 2006). Small size of these proteins allows an efficient use of computer design and point mutation approach for improving stability and functionality. For scaffold derived from defensin A and containing 29 amino acids, a library of such mutations was produced (Yang et al. 2003b).

In order to find scaffolds for new sensors, the scientists started active studies of the proteins that provide immune response in primitive organism (Binz et al. 2005). It is known that not all adaptive immune systems use the immunoglobulin fold as the basis for specific recognition molecules. Sea lampreys, for example, have evolved an adaptive immune system that is based on *leucine-rich repeat proteins*. Many other proteins, not necessarily involved in adaptive immunity, mediate specific high-affinity interactions. Their transformation into operative fluorescence sensors is the task for future research.

7.4.6 Prospects

Understanding the fact that different protein families unrelated to immunoglobulins can provide the basis for specific recognition molecules and can compete with them in many valuable properties has stimulated active research. Such proteins were found primarily among natural ligand-binding proteins. For adaptation to particular target an approach based on using the protein structure as a scaffold and applying point and random mutations to provide the changes at particular sites can be efficient. Meantime, the examples presented above show that unlimited possibilities offered by the techniques of random and directed mutations are not enough for making optimal binders, and the knowledge of molecular interactions and of their dynamics is needed. A rigid scaffold should provide an extraordinary stable protein architecture tolerating multiple substitutions or insertions at the primary structural level. These substitutions should determine affinity and specificity in target binding.

Scaffold-based affinity sensors promise good prospects in biosensor technologies but only on condition that the problem of coupling with fluorescence reporter response is properly addressed and resolved. Protein-ligand binding events usually involve in different proportions the combination of binding pocket solvent exclusion (Liu et al. 2005) and conformational change (Flores et al. 2006). Recent studies (Yesylevskyy et al. 2006) show that the number of proteins with global changes of conformation and its dynamics on ligand binding is very limited. Therefore coupling the binding events with conformational changes cannot be a general mechanism of these sensors operation. Their prospect will depend strongly on other mechanisms of signal transduction involving those based on direct contact of the target with reporter dye.

7.5 Designed and Randomly Synthesized Peptides

In previous Section, we discussed the possibilities of making fluorescence sensors based on functional ligand-binding proteins. We observed successful results in attempts to transform them into sensors by producing minor modifications of their structure that mainly involved target binding sites and the sites of reporter binding. Here we discuss and evaluate the possibilities arising from the use of synthetic peptides. They allow *artificial selection of scaffolds* as either folded domains or flexible peptide chains. The peptides possess the necessary properties as recognition units: flexibility to adapt sterically to any target, rigidity in secondary structure to conserve the binding aptitude and the propensity to form different kinds of non-covalent bonds with potential target.

To be successful in generation of designed binding molecules, this approach has to rely strongly on the ability to create and operate with large libraries together with powerful library selection technologies. The advances in protein engineering, selection and evolution technologies can be actively used. But the main advantage of this approach is the possibility of obtaining the sensing molecules of the *minimum possible size*. This allows a large-scale application of standard solid-phase techniques of peptide synthesis, which is a rather simple standard technology.

Operating with synthetic peptides has many technical advantages. Peptides offer functional robustness superior to that of most proteins and are well suited for long-term storage in dry, dissolved or immobilized forms. Importantly, they allow full control of the labeling process including a complete labeling at a single site. An oriented immobilization in a protein chip formats is readily obtained.

7.5.1 Randomly Synthesized Peptides, Why They Do Not Fold?

Synthetic peptides with random location of amino acid residues are commonly unfolded. The formation of their native-like structures is a low-probable event that can be observed for very rare sequences. This is because of strong connection between the amino acid sequence and the three-dimensional organization, known as the *folding code* (Demchenko and Chinarov 1999). The folding code is highly *degenerate* and includes

both steric and energetic factors. This means that some substitutions (even many of them) still lead to correct folding. Even larger substitutions are allowed if they are compensated in structural or thermodynamic sense by other substitutions. The folding code has *distributed* character, which means that it is not reduced to interactions between particular residues but involves extended elements of structure. In addition, kinetic variables on different hierarchical levels may not only determine the pathway of folding but also the resultant folded structure (Yesylevskyy et al. 2005; Demchenko 2001a).

Because of that, the prediction of folded structures is difficult. Moreover, the folding can be strongly influenced by intermolecular interactions (Demchenko 2001b). All these factors complicate the design of protein and peptide 3D structures *ab initio*. No less difficult is to design the interaction with the target molecule even if the structure is well known. Therefore, two strategies in the production of peptide binders were suggested and used:

(a) *Rational design based on already known folded motifs*. This means that if this motif is known being observed in native proteins, then it is highly probable that it will fold in the same way when produced as the structure of minimal size by synthetic means. By selecting this fold motif as a scaffold structure, one can introduce different modifications inducing or modifying the target recognition and fluorescence response properties. This strategy is commonly known as the *template-based approach* (Singh et al. 2006).
(b) *Selection from a large combinatorial library*. In this case, making the combinatorial peptide library and establishing the selection criteria are needed. The binding to the target could be the major selection criterion, so that this selection could be realized, for instance, by affinity chromatography.

7.5.2 Template-Based Approach

The well-defined secondary and tertiary structures of peptides and proteins are formed and stabilized by interactions in the main chain and by contacts between side groups. Despite of huge conformational space that allows astronomical number of peptide conformations, the number of folding motifs is very limited (Schulz and Schirmer 1979). The selection of topological peptide template can be made based on the known 3D structures of proteins. The recent advances in the chemistry of coupling reagents, protecting groups, and solid-phase synthesis have made the chemical synthesis of peptides with conformationally controlled and complex structures feasible (Singh et al. 2006).

These peptide templates can be used to construct novel structures with tailor-made functions. Such peptide-template-based approach demonstrates the utility in achieving molecular recognition of different targets. A statistical picture of amino acids found at protein-protein interaction sites indicates that proteins recognize and interact with one another mostly through the restricted set of specialized interface amino acid residues, Pro, Ile, Tyr, Trp, Asp and Arg (Sillerud and Larson 2005). They represent the three classes of amino acids: hydrophobic, aromatic and charged (one anionic and one cationic). They can be used for constructing the peptide recognition sites.

The automatic *solid phase peptide synthesis* is the key technology of producing the template-designed peptide sensors. The standard procedures allow obtaining peptides as long as of 20–30 residues, which can be sufficient for making the designed folds. These techniques allow *parallel synthesis* on solid support. Combining the surface chemistry with the recent technology of microelectronic semiconductor fabrication, the spatially addressable peptide microarrays can be obtained (Kodadek 2002). One can choose between two synthesis methodologies: pre-synthesized peptide immobilization onto a glass or membrane substrate and peptide synthesis *in situ*.

7.5.3 The Exploration of 'Mini-Protein' Concept

It was interesting to note that a peptide as small as 20 residues can possess a cooperatively folded tertiary structure (Gellman and Woolfson 2002). Such mini-proteins could serve as a fruitful platform for protein design by positioning all amino acids necessary for biomolecular recognition. Particularly, they can display a high DNA binding affinity and specificity (Pflum 2004). A 38-amino acid peptide was described as an α-helical hairpin stabilized by two disulfide bridges and presented as a scaffold for future sensor developments (Barthe et al. 2004).

It was proposed that a synthetic 42-residue helix-loop-helix polypeptide that dimerizes to form four-helix bundles could form a scaffold for molecular sensors (Enander et al. 2002). Different functional groups can be incorporated covalently into this scaffold in a site-selective manner. Incorporation of a receptor group interacting with the binding site of a protein together with an environment-sensitive dye allows obtaining a sensor for this protein (Fig. 7.15).

This fully designed sensor with an inhibitor of carbonic anhydrase as a recognition unit and a reporting fluorescent dye can detect the binding of carbonic anhydrase (Enander et al. 2002). Essentially, the linker structure and length modulate dissociation constant in a range of two orders of magnitude. The binding results in a significant increase of fluorescence intensity, which arises from a disruption of the homodimer in the presence of the target (Enander et al. 2004a). This concept can be applicable to numerous targets, for which the ligand is a small compound that can be grafted on the peptide scaffold. The potential of this approach for microarray applications was demonstrated by designing an affinity array (Enander et al. 2004b).

7.5.4 Molecular Display Including Phage Display

Phage display is a powerful method for the discovery of peptide ligands that are used for analytical tools, drug discovery, and target validations (Uchiyama et al. 2005). Phage display technology can produce a great variety of peptides and generate novel peptide ligands. A number of other display platforms include bacterial and yeast display, ribosome display, and mRNA display (Levin and Weiss 2006).

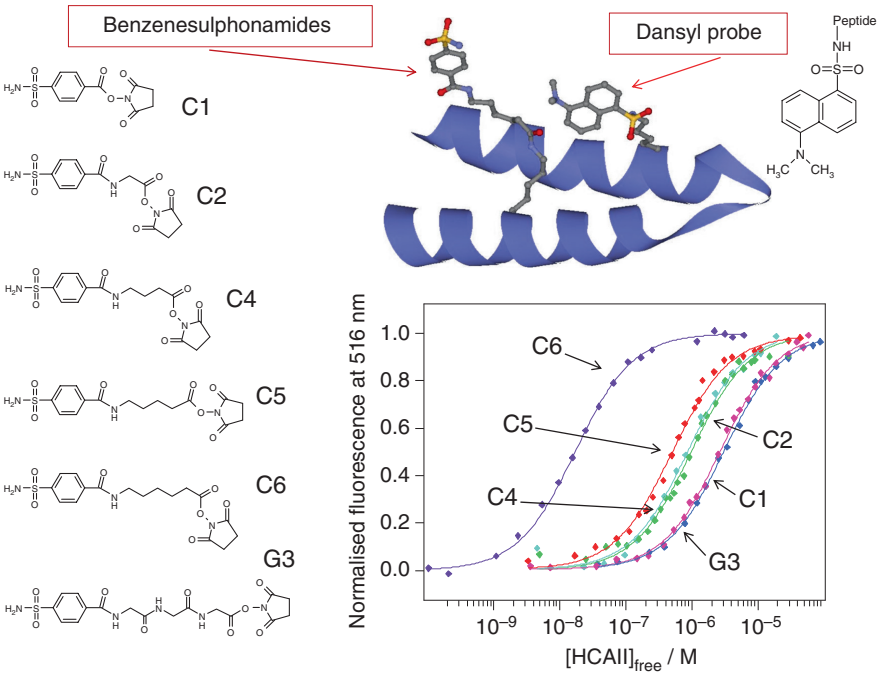

Fig. 7.15 Schematic representation of the helix-loop-helix polypeptide scaffold forming on dimerization a four-helix-bundle and proposed as a versatile sensing platform (Enander et al. 2004b). The scaffold is shown with a dansyl probe and benzenesulfonamide attached at amino acid positions 15 and 34, respectively. Attachment of a bifunctional spacer of different length allows linking covalently the benzenesulfonamide residue to a lysine residue side chain in the polypeptide scaffold. This construct was used for the detection of human carbonic anhydrase II. The graph representing fluorescence response to target binding as a function of a spacer structure and length used for benzenesulfonamide attachment

Ribosome display (Zahnd et al. 2007) is an *in vitro* selection and evolution technology for proteins and peptides from large libraries. The diversity of the library is not limited by the transformation efficiency of bacterial cells. The random mutations can be introduced easily after each selection round. This allows facile *directed evolution* of binding proteins over several generations.

Affinity selection of peptides displayed on phage particles can be used for mapping molecular contacts between small molecule ligands and their protein targets (Rodi et al. 2001). Important observations were made in these studies that the binding properties of peptides displayed on the surface of phage particles could mimic the binding properties of peptide segments in naturally occurring proteins. Conformation of these segments can be relatively unimportant for determining the binding properties of these disordered peptides because they adopt 'induced' conformation upon binding the target. Such '*induced fitting*' to the target (Demchenko 2001b) can be the basis of its molecular recognition.

The selection of peptide binders from the library does not need to know the 3D structures of interacting partners. Moreover, these structures can be flexible. This allows a rapid large-scale identification of potential ligand binding sites and also an easy introduction of fluorescence reporter responsive to target binding in a number of parameters (wavelength ratiometry, lifetime, anisotropy). Dynamic formation of optimal non-covalent bonds compensates the entropy loss associated with the loss of conformation mobility.

If *in vitro* selection techniques could produce short polypeptides that tightly and specifically bind to any of a wide range of macromolecular targets, the possibilities for sensor developments would be broad. Some applications have already been demonstrated. One of them is to construct the '*peptide beacons*' (Oh et al. 2007), which is discussed in Sect. 8.5. This sensing architecture is based on the increase of rigidity when bound to a macromolecular target. It is similar to DNA beacons and is based on the change of relative distance between fluorescent dye and the quencher on target binding. Based on this principle a robust optical sensor was developed for anti-HIV antibodies (Oh et al. 2007) and the antibodies to p53 protein that are important biomarkers for cancer (Neuweiler et al. 2002).

7.5.5 Peptide Binders for Protein Targets and the Prospects of Peptide Sensor Arrays

Labeled peptides with their flexible structures in solutions are very attractive as analytical tools for detecting different protein targets, particularly the antibodies. A prototype of self-referenced protein sensor based on peptide labeled with λ-ratiometric 3-hydroxychromone dye was developed (Enander et al. 2008). Using a model of high-affinity interaction between an 18-aminoacid antigenic peptide derived from tobacco mosaic virus coat protein and a recombinant antibody fragment, Fab 57P, a dramatic change of fluorescence spectrum was observed indicating their interaction by changing the relative intensities of two bands. The non-specific binding does not produce this effect (Fig. 7.16).

The ratio of intensities of two bands (I_{N*}/I_{T*}) in the dye fluorescence spectrum changed dramatically (from 0.92–0.94 to 0.60) on interaction with specific and remained unchanged in the presence of nonspecific antibody fragments. Essentially, the labeling was produced outside the antibody binding site and did not influence the binding so that it is the interaction at the periphery of the binding site that produced this change. This result shows that the response of fluorescence dye in such constructs is strongly position-dependent and that rational design should be complemented by comparative studies of systems with different dye locations.

Recently in the studies of different peptide-antibody system it was shown that on interaction with the antibody fragment, the peptide sensor labeled at N-terminal showed up to 47 % change in the ratio of its two emission bands. Competition with

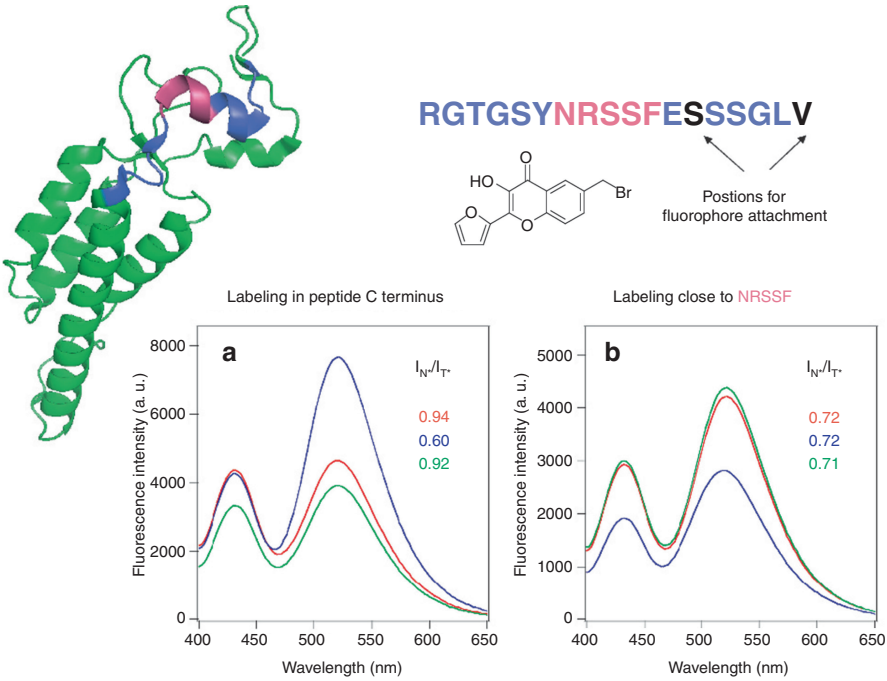

Fig. 7.16 Synthetic peptide for detecting protein target (Enander et al. 2008). The peptide representing the antigenic segment 134–151 of tobacco mosaic virus protein (shown in *pink*) interacts with the specific antibody fragment Fab57P as a model target. The fluorescence spectra of 3-hydroxychromone dye covalently attached to indicated sites in peptide sequence in the absence (*red*) and at presence (*blue*) of saturating amounts of specific antibody fragment. An addition of nonspecific antibody (*green*) serves as a control. The effect of dramatic change in the ratio of fluorescence intensities of two bands is specific to dye location is observed in (**a**) and absent in (**b**)

two unlabeled peptides of different lengths led to a dynamic displacement of the construct governed by the relative binding constants (Choulier et al. 2010).

In our view, fluorescent indicators based on synthetic peptides are very interesting alternatives to protein-based sensors. They can be synthesized chemically, are stable, and can be easily modified in a site-specific manner for fluorophore coupling at desired sites and for immobilization on solid supports (Choulier and Enander 2010). The key issue is the generation of reporting signal to target binding, which can be provided by their labeling and without target labeling by λ-ratiometric dyes.

The peptide based sensors are potentially useful for diagnosis of viral, bacterial, parasitic and autoimmune diseases by detecting the correspondent antibodies (Gomara and Haro 2007). Synthetic peptides can provide uniform, chemically well-defined antigens for antibody analysis, reducing inter- and intra-assay variation. The success of this approach depends on the extent to which synthetic peptides are able to mimic the antigenic determinants (Timmerman et al. 2005).

7.5.6 Antimicrobial Peptides and Their Analogs

Some natural peptides possess functionally important recognition properties and it is straightforward to use them as well as their analogs as the binders. Numerous bacteria, plants, and higher organisms produce antimicrobial peptides as a part of their innate immune system, providing a chemical defense mechanism against microbial invasion. Many of these peptides exert their antimicrobial activity by binding to components of the microbe's surface and disrupting the membrane. They can be incorporated into screening assays for detection of pathogenic species (Ngundi et al. 2006). It was shown that the surface-immobilized peptides, such as polymyxins B and E, can be used to detect pathogenic bacteria in two assay formats: sandwich and direct.

Different mutant forms of short antimicrobial peptides have been obtained and selected. They are promising as remedies to fight against the antibiotic-resistant microbes. Using *antimicrobial peptides* as recognition elements in an array biosensor, detection of these microbes can be achieved (Kulagina et al. 2006).

7.5.7 Advantages of Peptide Technologies and Prospects for Their Development

Peptides as chemical products possess many advantages over protein sensors based on ligand-binding proteins, enzymes or antibodies. They are readily obtained in large amounts by chemical synthesis, and the introduction of fluorescent dye can be a part of this synthesis but not only the modification at targeted sites, as in proteins.

We observe also that two methods of functional peptide design and production, chemical synthesis and phage display, enrich each other (Uchiyama et al. 2005). The best binders selected from combinatorial libraries can be produced by chemical synthesis on a large-scale level. The synthesis can be robotic. It can be provided directly on arrays to yield the product with highly reproducible properties. In comparison, the large-scale production of mutant recombinant proteins and their subsequent modification are tedious and very expensive. With peptides, all the problems of poor expression levels of the mutated proteins, deleterious effect on binding affinity of the mutation or of fluorophore coupling or low yield of this coupling are avoided.

Synthetic peptides possess a better thermal and chemical stability. They can be easier integrated into nanoparticles, porous materials and polymer gels, or deposited in array format for the simultaneous detection of many targets (Kodadek 2002). These technologies are expected to combine the low cost, speed and convenience, with a wide range of applications in diagnosis and the environment protection.

7.6 Nucleic Acid Aptamers

The fact that complementary pairing of nucleic acid bases, which are G-C and A-T in DNAs (or G-C and A-U in RNAs), resulting in a formation of a double-strand association complex (hybridization) between the formed nucleotide sequences, is the basis of the recognition process in nucleic acid sensors, and is in the heart of different DNA or RNA sensors. Here we will learn about new well-unexpected properties of nucleic acids. Being designed and selected by their affinities they can interact with high specificity with a broad variety of structurally unrelated molecular targets.

Aptamers are single-stranded DNA or RNA oligonucleotide sequences that possess the ability of recognizing various molecular targets, including peptides and proteins (Hamula et al. 2006; Tombelli et al. 2005). Commonly these properties of oligonucleotides are not observed or are very weak, but after the appearance of *selection-amplification techniques* operating with large libraries, a number of aptamers with very strong and extremely selective binding abilities increased tremendously. Much like in peptide selection, for finding the best binders one has to create a large pool of similar compounds, a *combinatorial library*, and to screen this library.

Polyanionic nature of nucleic acids does not deprive them from formation of stable three-dimensional structures. These structures are stabilized by intramolecular formation of short double-helical segments composed of complementary nucleic acid bases. Such structures may exhibit an ideal combination of rigidity and flexibility in intermolecular interactions.

7.6.1 Selection and Production of Aptamers

Aptamers can be identified in oligonucleotide pools by an *in vitro* selection process known as SELEX (*systematic evolution of ligands by exponential enrichment*) (Zheng et al. 2006; Hamula et al. 2006; Song et al. 2008). At first the library of oligonucleotides with random location of bases has to be obtained. It may contain as much as 10^{15}–10^{16} different molecules, and SELEX involves an iterative process of search for the best binders and of their selection (Gopinath 2007). SELEX involves repetitive rounds of two processes: (a) partitioning of aptamers from non-aptamers by an affinity method and (b) amplification of aptamers by the *polymerase chain reaction* (PCR) (Fig. 7.17).

The size of aptamers could vary from tens to thousands of nucleotides. Typically, it is smaller than 200 bases, and this is sufficient for their optimal performance. Being single-chain molecules they can fold to make segments of double-helical structure separated by loops (O'Sullivan et al. 2002). The development of *in vitro* selection and amplification techniques has allowed the identification of specific aptamers, which bind to the target molecules with high affinities. These affinities are frequently comparable with those of monoclonal antibodies, so that their dissociation constants can be observed in nanomolar to picomolar range. Compared to antibodies, the cross-reactivity of aptamers in binding protein targets is typically

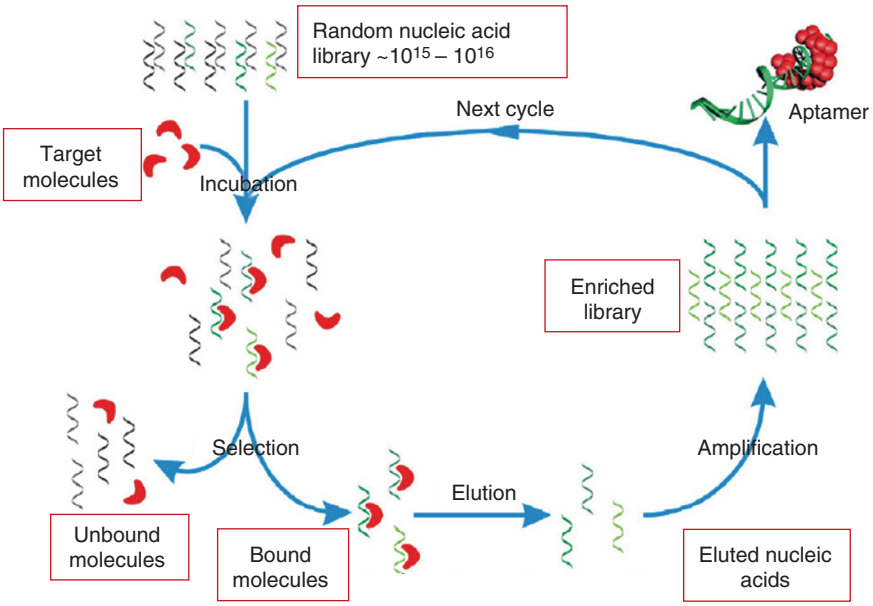

Fig. 7.17 Scheme for SELEX enrichment process (Song et al. 2008). A random nucleic acid library is incubated with a target molecule, and unbound molecules are separated from bound molecules. Bound nucleic acids are eluted, amplified by PCR (polymerase chain reaction) and serve as an enriched library for the next cycle. For every target, 6–12 consecutive cycles are performed and the final enriched library is cloned and sequenced

minimal (Hicke et al. 2001). Thus, they can discriminate protein targets containing only several amino acid substitutions.

It is important that since aptamers are selected wholly *in vitro*, their specificities can be crafted by the addition of negative selection steps. Presently the high-throughput selection of aptamers can be accomplished by robots. Due to the fact that they can also be potent pharmacological agents (their specific binding reduces protein activity) the amount of selected and identified aptamers has grown tremendously. Aptamer databases were created to help their systematization (Thodima et al. 2006).

7.6.2 Attachment of Fluorescence Reporter, Before or After Aptamer Selection?

Aptamers can be labeled with fluorescence reporters after the SELEX procedure selects the optimal binders or even before the SELEX procedure (Fig. 7.18). All classical methods of nucleic acids post-translational modification can also be applied for labeling aptamers as well as incorporation of naturally emitting 2-aminopurine (Katilius et al. 2006) and base-substituting dyes. Their fluorescence quantum yield strongly depends on the base stacking interactions when incorporated into

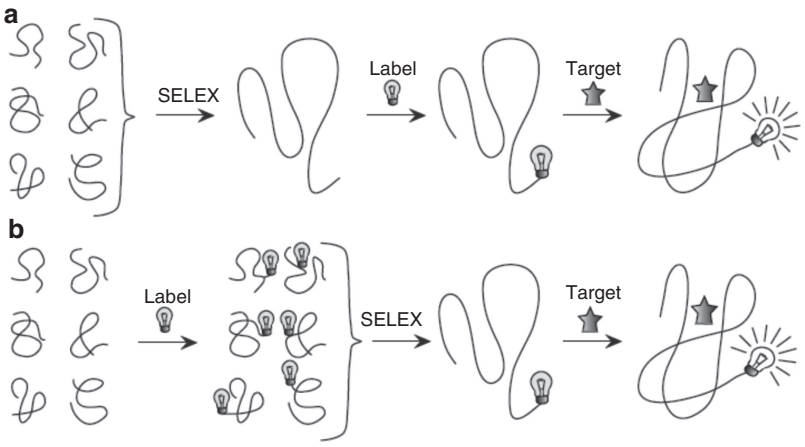

Fig. 7.18 Design of signaling aptamers. (**a**) Labeling an aptamer after SELEX procedure. The site of labeling is selected with the account of expected strong conformation changes that could change the fluorescence property of the attached dye. (**b**) Signaling aptamers are generated by SELEX using a random-sequence library in which each DNA or RNA molecule is labeled with one or a few dye molecules

double or single stranded DNA. This property can be used to generate a binding-specific fluorescence signal if the aptamers possess the modified fluorescent nucleotide analogues in positions that undergo conformational changes (as shown in Fig. 7.18a). Such aptamers that combine recognition and reporting functions are called *signaling aptamers*. The labeling of nucleic acids has been well described in the literature (Cox and Singer 2004).

Similarly to synthetic peptides, for DNA and RNA aptamers the problem of introducing fluorescence reporters can be solved in a most simple and elegant way. The dyes can be introduced covalently into their structures before the selection process (Fig. 7.18b). There is no restriction regarding such modification, and not only single labeling with the environment-sensitive dye but also double labeling with the emitter and quencher or with FRET donor and acceptor can be performed easily. Such procedure was described for ATP detecting aptamers (Jhaveri et al. 2000). Nucleotides bearing fluorescent labels can constitute a random pool of sequences, from which the ligand-binding species are selected. Then the binding species are screened for aptamers that signal the presence of cognate ligands.

With these remarkable properties, the aptamers allow all the possibilities for fluorescence reporting, including multiple dye labeling with the observation of excimer formation, PET and FRET (see Chap. 8). Selection of already labeled aptamers allows minimizing the possible negative effects of post-selection modifications on the aptamer binding to the target (Hesselberth et al. 2000). But the most attractive could be an idea to make the reporter dye that can be involved directly in

the process of target recognition. This could allow recording direct changes in the parameters of their fluorescence.

7.6.3 *Obtaining Fluorescence Response and Integration into Sensor Devices*

Due to the facts that aptamers are relatively small and flexible molecules and that they may change significantly their conformation on target binding, all the arsenals of fluorescence reporting methods described in Chap. 3 can be applied to aptamer sensing.

Generating fluorescence response in aptamers is facilitated by the fact that very often they are largely unstructured in solutions. They fold into the well-defined three-dimensional structures upon binding their target molecules (Hermann and Patel 2000; Stojanovic and Kolpashchikov 2004). This allows many possibilities for introducing the reporting signal. Examples of their realization are illustrated in Fig. 7.19.

The fluorescence response can be provided by the spectral shifts or in a two-band ratiometric manner. In addition, the retardation of the dye rotation can be observed by the increase of anisotropy. Moreover, the quenching effects can be obtained in

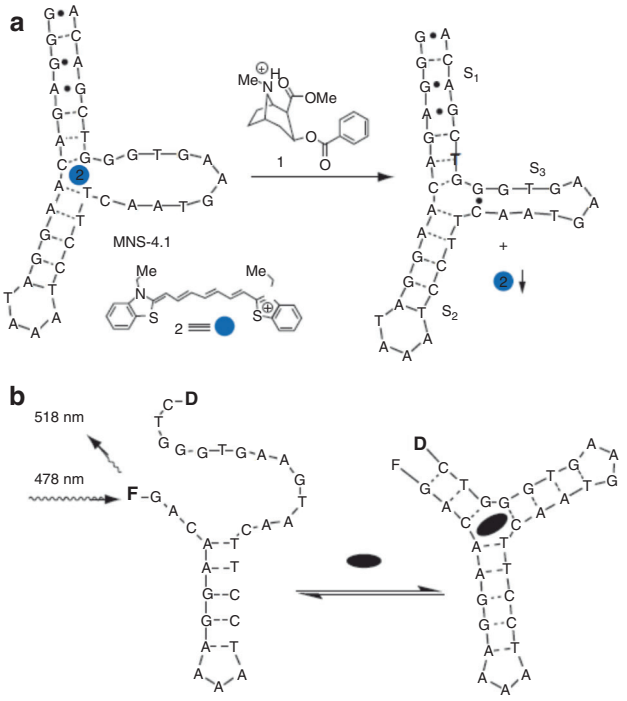

Fig. 7.19 The examples of two sensors responding to the binding of cocaine (Stojanovic et al. 2001; Stojanovic and Landry 2002). (**a**) Competitive assay based on displacement by cocaine (*1*) of a cyanine dye (*2*). The dye changes its absorbance and it aggregates. (**b**) The assay is based on inducing by cocaine binding of conformational change that approximates 5′ and 3′ ends. This results in quenching of fluorescence of fluorescein (*F*) emission by dabcyl dye (*D*)

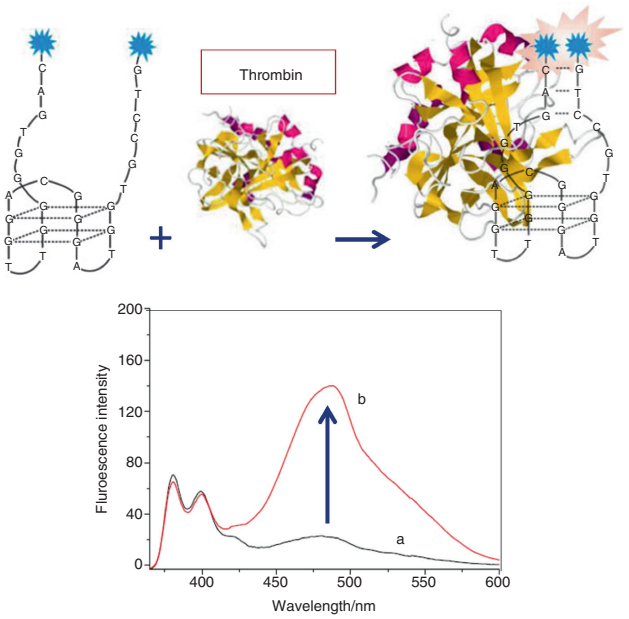

Fig. 7.20 Schematic diagram for detection of thrombin using the 27-meric aptamer with pyrene molecules labeled at both ends of the aptamer (Zhao and Cheng 2013). The binding of thrombin induces the conformation change of the aptamer, causing the pyrenes to form an excimer. Below: The emission spectra of the aptamer probe in the absence of thrombin (**a**) and in the presence of thrombin (**b**). The excimer gives fluorescence emission at about 485 nm with an excitation at 349 nm, allowing the detection of thrombin

lifetime domains. It is surprising in this respect that many researchers prefer less informative intensity sensing trying to provide quantitative analysis and facing the problem of proper response calibration. The double labeling with the emitting dye and the quencher can be applied for that. More reports appear on the introduction of λ-ratiometric sensing, for instance, in application of pyrene excimers (Fig. 7.20).

In fact, the *double labeling* is not a great problem if the assay is made in solution and both 5′-end and 3′-end are available for labeling. For providing the necessary response, the fluorophore and the quencher in one of the forms (with unbound or bound target) should be close together. Luckily, this happens (or can be designed) in some aptamers that structurally resemble the 'beacons', and an example of that is the sensor for thrombin (Li et al. 2002). Folding of DNA chain around the target molecule brings the 5′-end and 3′-end together, which results in quenching. The same authors showed that incorporation of emissive FRET pair at the same sites allows obtaining the wavelength-ratiometric response to target binding.

Structure-switching signaling aptamers are often designed so that they use duplex-complex transition in the conditions of homogeneous assay (Nutiu and Li 2004, 2005a). Duplex in this case is represented by a double-helical structure labeled with fluorescent dye and a complementary sequence labeled by a quencher. In this structure, the fluorescence is quenched, and de-quenching occurs when the conformation change occurs and a new complex with the target is formed.

The followers of 'sandwich' methodology also contribute to the field of aptamers sensing. In one of the studies (Heyduk and Heyduk 2005) the sensor was developed that involves protein-induced co-association of two aptamers recognizing two distinct epitopes of the protein. The aptamers contain short dye-labeled complementary 'signaling' oligonucleotides attached to the aptamer by non-DNA linker. Co-association of two aptamers with the target protein results in bringing

the two fluorescent oligonucleotide derivatives into proximity, producing a large change of FRET signal between the fluorophores.

An interesting possibility of obtaining fluorescence response on target binding is to apply the dyes *replacing DNA bases*. These dyes should report on the rupture-formation of the double helix. The fluorescence of 2-aminopurine is sensitive to conformational changes of DNA. Highly fluorescent donor-acceptor *purines* were synthesized recently (Butler et al. 2007). Their absorption spectra located at 320–340 nm appear weakly solvent dependent, while the emission maxima at 360–400 nm show significant long-wavelength shifts upon increases in polarity. They show nearly 100 % fluorescence quantum yields and lifetimes up to 3 ns in organic solutions with only moderate decrease in highly polar solvents, which may be unique for such simple nucleobases. Their application in sensing is expected to follow.

In contrast to purines, the synthesis of responsive isosteric fluorescent *pyrimidine* analogues was not so much successful, but the progress also has been made. In a recent study (Srivatsan and Tor 2007), appending five-membered aromatic heterocycles at the 5-position on a pyrimidine core, a family of responsive fluorescent nucleoside analogues was reported. They contain furan group as a strong electron donor, which allows exhibiting emission in the visible range. So constructed, ribonucleoside triphosphates are accepted by T7 RNA polymerase as substrates for *in vitro* transcription reactions and are very efficiently incorporated into RNA oligonucleotides with generation of fluorescent constructs.

It is certain that fluorescent base replacements of DNA and RNA will continue to find useful applications in sensing techniques that involve specific binding of nucleic acids. They are able to mimic natural nucleobases and, at the same time, to report on their interactions with other bases and on binding with proteins.

7.6.4 Aptamer Applications

Small molecule sensing is performed more efficiently with aptamers than with peptides. This can be illustrated by successful isolation from a population of random RNA sequences the subpopulations that bind specifically to a variety of organic dyes. According to rough estimates, one in 10^{10} RNA molecules folds in such a way as to create a specific binding site for small ligands, such as amino acid derivatives, cocaine or ATP (Nutiu and Li 2005b).

Aptamers have shown much promise towards detection of a variety of *protein targets*, including cytokines. Specifically, for the determination of cytokines and growth factors (Guthrie et al. 2006), several assays making use of aptamers have been developed, including aptamer-based analogs of ELISA, antibody-linked oligonucleotide assay and fluorescence assays based on anisotropy and FRET (Hamula et al. 2006).

Specific detection and quantitation of *cancer-associated proteins* (inosine monophosphate dehydrogenase II, vascular endothelial growth factor, basic fibroblast growth factor) in the context of human serum and in cellular extracts has been realized with aptamers. It is expected that this technology will improve diagnosis of cancer by enabling direct detection of the expression and modification of proteins closely correlated with disease (McCauley et al. 2003).

Aptamers are useful in the studies of *protein-protein interactions*, where a competitive assay format can be applied, in which the aptamers are displaced from protein-protein contact areas.

Aptamer microarrays are becoming one of the most efficient sensing technologies for multiplex analysis of numerous proteins in parallel, furthering the notion that such arrays may be useful in *proteomics*. Their fabrication is now developed to a great detail (Collett et al. 2005). Fluorescence polarization anisotropy can be used for the measurements of target protein binding both in solutions and on solid support (McCauley et al. 2003).

The solid-phase aptamer-protein interactions are similar to binding interactions seen in solution. Usually when the aptamers are used in heterogeneous sensing platforms, they can be the nucleic acid sequences of different lengths, with one of the ends (either 3′ or 5′-end) being normally used for the binding of the aptamer to the solid support. The other end can be used for carrying a dye. Biotin can be attached to one of the ends, so the aptamers can be spotted on streptavidin-coated slides benefiting from self-assembly based on a very strong streptavidin-biotin interaction (Collett et al. 2005)

In addition to sensor technologies, selected oligonucleotides can be used as '*aptazymes*', the species that possess biocatalytic properties and allow the direct transduction of molecular recognition into catalysis. Together with aptamers they can be used in different bioassays for the detection and quantitation of a wide range of molecular targets (Hesselberth et al. 2000).

7.6.5 Comparison with Other Binders: Prospects

No more than two decades have passed between the introduction of aptamers technology and its development into one of the most successful fields of molecular sensing. There is no restriction in developing the aptamers as the *sensors to any target*. Selected aptamers can bind to their targets with high affinity and discriminate between closely related target molecules. Aptamers can thus be considered as a valid alternative to antibodies as well as to any peptide or protein bio-mimetic receptors. The unique binding properties of nucleic acids, which are amenable to various modifications, make aptamers perfectly suitable for not only sensing, but also for other uses in biotechnology, including pharmaceutical applications (Proske et al. 2005). Such combination of already realized and potential applications as analytical, diagnostic and therapeutic tools (Tombelli et al. 2005) still further stimulates their development.

Out of all macromolecular binders, only the antibodies can presently compete with library-selected aptamers and peptides in versatility of adaptation to any particular target. Regarding other aspects, such as production, storage and application, the aptamers possess many potential *advantages* compared to antibodies. They are technologically more attractive because of their much smaller size. Their large-scale production is expected to be more reproducible and much cheaper. They possess higher stability to environmental factors, which allows the long-term storage without loss of

functional properties. Co-synthetic structural modifications including introduction of fluorescent groups can be achieved much easier. They show superiority to antibodies in specific protein detection (Stadtherr et al. 2005). Moreover, being selected for tripeptide sequences they can recognize these sequences in a large protein, which makes possible a simultaneous multi-site protein recognition (Niu et al. 2007).

The aptamers share with synthetic peptides the benefits regarding manipulation and incorporation into sensor constructs, and the main difference between them is on the selection step. The advantage of nucleic acid aptamer libraries over protein or peptide libraries is their large size (up to 10^{15}–10^{16} different sequences) and the easy identification of selected binders by enzymatic amplification with polymerases. The *larger library* offers more molecular diversity and higher probability of finding the optimal binders. Automated selection procedures now allow rapid identification of DNA and RNA sequences that can target a broad range of extra- and intracellular proteins with nanomolar affinities and high specificities.

All these advantages are not always clearly seen if the aptamers are accommodated into traditional techniques developed for antibodies, such as ELISA. The new techniques exploring their advantages in full are being developed (MacKay et al. 2014). They include microarray and microfluidic technologies. It is expected that they will be highly competitive and demonstrate a full potential for successful realization of extremely valuable properties of aptamers.

7.7 Peptide Nucleic Acids

All current techniques for quantifying specific DNA or RNA exploit the base pair fitting between target polynucleotide and a complementary nucleic acid sequence serving as the sensor recognition unit. The major effort of researchers is now directed towards developing the techniques that could dramatically increase the sensitivity of response to this primary interaction. This search was extended to synthetic polymers. It was found that the neutral polymer called ‘peptide nucleic acid’ demonstrates superior to DNA or RNA binding properties.

7.7.1 Structure and Properties

Peptide nucleic acid (PNA) is an artificial polymer that contains the same side groups (bases) as DNA and RNA and is capable of forming the highly stable complexes with complementary sequences of nucleic acids. Peptide nucleic acid is not an acid! It is a neutral oligomer, in which the entire charged backbone is replaced by an uncharged *N*-(2-aminoethyl) glycine scaffold. The nucleotide nitrogenous bases are attached to them via a methylene carbonyl linker. Therefore, PNA can be regarded as DNA with a *neutral peptide backbone* instead of a negatively charged sugar-phosphate backbone of natural nucleic acids (Shakeel et al. 2006). The size

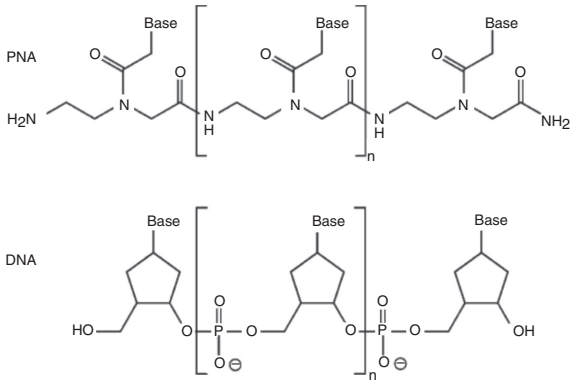

Fig. 7.21 Comparison of PNA and DNA structures showing structural similarity between them. Similar size of repeat units allows hybridization between the chains in the case of complementarity of side groups (nucleic acid bases). Because of absence of Coulombic repulsion, PNA binds to DNA stronger than a complementary DNA chain

and shape of this polymer allows ideal hybridization based on the base-base interaction with DNA and RNA (Fig. 7.21).

Because of the negative charge absence, peptide nucleic acids exhibit superior *hybridization properties* than the natural nucleic acids. PNA is chemically stable and resistant to enzymatic cleavage, which provides its stability towards degradation in a living cell. PNA is capable of recognizing specific sequences of DNA and RNA obeying the Watson-Crick hydrogen bonding scheme, and the hybrid complexes exhibit extraordinary thermal stability and unique ionic strength effects (Shakeel et al. 2006).

7.7.2 DNA Recognition with Peptide Nucleic Acids

The great interest to PNA as a recognition functionality for DNA or RNA detection appeared after it was demonstrated that *both ssDNA and DNA-PNA hybrids bind cationic conjugated polymer* (polythiophene derivative) with a dramatic change of its fluorescence. A combination of complementary functions of specific base-to-base PNA recognition with the extraordinary reporting function of conjugated polymer suggests a revolutionary change in DNA detection methodology (see Sect. 12.4).

A combination of surface-bound PNA probes and soluble fluorescent cationic conjugated polymers was suggested for detecting and identifying unlabelled target nucleic acid on microarrays (Raymond et al. 2005). Application of PNA instead of DNA on supported arrays has the advantage in the absence of interaction between PNA and cationic polymer, and only in the target DNA presence such interaction appears in the form of ‘triplex’ (Fig. 12.13).

In addition to active role in DNA recognition and passive role in reporting, PNA can play an active role when labeled with the dye that can serve the FRET acceptor. Then in combination with the conjugated polymer that serves an antenna and an energy donor, a *superquenching* effect (Sect. 8.4) can be achieved with substantial increase of response sensitivity (Liu and Bazan 2005).

Interaction of PNA with *double-stranded DNA* is the prospective trend in development of DNA sensing technologies. PNA is able to form specific higher-order (i.e. three- and four-stranded) complexes with DNA. This makes it an ideal structural probe for designing strand-specific dsDNA biosensors (Baker et al. 2006). The formation of higher-order complexes can be detected by dye-labeling of PNA. Addition to this system of cationic conjugated polymer allows providing the amplification of reporting effect.

This finding has important consequences. Commonly, the DNA hybridization assays require thermal denaturation producing the dissociation of the two strands, which is necessary for subsequent hybridization. Introduction into a sensing technology of a detection method for dsDNA that eliminates the need for thermal denaturing steps must have good prospects.

The *single nucleotide polymorphism* (SNP) is the major type of variation in the human genome that can characterize the identity of a person on a genetic level. The strategy employing a combination of PNA recognition units, an optically amplifying conjugated polymer detectors, and S1 nuclease enzyme is capable of detecting SNPs in a simple, rapid, and sensitive manner (Baker et al. 2006). The recognition is accomplished by sequence-specific hybridization between the uncharged, fluorescein-labeled PNA probe and the DNA sequence of interest. After subsequent treatment with S1 nuclease, the cationic polymer associates with the remaining anionic PNA/DNA complex, leading to sensitized emission of the dye-labeled PNA probe via FRET mechanism. An improvement of this assay can be provided by additional application of nonionic detergent (Al Attar et al. 2008).

The techniques addressing detection of single mismatches in hybridization assays can benefit from the possibility of using PNA segments in which one base is *substituted with a fluorescent dye*. This dye serves as a replacement of a canonical nucleobase with the ability of performing a reporting function (Socher et al. 2008). If a complementary DNA molecule (except at the site of the dye) hybridizes to the probe, the dye exhibits intense fluorescence emission because the stacking in the duplexes enforces its coplanar arrangement. However, a base mismatch at either position immediately adjacent to the dye dramatically decreases fluorescence, presumably because the dye becomes allowed to undergo torsional motions that lead to rapid depletion of the excited state. The number of dyes tested for this functional response (called '*forced intercalation*') increases (Bethge et al. 2008).

7.8 Molecularly Imprinted Polymers

The multi-point noncovalent binding that is necessary for selective detection of analyte in a mixture with structurally close molecules can be achieved not only with the binding sites formed by natural or synthetic molecules. The recognition element of a sensor can also be a *hole accommodating the target molecule* formed in the structure of synthetic polymer. If such accommodation can be made by providing a number of sterically fitting noncovalent interactions with the polymer matrix, this may allow realizing sufficient affinity for binding of the target and selectivity against non-target molecules (Alexander et al. 2006; Sellergren and Andersson 2000).

In a strict sense, *imprinted polymers* are not the 'molecular sensors', they are the organized macroscopic bodies in which many recognition sites for the same target can be formed by one or several polymer molecules. If the primary events of the target binding are recorded, they can constitute the platform for the development of the sensors that combine target binding and fluorescence response. This simple idea turned-out to be very profitable. It is frequently used in both chromatographic separation technology and in drug delivery. In sensor technologies, it offers very interesting prospects.

7.8.1 The Principle of Imprinted Polymer Formation

Imprinted polymers are produced by assembling and co-polymerizing of synthetic monomers and oligomers to form a polymeric network in the presence of target molecule (the analyte itself or a molecule with a similar structure). This process is often called a '*template-directed polymerization'*. The target serves as a molecular template by creating a *cavity* in polymer matrix. This cavity is complementary to the template. In addition to sterical fitting, it allows formation of many noncovalent interactions with the target that become fixed during polymerization step (Haupt and Mosbach 2000). After the polymer matrix is formed, the target is washed-out leaving the 'imprinted' binding sites that are complementary in size and shape to the analyte.

When it is introduced into the polymer, such *molecular memory* allows selective rebinding of the target, i.e. realizing molecular recognition (see Fig. 7.22). The

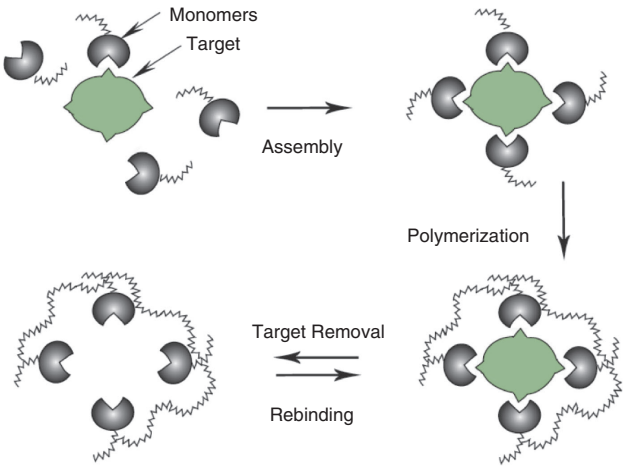

Fig. 7.22 The steps of recognition sites formation in imprinted polymer. On the first step, the monomeric or oligomeric units are incubated with the target, so that their noncovalent bonds are formed. Then, polymerization fixes this arrangement and the target is washed-out leaving the hole that can be occupied by the target

recognition units produced in this way in polymers challenge their natural counterparts that were discussed above, such as the ligand-binding proteins and antibodies.

The progress in polymerization techniques, in formation of molecular imprints and in the techniques of analytes trapping/detrapping is described in many publications (Mosbach and Haupt 1998; Haupt and Mosbach 2000). Imprinted polymers can be used in different formats, not only as films but also as microspheres and nanoparticles (Yoshimatsu et al. 2007).

7.8.2 The Coupling with Reporting Functionality

For operation of imprinted polymer as a sensor for detection of nonfluorescent molecules, the *fluorescence reporter should be incorporated* into polymer matrix (Rathbone and Bains 2005; Stephenson and Shimizu 2007). This has to be done in a way allowing providing the response to target binding by detectable change of fluorescence properties. If the target itself contributes to reporter function (being a fluorescent dye, quencher or FRET acceptor), the sensor performance is easy. For instance, the traces of cancerogenic benzo[a]pyrene in water can be detected by polymer binding, since this binding results in enhancement of intrinsic benzo[a] pyrene phosphorescence mediated by heavy atom incorporated into the polymer (Traviesa-Alvarez et al. 2007). On a general scale, the reporting on target binding to polymer sites is a very difficult task.

A number of methods have been suggested for achieving the transduction of binding event into *fluorescence signal* (Alexander et al. 2006), but no satisfactory solution of this problem appeared by now (Stephenson and Shimizu 2007). It is hard, for instance, to explore the anisotropy sensing, because no free segmental rotation could be allowed in the polymer. Meantime, in view of limitations in other possibilities, such attempts have been made (Hunt and Ansell 2006). Much simpler is the realization of competitor displacement assay with fluorescent competitor (Navarro-Villoslada et al. 2007).

Many researchers attempted the incorporation of fluorescent dyes on the step of polymerization process. Without transduction mechanism, this does not resolve the problem of fluorescence reporting. Most of these attempts regard intensity sensing, and the fluorescent dye is included into the polymer as a monomeric unit or as a substituent to induce the quenching/enhancement on target binding.

Probably, the best solution that is seen at present is the application of competition assay that involves FRET donor incorporated into polymer matrix and the competitor, which is the target with attached fluorophore (Descalzo et al. 2013).

7.8.3 Applications

It is amazing, that there is virtually no limit to size and chemical nature of analyzed compounds that can be detected with molecularly imprinted polymers. They have been developed for small organic molecules, such as steroids, for amino acids,

sugars, drugs, pesticides, and also for proteins and even the cells (Haupt and Mosbach 1999). In contrast to macromolecules, these binders are resistant to adverse environmental conditions such as heat and extremes of pH. Their affinity and selectivity can approach that observed for biospecific recognition (Hillberg et al. 2005).

Imprinted polymers are extensively used in many *separation techniques*, such as thin-layer chromatography, high-performance liquid chromatography and solid-phase extraction. They offer good potential for applications in sensor array technologies (Shimizu and Stephenson 2010). Their more intensive application in fluorescence sensing must follow the development of proper methods for signal transduction and fluorescence detection.

Substantial progress in sensing with imprinted polymers is expected from the combination of the imprinting methodology with the responsive properties of conjugated polymers. The prototype of this material was described (Li et al. 2007). It was tested for the detection of 2,4,6-trinitrotoluene and related nitroaromatic compounds. The described polymeric sensor shows remarkable air stability and photostability, high fluorescence quantum yield, and reversible analyte binding. Displaying their intrinsic signal amplification capability, fluorescent conjugated polymers are an attractive basis for the design of low detection limit sensing devices.

7.9 Sensing and Thinking: Selecting the Tool for Optimal Target Recognition

The ultimate goal in fluorescence sensing technologies is **to possess generic methodology allowing sensing any target and any combination of targets simultaneously by using simple unified detection technique**. It could be ideal to select a family of molecular or nanoscale sensors, for which the binding properties of large number of potential analytes could be induced, but which could use the same unified signal-transduction mechanism.

The analysis presented above clearly shows that this goal in observable future is not achievable. Synthetic coordination compounds show optimal performance for detecting only small molecules and ions with some prospects of binding to ‘hot spots’ of larger molecules. Antibodies and ligand-binding proteins recognize these larger molecules easier. The biopolymer molecules of larger complexity can be recognized by ligand-binding proteins or antibodies, but only based on their short-scale molecular features such as antigenic determinants. Molecular recognition should extend to macromolecules with large contact surfaces, to well-specified molecular patterns on cell surfaces and to extended segments of nucleic acid sequence.

In this respect, biopolymers such as proteins, peptides and nucleic acids often demonstrate the necessary flexibility for forming the interaction sites with a huge number of potential targets. The applications of two principles, *rational design* and *combinatorial library selection*, complement each other. Combination of rigid scaffolds with ‘rationally’ located flexible recognition units and fluorescence reporters

allows achieving highly selective binding and efficient reporting together with the possibility of fine-tuning the affinity to the desired range of target concentrations.

Questions and Problems

1. Why the small-molecular sensors with direct fluorescence response are better fitting to sensing ions than the neutral molecules? What intrinsic signal transduction mechanisms are employed in these sensors? (The reader may refer to Sects. 8.1 and 8.2).
2. Why cyclodextrins bind cholesterol and its derivatives and can extract cholesterol from biomembranes? What are the requirements for such binding?
3. What is the difference in target binding to cyclodextrin monomers and dimers in terms of selectivity and affinity?
4. How can the calixarene selectivity be tuned in order to recognize a particular analyte?
5. How calixarenes and porphyrins interact between each other? Based on these molecules the smart receptors for protein targets can be designed. What principles are implied in this design?
6. Explain the structure of a typical IgG antibody. How flexibility and rigidity of its structure co-participate in realizing the binding function?
7. How the principle of combined flexibility and rigidity is realized in ligand-binding proteins?
8. What are the advantages of synthetic peptides over proteins in sensing technologies? How to obtain them as high-affinity receptors?
9. Compare the affinities to a hypothetical rigid target of a flexible tetrapeptide Leu-Leu-Leu-Asp and of the same sequence incorporated into a rigid structure. Use formulas from Chap. 2 and the rough estimates of free energy change of 2–3 kJ/mol for the formation of salt bridge, 10 kJ/mol for hydrophobic interaction between amino acids and 3–4 kJ/mol as an entropy penalty for suppression of rotation around a single bond.
10. Explain the realization of different technologies for providing the fluorescence response in the cases: (a) aptamers in solution; (b) aptamers attached with one of the terminals to solid support.
11. What is the mechanism behind the use of intercalating dyes for obtaining the response to aptamer-target binding? What are the disadvantages of this approach?
12. The melting of PNA-DNA double helix (duplex), will it occur at higher or lower temperatures than the DNA duplex (dsDNA)?
13. Explain the mechanism of fluorescence response generation in the system PNA-ssDNA-conjugated polymer in the cases: (a) PNA is unlabeled; (b) PNA is labeled with fluorescent dye.
14. For detecting the single nucleotide substitutions, which possibility would you choose to use: short or long receptor sequences? High or low binding affinity?
15. In the case of imprinted polymer, what are the possibilities to provide fluorescence response in the following cases: (a) if the polymer does not contain

fluorescence reporter? (b) if it contains the reporter that is not contacting with the bound target? (c) if fluorescence reporter is located within the target-binding cavity?

16. Suggest the possibilities to locate the reporter in the imprinted polymer cavities available for direct contact with the target. What detection techniques could you suggest to use in this case?

References

Al Attar HA, Norden J, O'Brien S, Monkman AP (2008) Improved single nucleotide polymorphisms detection using conjugated polymer/surfactant system and peptide nucleic acid. Biosens Bioelectron 23(10):1466–1472

Alexander C, Andersson HS, Andersson LI, Ansell RJ, Kirsch N, Nicholls IA, O'Mahony J, Whitcombe MJ (2006) Molecular imprinting science and technology: a survey of the literature for the years up to and including 2003. J Mol Recognit 19(2):106–180

Al-Hassan KA, Khanfer MF (1998) Fluorescence probes for cyclodextrin interiors. J Fluoresc 8(2):139–152

Azzazy HM, Highsmith WE Jr (2002) Phage display technology: clinical applications and recent innovations. Clin Biochem 35(6):425–445

Badjic JD, Nelson A, Cantrill SJ, Turnbull WB, Stoddart JF (2005) Multivalency and cooperativity in supramolecular chemistry. Acc Chem Res 38(9):723–732

Baker ES, Hong JW, Gaylord BS, Bazan GC, Bowers MT (2006) PNA/dsDNA complexes: site specific binding and dsDNA biosensor applications. J Am Chem Soc 128(26):8484–8492

Balabai N, Linton B, Napper A, Priyadarshy S, Sukharevsky AP, Waldeck DH (1998) Orientational dynamics of beta-cyclodextrin inclusion complexes. J Phys Chem B 102(48): 9617–9624

Barthe P, Cohen-Gonsaud M, Aldrian-Herrada G, Chavanieu A, Labesse G, Roumestand C (2004) Design of an amphipathic alpha-helical hairpin peptide. C R Chim 7(3–4):249–252

Benhar I (2007) Design of synthetic antibody libraries. Expert Opin Biol Ther 7(5):763–779

Bethge L, Jarikote DV, Seitz O (2008) New cyanine dyes as base surrogates in PNA: forced intercalation probes (FIT-probes) for homogeneous SNP detection. Bioorg Med Chem 16(1): 114–125

Biedermann F, Elmalem E, Ghosh I, Nau WM, Scherman OA (2012) Strongly fluorescent, switchable perylene bis(diimide) host-guest complexes with cucurbit[8]uril in water. Angew Chem Int Ed Engl. doi:10.1002/anie.201205393

Binz HK, Pluckthun A (2005) Engineered proteins as specific binding reagents. Curr Opin Biotechnol 16(4):459–469

Binz HK, Amstutz P, Pluckthun A (2005) Engineering novel binding proteins from nonimmunoglobulin domains. Nat Biotechnol 23(10):1257–1268

Bishop KJ, Wilmer CE, Soh S, Grzybowski BA (2009) Nanoscale forces and their uses in self-assembly. Small 5(14):1600–1630

Boersma YL, Plückthun A (2011) DARPins and other repeat protein scaffolds: advances in engineering and applications. Curr Opin Biotechnol 22(6):849–857

Breslow R, Dong SD (1998) Biomimetic reactions catalyzed by cyclodextrins and their derivatives. Chem Rev 98(5):1997–2011

Brune M, Hunter JL, Corrie JET, Webb MR (1994) Direct, real-time measurement of rapid inorganic phosphate release using a novel fluorescent probe and its application to actomyosin subfragment 1 ATPase. Biochemistry 33:8262–8271

Butler RS, Myers AK, Bellarmine P, Abboud KA, Castellano RK (2007) Highly fluorescent donor-acceptor purines. J Mater Chem 17(19):1863–1865

Casadei J, Powell MJ, Kenten JH (1990) Expression and secretion of aequorin as a chimeric antibody by means of a mammalian expression vector. Proc Natl Acad Sci U S A 87(6): 2047–2051

Chen CT, Huang WP (2002) A highly selective fluorescent chemosensor for lead ions. J Am Chem Soc 124(22):6246–6247

Chmielewski MJ, Buhler E, Candau J, Lehn JM (2014) Multivalency by self-assembly: binding of concanavalin A to metallosupramolecular architectures decorated with Multiple Carbohydrate Groups. Chemistry 20(23):6960–6977

Choulier L, Enander K (2010) Environmentally sensitive fluorescent sensors based on synthetic peptides. Sensors 10(4):3126–3144

Choulier L, Shvadchak VV, Naidoo A, Klymchenko AS, Mely Y, Altschuh D (2010) A peptide-based fluorescent ratiometric sensor for quantitative detection of proteins. Anal Biochem 401(2):188–195

Collett JR, Cho EJ, Ellington AD (2005) Production and processing of aptamer microarrays. Methods 37(1):4–15

Cox WG, Singer VL (2004) Fluorescent DNA hybridization probe preparation using amine modification and reactive dye coupling. Biotechniques 36(1):114–122

de Lorimier RM, Smith JJ, Dwyer MA, Looger LL, Sali KM, Paavola CD, Rizk SS, Sadigov S, Conrad DW, Loew L, Hellinga HW (2002) Construction of a fluorescent biosensor family. Protein Sci 11(11):2655–2675

de Silva AP, Gunaratne HQN, Gunnaugsson T, Huxley AJM, McRoy CP, Rademacher JT, Rice TE (1997) Signaling recognition events with fluorescent sensors and switches. Chem Rev 97:1515–1566

Demchenko AP (2001a) Concepts and misconcepts in the analysis of simple kinetics of protein folding. Curr Protein Pept Sci 2(1):73–98

Demchenko AP (2001b) Recognition between flexible protein molecules: induced and assisted folding. J Mol Recognit 14(1):42–61

Demchenko AP, Chinarov VA (1999) Tolerance of protein structures to the changes of amino acid sequences and their interactions. The nature of the folding code. Protein Pept Lett 6(3): 115–129

Descalzo AB, Somoza C, Moreno-Bondi MC, Orellana G (2013) Luminescent core–shell imprinted nanoparticles engineered for targeted förster resonance energy transfer-based sensing. Anal Chem 85(11):5316–5320

Douhal A (2004) Ultrafast guest dynamics in cyclodextrin nanocavities. Chem Rev 104(4): 1955–1976

Dsouza RN, Pischel U, Nau WM (2011) Fluorescent dyes and their supramolecular host/guest complexes with macrocycles in aqueous solution. Chem Rev 111(12):7941–7980

Dwyer MA, Hellinga HW (2004) Periplasmic binding proteins: a versatile superfamily for protein engineering. Curr Opin Struct Biol 14(4):495–504

Edwards BM, Barash SC, Main SH, Choi GH, Minter R, Ullrich S, Williams E, Du Fou L, Wilton J, Albert VR, Ruben SM, Vaughan TJ (2003) The remarkable flexibility of the human antibody repertoire; isolation of over one thousand different antibodies to a single protein, BLyS. J Mol Biol 334(1):103–118

Eklund M, Axelsson L, Uhlen M, Nygren PA (2002) Anti-idiotypic protein domains selected from protein A-based affibody libraries. Proteins Struct Funct Genet 48(3):454–462

Enander K, Dolphin GT, Andersson LK, Liedberg B, Lundstrom I, Baltzer L (2002) Designed, folded polypeptide scaffolds that combine key biosensing events of recognition and reporting. J Org Chem 67(9):3120–3123

Enander K, Dolphin GT, Baltzer L (2004a) Designed, functionalized helix-loop-helix motifs that bind human carbonic anhydrase II: a new class of synthetic receptor molecules. J Am Chem Soc 126(14):4464–4465

Enander K, Dolphin GT, Liedberg B, Lundstrom I, Baltzer L (2004b) A versatile polypeptide platform for integrated recognition and reporting: affinity arrays for protein-ligand interaction analysis. Chemistry 10(10):2375–2385

Enander K, Choulier L, Olsson AL, Yushchenko DA, Kanmert D, Klymchenko AS, Demchenko AP, Mely Y, Altschuh D (2008) A peptide-based, ratiometric biosensor construct for direct fluorescence detection of a protein analyte. Bioconjug Chem 19(9):1864–1870

Engfeldt T, Renberg B, Brumer H, Nygren PA, Karlstrom AE (2005) Chemical synthesis of triple-labelled three-helix bundle binding proteins for specific fluorescent detection of unlabelled protein. Chembiochem 6(6):1043–1050

Fasting C, Schalley CA, Weber M, Seitz O, Hecht S, Koksch B, Dernedde J, Graf C, Knapp EW, Haag R (2012) Multivalency as a chemical organization and action principle. Angew Chem Int Ed 51(42):10472–10498

Flores S, Echols N, Milburn D, Hespenheide B, Keating K, Lu J, Wells S, Yu EZ, Thorpe M, Gerstein M (2006) The database of macromolecular motions: new features added at the decade mark. Nucleic Acids Res 34:D296–D301

Flower DR, North ACT, Sansom CE (2000) The lipocalin protein family: structural and sequence overview. Biochim Biophys Acta Protein Struct Mol Enzymol 1482(1–2): 9–24

Fonin AV, Stepanenko OV, Povarova OI, Volova CA, Philippova EM, Bublikov GS, Kuznetsova IM, Demchenko AP, Turoverov KK (2014) Spectral characteristics of the mutant form GGBP/H152C of D-glucose/D-galactose-binding protein labeled with fluorescent dye BADAN: influence of external factors. PeerJ 2:e275

Gellman SH, Woolfson DN (2002) Mini-proteins Trp the light fantastic. Nat Struct Biol 9(6):408–410

Gilardi G, Zhou LQ, Hibbert L, Cass AEG (1994) Engineering the maltose-binding protein for reagentless fluorescence sensing. Anal Chem 66(21):3840–3847

Glasner ME, Gerlt JA, Babbitt PC (2007) Mechanisms of protein evolution and their application to protein engineering. Adv Enzymol Relat Areas Mol Biol 75:193–239, xii–xiii

Gomara MJ, Haro I (2007) Synthetic peptides for the immunodiagnosis of human diseases. Curr Med Chem 14(5):531–546

Goodchild S, Love T, Hopkins N, Mayers C (2006) Engineering antibodies for biosensor technologies. Adv Appl Microbiol 58:185–226

Gopinath SCB (2007) Methods developed for SELEX. Anal Bioanal Chem 387(1):171–182

Gopinath SC, Tang T-H, Citartan M, Chen Y, Lakshmipriya T (2014) Current aspects in immunosensors. Biosens Bioelectron 57:292–302

Guntas G, Ostermeier M (2004) Creation of an allosteric enzyme by domain insertion. J Mol Biol 336(1):263–273

Guthrie JW, Hamula CLA, Zhang HQ, Le XC (2006) Assays for cytokines using aptamers. Methods 38(4):324–330

Hamada H, Kameshima N, Szymanska A, Wegner K, Lankiewicz L, Shinohara H, Taki M, Sisido M (2005) Position-specific incorporation of a highly photodurable and blue-laser excitable fluorescent amino acid into proteins for fluorescence sensing. Bioorg Med Chem 13(10): 3379–3384

Hamula CLA, Guthrie JW, Zhang HQ, Li XF, Le XC (2006) Selection and analytical applications of aptamers. TrAC Trends Anal Chem 25(7):681–691

Haupt K, Mosbach K (1999) Molecularly imprinted polymers in chemical and biological sensing. Biochem Soc Trans 27(2):344–350

Haupt K, Mosbach K (2000) Molecularly imprinted polymers and their use in biomimetic sensors. Chem Rev 100(7):2495–2504

Hazra P, Chakrabarty D, Chakraborty A, Sarkar N (2004) Intramolecular charge transfer and solvation dynamics of Nile Red in the nanocavity of cyclodextrins. Chem Phys Lett 388(1–3):150–157

Hermann T, Patel DJ (2000) Biochemistry – adaptive recognition by nucleic acid aptamers. Science 287(5454):820–825

Hesselberth JR, Miller D, Robertus J, Ellington AD (2000) In vitro selection of RNA molecules that inhibit the activity of ricin A-chain. J Biol Chem 275(7):4937–4942

Heyduk E, Heyduk T (2005) Nucleic acid-based fluorescence sensors for detecting proteins. Anal Chem 77(4):1147–1156

Hicke BJ, Marion C, Chang YF, Gould T, Lynott CK, Parma D, Schmidt PG, Warren S (2001) Tenascin-C aptamers are generated using tumor cells and purified protein. J Biol Chem 276(52):48644–48654

Hillberg AL, Brain KR, Allender CJ (2005) Molecular imprinted polymer sensors: implications for therapeutics. Adv Drug Deliv Rev 57(12):1875–1889

Hossain MA, Mihara H, Ueno A (2003) Fluorescence resonance energy transfer in a novel cyclodextrin-peptide conjugate for detecting steroid molecules. Bioorg Med Chem Lett 13(24):4305–4308

Hosse RJ, Rothe A, Power BE (2006) A new generation of protein display scaffolds for molecular recognition. Protein Sci 15(1):14–27

Hunt CE, Ansell RJ (2006) Use of fluorescence shift and fluorescence anisotropy to evaluate the re-binding of template to (S)-propranolol imprinted polymers. Analyst 131(5):678–683

Hust M, Dubel S (2004) Mating antibody phage display with proteomics. Trends Biotechnol 22(1):8–14

Jennings K, Diamond D (2001) Enantioselective molecular sensing of aromatic amines using tetra-(S)-di-2-naphthylprolinol calix[4]arene. Analyst 126(7):1063–1067

Jespers L, Bonnert TP, Winter G (2004) Selection of optical biosensors from chemisynthetic antibody libraries. Protein Eng Des Sel 17(10):709–713

Jhaveri S, Rajendran M, Ellington AD (2000) In vitro selection of signaling aptamers. Nat Biotechnol 18(12):1293–1297

Jin T, Fujii F, Yamada E, Nodasaka Y, Kinjo M (2006) Control of the optical properties of quantum dots by surface coating with calix n arene carboxylic acids. J Am Chem Soc 128(29): 9288–9289

Joseph R, Rao CP (2011) Ion and molecular recognition by lower rim 1, 3-di-conjugates of calix [4] arene as receptors. Chem Rev 111(8):4658–4702

Kachkovskiy GO, Shandura MP, Drapaylo AB, Slominskii JL, Tolmachev OI, Kalchenko VI (2006) New calix[4]arene based hydroxystyryl cyanine dyes. J Inclusion Phenom Macrocyclic Chem 56(3–4):315–321

Katilius E, Katiliene Z, Woodbury NW (2006) Signaling aptamers created using fluorescent nucleotide analogues. Anal Chem 78(18):6484–6489

Khan F, Pickup JC (2013) Near-infrared fluorescence glucose sensing based on glucose/galactose-binding protein coupled to 651-Blue Oxazine. Biochem Biophys Res Commun 438(3):488–492

Kodadek T (2002) Development of protein-detecting microarrays and related devices. Trends Biochem Sci 27(6):295–300

Korndorfer IP, Schlehuber S, Skerra A (2003) Structural mechanism of specific ligand recognition by a lipocalin tailored for the complexation of digoxigenin. J Mol Biol 330(2):385–396

Kubinyi M, Vidoczy T, Varga O, Nagy K, Bitter I (2005) Absorption and fluorescence spectroscopic study on complexation of oxazine 1 dye by calix 8 arenesulfonate. Appl Spectrosc 59(1):134–139

Kulagina NV, Shaffer KM, Anderson GP, Ligler FS, Taitt CR (2006) Antimicrobial peptide-based array for Escherichia coli and Salmonella screening. Anal Chim Acta 575(1):9–15

Lakowicz JR (2006) Principles of fluorescence spectroscopy, 3rd edn. Springer, New York

Leray I, Lefevre JP, Delouis JF, Delaire J, Valeur B (2001) Synthesis and photophysical and cation-binding properties of mono- and tetranaphthylcalix 4 arenes as highly sensitive and selective fluorescent sensors for sodium. Chemistry 7(21):4590–4598

Levin AM, Weiss GA (2006) Optimizing the affinity and specificity of proteins with molecular display. Mol Biosyst 2(1):49–57

Li JJ, Fang X, Tan W (2002) Molecular aptamer beacons for real-time protein recognition. Biochem Biophys Res Commun 292(1):31–40

Li J, Kendig CE, Nesterov EE (2007) Chemosensory performance of molecularly imprinted fluorescent conjugated polymer materials. J Am Chem Soc 129(51):15911–15918

Liu B, Bazan GC (2005) Methods for strand-specific DNA detection with cationic conjugated polymers suitable for incorporation into DNA chips and microarrays. Proc Natl Acad Sci U S A 102(3):589–593

Liu Y, Song Y, Chen Y, Li XQ, Ding F, Zhong RQ (2004) Biquinolino-modified beta-cyclodextrin dimers and their metal complexes as efficient fluorescent sensors for the molecular recognition of steroids. Chemistry 10(15):3685–3696

Liu Y, Liang P, Chen Y, Zhao YL, Ding F, Yu A (2005) Spectrophotometric study of fluorescence sensing and selective binding of biochemical substrates by 2,2′-bridged biso(beta-cyclodextrin) and its water-soluble fullerene conjugate. J Phys Chem B 109(49):23739–23744

Looger LL, Dwyer MA, Smith JJ, Hellinga HW (2003) Computational design of receptor and sensor proteins with novel functions. Nature 423(6936):185–190

MacKay S, Wishart D, Xing JZ, Chen J (2014) Developing trends in aptamer-based biosensor devices and their applications. IEEE Trans Biomed Circuits Syst 8(1):4–14

Makabe A, Kinoshita K, Narita M, Hamada F (2002) Guest-responsive fluorescence variations of gamma-cyclodextrins labeled with hetero-functionalized pyrene and tosyl moieties. Anal Sci 18(2):119–124

Mammen M, Choi S-K, Whitesides GM (1998) Polyvalent interactions in biological systems: implications for design and use of multivalent ligands and inhibitors. Angew Chem Int Ed 37(20):2754–2794

Martinez-Veracoechea FJ, Frenkel D (2011) Designing super selectivity in multivalent nanoparticle binding. Proc Natl Acad Sci 108(27):10963–10968

Marvin JS, Hellinga HW (1998) Engineering biosensors by introducing fluorescent allosteric signal transducers: construction of a novel glucose sensor. J Am Chem Soc 120(1):7–11

Marvin JS, Hellinga HW (2001a) Conversion of a maltose receptor into a zinc biosensor by computational design. Proc Natl Acad Sci U S A 98(9):4955–4960

Marvin JS, Hellinga HW (2001b) Manipulation of ligand binding affinity by exploitation of conformational coupling. Nat Struct Biol 8(9):795–798

Marvin JS, Corcoran EE, Hattangadi NA, Zhang JV, Gere SA, Hellinga HW (1997) The rational design of allosteric interactions in a monomeric protein and its applications to the construction of biosensors. Proc Natl Acad Sci U S A 94(9):4366–4371

McCauley TG, Hamaguchi N, Stanton M (2003) Aptamer-based biosensor arrays for detection and quantification of biological macromolecules. Anal Biochem 319(2):244–250

McQuade DT, Pullen AE, Swager TM (2000) Conjugated polymer-based chemical sensors. Chem Rev 100(7):2537–2574

Medintz IL, Deschamps JR (2006) Maltose-binding protein: a versatile platform for prototyping biosensing. Curr Opin Biotechnol 17(1):17–27

Medintz IL, Goldman ER, Lassman ME, Mauro JM (2003) A fluorescence resonance energy transfer sensor based on maltose binding protein. Bioconjug Chem 14(5):909–918

Meyer T, Knapp EW (2014) Database of protein complexes with multivalent binding ability: bivalbind. Proteins Struct Funct Bioinf 82(5):744–751

Miao Z, Ren G, Liu H, Jiang L, Cheng Z (2010) Cy5.5-labeled Affibody molecule for near-infrared fluorescent optical imaging of epidermal growth factor receptor positive tumors. J Biomed Opt 15(3):036007

Mohanty J, Bhasikuttan AC, Nau WM, Pal H (2006) Host-guest complexation of neutral red with macrocyclic host molecules: contrasting pK(a) shifts and binding affinities for cucurbit 7 uril and beta-cyclodextrin. J Phys Chem B 110(10):5132–5138

Mondal SK, Sahu K, Ghosh S, Sen P, Bhattacharyya K (2006) Excited-state proton transfer from pyranine to acetate in gamma-cyclodextrin and hydroxypropyl gamma-cyclodextrin. J Phys Chem A 110(51):13646–13652

Mosbach K, Haupt K (1998) Some new developments and challenges in non-covalent molecular imprinting technology. J Mol Recognit 11(1–6):62–68

Mulder A, Huskens J, Reinhoudt DN (2004) Multivalency in supramolecular chemistry and nanofabrication. Org Biomol Chem 2(23):3409–3424

Muyldermans S (2001) Single domain camel antibodies: current status. J Biotechnol 74(4): 277–302

Nanduri V, Kim G, Morgan MT, Ess D, Hahm BK, Kothapalli A, Valadez A, Geng T, Bhunia AK (2006) Antibody immobilization on waveguides using a flow-through system shows improved

Listeria monocytogenes detection in an automated fiber optic biosensor: RAPTOR (TM). Sensors 6(8):808–822
Nau WM, Florea M, Assaf KI (2011) Deep inside cucurbiturils: physical properties and volumes of their inner cavity determine the hydrophobic driving force for host–guest complexation. Isr J Chem 51(5–6):559–577
Navarro-Villoslada F, Urraca JL, Moreno-Bondi MC, Orellana G (2007) Zearalenone sensing with molecularly imprinted polymers and tailored fluorescent probes. Sens Actuators B 121(1):67–73
Neuweiler H, Schulz A, Vaiana AC, Smith JC, Kaul S, Wolfrum J, Sauer M (2002) Detection of individual p53-autoantibodies by using quenched peptide-based molecular probes. Angew Chem Int Ed Engl 41(24):4769–4773
Ngundi MM, Kulagina NV, Anderson GP, Taitt CR (2006) Nonantibody-based recognition: alternative molecules for detection of pathogens. Expert Rev Proteomics 3(5):511–524
Nishiyabu R, Kubo Y, James TD, Fossey JS (2012) Boronic acid building blocks: tools for sensing and separation. Chem Commun 47(4):1106–1123
Niu WZ, Jiang N, Hu YH (2007) Detection of proteins based on amino acid sequences by multiple aptamers against tripeptides. Anal Biochem 362(1):126–135
Nutiu R, Li YF (2004) Structure-switching signaling aptamers: transducing molecular recognition into fluorescence signaling. Chemistry 10(8):1868–1876
Nutiu R, Li YF (2005a) Aptamers with fluorescence-signaling properties. Methods 37(1):16–25
Nutiu R, Li YF (2005b) In vitro selection of structure-switching signaling aptamers. Angew Chem Int Ed 44(7):1061–1065
O'Sullivan PJ, Burke M, Soini AE, Papkovsky DB (2002) Synthesis and evaluation of phosphorescent oligonucleotide probes for hybridisation assays. Nucleic Acids Res 30(21):e114
Ogoshi T, Harada A (2008) Chemical sensors based on cyclodextrin derivatives. Sensors 8(8):4961–4982
Oh KJ, Cash KJ, Hugenberg V, Plaxco KW (2007) Peptide beacons: a new design for polypeptide-based optical biosensors. Bioconjug Chem 18(3):607–609
Organero JA, Tormo L, Sanz M, Roshal A, Douhal A (2007) Complexation effect of gamma-cyclodextrin on a hydroxyflavone derivative: formation of excluded and included anions. J Photochem Photobiol A 188(1):74–82
Oshovsky GV, Reinhoudt DN, Verboom W (2007) Supramolecular chemistry in water. Angew Chem Int Ed 46(14):2366–2393
Ozaki H, Nishihira A, Wakabayashi M, Kuwahara M, Sawai H (2006) Biomolecular sensor based on fluorescence-labeled aptamer. Bioorg Med Chem Lett 16(16):4381–4384
Pagliari S, Corradini R, Galaverna G, Sforza S, Dossena A, Montalti M, Prodi L, Zaccheroni N, Marchelli R (2004) Enantioselective fluorescence sensing of amino acids by modified cyclodextrins: role of the cavity and sensing mechanism. Chemistry 10(11):2749–2758
Peczuh MW, Hamilton AD (2000) Peptide and protein recognition by designed molecules. Chem Rev 100(7):2479–2493
Pflum MKH (2004) Grafting miniature DNA binding proteins. Chem Biol 11(1):3–4
Pickup JC, Khan F, Zhi Z-L, Coulter J, Birch DJ (2013) Fluorescence intensity-and lifetime-based glucose sensing using glucose/galactose-binding protein. J Diabetes Sci Technol 7(1):62–71
Proske D, Blank M, Buhmann R, Resch A (2005) Aptamers – basic research, drug development, and clinical applications. Appl Microbiol Biotechnol 69(4):367–374
Pu K-Y, Shi J, Cai L, Li K, Liu B (2011) Affibody-attached hyperbranched conjugated polyelectrolyte for targeted fluorescence imaging of HER2-positive cancer cell. Biomacromolecules 12(8):2966–2974
Purrello R, Gurrieri S, Lauceri R (1999) Porphyrin assemblies as chemical sensors. Coord Chem Rev 192:683–706
Quiocho FA, Ledvina PS (1996) Atomic structure and specificity of bacterial periplasmic receptors for active transport and chemotaxis: variation of common themes. Mol Microbiol 20(1):17–25
Rathbone DL, Bains A (2005) Tools for fluorescent molecularly imprinted polymers. Biosens Bioelectron 20(7):1438–1442

Raymond FR, Ho HA, Peytavi R, Bissonnette L, Boissinot M, Picard FJ, Leclerc M, Bergeron MG (2005) Detection of target DNA using fluorescent cationic polymer and peptide nucleic acid probes on solid support. BMC Biotechnol 5:10

Renberg B, Shiroyama I, Engfeldt T, Nygren PA, Karlstrom AE (2005) Affibody protein capture microarrays: synthesis and evaluation of random and directed immobilization of affibody molecules. Anal Biochem 341(2):334–343

Renberg B, Nordin J, Merca A, Uhlen M, Feldwisch J, Nygren PA, Karlstrom AE (2007) Affibody molecules in protein capture microarrays: evaluation of multidomain ligands and different detection formats. J Proteome Res 6(1):171–179

Renard M, Belkadi L, Hugo N, England P, Altschuh D, Bedouelle H (2002) Knowledge-based design of reagentless fluorescent biosensors from recombinant antibodies. J Mol Biol 318:429–42

Richter A, Eggenstein E, Skerra A (2014) Anticalins: exploiting a non-Ig scaffold with hypervariable loops for the engineering of binding proteins. FEBS Lett 588(2):213–218

Rodi DJ, Agoston GE, Manon R, Lapcevich R, Green SJ, Makowski L (2001) Identification of small molecule binding sites within proteins using phage display technology. Comb Chem High Throughput Screen 4(7):553–572

Ronnmark J, Kampf C, Asplund A, Hoiden-Guthenberg I, Wester K, Ponten F, Uhlen M, Nygren PA (2003) Affibody-beta-galactosidase immunoconjugates produced as soluble fusion proteins in the Escherichia coli cytosol. J Immunol Methods 281(1–2):149–160

Roshal AD, Grigorovich AV, Doroshenko AO, Pivovarenko VG, Demchenko AP (1999) Flavonols as metal-ion chelators: complex formation with Mg2+ and Ba2+ cations in the excited state. J Photochem Photobiol A 127(1–3):89–100

Sadhu KK, Bag B, Bharadwaj PK (2007) A multi-receptor fluorescence signaling system exhibiting enhancement selectively in presence of Na(I) and Tl(I) ions. J Photochem Photobiol A 185(2–3):231–238

Schulz GE, Schirmer RH (1979) Principles of protein structure. Springer, New York

Sellergren B, Andersson LI (2000) Application of imprinted synthetic polymers in binding assay development. Methods 22(1):92–106

Shakeel S, Karim S, Ali A (2006) Peptide nucleic acid (PNA) – a review. J Chem Technol Biotechnol 81(6):892–899

Shimizu KD, Stephenson CJ (2010) Molecularly imprinted polymer sensor arrays. Curr Opin Chem Biol 14(6):743–750

Sillerud LO, Larson RS (2005) Design and structure of peptide and peptidomimetic antagonists of protein-protein interaction. Curr Protein Pept Sci 6(2):151–169

Singh Y, Dolphin GT, Razkin J, Dumy P (2006) Synthetic peptide templates for molecular recognition: recent advances and applications. Chembiochem 7(9):1298–1314

Skerra A (2007) Alternative non-antibody scaffolds for molecular recognition. Curr Opin Biotechnol 18(4):295–304

Sliwa W, Deska M (2011) Functionalization reactions of calixarenes. Arkivoc 1:496–551

Socher E, Jarikote DV, Knoll A, Roglin L, Burmeister J, Seitz O (2008) FIT probes: peptide nucleic acid probes with a fluorescent base surrogate enable real-time DNA quantification and single nucleotide polymorphism discovery. Anal Biochem 375(2): 318–330

Song S, Wang L, Li J, Fan C, Zhao J (2008) Aptamer-based biosensors. TrAC Trends Anal Chem 27(2):108–117

Srivatsan SG, Tor Y (2007) Fluorescent pyrimidine ribonucleotide: synthesis, enzymatic incorporation, and utilization. J Am Chem Soc 129(7):2044–2053

Stadtherr K, Wolf H, Lindner P (2005) An aptamer-based protein biochip. Anal Chem 77(11):3437–3443

Stephenson CJ, Shimizu KD (2007) Colorimetric and fluorometric molecularly imprinted polymer sensors and binding assays. Polym Int 56(4):482–488

Stojanovic MN, Kolpashchikov DM (2004) Modular aptameric sensors. J Am Chem Soc 126(30):9266–9270

Stojanovic MN, Landry DW (2002) Aptamer-based colorimetric probe for cocaine. J Am Chem Soc 124(33):9678–9679
Stojanovic MN, de Prada P, Landry DW (2001) Aptamer-based folding fluorescent sensor for cocaine. J Am Chem Soc 123(21):4928–4931
Szejtli J (1998) Introduction and general overview of cyclodextrin chemistry. Chem Rev 98(5):1743–1753
Thodima V, Pirooznia M, Deng YP (2006) RiboaptDB: a comprehensive database of ribozymes and aptamers. BMC Bioinf 7:S6
Timmerman P, Beld J, Puijk WC, Meloen RH (2005) Rapid and quantitative cyclization of multiple peptide loops onto synthetic scaffolds for structural mimicry of protein surfaces. Chembiochem 6(5):821–824
Tolosa L, Ge XD, Rao G (2003) Reagentless optical sensing of glutamine using a dual-emitting glutamine-binding protein. Anal Biochem 314(2):199–205
Tombelli S, Minunni A, Mascini A (2005) Analytical applications of aptamers. Biosens Bioelectron 20(12):2424–2434
Traviesa-Alvarez JM, Sanchez-Barragan I, Costa-Fernandez JM, Pereiro R, Sanz-Medel A (2007) Room temperature phosphorescence optosensing of benzo a pyrene in water using halogenated molecularly imprinted polymers. Analyst 132(3):218–223
Tsou LK, Jain RK, Hamilton AD (2004) Protein surface recognition by porphyrin-based receptors. J Porphyrins Phthalocyanines 8(1–3):141–147
Uchiyama F, Tanaka Y, Minari Y, Toku N (2005) Designing scaffolds of peptides for phage display libraries. J Biosci Bioeng 99(5):448–456
Ueda H, Dong J (2014) From fluorescence polarization to quenchbody: recent progress in fluorescent reagentless biosensors based on antibody and other binding proteins. Biochim Biophys Acta 1844(11):1951–1959
Valeur B (2002) Molecular fluorescence. Wiley VCH, Weinheim
Valeur B, Leray I (2007) Ion-responsive supramolecular fluorescent systems based on multichromophoric calixarenes: a review. Inorg Chim Acta 360(3):765–774
Vogt M, Skerra A (2004) Construction of an artificial receptor protein (“anticalin”) based on the human apolipoprotein D. Chembiochem 5(2):191–199
Wang R, Bardelang D, Waite M, Udachin KA, Leek DM, Yu K, Ratcliffe CI, Ripmeester JA (2009) Inclusion complexes of coumarin in cucurbiturils. Org Biomol Chem 7(11):2435–2439
Weiss GA, Lowman HB (2000) Anticalins versus antibodies: made-to-order binding proteins for small molecules. Chem Biol 7(8):R177–R184
Wenz G, Han BH, Muller A (2006) Cyclodextrin rotaxanes and polyrotaxanes. Chem Rev 106(3):782–817
Wiederstein M, Sippl MJ (2005) Protein sequence randomization: efficient estimation of protein stability using knowledge-based potentials. J Mol Biol 345(5):1199–1212
Wosnick JH, Swager TM (2004) Enhanced fluorescence quenching in receptor-containing conjugated polymers: a calix 4 arene-containing poly(phenylene ethynylene). Chem Commun 23:2744–2745
Wu X, Li Z, Chen X-X, Fossey JS, James TD, Jiang Y-B (2013) Selective sensing of saccharides using simple boronic acids and their aggregates. Chem Soc Rev 42(20):8032–8048
Yang RH, Chan WH, Lee AWM, Xia PF, Zhang HK, Li KA (2003a) A ratiometric fluorescent sensor for Ag-1 with high selectivity and sensitivity. J Am Chem Soc 125(10):2884–2885
Yang RH, Li KA, Wang KM, Zhao FL, Li N, Liu F (2003b) Porphyrin assembly on beta-cyclodextrin for selective sensing and detection of a zinc ion based on the dual emission fluorescence ratio. Anal Chem 75(3):612–621
Yang W, Fan H, Gao X, Gao S, Karnati VVR, Ni W, Hooks WB, Carson J, Weston B, Wang B (2004) The first fluorescent diboronic acid sensor specific for hepatocellular carcinoma cells expressing sialyl Lewis X. Chem Biol 11(4):439–448
Yesylevskyy SO, Klymchenko AS, Demchenko AP (2005) Semi-empirical study of two-color fluorescent dyes based on 3-hydroxychromone. J Mol Struct THEOCHEM 755(1–3): 229–239

Yesylevskyy SO, Kharkyanen VN, Demchenko AP (2006) The change of protein intradomain mobility on ligand binding: is it a commonly observed phenomenon? Biophys J 91(8): 3002–3013

Yoshimatsu K, Reimhult K, Krozer A, Mosbach K, Sode K, Ye L (2007) Uniform molecularly imprinted microspheres and nanoparticles prepared by precipitation polymerization: the control of particle size suitable for different analytical applications. Anal Chim Acta 584(1):112–121

Zahnd C, Amstutz P, Pluckthun A (2007) Ribosome display: selecting and evolving proteins in vitro that specifically bind to a target. Nat Methods 4(3):269–279

Zeytun A, Jeromin A, Scalettar BA, Waldo GS, Bradbury AR (2003) Retraction: fluorobodies combine GFP fluorescence with the binding characteristics of antibodies. Nat Biotechnol 21(12):1473–1479

Zhang M, Yan X, Huang F, Niu Z, Gibson HW (2014) Stimuli-responsive host–guest systems based on the recognition of cryptands by organic guests. Acc Chem Res 47(14):1995–2005

Zhao Q, Cheng L (2013) Detection of thrombin using an excimer aptamer switch labeled with dual pyrene molecules. Anal Bioanal Chem 405(25):8233–8239

Zheng GX, Shao Y, Xu B (2006) Synthesis and characterization of polyaniline coated gold nanoparticle and its primary application. Acta Chim Sin 64(8):733–737

Zhou H, Baldini L, Hong J, Wilson AJ, Hamilton AD (2006) Pattern recognition of proteins based on an array of functionalized porphyrins. J Am Chem Soc 128(7):2421–2425

Chapter 8
Mechanisms of Signal Transduction

In previous chapters we discussed two essential functional components of every fluorescence sensor – the binding-recognition units (*binders* or *receptors*) and the units providing the response signal (*reporters*). Here we focus on the coupling between these functionalities. Such coupling must involve signal transduction resulting in changes on target binding of the reporter emission. The coupling mechanisms can be based on the excited-state reactions, such as electron transfer (intramolecular or intermolecular), intramolecular charge transfer, proton transfer or excited-state energy transfer. Conformational changes in receptor unit coupled with target binding may generate the reporter signal if they influence these reactions. In the case of several binding sites coupled with response functionality, nonlinear response functions can be obtained and simple logical operations realized.

The coupling between binding and reporting functionalities provides transduction of signal on the event of target binding into detectable output signal. It is essential that the process of molecular recognition occurs between the groups of atoms of interacting molecules, particles or interfaces in the *ground electronic states*. In contrast, fluorescence reporting requires *excited states*. The latter often exhibit profound changes in electronic structures and their energies. Thus, the coupling mechanisms should exist that connect the two types of events, one molecular and ground-state, and the other – electronic and excited-state. We call the realization of this coupling the *transduction* and the molecular or supramolecular structure responsible for that – the *transducer*.

8.1 General Principles of Signal Transduction

According to a more general definition of a *transducer*, it is a device that is activated by a signal from one system and provides this signal (often in another form) to a different system. Therefore, collecting and recording of fluorescent emission and transforming it into electrical signal by the measurement system is also a signal transduction (Fig. 8.1).

A.P. Demchenko, *Introduction to Fluorescence Sensing*,
DOI 10.1007/978-3-319-20780-3_8

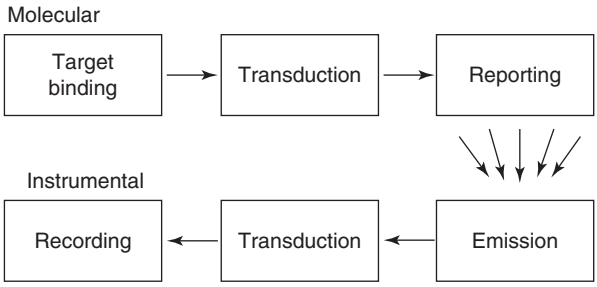

Fig. 8.1 Two levels of signal transduction in fluorescence sensing (molecular and instrumental)

Here we will concentrate on the mechanisms of transduction within the sensor unit on molecular and supramolecular scales, whereas the signal transduction on the instrumental level, which is different in its essence, will be discussed in Chap. 11. We limit our discussion to the mechanisms of *direct sensing*, in which the target-binding and fluorescence signal-generating events are coupling directly, without additional manipulation or reagent addition (Sect. 1.6). In this case, the informative signal is coupled directly with electronic or nuclear motion in the sensor occurring on target binding.

8.1.1 Target Binding and the Release of Information-Containing Signal

In many cases the transduction on molecular level results in perturbation of electronic structures of fluorescence reporters leading to the changes of parameters of their emission (as described in Chap. 3). The mechanisms of such coupling with primary events of target binding are variable and include intra- and intermolecular processes of *transfer of electronic charge*. All that gives the researchers a variety of possibilities for optimizing all three functions of fluorescence sensor: recognition, transduction and reporting.

An additional possibility for signal transduction is the coupling of *conformational variables* and the nanoscale association phenomena with individual and collective response of fluorescence emitters. The latter may involve activation of the energy transfer in different formats. This approach is frequently used and therefore deserves a detailed analysis. Finally we will show that the relay mechanisms of signal transduction allow not only providing a simple connection of binding and reporting events, but also performing more complicated logical operations. Such systems may become the elements of future molecular computers.

The ground-state and excited-state transformations are commonly governed by different types of molecular forces, which sometimes allows obtaining multiparametric response from a single dye. Introduction of two fluorophores (similar and differing in optical parameters) and generation of fluorescent nanocomposites expand dramatically the range of applications. Different means to generate the informative response in excitation and emission spectra using all these individual and composed reporters are extensively discussed elsewhere (Demchenko 2010). Here we briefly summarize some of these possibilities.

8.1.2 Signal Transduction with the Use of Single Emitters

A variety of organic dyes can respond to the changes in their weak interactions with surrounding molecules or groups of atoms. The *ground-state interactions* generate the differences in both the absorption and excitation spectra. In the ground state, the species displaying multiple light-absorbing states are usually in equilibrium, which allows the spectroscopic response to follow the structural transformations in the studied system and generate the reporting signal. The two forms of the dye belonging to two states of the system and differing only by their intermolecular interactions can be considered as distinct species with their own characteristic excitation and emission spectra (see Fig. 3.21). Different situation is observed when the ground-state interactions are the same but the spectral change on target binding appears as a result of the *excited-state reaction*. In this case, the new bands belonging to reactant and reaction product forms appear in fluorescence emission spectra only. Other parameters (anisotropy, lifetime) may change also, providing informative signal.

8.1.2.1 The Fluorophores in Protic Equilibrium

The ionization of attached groups (usually aromatic hydroxyls) may change dramatically the spectroscopic properties of organic dyes leading to the appearance of new bands in absorption and emission spectra. The variation of their excitation spectra reflects the ground-state *proton dissociation*. Since the acidity of dissociating hydroxy groups is commonly much higher in the excited than in the ground state, the pH range of sensitivity of this group attached to aromatic moiety can be dramatically shifted to lower pH in emission spectra (Laws and Brand 1979; Davenport et al. 1986). This allows providing the wavelength-ratiometric recording in an extended pH range. Presently the most extensively used dyes are the benzo[c]xanthene derivatives, such as C-SNAFL-1 (Whitaker et al. 1991; Mordon et al. 1995). The strongly red-shifted second band in emission spectra due to deprotonation of hydroxy group in the excited state can respond to local shift in association-dissociation equilibrium at the site of target binding and can be efficiently used in sensing technologies.

One of examples of such developments is the molecular sensor for *anions* based on switching in protonation-deprotonation equilibrium in a designed coumarin dye mediated by anion binding (Choi and Hamilton 2001).

8.1.2.2 Switching Between Fluorescent and Phosphorescent Emissions

Phosphorescence is usually observed with strong Stokes shifts, long emission lifetimes (up to milliseconds and seconds) and strong temperature-dependent quenching. In the λ-ratiometric sensing technologies only those dyes can be used that display strong room-temperature phosphorescence with the steady-state intensity comparable to that of fluorescence. They include platinum and palladium ions incorporated into porphyrins (Papkovsky and O'Riordan 2005) and chelating complexes of ruthenium

(Castellano et al. 1998; O'Neal et al. 2004) that can be included into solid polymer matrices. Since phosphorescence band is strongly shifted to longer wavelengths, a very precise, convenient and self-calibrating detection can be achieved in a steady-state λ-ratiometric recording (Hochreiner et al. 2005). However, the dyes exhibiting fluorescence and phosphorescence (or long-lived luminescence) demonstrate different temperature-dependent quenching for the two types of these emissions.

8.1.2.3 Hydrogen Bonding in the Ground and Excited States

The presence of *H-bond* donor and acceptor groups coupled to aromatic structures possessing π-electrons offers new possibilities for λ-ratiometric sensing based on the formation/breaking of intermolecular H-bonds. These bonds may influence the *intramolecular charge-transfer* (ICT) character of the excited states with the correspondent spectral shifts. Such effects are usually smaller than that on protonation and occur in the same direction (Wang et al. 2002). In excitation spectra on interaction with H-bond donor at the acceptor site one can observe the shifts of spectra to longer wavelengths and on interaction with proton acceptor at the donor site – to shorter wavelengths. Carbonyl groups attached to π-electronic systems are known for generating the strongest H-bonding sensors that are sensitive to solvent environment (Shynkar et al. 2004). The electron lone pairs on oxygen atoms allow arrangement of two such bonds, the stronger and weaker ones. Their formation is clearly observed as a strong two-step deformation of fluorescence spectra (Pivovarenko et al. 2000) (see Fig. 4.9).

8.1.2.4 Ground-State Charge Transfer

Strong electrostatic interaction in the ground state may shift the electronic density within the dye molecule resulting in the shifts of excitation and emission spectra. This approach was used for the first time by the group of Roger Tsien in the development of their famous Ca^{2+} binding probes Fura 2 and Indo 1 (Grynkiewicz et al. 1985). They operate according to this principle – the induction of transfer of electronic charge by the bound ions. In these stilbene-like dyes the bound Ca^{2+} ions interact with the electron-donor nitrogen atom incorporated into fluorophore generating the new excitation band shifted to shorter wavelengths.

8.1.2.5 Excited-State Intramolecular Charge Transfer (ICT)

This mechanism is very frequently used for generating the response in different types of sensors. It deserves special analysis, which will be made in the next Section. Here we stress that it can generate two well distinguished emissive forms belonging to reactant and reaction product. It can be realized only at a small distance within the π-electron conjugated dye molecule. The optimal structures of ICT dyes are known. They should contain an electron donating group (often a dialkylamino group) and an electron-withdrawing group (often, carbonyl) located at opposite sides.

8.1.2.6 Electrochromism

When the dye interacts with closely located charged group or with array of these groups (such as in biological membranes) this interaction changes the energies of electronic transitions and results in spectral shifts. This phenomenon is caused by the direct interaction of the ground- and excited-state dipoles with the applied electric field and is known as *electrochromism* (also called as *Stark effect*) (Bublitz and Boxer 1997). It allows designing the so-called molecular voltage sensors (Demchenko and Yesylevskyy 2009). Their maximal response should be observed when the dye exhibits substantial change of its dipole moment $\vec{\mu}$ on electronic excitation, which implies a substantial redistribution of the electronic charge density. This effect also depends on the polarity of the probe environment (dielectric screening reduces this effect) and on its orientation with respect to this field. Specially designed dyes can be applied for recording the electrostatic potential in biomembranes (Demchenko et al. 2009). This effect produces spectral shifts that are commonly observed in excitation spectra with recording of variations of fluorescence intensities at its two slopes. The more convenient for detection are the shifts in fluorescence spectra, but for these dyes such shifts are much smaller (Minta et al. 1989). Below we will see that the ESIPT reaction can dramatically amplify the electrochromic effect.

8.1.2.7 Excited-State Intramolecular Proton Transfer (ESIPT) and Its Electrochromic Modulation

An extended overview of this mechanism that is increasingly popular in applications will be presented in the next Section. The dyes exhibiting ESIPT are very attractive as mediators of sensor signal and its transformation into generated new band in fluorescence spectrum. Here the two spectrally resolvable excited states are connected by the excited-state reaction that can produce emissive species with dramatic (often by 100 nm and more) long-wavelength shifts of fluorescence spectra. Switching between these emissions is a very sensitive indicator of the change in *polarity*. The *electrochromic* effect can be also coupled with the ESIPT reaction, which allows displaying it as the ratio of intensities of two bands in emission spectra (Klymchenko and Demchenko 2002).

Summarizing, we indicate both the strong and weak points in using molecular sensors based on fluorescence response of single fluorophores. Strong points are: (a) single labeling that is much easier to perform and to control the yield and specificity of labeling in chemical and biological systems; (b) easily detectable λ-ratiometric signal that can be realized in all instrumental formats (fluorimeters, microscopes, plate readers, etc.) and (c) internal calibration realized on molecular scale that allows the output signal to be independent of variation of instrumental factors, fluorophore concentration, etc.

The weak points are also essential. There are very limited number of fluorophores that allow realizing this type of response, which limits the range of available

wavelengths and lifetimes. Presently the best in two-band ratiometric response are the 3-hydroxychromone dyes exhibiting ESIPT reaction (Klymchenko and Demchenko 2002; Demchenko 2006, 2009, 2010), but the species of this family with excitation wavelengths occupying the range of 380–430 nm are used only. Extension of their emission to red-NIR region are presently not available. The proteins of green fluorescent protein (GFP) family (Subach and Verkhusha 2012) and responsive polymers (Cho et al. 2013) are expected to enrich the range of single-fluorophore ratiometric reporters.

8.1.3 Signal Transduction with the Use of Coupled Emitters

In application of two coupled emitters the researcher can choose one of the two basic strategies. First is the introduction of the second fluorophore as the *reference* (as it was discussed in Sect. 3.2). The reference should not interact with the reporting fluorophore and there can be a broad choice of its location in one of the interacting partners at the periphery of their contact area. The other strategy consists in using actively the interaction between the two fluorophores. In that case the restrictions should be imposed for optimizing the response to this interaction.

8.1.3.1 Reporting with the Reference

The role of reference is solely to indicate its own presence in particular medium or at particular site and provide robust signal that must be distinguished from that of reporting fluorophore (within the range of variation of the latter).

Therefore, the dye should possess strongly different emission spectrum but of comparable intensity to that of reporter band. For optimal operation of such system, the direct interactions between the reference and reporter dyes (e.g. leading to PET or FRET) in this approach should be avoided. The requirement on rigid attachment of reference fluorophore to a sensor unit may not be necessary, and its presence in detectable concentrations in illuminated volume is sufficient. An example of the absence of such connection can be the pair of fluorescence probes for detecting of Ca^{2+} ions in cellular studies. Two dyes, of similar structure, one responsive to ion binding, and the other inert, can be incorporated into the cell for λ-ratiometric imaging of ions (Cooley et al. 2013). The problem is only in potentially different distribution of such dyes in heterogeneous systems that are the cells, which may lead to incorrect data.

8.1.3.2 Interaction Between Two Similar Emitters: The Excimers

In this case, two (monomer and excimer) emissions can interconvert, so that one band decreases and the other increases, and this signal should report on target binding (see Sect. 3.5). Excimer emission spectrum is easy to observe because it is very

different from that of the monomer. The interplay of intensities at two selected wavelengths, λ_1 and λ_2, with their change in converse manner and can be easily detected (see Fig. 3.12). However, the double labeling is needed, which is facilitated by the fact that the two partners are of the same structure and their choice is limited to anthracene and pyrene derivatives. Transduction mechanism is also not easy to achieve. The excimer formation requires close location and proper orientation between the partners, specifically, the sandwich-type association between two heterocycles rich in π-electrons. Therefore, molecular recognition between interacting partners (e.g. macromolecules) should be coupled either with molecular assembly (each of these partners containing the monomer), or with the conformational change in one of them bringing together or forcing apart these aromatic groups (Yang et al. 2003).

8.1.3.3 The FRET-Based Mechanism of Signal Transduction

Resonance energy transfer to fluorescent acceptor is a different possibility to benefit from λ-ratiometric recording in response to spectral overlap and distance variations coupled to recognition event (see Sect. 3.6). For the observation of FRET the direct contact between donor and acceptor is not needed, they can interact through space and can be located at separation distances within 1–10 nm from each other. The fact that the fluorescence response depends strongly on the properties of both donor and acceptor and on their distance and orientation allows many possibilities for its modulation and adaptation to the desired conditions. Two labels can be located in one of interacting partner indicating its conformational change, in both partners indicating their close contact and in one of the partners and the competitor. A variety of donor-acceptor pairs for FRET applications have been developed (Fan et al. 2013).

Concluding, we stress that there is a broad choice of interacting and non-interacting partners and they can be chosen depending on researcher's task. They can be independent emitters and one of them can serve as a reference for the other. They can interact strongly in the excited state, forming excimers. For a much broader range of interacting partners the reporter signal can be mediated at a distance on a scale of molecular dimensions via FRET.

8.1.4 Collective Emitters in Signal Transduction

These issues were well elaborated in Chap. 6, and here we repeatedly stress several important points.

(a) When assembled into a single nanoscale composite, individual emitters can be either non-interacting with the absence of changes of their light-emitting properties or interacting with the exchange or directional flow of excited-state energy between them.

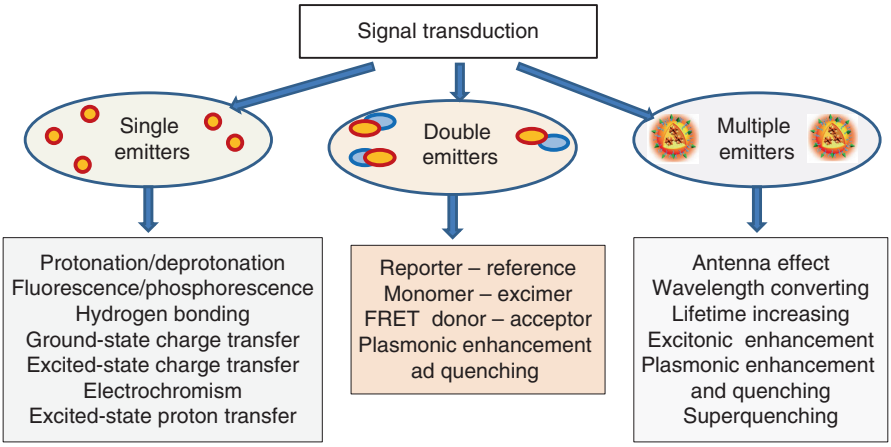

Fig. 8.2 Schematic presentation of diversity in signal transduction mechanisms that can be realized operating with single, double and multiple emitters

(b) The mechanism of interaction can be both of dipole-resonance nature (Forster-type) operating at a distance or of excitonic nature. In both cases the collective effects of switching on and off of emission can be coupled with sensor response.
(c) Designing fluorescence nanocomposites, one can easily manipulate with emission wavelength (and also anisotropy and lifetime) realizing innumerable possibilities for sensing and imaging.

We finish this section with a scheme that is definitely incomplete but allows navigating in the space of innumerous possibilities in sensor signal transduction and reporting (Fig. 8.2). Regarding the details, the readers can also refer to Chaps. 4, 5 and 6.

8.2 Basic Signal Transduction Mechanisms: Electron, Charge and Proton Transfer

Fluorescent, or in general, luminescent states of molecules or nanoparticles are the *electronic excited states*. Electrons in these states are very reactive, and this allows proceeding the reactions that commonly do not happen in the ground states. The most fundamental of these reactions are the electron, charge and proton transfers. These reactions are reversible in a sense that in a cycle [ground-state excitation → excited-state reaction → relaxation to reaction product ground state → transition to initial ground state] the same initial ground state species are restored. The interest to these reactions from the side of sensing technologies is due to the fact, that they allow one-step deactivation of excited state (quenching) and, in some cases, the spectral shifts and, notably, the generation of new emission bands belonging to the products of these reactions. These reactions can be modulated by target

binding to a sensor because of their dependence on non-covalent interactions at the reaction sites with the groups of atoms, molecules and surfaces that behave not only as enhancers or quenchers of their emission but also as switchers of these reactions. This allows realizing many different mechanisms of signal transduction.

Essentially, such transduction should provide the coupling between two types of events: one occurring in the *ground states* (target binding) and the other in the *excited states* (changes in parameters of the emission). The former can be described in molecular terms, and the later, if it involves perturbation of electronic sub-system, needs quantum-mechanical description. Three general trends in signal transduction are broadly used to date:

(1). Direct contact of target with functional fluorophore derivative that influences the energies of electronic states and results in electron-transfer quenching or in the transformations of spectra based on intramolecular charge transfer (ICT). The best realization of this trend is achieved with sensing ions because of their strong charge-perturbation effect (Valeur and Leray 2007).
(2). Induction of conformational changes in the sensor unit that can be realized in modulation of ICT, ESIPT or FRET with correspondent change in emission.
(3). Using intermolecular interaction between fluorescent emitters or emitter and quencher, so that both are involved in the sensing process.

8.2.1 Photoinduced Electron Transfer (PET)

Electronic excitation is the gain of energy by electronic structure, which allows its participation in different reactions. Because of that, the excited species can be considered as redox sites that can donate or capture electrons from other sites, being either oxidants or reductants. *Photoinduced electron transfer* (PET) is the process by which electron moves from one excited site to another site. Important requirements for this reaction are the closeness in space of two sites and matching their oxidation-reduction potentials. The distances for this reaction are much shorter than for FRET, since it needs the crossing of electronic wave functions of initially excited and product states. PET can be facilitated by covalent bonding between donor and acceptor via a short linkage (spacer).

In PET systems only one of the states (reactant or product) is commonly light-emissive, and usually it is the reactant state, which is initially excited. Consequently, the reaction *leads to quenching* of fluorescence emission. The electron exchange is not a 'profit-free' exchange between electronic systems. It is reversible, but when it starts from singlet (fluorescent) excited state the return is back to the ground state.

This reaction can occur between the excited dye and a redox active molecule or group of atoms within the same molecular structure or between two structures. If the electron donor has a high HOMO (*highest occupied molecular orbital*) level, its transfer is efficient to acceptor with LUMO (*lowest unoccupied molecular orbital*) level (Fig. 8.3). The solvent can also participate in this process influencing the energies of correspondent states (see Sect. 3.7).

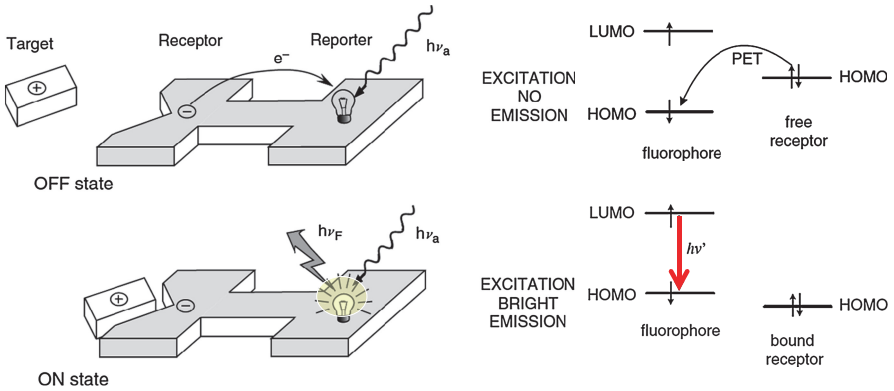

Fig. 8.3 Signal transduction in the simplest PET-based sensor. In a free sensor molecule the fluorescence is quenched due to efficient electron transfer from donor to acceptor fragments separated by a spacer. Cation binding produces strong electrostatic attraction of electron from the donor fragment preventing the electron transfer. Fluorescence is enhanced

Known *redox potentials* of interacting partners can be used to choose them, so that the PET receptor will transfer an electron to/from the excited LUMO/fluorophore preventing emission. The transduction effect on binding the target species can be in the form of a change of redox potential of the receptor that suppresses PET reaction giving rise to emission of the donor. In signal transduction systems based on PET, the relay is in fact a spacer that separates the electronic systems of donor and acceptor.

Both donor and acceptor can be the fluorescent dyes that may serve as reporters; in these cases also the excited-state energy will be lost as a result of PET. On excitation, the electronic potential of any dye changes dramatically and it may become better electron donor or acceptor than its closely located PET partner. This could lead to PET occurring usually much faster than the emission and that is why the fluorescence can be totally quenched.

This process can be exploited in sensor designs of different complexity (de Silva et al. 2001; Valeur and Leray 2000). Consider the simple case, in which the fluorescent reporter segment is an electron acceptor and the donor is the group of atoms, which is a part of the binding site. Let the target be a metal cation bearing positive charge (see Fig. 8.3). When the target binding site is not occupied, the absorption of light quantum by the reporter makes it a strong electron acceptor. The electron jumps to it from the receptor site resulting in quenching. This state can be called the OFF state. When the ion is bound, the situation becomes different. The ion attracts the oppositely charged electron from the receptor, and PET to excited reporter becomes energetically unfavorable. In the absence of PET the reporter dye remains a bright emitter. This is the ON state. The relative fluorescence intensity can be calibrated as a function of ion concentration.

Such simple realization of PET has found application mostly in the *sensing of ions* (Sect. 12.3). In a typical ion sensor, two electronic systems, one participating in ion recognition and the other used for reporting, are connected by a short spacer

(Valeur and Leray 2000). Cation binding produces the strong attraction of electron with the suppression of PET.

Sensing of *neutral molecules* in this way has also been made, though with limited success (Granda-Valdes et al. 2000). The schemes that are more complicated allow excluding the target analyte binding from direct influence on PET. For instance, this can be done by influencing the ionization of an attached group (Koner et al. 2007; Tomasulo et al. 2006) and thus extending this transduction mechanism to a much broader range of analytes.

PET can occur not only through bonds but also *through space*, and for this process the most important is the close distance between donor and acceptor. Therefore, in sensing event the donor and acceptor groups can be put together or moved apart due to a conformational change in the sensor (Sect. 8.5).

One more possibility offered by PET mechanism is the *association or dissociation* of nanoparticles: on association they can play a role of PET donor or acceptor. *Noble metal* nanoparticles have proved to be the most efficient electron acceptors from different types of fluorescent donors, including semiconductor quantum dots. The latter can be reduced or oxidized at relatively moderate potentials, which tend to vary slightly with the physical dimensions of these nanocrystals (Burda et al. 2005). Therefore, they can be used as efficient electron donors, and this possibility of signal transduction makes them efficient fluorescence reporters. Transition metal cations (such as Cu^{+2}) and free radicals quench fluorescence according to PET mechanism. This property can be used for their detection.

The PET quenching in *conjugated polymers* deserves special attention. Extremely low amounts of cationic electron acceptors quench the fluorescence of polyanionic conjugated polymer on a time scale shorter than picosecond, so that a greater than million-fold sensitivity to the quenching is achieved in comparison with the so-called 'molecular excited states' (Chen et al. 1999). Novel materials such as quantum dots suggest new strategies for optimal exploration of PET phenomenon in sensing. Below we will discuss in more detail three important cases of PET that are frequently used in sensing.

(a) *Electron transfer between molecular fragments of the same dye molecule*. If a single dye molecule contains two localized electronic systems, the one-electron oxidation-reduction in the excited state results in quenching. A proper construction of sensor units allows achieving a complete "ON-OFF" sensor behavior (de Silva et al. 2001). The PET process can be modulated by the target binding at the electron donor or acceptor sites by changing the donor or acceptor strength. Therefore, it is well understood why this mechanism can be applied most efficiently to ion sensing if the ion binds by the ion-chelating group coupled with a π–electronic system. Its application in biomolecular sensing is more difficult since this needs a rather strong electrostatic perturbation of electronic properties.

(b) *Intermolecular electron transfer*. At short distances an electron can be captured by an excited-state fluorophore acting as electron acceptor from a closely located ground-state electron donor, which also results in quenching. The application of fluorescence response based on this principle to DNA beacon

technology (Knemeyer et al. 2000) allowed achieving direct homogeneous assay without double labeling of molecular beacons. The role of fluorescence quencher is played by properly located guanosine residue (Heinlein et al. 2003).

In sensor proteins, the conformational changes that form or disrupt the PET donor-acceptor pair may produce a dramatic change in fluorescence response. In this case, the attached organic dye can serve as a PET acceptor, and intrinsic aromatic amino acids, Trp and Tyr, can be used as the ground-state electron donors (Marme et al. 2003). Based on this principle, the antibody fragments were suggested as versatile molecular sensors (Abe et al. 2011; Jeong and Ueda 2014). Due to PET from Trp residue to attached organic dye their fluorescence is quenched. Its enhancement is observed on antigen binding due to disruption of Trp-dye contact.

It is essential to emphasize that in contrast to FRET, in PET quenching the donor and the acceptor should be located at much closer mutual distance, usually forming a direct contact (Heinlein et al. 2003; Jeong and Ueda 2014). PET quenching may also occur on the formation of dye dimers and aggregates and be the origin of "*concentrational quenching*" effects (Sect. 6.1). In this case it occurs between the unexcited and excited monomers, and this effect can also be used in sensing (Johansson and Cook 2003).

(c) *Quenching by spin labels*. Stable nitroxide radicals are known as strong fluorescence quenchers. Their basic mechanism of quenching is also electron transfer, and its realization also requires a close proximity of quencher to fluorescent dye. But in this case, the fluorophore always serves as electron donor and nitroxide as an acceptor. Such quenching effect is known for a long time (Blough and Simpson 1988), and the covalent spin-labeling of proteins and polynucleotides have been described. Whereas the spin-labeled lipids are frequently used for determining the location of proteins and other fluorescent compounds in the membranes (Chattopadhyay and London 1987), the applications of nitroxide radicals in sensing technologies are still very rare. Meanwhile, regarding the double-labeling methods, they offer some advantages, mainly because of much smaller size of nitroxide group than that of common fluorescent dyes and due to the total "ON-OFF" effect of quenching. In addition to sensing based on proximity, they offer an interesting possibility of sensing based on variation of redox potential of their surrounding (Blough and Simpson 1988), since the reduction of nitroxide removes its ability of quenching. Based on this property the method for determination of ascorbic acid has been suggested (Lozinsky et al. 1999). Double (spin and fluorescence) sensing molecules afford various utilization possibilities (Bognar et al. 2006).

8.2.2 Intramolecular Charge Transfer (ICT)

Intramolecular charge transfer (ICT) is, in principle, also an electron transfer. The difference is that ICT occurs within the same electronic system or between the systems with high level of *electronic conjugation* between the partners, and it has its

own characteristic features. The electronic states achieved in this reaction are not the 'charge-separated' but '*charge-polarized*' states. Still they are the localized states with distinct energy minima.

The two, PET and ICT, states are easily distinguished by their absorption and emission spectra. In PET, the strong quenching occurs without spectral shifts. In contrast, the ICT states are often fluorescent but exhibit the changes of intensities. In addition, their excitation and emission spectra may exhibit significant shifts that depend on the environment. This allows providing the wavelength-ratiometric recording (see Sect. 3.7). In some cases a switching of intensity between *two emission bands*, normal (often called the *locally excited*, LE) and achieved in ICT reaction, can occur. This is even more attractive for ratiometric measurement.

Commonly the ICT states are observed when the organic dye contains an *electron donating group* (often a dialkylamino group) and an *electron-withdrawing group* (often, carbonyl). If these groups are located at opposite sides of molecule, an electronic polarization is induced. Because electron donor becomes in the excited state a stronger donor and an acceptor a stronger acceptor, an electronic polarization can be substantially increased in the excited-state. A created large dipole moment interacts with medium dipoles resulting in strong Stokes shifts.

The change in the medium conditions can produce the *LE-ICT switching*. Fluorescence from the normal LE state is commonly observed in low-polar solvents and in cryogenic conditions, where the spectra may contain residuals of vibrational structure. At an increase of polarity and temperature the ICT fluorescence appears, which has a broad and structureless long-wavelength shifted fluorescence band. In polar solvents, these shifts become larger because the solute-solvent dipole interactions are stronger. That is why the so-called '*polarity probes*' (Sect. 4.3) are in fact the ICT dyes. In addition, the ICT states are very sensitive to electric field effects and, therefore, to the presence of nearby charges.

From this discussion, it is clear that the realization of ICT offers many possibilities. However, the application of this effect cannot be as broad as that of PET, and only organic dyes (and not all of them) can generate an efficient ICT emission (see Sect. 4.3). Nevertheless, within this family of dyes one may find many possibilities for producing fluorescence reporter signal in sensing. They are:

(1) *Switching between LE and ICT emissions by direct influence of target charge* (Fig. 8.4). This switching can be produced by binding an ion to either electron donor or acceptor site. The processes occurring on interaction of ion-chelation group (as receptor) with a cation are well described (Valeur 2002). When an electron-donor group is attached to receptor, the cation reduces the electron-donating character of this group. Owing to the resulting reduction of electronic conjugation, a blue shift occurs in the absorption spectra together with decrease of the molar extinction. Conversely, a cation interacting with the acceptor group enhances the electron-withdrawing character of this group; the absorption spectrum is thus red-shifted and the molar extinction is increased. The fluorescence spectra are in principle shifted in the same direction as those of absorption spectra.

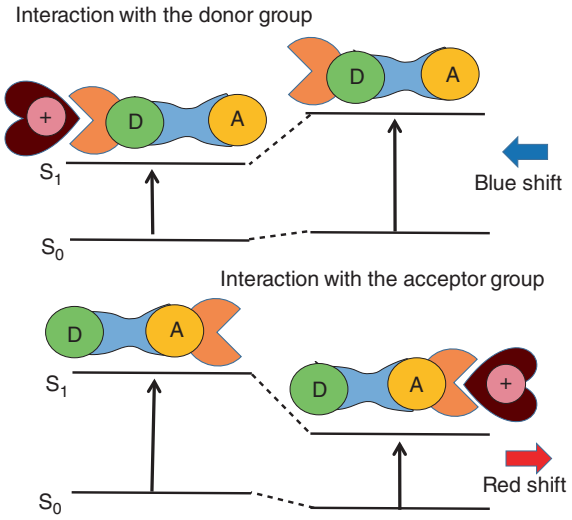

Fig. 8.4 Spectral shifts of ICT sensors resulting from interaction of a bound cation (+) with an electron-donating (*D*) or electron-withdrawing (*A*) group (Valeur and Leray 2000)

An anion produces the opposite effect. As a more recent example, the dye exhibiting ICT reaction was suggested as a sensor to fluoride (Yuan et al. 2007). Fluoride binds to electron-acceptor group and switches its emission from that at 500 nm to that at 380 nm.

The excited-state charge transfer makes the electron-donor site strongly positively charged. If a cation binds at this site, it exhibits a strong electrostatic repulsion, up to its dissociation. If this electron ejection happens on a time scale faster than the emission, no binding will be detected in fluorescence spectra. Therefore, more efficient will be to locate the cation binding site close to electron acceptor group, where the binding in the excited state becomes stronger. Following the same logics, the sites for anion recognition should be located at the electron-donor sites. A variety of chelator groups have been suggested as the recognition units for ions, such as crown ethers, cryptands, coronands and calix[4]arenes (Choi et al. 1999; de Silva et al. 1997; Valeur and Leray 2000). The electron donor or acceptor groups can be incorporated into these structures.

(2) *Coupling of ICT emission with dynamic variables*. The ICT states can be stabilized and modulated by the dynamics of surrounding molecules and groups of atoms. The ICT state possesses strongly increased dipole moment and, in the absence of strong interactions with surrounding dipoles, its energy may lie higher than that of the LE state. Thus, the LE emission at shorter wavelengths will be observed in low-polar or highly viscous environments, where the strong dipole interactions are absent or cannot form by dipole rotations at the time of emission (Fig. 3.18). In contrast, in highly polar environments the surrounding dipoles tend to re-organize to their equilibrium configuration, stabilizing the ICT state. This allows the ICT emission to be energetically favorable and therefore intensive. Because of stronger interaction, a decrease of excited-state

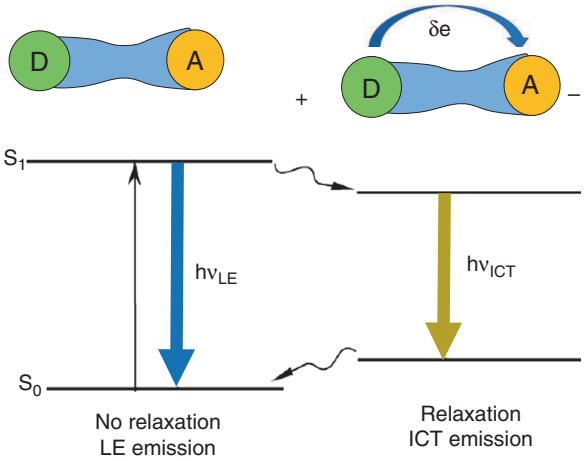

Fig. 8.5 The simplified energy diagram showing the influence of molecular relaxations (with lifetime τ_R) on the energies of LE and ICT states. The ICT states involve motion of partial charge (δe) within short distances generating strong dipoles that can be stabilized in polar media in the course of relaxation (mainly by orientation of surrounding dipoles) resulting in substantial shifts of fluorescence spectra to lower energies (longer wavelengths)

energy occurs, and the emission is shifted to longer wavelengths. Thus, an efficient transduction with the detectable change of reporter spectrum can be provided by the change in dynamics of molecules and groups of atoms at its location (Fig. 8.5).

(3) *Increased environment sensitivity of ICT emission.* Position of ICT energy level strongly depends on the strength of dipole-dipole interactions that is the major effect determining the effect of *solvent polarity*. Exploration of this property allows extending sensing possibilities to detecting nonionic targets. If the target is a neutral compound, its binding can influence the local polarity in the vicinity of reporter dye. This can be easily done if the testing has to be made in water. Since water is frequently used as a medium for sensing different analytes, it is worth to mention that it is not only a highly polar liquid but also the medium with very rapid (~1 ps) dielectric relaxations. In sensing in water, different coupled processes can be used, such as providing conformational change changing the environment of reporter dye or screening the dye from direct contact with water.

(4) Q*uenching of intramolecular charge transfer (ICT) states*. The intramolecular charge transfer excited states are characteristic for fluorophores that possess strong electron-donating and electron-accepting groups, and strong quenching of their ICT emission can often be observed in polar media and especially in water (Yatsuhashi et al. 1998; Bhattacharyya and Chowdhury 1993). Different factors, such as transition of the dye to low-polar environment can induce fluorescence enhancement in these systems.

(5) *Modulation of electronic conjugation within the dye exhibiting ICT emission*. This can be done by changing the planarity between electron-donor and acceptor

fragments, since the planar structure produces the best π-π electronic coupling. Such disruption of planarity with the appearance of ICT emission is well studied in many systems, and correspondent states got the special name *twisted intramolecular charge-transfer* (TICT) states (Grabowski et al. 2003). Planarity can be modulated by covalent modifications of the dye and changing their configurations, which also suggests many possibilities to generate the sensor response. The switching to TICT state can be used in sensing.

The explained above general principles of efficient usage of ICT mechanism in sensing is best demonstrated on the example of designing the Zn^{+2} ion sensor of new generation (Sumalekshmy et al. 2007). The two compounds, whose formulas are presented below (Fig. 8.6), one containing two protons (**1**) and the other one is substituted by fluorine atoms (**2**). These compounds generate strong shifts in absorption and fluorescence spectra on the binding of zinc ion, and that allows precise ratiometric recording. Compound **2** demonstrates 1:1 ligand-Zn^{+2} binding mode and yields a dissociation constant of $K_d = 2.4$ μM. This compound is strongly asymmetric, which allows an increase of ICT upon excitation, generating in the excited state

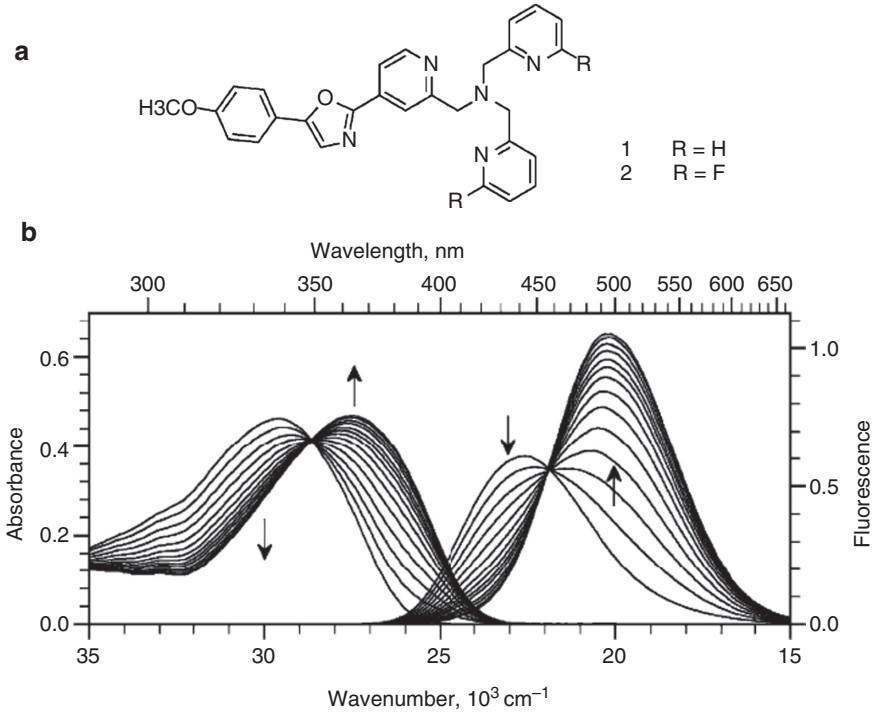

Fig. 8.6 The ICT-based sensor for zinc ions (Sumalekshmy et al. 2007). (**a**) The basic sensor molecule (1) and its fluorinated derivative (2). (**b**) Absorption (*left*) and fluorescence emission (*right*) spectra for the titration of compound (2) with zinc ions in micromolar concentration range in methanol. Addition of zinc ions results in the absorption band shifted from 339 to 362 nm, and fluorescence spectra from 441 to 497 nm. Quantum yield grows from 35 to 71 %

a strong dipole moment. In this configuration, the metal ion binds to the acceptor rather than to the donor binding site, so that the ion binding increases but not decreases the charge-transfer character of the excited state together with substantial shifts of spectra to longer wavelengths. Such increase, instead of commonly observed quenching in polar media, makes the Zn-bound state even more intensive in emission. This example demonstrates that the general principles work and can be applicable to a broad range of donor-acceptor fluorophores modified with tailored chelating sites for selective sensing of charged targets.

The transition from LE to ICT emission is not always detected as the appearance of a new band. However, in some aromatic dyes possessing strong electron-donor and electron acceptor substituents the ICT band is clearly distinguished showing this excited-state reaction as the transition between two localized states (El-Kemary and Rettig 2003; Rurack 2001; Yoshihara et al. 2003). The ability of these dyes to generate the *two-band emission* is an extremely valuable property for the design of wavelength-ratiometric reporters. An example could be the dimethylamino analogue of boron-dipyrromethene dye exhibiting well-resolvable LE and ICT emissions (Fig. 8.7). Its dual emission is well resolved, though the quantum yield is low. Substitution of dimethylamino group into azacrown transforms it into ion sensor. Coordination of the cation to the nitrogen donor atom of the crown inhibits the charge-transfer process, leading to a cation-dependent enhancement of the LE emission (Kollmannsberger et al. 1998).

The Ca^{2+}-chelating dyes Fura 2 and Indo-1 (Grynkiewicz et al. 1985) serve as good examples of influence of target binding on the ground-state *intramolecular charge transfer* (ICT) behavior of stilbene-like dyes. The ion binding results in redistribution of absorbed quanta between long and short-wavelength excitation bands. The appearance on Ca^{2+} binding of a new short-wavelength band at 405 nm

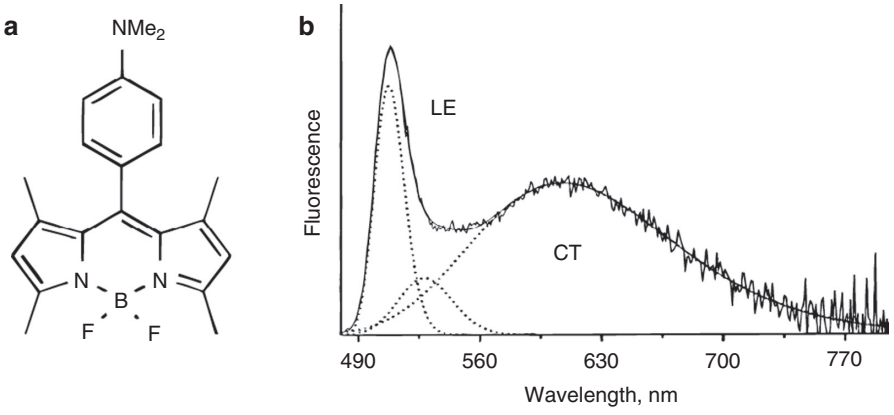

Fig. 8.7 The prototype of wavelength-ratiometric ion sensor based on intramolecular charge transfer (Kollmannsberger et al. 1998). (**a**) The structure of dimethylamino-substituted boron-dipyrromethene dye. (**b**) Its fluorescence spectrum in diethyl ether and its deconvolution into LE and CT (ICT) contributions

(490 nm for a free dye) is the result of IST reaction that occurs on interaction of chelated Ca^{2+} ion with the electron-donor nitrogen atom.

In principle, if the excitation spectra are so different, fluorescence spectra should be different too. But only in the case of Indo-1 the two-band response is observed also in fluorescence. The story is that in the excited states of these dyes due to redistribution of electronic density there appears the positive charge close to the bound ion. This results in ion ejection, and only the ion-free form remains present in emission. In contrast to other molecular Ca^{2+} sensors, in Indo-1 the electrostatic repulsion in the excited state between nitrogen atom and the bound ion is not sufficient for its ejection from the binding site and this interaction generates a new band in emission. Indo-1 is excited in the near-UV (about 345 nm), and until present all the attempts to synthesize the Ca^{2+} probe with similar properties but with the excitation and emission spectra shifted to the visible range were not successful. It was reported only that positioning of ion-binding group at the electron-acceptor site of coumarin dye reversed the effect (Bourson et al. 1993).

8.2.3 Excited-State Proton Transfer

Excited states of dye molecules differ from correspondent ground states by the ability to donate proton to the medium or to accept proton. Proton is a particle with a positive charge, so the protonation or deprotonation of a molecule neutral in the ground state makes a charged one in the excited state. Molecules that increase their acidity and more easily loose the protons in the excited states are called '*photo-acids*', and those that increase their basicity are called '*photo-bases*'. These reactions occur with the participation of solvent. In aqueous solutions two or more forms based on *protonation equilibria* can be observed that differ as a function of pH. In many organic dyes both proton-bound and proton-dissociated forms are strongly fluorescent and demonstrate different positions of their spectra (Arnaut and Formosinho 1993), so if these effects are coupled with the sensing events, they are easily recorded.

The equilibrium between two excited-state forms is established on a very short (picosecond) time scale, and in aqueous solution it can be shifted not only by the change of pH but also by the solvent access to the dye and by the dye local environment. Coupling the target binding to these changes can generate the sensor response.

Very efficient could be the response when the same molecule contains both proton-donor and proton-acceptor groups in a close proximity and connected by H-bond. Such reaction is called the *excited-state intramolecular proton transfer* (ESIPT). It does not require protic environment and may occur in any solvent, in solid matrix, even in vacuum. The strict requirement is only on the structure of molecule exhibiting ESIPT (Formosinho and Arnaut 1993) Proton-donor group is almost invariably a hydroxyl, and the basic proton acceptor must be either heterocyclic nitrogen atom or the oxygen in the form of carbonyl. The two groups, hydrogen-bonded in the ground state, form in the excited state a pathway for proton transfer.

The excitation leads to dramatic redistribution of electronic density in the fluorophore, so that the proton donors become stronger donors and acceptors – stronger acceptors. Hence appears the driving force for ESIPT (Kwon and Park 2011; Demchenko et al. 2013).

In many systems, ESIPT is very fast and irreversible on fluorescence lifetime scale and therefore it produces a single ESIPT band in fluorescence spectrum, which lacks switching ability needed for sensing. However, there are a number of dyes with a very attractive property of producing two bands in emission, one belonging to initially excited LE state, and the other – to the product of ESIPT reaction. Such dyes have been found among hydroxyphenyl benzothiazole, benzoxazole and benzimidazole derivatives. Their two-band switching, dependent on pH and binding of ions, can potentially be explored in sensing (Henary et al. 2007).

Switching between normal and ESIPT emissions can be achieved by changing aggregation state of the dye. For instance, 2(2′-hydroxyphenyl)benzoxazole (HBO), a typical dye of this group, forms dispersed aggregates in water exhibiting green ESIPT emission, whereas the dye solution demonstrates blue normal emission (Huang et al. 2006). It must be noted, that on a general scale these dyes did not find many applications, mainly because of the presence of several ground-state and excited-state forms and of strong quenching of some of these forms.

In Sect. 4.3 we described the family of 3-hydroxychromone (3HC) dyes that possess the property to observe normal and ESIPT emissions as two well-resolvable and intensive fluorescence bands. The great interest to these dyes from the side of sensing technologies is due to easy switching between two forms in response to variations of their weak intermolecular interactions with the environment. Now, after describing the properties of ICT state we can explain that, in accordance with predictions of Kasha (Kasha 1986), the observed ‘normal’ emission is in fact the emission from ICT state that is separated from ESIPT state by a small energy barrier (Demchenko et al. 2013). The power of these dyes is in the fact that directly, without any side reactions, they combine ICT and ESIPT mechanisms to report on the change of weak interactions with their environment by intensity variations of two bands with different colors in their emission. Azacrown-substituted analogs of these dyes were tested as ion sensors, and the two-wavelength ratiometric response was observed both in excitation and in emission spectra (Roshal et al. 1998, 1999). Smart derivatives of these dyes have found important applications in molecular and cellular studies (Demchenko 2006; Demchenko et al. 2013).

8.2.4 Prospects

Photoinduced electron transfer can be considered as the most general photophysical mechanism of signal transduction in fluorescence sensing. It can be realized with all fluorescence and luminescence emitters including all kinds of emitting nanoparticles and in this sense can provide the optimal way of communication between inorganic and organic worlds in the form of exchange of electrons. Usually this exchange

results in complete quenching, and different configurations of participating PET donors and acceptors find application as the response elements in sensing.

Being so easily achieved and so broadly observed, the PET effect is well suited only to intensity sensing, since the quenched states cannot provide reference for time-resolved, anisotropy or wavelength-shifting measurements. There is an active search for PET sensors with dual (LE and PET) emissions and the first promising results have been reported (Rurack et al. 2002). This raises expectations in a success on this trend.

In contrast, ICT has a basic ability to generate new bands in emission or produce strong spectral shifts, but this mechanism is available only to organic dyes. Moreover, these dyes should possess certain very necessary elements of structure, such as electron donor and acceptor groups separated in space for providing a high dipole moment. It is known that fluorescence in such systems can be strongly quenched in highly polar media, so the design of the best fluorescence reporters based on ICT (or, probably, on TICT) remains for the future.

Protonation-deprotonation of fluorescent dyes has found straightforward application in pH sensing, and it can be used on a broader scale when it is coupled with other reactions induced by target binding in water. Signal transduction with the aid of ESIPT is free from this limitation; the informative signal can be obtained in different solvents and upon modulation of solvent/sensor environment. This prospective trend has to be further developed.

8.3 Signal Transduction Via Excited-State Energy Transfer

The popularity of *Förster resonance energy transfer* (FRET) is explained not only by an immense range of possibilities for constructing the advanced molecular and nano-scale sensing devices, but also by a variety of fluorescence detection methods that can be used. FRET can be monitored by intensity changes (quenching of fluorescence of the donor and enhancement of the acceptor) and also by the change of polarization and lifetime of fluorescence emission. Variation of inter-fluorophore distances and their spectroscopic parameters can modulate FRET within the nanocomposite from its complete absence to highest probability of occurrence. In Sect. 3.6 the physical background of FRET phenomenon was presented and in Sects. 6.2 and 6.3 the peculiarities of its observation in nanostructures and nanocomposites were analyzed. Below we will discuss several possibilities realized for generation of efficient sensing and imaging signals.

8.3.1 Variation of Distance Between Individual Fluorophores

Many constructions designed for fluorescence sensing with FRET-based reporting explore strict stoichiometry between FRET donor and acceptor groups that are provided by either covalent linkage between them (often on a protein or oligonucleotide

matrix) or by formation of intermolecular complexes. In these cases the change in distance and orientation between interacting partners can report on the sensing event. This can be achieved when both donor and acceptor fluorophores belong to the sensor and a conformational change in the sensor on target binding causes the changes of their relative distance. Alternatively, donor and acceptor can belong to different interacting partners. One of them can label the sensor and the other the target or its analog (in displacement assay), and upon their binding the two fluorophores come to close proximity. The reader may refer to Fig. 3.16 and related text for more detailed discussion.

Should the target itself absorb light, it can be used as an emissive or quenching FRET acceptor and the problem may be reduced to selecting a proper donor that can be used as a reporting element of the sensor. And, of course, the labeled target analog can be used in displacement assay. In a more general case a double labeling is needed of the sensor, the target or of its analog as a competitor. Enzyme assays based on cleavage of double labeled substrates are also popular. Meantime, since the fluorogenic molecules are modified (destroyed) during the assay, this procedure cannot be formally considered as "sensing" but as a traditional biochemical analysis.

8.3.2 Variations of Spectroscopic Parameters

Modulation of FRET response at a fixed donor-acceptor distance by changing the *absorption spectrum* of the acceptor (see Fig. 3.17a, b) may have important advantages in fluorescence sensing and imaging. In organic dyes the absorption spectra shift on the formation of the charge-transfer complexes and, more efficiently, on their transition between pH-dependent protonated and deprotonated forms (Yao et al. 2007; Povrozin et al. 2009). The large spectral separation and high emission intensities of these forms in the visible allow generating strong sensor signal (Takakusa et al. 2003). The composites assembled of quantum dot donor and covalently attached squarene dye demonstrate such ability (Snee et al. 2006). In sensor design the effect of target binding can be coupled either with pH change or with pK_a shifts of smart FRET receptors.

In this case also the binary constructions with fixed fluorophore locations are used. The FRET efficiency can depend on the site of attachment of the ligand binding site – to donor or to acceptor (Guliyev et al. 2009). When a fluorophore responsive to ion binding is located at the acceptor site and the donor is excited, an efficient chemosensor can operate with the advantage of its strong Stokes-shifted emission Fig. 8.8a). In this case the observation of donor emission is not needed and the dual emission response or response in any other fluorescence parameter to target binding can be provided by the acceptor. Here the advantage is a stronger separation of excitation and emission bands and broader selection of excitation and emission fluorophores. In the case when the target-responsive unit is located at the energy donor site and the acceptor is just a passive emitter (Fig. 8.8b), then the emission

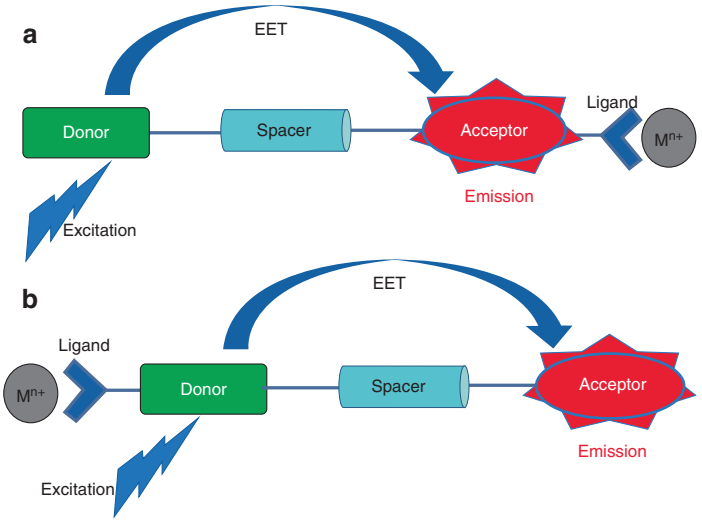

Fig. 8.8 Two different designs for excitation energy transfer (EET) coupled ion sensing (Guliyev et al. 2009). (**a**) The ligand binding and correspondent fluorescence response occurs at the FRET (EET) acceptor site and the donor plays a passive role. The informative signal comes from emission of the acceptor. (**b**) The ligand binding and correspondent fluorescence response occurs at the donor site. The ligand binding changes the excitation spectrum of the donor collected at the emission wavelength of the acceptor

can be collected at unaltered emission band of the acceptor and informative signal comes from the fluorescence excitation band that is changed on interaction with the target. The variability of fluorescence parameters that can be achieved in both cases is beneficial for multiplex sensing.

The commonly observed irreversible acceptor photobleaching can be useful when the FRET pairs are formed by highly photostable donor and easily photodegradable acceptor. Formation of bonding of intracellular molecules and structures can be observed when these potential partners are labeled by FRET donor and acceptor and the two images are taken at the wavelength of donor emission before and after the acceptor is bleached (Jares-Erijman and Jovin 2003; Van Munster et al. 2005).

There are also the possibilities to eliminate FRET by removing the acceptor absorption in a reversible way. The technique is called "satFRET" and involves the *excited-state saturation* of the acceptor (Beutler et al. 2008). With photochromic dyes the structure of FRET acceptor can be switched by light between two states reversibly: one state with the excitation band overlapping emission band of the donor and the other, in which this band is lacking. This allows realizing *photochromic FRET* (pcFRET) (Giordano et al. 2002). Dithienylethene can serve as such acceptor. It can switch to the colorless open form under the action of visible (green) light and switch back to closed light-absorbing form under the action of ultraviolet light. This switching influences dramatically the fluorescence intensity of the donor. Only several absorbed photons are required for such switching in

contrast to ~10^4–10^6 photons needed for irreversible photobleaching. In this technique, quantum dots can serve as FRET donors (Díaz et al. 2012). Some members of GFP family can exhibit light-activation and can be used as photochromic FRET acceptors (Bourgeois and Adam 2012).

8.3.3 FRET-Gating

Another interesting possibility that can be used in sensing is the '*FRET-gating*', when the adding or removing of the intermediate in the multi-step FRET process modulates the fluorescence response by changing the link between donor and acceptor (see Fig. 3.17c). The following literature example illustrates this possibility (Wang et al. 2004). It was shown that the excitation of cationic water-soluble conjugated polymer results in inefficient FRET to ethidium bromide dye intercalated within the bases of double-stranded DNA. When fluorescein label is attached to one terminus of the DNA, the link between donor and acceptor appears and an efficient FRET starts to be observed from the polymer through fluorescein to ethidium bromide. These experiments show that the proximity and conformational freedom of fluorescein provide a FRET gate to dyes intercalated within DNA. The conjugated polymer donor possessing strong absorbance also serves for amplification of this emission.

The overall process provides a substantial improvement over previous homogeneous conjugated polymer based DNA sensors. It is interesting also to note that multistep energy transfer of intrinsically excited DNA occurs between its bases, and this is one of important mechanisms of its protection against photodamage (Yashchuk et al. 2006).

Thus we observe that it is easy to intervene into a cascade system depicted in Fig. 6.7 by removing and then adding the intermediates in FRET process. When the donor and acceptor are in proximity but their spectral overlap is insufficiently small for the transfer, then an introduction of the third partner that can serve an acceptor to primary donor and donor to terminal acceptor results in the appearance of efficient transfer. New versions of this technology were reported (Aneja et al. 2008).

8.3.4 Exploration of Collective Effects in FRET

Collective effects in FRET may involve interactions between similar and different fluorophores (and also different types of quenchers) that influence different parameters of fluorescence emission (see Sect. 6.2). There are many possibilities to intervene into *homo-FRET* and *hetero-FRET* processes in nanocomposites in order to mediate the sensing effect.

The general scheme that combines the effects of *light harvesting* achieved by energy exchange between similar dyes via homo-FRET and *wavelength converting* chain reaction achieved by multi-step hetero-FRET is presented in Fig. 8.9. On light

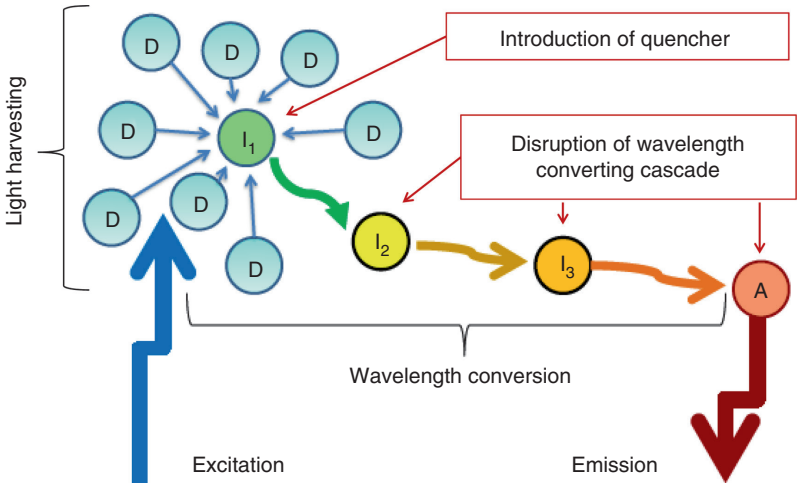

Fig. 8.9 Effects of light harvesting and wavelength conversion and the positions, at which the signal transduction can be realized in sensing. When many similar dyes exchange their energies (homo-FRET), introduction of quencher quenches the fluorescence of the whole system. Since hetero-FRET occurs from short-wavelength to long-wavelength emitters (denoted here as *D* and $I_1 - I_2 - I_3$ chain), many closely located short-wavelength emitters D can transfer their energy to species emitting at longer wavelengths until reaching the final acceptor A that emits light at the longest wavelength. The quencher can be introduced at any of these steps. Moreover, removal-inclusion of one of intermediates (FRET gating) modulates strongly the output signal

harvesting step the energy collected by coupled FRET donors serving as antennas instead of being released as the emission or transferred into the wavelength converting chain can be efficiently quenched. Such quenching will not depend on particular primary excited fluorophore in the system (see also Fig. 6.5) and this results in total quenching of the whole system – "*superquenching*" (see next Section). The target binding-release in the sensor construction can be coupled with quenching-dequenching events.

If the wavelength convertor chain exists in multi-fluorophore nanocomposite, then new possibilities for signal transduction appear. The primary donor may release its excitation energy into this chain, and on any step of energy transfer there is a possibility of strong modulation of fluorescence reporter signal. This can be done in different ways: (a) introduction of quencher that quenches fluorescence of a particular intermediate and (b) removing-insertion of an intermediate.

As we discussed above, these effects can be realized on the level of the dye pairs. Essential contrasting feature of multi-fluorophore systems is the absence of necessity of keeping an exact stoichiometry and distances in dye locations that require double labeling that is often a serious complication. All the participants here can be located within the critical range for efficient FRET and the researcher can play with their relative concentrations. For achieving the highest output in emission intensity, the primary donor concentration may be taken to be the highest. If the quencher

suppresses the emission of specific intermediate and the energy to this intermediate is transferred only partially, then emission of the donor or of the intermediate previous in the wavelength converting chain can be revealed.

Due to efficient multi-step FRET and pumping the wavelength converting chain by applying high relative concentrations of primary donors, the last fluorophores in this sequence can be represented by a small number of copies, or even by one fluorophore. This allows easy application of *FRET gating*. This can be realized in different formats, for instance, in competition assays.

8.3.5 Prospects

The *Förster resonance energy transfer* has often been considered as an important tool to generate fluorescence sensors based on distance dependence of the transfer and possibility to change it during the sensing event. Now we observe active development of research methodology that uses this phenomenon for a related but different purpose – for dramatic *improvement of fluorescent reporting* unit facilitating signal transduction and reporting at an increased level of sensitivity. This became possible due to the introduction as fluorescent emitters of different kind of nanoparticles that are much superior to organic dyes in photophysical behavior but are inferior in responsive abilities. Their conjugation and use of FRET to improve the response properties opens up an amazingly broad field for research and development.

The FRET mechanism allows operating with all the parameters of fluorescence emission: positions of band maxima, anisotropies and lifetimes in (almost) desired ranges (see Sect. 6.2). An efficient switch of emission throughout all visible to near-infrared range can be achieved in this way, which opens new possibilities in sensing and imaging.

8.4 Superenhancement and Superquenching

In this section we discuss the possibility to modulate the response of fluorescence emitters arranged into ensemble in much broader ranges than it is possible with a single reporter unit. Our aim is achieving the most efficient signal transduction and most intensive signal output. We try to explore collective properties in fluorophore ensembles that are absent in the composed units. Several strategies have been proposed and realized to generate amplified fluorescence response in sensor systems, which can be the transitions from the highest possible brightness to its extremely low level or the reverse.

Basic mechanisms of achieving the fluorophore brightness can be realized by assembling them into nanoparticles. They were discussed in Sect. 5.2. Here, by assuming that the highest brightness is achieved, we will discuss, how it could be manipulated for generating the most efficient analytical signal. We will operate with

the term "*superquenching*" that will indicate the quenching of the whole ensemble of coupled emitters in a single event. The term "*superenhancement*" could mean the restoration of a bright fluorescence emission ion this ensemble, "superdequenching".

8.4.1 The Essence of Superquenching

Here we consider superquenching as a general effect that can be realized in any assembly of fluorophores connected by electronic conjugation or FRET (Fig. 8.10). If the system of similar emitters is connected by homo-FRET, then the energy can migrate between them and it can be emitted by any different emitter within this system. Then if the quencher is present in the system, it becomes the trap for this energy. Such quencher can be non-fluorescent FRET acceptor, metal nanoparticle or molecular complex exhibiting static quenching. The dynamic range of change in intensity is much greater than on quenching of individual fluorophore.

Thus, '*superquenching*' is the collective effect, which with the introduction of fluorescence quencher results in the quenching of the whole ensemble of emitters

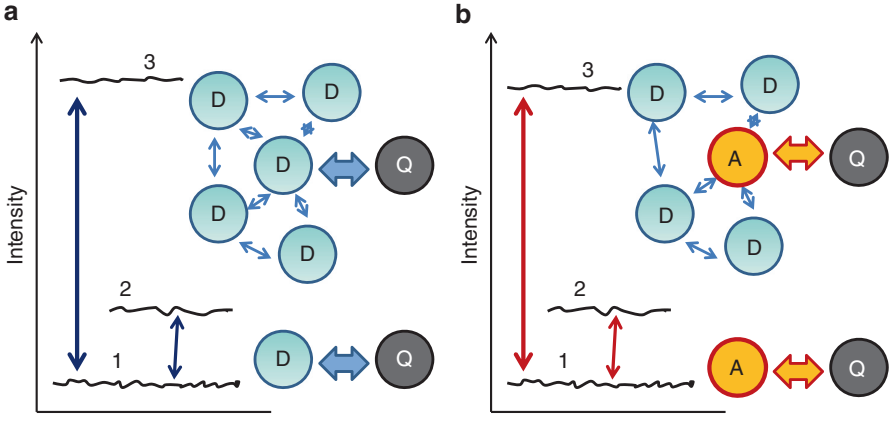

Fig. 8.10 Mechanisms of 'superenhancement' and 'superquenching' in a system of fluorophores connected by FRET. (**a**) The fluorophore D emits light intensity on level 2 and its interaction with the quencher Q results in emission decreased to level 1. When the system of a large number of fluorophores D is excited, its emission is much higher, on level 3, and the interaction of only one fluorophore with the quencher results in quenching of the whole ensemble of these emitters. The vertical arrows indicate the dynamic ranges of sensor response in both cases. (**b**) The same, but the FRET acceptor A is present in the system that collects all excitation energy from donors D and emits light at a red-shifted wavelength. When the quencher is present and A is alone, the dynamic range of response as the difference between intensity levels 2 and 1 is small. It becomes very significant when the system of donors D is excited and transfers its energy to acceptor A

(Lu et al. 2002; Demchenko 2013). Essential is the fact that the bright emission can be provided by the whole ensemble of dye molecules and that a single additional molecule can report on intermolecular interaction by inducing the effect of quenching in the whole system. It has the same origin as the '*concentrational quenching*' in dye aggregates (Johansson and Cook 2003), discussed in Sect. 6.1, but in this case it can be used for controlled sensor response.

We can consider a different realistic case, in which in contrast to that considered above (Fig. 8.10a) the excitation energy is collected not by the quencher but by light emitting FRET acceptor (Fig. 8.10b). In this case all the energy collected by the acceptor can be transferred in one step to the quencher. Here again, the profit is great. Instead of quenching the low-intensity signal of a single dye, an intensity appearing on a much greater level can be quenched. In the case of existence of multi-step FRET cascade (see Fig. 8.9), the quencher can be applied to any member of this cascade with equally dramatic superquenching (Demchenko 2013).

8.4.2 Realization of Superquenching

Superquenching can be realized in all cases of formation of the collective behavior between interacting fluorophores, particularly in all types of nanocomposites connected by *homo-FRET*. This collective response can be seen, for example, in dye-doped nanoparticles for instance, when the particles incorporate a dye responsive to pH. All the dyes together respond to a change of pH producing a strongly amplified effect (Kim et al. 2006).

We already discussed the issue of superquenching in the case of *conjugated polymers* (Sect. 5.3, see Fig. 5.11). This is a demonstrative example of excitonic coupling between fluorophores assembled into polymeric chains with high level of delocalization of excited-state electron density. The coupling of fluorescence emitters allows the excitation to migrate between different fluorophores in the system.

Another type of superquenching is observed in *J-aggregates* of cyanine dyes. Such collective effects were observed for cyanine dyes covalently attached as side groups to water-soluble cationic polymer (Jones et al. 2001). The cyanine dye fluorophores strongly associate in a J-aggregate structure characterized by a sharp red-shifted absorption (compared to the monomer) and a similarly sharp red-shifted fluorescence. Collective effect in quenching by very large Stern-Volmer constants for fluorescence quenching by oppositely charged electron acceptors or energy transfer dyes. The superquenching of the J-aggregate polymer fluorescence was demonstrated in a competitive bioassay.

Superquenching was reported in lanthanide-polymeric conjugates incorporated into nanoparticles (Li et al. 2014). There is unlimited range of possibilities to explore this phenomenon.

8.5 Signal Transduction Via Conformational Changes

There are many possibilities to incorporate conformational changes triggered by target binding into the process of signal transduction. Many such changes in flexible molecular structures occur with low activation energies, so the switch between two conformations can be coupled to target binding. Those of them that cannot proceed in the ground states can sometimes be observed in the excited states, where the activation barriers for rotations around certain bonds are dramatically reduced. Thus, the responding sensors involving both large-scale and small-scale conformational changes can be constructed. The excited-state electron transfer and energy transfer on molecular level are distance- and orientation-dependent. Therefore the change in the distances and orientations between the partners in these reactions can be used as the tools in signal transduction.

8.5.1 Excited-State Isomerism in the Reporter Dyes and Small Molecules

There are several classes of dye molecules that are highly stable in the ground state but easily isomerize in the excited state. One of classical examples for that is stilbene. In a *trans*-form it is strongly fluorescent, but in solutions that allow its rapid isomerization into *cys*-stilbene its fluorescence is very weak. Based on this fact, one can make a sensor, in which the target binding will influence the stilbene isomerization. Such possibility can be suggested based on results obtained with anti-*trans*-stilbene antibodies (Simeonov et al. 2000). In a complex with antibodies it exhibits bright emission indicating that its isomerization is suppressed. For our purpose, the antibody may serve a prototype of a target to show the efficient modulation of response on its binding. The other feasible idea is to modify stilbene with target-recognition moiety and use such stilbene-antibody associate as a sensor. Following this way a sensor for mercury ions was constructed (Matsushita et al. 2005). Stilbene fluorescence is bright but becomes strongly quenched by these ions.

In some cases the effect of binding can be coupled with the redistribution of *rotamers* (Henary et al. 2007) and on the conformational change in the sensor unit *bringing two distant pyrene groups together* with the formation of excimer (Schazmann et al. 2006). The designed molecules exhibiting conformational change can be labeled with two dyes to provide response to ion binding by *intramolecular FRET* (Petitjean and Lehn 2007).

8.5.2 Conformational Changes in Conjugated Polymers

In Sect. 5.3 we reviewed the properties of conjugated polymers as fluorescence reporters and argued that their response can be based on two unique features, ‘superquenching’ and the dependence of fluorescence emission on *chain conformation*. The modulation of chain conformation on target binding has found many

applications, especially in detection of nucleic acids (Sect. 12.4). Here we stress that the chain conformation produces dramatic impact on the properties of π-conjugated system that influences the fluorescence, since it determines the conjugation length (Pecher and Mecking 2010).

The conformation-dependent fluorescence of conjugated polymers was shown by many researchers. It is important that these polymeric molecules allow many different modifications with the attachment of side groups and these groups may determine the conformational state of the backbone and thus the fluorescence signal. Of special interest are the modifications with the charged side groups that transform the low-polar polymers into polyelectrolytes and allow target binding based on electrostatic interactions.

The presented below example demonstrates that (Fig. 8.11). It was shown that electrostatic interactions with negatively and positively charged peptides altered the fluorescence spectrum of poly[3-[(*S*)-5-amino-5-carboxyl-3-oxapentyl]-2, 5-thiophenylene hydrochloride] shown in Fig. 8.10a (Nilsson et al. 2003). The addition of a positively charged peptide in a random-coil formation forces the polymer to adopt a nonplanar conformation, which leads to increased and blue-shifted intensity of the emitted light. After the addition of a negatively charged peptide with a random-coil conformation, the backbone of the polymer adopts a planar conformation and an aggregation of the polymer chains occurs, seen as a red shift and a decrease of the intensity of the emitted light. A calcium ion sensor was suggested based on different conformation of this polymer in the unbound form and on its binding to Ca^{+2}-free and Ca^{+2}-bound forms of calmodulin.

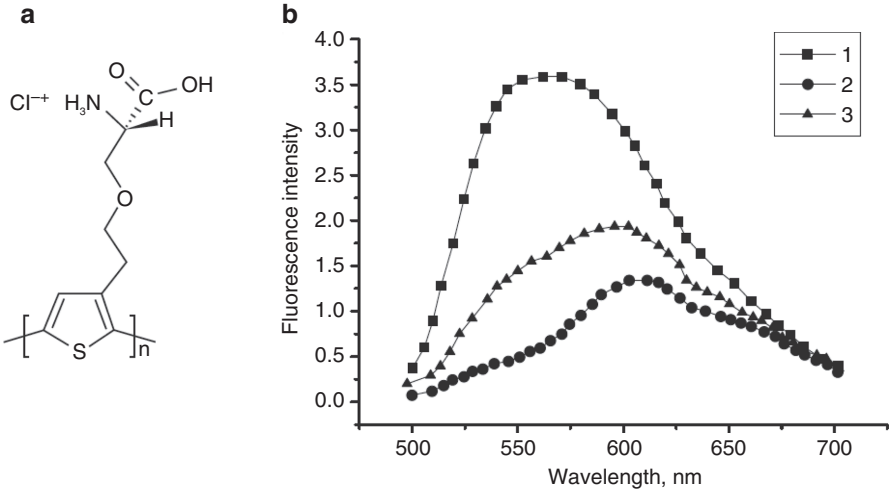

Fig. 8.11 The conjugated polyelectrolyte poly[3-[(*S*)-5-amino-5-carboxyl-3-oxapentyl]-2,5-thiophenylene hydrochloride] (**a**) and its fluorescence spectrum (**b**) (Nilsson and Inganas 2004). The fluorescence spectrum in unbound form (*1*) changes on binding to calmodulin. In the bound form, the fluorescence spectrum responds to the presence of Ca^{+2} ions as shown in comparison of Ca^{+2}-free (*2*) and Ca^{+2}-bound (*3*) forms

With proper modification of side groups, these polymers can specifically recognize charged molecules, such as ATP (Li et al. 2005). But the most significant effect is recorded on binding to regular protein fibrils that appear in some pathologies, such as Alzheimer's disease. These pathological protein aggregates exhibit β-sheet structure, and the polymer binding to them produces remarkable changes in their spectra (Herland et al. 2008).

A family of glycopolythiophenes containing sialic acid or mannose ligands were prepared and evaluated for their ability to bind lectins, virus, and bacteria (Baek et al. 2000). The binding interactions result in an unusual red-shift in the visible absorption of the polymer backbone, suggesting an extension of the effective conjugated length upon interaction of the ligand with its receptor.

The binding of conjugated polymer with cationic substituents to DNA is based on electrostatic interaction and depends on the DNA conformation. The polymer on binding to DNA has to change its conformation and thus generate the sensing signal (Fig. 12.13). This methodology found application in DNA hybridization assays, in which conjugated polymer started to play a role of 'hybridization transducer' (Dore et al. 2006). It was successfully applied to nucleic acid aptamers as sensors (Ho and Leclerc 2004). Since single-stranded DNA (ss-DNA) can specifically bind to various targets, including a complementary ss-DNA, ions, proteins, drugs, and so forth and on this binding the oligonucleotide probe often undergoes a conformational transition, the range of application of this methodology can be very broad (De Schryver et al. 2005).

8.5.3 Conformational Changes in Peptide Sensors and Aptamers

In the mechanism of recognition between flexible peptides and nucleotides and their well-organized targets there is nothing artificial. A great number of 'natively unfolded' proteins were discovered in recent decades, which even required revising the paradigm on interactions of proteins with their substrates and ligands. It became clear that the '*lock-and-key'* and '*induced fit*' mechanisms should be complemented by the mechanism of '*induced and assisted folding*' (Demchenko 2001). Many cases were found, in which the natively unfolded protein on its specific interaction with another protein or nucleic acid exhibits the unfolding → folding conformational change to form a stable and well organized complex (Fig. 8.12a).

There is a special class of proteins, called molecular chaperones, which, interacting with unfolded proteins, provide their transition into the folded state. Moreover, examples were found of interacting partners, so that both of them are unfolded, and upon interaction, they find a common pathway to the folded states (Fig. 8.12b). In both these cases, the interactions between the partners can be very specific, starting from their initial contacts. The whole process follows strict thermodynamic and kinetic rules and involves millions of decisions of the chains for abortion or for

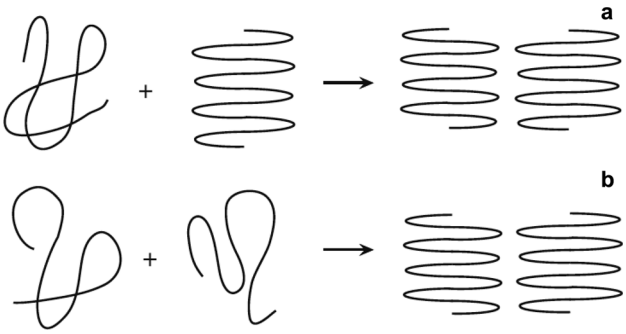

Fig. 8.12 Illustration of mechanisms of 'induced and assisted folding'. (**a**) Unfolded protein folds upon interaction with the other folded protein used as template. (**b**) Two unfolded proteins assist each other to attain folded conformations. In both cases, specific recognition occurs on the level of groups of atoms. It is sequentially enforced in the course of folding

re-enforcements of contacts. Therefore, the formed complex is also very specific, satisfying the requirement for molecular recognition.

The strategy to make virtually any protein the sensor with signal transduction based on *target-induced folding* was developed (Kohn and Plaxco 2005). Rational genetic engineering can destabilize the protein structure in such a way that it becomes naturally unfolded. Binding the target should make the folded state thermodynamically more stable and induce the unfolding-folding transition. These results make a fair background for understanding how the unfolded peptide selected from the library without regular structure and at the absence of formed binding site, can serve as a very specific binder. The specificity of interaction appears if the design allows a strong coupling of the chain folding and recognition.

Such a profound change in conformation of recognition unit provides many possibilities for signal transduction in sensing. Many fluorescence reporting mechanisms can be applied to such systems. Meantime, one precaution has to be made. Modification with fluorescent dye can be a strong intervention into the process of folding. Therefore, such modification has preferably to be made in a site that has a minimal involvement into the process of folding. Alternatively, the modification should be made on the step of selecting the prospective receptors from a combinatorial library, so that the selection has to be made with the account of folding and recognition properties of peptide-dye conjugate.

Zinc finger presents a classical example of transforming the designed peptide into a sensor. It is derived from small (25–30 residue) protein domain that selectively binds zinc ion with a dissociation constants in the picomolar range. In the absence of zinc, the peptide is unfolded and it folds to coordinate the Zn ion (Fig. 8.13). The primary coordination sphere involves two His and two Cys residues. The chemical synthesis of this peptide was easily performed with incorporation

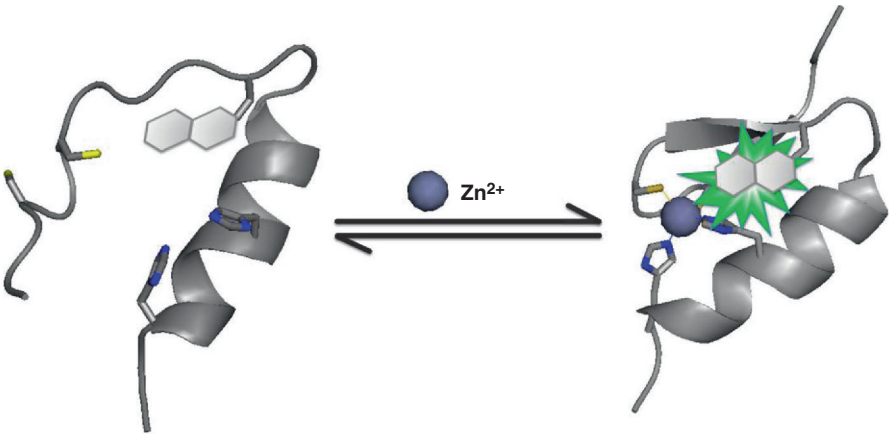

Fig. 8.13 The zinc-induced folding of zinc finger peptide (Walkup and Imperiali 1996). The conformational change in peptide is detected with the environment-sensitive dye. In unfolded state (*left*) the dye is exposed to water and indicates its position in a polar environment. Its environment changes to low-polar (*right*) on the folding of peptide triggered by zinc ion

of fluorescence reporters into this structure. In this case, the signal transduction does not involve the interaction of reporter with coordinated zinc and can be provided by the dyes that interact between themselves and report based on FRET or PET mechanisms (Walkup and Imperiali 1996). Therefore many modifications are possible to improve the performance of such sensors.

The conformational adaptation of receptor in forming the complex with target is present in sensing *aptamers*. In Sect. 7.6 we described in detail the selection, synthesis and operation of nucleic acid aptamers. Here we will focus on mediation and generation of fluorescence signal coupled with conformational change in these sensor molecules. Many aptamers (especially with a short sequence) are without or with only small segments of regular structure in their free states in solutions. A number of studies demonstrated that the target binding is coupled with their ordering into well-defined three-dimensional structure (Hermann and Patel 2000; Stojanovic and Kolpashchikov 2004). This suggests many possibilities for providing fluorescence response with realization of principle of direct sensing.

An interesting possibility for signal transduction can be found with aptamers. Since they reorganize and in many cases form the double-helical structure on target binding, this process can be detected by the dyes that can *specifically intercalate* into this structure. Particularly, such response can be obtained with intercalating rubidium chelating complexes that can provide dramatic increase in phosphorescence (Puleo et al. 2006). This eliminates the necessity of covalent labeling of aptamers. The response to conformational change in aptamers can also be detected with the aid of cationic conjugated polymer (Ho and Leclerc 2004).

8.5.4 Molecular Beacons

Molecular beacons (the other name 'molecular hairpins') are the direct molecular sensors designed for detection of specific nucleic acid sequences based on formation of complementary double helix structures. Nucleic acids are widely known for their ability to form Watson-Crick double helical structures that are stabilized by hydrogen bonds between complementary base pairs. Formation of these structures is strongly sequence-specific. The double helix can be formed between two different chains with complementary structures but also in a single chain when it folds to itself to form a double helix. This allows to make sensors out of single-chain nucleic acids that fold into a specially designed structure containing two structural components, a loop and a stem (Fig. 8.14). They can be considered as a special case of aptamers, with specificity to recognize the sequences in nucleic acids.

The loop is the recognition element containing complementary nucleic acid sequence to the target sequence that has to be detected in a pool of many different oligonucleotides. The stem is formed of two complementary sequences that fold to themselves to flank the loop. Hybridization of the loop part with the target DNA or RNA sequence generates a conformational change in this

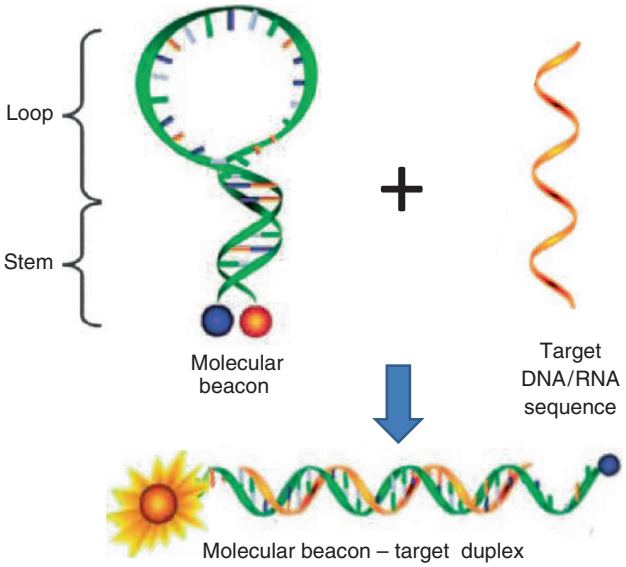

Fig. 8.14 Schematic representation of the generation of fluorescence signal by the hybridization of nucleic acid sequences with molecular beacons. A molecular beacon is a hairpin-shaped nucleic acid with the sequence of the loop complementary to the sequence in the target nucleic acid. In the absence of the target, the two dyes, donor (D) and acceptor (A) that can be a fluorophore and a quencher are located closely and interact. When the loop hybridizes with a target sequence, the stem is disrupted and the two labels move apart generating a fluorescence response of the donor

structure, its stretching-out. As a result, the chain segments forming stem disconnect and move apart. This motion is detected being transformed into fluorescence signal. Since the nucleic acid sequence of the loop can be made complementary to that of any nucleic acid target, molecular beacons can be used as a generic technology for recognition of specific nucleic acid sequences (Tyagi and Kramer 1996).

The distance between 3′ and 5′ ends, being very short in folded beacon, dramatically increases on target binding. So, the fluorescence reporter signal can be generated based on recording the disconnection between stem segments. The dye can be attached to one of these chain terminals or to both of them. There are several possibilities to generate the reporter signal.

1. The *increase of distance* between two beacon ends can be used in detection by FRET to non-fluorescent acceptor (quencher). The introduction of two labels, donor and acceptor, is needed in this case. In the sensing event (hybridization with complementary sequence) the separation between two dyes increases causing fluorescence enhancement. This approach was explored in a number of works (Marras 2006)
2. More advantageous is the detection technique in which both *FRET donor and acceptor are fluorescent*. This possibility was realized with the use of cyanine dyes Cy3 and Cy5 (Ueberfeld and Walt 2004). When the donor and acceptor dyes are in close proximity, an emission of the acceptor is observed. On hybridization this emission disappears and emission of the donor is enhanced. It was found that the ratio of donor-acceptor intensities is independent of the amount of the probe and provides a quantitative measure of the free target concentration.
3. The quenching of fluorescence signal is achieved by *photoinduced electron transfer* (PET) quenching (see Sect. 8.2). In PET quenching the emitting dye and the quencher (electron donor or acceptor) should be present in stem structure at a very close distance from each other (Heinlein et al. 2003), in contrast to much larger distance (of several nanometers) that is needed in FRET sensing. Since in the folded state of molecular beacon the distance between two chain terminals is very short, a complete quenching can be achieved, so that fluorescence enhancement appears on hybridization. The advantage of this technology is in the possibility to avoid second labeling. The nucleic acid guanosine base can play this role of PET quencher of complementary dye in beacon construction (Knemeyer et al. 2000).
4. One of hairpin ends can be *immobilized on metal surface* (Dudley et al. 2002). If the other terminal contains the dye the fluorescence of this dye will be quenched due to contact with the surface (also due to PET mechanism). Fluorescence enhancement will be observed on hybridization.

The sensing DNA or RNA oligonucleotide can be successfully substituted by artificial oligomers – *peptide nucleic acids* (see Sect. 7.7). In their structures the negatively charged ribose or deoxy ribose phosphate is replaced by an uncharged N-(2-aminoethyl)-glycine scaffold, to which the nucleobases are attached via a methylene carbonyl linker (Brandt and Hoheisel 2004). The target recognition by these beacons is less sensitive to ionic strength and their fluorescence is not affected by DNA-binding proteins.

The principle of molecular beacon acquires more and more general importance. A successful result on its application in detecting proteins has been reported recently (Thurley et al. 2007). The *peptide beacon* (Fig. 8.15) uses the ability of a designed peptide to change its conformation between target-bound and target-free forms with fluorescence reporting based on double labeling. In another development, a short peptide beacon was suggested for detecting nucleic acids (Wu et al. 2012). Two pyrene units were appended to a synthesized construct. On their intercalation into DNA double helix the contact between them is disrupted with disappearance of excimer and appearance of monomer band in emission. Such DNA sensor was shown to enter spontaneously into the living cells.

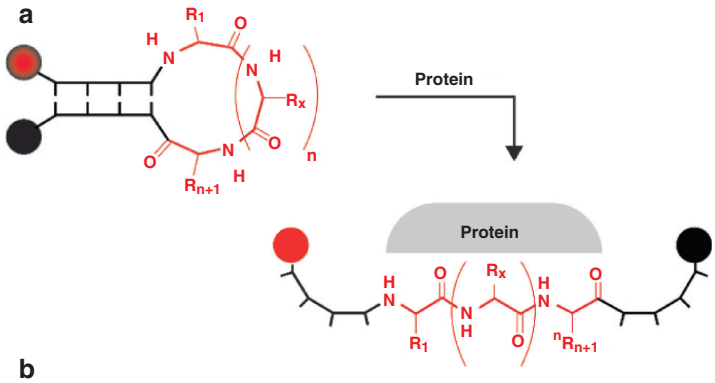

Fig. 8.15 The prototype of peptide molecular beacon for detecting proteins (Thurley et al. 2007). The same principle as in DNA beacons is applied here. Whereas the recognition part is peptide, the stem part is made of complementary peptide nucleic acid (PNA) sequences. (**a**) The principle of beacon formation. R_i are the side groups of amino acids. (**b**) The sequences of peptide molecular beacons. *Lower case letters* indicate PNA nucleotides. Pyb is pyrene butanoic acid NIR is the near-IR dye and Dabcyl is the quencher

8.5.5 Proteins Exhibiting Conformational Changes

Flexibility of protein structures coupled with target recognition is used in different sensing technologies (Ha and Loh 2012; Plaxco and Soh 2011). These structures were optimized in evolution for performing biological functions, which requires highly selective ligand binding. As the target recognition units, they can display different modes of conformational change: rigid-body domain movement, limited structural rearrangement, global fold switching, and folding–unfolding. Such changes can be induced by target binding, but may not induce any structural changes. There is an active search for the most efficient coupling of recognition with sensor response in the case of fluorescence sensing. The major problem here is to transform the act of ligand binding to the measurable response signal.

This task is not easy, even in the case of *ligand-binding proteins* that exhibit global conformational changes, such as the *hinge-bending motions* of domains, rigid elements of their structures. The analysis of intra- and inter-domain dynamics of 157 ligand-binding proteins (Yesylevskyy et al. 2006) allows formulating the necessary conditions, which should be satisfied in order to couple the *intramolecular dynamics* of such biosensor in order to transfer the signal from the binding site to the reporter group. This can only be achieved if (a) the protein undergoes significant conformational change upon the ligand binding; (b) the intra-domain conformational changes are small in comparison with the relative motion of domains and (c) the strength of the inter-domain contacts is significant in the ligand-bound conformation and very small in the ligand-free conformation.

The technique developed in (Yesylevskyy et al. 2006) can be applied to the candidate proteins to see if these conditions are fulfilled for them. This can allow minimizing the possible design errors caused by the choice of the protein, which is not suitable for the design of sensors, where the reporter group is not in contact with the ligand. An algorithm was developed, which allows physically consistent simulations of slow large-scale protein dynamics that is based on subdividing the protein into the hierarchy of the rigid-body-like clusters (Yesylevskyy et al. 2007). A closed conformation, staring from the open one, can be predicted in agreement with their known crystallographic structures. Such techniques are promising in deciphering the character of protein motions involved in the signal transduction from the ligand binding site to the fluorescence reporter.

It was shown in (Yesylevskyy et al. 2006) that the periplasmic *ligand-binding proteins* and *calmodulin* are the most probable targets for the biosensor design. Being composed of two well separated domains, they undergo large hinge-bending motion upon ligand binding. In the open ligand-free state the domains are far from each other, while in the closed ligand-bound state the domain become tightly packed. The ligand is often captured in the cleft between the domains.

One of such proteins, the *Maltose binding protein* (MBP) (Fig. 8.16) is the most successful sensor protein, which is extensively studied and widely used (de Lorimier et al. 2002). Its mutated forms and other monosaccharide binding proteins are a part of active efforts in glucose sensor development (Fonin et al. 2014). Many genetic mutants of MBP were produced to modulate specificity and affinity

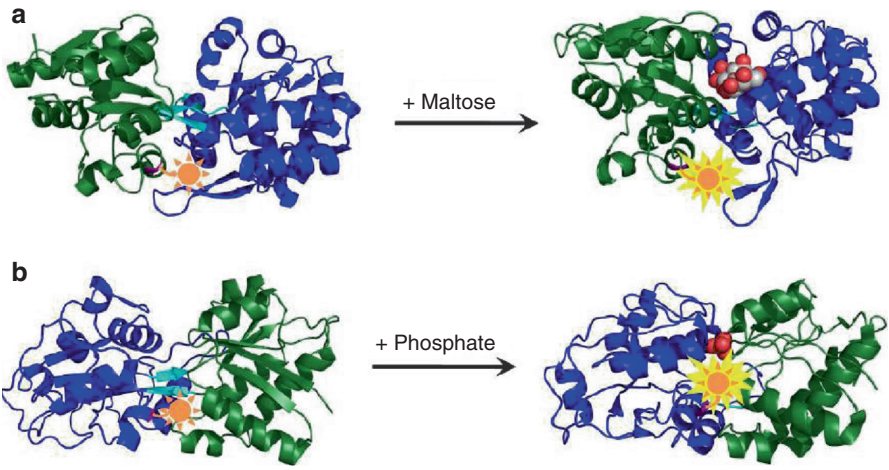

Fig. 8.16 The change in conformation in maltose-binding protein (**a**) and phosphate-binding protein (**b**) from an apo state (*left*) to a ligand-bound state (*right*) by a bending-twisting motion of the N domain (*green*) and C domain (*blue*) about the hinge region (*cyan*) (Tainaka et al. 2010). A fluorescent reporter group (*orange*) to monitor ligand binding has been attached to an allosteric site or a peristeric site, respectively

in target recognition and different spectroscopic techniques of signal transduction and reporting (Medintz and Deschamps 2006; Gilardi et al. 1994). In particular, a competitor displacement assay was suggested for maltose binding, in which the competitor was the labeled β-cyclodextrin derivative (Medintz et al. 2003). The use of quantum dot – organic dye pair allowed to use distance-dependent interactions between them resulting in PET quenching or FRET (Medintz and Deschamps 2006). Located distantly in open conformation, they become close neighbors in a closed conformation. A different construction using conformation-dependent FRET efficiency from ruthenium complex to quantum dot was also found efficient (Raymo and Yildiz 2007). In contrast, the application of environment-sensitive dyes did not result in expected spectral shifts and the significant response was obtained in intensity and lifetime only (de Lorimier et al. 2002; Fonin et al. 2014; Pickup et al. 2013). This may be the result of strong quenching hiding the spectral sensitivity, see Fig. 3.20.

Calmodulin is the calcium binding protein that, possessing a rather flexible conformation, changes it dramatically upon binding of four Ca^{2+} ions (Fig. 8.17a). Tsien and coworkers have designed a genetically encoded calcium sensor comprising four components: calmodulin, a polypeptide named M13 that binds the calcium-bound form of calmodulin, and two fluorescent proteins selected as FRET donor and acceptor and serving as reporters on conformational change occurring on ion binding (Fig. 8.17b). This change results in the appearance of fluorescence emission of FRET acceptor with easily observable spectral shift.

The small number of these successful cases is an indication of difficulties in extending of this principle of sensing on other ligand-binding proteins. Therefore an

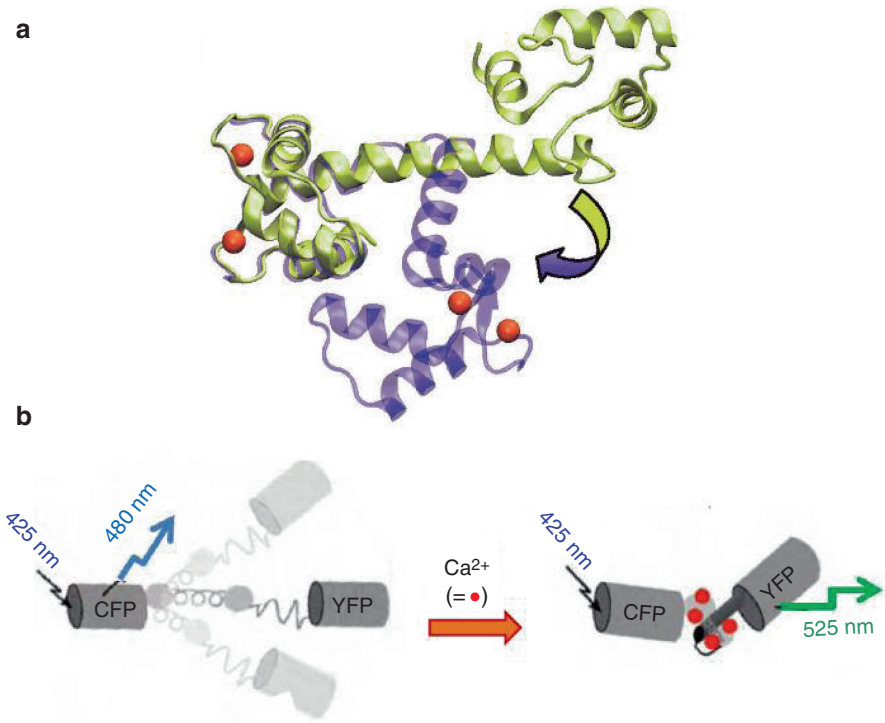

Fig. 8.17 The cell calcium sensor obtained by protein engineering. (**a**) Calmodulin in open ligand-free conformation (*yellow*) and closed ligand-bound conformation (*semitransparent blue*) are aligned by the first domain. The ligand Ca^{2+} ions are shown as red balls. The motion of the second domain induced by the ligand binding is clearly visible and indicated by *arrows*. (**b**) The "chameleon" that changes the fluorescence spectrum in response to Ca^{2+} ions binding. It is composed of calmodulin (responding to ion binding by conformational change) and green (GFP) and yellow (YFP) fluorescence proteins that are fused to N and C terminals of calmodulin via calmodulin-binding peptide M13 (Miyawaki et al. 1999; Miyawaki et al. 1997). The binding of Ca^{2+} ions induces conformational change in calmodulin that brings together the FRET donor and acceptor domains resulting in switching from the donor to acceptor emission

interesting strategy was suggested to decrease protein stability of a protein up to partial unfolding by inducing some structural changes, thus allowing the target to induce the switching to folded form with correspondent spectroscopic response (Ha and Loh 2012; Plaxco and Soh 2011).

Successful application of sensors based on protein molecules exhibiting conformational changes allows avoiding direct contact of fluorescence reporter with the target but depends critically on a position of right reporter at a right place. An example is the response of two-color ratiometric dye to the conformational change of enzyme inhibitor α_1-antitrypsin with elastase (Fig. 8.18). Ratiometric response of the dye is the result of change of its interaction with molecular environment (Boudier et al. 2009). This interaction leads to dramatic change in the band intensity ratio, suggesting an increased exposure of the label to the bulk water on formation of the complex.

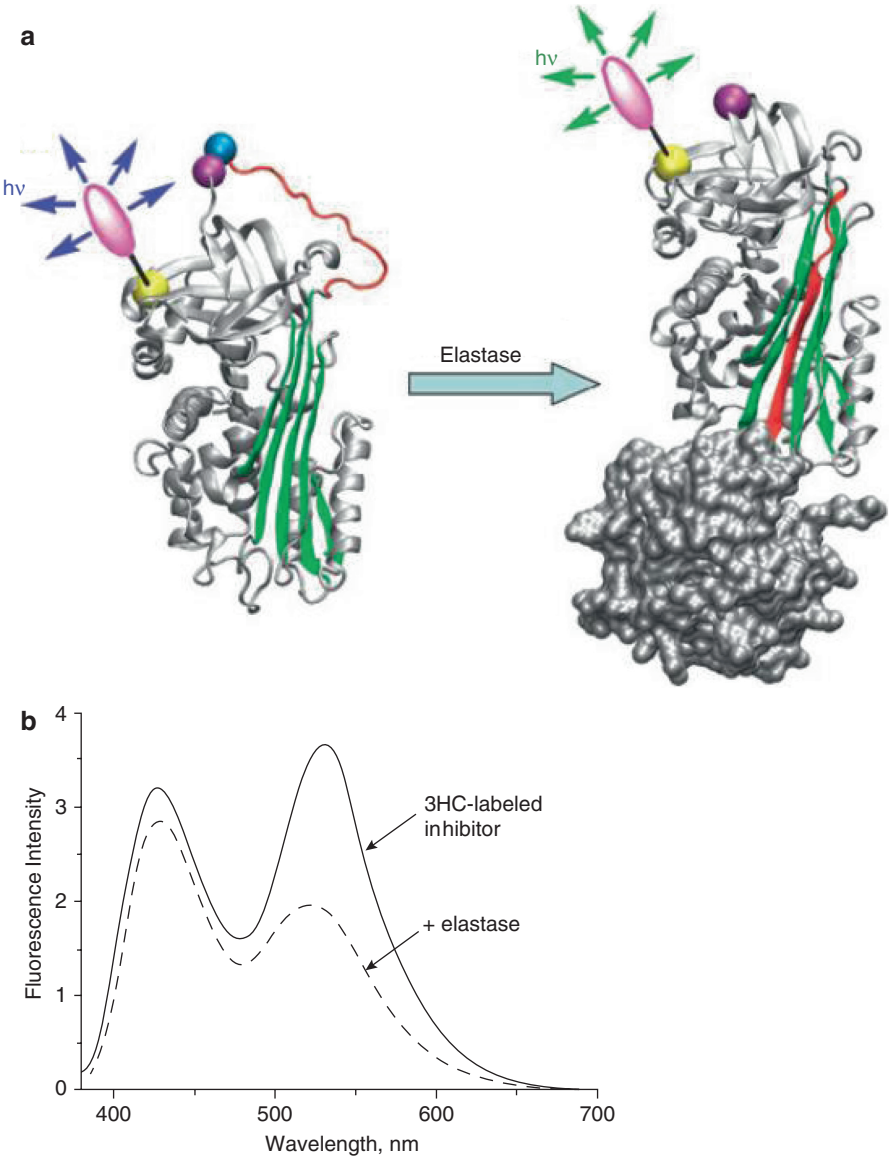

Fig. 8.18 An example of the application of environment-sensitive dye for the detection of conformational change in protein (Boudier et al. 2009). (**a**) The structure of human α_1-antitrypsin. The 3-hydroxychromone (3HC) label was attached by Cys-232 residue of the protein. Elastase enzyme interacts with α_1-antitrypsin and cleaves the peptide bond in the inhibitor's loop resulting in the conformation change. (**b**) Steady-state fluorescence emission spectra of 10 μM of the labeled α_1-antitrypsin in the absence (—) and in the presence (– – –) of elastase

8.5.6 Prospects

Conformational changes in the receptor molecular unit together with implementation of reporting mechanism based on electron, proton or energy transfer provided by fluorescence reporters allow realizing the principle of direct sensing (Sect. 1.6). Based on these changes we are able to obtain direct response to target binding in the form of changing the parameters of emission. Dependent upon the system design, it is possible to select conformational isomerizations in the reporting dye or the changes in conformation of conjugated polymers with their strong effects on *electronic conjugation* between the fragments of dye molecule or the monomers in a polymeric structure.

The folding reactions in polypeptides and ologonucleotides selected as the best binders from great libraries offer a dramatic progress in sensing technologies. These flexible sensors should be selected for being committed to be folded only in complexes with the targets. Though they are structureless or possess only a small amount of three-dimensional structure, they can be selected to contain all geometrical and bonding features for correct target recognition. Sensing by '*induced folding*' must find many applications as a simple, universal and economical way to address many targets.

Molecular beacons are a specialized version of aptamers that realize transition from intramolecular (hairpin) to intermolecular (complex) folded state of oligonucleotide. Detecting response to this change is easy and can be provided in a number of ways. And finally, regarding the *ligand binding proteins* and their genetic versions, their conformational changes are very specific, as specific as their recognition. Time will show if a generic methodology will be developed on their basis.

8.6 Signal Transduction Via Association and Aggregation Phenomena

Since it is well documented that reduction of size and dimensionality of different types of nanoparticles results in quantum confinement effects that influence dramatically their spectroscopic properties, it was natural to suggest that aggregation of these particles will provide the necessary signal for sensing. In clustered assemblies of the particles the new collective properties can be observed, such as the *coupled plasmon absorbance*, interparticle electron and energy transfer and the appearance of electrical conductivity (Barbara et al. 2005). Thus, possessing unique responsive properties, nanoparticles can change them in the course of aggregation coupled with target binding.

The strong color that can be detected visually on illumination of nanoparticles is due to a combination of two optical phenomena: light *absorption* and *scattering* (Yguerabide and Yguerabide 1998). Due to this fact, the correct term could be the '*extinction*' instead of 'absorption', since it describes both absorption and scattering components to the observed colors.

8.6.1 *Association of Nanoparticles on Binding Polyvalent Target*

One of the easiest possibilities to detect bivalent or polyvalent target is to provide a sensing system in which this target (or competitor that can be substituted by the target) can simultaneously react with the binding sites on several nanoparticles. This reaction may induce aggregation or at least cluster formation, in analogy to a well-known immunoprecipitation method, where a bivalent antibody reacting with polyvalent antigen induces formation of precipitate. With the introduction into the sensor development of nanoparticles this principle has got a new stimulus for development. An easily detectable change in optical properties of gold and silver nanoparticles occurs on their association due to *plasmon-plasmon interactions* between adjacent particles (Jans and Huo 2012; Saha et al. 2012; Valentini and Pompa 2013). The characteristic visually detected red color of gold colloid changes to bluish-purple color upon colloid aggregation (Fig. 8.19).

This property has found application in *polynucleotide detection* (Elghanian et al. 1997). On introduction into the test system of target polynucleotide, the gold nanoparticles labeled with nucleotides possessing attached complementary sequences start to associate. This induces a dramatic change of visually detected color from red to blue.

Because of extremely strong light absorption of gold nanoparticles, the straightforward application of this colorimetric method allows achieving a detection limit of ~10 femtomoles of oligonucleotide. This is already 50 times more sensitive than sandwich hybridization detection methods based on fluorescence detection. In order to further increase this sensitivity the intensity and color of scattered light was suggested to be recorded (Storhoff et al. 2004). This scatter-based method is so sensitive that it allows detection of zeptomole quantities of nucleic acid targets.

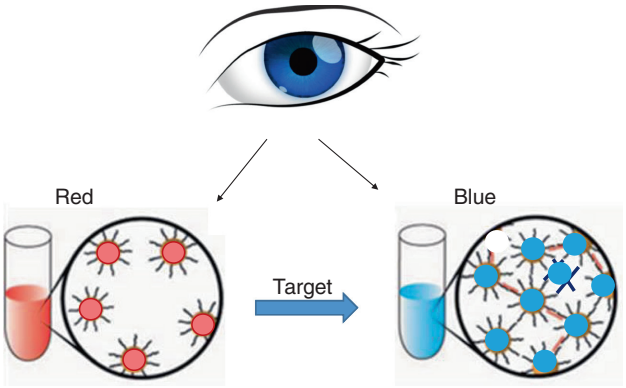

Fig. 8.19 The change of visually detected reflected/scattered color of gold nanoparticles on their association caused by their binding by polyvalent target

There are many other detection methods suggested with the use of color change of noble metal nanoparticles (Jans and Huo 2012; Saha et al. 2012). The color change based on analyte-induced aggregation/desaggregation test was suggested for the detection of low concentrations of *heavy metal ions* (Pb^{2+}, Cd^{2+}, Hg^{2+}) in aqueous solutions. The ensemble in this case consists of gold nanoparticles functionalized with alkanethiol chains carrying carboxylate groups at the distal terminal ends. Aggregation of the particles upon the addition of metal ions occurs due to ion coordination by these groups belonging to two neighbor particles. Dextran-coated gold nanoparticles aggregated with concanavalin A were used for competitive *glucose sensing* in an extended millimolar-micromolar range (Aslan et al. 2004).

8.6.2 Association-Induced FRET and Quenching

The change in physical separation between nanoparticles induces the changes in energy- and electron transfer efficiency. One of the typical applications of using *association between quantum dots* is the sensing potassium ions by observing FRET with the change of color between small (green) and large (red) CdSe/ZnS nanocrystals (Chen et al. 2006). This assay showed excellent sensitivity.

Association of *conjugated polymers* in solutions commonly leads to quenching. Since such association can be modulated by target binding (Jiang et al. 2007), this provides additional possibility for fluorescence sensing with efficient response.

Quantum dots that emit at 525 and 585 nm are used to encode aptamer-linked nanostructures sensitive to adenosine and cocaine, respectively. In addition to quantum dots, the nanostructures also contain gold nanoparticles that serve as quenchers. Addition of target analytes disassembles the nanostructures and results in increased emission from quantum dots. Simultaneous colorimetric and fluorescent detection and quantification of both molecules in one pot was demonstrated (Liu et al. 2007).

8.7 Smart Sensing with Logical Operations

Sensing and computing are always connected and both exhibit dramatic advancement in miniaturization leading them to molecular level. In information technology, miniaturization is responsible for outstanding progress seen in recent decades. But it still remains to be based on macroscopic concepts and its realization in silicon-based devices, the reduction of size of which is approaching limit. The next and definitely ultimate limit of miniaturization is that of molecules, since molecules are the smallest bodies in which information transfer can be achieved in the form of directed translocation of charge. Information inputs and outputs on molecular level can be provided by optical means, and this makes an additional strong connection between sensing and computing (Daly et al. 2014). Thus, will it be helpful to examine the background of optical sensing from a computer science viewpoint? The target could be the input, the emission – the output, the sensor serving as the processor device, and the excitation as the trigger and the power supply.

8.7.1 Why Logical Operations in Fluorescence Sensing?

In previous chapters we always implicitly assumed that with the sensor response function being of any shape, the transduction function (that connects the number of formed complexes with response that they produce) is always linear (or weighted linear as explained in Sect. 2.5). This means the existence of *strict proportionality* between the amount of *bound* target and the detected signal. However, the transduction mechanism can be more complicated and operate instead of one, with a number of output parameters, analyze their combinations and interferences. Speaking in the language of information technology, such analysis can include *logic gates* operations (Magri et al. 2007; Andréasson and Pischel 2010).

The introduction of the language of information science into sensing technology, if it is not a mental exercise, should have some important reason. The reason is, that using this language we can design and classify the sensors with *nonlinear and multiparametric operation*. For instance, if we need in a given system to obtain the response to the presence of one analyte on the background of the presence of second analyte and the absence of third analyte, in a traditional way we have to apply three separate sensors and then analyze three output signals. The results will contain extra information and it will be difficult to analyze. But we are, in principle, able to devise molecular or supramolecular construction that will do that itself and provide us an already processed single output, such as depicted in Fig. 8.20.

Molecule presented in Fig 8.20b is the *logic gate* operating according to the design principles of modular photoinduced electron transfer (PET) systems (Magri et al. 2006). More specifically, it possesses a "receptor 1-spacer 1-fluorophorespacer 2-receptor 2-spacer 3-receptor 3" format. The receptors incorporated in the design are a benzo-15-crown-5 ether as receptor 1 for Na^+, a tertiary amine as receptor 2 for H^+, and a phenyliminodiacetate as Receptor 3 for Zn^{2+}. An anthracene moiety is used as the fluorophore. The three spacer units between adjacent receptors and the fluorophore are methylene spacers. They minimize the distance between the receptors and the fluorophore, facilitating conditions for efficient PET, notably if there are folded conformers. Such construction delivers the highest fluorescence output when all three receptors are occupied with their respective inputs, i.e., sodium ions, protons and zinc ions.

This arrangement and many others presented later in the literature (Magri et al. 2007; Andréasson and Pischel 2010) demonstrate the possibility of deriving a single optical output signal from a complex analytical situation, such as simultaneous sensing of ΔpH, glutamate and zinc concentrations in neuron terminals (Hettie et al. 2014). This approach might indeed lead to a "*lab-on-a-molecule*" with interesting future implications for multi-parameter sensing. Different complex operations become possible on this pathway, including design and operation of chemical sensors with non-linear and modulated performance. Some of molecular and nano-scale devices can already perform logic operations of remarkable complexity.

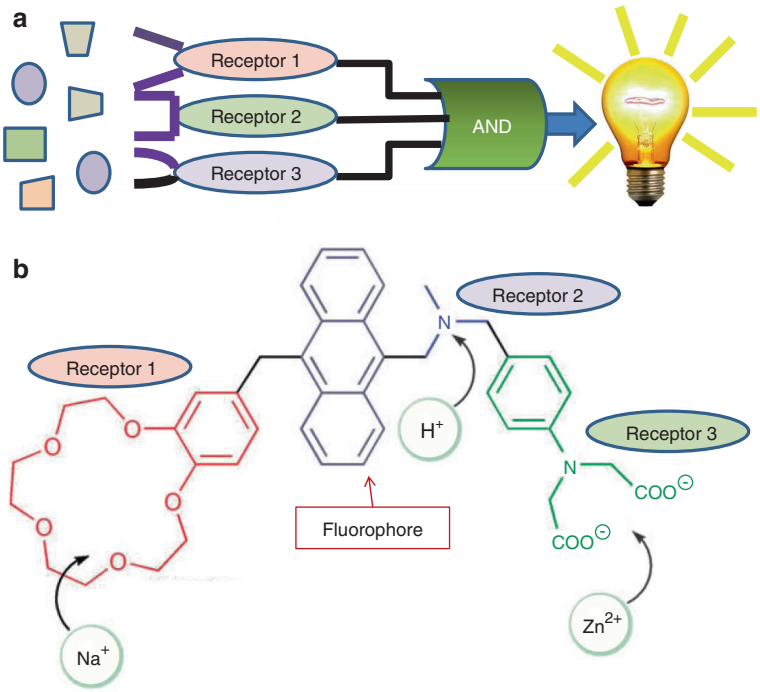

Fig. 8.20 Schematic presentation of sensor performance with molecular AND logic gate (**a**). The sensor consists of several (shown 3) types of target binding sites. On signal transduction step a logical operation is performed to provide an output signal reporting on a designed combination of occupations of these sites. (**b**) An example of such sensor performing AND logical operation (Magri et al. 2006). This molecular construction produces the highest fluorescence output when all three receptors (sodium ions, zinc ions and protons) are saturated with their ligands

8.7.2 Logical Operations on Molecular Scale

The *logic gate* operations on molecular scale are formally the same as that performed in digital computing (Magri et al. 2007), the sensors can perform basically similar operations. They are based on Boolean algebra, which is in the background of computing dealing with 0 and 1 binary code. With a single input (e.g. analyte binding) and single output (e.g. switch-on of fluorescence intensity), only two operations are possible, There are: YES when input is 0 or 1 and output is the same and NOT, which is the opposite: when input is 0 or 1, the output is 1 or 0. Thus, the simple PET system (see Fig. 8.3) can already serve as a logic gate. The PET-based luminescent switches may be triggered by various chemical and physical stimuli: protons, metal cations, anions, different organic molecules and nanoparticles.

With two inputs (such as two different targets bound to two different sites), more complicated logical operations are possible. When both inputs are 1 and 1, AND operation gives output 1, OR operation gives 1 and NOR operation gives 0. When both inputs are 0 and 0, AND operation gives 0, OR operation gives 0 and NOR operation gives 1. If, in contrast, the first input is 1 and second input is 0, then AND operation gives 0, OR operation gives 1 and NOR operation gives 0. In INHIBIT logic gate, if both inputs are either 0 or 1, the output will be 0, and if they are different, the output will be 1.

Detailed description of molecular basis of these operations can be found in the literature, and they are typically explained on examples of ion binding to fluorophore-attached chelating groups (Szacilowski 2012; Andréasson and Pischel 2010). OR is the operation, that can be achieved with a sensor receptor without selectivity in input stimuli, e.g. when it does not recognize between the binding of two or several different ions producing the same output. Molecular AND logic gates can be constructed of two receptors and a fluorescent unit linked covalently with both the receptors. In contrast to the OR gate, in AND gate the fluorescence should be switched on only when both receptors bind corresponding substrates.

Implementation on molecular scale of other functions is more complicated and can involve combination of receptors and/or reporters. For instance, molecular-scale implementation of an XOR gate requires a chemical system, which responds to two different stimuli in a complex way: any of these two stimuli should switch on the gate, while concomitant presence of both triggering molecules should leave the system in the OFF state. This gate is in the core of complex logic systems: binary comparators and arithmetic units (half adder, half subtractor, full adder, etc.). Design of molecular structures that could be such signal transformers is sometimes a difficult task. Meantime, with different and multi-target inputs and also the combination of emitters and of the mechanisms of signal transduction, such functions can be realized.

8.7.3 Exploration of Basic Signal Transduction Mechanisms

Photoinduced electron transfer (PET) has proved to be the efficient mechanism in performing basic logic operations (de Silva and Uchiyama 2011; Magri et al. 2007) because it can be easily realized in small-molecular organic donor-spacer-acceptor systems. There are many examples using this photophysical process for molecular-level implementation of single-input logic gates such as YES and NOT. Molecular versions of double-input logic gates such as AND, OR, NOR, NAND, INHIBIT, and XOR were realized. A prototypical number-processing system can attain a half-adder function. Presented in Fig. 8.20 is an example of molecular construction with AND logic gate.

Many possibilities appear when a nanocomposite is assembled with luminophores excited at different wavelengths and, being *connected by FRET*, emitting on different wavelength and time scales. Thus, quantum dots were combined with the long-lifetime terbium complexes (Tb), a near-IR Alexa Fluor dye (A647), and self-assembling peptides (Claussen et al. 2013b). Such composite based on time-gated FRET demonstrates the functioning of a combinatorial and sequential logic device (Fig. 8.21).

Upon excitation, the Tb-QD-A647 FRET-complex produces the time-dependent photoluminescent signatures from multi-FRET pathways enabled by the capacitor-like behavior of the Tb. This system allows manipulating with the dye/

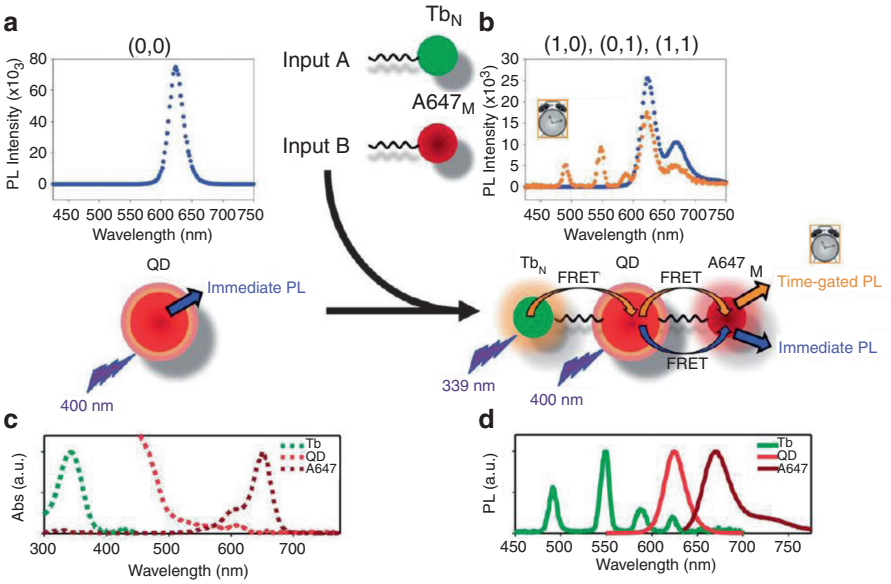

Fig. 8.21 Logic device based on variability in wavelength-dependent input and time-gated output in a system connected by FRET (Claussen et al. 2013a). Device consists of terbium(III) complex (Tb, *left green*) and Alexa Fluor 647 dye (A647, *right red*) conjugates co-assembled around a *central quantum dot* (QD, *center red*) via peptide linkers. Four input states can be realized. (**a**) Initial input state (0,0) contains QD with no Input A (A647) nor Input B (Tb). The (**b**) subsequent states ((0,1), (1,0), (1,1)) contain distinct valences of Input A and Input B. Inset photoluminescence (PL) plots display the output PL intensity immediately (*blue plot*) and 55 ms (*orange plot*) after UV excitation. QD peak PL ~625 nm; Tb peaks at ~490, 550, 585, and 620; A647 peak PL ~670 nm. Note, the contribution of the Tb peak at 620 nm to the QD peak at 625 nm is deconvolved and accounted for in all logic gates. Immediate PL monitoring (*blue*) results in (**a**) either direct QD PL or in (**b**) QD-A647 FRET and emission from both. Time-delayed PL monitoring (*orange* – indicated by the clock) results in a convolution of Tb, QD, and A647 PL (**b**). Changing the valence of TbN- or A647M per QD provides for control over the magnitude, and to some extent influence, of these inputs on device emission. For time-gated monitoring, the Tb is preferentially excited at 339 nm, while for immediate PL monitoring the QD is excited at 400 nm, which excludes the excitation of Tb. Normalized absorption (**c**) and emission (**d**) spectra for the Tb, QD and A647

Tb inputs by variation of excitation wavelength and time-gating signal collection. Fluorescent output is converted into Boolean logic states to create complex arithmetic circuits including the half-adder/half-subtractor, 2:1 multiplexer/1:2 demultiplexer, and a 3-digit, 16-combination keypad lock. The key element of this nano-device is the Tb luminophore that, with its millisecond lifetime, serves as a memory element capable of "storing/carrying" information, while directly sensitizing the QDs and indirectly sensitizing any downstream FRET acceptors attached to the QD (Claussen et al. 2013a). Application of long-lifetime emitting lanthanides expands dramatically the toolbox for constructing new logical elements (Pu et al. 2014).

8.7.4 Applications in Sensing and Imaging Technologies

Design of logic gate elements are closely related to the development of multiplexing (many inputs) and multiparametric (many outputs) sensor technologies and expand their possibilities. Applying single type of sensor units, direct detection of two or even three analytes at once becomes possible. Moreover, a response can be programmed based on concentration ratios of several analytes with established threshold, above which the output signal is released.

The suggested constructs are mainly based on the products of synthetic organic chemistry. They are made by assembling several ion recognition sites with two or more organic heterocycles that provide the signal transduction and response. This transduction is based on the basic mechanisms that were discussed above, PET, ICT and FRET. It was shown that efficient signal processing can be achieved with one or several fluorophores and electron donors or acceptors coupled with ion binding sites (Straight et al. 2007). Even the combination of ion chelating group and pH-titrated group may be surprisingly efficient for providing two inputs (concentrations of ions and of protons).

In the construction of logic gates, special attention has started to be paid to *photochromes* (Gust et al. 2006). They are organic molecules that are isomerized by light between two stable forms. They can be covalently linked to other dyes, so that the changes in their properties resulting from photoisomerization can be used to switch the electron and energy transfer on or off. With the aid of photochromes the problem of not only the transformation but also of the storage of information on molecular level can be resolved.

Other developments of *molecular logic gates* include designing constructs involving DNA (Okamoto et al. 2004), deoxyribozymes (Stojanovic and Stefanovic 2003), peptide nucleic acid (PNA) (Cheah et al. 2005), DNA aptamers (Yoshida and Yokobayashi 2007) and cationic conjugated polymer/DNA assemblies with ethidium bromide as intercalating reporter dye (Zhou et al. 2005). For connecting the elements performing logic functions, different types of '*molecular wires*' were developed. They can explore the excitonic conduction mechanism that can be realized in conducting polymers (Yashchuk et al. 2000). In connecting the functional

elements, these neutral (electron + hole) quasi-particles can display a one-way conductivity.

Realizing the multi-channel outputs in '*molecular computing*' requires from fluorescent reporter to be present in several recognizable emissive states (Perez-Inestrosa et al. 2007). This problem, in principle, can be resolved with color-changing fluorescent dyes based on different excited-state processes (see above, Sect. 8.1).

Interestingly, smart molecules allow not only computing but also *protecting the information* on the molecular scale (Margulies et al. 2007). By exploiting the principles of molecular Boolean logic, a molecular device can be developed that mimics the operation of an electronic keypad lock, e.g., a common security circuit used for numerous applications, in which access to an object or data is to be restricted to a limited number of persons. The 'password' should include not only the proper combination of the inputs but also the correct order by which they are introduced. It was shown that different 'passwords' can be coded by a combination of two chemical and one optical input signals, which can activate, separately, blue or green fluorescence output channels from pyrene or fluorescein fluorophores. The information in each channel is a single-bit light output signal that can be used to authorize a user, to verify authentication of a product, or to initiate a higher-level process.

Such smart sensors are highly needed in cellular research. Tunable fluorescent molecular logic gates with applications to neuronal imaging focus on the studies of neurodegenerative diseases (Hettie et al. 2014). The three-input AND molecular logic gates are based on the coumarin-3-aldehyde scaffold and designed to give a turn-on fluorescence response upon the co-release of glutamate and zinc ions from secretory vesicles via exocytosis.

There are attempts to expand the utility of digital logics concept to processes outside optical input and optical or electronic output. As their result, a two-module molecular de-multiplexer was synthesized, in which the output is switching between near-IR emission and photochemical generation of cytotoxic singlet oxygen (Erbas-Cakmak et al. 2013). In the neutral form, the designed compound fluoresces brightly under excitation at 625 nm. However, acid addition moves the absorption bands of the two modules in opposite directions, resulting in an effective reversal of excitation energy transfer direction with suppression of fluorescence and a concomitant upsurge of singlet oxygen generation. Since the switching occurs exactly in the same pH range as the difference in intrinsic pH between normal and cancer cells, under the same excitation conditions the cancer cells can be selectively destroyed by singlet oxygen action, whereas the cells in the surrounding healthy tissue may rest without damage and fluoresce brightly. Realizing such ideas on switching between diagnostic and therapeutic modes is highly needed in theranostics (see Sect. 14.4). And the fact that this can be done on the level of composite organic molecule allows making very optimistic predictions.

8.7.5 Prospects

We observe that organic molecules, nanostructures and their compositions allow not only transduction of sensor output signal into emissive form but also are able to provide its non-linear transformation, simulating the operation of elementary digital computational devices. There is a possibility to go deeper and to request from designed molecules to perform smart logical operations, serving as logic gates. The excited-state reactions of electron, proton and energy transfers offer such possibility. The fact that these reactions are triggered by light and allow optical output and can be coupled by design in different ways may allow solving important problem of intelligent transformation of reporter signal already on molecular or nano-scale level.

As a result of these complicated multiparametric logical operations an already processed output signal can be obtained. No doubt, digital logics will be a common language in these developments.

The term '*lab-on-a-molecule*' is ready for use to coin the multifunctional and multiparametric sensors (Daly et al. 2014), although the real distance to their practical use is not so short. Many of the fluorescent molecular device designs, e.g. based on PET switching principle were established for small molecules. They can serve as starting points for achieving new steps of complexity and perfectness on nanoscale (Claussen et al. 2013a).

8.8 Sensing and Thinking: How to Couple the Recognition and Reporting Functionalities?

Summing up, we list the basic mechanisms of signal transduction that operate in fluorescence sensors coupling the target binding and fluorescence (luminescence) response.

Very short on the scale of distances is the *intramolecular charge transfer* (ICT). It can operate within π-conjugated electronic system and is able to transform directly the weak interaction energy of target binding into the spectral shifts. Elementary act in intramolecular proton transfer (ESIPT) occurs at even shorter distances (proton is much heavier than electron and its wavefunction is shorter), but in organic dyes this transfer is often coupled with conformational isomerizations, making-breaking of hydrogen bonds and ICT. The 3-hydroxychromone family of dyes is unique among well-described systems, in which ESIPT is coupled only with ICT, and this allows obtaining strong two-band ratiometric response. Both of these basic phenomena (and their frequently observed coupling) can generate wavelength-dependent switching of fluorescence intensity and provide response in a broad dynamic range.

Photoinduced electron transfer (PET) can operate also at short distances between localized electronic systems. It can be both intramolecular and intermolecular. Intramolecular transfer requires separation between donor and acceptor fragments by only one or two single bond bridges, and intermolecular transfer needs direct

contact between them. All these mechanisms are basic and universal, but for their realization they need proper molecular structures, that can be the most efficiently provided by organic dyes.

The *Förster resonance energy transfer* (FRET) can operate at greater distances, up to 8–10 nm. It is much more universal and can be realized with all kinds of emissive molecules and particles as the donors and all kinds of light-absorbing acceptors if the conditions regarding distance, orientation and spectral overlap are satisfied. Collective effects in FRET allow achieving efficient light-harvesting and wavelength-shifting that allows broad-range manipulations with the wavelength and sensitivity of response.

Conformational isomerizations add a new dimension to signal transduction. They offer many possibilities for coupling the target binding with the response. They are especially important in the cases of large and neutral target molecules, the binding of which does not produce the perturbation sufficient for direct modulation of IST, PET or ESIPT. Target-induced *aggregation of nanoparticles* is an additional possibility of detecting the large-size and multivalent binding targets.

The ability of molecular sensors to perform elementary logical operations opens new horizons for exploration and promises new advanced products.

Questions and Problems

1. Explain the relation between photoinduced electron transfer (PET) and fluorescence quenching. Does PEt always lead to quenching? Is quenching always the result of PET?
2. What is the distance dependence for PET? What other factors determine PET efficiency? Suggest several examples for using these factors in the construction of sensors.
3. Based on what criteria would you differentiate ICT and PET? Suggest the sensor designs that can be realized with PET but cannot with ICT and vice versa. What methods of fluorescence detection shown in Fig. 3.4 are applicable for the detection of response based on PET and what on ICT?
4. Identify the electron-donating and electron-withdrawing groups in the structure of ketocyanine dye described in Sect. 4.3. Suggest how the dipole moment is oriented in this molecule.
5. How LE and ICT emissions depend on solvent polarity? Can the switching between them be induced by changing the temperature? If yes, in what direction is this change and what is its mechanism?
6. What are the differences in requirements for observation and in reaction mechanisms between intermolecular and intramolecular proton transfers?
7. List and explain *collective* effects in FRET. What will be the spectroscopic effects in the following cases: (a) dye molecules of only one type are present in the system; (b) molecules of one type with the added quencher; (c) molecules of one type (donors) with the added acceptor.
8. Explain the antenna effect. Is the energy transfer between the donors (homo-FRET) important for manifestation and application of antenna effect?
9. Evaluate the properties of different dyes and nanoparticles as FRET donors and acceptors. Select the optimal donor-acceptor pairs for (a) the measurements

of intensity; (b) the two-band ratiometric measurements; (c) the measurements of lifetimes.

10. What is the induced folding of macromolecules? How can it be used in sensing?
11. Can molecular beacons be immobilized on a surface? What transduction mechanisms can be used when molecular beacon is in solution and when it is immobilized?
12. Try to suggest the structures alternative to molecular beacons performing the same function – hybridization with single strand DNA with the reporting based on conformational change.
13. What are the advantages and disadvantages of maltose binding protein as a scaffold for the design of various sensors? What are the optimal detection methods to be used with this protein as the sensor: (a) with single labeling? (b) with double labeling?
14. Why the aggregates of noble metal nanoparticles change their color?
15. Analyze the inputs, the outputs and the transduction mechanisms in operation of sensor depicted in Fig. 8.21. What is the role of FRET? Can the Tb luminophore be substituted?

References

Abe R, Ohashi H, Iijima I, Ihara M, Takagi H, Hohsaka T, Ueda H (2011) "Quenchbodies": quench-based antibody probes that show antigen-dependent fluorescence. J Am Chem Soc 133(43):17386–17394

Andréasson J, Pischel U (2010) Smart molecules at work—mimicking advanced logic operations. Chem Soc Rev 39(1):174–188

Aneja A, Mathur N, Bhatnagar PK, Mathur PC (2008) Triple-FRET technique for energy transfer between conjugated polymer and TAMRA dye with possible applications in medical diagnostics. J Biol Phys 34(5):487–493

Arnaut LG, Formosinho SJ (1993) Excited-state proton-transfer reactions. 1. Fundamentals and intermolecular reactions. J Photochem Photobiol A Chem 75(1):1–20

Aslan K, Lakowicz JR, Geddes CD (2004) Tunable plasmonic glucose sensing based on the dissociation of Con A-aggregated dextran-coated gold colloids. Anal Chim Acta 517(1–2):139–144

Baek MG, Stevens RC, Charych DH (2000) Design and synthesis of novel glycopolythiophene assemblies for colorimetric detection of influenza virus and E. coli. Bioconjug Chem 11(6):777–788

Barbara PF, Gesquiere AJ, Park SJ, Lee YJ (2005) Single-molecule spectroscopy of conjugated polymers. Acc Chem Res 38(7):602–610

Beutler M, Makrogianneli K, Vermeij RJ, Keppler M, Ng T, Jovin TM, Heintzmann R (2008) satFRET: estimation of Forster resonance energy transfer by acceptor saturation. Eur Biophys J 38(1):69–82

Bhattacharyya K, Chowdhury M (1993) Environmental and magnetic field effects on exciplex and twisted charge transfer emission. Chem Rev 93:507–535

Blough NV, Simpson DJ (1988) Chemically mediated fluorescence yield switching in nitroxide-fluorophore adducts: optical sensors of radical/redox reactions. J Am Chem Soc 110:1915–1917

Bognar B, Osz E, Hideg K, Kalai T (2006) Synthesis of new double (spin and fluorescence) sensor reagents and labels. J Heterocycl Chem 43(1):81–86

Boudier C, Klymchenko AS, Mely Y, Follenius-Wund A (2009) Local environment perturbations in alpha1-antitrypsin monitored by a ratiometric fluorescent label. Photochem Photobiol Sci 8(6):814–821. doi:10.1039/b902309g

Bourgeois D, Adam V (2012) Reversible photoswitching in fluorescent proteins: a mechanistic view. IUBMB Life 64(6):482–491. doi:10.1002/iub.1023

Bourson J, Pouget J, Valeur B (1993) Ion-responsive fluorescent compounds. 4. Effect of cation binding on the photophysical properties of a coumarin linked to monoaza- and diaza-crown esters. J Phys Chem 97:4552–4557

Brandt O, Hoheisel JD (2004) Peptide nucleic acids on microarrays and other biosensors. Trends Biotechnol 22(12):617–622

Bublitz GU, Boxer SG (1997) Stark spectroscopy: applications in chemistry, biology, and materials science. Annu Rev Phys Chem 48:213–242

Burda C, Chen XB, Narayanan R, El-Sayed MA (2005) Chemistry and properties of nanocrystals of different shapes. Chem Rev 105(4):1025–1102

Castellano FN, Dattelbaum JD, Lakowicz JR (1998) Long-lifetime Ru(II) complexes as labeling reagents for sulfhydryl groups. Anal Biochem 255(2):165–170

Chattopadhyay A, London E (1987) Parallax method for direct measurement of membrane penetration depth utilizing fluorescence quenching by spin-labeled phospholipids. Biochemistry 26(1):39–45

Cheah IK, Langford SJ, Latter MJ (2005) Concept transfer – from genetic instruction to molecular logic. Supramol Chem 17(1–2):121–128

Chen LH, McBranch DW, Wang HL, Helgeson R, Wudl F, Whitten DG (1999) Highly sensitive biological and chemical sensors based on reversible fluorescence quenching in a conjugated polymer. Proc Natl Acad Sci U S A 96(22):12287–12292

Chen CY, Cheng CT, Lai CW, Wu PW, Wu KC, Chou PT, Chou YH, Chiu HT (2006) Potassium ion recognition by 15-crown-5 functionalized CdSe/ZnS quantum dots in H2O. Chem Commun 3:263–265

Cho YS, Kim KM, Lee D, Kim WJ, Ahn KH (2013) Turn-on fluorescence detection of apoptotic cells using a zinc (II)-dipicolylamine-functionalized poly (diacetylene) liposome. Chem Asian J 8(4):755–759

Choi K, Hamilton AD (2001) A dual channel fluorescence chemosensor for anions involving intermolecular excited state proton transfer. Angew Chem Int Ed 40(20):3912–3915

Choi SU, Ryu SY, Yoon SK, Jung NP, Park SH, Kim KH, Choi EJ, Lee CO (1999) Effects of flavonoids on the growth and cell cycle of cancer cells. Anticancer Res 19(6B):5229–5233

Claussen JC, Algar WR, Hildebrandt N, Susumu K, Ancona MG, Medintz IL (2013a) Biophotonic logic devices based on quantum dots and temporally-staggered Förster energy transfer relays. Nanoscale 5(24):12156–12170

Claussen JC, Hildebrandt N, Susumu K, Ancona MG, Medintz IL (2013b) Complex logic functions implemented with quantum dot bionanophotonic circuits. ACS Appl Mater Interfaces 6(6):3771–3778

Cooley LA, Martin VV, Gee KR (2013) Development and in vitro characterization of ratiometric and intensity-based fluorescent ion sensors. In: Chemical neurobiology. Meth Mol Biol v. 995 Springer New York, pp 133–145

Daly B, Ling J, de Silva AP (2014) Information gathering and processing with fluorescent molecules. Front Chem Sci Eng 8(2):240–251

Davenport LD, Knutson JR, Brand L (1986) Excited-state proton transfer of equilenin and dihydro equilenin: inreractions with bilayer vesicles. Biochemistry 25:1186–1195

de Lorimier RM, Smith JJ, Dwyer MA, Looger LL, Sali KM, Paavola CD, Rizk SS, Sadigov S, Conrad DW, Loew L, Hellinga HW (2002) Construction of a fluorescent biosensor family. Protein Sci 11(11):2655–2675

De Schryver FC, Vosch T, Cotlet M, Van der Auweraer M, Mullen K, Hofkens J (2005) Energy dissipation in multichromophoric single dendrimers. Acc Chem Res 38(7):514–522

de Silva AP, Uchiyama S (2011) Molecular logic gates and luminescent sensors based on photoinduced electron transfer. In: Luminescence applied in sensor science. Springer Berlin-Heidelberg, pp 1–28

de Silva AP, Gunaratne HQN, Gunnaugsson T, Huxley AJM, McRoy CP, Rademacher JT, Rice TE (1997) Signaling recognition events with fluorescent sensors and switches. Chem Rev 97:1515–1566

de Silva AP, Fox DB, Moody TS, Weir SM (2001) The development of molecular fluorescent switches. Trends Biotechnol 19(1):29–34

Demchenko AP (2001) Recognition between flexible protein molecules: induced and assisted folding. J Mol Recognit 14(1):42–61

Demchenko AP (2006) Visualization and sensing of intermolecular interactions with two-color fluorescent probes. FEBS Lett 580(12):2951–2957
Demchenko AP (2009) Introduction to fluorescence sensing. Springer, Amsterdam
Demchenko AP (2010) The concept of lambda-ratiometry in fluorescence sensing and imaging. J Fluoresc 20(5):1099–1128
Demchenko AP (2013) Nanoparticles and nanocomposites for fluorescence sensing and imaging. Meth Appl Fluoresc 1(2):022001
Demchenko AP, Yesylevskyy SO (2009) Nanoscopic description of biomembrane electrostatics: results of molecular dynamics simulations and fluorescence probing. Chem Phys Lipids 160(2):63–84
Demchenko AP, Mely Y, Duportail G, Klymchenko AS (2009) Monitoring biophysical properties of lipid membranes by environment-sensitive fluorescent probes. Biophys J 96(9):3461–3470
Demchenko AP, Tang KC, Chou PT (2013) Excited-state proton coupled charge transfer modulated by molecular structure and media polarization. Chem Soc Rev 42(3):1379–1408. doi:10.1039/c2cs35195a
Díaz SA, Giordano L, Jovin TM, Jares-Erijman EA (2012) Modulation of a photoswitchable dual-color quantum dot containing a photochromic FRET acceptor and an internal standard. Nano Lett 12(7):3537–3544. doi:10.1021/nl301093s
Dore K, Leclerc M, Boudreau D (2006) Investigation of a fluorescence signal amplification mechanism used for the direct molecular detection of nucleic acids. J Fluoresc 16(2):259–265
Dudley AM, Aach J, Steffen MA, Church GM (2002) Measuring absolute expression with microarrays with a calibrated reference sample and an extended signal intensity range. Proc Natl Acad Sci U S A 99(11):7554–7559
Elghanian R, Storhoff JJ, Mucic RC, Letsinger RL, Mirkin CA (1997) Selective colorimetric detection of polynucleotides based on the distance-dependent optical properties of gold nanoparticles. Science 277(5329):1078–1081
El-Kemary M, Rettig W (2003) Multiple emission in coumarins with heterocyclic substituents. Phys Chem Chem Phys 5:5221–5228
Erbas-Cakmak S, Bozdemir OA, Cakmak Y, Akkaya EU (2013) Proof of principle for a molecular 1: 2 demultiplexer to function as an autonomously switching theranostic device. Chem Sci 4(2):858–862. doi:10.1039/c2sc21499g
Fan J, Hu M, Zhan P, Peng X (2013) Energy transfer cassettes based on organic fluorophores: construction and applications in ratiometric sensing. Chem Soc Rev 42(1):29–43
Fonin AV, Stepanenko OV, Povarova OI, Volova CA, Philippova EM, Bublikov GS, Kuznetsova IM, Demchenko AP, Turoverov KK (2014) Spectral characteristics of the mutant form GGBP/H152C of D-glucose/D-galactose-binding protein labeled with fluorescent dye BADAN: influence of external factors. PeerJ 2:e275
Formosinho SJ, Arnaut LG (1993) Excited-state proton-transfer reactions. 2. Intramolecular reactions. J Photochem Photobiol A Chem 75(1):21–48
Gilardi G, Zhou LQ, Hibbert L, Cass AE (1994) Engineering the maltose binding protein for reagentless fluorescence sensing. Anal Chem 66(21):3840–3847
Giordano L, Jovin TM, Irie M, Jares-Erijman EA (2002) Diheteroarylethenes as thermally stable photoswitchable acceptors in photochromic fluorescence resonance energy transfer (pcFRET). J Am Chem Soc 124(25):7481–7489. doi:ja016969k [pii]
Grabowski ZR, Rotkiewicz K, Rettig W (2003) Structural changes accompanying intramolecular charge transfer: focus on twisted intramolecular charge transfer states and structures. Chem Rev 103:3899–4031
Granda-Valdes M, Badia R, Pina-Luis G, Diaz-Garcia ME (2000) Photoinduced electron transfer systems and their analytical application in chemical sensing. Quim Anal 19:38–53
Grynkiewicz G, Poenie M, Tsien RY (1985) A new generation of Ca2+ indicators with greatly improved fluorescence properties. J Biol Chem 260(6):3440–3450
Guliyev R, Coskun A, Akkaya EU (2009) Design strategies for ratiometric chemosensors: modulation of excitation energy transfer at the energy donor site. J Am Chem Soc 131(25):9007–9013
Gust D, Moore TA, Moore AL (2006) Molecular switches controlled by light. Chem Commun 11:1169–1178

Ha JH, Loh SN (2012) Protein conformational switches: from nature to design. Chemistry A Eur J 18(26):7984–7999
Heinlein T, Knemeyer J-P, Piestert O, Sauer M (2003) Photoinduced electron transfer between fluorescent dyes and guanosine residues in DNA-hairpins. J Phys Chem B 107:7957–7964
Henary MM, Wu YG, Cody J, Sumalekshmy S, Li J, Mandal S, Fahrni CJ (2007) Excited-state intramolecular proton transfer in 2-(2'-arylsulfonamidophenyl)benzimidazole derivatives: the effect of donor and acceptor substituents. J Org Chem 72(13):4784–4797
Herland A, Thomsson D, Mirzov O (2008) Decoration of amyloid fibrils with luminescent conjugated polymers. J Mater Chem 18:126–132
Hermann T, Patel DJ (2000) Biochemistry – adaptive recognition by nucleic acid aptamers. Science 287(5454):820–825
Hettie KS, Klockow JL, Glass TE (2014) Three-input logic gates with potential applications for neuronal imaging. J Am Chem Soc 136(13):4877–4880
Ho HA, Leclerc M (2004) Optical sensors based on hybrid aptamer/conjugated polymer complexes. J Am Chem Soc 126(5):1384–1387
Hochreiner H, Sanchez-Barragan I, Costa-Fernandez JM, Sanz-Medel A (2005) Dual emission probe for luminescence oxygen sensing: a critical comparison between intensity, lifetime and ratiometric measurements. Talanta 66(3):611–618
Huang J, Peng AD, Fu HB, Ma Y, Zhai TY, Yao JN (2006) Temperature-dependent ratiometric fluorescence from an organic aggregates system. J Phys Chem A 110(29):9079–9083
Jans H, Huo Q (2012) Gold nanoparticle-enabled biological and chemical detection and analysis. Chem Soc Rev 41(7):2849–2866
Jares-Erijman EA, Jovin TM (2003) FRET imaging. Nat Biotechnol 21(11):1387–1395
Jeong H-J, Ueda H (2014) Strategy for making a superior Quenchbody to proteins: effect of the fluorophore position. Sensors 14(7):13285–13297
Jiang H, Zhao XY, Schanze KS (2007) Effects of polymer aggregation and quencher size on amplified fluorescence quenching of conjugated polyelectrolytes. Langmuir 23(18):9481–9486
Johansson MK, Cook RM (2003) Intramolecular dimers: a new design strategy for fluorescence-quenched probes. Chemistry 9(15):3466–3471. doi:10.1002/chem.200304941
Jones RM, Bergstedt TS, Buscher CT, McBranch D, Whitten D (2001) Superquenching and its applications in J-aggregated cyanine polymers. Langmuir 17(9):2568–2571
Kasha M (1986) Proton-transfer spectroscopy – perturbation of the tautomerization potential. J Chem Soc Faraday Trans II 82:2379–2392
Kim S, Pudavar HE, Prasad PN (2006) Dye-concentrated organically modified silica nanoparticles as a ratiometric fluorescent pH probe by one- and two-photon excitation. Chem Commun (Camb) 19:2071–2073
Klymchenko AS, Demchenko AP (2002) Electrochromic modulation of excited-state intramolecular proton transfer: the new principle in design of fluorescence sensors. J Am Chem Soc 124(41):12372–12379
Knemeyer JP, Marme N, Sauer M (2000) Probes for detection of specific DNA sequences at the single-molecule level. Anal Chem 72(16):3717–3724
Kohn JE, Plaxco KW (2005) Engineering a signal transduction mechanism for protein-based biosensors. Proc Natl Acad Sci U S A 102(31):10841–10845
Kollmannsberger M, Rurack K, Resch-Genger U, Daub J (1998) Ultrafast charge transfer in amino-substituted boron dipyrromethene dyes and its inhibition by cation complexation: a new design concept for highly sensitive fluorescent probes. J Phys Chem A 102(50):10211–10220
Koner AL, Schatz J, Nau WM, Pischel U (2007) Selective sensing of citrate by a supramolecular 1,8-naphthalimide/calix[4]arene assembly via complexation-modulated pK(a) shifts in a ternary complex. J Org Chem 72(10):3889–3895
Kwon JE, Park SY (2011) Advanced organic optoelectronic materials: harnessing Excited-State Intramolecular Proton Transfer (ESIPT) process. Adv Mater 23(32):3615–3642

Laws WR, Brand L (1979) Analysis of two-state excited-state reactions. The fluorescence decay of 2-naphthol. J Phys Chem 83:795–802
Li C, Numata M, Takeuchi M, Shinkai S (2005) A sensitive colorimetric and fluorescent probe based on a polythiophene derivative for the detection of ATP. Angew Chem Int Ed Engl 44(39):6371–6374
Li Q, Zhang J, Sun W, Yu J, Wu C, Qin W, Chiu DT (2014) Europium-complex grafted polymer dots for amplified quenching and cellular imaging applications. Langmuir 30(28), 8607–8614
Liu J, Lee JH, Lu Y (2007) Quantum dot encoding of aptamer-linked nanostructures for one-pot simultaneous detection of multiple analytes. Anal Chem 79(11):4120–4125
Lozinsky E, Martin VV, Berezina TA, Shames AI, Weis AL, Likhtenshtein GI (1999) Dual fluorophore-nitroxide probes for analysis of vitamin C in biological liquids. J Biochem Biophys Methods 38(1):29–42
Lu L, Helgeson R, Jones RM, McBranch D, Whitten D (2002) Superquenching in cyanine pendant poly(L-lysine) dyes: dependence on molecular weight, solvent, and aggregation. J Am Chem Soc 124(3):483–488
Magri DC, Brown GJ, McClean GD, de Silva AP (2006) Communicating chemical congregation: a molecular AND logic gate with three chemical inputs as a “lab-on-a-molecule” prototype. J Am Chem Soc 128(15):4950–4951
Magri DC, Vance TP, de Silva AP (2007) From complexation to computation: recent progress in molecular logic. Inorg Chim Acta 360(3):751–764
Margulies D, Felder CE, Melman G, Shanzer A (2007) A molecular keypad lock: a photochemical device capable of authorizing password entries. J Am Chem Soc 129(2):347–354
Marme N, Knemeyer JP, Sauer M, Wolfrum J (2003) Inter- and intramolecular fluorescence quenching of organic dyes by tryptophan. Bioconjug Chem 14(6):1133–1139
Marras SA (2006) Selection of fluorophore and quencher pairs for fluorescent nucleic acid hybridization probes. Methods Mol Biol 335:3–16
Matsushita M, Meijler MM, Wirsching P, Lerner RA, Janda KD (2005) A blue fluorescent anti body-cofactor sensor for mercury. Org Lett 7(22):4943–4946
Medintz IL, Deschamps JR (2006) Maltose-binding protein: a versatile platform for prototyping biosensing. Curr Opin Biotechnol 17(1):17–27
Medintz IL, Goldman ER, Lassman ME, Mauro JM (2003) A fluorescence resonance energy transfer sensor based on maltose binding protein. Bioconjug Chem 14(5):909–918
Minta A, Kao JP, Tsien RY (1989) Fluorescent indicators for cytosolic calcium based on rhodamine and fluorescein chromophores. J Biol Chem 264(14):8171–8178
Miyawaki A, Llopis J, Heim R, McCaffery JM, Adams JA, Ikura M, Tsien RY (1997) Fluorescent indicators for Ca2+ based on green fluorescent proteins and calmodulin. Nature 388(6645):882–887
Miyawaki A, Griesbeck O, Heim R, Tsien RY (1999) Dynamic and quantitative Ca2+ measurements using improved cameleons. Proc Natl Acad Sci U S A 96(5):2135–2140
Mordon S, Devoisselle JM, Soulie S (1995) Fluorescence spectroscopy of pH in vivo using a dual-emission fluorophore (C-SNAFL-1). J Photochem Photobiol B 28(1):19–23
Nilsson KPR, Inganas O (2004) Optical emission of conjugated polyuelectrolite. Calcium-induced conformational changes in calmodulin and calmodulin-calcineurin interactions. Macromolecules 37:9109–9113
Nilsson KP, Rydberg J, Baltzer L, Inganas O (2003) Self-assembly of synthetic peptides control conformation and optical properties of a zwitterionic polythiophene derivative. Proc Natl Acad Sci U S A 100(18):10170–10174
O’Neal DP, Meledeo MA, Davis JR, Ibey BL, Gant VA, Pishko MV, Cote GL (2004) Oxygen sensor based on the fluorescence quenching of a ruthenium complex immobilized in a biocompatible poly(ethylene glycol) hydrogel. IEEE Sens J 4(6):728–734
Okamoto A, Tanaka K, Saito I (2004) DNA logic gates. J Am Chem Soc 126(30):9458–9463
Papkovsky DB, O'Riordan TC (2005) Emerging applications of phosphorescent metalloporphyrins. J Fluoresc 15(4):569–584

Pecher J, Mecking S (2010) Nanoparticles of conjugated polymers. Chem Rev 110(10):6260–6279
Perez-Inestrosa E, Montenegro JM, Collado D, Suau R, Casado J (2007) Molecules with multiple light-emissive electronic excited states as a strategy toward molecular reversible logic gates. J Phys Chem C 111(18):6904–6909
Petitjean A, Lehn JM (2007) Conformational switching of the pyridine-pyrimidine-pyridine scaffold for ion-controlled FRET. Inorg Chim Acta 360(3):849–856
Pickup JC, Khan F, Zhi Z-L, Coulter J, Birch DJ (2013) Fluorescence intensity-and lifetime-based glucose sensing using glucose/galactose-binding protein. J Diabetes Sci Technol 7(1):62–71
Pivovarenko VG, Klueva AV, Doroshenko AO, Demchenko AP (2000) Bands separation in fluorescence spectra of ketocyanine dyes: evidence for their complex formation with monohydric alcohols. Chem Phys Lett 325(4):389–398
Plaxco KW, Soh HT (2011) Switch-based biosensors: a new approach towards real-time, in vivo molecular detection. Trends Biotechnol 29(1):1–5
Povrozin YA, Markova LI, Tatarets AL, Sidorov VI, Terpetschnig EA, Patsenker LD (2009) Near-infrared, dual-ratiometric fluorescent label for measurement of pH. Anal Biochem 390(2):136–140
Pu F, Ren J, Qu X (2014) "Plug and play" logic gates based on fluorescence switching regulated by self-assembly of nucleotide and lanthanide ions. ACS Appl Mater Interfaces 6(12):9557–9562
Puleo CM, Liu K, Wang TH (2006) Pushing miRNA quantification to the limits: high-throughput miRNA gene expression analysis using single-molecule detection. Nanomedicine 1(1): 123–127
Raymo FM, Yildiz I (2007) Luminescent chemosensors based on semiconductor quantum dots. Phys Chem Chem Phys 9(17):2036–2043
Roshal AD, Grigorovich AV, Doroshenko AO, Pivovarenko VG, Demchenko AP (1998) Flavonols and crown-flavonols as metal cation chelators. The different nature of Ba2+ and Mg2+ complexes. J Phys Chem A 102(29):5907–5914
Roshal AD, Grigorovich AV, Doroshenko AO, Pivovarenko VG, Demchenko AP (1999) Flavonols as metal-ion chelators: complex formation with Mg2+ and Ba2+ cations in the excited state. J Photochem Photobiol A Chem 127(1–3):89–100
Rurack K (2001) Flipping the light switch 'on' – the design of sensor molecules that show cation-induced fluorescence enhancement with heavy and transition metal ions. Spectrochim Acta A 57:2161–2195
Rurack K, Danel A, Rotkiewicz K, Grabka D, Spieles M, Rettig W (2002) 1,3-Diphenyl-1H-pyrazolo[3,4-b]quinoline: a versatile fluorophore for the design of brightly emissive molecular sensors. Org Lett 4(26):4647–4650
Saha K, Agasti SS, Kim C, Li X, Rotello VM (2012) Gold nanoparticles in chemical and biological sensing. Chem Rev 112(5):2739–2779
Schazmann B, Alhashimy N, Diamond D (2006) Chloride selective calix[4]arene optical sensor combining urea functionality with pyrene excimer transduction. J Am Chem Soc 128(26): 8607–8614
Shynkar VV, Klymchenko AS, Piemont E, Demchenko AP, Mely Y (2004) Dynamics of intermolecular hydrogen bonds in the excited states of 4'-dialkylamino-3-hydroxyflavones. On the pathway to an ideal fluorescent hydrogen bonding sensor. J Phys Chem A 108(40):8151–8159
Simeonov A, Matsushita M, Juban EA, Thompson EHZ, Hoffman TZ, Beuscher AE, Taylor MJ, Wirsching P, Rettig W, McCusker JK, Stevens RC, Millar DP, Schultz PG, Lerner RA, Janda KD (2000) Blue-fluorescent antibodies. Science 290(5490):307–313
Snee PT, Somers RC, Nair G, Zimmer JP, Bawendi MG, Nocera DG (2006) A ratiometric CdSe/ZnS nanocrystal pH sensor. J Am Chem Soc 128(41):13320–13321
Stojanovic MN, Kolpashchikov DM (2004) Modular aptameric sensors. J Am Chem Soc 126(30):9266–9270
Stojanovic MN, Stefanovic D (2003) Deoxyribozyme-based half-adder. J Am Chem Soc 125(22):6673–6676

Storhoff JJ, Lucas AD, Garimella V, Bao YP, Muller UR (2004) Homogeneous detection of unamplified genomic DNA sequences based on colorimetric scatter of gold nanoparticle probes. Nat Biotechnol 22(7):883–887

Straight SD, Liddell PA, Terazono Y, Moore TA, Moore AL, Gust D (2007) All-photonic molecular XOR and NOR logic gates based on photochemical control of fluorescence in a fulgimide-porphyrin-dithienylethene triad. Adv Funct Mater 17(5):777–785

Subach FV, Verkhusha VV (2012) Chromophore transformations in red fluorescent proteins. Chem Rev 112(7):4308–4327

Sumalekshmy S, Henary MM, Siegel N, Lawson PV, Wu Y, Schmidt K, Bredas JL, Perry JW, Fahrni CJ (2007) Design of emission ratiometric metal-ion sensors with enhanced two-photon cross section and brightness. J Am Chem Soc 129(39):11888

Szacilowski K (2012) Infochemistry: information processing at the nanoscale. John Wiley & Sons., Chichester, West Sussex, UK

Tainaka K, Sakaguchi R, Hayashi H, Nakano S, Liew FF, Morii T (2010) Design strategies of fluorescent biosensors based on biological macromolecular receptors. Sensors 10(2):1355–1376

Takakusa H, Kikuchi K, Urano Y, Kojima H, Nagano T (2003) A novel design method of ratiometric fluorescent probes based on fluorescence resonance energy transfer switching by spectral overlap integral. Chemistry 9(7):1479–1485

Thurley S, Roglin L, Seitz O (2007) Hairpin peptide beacon: dual-labeled PNA-peptide-hybrids for protein detection. J Am Chem Soc 129(42):12693

Tomasulo M, Yildiz I, Kaanumalle SL, Raymo FM (2006) pH-sensitive ligand for luminescent quantum dots. Langmuir 22(24):10284–10290

Tyagi S, Kramer FR (1996) Molecular beacons: probes that fluoresce upon hybridization. Nat Biotechnol 14(3):303–308

Ueberfeld J, Walt DR (2004) Reversible ratiometric probe for quantitative DNA measurements. Anal Chem 76(4):947–952

Valentini P, Pompa PP (2013) Gold nanoparticles for naked-eye DNA detection: smart designs for sensitive assays. RSC Adv 3(42):19181–19190

Valeur B (2002) Molecular fluorescence. Wiley VCH, Weinheim

Valeur B, Leray I (2000) Design principles of fluorescent molecular sensors for cation recognition. Coord Chem Rev 205:3–40

Valeur B, Leray I (2007) Ion-responsive supramolecular fluorescent systems based on multichromophoric calixarenes: a review. Inorg Chim Acta 360(3):765–774

Van Munster EB, Kremers GJ, Adjobo-Hermans MJ, Gadella TW Jr (2005) Fluorescence resonance energy transfer (FRET) measurement by gradual acceptor photobleaching. J Microsc 218(Pt 3):253–262

Walkup GK, Imperiali B (1996) Design and evaluation of a peptidyl fluorescent chemosensor for divalent zinc. J Am Chem Soc 118:3053–3054

Wang S-L, Lee T-C, Ho T-I (2002) Excited state proton transfer and steric effect on the hydrogen bonding interaction of the styrylquinoline system. J Photochem Photobiol A Chem 151:21–26

Wang S, Gaylord BS, Bazan GC (2004) Fluorescein provides a resonance gate for FRET from conjugated polymers to DNA intercalated dyes. J Am Chem Soc 126(17):5446–5451

Whitaker JE, Haugland RP, Prendergast FG (1991) Spectral and photophysical studies of benzo[c] xanthene dyes: dual emission pH sensors. Anal Biochem 194(2):330–344

Wu J, Zou Y, Li C, Sicking W, Piantanida I, Yi T, Schmuck C (2012) A molecular peptide beacon for the ratiometric sensing of nucleic acids. J Am Chem Soc 134(4):1958–1961

Yang RH, Chan WH, Lee AWM, Xia PF, Zhang HK, Li KA (2003) A ratiometric fluorescent sensor for Ag-1 with high selectivity and sensitivity. J Am Chem Soc 125(10):2884–2885

Yao S, Schafer-Hales KJ, Belfield KD (2007) A new water-soluble near-neutral ratiometric fluorescent pH indicator. Org Lett 9(26):5645–5648

Yashchuk VMN, Syromyatnikov VG, Ogul'chansky TY, Kolendo AY, Prot T, Blazejowski J, Kudrya VY (2000) Multifunctional macromolecules and structures as one-way exciton conductors. Mol Cryst Liq Cryst 353:287–300

Yashchuk V, Kudrya V, Losytskyy M, Suga H, Ohul'chanskyy T (2006) The nature of the electronic excitations capturing centres in the DNA. J Mol Liq 127(1–3):79–83

Yatsuhashi T, Nakajima Y, Shimada T, Tachibana H, Inoue H (1998) Molecular mechanism for the radationless deactivation of the interamolecular charge-transfer excited singlet state of amino-fluorenones through hydrogen bonds with alcohols. J Phys Chem A 102:8657–8663

Yesylevskyy SO, Kharkyanen VN, Demchenko AP (2006) The change of protein intradomain mobility on ligand binding: is it a commonly observed phenomenon? Biophys J 91(8): 3002–3013

Yesylevskyy SO, Kharkyanen VN, Demchenko AP (2007) The blind search for the closed states of hinge-bending proteins. Proteins 71(2):831–843

Yguerabide J, Yguerabide EE (1998) Light-scattering submicroscopic particles as highly fluorescent analogs and their use as tracer labels in clinical and biological applications – II. Experimental characterization. Anal Biochem 262(2):157–176

Yoshida W, Yokobayashi Y (2007) Photonic boolean logic gates based on DNA aptamers. Chem Commun 2:195–197

Yoshihara T, Galievsky VA, Druzhinin SI, Saha S, Zachariasse KA (2003) Singlet excited state dipole moments of dual fluorescent N-phenylpyrroles and 4-(dimethylamino)benzonitrile from solvatochromic and thermochromic spectral shifts. Photochem Photobiol Sci 2:342–353

Yuan MS, Liu ZQ, Fang Q (2007) Donor-and-acceptor substituted truxenes as multifunctional fluorescent probes. J Org Chem 72(21):7915–7922

Zhou YC, Zhang DQ, Zhang YZ, Tang YL, Zhu DB (2005) Tuning the CD spectrum and optical rotation value of a new binaphthalene molecule with two spiropyran units: mimicking the function of a molecular “AND” logic gate and a new chiral molecular switch. J Org Chem 70(16):6164–6170

Chapter 9
Supramolecular Structures and Interfaces Designed for Sensing

An important step to perfection of fluorescent sensors can be made by their self-assembly into supramolecular structures and by their attachment to flat or porous surfaces and to different types of particles (Fig. 9.1). Scaling up from small single molecules to larger molecular ensembles aims at achievement of two

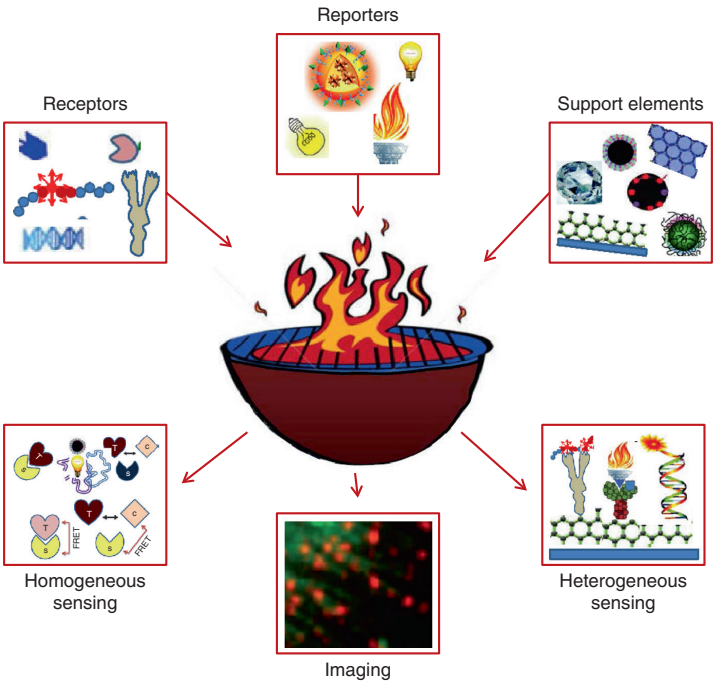

Fig. 9.1 Formation of supramolecular fluorescence sensor systems from different building blocks and obtaining at the outcome the technologies for homogeneous and heterogeneous sensing and imaging with strongly improved performance

A.P. Demchenko, *Introduction to Fluorescence Sensing*,
DOI 10.1007/978-3-319-20780-3_9

important goals: *improvement of molecular recognition*, especially with the targets of large size and complexity, and *exploration of collective properties* of fluorescence reporters that offer enhanced sensitivity. On this step, a substantial improvement in performance can be attained and new important functionalities added. These technological breakthroughs are a part of '*bottom-up*' approach to technological products with advanced functions (Balzani et al. 2003). The central theme in self-assembly is to direct an outcome of an otherwise spontaneous reaction and to exert control over all its steps. For controlling and directing the assembly a combination of physical and chemical means is often required.

In this Chapter we will see, how the new functions can be realized in supramolecular structures by combining functional and passive support materials. Covalent linkage, directional assembly and coupling to surface can modify dramatically the performance of fluorescence sensors. Molecular recognition can be efficiently improved by assembling correspondent functionalities. Also, discussed in Chap. 6, collective properties of fluorescence reporters can be optimized on the level of supramolecular structures. Serving as support media and templates, DNA, proteins and lipid bilayers allow precise positioning of different functional units, and, based on biospecific interaction, precise self-assembly can be realized. In assembled structures, carbon nanoparticles (graphenes, fullerenes, nanotubes and dots) can play additional role as fluorescence quenchers. Synthetic polymers being polyelectrolytes or possessing alternating hydrophylic-hydrophobic domains can form a variety of self-assembled structures ready for targeted functionalization by covalent linkage. This Chapter provides demonstrative examples on exploration of these possibilities.

9.1 Self-Assembled Supramolecular Systems

With the increase of size and complexity, the preparation of molecular conjugates by covalent synthesis becomes a very difficult, time-consuming and even unrealizable choice. In contrast, supramolecular chemistry based on self-assembly may offer the creation of nanoscale systems with a broad range of sensor applications. Self-assembly of composite sensor units is based on the same principles as the sensing itself – on complementarity between interacting partners and formation of non-covalent interactions between them, such as hydrogen bonds, salt bridges, solvation forces, π-π stacking and coordination of metal ions. Due to multiplicity of these bonds (see *multivalency* effect, Sect. 7.1), the interactions between the partners can compete in strength with covalent bonds.

Supramolecular chemistry has developed into a strong interdisciplinary field of research (Lehn 1995). One of its rules is the *requirements for topological saturation*. Saturation by non-covalent interactions should provide collective effect that has to bring to the system a necessary structural stability. Additional stability may be achieved with covalent cross-links formed after the assembly. A 'hot spot' should remain only for recognition site and, if necessary, for providing binding to a surface or location in heterogeneous structure, such as the living cell.

9.1.1 *Affinity Coupling*

In general, there are two principles of formation of supramolecular structures: affinity coupling and self-assembly. The examples of *affinity coupling* are the interactions antigen-antibody and biotin-avidin (or streptavidin) that are the most frequently used for creation of supramolecular structures. The advantage of antibodies is their versatility, since antigenic determinants can be inherently present or artificially incorporated into any structure of protein, nucleic acid or carbohydrate origin. They can be obtained as binding sites of many artificial molecules including organic dyes. The possibilities of manipulating with them have grown with introduction of monovalent single-chain *antibody fragments* (Piervincenzi et al. 1998). Thus, for efficient highly selective high-affinity coupling, one of assembling units should contain antibody or its fragment and the other – antigenic determinant recognized by it. With a broad variation of affinities ($K_d \approx 10^{-8}$–10^{-13} M) the antigen-antibody interactions may not in all cases be sufficiently strong for formation of stable supramolecular structures.

Binding of *avidin* or *streptavidin* with biotin is different. Protein avidin can be found in the white of chicken eggs. It binds a rather small molecule *biotin* of 244.3 Da (also known as vitamin B7) with a uniquely high affinity ($K_d \approx 10^{-14}$–10^{-15} M). *Streptavidin* is a bacterial analog of avidin, it has similar properties as avidin but can be produced in bacteria. It is a globular 60 kDa protein with a high (compared to other proteins) thermal and pH-stability (Fig. 9.2).

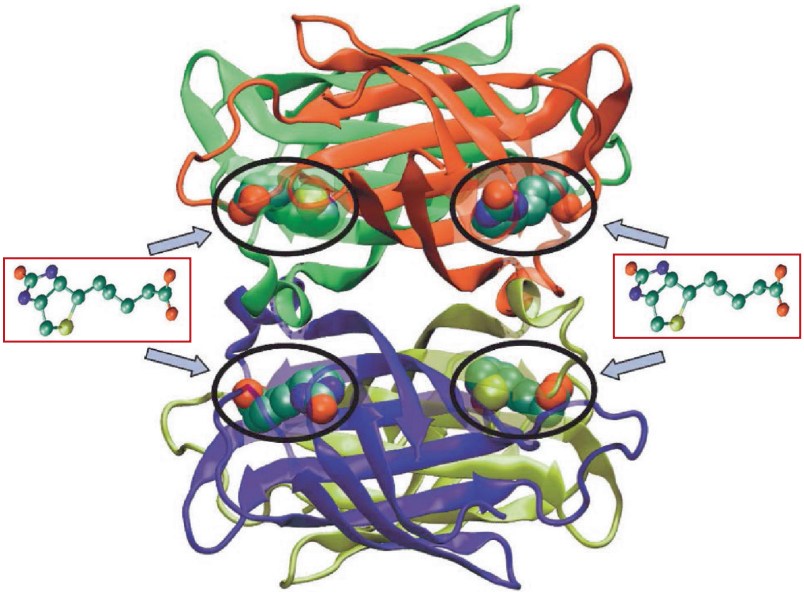

Fig. 9.2 The streptavidin-biotin system. Streptavidin tetramer (PDB code 1SWE) in complex with biotin. The protein is shown in cartoon representation. The biotin molecules are in space fill representation and their location is *circled* and marked by *arrows*. Streptavidin monomers are colored red, green, blue and yellow respectively. The parts of the protein, which are in front of the biotin molecules are made semi-transparent for clarity

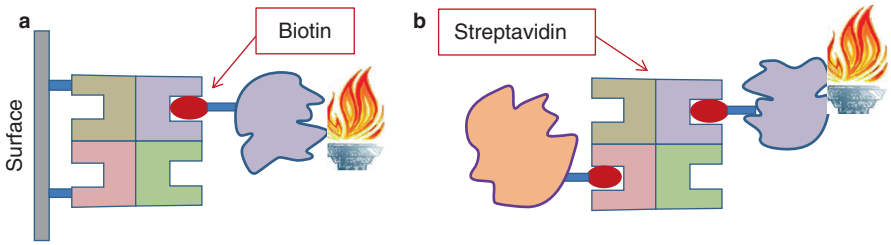

Fig. 9.3 Typical supramolecular complexes that can be assembled using tetrameric streptavidin-biotin junction. (**a**) The complex obtained with streptavidin covalently attached to the surface. (**b**) The complex combines two nanoscale structures. One of them is shown to contain fluorescence reporter

Since each avidin molecule can bind four biotins or biotin-labeled units, the complex, precisely arranged and very stable supramolecular constructions can be designed. Therefore if streptavidin is a part of one component of the structure and biotin is attached to its another component, these components find each other in solution and associate irreversibly with formation of a series of noncovalent bonds between complementary groups of interacting surfaces that are formed together and are, therefore, as strong as covalent bond (Fig. 9.3).

Streptavidin-biotin pair has now become a standard tool for providing strong and specific assembling of supramolecular structures. In contrast to antibodies, their complementary surfaces do not allow much structural variation, but there are many possibilities of reacting or substituting the groups that are outside their contact areas.

In biological world, a number of additional partner pairs can be formed that are characterized by high affinities. Such are the pairs lectin – carbohydrate or enzyme – suicide inhibitor possessing subnanomolar dissociation constants. However, they did not find extensive practical use. So, streptavidin – biotin pair remains the most requested in generating molecular junctions.

It is surprising that by now organic synthetic chemistry could not suggest a proper substitute to streptavidin-biotin pair that could compete in simplicity, stability and prize. Presently the binding properties of biotin but not of avidin or streptavidin can be simulated with designed peptides. Trivalent vancomycin/D-Ala-D-Ala- complex may probably be suggested as a pair with relatively tight binding of smaller molecular weight units (Rao et al. 1998).

Affinity coupling is an extremely valuable tool in intracellular research. For many of these studies it is needed that the fluorescently labeled partner should be introduced from outside into the cell, where it should find its second partner out of thousands of types of other molecules. Unfortunately, neither streptavidin-biotin nor antigen-antibody pair can be efficiently used for this task. The solutions to this problem and their illustrations will be discussed in Chap. 13.

9.1.2 Self-Assembly

Self-assembly involves the use of topological complementarity and saturation of intermolecular interactions between the partners on a broader scale with possible adaptation of conformation of partners for achieving this saturation (Lehn 1995).

Self-assembling and self-organizing methodologies are the powerful tools for the "*bottom-up*" approach for the realization of complex structures with functional properties. Recently, this concept has been extended to the design of fluorescent chemosensors providing new exciting potentialities for the development of innovative sensing systems (Mancin et al. 2006). The idea of this approach is, again, borrowed from Nature. Living cells do not appear as a result of 'nanofabrication'. All the processes leading to formation of supramolecular structures, such as chromatin, membranes, microfilaments or viruses, start from synthesis of *individual molecules* and their *subsequent assembly*. Being the building blocks for such assembly, biomolecules are adapted for assembly by their inner structures forming the contact surfaces. The same is required from artificial systems.

In such self-assembling systems, the principle of molecular recognition (Sect. 7.1) is actively explored. In addition to steric complementarity there should be maximal intermolecular contact with maximal saturation by noncovalent bonds. Throughout this Chapter the reader can evaluate relative importance of different types of these interactions for particular structures. Thus, amphiphilic structures favorable for *hydrophobic interactions* are essential for self-assembly by incorporation into micelles and lipid bilayers, but they are 'lubricants' that lack specificity that may be often necessary. *Electrostatic interactions* can provide the necessary recognition pattern, especially when they are assembled to clusters. They govern the layer-by-layer formation of multi-layer scaffolds. Here we will discuss the third very important type of noncovalent intermolecular interactions, the hydrogen bonds.

Hydrogen bonds are the short-range, unidirectional and specific. Individual bonds being in energy of the order of 10–15 kJ/mol are rather week, but their collective action can result in a much stronger effect. Enough to mention, that these bonds provide stability to α-helix in proteins and to double helix in DNA. In self-assembling molecular structures, quadruple bonds of acceptor-acceptor-donor-donor (AADD) type were suggested as a powerful strategy for creating nanocomposite structures (Corbin et al. 2002). Constructed following this principle, ureidodeazapterin-based module (Fig. 9.4) reveals an unprecedented stability of dimers based on their AADD self-complementary with the dimerization constant $K_{dimer} > 5 \times 10^8$ M^{-1}. Linking covalently two such units together with a semi-rigid spacer, a number of stable dendritic structures can be obtained.

There is a very strong request for new modules and strategies that can amplify the relatively weak strength of a hydrogen bond to give more stable assemblies.

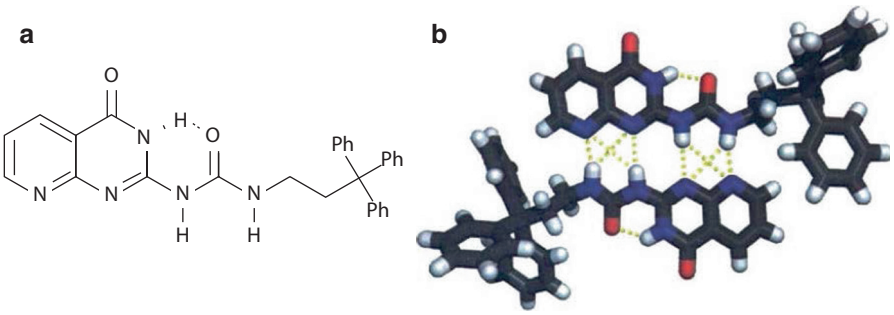

Fig. 9.4 Heterocyclic structure containing two donors and two acceptor for hydrogen bonding (**a**) and the model of formation of hydrogen-bonded dimer (**b**) (Corbin et al. 2002)

The presented above example demonstrates clearly, how to achieve that. Collective effects of rather week bonds can bring the results that are quite satisfactory for formation of stable and specific supramolecular structures. Experimental evidence exists that such *multivalent interactions* can increase the affinity compared to univalent interactions by many orders of magnitude (Baldini et al. 2007).

Many different hydrogen-bonded supramolecular structures comprising tens hydrogen bonds have been suggested (Vriezema et al. 2005). These structures can be less stable in water and other protic solvents, in view that these solvents themselves can be good hydrogen bonding partners.

The full advantage of *hydrogen-bonding complementarity* can be explored in precise and programmable self assembly based on DNA double helix (Seeman 2003). The partners that contain complementary sequences can assemble in a thermally reversible manner over a range of length scales. DNA can be conjugated to other materials (molecules and nanoparticles) or attached to solid support. It is expected that the organizational capabilities of structural DNA nanotechnology, that are just beginning to be explored, will find broad application.

9.1.3 Two-Dimensional Self-Assembling of S-Layer Proteins

Peptides and proteins provide a variety of opportunities for controlled and specific self-assembly. Mechanistically, peptide self-assembly can result from amphiphilic properties and from complementarity of partner structures. This complementarity can pre-exist in components, but can also appear in the course of interaction, the process that is known as '*induced folding*' (Demchenko 2001). Designed peptides forming the dimers can be used for assembling the nanoparticles (Aili et al. 2007).

The proteins that can assemble into *two-dimensional crystals* deserve special attention (Sleytr et al. 2007). Such proteins form the surface layers (S-layers) characteristic for prokaryotic organisms (archaea and bacteria). They vary in molecular mass of subunits (40–200 kDa) and the thickness of the formed layer (from 5–20 up to 70 nm). As S-layers are the periodic structures, they exhibit identical physicochemical proper-

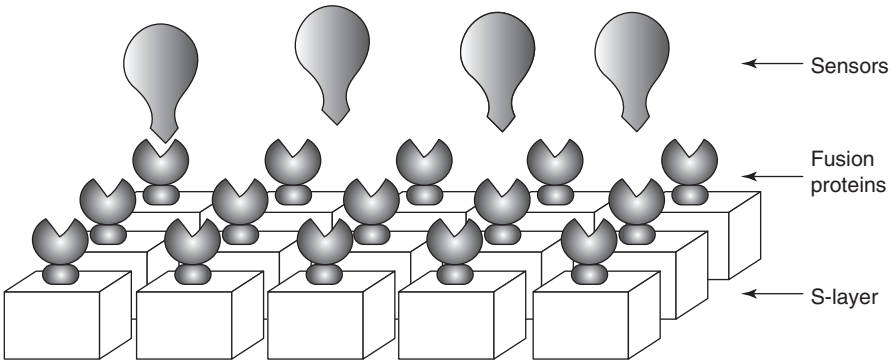

Fig. 9.5 Schematic representation of two-dimensional structures formed of engineered S-layer proteins fused to functional or structure-forming protein (e.g. streptavidin). The latter can form supramolecular structures by affinity coupling (such as streptavidin with biotin) or by self-assembly. Different possibilities can be realized in these constructions, such as biotinylated nanoparticles or antibodies. This ensures the binding of receptor elements in defined spacing and orientation

ties for each molecular unit down to the subnanometer level and possess pores of identical size and morphology. Protein engineering allows obtaining their truncated forms and also covalently coupled hybrids with other proteins, of which the most interesting is the coupling with streptavidin. The latter allows obtaining complicated constructions based on two-dimensional S-layers as the building blocks.

Many applications of *S-layers* in nanobiotechnology depend on the ability of isolated subunits to re-crystallize into monomolecular layers in suspension or on suitable surfaces and interfaces, such as liposomes (see Sect. 9.5). Because of these properties and using the possibility of modifications with various protein reagents, S-layer lattices can be exploited as scaffolding and patterning elements for generating more complex supramolecular assemblies and structures. One of such possibilities is illustrated in Fig. 9.5.

9.1.4 Template-Assisted Assembly

The self-organization of essential sensor components on a proper template is an important approach to the realization of functioning of self-assembled structures as sensors. In this case, the receptor and the reporter do not always need to interact directly. The communication between them can be provided by *spatial proximity* of these two units on the template only, so that a signal transduction mechanism can be intermolecular but efficient. Thus, template can play important role both in formation of functional supramolecular structure and in maintenance of its integrity.

The main advantages of template-assisted assembly are the possibility of choosing the template and its immobilization strategy selecting from broad possibilities in optimization

of sensor performance. Depending on the template, *little or no synthetic modifications of the receptor and reporter are needed*, and this allows an easy selection of their optimal configuration. The spatial proximity of a large number of sensor units in the assembly, leads to collective effects and properties that may contribute to the improvement of the sensors performances. Different types of template have been used to guide the self-organization of sensors, spanning from micellar aggregates to monolayers, to glass surfaces, and, more recently, to nanoparticles. Each of these templates has its own peculiar features that are reflected in a characteristic performance of the resulting sensor.

Additional benefit of template-assisted assembly is the possibility of *micropatterning* – the formation on the surface of molecular clusters with desirable properties. The active areas for accommodating these clusters with the size of 100 nm or less can be pre-fabricated on the surface. This approach with the aid of surface chemistry merges fabrication and self-assembly and thus combines bottom-up and top-down approaches (Henzie et al. 2006).

9.1.5 Prospects

New rapidly developing chemistry based on the principles of self-assembly and self-organization tends to complement, and to significant extent, to substitute common organic synthetic chemistry in an attempt to produce supramolecular systems of great complexity and high level of functionality. The new strategy requires the design and synthesis of a limited number of relatively simple building blocks that are then allowed to self-organize into complex structures. Following it, without strong synthetic effort, one can assemble the recognition unit together with the signal transduction and reporting unit into one block with superior properties. In this case, there may be no need for covalent links between these units; they only have to be designed according to a productive strategy, and noncovalent interactions between them are quite sufficient for functioning.

It could be ideal to develop one or several ‘standard’ reporting units that could be compatible to self-assemble with the library of receptors raised to detect a huge variety of targets. Then it may be possible to use unified technique for their detection. The scientists indicate that, despite the fact that there are interesting examples of large self-assembled structures, there is still a general lack of understanding how to introduce the standardized procedures for the step-by-step synthesis of nano-sized composites. This direction, meantime, is the only way to fill the gap between miniaturization of macroscopic approaches (known as ‘top-down’ principle) and chemical synthesis that has a limit on increasing complexity of molecular structures.

9.2 Building Blocks for Supramolecular Sensors

Supramolecular structures with the function of fluorescence sensing are seen as self-organized complexes between or with designed partners, in which recognition and reporting can be coupled in a most efficient way. In an effort for developing

better sensors an important role is given to nanoscale support materials. They include different types of molecules and particles representing inorganic, organic and biological worlds (Oshovsky et al. 2007).

9.2.1 Graphene and Graphene Oxide

Enormous enthusiasm of researchers involved in molecular electronics that predict *carbon* to substitute *silicon* to be the basis of technological revolution, is supported by scientists working in the field of sensing technologies. Nanoscale carbon materials can be very strong light absorbers, light emitters and light quenchers. Their light emitting properties were discussed in Sect. 5.4. Meantime, the role of carbon materials as the building blocks is much broader, especially when it is coupled with *quenching* that can give an output signal in sensing.

The basic platform of nanoscale carbon is *graphene* (Fig. 9.6). Its carbon atoms form a densely packed regular two-dimensional pattern of atomic width. The sp^2 bonding is the same as in polycyclic aromatic hydrocarbons and allow delocalization of electrons that are responsible for unique electron conduction. Graphene sheet is an ideal absorber of different types of molecules, especially of aromatic nature, of biological macromolecules and nanoparticles. Different aromatic compounds demonstrate

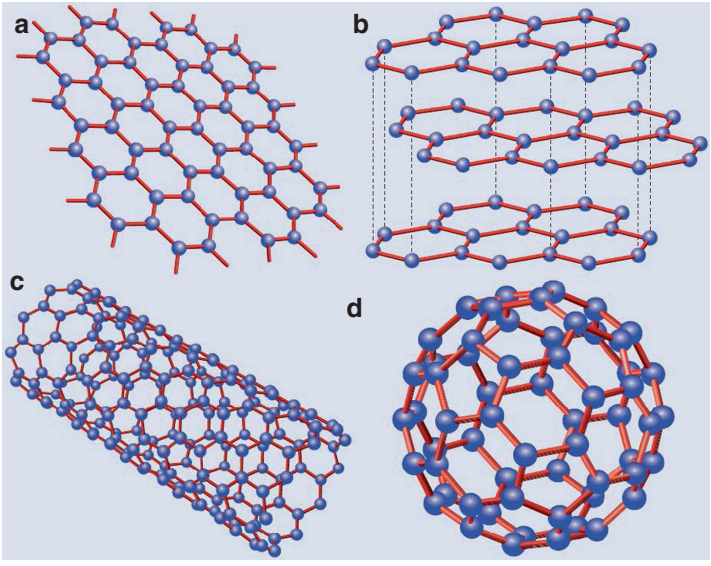

Fig. 9.6 Basic nanostructures formed of carbon (Neto et al. 2006). Graphene (**a**) is a 2D honeycomb lattice of carbon atoms. Other well-known forms of carbon all derive from graphene: graphite is a stack of graphene layers (**b**); carbon nanotubes are the rolled-up cylinders of graphene (**c**); and fullerenes (C60 is shown, **d**) are the balls consisting of wrapped graphene through the introduction of pentagons into hexagonal lattice

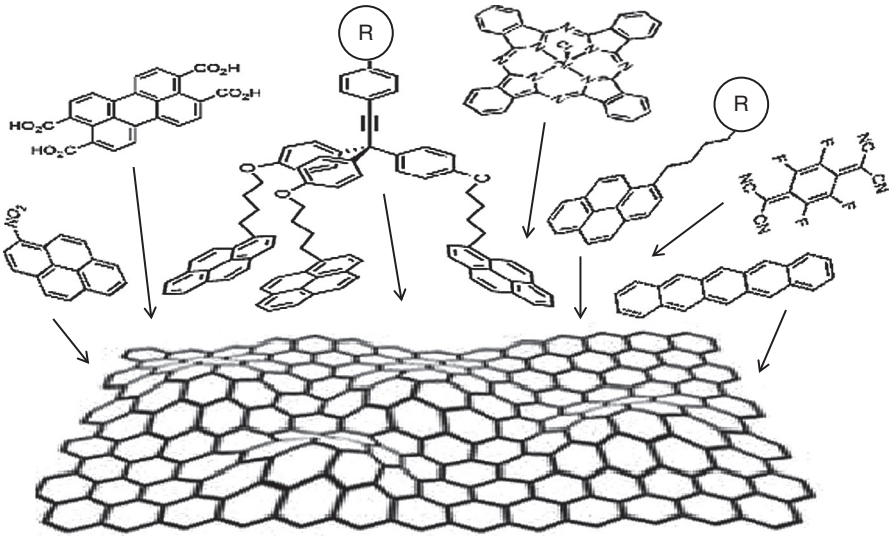

Fig. 9.7 Molecules containing exposed aromatic groups interacting with graphene sheet

increased affinity to graphene being stabilized by π-π stacking interactions. Figure 9.7 illustrates examples of these interactions for the compounds discussed in ref. (Mann and Dichtel 2013). Those molecules that being bound to graphene sheet lose their fluorescence (e.g. pyrene derivatives), can regain it after dissociation, If the target recognition is coupled with this event, such fluorescence enhancement can be used as the reporter response. Other possibilities arise if the reporting is based on association-dissociation of fluorescently bound receptor. Thus, DNA molecule can be bound if it is single-stranded and it dissociates if it acquires the double-helix form, and several reported methods of studying DNA hybridization are based on that (Deng et al. 2014).

The sticky ends of graphene sheets are amenable to different covalent modifications. The familiar *graphite* can be viewed as the structure composed of many layers of such graphene sheets. Hiding sticky ends, graphene sheet can be rolled up into cylinder forming *carbon nanotube*, and with the inclusion of pentagon elements it can form *fullerenes*, the structures in the form of hollow spheres.

Graphene oxide (GO) and *reduced graphene oxide* (rGO) were previously considered as graphene derivatives and predecessors in its synthesis, but now their special role is broadly recognized. In these graphene sheets, the polar groups are present that break up the regular graphene structure into connected islands. In addition to increasing the solubility, there appear additional sites of covalent binding and self-assembly.

Graphene and GO interact strongly with polymers (Salavagione et al. 2011), proteins (Zhang et al. 2013) and, notably, with single-stranded nucleic acids but not with double helices. Based on this feature, the methods of the DNA hybridization assays were developed (Lu et al. 2010). These techniques are simple: conjugate of sensing DNA with fluorescence label is exposed to the test system. The emission is quenched. If target DNA is present in this system, it forms double helix with the sensing sequence, which after dissociation from carbon surface starts to fluoresce.

Highly efficient quencher ability not only of nucleic acid but also for various organic dyes and quantum dots is a characteristic feature of graphene materials due to very efficient *electron transfer* from the excited dye to graphene sheet. In the case of organic dyes and polymers with heterocyclic side groups including single-stranded nucleic acids there is a strong interaction together with strong quenching through π-π stacking between the ring structures in correspondent partners that makes electron transfer quenching extremely efficient. In the case of DNA, the double strand conformation makes these interactions not possible.

Many possibilities can be realized exploring the quenching-enhancing effects on association-dissociation with graphene or GO surface. They are used as scaffolds to which the assembled recognition and reporting functionalities can be attached. In close proximity to the surface the emission of fluorescent dye or nanoparticle is quenched and the target binding results in disruption of this interaction leading to fluorescence enhancement.

9.2.2 Carbon Nanotubes

Tubular structures are probably mechanically the most rigid and functionally versatile modules that can be used both as nanoscale support materials and as transducers. Their inherent well-defined structural features, such as cylindrical dimensionality forming precisely established inner and outer volumes, are very useful for that. Especially attractive are the nanotubular structures that possess their own optical properties useful in sensing.

Those are *carbon nanotubes* that are very promising materials as molecular wires in electronics and also as the building blocks of various nanocomposites (see Fig. 9.6). These tubes have a tunable near-infrared emission (at 1200–1400 nm) that responds to changes in the local dielectric function (Choi and Strano 2007), but remains stable to permanent photobleaching. This emission can be quenched by appropriate redox-active dyes, and with proper construction this effect can be used in sensing (Satishkumar et al. 2007). Carbon nanotubes exhibit emission in the near-IR, which is already used in sensing (Barone et al. 2005). Meantime their most requested role in sensing technologies is as the platform for nanodevice assembly and also as a very potent fluorescence quencher (see Sect. 5.4).

The techniques of integration of nanotubes into various devices and designing the integrated sensing elements were developed (Mahar et al. 2007). This makes good prospect for the creation of smart sensors, in which the signal transduction is provided by fluorescence quenching and charge transfer. The first attempts along this line were successful (Barone et al. 2005).

9.2.3 Fullerenes

Fullerenes are known as very potent electron acceptors, and this property is used already in different optoelectronic devices (Wróbel and Graja 2011; Ito and D'Souza 2012). Though they look as point light absorbers, their own absorbance in the visible is very low (for C60 it is ~760 M^{-1} cm^{-1} at the band maximum ~455 nm). This suggests for these

particles a convenient role of electron acceptors in nanocomposites together with different types of fluorophores providing quenching-enhancement response. Though, there are practical difficulties due to low solubility of fullerenes and their tendency to aggregate.

The examples presented above show that carbonic nanostructures can play a very important role in fluorescence sensing technologies. These nanomaterials can serve not only as scaffolds, they can play an active role being used as the quenchers. Typically, most of these nanomaterials, despite the position of their absorption peak, are capable of quenching the fluorescence from different light emitters with varying emission wavelengths. An important role in this process is played by electron transfer and also by non-resonant energy transfer operating by electron-exchange mechanism, both resulting in quenching. Because of their advantage as universal quenchers, fluorescence-quenching nanomaterials eliminate the difficulty in selecting wavelength-matching fluorophore and quencher that may be a problem with conventional fluorescence-activated biosensors.

9.2.4 DNA Templates

Let us for the moment forget about a very important functional role of DNA and RNA and consider oligo- and polynucleotides of different lengths as scaffolds for the assembly of nanocomposite sensors. Their role is not limited to nucleic acid hybridization and may allow extremely broad range of applications in sensors operating on supramolecular level (Wilner and Willner 2012). Their great advantage is the possibility of *designed location* in the sequence of nucleic acid bases of different building blocks that can provide programmable arrangement of rigid structure-forming strands that can serve as scaffolds for further modifications.

DNA is a polymer made of building blocks, *nucleotides*, which are the purines: adenine (A) and guanine (G), and the pyrimidines: thymine (T) and cytosine (C). The nucleotides bind to each other to form a linear chain through the phosphodiester bonds. This represents a so-called single-stranded DNA molecule. Single strands can wrap around each other to form the well-known helical structure (double helix). The challenge in creating DNA nanostructures is to specify the appropriate DNA sequences in a way that the desired structure (geometry) forms have to be thermodynamically stable. The stability of double stranded DNA structure is provided by pairing of A with T and G with C stabilized with hydrogen bonds. Constructing the DNA-based templates can be modulated by temperature (the 'thermal annealing' uses controlled high-temperature DNA melting) and also by attached macromolecules and ions.

Design of specific topology based on sequence design with active use of these modulating factors have led to *DNA origamis* – the constructions formed of DNA with very complex structure and topology. Utilization of DNA origami can advance the assembly of materials by allowing programmable fabrication of non-periodic complex structures with ~6 nm resolution. There are different possibilities for constructing origamis. One uses already assembled DNA origami as a prefabricated template and then different materials can be attached. In another approach, assembly of the DNA origami structure can be used to drive the assembly of materials, i.e.

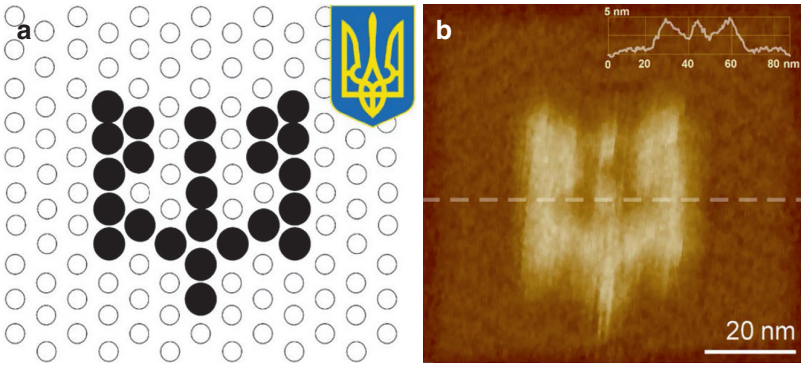

Fig. 9.8 DNA origami as a prefabricated template for streptavidin assembly (Kuzyk et al. 2009). (**a**) Schematic picture of the pattern for the assembly. The pattern is chosen to resemble the national emblem of Ukraine (*inset*). (**b**) High magnification AFM image to illustrate the high precision of assembly. The *inset* shows a height profile along the *dashed line*

both assemblies can take place simultaneously. Very strict precision of formation of designed structures can be achieved, as illustrated in Fig. 9.8.

We can admire such pieces of art realized on molecular level due to unique ability to locate strands and kinks of the structure in a *well precise manner*. But we also get a strong stimulus to create geometrically precise molecular composites for advanced sensing and imaging. The DNA is able to bind specifically different molecules and to position peptides, proteins or other supramolecular sensor components. Conjugation with peptide nucleic acids (see Sect. 7.7) can be explored on this new level of structure formation. The examples of the studies in right direction are the formations of porphyrin arrays on DNA template (Fendt et al. 2007). The designed pattern and precise spacing of their location adds unlimited possibilities in a bottom-up approach toward self-assembly.

Fluorescent analogs of DNA bases as well as intercalating dyes can serve as reporters. Short DNA-like oligomers with fluorophores replacing DNA bases can be synthesized either as the sequences with precise location of selected dyes or as the libraries with their random location (Kwon et al. 2015). Being attached to polymer beads, they generate different fluorescence colors due to multiple interactions between closely spaced fluorophores. The color changes on interaction with different analytes (Fig. 9.9).

9.2.5 Peptide Scaffolds

The ability to form three-dimensional structures of various complexity and of various functional use will stimulate the researchers for many years ahead. Innumerable possibilities for structure formation based on variation in a sequence formed by 20 amino acids can be used not only for the construction of sensor units (as we observed in Sect. 7.5) but also for making the scaffolds for supramolecular sensors. Here we

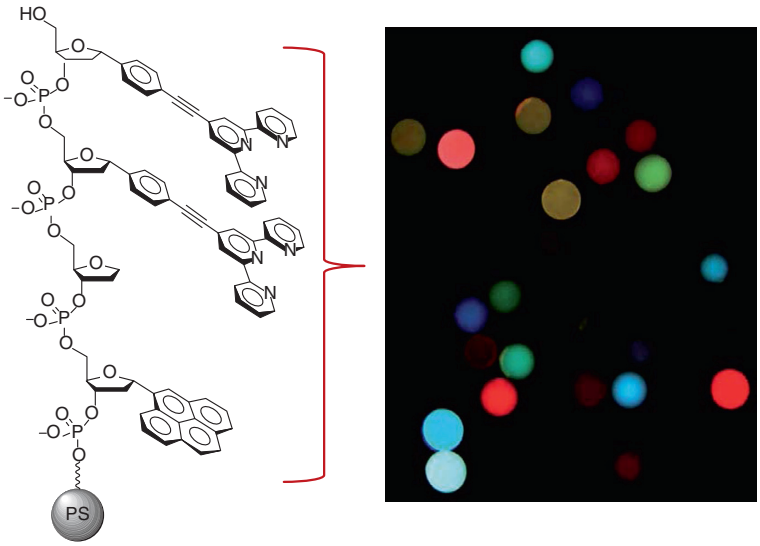

Fig. 9.9 An example of application of DNA-like sequences with fluorescence dye substitutes in sensing (Kwon et al. 2015). A tetrameric-length sequence is covalently attached to polyethylene glycol-polystyrene (*PS*) bead. One bead contains many copies of one sequence, and the library is composed of 1296 unique sequences. Sample image of this library (*right*) is captured by epifluorescence microscope at single excitation wavelength (340–380 nm) and the color pattern reports on the presence of analytes in the tested medium

present the example of formation of scaffolds for such sensors by association of peptides.

Peptides with the properties of forming the *self-assembled tubular structures* were first suggested as anti-microbial agents. Later it was realized that such peptide structures can serve as ideal scaffolds for supramolecular sensors (Gao and Matsui 2005). Surprisingly, it was found that even the peptides as short as Phe-Phe dipeptide can form stable nanotubes. Via their molecular-recognition functions, the self-assembled peptide nanostructures can be further organized to form nanowires, nanoparticles and even ‘nanoforests’ (on solid support). It has been demonstrated that cyclic peptides formed as planar rings by alternating L- and D- amino acids self-assemble via hydrogen bonding to tubular open-ended and hollow structures (Brea et al. 2007). The application of such molecular self-assemblies as the sensor building blocks use simple production methods, it is robust, practical and affordable. It is also beneficial that smart functionalities can be added at desired positions in peptide nanotubes through well-established chemical and peptide syntheses. They may include both recognition and reporting units with exploration of fluorescence-based technologies.

The other types of peptide-based scaffolds are their associates based on the principle of *amphiphilicity* (the separation of polar and unpolar sites). Their polar sites can be represented by 1–2 charged amino acids and hydrophobic part – by four or more sequential hydrophobic amino acids. They form ordered nanostructures similar to that formed by lipids (Jiang et al. 2007). There are many opportunities for hierarchical formation of supramolecular assemblies of larger complexity based on these peptide assemblies.

The principle of formation of the third type of these scaffolds is borrowed from the known examples of appearance in vivo of *amyloid fibrils* that are associated with a large number of human diseases. Application of peptides forming amyloid fibrils as scaffolds was suggested based on the facts of formation by them of *very rigid β-sheeted structures* (del Mercato et al. 2007).

The peptides assembled based on noncovalent intermolecular interactions allow realizing three most important types of these interactions: (a) electrostatic interactions based on complementarity of charged groups, (b) hydrogen bonding that involves complementarity of proton donor and acceptor groups and (c) hydrophobic interactions that provide stabilization of contacts between low-polar groups in polar media. Individually, these bonds are weak, but their collective action provides significant effects of stabilization of intermolecular complexes.

9.2.6 *Inorganic Colloidal Scaffolds*

In Chaps. 5 and 6 the properties of different nanoscale inorganic materials were overviewed. Being made of conducting, insulating or semiconducting materials and possessing different optical properties, they have something in common: they cannot be used 'naked' and they have to be 'decorated'. The steps in such *decoration* are illustrated in Fig. 9.10. In such already modified state they can be functionalized or assembled into nanocomposites. For performing such manipulations with them,

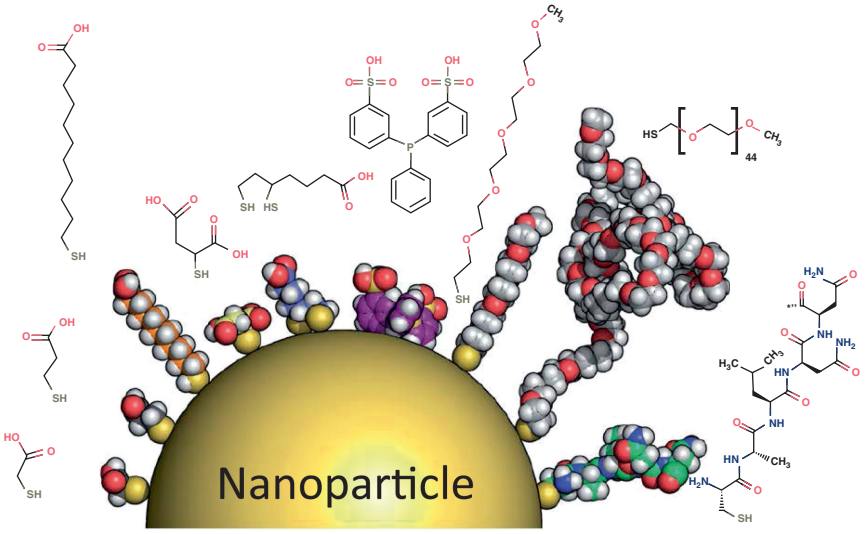

Fig. 9.10 A nanoparticle stabilized with different hydrophilic ligands (Sperling and Parak 2010). The space-filling models and chemical formulas were shown for those molecules (*left to right*): mercaptoacetic acid (MAA), mercaptopropionic acid (MPA), mercaptoundecanoic acid (MUA), mercaptosuccinic acid (MSA), dihydrolipoic acid (DHLA), bis-sulphonated triphenylphosphine, mPEG5-SH, mPEG45-SH (2000 g mol^{-1}) and a short peptide of the sequence CALNN

they have to be present in dispersed forms and stabilized against aggregation. Details of such stabilization reactions can be found in the literature (Sperling and Parak 2010). Different reagents can be used for this purpose, but the general principle is the following. The stabilizing agent should be bi-functional. It has to bind strongly to the particle surface and, simultaneously, prevent the aggregation.

Usually the stabilizing agent is present in the medium of nanoparticle synthesis, but the surface layer that it forms is not optimal for controlled assembly, the introduction of receptors, fluorescence reporters or other functionalities. Therefore the ligand molecules on the surface can be exchanged by others. Usually the incoming ligand molecule binds stronger to the inorganic nanoparticle surface and allows new possibilities for inducing new properties. A common example of *ligand exchange* is the treatment of Au nanoparticles that in an aqueous solution are synthesized by citrate reduction. They have negatively charged citrate ions adsorbed on their surface and are thus stabilized by electrostatic repulsion. On subsequent steps they can be replaced by sulphonated phosphines or mercaptocarboxylic acids (see following Section).

In a very common case, the partners that are selected for self-assembly are dissolved in non-mixing solvents of different polarities. Then the *phase transfer* steps are needed. Three strategies can be selected for that: ligand exchange, ligand modification and additional layers of molecules that stabilize the particles in the desired phase (Sperling and Parak 2010). Being a part of these approaches, silanization is used for surface modification and phase transfer. Organic polymers are often applied for formation of coating layers. Further steps of functionalization may involve covalent attachment of proteins, nucleic acids, etc.

9.3 Conjugation, Labeling and Cross-Linking

Integration of nanoparticles and their conjugation with biomolecules leads to novel hybrid systems, which may couple the recognition, cell penetration or catalytic properties of biomaterials with the attractive multifunctional characteristics of nanoparticles. In the development of supramolecular sensors, synthetic chemistry plays a very important role, but often on a high level of modification and integration of nanostructures. The is a need for modifying the molecular and supramolecular structural blocks by covalent attachment of recognition and reporting units and of additional stabilization of self-assembled structures with covalent bonds. Several key approaches on this pathway will be outlined below. With different types of particles a multi-point conjugation can be achieved (Aubin-Tam and Hamad-Schifferli 2008). The techniques have been developed for specific binding of nanoparticles with different small molecules (Algar et al. 2011), and also with DNA (Boeneman et al. 2010), peptides and proteins (Aubin-Tam and Hamad-Schifferli 2008; Prasuhn et al. 2010). Binding with whole bacterial cells (Moyano and Rotello 2011) becomes possible. Formation of supramolecular structures based on biospecific molecular recognition will be of special concern in our discussion.

9.3.1 Nano-bio Conjugation

The nanomeric size of fluorescent particles allows many different possibilities of chemical manipulations with them: formation of single biomolecule-particle conjugates (Katz and Willner 2004), attachment to nanoparticles of multiple molecules in a well-controlled manner (Peng et al. 2011) and also the formation of their heterocomposites of high complexity (Algar et al. 2011). Meantime, each type of nanoparticle structure requires its own conjugation chemistry.

Functional groups on polymer surfaces are the easy targets for bioconjugation, and exposed amino groups of PAMAM dendrimers are especially convenient for such modifications (Bergamini et al. 2010). Many possibilities exist for modifications of fluorescent conjugated polymers that are discussed in Sect. 5.3. The literature examples include their coupling with lipids with potential for gene delivery (Feng et al. 2010) and with short peptides that can be functionalized for cellular research (Pu et al. 2010). In the latter case, variation of peptide coverage changes the polymer emission color.

Regarding semiconductor quantum dots (Sect. 5.5), their bioconjugation is more difficult and several strategies for that have been developed (Biju et al. 2010; Jin and Hildebrandt 2012; Algar et al. 2011; Hötzer et al. 2012). Their further functionalization with the attachment of ligands to cellular receptors can be achieved via interaction of streptavidin-QD with biotinylated ligand (Lidke et al. 2007). As we observed above, the biotin-avidin (including neutravidin and streptavidin) interaction is a popular approach for connecting components in functional nanocomposites.

9.3.2 Techniques of Conjugation and Labeling

Covalent linkage was and remains the most frequently used means in self-assembly of inorganic, organic and organic–inorganic structures, their functionalization and labeling. The most frequently used reactions for covalent modification are described in Fig. 9.11.

Amino groups and *SH-groups* are the usual targets for *chemical modifications*, and their presence at the sites of desired modification with the absence in other sites may guarantee the necessary precision (Brinkley 1992). SH-targeting is more actively used with peptides and proteins because these groups present as Cys residues are less abundant than the amino groups (N-terminal and that of Lys residues). Solid phase synthesis of peptides and site-directed mutagenesis of large proteins are used for incorporation of SH- groups into desired sites of the sequence for subsequent attachment of fluorescent dyes according to well-known chemistry. Usually the fluorescence dyes are synthesized together with reactive group for labeling.

The three-dimensional structures of biological macromolecules, if they are known, are actively used for determination of the optimal labeling sites. Comparative

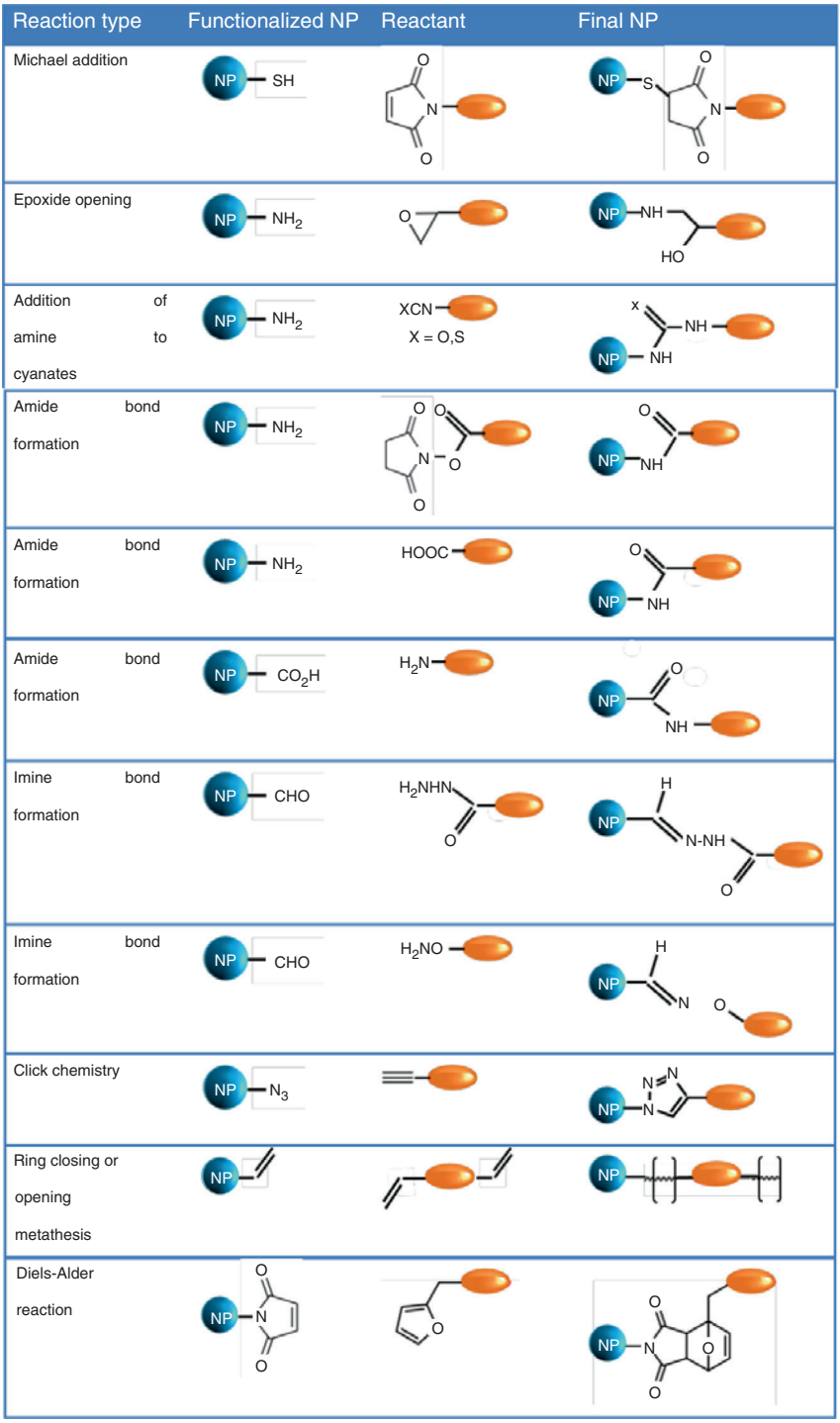

Fig. 9.11 Methods of conjugation and functionalization of inorganic nanoparticles (Erathodiyil and Ying 2011)

studies of sensor proteins, in which the *engineered* Cys *locations* were rationally designed based on the strongest differences of environments of these sites in unbound and bound forms derived from X-ray structures (Marvin et al. 1997) witness for usefulness of this approach. The retention of native protein structure during SH labeling is especially important for proteins that contain significant amount of S-S bonds that are necessary for supporting this structure, and, particularly, for antibodies. Thus, the skill is to select the location of introduced SH- group in such a way that could allow correct protein folding with correct formation of S-S bonds that are essential for structure and, simultaneously, to keep the introduced SH-group free and available for chemical modification. It was found (Renard et al. 2002) that a mild reducing treatment is necessary to reactivate mutant Cys residues before coupling with SH-reactive dye. The reaction of coupling in these conditions allows preserving the essential disulphide bonds of the antibody variable domains. In the same study, the structural and energetic criteria were applied to locate the sites of introduction of reactive Cys residues by mutagenesis. The authors selected the target residues as that belonging to topological neighborhood of the antigen in the structure of complex between antibody and antigen, its absence of functional importance for binding the antigen and its solvent accessibility. The feasibility of this rule was shown in experiment.

9.3.3 Co-synthetic Modifications

Co-synthetic incorporation of fluorescent dyes into polymer and biopolymer structures is less frequently used, though such procedures may be of choice for sensing peptides and also of oligonucleotides as aptamers. In Sect. 7.5 we observed that in some sensing technologies the large globular protein structures are not required, and the necessary effect of target recognition can be achieved by smaller peptides. They are more flexible in application and more tolerant to environment conditions with better performance regarding reproducibility and multi-use operation. In this case, peptides can be obtained by chemical solid-state synthesis and any possible variation of amino acid sequence can be easily achieved. They may include co-synthetic incorporation of fluorescent reporter groups at any position in the sequence, which makes unnecessary the site-specific modification of SH- or NH_2-groups (Link et al. 2003).

An alternative possibility, the incorporation of *non-natural amino acids* in a cell-free peptide and protein biosynthesis on ribosome, is also possible. In this case a non-natural aminoacyl-tRNA is constructed and incorporated into synthetic process (Katzen et al. 2005).

Regarding covalent labeling of nucleic acids, both 5′ and 3′ terminals are available for that. There are also many new possibilities to synthesize artificial fluorescent nucleic acid bases that can be incorporated co-synthetically.

9.3.4 *Chemical and Photochemical Cross-Linking*

Self-assembly, if necessary, can be combined with *chemical cross-linking* and photopolymerization (Mancin et al. 2006). This will provide higher stability to the formed structures and allow integrating molecules with different functions. Such applications are immense, and the reader is advised to consult classical monographs (Hermanson 1995) and reviews (Brunner 1993; Brinkley 1992), in which these modifications are described in sufficient detail.

These reactions, however, were not sufficient to satisfy the demands of bioconjugation chemistry, macromolecular science and, particularly, the design of supramolecular ensembles. All that stimulated the development of *click chemistry* that rapidly became a general tool for achieving modular and highly specific cross-linking occurring with high chemical yields and with a product being stable in physiological conditions. The azide alkyne cycloaddition reaction catalyzed by copper and occurring in mild conditions at room temperature fully satisfies the click chemistry concept. Moreover, this reaction can be fluorogenic (Le Droumaguet et al. 2010), i.e. it can generate fluorescent product from non-fluorescent predecessors (Fig. 9.12).

Essentially, this reaction is not limited to small molecules and organic dyes containing the complementary groups. It can provide the linkage between inorganic and organic macromolecular species. An acetylene-functionalized lipase has been attached to azide-functionalized water-soluble gold nanoparticles. The product containing about six enzyme molecules per nanoparticles retained in full its catalytic activity (Brennan et al. 2006). Another example was the demonstration that azide-functionalized gold nanoparticles can be specifically coupled to an alkyne-modified DNA duplex, resulting in a chain-like assembly of nanoparticles on the DNA template (Fischler et al. 2008), see Fig. 9.13.

Silica beads, quantum dots and other nanomaterials can be assembled with this reaction and decorated with different types of chemical and biological receptor and

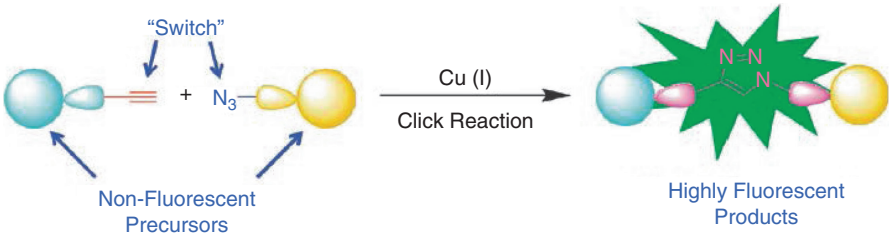

Fig. 9.12 Schematic representation of a typical fluorogenic click reaction (Li and Liu 2012). Non-fluorescent alkyne- and azide-containing starting materials are covalently coupled together to afford a highly fluorescent product

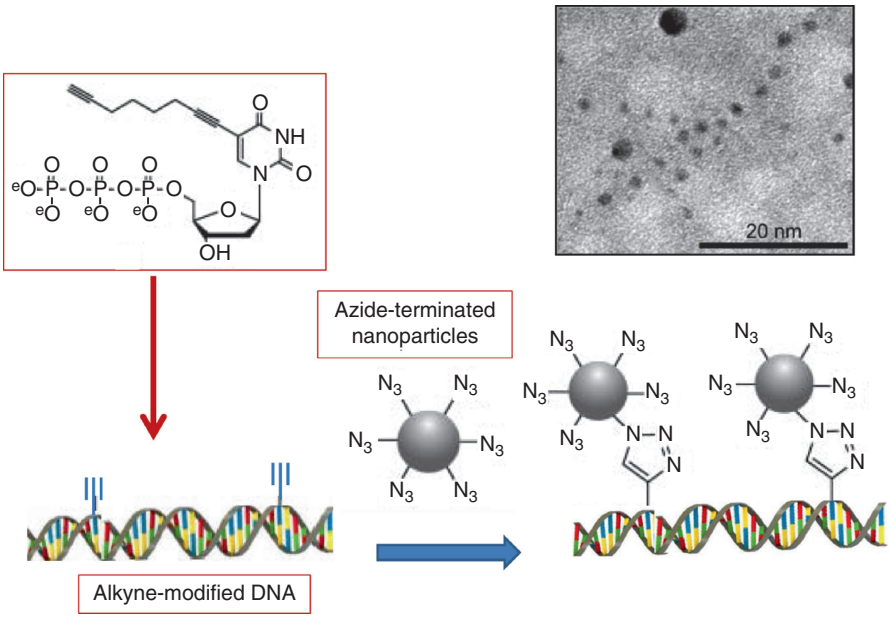

Fig. 9.13 Regular chain of gold nanoparticles formed on DNA scaffold with the aid of click reaction (Fischler et al. 2008). Azide terminate nanoparticles reacted with alkyne-modified DNA duplex. In the insert: the representative TEM micrograph validating one-dimensionally and equidistant assembly of nanoparticles

reporter units expanding the possibilities of fluorescence-based technologies (Le Droumaguet et al. 2010; He and Gao 2011).

9.4 Supporting and Transducing Surfaces

Surfaces play very special roles in fluorescence sensing. Despite the fact that, unlike potentiometric or cantilever sensors, their presence is not so critical for reporting event, the sensor assembly on the surface and the sensing based on interaction with it can allow realizing additional possibilities.

Formation of an organized assembly can be achieved by self-organization of receptors and fluorescent reporters on a *surface as a template* (Arduini et al. 2007). In this way one can form a construction, in which the target binding and reporting units do not interact directly and the communication between these two units is determined only by their spatial closeness ensured by the template. Already in this simple construction there are many possibilities for modification and optimization of the sensor by simple adjustment of the ratio of components. With the combination

of covalent binding and self-organizing methodologies, the more complicated multifunctional sensors can be constructed. In this Section we discuss different technologies for formation of surfaces with active and passive role in sensing.

9.4.1 Surfaces with Passive Role. Covalent Attachments

The role of surface as a passive support can be very important in many sensor constructions. When the sensor molecules, nanoparticles or supramolecular structures are immobilized on the surface, *they cannot diffuse* freely in solution and mix with other sensors. Many attractive analytical advantages can be derived from sensor attachment to the surface. We indicate several of such new possibilities.

(a) The sensors composed in this way allow their using for many times with simple sample addition-washing protocols or providing continuous monitoring in the flow.
(b) In such many-use systems, the reagent additions can be easily applied, for instance, the addition of fluorescent competitor.
(c) Due to fixed spatial separation between sensor molecules, the sensing of a large number of analytes (multiplex sensing) can be made on the same plate simultaneously. For such multiplex sensing the *microarrays* (sometimes called biochips) can be developed for simultaneous sensing of hundreds or even thousands of targets (see Sect. 11.3).

The choice of methods of surface immobilization depends on the chemical structures of sensor and the surface; these methods are well described in original literature and reviews (Sobek et al. 2006). They do not differ much from those methods that are used in other sensor technologies, where the surface immobilization is also needed, such as surface plasmon resonance. Meantime, each sensor and each application may demand its own solution; the demands on applied solid support are thereby as manifold as the applications themselves. Immobilization should satisfy many requirements, particularly, it should involve proper orientation of sensors and availability of receptor sites for target binding.

The *hydrogel layers* allow high density of sensor immobilization. Hydrogels are the three-dimensional (3D) polymer networks that swell, but do not dissolve in water. They can be made optically transparent and fluorescent-free, being formed of different hydrophilic polymers, such as polyacrylamide and polyethylene glycol (Svedhem et al. 2001). Their development into 3D microarrays for DNA hybridization and protein detection (Rubina et al. 2003, 2004) allowed increasing substantially the density of sensor locations. One of proposed procedures (Burnham et al. 2006) looks in the following way. Disulphide-crosslinked derivative of hydrogel is deposited on the surface of quartz or silicon. Then the application of reducing agent provides generation of reactive SH groups throughout the hydrogel leading to 'activated hydrogel'. These SH groups can be readily modified with attachment of proteins or other functional groups resulting in functional hydrogel.

For providing efficient affinity coupling with the use of biotin-streptavidin pair, the SH-reactive biotin derivative is applied. It yields *biotinylated hydrogel*, which is ready for binding streptavidin. The latter one is particularly useful for immobilization of biotinylated aptamers (Schaferling et al. 2003). Since biotinylated proteins are deposited from solution, such system is advantageous for deposition of proteins that need delicate conditions of treatment. Generally, in addition to increased binding capacity, immobilization within three-dimensional hydrogels offers many advantages over binding to flat two-dimensional surfaces, such as 'wet' and friendly polar environment with stabilizing effect of the gel matrix. A disadvantage is a slow rate of establishing the target-binding equilibrium that is limited by target diffusion in the gel.

Different materials that can serve as supporting media, transducers and even imprinted recognition elements can be made in a *sol–gel process*. Both inorganic and organic/inorganic composite materials can be obtained by this procedure. The colloidal suspensions or 'sols' are formed via hydrolysis of alkoxy metal groups in the precursors with subsequent polycondensation. The obtained transparent glass-like structures can attain different shapes and may be obtained with high porosity. The pore size distribution can be controlled by chemical composition and by the reaction conditions. Importantly, fluorescent dyes can be incorporated into these structures in several ways: by adsorption within the pores, by incorporation into reaction mixture (due to mild conditions of synthesis there is no decomposition of dyes) and also by covalent binding to finally obtained material. Covalent attachment should be preferred for obtaining the sensors of high stability.

9.4.2 Self-Assembled Monolayers

Self-assembled monolayers (SAMs) are monomolecular ordered structures that can form spontaneously on a chemically active surface (Ruckenstein and Li 2005; Flink et al. 2000). They can be prepared simply by adding a solution of monolayer-forming molecules onto the surface and washing off the excess. The monolayer is formed due to strong interaction energy of one of the groups (usually, terminal) of a monolayer former with an active surface (Sharpe et al. 2007). It can be additionally stabilized by side interactions in the monolayer.

Gold and silver surfaces form very stable and ordered monolayers with thiol-containing compounds because of strong binding energy between them (Fig. 9.14). In the case of alkane thiols deposited on gold, this energy can be as high as 100–150 kJ/mol. SAM of long chain alkane thiol produces a highly packed and ordered surface, which can provide a membrane-like microenvironment, useful for immobilizing biological molecules. In addition to the low molecular mass thiol derivatives, the self-assembled monolayers on gold can be formed by SH-substituted peptides, proteins, carbohydrates (Revell et al. 1998), DNA and peptide nucleic acids (Briones and Martin-Gago 2006).

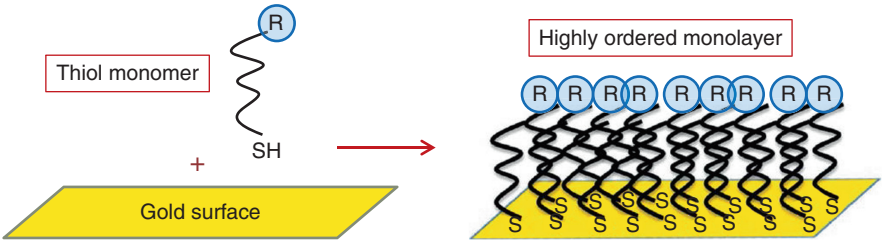

Fig. 9.14 Formation of thiol surface-adsorbed monolayer (SAM) on gold surface. SAMs are frequently used for spontaneous modifications of gold and silver surfaces with the compounds containing sulfur. R denotes the active group needed for further modifications, often they are carboxylic groups

It was reported that polythiophene monolayers on gold retain their fluorescent properties (Shinkai 2002), as well as some modified fluorescent dyes (Kriegisch and Lambert 2005). Meantime, a strong *quenching of fluorescence* of closely located dyes by PET and FRET mechanisms is a well-known property of gold surfaces. This property can be useful (Perez-Luna et al. 2002). One of such possibilities is the following. By immobilizing the analyte of interest (or its structural analogue) to a metal surface and exposing it to a labelled receptor (e.g. antibody), the fluorescence of the labelled receptor, being in close proximity to the metal, becomes quenched. If a free analyte is present, the labelled receptor dissociates from the metal surface with an increase of fluorescence intensity.

In many cases, the quenching by metal surface has to be avoided, and another type of support has to be used. *Alkyl silane* molecules (e.g. octadecyltrichlorosilane) form the self-assembled structures on silicon oxide surfaces, and also a number of different surfaces can be modified with alkyl carboxylates. Recent developments in the chemistry of SAMs on glass suggest new technologies for fluorescent sensor design. Trialkoxysilanes or halogenosilanes reacting with hydroxylated surfaces with the formation of SAMs offer such possibilities (Sullivan and Huck 2003).

Alkylsiloxanes are formed on the surface of silicon or glass. The reactive siloxane groups can form on a surface a cross-linked network by condensing with hydroxyl groups on the surface, water and neighboring siloxanes. This binding is more stable than of alkanethiolates on gold, but there is a stronger limitation on the chemistry of second functional group that will extend from the formed surface and will be needed for further modifications.

Designed polypeptides with variable repeat length containing N-terminal dicysteine were suggested as scaffolds for surface immobilization of quantum dots (Medintz et al. 2006). Many other methods have been developed for modification of the surfaces of these particles that attain increasing importance in sensing.

Hydrophobic surfaces can be covered with *phospholipid monolayers*, which can be formed spontaneously, and the stability of such structures can be increased by thermal treatment (Stine et al. 2005). Such coating may help solubilizing the

hydrophobic particles in polar media and also incorporating into them of target-binding functionalities.

Dense and highly regular two-dimensional distribution of exposed reactive functional groups of SAMs offers many possibilities for further attachment to solid support of the whole sensors or their *assembly on the surface* from receptor and reporter components. SAMs offer a simple and straightforward method to generate modified surfaces with transducing function. This property is of extreme value for making functional microfluidic devices (Sect. 11.5), in which due to a narrow size of produced channels a high surface-to-volume ratio can be generated. Even in these microscopic structures the deposition of SAMs is simple, it requires only the flow of a solution or of a gas stream of adsorbate molecules through the channels.

Thus, one of the actively used functions of SAMs is the *hosting of biosensor molecules and cells*. This includes confining and aligning of biological macromolecules and the immobilization of cells in a way preventing their adhesion. The other important problem is the immobilization of fluorescence reporters and providing signal transduction function to these reporters. Thus, the general role of SAMs is to form an interface between the surface and the molecular sensors or nanosensors. Such possibility can be realized both on flat surfaces and on the particles of different size.

Supramolecular interactions such as of π-π type have been recently exploited to make sensitive glass surfaces. It was reported on the functionalization of glass surfaces (quartz, glass slides and silica particles) with 2,7-diazapyrene derivatives for the detection of catecholamine neurotransmitters, such as dopamine (Cejas and Raymo 2005) (Fig. 9.15).

Thus, the most attractive feature of self-assembled monolayers is their ability to change easily the surface properties of the layer including its binding properties by tuning the chemistry of terminal group that appears on its surface without significant influence on the formation of these layers.

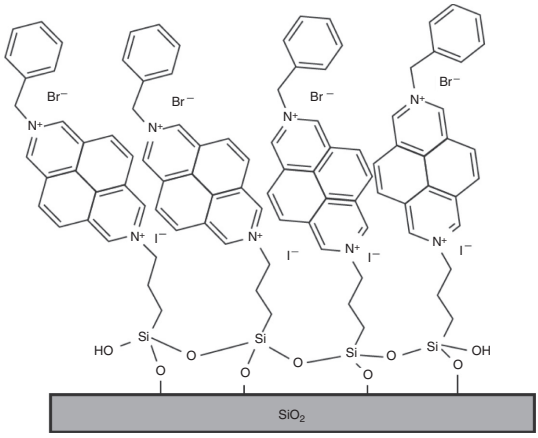

Fig. 9.15 Schematic structure of 2,7-diazapyrenium monolayers formed on silicon substrates that are able of selective binding of dopamine (Cejas and Raymo 2005)

9.4.3 *Langmuir-Blodgett Films*

Formation of *Langmuir-Blodgett films* is an alternative to self-assembly method of producing regular monolayers on solid support surface (Davis and Higson 2005). This method is less demanding to the strength of interaction of monolayer-forming molecules with the support but requires them to be *amphiphilic*, i.e. to be composed of polar and apolar parts separated in space. The monolayer is primarily formed at the air-liquid interface, and then it is transferred to the surface of solid plate by immersing it to this liquid (Fig. 9.16a).

By repeating the operation of immersion and emersion several times, several regular monolayers can be deposited. When primarily formed at the air-water interface and then transferred to hydrophobic support, these films expose polar groups. This is very useful for further modifications, such as attaching of various molecular and nano-composite sensors operating in aqueous media. Langmuir-Blodgett films with all their modifications made in solvent can be used in the air, which makes them applicable in the sensing of vapors.

There are many possibilities of forming Langmuir-Blodgett monolayers in mixed composition with the inclusion of fluorescent dyes (Hussain et al. 2006). In particular, amphiphilic analogs of polarity-sensitive dyes can be mixed with fatty acids to form stable monolayers (Alekseeva et al. 2005). Formation of stable films by luminescent complexes of europium have also been described (Xiang et al. 2006). Conjugated polymers can be used as monolayer formers (Mattu et al. 2006). All that suggests many attractive possibilities for fluorescence sensing, but, surprisingly, this methodology is used rarely.

It should be indicated that Langmuir-Blodgett films when formed do not allow easy incorporation of compounds dissolved in external solution. Such incorporation can be better provided on the step of their formation; the incorporated molecules

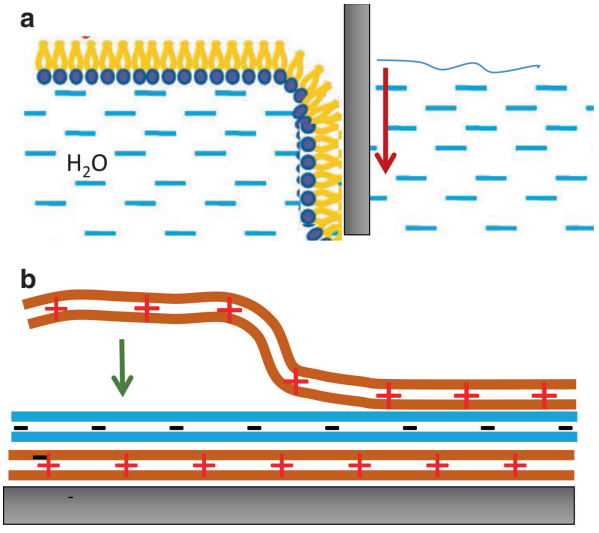

Fig. 9.16 Different methods of functional modification of the surface. (**a**) Langmuir-Blodgette films. The films are first formed on a liquid surface by ordering of amphiphilic molecules forming ordered layer and then transferred to solid–liquid interface. (**b**) Films obtained by layer-by-layer procedure, in which the layering on the solid surface is provided based on electrostatic interaction of deposited polymer layer with the previously formed layer

should be amphiphilic and possess some similarity with the major component of the film. There is also a possibility to make a second layer on top of the film. If this layer is formed by phospholipids, many possibilities appear for incorporation of a broad variety of different molecules, including biomembrane proteins. There are the results (Davis and Higson 2005) showing that single-strand DNA molecules can be incorporated into the films formed by octadecylamine and that they can be hybridized with complementary strands.

9.4.4 Layer-by-Layer Approach

Layer-by-layer technique is a version of self assembly that is available to polyelectrolytes and uses the property of a molecular layer formed by charged polymer to absorb a molecular layer of a polymer with an opposite charge (Ariga et al. 2006; Chaki and Vijayamohanan 2002; El-khouri et al. 2012). Such layer-by-layer technique allows obtaining multilayers with precise thickness (Fig. 9.16b). Since many natural and synthetic polymers contain the charges, this technique is useful for formation the surfaces with desired properties. In addition, the distance from the surface monolayer to solid support can be precisely controlled. A smaller-size charged molecules including fluorescent dyes (Egawa et al. 2006) can participate in the formation of layers.

The layer-by-layer structures are not limited to flat surfaces but can be assembled onto different *charged particles*. In comparison with Langmuir-Blodgett films, they do not show a very high degree of order. These films are highly stable, due to the multiple interactions providing the charge neutralization. Meantime, the order in polymer layers themselves cannot be very high, which makes the structures rather amorphous. In aqueous solutions, they can be affected by pH and ionic strength, which is not always a favorable property.

The layers formed by *conjugated polymers* deserve special attention. Polyelectrolytic nature of many of them makes very good prospects for making ‘responsive’ layers with their inclusion. It is known that their fluorescence superquenching effect in thin films is much greater compared to that in isolated conjugated polymer molecules in solution. This is because the efficient exciton length is larger in two dimensions than in one-dimensional polymer chain. Precise deposition of quenchers that could be a part of reporting mechanism is possible in this system.

The layer-by-layer approach can be extended to *nanoparticles*. The stepwise construction of a novel kind of self-assembled organic/inorganic multilayers based on multivalent supramolecular interactions between guest-functionalized dendrimers and host-modified gold nanoparticles was reported (Crespo-Biel et al. 2005). Such supramolecular layer-by-layer assembly yields the growth of plasmon absorption band in proportion to a number of layers. The interactions between optically responsive monolayers can be studied as a function of distance between them that is regulated by a number of intermediate inert layers. It was found (Ianoul and Bergeron 2006) that in order to minimize the quenching of fluorescence signal, 20 polyelectrolyte monolayers are necessary to be deposited between the nanoparticles and the dye by a layer-by-layer deposition technique producing a 15–20 nm separation cushion.

The combination of the layer-by-layer method of multilayer formation with other fabrication techniques such as spraying, spin-coating and photolithography offers many new possibilities for creation of sensor arrays (Ariga et al. 2007).

9.4.5 Prospects

Design of fluorescence sensors using functionalized surfaces has many technical advantages. It also extends the possibilities of sensing, particularly to the gas phase. With surface immobilization it is much easier to perform the sensors that allow multiple uses, continuous application of tested medium and target monitoring, washing-out the non-target species or reagent additions. The surface deposition allows spatial separation of sensors to different targets and therefore to provide multiplex sensing.

These are 'trivial' and most easily understood advantages of 'passive' surfaces. Even for them, there is a lot of potential for improvement by making the right choice among different possibilities. The surface covered with polymer hydrogel is very attractive since it allows a 'three-dimensional' incorporation of sensor units into the gel matrix. However, this can be done only for small-size sensor molecules or particles, and the response of these sensors is slow because of retarded diffusion. In contrast, being attached to SAMs, the sensor recognition sites are equally exposed and their response is faster, but the limited number of receptors inherent to a planar surface restricts the sensor density.

Surfaces can play an active role by participating in signal transduction, and such participation is versatile. The gold and silver surfaces are very good as SAM formers and also as fluorescence quenchers, and this favorable combination can be used in the design of many sensors exploring the variation of distance between the surface and fluorescent dye (or nanoparticle). This and other, more inert, surfaces can be modified with the introduction of SAM made of fluorescent molecules or of a layer formed by fluorescent conjugated polymer. This offers many additional possibilities. A variety of amphiphilic, 'fatty-acid-type' molecules can form Langmuir-Blodgett monolayers and multilayers with incorporation of fluorescent dyes, and this possibility should not be overlooked.

In addition, the last point. Surface can be extensively used as a platform for solid-phase synthesis of peptides and oligonucleotides with analyte receptor functions. Affinity coupling and self-assembly as important steps for making the sensors of high complexity can be efficiently provided on the surface. The thin film technology is also one of the most powerful strategies for immobilization of sensor units on artificial devices such as optodes.

9.5 Functional Lipid and Polymer Bilayers

The membrane of a living cell is probably one of the brightest examples of how Nature uses self-assembly of relatively simple building blocks to create highly organized structures. Membrane can be viewed as a structure formed of lipids with different integral proteins and glycolipids incorporated into it. Lipids alone can form

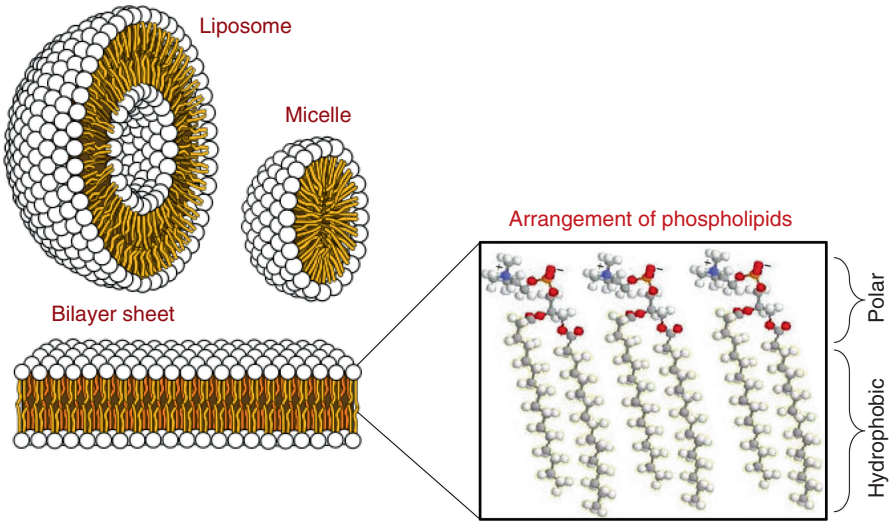

Fig. 9.17 Popular schematic view (Wikipedia) of liposome, micelle and flat bilayer sheet formed by lipid molecules. Stability of these structures is determined by amphiphilic properties of constituting molecules and their arrangement in monolayer (*shown right*). Polar heads tend to be exposed to aqueous solvent, whereas hydrophobic tails tend to be screened from it forming the central part of bilayer

artificial self-assembled structures that in many properties resemble the cell membranes, the basic element of which is the *lipid bilayer*.

Lipid bilayers (Fig. 9.17) can form the structures of different curvatures, from planar membranes to small nanoparticles (of the smallest size of ~50 nm) with a closed volume. The latter are called the *lipid vesicles* or *liposomes*. Their stability allows to fill their inner volume and to use them as drug carriers. Bilayers themselves allow incorporation of membrane proteins, making them convenient models of biological membranes.

Common phospholipids forming these structures are the molecules with polar heads and two long (16–18 carbon atoms) hydrocarbon tails. The bilayer consists of two monolayers, in which the apolar tails get together and polar heads stretch out to form two outer surfaces extending to aqueous solvent. When a vesicle is formed, some of the heads appear facing the inner volume and the others extend to the outer surface. The small low-polar molecules can be dissolved between hydrophobic tails in the inner part of bilayer. Bilayer membranes, especially in the form of vesicles, offer very interesting possibilities for fluorescence sensing.

9.5.1 Liposomes as Integrated Sensors

Liposomes are the self-organized membrane structures. They can spontaneously form in water from suspension of hydrated lipids (phospholipids or sphingolipids) by sonication, injection through porous membrane or just by gentle agitation. They possess very important collective properties. If they are made of a single type of

lipid, they exhibit remarkable cooperativity in structural transitions. Thus, as a function of temperature the phospholipid molecules can change the structural arrangement in the bilayer at fixed temperature within the transition range as narrow as 0.6°C. These transitions between structural forms are extremely sensitive to incorporation of some other molecules, such as cholesterol.

The structural and dynamic properties of the bilayers can change in a specific manner on incorporation of many different compounds (and the general anesthetics are the well-known examples). Important to note, all these changes involve only arrangements and dynamics of lipids and do not produce the change of overall structure and integrity of liposome. Being very thin (about 4 nm in width) the bilayers possess tremendous depth-dependent gradients of polarity, hydration and electric fields. They are practically impermeable to ions, even to protons.

The latter properties make the bilayers the ideal transducers in sensor technologies. From the time of discovery, liposomes are the objects of active research with various fluorescent dyes serving as the 'probes' for their structure and dynamics. The targeted synthesis of smart derivatives of wavelength-ratiometric two-color fluorescent dyes made possible their spontaneous incorporation into the bilayer in desired depth and orientation (Klymchenko et al. 2002) (Fig. 9.18). This allowed determining the polarity and hydration in the bilayer for the first time as easily distinguishable parameters (Klymchenko et al. 2004a, b), and characterization of its electrostatic potential (Klymchenko et al. 2003).

Thus, we know that liposome can interact with different molecules, and this interaction changes its collective structural and dynamic properties, without changing its integrity. We know also that these interactions can depend strongly on lipid composition of the membrane, and in this sense can be very specific. We possess

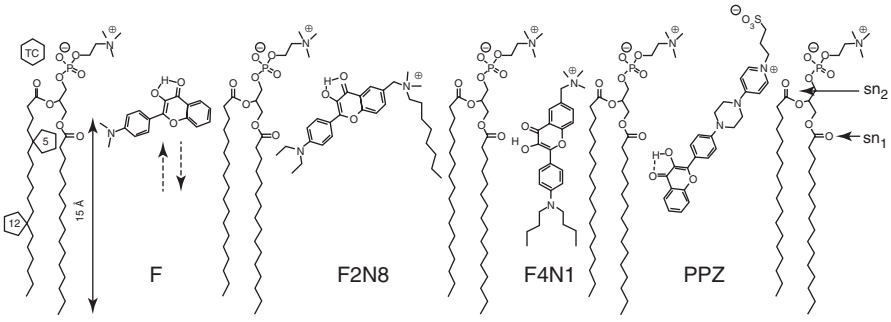

Fig. 9.18 The first-generation 3-hydroxychromone dyes for biomembrane studies (Klymchenko et al. 2002). Dye **F** does not occupy a well-determined position (its motion is shown by *arrows*). Dependent on its position, it may or may not form hydrogen bond with water. Location of Dye **F2N8** is at the polar interface. Dye **F4N1** in vertical orientation goes deeper into the bilayer, on the level of the lipid sn_1 carbonyls. Dye **PPZ** is in inverted orientation, it goes deeper than the carbonyl groups. Such location is supported by the results on quenching by nitroxide paramagnetic quenchers that were covalently attached to the lipids (shown in the *left part* of the figure)

novel fluorescence dyes as the tools to provide the most sensitive response to these interactions. What remains, is to make the sensors. It was demonstrated that the lipid bilayer itself can serve as the sensor element that allows for the efficient detection and characterization of molecules that interact with the membrane and changes its structure. Possessing high cooperativity, the *whole bilayer structure* can serve as a composed nanosensor combining the binding and reporting functions, so the transduction occurs due to cooperative properties of the bilayer. Located in the bilayer fluorescent dyes provide the reporting signal.

This idea was explored for the development of prototype sensor for *cholesterol*. The changes in lipid membranes on incorporation of cholesterol are well-known. They are especially great for bilayers made of lipid sphingomyelin that are able to form with cholesterol the very rigid structures, "rafts". We formed the vesicles made of sphingomyelin, incorporating functional 3HC dyes and observed dramatic changes of fluorescence color on incorporation of cholesterol (Turkmen et al. 2005). These experiments were reproduced with a number of dyes and one of these results is presented in Fig. 9.19.

We observe that on incorporation of cholesterol the blue (500 nm) band looses about 80 % of its relative integral intensity. This dramatic change of color can be easily detected even visually and, of course, with the application of a simple fluorescence detection technique. The absence of the effect of cholesterol on the spectra in phosphatidylcholine vesicles demonstrates that specific raft-forming structure is needed for generation of spectroscopic changes.

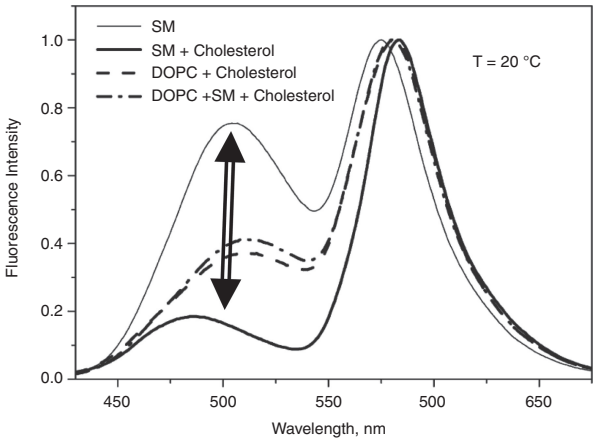

Fig. 9.19 The prototype for two-band ratiometric fluorescence sensor for cholesterol that uses sphingomyelin (*SM*) bilayer vesicles with functionalized 3HF dye (Turkmen et al. 2005). *Thin solid line* represents the spectrum in SM bilayer. Upon addition of cholesterol, the relative intensity of the short-wavelength band dramatically (by ~80 %) decreases (*thick solid line*). This does not happen when cholesterol is added to phosphatidylcholine (*DOPC*) vesicles (compare *dash* and *dot-dash lines*). The *arrow* shows dynamic range of this effect

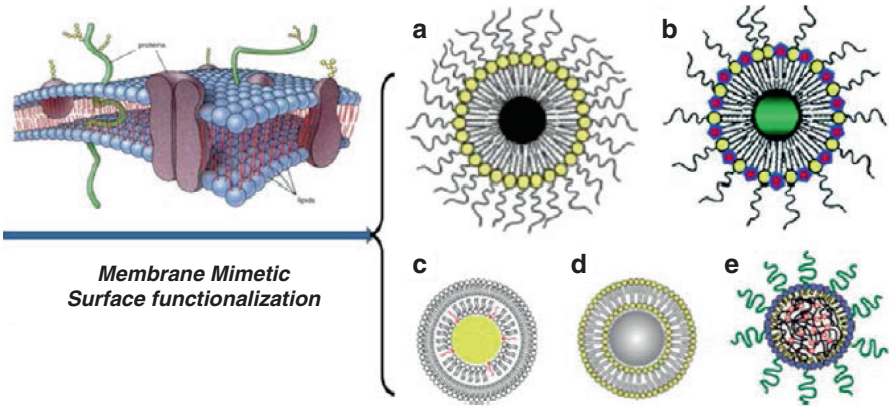

Fig. 9.20 Schematic representation of typical membrane mimetic surface functionalization of nanoparticles (Weingart et al. 2013). (**a**) Magnetic nanoparticle. (**b**) Quantum dot. (**c**) Gold nanoparticles. (**d**) Silica nanoparticle. (**e**) Polymeric nanoparticle

9.5.2 Stabilized Phospholipid Bilayers

The weak points of liposomes are well known to those who work with them. It is not easy to make them homogeneous in size, and their long-term stability is bad. Therefore, the idea appeared to stabilize them by forming them around micro- or nanoparticles, to form *core-shell liposomes*. The cores of these particles may be of noble metals, polymeric or composed of quantum dots with the exploration in full of their signal transduction and fluorescence possibilities. In such construction the particle serves as the 'core', it is surrounded by lipid bilayer as the 'shell' (Mornet et al. 2005; Troutier and Ladavière 2007; Weingart et al. 2013), see Fig. 9.20.

The core determines the particle size and shape and protects it from spontaneous decomposition. It can be selected in order to obtain additional valuable properties. For instance, it can be made magnetic (Shinkai 2002), which will facilitate separation of sensor particles from tested media and their repeated use. Alternatively, being a polymer or silica bead doped with fluorescent dye or quantum dot, it can provide fluorescent emission. The procedures of making these composites are simple due to spontaneous formation of bilayers (Mornet et al. 2005). The nanocomposites based on silica core and phospholipid bilayer shell are quite popular in fluorescence sensing technologies (Chemburu et al. 2010).

Different types of nanoparticles can play the role of a core in such nanocomposites (Weingart et al. 2013). The stabilizing core effect on phospholipid bilayers is frequently observed. The membrane-inserted sensor functionalities can be engineered in bilayers formed on the surface of polymer latex beads (Fig. 9.21). These composites called *lipobeads* can be transformed into fluorescent sensors by incorporation into the bilayer of various fluorescent dyes that possess sensing properties or are conjugated with recognition units. Such lipobead nanosensors were suggested for intracellular measurements of pH, Ca^{2+}, and O_2 (Ma and Rosenzweig 2005).

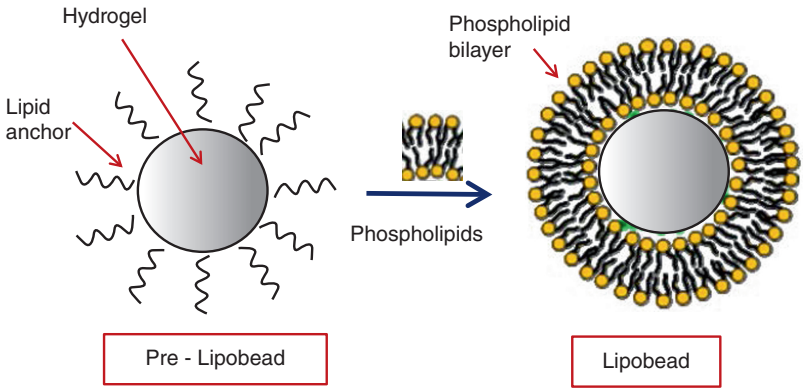

Fig. 9.21 Schematic illustration of the self-assembly of a lipid membrane around a hydrogel-phospholipid conjugate (Ng et al. 2001)

There are large possibilities in the modification of the surfaces of these particles with bioactive molecules for the development of biosensors.

The membrane shell can possess both receptor and reporter properties and can be modified for that in many ways. Lipid self-assembly on particles allows receptor insertion and amplification of receptor-target recognition. One of such incorporated receptors can be monosialoganglioside GM1, which can specifically bind *cholera toxin* (Carmona-Ribeiro 2001). Utility of self-assembled vesicles, bilayers or monolayers at interfaces is limited only by our own imagination.

The *planar surfaces* of optical waveguides and microfluidic devices can also be modified by depositing the lipid bilayers resulting in their stabilization and allowing incorporation of different types of recognition units. Among recent developments is the formation of bilayer membrane that recognizes cholera toxin directly on the surface of a planar optical waveguide (Kelly et al. 2006). This approach can be extended to the development of sensor arrays on planar support (Yamazaki et al. 2005). Incorporation of integral membrane proteins into the arrayed membranes enables the study of ligand/receptor binding, as well as the interactions with intact living cells.

9.5.3 Polymersomes

Polymersomes are *synthetic analogs of liposomes* made of amphiphilic vesicle-forming block copolymers. The advantage of polymersomes over liposomes is their increased stability, which contributes to the increased lifetimes of these structures. In contrast to common liposomes that have high tendency to collapse with time, polymersomes can be made to be stable eternally. This can be achieved by their chemical cross-linking (Discher et al. 2002).

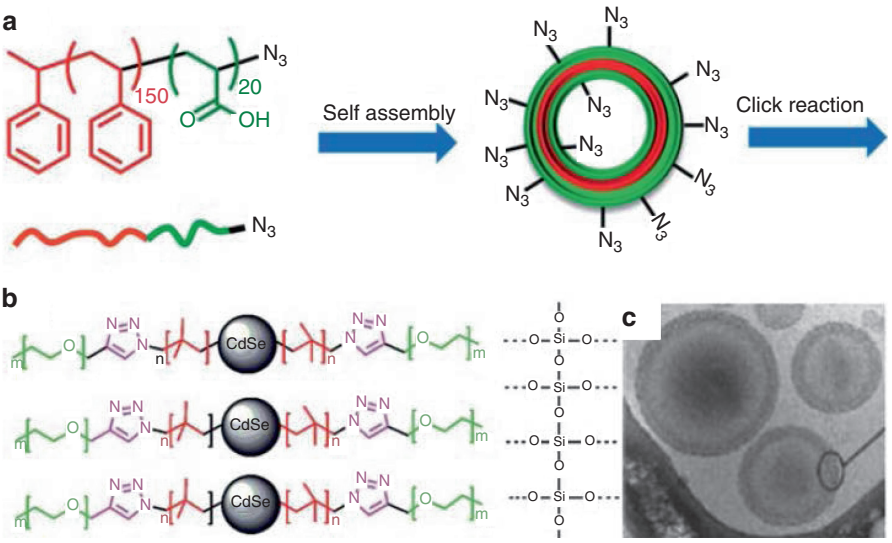

Fig. 9.22 Click reactions stabilizing polymersomes (Li and Binder 2011). (**a**) Modification of polymersomes for click reaction by introduction of azide groups for forming shell-stabilized polymersomes. (**b**) Synthesis of diblock copolymers on the surface of nanoparticles can be provided with the aid of click reaction. (**c**) The formed nanocomposites can be covered with silica shell

For the formation of bilayers, the polymersomes have to be assembled according to the same principle as the lipid vesicles. In this case they consist of two blocks – polar heads and hydrophobic tails. The vast amount of available monomers and the ability to vary the ratio of the two blocks make it possible to tune the properties of the resulting vesicles, for example, vesicle size, polarity, stability, etc. In general, the membranes of block copolymer vesicles possess higher thickness and less fluidity compared to liposomes (Antonietti and Forster 2003). These properties can vary in broad ranges depending on the polymer composition (Bermudez et al. 2002).

Formation of polymersomes and subsequent manipulations with them can be provided with the aid of click reaction (Fig. 9.22). This allows obtaining core-shell nanocomposites of various structures and properties (Li and Binder 2011).

Polymersomes are still waiting for their intensive exploration in sensing and imaging technologies.

9.5.4 Formation of Protein Layers Over Lipid Bilayers

The layers formed by two-dimensional crystallization of *S-layer proteins* usually need some support for their formation. It was demonstrated that they can be readily formed over liposomes (Moll et al. 2002). This allows activating an important line of development in combining the S-layer and lipid membrane technologies (Huber

et al. 2006). Although, the development of S-layer technologies was focused primarily on liposomal drug delivery systems, an important field of future applications emerges in sensor technologies.

The interaction of S-layer proteins with lipid molecules is noncovalent. Electrostatic interaction between exposed carboxy groups on the inner face of the S-layer lattice and the zwitterionic lipid head groups at the outer face of liposomes is primarily responsible for the binding and defined orientation of the S-layer subunits. As a result, they can form a closed shell around liposome and this allows obtaining the composites with essentially increased stability. However, these interactions do not reduce substantially the lipid mobility in the plane of bilayer. A formed closed lattice structure is amendable to different modifications. Moreover, since S-layer proteins can be genetically modified and fused with other structure-forming proteins, the supramolecular functional constructs can be assembled.

9.5.5 Prospects

There are many very positive features offered by lipid bilayers and their analogs. These structures can be formed spontaneously and they allow spontaneous incorporation into them of different functional molecules, both receptors and reporters. They can respond to target binding by the changes of their integral and easily measurable properties, such as the lipid order and dynamics. When they form the particles with closed inner volumes (liposomes), these particles can retain in this volume many different molecules or particles with diverse functional possibilities. The composites containing single particles surrounded by the bilayer are of special importance because they allow achieving a strongly increased stability of the bilayer towards aggregation or decomposition and also because of possibility to provide additional useful properties to the core particles. Synthetic lipid analogs and bilayer-forming polymers expand these possibilities.

9.6 Sensing and Thinking: Extending Sensing Possibilities with Smart Nano-ensembles

Reading this Chapter we observe a myriad of opportunities for manipulating with interactions of molecules, nanoparticles and surfaces. Since there is no limit regarding the sensor construct, the choice of optimal solution can be made on a very broad scale. This may involve not only molecular complexes and responding nanoparticles, but also the self-assembled supramolecular structures, composite nanoparticles (that combine recognition and response properties) and various types of surfaces and interfaces. Clearly, this relatively new field of development of fluorescence sensors is far from being mature. Whereas the advance in recognition units and fluorescence reporters, though promising many improvements, follows already well-established trends,

the optimization of their performance based on the principles of integration and self-assembly promises new exciting discoveries that will result in new useful products.

Synthetic strategies based on covalent linking, affinity coupling and self-assembly offer many advantages. They include the minimization of synthetic work, the ease of modification and optimization of the sensor, the possibility to tune its properties by a simple adjustment of the ratio of components. The applications of these new concepts tend not only to combine the target binding and the response but also to improve this response by creating optimal supramolecular ensemble allowing activating optimal communication and signal transduction between its structural elements. The recognition units can be formed by assembly of functional molecules with the appearance of new recognition properties.

Incorporation onto planar surfaces and nano-sized structures provides the support for functional materials that allows their stabilization and integration into self-assembled nanoscale recognition units. The use of nanoparticles can make these recognition units nano-sized and multi-valent. In addition, the self-assembled systems allow great possibilities for introduction of fluorescence response functionality and thus for providing additional important properties. In the assembly, the receptor and the reporter units may not interact directly and the signal on target binding can be transmitted due to their spatial closeness ensured by the template and even indirectly via the change of integral property of nanoscale system.

Improving the functionality is always increasing the complexity. For overcoming the observed difficulties, the libraries of sensor building blocks have to be created. The well established streptavidin-biotin pair is not optimal for many applications, therefore new pairs for molecular assembly, especially of synthetic origin, should appear offering new possibilities. Their libraries are expected to be made available and then easily combined to produce the most suitable system for the desired use.

Questions and Problems

1. Evaluate the prospective application of carbon nanotubes. Can they serve as support materials? Or as optical signal transducers? Or as the FRET donors or acceptors with organic dyes?
2. Why the nanoscale materials with core–shell composition are so attractive? How they can combine recognition and response properties?
3. What is the advantage of DNA scaffold compared to that made of synthetic polymers? How does the DNA structure allow incorporation of bulky substituents? Provide the modeling and compare your predicted structures with the results on porphyrins-DNA composites described in ref. (Fendt et al. 2007).
4. Is it possible to design the partner for self-assembly, based on the known three-dimensional structure of the other partner? On what principles this design should be based?
5. How many intermolecular hydrogen bonds should be formed to make the dimeric structure stable?
6. Explain, why the support surface formed by S-layer protein allows obtaining the structures, in which the sensor elements can face only one side. What factors could determine the sidedness?

7. Why the operation of sensors based on micellar structures does not allow a broad-range variation of micelle-forming detergent concentrations? Explain the 'concentration-of-the-target' effect of micelles.
8. What are the structural and energetic requirements for the formation of self-assembled monolayers?
9. What are the advantages of hydrogel layers? What additional limitations are imposed on the use of this support material?
10. Can the Langmuir-Blodgett films be formed on a polar surface? Can they be formed in the presence of detergent? How to incorporate fluorescent dye into these films?
11. In what medium the layer-by-layer assembly should be made?
12. List the most important properties of phospholipid bilayers and vesicles (liposomes) made of them. What are the reasons and what are the means to stabilize them? What new properties can be obtained?
13. How could you define the recognition element and signal transduction mechanism in liposome cholesterol sensor?
14. On what length scales can you estimate the applications of 'top-down' and 'bottom-up' approaches? Does the gap between them exist, and how it can be filled?

References

Aili D, Enander K, Baltzer L, Liedberg B (2007) Synthetic de novo designed polypeptides for control of nanoparticle assembly and biosensing. Biochem Soc Trans 35:532–534

Alekseeva VI, Marinina LE, Savvina LP, Ibrayev NH (2005) Spectral and luminescent properties of nile red dye in Langmuir-Blodgett films. Mol Cryst Liq Cryst 427(1):471–478

Algar WR, Prasuhn DE, Stewart MH, Jennings TL, Blanco-Canosa JB, Dawson PE, Medintz IL (2011) The controlled display of biomolecules on nanoparticles: a challenge suited to bioorthogonal chemistry. Bioconjug Chem 22(5):825–858. doi:10.1021/bc200065z

Antonietti M, Forster S (2003) Vesicles and liposomes: a self-assembly principle beyond lipids. Adv Mater 15(16):1323–1333

Arduini M, Rampazzo E, Mancin F, Tecilla P, Tonellato U (2007) Template assisted self-organized chemosensors. Inorg Chim Acta 360(3):721–727

Ariga K, Nakanishi T, Michinobu T (2006) Immobilization of biomaterials to nano-assembled films (self-assembled monolayers, Langmuir-Blodgett films, and layer-by-layer assemblies) and their related functions. J Nanosci Nanotechnol 6(8):2278–2301

Ariga K, Hill JP, Ji QM (2007) Layer-by-layer assembly as a versatile bottom-up nanofabrication technique for exploratory research and realistic application. Phys Chem Chem Phys 9(19):2319–2340

Aubin-Tam M-E, Hamad-Schifferli K (2008) Structure and function of nanoparticle–protein conjugates. Biomed Mater 3(3):034001

Baldini L, Casnati A, Sansone F, Ungaro R (2007) Calixarene-based multivalent ligands. Chem Soc Rev 36(2):254–266

Balzani V, Credi A, Venturi M (2003) Molecular logic circuits. Chemphyschem 4(1):49–59

Barone PW, Baik S, Heller DA, Strano MS (2005) Near-infrared optical sensors based on single-walled carbon nanotubes. Nat Mater 4(1):86–92, doi:nmat1276 [pii] 10.1038/nmat1276

Bergamini G, Marchi E, Ceroni P (2010) Luminescent dendrimers as ligands and sensors of metal ions. In: Demchenko AP (ed) Advanced fluorescence reporters in chemistry and biology II:

molecular constructions, polymers and nanoparticles, vol 9. Ser Fluoresc, Springer Berlin-Heidelberg; pp 253–284
Bermudez H, Brannan AK, Hammer DA, Bates FS, Discher DE (2002) Molecular weight dependence of polymersome membrane structure, elasticity, and stability. Macromolecules 35(21):8203–8208
Biju V, Itoh T, Ishikawa M (2010) Delivering quantum dots to cells: bioconjugated quantum dots for targeted and nonspecific extracellular and intracellular imaging. Chem Soc Rev 39(8):3031–3056. doi:10.1039/b926512k
Boeneman K, Deschamps JR, Buckhout-White S, Prasuhn DE, Blanco-Canosa JB, Dawson PE, Stewart MH, Susumu K, Goldman ER, Ancona M, Medintz IL (2010) Quantum dot DNA bioconjugates: attachment chemistry strongly influences the resulting composite architecture. ACS Nano 4(12):7253–7266. doi:10.1021/nn1021346
Brea RJ, Vazquez ME, Mosquera M, Castedo L, Granja JR (2007) Controlling multiple fluorescent signal output in cyclic peptide-based supramolecular systems. J Am Chem Soc 129(6):1653–1657
Brennan JL, Hatzakis NS, Tshikhudo TR, Dirvianskyte N, Razumas V, Patkar S, Vind J, Svendsen A, Nolte RJ, Rowan AE (2006) Bionanoconjugation via click chemistry: the creation of functional hybrids of lipases and gold nanoparticles. Bioconjug Chem 17(6):1373–1375
Brinkley M (1992) A brief survey of methods for preparing protein conjugates with dyes, haptens, and cross-linking reagents. Bioconjug Chem 3(1):2–13
Briones C, Martin-Gago JA (2006) Nucleic acids and their analogs as nanomaterials for biosensor development. Curr Nanosci 2(3):257–273
Brunner J (1993) New photolabeling and cross-linking methods. Annu Rev Biochem 62:483–514
Burnham MR, Turner JN, Szarowski D, Martin DL (2006) Biological functionalization and surface micropatterning of polyacrylamide hydrogels. Biomaterials 27(35):5883–5891
Carmona-Ribeiro AM (2001) Bilayer vesicles and liposomes as interface agents. Chem Soc Rev 30(4):241–247
Cejas MA, Raymo FM (2005) Fluorescent diazapyrenium films and their response to dopamine. Langmuir 21(13):5795–5802
Chaki NK, Vijayamohanan K (2002) Self-assembled monolayers as a tunable platform for biosensor applications. Biosens Bioelectron 17(1):1–12
Chemburu S, Fenton K, Lopez GP, Zeineldin R (2010) Biomimetic silica microspheres in biosensing. Molecules 15(3):1932–1957
Choi JH, Strano MS (2007) Solvatochromism in single-walled carbon nanotubes. Appl Phys Lett 90(22)
Corbin PS, Lawless LJ, Li ZT, Ma YG, Witmer MJ, Zimmerman SC (2002) Discrete and polymeric self-assembled dendrimers: hydrogen bond-mediated assembly with high stability and high fidelity. Proc Natl Acad Sci U S A 99(8):5099–5104
Crespo-Biel O, Dordi B, Reinhoudt DN, Huskens J (2005) Supramolecular layer-by-layer assembly: alternating adsorptions of guest- and host-functionalized molecules and particles using multivalent supramolecular interactions. J Am Chem Soc 127(20):7594–7600
Davis F, Higson SPJ (2005) Structured thin films as functional components within biosensors. Biosens Bioelectron 21(1):1–20
del Mercato LL, Pompa PP, Maruccio G, Della Torre A, Sabella S, Tamburro AM, Cingolani R, Rinaldi R (2007) Charge transport and intrinsic fluorescence in amyloid-like fibrils. Proc Natl Acad Sci U S A 104(46):18019–18024
Demchenko AP (2001) Recognition between flexible protein molecules: induced and assisted folding. J Mol Recognit 14(1):42–61
Deng X, Tang H, Jiang J (2014) Recent progress in graphene-material-based optical sensors. Anal Bioanal Chem 406(27):6903_6916
Discher BM, Bermudez H, Hammer DA, Discher DE, Won YY, Bates FS (2002) Cross-linked polymersome membranes: vesicles with broadly adjustable properties. J Phys Chem B 106(11):2848–2854
Egawa Y, Hayashida R, Anzai JI (2006) Multilayered assemblies composed of brilliant yellow and poly(allylamine) for an optical pH sensor. Anal Sci 22(8):1117–1119

El-khouri R, Szamocki R, Sergeeva Y, Felix O, Decher G (2012) Multifunctional layer-by-layer architectures for biological applications. Funct Polymer Films 2:11–71

Erathodiyil N, Ying JY (2011) Functionalization of inorganic nanoparticles for bioimaging applications. Acc Chem Res 44(10):925–935

Fendt LA, Bouamaied I, Thoni S, Amiot N, Stulz E (2007) DNA as supramolecular scaffold for porphyrin arrays on the nanorneter scale. J Am Chem Soc 129(49):15319–15329

Feng X, Tang Y, Duan X, Liu L, Wang S (2010) Lipid-modified conjugated polymer nanoparticles for cell imaging and transfection. J Mater Chem 20(7):1312–1316

Fischler M, Sologubenko A, Mayer J, Clever G, Burley G, Gierlich J, Carell T, Simon U (2008) Chain-like assembly of gold nanoparticles on artificial DNA templates via 'click chemistry'. Chem Commun 2:169–171

Flink S, van Veggel F, Reinhoudt DN (2000) Sensor functionalities in self-assembled monolayers. Adv Mater 12(18):1315–1328

Gao XY, Matsui H (2005) Peptide-based nanotubes and their applications in bionanotechnology. Adv Mater 17(17):2037–2050

He H, Gao C (2011) Click chemistry on nano-surfaces. Curr Org Chem 15(21):3667–3691

Henzie J, Barton JE, Stender CL, Odom TW (2006) Large-area nanoscale patterning: chemistry meets fabrication. Acc Chem Res 39(4):249–257

Hermanson GT (1995) Bioconjugation techniques. Academic, San Diego

Hötzer B, Medintz IL, Hildebrandt N (2012) Fluorescence in nanobiotechnology: sophisticated fluorophores for novel applications. Small 8(15):2297–2326. doi:10.1002/smll.201200109

Huber C, Liu J, Egelseer EM, Moll D, Knoll W, Sleytr UB, Sara M (2006) Heterotetramers formed by an S-layer-streptavidin fusion protein and core-streptavidin as a nanoarrayed template for biochip development. Small 2(1):142–150

Hussain SA, Paul PK, Bhattacharjee D (2006) Role of microenvironment in the mixed Langmuir-Blodgett films. J Colloid Interface Sci 299(2):785–790

Ianoul A, Bergeron A (2006) Spatially inhomogeneous enhancement of fluorescence by a monolayer of silver nanoparticles. Langmuir 22(24):10217–10222

Ito O, D'Souza F (2012) Recent advances in photoinduced electron transfer processes of fullerene-based molecular assemblies and nanocomposites. Molecules 17(5):5816–5835

Jiang H, Zhao XY, Schanze KS (2007) Effects of polymer aggregation and quencher size on amplified fluorescence quenching of conjugated polyelectrolytes. Langmuir 23(18): 9481–9486

Jin Z, Hildebrandt N (2012) Semiconductor quantum dots for in vitro diagnostics and cellular imaging. Trends Biotechnol 30(7):394–403, doi:S0167-7799(12)00056-X [pii] 10.1016/j.tibtech.2012.04.005

Katz E, Willner I (2004) Integrated nanoparticle–biomolecule hybrid systems: synthesis, properties, and applications. Angew Chem Int Ed 43(45):6042–6108. doi:10.1002/anie.200400651

Katzen F, Chang G, Kudlicki W (2005) The past, present and future of cell-free protein synthesis. Trends Biotechnol 23(3):150–156

Kelly TL, Lam MCW, Wolf MO (2006) Carbohydrate-labeled fluorescent microparticles and their binding to lectins. Bioconjug Chem 17(3):575–578

Klymchenko AS, Duportail G, Ozturk T, Pivovarenko VG, Mely Y, Demchenko AP (2002) Novel two-band ratiometric fluorescence probes with different location and orientation in phospholipid membranes. Chem Biol 9(11):1199–1208

Klymchenko AS, Duportail G, Mely Y, Demchenko AP (2003) Ultrasensitive two-color fluorescence probes for dipole potential in phospholipid membranes. Proc Natl Acad Sci U S A 100(20):11219–11224

Klymchenko AS, Duportail G, Demchenko AP, Mely Y (2004a) Fluorescence probing of polarity, hydration and electrostatics in lipid bilayers with 3-hydroxyflavone dyes. Biophys J 86(1):31A–31A

Klymchenko AS, Mely Y, Demchenko AP, Duportail G (2004b) Simultaneous probing of hydration and polarity of lipid bilayers with 3-hydroxyflavone fluorescent dyes. Biochimica Et Biophysica Acta-Biomembranes 1665(1–2):6–19

Kriegisch V, Lambert C (2005) Self-assembled monolayers of chromophores on gold surfaces. In: Supermolecular dye chemistry, Topics Curr Chem 258:257–313
Kuzyk A, Laitinen KT, Törmä P (2009) DNA origami as a nanoscale template for protein assembly. Nanotechnology 20(23):235305
Kwon H, Jiang W, Kool ET (2015) Pattern-based detection of anion pollutants in water with DNA polyfluorophores. Chem Sci 6(4):2575–2583
Le Droumaguet C, Wang C, Wang Q (2010) Fluorogenic click reaction. Chem Soc Rev 39(4):1233–1239
Lehn J-M (1995) Supramolecular chemistry. VCH, Weinheim
Li N, Binder WH (2011) Click-chemistry for nanoparticle-modification. J Mater Chem 21(42):16717–16734
Li C, Liu S (2012) Polymeric assemblies and nanoparticles with stimuli-responsive fluorescence emission characteristics. Chem Commun 48(27):3262–3278
Lidke DS, Nagy P, Jovin TM, Arndt-Jovin DJ (2007) Biotin-ligand complexes with streptavidin quantum dots for in vivo cell labeling of membrane receptors. Methods Mol Biol 374:69–79
Link AJ, Mock ML, Tirrell DA (2003) Non-canonical amino acids in protein engineering. Curr Opin Biotechnol 14(6):603–609
Lu CH, Li J, Liu JJ, Yang HH, Chen X, Chen GN (2010) Increasing the sensitivity and single-base mismatch selectivity of the molecular beacon using graphene oxide as the "nanoquencher". Chemistry 16(16):4889–4894
Ma AH, Rosenzweig Z (2005) Synthesis and analytical properties of micrometric biosensing lipobeads. Anal Bioanal Chem 382(1):28–36
Mahar B, Laslau C, Yip R, Sun Y (2007) Development of carbon nanotube-based sensors – a review. IEEE Sensors J 7(1–2):266–284
Mancin F, Rampazzo E, Tecilla P, Tonellato U (2006) Self-assembled fluorescent chemosensors. Chemistry 12(7):1844–1854
Mann JA, Dichtel WR (2013) Noncovalent functionalization of graphene by molecular and polymeric adsorbates. J Phys Chem Lett 4(16):2649–2657
Marvin JS, Corcoran EE, Hattangadi NA, Zhang JV, Gere SA, Hellinga HW (1997) The rational design of allosteric interactions in a monomeric protein and its applications to the construction of biosensors. Proc Natl Acad Sci U S A 94(9):4366–4371
Mattu J, Johansson T, Holdcroft S, Leach GW (2006) Highly ordered polymer films of amphiphilic, regioregular polythiophene derivatives. J Phys Chem B 110(31):15328–15337
Medintz IL, Sapsford KE, Clapp AR, Pons T, Higashiya S, Welch JT, Mattoussi H (2006) Designer variable repeat length polypeptides as scaffolds for surface immobilization of quantum dots. J Phys Chem B 110(22):10683–10690
Moll D, Huber C, Schlegel B, Pum D, Sleytr UB, Sara M (2002) S-layer-streptavidin fusion proteins as template for nanopatterned molecular arrays. Proc Natl Acad Sci U S A 99(23):14646–14651
Mornet S, Lambert O, Duguet E, Brisson A (2005) The formation of supported lipid bilayers on silica nanoparticles revealed by cryoelectron microscopy. Nano Lett 5(2):281–285
Moyano DF, Rotello VM (2011) Nano meets biology: structure and function at the nanoparticle interface. Langmuir 27(17):10376–10385. doi:10.1021/la2004535
Neto AC, Guinea F, Peres NM (2006) Drawing conclusions from graphene. Phys World 19(11):33
Ng CC, Cheng YL, Pennefather PS (2001) One-step synthesis of a fluorescent phospholipid-hydrogel conjugate for driving self-assembly of supported lipid membranes. Macromolecules 34(17):5759–5765
Oshovsky GV, Reinhoudt DN, Verboom W (2007) Supramolecular chemistry in water. Angewandte Chemie-International Edition 46(14):2366–2393
Peng H-C, Kang C-C, Liang M-R, Chen C-Y, Demchenko A, Chen C-T, Chou P-T (2011) En route to white-light generation utilizing nanocomposites composed of ultrasmall CdSe nanodots and excited-state intramolecular proton transfer dyes. ACS Appl Mater Interfaces 3(5):1713–1720

Perez-Luna VH, Yang SP, Rabinovich EM, Buranda T, Sklar LA, Hampton PD, Lopez GP (2002) Fluorescence biosensing strategy based on energy transfer between fluorescently labeled receptors and a metallic surface. Biosens Bioelectron 17(1–2):71–78

Piervincenzi RT, Reichert WM, Hellinga HW (1998) Genetic engineering of a single-chain antibody fragment for surface immobilization in an optical biosensor. Biosens Bioelectron 13(3–4):305–312

Prasuhn DE, Deschamps JR, Susumu K, Stewart MH, Boeneman K, Blanco-Canosa JB, Dawson PE, Medintz IL (2010) Polyvalent display and packing of peptides and proteins on semiconductor quantum dots: predicted versus experimental results. Small 6(4):555–564. doi:10.1002/smll.200901845

Pu K-Y, Li K, Liu B (2010) Multicolor conjugate polyelectrolyte/peptide complexes as self-assembled nanoparticles for receptor-targeted cellular imaging. Chem Mater 22(24):6736–6741. doi:10.1021/cm102788b

Rao JH, Lahiri J, Isaacs L, Weis RM, Whitesides GM (1998) A trivalent system from vancomycin center dot D-Ala-D-Ala with higher affinity than avidin center dot biotin. Science 280(5364):708–711

Renard M, Belkadi L, Hugo N, England P, Altschuh D, Bedouelle H (2002) Knowledge-based design of reagentless fluorescent biosensors from recombinant antibodies. J Mol Biol 318(2):429–442

Revell DJ, Knight JR, Blyth DJ, Haines AH, Russell DA (1998) Self-assembled carbohydrate monolayers: formation and surface selective molecular recognition. Langmuir 14(16):4517–4524

Rubina AY, Dementieva EI, Stomakhin AA, Darii EL, Pan'kov SV, Barsky VE, Ivanov SM, Konovalova EV, Mirzabekov AD (2003) Hydrogel-based protein microchips: manufacturing, properties, and applications. Biotechniques 34(5):1008–1014, 1016–1020, 1022

Rubina AY, Pan'kov SV, Dementieva EI, Pen'kov DN, Butygin AV, Vasiliskov VA, Chudinov AV, Mikheikin AL, Mikhailovich VM, Mirzabekov AD (2004) Hydrogel drop microchips with immobilized DNA: properties and methods for large-scale production. Anal Biochem 325(1):92–106

Ruckenstein E, Li ZF (2005) Surface modification and functionalization through the self-assembled monolayer and graft polymerization. Adv Colloid Interface Sci 113(1):43–63

Salavagione HJ, Martínez G, Ellis G (2011) Recent advances in the covalent modification of graphene with polymers. Macromol Rapid Commun 32(22):1771–1789

Satishkumar BC, Brown LO, Gao Y, Wang CC, Wang HL, Doorn SK (2007) Reversible fluorescence quenching in carbon nanotubes for biomolecular sensing. Nat Nanotechnol 2(9):560–564

Schaferling M, Riepl M, Pavlickova P, Paul H, Kambhampati D, Liedberg B (2003) Functionalized self-assembled monolayers on gold as binding matrices for the screening of antibody-antigen interactions. Microchimica Acta 142(4):193–203

Seeman NC (2003) At the crossroads of chemistry, biology, and materials: structural DNA nanotechnology. Chem Biol 10(12):1151–1159

Sharpe RBA, Burdinski D, Huskens J, Zandvliet HJW, Reinhoudt DN, Poelsema B (2007) Template-directed self-assembly of alkanethiol monolayers: selective growth on preexisting monolayer edges. Langmuir 23(3):1141–1146

Shinkai M (2002) Functional magnetic particles for medical application. J Biosci Bioeng 94(6):606–613

Sleytr UB, Egelseer EM, Ilk N, Pum D, Schuster B (2007) S-Layers as a basic building block in a molecular construction kit. FEBS J 274(2):323–334

Sobek J, Bartscherer K, Jacob A, Hoheisel JD, Angenendt P (2006) Microarray technology as a universal tool for high-throughput analysis of biological systems. Comb Chem High Throughput Screen 9(5):365–380

Sperling R, Parak W (2010) Surface modification, functionalization and bioconjugation of colloidal inorganic nanoparticles. Philos Trans R Soc A Math Phys Eng Sci 368(1915):1333–1383

Stine R, Pishko MV, Hampton JR, Dameron AA, Weiss PS (2005) Heat-stabilized phospholipid films: film characterization and the production of protein-resistant surfaces. Langmuir 21(24):11352–11356

Sullivan TP, Huck WTS (2003) Reactions on monolayers: organic synthesis in two dimensions. Eur J Org Chem 1:17–29

Svedhem S, Hollander CA, Shi J, Konradsson P, Liedberg B, Svensson SCT (2001) Synthesis of a series of oligo(ethylene glycol)-terminated alkanethiol amides designed to address structure and stability of biosensing interfaces. J Org Chem 66(13):4494–4503

Troutier A-L, Ladavière C (2007) An overview of lipid membrane supported by colloidal particles. Adv Colloid Interface Sci 133(1):1–21

Turkmen Z, Klymchenko AS, Oncul S, Duportail G, Topcu G, Demchenko AP (2005) A triterpene oleanolic acid conjugate with 3-hydroxyflavone derivative as a new membrane probe with two-color ratiometric response. J Biochem Biophys Methods 64(1):1–18

Vriezema DM, Aragones MC, Elemans J, Cornelissen J, Rowan AE, Nolte RJM (2005) Self-assembled nanoreactors. Chem Rev 105(4):1445–1489

Weingart J, Vabbilisetty P, Sun X-L (2013) Membrane mimetic surface functionalization of nanoparticles: methods and applications. Adv Colloid Interface Sci 197:68–84

Wilner OI, Willner I (2012) Functionalized DNA nanostructures. Chem Rev 112(4):2528–2556

Wróbel D, Graja A (2011) Photoinduced electron transfer processes in fullerene–organic chromophore systems. Coord Chem Rev 255(21):2555–2577

Xiang XM, Qian DJ, Li FY, Chen HT, Liu HG, Huang W, Feng XS (2006) Fabrication of europium complexes with 4′-(4-methylphenyl)-2,2′: 6′,2″-terpyridine and 4,4′-dinonyl-2,2′-dipyridyl at the air-water interface and their emission properties in Langmuir-Blodgett films. Colloids and Surfaces a-Physicochemical and Engineering Aspects 273(1–3):29–34

Yamazaki V, Sirenko O, Schafer RJ, Nguyen L, Gutsmann T, Brade L, Groves JT (2005) Cell membrane array fabrication and assay technology. BMC Biotechnol 5:18

Zhang Y, Wu C, Guo S, Zhang J (2013) Interactions of graphene and graphene oxide with proteins and peptides. Nanotechnol Rev 2(1):27–45

Chapter 10
Non-conventional Generation and Transformation of Response

Most of our discussion in previous Chapters was concentrated on the sensors that can be excited by light and emit informative light signal. Meantime, this is not the only possibility for obtaining the reporting information. The dye, or *luminophore* in general, can be also excited to emissive state in a chemical reaction (*chemiluminescence*), in biochemical transformation (*bioluminescence*) and reaction at electrode (*electroluminescence*, and more specifically, *electrochemiluminescence*). Light emission can be excited by radioactive light source (*radioluminescence*). Reporting can be provided by deactivation of the excited state not only in the form of emission or photoinduced chemical transformations but also in the form of electron transfer to conducting surface generating photocurrent (Fig. 10.1).

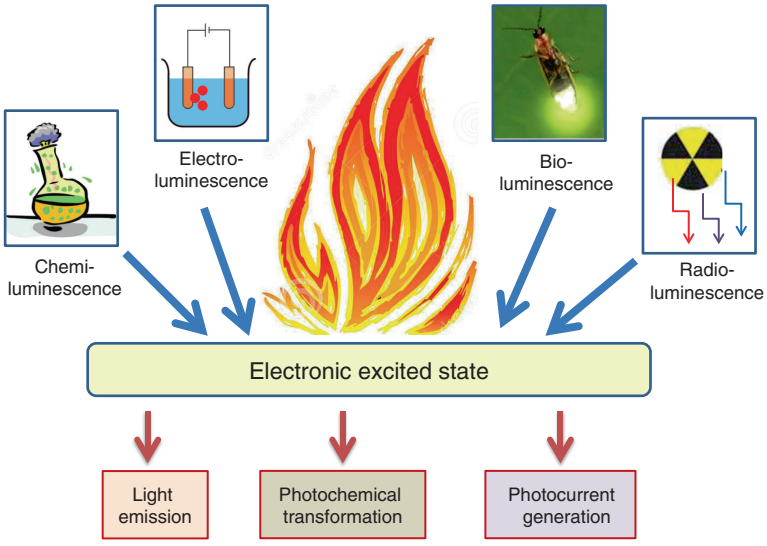

Fig. 10.1 Possibilities of non-optical electronic excitation of luminophores resulting in their emissive and non-emissive transformations

A.P. Demchenko, *Introduction to Fluorescence Sensing*,
DOI 10.1007/978-3-319-20780-3_10

This allows producing electrical signal directly, avoiding emission and detection of light. Moreover, emission of microscale semiconductor or polymeric light source can be directly coupled with the sensing event. Such coupling can be provided with the response of miniaturized detector.

Excitation via *evanescent field* effect is a powerful tool to introduce spatial resolution into the sensor system; it can be combined with different sensing technologies. Being introduced into heterogeneous assays, it allows providing a direct response to the target binding.

Though the systems exploring these possibilities develop quite rapidly, they cannot easily overcome the problems arising due to low sensitivity of produced or detected signal on the background of high noise level that is obviously present in miniaturized systems. Therefore this Chapter is complemented by the section describing the mechanisms of amplification of luminescence signal by coupling it with *plasmonic interactions*, which are, in some sense, also non-conventional.

10.1 Chemiluminescence and Electrochemiluminescence

Chemiluminescence is the emission that occurs as a result of chemical reaction and commonly is observed in solutions, being started by mixing the reagents. In contrast, *electrochemiluminescence* is the emission coupled with redox reaction at electrode. So it can usually be observed in solution in a thin pre-electrode layer. Both of them are the chemical reactions, in which the reagents are consumed and in which the chemical stoichiometry is observed. Each product of this reaction appears in the excited state and gets enough energy for emitting light, but because of different coupled deactivation events, the quantum yields of this emission rarely exceed 1 %. Generated are the excited states that are basically the same as in luminescence based on photon absorption, but no light source is needed. This also means the absence of optical background and, with the possibility of collecting the emitted quanta with their broad spectral distribution, achieving very high sensitivity of detection.

10.1.1 Chemiluminescence

Chemiluminescence is also known as ‘cold-light’ emission. It occurs when in a chemical reaction an intermediate is formed that decomposes into product with its electrons appearing in the excited state. Such species are able to relax to the ground state with the emission of light in the visible range of spectrum. Since the excited states are generated in chemical reactions, which are much slower than the electronic events the intensity of emitted light here is proportional to the reaction rate on a chemical step.

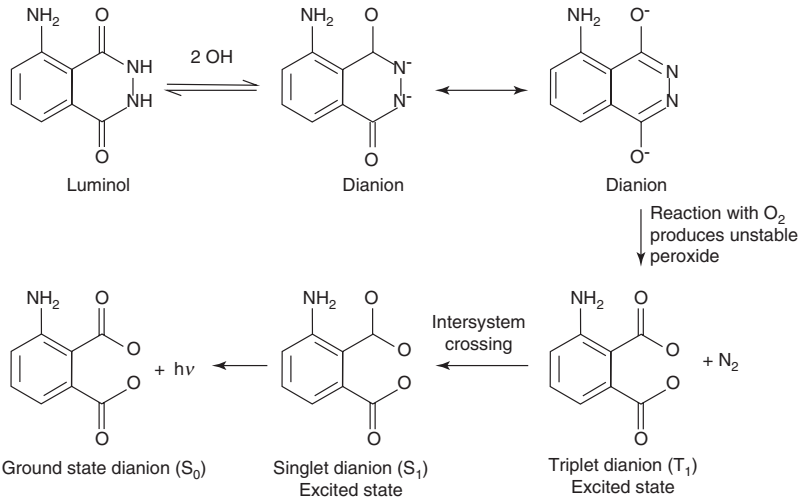

Fig. 10.2 The scheme of luminol transformations leading to chemiluminescence. First, luminol is activated with an oxidant to dianion. Usually, a solution of hydrogen peroxide (H_2O_2) and a hydroxide salt in water is used as the activator. In the presence of a catalyst (such as an iron-containing compound), the hydrogen peroxide is decomposed to form oxygen and water. The oxygen produced in this reaction reacts with luminol dianion to yield an organic peroxide. The latter is very unstable and immediately decomposes with the loss of nitrogen to produce 5-aminophthalic acid with electrons in an excited state. As the excited state relaxes to the ground state, the excess energy is liberated as a photon visible as blue light

A classical example of such reaction is the reaction of *luminol* (5-amino-2,3-dihydro-1,4-phthalazinedione) and strong oxidizer, such as hydrogen peroxide, in the presence of sensitizers, such as iron and copper (Fig. 10.2). A strong blue emission is produced in this reaction.

This reaction can be primarily used for the determination of *organic peroxides* (Baj and Krawczyk 2007) but is not limited to them. Any compound that influences the rate of reaction producing the luminescence can be determined, and the major problem is the selectivity of this assay. It was reported on application of this reaction for the determination of carbon monoxide in blood serum samples (Xie et al. 2007) and of sugars in food (Li and He 2007).

It was found that silver, gold and platinum nanoparticles enhance chemiluminescence in luminol – hydrogen peroxide system. This fact opens many possibilities for determining the compounds that not only inhibit the reaction but also influence the binding of its substrates to the particle surface. The list of such compounds includes uric acid, ascorbic acid, estrogens and phenols (Xu and Cui 2007). Enzyme horse radish peroxidase can also catalyze this process, and very efficiently (see below).

Interestingly, luminol is used with a great success by forensic investigators for chemiluminescent detection of *trace amounts of blood* left at crime scenes. The area

under investigation can be sprayed with solutions of luminol and activator. The detection is based on the fact that the iron cations are the necessary components of blood protein hemoglobin, which is present in any blood. They catalyze the chemical reaction of luminol. This leads to blue glow that is easily detected in the dark revealing the location of even infinitesimal amounts of blood.

10.1.2 Enhanced Chemiluminescence

The use of chemiluminescence in detection technologies is not limited by direct influence of target on the reaction producing the emission. The application in sensing can be realized by labeling the sensor unit with the catalyst and adding all the substrates of the reaction into the test medium. *Horseradish peroxidase* is an enzyme that is used in many technologies, including chemiluminescence. It transforms peroxides with the generation of oxygen. When it is coupled to one of the partners interacting in sensing event and the substrate, the transformation of which changes its absorption or emission, is added, an amplified signal can be generated. When this enzyme is coupled to the receptor molecule, then the presence of this complex can be detected with great sensitivity in a micro-flow format (Yakovleva et al. 2003). In this technique for producing chemiluminescent signal the enzyme catalyzes the conversion of added substrate (usually, luminol derivative) into a sensitized reagent. Its further oxidation by hydrogen peroxide produces excited species that emit light, allowing ultrasensitive detection. In detecting protein targets a femtomolar level of sensitivity can be achieved.

Chemiluminescent detection increases the sensitivity of *immunoassays*. For instance, peroxidase can be attached to antibody that specifically recognizes the antigen. Thus, in ELISA assay with peroxidase labeling, the substitution of colorimetric detection by chemiluminescence allows achieving a ten-fold increase of sensitivity (Zhang et al. 2006a). Chemiluminescent detection can be realized in microarray format with broad area of applications (Seidel and Niessner 2014).

Chemiluminescence is attractive in many respects, but one point is not so pleasant for a spectroscopist. On its application, emission intensity is often very low. In such cases with optical excitation, one has to do the obvious thing – to increase intensity of incident light. In chemiluminescence this cannot be done because there is no external light.

10.1.3 Nanoparticle-Based Platforms in Chemiluminescence

The method of chemiluminescence progresses by absorbing ideas from other luminescence techniques. Thus, a resonance energy transfer (FRET) between *chemiluminescent donors* and luminescent quantum-dots as acceptors was suggested as improvement of this methodology (Huang et al. 2006). Although high resolution in time is not applicable to this method, many attempts are made to reduce the response time by decreasing the reaction volume and increasing the speed of mixing.

Integration into this techniques of nanoparticles and nanocomposites brought very interesting results. In one of examples, gold nanoparticles were used to comprise the aptamer covalently labeled with a chemiluminescent reagent, N-(4-aminobutyl)-N-ethylisoluminol (ABEI) and resonance-transfer quenching of produced emission was used as reporter signal (Qin et al. 2013). A detection range of ~10^{-10}–10^{-11} M was achieved. Carbon nanoparticles (Gao et al. 2014) and graphene sheets (Su and Lv 2014) were suggested for use as efficient FRET-based quenchers of chemiluminescence. Presently nanomaterial-amplified chemiluminescence became a broad field of research (Li et al. 2011) and we expect the development of new analytical methods on this basis.

A new story was opened with the publications that quantum dots (Wang et al. 2005; Li et al. 2007) and carbon nanoparticles (Lin et al. 2012) themselves can be directly oxidized by oxidants and produce chemiluminescence emission. The suggestions to use these effects in sensing followed (Tang et al. 2014).

One remark may be interesting to the reader. Basically, the excited states generated in chemical reaction and on absorption of light quanta do not differ. Therefore, the mechanism of resonance energy transfer (FRET) is the same, and no special terms are needed for its description. But there is one technical difference: the problem of direct excitation of the acceptor does not exist here. To get benefit of that by detecting the donor-acceptor switching of emission is not easy because of low intensity of emitted quanta.

10.1.4 Electrochemiluminescence

Electrogenerated chemiluminescence (ECL) also called *electrochemiluminescence* is a chemiluminescence produced directly or indirectly as a result of electron transfer between an electrode and some solution species or species bound to the electrode surface (Kulmala and Suomi 2003; Miao 2008). These electron transfer reactions generate excited states that emit luminescent light. Thus, this process is essentially the conversion of electrical energy into the radiative energy. In fact, in this case we observe a redox chemical reaction at the electrode, but in contrast to chemiluminescence that was discussed above, we achieve structural resolution (the reaction occurs at the electrode but not in the whole volume) and the possibility of starting/terminating reaction by switching on/off the voltage.

Many dyes and metal complexes that produce photoexcited luminescence or chemiluminescence can also generate ECL (Richter 2004). One of these examples is tris-(2,2'-bipyridine) chelate, $Ru(bpy)_3^{2+}$, which is already well-known to the reader as the luminescent metal chelating complex (Sect. 4.5). The complexes of ruthenium (III), such as $Ru(bpy)_3^{2+}$, are excited along the one-electron oxidation-reduction pathway. Application of voltage to an electrode in its presence results in light emission that is similar to that observed on photoexcitation and that can be detected at very low concentrations, 10^{-11} M.

ECL reactions are rather efficient. Their *quantum yield* can be defined as the ratio of the number of emitted quanta to the number of redox events leading to generation

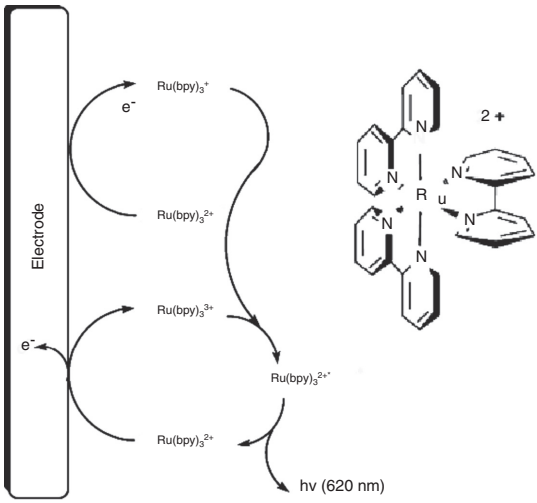

Fig. 10.3 Structure of $Ru(bpy)_3^{2+}$ and proposed mechanism giving rise to its electrochemiluminescence (ECL) emission (Richter 2004). $Ru(bpy)_3^{2+*}$ represents an excited molecule that emits light

of excited states. The ECL reaction for $Ru(bpy)_3^{2+}$ has quantum efficiency of 5 %. This value is frequently used as a reference for determination of quantum yields by a comparative approach (Richter 2004). The other remarkable feature of ECL reactions is their *reversibility*. In contrast to substrates of chemiluminescence reactions in solutions, $Ru(bpy)_3^{2+}$ is not consumed during the photochemical cycle, it relaxes to its ground state (Fig. 10.3), which allows single molecule to participate in many reaction cycles.

Indirect generation of ECL is also possible. In this case, a 'co-reactant' is needed, which is a substance that attains strong oxidation or reduction potential in reaction at electrode. The produced intermediate interacts with ECL luminescent species to generate their excited states. The use of co-reactant is rather limited in aqueous solvents, since the available potential range in water is too narrow to generate the required energetic precursors (Richter 2004). A useful co-reactant in aqueous medium is the oxalate anion and also tri-n-propylamine that work together with $Ru(bpy)_3^{2+}$. Usually such reactions are performed at high and constant concentrations of co-reactant.

Many inorganic complexes and organic molecules have been tested in ECL systems (Richter 2004), meantime $Ru(bpy)_3^{2+}$ remains the most requested luminophore for different applications. With its use as a single reporter it is not easy to explore multiple labeling or introduction of internal standard. By attaching suitable groups to the bipyridine moieties, it can be used to label antibodies for application in sandwich assays (Miao and Bard 2003) or for labeling the single-strand DNA to be used in hybridization techniques (Dennany et al. 2003). Introduction into $Ru(bpy)_3^{2+}$ system of the ion-chelating groups allows obtaining the ion sensors operating similarly to that producing fluorescence response (Richter 2004).

Many other versions of common fluorescence detection techniques were adapted for ECL technique (Fahnrich et al. 2001). ECL demonstrates remarkable flexibility in the direction of miniaturization and imaging. It can be used in the form of microelectrode and ultra-microelectrode technique to produce images on electrode

surfaces and also as a light source for near-field optical microscopy (Zu et al. 2001). Sensor microarrays can be deposited on electrode surface (Venkatanarayanan et al. 2012).

Application of novel nanomaterials is a new step in development of ECL method. The most successful in this respect are graphenes, nanotubes and carbon dot particles that combine high electrical conductivity with high level of available surface to volume ratio (Deng and Ju 2013; Su and Lv 2014).

10.1.5 Cathodic Luminescence

A special version of ECL is the *cathodic luminescence* (Kulmala and Suomi 2003; Suomi and Kulmala 2011). Its mechanism is basically different from that discussed above. Instead of being based on electron-transfer chemiluminescent reactions of electrochemically generated reactants in solutions it involves direct formation of excited states at the electrode surface. This type of high voltage cathodic luminescence results from *injection of hot electrons* into the aqueous electrolyte solution with the formation of hydrated electrons (Fig. 10.4).

This technique, though totally depending on electrode phenomenon, is closer to common photoluminescence in several aspects. First, it allows high spatial resolution and, particularly, the excitation of those luminophores that are *close to electrode surface*. Here the distance limit is about 50 nm from the tunnel emission

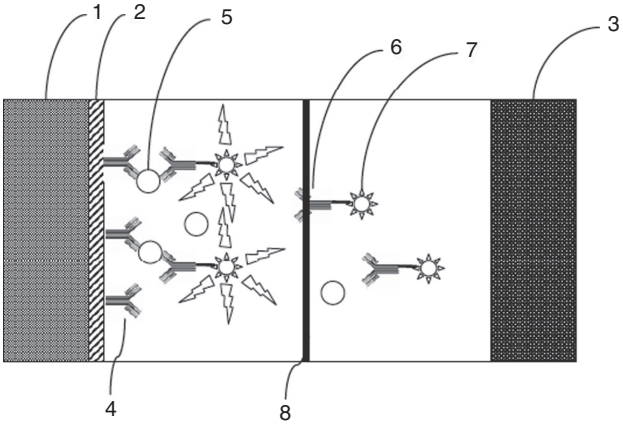

Fig. 10.4 The measuring principles of an immunoassay (sandwich format) employing thin insulating film-coated tunnel emission electrodes (Kulmala and Suomi 2003). The working electrode consists of a base material (*1*) and an insulating film (*2*) coated with antibodies (*4*) that are specific to an analyte (*5*). The counter electrode (*3*) does not participate in generating the response. The second antibody (*6*) specific to the analyte is attached to label (*7*). This results in the formation of immunocomplexes (*4*)–(*5*)–(*6*)–(*7*) on the surface of the insulating film. The analyte level can be quantified after this reaction step by electric pulse excitation of the label molecules (*7*) involved in the complex formation. Line (*8*) marks the distance from electrode, within which the excitation is possible

electrode surface. This allows obtaining reporter signal only from those labels that are attached to species adsorbed to the surface. The other labeled species, remaining in solution, are not excited during the lifetime of hot electrons, so they do not provide the signal. This allows carrying out homogeneous assays, which avoids washing-out the unbound species.

The other attractive feature of this technique is the possibility of time-resolved study. Likewise in photoexcitation, an electric pulse on an electrode starts the emission, and it can be then observed as a *time-resolved decay*. This allows detecting signals simultaneously from several labels, and they may be resolved by differences in decay times. If it is necessary to resolve contributions from sensors emitting at different wavelengths, this possibility also exists. Wavelength and time discrimination can be combined in efficient separation of signals emerging from different labels.

The special feature of hot electron injection into aqueous solutions is that luminophores having very different *optical and redox properties* can be simultaneously excited (Kulmala and Suomi 2003). This opens many possibilities for their selection. The absence of results of systematic studies do not allow drawing general conclusions, but since it was reported that this type of electrogenerated emission can be obtained from organic dyes, metal chelates and also quantum dots, it can be expected that the range of applicable reporters is rather broad.

The most intensively studied in this application were the luminescent lanthanide metal complexes with aromatic ligands. An injection of hot electrons into aqueous solution provides a possibility to excite them electrochemically by a *ligand-sensitized mechanism*. Like in photoexcitation, the ligand is excited first, and then it transfers the energy to the central ion that finally emits light. The best studied in this respect are Tb(III) phenolic chelates. With lifetime of 1.7–2.4 ms, these complexes allow efficient use of time-resolved measuring techniques. It was stated that the time-resolved ECL measurements provide excellent signal-to-noise ratio and about the same sensitivity of detection as the time-resolved photoluminescence of lanthanide(III) chelates (Kulmala and Suomi 2003; Suomi and Kulmala 2011). This methodology has been successfully applied to immunoassays.

10.1.6 Essentials of the Techniques and Their Prospects

Simple and cheap chemiluminescent techniques have found many followers and are frequently used in clinical diagnostics. Electrogenerated chemiluminescence offers further increase of simplicity making the flow cells with sample injection unnecessary but requires locating the receptors at the surface of conducting materials. Both of these techniques involve the generation of excited states by the species that undergo highly energetic electron transfer reactions. In chemiluminescence the process leading to production of light is an essentially irreversible chemical reaction that has to be started by reagent mixing (usually, their injection into a flow cell). The intensity is measured in a steady-state regime, and the emission decay-associated time-resolved measurements here are not possible. The optical technique in this case is amazingly simple; it needs neither light excitation unit nor wavelength filtering in the emission

beam. The microscopic volume flow-injection cell can be located on top of photomultiplier detector, and this is the most important part of instrumentation.

Since in electrochemiluminescence the emission is initiated and controlled by switching the electrode voltage, the time-resolved or time-gated luminescence can be easily detected with reporters exhibiting long lifetimes. No separation of bound and unbound target is needed, since only the target bound in thin pre-electrode layer can be detected. Such combination of spatial and temporal selection allows achieving discrimination against background emission without any wavelength selection. This allows using very simple instrumentation.

Regarding the prospects, we have to consider that starting the response reaction 'by syringe' is less attractive than by light or by electrical pulse, especially concerning miniaturization and multiplex applications. Future developments will show if the sensor technologies based on chemically or electrochemically generated luminescence will raise a strong competition to the techniques using optical excitation. Simplicity of instrumentation is an attractive feature, but it cannot be considered as decisive. The limiting factor for this technology at present is a rather small choice of available reagents that can be used as reporters.

10.2 Bioluminescence

Bioluminescence is also chemiluminescence, but it takes place in various living organisms, the most known of which are the fireflies. It is a rather widespread phenomenon in living world, involving broad range of species, from bacteria to fishes. In contrast to common chemiluminescence, bioluminescence reactions are highly efficient, with quantum yields approaching 88 %. Their applications in sensing can be as exotic as these reactions themselves.

10.2.1 The Origin of Bioluminescence

The luminescent organisms synthesize specific substrate *luciferin* together with the enzyme *luciferase*. This enzyme catalyzes formation of intermediate complex of luciferin with ATP (adenosine triphosphate, the ubiquitous intracellular energy source). This complex, when combined with oxygen, oxidizes producing a very strong 'cold' emission.

The general reaction scheme of this two-step reaction is the following:

$$\text{luciferin} + \text{ATP} + \text{luciferase} \rightarrow \text{luciferase} \bullet \text{luciferyl adenylate} + \text{PP}_\text{i}$$

$$\text{luciferase} \bullet \text{luciferyl adenylate} + \text{O}_2 \rightarrow \text{luciferase} + \text{oxyluciferin} + \text{AMP} + \text{CO}_2 + \textit{light}$$

The first step is the formation of an enzyme-bound luciferyl-adenylate and release of inorganic phosphate, PP_i. The second step is an oxidative decarboxylation

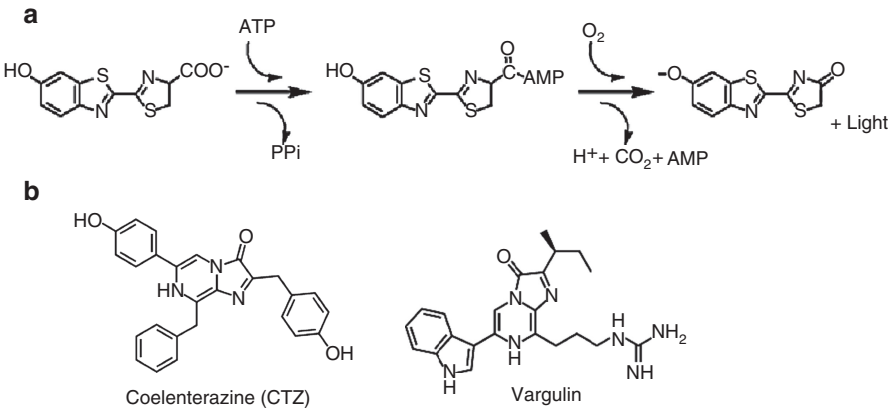

Fig. 10.5 The two-step chemical reaction catalyzed by firefly luciferase resulting in generation of emission of light (**a**) and the newly characterized luciferase substrates that can also operate in cell-free system (**b**)

of luciferyl adenylate that results in production of oxyluciferin, AMP, carbon dioxide and emission of light. The chemistry of this transformation for firefly *luciferin-luciferase system* is presented in Fig. 10.5.

It should be noted that both luciferin and luciferase are generic terms for a substrate and its associated enzyme that catalyze the light-producing reaction. Their particular molecular structures are variable among different species. The best studied and the most frequently used firefly luciferase is the monomeric protein with molecular mass 62 kDa. It emits yellow-green light with the peak of emission at 560 nm. Meantime, search among natural species and chemical modifications continue for increasing the analytical value of bioluminescence. Some of new luciferase substrates are shown in Fig. 10.5 (Paley and Prescher 2014).

10.2.2 Genetic Manipulations with Luciferase

By means of genetic engineering, the reaction giving rise to bioluminescence can be produced in different animals, e.g. in nude mice. Of course, making different animals luminescent can be a good fun resulting in possibly good applications. Meantime, probably more important on the present step is to make the luminescent whole-cell biosensors based on responsive bacteria and yeasts (Sect. 11.6). This allows achieving several aims:

(a) To provide *analytical detection* of compounds that are present in trace amounts but those that produce significant biological effect, such as steroid hormones (Fine et al. 2006).
(b) To obtain *integral response* to particular substance on a cellular level. This response will contain information not only on concentration of this substance but also on its influence on cell, on its efficiency, tolerance, etc.

(c) To provide on the level of cellular effects the *parallel screening* of many different compounds, including those suspected as hazards and those tested as potential drugs.

The milestone on this trend could be the design of efficient 'mini-luciferase', a small fragment of this enzyme that could retain the catalytic properties but be more convenient in use. Some success on this trend was achieved already (Paulmurugan and Gambhir 2007).

10.2.3 Bioluminescence Producing Resonance Energy Transfer

The excited states producing bioluminescent emission can also transfer the energy to other emitters in a mechanism based on *Förster resonance energy transfer* (FRET). This mechanism is of general origin and does not involve any specificity in generation of excited states, whether it is by light or by chemical reaction. In this regard, the new term, 'bioluminescence resonance energy transfer' (BRET) that was introduced by some authors for describing this type of energy transfer seems to be incorrect. For sensing technologies, this type of energy transfer is interesting since it can transform many fluorophores that are useful in sensing into a new class of bioluminescent probes.

Particularly, this opens an interesting possibility of activating the sensors via internal bioluminescent molecular 'light source'. This idea was efficiently realized with quantum dots (So et al. 2006). The '*self-illuminating quantum dots*' that represent their hybrids with luciferase were produced and tested. Since excitation source in this case is not needed, the dots incorporated into the cells provide much more efficient sensing than in a common manner of excitation. 'From inside' they are excited with a great selectivity, which allows virtually eliminating the light scattering and autofluorescence (of cellular pigments, porphyrins and flavins).

The other interesting application was found in research with the aim of determining the *interactome* (the whole pattern of interactions of macromolecules inside the living cell). A bioluminescent luciferase can be genetically fused to one candidate protein, and a green fluorescent protein mutant fused to another protein of interest. Interactions between the two labelled partner proteins can bring the luciferase and green fluorescent protein close enough for resonance energy transfer to occur, thus changing the color of the bioluminescent emission. The energy transfer from bioluminescent donor should be particularly useful for testing the protein interactions within a variety of native cells, especially with integral membrane proteins or proteins targeted to specific organelles (Xu et al. 1999). The studies of proteases and of other enzymes are also the domain of application of this techniques (Wu et al. 2014b).

Molecular imaging of protein-protein interactions in living cells modulated by binding small molecules raises not only theoretical but also practical interest in clinical diagnostics and development of new drugs. For in vivo monitoring of estrogen-like compounds, the homogeneous assay can use the combination of

luciferase with a protein of green fluorescent protein family. The procedure for evaluating the presence of estrogen-like compounds has been developed and optimized. The estrogen alphareceptor (ERalpha) forms homodimers as a result of binding the estrogen-like compounds, such as 17-beta estradiol. The fusion of bioluminescent donor and acceptor to monomers allows to visualize the estrogen binding (Michelini et al. 2004).

10.2.4 Prospects

The attractive feature of bioluminescence is the possibility of providing target detection and imaging inside the living cell in the absence of external excitation (Roda et al. 2004; Frangioni 2006). This requires genetic manipulation with luciferase enzyme and the presence of all necessary substrates of catalyzed reaction. The encountered difficulties have been successfully passed, so that even 'miniluciferase' and peptides that, upon assembly, restore the enzyme activity are now available. With the aid of this tool, bacterial, yeast and human cultured cells can be transformed into efficient 'whole-cell' biosensors (Sect. 11.6). Sensing inside the cell can occur according to the energy-transfer mechanism that does not require external excitation, and very promising results on this trend have already been obtained.

The other unique property of luciferin-luciferase reaction is its sensitivity of detecting ATP concentrations on the level of ~10^{-17} M. Such extreme sensitivity is useless for testing inside the living cells, where the ATP concentrations are commonly on the level of ~1–10 mM, but can be used for finding microorganisms in extremely diluted media and, probably, for searching for life on other planets.

Emphasizing strong attractive features of bioluminescence we have to count on low and sometimes very low level of collected emission intensity. This limits applications in resonance energy transfer, in which bioluminescent sites serve as donors and also for in vivo studies, in which high luminophore dilutions are unavoidable.

10.3 Radioluminescence and Cherenkov Effect

Radioluminescence is a phenomenon whereby high energy electromagnetic radiation is converted into visible light. Many fluorophores can be excited not only in conventional optical way but also by absorbing the X-ray radiation. Moreover, plastic scintillators transform the traces of α, β and γ radioactive decay into visible light. As such particle passes through the scintillator, it deposits energy in atoms and molecules along its path, creating excited atomic or molecular states through a nonradiative process. Radiative decay (luminescence) of these excited molecules produces numerous photons from each particle. These photons can be used to excite other luminophores.

10.3.1 Radioluminescence

Radioluminescence excited by isotopes with *β decay* (e.g. tritium) was used already for a long time as a low-level light source for night illumination of instrument dials or in other applications where light must be produced for long periods without external energy sources. With the introduction of new technologies and new highly sensitive detectors we observe rejuvenation of this type of light generation in sensing and imaging.

The *X-ray excited optical luminescence* is a novel technique that is on the step of active development. As the X-rays possess excellent soft tissue penetration, this offers an appealing approach for use as an imaging modality. In the developments of sensing and imaging applications one can benefit from the experience of designing bulk materials and single crystals as *scintillator phosphors*. Meantime, for *in vitro* and *in vivo* imaging methodologies they should be applied in the form of nanoparticles. Presently only scarce information exists on nanoscale converters of electromagnetic energy that must be designed based on a good understanding of the factors that control their luminescence. Promising with respect to efficiency are the lanthanide nanocrystals $NaGdF_4:Eu^{3+}$ that exhibit great X-ray excited luminescence together with possibilities of their use in other detection modalities (Sudheendra et al. 2014). The IR emission of lanthanide-based composites allows obtaining good contrast (Fig. 10.6).

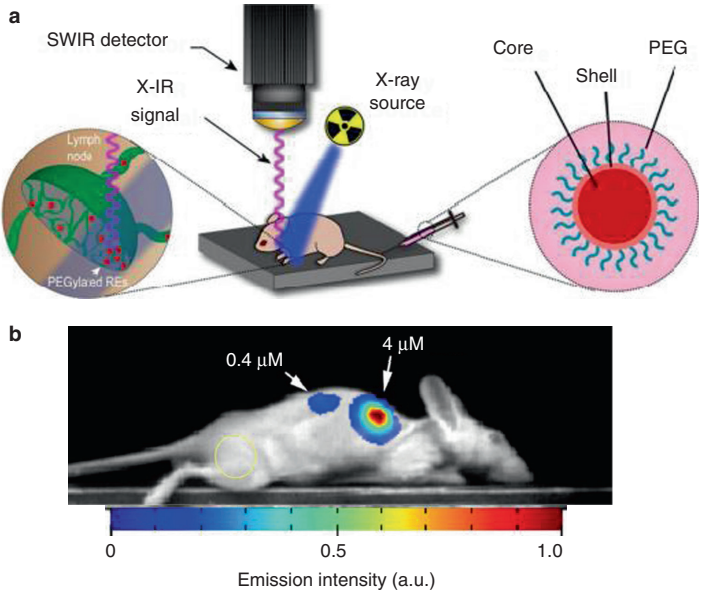

Fig. 10.6 Imaging with X-ray excited IR-luminescent (X-IR) nanocomposites (Naczynski et al. 2015). (**a**) Scheme of experiment. (**b**). Distinct focal luminescence was visualized away from the injection site near the animal's axillary and brachial lymph nodes. After dissection, X-IR signal could be traced to the local lymph nodes draining from the injection site (axillary lymph node shown in the inset). In contrast, contralateral lymph nodes did not show any notable X-IR signal

The *X-ray luminescence optical tomography* (XLOT) is an emerging hybrid imaging modality, in which X-ray excitable nanoparticles (phosphor particles) emit optical photons when stimulated with a collimated X-ray beam generating a three-dimwnsional image (Ahmad et al. 2014). By scanning a narrow X-ray beam through the tissue sample, by collecting the luminescence at every position and attaining luminescent imaging at multiple angles and/or multiple X-ray excitation patterns, one can construct the 3D distribution of emitters in the tissue. Deep penetration of X-rays exciting the luminophores and their negligible scattering in heterogeneous media offers advantages in tomography applications over optically excited luminophores. These advantages are in increased spatial resolution in visible and near-IR images that can be made very sharp by collimating the X-ray excitation beam. A disadvantage is the necessity to keep the radiation dose as small as possible, since it can produce damaging effect.

The modification of X-ray excitable probes with targeting agents and antibodies will extend the use of this novel technique for deep tissue molecular and cellular imaging. Radioluminescence can be combined with other methods of visualization and treatment in vivo by designing nanocomposites, particularly with superparamagnetic modality or the ability of carrying/release of drugs.

10.3.2 Self-Illumination by Radioactive Decay

Every developer of instrumentation in fluorescence sensing dreams of a light source that could be simple, reliable and work eternally without a need for electric power. The first steps towards this goal have been made (Holthoff et al. 2005). The light source suggested for application in sensor array format consists of a sealed *source of β radiation* (^{90}Sr) and a plastic scintillator. ^{90}Sr has a half-life of 28.5 years, and it emits β particles with a maximum energy of 0.546 MeV. This radiation generates blue light (λ_{max} 435 nm) from the plastic scintillator, and the blue light excites the analyte-responsive luminophores within the chemical responsive sensor arrays.

The *Cerenkov radiation* is the visible wavelength light produced by any charged particle travelling through a dielectric medium faster than the speed of light in that medium. Thus, its efficiency depends on *refractive index* of that medium, in which the radiation propagates and is retarded. Molecules in the medium polarized by the passage of the charged particle relax, producing visible light (Fig. 10.6a). Unlike common fluorescence emission spectra that originate from the transitions between quantized energy states and have characteristic spectral peaks, the Cerenkov radiation spectra are continuous. The relative intensity of this radiation is proportional to its energy, and because of that the emissions at higher energies (ultraviolet/ blue) are the most intense.

The amount of light detected in such emission is significantly lower than that in other optical imaging techniques. However, essential advantages shared by chemiluminescence and bioluminescence are in high signal to background ratios because of the lack of an incident light source. Together with the absence of non-specific

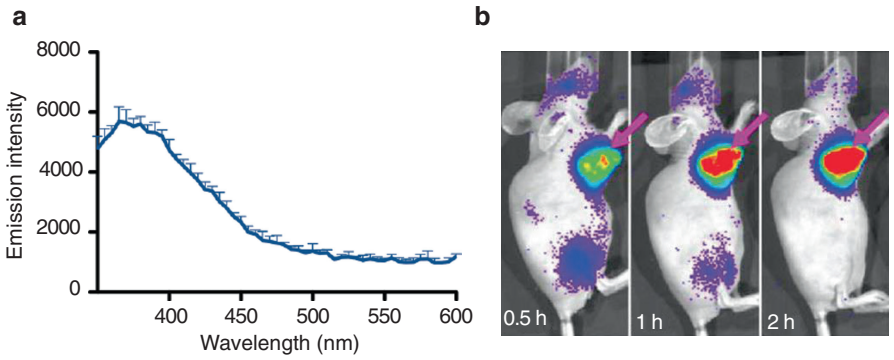

Fig. 10.7 Cerenkov light imaging (Thorek et al. 2012). (**a**) The profile of the Cerenkov radiation is centered at the blue, as shown with ^{68}Ga (18.5 MBq) in 0.1 M HCl diluted in water. (**b**) The Cerenkov luminescence imaging of nude mice bearing C6-FLuc tumor injected via tail vein with the clinically approved tracer for the detection of tumors ^{18}F-FDG at 0.5, 1, 2 h post-injection

background signal, the positron (β^+)-emitting radionuclides (e.g., ^{11}C, ^{18}F, ^{64}Cu, ^{68}Ga) allow sensitive, noninvasive measurement of the distribution of their picomolar quantities in small animals and humans. So, the isotopes that can be used in positron emission tomography can be also used here, but the emission can be detected using the sensitive CCD optical imaging systems. They can provide imaging signals at the sites of their accumulation (Fig. 10.7).

Because the ultraviolet/blue wavelengths of Cerenkov radiation are strongly light absorbing and exhibiting multiple scattering in heterogeneous living tissues, an idea was realized to transform this emission to the long wavelength red region. As in other cases depicted in Chap. 7, this can be done by using the energy transfer to nanoparticles emitting in the red and near-IR (Fig. 10.8).

Such strongly Stokes-shifted emission of quantum dots was successfully applied in animal imaging (Dothager et al. 2010). In a recent development (Sun et al. 2014), the self-illuminating quantum dot system was constructed by doping

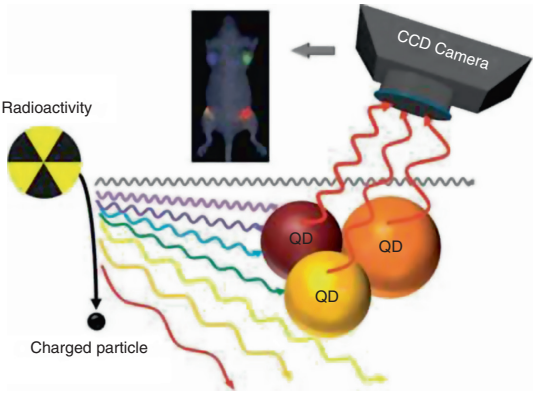

Fig. 10.8 Radiation-excited luminescent quantum dots for optical imaging (Liu et al. 2010)

positron-emitting radionuclide ^{64}Cu into CdSe/ZnS core/shell nanoparticles via a cation-exchange reaction. Exhibiting efficient Cerenkov resonance energy transfer, they can accurately reflect their biodistribution during circulation in the living body.

10.4 Two-Photon Excitation and Stimulated Emission

Being well known to physicists, the phenomena observed on manipulation with optical flux density and with two-step transition to the excited state followed by spontaneous emission from this state were almost forgotten in sensor development. Now the situation changes dramatically and the great advantages in exploration of these phenomena have started to find proper application. Great contribution to this field is provided by material chemists. They develop two-photonic dyes and up-conversion materials with unique properties.

10.4.1 Two-Photon and Multi-Photon Fluorescence

An interesting phenomenon is behind this technique. A fluorophore can be excited not only by the light quantum with the energy that corresponds to the energy of its electronic transition but also by *two or more quanta*, the total energy of which correspondng to the energy of this transition (Fig. 10.9). For such summation of their energies these quanta should appear together in a right place at a right time and their simultaneous absorption should occur in a single event.

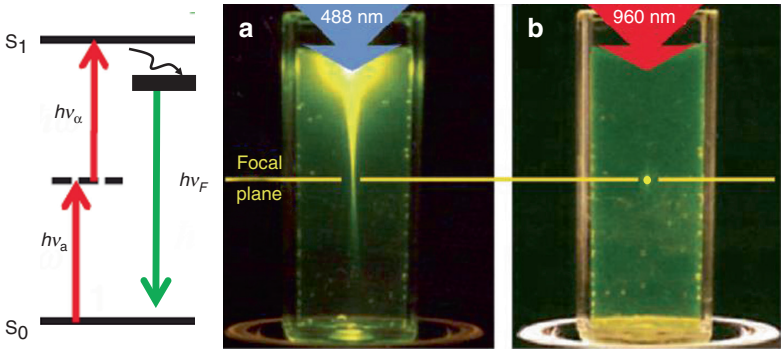

Fig. 10.9 Energy level diagram for two-photon excitation. The 'intermediate' energy level after absorption of the first quantum is 'virtual', non-existent in reality and only the precise matching of two quanta in time and space may result in addition of their energies. On absorption of this double energy a normal emission occurs after some step of relaxation. This emission is observed at much shorter wavelengths than the excitation. Right: Photograph illustrating the much sharper contrast of two-photon (**b**) versus one photon (**a**) excitation. In the second case the bright spot is seen only at the focal plane

Such events are commonly very rare. For increasing their probability, intense flux of photon energy is needed. The light beam has to be focused into a very *small volume*, and the high temporal *flux density* can be achieved by the application of ultra-short pulses that allow concentrating the high peak energy. For the present sensing technologies, only the excitation with two or three photons of *equal energies* is practically useful, since this can be provided with one laser. The energy of two-photon excitation has to correspond to one-half of electronic transition energy, so that for exciting the dye absorbing light at 400 nm (25,000 cm^{-1}) the laser emitting at about 800 nm (12,500 cm^{-1}) should be applied (So et al. 2000).

What is the advantage of this technique? In contrast to common single-photon excitation, in which the emission changes linearly with the intensity of excitation light, the fluorescence emission on two-photon excitation varies with the *square power* of the excitation intensity. This quadratic relationship between excitation and emission allows focusing the excitation power to a very small volume almost without observing the emission outside this volume. In this way, we achieve a very high *spatial resolution*. Selectively excited can be the species located in very small focal volumes (counted in femtoliters!), while the rest of the sample remains in the dark. With these developments, new possibilities are opened in three coupled areas: fluorescence microscopy (see Sect. 13.1), detection of single molecules (Sect. 13.3) and analytical methods that enable small-volume detection.

In addition to these attractive features, the problems with the *scattered light* become eliminated. This is because the scattered light appears at the wavelength of excitation, which is commonly in the near-IR; this is quite a different spectral region from which fluorescence is observed. A high penetration of light of 800–1000 nm in human tissues together with possibility of activating the highly localized photochemical reactions opens new possibilities for non-invasive clinical diagnostics and photodynamic treatment of disease (Papkovsky et al. 2000), see Fig. 14.4.

Selecting the dye for two-photon spectroscopy or microscopy one has to know that in these excitation conditions some properties are different from that observed at excitation by single photons. Due to different quantum mechanical selection rules, the two-photon and single-photon *excitation spectra* are not equivalent, and for two photons they are often much broader. The relative *molar absorbances* of many dyes may exhibit an unexpected variation: high brightness with single photons may transform to low brightness at two-photon excitation. An unusually high and wavelength-independent *anisotropy* was detected in the studies of asymmetrical polymethine and fluorene molecules (Fu et al. 2006).

A special effort is being made for synthesizing organic dyes with especially high two-photonic absorbance (Webster et al. 2008). Recently, a very detailed study of both symmetric and asymmetric cationic cyanine dyes have been performed and general regularities of their structure-property relations established (Fu et al. 2007). Enhancing the two-photon absorbance can be achieved by extending the polymethine chain and also by the increase in the donor strengths of the terminal groups.

A strong enhancement of the two-photon absorption cross-section of pseudoisocyanine dyes was observed in aqueous solution in the course of their formation of

supramolecular *J-aggregates* (Belfield et al. 2006). This enhancement is attributed to a strong coupling of their molecular transition dipoles. Forming J-aggregates, some styryl dyes were found to be good two-photon emitters for the DNA detection and imaging (Yashchuk et al. 2007).

The major characteristic of two-photonic fluorophores is their two-photonic absorption cross-section measured in *Goeppert-Mayer units*, (1 GM = 10^{-50} cm^4 s/photon). We can make comparative estimates taking as the reference one of the brightest organic dyes, Rhodamine B. It is characterized by only 210 GM units, and for many common organic dyes it is much lower. In contrast, the new dyes synthesized with the knowledge of physical two-photonic action, demonstrate the GM values higher by many orders. Thus, for one specially designed polymethine dye the value of 2280 GM was achieved (Fu et al. 2007), and for fluorene-bridged squaraine dimer it reached the value 2750 GM (Moreshead et al. 2013), Theoretical analysis suggests that for achieving high GM values the presence in the same molecule of several sites producing substantial charge transfer in their extended π-conjugated system is needed (Przhonska et al. 2010). Also, it was recently shown (Collini 2012) that the aggregated forms of these dyes with suitable alignment of the active units that allow proper intermolecular interactions may exhibit dramatically enhanced two-photonic cross-section.

With these values, probably, the highest limit for organic dyes is reached or almost reached. Based on understanding achieved in the studies with organic dyes, much higher values were obtained with specially designed conjugated polymers. With one of the nanoparticles composed of them, a record value of 200,000 GM was achieved (Wu et al. 2007). Other types of fluorescent nanoparticles demonstrate rather high values. Thus, for CdSe quantum dots the GM values 780–10,300 were reported (Pu et al. 2006). Quite significant is the two-photon absorption ability and correspondent intense fluorescence of carbon nanoparticles. The reported two-photon cross-sections are 39,000 GM for C-dots (Cao et al. 2007) and 48,000 GM for graphene dots (Liu et al. 2013).

High two-photon absorption cross-section is not only the question of brightness. With its higher values the less expensive techniques can be used. Usually the two-photon excited fluorescence is excited by *ultra-short laser pulses*. As we have seen above, this is not because the high resolution in time is actually needed but because within shortest pulses the highest density of photons can be concentrated, increasing probability of two-photon absorption. The ideal though expensive possibility for that is to use the basic frequency of Ti-sapphire laser that is able to provide pulses as short as 100 fs in a tuning range 800–1000 nm. This allows exciting with two photons of all light-emitters that possess absorption bands in the violet-blue spectral range.

Lasers with picosecond and nanosecond pulse widths can also be used, but less efficiently. There is a much broader choice of them, starting from mode-locked Nd:YAG and the dye lasers that can be pumped by Nd:YAG and ending with recently developed pulsed diode lasers. Lasers with long pulse duration may not only decrease the peak pulse density but also increase the possibility of up-conversion

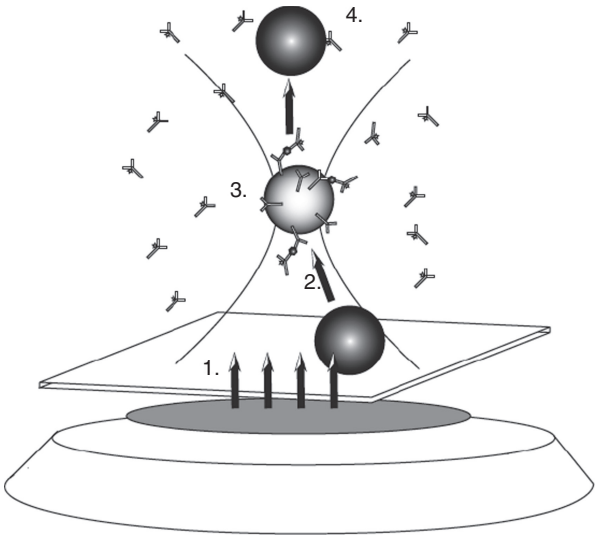

Fig. 10.10 The operation principle of a sensor based on two-photon excitation. A latex particle is pushed by optical forces of excitation light (*1*, *2*) and moving through a very small (1 fl) detection volume (*3*) of two-photon excitation generating the fluorescence response signal. Once measured the particles are pushed away by the same optical forces (*4*). Courtesy of Prof. Pekka Hänninen, University of Turku

(excitation from excited state) that may decrease the quantum yield. These effects depend upon the applied dye.

In contrast to common belief that only femtosecond pulses could be used for two-photon excitation, the group of Finnish researchers (Hanninen et al. 2000) used a Nd:YAG laser producing sub-nanosecond pulses for excitation of fluorescence. The *latex microparticles* were used as matrices for carrying the binder units to detect the target binding. When a microparticle appears in the focal volume of two-photon excitation, the confocally arranged scattering detector monitors its arrival, and then two-photon excited fluorescence measurement is triggered. The signal from particles is recorded one by one, and their statistical analysis performed. Such procedure allows avoiding any separation or washing steps showing that the sensor technology based on two-photon excitation can be realized in a simple and cost-effective way (Fig. 10.10).

This methodology has been demonstrated for immunoassays, pathogen detection assays (viral assays) and some research assays, and its success initiated many suggestions for the application on a larger scale. The microparticles can be encoded with different luminescent dyes, and thus the separation-free multi-target analysis becomes possible in a single assay.

10.4.2 Amplified Stimulated Emission

Many of fluorescent molecules and nanoparticles exhibit in solutions under extensive illumination the *amplified stimulated emission* (ASE). This phenomenon is in the background of operation of dye lasers. Under intensive light (pumping by external laser) the reversal in population of the ground and excited state can be

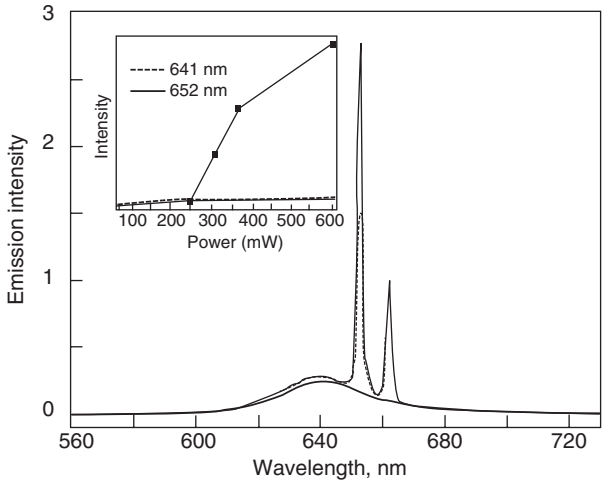

Fig. 10.11 Fluorescence from the CdSe NCs showing normal and amplified stimulated emissions at intensive excitations (Somers et al. 2007). The spectrum transforms into discrete sharp lines once the lasing threshold is crossed. Inset shows the non-linear increase in intensity at threshold pump intensity at 652 nm while the fluorescence at 641 nm shows a linear response. The sensor response could be in the appearance-disappearance of the ASE peak

achieved. Depopulation from highly populated excited state produces bright emission with a very characteristic spectrum (Fig. 10.11). On the background of broad and structureless 'normal' emission band there appear very sharp and highly intensive lines due to generation of amplified emission. Commonly it is a single line, and its position in comparison to a band maximum of normal emission is shifted towards longer wavelengths. If the responsive dyes or nanoparticles are a part of a laser cavity, then their linear single photon response can be replaced with the nonlinear one with dramatic increase of intensity due to amplified emission of many photons.

Therefore the following mechanism of sensing can be realized (Fig. 10.12). The appearance of sharp lines in emission spectra above the minimum pump energy at which ASE can be observed (*lasing threshold*) can be referenced against the intensity of normal emission at another wavelength. The transduction mechanism in sensing becomes the influence of the target on the threshold position. The mechanism for increased ASE sensitivity can be mediated via the influence on excited-state kinetics. The lasing threshold depends strongly on material emission lifetime: short lifetimes result in higher lasing thresholds. Longer lifetimes results in lower lasing thresholds due to higher probability of populating the excited state.

The ASE phenomenon for a long time has not been requested in sensor technologies. Meantime, it can be applied in a straightforward manner if a system is found, in which a sensing signal can be introduced as a switch between spontaneous and stimulated emissions. Unfortunately, many organic dyes, the ASE of which was studied in most detail, are not attractive for this application because of their low photostability in solutions. The problem of signal transduction in sensor applications of ASE emitters can be solved with CdSe nanoparticles (Somers et al. 2007).

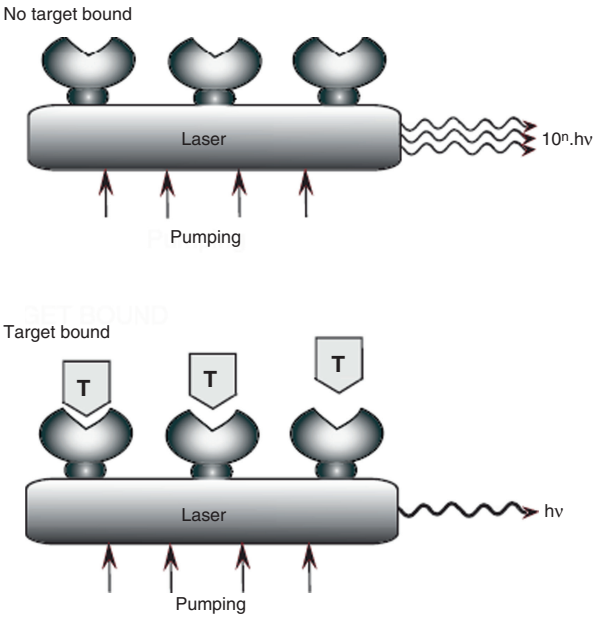

Fig. 10.12 Design concept of application of amplified stimulated emission in sensing. A single photon emitting center is replaced by a laser, which can be turned off or on by the recognition of a target. The strategy allows for high gain responses in the presence of target (*T*) at low concentrations

However, if semiconductor nanoparticles are used, their lasing threshold is too high. The situation is changing now. With *nanoplatelets* (the nanometer-sized sheets and ribbons) the thresholds as low 6 μJ/cm^2 and gain as high as 600 cm^{-1} were achieved (She et al. 2014).

It is known also that the stimulated emission can be produced by *two-photon excitation* (He et al. 2006). It was shown that novel types of semiconductor nanoparticles can demonstrate decreased lasing threshold in these conditions of excitation (Guzelturk et al. 2014) there is a principal possibility to introduce a spatial resolution into this interesting methodology.

Promising in respect of development of this technology are *conjugated polymers* (Scherf et al. 2001). With their long-lifetime emission, many emissive excitons are generated. Introduction of a quencher decreases the exciton lifetime, thereby resulting in increased lasing threshold. The amplified sensing response can be therefore obtained by pumping the conjugated polymer material close to the intrinsic lasing threshold and observing the switching between spontaneous and stimulated emissions.

These ideas were practically realized in the design of a sensor responsive to vapors of *trinitrotoluene* (TNT), which is a dangerous explosive that can be used in terrorist attacks. In specially designed conjugated polymer films the ASE observation allowed to increase sensitivity to TNT manifold (Rose et al. 2005). The adsorption of trace vapors of these explosives on thin polymer films introduce non-radiative deactivation pathways that compete with stimulated emission. As it was expected, the induced cessation of the lasing action, and associated sensitivity enhancement, is the most pronounced when the films are pumped at intensities near their lasing threshold. So, lasers can become the sensors.

10.5 Direct Optical Generation of Electrical Response Signal

From reading the previous sections, we can derive that there are many alternatives to common optical excitation by visible light. Here we will provide a close look at the side of detection of reporter signal. Are there alternatives to generation of light emission that has to be detected by electronic recording? It has to be acknowledged that electrochemical methods being the strong competitors to fluorescence (luminescence) sensing offer the most straightforward approach to signal conversion, from target interaction to electrical signal in an electrode-coupled reaction. Is there any possibility to merge these technologies in order to select the optimal solution? We will try to respond to this question below.

10.5.1 Light-Addressable Potentiometric Sensors

These possibilities were realized with the development of the *light-addressable potentiometric sensor* (LAPS). In the dark state of semiconductor layers the electric conductivity is absent because of the absence of free electrons. They appear at light illumination, and this may induce the photocurrent. The electric current itself and its variation can be observed only in the case if the film is illuminated by light and the energy of light quanta is sufficient for electron transfer to a conduction zone. If semiconductor is represented by a thin film exposed to a medium with variable concentration of protons or ions, due to polarization of charges the electrical conductance can change. The number of these electrons will depend on polarization of semiconductor surface that can be produced by ions in the test sample. Thus, with laser excitation we can get direct electrical response.

The light-addressable potentiometric sensor *instruments* are based on this principle (Fig. 10.13). The sensor plate is made of thin semiconductor layer with an insulating layer on the front surface exposed to a tested medium and an ohmic contact on the back surface. The photocurrent is modulated by modulating the intensity of the light beam with a frequency typically in the range of 10–20 kHz. The amplitude of the external photocurrent depends on the surface charge of the biased sensor structure. Depending on the utilized transducer layer, different targets can be detected.

The *sensing surface* of the LAPS can be modified to implement sensitivity and selectivity to various chemical species. It can be represented by ion-selective membrane. This membrane can be substituted by arrayed combination of materials, thus a single sensor plate can be used as a multi-analyte sensor (Yoshinobu et al. 2005). By recording both the position of the light beam and the amplitude of the photocurrent one can generate images of the target distribution above the sensor surface.

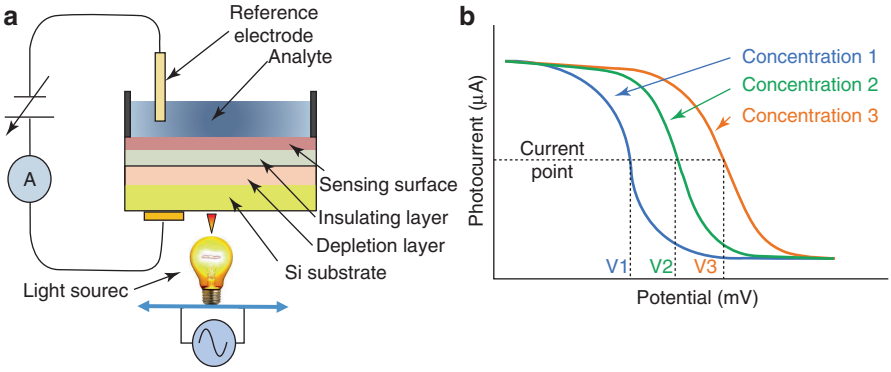

Fig. 10.13 Schematic presentation of a light-addressable potentiometric sensor (LAPS) device (**a**) and the dependence of target concentration on photocurrent (**b**) (Zhang et al. 2012). The laser scans the semiconductor thin film that, through an insulating layer, is exposed to sample that can induce polarization effect by variation of pH or concentrations of ions. The laser scans the whole semiconductor surface, and only an illuminated site can produce the response in the change of photocurrent. The curve of photocurrent versus bias voltage shifts horizontally with the increase of target concentration. The indicated current point can be used for quantitative assay

Scanning with laser will provide the necessary spatial selectivity producing the two-dimensional image that can achieve a ~1 μm resolution. These chemical imaging systems can be used e.g., for the study of biological systems like cultured neurons or brain slices on microscale level. The constructed devices based on semiconductor laser technique can be of a very small size (Das et al. 2013; Werner et al. 2014).

Since the effects of charge movements are involved, the LAPS devices have been developed for sensing pH and small ions (Das et al. 2013), but the application can extend to other reactions coupled with the consumption, generation or just motion of charged species. Even the DNA hybridization assays can be realized based on this principle (Wu et al. 2014a).

If a living cell is deposited on top of an insulating layer, its electrical activity can be detected (Xu et al. 2006). By scanning the laser along the LAPS sensor the surface potentials at any desired position can be mapped. Based on that, the changes of action potential towards different drugs can be detected.

Thus, there is a possibility for merging photochemistry and electrochemistry in order to substitute the optical response into electrical one. The benefit here is in avoiding generation of optical signal in a relay leading to recording the informative signal on sensor-target interaction. This must lead to simplification in the detection and analysis of informative response in electronic system. However, miniaturization of devices based on this principle and development of multi-analyte heterogeneous assays needs new technical solutions.

10.5.2 The Photocells as Potential Sensors

There is a principal possibility to avoid the electrode technique generating electrical current directly. The photoinduced electron transfer (PET) is an important signal transduction mechanism that is in the background of many sensor technologies (Sect. 8.2). Being a short-distance effect, it usually involves the electron movement from one molecule or its fragment to the other molecule or fragment and results in quenching. Usually, the reporting signal is optical, it is the ON-OFF switching in emission intensity. We observed also that electron can be transferred also to *conducting surface*, such as the metal surface. Thus, in principle, an *electric signal* can be generated by the transfer of electrons from an excited dye.

In semiconductors the electrons injected into their conductance bands can generate electric currents. The devices based on this principle have been developed for solar energy conversion (Gratzel 2007). Absorbing the energy of light, different organic dyes, quantum dots or luminescent metal chelates serving as the light harvesters provide heterogeneous electron transfer from their electronically excited states into the wide conduction band of the semiconductor. Then the electrons migrate to the collector electrode generating electrical current. The efficiency of these solar energy transducers have reached the ten percent level and continues to grow. The wide band gap oxide semiconductors of mesoporous or nanocrystalline morphology, usually nanocrystalline TiO_2, were selected for their optimal use. These photocell devices got the name *Gratzel cells* (Peter 2007). There are many possibilities to control and to amplify this signal, for instance, by shifting between two states of the sensor – PET quenching (and inducing photocurrent) and fluorescent (but with zero photocurrent). They are still waiting for their technical solution.

Much simpler could be realization of a scheme, in which the dye molecules are changing their characteristic absorbance in the presence of a target. In this way they can generate an inner filter effect, modulating the light intensity illuminating the photocell.

Summarizing, we have shown only two possibilities for merging photochemistry and electrochemistry in order to substitute the optical response into electrical one. This field is open for active exploration. It should be counted that the use of electrode instead of light detection unit leads to smaller instruments and reduced cost of their production. Photocell technology develops rapidly and it should be reasonable to get benefit from that. Microfabrication is more suited for the construction of electrochemical than of optical detectors. This raises a strong motivation to look for simpler and cheaper detection methods than the detection of light.

10.6 Evanescent-Wave Fluorescence Sensors

Evanescent wave excitation is primarily the possibility to achieve spatial selection in optical excitation, since this technique allows exciting those species that are located close to interface between two media (such as water and glass). The power

of this approach is in its ability to be combined with different sensor technologies offering their improvement and, often, their dramatic transformation.

10.6.1 Excitation by Evanescent Field

The phenomenon of *refraction of light* at an interface between the media of different refractive indices is known from textbooks. The refraction strongly depends on the angle of incident beam, so with the increase of this angle there appears the condition when the light is totally reflected (Fig. 10.14a). This occurs when the angle, at which the light propagating in a medium of higher refractive index n_2 encounters a medium of lower refractive index n_1, is higher than a certain critical angle θ_c. The latter is determined by equation $\theta_c = \sin^{-1}(n_1/n_2)$. It is interesting to note that the so attractive sparkling properties of finely processed diamonds are due exactly to this phenomenon.

However, the *total internal reflection* is not truly total and the geometrical principle is not totally valid. A small amount of electromagnetic field propagating with the frequency of light in the medium with n_2 still penetrates at a short distance into the medium of lower n_1 in the form of standing wave known as *evanescent wave* (Taitt et al. 2005). This evanescent wave is identical in frequency to the incident light and strongly decays with distance from the interface (Fig.10.14b).

Evanescent wave decays exponentially as a function of distance. In practically realizable situations, it can propagate to a distance of 100–200 nm, which depends

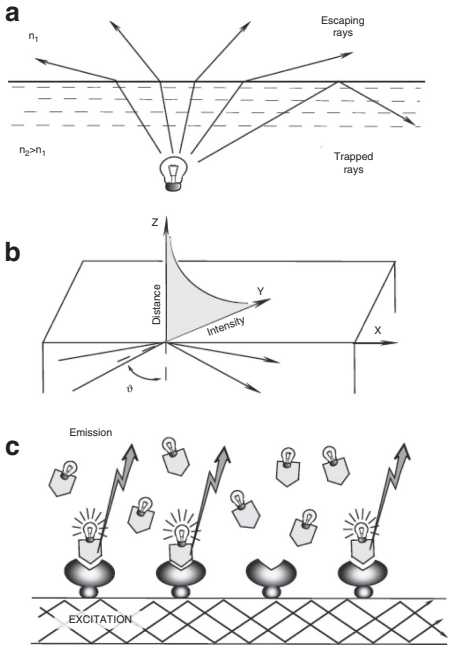

Fig. 10.14 The total internal reflection and its application in sensing using optical waveguides. (**a**) Transmission and reflection of light entering from a medium with higher refractive index n_2 to a medium with lower refractive index n_1. The rays incident at angles higher than a critical angle $\theta_c = \sin^{-1}(n_1/n_2)$ are totally reflected. (**b**) The rays internally reflected into the medium with n_2 produce evanescent wave in the medium with n_1. This wave decays exponentially as a function of distance from the surface on a nanometer scale. (**c**) Evanescent wave is formed in optical waveguide by internally reflected light rays propagating inside it. Generated evanescent wave is able to provide optical excitation of the dyes located close to the surface. This phenomenon is used in sensing by selective detection of surface-immobilized labeled species

on refractive indices, incidence angle and the wavelength. Its energy is sufficient to excite fluorescence of species located within the range of action of this field.

When special materials and special configuration of excitation beam were developed, this phenomenon has found important application in sensing. The technique used for that is called the *evanescent field excitation* (by the physical principle) and *total internal reflection* spectroscopy/microscopy (by the method of its realization). This principle can be realized on optical waveguides (see Sect. 11.2) and in fluorescence microscopy format (Sect. 13.1).

The basic mode of operation of evanescent-wave sensors is illustrated in Fig. 10.14c. The light propagates along optical waveguide without leaving it, exhibiting total internal reflection from its walls. The sensors (that may be composed of receptor units only) are attached to the *waveguide surface* and extend to the solvent. The difference between refractive indices of solvent water medium ($n_1 = 1.33–1.37$) and fused silica from which the optical waveguides are usually made ($n_2 = 1.46$) is quite significant for providing this optical trapping. The labeled targets that are bound to the sensor can be detected by their fluorescence emission. If the labeled species are not bound and are not under the influence of evanescent field, they are not excited and remain in the dark.

Since only the bound species demonstrate the fluorescence response and those remaining in solution do not respond, for providing or modulating the reporting signal there appears the possibility to avoid washing-out the unbound species, since being at a sufficient distance they remain in the dark. With the exploration of this effect, many different sensor configurations based on different principles can be realized. For instance, the labeled species can be not necessarily the target but the competitor. Another possibility is to make fluorescent the sensors attached to *waveguides*, and the target or its competitor in this case can be the quencher. Moreover, under specific conditions of illumination, this effect can be used in microscopy. In this case, only the area of studied object that is attached to a glass support will selectively produce the response.

10.6.2 Applications in Sensing

Evanescent wave sensing technology cannot be considered separately from other developments in fluorescence sensing. Moreover, it can be used as a platform for adaptation of different already developed approaches and allows their substantial improvement. Since all these sensors can measure surface-specific binding events by collecting the emission selectively from the surface, many *heterogeneous assays* can be transformed into direct sensors. Versatility of this technology is seen from its application using both fiber optic and planar array fluorescence sensors (Sect. 11.2).

The most extensive application this technology has found in *immunoassays*. Evanescent wave biosensors utilizing antibody-based sandwich fluorescence assays have been described for detection of gram-negative and gram-positive bacteria,

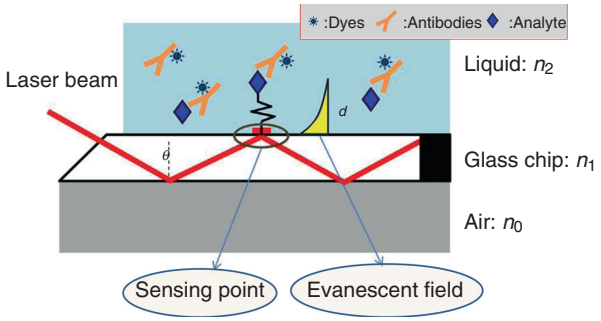

Fig. 10.15 Principle schematic of evanescent wave planar optical waveguide chip (Xiao-Hong et al. 2014). Evanescent field penetrates into test liquid and is able to excite fluorophores that are located close to waveguide surface providing the necessary selectivity

viruses, and different proteins including toxins. In fact, any compounds to which immunoassays are applicable can be determined by application of this method. Competitive and displacement assays can be established for detection of small molecular weight compounds, such as hormones and neurotransmitters. The reader can find many references in a review addressing this field (Taitt et al. 2005). The recent developments include miniaturization of this technique, transforming it into format of re-usable chips (Fig. 10.15).

One of the most interesting application areas is the *hybridization*-based detection of target DNA/RNA molecules. It was shown that molecular beacon technique is quite applicable also in this case (Liu and Tan 1999). Biotinylated molecular beacons were designed and immobilized on an optical fiber core surface via biotin-avidin or biotin-streptavidin interactions. They can be used to directly detect, in real-time, the target DNA/RNA molecules without using competitive assays. The sensor demonstrates rapid, stable, highly selective, and reproducible performance.

Spatial resolution offered by this technology is extremely attractive for the assays, in which the binding of labeled target or competitor can be recorded in narrow pre-surface layer. The other application is in cellular research with the development of specialized *evanescent field microscope* (Sect. 13.1). In general, evanescent-field sensing can be considered as universal platform that may encompass different sensing technologies targeted to many analytes and provide very sharp images with spatially selective excitation.

10.7 Plasmonic Enhancement of Luminescence Emission

A strong enhancement of fluorescence emission intensity is observed when fluorescent molecules or nanoparticles appear close to nanoparticles of gold and silver even without their direct interaction. Such enhancement occurs without increase and even with some decrease of emission lifetime indicating the suppression of

nonradiative channel of excited-state decay. Interaction of light with these nanoparticles generates resonance conditions influencing fluorescence emitters and leading to their *plasmonic enhancement*. Such resonance conditions exist in the case of flat thin metal surfaces used in surface plasmon resonance (SPR) but are much stronger and fluorophore emission attains new features (Merlen et al. 2010; Li et al. 2015; Howes et al. 2014).

Presently these effects became a hot topic both in research and in sensor development, promising many new possibilities. They increase dramatically the total emission per reporter molecule. Because of that they extend into the methods that provide an enhanced sensitivity and a wider dynamic range for chemical analysis, medical diagnostics, and in vivo molecular imaging.

10.7.1 Surface Plasmon Resonance and Surface Plasmon-Field Enhanced Fluorescence

The effect of fluorescence excitation by *evanescent wave* was discussed above (Sect. 10.6). This wave appears at an interface between the media of different refractive indices and extends into the medium with lower refractive index when the incident light beam is directed at an angle higher than critical, so that all incident light is reflected. It is known also that the evanescent field is dramatically enhanced when a thin (about 50 nm) layer of noble metal (gold or silver) is deposited on the solid glass surface (Neumann et al. 2002). Such enhancement appears due to the presence of propagating in two dimensions charge oscillations on the surface of thin metal films – *propagating plasmons-polaritons*. This effect depends on the refraction index in contacting medium and is sensed at a rather long length (up to ~200 nm) decaying exponentially with distance. The resonance conditions are observed only at certain angle of incident light and this angle changes with refraction index. The target binding to surface changes the refraction index changing this angle. Detection of this change is used in *surface plasmon resonance* (SPR) sensing technique (Couture et al. 2013).

The enhancement of evanescent field occurs due to resonant coupling between the incident radiation and the surface plasmon wave. The well-known resonant enhancement of *Raman scattering* bands is also related to this phenomenon (Le Ru and Etchegoin 2012).

With the knowledge of these findings, the reader must come with the idea of combining the benefits offered by surface-selective evanescent-wave excitation with the possibility of plasmonic enhancement of this emission. Technical realization of this possibility has led to establishment of *surface plasmon field-enhanced* fluorescence spectroscopy (SPFS). It exploits the strong SPR-generated evanescent field for excitation of surface-confined fluorescent dye (Ekgasit et al. 2004). The resonant excitation of an evanescent surface plasmon mode is used here to excite the dyes chemically attached to the target biomolecules and located on their binding close to the metal/solution interface. In this area, the dye is exposed to the strong optical fields giving rise to significantly enhanced emission (Fig. 10.16).

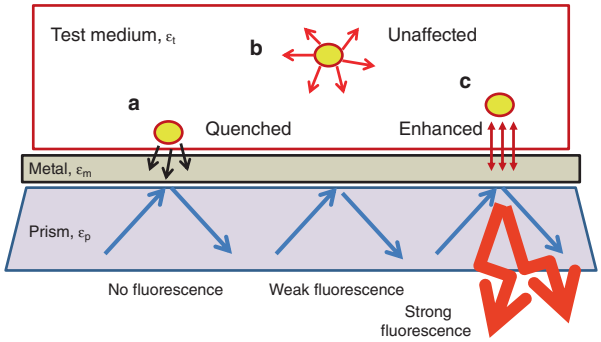

Fig. 10.16 Behavior of dyes located in the test medium of dielectric function ε_t (commonly, water) excited near thin metal surface of ε_m deposited on prism of ε_t. The excitation is provided through the prism at optimal angle. (**a**) The dye is located close to the surface. The dominant decay channel is the energy transfer to metal resulting in quenching. (**b**) The distance to metal is large. The dye produces free-space emission of photons. (**c**) A strongly enhanced highly directional fluorescence emission is observed. It propagates through the prism in a cone of angles

The *distance dependence* here is very important, since at very short distances the energy transfer to metal plasmons results in quenching. The enhanced local field decays exponentially with distance, so if the distance is very large the dye spontaneous emission is unaffected. There is an optimal distance at which fluorescence is strongly enhanced propagating within a cone of angles within the prism. If the labeled target is located within this area, it can be detected by an increased number of emitted photons. The use of fluorescence detection schemes in combination with the resonant excitation of surface plasmons has been shown to increase dramatically the sensitivity for bioanalyte detection (Neumann et al. 2002).

Since it is technically possible to monitor simultaneously the *reflected light* (for obtaining the SPR signal) and surface Plasmon enhanced *emitted light* from the same surface, this approach can provide two complementary channels of information. Many benefits can be obtained from such marriage. For instance, the unlabeled targets of large mass, producing a strong change of refractive index in the interfacial region, are active in SPR. In contrast, the small-size fluorescent dyes produce in the same region a strongly amplified effect in fluorescence without detectable change in SPR signal. In this configuration, which requires angle-resolved incident light (Neumann et al. 2002), the sensitivity of fluorescence-based response can be much higher than that of SPR. Both of them allow not only equilibrium measurements but also studying the association-dissociation kinetics with the use of flow cells.

An interesting property of surface-plasmon fluorescence spectroscopy is the ability to generate the *angle-resolved emission* (Ming et al. 2012). It was shown (Gryczynski et al. 2005), that upon excitation of quantum dots, the surface plasmons emitted a hollow cone of radiation (due to symmetry conditions) into an attached hemispherical glass prism located at a narrow angle. This directional radiation preserves the spectral properties of QD emission and is highly polarized irrespective of the excitation polarization. The development of these new techniques in combination with the use of highly photostable quantum dots addresses the issue of bioassay sensitivity and offers substantial improvement.

10.7.2 Modulation of Light Emission by Plasmonic Nanoparticles

If instead of solid layer, the dye interacts with metal nanoparticles, additional important factors can modulate the emission in this system. Particularly, the *scattering* of incident radiation on nanoparticles and *plasmon confinement* effect induce new unusual features to emitted radiation. These effects are described in many publications (Darvill et al. 2013; Stewart et al. 2008; Li et al. 2015). Figure 10.17 illustrates the fact that strong plasmonic enhancement can be obtained only with the use of small metal nanoparticles possessing high density of conduction electrons. The very small clusters of several atoms demonstrate instead of plasmon effect their own emission (Sect. 4.6), and larger particles reveal the large-scale electron conductance. In contrast to these cases, in small nanoparticles the oscillation of conduction electrons under the influence of electromagnetic field is restricted in space generating the *surface plasmon oscillations* (Eustis and El-Sayed 2006).

It turned out that the most efficient are the effects generated by nanoparticles smaller than the wavelength of incident light (Li et al. 2015). In this case, the collective oscillations of electrons occur in phase in sub-wavelength volume and very high values of local electromagnetic field intensity are created around the metal nanostructures. This results in large absorption and scattering cross-section, as well as in amplified emission. This condition is called *localized surface plasmon resonance* (LSPR).

Plasmons transform incident light into very strong electromagnetic fields within sub-wavelength regions (near-fields). The high near-field intensities affect the electronic dynamics of fluorophore molecule, resulting in modifications in the decay rate and quantum yield. The increase in emission intensity in optimal conditions reaches very significant values, up to two orders of magnitude (Lakowicz

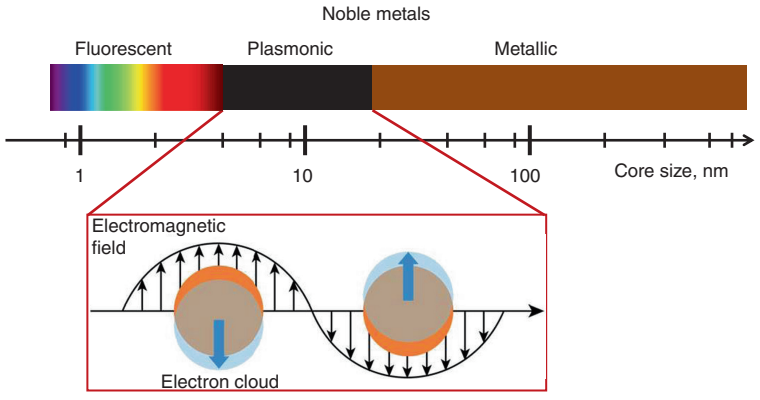

Fig. 10.17 The size-dependent optical properties of noble metal materials. In the particles of nanometer size the oscillations of conduction electrons in the electromagnetic field of the incident light generate localized plasmons producing strong local electromagnetic field effects that can modulate optical properties of nearby molecules and nanoparticles

2005; Aslan et al. 2005), and the reported three orders of magnitude can be considered as record values (Kinkhabwala et al. 2009). In these conditions weak fluorescence emitters can be converted into good ones. Important also is the generality of this phenomenon observed not only for organic dyes but also for semiconductor quantum dots (Gryczynski et al. 2005; Lee et al. 2009), conjugated polymers (Park et al. 2007), lanthanide-chelator luminophores (Zhang et al. 2006b), etc. It is characteristic of not only fluorescence but also of phosphorescence and chemiluminescence. It influences dramatically the FRET efficiency in a donor-acceptor system made of organic dyes adsorbed on silver or gold nano-island films (Giorgetti et al. 2009).

Much effort has been provided to establish the *optimum distance* between the dye and the surface of metal particle for maximal amplification effect. Whereas fluorescence from a molecule directly adsorbed onto the surface of a metallic nanoparticle is strongly quenched (as will be discussed below), at a distance of few nanometers from the nanoparticles it can be strongly enhanced. However, if the distance is too large, the enhancement effect has again to vanish. The experiments focused on such distance optimization were performed with metal particles covered with inert material of variable thickness with the dye adsorbed or covalently attached to its surface. Silica shells (Tovmachenko et al. 2006; Mishra et al. 2013) and inert stearic acid spacer layers (Ray et al. 2007) were used to evaluate this distance dependence. Elegant experiments on a single molecular level were also provided (Fig. 10.18). The results presented in different publications exhibit rather broad variation in estimation of such optimal distance, from 5–10 to more than 20 nm. This is probably because this distance depends on orientation and spectral fitting of

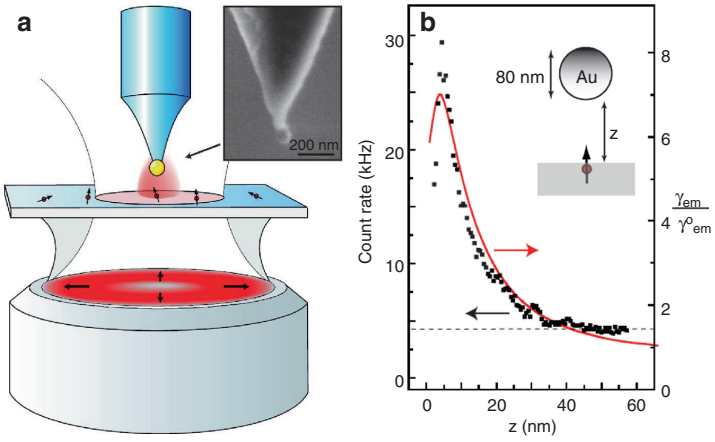

Fig. 10.18 Experimental arrangement in the single-molecular study of the distance effect in plasmon enhancement of fluorescence (**a**) and the obtained results (**b**) (Anger et al. 2006). Au nanosphere was attached to the end of a pointed optical fiber and scanned over a single fluorophore (*Nile Blue*) molecule dispersed in poly(methylmethacrylate) on a glass slide. Variation of fluorescence intensity (*left axis*, *dark dots*) is recorded as a function of the spacing z between the Au nanosphere and a dye molecule. The red curve (*right axis*) shows the emission rate γ_{em} normalized against the value (γ_{em}^0) in free space

the dye and plasmon particle, the plasmon system, the excitation and emitted wavelengths (Fort and Grésillon 2008; Cade et al. 2009).

The intensity enhancement on interaction with localized surface plasmons depends also on the *wavelength of incident light*. The single-molecular studies using individual gold and silver particles excited at different laser-frequencies in configuration similar to that described in Fig. 10.18 have shown that the maximal enhancement should be observed when the emission frequency is *red-shifted* from the surface plasmon resonance of the particle (Bharadwaj and Novotny 2007).

10.7.3 The 'Nanoantenna' Mechanism of Fluorescence Enhancement by Local Field

The plasmonic modification of fluorescence intensity combines two mechanisms. One of them is from *absorption side* and it occurs due to strongly enhanced local (on the scale of nanometers) electromagnetic field augmenting the probability of fluorophore excitation.

In order to better understand the origin of this component of plasmonic enhancement one can use the term 'optical *extinction cross section*', which is the sum of the absorption and scattering cross sections for photons. This term is frequently used by physicists for describing the interaction strength between optical species and light. It can be imagined as a hypothetical area surrounding a particle with very special properties and indicates a higher probability of light being absorbed or scattered by an optically active species. Whereas organic fluorophores and semiconductor QDs possess quite similar ratios of extinction cross sections versus their physical cross sections (which means that their extinction cross sections do not go beyond their actual sizes), for plasmonic nanocrystals this ratio is larger by 2–3 orders of magnitude (Ming et al. 2012). This means that very strong *electromagnetic field* is created around plasmonic particle on its interaction with light, exceeding substantially its size. For fluorophore located within this area the effect will be similar to that occurring on manifold increase of incident light intensity. Therefore plasmonic nanoparticles are often called *nanoantennas*.

The plasmonic particles are very strong light absorbers and scatterers and the relative contribution of these effects is *size-dependent* (Fig. 10.19). For smallest particles, less than ~15 nm, the effect of light absorption dominates. In contrast, for greater nanoparticles the scattering cross-section becomes larger, especially at wavelengths longer than of the plasmon resonance (λ_{LSPR}). The strongest enhancement effects were reported for them (Yagai et al. 2007). Since the optical cross section of the nanoparticle at the resonance energies is strongly enhanced relative to its off-resonance value, the light scattering, being increased with nanoparticle size, should also depend upon the energy of plasmon excitation. It is maximal at resonance wavelength.

The plasmonic properties depend strongly on the type of material (gold or silver) and the shape of particles. For silver spherical particles the resonance is in blue-green and for

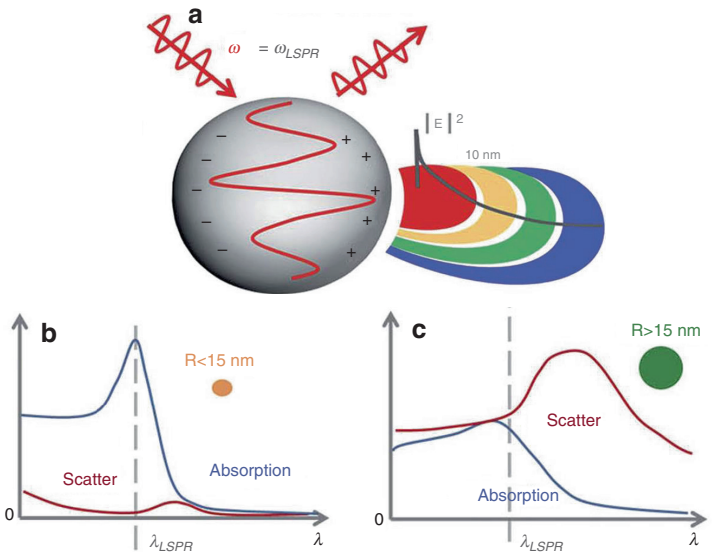

Fig. 10.19 Localized surface plasmon resonance (LSPR) observed when the metal nanoparticle is smaller than the incident light wavelength, making the electron oscillations in phase (Li et al. 2015). (**a**) The collective oscillations lead to large absorption and scattering cross-section, as well as to amplified local electromagnetic field. (**b**) For small particles (less than ~15 nm), absorption cross-section dominates over scattering. (**c**) For larger nanoparticles (greater than ~15 nm), the scattering cross-section becomes much stronger. The electromagnetic field is taken as polarized in the plane of incidence in the figures

gold particles in orange-red region (Fig. 10.20). If the particles are not spherical, their resonance regions are much broader extending to red and near-IR range of spectrum. In particles with sharp edges the local fields are strongly enhanced at these edges.

Thus, plasmonic nanocrystals are very efficient 'concentrators' of electromagnetic fields generated by incident light in the vicinity of their physical boundary.

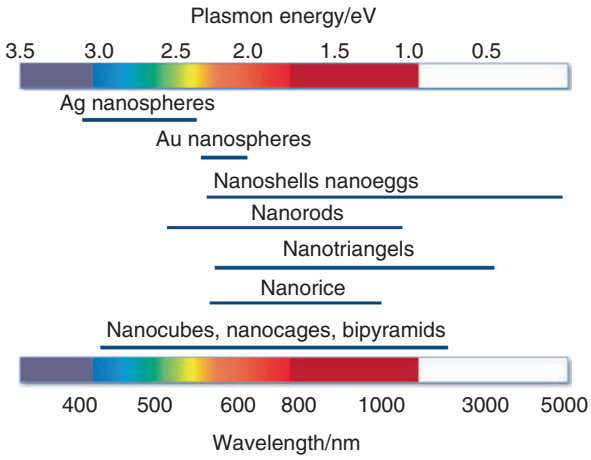

Fig. 10.20 Spectral dependence of the plasmon resonance of differently shaped nanoparticles (Höppener and Novotny 2012). Note that for Ag and Au nanospheres the resonance ranges are different and that for Au nanostructures of different shape the range of resonance energies is broader and mostly shifted to the red

The fluorophores located in this vicinity obtain dramatic increase of excitation energy resulting in enhancement of their emission.

10.7.4 The Plasmonic Modulation of Emission

In addition to modulation by intense local electromagnetic field of fluorophore excitation properties, new effects appear in emission due to *resonance enhancement* of the radiation of oscillating dipole of excited fluorophore by metal particle. Because of that, strong additional emission enhancement becomes possible for weak emitters increasing their quantum yield up to the level of bright emitters. Also the emission parameters including the lifetime, resonance wavelength and even the shape of spectra can be altered (Lakowicz 2005). These facts indicate the existence of a strong resonance coupling that allows transfer of excitation energy.

In vicinity of plasmonic nanocrystal the excited fluorophore can emit a photon, undergo nonradiative decay or relax rapidly by exciting the localized plasmon resonance of the plasmonic nanocrystal via energy transfer. Once the localized plasmon is excited, it can either reradiate or decay nonradiatively owing to internal damping. Owing to the localized density of photonic states, the plasmon resonance can alter both the radiative and nonradiative decay rates of excited fluorophore.

The basic effect of plasmon enhancement of emission intensity is very different from that observed in common free-space fluorescence, where on enhancement or quenching the quantum yield, Φ_o, and lifetime, τ_0, are changed in the same direction. As described in Sect. 4.1, the following equations relate Φ_o and τ_0 to radiative and non-radiative rate constants:

$$\Phi_0 = k_r / \left(k_r + \Sigma k_{nr}\right) = 1 / \left[1 + \left(\Sigma k_{nr} / k_r\right)\right] \tag{10.1}$$

$$\tau_0 = 1 / \left(k_r + \Sigma k_{nr}\right) \tag{10.2}$$

where Φ_o and τ_0 are the free-space quantum yield and lifetime, respectively, k_r is the radiative rate, k_{nr} is the nonradiative rate. For molecules in free space conditions, the *fluorescence power* P_{0fl} (the efficiency of fluorescence emission in energy units) is determined as follows

$$P_{0\,fl} = \sigma_{abs} \cdot N \cdot I_0 \cdot \Phi_0 \tag{10.3}$$

where σ_{abs} is the absorption cross-section, N is the number of the molecules in the beam spot, I_0 is the incident intensity. However, if the molecules are placed near a metal particle, then additional factors appear. The fluorescence power P_{fl} is determined as follows (Dvoynenko and Wang 2007):

$$P_{fl} = \sigma_{abs} \cdot N \cdot I_0 \cdot M^2 \cdot \Phi \tag{10.4}$$

where $M(\omega_{ex}) = \left|E_{loc}(\omega_{ex}) / E_0(\omega_{ex})\right|$ is the enhancement factor of local field, $E_{loc}(\omega_{ex})$ is the amplitude of the local field at the excitation frequency (ω_{ex}), $E_0(\omega_{ex})$ is the amplitude of the incident field, Φ is the modified quantum yield of fluorescence. The first effect modifying the intensity by the factor $M(\omega_{ex})^2$ is obvious: this is the modification of the excitation rate. The second effect is the *modification of quantum yield*. It is not so obvious because this change is caused by the change of the radiation rate as well as nonradiative rate. Here the quantum yield Φ has the form

$$\Phi = M(\omega_{em})^2 k_r / \left(M(\omega_{em})^2 k_r + k_{nr} + k_{FRET}\right) \tag{10.5}$$

where $M(\omega_{em})$ is the enhancement of local field at the emission frequency (ω_{em}), k_{FRET} is the nonradiative rate because of the Forster resonance energy transfer (FRET). $M(\omega_{em})^2$ is equal to the enhancement of the radiative rate because of the reciprocity relation in classical electrodynamics (Méndez et al. 1997). The increase of the radiative rate occurs in particular due to a transformation of evanescent waves to propagative ones by the polarization of a metal particle that was schematically presented in Fig. 10.17. The polarized particle is a source of a scattered waves and the local field enhancement is mainly due to the evanescent waves.

Comparing Eqs. (10.4) and (10.5) with Eq. (10.3) one can find that the *fluorescence power* can be increased by the increase of the excitation rate provided by interaction with plasmon. As regards to the *quantum yield*, its increase is quite tricky. Comparing Eqs. (10.1) and (10.5) it is seen that the quantum yield Φ can be increased for molecules having in free space a low value of the quantum yield Φ_o. Thus, interaction with plasmons can transform bad emitters into good emitters. Examples of such transformation are numerous and not only in fluorescence. One of them is the plasmon enhancement of electroluminescence (Gu et al. 2011), which can be explained only by this way. However, if the quantum yield Φ_o is very high, then $\Phi < \Phi_o$ in all cases and plasmon enhancement of fluorescence is limited to augmenting the excitation rate.

The *quenching* of fluorescence happens if in a plasmon system the local field enhancement is low ($M(\omega_{ex}) \quad 1$). For example, this takes place in the case of a smooth surface or smooth metal film. At small distances between molecules and metal surface the FRET rate is much higher than any radiation rate ($k_{FRET} >> k_r$) and as results the fluorescence intensity drops dramatically. In contrast, the Raman intensity does not show any quenching effect and, thus, the ratio between Raman and fluorescence intensities can be an indicator of the lifetime and of molecule-metal distance (Dvoynenko et al. 2010).

In contrast to common free-space emission, the *quantum yield* here is not proportional to *lifetime* because of the presence of strong metal-modified radiative decay kinetics with the rate determined by $M(\omega_{em})^2$ factor. This is why the fluorophore metal-modified lifetime, τ_m, is *decreased* with an *increased* radiative decay rate. It can be seen that as the value of $M(\omega_{em})^2$ increases, the quantum yield, Φ_m also

increases, instead of commonly expected decrease. These predictions were confirmed in experiment (Aslan et al. 2005).

The calculation of *optimal distance* providing maximum value of the fluorescence enhancement is difficult, since it depends on many factors. Particularly, it depends on the quantum yield of the free molecule Φ_0. As it can be derived from Eq. (10.5), a low value of Φ_0 decreases this optimal distance, while for a high value of Φ_0 this distance is experimentally estimated to be 5–10 nm (Anger et al. 2006). However, strictly speaking this distance depends on a plasmonic system. Two coupled spheres (particles) can dramatically change this rule because $M(\omega_{ex})$ can be higher by one order of magnitude as compared to a single particle and the fluorescence enhancement can be observed even at smaller molecule-metal distances.

Metallic nanoparticles (especially silver, gold and copper) are known to *scatter light* efficiently and in an angular-dependent fashion. It is this property that is used in the enhancement of the local field and radiative rate. The silver particles are several-fold better scatterers than gold (Yguerabide and Yguerabide 1998). Subsequently, light scattering by silver and gold nanoparticles can be detected at concentrations as low as 10^{-16} M (see Sect. 8.6). The scattered light by metallic nanoparticles is the highest at observation angles of 0 and 180° with respect to the incident light, i.e. in the backward and forward directions. The angular dependence of the scattered light depends on the size, shape and composition of the nanoparticles. It is essential that enhanced fluorescence emission reproduces exactly this angular dependence. In addition, this angular dependence can be changed on the binding of labeled target protein. It was suggested to use this property for development of *angle-ratiometric fluorescence sensing* (Aslan et al. 2007b).

In plasmonic systems, it is often very difficult to separate the effects of enhancement and quenching, but the general rules for obtaining enhancement can be formulated. The fluorophores should optimally fit by their absorption and emission spectra to the wavelength range of resonance scattering of plasmon nanoparticles, they should be located at an optimal distance and in optimal orientation to nanoparticle of its dipole. The plasmon particle should be of such size and shape that it should be more scatterer than absorber and that its size, shape and interactions with other plasmon particles should better fit to resonance conditions. Hence nanostars, nanorods, and nanoshells and their associates generally have increased enhancement effect compared to nanospheres (Ming et al. 2012).

10.7.5 Extended Range of Observations

Metal enhancement is demonstrated for *two-photon excited* fluorescent dyes. Simultaneous absorption of two photons occurs if the density of incident photons is high (Sect. 10.4), which can be achieved by pulsed lasers with high peak power and their sharp focusing. It was shown that metal nanoparticles can provide such an enhancement of excitation rate due to very high absorption cross-section that may be sufficient for generating the two photon emission near their surfaces (Gryczynski

et al. 2002). This fact suggests the possibility that such approach will change the two-photon microscopy (Sect. 13.1) by making unnecessary the scanning with ultra-short laser pulses; so that the wide-field optics may possibly be used.

Notably, the effect of metal-nanoparticle emission enhancement is not limited to fluorescence only. It was also discovered for *chemiluminescence* (Chowdhury et al. 2006). This indicates that the surface plasmons can be directly excited from chemically induced electronic excited states and excludes the possibility that they are created by incident excitation light. Such observation has to stimulate new developments in chemiluminescence sensing methods (Sect. 10.1), the methods that use very cheap instrumentation but suffer from low levels of emission signals.

Phosphorescence emission can also be enhanced on interaction with the metal (Zhang et al. 2007), and this effect is clearly observed with metal nanoparticles (Zhang et al. 2006b). Since the triplet states that give rise to phosphorescence are chemically reactive, the proximity of metal nanoparticles produce their activation and acceleration, in particular, generating singlet oxygen and superoxide radicals (Zhang et al. 2007). On the other side, the shorter lifetime of the metal-enhanced *fluorescence* results in less time for the excited state photoreactions, and thus more excitation-emission cycles can occur prior to photobleaching. Thus, the increased *photostability* of fluorescent dyes is an important additional benefit.

10.7.6 Applications of Metal Enhancement

Current literature contains numerous examples of successful applications of sensor techniques based on plasmonics. Their obvious advantage is dramatically increases sensitivity making unnecessary in many cases additional pre-treatment (such as PCR technique) or post-treatment, such as developing chromogenic or fluorogenic products (such as in ELISA). These techniques allow real-time measurement of reaction kinetics of binding events when the plasmonic chip is integrated into a flow-cell. Both spotted and suspension arrays (see Chap. 11) can be applied for simultaneous detection of multiple analytes.

A straightforward use of metal enhancement is for providing an *increased sensitivity* to traditional detection techniques. An example is the recent work (Aslan et al. 2006), in which the application of this approach resulted in detection of only several femtomoles (10^{-15} mol) of RNA rapidly and without the use of time- and reagent-consuming PCR procedure. It has a strong potential to be developed into different single-molecular detection methodologies.

The other important advantage in sensing applications is the *localized nature* of the enhancement effect. The enhanced evanescent field mode of excitation localizes the excitation volume in close proximity to the metal nanostructures. As in other evanescent-field excitation techniques, this allows exciting only the bound species and eliminates the need for any washing steps. In contrast to plain surfaces, the nanoparticles possess dramatically larger surface areas. Together with their effect as scatterers, this offers broader flexibility in the assay development.

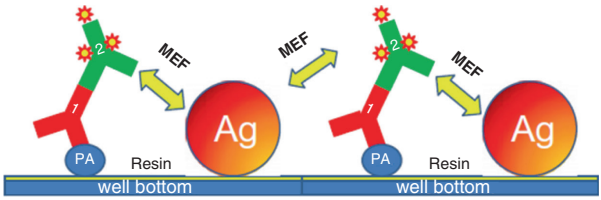

Fig. 10.21 Scheme of the anthrax protective antigen (*PA*) exotoxin assay based on metal-enhanced fluorescence (Dragan et al. 2012). When the multiprotein complex. *PA* primary antibody. (*1*) and labeled with fluorescein secondary antibody (*2*) is attached to the plate bottom resin, the enhancement of fluorescein emission is induced by close proximity to the silver nanoparticles deposited within plate wells

As an example of analytical application of this new technique, the recently developed method to detect low levels of the anthrax protective antigen (PA) exotoxin in biological fluids with analytical sensitivity of less than 1 pg/ml (Dragan et al. 2012) can be cited. Technologically, the proposed assay uses standard 96-well plastic plates modified with silver island films grown within the wells. In a configuration shown in Fig. 10.21, the fluorescent probe covalently attached to the secondary antibody plays a crucial role of indicating the recognition event by demonstrating its metal-enhanced fluorescence.

An immense variety of potentially useful *nanocomposites* can be constructed exhibiting enhanced emission. An interesting possibility, for example, can be realized when the dye is incorporated into silica core of the beads that are coated by silver layer to generate porous but continuous metal nanoshells (Zhang et al. 2006b). Being brightly emissive, such particles are simultaneously protected from the quenching effect of the solvent. The synthesis of hybrid nanoprobes composed of gold-nanorods, CdSe/ZnS quantum dots and iron oxide nanoparticles was reported (Basiruddin et al. 2011). They were shown to combine plasmonic, fluorescent and magnetic properties into a single molecular construct.

In this regard, the approach based on metal particle enhancement has a strong potential for application in *high throughput screening* and other assays dealing with great number of samples and determining many parameters. Such possibility of *multiplex detection* was demonstrated for the DNA microarrays, in which the surface-bound silver nanoparticles were used as fluorescence enhancers (Sabanayagam and Lakowicz 2007).

10.7.7 Microwave Acceleration of Metal-Enhanced Emission

Low-power microwave heating is increasingly used in different techniques of chemical synthesis for accelerating the reaction rates (Tokuyama and Nakamura 2005). Microwaves with the frequency of 0.3–300 GHz lie between the infrared and radio-frequency electromagnetic radiations. They are strongly absorbed by mobile dipoles

in the medium, so that polar systems of any size are selectively heated, and non-polar remain transparent to this radiation. Home kitchen microwaves operate based on this principle. For metals, the attenuation of microwave radiation arises from the motions of extremely mobile conductance electrons. The charge carriers in the metal, which are displaced by the electric field, are subjected to resistance due to collisions with the lattice phonons. They provide energy to the lattice resulting in the local heating. This so-called Ohmic heating of the metal nanoparticles occurs in addition to the heating of any medium, such as water surrounding the nanoparticles.

Essentially, the *localized heating* around the metal nanostructures can be achieved without heating of the whole volume. This accelerates the local diffusion and specific binding (recognition) between macromolecules close to them. Thus, the speed of receptor-target binding can be increases, which is highly needed for increasing efficiency of operation of sensors. Thus, the combination of metal enhancement and localized heating by microwaves makes the sensing both very sensitive and rapid (Aslan and Geddes 2005).

When the time-consuming steps of sample pre-treatment and after-treatment are eliminated or substantially reduced, then the *assay duration* becomes the step limited by the sensor-target incubation time. The process of recognition between the target and receptor involves many trial-and-error steps on molecular level, so that many minutes and sometimes hours are needed for establishing the equilibrium between free and bound target. The slow rate is particularly characteristic for the most popular assays involving macromolecules, in which the multi-point specific contacts need to be established, such as the DNA hybridization assays and immunoassays. It was recently demonstrated that for both these types of assays with the application of microwaves the incubation times can be reduced manifold, to seconds.

Thus, it was shown (Aslan et al. 2006; Aslan et al. 2007a) that by combining the metal enhancement effects of silver nanoparticles on dye emission with low-power, localized microwave heating, a model *DNA hybridization assay* to detect 23-mer targets can be kinetically complete within 20 s. This gives acceleration up to 600-fold, as compared to an identical hybridization assay run without microwaves and does not lead to any destruction or denaturation of interacting partners. Simultaneously, by metal enhancement, a greater than ten-fold increase in assay sensitivity was achieved. The speed of assay together with high sensitivity is especially important in the identification of such dangerous bioagents, as Anthrax (DNA) or Ebola (RNA) viruses.

The limiting factors in current *immunoassays* are their low sensitivity and slow speed. For increasing the sensitivity, additional operations (such as catalytic amplification) are frequently introduced, and they still further increase the time of test duration. Therefore the microwave-heated metal-enhanced technique is an attractive technology for the future. This approach allows reducing the incubation times in immunoassays from many minutes to few seconds with dramatic increase of sensitivity (Aslan et al. 2007c). In view of these findings, it is highly probable that this new technology will fundamentally change the ways by which the immunoassays and other diagnostic tools are employed in clinical medicine, adding speed and sensitivity.

10.7.8 Prospects

In present days, we are on the most romantic step of exploration of the phenomenon of metal enhancement of fluorescence. This is definitely a new and very prospective tool in sensing technologies that showed already the superiority over traditional detection techniques. Meantime it is still difficult to predict whether a particular sized metal structure will strongly quench or strongly enhance the fluorescence or other type of emission of a definite molecular dye or nanocomposite, and to what extent. There are many factors influencing this enhancement and, notably, the interplay between *enhancement* and *quenching*. These factors can belong to the emitter (quantum yield, lifetime), to the metal (plain surface or nanoparticles, particle size and shape, their resonance absorption energy) and to both of them (their orientation and distance).

In the case of fluorescent molecules located at very short distances from a metal surface, the *quenching* takes place. Electromagnetic-field *enhancement* occurs at longer distances. As a result, there is an optimal dye to metal distance for fluorescence enhancement. With good understanding of this phenomenon, switching between enhancement and quenching can provide the broadest dynamic range hardly available to any other sensing technique.

It is presently certain that the phenomenon of metal enhancement is of *general origin*. It appears irrespective of the nature of excited state (singlet or triplet) and of the way of excitation (optical or in a chemical reaction). This adds many new dimensions to research and practical use of this phenomenon.

Such bright perspective stimulates detailed studies in all aspects, including the sizes, shapes and composition of metal nanostructures, and also the nature, spectroscopic properties and location of fluorophores. The role of augmentation of optical intensity incident on the dye molecule through near field enhancement, of modification of the radiative decay rate of the emitter and of increasing the coupling efficiency of the fluorescence emission to the far field through nanoparticles scattering deserve detailed studies.

An immense variety of nanocomposites exhibiting plasmon-enhanced emission can be constructed. They can be made of similar and dissimilar emitters but with necessary participation of plasmonic nanoparticles in their special arrangement. This allows achieving important goal to increase the output signal and thus to reach the lower limits of target detection.

10.8 Sensing and Thinking: Eliminating Light Sources and Photodetectors: What Remains?

This is a provocative question. In every detection method considered above we need necessarily the input of energy and also the output of energy carrying informative signal. Simply the inputs and outputs of this energy could not be necessarily optical radiations and therefore possibilities for research and development can be much broader.

In this Chapter we tried to compare seemingly incomparable techniques. They offer the complementing to fluorescence sensing in different, sometimes unexpected, directions. The reader is encouraged to analyze them and to develop his/her own opinion, which of them offer substantial progress with a broad-scale practical implementation, and which will end up in research laboratories. Different criteria for such comparison can be used, in addition to common detection limit and sensitivity. (a). Speed of analysis. (b). Spatial resolution with extension to microarray techniques. (c). Possibility of extension to microbead assays and suspension arrays. The reader may consider different constructions combining two or several of these non-conventional approaches.

Questions and Problems

1. List the methods of exciting luminescence beside the optical excitation. Explain the origin of excitation energy in these cases
2. What kind of chemical species can emit light in the form of chemiluminescence? Why chemiluminescence is restricted to a very narrow range of reactions? What kinds of chemical substances can interfere into these assays for providing the sensor response? Evaluate the possibilities of this method for sensing multiple samples.
3. Are the mechanisms of quenching of chemiluminescence and bioluminescence emission similar to that of common luminescence, or different?
4. Why the spectral resolution for detection of chemiluminescence is commonly not needed and the sample cell can be located on top of the detector?
5. Estimate the achievable time resolution in chemiluminescence and electrochemiluminescence methods.
6. What are the reasons to introduce the luciferin-luciferase system into different living cells by genetic engineering? Evaluate possible applications of this approach.
7. What are the possibilities of using the intrinsically illuminated nanoparticles?
8. Analyze the possibilities of application of high-energy radiation for exciting luminescence emission.
9. What are the conditions for obtaining the two-photonic excitation? Can these two photons be of different energies?
10. Can the two-photon emission be polarized and can it allow application in polarization assays?
11. What are the differences in excitation of two-photon and up-conversion luminophores? Does up-conversion allow achieving high spatial resolution? What are the special properties of up-converting luminophores as the FRET donors? Can they serve also as FRET acceptors?
12. What are the requirements for observation of amplified stimulated emission? How fluorescence reporting can be introduced into this process?
13. What are the possibilities instead of generating reporter emission and recording it with photodetector to obtain directly the electrical signal?
14. Explain the performance of LAPS. What are the areas of its application? For multiplex applications, do we need to make a separate system containing the semiconductor plate and the electrodes for every analyte?

15. What is the distance dependence for evanescent wave excitation? Compare it with the sizes of macromolecules, nanoparticles, cells.
16. What is special in metal nanoparticles so that they provide the effect of enhancement of fluorescence? What is its dependence on the particle size and the dye-particle distance?
17. Explain the mechanism by which the enhancement of fluorescence intensity can be coupled with shortening of lifetime.
18. Why the microwave heating can be local and focused on only metal particles in solutions? How it can decrease the duration of the assays?

References

Ahmad M, Pratx G, Bazalova M, Lei X (2014) X-Ray luminescence and X-Ray fluorescence computed tomography: new molecular imaging modalities. Access, IEEE 2:1051-1061. doi:10.1109/access.2014.2353041

Anger P, Bharadwaj P, Novotny L (2006) Enhancement and quenching of single-molecule fluorescence. Phys Rev Lett 96(11):113002

Aslan K, Geddes CD (2005) Microwave-accelerated metal-enhanced fluorescence: platform technology for ultrafast and ultrabright assays. Anal Chem 77(24):8057–8067

Aslan K, Gryczynski I, Malicka J, Matveeva E, Lakowicz JR, Geddes CD (2005) Metal-enhanced fluorescence: an emerging tool in biotechnology. Curr Opin Biotechnol 16(1):55–62

Aslan K, Huang J, Wilson GM, Geddes CD (2006) Metal-enhanced fluorescence-based RNA sensing. J Am Chem Soc 128(13):4206–4207

Aslan K, Malyn SN, Bector G, Geddes CD (2007a) Microwave-accelerated metal-enhanced fluorescence: an ultra-fast and sensitive DNA sensing platform. Analyst 132(11):1122–1129

Aslan K, Malyn SN, Geddes CD (2007b) Angular-dependent metal-enhanced fluorescence from silver colloid-deposited films: opportunity for angular-ratiometric surface assays. Analyst 132(11):1112–1121

Aslan K, Malyn SN, Geddes CD (2007c) Microwave-accelerated surface plasmon-cCoupled directional luminescence: application to fast and sensitive assays in buffer, human serum and whole blood. J Immunol Methods 323(1):55–64

Baj S, Krawczyk T (2007) Chemiluminescence detection of organic peroxides in a two-phase system. Anal Chim Acta 585(1):147–153

Basiruddin S, Maity AR, Saha A, Jana NR (2011) Gold-nanorod-based hybrid cellular probe with multifunctional properties. J Phys Chem C 115(40):19612–19620

Belfield KD, Bondar MV, Hernandez FE, Przhonska OV, Yao S (2006) Two-photon absorption of a supramolecular pseudoisocyanine J-aggregate assembly. Chem Phys 320(2):118–124

Bharadwaj P, Novotny L (2007) Spectral dependence of single molecule fluorescence enhancement. Opt Express 15(21):14266–14274

Cade NI, Ritman-Meer T, Kwaka K, Richards D (2009) The plasmonic engineering of metal nanoparticles for enhanced fluorescence and Raman scattering. Nanotechnology 20(28):285201

Cao L, Wang X, Meziani MJ, Lu F, Wang H, Luo PG, Lin Y, Harruff BA, Veca LM, Murray D, Xie SY, Sun YP (2007) Carbon dots for multiphoton bioimaging. J Am Chem Soc 129(37):11318–11319. doi:10.1021/ja073527l

Chowdhury MH, Aslan K, Malyn SN, Lakowicz JR, Geddes CD (2006) Metal-enhanced chemiluminescence: radiating plasmons generated from chemically induced electronic excited states. Appl Phys Lett 88(17)

Collini E (2012) Cooperative effects to enhance two-photon absorption efficiency: intra- versus inter-molecular approach. Phys Chem Chem Phys 14(11):3725–3736. doi:10.1039/c2cp24030k

Couture M, Zhao SS, Masson J-F (2013) Modern surface plasmon resonance for bioanalytics and biophysics. Phys Chem Chem Phys 15(27):11190–11216. doi:10.1039/C3CP50281C

Darvill D, Centeno A, Xie F (2013) Plasmonic fluorescence enhancement by metal nanostructures: shaping the future of bionanotechnology. Phys Chem Chem Phys 15(38): 15709–15726

Das A, Das A, Chang LB, Lai CS, Lin RM, Chu FC, Lin YH, Chow L, Jeng MJ (2013) GaN thin film based light addressable potentiometric sensor for pH sensing application. Appl Phys Express 6(3):036601

Deng S, Ju H (2013) Electrogenerated chemiluminescence of nanomaterials for bioanalysis. Analyst 138(1):43–61

Dennany L, Forster RJ, Rusling JF (2003) Simultaneous direct electrochemiluminescence and catalytic voltammetry detection of DNA in ultrathin films. J Am Chem Soc 125(17):5213–5218

Dothager RS, Goiffon RJ, Jackson E, Harpstrite S, Piwnica-Worms D (2010) Cerenkov radiation energy transfer (CRET) imaging: a novel method for optical imaging of PET isotopes in biological systems. PLoS One 5(10):e13300

Dragan AI, Albrecht MT, Pavlovic R, Keane-Myers AM, Geddes CD (2012) Ultra-fast pg/ml anthrax toxin (protective antigen) detection assay based on microwave-accelerated metal-enhanced fluorescence. Anal Biochem 425(1):54–61

Dvoynenko MM, Wang J-K (2007) Finding electromagnetic and chemical enhancement factors of surface-enhanced Raman scattering. Opt Lett 32(24):3552–3554

Dvoynenko M, Kazantseva Z, Strelchuk V, Kolomys O, Venger E, Wang J-K (2010) Molecular ruler based on concurrent measurements of enhanced Raman scattering and fluorescence. Opt Lett 35(22):3808–3810

Ekgasit S, Thammacharoen C, Yu F, Knoll W (2004) Evanescent field in surface plasmon resonance and surface plasmon field-enhanced fluorescence spectroscopies. Anal Chem 76(8):2210–2219

Eustis S, El-Sayed MA (2006) Why gold nanoparticles are more precious than pretty gold: noble metal surface plasmon resonance and its enhancement of the radiative and nonradiative properties of nanocrystals of different shapes. Chem Soc Rev 35(3):209–217

Fahnrich KA, Pravda M, Guilbault GG (2001) Recent applications of electrogenerated chemiluminescence in chemical analysis. Talanta 54(4):531–559

Fine T, Leskinen P, Isobe T, Shiraishi H, Morita M, Marks RS, Virta M (2006) Luminescent yeast cells entrapped in hydrogels for estrogenic endocrine disrupting chemical biodetection. Biosens Bioelectron 21(12):2263–2269

Fort E, Grésillon S (2008) Surface enhanced fluorescence. J Phys D Appl Phys 41(1):013001

Frangioni JV (2006) Self-illuminating quantum dots light the way. Nat Biotechnol 24(3):326–328

Fu J, Przhonska OV, Padilha LA, Hagan DJ, Van Stryland EW, Belfield KD, Bondar MV, Slominsky YL, Kachkovski AD (2006) Two-photon anisotropy: analytical description and molecular modeling for symmetrical and asymmetrical organic dyes. Chem Phys 321(3): 257–268

Fu J, Padilha LA, Hagan DJ, Van Stryland EW, Przhonska OV, Bondar MV, Slominsky YL, Kachkovski AD (2007) Molecular structure – two-photon absorption property relations in polymethine dyes. J Opt Soc Am B 24(1):56–66

Gao H, Wang W, Wang Z, Han J, Fu Z (2014) Amorphous carbon nanoparticle used as novel resonance energy transfer acceptor for chemiluminescent immunoassay of transferrin. Anal Chim Acta 819:102–107

Giorgetti E, Cicchi S, Muniz-Miranda M, Margheri G, Del Rosso T, Giusti A, Rindi A, Ghini G, Sottini S, Marcelli A, Foggi P (2009) Forster resonance energy transfer (FRET) with a donor-acceptor system adsorbed on silver or gold nanoisland films. Phys Chem Chem Phys 11(42):9798–9803

Gratzel M (2007) Photovoltaic and photoelectrochemical conversion of solar energy. Philos Transact A Math Phys Eng Sci 365(1853):993–1005

Gryczynski I, Malicka J, Shen YB, Gryczynski Z, Lakowicz JR (2002) Multiphoton excitation of fluorescence near metallic particles: enhanced and localized excitation. J Phys Chem B 106(9):2191–2195

Gryczynski I, Malicka J, Jiang W, Fischer H, Chan WCW, Gryczynski Z, Grudzinski W, Lakowicz JR (2005) Surface-plasmon-coupled emission of quantum dots. J Phys Chem B 109(3):1088–1093

Gu X, Qiu T, Zhang W, Chu PK (2011) Light-emitting diodes enhanced by localized surface plasmon resonance. Nanoscale Res Lett 6(1):1–12

Guzelturk B, Kelestemur Y, Olutas M, Delikanli S, Demir HV (2014) Amplified spontaneous emission and lasing in colloidal nanoplatelets. ACS Nano 8(7):6599–6605

Hanninen P, Soini A, Meltola N, Soini J, Soukka J, Soini E (2000) A new microvolume technique for bioaffinity assays using two-photon excitation. Nat Biotechnol 18(5):548–550

He GS, Zheng Q, Prasad PN, Grote JG, Hopkins FK (2006) Infrared two-photon-excited visible lasing from a DNA-surfactant-chromophore complex. Opt Lett 31(3):359–361

Holthoff WG, Tehan EC, Bukowski RM, Kent N, MacCraith BD, Bright FV (2005) Radioluminescent light source for the development of optical sensor arrays. Anal Chem 77(2):718–723

Höppener C, Novotny L (2012) Exploiting the light–metal interaction for biomolecular sensing and imaging. Q Rev Biophys 45(02):209–255

Howes PD, Rana S, Stevens MM (2014) Plasmonic nanomaterials for biodiagnostics. Chem Soc Rev 43(11):3835–3853

Huang XY, Li L, Qian HF, Dong CQ, Ren JC (2006) A resonance energy transfer between chemiluminescent donors and luminescent quantum-dots as acceptors (CRET). Angew Chem Int Ed 45(31):5140–5143

Kinkhabwala A, Yu Z, Fan S, Avlasevich Y, Müllen K, Moerner W (2009) Large single-molecule fluorescence enhancements produced by a bowtie nanoantenna. Nat Photonics 3(11):654–657

Kulmala S, Suomi J (2003) Current status of modern analytical luminescence methods. Anal Chim Acta 500(1–2):21–69

Lakowicz JR (2005) Radiative decay engineering 5: metal-enhanced fluorescence and plasmon emission. Anal Biochem 337(2):171–194

Le Ru EC, Etchegoin PG (2012) Single-molecule surface-enhanced Raman spectroscopy. Annu Rev Phys Chem 63:65–87

Lee SY, Nakaya K, Hayashi T, Hara M (2009) Quantitative study of the gold-enhanced fluorescence of CdSe/ZnS nanocrystals as a function of distance using an AFM probe. Phys Chem Chem Phys 11(21):4403–4409

Li BX, He YZ (2007) Simultaneous determination of glucose, fructose and lactose in food samples using a continuous-flow chemiluminescence method with the aid of artificial neural networks. Luminescence 22(4):317–325

Li Y, Yang P, Wang P, Huang X, Wang L (2007) CdS nanocrystal induced chemiluminescence: reaction mechanism and applications. Nanotechnology 18(22):225602

Li Q, Zhang L, Li J, Lu C (2011) Nanomaterial-amplified chemiluminescence systems and their applications in bioassays. TrAC Trends Anal Chem 30(2):401–413

Li M, Cushing SK, Wu N (2015) Plasmon-enhanced optical sensors: a review. Analyst 140(2):386–406

Lin Z, Xue W, Chen H, Lin J-M (2012) Classical oxidant induced chemiluminescence of fluorescent carbon dots. Chem Commun 48(7):1051–1053

Liu X, Tan W (1999) A fiber-optic evanescent wave DNA biosensor based on novel molecular beacons. Anal Chem 71(22):5054–5059

Liu H, Zhang X, Xing B, Han P, Gambhir SS, Cheng Z (2010) Radiation-luminescence-excited quantum dots for in vivo multiplexed optical imaging. Small 6(10):1087–1091

Liu Q, Guo B, Rao Z, Zhang B, Gong JR (2013) Strong two-photon-induced fluorescence from photostable, biocompatible nitrogen-doped graphene quantum dots for cellular and deep-tissue imaging. Nano Lett 13(6):2436–2441. doi:10.1021/nl400368v

Méndez E, Greffet J-J, Carminati R (1997) On the equivalence between the illumination and collection modes of the scanning near-field optical microscope. Opt commun 142(1):7–13

Merlen A, Lagugné-Labarthet F, Harté E (2010) Surface-enhanced raman and fluorescence spectroscopy of dye molecules deposited on nanostructured gold surfaces. J Phys Chem C 114(30):12878–12884

Miao W (2008) Electrogenerated chemiluminescence and its biorelated applications. Chem Rev 108(7):2506–2553

Miao WJ, Bard AJ (2003) Electrogenerated chemluminescence. 72. Determination of immobilized DNA and C-reactive protein on Au(111) electrodes using Tris(2,2'-bipyridyl)ruthenium(II) labels. Anal Chem 75(21):5825–5834

Michelini E, Mirasoli M, Karp M, Virta M, Roda A (2004) Development of a bioluminescence resonance energy-transfer assay for estrogen-like compound in vivo monitoring. Anal Chem 76(23):7069–7076

Ming T, Chen H, Jiang R, Li Q, Wang J (2012) Plasmon-controlled fluorescence: beyond the intensity enhancement. J Phys Chem Lett 3(2):191–202

Mishra H, Mali BL, Karolin J, Dragan AI, Geddes CD (2013) Experimental and theoretical study of the distance dependence of metal-enhanced fluorescence, phosphorescence and delayed fluorescence in a single system. Phys Chem Chem Phys 15(45):19538–19544

Moreshead WV, Przhonska OV, Bondar MV, Kachkovski AD, Nayyar IH, Masunov AE, Woodward AW, Belfield KD (2013) Design of a new optical material with broad spectrum linear and two-photon absorption and solvatochromism. J Phys Chem Lett 117(44):23133–23147

Naczynski DJ, Sun C, Türkcan S, Jenkins C, Koh AL, Ikeda D, Pratx G, Xing L (2015) X-ray induced shortwave infrared biomedical imaging using rare-earth nanoprobes. Nano Lett 15: 96–102

Neumann T, Johansson ML, Kambhampati D, Knoll W (2002) Surface-plasmon fluorescence spectroscopy. Adv Funct Mater 12(9):575–586

Paley MA, Prescher JA (2014) Bioluminescence: a versatile technique for imaging cellular and molecular features. Med Chem Commun 5(3):255–267

Papkovsky DB, O'Riordan T, Soini A (2000) Phosphorescent porphyrin probes in biosensors and sensitive bioassays. Biochem Soc Trans 28:74–77

Park HJ, Vak D, Noh YY, Lim B, Kim DY (2007) Surface plasmon enhanced photoluminescence of conjugated polymers. Appl Phys Lett 90(16):161107

Paulmurugan R, Gambhir SS (2007) Combinatorial library screening for developing an improved split-firefly luciferase fragment-assisted complementation system for studying protein-protein interactions. Anal Chem 79(6):2346–2353

Peter LM (2007) Dye-sensitized nanocrystalline solar cells. Phys Chem Chem Phys 9(21): 2630–2642

Przhonska OV, Scott Webster S, Padilha LA, Hu H, Kachkovski AD, Hagan DJ, Stryland EW V (2010) Two-photon absorption in near-IR conjugated molecules: design strategy and structure-property relations. In: Demchenko AP (ed) Advanced fluorescence reporters in chemistry and biology. I. Fundamentals and molecular design, vol 8, Springer series on fluorescence. Springer, Heidelberg pp 105–148

Pu S-C, Yang M-J, Hsu C-C, Lai C-W, Hsieh C-C, Lin SH, Cheng Y-M, Chou P-T (2006) The empirical correlation between size and two-photon absorption cross section of CdSe and CdTe quantum dots. Small 2(11):1308–1313. doi:10.1002/smll.200600157

Qin G, Zhao S, Huang Y, Jiang J, Liu Y-M (2013) A sensitive gold nanoparticles sensing platform based on resonance energy transfer for chemiluminescence light on detection of biomolecules. Biosens Bioelectron 46:119–123

Ray K, Badugu R, Lakowicz JR (2007) Sulforhodamine adsorbed Langmuir-Blodgett layers on silver island films: effect of probe distance on the metal-enhanced fluorescence. J Phys Chem C 111(19):7091–7097

Richter MM (2004) Electrochemiluminescence (ECL). Chem Rev 104(6):3003–3036

Roda A, Pasini P, Mirasoli M, Michelini E, Guardigli M (2004) Biotechnological applications of bioluminescence and chemiluminescence. Trends Biotechnol 22(6):295–303

Rose A, Zhu ZG, Madigan CF, Swager TM, Bulovic V (2005) Sensitivity gains in chemosensing by lasing action in organic polymers. Nature 434(7035):876–879

Sabanayagam CR, Lakowicz JR (2007) Increasing the sensitivity of DNA microarrays by metal-enhanced fluorescence using surface-bound silver nanoparticles. Nucleic Acids Res 35(2):e13
Scherf U, Riechel S, Lemmer U, Mahrt R (2001) Conjugated polymers: lasing and stimulated emission. Curr Opin Solid State Mater Sci 5(2):143–154
Seidel M, Niessner R (2014) Chemiluminescence microarrays in analytical chemistry: a critical review. Anal Bioanal Chem 406:5589–5612
She C, Fedin I, Dolzhnikov DS, Demortière A, Schaller RD, Pelton M, Talapin DV (2014) Low-threshold stimulated emission using colloidal quantum wells. Nano Lett 14(5):2772–2777
So PTC, Dong CY, Masters BR, Berland KM (2000) Two-photon excitation fluorescence microscopy. Annu Rev Biomed Eng 2:399–429
So MK, Xu CJ, Loening AM, Gambhir SS, Rao JH (2006) Self-illuminating quantum dot conjugates for in vivo imaging. Nat Biotechnol 24(3):339–343
Somers RC, Bawendi MG, Nocera DG (2007) CdSe nanocrystal based chem-/bio-sensors. Chem Soc Rev 36(4):579–591
Stewart ME, Anderton CR, Thompson LB, Maria J, Gray SK, Rogers JA, Nuzzo RG (2008) Nanostructured plasmonic sensors. Chem Rev 108(2):494–521
Su Y, Lv Y (2014) Graphene and graphene oxides: recent advances in chemiluminescence and electrochemiluminescence. RSC Advances 4(55):29324–29339
Sudheendra L, Das GK, Li C, Stark D, Cena J, Cherry S, Kennedy IM (2014) NaGdF4: Eu3+ Nanoparticles for enhanced X-ray excited optical imaging. Chem Mater 26(5):1881–1888
Sun X, Huang X, Guo J, Zhu W, Ding Y, Niu G, Wang A, Kiesewetter DO, Wang ZL, Sun S (2014) Self-illuminating 64Cu-Doped CdSe/ZnS nanocrystals for in vivo tumor imaging. J Am Chem Soc 136(5):1706–1709
Suomi J, Kulmala S (2011) Hot electron-induced electrogenerated chemiluminescence. In: Reviews in fluorescence 2009. Springer: New York, pp 47–73
Taitt CR, Anderson GP, Ligler FS (2005) Evanescent wave fluorescence biosensors. Biosens Bioelectron 20(12):2470–2487
Tang Y, Su Y, Yang N, Zhang L, Lv Y (2014) Carbon nitride quantum dots: a novel chemiluminescence system for selective detection of free chlorine in water. Anal Chem 86(9):4528–4535
Thorek DL, Robertson R, Bacchus WA, Hahn J, Rothberg J, Beattie BJ, Grimm J (2012) Cerenkov imaging-a new modality for molecular imaging. Am J Nucl Med Mol Imaging 2(2):163
Tokuyama H, Nakamura M (2005) Acceleration of reaction by microwave irradiation. J Synth Org Chem Jpn 63(5):523–538
Tovmachenko OG, Graf C, van den Heuvel DJ, van Blaaderen A, Gerritsen HC (2006) Fluorescence enhancement by metal-core/silica-shell nanoparticles. Adv Mater 18(1):91–95
Venkatanarayanan A, Crowley K, Lestini E, Keyes TE, Rusling JF, Forster RJ (2012) High sensitivity carbon nanotube based electrochemiluminescence sensor array. Biosens Bioelectron 31(1):233–239
Wang Z, Li J, Liu B, Hu J, Yao X, Li J (2005) Chemiluminescence of CdTe nanocrystals induced by direct chemical oxidation and its size-dependent and surfactant-sensitized effect. J Phys Chem B 109(49):23304–23311
Webster S, Fu J, Padilha LA, Przhonska OV, Hagan DJ, Van Stryland EW, Bondar MV, Slominsky YL, Kachkovski AD (2008) Comparison of nonlinear absorption in three similar dyes: polymethine, squaraine and tetraone. Chem Phys 348(1):143–151
Werner CF, Yoshinobu T, Miyamoto K-I, Schoening MJ, Wagner T (2014) Semiconductor-based sensors for imaging of chemical processes. In: Sensors and measuring systems 2014; 17. ITG/GMA Symposium; Proceedings of, 2014. VDE, pp 1–5
Wu C, Szymanski C, Cain Z, McNeill J (2007) Conjugated polymer dots for multiphoton fluorescence imaging. J Am Chem Soc 129(43):12904–12905
Wu C, Bronder T, Poghossian A, Werner CF (2014) Schoening MJ DNA-hybridization detection using light-addressable potentiometric sensor modified with gold layer. In: Sensors and measuring systems 2014; 17. ITG/GMA Symposium; Proceedings of, 2014a. VDE, pp 1–4
Wu N, Dacres H, Anderson A, Trowell SC, Zhu Y (2014b) Comparison of static and microfluidic protease assays using modified bioluminescence resonance energy transfer chemistry. PLoS One 9(2), e88399

Xiao-Hong Z, Lan-Hua L, Wei-Qi X, Bao-Dong S, Jian-Wu S, Miao H, Han-Chang S (2014) A reusable evanescent wave immunosensor for highly sensitive detection of bisphenol a in water samples. Sci Rep 4:4572. doi:10.1038/srep04572

Xie X, He X, Song Z (2007) A sensitive chemiluminescence procedure for the determination of carbon monoxide with myoglobin-luminol chemiluminescence system. Appl Spectrosc 61(7):706–710

Xu SL, Cui H (2007) Luminol chemiluminescence catalysed by colloidal platinum nanoparticles. Luminescence 22(2):77–87

Xu Y, Piston DW, Johnson CH (1999) A bioluminescence resonance energy transfer (BRET) system: application to interacting circadian clock proteins. Proc Natl Acad Sci U S A 96(1):151–156

Xu Y, Cai H, Liu QJ, Qin LF, Wang LJ, Wang P (2006) A novel structure of LAPS array for cell-based biosensor. Rare Metal Mater Eng 35:51–54

Yagai S, Kinoshita T, Higashi M, Kishikawa K, Nakanishi T, Karatsu T, Kitamura A (2007) Diversification of self-organized architectures in supramolecular dye assemblies. J Am Chem Soc 129(43):13277–13287

Yakovleva J, Davidsson R, Bengtsson M, Laurell T, Emneus J (2003) Microfluidic enzyme immunosensors with immobilised protein A and G using chemiluminescence detection. Biosens Bioelectron 19(1):21–34

Yashchuk VM, Gusak VV, Drnytruk IM, Prokopets VM, Kudrya VY, Losytskyy MY, Tokar VP, Gumenyuk YO, Yarmoluk SM, Kovalska VB, Balanda AO, Kryvorotenko DV (2007) Two-photon excited luminescent styryl dyes as probes for the DNA detection and imaging. Photostability and phototoxic influence on DNA. Mol Cryst Liq Cryst 467:325–338

Yguerabide J, Yguerabide EE (1998) Light-scattering submicroscopic particles as highly fluorescent analogs and their use as tracer labels in clinical and biological applications – II. Experimental characterization. Anal Biochem 262(2):157–176

Yoshinobu T, Iwasaki H, Ui Y, Furuichi K, Ermolenko Y, Mourzina Y, Wagner T, Nather N, Schoning MJ (2005) The light-addressable potentiometric sensor for multi-ion sensing and imaging. Methods 37(1):94–102

Zhang S, Zhang Z, Shi W, Eremin SA, Shen J (2006a) Development of a chemiluminescent ELISA for determining chloramphenicol in chicken muscle. J Agric Food Chem 54(16):5718–5722

Zhang YX, Aslan K, Previte MJR, Malyn SN, Geddes CD (2006b) Metal-enhanced phosphorescence: Interpretation in terms of triplet-coupled radiating plasmons. J Phys Chem B 110(49):25108–25114

Zhang YX, Aslan K, Previte MJR, Geddes CD (2007) Metal-enhanced superoxide generation: a consequence of plasmon-enhanced triplet yields. Appl Phys Lett 91(2):023114

Zhang W, Zhao Y, Ha D, Cai W, Wang P (2012) Light-addressable potentiometric sensor based on precise light intensity modulation for eliminating measurement error caused by light source. Sensors and Actuators A: Physical 185(0):139–144. doi: http://dx.doi.org/10.1016/j.sna.2012.07.012

Zu YB, Ding ZF, Zhou JF, Lee YM, Bard AJ (2001) Scanning optical microscopy with an electrogenerated chemiluminescent light source at a nanometer tip. Anal Chem 73(10):2153–2156

Chapter 11
The Sensing Devices

In order to be analyzed, the signal from fluorescence reporter should be first generated by optical or other means and then detected by designed instrumentation. In this Chapter we concentrate on different types of instruments that are used in fluorescence sensing. Some of them are universal (e.g. steady-state and time-resolved spectrofluorimeters) and others (e.g. spotted microarrays and their readers) are specialized on obtaining very limited information on a large number of samples simultaneously. Depending on the purpose, different light sources and detectors can be selected, and the general trend is to decrease in power voltage and achieve miniaturization. Optical waveguides and optodes become increasingly popular. For sensing multiple analytes the choice between spotted and suspension microarrays can be made in view of different instrumentation required. We overview microfluidic devices that may couple sensor response with different reagent supply and chemical transformations and may host as biosensors the whole living cells. Optimizing convenience, sensitivity and precision for obtaining the proper sensor is the subject that will be finally discussed.

The sensor technique should optimally satisfy the requirements of selectivity, sensitivity, stability and, often preferably, convenience in performance. In addition, measurements in kinetic regime, scanning the image of nano-structured material or living cell or simultaneous detection of hundreds and thousands of analytes put additional requirements on instrumentation and on its versatility. Because of innumerable amount of potential targets and inestimable variety of experimental conditions in which the measurements have to be made, no single solution could exist regarding assay format and proper instrumentation. In Fig. 11.1 several formats that are the most frequently used in fluorescence sensing technologies are depicted.

Cuvette-type spectroscopy in solutions is applicable to any homogeneous assay, it allows recording of all possible fluorescence parameters and applicable for polarization and time-resolved measurements. It allows achieving the highest possible

A.P. Demchenko, *Introduction to Fluorescence Sensing*,
DOI 10.1007/978-3-319-20780-3_11

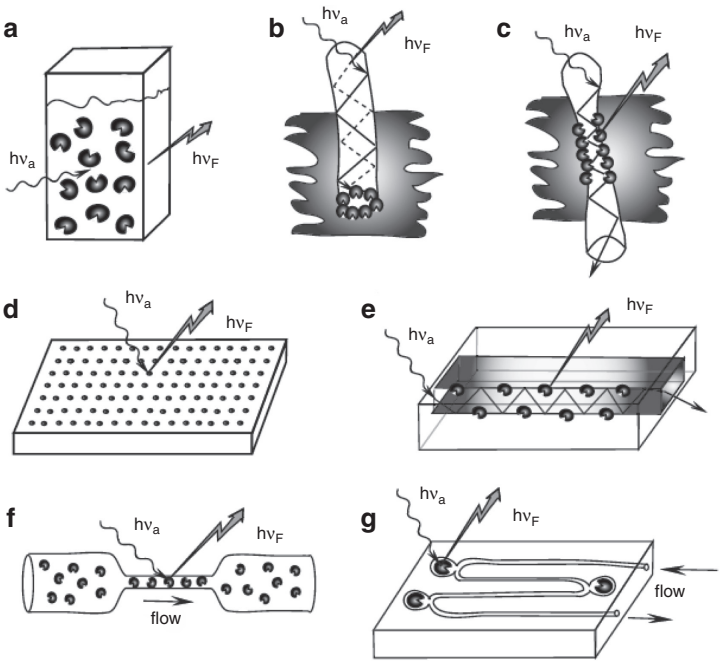

Fig. 11.1 Different instrument formats that are frequently used in fluorescence sensing. (**a**) Sensing in a spectrofluorimeter cuvette. The most precise technique that needs large amount of sample. The samples are detected one by one. The flow-through detection is possible. (**b**) Optical waveguides in tip configuration. Both the light source and fluorescence detection unit operate at a distal terminal of waveguide. (**c**) Optical fiber sensor utilizing the evanescent wave excitation and collection of fluorescence signal outside the fiber. (**d**) Flat supported microarray. It allows attachment of a number of different sensor units. Scanning the excitation beam allows read-out of fluorescence. (**e**) Planar optical waveguide. Miniaturized sample-saving technique that allows efficient collection of out-the-waveguide fluorescence. (**f**) Microsphere-based array. Sensor units are attached to micro-beads that are detected one by one passing through a narrow capillary. (**g**) Microfluidic device. Fabricated microscopic channels and reservoirs allow in addition to sensing the preparations of sample (separations, reagent additions)

spectral resolution sensitivity but requires large amount of sample and does not allow spatial resolution (recording of images) or simultaneous detection of a large number of samples.

Cuvette format does not satisfy the requests of many applications in sensing. Therefore, many efforts have been made for miniaturization of fluorescence sensing techniques, which became the leading topic of technology development over last decade. Various *lab-on-a-chip* techniques have been developed (Vinet et al. 2002). They allowed solving in a consistent way the problems of miniaturization, integration and systematization of various sensor types with the possibility to apply modern technologies of micro-fabrication. A variety of pocket-size lab-on-a-chip instruments have appeared (Gardeniers and van den Berg 2004), they started to occupy strong positions in practical use. Their development strongly follows the tendency of *multi-parameter* and *multi-analyte* monitoring in parallel. The use of

nanoliter plates became possible, resulting in reduced sample volume and reduced amount of necessary reagents together with improvement of detection technique.

11.1 Instrumentation for Fluorescence Spectroscopy

In this Section we will provide a short description of optical elements that are used in conventional instrumentation and that are needed for the development of miniaturized devices. A more detailed information about them can be found in the textbooks and reviews (Bacon et al. 2004; Lakowicz 2006; Valeur 2002). Their miniaturization and adaptation to the need of sensor applications will be in the main focus. The sources of error peculiar to fluorescence and suited fluorescence standards are well described in the literature (Resch-Genger et al. 2005).

11.1.1 Standard Spectrofluorimeter

Cuvette-type fluorescence detection is commonly provided using standard fluorimeter described in Fig. 11.2. It is usually equipped with excitation and emission monochromators that allow easy setting of excitation and emission wavelengths

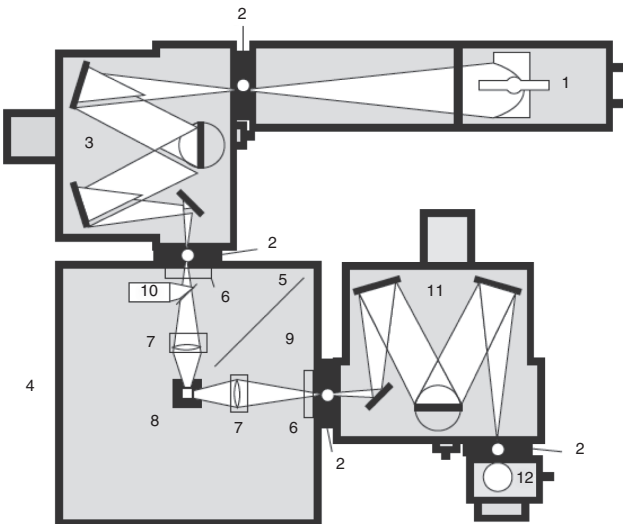

Fig. 11.2 Schematics of conventional spectrofluorimeter. The light emitted by light source *1* with continuous spectrum illuminates via slit *2* the monochromator *3* that enters the sample chamber *4* with inner space *5* and passing through polarizer *6* is focused with lens *7* on cuvette *8*. Emission light passing through similar optical elements *9* enters monochromator *11* , where after decomposition into spectrum it is recorded by photomultiplier tube *12*. Many instruments use the reference channel with photodetector 10 to compensate the fluctuations in intensity of the light source

and scanning them for obtaining the spectra. Polarizers placed in excitation and emission beams allow recording the spectra at horizontal and vertical polarizations and measurement of anisotropy.

These instruments use the *cuvettes* for liquid samples from 4 ml down to 0.04 ml. Though different samplers for automatic cuvette filling can be used with them, the samples are measured one by one or in a flow of one sample with a rather low productivity. Thus, these versatile and high-precision instruments are needed mostly for sensor development but not for routine sensing itself.

The *microplate readers* used for scanning the spotted arrays are built based on the same schematics as spectrofluorimeters, but with some modifications. The difference is mostly in geometry of incidence and fluorescence beams. The microplate (e.g. array) is located horizontally. The incident beam illuminates the plate from the top, allowing its scanning in $\boldsymbol{x}$ and $\boldsymbol{y}$ directions. The emission light is also collected from the top by using a special mirror that directs it to emission monochromator or, through the filter, to the detector.

Miniaturization and simplification of such instruments may occur in many directions. Simplified instruments may contain instead of monochromators the wavelength-selective optical filters on excitation and emission beams and also miniaturized and economical light sources and light detectors. The size of the sample chamber can be dramatically reduced and, as we will see below, substituted with an optical waveguide.

11.1.2 Light Sources

The fluorescence reporter is commonly excited by light, therefore the light source is a necessary part of spectroscopic instrumentation (luminescence excited by electric field and in chemical reactions is discussed in Chap. 10). There may be different requirements for the light source dictated by the methods of observation of response. Often a spectral resolution is needed, which can be provided by light source itself (producing monochromatic light) or by a lamp with broad-band spectrum with the aid of additional optical devices (monochromators and filters). Pulsed or frequency-modulated excitation is commonly used for the time-resolved measurements, and polarized light is needed for detection in anisotropy. Spectral, temporal or polarization resolution (or combination of them) is used for reducing background signal and reducing light-scattering effects.

The requirements for the light sources may be varied, but all of them have to provide a basic function of delivering sufficient radiant energy at a particular wavelength or in the wavelength range of interest. They must maintain a constant or regulated light intensity over the whole time interval of measurement. This requires keeping a working balance between the intensity and degree of *monochromaticity*. Additional requirement for collimation, polarization, rejection of stray light, etc.

Table 11.1 Lasers that are frequently used as light sources

Laser	Abbreviation	Operation wavelengths, nm	Operation mode
Nitrogen	N_2	337	Pulsed
Argon	Ar^+	351, 364, 454, 458, 488, 514	CW
Titanium-Sapphire	Ti-Sapphire	650–1100	Pulsed, quasi-CW
Helium-Neon	He-Ne	543, 1150	CW
He-Cadmium	He-Cd	325, 441, 563	CW
Diode-Blu-ray	GaN	405	CW
Diode-green	(Pointer)	515–520	CW
Diode-red	(DVD)	650	CW
Diode-near-IR	(CD)	780	CW

should also be accounted. Lasers are the light sources that satisfy ideally the requirement of monochromaticity (Table 11.1).

Lasers operate in continuous wave (CW) and pulsed modes. Also quasi-CW operation is known. Pulsed mode may be realized by various methods as Q-switching, mode-locking, pulsed pumping (Allen 2013). Pulsed solid-state lasers and wavelength-tunable dye lasers made a strong contribution to spectroscopy. Now there came the era of semiconductor lasers. Their small size and simplicity of maintenance is just what is needed for sensor technologies.

With the rapid decrease of price for instrumentation, the *time-resolved detection* methods gain a lot of popularity. The power of this technique lies mainly in its important features allowing discriminating the scattered light and most of background emission. Lasers for picosecond-nanosecond time-resolved spectroscopy should meet the following requirements. Pulse duration should be short compared to lifetime τ_F. This can allow achieving high time resolution in fluorescence signal. Meantime the time span between the pulses should be at least several times longer than the lifetime; this is because the new pulse has to arrive only when the system returns to the ground state after excitation by previous pulse. 50–100 MHz is a reasonable compromise for common fluorescent dyes. If the long-living emission in microsecond-millisecond time range has to be observed (such as of lanthanide chelates, phosphorescent dyes and metalloporphyrin labels) the same principle should be maintained but on a much longer time scale, so the economical pulsed lamps can be used in this case.

Lasers for *two-photon microscopy* in addition to these requirements should possess high peak power for providing high instant photon density (since two-photon excitation depends as a square power of intensity) and low average power to prevent thermal damage. Since the image is scanned point-by-point, sufficient number of laser pulses should be provided at every point for collecting enough number of emission quanta. Therefore, for most practical situations the femtosecond pulse laser with pulse duration of 100–200 fs may be the best (but expensive) choice. The mode-locked Ti:sapphire lasers became very popular in this application. Neodymium-based systems excited by laser diodes have recently become their strong competitors; the latter are more reliable and much simpler in adjustment. For

two-photon excitation of the dyes excited by visible light the laser light must be about twice (with some deviations) the wavelength of the one-photon peak absorption, roughly 700–1200 nm.

Regarding miniaturization, gallium arsenide-based vertical-cavity surface-emitting lasers (VCSELs) can be considered as optimal excitation sources, but presently they are developed into mature and reliable devices only for the near-IR region (850 nm and longer). The VCSEL chip is small ($0.3 \times 0.3 \times 0.1$ mm), requires only one-tenth of the operating current of edge-emitting lasers, can operate in pulsed (<1 ns) regime providing high peak intensity at low-power operation and does not require cooling.

A revolutionary change in fluorescence sensing instrumentation comes with the development of semiconductor *light emitting diodes* (LEDs) that can be miniaturized to occupy millimeter dimensions and feature reduced power of operation (Moe et al. 2005). They can efficiently provide electrical power conversion into monochromatic (bandwidth of tens of nanometers) visible or IR light emission. The reverse process, the electrical power generation upon their illumination, is also possible, which allows using them not only as the light sources but also as the light detectors. The findings that materials with such properties can be made not only of inorganic semiconductors but also of organic polymers (Samuel and Turnbull 2007), opened the way for their easy and inexpensive fabrication. With their use, the whole spectrofluorimeter attains pocket-size dimension. Because of much wider emission bandwidth and inferior beam quality, the LEDs are not very competitive with the lasers in spectroscopic instrumentation, but their apparent merits pose them as the light sources of choice in different sensor devices (Dasgupta et al. 2003), including those using time-resolved fluorescence detection (Liu et al. 2004).

A critical issue in miniaturization of light source is its power supply unit. Recently it was suggested to avoid it totally by using the energy of radioactive decay. The light source can be the *plastic scintillator*, in which the light is produced by β-particles generated in radioactive decay of ^{90}Sr (Holthoff et al. 2005). With the lifetime of isotope ^{90}Sr of 28.5 years, these light sources can shine with no external supply of energy, being almost eternal on the scale of our lives.

11.1.3 Light Detectors

Photodetectors convert the energy of light to electrical signal that can be recorded in analog or digital form. Their response should be a linear function of light intensity over at least several orders of magnitude. An adequate *signal-to-noise* (S/N) ratio should also be maintained. In fluorescence spectroscopy quantum light detectors are used which are characterized by the *quantum efficiency* (QE), which is the intrinsic ability of a detector to convert photons into electrons. It is expressed as the ratio of number of generated electrons to number of incident photons in percent. In the case where all other detector characteristics are equal, the detector with the highest QE possible is the best choice.

Presently, in addition to vacuum photocathode devices, such as *photomultiplier tubes* (PMT), there appeared a number of different types of semiconductor photodetectors. In general, vacuum technology being superior in absolute sensitivity and in low noise level shows its limitations in terms of size, operating voltage and robustness. Therefore, in an attempt to decrease the size and cost of instrumentation, the PMTs become presently more and more substituted by new semiconductor photodetectors, such as *photodiodes* (Yotter and Wilson 2003).

In *vacuum devices*, the photons are incident on an active region of photocathode, and this triggers the flow of electrons, which is amplified in several cascade steps. The number of photoelectrons is less than the number of incident photons by the factor QE that for the best photocathodes may exceed 45 %. These devices can be used both for detection of slowly varying and pulsed light fluxes. PMTs can operate along analog and digital modes of processing the output signal. Analog modes are based on measurement of the output current and are frequently used for detection of relatively high light levels. When the incident light is modulated, the alternative current mode extracts only the alternative current component.

For detecting very weak light the most effective is so called *single-photon counting* mode. This is an inherently digital mode based on counting the output current pulses initiated by photoelectrons released from photocathode. Each single photoelectron produces at the PMT output a single pulse. Since the quantum efficiency is always less than unity (100 %), the average number of photoelectrons is always less than the average number of incident photons. Therefore, this mode of the PMT operation should be called the single photoelectron counting mode. Noise level of PMT operating in any mode can be decreased by cooling.

In microchannel plate photomultipliers, which are the PMT versions, the electrons from photocathode pass through a narrow semi-conductive channel. Multiple secondary electrons are generated when they hit the channel, and this can happen many times with an avalanche effect producing a gain exceeding 10^8. However, these devices are expensive and need a very high operating voltage of 2400–3000 V, which, together with their high cost, limits their application in miniaturized schemes.

The *solid-state semiconductor devices* use a different principle, a photon-induced electron–hole pair generation in semiconductor material. When the energy of absorbed photon is large enough to raise an electron from the valence band to a conduction band, they create positive charges, 'holes', in the valence band. The applied electric field by separating the electrons and holes produces the electric current that is proportional to photon flux. The small size and low voltage requirement makes these detectors preferable in all cases of steady-state fluorescence measurements where light intensity may be high enough and a high precision of the measurement is not needed.

The low sensitivity of photodiodes is due to the fact that no amplification or any other gain mechanism is implied in their operation. The certain gain mechanism can be realized only in the so-called '*avalanche photodiodes*' (APD). These devices operate in a mode similar to Geiger counter. When a bias above the diode breakdown voltage is applied, no current follows until a photon generates a photoelectron that causes a so-called avalanche breakdown and an appearance of large current. Then the bias across the diode is reduced to terminate the current and is re-started again to

count another photon. Therefore, these devices can operate in a single photon counting mode. They allow low-voltage operation (on the level of 30–40 V), which allows miniaturization of the whole system leading to such applications as even the implantation of integrated wireless sensor into a human body.

Other silicon-based detectors, such as PIN (*p-i-n*) photodiodes can be made as small as thin films. Meantime, they are not sensitive enough for use with low-power light sources and faint fluorescence emission. For improvement of PIN photodiodes a signal processing algorithm called as 'lock-in amplification' was developed (Tung et al. 2004), and with this improvement they provide at least equally high signal-to-noise ratios as a PMT without signal processing.

A two-dimensional matrix of detectors is needed to produce an image. For *fluorescence imaging* the currently available instrumentation is based on one of two principles. One involves laser scanning and detection with PMT, and the other – the combination of lamp for excitation and *charge-coupled device* (CCD) for detection (Spibey et al. 2001). The latter possibility is preferable when the multi-color applications require variations in excitation wavelength. Charge-coupled device sensors in the form of cameras and array detectors are explored in many applications. They exhibit low noise, broad spectral range and linearity of response over many orders of magnitude. They can be interfaced directly to the computer. Such intensified and electron-multiplying CCD-based devices are meantime expensive, bulky and requiring cooling. Therefore, their application areas are mainly limited to basic research.

The *complementary metal-oxide-semiconductor* (CMOS) imagers have recently reached the level of CCD performance being much cheaper and more convenient in use. Their rapid development was stimulated by mass production of digital cameras and smartphones. They offer superior integration, power dissipation and system size making them a natural fit for different handheld devices with wireless capability. The productive but very inexpensive spectrofluorimeters (Yu et al. 2014), Fig. 11.3,

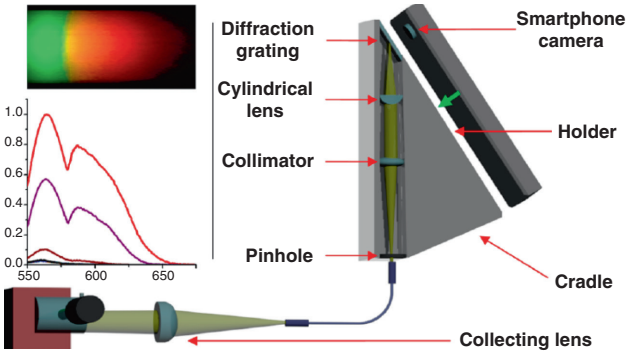

Fig. 11.3 A high resolution and sensitive fluorescence spectrometer based on a conventional smartphone (Yu et al. 2014). Using a simple interface its internal camera functions as an imaging detector. By placing a transmission diffraction grating directly in front of the camera, along with optics for collimating light emitted from a liquid fluorescent sample onto the grating, an emission spectrum is distributed across the pixels of a CMOS imager

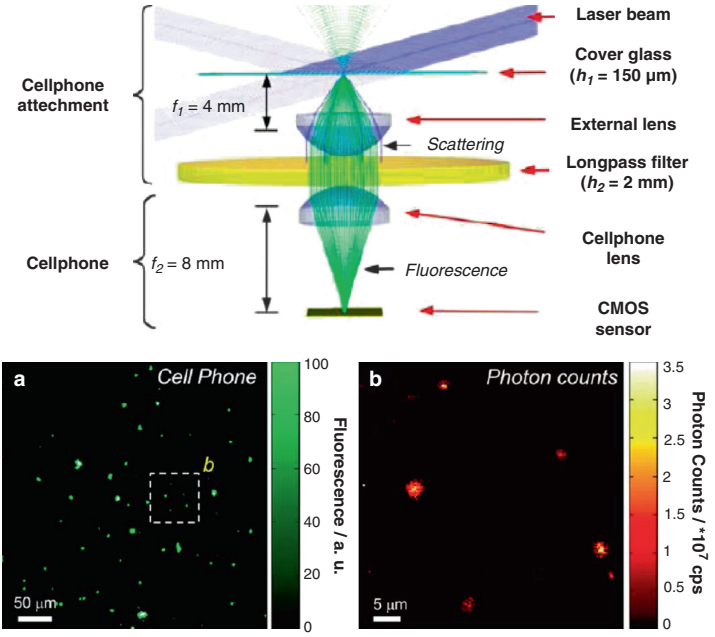

Fig. 11.4 The cellphone-based fluorescence microscope (Wei et al. 2013). In a ray-tracing diagram the excitation and scattered beams are indicated with solid blue rays, while the fluorescent emission is highlighted with solid green rays. Below: (**a**) fluorescent image of labeled virus particles and (**b**) photon-counting map corresponding to the dashed area in (**a**)

fluorescence imaging (Andreou et al. 2011) and time-resolved (Guo and Sonkusale 2011) systems have been suggested using smartphones or their CMOS matrices as detector units.

Constructing a microscope of very simple design (Fig. 11.4), such sensitivity and spatial resolution can be achieved that even single viruses can be detected (Wei et al. 2013).

Concluding, there exist a variety of detectors for light quanta satisfying very different needs. Photodiodes are the simplest, cheapest elements that can be incorporated into any analytical system. If higher sensitivity coupled with low noise is needed, one has to choose photomultiplier, but the advantages of photodiodes will be definitely lost. CCD cameras and CMOS imagers add the potential of spatial and spectral resolution that is required in many applications.

11.1.4 Passive Optical Elements

Light sources and light detectors are traditionally called active optics. In contrast, mirrors, lenses, optical filters and waveguides belong to passive optics. *Mirrors and lenses* improve the detection by focusing the light in the desired illumination

volume. So do *planar waveguides* that can also allow beam splitting in the emission channel for multi-wavelength detection in combination with optical filters.

Precisely polished quartz lenses are commonly used in bench-top instrumentation. Fabrication of plastics allowed to reduce their cost and also to allow their fitting to miniaturized sensor devices. Their fabrication directly into a glass chip allowed substituting a microscope (Roulet et al. 2002).

Optical fibers and waveguides are often much more convenient to use than the traditional lens systems, since they allow extending the possibilities of realizing different instrument configurations (Monro et al. 2001). *Optical fibers* are preferable for measurements at a distance from analytical instrumentation, e.g. in aggressive media, for providing connection between sensor tip and an instrument and waveguides – in miniaturized systems. Both operate on the principle of total internal reflection generating evanescent wave (see Sect. 10.6).

Optical waveguides became very important integrating elements that allow miniaturization of all instrumentation. Such integration may include miniature light sources and detectors to produce microfluidic devices, in which all optical elements can be aligned during fabrication. They may also serve as miniature support materials for immobilization of sensor molecules on their surfaces. Fabricated microlenses can be located on top of optical waveguides for providing optimal light collection.

The application of *organic polymers* as materials for all passive optical elements used for various coupling, routing and filtering applications became widespread. With their aid, many different instrument configurations have become possible (Sadana and Ramakrishnan 2002). Inorganic materials such as oxidized porous silicon can also be used with a great success (Mogensen et al. 2004). These new materials prove to be powerful basic building blocks for constructing miniature sensor modules. They can be fabricated in automated low-cost processes such as replication and thin-film deposition.

In miniaturized devices it is especially important to optimize all elements of optical train including emission filters (Dandin et al. 2007). In the process of optimizing the detection by removing the interfering light contributions, they should not remove a significant portion of a light signal.

11.1.5 Integrated Systems

The sensor devices for many practical applications should be produced in mass. They should be different from analytical instrumentation used in research labs with respect to compactness, convenience of use and the price. Miniaturization of all optical elements, their fabrication from inexpensive materials and in the form of integrated units are the present tendencies in instrument design. Therefore, the emerging generation of fluorescence sensors vaguely resembles the spectrofluorimeter depicted in Fig. 11.2. Miniaturization and application of direct contact between optical elements changes dramatically these instruments, though maintaining the

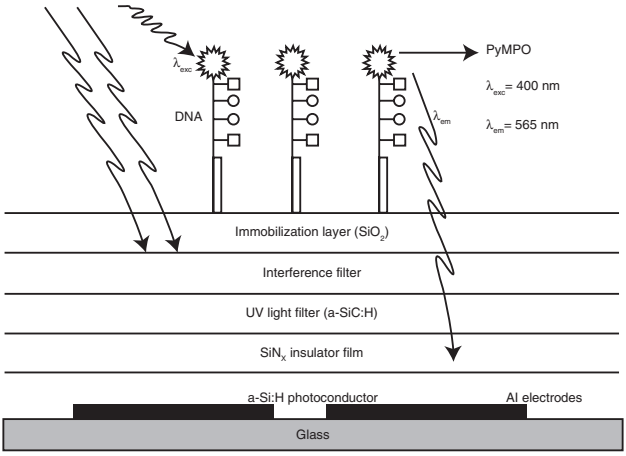

Fig. 11.5 Sensor unit based on on-chip thin film amorphous silicon photodetector for the quantification of hybridized DNA (Fixe et al. 2004). Schematic diagram showing assembly of layers. The unit integrates the target (DNA labeled with PyMPO dye) binding with the detection of its fluorescence using a-Si:H semiconductor thin film detector via the thin-film cut-off and interference optical filters transmitting only the emission light

basic function of exciting the sample with monochromatic light and detecting often spatially resolved and monochromatic emission.

An example is one of these developments, in which the target binding to sensor molecules attached to immobilization layer results in detection provided by a thin film detector via thin films serving as the optical filters (Fig. 11.5). Such systems allow excluding the necessity of out-of-chip data acquisition (Fixe et al. 2004).

Such dramatic miniaturization occurs not without the loss of absolute sensitivity. Maintaining high absolute sensitivity and high signal-to-noise ratio is the general requirement that should be observed. A productive idea for realizing that is to use on the level of detection a discrimination of non-random statistics given by the useful signal and the random signal produced by the noise (Mogensen et al. 2004).

11.1.6 Prospects

In contrast to classical spectroscopic instrumentation, the miniaturized integrated sensor devices evolve with a tremendous rate. The basic scheme of a spectrofluorimeter will probably remain for some time in the background of future devices, but the most significant changes will occur with these elements themselves. These devices can be fabricated by standard semiconductor and polymer technologies, be of a very small size and operate at low voltages. A variety of sensor configurations performing these functions is possible by selection in the diversity of optical and electronic elements and using them as the construction blocks. By combining such functions as power supply, excitation, focusing, filtering, detection, signal

processing and communication in the small integrated units, the price of these instruments will go down and the application areas will become unobservable broad. It is expected that both the light sources and the detectors will be fabricated based on semiconductor technology and all other elements, such as filters, gratings and lenses, will be deposited during the fabrication. This will move optical instrumentation from bench-top through lap-top to finger-top size. The latter is already achieved in pioneering works.

Still further miniaturization of devices will need the development of new tools and their association for manipulating and controlling the light onto very small areas (Monat et al. 2007). They may involve application of photonic crystals and with their aid the light paths can be confined to sub-wavelength scale. The novel optical nano-devices will provide the basic building blocks of completely new architectures and platforms that will have an impact on numerous applications.

11.2 Optical Waveguides and Optodes

The *fiber optics technology* has found important application in sensing for the delivery at a distance of excitation light, for acquisition of optical signal and for its coupling with the detection system. These techniques develop rapidly being stimulated by the progress in optical telecommunications. In both cases, transmission of optical signal along the fiber can occur without losses, if necessary, to hundreds and thousands kilometers.

The light travels along the cores of optical waveguides almost without losses because of *total internal reflection*. Total reflection occurs at an interface of two optical media when the index of refraction of the outer medium is smaller than the index of refraction of the core (see Sect. 10.6). Fluorescence sensing technology benefits from using the fibers ranging in length from centimeters to hundreds of meters. The property of light beams is such that they do not interact and do not interfere with each other if they propagate in the same or opposite directions. This is a great advantage of optical waveguides over electrical circuits, in which such independence is not possible to achieve.

Transmission properties of the fibers are known to be wavelength-dependent. Presently most of the fibers are made of inexpensive materials plastic and silica; their transparency range occupies the whole visible and near-IR part of the spectrum. Since optical fibers transmit the light of different colors and lifetimes independently, this allows using the whole arsenal of fluorescence responses. In addition, the fiber optical sensing allows using the fibers as the platforms for *evanescent-wave detection*, thus providing essential enrichment to all sensing technology.

The *optical fiber sensing devices* are frequently applied in a continuous monitoring of different industrial processes and, on a more limited scale, in environmental monitoring of air and water quality (Bosch et al. 2007; Taitt et al. 2005). They are attractive for clinical diagnostics. Since they allow high degree of miniaturization and considerable geometric versatility, this makes them appealing both for the field

and for the point-of-care analyses. In industrial applications, they are particularly useful for making measurements in potentially hazardous, radioactive or explosive environments with the transfer of optical signal by the fibers for measurement at a safe distance.

Sensing with waveguides and classical measurements with spectrofluorimeter can employ the same principles. Moreover, it may use the same equipment, in which the delivery of excitation light 'by air' within the instrument is substituted by delivery in a waveguide from a distant 'probe'. Application of optical fibers and waveguides allows constructing the 'probes', in which the beam of excitation light is guided out from the instrument, provides distant target detection and then as a fluorescence response is guided in to reach the instrument for recording the signal.

Meantime, this is only one possibility out of many others. The waveguides can also perform in a way, in which common spectrofluorimetry can never operate. Assembled together the fibers can form optical arrays that are easily integrated with a multitude of different sensing schemes (Epstein and Walt 2003). These arrays can allow multiparametric analyte detection. Moreover, many of such sensors put together can form an image. Imaging fiber bundles comprised of thousands of fused optical fibers are the basis for an optically connected, individually addressable parallel sensing platform (Yagai et al. 2007).

11.2.1 Optical Fiber Sensors with Optode Tips

There are two major possibilities to use optical waveguides in sensing. One is to use the fiber terminal for attaching the sensor molecules that have to be excited by light through the waveguide and then produce emission signal that has to be returned by the same waveguide to the instrument detector. The other possibility is to use for excitation the sensor molecules or particles attached to the periphery of a waveguide for excitation by evanescent wave.

Optical fiber sensing instrument based on the first principle may consist of three main parts: (a) the probe called *optode* (see Fig. 11.6), which provides the fluorescence response by modulating the optical signal on target-sensor interaction; (b)

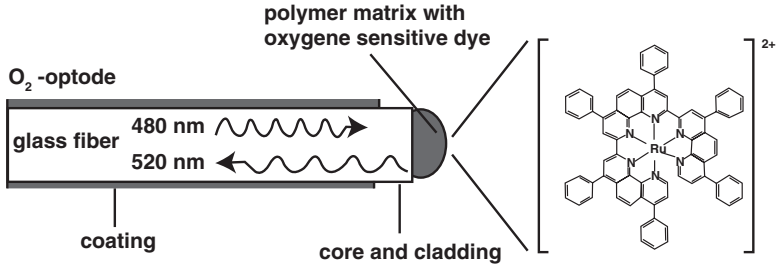

Fig. 11.6 Principle setup of fiber optic chemosensors (optodes) (Glindkamp et al. 2010). An example of pO_2–optode used in disposable bioreactors

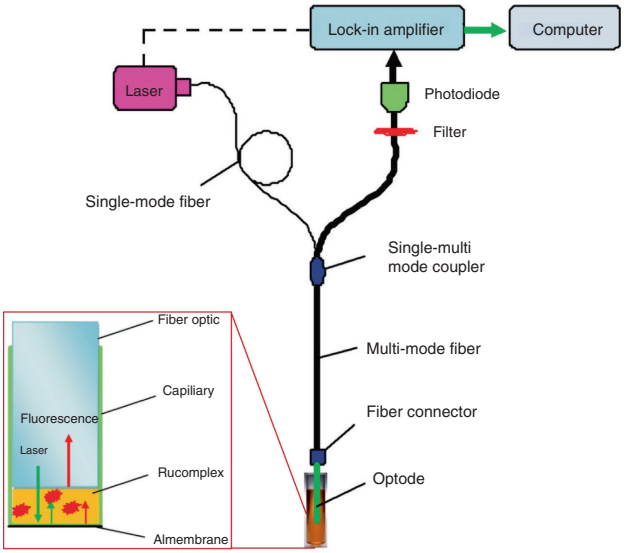

Fig. 11.7 Schematic diagram of the all-fiber structure based photoluminescence measurement system (Long and Shi 2014). For rapid and sensitive temperature detection in small volume samples (<5 μl), this system uses Ruthenium (II) complex as a temperature indicator. The luminescence intensity diminishes monotonically from 0 to 80 °C, and the response to temperature is rapid and completely reversible

an optical link (waveguide) that carries the optical signal from the instrument to the probe and vice versa and (c) an optoelectronic system that contains the hardware and software for interrogating the probe and for processing the signal. The light modulated by the optode and carried by the fiber should bring the information on the presence of target and allow its quantitative determination (Fig. 11.7).

It is easy to fabricate optode for sensing if the target analyte is fluorescent itself. In the case if the target molecules are optically silent, one has to develop the recognition process on optode tip that could involve fluorescence signal generation. In oxygen sensing (Fig. 11.6), for instance, this could be the decrease of intensity and lifetime on quenching by oxygen of long-lifetime luminescence reporter, in pH sensing – the change of spectra of attached acid–base fluorescence indicator and in temperature sensing (Fig. 11.7) – the effect of thermal quenching. In other cases, one has to use more complicated receptor-transducer-reporter combinations like those described in previous chapters of this book.

Optical fibers have been used to develop the sensors based on nucleic acids and cells (Brogan and Walt 2005). Sensors employing DNA probes have been developed for various genomics applications and microbial pathogen detection. Live cell-based sensors have enabled the monitoring of environmental toxins, and have been used for fundamental studies on populations of individual cells. Both single-core optical fiber sensors and optical fiber sensor arrays have been used for these purposes. Many original papers and reviews describe various applications of this technique in biosensing including the detection of enzymes, whole cells, antibodies, nucleic acids, and biomimetic polymers (Wang and Wolfbeis 2012).

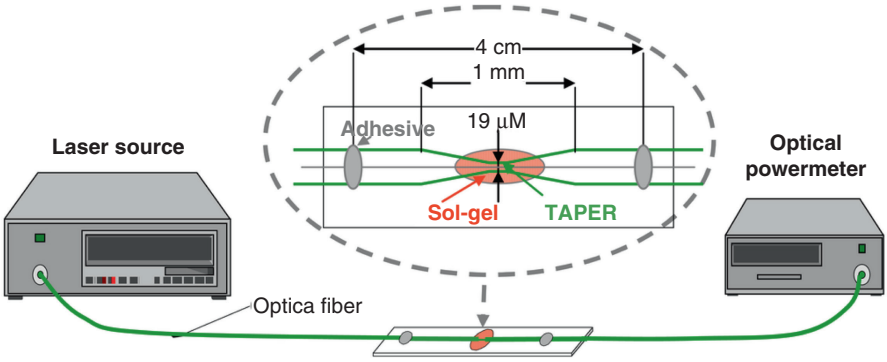

Fig. 11.8 Typical evanescent wave sensor working in transmissive setups using optical fiber as the sensor element (Elosua et al. 2006). Here the sensor is connected between the interrogating signal source and the detector, the sensing signal being based on the modulation of the light intensity

11.2.2 Evanescent-Field Waveguides

In addition to sensor devices based on optode tips, there are the devices that use a part of *optical fiber* (usually close to its distant end) as the sensing surface with the operation based on *evanescent-field* transduction (Fig. 11.8).

Due to evanescent field propagating out from the waveguide at a distance up to 100–200 nm, only the labeled molecules that are bound to the surface will be selectively excited. Tapered waveguide areas at its distant terminus can be used as the solid support for the proper sensors (Leung and Cavalieri 2003). It was shown that this technique works well in a sandwich configuration and can compete with traditional immunoassays. Decrease of fiber diameter (tapering) to the level of several microns increases dramatically the magnitude of evanescent field and therefore the sensitivity of assay. It can be stated that optical fiber-based sensors combine the use of a target recognition element with an optical fiber or optical fiber bundle. They can be used for a variety of analytes ranging from metals and chemicals to physiologically active materials (Monk and Walt 2004).

Similar in performance to optical fibers are the *waveguides of planar geometry* (Bradshaw et al. 2005). They are also based on evanescent wave excitation principle. Their advantage is that they can be easily fabricated in the form of thin films. Planar waveguides provide the possibility of immobilizing multiple capture biomolecules onto a single surface and therefore, offer the exciting prospect of multianalyte detection. They found important application in microfluidic devices, as we will see below (Sect. 11.5).

An ultimate sensitivity of optical waveguide sensing technique is achieved mainly due to the background signal suppression. It was reported (Plowman et al. 1999) on a construction of a dual-channel fluoroimmunoassay that was able to detect femtomolar (i.e. less than 1 part per trillion, w/w) target concentrations. It operated on etched channel silicon oxynitride thin-film impregnated optical waveguide that was tested both in direct (fluorescent-labeled protein binding to immobilized receptor) and sandwich-type assays.

Optical fiber-based techniques operate in a similar way with the planar waveguide sensors and in comparison with them they have certain advantages and disadvantages. Overall, they are flexible and light, easy to manipulate with ingoing and outgoing light, they can be operated from long distances and they are very cheap. On the other hand, due to their core-cladding geometry, it is difficult to access from outside the evanescent field, which is the main fiber parameter that is needed for sensing. One way to overcome this problem is to taper the fiber (reduce its diameter to few microns or less). Recently tapered fiber or silica nanowires have drawn great attention for sensing applications (Domachuk and Eggleton 2004). Due to their unique waveguiding properties, they have the potential to become the most sensitive waveguide sensors.

11.3 Multi-analyte Spotted Microarrays

Miniaturization is, of course, not the only aim in constructing new generations of sensors. Novel sensors can do much more – they can detect many analytes simultaneously, adapt to several analyte concentration ranges, provide multi-analyte comparison between the samples. For proceeding in depth with these tasks and correspondent devices, we have to introduce the principle of *multiplexing*. A system is defined as *multiplexed* if a number of sensing elements is larger than their possible number in the case of their individual operation (i.e. supplied individually by light sources, detectors, etc.). The sensors can be multiplexed by *location* (sensing the same target in different areas) or by *target* (sensing simultaneously different targets). A multiple spotting technique can be applied (Fig. 11.9). It allows for direct comparison of numerous different analytes on a single array.

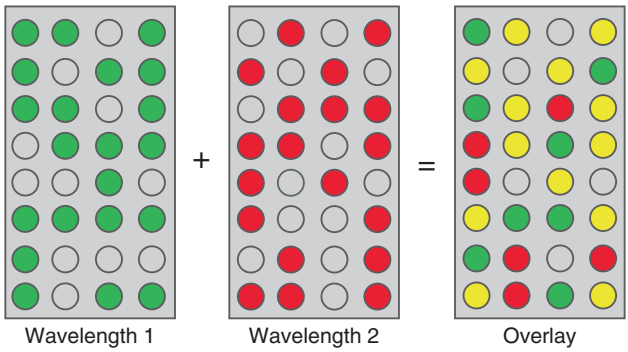

Fig. 11.9 Schematic representation of multicolor detection with planar spotted microarrays (Herbáth et al. 2014). The scanners are able to record fluorescence in 2 (or more) channels recording emission from species labeled with different dyes. Then the images can be overlaid for determining analytes that are simultaneously present in studied samples. Accordingly, the array before and after exposing to tested samples can be scanned for formation of difference image

Such multiplexed operation by location can be performed by microarrays. The *spotted microarrays* are the assemblies of a great number (hundreds and thousands) of sensor instruments in which every instrument is represented by a spot on a surface formed by the deposition of one type of sensor molecules or particles. The analyzed sample is exposed to whole microarray, so the binding of different targets to correspondent sensor instruments occurs in essentially the same conditions. The read-out of reporter signal is made using the specialized fluorescence microscope instruments – the *readers*.

In biosensing technologies the term '*spotted microarrays*' is often substituted with a term of much broader meaning, '*biochips*'. Biochips are highly miniaturized micro-scale analytical devices in detection of proteins and, mainly, nucleic acids exhibiting massive parallelism of function. The microarray technologies have become very popular in biosensing applications, and their development is stimulated by practical needs in genetic analysis (Dharmadi and Gonzalez 2004; Epstein and Butow 2000), detection of antigens and antibodies of different specificities (Luppa et al. 2001) and in drug discovery. The advantages of microarray technology are the miniaturization, reduction of volume of reagents and of reaction volume. Unified automated procedures can be applied to all steps of manipulation with the arrays.

11.3.1 Fabrication

Design and fabrication of microarrays requires operating with materials with great precision on the micrometer and even on the nanometer scale. The rapidly developing semiconductor and integrated circuit research and industry acquired a wealth of experience in nano-scale manipulations that can be successfully applied in sensing devices. In a recently published review (Blattler et al. 2006) the leading techniques for *generating nanopatterns* with biological recognition function are described. They include parallel techniques, such as extreme ultraviolet interference lithography, soft-lithographic techniques (e.g., replica molding and microcontact printing), nanoimprint lithography, nanosphere lithography (e.g., colloid lithography or colloidal block-copolymer micelle lithography). In addition, direct-writing techniques including e-beam lithography, focused ion-beam lithography and dip-pen nanolithography can be used.

Details on how the *nanopatterns* are generated, how the sensing function is imparted to these patterns and examples of how these surfaces can and are being used for immobilization of sensor molecules and particles can be found in different publications (Bally et al. 2006; Venkatasubbarao 2004). The support materials could be either glass or plastic, and of major importance is their surface chemistry. The methods of *sensor application* should allow optimal exposing of sensors to capture targets but also to minimize the non-specific adsorption of non-target components of the studied sample (Sobek et al. 2006). Following the progress in these activities one may observe that every step brings substantial progress in increasing

the spot density, by making them three-dimensional (using hydrogel support) and by increasing the sensitivity of response.

Microarray fabrication allows different possibilities for application of sensor molecules and nanoparticles. Deposition of oligonucleotides, PNA and peptides can be provided in two ways – by covalent attachment and by on-site synthesis (Venkatasubbarao 2004). In the latter case, growth of polymer chain occurs directly on the surface of glass support. Direct spotting is used for attachment of proteins and long-chain DNA. For DNA attachment, the slide surface can be modified with attachment of amino groups, and the DNA is kept bound by ionic interactions. Protein sensors (Romanov et al. 2014) are usually deposited on the array surface based on affinity interaction between biotin and streptavidin. Other partners for affinity coupling mentioned in Chap. 9 can be also of use.

11.3.2 Problems with Microarray Performance

The *spotted microarrays*, providing a powerful analytical tool for the simultaneous analyses of thousands of sensor responses in a single experiment, allow application of all fluorescence detection methods described in Chap. 3. Meantime, there appear many problems that are related to the sensitivity, accuracy, specificity and reproducibility of microarray results. These problems are of special concern when the technologies based on preliminary labeling of all components of analyzed sample are applied (Draghici et al. 2006). Since this is presently the dominant approach in DNA hybridization assay and alternative methods (such as molecular beacons) are introduced slowly into practice, there remains considerable uncertainty and skepticism regarding the data obtained using this technology (Wilkes et al. 2007).

Comparison of results of seemingly identical experiments from different laboratories or even from different days shows that their matching is not always satisfactory. Even stronger inconsistencies can be observed when the data from different array platforms are compared. For improving confidence in these data, optimization on every step of microarray performance and standardization of optimized procedures are needed.

In real systems, the concentrations of analyzed compounds vary in broad ranges. They may exceed in either direction the size of the analytical window determined by the binding constant, which is within two orders of magnitude (see Sect. 2.2). For covering an extended range of target concentrations a number of sensor units with the same specificity but different affinities can be constructed for analyzing every target. This has to increase the size of array. In addition, the attempts to extend the target detection to weaker affinities, with dissociation constant, K_d, lower than ~10^{-7} M, leads the detection methods to direct sensing, which requires establishing the dynamic equilibrium between free and bound analyte and limits the application of washing and other manipulations with the arrays.

A significant related problem arises from the fact that on target binding on microarrays the true *association-dissociation equilibrium* is not reached (Carletti et al. 2006). The characteristic time for DNA hybridization equilibrium, $t_{1/2}$, is 41 days

estimated for a target human genome. Similar hybridization times are expected for the whole-transcriptome chips hybridized with tissue DNA. These conditions are commonly not reached. Non-equilibrium binding introduces a stochastic factor into hybridization dynamics, and kinetic variables, such as differential diffusion rates of sample components, may influence the result.

Since the spotted sensor concentration and optical alignment to the spot readout may vary from sample to sample, the problem of *internal calibration* is of special importance for microarrays. Similar problems exist also in fluorescence imaging of the cells due to commonly observed spatial variation of intracellular sensor concentration and in flow cytometry, in which a commonly observed broad distribution of data is due to variations of cell volume and of the extent of fluorescence probe uptake. In all these cases the sensor (and reporter dye) concentration is variable (or unknown) and it can change in time.

Often the reporter dye responds not only to analyte binding but also to many other factors affecting its molecular environment due to unavoidable sensitivity of its emission to various parameters of physical and chemical origin. Therefore, it is not possible to provide the response only to analyte binding and achieve suppressing of all other influences. Because of that, the measured fluorescence intensities in microarrays may vary significantly and may not reflect the actual differences in target concentrations in analyzed samples.

The problem of *calibration of response signal* on arrays has been discussed (Demchenko 2005a, b) and it was shown (see Chap. 3) that different fluorescence sensing techniques are affected differently by these problems. Comparative analysis based on three important properties – insensitivity to instrumental factors, insensitivity to the amount/concentration of sensor molecules and insensitivity to intrinsic factors influencing the fluorescence, such as the fluorescence quenching, as given in Table 3.1, demonstrates convincing reasons for substituting intensity sensing by more advanced methods of detection. Internal calibration is possible with application of two dyes (with the reference in intensity sensing and with fluorescent acceptor in FRET) and with single dye in anisotropy and lifetime sensing. Meantime, the most efficient could be the application of single dye with wavelength-ratiometric response.

11.3.3 Read-Out and Data Analysis

Each member of the array (spot) is easily identified by its position in the ($\boldsymbol{x}$,$\boldsymbol{y}$) coordinate space, which can be done with microscope-based two-coordinate readers. The analysis of read-out information from microarrays is a non-trivial task because of large data size and of many levels of its variation introduced by different stages of experiments. Visually, it is very hard to analyze the array that consists of several tens of thousands of elements. The analysis can be further complicated by heterogeneity in response, for instance, by variations of affinities of sensors binding the same target (Elbs et al. 2007). Comparison of different data sets obtained at different time and with different instrumentation may appear even more difficult. Statistical analysis cannot improve the primary data; it can only suggest their most

probable interpretation. Therefore, the primary data have to be of the best quality, they should be as least affected by systematic and experimental errors as possible.

On the step of analysis, *different algorithms* can be applied with the correspondent software. Their description can be found in the literature (Leung and Cavalieri 2003). Some of them are rather complicated, but some are available to those users who do not have experience in programming. Such is the visual programming (Curk et al. 2005) that offers an intuitive means of combining known analysis and visualization methods into powerful applications. For a detailed description of different algorithms of analysis of microarray data (such as data filtering, hierarchical clustering, principal component analysis) the reader is advised to refer to a comprehensive review (Quackenbush 2001).

11.3.4 Applications of Spotted Microarrays

The applications of microarrays are well presented in other sections of this book, so here we will provide only their brief listing. The primary application this technology has found in *DNA hybridization assays*, where a comparative method based on simultaneous application of studied and control samples labeled with different dyes is commonly used (Dudley et al. 2002). Usually the whole-pool labeling is provided in these tests. In this respect, molecular beacons and tests using PNA and conjugated polymers have started to demonstrate their advantage mainly due to the absence of necessity to label the whole analyte pool.

Protein-detecting microarrays (Tomizaki et al. 2005; Pratsch et al. 2014) must produce an enormous impact on the functional analysis of cellular activity and regulation, especially at the level of protein expression and protein-protein interaction, and might become an invaluable tool in disease diagnostics. However, the biochemical diversity and the sheer number of proteins are such that an equivalent analysis is much more complex and thus difficult to accomplish (see Sect. 15.1 for more detail). Essentially, proteins do not demonstrate simple chemistry or uniformity of labeling, which requires the construction of microarrays based on different principles rather than the analyte pool labeling before application.

Microarrays based on *application of antibodies* (Fig. 11.10) have been applied for many purposes (Kusnezow et al. 2003; Herbáth et al. 2014). The antibodies exhibit strong competition from the side of other molecules and particles used for molecular recognition, of aptamers in particular (Collett et al. 2005).

Quantification of *protein-protein interactions* has become an easy task with the application of double labeling and recording FRET response in two-color sensor arrays (Schäferling and Nagl 2011), such as shown in Fig. 11.9. Extension of these studies to interactome level (Sect. 15.1) requires more effort in multiplexed assays, in which spotted microarrays play a leading role (Betzen et al. 2014).

Arrays for recognition and quantitative determination of *glycans* are very important instruments for revealing glycan functions that play an important role in intercellular communication, generating immune response, binding viruses (Rillahan and Paulson 2011). Series of glycan binding proteins, mostly lectins of plant origin, are actively used in constructing the microarrays addressing the functional *glycomics* area.

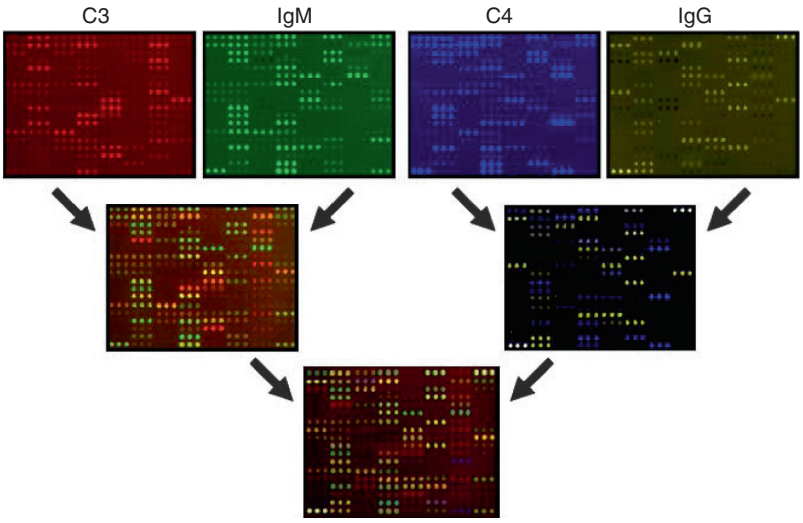

Fig. 11.10 An example of multiplex measurements based on overlay of four detection channels (Herbáth et al. 2014). Here the complement protein (*C3*, *C4*) and antibody (*IgM* and *IgG*) levels were analyzed simultaneously on antigen microarrays with triplicate measurements

Arrays possessing *small molecules* as recognition units (Hong et al. 2014) have been recently suggested as a tool for discovering protein–small molecule interactions (Fig. 11.11).

Such large-scale binding assays that involve different small organic molecules, peptides and glycans are used for providing high quality information from the direct

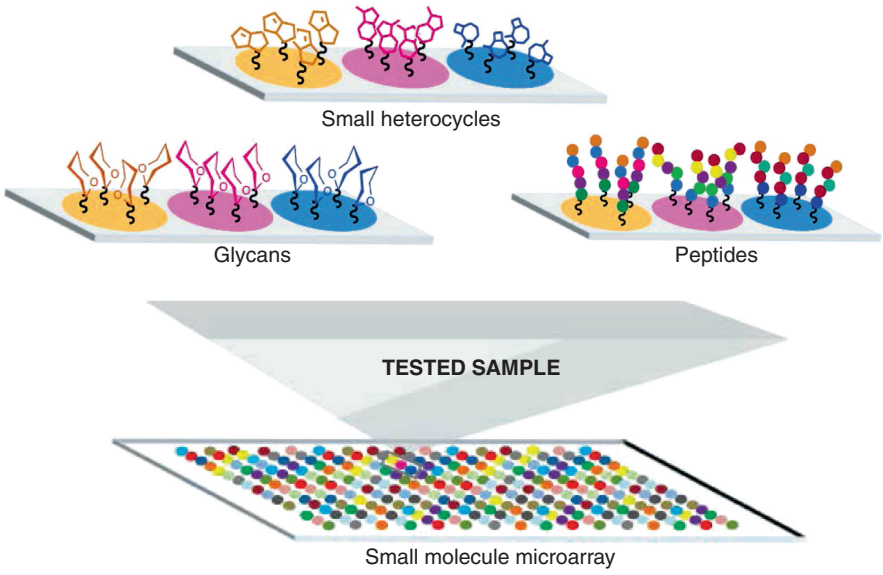

Fig. 11.11 Arrays of small molecules (heterocyclic compounds, glycans, peptides, etc.) recognizing protein targets and probing different sites on their surfaces

binding interaction between proteins of interest and a collection of small molecules in a high-throughput fashion. In order to project forward to possible areas in which such arrays could contribute, much effort has to be directed towards establishing the representative libraries of binders (Wu et al. 2011) and their deposition on arrays (Voskuhl et al. 2014). No less important is developing the most efficient response mechanism, which can be the λ-ratiometry of color-changing dyes (Demchenko 2005a).

11.3.5 Prospects

In the times less than a decade microarray technology made a tremendous progress in its development using actively the methods derived from microelectronics in combination with advanced synthetic chemistry. The *photolithography* is used for on-chip synthesis of highly dense arrays or pre-synthesized peptides and oligonucleotides. Alternatively, they are put down by *electronically addressed deposition*. Both approaches lead to densely located surface-exposed molecular sensor elements that could detect hundreds and thousands of targets simultaneously.

The power of array technology is in obtaining of such a huge number of information in the same conditions and (almost) simultaneously, that minimizes the systematic errors in their detection. Most of the recent applications of these devices are in DNA and RNA hybridization assays, in detection of antigens and antibodies and in drug discovery. They extend rapidly into the studies of *proteome* with the aim of construction of extended maps of protein-protein interactions, *interactome* (Sect. 15.1). The technique is expending into the areas of diagnostics, forensic analysis and monitoring the environment.

With this success, one has to take into account the weak points of this technology. Reading the microarrays requires bulky and expensive instrumentation, and manipulations with the samples are quite laborious. The incubation time is long, and the method is subjective to many types of errors. These problems are addressed to future research.

Fluorescence reporting offers a very high sensitivity of detection within *picoliter volumes*. Further reduction of this volume leads to natural limit of single molecules. On this pathway we observe the appearance of '*nanoarrays*', in which the size of every spot can be decreased by three orders of magnitude in comparison to common microarrays (Lynch et al. 2004). It is possible but not always reasonable to reach even smaller volumes due to the necessity of applying much more expensive instrumentation for the reading. Also, it is important that determining of target concentrations is needed with some statistical value. Meantime, in living cells there occur the interactions of individual molecules. They may not always follow thermodynamic rules, and it is interesting to observe, what kind of new effects can then be detected.

11.4 Suspension Arrays and Barcoding

Plain spotted arrays on solid support are not the only means for *multiplex detection*. The sensors may remain in solution (suspension) if there is a possibility to recognize any particular sensor in this system and distinguish it from the sensors of other specificities. If the nanoparticles or larger microspheres carrying particular sensors are recognized by distinct spectroscopic properties, this allows mixing many types of uniquely optically encoded particles (Wilson et al. 2006). Detecting the binding of specific analytes to each of their diverse types can be provided using chromatography or flow cytometry (Lim and Zhang 2007).

11.4.1 Construction of Suspension Arrays

Such *suspension arrays* may contain many thousand types of sensor particles possessing their recognition features, "*barcodes*" (see Sect. 6.4). Dyes (and nanoparticles) emitting at different wavelengths forming in combination a characteristic pattern may serve for constructing these barcodes (Jun et al. 2012).

It is convenient to obtain the barcode pattern by exciting fluorescence at single wavelength, which can be realized when the dyes in different proportions are incorporated into silica particles and coupled by FRET cascade reaction (Ma et al. 2007). In such compositions, when the FRET donor is excited and the recognition is provided by the acceptors, a huge number of combinations are possible. In theory, six colors at six different intensities should provide nearly 40,000 unique barcodes (Wilson et al. 2006). In practice it is hard to achieve such values in view of spectral overlaps between the dyes and variability of fluorescence intensities introduced both on the production and reading steps. In this respect, quantum dots have much better prospects than organic dyes because they possess much narrower spectra covering the whole visible range, they can be excited by a single wavelength and, in addition, they exhibit higher photostability (Eastman et al. 2006).

Microspheres made of synthetic polymer or silica can serve as good carriers of such sensors (Borisov et al. 2010). The sample containing a mixture of potential analytes together with non-analyte compounds can be exposed to the mixture of such sensing beads, so that specific binding of every analyte should occur to the appropriate bead.

Applying this technology seems to be easy, but it remains to resolve two problems. One is *to provide uniquely addressable coding* of microspheres carrying particular sensors, so that they could be recognized in their mixture. The other problem is to obtain the information on target binding to the sensors *on every bead individually* and to provide its quantitative analysis. Solutions of these problems will be discussed below.

11.4.2 Barcodes for Microsphere Suspension Arrays

The principle is that each target-specific element in the array has to be represented by a subpopulation of particles with distinct and well recognizable optical properties, their '*barcodes*'. Dyes (and nanoparticles) emitting at different wavelengths may serve as these barcodes. For instance, simultaneous detection of multiple bacterial targets can be achieved by using antibodies marked by silica particles containing three co-located dyes in different proportions and coupled by FRET (Ma et al. 2007). The dyes allow excitation at single wavelength (of the donor) and recognition of the particles by their different colors of fluorescence emission is provided by the acceptor. In this and similar cases FRET mechanism is not used for reporting function of a sensor but as a 'wavelength convertor' that allows obtaining a family of 'barcodes' that can be recognized by variable fluorescence spectra.

In addition to possibilities to spectral-fluorescence barcoding, other possibilities to identify the particles can be suggested. A two-dimensional graphical code similar to the barcodes found in supermarkets can be generated in a laminar flow in a microfluidic system (Pregibon et al. 2007). This method based on continuous-flow lithography combines particle synthesis and encoding with probe incorporation into a single process initiated and controlled by photopolymerization with introduction of photomask. Over a million of unique codes can be generated in this way.

11.4.3 Reading the Information from Microspheres

The marked sensor particles should be counted individually, and not only their recognition but also their response to target binding should be recorded. There are two possibilities for that. One is to count and measure the microspheres *one by one*, as they pass through the detector unit. The other is to read them with *microscope imaging system*. Both of them can be successfully realized in common equipment (flow cytometers and scanning microscopes correspondingly) as well with the aid of specially designed instrumentation (Wilson et al. 2006), see Fig. 11.12.

Flow cytometers are the instruments developed for measuring cells and particles in the flow (Fig. 11.12a). This technique that was originally developed for cell counting and sorting is ideally suited for the analysis of beads arrays. In the heart of these instruments is a very thin glass capillary that can be illuminated with several lasers and allow detection of scattered light and fluorescence emission at several wavelengths from microscopic objects (particles or cells) passing through this capillary. The results in flow cytometry are usually displayed on a computer window in two dimensions with dots representing the counted objects as a function of light-scattering and fluorescence intensity or fluorescence intensities at two different wavelengths.

Modern *flow cytometers* can measure and sort more than 20,000 cells or particles per second with continuous detection of many (ten or more) light emission and laser-scattering signals. Since this method allows for large-scale screening applications, it can be very useful for multiplexed assays and are able to provide a combined output that involves barcode reading and reporter signal (Yu et al. 2012).

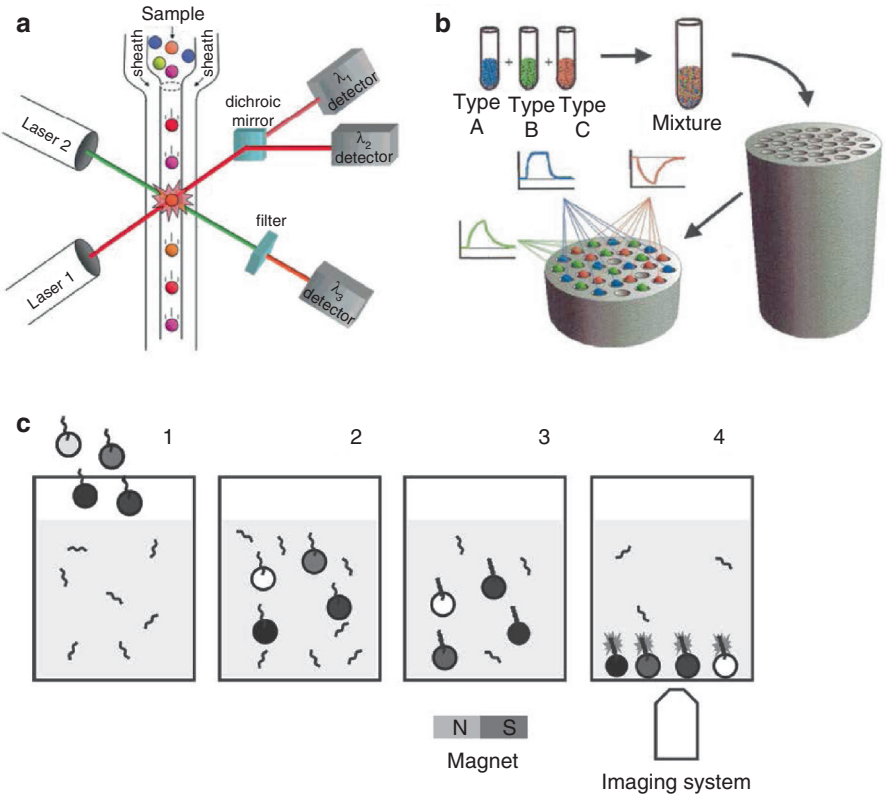

Fig. 11.12 Reading the analytical information from suspension arrays (Borisov et al. 2010). (**a**) Using a flow cytometer. The sample microspheres are hydrodynamically focused in a fluidic system and read-out by two laser beams. Laser 1 excites the encoding dyes and the fluorescence is detected at two wavelengths. Laser 2 is used to quantify the analyte. (**b**) Scheme of randomly ordered bead array concept. Beads are pooled and adsorbed into the etched wells of an optical fiber. (**c**) Scheme of randomly-ordered sedimentation array. A set of encoded microspheres is added to the analyte solution (*1*). Subsequent to binding of the analyte (*2*), microparticles sediment (*3*) and assemble at the transparent bottom of a sample tube generating a randomly ordered array (*4*). This array is evaluated by microscope optics and a CCD-camera

Using automated sample handling, these measurements can be provided in real time with subsecond kinetic resolution. Therefore, merging microarray concept with flow cytometry looks very natural (Tung et al. 2004).

It is also possible to use microbeads carrying different indicator or receptor molecules that are randomly loaded into the wells of chemically etched *optical fiber* or *silicon chips* (Fig. 11.12b). The beads are loaded onto the fiber in a simple dipping and evaporation technique. A typical fiber bundle consists of 5,000–50,000 individual fibers which are read out with an imaging system based on microscope optics and a CCD camera. The system has separated color channels to identify each bead and detect the reporter fluorophores or indicator dyes.

A different suspension array concept is based on sedimentation and microscopic imaging employs *magnetic microbeads* (Fig. 11.12c). They settle to the bottom of a

microplate well by magnetic forces and form randomly ordered arrays, which are examined by fluorescence microscopy and automated imaging analysis. These particles can be magnetically guided to a place of interest by an external magnetic field. The magnetic beads usually consist of inorganic or metallic nanoparticles which are distributed in a dye-doped polymeric bead. Since the dye properties (e.g., luminescence brightness, solubility, etc.) are affected by the presence of magnetic additive, the particle synthesis becomes more challenging. Meantime, these particles cover already a wide range of applications such as immunoassays, cell labeling, imaging and purification, or represent at least a good basis for further modifications.

Reading barcodes with *imaging devices* is a possibility that can be realized with inverted epifluorescence microscopes equipped with CCD cameras. Decoding should be provided by image-recognition software.

11.4.4 Applications

Example of application of barcoded particles is presented in Fig. 11.13. Unique recognition signal for each individual target is realized by varying the numbers and ratios of different quantum dots in particles containing recognition units for each

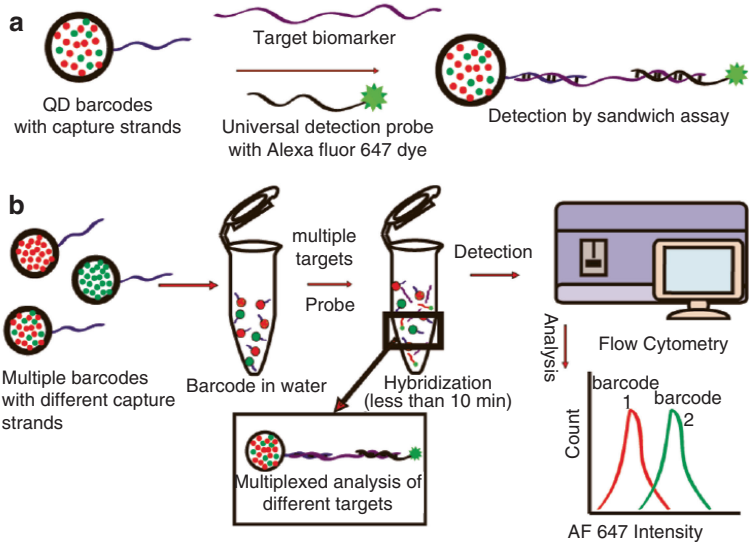

Fig. 11.13 Schematic diagram of assay based on suspension arrays using quantum dot barcodes (Giri et al. 2011). (**a**) The basic principles of detection the pathogenic DNA sequence. (**b**) Flowchart shows the sequential steps involved in the assay. Every type of barcoded microbead is loaded with DNA strand recognizing specific pathogenic DNA. Incubation with sample containing potential targets and hybridization with secondary DNA labeled with fluorescent dye allows rapid and efficient analysis by flow cytometry

analyte DNAs. The probe nucleic acid sequences are coupled to particles with unique recognition patterns. Analyte binding generates the appearance of new fluorescence band that is well separated from a barcoding spectrum. Thus, after capture of target DNA by the coded microbeads, the single-bead spectroscopy studies reveals both the presence and the identity of the target DNA producing emission signals with variable intensities. The DNA hybridization studies demonstrate that the coding and target signals can be simultaneously read at the single-bead level (see Fig. 6.14). They open new opportunities in gene expression studies, high-throughput screening, and medical diagnostics.

An example of such applications is the rapid screening of genetic biomarkers of infectious agents such as HIV, malaria, hepatitis B and C, and syphilis (Giri et al. 2011). Multicolor detection by flow cytometry allows recognition of barcode together with the dye labeling the secondary recognition DNA fragment in sandwich assay. Using quantum dot barcodes allows providing characteristic pattern for every type of suspended particles by exciting at single wavelength and constructing characteristic two-dimensional contour plots. With the possibility of developing the cost-effective miniature barcode read-out devices such technique has to find application as a point-of-care diagnostic platform.

Another important application of bead/suspension arrays is for discovery of protein biomarkers (Zhang et al. 2014). Up to a few hundreds of color-coded polystyrene bead sets can be used, so that each bead set conjugated with a unique antibody is internally dyed with different ratios of two spectrally distinct fluorophores. This technology has been applied for identification of novel biomarkers used for prediction of progression and diagnosis of cancer.

11.4.5 Prospects

Microsphere suspension arrays, with the solution of barcode problem, are becoming strong competitors to flat spotted microarrays. They are potentially superior in *speed of analysis*, since kinetics of target binding to them can be easily accelerated by efficient mixing in solution. There are additional benefits of this technology, such as *larger surface area* for functionalization of microparticles relative to flat supports, flexibility and simplicity of manipulation (e.g. microspheres can be made magnetic). Microspheres are much better reproducible in fabrication than the flat arrays. Whereas the same chemistry has to be used for different sensor binding to flat arrays, microsphere arrays are free from this limitation. Moreover, one can easily make the necessary array composition by just mixing the stocked microspheres loaded with necessary sensors.

The availability of instruments for reading the microsphere arrays must stimulate further development of this technology. Regardless of principle of fluorescence detection, no sample pre-treatment or after-treatment such as washing may be needed. This is common for flow cytometry, and its ability to resolve free and bound probes (by realizing sandwich assays, by target labeling, the change in

light-scattering, etc.) allow different assay formats to be applied. Thus, suspensions may compete successfully with solid chips.

11.5 Microfluidic Devices

Reduction of size and volume of sensor and chemical reactor devices by several orders of magnitude can be achieved with present technologies. This stimulates developing the technologies that allow sample manipulation together with sensing in a greatly reduced volume. *Microfluidic devices* that are often called *micrototal analysis systems* (μ-TAS) and *lab-on-a-chip devices* have already been developed in a number of laboratories and they promise even greater future (Dittrich et al. 2006). In addition to miniaturization, they offer many useful properties. It is the reduction of diffusion lengths in the sample, which increases the rates of target binding and of different chemical or biochemical transformations. Confined geometries prevent from high dilutions, and planar active surfaces allow achieving a high surface-to-volume ratio and providing high-density immobilization of participants in the sensing process. The surface-related effects can be made dominant in sample handling and sensor-based applications.

Though many detection methods can operate together with microfluidic systems, fluorescence is of primary use. The recently developed technologies allow serial and inexpensive production of integrated microfluidic systems that incorporate the whole necessary range of optical detection elements, including light sources and optical detectors. A broad variety of sensors can be incorporated into these devices, from small molecules to nanoparticles and up to intact living cells.

11.5.1 Fabrication and Operation of a Lab-on-a-Chip

The '*lab-on-a-chip*' concept involves fabrication of devices in which all elements will be miniaturized, including sample supply, excitation source and fluorescence readout unit. Both inorganic (silica) and organic polymers can be used as the bodies of these devices and different automatic micro-fabrication techniques, such as replica and injection molding, embossing, and laser ablation are used for producing fluidic channels and introduction of reactive and optical elements (Dittrich et al. 2006). Their mass production can make them disposable and one-use (Fiorini and Chiu 2005).

The inner surfaces of fluidic channels and volumes are modified for capture of sorbent, catalyst and sensor molecules with the aid of laser-activated photochemical reactions that allows achieving a high precision. They represent the solid phase that can be combined with moving phase consisting of different types of molecules and nanoparticles of different size. Particularly, quantum dots and other fluorescent

nanoparticles can be used in this combination. Moreover, all the advantages of multiplex analysis using barcoded microspheres can be realized here (Lim and Zhang 2007).

The pumping and valving of fluid flow, the mixing of different reagents, and the separation and detection of different chemical species have to be implemented in a microfluidic format, and this is technically achievable. Filling and manipulation of these devices can be made due to capillary forces and by centrifugation using developed compact disc (CD)-based centrifuge platforms (Madou et al. 2006). Microscopic pumps and valves can be made based on different principles, such as pneumatic, electromagnetic (Wang et al. 2004) and photo-switchable with laser beams (Nagai et al. 2007). A strong effort is presently made for making interfacing and interconnecting with macroscopic lab devices as simple and convenient as possible or even for substituting them completely.

An important possibility to manipulate in microfluidic devices provided by optical forces drive the particles of higher refractive index than the surrounding medium to the region of maximum optical density. Application of this effect have led to rapid development of '*optofluidics*' (Monat et al. 2008).

An example of supramolecular *microfluidic optical chemosensor* (μFOC) is presented in Fig. 11.14. A serpentine channel has been patterned with a sol–gel film that incorporates a cyclodextrin supramolecule modified with a Tb^{3+} macrocycle. Bright emission from the Tb^{3+} ion is observed upon exposure of the μFOC to biphenyl in aqueous solution. The presence of biphenyl in the cyclodextrin receptor site triggers Tb^{3+} emission by an absorption-energy transfer-emission process. These results demonstrate that the intricate signal transduction mechanisms are successfully preserved in microfluidic environments and can be detected by steady-state and time-resolved spectroscopic measurements directly on the optical chemosensor patterned within the microfluidic network.

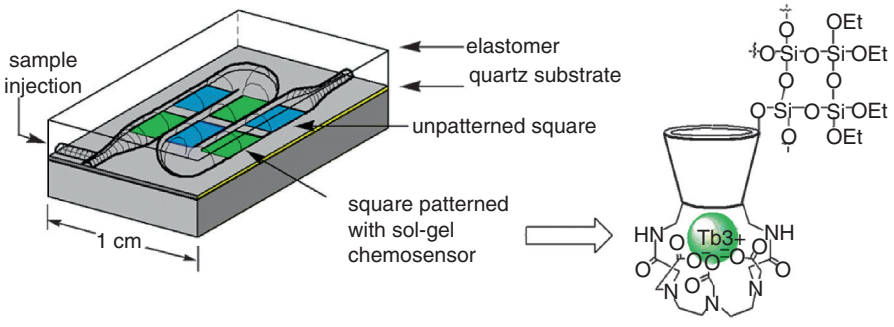

Fig. 11.14 Microfluidic optical chemosensor fabricated in a serpentine channel configuration (Rudzinski et al. 2002). The supramolecular chemosensor is a cyclodextrin decorated by a macrocycle in which a Tb^{3+} ion resides. The conical bucket schematically represents the cyclodextrin receptor site. The target binding is detected by the appearance of its characteristic luminescence bands

11.5.2 Microfluidic Devices as Microscale Reactors and Analytical Tools

The lab-on-a-chip devices allow *different manipulations* with extremely low sample and reagent quantities that can be provided directly inside the device, and all this process can be coupled with sensing. From the side of synthetic chemists, the interest in miniaturized analytical systems was stimulated by the fact that physical processes can be more easily controlled and harnessed when instrumental dimensions are reduced to the micrometre scale. Such systems might be revolutionized in the fields of high-throughput synthesis and chemical production (deMello 2006).

Important characteristic feature of these devices is that *chemical reactions* and *sensing events* can be coupled or preceded by *sample preparation* and *separation steps*. Such combination allows not only to simplify the assay but also to minimize the non-specific adsorption and side reactions. The measurement is often coupled with preparation of sample. Pre-treatment of sample is commonly needed to remove the sample components that do not contain the analyte but that may complicate the analysis. This may be a separate procedure. But researchers often try to combine it with the measurement, especially when dealing with such heterogeneous species as human blood. As an example, steroid screening can be made starting from the *whole blood* sample; the membrane filter can be incorporated directly into the microdevice (Thorslund et al. 2006).

Using lab-on-a-chip concept, miniaturized devices for *DNA analysis* can be constructed that are able to provide dielectrophoresis for purification of DNA, artificial gel structures for rapid DNA separation, and nanofluidic channels for direct visualization of single DNA molecules. The marriage of microfluidics with detection technologies that rely on highly selective nucleic acid hybridization provide improvements in bioanalytical methods for the purposes such as detection of pathogens or mutations and drug screening. Importantly, such a complex and multi-step process as the *polymerase chain reaction* (PCR), that requires not only reagent change but also temperature cycling, can be conducted in continuous-flow microchips (Zhang et al. 2006).

Microfluidic immunosensor systems can be realized in both homogeneous and heterogeneous assay formats (Bange et al. 2005), which is important for clinical applications. Sandwich immunoassays can also be adapted to microarray format that allows detection of many target compounds as antigens.

11.5.3 Fluorescence Detection in Microfluidic Devices

There are two tendencies in realization of fluorescence detection in microfluidic devices. One is to make an integrated optical chip located in close contact with microfluidic part but separated from it. This allows making microfluidic part disposable but optical part re-useable. As an illustration, one of suggested devices

(Chediak et al. 2004) contained a semiconductor LED, a CdS optical filter and a silicone photodiode integrated in the same unit, so that a microfluidic reactor is located in close proximity.

The other tendency is to make all the elements that are necessary for efficient instrument performance assembled *in one chip*, including sample separation, chemical modification and binding to immobilized sensor molecules. For visualization of results different fluorescence excitation and detection techniques can be used (Kovarik et al. 2011). In this configuration, the microfluidic units have to become the true *micro-total-analytical-systems* (μTASs) that will be self-consistent devices independent of interfacing to external macro-scale equipment. A strong move in this direction is observed. One of these lab-on-a-chip systems integrates five different components monolithically assembled on one substrate. They represent three main domains of microchip technology: optics, fluidics and electronics (Balslev et al. 2006).

Multi-analyte sensing in these systems is possible in different configurations of microfluidic chip. One, for instance, involves the sensor molecules immobilized on walls of *capillary channels*, so that a microliter droplet of sample fills the channels by capillary forces (Henares et al. 2007). Optical image is then obtained with fluorescent microscope. The other possibility is to apply optical waveguides exposed to the sample filling the channels for providing evanescent-field detection (Irawan et al. 2006). The planar waveguides can be monolithically integrated with the microfluidic channels. They also offer the possibility of creating multiple parallel assays on a single platform. A mobile-phase sensing can be performed with barcoded microspheres, and this provides the link between micro(nano)arrays and microfluidics.

The marriage of *microarray* technologies with the emerging field of *microfluidics* is especially attractive. Combining the highly parallel analysis of many targets in the sample with the advantages of microfluidics, such as reduction in reagent cost, reductions in hybridization assay times, high-throughput sample processing, and also integration and automation capabilities of the front-end sample processing steps is very prospective (Situma et al. 2006). This potential marriage requires many additional efforts, such as developing the low-cost manufacturing methods of the fluidic chips and providing their proper interfaces to the macro-world in addition to optimizing the interactions of microspheres with microchannel walls.

11.5.4 Prospects

Micrometer-scale analytical devices combining separation of sample components, their chemical reactions and detection properties are more attractive than their macro-scale counterparts for various reasons. They use smaller volumes of reagents and are therefore cheaper, quicker and less hazardous to use, and more environmentally appealing. They are well suited to point-of-care testing or field applications (Jung et al. 2015). Dramatically reduced volume and comparatively extended inner

surface create unique possibilities for sample manipulation, separation of its components, chemical reactivity and sensing.

The microfluidic devices are already capable of performing difficult chemical and biological manipulations combined with analytical detection. Such device can serve the function of a whole analytical laboratory and, in addition to sensing, can provide sample preparation and separation of sample components, which can be done with active participation of modified surfaces of microchannels. The benefits of miniaturization are the low sample and reagent consumption and extremely fast analysis times. The operation of such devices requires a very sensitive detection that can be provided by integrated fluorescence detection technique. It will allow exploration of many possibilities that are especially attractive for miniaturized devices, such as evanescent-field and near-field excitation. The single-molecule and single-particle detection will provide an ultimate sensitivity.

11.6 Devices Incorporating the Whole Living Cells

The idea to use the whole cells as highly integrated biosensors responding to different stimuli with their incorporation into *microfluidic devices* is especially attractive (Melamed et al. 2012). This is because these devices offer an efficient and relatively easy way to incorporate the cells and to maintain them in native conditions by supplying the culture media. The inner volume of microfluidic channel can be as small as to allow location of one or several cells, so that their individual properties can be studied. The size of miniaturized optical system becomes closer to that of the cell, and therefore the excitation and collection of emission light can be more efficient than in microscope. Meantime, such device is not a substitute for microscope because of the absence of inherent imaging possibilities; they can be applied externally. Commonly, the cell is illuminated as a whole and its response is detected as an integrated signal. So the selectivity of response is determined by incorporated fluorescent dyes (or biosynthesis of reporters within the cells), their location in the cell and their response to applied stimuli.

In this technology the whole cell may be considered as the top level of biosensor. This is because it can respond to a wide variety of functionally important stimuli in a *highly integrated* but *specified* manner. It can enhance, integrate or suppress the effects of different chemical stimuli, which allows detecting them as the targets. In many cases, the signal generated by target binding to cell receptors can be transformed into *generalized and amplified signal of cell response* and expressed in such integrated variables as *toxicity*. This opens many possibilities for determining and testing different hazardous compounds and drugs.

A lot of important information about cellular functions and their responses have been obtained with the use of two powerful methods – fluorescence microscopy and flow cytometry (see Chap. 13 for more details). Scanning confocal and two-photon microscopies can allow obtaining valuable information about the cells in two complementary aspects. Microscopy allows studying the cell ultrastructure and following

the distribution of metabolites and ions, etc. But this can be done only for one cell at a time, so it is hard to derive the statistical distribution of measured parameters within cell population. Flow cytometry, in contrast, allows obtaining such statistical information but for a limited number of parameters. Introduction of microfluidic concept into cellular research brought a new possibility: to study an extended number of parameters for one or small number of living cells trapped in the lab-on-a-chip channels.

11.6.1 Cellular Microorganisms or Human Cultured Cell Lines?

Many different cells, microbial, yeast and of mammalian cell lines, were suggested for whole-cell sensor applications (O'Shaughnessy and Pancrazio 2007; Yagi 2007). They may display different sensitivity to target compounds, so different cells may be needed for different ranges of variation of target concentration. *Bacterial cells* are of active use, particularly for environmental monitoring of pollutants. They are less demanding regarding cultivation conditions. Recent findings, however, showed that the cloned bacterial populations are always physiologically, phenotypically and genotypically heterogeneous. This emphasizes the need for sound statistical approaches for the interpretation of reporter response in individual bacterial cells (Tecon and van der Meer 2006). In order to reduce this heterogeneous response and to determine a number of targets within the same format, the sensor arrays with individual cells immobilized in fabricated patterned hydrogel microwells have been developed.

Advantages of *bacterial* and *yeast cells* follow from their specific properties:

1. They can be easily *genetically engineered* with the incorporation of genes that are cable to synthesize required recognizing or reporting molecules.
2. Some targets such as pollutants can activate their metabolic pathways by influencing the expression of single genes (Belkin et al. 1997). And, in a more general sense, they can offer insight into the *physiological effect* of an analyte (Stenger et al. 2001).
3. They can be *bioluminescent* naturally or modified so that a bioluminescent reporting gene is fused to a promoter sequence of the gene of the relevant pathway (see Sect. 10.2). Such modified bacteria offer a solution of a problem of generating a reporter signal. Alternatively, fluorescent proteins of GFP type can be fused with desired proteins to generate fluorescence response.

Several approaches for *transduction of cellular signals* are explored. Versatility of fluorescent dyes together with the new possibilities offered by fluorescent nanoparticles allows tracking cellular response on nuclear, mitochondrial, cytoplasmic and biomembrane levels. The methods based on well-developed determinations of membrane potential (Farinas et al. 2001) or intracellular release of Ca^{2+} ions can be successfully applied.

11.6.2 Living and Fixed Cells

In all analytical tools, *live cells* should be treated gently so that incorporation of different molecules and particles as sensors should be compatible with cell viability. Whereas passive diffusion can be realized with small molecules, large molecules such as polypeptide and protein sensors need special cationic leader peptides (such as HIV-derived TAT peptide) to facilitate their entry into the cell. Regarding larger particles such as quantum dots, for their incorporation there is no general procedure, and the strategy should be selected depending on the cell type. There could be uptake by *endocytosis*, direct *microinjection* of nanoliter volumes, *electroporation* (using the charge for physical delivery through the membrane) and mediated uptake (by incorporation into phospholipid vesicles or attachment of cationic peptides) (Eastman et al. 2006; Derfus et al. 2004). All that can be realized in microfluidic devices. For maintaining the cell living conditions, culture medium with all necessary nutrients can be supplied through the microchannels.

In contrast, *fixed cells* that are often used in microscopic studies are in fact dead cells with chemically cross-linked components to maintain cellular architecture. Nanosensor particles of various sizes can enter the fixed cell easily through the pores that can be created chemically. Different technologies in cellular research, such as flow cytometry, often involve the determination of intracellular antigens using corresponding antibodies. This procedure is possible only after the cell fixation, and permeabilisation treatment is needed to allow the antibodies entry inside the cell. For the sake of biosensor applications, the researcher can make selection between these two, living and fixed, conditions.

11.6.3 Single Cells in Microfluidic Devices

Microfluidic chips are ideal platforms for housing and handling small numbers of living cells (see Fig. 11.15 as an example). A large variety of microfluidic systems is available for cell analysis that allow not only a short-term manipulation with them but *maintaining their long-term culture* (for >2 weeks) and observing the whole range of their differentiation. This possibility was shown for muscle cells spanning the whole process of differentiation from myoblasts to myotubes (Tourovskaia et al. 2005). The microfluidic system provides accurate control of the perfusion rates and biochemical composition of the environment surrounding the cells, so that no difference is observed in differentiation between microfluidic and traditional cultures. Microfluidic systems allow performing a number of cell-based tests in parallel and monitoring them for a long term continuously (Hung et al. 2005).

We can observe that *microfluidic devices* used in research rapidly fill the gap between single-cell studies performed by microscopy and mechanistic studies of

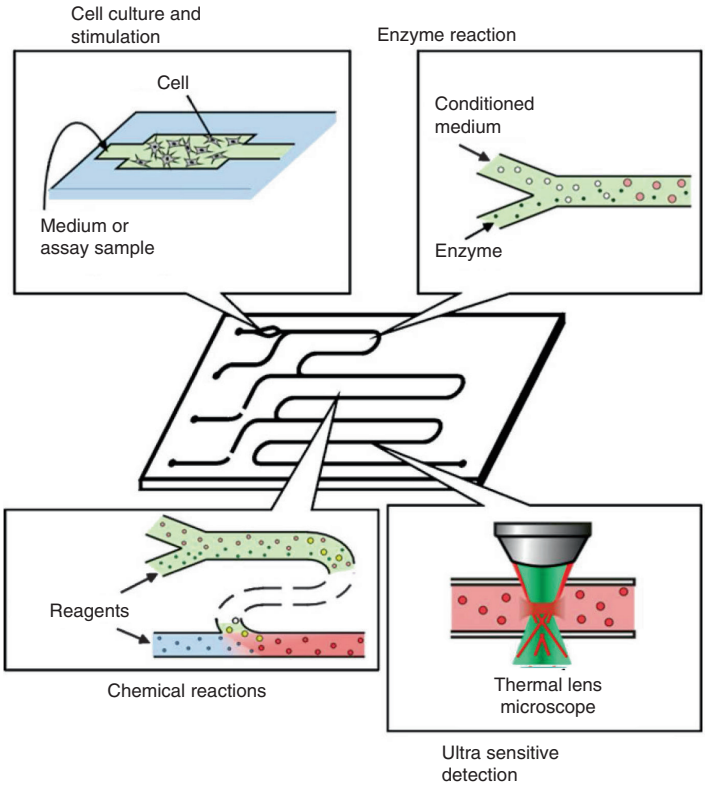

Fig. 11.15 A design of microchip-based bioassay system, in which cell culture, chemical reactions, and detection were integrated into a glass microchip (Goto et al. 2005). The chip has a microchamber for cell culture, microchannels for chemical and enzymatic reactions, and a detection area with six holes: one medium inlet, three reagent inlets, one cell introduction hole, and one outlet

cellular processes that are usually carried out with large populations of cells (Lidstrom and Meldrum 2003). This is important because the parameters that are measured as averages of large populations can be misleading. For instance, an apparently linear response to a signal could, in fact, reflect an increasing number of cells in the population that have switched from 'OFF' to 'ON', rather than a graded increase in response by all the cells. The studies in parallel of a *significant number of individual cells* is challenging, but new technologies allow them to become a reality.

Optical waveguides are the basic and the most important optical elements that must be integrated into lab-on-a-chip microsystems together with living cells. The common methods for waveguide fabrication are the conventional deposition

techniques on glass substrates. However, polymers are more favorable substrates for microfluidic devices due to the fabrication flexibility that they offer and to their low cost. Consequently, the fabrication of optical waveguides on polymeric substrates has the potential to solve a major integration problem (Leeds et al. 2004).

The deposition of living cells on top of waveguides in a microfluidic chip can potentially give valuable information about cell life and its perturbations. It has to be counted, however, that the evanescent field interaction depth is small (~200 nm) and decaying with distance from the waveguide, so in view of the larger cell size the full integral response of the cell is difficult to achieve.

The *manufacturing of microfluidic chip* for cell handling has to meet several requirements. On one hand, the design of the chip has to ensure the microfluidic functions (reproducible loading and unloading, washing, filling and processing), and on the other hand it has to ensure low costs and easy handling. Extremely important is to make cell-friendly microenvironment that can be achieved by covering the device channels with peptides or biocompatible polymer hydrogels. There were only few attempts to integrate many functions together on a microfluidic platform and the challenge lies ahead. A solution can be found in building systems with modular design. This design should still allow easy fabrication, for instance, by writing waveguides on polymers using UV treatment.

11.6.4 Bacterial Cells with Genetically Incorporated Sensors

Bacterial cells allow many possibilities for synthesis of *genetically engineered guest proteins*. These proteins may serve as molecular sensors inside the cells. Microfluidic device in this case serves as a support and detection medium. As an example could serve a microsystem wherein *E. coli* cells were genetically engineered to express the desired capture proteins on the membrane surface and were spatially arrayed as sensing elements in a microfluidic device (Oh et al. 2006). Through the co-expression of peptide-based capture ligands on the cell surface and fluorescent protein in the cytoplasm, an effective means of directly linking the fluorescence intensity to the density of capture ligands was demonstrated.

In line with inducing the ability of testing specific targets, the strong attempts are made for improving the *general toxicity tests*. In this respect also, genetic engineering becomes more and more important. Using the recombinant DNA technology the toxicity-responsive gene promoter is fused to a gene coding a protein that can be easily quantified. Usually this is either GFP-family protein with detection in fluorescence or luciferase producing bioluminescent emission. Photosynthetic bacteria with their built-in mechanisms of synthesis of fluorescent pigments can be also actively used (Yagi 2007). Unfortunately, promoter activation and generation of cellular response takes several hours, which is not very attractive for in-field analysis.

The examples of application of bacterial sensing system take advantage of the recognition of the regulatory protein, ArsR, for arsenite and antimonite to

produce the reporter protein, which in this case is GFPuv (Rothert et al. 2005). The fluorescence emitted by the GFPuv in the cells can be directly related to the concentration of the analyte in the cell, making this sensing system useful in the detection of arsenite and/or antimonite in a variety of samples. Alternatively, the analyte may intervene into metabolic processes in living cells, and this provides the means for its highly sensitive detection.

11.6.5 The Cultured Human Cells

This technique based on bacterial cells for detection of toxic compounds has some limits, since these cells do not respond to many compounds that are toxic for men. Those are the compounds that influence nervous system, immunity and cell differentiation. In addition, some pollutants become toxic after processing in the liver. Therefore the application of *cultured human cell lines* is very actual. Cardiac myocytes and neurons are of primary concern, and the parameters such as membrane potential are attractive as the means of response (O'Shaughnessy and Pancrazio 2007).

11.6.6 The Whole Cell Arrays

In many tests, in particular for pathogen detection, there were attempts to apply *microarray technology* with incorporated living cells (Ron 2007; Yoo et al. 2007). Genetically modified bacteria were used for this purpose. The modifications include the inducing or augmentation of recognition of pathogen together with induction of response in bioluminescence.

A significant problem is the viability of cells on arrays, since for long-term cellular monitoring the cells need continuous perfusion. Special devices were designed that allow performing many functions including repeated cell growth/passage cycles, reagent introduction, and real-time optical analysis (Hung et al. 2005).

11.6.7 Prospects

The living cell can be viewed as a constellation of potential molecular sensors with complex correlations between them. The cell-based biosensors can provide all the information that is available to molecular sensors regarding quantitative response to analyte concentration. In addition, their response may also contain integrated functionally relevant information, for instance, the response to a toxic compound by a general stress. Being incorporated into microfluidic devices, the cells are able to respond dynamically and rapidly and allow long-term temporal observations.

Detection of physiologically active compounds is the major field of applications of whole-cell biosensors (Stenger et al. 2001). And importantly, in contrast to all other types of chemical sensors and biosensors the cells can detect the *unknown threat agents* by their functional response.

11.7 Sensing and Thinking: Optimizing Convenience, Sensitivity and Precision for Obtaining the Proper Sensor Response

In practice, working with sensors is always dealing with the devices that are required to connect the events occurring on molecular and supramolecular or cellular level with the quantitative measure that we need to obtain and understand. These devices can be evaluated according to a number of parameters, such as sensitivity, speed of response, reversibility, repeatability, reproducibility, possibility of continuous monitoring, portability, the ease of operation and price. Until now, many techniques in analytical chemistry are adapted for the cuvette assay format (Lakowicz 2006; Valeur 2002), which is reasonable for detecting a single analyte and is not applicable for multi-analyte arrays. Still common is the bench-top instrumentation that allows such precise but low productive measurements.

Presently we witness dramatic changes. We observe that similar (or at least quite satisfactory) precision in analysis can be achieved with highly miniaturized instrumentation. Furthermore, its use can lead to dramatic increase of efficiency of analysis regarding the possibility of sensing many targets together and thus to characterize the sample of very complicated composition. Further on, the new instrumentation demonstrates extreme flexibility in addressing different analytical tasks. And finally, it can be mass produced, cheap and available for personal use.

Questions and Problems

1. Explain the functioning of every element of spectrofluorimeter. Find for each of these elements their miniaturized counterpart.
2. Explain the physical mechanism of light propagation without losses in optical fiber and plain waveguide. Is there any difference? What will happen if $n_2 < n_1$? If $n_2 = n_1$? (see Fig. 10.14).
3. Which principles of incorporation of fluorescence reporters can be and which cannot be realized with microarrays on planar solid support? (a). The same environment-sensitive reporters coupled to the sensors attached to all the spots. (b). Competitors specific to different sensors labeled with the same dyes? (c). Sandwich assays with detectors labeled with the same dyes. Can FRET be applied to these microarrays? If yes, in what configurations?
4. Compare the microsphere-based microarrays with spotted microarrays on flat solid support regarding their capacity and convenience of application.
5. Why the equilibrium in sensor-target interactions is established much faster in microsphere-based microarrays than in microarrays on solid support?

6. How to detect the target binding to arrayed microspheres when the whole visible wavelength range is occupied with emission needed for barcoding?
7. Estimate the optimal size of microspheres in view of convenience of manipulation and detection.
8. What are the means to manipulate with liquid flow in microfluidic channels.
9. Where should the sensors be located in lab-on-a-chip devices? (a) Attached to the inner volume of the channels. (b) In the moving phase. (c) On the incorporated optical waveguides. (d) In the outlet sample volume. Compare different possibilities.
10. How to apply the optical units to lab-on-a-chip devices? (a) Unit providing monochromatic excitation. (b) Unit providing collection and detection of fluorescence.
11. What is the target-related difference between molecular and whole-cell sensors? Suggest the range of targets that are optimal for molecular sensing. Do the same for the cell-based sensing.
12. How the fluorescence response can be introduced into/onto the cells captured in microfluidic devices?

References

Allen L (2013) Essentials of lasers: the commonwealth and international library: selected readings in physics. Pergamon press, London

Andreou AG, Zhang Z, Ozgun R, Choi ET, Kalayjian ZK, Marwick MA, Christen JB, Tung L (2011) Contactless fluorescence imaging with a CMOS image sensor. In: Circuits and systems (ISCAS), 2011 IEEE International Symposium on, Rio de Janeiro 2011. IEEE, pp 2341–2344

Bacon CP, Mattley Y, DeFrece R (2004) Miniature spectroscopic instrumentation: applications to biology and chemistry. Rev Sci Instrum 75(1):1–16

Bally M, Halter M, Voros J, Grandin HM (2006) Optical microarray biosensing techniques. Surf Interface Anal 38(11):1442–1458

Balslev S, Jorgensen AM, Bilenberg B, Mogensen KB, Snakenborg D, Geschke O, Kutter JP, Kristensen A (2006) Lab-on-a-chip with integrated optical transducers. Lab Chip 6(2): 213–217

Bange A, Halsall HB, Heineman WR (2005) Microfluidic immunosensor systems. Biosens Bioelectron 20(12):2488–2503

Belkin S, Smulski DR, Dadon S, Vollmer AC, Van Dyk TK, Larossa RA (1997) A panel of stress-responsive luminous bacteria for the detection of selected classes of toxicants. Water Res 31(12):3009–3016

Betzen C, Hoheisel JD, Kastelic D (2014) Methods for analyzing and quantifying protein-protein interaction. Expert Rev Proteomics 11(1):107–120

Blattler T, Huwiler C, Ochsner M, Stadler B, Solak H, Voros J, Grandin HM (2006) Nanopatterns with biological functions. J Nanosci Nanotechnol 6(8):2237–2264

Borisov SM, Mayr T, Mistlberger G, Klimant I (2010) Dye-doped polymeric particles for sensing and imaging. In: Demchenko AP (ed) Advanced fluorescence reporters in chemistry and biology II: molecular constructions, polymers and nanoparticles. Springer Ser Fluoresc 9:193–228

Bosch ME, Sanchez AJR, Rojas FS, Ojeda CB (2007) Recent development in optical fiber biosensors. Sensors 7(6):797–859

Bradshaw JT, Mendes SB, Saavedra SS (2005) Planar integrated optical waveguide spectroscopy. Anal Chem 77(1):28A–36A
Brogan KL, Walt DR (2005) Optical fiber-based sensors: application to chemical biology. Curr Opin Chem Biol 9(5):494–500
Carletti E, Guerra E, Alberti S (2006) The forgotten variables of DNA array hybridization. Trends Biotechnol 24(10):443–448
Chediak JA, Luo ZS, Seo JG, Cheung N, Lee LP, Sands TD (2004) Heterogeneous integration of CdS filters with GaN LEDs for fluorescence detection microsystems. Sens Actuators A Phys 111(1):1–7
Collett JR, Cho EJ, Ellington AD (2005) Production and processing of aptamer microarrays. Methods 37(1):4–15
Curk T, Demsar J, Xu QK, Leban G, Petrovic U, Bratko I, Shaulsky G, Zupan B (2005) Microarray data mining with visual programming. Bioinformatics 21(3):396–398
Dandin M, Abshire P, Smela E (2007) Optical filtering technologies for integrated fluorescence sensors. Lab Chip 7(8):955–977
Dasgupta PK, Eom IY, Morris KJ, Li JZ (2003) Light emitting diode-based detectors absorbance, fluorescence and spectroelectrochemical measurements in a planar flow-through cell. Anal Chim Acta 500(1–2):337–364
Demchenko AP (2005a) The future of fluorescence sensor arrays. Trends Biotechnol 23(9):456–460
Demchenko AP (2005b) The problem of self-calibration of fluorescence signal in microscale sensor systems. Lab Chip 5(11):1210–1223
deMello AJ (2006) Control and detection of chemical reactions in microfluidic systems. Nature 442(7101):394–402
Derfus AM, Chan WCW, Bhatia SN (2004) Intracellular delivery of quantum dots for live cell labeling and organelle tracking. Adv Mater 16(12):961
Dharmadi Y, Gonzalez R (2004) DNA microarrays: experimental issues, data analysis and application to bacterial systems. Biotechnol Prog 20:1309–1324
Dittrich PS, Tachikawa K, Manz A (2006) Micro total analysis systems. Latest advancements and trends. Anal Chem 78(12):3887–3907
Domachuk P, Eggleton BJ (2004) Photonics – Shrinking optical fibres. Nat Mater 3(2):85–86
Draghici S, Khatri P, Eklund AC, Szallasi Z (2006) Reliability and reproducibility issues in DNA microarray measurements. Trends Genet 22(2):101–109
Dudley AM, Aach J, Steffen MA, Church GM (2002) Measuring absolute expression with microarrays with a calibrated reference sample and an extended signal intensity range. Proc Natl Acad Sci U S A 99(11):7554–7559
Eastman PS, Ruan WM, Doctolero M, Nuttall R, De Feo G, Park JS, Chu JSF, Cooke P, Gray JW, Li S, Chen FQF (2006) Qdot nanobarcodes for multiplexed gene expression analysis. Nano Lett 6(5):1059–1064
Elbs M, Hulko M, Frauenfeld J, Fischer R, Brock R (2007) Multivalence and spot heterogeneity in microarray-based measurement of binding constants. Anal Bioanal Chem 387(6):2017–2025
Elosua C, Matias IR, Bariain C, Arregui FJ (2006) Volatile organic compound optical fiber sensors: a review. Sensors 6(11):1440–1465
Epstein CB, Butow RA (2000) Microarray technology – enhanced versatility, persistent challenge. Curr Opin Biotechnol 11(1):36–41
Epstein JR, Walt DR (2003) Fluorescence-based fibre optic arrays: a universal platform for sensing. Chem Soc Rev 32(4):203–214
Farinas J, Chow AW, Wada HG (2001) A microfluidic device for measuring cellular membrane potential. Anal Biochem 295(2):138–142
Fiorini GS, Chiu DT (2005) Disposable microfluidic devices: fabrication, function, and application. Biotechniques 38(3):429–446
Fixe F, Chu V, Prazeres DMF, Conde JP (2004) An on-chip thin film photodetector for the quantification of DNA probes and targets in microarrays. Nucleic Acids Res 32(9):e70

Gardeniers JGE, van den Berg A (2004) Lab-on-a-chip systems for biomedical and environmental monitoring. Anal Bioanal Chem 378(7):1700–1703

Giri S, Sykes EA, Jennings TL, Chan WC (2011) Rapid screening of genetic biomarkers of infectious agents using quantum dot barcodes. ACS Nano 5(3):1580–1587

Glindkamp A, Riechers D, Rehbock C, Hitzmann B, Scheper T, Reardon KF (2010) Sensors in disposable bioreactors status and trends. In: Disposable bioreactors. Springer Berlin-Heidelberg, pp 145–169

Goto M, Sato K, Murakami A, Tokeshi M, Kitamori T (2005) Development of a microchip-based bioassay system using cultured cells. Anal Chem 77(7):2125–2131

Guo J, Sonkusale S (2011) A CMOS imager with digital phase readout for fluorescence lifetime imaging. In: ESSCIRC (ESSCIRC), 2011 Proceedings of the, 2011. IEEE, Helsinki, pp 115–118

Henares TG, Takaishi M, Yoshida N, Terabe S, Mizutani F, Sekizawa R, Hisamoto H (2007) Integration of multianalyte sensing functions on a capillary-assembled microchip: Simultaneous determination of ion concentrations and enzymatic activities by a "drop-and-sip" technique. Anal Chem 79(3):908–915

Herbáth M, Papp K, Balogh A, Matkó J, Prechl J (2014) Exploiting fluorescence for multiplex immunoassays on protein microarrays. Methods Appl Fluoresc 2(3):032001

Holthoff WG, Tehan EC, Bukowski RM, Kent N, MacCraith BD, Bright FV (2005) Radioluminescent light source for the development of optical sensor arrays. Anal Chem 77(2):718–723

Hong JA, Neel DV, Wassaf D, Caballero F, Koehler AN (2014) Recent discoveries and applications involving small-molecule microarrays. Curr Opin Chem Biol 18:21–28

Hung PJ, Lee PJ, Sabounchi P, Lin R, Lee LP (2005) Continuous perfusion microfluidic cell culture array for high-throughput cell-based assays. Biotechnol Bioeng 89(1): 1–8

Irawan R, Tay CM, Tjin SC, Fu CY (2006) Compact fluorescence detection using in-fiber microchannels – its potential for lab-on-a-chip applications. Lab Chip 6(8):1095–1098

Jun BH, Kang H, Lee YS, Jeong DH (2012) Fluorescence-based multiplex protein detection using optically encoded microbeads. Molecules 17(3):2474–2490

Jung W, Han J, Choi J-W, Ahn CH (2015) Point-of-care testing (POCT) diagnostic systems using microfluidic lab-on-a-chip technologies. Microelectronic Eng 132:46–57

Kovarik ML, Gach PC, Ornoff DM, Wang Y, Balowski J, Farrag L, Allbritton NL (2011) Micro total analysis systems for cell biology and biochemical assays. Anal Chem 84(2): 516–540

Kusnezow W, Jacob A, Walijew A, Diehl F, Hoheisel JD (2003) Antibody microarrays: an evaluation of production parameters. Proteomics 3(3):254–264

Lakowicz JR (2006) Principles of fluorescence spectroscopy, 3rd edn. Springer, New York

Leeds AR, Van Keuren ER, Durst ME, Schneider TW, Currie JF, Paranjape M (2004) Integration of microfluidic and microoptical elements using a single-mask photolithographic step. Sens Actuators A Phys 115(2–3):571–580

Leung YF, Cavalieri D (2003) Fundamentals of cDNA microarray data analysis. Trends Genet 19(11):649–659

Lidstrom ME, Meldrum DR (2003) Life-on-a-chip. Nat Rev Microbiol 1(2):158–164

Lim CT, Zhang Y (2007) Bead-based microfluidic immunoassays: the next generation. Biosens Bioelectron 22(7):1197–1204

Liu Y, Song Y, Chen Y, Li XQ, Ding F, Zhong RQ (2004) Biquinolino-modified beta-cyclodextrin dimers and their metal complexes as efficient fluorescent sensors for the molecular recognition of steroids. Chemistry 10(15):3685–3696

Long F, Shi H (2014) Simple and compact optode for real-time in-situ temperature detection in very small samples. Sci Rep 4

Luppa PB, Sokoll LJ, Chan DW (2001) Immunosensors – principles and applications to clinical chemistry. Clin Chim Acta 314(1–2):1–26

Lynch M, Mosher C, Huff J, Nettikadan S, Xu J, Henderson E (2004) Functional nanoarrays for protein biomarker profiling. NSTI Nanotech 2004, vol 1, Technical proceedings, Cambridge, Massachusetts, USA, pp 35–38

Ma Q, Wang XY, Li YB, Shi YH, Su XG (2007) Multicolor quantum dot-encoded microspheres for the detection of biomolecules. Talanta 72(4):1446–1452

Madou M, Zoval J, Jia GY, Kido H, Kim J, Kim N (2006) Lab on a CD. Annu Rev Biomed Eng 8:601–628

Melamed S, Elad T, Belkin S (2012) Microbial sensor cell arrays. Curr Opin Biotechnol 23(1):2–8

Moe AE, Marx S, Banani N, Liu M, Marquardt B, Wilson DM (2005) Improvements in LED-based fluorescence analysis systems. Sens Actuators B Chem 111:230–241

Mogensen KB, Eriksson F, Gustafsson O, Nikolajsen RPH, Kutter JP (2004) Pure-silica optical waveguides, fiber couplers, and high-aspect ratio submicrometer channels for electrokinetic separation devices. Electrophoresis 25(21–22):3788–3795

Monat C, Domachuk P, Grillet C, Collins M, Eggleton BJ, Cronin-Golomb M, Mutzenich S, Mahmud T, Rosengarten G, Mitchell A (2008) Optofluidics: a novel generation of reconfigurable and adaptive compact architectures. Microfluid Nanofluid 4(1–2):81–95

Monat C, Grillet C, Domachuk R, Smith C, Magi E, Moss DJ, Nguyen HC, Tomljenovic-Hanic S, Cronin-Golomb M, Eggleton BJ, Freeman D, Madden S, Luther-Davies B, Mutzenich S, Rosengarten G, Mitchell A (2007) Frontiers in microphotonics: tunability and all-optical control. Laser Phys Lett 4(3):177–186

Monk DJ, Walt DR (2004) Optical fiber-based biosensors. Anal Bioanal Chem 379(7–8): 931–945

Monro TM, Belardi W, Furusawa K, Baggett JC, Broderick NGR, Richardson DJ (2001) Sensing with microstructured optical fibres. Meas Sci Technol 12(7):854–858

Nagai H, Irie T, Takahashi J, Wakida S (2007) Flexible manipulation of microfluids using optically regulated adsorption/desorption of hydrophobic materials. Biosens Bioelectron 22(9–10): 1968–1973

O'Shaughnessy TJ, Pancrazio JJ (2007) Broadband detection of environmental neurotoxicants. Anal Chem 79(23):8838–8845

Oh SH, Lee SH, Kenrick SA, Daugherty PS, Soh HT (2006) Microfluidic protein detection through genetically engineered bacterial cells. J Proteome Res 5(12):3433–3437

Plowman TE, Durstchi JD, Wang HK, Christensen DA, Herron JN, Reichert WM (1999) Multiple-analyte fluoroimmunoassay using an integrated optical waveguide sensor. Anal Chem 71(19):4344–4352

Pratsch K, Wellhausen R, Seitz H (2014) Advances in the quantification of protein microarrays. Curr Opin Chem Biol 18:16–20

Pregibon DC, Toner M, Doyle PS (2007) Multifunctional encoded particles for high-throughput biomolecule analysis. Science 315(5817):1393–1396

Quackenbush J (2001) Computational analysis of microarray data. Nat Rev Genet 2(6):418–427

Resch-Genger U, Hoffmann K, Nietfeld W, Engel A, Neukammer J, Nitschke R, Ebert B, Macdonald R (2005) How to improve quality assurance in fluorometry: fluorescence-inherent sources of error and suited fluorescence standards. J Fluoresc 15(3):337–362

Rillahan CD, Paulson JC (2011) Glycan microarrays for decoding the glycome. Annu Rev Biochem 80:797

Romanov V, Davidoff SN, Miles AR, Grainger DW, Gale BK, Brooks BD (2014) A critical comparison of protein microarray fabrication technologies. Analyst 139(6):1303–1326

Ron EZ (2007) Biosensing environmental pollution. Curr Opin Biotechnol 18(3):252–256

Rothert A, Deo SK, Millner L, Puckett LG, Madou MJ, Daunert S (2005) Whole-cell-reporter-gene-based biosensing systems on a compact disk microfluidics platform. Anal Biochem 342(1):11–19

Roulet JC, Volkel R, Herzig HP, Verpoorte E, de Rooij NF, Dandliker R (2002) Performance of an integrated microoptical system for fluorescence detection in microfluidic systems. Anal Chem 74(14):3400–3407

Rudzinski CM, Young AM, Nocera DG (2002) A supramolecular microfluidic optical chemosensor. J Am Chem Soc 124(8):1723–1727
Sadana A, Ramakrishnan A (2002) A kinetic study of analyte-receptor binding and dissociation for biosensor applications: a fractal analysis for cholera toxin and peptide-protein interactions. Sens Actuators B Chem 85(1–2):61–72
Samuel IDW, Turnbull GA (2007) Organic semiconductor lasers. Chem Rev 107(4):1272–1295
Schäferling M, Nagl S (2011) Förster resonance energy transfer methods for quantification of protein–protein interactions on microarrays. In: Protein microarray for disease analysis. Springer Berlin-Heidelberg pp 303–320
Situma C, Hashimoto M, Soper SA (2006) Merging microfluidics with microarray-based bioassays. Biomol Eng 23(5):213–231
Sobek J, Bartscherer K, Jacob A, Hoheisel JD, Angenendt P (2006) Microarray technology as a universal tool for high-throughput analysis of biological systems. Comb Chem High Throughput Screen 9(5):365–380
Spibey CA, Jackson P, Herick K (2001) A unique charge-coupled device/xenon arc lamp based imaging system for the accurate detection and quantitation of multicolour fluorescence. Electrophoresis 22(5):829–836
Stenger DA, Gross GW, Keefer EW, Shaffer KM, Andreadis JD, Ma W, Pancrazio JJ (2001) Detection of physiologically active compounds using cell-based biosensors. Trends Biotechnol 19(8):304–309
Taitt CR, Anderson GP, Ligler FS (2005) Evanescent wave fluorescence biosensors. Biosens Bioelectron 20(12):2470–2487
Tecon R, van der Meer JR (2006) Information from single-cell bacterial biosensors: what is it good for? Curr Opin Biotechnol 17(1):4–10
Thorslund S, Klett O, Nikolajeff F, Markides K, Bergquist J (2006) A hybrid poly(dimethylsiloxane) microsystem for on-chip whole blood filtration optimized for steroid screening. Biomed Microdevices 8(1):73–79
Tomizaki KY, Usui K, Mihara H (2005) Protein-detecting microarrays: current accomplishments and requirements. Chembiochem 6(5):783–799
Tourovskaia A, Figueroa-Masot X, Folch A (2005) Differentiation-on-a-chip: a microfluidic platform for long-term cell culture studies. Lab Chip 5(1):14–19
Tung YC, Zhang M, Lin CT, Kurabayashi K, Skerlos SJ (2004) PDMS-based opto-fluidic micro flow cytometer with two-color, multi-angle fluorescence detection capability using PIN photodiodes. Sens Actuators B Chem 98(2–3):356–367
Valeur B (2002) Molecular fluorescence. Wiley VCH, Weinheim
Venkatasubbarao S (2004) Microarrays – status and prospects. Trends Biotechnol 22(12): 630–637
Vinet F, Chaton P, Fouillet Y (2002) Microarrays and microfluidic devices: miniaturized systems for biological analysis. Microelectron Eng 61–2:41–47
Vosch T, Antoku Y, Hsiang JC, Richards CI, Gonzalez JI, Dickson RM (2007) Strongly emissive individual DNA-encapsulated Ag nanoclusters as single-molecule fluorophores. Proc Natl Acad Sci U S A 104(31):12616–12621
Voskuhl J, Brinkmann J, Jonkheijm P (2014) Advances in contact printing technologies of carbohydrate, peptide and protein arrays. Curr Opin Chem Biol 18:1–7
Wang X-D, Wolfbeis OS (2012) Fiber-optic chemical sensors and biosensors (2008–2012). Anal Chem 85(2):487–508
Wang Z, El-Ali J, Engelund M, Gotsaed T, Perch-Nielsen IR, Mogensen KB, Snakenborg D, Kutter JP, Wolff A (2004) Measurements of scattered light on a microchip flow cytometer with integrated polymer based optical elements. Lab Chip 4(4):372–377
Wei Q, Qi H, Luo W, Tseng D, Ki SJ, Wan Z, Göröcs ZN, Bentolila LA, Wu T-T, Sun R (2013) Fluorescent imaging of single nanoparticles and viruses on a smart phone. ACS Nano 7(10):9147–9155
Wilkes T, Laux H, Foy CA (2007) Microarray data quality – review of current developments. OMICS 11(1):1–13

Wilson R, Cossins AR, Spiller DG (2006) Encoded microcarriers for high-throughput multiplexed detection. Angew Chem Int Ed Engl 45(37):6104–6117

Wu H, Ge J, Uttamchandani M, Yao SQ (2011) Small molecule microarrays: the first decade and beyond. Chem Commun 47(20):5664–5670

Yagai S, Kinoshita T, Higashi M, Kishikawa K, Nakanishi T, Karatsu T, Kitamura A (2007) Diversification of self-organized architectures in supramolecular dye assemblies. J Am Chem Soc 129(43):13277–13287

Yagi K (2007) Applications of whole-cell bacterial sensors in biotechnology and environmental science. Appl Microbiol Biotechnol 73(6):1251–1258

Yoo SK, Lee JH, Yun SS, Gu MB, Lee JH (2007) Fabrication of a bio-MEMS based cell-chip for toxicity monitoring. Biosens Bioelectron 22(8):1586–1592

Yotter RA, Wilson DM (2003) A review of photodetectors for sensing light-emitting reporters in biological systems. IEEE Sens J 3(3):288–303

Yu H-W, Kim IS, Niessner R, Knopp D (2012) Multiplex competitive microbead-based flow cytometric immunoassay using quantum dot fluorescent labels. Anal Chim Acta 750:191–198

Yu H, Tan Y, Cunningham BT (2014) Smartphone fluorescence spectroscopy. Anal Chem 86(17):8805–8813

Zhang C, Xu J, Ma W, Zheng W (2006). PCR microfluidic devices for DNA amplification. Biotechnology advances, 24(3), 243–284

Zhang X, Soori G, Dobleman TJ, Xiao GG (2014) The application of monoclonal antibodies in cancer diagnosis. Expert Rev Mol Diagn 14(1):97–106

Chapter 12
Focusing on Targets

The great power of fluorescence sensing technologies is their ability to be used for an immense variety of tasks, starting from characterizing physical properties (temperature, pressure, viscosity) in different media (liquids, gasses, supercritical and ionic fluids) up to determination of different metabolites in living cells and detection of harmful microbes. Many different tools were developed for quantitative assays of different molecules of natural or synthetic origin. Using efficient molecular recognition units, fluorescence methods allow determining not only net concentrations of biological macromolecules (nucleic acids, proteins, glycans) but also quantitizing them as individual species with their unique structures and functions.

In this Chapter the reader may not find exhaustive coverage of data on sensing of all possible targets. This information is immense with the tendency of its exponential expansion day by day. The aim is different – to show the diversity of tasks and diversity of possibilities for their solutions. Responding to intermolecular interactions, fluorescent dyes can recognize the surrounding medium and determine its physical parameters, such as temperature and pressure. Being incorporated into the structures adsorbing gas molecules, they are able to identify the gas composition. Fluorescence sensors are also applicable in solutions being efficient in the broadest possible range of target concentrations. Increasing the complexity of target molecules requires adequate improvement of the binding and reporting properties of sensors. Molecules of biological value, and especially proteins, nucleic acids and glycopolymers, are the targets, where the principles of biomolecular recognition are of great utility. And, finally, we have to identify bacteria and viruses, achieving ultimate speed and ultimate sensitivity of their detection. This is also a resolvable task for fluorescence sensors. Diversity of most efficient solutions regarding these tasks is demonstrated here. The concluding section “Sensing and thinking” with a list of questions and problems has to encourage the readers in finding their own solutions.

A.P. Demchenko, *Introduction to Fluorescence Sensing*,
DOI 10.1007/978-3-319-20780-3_12

12.1 Temperature, Pressure and Gas Sensing

There are many methods to measure the *thermodynamic properties of matter*, which seem to be simple, convenient and reliable. Meantime, fluorescence sensing occupies a strong niche in all the cases when the response should be obtained on a molecular level: in microscopic volumes, at interfaces, in the conditions of strong gradients of these parameters. They are of preference if we need to create an image in these parameters or if there is a necessity to make the measurements distantly or with a high resolution in time.

The design of fluorescence or luminescence sensors can be very simple, since their response can be formed by collective effects produced by collisional interaction of individual molecules due to their thermal motion. Temperature and pressure are the thermodynamic parameters that characterize these systems and have to be determined for many practical needs. Their gradients in solids, liquids, their surfaces and interfaces are also important in many research and industrial applications.

12.1.1 Molecular Thermometry

The measurement of temperature is ubiquitous in common life, as well in all fields of science, engineering, medicine. Nowadays most of temperature measurements are based on the temperature-dependent electrical signals and use thermocouples, thermistors or resistance thermometers. For remote measurements, the detection of IR radiation (pyrometry) is frequently used. These methods have essential limitations. For instance, accurate measurement of temperature distribution, 'thermal image', cannot be easily obtained with thermo-electrical devices, and it is hard to measure IR radiation at low temperatures (due to low signal), in water or in humid media (because of strong absorbance of water molecules in the whole IR region). All this range of applications offers a broad area of activity for the type of sensors described in this book. In all these conditions, the methods based on luminescence demonstrate their advantage. They allow the sensing response (a) to be generated on a *molecular level*, (b) to be detected remotely and, if necessary, with (c) to achieve very *high spatial resolution*.

Since the *thermal quenching* of all kind of luminescence is a very common phenomenon, both fluorescent and phosphorescent dyes as well as luminescent metal-ligand complexes can be used for *sensing the temperature* (Wang et al. 2013b). Thermal quenching is a dynamic process that reduces both intensity and lifetime in a coupled manner, so both these parameters can be measured and calibrated on a temperature scale. The advantage of intensity measurement is the simplicity and of lifetime detection – the independence of response on instrumental and photobleaching effects.

The sensors can be constructed using the temperature-dependent structural properties of self-assembled or polymeric materials, into which the environment-sensitive dyes can be embedded. This idea was realized with a series of thermally responsive polymers (Ellison and Torkelson 2002).

The *calibration* of probe response is complicated if a single channel measurement of intensity is made only. It could be natural to make the response signal ratiometric. The intensity measurements needs for that the application of a reference, and such reference signal can be introduced in different ways. As in other application areas, the best solution could be to use a single dye with two response channels so that the two signals could exhibit different temperature dependence.

The dyes exhibiting *fluorescence* and *phosphorescence* simultaneously or the systems allowing detection of both fluorescence and long-lived luminescence of metal complexes deserved special attention. This is because for the two types of these emissions the thermal quenching is different; the emission with *longer lifetime* is *quenched stronger*. Because of that, the ratio of their intensities is temperature-dependent and can be calibrated as an empirical ratiometric parameter in temperature units. Since the phenomenon of thermal quenching is very general, many possibilities exist in optimal design of such temperature sensors. The complexes of rare earth ions incorporated into different glasses and crystals were reported to be efficient thermometers operating based on this principle. They can be efficient at the temperatures up to 600 °C with the resolution of the order of 1 °C (Wade et al. 2003).

The *monomer-exciplex equilibrium* between perylene and N-allyl-N-methylaniline embedded into polymer matrix is temperature-dependent. The monomer emits blue light and the exciplex green light. On the temperature increase, this equilibrium is shifted towards the monomer. The linear temperature dependence of the ratio of these emission intensities can be used for reading the temperature (Chandrasekharan and Kelly 2001).

Other excited-state reactions, such as the *excited-state intramolecular proton transfer* (ESIPT), can also be used in sensing. The aggregates of 2-(2′-hydroxyphenyl) benzoxazole (HBO) show a fluorescent ratiometric change in a range of temperature from 15 to 60 °C. The reversibility and robustness as well as the stability of the aqueous dispersion of aggregates show very good performances, which may be useful in the applications of molecular thermometers (Huang et al. 2006a).

The reader may expect that the thermometers using molecular mechanism of response should, in principle, achieve a *molecular-scale spatial resolution*. Such molecular thermometers have the potential of measuring the temperature gradients inside the living cells (Gota et al. 2008). In fact, there are two possibilities for such measurements. One is to use a protein or a nucleic acid with the defined range of thermal transition and to label it with an environment-sensitive fluorescent dye or a FRET pair (Ke et al. 2012). Such construct can be a good molecular thermometer in the range of this transition on a condition that no uncontrollable factors such as ligand binding or local pH could influence it.

The other possibility is to incorporate the temperature-responsive fluorescent nanoparticles calibrated in wavelength shift, lifetime or two-wavelength ratiometric ratio (Jaque et al. 2014). Such molecular thermometers are particularly needed for the sensing *on a tissue level*. They can provide control of clinical treatment of tumors by hyperthermia. It is know that the tumors are commonly more sensitive to high temperatures than the normal cells. Because of that, they can be selectively destroyed by thermal treatment. In order to avoid destroying the normal cells, the temperature has to be kept locally in narrow ranges (at about 42.5 °C). The dyes and nanoparticles with near-IR emission that fits the wavelength range of transparency of human skin and tissues can be used for such monitoring. It was shown that the nanoscale gold thermometers can effectively determine the local temperatures inside or around the targeted cancer cell (El-Sayed et al. 2006; Huang et al. 2006b).

The luminescent temperature sensing has found many *industrial applications*, particularly in aerodynamics and space technologies and also in polymer processing industry (Wang et al. 2013b). This is mainly because of the ability of visualizing the temperature gradients in the sample. This property may be useful in the case of necessity to test any industrial unit under gas or liquid flow conditions and to observe and quantify the thermal gradients that appear on this testing. One can resolve such problems in a very simple and elegant way. The surface can be covered with luminescent dye using the brush or sprayer, and after illumination, one can make the pictures. The luminescence response of such surface being calibrated and recorded provides information on the distribution of temperature (Chandrasekharan and Kelly 2001).

Up-converting materials are capable of absorbing near-infrared light and converting it into short-wavelength luminescence. The efficiency of this remarkable effect is highly temperature dependent and thus can be used for temperature determination (thermometry) on a nanometer scale. All the up-converting materials discovered so far display several (mainly two) narrow emission bands (see Sect. 5.6) each of which has its own temperature dependence. The ratio of the intensity of two of these bands provides a referenced signal for optical sensing of temperature, for example inside the cells (Fischer et al. 2011).

12.1.2 Molecular Barometry

The luminescence quenching effect depends not only on the temperature, but also, for long-living (microsecond-millisecond) emission, on pressure-dependent concentration of molecular oxygen in the medium, which allows *measuring the pressure*. The mechanism of this quenching is collisional, which allows both spectroscopic and lifetime measurements (Gouterman 1997).

The oxygen diffusion and its permeability in a thin polymer film coating can be put into the background of developing the pressure-responsive thin polymer films. Any object (even of the size of airplane or a bridge) can be covered with such a film,

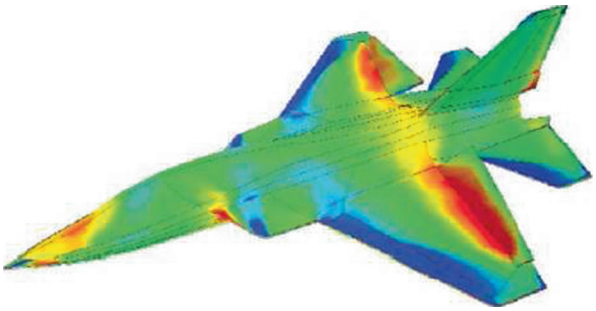

Fig. 12.1 Fluorescence picture of a model of an aeroplane painted with a pressure-sensitive paint, placed in a wind tunnel and imaged via fluorescence (Wolfbeis 2005). Pressure distribution is indicated via the spectrum-like sequence of pseudo-colours (*red*: high pressure; *blue*: low pressure)

and the pressure distribution on it following any applied strain can be detected by observing the luminescence response (Fig. 12.1).

Since the observed emission is influenced also by the temperature, a two-parameter temperature-pressure responsive layer can be suggested based on the response of two dyes. One of them, for instance, can be a platinum-porphyrin type complex and the other a europium chelate complex. Then, one of these emitters responds to pressure (with a small temperature dependence) and the other responds to temperature (with no dependence on pressure).

12.1.3 The Sensors for Gas Phase Composition

Determination of gases and vapors is a topic of great interest in various areas, including the monitoring of air quality, control of hazardous gases and vapors in industrial environmental and physiological investigations. Many fluorescent molecular probes have been rationally designed to change the fluorescence intensity or color in the presence of certain gases. To date, fluorescent probes for CO_2, SO_2, O_3, NO, CO, H_2S, singlet oxygen and many more complex molecules are known (Zhou et al. 2015). For generating the sensor signal, gases and vapors should be *adsorbed* at the surface or *absorbed* within a solid material used for recognition and producing the change in properties recorded as the response in fluorescence or other type of luminescence (Apostolidis et al. 2004). A simple and efficient *gas sens*or can be constructed based on a very thin polymer film or a film with a high level of porosity deposited on a solid support. Presently, the general tendency is to use the effect of quenching in a conjugated polymer (Kwan et al. 2004) or the lifetime sensing, in which the reporter function is played by ruthenium complexes exhibiting long-lifetime luminescence. This allowed developing a sol–gel complex for humidity sensing (McGaughey et al. 2006). The formation with such complex of a FRET pair with pH-active aso dye allowed creating the sensor for carbon dioxide (von Bultzingslowen et al. 2003).

Gasses are composed of small neutral molecules, and the specially prepared surfaces are needed for their adsorption. In some cases the *hydrogen bonds* can be involved in their recognition. They are rather weak noncovalent interactions formed between two partners – the donor (e.g. hydroxyl) and the acceptor (e.g. carbonyl). Transduction of signal on hydrogen-bonding interactions can be made with direct involvement of a dye containing proton acceptor group (Sect. 4.3), and this can be the method to generate the response. Such effect can be facilitated by incorporation of strong hydrogen bond donor (e.g. hexafluoroisopropanol) into conjugated polymer (Amara and Swager 2005). The target binding perturbs the electronic system of polymer and activates the ICT quenching. The film made of this polymer showed the quenching upon exposure to pyridine vapor.

Monitoring the *oxygen* concentrations is particularly important in chemical or clinical analysis and environmental control. Recently, a variety of devices and sensors based on the quenching of photoluminescent states of organic dyes have been developed to measure partial pressure of oxygen on the solid surface (Wang and Wolfbeis 2014). Many optical oxygen sensors are composed of organic dyes, such as polycyclic aromatic hydrocarbons (pyrene, pyrene derivative etc.), transition metal complexes (Ru^{2+}, Os^{2+}, Ir^{3+} etc.), metalloporphyrins (Pt^{2+}, Pd^{2+}, Zn^{2+} etc.) and fullerene (C-60 and C-70) immobilized in oxygen permeable polymer films (Amao 2003)

Many *explosives* are electron-deficient highly nitrated organic compounds, such as nitroaromatics, nitramines or nitrates. Their detection is a major security concern, therefore the tests need to be performed rapidly and 'non-invasively' in public places by detecting their trace amounts in vapors. Much effort has been made for that, and the major trend is to exploit the electron-acceptor properties of these molecules in the systems producing fluorescence quenching by photoinduced electron transfer. The thin films of conjugated polymer were suggested to apply for this purpose. This approach allowed developing a device that is able to detect the vapors of *trinitrotoluene* (TNT) on the femtogram level (Thomas et al. 2005).

Gas sensors based on *oligodeoxyfluorosides* (ODFs) were recently introduced. ODFs are emissive oligomers composed of multiple fluorophores assembled on a DNA backbone. The properties of a certain ODF sequence, such as emission color or sensitivity to chemical compounds, are encoded by the sequence of fluorophores attached to the sugar-phosphate backbone of DNA. Combinatorial libraries of ODFs can be generated using the solid-phase phosphoramidite chemistry. Screening of ODF libraries toward different volatiles resulted in the identification of sensors for toxic gases (Koo et al. 2011a) and also for volatile metabolites of bacteria (Koo et al. 2011b) and vapor-phase identification of petroleum products in contaminated soil (Jiang et al. 2013).

In conclusion, it should be added that fluorescence or luminescence-based gas sensors are often needed in a combination that could allow obtaining the recognition pattern for many ingredients and that the low-specificity binding can be useful for forming this pattern. Such '*electronic nose*' approach will be discussed in Sect. 15.5. It should be noted, however, that in this respect the optical detection techniques are in strong competition with that based on semiconductor thin films that allow direct detection of electrical signal. The future will show, which of these technologies will demonstrate stronger potential for improvement and better ability for applications.

12.2 Probing the Properties of Condensed Matter

The choice of proper medium is important for all the technologies that involve chemical synthesis and separation/purification of reaction products. The dye molecules exhibiting sensitivity of their emission to variations of many properties in their molecular environment, such as *polarity*, *fluidity*, *molecular order* and *mobility*, can be used to characterize these properties. The distinction between probes and sensors is not always clear in these cases. When these integrated parameters characterizing the liquid medium are to be obtained, we will consider these dyes as *probes*. Meantime, the same parameters can be used for providing the response in these media to particular targets. In the latter cases, they can be employed as sensors.

12.2.1 Polarity Probing in Liquids and Liquid Mixtures

Fluorescence probes are frequently used for characterizing *polarity* and *viscosity* of various condensed media. Since in this case the response is provided by molecular structures and on molecular level, it some systems it may appear different from that obtained by macroscopic technique because it may reflect variations of molecular structures of solvents and solutions. For instance, the commonly measured *viscosity* as the resistance to liquid flow may not perfectly match to the data obtained by detection of mobility on molecular level. Therefore it is often called '*microviscosity*' or '*nanoviscosity*'. Meantime, in many applications a *continuous approximation* is applied, in which the fluorescence response of 'nanoviscosity' is calibrated in standard solvents with the known 'macroscopic' viscosity. This allows using the same poise units.

The same is with the term '*polarity*'. Physical definition of polarity is quite different from that used by chemists and physical chemists. It is based on the analysis of intermolecular interactions (see Sect. 4.3) and can be studied with fluorescent dyes (Suppan and Ghoneim 1997). Physical description is very important for the development of new dyes as molecular reporters and probes, since their molecular parameters are included into the physical analysis of spectroscopic data. In contrast, the chemists often use the polarity scaling that is calibrated on the basis of distribution of matter between water and hexane (e.g. P-scale). Finally, physical chemists prefer empirical scaling based on an empirical correlation of polarity with some spectroscopic property, usually the shifts of absorption or fluorescence spectra of the applied probes (Reichardt and Welton 2011).

The specially designed or selected probe molecules possess the most remarkable properties to exhibit the solvent-dependent shifts of absorption or fluorescence spectra. On the basis of these effects several *empirical solvent polarity scales* were suggested (Catalan 1997; Reichardt and Welton 2011). They are not totally equivalent, and the scatter of experimental data against these scales is significant, even within the families of structurally related solvents. It can be observed that the classical scale based on the absorption wavelength shifting for *non-fluorescent betaine*,

$E_T(30)$, and its normalized version, E_T^N, (Reichardt and Welton 2011), remains the most reliable among many suggested scales. The newly suggested dyes as polarity calibrators based on absorption or fluorescence are neither universal enough to cover the broadest range of solvents nor specific enough to investigate the mechanisms of deviations from simple regularities provided by specific features of every solvent.

The use of *pyrene* as a probe allows exploring the polarity-dependent change in relative intensity of two vibronic bands in its fluorescence spectrum (Dong and Winnik 1984). Among the wavelength-shifting dyes the strongest polarity-dependent effect is observed for the dye called Fluoroprobe, possessing a strong intramolecular charge transfer (Hermant et al. 1990). Next in efficiency are ketocyanines and dialkylaminonaphthalenes, such as Prodan (Sect. 4.3). Unfortunately, Fluoroprobe is severely quenched in protic solvents, and the two other types of dyes in these solvents exhibit the shifts due to hydrogen bonding, almost as strong as the whole polarity scale.

The two-band emissive *3-hydroxychromone dyes* allow not only obtaining a highly sensitive ratiometric response to polarity but also providing the means for discriminating polarity and hydrogen bonding effects (Demchenko 2006). Their two-band ratiometric response is so sensitive that a series of different dyes had to be developed for determination of polarity in its narrow ranges. Several dyes with small variation in structure (the major variation in the ICT property of the N* state) can cover the whole polarity scale (Fig. 12.2).

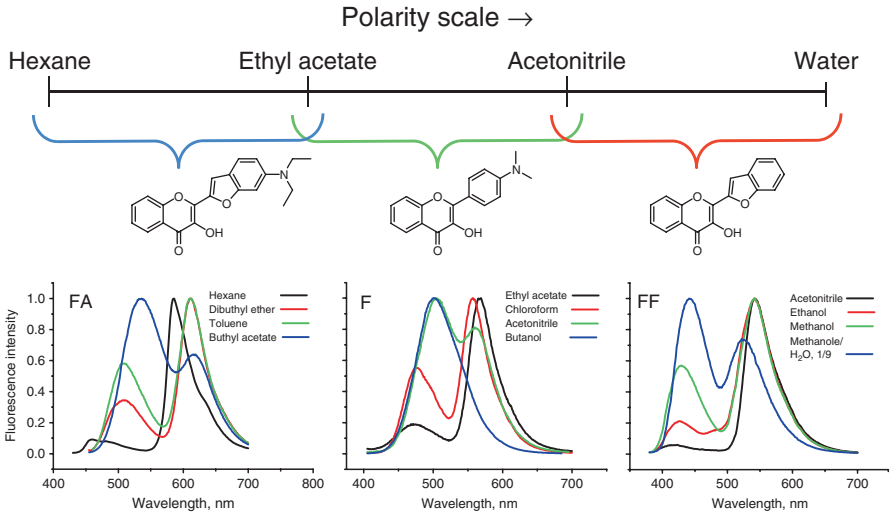

Fig. 12.2 Polarity scale marking the range of two-band ratiometric response of typical 3-hydroxychromone derivatives and their representative spectra in selected solvents (Demchenko et al. 2013). The higher is the solvent polarity, the dye with smaller excited-state dipole moment is needed for switching between two emission bands

It must be acknowledged that the empirical scaling is useful in the studies of solvent mixtures, interfaces and micro-heterogeneous systems, such as micelles (Yesylevskyy and Demchenko 2011). In the broadest sense, *polarity* is an efficient variable describing the interaction forces of the probe with the solvent and its components. Their description must involve several molecular properties (electronic and nuclear polarizabilities, abilities to form specific bonding), and therefore it is difficult to provide a strict definition of polarity and provide its measurement in a straightforward manner. The empirical methods use the description of polarity with a single parameter and therefore they are simple in application. Providing satisfactory description of polarity-related properties in many systems, they are very popular.

The necessary condition for the dyes to exhibit spectral shifts in response to variation of solvent polarity is a strong change of their dipole moments on electronic excitation. There occurs the response of dye environment to this change, as a change of electronic and nuclear polarizations that determine the polarity. After classical works of Gregorio Weber, most of the activities were focused on finding the dyes with a dipole moment *increase*. Meantime, the dyes with dramatic *decrease* of the dipole moment also exist. Those are the cyanine dyes. These dyes with red and near-IR absorption and emission promise prospects for using two-photon absorption and as FRET acceptors in different sensor technologies, especially for *in-vivo* sensing. The long-chain cyanine dyes respond to changes of polarity by their two-band response in *excitation spectra* (Lepkowicz et al. 2004).

As it is shown in Fig. 12.3, an increase in the length of polymethine chain leads to a symmetry breaking and the appearance of two forms with symmetrical and

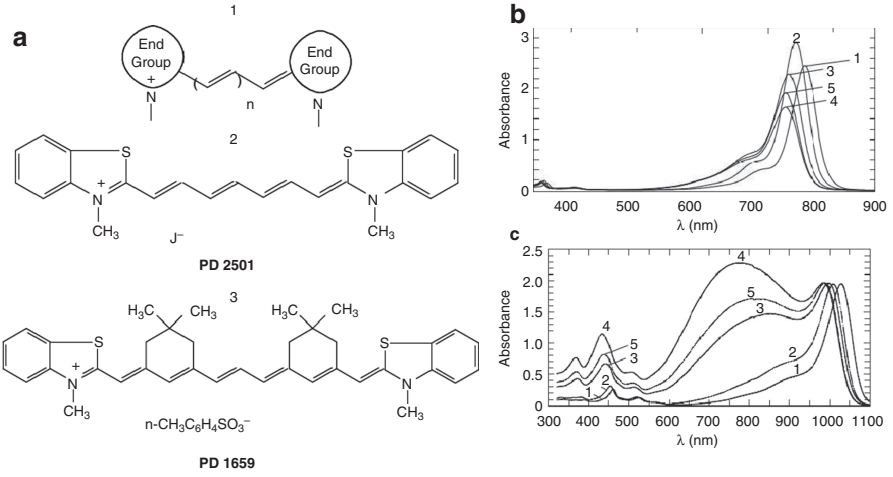

Fig. 12.3 Selected representatives of polarity-sensitive near-IR polymethine dyes. A. The structures of PD 2501 and PD 1659 dyes. B. Their Absorption spectra for PD 2501 (**a**) and PD 1659 (**b**) in o-dichlorobenzene (*1*), methylene chloride (*2*), ethanol (*3*), acetonitrile (*4*) and methanol (*5*) (Reproduced with permission from (Lepkowicz et al. 2004))

asymmetrical distributions of the charge density in the ground state. This distribution depends on the substituents in the chain and for some dyes is strongly polarity-dependent.

12.2.2 Viscosity and Molecular Mobility Sensing

For sensing *molecular dynamics* in condensed-phase systems such as liquids, polymers and glasses, a fluorescent dye should respond by the change in its spectroscopic parameters to the change of *translational or rotational diffusion* in this system. The oldest and simplest method to measure solvent viscosity is to apply the dye exhibiting molecular rotation with the detection of anisotropy and application of Eq. (3.8) connecting determined *rotational correlation time* with solvent viscosity.

The other possibility is to use the dyes possessing *mobility of their segments*. In low-viscosity medium these dyes are free to rotate, and such rotation induces the quenching (Baptista and Indig 1998). In rigid media such dynamics is frozen and a bright emission appears. Typical in this respect is the behavior of triphenylmethane dyes, such as Crystal Violet and Malachite Green. They possess the three-blade propeller-like phenyl rings joined by the central carbon atom. Viscosity-dependent flexibility of these dyes comes from their peculiar structure that allows mobility of phenyl rings resulting in fluorescence quenching. Therefore, the lifetimes τ_F depend strongly on the solvent viscosity and, due to the absence of groups forming specific noncovalent bonds, practically do not depend on other solvent properties. Being about 40 ns in rigid environments, τ_F drops to several picoseconds in room-temperature methanol ($\eta \sim 0.6$ cP).

Isomerization dynamics can be coupled with the dynamics of formation-breaking of complexes with solvent molecules. Such effects were observed in asymmetric polymethine dyes and applied for studies of microviscosity of membranes and living cells (Volovik et al. 1994). The two forms, one detected in solid, the other – in liquid environments, differ strongly in fluorescence spectra. So, in fluorescence spectra excited at 600 nm the 'solid' band observed in solid media is located at 700–710 nm and 'liquid' band is the only feature of the spectrum in liquid media, it is located at 760–770 nm. In solid media the spectrum weakly depends on the solvent, and in liquids this dependence does not exist at all (Fig. 12.4). In viscous media (e.g. glycerol) both of these forms coexist, so that the ratio of their intensities can be calibrated as a function of viscosity. Amazingly, neither position of these bands nor the intensity ratio shows notable dependence on any solvent parameter except viscosity (Volovik et al. 1994).

An attempt to provide wavelength-ratiometric response to viscosity was recently made also with the aid of substituted styryl pyridinium probe (Wandelt et al. 2005). This dye is soluble and strongly fluorescent in aqueous solution, displaying dual excitation peaks at 469 and 360 nm detected at emission wavelengths 500–650 nm,

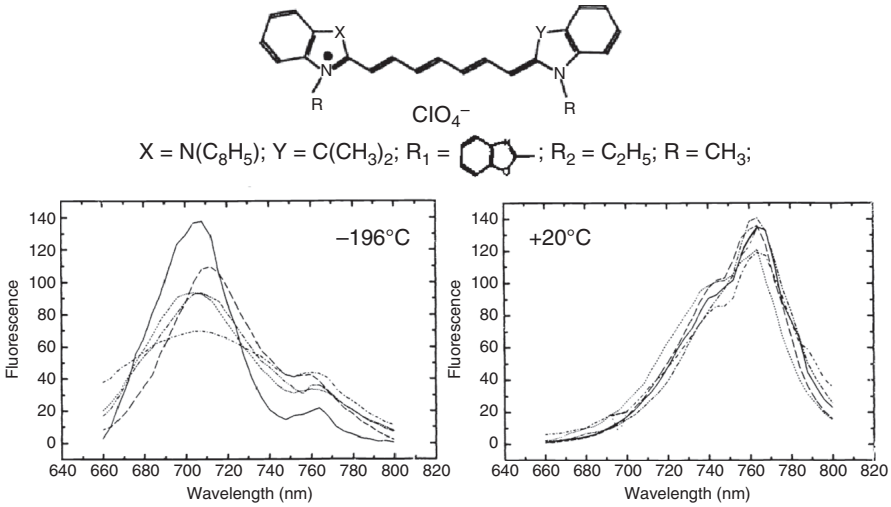

Fig. 12.4 Fluorescence spectra of asymmetric polymethine dye at −196 °C and +20 °C in ethanol (– – – - -), acetone (– – – – –), acetonitrile (- – -), dimethylformamide (– · - · - ·) and chlorobenzene (—) (Volovik et al. 1994)

indicating the formation of ground-state complexes with the solvent. The dye could be irreversibly loaded to a living cell, which allowed obtaining distribution of viscosity in the cytoplasm using fluorescence imaging microscopy with a spectrofluorimeter in dual-excitation single-emission mode.

An alternative way for providing viscosity sensing is to use highly dipolar 'polarity-sensitive' dyes and to study the *rates of dielectric relaxations* in their environment with the aid of time-resolved spectroscopy (Vincent et al. 1995) or by the observation of the Red-edge effects (Demchenko 2002). The problem here is that high and wavelength-selective temporal resolution is needed in the conditions when the dielectric relaxation rates match the time scale of fluorescence lifetimes. For low-viscosity liquids it is the scale of several picoseconds, which is very inconvenient for routine measurements. These methods can be used in highly viscous systems in which the relaxations are nanosecond or longer.

Viscosity-sensitive response can be achieved with *fluorescent molecular rotors*. They are fluorescent dyes exhibiting viscosity-dependent isomerization in the excited state that modulate fluorescence response. An example of such molecules is 4-tricyanovinyl-[N-(2-hydroxyethyl)-N-ethyl]aniline (TC1). Such molecules can be covalently bound to a fiber-optic tip without loss of viscosity sensitivity. Covalently bound fluorescent molecular rotors exhibit a viscosity-dependent intensity increase similar to molecular rotors in solution. An optical fiber-based fluorescent viscosity sensor may be used in real-time measurement applications ranging from biomedical applications to the food industry (Haidekker and Theodorakis 2007).

The problem of introducing the reference for ratiometric measurements that is common for all intensity-based sensors is actual also for viscosity sensors. It can be solved, for instance, by fusing viscosity-sensitive and viscosity-insensitive dye with resultant ratiometric detection (Fischer et al. 2007). Meantime, the best solution could be provided by viscosity-sensitive ratiometric dyes that require no reference, as it was shown in previous studies (Volovik et al. 1994).

In addition, the conjugation of fluorescent molecular rotors to specific recognition groups allows them to target specific sites in cells, for example the cell membrane or cytoplasm (Kuimova 2012). Membrane viscosity characterizes dynamic processes determining the membrane transport and cytoplasm viscosity is an important characteristics of intracellular diffusion of enzymes and metabolites. Molecular rotors are therefore emerging as important functional biosensors for local microviscosity measurements (Nipper et al. 2008), but intensity sensing seems inappropriate in view of uncertain distribution of the probe dyes within the cells. For molecular rotors primary solution for obtaining the dye concentration independent response must be the lifetime sensing (Kuimova et al. 2008).

Thus, fluorescence probes allowed obtaining polarity and viscosity scales of common liquids that can be used for evaluation and selection of different liquid compositions and for characterization of heterogeneous media and even the condensed media with poorly understood molecular properties, such as ionic liquids and supercritical liquids.

12.2.3 Probing the Ionic Liquids

Room-temperature ionic liquids have recently acquired a lot of interest in view of their attractive properties as the media for chemical reactions involving synthesis, catalysis and extraction (Chiappe and Pieraccini 2005). They are usually composed of organic cation (alkylammonium, alkylphosphonium, imidazolium, pyridinium, isoquinolinium) and an inorganic anion. They remain liquid over a wide temperature range, including room temperature, and in normal conditions they behave as molten salts. Many ionic liquids are colorless and optically transparent over a wide spectral range, from UV to near-IR, which does not create any problems for their optical studies.

High viscosity and the absence of sharp freezing point suggest a ‘supercooled’ nature of ionic liquid media and their nano-structuring. Therefore, the study of their molecular dynamics with fluorescence probes attracted much attention. The time-resolved spectroscopy with excitation-wavelength selection (Funston et al. 2007) allowed to show that in the origin of high viscosity of these solvents is the very slow rate of dielectric relaxations, which are in the range of hundreds of nanoseconds. This is by a factor of 10^4–10^5 slower than in common liquids (Hu and Margulis 2006).

It was shown, that ionic liquids exhibit both static and dynamic disorder. *Static disorder* is the characteristics of the system when on a relatively long time scale

each molecule reveals the peculiar local and stable characteristic of its environment that may be different from that of another molecule situated within this system. A *dynamic disorder* appears when the probe molecules are located in different environments but these environments interchange dynamically on a time scale of emission. Static disorder is characteristic of solid systems (e.g. glasses) and it is characteristic for the polymers in glassy states, whereas dynamic disorder is observed in molten polymer states. They can be easily distinguished and characterized with fluorescent dyes using the Red Edge wavelength-selective fluorescence spectroscopy (Demchenko 2002).

Interesting features of excited-state reactivity were revealed with *3-hydroxyflavone* probe (Kimura et al. 2010). It was confirmed that *solvation dynamics* corresponds to that in high viscosity solvents and is much slower than the fluorescence emission. Meantime, the excited-state proton transfer reaction proceeds on a much faster scale, in the absence of dynamic equilibrium with the solvent (Demchenko et al. 2013). The fact that reaction dynamics can be decoupled from solvation dynamics may be an important feature of chemical reactivity in ionic liquids as the solvent media.

12.2.4 The Properties of Supercritical Fluids

Supercritical fluid is a unique state of condensed matter, which can be reached in liquids by simultaneous increase of temperature (T) and pressure (P) above their critical points T_c and P_c. In these conditions, the liquid and gas phases coalesce into a single phase. Its properties, such as density, viscosity and the diffusion rate, can be tuned continuously in broad ranges by simply adjusting T and P values without changing the solvent composition. Combination of liquid-like but tunable solvation properties with gas-like rates of molecular diffusion makes supercritical fluids very attractive solvent media for chemical reactions. In this respect, supercritical CO_2, being both efficient and non-toxic, presents an attractive example of the medium for the future 'green' chemical synthetic technologies.

A high level of *fluctuations of physical properties* is characteristic for critical phenomena. Dynamic molecular clusters are forming and breaking in these systems. Such clusters have also to surround the solute molecules that can be the fluorescent dyes. As in liquid solvents, polarity may serve as an important characteristic predicting the solubility and reactivity of different compounds.

The studies with solvent-sensitive fluorescent dyes have shown that close to the critical temperature and pressure, the local solvent density around a solute molecule is higher than the actual bulk value. Such enhanced solvent density was explained as the witness of such 'clustering' or 'local density augmentation' (Abbott et al. 2007).

An interesting effect was observed in the pressure dependence of fluorescence of wavelength-ratiometric 3-hydroxychromone dye exhibiting the ESIPT reaction in supercritical CO_2 (Barroso et al. 2006). Figure 12.5 shows that the fluorescence spectra, normalized at the normal emission maximum (422–428 nm) nm,

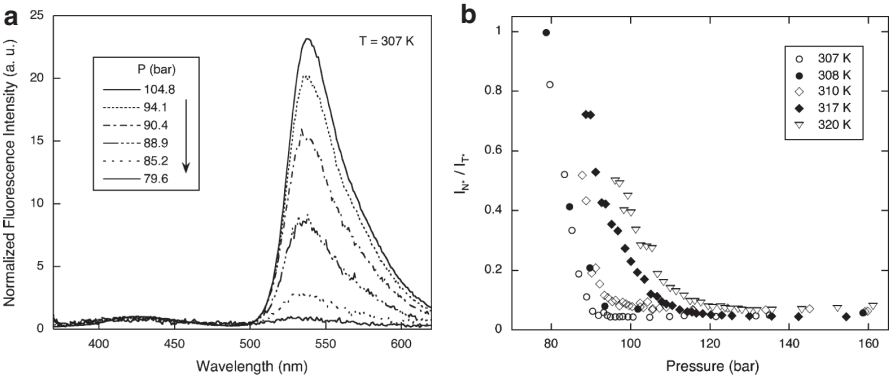

Fig. 12.5 The results of fluorescence studies in supercritical CO_2 at different pressures and T 307 K (Barroso et al. 2006). The λ-ratiometric dimethylamino-3-hydroxyflavone dye (see Fig. 12.2) was used as the probe. (**a**) The spectra normalized to the maximum of the normal band (428 nm) to emphasize the change in the relative intensities of the normal and tautomer bands. (**b**) The pressure dependence of ratiometric response at different temperatures. Excitation wavelength was 350 nm

demonstrate a dramatic increase in the tautomer band (535–538 nm) intensity with an increase in the pressure of the system. As the density exceeds 0.7 g/mL, the relative intensity of the two bands tends to a constant value, indicating the polarity similar to that of apolar organic solvents, such as toluene and di-*n*-butyl ether. At lower densities, the substantial decrease of the total fluorescence intensity (a 600-fold decrease as the pressure decreases from 100 to 80 bar) is accompanied by an even more accentuated decrease of the tautomer fluorescence.

If the intensity ratio is considered only, such behavior could mean a dramatic increase of polarity. Meantime, the true explanation is different. An impressive dynamic fluorescence quenching at low pressures makes the fluorescence rates comparable or even shorter than the rates of ESIPT reaction (see Sect. 3.8), so the excited species simply have no time for transition to a tautomer state exhibiting the long-wavelength band in emission. The origin of such dramatic quenching at low pressures is probably related to a more 'naked' environment of fluorescent dye and its greater exposure to collisions with CO_2 molecules possessing high kinetic energies.

12.2.5 The Structure and Dynamics in Polymers

Polymers are the well-known systems in which estimation of molecular parameters characterizing segmental dynamics and interactions is important for understanding their macroscopic properties. This can be done by fluorescence probe techniques. Their application allows to study the dynamic processes of interest, such as polymerization kinetics and mechanisms, thermal transitions, photodegradation, swelling

in solvents, and so forth (Bosch et al. 2005). In polymer studies the fluorescent probes that sense both polarity and viscosity (or molecular void volume in solid samples) are of special value. Usually these are the dyes that exhibit photoisomerization dynamics, such as 2-(4-dimethylaminostryl)benzoxazole and its butadienyl analogues (Fayed and Etaiw Sel 2006)

Fluorescence polarity-sensitive probes and fluorescent molecular rotors as viscosity probes have found many applications for monitoring the reaction of polymerization (Quirin and Torkelson 2003) and for controlling desorption of water from polymer films (Ellison et al. 2004). Very important is their application for characterizing and monitoring the structural transitions in polymers.

One of the most interesting applications of fluorescence probe method is the study of the local dynamics of a polymer matrix at the onset of the *glass transition* (Deschenes and Vanden Bout 2001). In these experiments, the molecules of organic dye Rhodamine 6G dispersed within a thin poly(methacrylate) film were observed at temperatures slightly above the melting temperature of the polymer. Fluorescence polarization was used to follow a slow rotational diffusion of individual molecules over several hours. This study demonstrated in these conditions the presence of both static and dynamic disorder.

Some polymers can exist in *highly elastic state*. Being macroscopically solid, they differ substantially in dynamic properties from that in glassy state. Application of polymethine dye as a probe and investigation of static and time-resolved spectra allowed to reveal and characterize the relaxation processes in one of them, polyurethane acrylate, on the nanosecond time scale (Przhonska et al. 1999). The dye developed and used in these studies has a unique property of ICT-dependent change in the conjugation length in the excited state, which leads to strong Stokes shifts, even in rigid polymer media. Its application allowed revealing the important features of molecular dynamics in elastic polymers that could not be detected with common dyes.

A new field of applied research is the study of structural transformations (e.g. glass transitions) of polymers in the forms of thin films and nanoparticles (Masuhara et al. 2006). Among other areas, these data are needed for sensor technologies themselves.

An important application of fluorescent probes is in optimization of polymer properties by rapid screening of many samples varying in composition, technology of preparation, etc., so that the combinatorial discovery cycles can be developed (Potyrailo 2006). Selection of fluorescence dyes for this purpose depends upon the desired properties to be optimized.

12.2.6 Fluorescence Probing the Interfaces

In many cases, it is important to characterize the structure, dynamics and interactions at liquid-liquid, liquid–solid and solid-solid interfaces and at the liquid and solid surfaces exposed to air (Yesylevskyy and Demchenko 2011). Most straightforward

in these cases is to locate at the interface region the small environment-sensitive dye molecules (probes). It can provide information on static properties such as polarity, hydrogen bonding ability and electrostatic potentials, and also on the dynamic properties, such as the rates of segmental motions and the rates of dielectric relaxations (rotations of dipoles surrounding the probe).

In *liquid-liquid interfaces*, the strongly *amphiphilic* dye molecules (containing both apolar and polar sites) can concentrate at the interface between two non-miscible liquids and report about the properties of their interface. Sulforhodamine dye located at the interface demonstrates intermediate polarity between two phases as it is witnessed by time-resolved spectroscopy with total internal reflection observation (Ishizaka et al. 2001).

In *solid–liquid interfaces* some interactions that are saturated in bulk liquid can remain unsaturated with some new interactions formed. The same is with *solid-solid interfaces*. Commonly in these cases, the dye is attached to the surface of one component before depositing the other component. Sometimes the third component is used that serves for providing adhesion between interacting surfaces, and it can be used for introduction of fluorescence sensing dye. In the studies of the surfaces exposed to gas phase the dyes can be incorporated in a similar way.

The *small-size organic dye* molecules are commonly used to study interfaces, including the nanoparticles, the surfaces of protein molecules and biomembranes (Epand and Kraayenhof 1999). This is because the interfaces are the sites of greatest gradients of all molecular properties and in view of the fact that the probe sizes should be commeasurable with the sizes of molecules and groups of atoms forming these gradients. The dyes are usually used as the environment-sensitive probes. In addition to spectroscopic properties, the dye solubility in both media with strong preference to interface is particularly important. It can be enhanced by covalent modification with correspondent 'affinity' groups.

In *solid-solid compositions*, the silane coupling agents are commonly applied to glass fibers to promote fiber/resin adhesion and to enhance durability in composite parts. In one of the studies (Lenhart et al. 2000) a multilayer coupling agent on glass was doped with the trace levels of dimethylaminonitrostilbene (DMANS) dye. A 53-nm blue shift in fluorescence spectrum from the position for immobilized DMSCA can be followed during cure of an epoxy resin overlayer, which indicates a substantial decrease of polarity and increase of rigidity of dye environment. Such effects were observed only in the case of very thin silane layers. Thicker layers showed smaller fluorescence shifts during cure, suggesting incomplete resin penetration into these layers (Lenhart et al. 2002). This result shows the potential of such approach to monitor the properties of the fiber/resin interface during the composite processing.

In another study (Olmos et al. 2003, 2005) the interfaces between glass fibers or silica particles coated with silanes and epoxy polymer were studied using dansyl and pyrene labels. An increased heterogeneity of interactions and structural rigidity were indicated in comparison to epoxy bulk. Comparing the curing reaction in the polymer bulk and at the interface, it could be concluded that the epoxy curing at the interface proceeded faster but only during the first stages of the reaction.

12.3 Detection of Small Molecules and Ions

The broadest diversity of approaches involving the design and operation of recognition units, reporters and transduction mechanisms are used in these applications. They involve both synthetic chemical sensors and biosensors.

12.3.1 pH Sensing

pH is the measure of *proton concentration* in the studied medium. It is also an indicator of ionization state of many compounds dissolved in water and modulator of their reactions. It is also an essential parameter in cell physiology determining the rates of many biochemical reactions that operate within a narrow (commonly, neutral) pH range. Therefore, many fluorescent pH indicators and sensors are developed and actively used.

Sensing pH is based on the fact, that in some fluorescent dyes the ionization of attached groups changes dramatically the spectroscopic properties leading to the appearance of new bands in absorption and in emission. The titration ranges in absorption and in emission usually do not correspond. Because the acidity of these groups is much higher in the excited than in the ground state, the pH range of sensitivity in emission becomes dramatically shifted to lower pH. If the two forms are fluorescent, one can obtain with a single-band excitation the two emission bands that belong to neutral and proton-dissociated forms. During gradual pH change with fluorescence detection, one of the forms disappears and the other one appears in a coupled manner. The equilibrium between these forms can be established on a very fast time scale (Laws and Brand 1979; Davenport et al. 1986). This allows λ-ratiometric recording (Demchenko 2014).

Among the dyes suggested as fluorescent indicators of pH, benzo[c]xanthene derivatives such as C-SNAFL-1 (Whitaker et al. 1991; Mordon et al. 1995) are the most extensively used. Their excitation spectra may reflect the ground-state proton dissociation, and in emission spectra the pH-dependent appearance of strongly red-shifted second band is due to deprotonation of hydroxy group in the excited state. A number of other dyes have been synthesized that have the ability to change their ionization state in the ground and excited states as a function of pH. Among them is the new water-soluble 3-hydroxychromone dye, 3,4′-dihydroxy-3′,5′-bis(dimethylaminomethyl)flavone that exhibits two-band ratiometric response in a broad pH range (Valuk et al. 2005).

The *range of detectable titration* of ionizable groups obeys to the rule of equilibrium between two states (Sect. 2.3), and therefore the range of pH sensitivity in titration of a single group is limited to two sequential digits of pH. For increasing it, several ionisable groups ranging on a pH scale can be attached to a dye. Based on this principle, an optode-based sensor showing an almost linear pH response in the range from two to ten was constructed (Li et al. 2006). It uses amino-functionalized corrole immobilized in a sol–gel glass matrix. Other researchers (Niu et al. 2005) constructed a ratiometric fluorescence sensor with broad dynamic range based on

two fluorescent dyes that were sensitive in different pH-ranges. The dyes were co-polymerized with acrylamide, hydroxyethyl methacrylate and triethylene glycol dimethacrylate on the silanized glass surface. The sensor covers a broad dynamic range of pH 1.5–9.0.

Following the excitation in the range 370–405 nm, the emission spectrum of a cell-permeable macrocyclic Eu(III) complex incorporating an N-methylsulfonamide moiety changes with pH, allowing ratiometric pH measurements in the range six to eight (Pal and Parker 2007). A number of other pH sensors based on emission of lanthanide chelates have been suggested (Bunzli and Piguet 2005). They use the change of Eu(III) fluorescence due to pH-dependent change in ionization state of chelating units.

Since many processes *in the living cell* depend on pH, its values (pH_i) are highly regulated and kept constant near the neutral values (exceptions are certain organelles such as lysosomes, in which pH is acidic). This regulation fails in some pathological conditions leading to acidosis or alkalosis. That is why an effort has been made to synthesize the cell-permeable fluorescence sensitive dyes (Han and Burgess 2009) and to develop the pH-sensitive fluorescent proteins. Such pH-sensitive member of GFP family has been described (McAnaney et al. 2002, 2005). It exhibits dual emission properties due to pH-sensitive excited-state proton transfer (ESPT) rate.

12.3.2 Oxygen

Oxygen sensing is needed in many areas of research and industry (Wang and Wolfbeis 2014). Oxygen is known as a very potent *collisional quencher* of long-living luminescence, so if the lifetime of sensor emission is sufficiently long on the scale of oxygen diffusion, the quenching rate is proportional to its concentration in the studied medium. Such decrease of quantum yield and lifetime is used as the major principle applied in oxygen sensing (Nagl et al. 2007; Quaranta et al. 2012). The most typical are the lifetime-based methods, since they allow avoiding the problem of self-calibration of output signal.

For the purpose of spectroscopic analysis of oxygen, the probes exhibiting both *fluorescence and phosphorescence* on the same intensity scale are very attractive. The short-living fluorescence is not affected by the presence of oxygen and may serve as the reference, whereas the long-living phosphorescence can provide the necessary response in quenching. Since phosphorescence band is strongly shifted to longer wavelengths, a very precise, convenient and self-calibrating detection can be achieved in a steady-state recording at two emission wavelengths. This makes alternative to lifetime measurements and may offer similar precision but needs a simpler instrumentation. The λ-ratiometric imaging of oxygen in living cells can be provided based on this principle (Fig. 12.6).

Of course, the two dyes, one phosphorescent and the other fluorescent, incorporated into one nanoparticle, can also be used for wavelength-ratiometric sensing of oxygen. A disadvantage in this case could be their different photostabilities. If one of the dyes is bleached, this will change the ratio of two signals in emission unrelated to oxygen sensing.

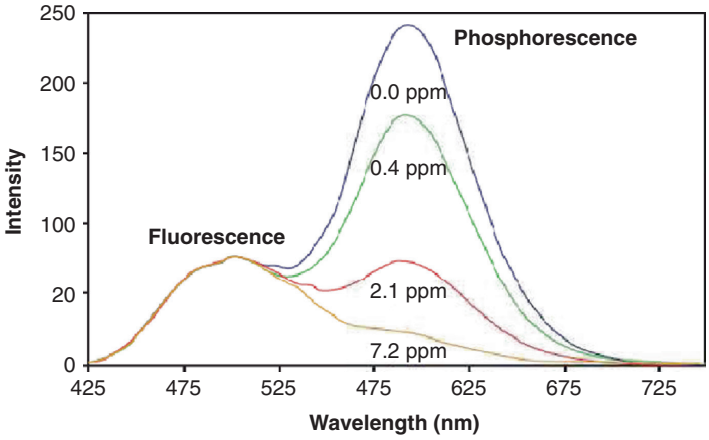

Fig. 12.6 An example of a wavelength-ratiometric phosphorescent oxygen indicator, which displays an oxygen-quenchable phosphorescence and a fluorescence emission that does not depend on the presence of oxygen (Hochreiner et al. 2005)

Different detection formats need to be realized in oxygen sensing. Thus, for application in cell culture bioreactor an external *fiber-optic probe* has to be incorporated (O'Neal et al. 2004). The suggested probe takes advantage of the oxygen-stimulated fluorescence quenching of dichloro(tris-1,10-phenanthroline) ruthenium (II) hydrate. This fluorophore was immobilized in a photo-polymerized hydrogel made of poly(ethylene glycol) diacrylate. The sensor showed a high degree of reproducibility across a range of oxygen concentrations that are typical for cell culture experiments.

12.3.3 Heavy Metals

Industrial pollution raises the necessity of determining the concentrations of *heavy metal ions* on a very low level, down to nanomoles, since even in such concentrations these ions can accumulate and display a negative effect. The most needed ions to be determined are Hg^{2+}, Cu^{2+}, Cd^{2+}, Co^{2+}, Pb^{2+} (Aragay et al. 2011).

The heavy metal ions are known as potent *fluorescence quenchers* (the quenching mechanism is the induction of intersystem crossing, the Kasha effect), and therefore the first-generation sensors were based on this effect. Further developments suggested the 'turn-on' sensors with the increase of intensity on ion binding (Liu et al. 2013). Such sensors were developed for copper (Konishi and Hiratani 2006), mercury (Huang and Chang 2006) an many other ions (Dutta and Das 2012) in aqueous solutions. Metal nanoparticles and quantum dots are becoming involved in the construction of nanosensors, and they offer an increase of sensitivity in detection. Meantime, the sensors that could fully satisfy practical needs have still to appear.

One of the most important applications of fluorescent detection methods are in control for heavy metal contamination of food and beverages. A series of organic

dyes combining ion recognition with fluorescence reporting have been synthesized for this purpose. Some of them possess nanomolar sensitivity of detection or the sensitivity quite sufficient for distinguishing non-toxic and toxic levels of contaminants (Domaille et al. 2008).

Fluorescence-based sensing systems for heavy metal ions have started to be developed based on *genetically engineered* living yeast cells. Such sensor was suggested for the detection of copper (Vopálenská et al. 2015).

12.3.4 Glucose

Glucose sensing is important both in food processing industry and in clinical chemistry. Close monitoring of *blood glucose* on the level of 10 mM is needed for diabetes patients and its increase requires immediate treatment. The existing devices based on enzyme sensors and electrochemical detectors have shown their limitations, and this fact encourages alternative approaches, one of which is the fluorescence sensing (Pickup et al. 2005; Steiner et al. 2011).

In this book, the clinical applications of chemical receptors for monitoring glucose level are overviewed in Sect. 14.1. The small-molecule sensors are represented by *boronic acid derivatives* (which bind the diols of sugars, see Sect. 7.2) coupled to organic fluorescence dyes, so that the direct mechanisms of their response based on PET or ICT can be used with the detection in intensity, spectral shift or lifetime. *Bioanalytical recognition units* include the lectin concanavalin A (Con A), enzymes such as glucose oxidase, glucose dehydrogenase and hexokinase/glucokinase, bacterial glucose-binding protein. In these cases, the most popular mechanism of response is FRET between a fluorescent donor and an acceptor within a protein that undergoes glucose-induced changes in conformation or re-arrangement of subunits.

Competitive displacement assays were also developed. They use fluorescently labeled dextran as a competitor in glucose binding to concanavalin A (Ballerstadt et al. 2004) or apo-glucose oxidase (Chinnayelka and McShane 2004). Plasmonic amplification of such assay based on gold colloid particles was reported (Aslan et al. 2004).

Though simple when performed in test tube, many of these methods a still far from the patient's use. They require taking the blood sample or invasion into the human tissue. The attempts to provide *noninvasive glucose monitoring* by the measurement of cell autofluorescence due to NAD(P)H, and fluorescent markers of mitochondrial metabolism are of interest. Two alternative approaches have a strong potential for development. One is to use biological fluids, the collection of which does not need invasion, such as saliva, sweat and tears. The introduction of contact lenses that light-up the increase of glucose level in tears is a remarkable step in this direction (Badugu et al. 2003).

The other approach is an attempt to provide in vivo monitoring based on the response of the safe near-IR dyes (Ballerstadt et al. 2004). The near-IR light can transmit through the skin and may provide an optical excitation and readout.

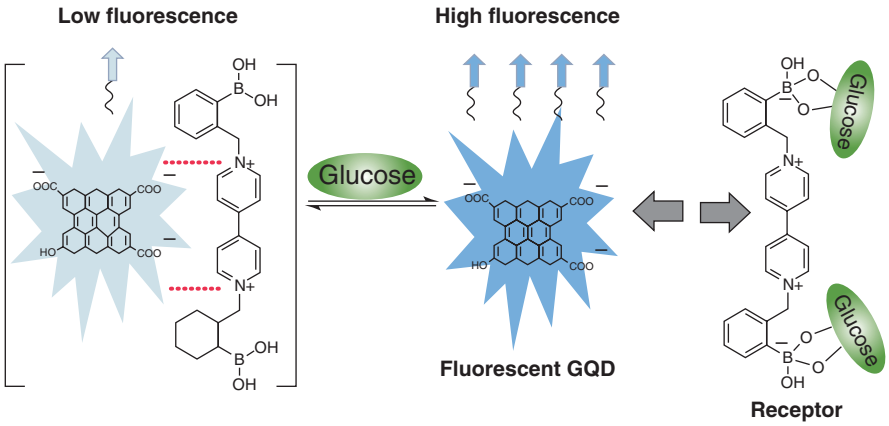

Fig. 12.7 Proposed glucose-sensing mechanism based on a cationic boronic acid-substituted bipyridinium salt receptor and fluorescent carboxyl-substituted graphene dot (Li et al. 2013)

New materials have started to be used in a search for the optimal glucose sensor. One of such proposals is to use graphene dots (see Sect. 5.4) as fluorophores the emission of which can be de-quenched on binding glucose to boronic acid sensor (Fig. 12.7).

12.3.5 Hydrogen Peroxide

Hydrogen peroxide (H_2O_2) with an oxygen-oxygen single bond is a strong *oxidizer* that is used in different industrial technologies. In trace amounts it is naturally produced in living bodies serving a second messenger in cellular signal transduction. It can also be a marker for oxidative stress. Overproduction of H_2O_2 is implicated with various diseases including cancer, diabetes, and cardiovascular and neurodegenerative disorders. Therefore, quantitative detection of H_2O_2 and other *reactive oxygen species* (ROS) is important in various areas of human life (Chen et al. 2011).

Luminescence probing is a common method for determining *hydrogen peroxide* (Schäferling et al. 2011). Both fluorescent small molecules (Abo et al. 2011) and nanoparticles with long emission decays are actively used in single-photon (Dickinson et al. 2010) and two-photon (Chung et al. 2011) modes of exciting fluorescence. These methods are applicable for imaging H_2O_2 in living cells and tissues, and with addition of affinity functionalities, they can detect its generation and transformation in different cellular compartments. Some of the novel dyes display wavelength-ratiometric response both in absorption and emission (Lin et al. 2008), which is very advantageous in sensing.

12.3.6 Cholesterol

Cholesterol is an important substance in clinical diagnostics due a strong correlation between total cholesterol in human blood serum and heart and blood vessels diseases. A large number of clinical disorders are related to arteriosclerosis, in which the role of cholesterol is very important. Presently the detection of cholesterol is based on the action of enzymes cholesterol oxidase and cholesterol esterase, so that hydrogen peroxide liberated in this reaction is the target for amperometric detection (Vidal et al. 2003).

The attempts to establish the *direct sensing* methods that avoid manipulation with enzymes include the application of cyclodextrin dimers labeled with fluorescent reporter dye (Liu et al. 2004) and europium-tetracycline complex (Silva et al. 2008).

The present author has made an attempt to use the well-known property of cholesterol to incorporate into lipid bilayers and to form very strong complexes (called 'rafts') when this lipid is sphingomyelin (see Fig. 9.19). We produced sphingomyelin vesicles with embedded wavelength-ratiometric 3-hydroxychromone dyes, and observed dramatic changes in florescence color upon incorporation of cholesterol molecules into these bilayer structures (Turkmen et al. 2005).

12.4 Nucleic Acid Detection and Sequence Identification

The detection and characterization of DNA and RNA is needed in many applications, which include all branches of biology, medicine, environmental control and forensic detection. Such extremely broad range of applications requires the search of diverse methodologies that should be optimal for every particular task. The last decade saw the active development of DNA high-throughput technologies. They are based on principles that are discussed in Chap. 11. The microarrays were successfully applied for genotyping and gene expression studies. The limitations in operation of this technology and insufficient reproducibility of its data required finding new solutions. The high performance techniques offered by modern biotechnology and nanotechnology will be discussed here.

12.4.1 Detection of Double-Stranded DNA

The request for detection of nucleic acids is often focused on finding and quantization of *double-strand DNA* (dsDNA) in solutions (homogeneous detection), or by visualization and quantification (staining) in electrophoretic gels, blots, arrays, and directly in living cells. In a living cell, genomic DNA commonly exists in dsDNA form, which allows its easy detection by fluorescence dyes. A number of cell-permeable and cell-impermeable dyes were developed for this purpose (Spence and Johnson 2010). The most attractive among them are the dyes that exhibit almost no fluorescence in water but a very high emission when they are bound with high affinity to DNA (with

enhancement by a factor of ~10^3 and higher). Particularly, acridine dyes and ethidium bromide possess this property (Haugland 2005), see Sect. 4.2. They can be used in *Fluorescent Intercalator Displacement* (FID) assays for the studies of interactions of different ligands with DNA. Displacing these dyes from their complexes with DNA results in their easily observed quenching, which allows in competition experiments (see Sect. 2.3) to obtain binding parameters of these ligands.

Affinity of these dyes towards DNA can be dramatically (by 10^3–10^4 times) increased upon the use of the *dimers of these dyes* instead of previously applied monomers. These dimers, such as EthD, YOYO and TOTO (Thiazole Orange dimer), carry four positive charges allowing strong electrostatic interaction with the negatively charged DNA (Fig. 12.8). Their binding is so strong, that electrophoresis of DNA labeled with nanomolar quantities of these dyes can be performed without the dye loss (Glazer et al. 1990). The affinity towards DNA and the brightness of fluorescence response are sufficient for single-molecular detection.

Free YOYO dye in aqueous buffer has absorption maximum at λ_{max} 458 nm and very low intensity of fluorescence emission at λ_{max} 564 nm. As for other intercalating dyes, this intensity increases (by 3200 times) upon binding to double-stranded DNA

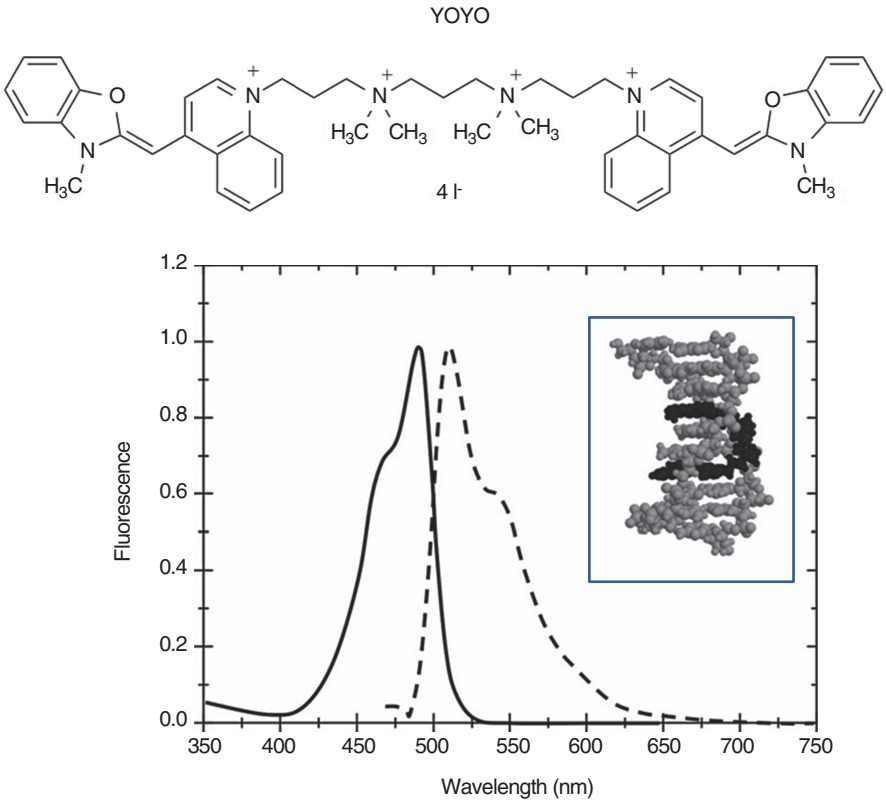

Fig. 12.8 Fluorescence excitation (*solid*) and emission (*dashed*) spectra of YOYO and the model of its intercalation into double-helix DNA structure

with some spectral changes (absorption: λ_{max} 489 nm, emission: λ_{max} 509 nm). The mode of incorporation (intercalation) into dsDNA is shown in the insert of Fig. 12.8.

In general, there are two major modes of binding of the dyes on the dsDNA molecules. One mode is the *intercalation* between the nucleic acid bases. In the double helix, the bases form planar couples stabilized by hydrogen bonds. *Intercalation* is the inserting and stacking of planar small-size molecules between the base pairs of the DNA double helix due to hydrophobic and van der Waals interaction. Intercalation is a noncovalent binding, in which the molecule is held perpendicular to the helix axis. This type of binding is characteristic for acridine, ethidium and thiazole dyes and their dimers. The planar dye molecule of the same size as the base pair accommodates between the neighboring base pairs. The major effect of fluorescence enhancement of these dyes is their screening from the quenching effect of water. In the cases of the dye dimers, the two heterocyclic parts intercalate between the base pairs, and the linker accommodates to the minor groove.

The other type of DNA-staining dyes are the dyes that bind directly to the *minor groove* of the double helix. In this case, the binding of dye molecules is mostly electrostatic, and great enhancement of their fluorescence upon the binding can be due to both displacement of water from their contact areas with DNA and to the suppression of their internal segmental mobility. The most know dye of this type is blue-emissive 4′,6-diamidino-2-phenylindole, or DAPI, which is extensively used in fluorescence microscopy to stain DNA in cell nucleus (Kapuscinski 1995). Other examples are the dyes known as Hoechst dyes (e.g. Hoechst 33258 or Hoechst 33342) which possess three positive charges per molecule. They are cell membrane permeable, and their positive feature is the strong Stokes shifts that allow exciting fluorescence at about 350 nm and observing it in the 500 nm region.

There are different *cyanine dyes* (Sect. 4.2) that are frequently used for DNA detection (Tatikolov 2012). Their advantage is the presence of low-polar groups together with the positive charge that provides specific affinity towards nucleic acids together with high brightness necessary for ultrasensitive detection. Fluorescence enhancement on their binding is due to dye fixation in trans-conformation. They demonstrate remarkable diversity of the binding patterns. The short-chain monomethine dyes act as intercalators, while the increase in polymethine chain length leads to increasing the potency for groove binding (Yashchuk et al. 2007; Kovalska et al. 2006). Their sensitivity can be even further increased by formation on this interaction of cyanine dye aggregates (Ogul'chansky et al. 2000; Yarmoluk et al. 2002).

12.4.2 Distinguishing Double-Stranded and Single-Stranded DNA and RNA

Many fluorescent dyes bind not only to dsDNA but also to *single-stranded DNA* (ssDNA) and RNA. Acridine orange is one of the earliest examples, for which such binding was described. The mechanisms of binding to double and single-stranded nucleic acids are so different, that there is a difference in emission color. When this dye binds to dsDNA, it exhibits green fluorescence, whereas bound to RNA its fluorescence

is red. Thus, the DNA in the nucleus stains green, while the RNA in cytoplasm – red. These observations were recently extended by an application of a number of acridinium derivatives, and those of them were found that bind to single strands of DNA and RNA with negligible binding to double-strand DNA (Kuruvilla and Ramaiah 2007).

Due to the presence of four positive charges, the ethidium dimer and also YOYO and TOTO dyes can also bind to ssDNA and RNA but with lesser affinity. To overcome these limitations, new fluorescent dyes were developed which can discriminate between ssDNA, dsDNA and RNA. Advanced variants of cyanine dyes marked by Life Technologies™ under names PicoGreen®, OliGreen® and RiboGreen® can be used to selectively quantify in solutions dsDNA, ssDNA and RNA respectively (Spence and Johnson 2010).

Many new possibilities appear in the studies of structures and interactions of nucleic acids using neutral 3-hydorxychromone (3HC) derivatives as color-changing λ-ratiometric dyes when they are attached to polycations. Using the labelled spermine as a probe, the binding to single-stranded or double-stranded DNA is easily distinguished by dramatic change in their double-band spectra (Klymchenko et al. 2008). As shown in Fig. 12.9, the response of 2-furyl-3HC dye

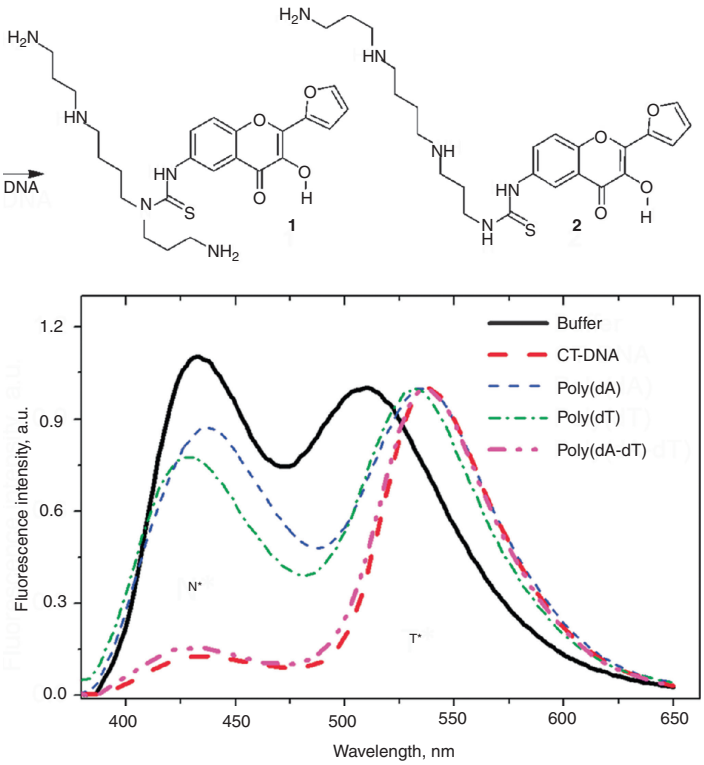

Fig. 12.9 Fluorescence spectra of spermine derivatives **1** and **2** labeled with 2-furyl-3HC dye interacting with single-strand (*blue*) and double-strand (*red*) DNAs (Klymchenko et al. 2008). Dramatic increase of relative intensity of long-wavelength ESIPT band intensity indicates incorporation of the label into a double-helical structure

label demonstrates the ratio of the two N* and T* emission bands to change up to 16-fold, so that the emission of the long-wavelength band increases dramatically. This suggests an efficient screening of the 3HC fluorophore from water molecules in the complex with DNA. In sharp contrast, only moderate changes in the dual emission on binding to a single-stranded DNA are observed, indicating a much higher fluorophore exposure to water at the binding site. Thus, the fluorophore being conjugated to spermine discriminates the binding of this polycation to dsDNA from that to ssDNA.

12.4.3 Sequence-Specific DNA Recognition

When the dyes bind to nucleic acids by intercalation, they do not exhibit sequence specificity. This is conceivable, since no specific interactions of the DNA bases participate in the dye binding. However, the required sequence specificity can be observed on *groove binding* in double helical structure. Here in addition to hydrophobic and van der Waals interaction, the electrostatic interaction between a dye molecule and charged phosphate groups can take place, as well as the hydrogen bonds formation with the base pairs and hydroxyl groups of sugar residues. Groove binders can be the *sequence-specific* also because of possibility to aggregate that extends the interactions within the groove (Vercoutere and Akeson 2002). An example of sequence-specific binding in the minor groove is DAPI, which preferentially bind to AT-rich regions.

Another example of site-selective binding to DNA is *pyrrole-imidazole polyamide* conjugates. These synthetic molecules have been developed on the basis of DNA-binding natural antibiotics and now are widely used in chemical biology. Conjugation of a fluorophore to pyrrole-imidazole polyamide chain gives many possibilities for site-selective DNA staining in fluorescence microscopy and other applications (Vaijayanthi et al. 2012).

Oligonucleotide or peptide nucleic acid (PNA) chains labelled with a fluorophore selectively bind to their complementary strands, which allows for the detection of specific DNA sequences in complex biological media. Fluorescent oligonucleotide probes are used in *fluorescence in situ hybridization* (FISH) to detect the presence of certain chromosomal DNA sequences. Additionally, the use of cyanine dyes such as thiazole orange (TO) covalently attached to the recognition chain as a base surrogate is more advantageous because of light-up response due to the phenomenon called *forced intercalation* (FIT). FIT probes have been used for wash-free detection of DNA and RNA sequences (Socher et al. 2008). They are effective in detection of viral mRNA molecules (Kummer et al. 2012).

An efficient recognition of complex DNA structures can be achieved with the proteins functioning as specific DNA binders and with their fragments retaining these properties. Their function requires structural motifs known as '*zinc fingers*'. The HIV-derived NCp7 protein is one of these examples. In an experiment illustrated below (Fig. 12.10), the truncated NCp7 peptide fragment (11–55) was prepared using solid phase peptide synthesis. At the last step of synthesis a carboxylic acid

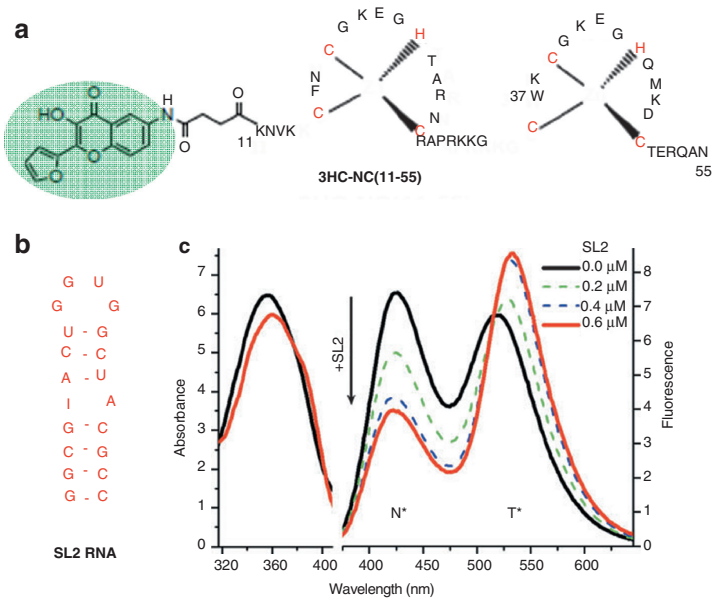

Fig. 12.10 Interaction of fragment NC(11–55) of the HIV-1 nucleocapsid protein labeled with 3HC dye (**a**) and SL2 RNA (**b**) (Shvadchak et al. 2009). (**c**) Changes in the absorption (*left*) and emission (*right*) spectra of 0.4 mM 3HC-NC(11–55) recorded in the absence (*black*) and in the presence of indicated concentrations of SL2 RNA. Excitation at 340 nm

analog of λ-ratiometric 3HC dye was covalently attached at the N-terminus of this peptide. This allowed obtaining direct reporting signal on oligonucleotide-peptide interaction (Shvadchak et al. 2009).

It was demonstrated that the addition of double-helical oligonucleotides to the solution of peptide conjugate leads to significant changes of the fluorescence spectra of the 3HC label: the N*/T* intensity ratio (see Sect. 4.3) decreases and the T* band (located at longer wavelengths) becomes dominant being shifted to the red. According to the data on the parent fluorophore in model solvents, the observed decrease in this ratio suggests the decrease in the environment polarity. Based on comparative studies with several oligonucleotides, it was shown that the labelled peptide displays a strong sequence-dependent fluorescence response. Thus, using the environment-sensitive 3HC dye one can observe not only the act of specific binding to nucleic acid sequence and determine the binding affinity (in titration experiment) but also get some information on the mechanism of molecular recognition.

12.4.4 The 'DNA Chip' Hybridization Techniques

Nothing is more specific than the recognition between specific DNA or RNA sequences that leads to the formation of double-helical structures. Such recognition is always in the background of *hybridization assays*. The two strands recognize

each other by formation of very selective hydrogen bonds between the complementary nucleic acid bases. Three such bonds are formed between guanine (G) and cytosine (C) base pairs, and two bonds are formed in complementary pairs of adenine (A) and thymine (T), for DNA, or adenine and uracil (U), for RNA. Due to collective effect produced on the affinity of interaction by multipoint binding, the formation of the first three-four base pairs is sufficient to trigger the process of hybridization. The formed hybrid double helices are highly specific and stable.

In order to possess the detection method that could satisfy many demands (such as in genomic analysis and/or clinical gene expression profiling), we have to resolve three technological problems. First, we need the *adequate transduction method* to generate a physically measurable signal from the hybridization event. Second, this method should be *extremely sensitive* to allow detection of formed hybrids on a picomolar level of concentrations and below. Third, this method should allow the use of *microarrays* (see Sects. 11.3 and 11.4) to apply essentially the same way of detection for all the spotted (or otherwise marked) sensor sequences.

With this prospective, we can critically analyze the 'DNA chip' technology that presently dominates in biomedical research and clinical diagnostics. It relies on a combination of amplification by *polymerase chain reaction* (PCR) or *reverse transcription polymerase chain reaction* (RT-PCR) of the whole pool of tested sequences and on application of organic dyes as the labels for the amplified products in this pool.

The common DNA chip technology is well described (Sassolas et al. 2008). It is based on the principle of *competitive hybridization* that can be realized in three essential steps (Fig. 12.11):

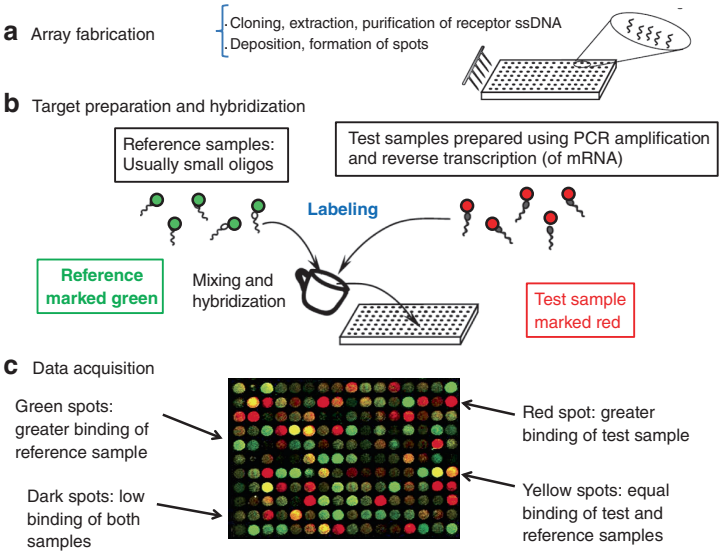

Fig. 12.11 Schematic showing the steps involved in fabrication (**a**), hybridization (**b**), and analysis (**c**) of a spotted DNA microarray with target sequences from a test sample and a reference sample that have been fluorescently labelled with different fluorophores, mixed and hybridized to the same array

(a) *The array fabrication*. The sensing ssDNA sequences possessing no label are immobilized or directly synthesized on the surface (slices or membranes) in multiple copies, forming the microarray. Each type of ssDNA sequence occupies the separate spot.
(b) The *preparation of the target and the reference*. A comparative study is commonly made (*competitive hybridization*). The pool of DNA or RNA fragments that contain potential targets are amplified by PCR or RT-PCR and are covalently labeled with a fluorescent dye. The same is done with the reference sample. In this case the labeling is made with the dye emitting with a different color. Often, cyanine dyes are used for such labeling (see Fig. 4.5). Cy3 serves as 'green' dye and Cy5 as 'red' dye. Then both labeled samples are mixed and hybridized to an array. The target sequences compete for the binding sites and those of them that are present in greater quantities in solution are predominantly bound.
(c) The *data acquisition and analysis*. It is provided by a special reader, recording in two channels the spectrally resolved fluorescence emission. The formed image is analyzed with the aid of special computer software.

Thus, the elementary units of DNA flat microarrays (biochips) are the spots, each containing numerous ssDNA chains of identical sequence terminally anchored to the support surface. The pattern of spots location allows finding each DNA sequence at a unique site. These chains hybridize selectively with free ssDNA chains having a complementary sequence. The microarray is exposed to a solution containing the fluorescently labeled DNA chains. The presence of specific sequences (targets) is signaled by hybridization on the corresponding spot as monitored by correlating the strength of the label signal with the position of the spot (Dharmadi and Gonzalez 2004).

Based on this principle, the functional and convenient DNA biochips have been applied to analyze genomes, to detect inherited and acquired diseases, such as cancer, to detect cellular responses to different stimuli, such as the effects of drugs on a genomic level. They have proved to be very useful for rapid detection of mutations, single nucleotide polymorphism (SNP) and also for gene discovery and expression monitoring.

Modern technology allows depositing as much as 10^5 of different oligonucleotides on a square centimeter chip, which shows the capability of extension to the whole *transcriptome profiling* (see Sect. 15.1). Arrays containing many thousands of unique probe sequences have been constructed, and sophisticated algorithms were developed for fluorescence readout data analysis.

This technique is still far from being ideal, and there exist at least two important critical steps that have to be improved. One is the use of PCR, and the other – the target labeling. The *PCR technique* allows producing many nucleic acid sequences using the target nucleic acid fragment as a template. With its aid, the detection limit reaches the subpicomolar range. Meantime, this reaction is time-consuming, it requires temperature cycling and consumes expensive materials (enzymes and labeled dNTPs). Furthermore, the selective and nonlinear target amplification in PCR may distort the results. Portability and miniaturization of this reaction remains a problem. Avoiding the PCR reaction can be possible only when the necessary level of sensitivity is achieved with alternative procedures.

Incorporation of sensor DNA into hydrogels makes them three-dimensional greatly increasing their capacity. This development has found many applications in research and in clinical diagnostics (Rubina et al. 2004).

The simple 'DNA chip' technology has opened exciting possibilities for applied genetic analysis for the diagnosis of infections, identification of genetic mutations, and forensic inquiries. Its most successful application is in transcriptome analysis (the poolof mRNA species), see Sect. 15.1. Meantime, we have to admit that the *target pool labeling* used here is the most primitive concept in sensing (Sect. 1.2). Its success in DNA hybridization assays is due to a lucky fact that the same chemistry can be used for labeling all nucleic acids present in the pool. Still it encounters different problems regarding calibration, accuracy and speed of analysis. The attempts to substitute it with the techniques based on more advanced concepts (as described in Chap. 1) is discussed below.

12.4.5 Sandwich Assays in DNA Hybridization

Sandwich assay avoids the necessity of pool labeling but requires recognition of the target at two different sites (Sect. 1.4). In nucleic acid detection one of the DNA terminal sequences can be recognized by the capture sequence (that is usually attached to support), and the remaining single-chain segment exposed to the solvent can be hybridized with the indicator sequence that contains fluorescence label. Illustration of this principle is presented in Fig. 12.12a, b. As in the case of immunoassays, this label can be not only the fluorescent dye but also a fluorescent nanoparticle that can provide increased brightness. The dye-silica doped nanoparticles were successfully used for DNA detection in this assay (Zhao et al. 2003). An impressive detection limit of 0.8 fm (femtomoles) and selectivity ratio of 14:1 against one-base mismatches have been achieved.

This approach can allow to make one more step forward and to develop the *wavelength-ratiometric* fluorescence nanosensor based on double labeling (Fig. 12.12c). The capture sequences, instead of being attached to a plain support, can be bound to fluorescent nanoparticles that serve as FRET donors. Indicator DNA is modified with the attachment of fluorescent dye that serves as FRET acceptor. When both of them are present in test medium without target DNA, they do not interact and we observe emission of the donor. In the presence of target DNA sequence, it hybridizes with both capture and indicator sequences, the FRET donor and acceptor approach each other and we observe the emission of the acceptor (Zhang et al. 2005). Many constructions like that can be devised, but their extension to high throughput screening in 'suspension array' format needs precise identification of nanoparticles carrying specific sensors, the 'barcoding'.

12.4.6 Molecular Beacon Technique

Quite different methodology is behind the molecular beacon techniques (Fig. 12.12d). They operate according to the principle of direct sensing, in which the *recognizing sequence* possesses also the *reporting function*. Reporting is coupled to

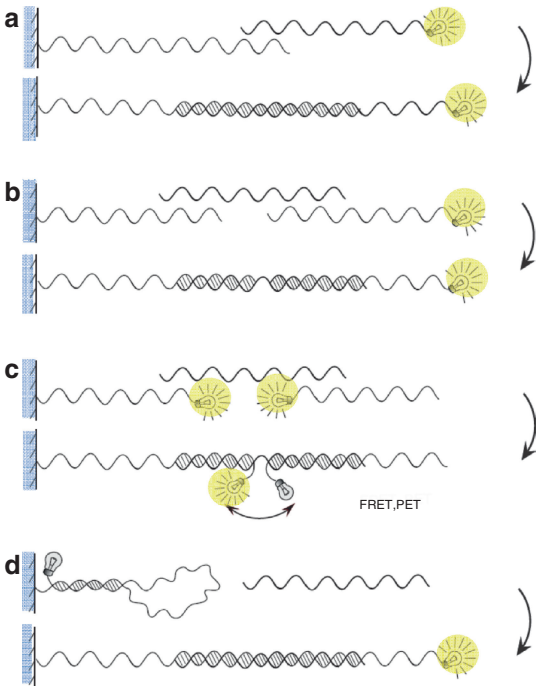

Fig. 12.12 Different principles that are followed in the design of DNA sensor arrays. (**a**) Target pool labeling. The sensor chain is unlabeled. (**b**) The sandwich assay. Neither target pool nor sensor chain is labeled. The indicator chain brings the label. (**c**) Both sensor and indicator sequences are labeled. Binding the target brings two labels together and allows realizing PET quenching or FRET emission wavelength switching effects. (**d**) Molecular beacon. The target binding to complementary loop structure disrupts the stem and removes the label from quenching by the neighboring groups or by the surface

conformational change in this sequence. In Sect. 8.5 the reader can find the detailed description of this mechanism, and below we concentrate on different possibilities of its realization and on some of obtained results.

Molecular beacons are the nucleic acids that contain two structural components, a loop and a stem forming a 'molecular hairpin' (see Fig. 8.14). The loop is the recognition element for complementary nucleic acid sequences of the target. The stem is formed of two complementary sequences that flank the loop, and that are end-labeled with a reporter dye and a quencher (Tyagi and Kramer 1996). The process of recognition in molecular beacons is associated with *disruption of intramolecular contacts* between DNA bases in the stem in favor of intermolecular contacts with the target formed by the loop. Because of this competition, this method is much more sensitive to single nucleotide substitutions than the simpler hybridization assays (Demidov and Frank-Kamenetskii 2004).

Hybridization of the target nucleotide sequence to the loop opens the stem-loop, inducing a separation between them removing the interaction between two labels or label and quencher (see Fig. 12.12d). Different signal transduction mechanisms, in addition to fluorescence de-quenching, were suggested to provide the response to analyte ssDNA or RNA binding (Guo et al. 2012). Moreover, the hairpin is the simplest but not the only possible structure of a molecular DNA sensor that combines target binding and reporting. Hybrid structures were proposed that contain DNA segments connected by a flexible polymer linker (Yang et al. 2006). Upon the hybridization, the labeled DNA segments appear in close proximity, so that the response in FRET is generated.

A great advantage of molecular beacons is the possibility of their use for *intracellular* studies (Wang et al. 2013a). The labeled hairpins are the molecular instru-

ments that do not need any support and contain everything for both recognition and reporting. There is a problem, however, that any nonspecific disruption of stem-loop structure would give a false positive result. This can happen due to degradation by nucleases, protein binding or other conditions making the stem structure unstable.

12.4.7 DNA Sensing Based on Conjugated Polymer

Cationic conjugated polymers exhibit strong electrostatic binding to nucleic acids with the change of their fluorescence properties. An example is polythiophene polymer which was used for colorimetric and fluorometric detection of nucleic acids (Ho et al. 2002). They can be *strongly fluorescent* in their native random coil conformation, but *fluorescence is quenched* when they combine with a single-stranded DNA chain to adopt a highly conjugated, planar conformation. The fluorescence appears again (λ_{exc} =420 nm, λ_{em} =525 nm) when a complementary oligonucleotide target is added to this molecular system. Such interaction is different with the double-stranded DNA. In this case, the polymer binds in a helical and non-planar configuration (a 'triplex') with the negatively charged phosphate backbone of the double-stranded DNA (Fig. 12.13a).

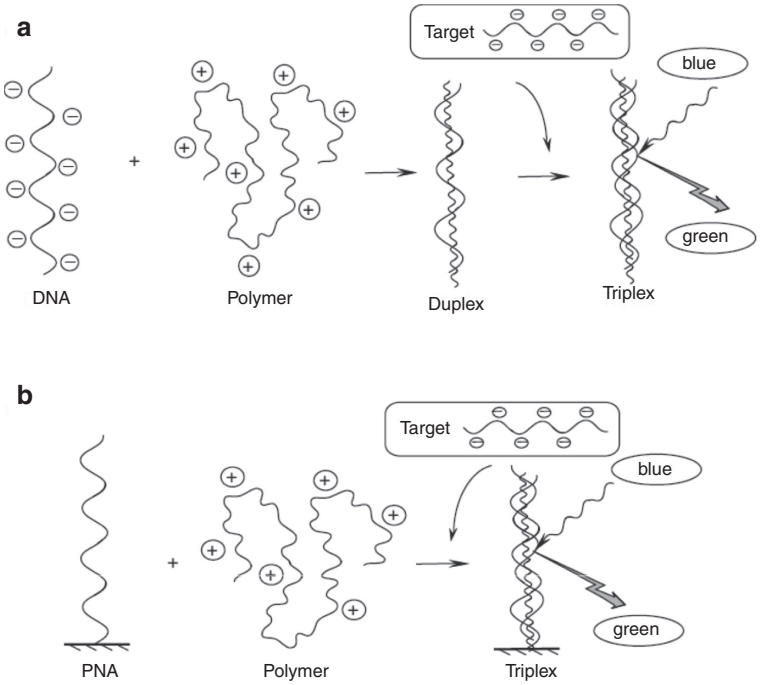

Fig. 12.13 Schematic representation of the transduction mechanism produced by conjugated polymer in the cases when the hybridization of target DNA is produced with DNA in solution (**a**) and with PNA on solid support (**b**) (After Dore et al. (2006))

Thus, the *conjugated polymer* can serve as a very sensitive indicator of hybridization. Moreover, since in exhibits a remarkable property of antenna effect in FRET (Sect. 6.2) and superquenching (Sect. 6.1), the sensitivity of response can be dramatically increased with the inclusion into this system of additional organic dye. It was shown, that tagging the sensor chain with *fluorescent dye serving as FRET acceptor* that emits with substantial wavelength shift allows detecting as much as only five copies of dsDNA in 3 ml in the presence of the entire human genome, in only 5 min (Ho et al. 2005). This approach is suitable for the rapid assessment of the identity of single nucleotide polymorphisms (SNPs) of different genes, and of pathogens without the need for nucleic acid amplification (Dore et al. 2006).

When the neutral *peptide nucleic acid* (Sect. 7.7) is immobilized as the recognition unit on the surface of planar array, it does not interact with the cationic polymer (Fig. 12.13b). The triplex formation occurs on hybridization with the target nucleic acid. Exploration of antenna effect and superquenching is also efficient in this case with the introduction of fluorescent dye serving as the quencher or as the FRET acceptor (Baker et al. 2006; Liu and Bazan 2005).

12.4.8 Quadruplex DNA

Specific detection of *quadruplex* DNA (or G4-DNA), in addition to single- and double-stranded DNA under biologically important conditions is an important issue. In contrast to triplex DNA, quadruplex structures are not exotic forms, they are fully stable and moreover fully natural, forming e.g. in telomeres and promoter regions of numerous genes. There is also quadruplex RNA. G4-DNA and RNA are formed by stacked arrays of guanine quartets connected by non-canonical hydrogen bonds. They are now considered as attractive targets for anticancer therapy (e.g., specific G4-DNA ligands are telomerase inhibitors).

Among the G4 specific fluorescent dyes are the porphyrins (Arthanari et al. 1998) and carbazole derivatives (Chang et al. 2004). A hot topic is the detection of DNA quadruplexes directly in living cells. Artificial constructions based on G4-quadruplexes are of analytical value and can serve the bases for different sensor constructs (Ma et al. 2012), particularly for detection of ions (Ruttkay-Nedecky et al. 2013).

12.4.9 Conclusive Remarks and Prospects

The DNA analytic techniques have led to revolutionary changes in modern biology and related areas. They allow both single target detection and the whole-cell expression of genes. They brought unique possibilities for identification of personality involving the characteristics of single nucleotide polymorphism (SNP), recognition of cancer cells and tissues and detection of pathogenic microorganisms. They allow

comparison of closely related species in plant and animal worlds. This huge amount of tasks requires development of different competitive technologies, what is actually observed.

The highly needed multiplexed microarray platforms provide parallel detection capabilities enabling the measurements of many thousands of simultaneous responses. The DNA microarrays are especially attractive due to achieved combination of high throughput, parallelism, miniaturization, speed, and automation. Inclusion of the expression profile of the whole genome eliminates the bias related to any preliminary selection. Moreover, the global nature of the DNA microarray technique holds tremendous promise for the discovery of complex genetic and metabolic networks. In this rapidly developing technology, the measurement is ahead of analysis and the sensitivity is ahead of accuracy. Overcoming these difficulties is expected soon.

The methods that offer avoiding the PCR amplification and labeling of the target pool are expected to complement and, in many important areas, to substitute the standard 'DNA chip' approach. These methods are expected to make the DNA tests considerably simpler, cheaper, and quicker and therefore more applicable for large-scale applications. This goal can be achieved on one condition: they have to demonstrate the superior sensitivity. This condition can be realized when the ultra-bright nanoparticles will substitute or complement organic dyes and when enzymatic amplification mechanisms will be substituted by photophysical ones. The dye-doped nanoparticles (Zhao et al. 2003), quantum dots as FRET donors (Zhang et al. 2005), conjugated polymers as self-amplified systems (Dore et al. 2006; Liu and Bazan 2005) the metal-enhancement support (Aslan et al. 2006), as well as enhancing support of porous semiconductor materials (Dorfman et al. 2006) are the trends pointed forward by pioneering research.

12.5 Recognition of Protein Targets

Proteins are biological macromolecules that are the most essential constituents of cells, the building blocks of all their organelles and the catalysts of all biochemical reactions. In different conditions and for different purposes there is a need to determine (a) the total protein content, (b) the specific proteins, such as particular enzyme or antibody, (c) all protein composition in a given system and (d) all human proteome. We will start with the simplest tasks and proceed with the more complicated ones.

12.5.1 Total Protein Content

Classical protein assays known from the textbooks on biochemistry, such as the Biuret, Lowry and Bradford methods based on the change of absorbance of bound dye, have a strong tendency to be substituted by rapid, sensitive and

precise methods employing the biosensors. The problem with the broad-scale protein determination is in great diversity and even uniqueness of every protein that complicates its recognition 'as a protein'. Nevertheless, such attempts continue using different recognition units, such as fluorescent dyes themselves (Harvey et al. 2001) or modified cyclodextrins combined with attached reporting dyes (Zhu et al. 2007).

12.5.2 Specific Protein Recognition

Presently, the most requested in sensing as the recognition elements for detection of proteins are the antibodies (Kusnezow et al. 2003) that recognize linear segments or conformationally unified clusters of 3–5 amino acids on the protein surface. In addition, the designed binding proteins, peptides and aptamers demonstrate their increased utility (Chap. 7). Because of dramatic variations of protein structures, of their surface topologies and of their surface modifications there is a great difficulty in unifying the strategies for protein-receptor interactions. The peptide-based molecular beacons have been developed (see Fig. 8.15), but they are of limited utility. Often a special recipe is needed to target a particular protein.

Detection of human serum albumin (HSA) in blood serum and urine is of diagnostic value (Sect. 14.1) and, therefore, many different methods were suggested addressing this issue. Since major function of albumin is carrying low-polar metabolites, different fluorescent dyes bind to this protein with high specificity and affinity. Immobilization and screening from quenching by water provides their fluorescence enhancement sufficient for strong fluorescence response (Kessler et al. 1997). Recently described HSA probes based on fluorescent molecular rotors showed up to 400-fold enhancement of fluorescence upon binding to the target (Wu et al. 2014) .

Complementary to the highly specific recognition described above is the strategy of cross-responsive arrays that are inspired by the mammalian olfactory system (Sect. 15.5). The high level of cross-reactivity still allows precise determination of particular target. This is because each target generates a unique composite pattern of interactions with olfactory receptors. In analogy, an array of nonspecific or weakly interacting agents would give rise to distinctive fingerprints in response to a target. This strategy can be the basis for identification of "hot spots" on protein surfaces. Following it, a smart sensor array (*chemical nose*) was developed for sensing specific proteins (You et al. 2007). It is based on reversible binding of anionic poly(paraphenyleneethynylene) (PPE) polymer with cationic gold nanoparticles (Fig. 12.14). These complexes are initially quenched, but in the presence of proteins they are disrupted giving a turn-on response. The varied affinities of protein to gold particles led to different scales of PPE displacement, so that fluorescence response generates fingerprint pattern for individual proteins. These affinities are determined by their respective structural features, allowing charged, hydrophobic, hydrophilic, and hydrogen-bonding interactions.

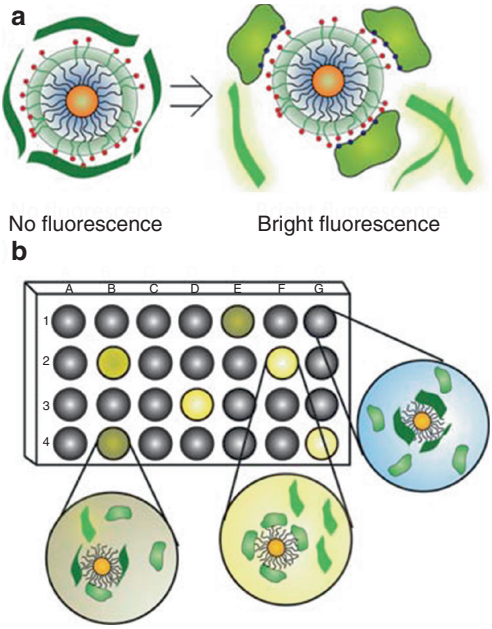

Fig. 12.14 Experiment on specific protein detection based on chemical nose concept (You et al. 2007). (**a**) The protein analyte releases fluorescent polymer from its complex with gold nanoparticle with concomitant restoration of fluorescence. (**b**) Pattern generation through differential release of fluorescent polymers from gold nanoparticles

12.5.3 High Throughput Protein Arrays

A strong demand for high-throughput analysis on proteomic level stimulates rapid development of *protein arrays* for simultaneous detection of many proteins. Due to their high throughput, they must have great potential to reduce the cycle time of drug discovery and to improve the efficiency of medical diagnostics. For real world use, a protein array have to become simple and inexpensive to manufacture, its fabrication should be amendable to automation, the size and shape of their spots must be controlled, they must be durable and reproducible in application. Their sensitivity should be on a competing level with that of ELISA, which means a picomolar detection limit.

Making these arrays by using the traditional way for DNA chips is much more difficult than of DNA or RNA microarrays because of three major problems. One is related to conformational lability of protein molecules and the necessity to immobilize them on support in native conformation. The other is the fluorescent labeling of protein pool. This requires from the researchers a broader view and the revision of basic concept of array operation. And the third problem is related to variable and often low output signal.

(a) The concept that the *best recognition partner of a protein is the protein* has to be revised. Individual proteins differ in stability, surface charge and reactivity of surface groups and other properties. This creates difficulties in their immobilization in the native form and orientation that could allow target binding. Protein stability in storage and application remains an important concern. The

novel strategies to fabricate the sensor molecules include single chain antibodies displayed by phage, protein- oligonucleotide conjugates, synthetic peptides and aptamers (see Chap. 7).

Protein sensors should be used with the account of new possibilities that exist for their application as recognition units (Sect. 7.3). It is also possible to construct arrays of full-length, functional proteins from a library of expression clones (Bertone and Snyder 2005). They may be of great use when the global observations of biochemical activities are needed, and hundreds or thousands of proteins can be simultaneously screened for protein-protein, protein-nucleic acid, and small molecule interactions.

(b) The *concept of pool labeling* should be abandoned, since it cannot reproduce the true protein concentration. Usually such labeling is provided by amino-reactive dyes in the form of their active ester or isothiocyanate derivatives. The proteins differ so much in the amount and chemical reactivity of their surface amino groups that no uniform fluorescent labeling is possible. Moreover, the site-dependent variation of fluorescence properties is observed for many fluorescent dyes.

(c) Direct reading the intensity of labeled dyes does not provide the necessary sensitivity. Therefore, the nanoparticles with brighter emission (Chap. 5) or some signal amplification mechanism with their involvement (Chap. 6) should be implemented into the process of fluorescence response.

These facts explain why despite the offer of different ligand-binding proteins, peptides and aptamers, the *antibodies* are still very much in vogue, as well as recombinant antibody fragments (Pavlickova et al. 2004). Many problems with the design and production of microarrays based on them have been resolved, including their immobilization in 3D hydrogels (Rubina et al. 2003). The prospects of their application on proteomic level will be critically discussed in Sect. 15.1.

The protein microarrays based on immobilized DNA and RNA *aptamers*, selected against many different protein targets, allow simultaneously detecting and quantifying the levels of individual proteins in complex biological mixtures. Each aptamer can be fluorescently labeled and immobilized on a glass substrate. Different methods including fluorescence polarization (anisotropy) can be used for detecting the target protein binding. The latter detection method can operate both in solution and on solid support.

Water-soluble *conjugated polymers* with pendant-charged residues provide an excellent scaffold for the design of sensor arrays, since they combine the binding and responsive properties (Thomas et al. 2007). The introduced side groups can provide specific protein binding through multivalent interactions, and their optical properties are sensitive to minor changes in their conformation with the possibility of fluorescence superquenching (Sect. 6.1).

The sensor arrays based on non-covalent interactions with *metal* and *semiconductor nanoparticles* and their conjugates with organic dyes and fluorescent polymer conjugates have started to be developed (Gill et al. 2008).

12.6 Polysaccharides, Glycolipids and Glycoproteins

Known under the common name of *glycans*, polysaccharides, and carbohydrate portions of glycolipids and glycoproteins constitute a large family of compounds that involve sugar elements (Jelinek and Kolusheva 2004). These molecules are present both inside and on the surface of cells and are integral constituents of a vast number of proteins that are involved in a myriad of cellular events. Carbohydrates and glycoconjugates of proteins and lipids participate in such processes as the normal and pathogenic cell adhesion, inflammation, signal transduction, etc. Therefore, a new field of *glycomics* has to follow in development the more advanced fields of genomics and proteomics with a strong extension into clinical diagnostics. In addition, control on carbohydrate level is needed in industrial biotechnologies and in many other industrial processes such as food processing and storage.

Before these highly needed arrays come into practice, many technical problems have to be resolved (Shin et al. 2005). These problems are much more difficult than with DNA and protein arrays. They can be outlined as follows:

(a) Glycans are rather *diverse chemical structures*, and there are no unified methods for their synthesis, modification and immobilization on the surface. Moreover, the designed sensors must be able to probe protein-carbohydrate, carbohydrate-carbohydrate, nucleic acid-carbohydrate and intact cell-carbohydrate interactions. This makes difficult to develop a unified strategy of sensor design. The questions to be resolved involve the proper surface preparation, the proper linking chemistry, and immobilization with proper orientation.
(b) The glycan interactions display *diverse affinities* and often are rather weak ($K_d \sim \mu M$-mM). Definitely, such strength of sensor-target interactions does not allow using in full the sandwich techniques that require washing steps. In addition, the researcher should often address the problem of nonspecific adsorption effects and false-positive signals. The application of competition assays can also be problematic.
(c) There is *no unified procedure* for fluorescent labeling, and the existing methods of introduction of reactive groups are not enough specific. Also, close fluorescent analogs of carbohydrates do not exist, and conjugation of fluorescent dyes may interfere strongly with the target recognition.

These difficulties do not detract the researchers, and with the implementation of new ideas and new technologies they have to be overcome. Several examples are presented below.

It was shown that with the aid of combinatorial methods of sensor design, a library can be constructed for specific binding of *lectins*, which are the specific carbohydrate binding proteins (Kolomiets et al. 2007). A 15,625-membered short peptide-dendrimer combinatorial library was produced and acylated with an alpha-C-fucosyl residue at its four N-termini and screened for binding to fucose-specific lectins. In this way, the targets on a sub-micromolar level can be identified.

Similarly to antibodies recognizing the surface antigens, the *glycan sensors* can recognize carbohydrate pattern on the surfaces of pathogenic microbes. It is known that a large number of bacterial toxins, viruses and bacteria target carbohydrate derivatives on the cell surface to attach and gain entry into the cell, and glycan sensors can detect them (Ngundi et al. 2006b). Because of that, they find important application for the determination of microbial contaminants in food.

Being made of *lectins*, the glycan sensors provide the profiling of carbohydrate expression on the surface of human cells (Zheng et al. 2005). Sensing the glycan markers of diseases is an important approach in clinical diagnostics (Dai et al. 2006). In this respect, *glycan microarrays* technology becomes promising in high-throughput identification of glycan-binding proteins and pathogenic microorganisms and even for decoding of the whole glycome (Rillahan and Paulson 2011).

12.7 Detection of Harmful Microbes

Rapid, sensitive, and selective detection of pathogenic bacteria and viruses is extremely important for proper diagnosis and treatment of diseases. Global biosecurity threats such as the spread of emerging infectious diseases (i.e. Ebola and avian influenza) and bioterrorism have dramatically increased the importance of this problem. The control for microbial contamination is not only a medical problem. It plays an important role in pharmaceutical clean room production and in food processing technology. What does the future hold and which biosensor technology platform is suitable for the real-time detection of infectious microbes?

12.7.1 Detection and Identification of Bacteria

The role of sensors in analysis of microbes is primarily in simplification and speeding up the assays. Conventional microbiological classification tests involving colony growth in culture media require tedious cultivation for several days and highly professional analysis of only one bacterial pathogen at a time. Alternatively, genic material of a pathogen can be detected by PCR, which is also time-consuming and prone to false-positive results. The sensors should substitute these tests and allow detecting multiple microbes, obtaining response in minutes and in the simplest possible way. Therefore, many assays, mostly immunoassays, were suggested for practical use.

Traditionally, these assays are based on recognition properties of *antibodies* against surface cell receptors. Critical analysis of these assays can be found elsewhere (Sapsford et al. 2006). On the present step of technology development their essential improvement can be provided. In detection of individual bacterial cells they are developing into potent biosensor technologies that allow high-affinity binding to bacterial surface together with very efficient fluorescence response. *Silica nanoparticles* responding in different colors have proved to be prospective for simultaneous and sensitive detection of multiple bacterial targets (Wang et al. 2007).

Antimicrobial peptides are the different types of recognition units. These peptides represent an innate immune system as a first line of defense against microbial invasion that evolved in bacteria, plants, and higher and lower animals. They exert their antimicrobial activity by binding to components of the microbe's surface and disrupting the membrane. Their recognition power to detect *E. coli* and *Salmonella* was demonstrated (Ngundi et al. 2006a).

An interesting approach for the detection of bacteria is the use of *carbohydrate-functionalized fluorescent polymers* (Disney et al. 2004). It is based on the fact, that many pathogens that infect humans use the cell surface carbohydrates as receptors to facilitate the cell-cell adhesion. The hallmark of these interactions is their multivalency, or the simultaneous occurrence of multiple interactions. Fluorescent polymers that occupy increasingly strong position in fluorescence sensing (Sect. 5.3) can be modified with different functional substituents. A carbohydrate-functionalized fluorescent polymer, which displays many carbohydrate ligands on a single polymer chain, was used to allow for multivalent detection of pathogens. With their application, the brightly fluorescent aggregates of bacteria can be easily observed.

The sensitive detection of pathogens via their *nucleic acid sequences* is another possibility for research and development. The microfluidic biosensor with disposable microchannels possessing defined areas for capture and detection of target pathogen RNA sequence was demonstrated (Kwakye and Baeumner 2003). Two different DNA probes complementary to unique sequences on the target pathogen RNA serve as the biorecognition elements. For signal generation and amplification, one probe is coupled to dye-encapsulated liposomes, while the second probe is coupled to superparamagnetic beads for target immobilization. The probes hybridize to target RNA and the liposome-target-bead complex is subsequently captured on a magnet. The amount of liposomes captured correlates directly to the concentration of target sequence and is quantified using a fluorescence microscope.

The environmental, clinical and food monitoring or detection of bioterrorist agents requires novel techniques that have to be very sensitive but also fast and easy in performance. Promising in this respect are the techniques based on combination of plasmonic enhancement and microwave heating (Aslan and Geddes 2015), see also Sect. 10.7.

12.7.2 Bacterial Spores

Many harmful microbes form protective spores (endospores) that allow them to survive through hard times and to transform into active microbes in favorable conditions for their development. Such dormant forms can be very dangerous since they can survive during extremely long periods of time. The spores are composed of DNA, the DNA-stabilizing agents (such as calcium dipicolinate) and the protecting shell that can be recognized by fluorescence sensors.

A novel fluorescence assay was developed for the detection of Bacillus thuringiensis (BT) spores based on *aptamer*-quantum dots binding (Ikanovic et al. 2007).

The assay is based on the fluorescence observed after binding an aptamer-quantum dot conjugate to BT spores. The SELEX technique was used in order to select and identify the DNA aptamer sequence specific for BT. The 60-base aptamer was then coupled to fluorescent zinc sulfide-capped, cadmium selenide quantum dots. The assay is semi-quantitative, specific and can detect BT at concentrations of about 1,000 colony forming units/ml.

12.7.3 Detection of Toxins

Harmful bacteria can be detected by the products that they synthesize. These products, the *toxins*, provide poisoning effects. This refers not only to the most dangerous infections. For instance, staphylococcal enterotoxins are a major cause of food poisoning. Here the role of sensor technologies is not only to provide rapid and sensitive tests but also to avoid extensive pretreatment or concentration of the sample prior to analysis. Though not fully conforming to these needs, immunosensor arrays based on immobilized antibodies have become the common approach for the detection of toxins (Rucker et al. 2005), and the most popular for detection is the competition format (Ngundi et al. 2006a).

Glycan arrays discussed in the previous section are emerging as the very powerful tools for detection of toxins that contain a carbohydrate component. Arrays of N-acetyl galactosamine (GaINAc) and N-acetylneuraminic acid (Neu5Ac) derivatives were immobilized on the surface of a planar waveguide and were used as receptors for protein toxins with a sensitivity on the level of 100 ng/ml (Ngundi et al. 2006b).

12.7.4 Sensors for Viruses

Viruses are the sub-microscopic infectious agents that are able to grow or reproduce only inside a host cell. Each viral particle consists of genetic material in the form of DNA or RNA and a protective coat made of proteins, called a capsid. Both these nucleic acids and capsid proteins can be the targets of viral infection. Of diagnostic importance are also the antibodies raised in the organism in response to virus infection.

The early detection of *human immunodeficiency virus* (HIV) is an extremely important problem in all efforts to prevent epidemic propagation of AIDS disease. Currently, the standard diagnostic tests for HIV infection are based on the ELISA technique, which is an expensive and inconvenient multi-step procedure. For this and other viral diseases the important method of detection is a serial determination of antiviral antibodies. A great variety of synthetic and phage-displayed peptides have been presently collected as test antigens (Palacios-Rodriguez et al. 2007), so what remains is to develop simpler methods that could be equal or superior in precision.

Interesting was the recent suggestion for the detection of anti-HIV antibodies based on *peptide beacons* (Oh et al. 2007). These peptides contain the sequence rec-

ognized by the antibodies and adopt different conformations in the free and antibody-bound forms, which influences the effect of bound quencher on the fluorescence of dye bound in a different position in peptide sequence. Application of techniques providing the signal amplification up to the sensitivity of ELISA is expected to follow.

Methods relying on *viral antigen* detection are expected to experience revolutionary changes with the application of novel fluorescence sensing technologies. The application of time-resolved detection of Eu^{3+}-doped luminescence nanoparticles was shown to improve dramatically the sensitivity of adenovirus detection (Valanne et al. 2005).

12.8 Sensing and Thinking: Adaptation of Sensor Units for Multi-scale and Hierarchical Range of Targets

Analyzing different applications of fluorescence sensors, we witness the interesting crossing points of microscopic and macroscopic concepts. Molecules that respond to thermal collisions with their neighboring molecules allow detecting the temperature and pressure gradients on the surface of airplanes, and the ion sensors are used for detecting pollution of large pieces of land. Regarding the size of instrumentation, it goes down irrespective of complexity and application. Simultaneously, with the increase of complexity in tasks and efficiency in response, the size of elementary sensing units grows from rather small and simple molecules to self-assembled supramolecular ensembles involving biomacromolecules and the structures formed by them.

Being aimed at development of a sensor for particular compound or series of compounds the researcher is able to select the optimal solution out of a broad variety of possibilities offered by synthetic organic and polymer chemistry and also by the chemistry and biochemistry of proteins, peptides and nucleic acids. In addition, all the recently developed techniques of manipulation with the genes and gene products can be applied in this field. Though fragmentary, the presented above analysis involves the major classes of inorganic, organic and biological compounds, for which a strong request exists for their detection. Providing the analogies, the reader can find the optimal approach in the search for a rationally designed sensor that needs to be made.

It is expected that the reader will share with the author a strong belief that the described systems and their newly created analogs have the full potential to complement or replace the classical analytical methods. This can be done by simplifying or eliminating the sample preparation protocols and making field-testing easier, faster, with significant decrease in costs per analysis together with an increase in fidelity, and precision.

Questions and Problems

1. What are the advantages and disadvantages in the application of luminescence to temperature and pressure sensing compared to other popular methods? Which method would you select for sensing temperature inside the oven? Inside the cryogenic device? Inside the water pipe? Inside the targeted cells in a living body?

2. Temperature and pressure are the parameters, the background of which is thermodynamic and is connected with averaging over great molecular ensemble. How then to understand their meaning on molecular level?
3. Why oxygen is so easily determined in gas mixtures? What are the means to use fluorescence detection for quantitative analysis of other gasses?
4. Explain the principle that can be used in the background of determining the explosive vapors.
5. Explain the difference between different definitions of the term 'polarity'. What is the mechanism behind fluorescence sensing of solvent polarity? Should the polarity of the probe molecule itself correspond to the polarity of studied medium?
6. How the sensor response to polarity and viscosity can be made ratiometric? Analyze the presented examples
7. What is the static and what is the dynamic disorder in fluid systems? Does dynamic disorder depend on observation time window?
8. What is the major effect discovered with the wavelength-ratiometric probe in supercritical CO_2? (a). Change of polarity? (b). Change of solvent reactivity? (c). Change of size and dynamics of solvent clusters?
9. What probes and what measurements can you suggest for studying the dynamic properties in polymers?
10. How can you define the polarity at an interface?
11. What determines the width of pH range detected by fluorescence pH sensors? What are the means to extend this range?
12. How to achieve the wavelength-ratiometric oxygen sensing in solutions? Can this approach be applied to other gasses?
13. On what major principles operate the sensors for heavy metal ions?
14. Why optimal *in vitro* glucose sensors are not the best when applied *in vivo*?
15. What are the differences in affinity, selectivity and the mechanisms of binding to ssDNA and dsDNA between monomers and dimers of acrydine dyes?
16. Explain advantages and disadvantages in application of planar arrays with target pool labeling (DNA chips). Why it is hard to apply the same methodology to make protein arrays? What are the major problems in making glycan arrays?
17. For the detection of bacteria, what in your view are the best recognition units (choose between antibodies, antimicrobial peptides, aptamers, etc.) and reporting units (choose between the dye-doped nanoparticles, conjugated polymers, the systems exhibiting FRET, etc.). Suggest the best composition of receptors and reporters.

References

Abbott AP, Hope EG, Palmer DJ (2007) Probing solute clustering in supercritical solutions using solvatochromic parameters. J Phys Chem B 111(28):8119–8125

Abo M, Urano Y, Hanaoka K, Terai T, Komatsu T, Nagano T (2011) Development of a highly sensitive fluorescence probe for hydrogen peroxide. J Am Chem Soc 133(27):10629–10637

Amao Y (2003) Probes and polymers for optical sensing of oxygen. Microchimica Acta 143(1):1–12

Amara JP, Swager TM (2005) Synthesis and properties of poly(phenylene ethynylene)s with pendant hexafluoro-2-propanol groups. Macromolecules 38:9091–9094
Apostolidis A, Klimant I, Andrzejewski D, Wolfbeis OS (2004) A combinatorial approach for development of materials for optical sensing of gases. J Comb Chem 6(3):325–331
Aragay G, Pons J, Merkoçi A (2011) Recent trends in macro-, micro-, and nanomaterial-based tools and strategies for heavy-metal detection. Chem Rev 111(5):3433–3458
Arthanari H, Basu S, Kawano TL, Bolton PH (1998) Fluorescent dyes specific for quadruplex DNA. Nucleic Acids Res 26(16):3724–3728
Aslan K, Geddes CD (2015) Pathogen detection using spatially focused microwaves and metal-enhanced fluorescence. In: Marks RS, Lobel L, Sall AA (eds), Viral diagnostics: advances and applications. CRC Press, Boca Raton, pp 201–252
Aslan K, Lakowicz JR, Geddes CD (2004) Tunable plasmonic glucose sensing based on the dissociation of Con A-aggregated dextran-coated gold colloids. Anal Chim Acta 517(1–2): 139–144
Aslan K, Huang J, Wilson GM, Geddes CD (2006) Metal-enhanced fluorescence-based RNA sensing. J Am Chem Soc 128(13):4206–4207
Badugu R, Lakowicz JR, Geddes CD (2003) A glucose sensing contact lens: a non-invasive technique for continuous physiological glucose monitoring. J Fluoresc 13(5):371–374
Baker ES, Hong JW, Gaylord BS, Bazan GC, Bowers MT (2006) PNA/dsDNA complexes: site specific binding and dsDNA biosensor applications. J Am Chem Soc 128(26):8484–8492
Ballerstadt R, Polak A, Beuhler A, Frye J (2004) In vitro long-term performance study of a near-infrared fluorescence affinity sensor for glucose monitoring. Biosens Bioelectron 19(8): 905–914
Baptista MS, Indig GL (1998) Effect of BSA binding on photophysical and photochemical properties of triarylmethane dyes. J Phys Chem B 102(23):4678–4688
Barroso M, Chattopadhyay N, Klymchenko AS, Demchenko AP, Arnaut LG, Formosinho SJ (2006) Dramatic pressure-dependent quenching effects in supercritical CO2 assessed by the fluorescence of 4′-dimethylamino-3-hydroxyflavone. Thermodynamic versus kinetics control of excited-state intramolecular proton transfer. J Phys Chem A 110(50):13419–13424
Bertone P, Snyder M (2005) Advances in functional protein microarray technology. FEBS J 272(21):5400–5411
Bosch P, Catalina F, Corrales T, Peinado C (2005) Fluorescent probes for sensing processes in polymers. Chemistry 11(15):4314–4325
Bunzli JCG, Piguet C (2005) Taking advantage of luminescent lanthanide ions. Chem Soc Rev 34(12):1048–1077
Catalan J (1997) On the E-T (30), pi*, P-y, S′, and SPP empirical scales as descriptors of nonspecific solvent effects. J Org Chem 62(23):8231–8234
Chandrasekharan N, Kelly LA (2001) A dual fluorescence temperature sensor based on perylene/exciplex interconversion. J Am Chem Soc 123(40):9898–9899
Chang C-C, Kuo I-C, Ling I-F, Chen C-T, Chen H-C, Lou P-J, Lin J-J, Chang T-C (2004) Detection of quadruplex DNA structures in human telomeres by a fluorescent carbazole derivative. Anal Chem 76(15):4490–4494
Chen X, Tian X, Shin I, Yoon J (2011) Fluorescent and luminescent probes for detection of reactive oxygen and nitrogen species. Chem Soc Rev 40(9):4783–4804
Chiappe C, Pieraccini D (2005) Ionic liquids: solvent properties and organic reactivity. J Phys Org Chem 18(4):275–297
Chinnayelka S, McShane MJ (2004) Resonance energy transfer nanobiosensors based on affinity binding between apo-enzyme and its substrate. Biomacromolecules 5(5):1657–1661
Chung C, Srikun D, Lim CS, Chang CJ, Cho BR (2011) A two-photon fluorescent probe for ratiometric imaging of hydrogen peroxide in live tissue. Chem Commun 47(34):9618–9620
Dai Z, Kawde AN, Xiang Y, La Belle JT, Gerlach J, Bhavanandan VP, Joshi L, Wang J (2006) Nanoparticle-based sensing of glycan-lectin interactions. J Am Chem Soc 128(31): 10018–10019

Davenport LD, Knutson JR, Brand L (1986) Excited-state proton transfer of equilenin and dihydro equilenin: interactions with bilayer vesicles. Biochemistry 25:1186–1195
Demchenko AP (2002) The red-edge effects: 30 years of exploration. Luminescence 17(1): 19–42
Demchenko AP (2006) Visualization and sensing of intermolecular interactions with two-color fluorescent probes. FEBS Lett 580(12):2951–2957
Demchenko AP, Tang KC, Chou PT (2013) Excited-state proton coupled charge transfer modulated by molecular structure and media polarization. Chem Soc Rev 42(3):1379–1408
Demchenko AP (2014) Practical aspects of wavelength ratiometry in the studies of intermolecular interactions. J Mol Struct 1077:51–67
Demidov VV, Frank-Kamenetskii MD (2004) Two sides of the coin: affinity and specificity of nucleic acid interactions. Trends Biochem Sci 29(2):62–71
Deschenes LA, Vanden Bout DA (2001) Single-molecule studies of heterogeneous dynamics in polymer melts near the glass transition. Science 292(5515):255–258
Dharmadi Y, Gonzalez R (2004) DNA microarrays: experimental issues, data analysis, and application to bacterial systems. Biotechnol Prog 20(5):1309–1324
Dickinson BC, Huynh C, Chang CJ (2010) A palette of fluorescent probes with varying emission colors for imaging hydrogen peroxide signaling in living cells. J Am Chem Soc 132(16): 5906–5915
Disney MD, Zheng J, Swager TM, Seeberger PH (2004) Detection of bacteria with carbohydrate-functionalized fluorescent polymers. J Am Chem Soc 126(41):13343–13346
Domaille DW, Que EL, Chang CJ (2008) Synthetic fluorescent sensors for studying the cell biology of metals. Nat Chem Biol 4(3):168–175
Dong DC, Winnik MA (1984) The Py scale of solvent polarities. Can J Chem 62(11):2560–2565
Dore K, Leclerc M, Boudreau D (2006) Investigation of a fluorescence signal amplification mechanism used for the direct molecular detection of nucleic acids. J Fluoresc 16(2): 259–265
Dorfman A, Kumar N, Hahm JI (2006) Highly sensitive biomolecular fluorescence detection using nanoscale ZnO platforms. Langmuir 22(11):4890–4895
Dutta M, Das D (2012) Recent developments in fluorescent sensors for trace-level determination of toxic-metal ions. TrAC Trends Anal Chem 32:113–132
Ellison CJ, Torkelson JM (2002) Sensing the glass transition in thin and ultrathin polymer films via fluorescence probes and labels. J Polym Sci Part B-Polym Phys 40(24):2745–2758
Ellison CJ, Miller KE, Torkelson JM (2004) In situ monitoring of sorption and drying of polymer films and coatings: self-referencing, nearly temperature-independent fluorescence sensors. Polymer 45(8):2623–2632
El-Sayed IH, Huang X, El-Sayed MA (2006) Selective laser photo-thermal therapy of epithelial carcinoma using anti-EGFR antibody conjugated gold nanoparticles. Cancer Lett 239(1): 129–135
Epand RM, Kraayenhof R (1999) Fluorescent probes used to monitor membrane interfacial polarity. Chem Phys Lipids 101(1):57–64
Fayed TA, Etaiw Sel D (2006) Fluorescence characteristics and photostability of benzoxazole derived donor-acceptor dyes in constrained media. Spectrochim Acta A Mol Biomol Spectrosc 65(2):366–371
Fischer D, Theodorakis EA, Haidekker MA (2007) Synthesis and use of an in-solution ratiometric fluorescent viscosity sensor. Nat Protoc 2(1):227–236
Fischer LH, Harms GS, Wolfbeis OS (2011) Upconverting nanoparticles for nanoscale thermometry. Angew Chem Int Ed 50(20):4546–4551. doi:10.1002/anie.201006835
Funston AM, Fadeeva TA, Wishart JF, Castner EW Jr (2007) Fluorescence probing of temperature-dependent dynamics and friction in ionic liquid local environments. J Phys Chem B 111(18): 4963–4977
Gill R, Zayats M, Willner I (2008) Semiconductor quantum dots for bioanalysis. Angew Chem Int Ed 47(40):7602–7625

Glazer AN, Peck K, Mathies RA (1990) A stable double-stranded DNA-ethidium homodimer complex: application to picogram fluorescence detection of DNA in agarose gels. Proc Natl Acad Sci U S A 87(10):3851–3855

Gota C, Uchiyama S, Yoshihara T, Tobita S, Ohwada T (2008) Temperature-dependent fluorescence lifetime of a fluorescent polymeric thermometer, poly(N-isopropylacrylamide), labeled by polarity and hydrogen bonding sensitive 4-sulfamoyl-7-aminobenzofurazan. J Phys Chem B 112(10):2829–2836

Gouterman M (1997) Oxygen quenching of luminescence of pressure sensitive paint. J Chem Educ 74:1–7

Guo J, Ju J, Turro NJ (2012) Fluorescent hybridization probes for nucleic acid detection. Anal Bioanal Chem 402(10):3115–3125

Haidekker MA, Theodorakis EA (2007) Molecular rotors–fluorescent biosensors for viscosity and flow. Org Biomol Chem 5(11):1669–1678

Han J, Burgess K (2009) Fluorescent indicators for intracellular pH. Chem Rev 110(5): 2709–2728

Harvey MD, Bablekis V, Banks PR, Skinner CD (2001) Utilization of the non-covalent fluorescent dye, NanoOrange, as a potential clinical diagnostic tool. Nanomolar human serum albumin quantitation. J Chromatogr B Biomed Sci Appl 754(2):345–356

Haugland RP (2005) The handbook. A guide to fluorescent probes and labeling technologies, 10th edn. Invitrogen Corp, Eugene

Hermant RM, Bakker NAC, Scherer T, Krijnen B, Verhoeven JW (1990) Systematic studies of a series of highly shaped donor-acceptor systems. J Am Chem Soc 112:1214–1221

Ho HA, Boissinot M, Bergeron MG, Corbeil G, Doré K, Boudreau D, Leclerc M (2002) Colorimetric and fluorometric detection of nucleic acids using cationic polythiophene derivatives. Angewandte Chemie 114(9):1618–1621

Ho HA, Dore K, Boissinot M, Bergeron MG, Tanguay RM, Boudreau D, Leclerc M (2005) Direct molecular detection of nucleic acids by fluorescence signal amplification. J Am Chem Soc 127(36):12673–12676

Hochreiner H, Sanchez-Barragan I, Costa-Fernandez JM, Sanz-Medel A (2005) Dual emission probe for luminescence oxygen sensing: a critical comparison between intensity, lifetime and ratiometric measurements. Talanta 66(3):611–618

Hu ZH, Margulis CJ (2006) A study of the time-resolved fluorescence spectrum and red edge effect of ANF in a room-temperature ionic liquid. J Phys Chem B 110(23):11025–11028

Huang CC, Chang HT (2006) Selective gold-nanoparticle-based "turn-on" fluorescent sensors for detection of mercury(II) in aqueous solution. Anal Chem 78(24):8332–8338

Huang J, Peng AD, Fu HB, Ma Y, Zhai TY, Yao JN (2006a) Temperature-dependent ratiometric fluorescence from an organic aggregates system. J Phys Chem A 110(29):9079–9083

Huang X, Jain PK, El-Sayed IH, El-Sayed MA (2006b) Determination of the minimum temperature required for selective photothermal destruction of cancer cells with the use of immunotargeted gold nanoparticles. Photochem Photobiol 82(2):412–417

Ikanovic M, Rudzinski WE, Bruno JG, Allman A, Carrillo MP, Dwarakanath S, Bhahdigadi S, Rao P, Kiel JL, Andrews CJ (2007) Fluorescence assay based on aptamer-quantum dot binding to Bacillus thuringiensis spores. J Fluoresc 17(2):193–199

Ishizaka S, Kim HB, Kitamura N (2001) Time-resolved total internal reflection fluorometry study on polarity at a liquid/liquid interface. Anal Chem 73(11):2421–2428

Jaque D, Rosal B, Rodríguez EM, Maestro LM, Haro-González P, Solé JG (2014) Fluorescent nanothermometers for intracellular thermal sensing. Nanomedicine 9(7):1047–1062

Jelinek R, Kolusheva S (2004) Carbohydrate biosensors. Chem Rev 104(12):5987–6015

Jiang W, Wang S, Yuen LH, Kwon H, Ono T, Kool ET (2013) DNA-polyfluorophore chemosensors for environmental remediation: vapor-phase identification of petroleum products in contaminated soil. Chem Sci 4(8):3184–3190

Kapuscinski J (1995) DAPI: a DNA-specific fluorescent probe. Biotech Histochem 70(5): 220–233

Ke G, Wang C, Ge Y, Zheng N, Zhu Z, Yang CJ (2012) L-DNA molecular beacon: a safe, stable, and accurate intracellular nano-thermometer for temperature sensing in living cells. J Am Chem Soc 134(46):18908–18911

Kessler MA, Meinitzer A, Petek W, Wolfbeis OS (1997) Microalbuminuria and borderline-increase albumin excretion determined with a centrifugal analyzer and the Albumin Blue 580 fluorescence assay. Clin Chem 43(6):996–1002

Kimura Y, Fukuda M, Suda K, Terazima M (2010) Excited state intramolecular proton transfer reaction of 4′-N, N-diethylamino-3-hydroxyflavone and solvation dynamics in room temperature ionic liquids studied by optical Kerr gate fluorescence measurement. J Phys Chem B 114(36):11847–11858

Klymchenko AS, Shvadchak VV, Yushchenko DA, Jain N, Mely Y (2008) Excited-state intramolecular proton transfer distinguishes microenvironments in single- and double-stranded DNA. J Phys Chem B 112(38):12050–12055

Kolomiets E, Johansson EMV, Renaudet O, Darbre T, Reymond JL (2007) Neoglycopeptide dendrimer libraries as a source of lectin binding ligands. Org Lett 9(8):1465–1468

Konishi K, Hiratani T (2006) Turn-on and selective luminescence sensing of copper ions by a water-soluble Cd10S16 molecular cluster. Angew Chem Int Ed Engl 45(31):5191–5194

Koo C-K, Samain F, Dai N, Kool ET (2011a) DNA polyfluorophores as highly diverse chemosensors of toxic gases. Chem Sci 2(10):1910–1917

Koo C-K, Wang S, Gaur RL, Samain F, Banaei N, Kool ET (2011b) Fluorescent DNA chemosensors: identification of bacterial species by their volatile metabolites. Chem Commun 47(41): 11435–11437

Kovalska VB, Volkova KD, Losytskyy MY, Tolmachev OI, Balanda AO, Yarmoluk SM (2006) 6,6′-Disubstituted benzothiazole trimethine cyanines–new fluorescent dyes for DNA detection. Spectrochim Acta A Mol Biomol Spectrosc 65(2):271–277

Kuimova MK (2012) Mapping viscosity in cells using molecular rotors. Phys Chem Chem Phys 14(37):12671–12686

Kuimova MK, Yahioglu G, Levitt JA, Suhling K (2008) Molecular rotor measures viscosity of live cells via fluorescence lifetime imaging. J Am Chem Soc 130(21):6672–6673

Kummer S, Knoll A, Socher E, Bethge L, Herrmann A, Seitz O (2012) PNA FIT-probes for the dual color imaging of two viral mRNA targets in influenza H1N1 infected live cells. Bioconjug Chem 23(10):2051–2060

Kuruvilla E, Ramaiah D (2007) Selective interactions of a few acridinium derivatives with single strand DNA: study of photophysical and DNA binding interactions. J Phys Chem B 111(23):6549–6556

Kusnezow W, Jacob A, Walijew A, Diehl F, Hoheisel JD (2003) Antibody microarrays: an evaluation of production parameters. Proteomics 3(3):254–264

Kwakye S, Baeumner A (2003) A microfluidic biosensor based on nucleic acid sequence recognition. Anal Bioanal Chem 376(7):1062–1068

Kwan PH, MacLachlan MJ, Swager TM (2004) Rotaxanated conjugated sensory polymers. J Am Chem Soc 126(28):8638–8639

Laws WR, Brand L (1979) Analysis of two-state excited-state reactions. The fluorescence decay of 2-naphthol. J Phys Chem 83:795–802

Lenhart JL, van Zanten JH, Dunkers JP, Zimba CG, James CA, Pollack SK, Parnas RS (2000) Immobilizing a fluorescent dye offers potential to investigate the glass/resin interface. J Colloid Interface Sci 221(1):75–86

Lenhart JL, van Zanten JH, Dunkers JP, Parnas RS (2002) Using a localized fluorescent dye to probe the glass/resin interphase. Polym Compos 23(4):555–563

Lepkowicz RS, Przhonska OV, Hales JM, Fu J, Hagan DJ, Van Stryland EW, Bondar MV, Slominsky YL, Kachkovski AD (2004) Nature of the electronic transitions in thiacarbocyanines with a long polymethine chain. Chem Phys 305(1–3):259–270

Li CY, Zhang XB, Han ZX, Akermark B, Sun L, Shen GL, Yu RQ (2006) A wide pH range optical sensing system based on a sol–gel encapsulated amino-functionalized corrole. Analyst 131(3):388–393

Li Y-H, Zhang L, Huang J, Liang R-P, Qiu J-D (2013) Fluorescent graphene quantum dots with a boronic acid appended bipyridinium salt to sense monosaccharides in aqueous solution. Chem Commun 49(45):5180–5182

Lin W, Long L, Yuan L, Cao Z, Chen B, Tan W (2008) A ratiometric fluorescent probe for cysteine and homocysteine displaying a large emission shift. Org Lett 10(24):5577–5580

Liu B, Bazan GC (2005) Methods for strand-specific DNA detection with cationic conjugated polymers suitable for incorporation into DNA chips and microarrays. Proc Natl Acad Sci U S A 102(3):589–593

Liu Y, Song Y, Chen Y, Li XQ, Ding F, Zhong RQ (2004) Biquinolino-modified beta-cyclodextrin dimers and their metal complexes as efficient fluorescent sensors for the molecular recognition of steroids. Chemistry 10(15):3685–3696

Liu Z, He W, Guo Z (2013) Metal coordination in photoluminescent sensing. Chem Soc Rev 42(4):1568–1600

Ma D-L, Shiu-Hin Chan D, Yang H, He H-Z, Leung C-H (2012) Luminescent G-quadruplex probes. Curr Pharm Des 18(14):2058–2075

Masuhara H, Asahi T, Hosokawa Y (2006) Laser nanochemistry. Pure Appl Chem 78(12): 2205–2226

McAnaney TB, Park ES, Hanson GT, Remington SJ, Boxer SG (2002) Green fluorescent protein variants as ratiometric dual emission pH sensors. 2. Excited-state dynamics. Biochemistry 41(52):15489–15494

McAnaney TB, Shi X, Abbyad P, Jung H, Remington SJ, Boxer SG (2005) Green fluorescent protein variants as ratiometric dual emission pH sensors. 3. Temperature dependence of proton transfer. Biochemistry 44(24):8701–8711

McGaughey O, Ros-Lis JV, Guckian A, McEvoy AK, McDonagh C, MacCraith BD (2006) Development of a fluorescence lifetime-based sol–gel humidity sensor. Anal Chim Acta 570(1):15–20

Mordon S, Devoisselle JM, Soulie S (1995) Fluorescence spectroscopy of pH in vivo using a dual-emission fluorophore (C-SNAFL-1). J Photochem Photobiol B 28(1):19–23

Nagl S, Baleizao C, Borisov SM, Schaferling M, Berberan-Santos MN, Wolfbeis OS (2007) Optical sensing and imaging of trace oxygen with record response. Angew Chem Int Ed Engl 46(13):2317–2319

Ngundi MM, Kulagina NV, Anderson GP, Taitt CR (2006a) Nonantibody-based recognition: alternative molecules for detection of pathogens. Expert Rev Proteomics 3(5):511–524

Ngundi MM, Taitt CR, McMurry SA, Kahne D, Ligler FS (2006b) Detection of bacterial toxins with monosaccharide arrays. Biosens Bioelectron 21(7):1195–1201

Nipper ME, Majd S, Mayer M, Lee JC, Theodorakis EA, Haidekker MA (2008) Characterization of changes in the viscosity of lipid membranes with the molecular rotor FCVJ. Biochim Biophys Acta 1778(4):1148–1153

Niu CG, Gui XQ, Zeng GM, Yuan XZ (2005) A ratiometric fluorescence sensor with broad dynamic range based on two pH-sensitive fluorophores. Analyst 130(11):1551–1556

O'Neal DP, Meledeo MA, Davis JR, Ibey BL, Gant VA, Pishko MV, Cote GL (2004) Oxygen sensor based on the fluorescence quenching of a ruthenium complex immobilized in a biocompatible poly(ethylene glycol) hydrogel. IEEE Sensors J 4(6):728–734

Ogul'chansky T, Yashchuk VM, Losytskyy M, Kocheshev IO, Yarmoluk SM (2000) Interaction of cyanine dyes with nucleic acids. XVII. Towards an aggregation of cyanine dyes in solutions as a factor facilitating nucleic acid detection. Spectrochim Acta A Mol Biomol Spectrosc 56(4):805–814

Oh KJ, Cash KJ, Hugenberg V, Plaxco KW (2007) Peptide beacons: a new design for polypeptide-based optical biosensors. Bioconjug Chem 18(3):607–609

Olmos D, Aznar AJ, Baselga J, Gonzalez-Benito J (2003) Kinetic study of epoxy curing in the glass fiber/epoxy interface using dansyl fluorescence. J Colloid Interface Sci 267(1):117–126

Olmos D, Aznar AJ, Gonzalez-Benito J (2005) Kinetic study of the epoxy curing at the silica particles/epoxy interface using the fluorescence of pyrene label. Polym Test 24(3):275–283

Pal R, Parker D (2007) A single component ratiometric pH probe with long wavelength excitation of europium emission. Chem Commun 5:474–476
Palacios-Rodriguez Y, Gazarian T, Rowley M, Majluf-Cruz A, Gazarian K (2007) Collection of phage-peptide probes for HIV-1 immunodominant loop-epitope. J Microbiol Methods 68(2):225–235
Pavlickova P, Schneider EM, Hug H (2004) Advances in recombinant antibody microarrays. Clin Chim Acta 343(1–2):17–35
Pickup JC, Hussain F, Evans ND, Rolinski OJ, Birch DJS (2005) Fluorescence-based glucose sensors. Biosens Bioelectron 20(12):2555–2565
Potyrailo RA (2006) Polymeric sensor materials: toward an alliance of combinatiorial and rational design tools? Angew Chem Int Edit 45(5):702–723
Przhonska O, Bondar M, Gallay J, Vincent M, Slominsky Y, Kachkovski A, Demchenko AP (1999) Photophysics of dimethylamino-substituted polymethine dye in polymeric media. J Photochem Photobio B Biol 52(1–3):19–29
Quaranta M, Borisov SM, Klimant I (2012) Indicators for optical oxygen sensors. Bioanal Rev 4(2–4):115–157
Quirin JC, Torkelson JM (2003) Self-referencing fluorescence sensor for monitoring conversion of non-isothermal polymerization and nanoscale mixing of resin components. Polymer 44(2):423–432
Reichardt C, Welton T (2011) Solvents and solvent effects in organic chemistry. Weinheim: Viley VCH
Rillahan CD, Paulson JC (2011) Glycan microarrays for decoding the glycome. Annu Rev Biochem 80:797
Rubina AY, Dementieva EI, Stomakhin AA, Darii EL, Pan'kov SV, Barsky VE, Ivanov SM, Konovalova EV, Mirzabekov AD (2003) Hydrogel-based protein microchips: manufacturing, properties, and applications. Biotechniques 34(5):1008–1014, 1016–1020, 1022
Rubina AY, Pan'kov SV, Dementieva EI, Pen'kov DN, Butygin AV, Vasiliskov VA, Chudinov AV, Mikheikin AL, Mikhailovich VM, Mirzabekov AD (2004) Hydrogel drop microchips with immobilized DNA: properties and methods for large-scale production. Anal Biochem 325(1):92–106
Rucker VC, Havenstrite KL, Herr AE (2005) Antibody microarrays for native toxin detection. Anal Biochem 339(2):262–270
Ruttkay-Nedecky B, Kudr J, Nejdl L, Maskova D, Kizek R, Adam V (2013) G-quadruplexes as sensing probes. Molecules 18(12):14760–14779
Sapsford KE, Ngundi MM, Moore MH, Lassman ME, Shriver-Lake LC, Taitt CR, Ligler FS (2006) Rapid detection of foodborne contaminants using an Array Biosensor. Sensors Actuators B Chem 113(2):599–607
Sassolas A, Leca-Bouvier BD, Blum LJ (2008) DNA biosensors and microarrays. Chem Rev 108(1):109–139
Schäferling M, Grögel DB, Schreml S (2011) Luminescent probes for detection and imaging of hydrogen peroxide. Microchimica Acta 174(1–2):1–18
Shin I, Park S, Lee MR (2005) Carbohydrate microarrays: an advanced technology for functional studies of glycans. Chemistry 11(10):2894–2901
Shvadchak VV, Klymchenko AS, de Rocquigny H, Mely Y (2009) Sensing peptide-oligonucleotide interactions by a two-color fluorescence label: application to the HIV-1 nucleocapsid protein. Nucleic Acids Res 37(3), e25
Silva FR, Samad RE, Gomes L, Courrol LC (2008) Enhancement of europium emission band of europium tetracycline complex in the presence of cholesterol. J Fluoresc 18(1):169–174
Socher E, Jarikote DV, Knoll A, Röglin L, Burmeister J, Seitz O (2008) FIT probes: peptide nucleic acid probes with a fluorescent base surrogate enable real-time DNA quantification and single nucleotide polymorphism discovery. Anal Biochem 375(2):318–330
Spence MTZ, Johnson ID (2010) The molecular probes handbook: a guide to fluorescent probes and labeling technologies, 11th edn. New York: Life Technologies Corporation
Steiner M-S, Duerkop A, Wolfbeis OS (2011) Optical methods for sensing glucose. Chem Soc Rev 40(9):4805–4839
Suppan P, Ghoneim N (1997) Solvatochromism. Royal Society of Chemistry, Cambridge

Tatikolov AS (2012) Polymethine dyes as spectral-fluorescent probes for biomacromolecules. J Photochem Photobio C Photochem Rev 13(1):55–90
Thomas SW, Amara JP, Bjork RE, Swager TM (2005) Amplifying fluorescent polymer sensors for the explosives taggant 2,3-dimethyl-2,3-dinitrobutane (DMNB). Chem Commun 36:4572–4574
Thomas SW 3rd, Joly GD, Swager TM (2007) Chemical sensors based on amplifying fluorescent conjugated polymers. Chem Rev 107(4):1339–1386
Turkmen Z, Klymchenko AS, Oncul S, Duportail G, Topcu G, Demchenko AP (2005) A triterpene oleanolic acid conjugate with 3-hydroxyflavone derivative as a new membrane probe with two-color ratiometric response. J Biochem Biophys Methods 64(1):1–18
Tyagi S, Kramer FR (1996) Molecular beacons: probes that fluoresce upon hybridization. Nat Biotechnol 14(3):303–308
Vaijayanthi T, Bando T, Pandian GN, Sugiyama H (2012) Progress and prospects of pyrrole-imidazole polyamide–fluorophore conjugates as sequence-selective DNA probes. Chembiochem 13(15):2170–2185
Valanne A, Huopalahti S, Soukka T, Vainionpaa R, Lovgren T, Harma H (2005) A sensitive adenovirus immunoassay as a model for using nanoparticle label technology in virus diagnostics. J Clin Virol 33(3):217–223
Valuk VR, Duportail G, Pivovarenko VG (2005) A wide-range fluorescent pH-indicator based on 3-hydroxyflavone structure. J Photochem Photobio A Chem 175(2–3):226–231
Vercoutere W, Akeson M (2002) Biosensors for DNA sequence detection. Curr Opin Chem Biol 6(6):816–822
Vidal JC, Garcia-Ruiz E, Espuelas J, Aramendia T, Castillo JR (2003) Comparison of biosensors based on entrapment of cholesterol oxidase and cholesterol esterase in electropolymerized films of polypyrrole and diaminonaphthalene derivatives for amperometric determination of cholesterol. Anal Bioanal Chem 377(2):273–280
Vincent M, Gallay J, Demchenko AP (1995) Solvent relaxation around the excited-state of indole – analysis of fluorescence lifetime distributions and time-dependence spectral shifts. J Phys Chem 99(41):14931–14941
Volovik Z, Demchenko A, Skursky S (1994) Solvent-dependent photophysics of non-symmetric polymethine dyes as fluorescence probes: dual emission and inhomogeneous broadening. Proc SPIE Int Soc Opt Eng 2137:600–607
von Bultzingslowen C, McEvoy AK, McDonagh C, MacCraith BD (2003) Lifetime-based optical sensor for high-level pCO(2) detection employing fluorescence resonance energy transfer. Anal Chim Acta 480(2):275–283
Vopálenská I, Váchová L, Palková Z (2015) New biosensor for detection of copper ions in water based on immobilized genetically modified yeast cells. Biosens Bioelectron 72:160–167
Wade SA, Collins SF, Baxter GW (2003) Fluorescence intensity ratio technique for optical fiber point temperature sensing. J Appl Phys 94(8):4743–4756
Wandelt B, Cywinski P, Darling GD, Stranix BR (2005) Single cell measurement of microviscosity by ratio imaging of fluorescence of styrylpyridinium probe. Biosens Bioelectron 20(9):1728–1736
Wang X-D, Wolfbeis OS (2014) Optical methods for sensing and imaging oxygen: materials, spectroscopies and applications. Chem Soc Rev 43(10):3666–3761
Wang L, Zhao WJ, O'Donoghue MB, Tan WH (2007) Fluorescent nanoparticles for multiplexed bacteria monitoring. Bioconjug Chem 18(2):297–301
Wang K, Huang J, Yang X, He X, Liu J (2013a) Recent advances in fluorescent nucleic acid probes for living cell studies. Analyst 138(1):62–71
Wang X-d, Wolfbeis OS, Meier RJ (2013b) Luminescent probes and sensors for temperature. Chem Soc Rev 42(19):7834–7869
Whitaker JE, Haugland RP, Prendergast FG (1991) Spectral and photophysical studies of benzo[c] xanthene dyes: dual emission pH sensors. Anal Biochem 194(2):330–344

White RR, Shan S, Rusconi CP, Shetty G, Dewhirst MW, Kontos CD, Sullenger BA (2003) Inhibition of rat corneal angiogenesis by a nuclease-resistant RNA aptamer specific for angiopoietin-2. Proc Natl Acad Sci U S A 100(9):5028–5033

Wolfbeis OS (2005) Materials for fluorescence-based optical chemical sensors. J Mater Chem 15(27–28):2657–2669

Wu Y-Y, Yu W-T, Hou T-C, Liu T-K, Huang C-L, Chen I-C, Tan K-T (2014) A selective and sensitive fluorescent albumin probe for the determination of urinary albumin. Chem Commun 50(78):11507–11510

Yang CJ, Martinez K, Lin H, Tan W (2006) Hybrid molecular probe for nucleic acid analysis in biological samples. J Am Chem Soc 128(31):9986–9987

Yarmoluk SM, Losytskyy MY, Yashchuk VM (2002) Nonradiative deactivation of the electronic excitation energy in cyanine dyes: influence of binding to DNA. J Photochem Photobiol B 67(1):57–63

Yashchuk VM, Gusak VV, Drnytruk IM, Prokopets VM, Kudrya VY, Losytskyy MY, Tokar VP, Gumenyuk YO, Yarmoluk SM, Kovalska VB, Balanda AO, Kryvorotenko DV (2007) Two-photon excited luminescent styryl dyes as probes for the DNA detection and imaging. Photostability and phototoxic influence on DNA. Mol Cryst Liq Cryst 467:325–338

Yesylevskyy SO, Demchenko AP (2011) Fluorescence probing in structurally anisotropic materials. In: Advanced fluorescence reporters in chemistry and biology III. Berlin/Heidelberg: Springer; pp 119–158. doi:10.1007/978-3-642-18035-4

You C-C, Miranda OR, Gider B, Ghosh PS, Kim I-B, Erdogan B, Krovi SA, Bunz UH, Rotello VM (2007) Detection and identification of proteins using nanoparticle–fluorescent polymer 'chemical nose'sensors. Nat Nanotechnol 2(5):318–323

Zhang CY, Yeh HC, Kuroki MT, Wang TH (2005) Single-quantum-dot-based DNA nanosensor. Nat Mater 4(11):826–831

Zhao X, Tapec-Dytioco R, Tan W (2003) Ultrasensitive DNA detection using highly fluorescent bioconjugated nanoparticles. J Am Chem Soc 125(38):11474–11475

Zheng T, Peelen D, Smith LM (2005) Lectin arrays for profiling cell surface carbohydrate expression. J Am Chem Soc 127(28):9982–9983

Zhou X, Lee S, Xu Z, Yoon J (2015) Recent progress on the development of chemosensors for gases. Chem Rev. doi:10.1021/cr500567r

Zhu X, Sun J, Hu Y (2007) Determination of protein by hydroxypropyl-beta-cyclodextrin sensitized fluorescence quenching method with erythrosine sodium as a fluorescence probe. Anal Chim Acta 596(2):298–302

Chapter 13
Sensing Inside the Living Cells

Microscopy in fluorescent light is quite different from common light transmission microscopy. The optical contrast needed in transmission is not important here and there is no need to enhance it by dye staining. Instead, the dyes can be applied in much lower concentrations so that they do not interfere with cellular life. They can form fluorescent image contrasting different structures and organelles, demonstrating distributions of different types of molecules and their dynamics. High resolution in images is achieved due to focusing the exciting light beam on particular site forming *focal plane* or *focal volume*, and this allows suppression of out-of-site emission. The illuminated volume can be dramatically reduced, which leads to detection of single molecules. In order to achieve localization of macromolecules and formation of image with molecular resolution, the fundamental restriction known as *diffraction limit* has been overcome by recently developed techniques.

All these achievements become very useful when they allow addressing fundamental problems of cellular biology and also when they allow characterizing the species inside the cell that are of diagnostic and prognostic value. Extremely important are the possibilities of imaging the interactions between macromolecules and their biocatalytic transformations. Manipulation with fluorescent dyes and nanoparticles allows many possibilities for their use as tags, probes and sensors (Schäferling 2012). The applied species can be intrinsic or extrinsic to the cell; they can be not only silent observers but also participants, modulators or disruptors of specific activities that form biological functions. They can be successfully studied and quantitatively characterized with fluorescence techniques.

A.P. Demchenko, *Introduction to Fluorescence Sensing*,
DOI 10.1007/978-3-319-20780-3_13

13.1 Modern Fluorescence Microscopy

The basic function of a *fluorescence microscope* is to provide the image of studied object in fluorescent light with the full rejection of incident light. Advancement in such instrumentation stimulated a great progress in imaging. For forming the image that is informative for sensing in fluorescent light, a variety of different dyes were suggested as the labels, tags, probes and sensors.

There is a choice to compose an image based on selected parameter characterizing their emission. Commonly it is the light intensity, but it can be also anisotropy, lifetime and ratio of intensities at selected wavelengths (λ-ratiometry). Microscopes allow the selection of excitation wavelengths (often, in a limited range) and detection at different emission wavelengths that are usually selected in a broader range by the filters. Thus, the studied object is illuminated by light of an (almost) desired wavelength, and then the much weaker emitted fluorescence is separated from the excitation light, an image is formed. This image can be recorded with a high contrast against the background.

There are two sources of this *background*, and the instrument constructors and researchers combine their efforts to eliminate (or, at least, to reduce) them. One is the intrinsic fluorescence of cellular components (*autofluorescence*). It is caused by such pigments, as reduced nicotinamide dinucleotide (NADH) and flavine adenine dinucleotide (FAD) that are always present in a living cell. Such background signal can be reduced by proper selection of excitation and emission wavelengths (usually, by shifting from near-UV and violet to green and longer wavelengths). Of course, the applied fluorescence reporter should have the highest brightness in these conditions.

The other source of background is fundamentally unavoidable but can be dramatically reduced by optical means. It is the excitation of emitting species that are illuminated by excitation beam but are *out of focus*. These emitters do not participate in the formation of image but spoil it. Actually, here the aims in microscopy are the opposite to that in common photography, where a photographer tries to keep both close and distant objects in focus. Here various optical principles and instrument constructions are employed to restrict the excitation and detection of fluorophores to a thin region of the sample (focal plane) and to make the fluorescence from this region much stronger than that coming from the regions outside it. Below, we will overview three technologies that provide dramatically increased response from the dyes located within the focal plane. These are the *total internal reflection microscopy*, the *confocal microscopy* and the *two-photon microscopy*. Elimination of background fluorescence from outside the focal plane can dramatically improve the signal-to-noise ratio, and consequently, the contrast of obtained images.

With all these advancements, the spatial resolution remains the most important factor to be considered. The fundamental limit is given by the length of light wave

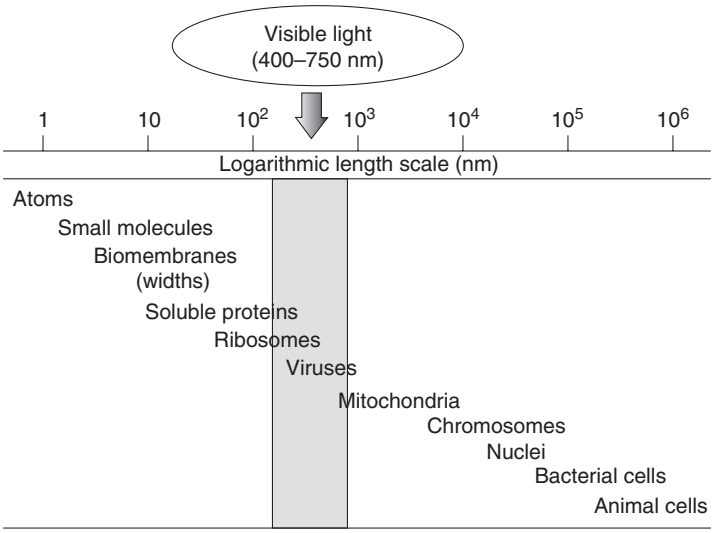

Fig. 13.1 The sizes of cells and of their components with respect of wavelength of visible light

and is known as the *diffraction limit*. It is associated with the name of Ernst Abbe, who in 1873 formulated this limit as the ability of a lens-based optical microscope to discern only those details that are larger than a half of the wavelength of light. The diagram presented below (Fig. 13.1) may help the reader in orienting in dimensions of cellular components and whole cells in comparison with the wavelength of light. The objects with dimensions smaller than 200–400 nm (presented to the left of grey vertical band) are not resolvable by conventional image-making microscopy.

Thus, two or more orders of magnitude separate the best resolution that can be obtained by conventional diffraction-limited optical techniques and the molecular level. However, there are two possibilities to overcome this limit in producing the fluorescence images. One is to make a waveguide with a pointed edge of nanometer dimension and to provide scanning with a 'nano-beam'; this is the *near-field fluorescence microscopy*. Recently, the other possibility to break the diffraction limit was suggested within the range if *scanning* and *wide-field optical nanoscopy*. Both these techniques will be also discussed below.

13.1.1 Epi-fluorescence Microscopy

The wide field *epi-fluorescence microscopy* is the most popular fluorescence method in cellular research. In this configuration the excitation and

observation of the fluorescence are from above (*epi*) the specimen, in contrast to common microscopes that collect transmitted light. With different fluorescent stains this technique allows identifying cells and cellular components with a high degree of specificity. This microscopy has become an important tool in the field of biology, opening the doors for more advanced technical designs. For example, with the labelled antibodies, different disease conditions can be identified.

The construction of epi-fluorescence microscope (Fig. 13.2) allows very efficient collection of fluorescent light that forms the image. The epi-configuration allows the microscope to let the excitation light illuminate the specimen and then sort out the much weaker emitted light from the scattered excitation light to make up the image. For that, the microscope has a filter that allows passing only the radiation with the desired wavelength that matches the fluorescing material. The emitted light is separated from the much brighter excitation light with a second filter. Here, the fact that the emitted light has a spectrum at longer wavelengths (being Stokes-shifted) is used. The bright fluorescing areas can be observed in the microscope against a dark background with a high contrast.

The major disadvantage of this microscope is that it allows collecting the image of a specimen with the three-dimensional distribution of fluorescent species as a two-dimensional picture formed by *both in-focus* and *out-of-focus* located fluorescence emitters. It produces 'photographic' imaging of the object, in which sometimes it is hard to judge, what is in front and what is behind. Thus, a significant part of spatial information can be lost.

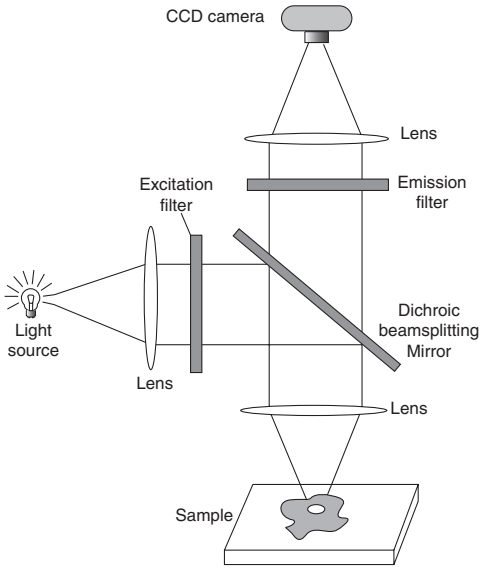

Fig. 13.2 Schematic representation of a simplest epi-fluorescence microscope. Incident excitation light, after passing the optical filter, is focused on the specimen from *above*. Fluorescent light is directed to the detector after passing the filter that rejects the reflected and scattered excitation light

13.1.2 Total Internal Reflection Fluorescence Microscopy (TIRF)

The *total internal reflection microscopy* takes advantage of the evanescent wave that exists when the light is totally internally reflected at the interface between two media having dissimilar refractive indices (see Sect. 10.6). In this technique, a prism of sapphire or special glass with high refractive index is used to illuminate the sample located on top of it. If the light is directed into the prism at an angle higher than the critical angle, the beam will not enter the studied specimen in low-refractive aqueous environment and will be totally internally reflected at the interface. Meantime, some of the light energy can propagate at a short distance and excite fluorescent dyes close to the interface. The reflection phenomenon develops at the interface a so-called *evanescent wave* that permeates about 100–200 nm outside the interface (Fig. 13.3). The light intensity of evanescent wave is sufficiently high to excite the dyes, but remains located within this short distance (see Sect. 10.6). Because of such shallow penetration depth of excitation energy, the *x*-*y* plane close to the interface becomes in fact the focal plane.

Depicted in Fig. 13.3 is the simplest configuration of microscope based on this principle that allows many modifications. They are well described in the literature and in information materials provided by the instrument manufacturers. Because the excitation of fluorophores in the bulk of the object is avoided and the fluorescence emission is confined to a very thin region, a much higher signal-to-noise ratio is achieved compared to conventional epi-fluorescence imaging. Some instruments

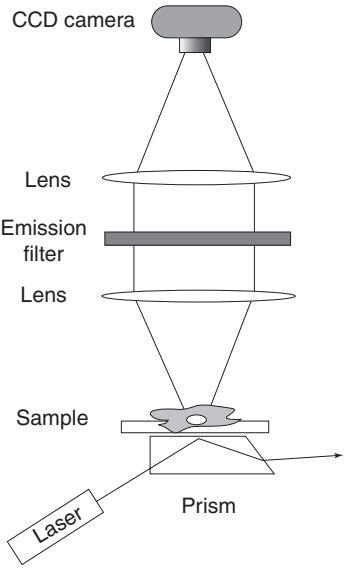

Fig. 13.3 Schematic representation of total internal reflection fluorescence microscope with illumination 'from below' and detection 'from above'. The incident beam does not penetrate into the medium where the specimen is located and excites its fluorescence by producing evanescent field in a narrow pre-surface area

allow varying the illumination incidence angle and, consequently, the penetration depth of the evanescent wave. This allows increasing the resolution along z axis and distinguishing the depths of dye location on a nanometer scale. Meantime, these variations are limited to the pre-surface area and do not allow seeing the whole cells.

13.1.3 Confocal Microscopy

Confocal microscopy offers a different principle of forming sharp images. The conventional focusing system is applied here, in which the excitation of out-of-focus located dyes by incident beam is not avoided, but an optical configuration of the instrument allows rejecting their emission. This is achieved with the application of *scanning* the focal plane with the use of *confocal pinhole* that provides geometric restriction to passing the out-of-focus emission (Fig. 13.4).

Application of this principle allows rendering very sharp fluorescence images due to dramatically improved signal-to-noise ratio. In confocal microscopy, the resolution along z axis is on the level of 1 μm, which is by one order of magnitude less than in total internal reflection microscopy. But the great advantage here is the possibility to *move the focal plane* providing scanning the object at different z levels, so that the cross-sections at various depths can be obtained. If necessary, by computational means these cross-sections can be transformed into the three-

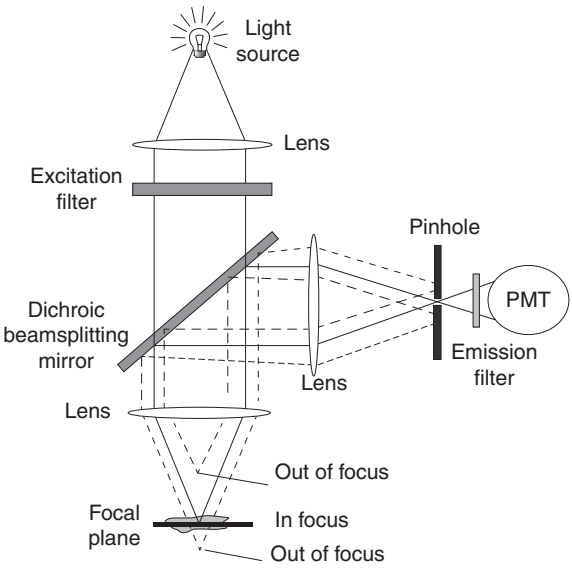

Fig. 13.4 Schematic representation of a typical confocal microscope showing the beam geometry that allows rejection of photons emitted from outside the focal plane

dimensional image of the object. A remarkable explosion in the popularity of confocal microscopy in recent years is due in part to the relative ease, with which the high-quality cross-sectional images can be obtained from the samples prepared for conventional optical microscopy.

One weak point of (the by now "classical") confocal microscopy is the need to use the high-intensity lasers for excitation and to illuminate with them a large volume, not only within the focal plane. Since the illumination is not limited to a focal plane, it generates not only fluorescence but also produces photobleaching and phototoxicity in the whole illuminated volume throughout the object. Involvement of these factors strongly depends on the properties of used dyes. Another major disadvantage of confocal microscopes is the restriction of the instantaneous illumination to a tightly focused spot (in the limit, an "Airy disk"). This circumstance has two consequences: (1) if linearity of response is to be preserved, one must limit the irradiance in the focal plane to a value that does not lead to saturation of the excited state; and (2) the very low duty cycle of excitation (fractional area of the objective field illuminated at any one time) leads to long acquisition times, a great disadvantage in studies of live cells.

An attempt to overcome at least one of these limitations is to form an image by simultaneous illumination of many pinholes, as in the "spinning disk" microscopes. Confocality is here provided by synchronous rotation of two discs (called Nipkow disks). One of these disks contains about 20,000 microlenses, and the other is placed with the same number of pinholes (Straub et al. 2000). Passing through the array of microlenses and focusing upon correspondent pinholes, the excitation laser beam can create about 1000 independent focal volume elements. By rotating the disk pair, a full high resolution confocal image can be acquired within 50 ms. The disadvantage of rotating disks is that the pattern of illumination and detection cannot be adjusted at will for particular purpose.

13.1.4 Programmable Array Microscope

The optical sectioning 'intelligent' *Programmable Array Microscope* (iPAM) can serve as an add-on module for conventional commercial wide field fluorescence microscope, converting it into a high-speed optical sectioning ("confocal") instrument (de Vries et al. 2015). It is unique in that it combines both large field of view and high speed, without compromising the imaging performance. In iPAM the structured illumination and structured detection operate in synchrony. A single digital micro-mirror device (DMD) acts as a spatial light modulator defining a pattern in both the fluorescence excitation and emission paths. A sequence of binary patterns of excitation light is projected into the focal plane of the microscope. The resulting fluorescent emission is captured as two distinct signals: *conjugate*, *c*

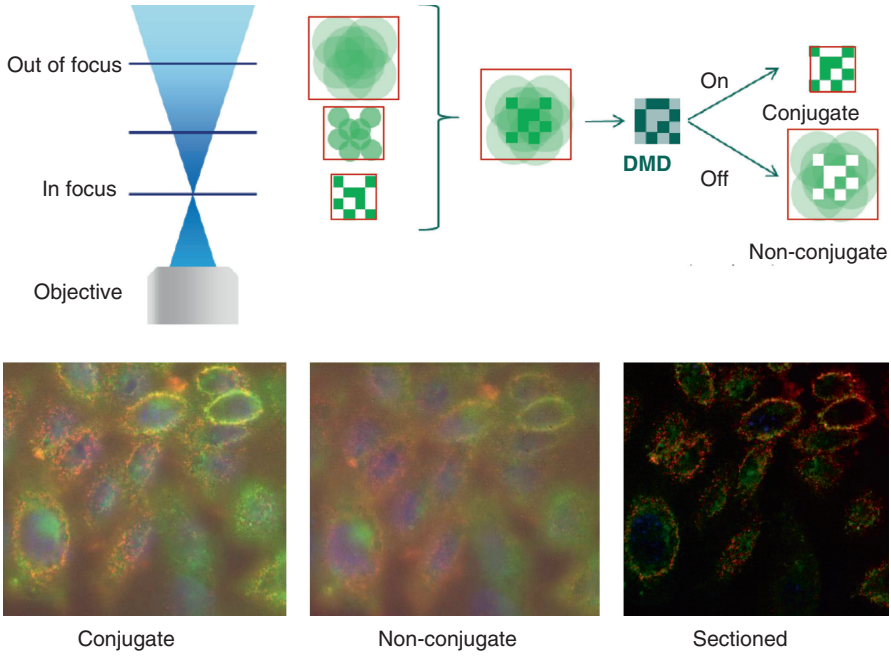

Fig. 13.5 Operation principle of programmable array microscope (*above*) and comparison of the conjugate, non-conjugate and the resulting sectioned images (*below*) (de Vries et al. 2015). The conjugate image reveals the extra in-focus detail in the image that is missing in the non-conjugate image. It is this in-focus component in the conjugate image which is left after (weighted) subtraction of the non-conjugate

("on-focus") consisting of light impinging on and deviated from the "on" elements of the DMD, and the *non-conjugate*, *nc* ("out-of-focus") light falling on and deviated from the "off" elements (Fig. 13.5).

Thus, the *c* image comprises the in-focus information and part of the out-of-focus background, while the *nc* image receives the rest of the out-of-focus background. The two distinct, deflected beams are optically filtered and detected either by two individual cameras or captured as adjacent images on a single camera after traversing an image combiner. The sectioned image is gained from a subtraction of the *nc* image from the *c* image, weighted in accordance with the pattern(s) used for illumination and detection and the relative exposure times of the cameras. The widefield image is given by the sum of the *c* and *nc* images.

This system can function at very high acquisition speed with low light intensities, preventing saturation and minimizing photobleaching of sensitive fluorophores. The programmable array allows optimization of the patterns (duty cycle, feature size and distribution), thus enabling a wide range of applications, ranging from patterned photobleaching to superresolution microscopy.

13.1.5 Two-Photon and Three-Photon Microscopy

In Sect. 10.4 of this book, we described the physical background of a phenomenon that brings the electronic system to an excited state by *absorption of two photons* simultaneously. Two photon excitation can occur only when the photon density is very high, which can be realized by confining the light flux on a spatial and temporal scale. Very short pulses of a well-focused laser can do this. In this case, the *laser focal point* is the only location along the optical path where the photon density is high enough to generate a significant occurrence of two-photon excited species.

The generation of two-photon excitation in a fluorophore-containing specimen at the microscope focal point is illustrated in Fig. 13.6. Above and below the focal point, the photon density is not sufficiently high for two photons to pass at the same instant within the absorption cross section of a single fluorophore. Only at the focal point, this density can be so high that the two photons will be absorbed simultaneously with sufficient probability.

This phenomenon has found a very important application in microscopy because it brings many benefits.

(a) In contrast to confocal microscopy, the two-photon microscopy allows concentrating all the excitation in a narrow focal plane. Outside this plane, the dyes are not excited simply because the photon flux is insufficient. This brings not only a sharp image but also the absence of photochemical reactions outside the focal plane, which would lead to photobleaching and phototoxicity.

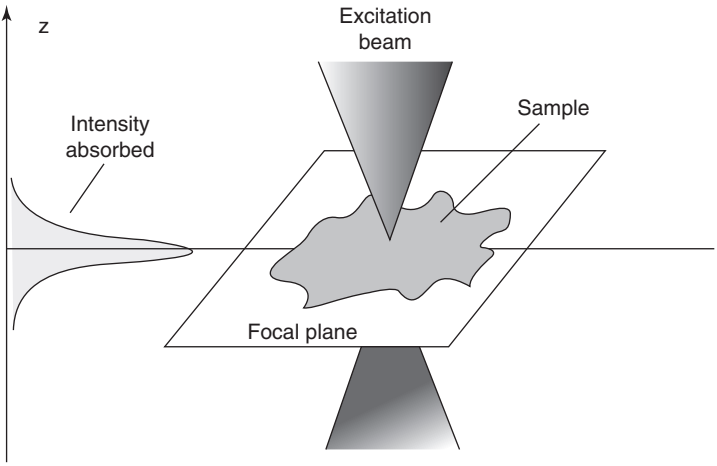

Fig. 13.6 Illustration of the principle of two-photon and three-photon microscopy. The focused light provides the high photon density that can be absorbed by only in-plane dyes, thus forming a sharp image. The near-IR laser can excite 'blue-green' and 'near-UV' emissions by two-photon and three-photon absorption, respectively

Thus, if we want to express in two words the key difference between confocal and two-photon microscopy, we must say: *in confocal microscopy the out-of-focus background is rejected, but in two-photon microscopy it does not appear!*

(b) In two-photon microscopy the wavelengths of excitation and emission differ dramatically (for instance, the dye with normal absorption band maximum at 520 nm can be excited by two photons of 1050 nm laser, and an emission detected at 560 nm). Therefore, *the scattered excitation light is easily rejected*.
(c) The cells and tissues are relatively transparent in the near-IR, so an intensive light for exciting two photons *can penetrate without essential losses* at substantial depths into the living tissue or even inside intact animal specimens. Additionally, because there is no absorption in out-of-focus specimen areas, more of the excitation light penetrates through the specimen to the plane of focus. Together with the formation of focal planes at substantial depths and with the possibility to move these planes this provides unique prospects in imaging.

The *three-photon excitation* has an interesting prospect in cellular research not only by producing the sharper image. Such three-photon excitation occurs in much the same way as the two-photon process, except that three photons must interact with the same dye simultaneously to produce emission. One of the benefits of that is the possibility to provide an excitation of two dyes absorbing light at two quite different wavelengths with the same laser. With the 1050 nm laser the blue-green dye can be excited by two photons at about 520 nm whereas a near-UV absorbing (at about 350 nm) dye can be excited simultaneously by three photons. Fluorescence of these two dyes can form a two-color image.

New possibilities appear with intracellular applications of reporting dyes operating by variation of lifetime. The two-photon excitation microscopy utilizes pulsed lasers, therefore it can be readily extended into the combination with fluorescence lifetime imaging. Detection of various analytes and establishing proximity relations between molecules often use the FRET methodology (Sect. 3.6), and the best applicable to cellular research FRET detection is the lifetime imaging. Different two-photon excited probes were developed for visualization of sub-cellular structures and measuring local pH and concentrations of analytes (Lim 2013; Zhang et al. 2013).

13.1.6 Time-Resolved and Time-Gated Imaging

The *fluorescence lifetime imaging* (FLIM) has become one of the most powerful techniques in cellular research (Berezin and Achilefu 2010; Kumar 2011). Lifetime is the fluorescence parameter that is extremely sensitive to intermolecular interactions. In sensing applications it can be used in different aspects, mostly in configurations that allow dynamic fluorescence quenching and FRET. Lifetime is the dye

concentration-independent parameter but the parameter that requires clever operation, since totally quenched species cannot be detected (Sect. 3.4). The purpose of FLIM is by measuring the lifetime at each point of the image to detect the variations of intermolecular interactions (Marriott et al. 1991). These variations can be correlated with the presence of target species and their interactions.

A number of fluorescence reporters have been suggested for lifetime imaging (Berezin and Achilefu 2010). This technique is especially applicable for working with the visible fluorescent proteins, such as GFP, since these proteins, being FRET donors, easily exhibit the dynamic quenching effects but do not respond so easily by spectral changes.

The time-resolved microscopy is implemented in one of the two ways. Both of them came from time-resolved spectroscopy. One uses the *time-domain* measurement and the detection with *single-photon counting* technique. Its simplest version is the *time-gated* technique that allows collecting the quanta within a selected time window (see Fig. 3.11). Close in methodology and simpler in performance is the *stroboscopic* technique, which is based on formation of the time window by opening and closing the detector voltage by synchronized pulses (strobes). The frequency domain measurement uses a different principle. It is based on excitation by *frequency-modulated light*, so that the lifetime information can be obtained from *phase shift* and *demodulation* of excitation light (Lakowicz 2006).

The application of *time-gated microscopy* is reasonable when there is a need to distinguish between the emissions possessing well separated lifetimes, and this necessitates acquiring and analysis of two sets of images (at short and long lifetimes). This technique is the best suited for the images formed by lanthanide chelates and metal-ligand complexes, possessing long lifetimes (Grichine et al. 2014). The time-resolved imaging allows more flexibility, and a combination of intensity and lifetime imaging allows improving the application of FRET (Hanley et al. 2002), which is a key approach to elucidating the proximity relations and dynamics inside the cell.

13.1.7 Wavelength-Ratiometric Imaging

In the studies of living cells and other heterogeneous microscopic objects, the great advantages of λ-ratiometry (Sects. 3.7 and 3.8) can be efficiently realized providing imaging in different colors of targets distributions and their transformations (Demchenko 2010). This technique was successfully stimulated by introduction of the first Ca^{2+} probes (Grynkiewicz et al. 1985) and continues its development and exploration addressing different targets and employing different mechanisms of wavelength-switching, such as ESIPT and FRET (see Chap. 8). One of such techniques was applied for detecting and characterizing the cell membrane transformations in the course of apoptosis with the use of the two-band electrochromic dye (Shynkar et al. 2007). In this work the two images in different colors are taken in

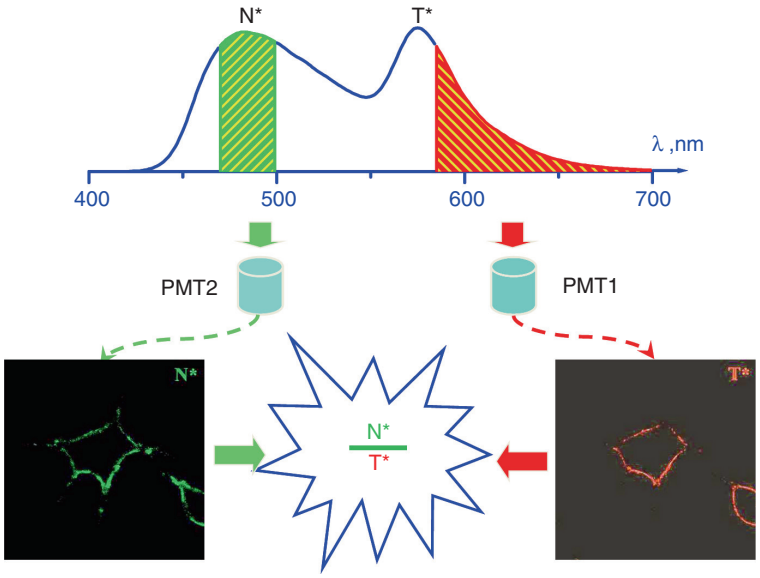

Fig. 13.7 One of the possibilities to construct ratiometric image in microscopy (Shynkar 2005). The fluorescence spectrum of 3HC biomembrane fluorescence probe F2N12S is presented *above*. The *green* and *red* parts of this spectrum are selected with filters and detected over the image with different detectors. Then the ratio of two images is obtained. Presented in pseudocolor it does not depend on the distribution of dye molecules but on the redistribution of intensity in their spectra

confocal microscope using different photodetectors and then the ratio of these images was obtained (Fig. 13.7).

The technique of obtaining multicolor λ-ratiometric images can be simplified by avoiding the use of expensive CCD cameras. The color cameras that must be familiar to every photographer and almost every cellular phone owner operate based on a principle of application of three different types of pixels or layers, each of them sensitive towards different wavelength ranges. With such easily available systems the sensor response of dual or even triple sensors (or by applying the color-switching sensors) can be monitored in a very straightforward manner (Stich et al. 2010). The chips incorporated into these cameras contain red/green/blue (RGB) channels that are sensitive to the red, green, and blue parts of the visible spectrum, so that the color picture is formed on a pixel-by-pixel basis out of relative intensities in these channels. Therefore up to three different emissions can be differentiated if they match the correspondent color channels of the camera. The only precondition is that the applied fluorescence reporters should emit at separable wavelengths, then their emissions can be analyzed separately and the ratiometric signal obtained. A comparative study of different imaging techniques for optical chemical sensors demonstrates good prospects for this new type of detectors (Meier et al. 2013).

Importantly, the multicolor λ-ratiometric images can be easily combined with polarization (Jameson and Ross 2010) and lifetime imaging (Peng et al. 2011).

13.1.8 Traditional Fluorescence Microscopy: Advances and Limitations

Several trends of traditional far-field (lens-based) optical imaging demonstrate its usefulness but approach the limit of perfectness in their development. All possibilities of fluorescence spectroscopy (spectral resolution, anisotropy, lifetime) can be realized in microscopy, Simple epi-fluorescence microscope remains basic in many studies competing with more advanced techniques. Out-of-focus emission spoils the image and therefore different microscopic techniques were devised offering *optical sectioning*, i.e. a way to reject out-of-focus light and maintain only in-focus information in the final image.

In a confocal microscope, the fluorescence is excited throughout the illuminated volume of the specimen, but only the signal originating in the focal plane passes through the confocal pinhole, allowing collecting the background-free data, but this greatly reduces the number of quanta reaching the detector. By contrast, the two-photon excitation generates the fluorescence only at the focal plane, and, since no background fluorescence is produced, a pinhole in front of the detector is not required. In both methods the spatial resolution along z axis is similar, it is about 500–600 nm. In this aspect, they are behind the total internal reflection microscopy, in which this resolution is about 100 nm but without the possibility to move the focal plane located at the interface. All three methods are adaptable for time-resolved measurements. The time-resolved imaging, with or without using of FRET, allows making important steps towards real intracellular sensing of many analytes.

The in-plane resolution in conventional fluorescence microscopy has reached the values of 200–300 nm and approached the diffraction limit. This does not allow resolving molecules and molecular structures having smaller dimensions, as seen in Fig. 13.1. Other limiting factors remain also important. The scanning confocal microscopy requires high power of excitation light, which is not tolerable by many organic dyes, and photostable inorganic nanocrystals are often larger in size than their macromolecular targets. Slow speed of collecting the images makes complicated working with live cells in their natural environment. Programmable array microscopy offers the possibility of overcoming these limitations.

The information content of obtained images becomes the key factor. It is not enough to localize the cell organelles and determine their number and sizes. An amount and localization of at least some out of many 1000 types of molecules is of major interest, and this constitutes the intracellular sensing.

13.2 Super-Resolution Microscopy

Improving the spatial resolution is a strong demand from the side of researchers and practical users of intracellular sensing. *Resolution* is the power to resolve objects from each other, and in optical imaging it is limited by the diffraction of light. However, the lens-based amplification in light microscopy has its limit.

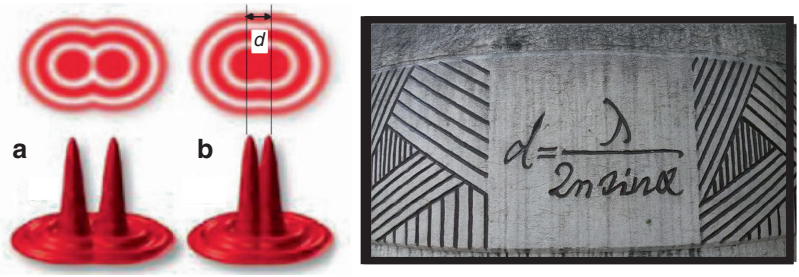

Fig. 13.8 The resolution between two fixed points on microscopic image separated larger (**a**) and close (**b**) to the diffraction limit (the point spread functions and their projections). When the two objects come closer they cannot be individually distinguished anymore. *Right*: The formula describing the diffraction limit engraved on Ernst Abbe memorial stone in Jena

13.2.1 Breaking the Diffraction Limit

The mathematical expression for the *diffraction limit* was formulated in 1863 by Ernst Abbe: the two spots in the microscope image (Fig. 13.8) cannot be resolved if their separation distance is smaller than the d value that equals to $\lambda/2n\sin\alpha$ in the focal plane (xy) and $2\lambda/n\sin2\alpha$ along the optical axis (z). Here λ is the wavelength of light and $n\sin\alpha$ is the numerical aperture of the lens. As most lenses have a numerical aperture of <1.5 (α is <70°), the theoretical resolution limit for cell imaging (where λ is ~400 nm) is 150 nm laterally and 500 nm axially. The current resolution obtainable with a *wide-field* microscope (in which illuminated is an observable area of several microns in diameter) approaches this limit.

For many years after its formulation, the diffraction limit was both a technological and a psychological barrier. Only recently, the attempts to lift this barrier became successful and resulted in new technologies of fluorescence imaging. One of them is the *near-field* technique that uses mechanical scanning with ultra-thin probe serving as a nano-sized light source. The ultra-high resolution can be achieved also in a different way by the formation of optical image in the *far-field* (at distances much larger than the wavelength of light) with a recently suggested special scanning technique called *stimulated emission depletion* (STED) microscopy. This technique allows demonstrating that, in principle, the resolution in confocal images can approach a molecular level. A number of other smart "molecular localization (PALM, STORM,…)" wide-field techniques increasing the resolution to several nanometers have also been suggested. These achievements were marked by the Nobel Prize in Chemistry 2014 that was awarded jointly to Eric Betzig, Stefan W. Hell and William E. Moerner *"for the development of super-resolved fluorescence microscopy"*.

13.2.2 Near-Field Scanning Microscopy

One of the super-resolution techniques is the *near-field scanning optical microscopy* that is commonly abbreviated as NSOM or SNOM (Dickenson et al. 2014; Lereu et al. 2012).

What is the *near field*? According to commonly used definition, the optical near field is the region of space of dimension less than a wavelength of a light source, within which the optical diffraction does not occur. In these conditions the light interacts with the matter before diffracting. Because of this interaction, the resolution does not depend upon the wavelength but is a function of only the size of the light source and the distance from the sample. The idea in the background of this method is to reduce the size of a light source to the dimension of tens of nanometers. With such nano-scale source, the scanning of microscopic object deposited on the surface can be made for obtaining the improved image.

Scanning near-field optical microscopy is presently seen as a powerful tool for nano-scale imaging (Rasmussen and Deckert 2005; De Serio et al. 2003). It promises high spatial resolution capability down to a few tens of nanometers. Of course, everything depends on the skills of researcher to provide the optical waveguide with nanometer-sized tip and to manipulate with it. The diameters of fiber optics tips can be made as small as 20–40 nm (Voronin et al. 2006), which is by one order of magnitude smaller than the wavelength of light used for fluorescence excitation. Such thin fibers attain very interesting properties that become useful in cellular studies. The photon cannot escape normally from the tip; it travels some distance along the fiber and further is substituted by an exciton or evanescent wave. This allows providing excitation of fluorescent species that are present in a small sensing volume within about 100 nm from the tip surface. As a result, only the species within this small volume can be excited (Fig. 13.9).

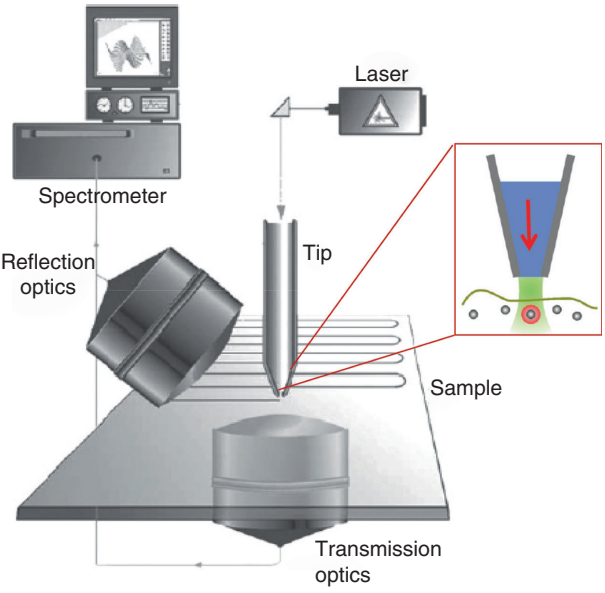

Fig. 13.9 The SNOM set-up operated in illumination mode (De Serio et al. 2003). Laser light is coupled into the sub-wavelength aperture, which illuminates the sample placed in the near field of the tip; scattered or fluorescent light from the sample is collected in the far field through an objective placed in either reflection or transmission

SNOM is a proximity method addressing a difficult task of combining high resolution with a single fluorophore sensitivity. It requires scanning the sample relative to the optical probe of sub-wavelength size at a distance of a few nanometers. The gap between the probe and sample is controlled by measuring the force interactions, so SNOM can provide both optical and topographical images on the sample surface simultaneously. The latter function is similar to that of *atomic force microscope* (AFM). A number of examples demonstrate the efficiency of SNOM. In one of the studies (Ma et al. 2006) the sub-10 nm resolution was achieved in detection of a single DNA molecule.

Being conceptually close to atomic force microscopy, this technique needs scanning the surface of the object by using some shear-force-feedback device and allows a three-dimensional representation of its surface, this time with a fluorescence response. Due to these technical restrictions, all the presently developed SNOM types are focused on scanning the surface of a sample and do not allow the three-dimensional possibilities of a confocal set-up. Since it is not diffraction-limited, such *near-field excitation* can provide the necessary spatial selectivity and resolution that is much higher than that achieved with common fluorescence excitation.

In *tip-enhanced near-field optical microscopy* (TENOM) the evanescent near-field in the vicinity of sharp metallic probes is used to interact with the sample (Mauser and Hartschuh 2014). Raster-scanning the probe yields both optical and topographic sample information. The antenna function of the probe provides efficient coupling between the far-field and the probe's near-field. As a result of such plasmon-induced effect, signal enhancement for objects in the vicinity of the probe can be achieved using a laser source and a detector in the far-field. This signal enhancement and the correspondingly improved detection sensitivity are essential, since high spatial resolution is connected to a shrinking sample volume and weaker signals.

The application of this technique is limited to scanning the surface only. For sensing inside the cell, however, it meets many problems associated with the multitude of reactions occurring in it and the mobility of its constituents.

13.2.3 Stimulated Emission Depletion (STED) Microscopy

Can the resolution be substantially improved in the *far-field*, in which the image is formed on optically created focal plane? In other words, can the improvements of resolution overcoming the diffraction limit be made based on already popular platforms of lens-based confocal and two-photon microscopies? The answer is yes. Single emitters can be localized within a focal plane with the precision higher than the half of wavelength.

Some improvements in resolution can be achieved by computational techniques. The emitters can be approximated as ideal point sources of fluorescent light, and their intensity distribution can be fitted to two-dimensional parameters of a point-spread function (Sharonov and Hochstrasser 2006). The application of such approach improves the image but requires definite assumptions, and therefore cannot provide the general solution of the problem. The recently developed STED microscopy (Hell 2007) being an experimental technique shows such possibility (Donnert et al. 2006; Blom and Widengren 2014).

The STED microscopy (Fig. 13.10) reduces the size of the excited region by using a very short excitation pulse, which is immediately followed by a 'depletion' pulse, tuned to a red-shifted emission line of the fluorescent dye that forms an image. This depletion pulse causes *stimulated emission*, moving electrons from the excited state (from which fluorescence occurs) to the ground energy state. The profile of the depletion beam is altered in such a way that it is focused to a ring instead of a spot, featuring a dark spot of zero laser intensity in the beam center. The only region of the sample that is allowed to emit light is the much smaller central portion

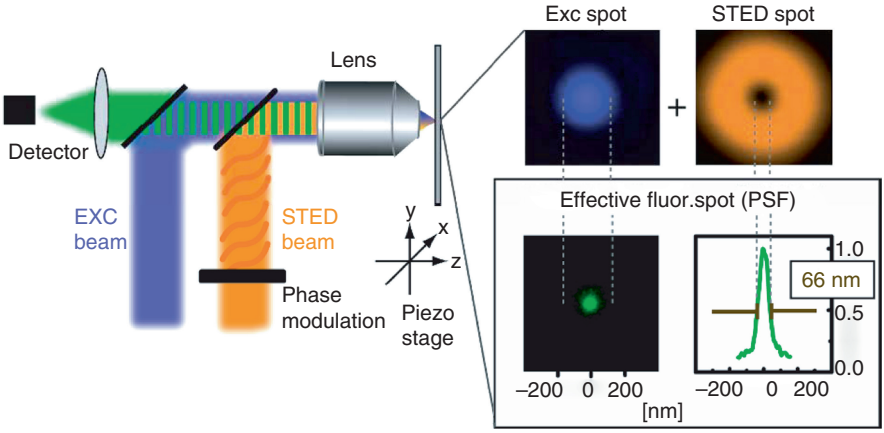

Fig. 13.10 The basic principle of STED microscopy. The excitation light beam (EXC beam, in *blue*) is steered by a mirror through the objective lens, and due to diffraction is focused to a spot ca. 200 nm in diameter on the sample. By scanning this blue excitation spot over the sample (the cell) and recording the fluorescent light emitted at longer wavelengths from the labeled molecules with a computer, one can form an image of the sample. The smaller the excitation spot is, the higher the resolution of the microscope. Due to diffraction, the excitation spot cannot be made smaller than ~200 nm by focusing with a lens, which limits the resolution of common microscope. To overcome this limit, a second beam is used (STED beam, in orange) to quench the fluorescent markers before they fluoresce. Because the STED beam is doughnut-shaped and centered over the excitation spot, one is able to preferentially quench the markers at the outer edge of the excitation spot and not those in the center. The result is a much smaller effective fluorescence spot (*green*), here reduced to a diameter of tens of nanometers

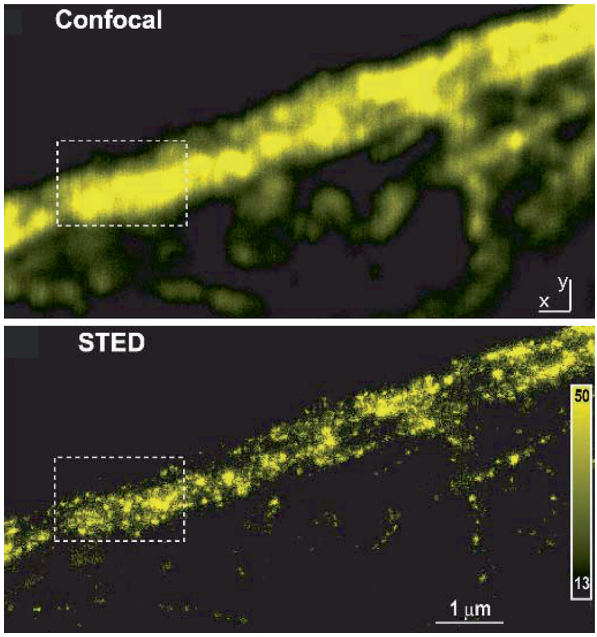

Fig. 13.11 Imaging neurofilaments in human neuroblastoma cell (Donnert et al. 2006). Contrary to the confocal recording, the STED recording displays details with 30 nm resolution

that is not irradiated by the depleting pulse. In this way a dramatic reduction of spot size can be achieved. Scanning this sub-diffraction spot across the specimen delivers images with a sharpened sub-diffraction resolution (Fig. 13.11).

Recent studies have shown that an equally high resolution of images can be achieved even without synchronization of lasers and using continuous-wave laser beams (Willig et al. 2007) providing excitation and depletion that allows achieving the three-dimensional sub-diffraction structural resolution (Fig. 13.12). High temporal resolution of the image allows observing the fast motions of nanoparticles (Westphal et al. 2007).

The STED microscopy is considered as the first implementation of a more general concept that under ideal conditions offers *unlimited improvement of spatial resolution*. By making the STED doughnut very intense, it is in principle possible to shrink the fluorescent spot to molecular size, thus attaining molecular resolution – an exciting goal for the near future. However, the range of applications of initially developed STED technology is limited by the high cost of instrumentation and, most importantly, by the necessity to use high light intensities to induce stimulated emission, which imposes more stringent demands than usual on photostability of applied fluorescence dyes. New developments allowed overcoming this limitation (Bergermann et al. 2015). The use of parallel STED with lower light levels, high speed and 100,000 spots simultaneously has become possible.

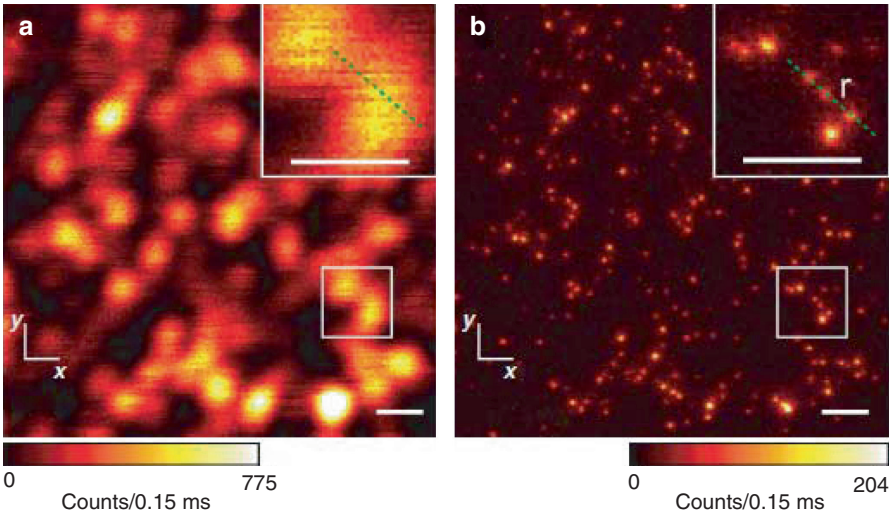

Fig. 13.12 Comparison of nanoscale images of fluorescent 20-nm-diameter beads obtained with confocal (**a**) and corresponding CW-STED (**b**) images. The images were recorded simultaneously with an excitation power of 11 mW (at 635 nm) at the sample and by turning the STED laser (825 mW, 730 nm) on and off line by line. *Insets*, magnification of the *boxed area*. Scale bars, 500 nm (Willig et al. 2007)

STED is in principle possible with every fluorescence dye. The only requirement is the proper adjustment of imaging conditions to their photophysical properties. Live cell imaging with fluorescent proteins has been demonstrated (Morozova et al. 2010), and posttranslational labeling with fluorescence dyes emitting in the red and near-IR and more suitable for STED appears to be a promising alternative (Lukinavičius et al. 2013; Wurm et al. 2012).

Thus, STED microscopy using platform of conventional far-field light microscopy radically distinguishes itself from it in the fact that its resolution is no longer fundamentally limited by the wavelength of light. It opened a new chapter in the story, in which the fundamental questions of biological processes on a nanoscale can potentially be answered with focused light. STED was the first "*deterministic*" method that uses to enhance the resolution the non-linear response of fluorophores. Essentially, in STED the raw detection of nanoscale-separated positions is the result of a pure physical (optical switching by stimulated emission) process, therefore no data processing is required. Additional mathematical processing is possible as an extra step to enhance the image quality and even further separate labeled fluorescent molecules.

The STED format is a part of more general concept for obtaining superresolution images, RESOLFT (*reversible saturable optical fluorescence transitions*). In addition to stimulated emission, any photo-induced reversible transition between signal-

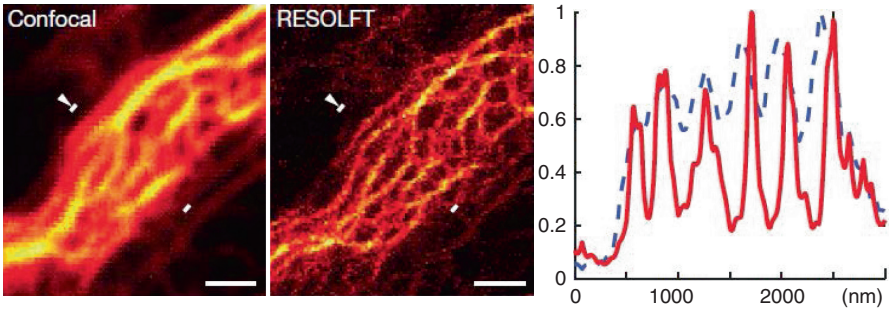

Fig. 13.13 Result of application of RESOLFT nanoscopy to the study of living cells (Grotjohann et al. 2011). Mammalian (PtK2) cell expressing keratin-19–rsEGFP imaged in the confocal (*left*) and the RESOLFT (*middle*) mode. Graph shows the normalized fluorescence profiles between the *two white markers* with the *white arrowhead* indicating the direction (*solid red*, RESOLFT; *dashed blue*, confocal)

ling and non-signalling states and providing temporal selection of emitters can be used, extending the possibilities of "*deterministic*" scanning format. The switchable enhanced fluorescent proteins were found useful for this technology (Grotjohann et al. 2011). Since the light intensities required for photochromic switching can be by many ordered of magnitude lower than for stimulated emission, its exploration opens many new possibilities for life cell imaging (Fig. 13.13).

In the sub-section below we will discuss quite different methodology that is in the background of "*stochastic*" methods. The latter rely on stochastic switching or fluctuating response of chromophore to light-activation in order to localize the individual emitters in the wide-field image.

13.2.4 Stochastic Methods in Super-Resolution Imaging (PALM, STORM, etc.)

Super-resolution in microscopic images can be achieved also by random switching between emissions of fluorescent probes contrasting the studied object and located at the distances greater than the diffraction limit. The trick is to excite sequentially several sub-populations of these probes and then making the composed image. Individual probes located at sufficiently large distances are imaged at the centers of their diffraction limited spots that can be located with nanoscale precision. Then the series of images are created by repeating the excitation/measure/bleaching sequence many times. The superposition of acquired images provides the super-resolved image.

The popular versions of such stochastic switching approach are *photoactivation-localization microscopy* (PALM), *stochastic optical reconstruction microscopy* (STORM), *fluorescence photo-activation localization microscopy* (FPALM), *super-resolution optical fluctuation imaging* (SOFI) and *single-molecule super-localization*

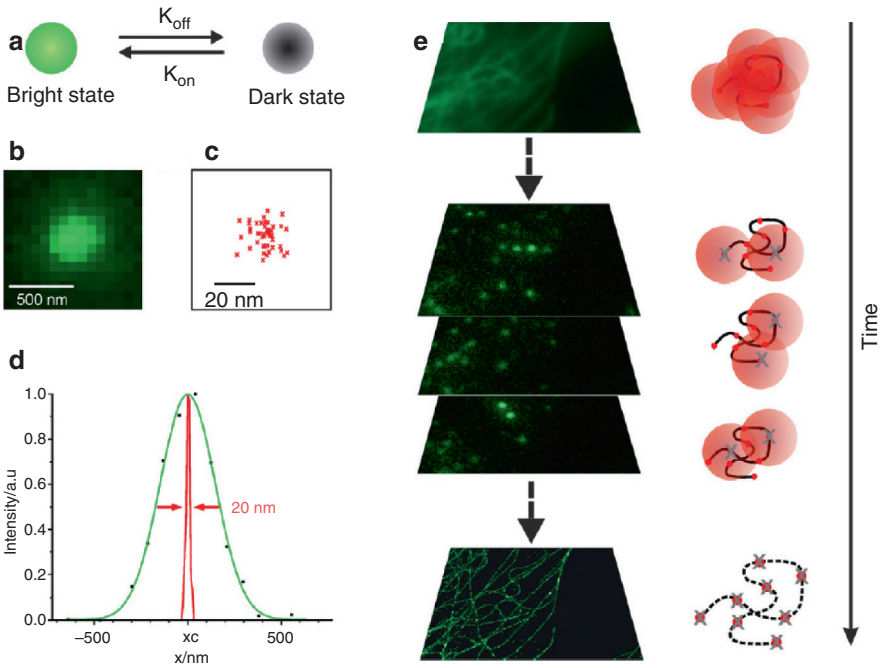

Fig. 13.14 Super-resolution microscopy by stochastic photo-switching and single-fluorophore localization (Hohlbein et al. 2010). Localization-based super-resolution techniques employ fluorescent probes that exist in at least two discernible states, e.g. a fluorescent (*bright*) state and a non-fluorescent (*dark*) state. Multiple closely spaced emitters are indistinguishable. The position of a point source can be recovered only if the photons that it emits have been identified from those arising from the neighboring molecules. Therefore the dyes exhibiting controllable transition between light and dark states (**a**) are chosen (photoswitching, photoactivation or photoconversion). (**b**) Blurred emission profile of a single fluorophore in widefield microscopy and its point spread function (**c**). Both multiple single-molecule localizations with high precision can be approximated with a Gaussian function, demonstrating the increase in spatial resolution (**d**). (**e**) Sequential steps in achieving the sub-diffraction resolution images by temporal confinement of fluorescence emission of all fluorophores in a sample, combining stochastic photo-switching with high-precision single-molecule localization

and active control (SMACM) (Moerner 2012; Hohlbein et al. 2010; Hensel et al. 2013). They share the same principle of image formation but differ in experimental detail and, essentially, by the mechanism of switching and the type of switchable probe. The idea behind these methods can be schematically illustrated in Fig. 13.14.

Consider a typical wide-field fluorescence image. Clearly, it is impossible to super-resolve its underlying structure because the fluorescent labels are in high concentration and their distorted images overlap. Using controllable operation with these fluorophores, it becomes possible to temporarily reduce their number by either blinking or photobleaching to guarantee that only a sparse subset of molecules are emitting. Those selected species can be localized with sub-diffraction precision as single emitters. Once the molecules of first subset are photobleached or enter a dark

state, another subset can be activated or stochastically turned on and localized. This process is repeated and the resulting localizations are summed to give a super-resolution reconstruction of the underlying structure.

When applied to cellular research, the PALM technique is based on *photoactivatable* fluorescent proteins. After photoactivation of particular subset, molecules are rapidly photobleached during readout and this process is switched to other subsets until the entire ensemble has been probed. Because fluorophores are switched off by photobleaching, each molecule of the ensemble can be detected only once, but by using reversibly *photochromic* fluorescent proteins, the possibility for multiple readout of each fluorophore can be realized (Wang et al. 2014).

STORM is based on labeling with photoswitchable synthetic dyes. This technique exploits the property of certain fluorophores to enter into a relatively stable (milliseconds-seconds) dark state upon illumination, which can be caused by different photochemical processes (Ha and Tinnefeld 2012). After switching off the majority of fluorophores by the readout-laser, sub-ensembles are recovered by photoactivation in a stochastic manner and switched off again during readout. Thus, single molecule can blink on and off many times before photobleaching. The STORM technique allows photoactivation to be performed by energy transfer from another dye in close proximity (photochromic blinking), which provides flexible means for multicolor imaging. Meantime, in many fluorescent dyes the reversible inactivation-activation cycle can be realized based on their property to switch from emissive to long-living dark states by thiol-containing reducing agents, which is realized in *direct-STORM* (dSTORM) technique (Heilemann et al. 2009). With the use of different molecular tags (see Sect. 13.4) this method has strong potential for the studies of localizations and interactions within living cells (van de Linde et al. 2011).

The methods using stochastic switching for determining fluorophore localization are often combined under the name *single-molecule localization microscopy* (Fürstenberg and Heilemann 2013). Using stochastic switching approach a super-resolution image can be obtained in a wide-field mode (Fig. 13.15).

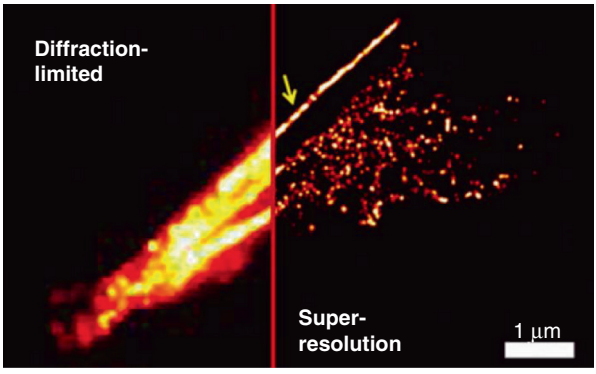

Fig. 13.15 An example of achieving super-resolution image by stochastic switching approach (Moerner 2012). The images are of microtubules in a mammalian cell acquired by photoactivation of genetically targeted small molecules. Single microtubule is indicated by arrow. Its measured size is 85 nm

13.2.5 Structured Illumination Microscopy (SIM)

Resolution improvement by a factor of 2 can be achieved in a simple wide field microscope using *structured illumination*, where a fine grating is projected onto the sample and the final image is reconstructed from a set of images taken at different grating positions. Different SIM modifications (mainly grid projection and aperture correlation) were suggested to get benefit from this possibility. Actually that does not go beyond the diffraction limit, and only with the induction of nonlinear response by the application of labeling with switchable fluorophores (the idea is similar to that applied in stochastic methods) this technique reached the level of nanoscale resolution (Rego et al. 2012).

13.2.6 Critical Comparison of the Techniques

Super-resolution imaging methods breaking the diffraction limit have received increasing attention and enthusiasm among biologists addressing cellular processes at the nanoscale. Novel fluorescence microscopy methods allow dramatic increase in spatial resolution. However, the benefits offered by these methods are associated with substantial increase in complexity of the instrumentation and also with manipulation with biological samples involved.

To date, all fluorescence superresolution methods are based on separating the emitters to a resolvable distance and then forming the images by temporarily establishing distinguishable fluorescent "ON" states and dark "OFF" states. Switching between the formed sub-populations should result in spatial regions of sub-diffraction size achieved in a *targeted* or *stochastic* fashion. In STED/RESOLFT technique the specific spatial patterning and time-sequential readout of neighboring molecules in sub-diffraction regions is achieved by scanning with light beam. Since stimulated emission is a very general physical phenomenon, no special requirements are imposed on fluorophores, which allows very broad flexibility in their choice.

In contrast, in stochastic methods based on *single-molecule localization* (PALM, STORM, etc.), parallelism is achieved by widefield acquisition. This requires special probes that have to be photo-activated or photo-switched. In these methods, conventional probes can be used only if they are irreversibly or reversibly photoinactivated during experiment. For achieving satisfactory level of resolution, often many thousands of images differing in amount and localization of emitters have to be processed. The choice of fluorescence reporters is important in both types of these techniques (Ha and Tinnefeld 2012); they should be adapted to the task of experiment.

Both types of approaches are quite successful in achieving the ultra-high level of optical resolution, which was demonstrated to be on a comparable level. The "sto-

chastic" approach is attractive by simplicity of its concept and greater availability of instrumentation for imaging single molecules. It allows larger possibilities in the studies of molecular motions and interactions in living cells. However, recent developments in STED technique allows competing successfully also on these issues. These methods possess potential for further improvements in instrumentation and analysis that could enhance the speed of the experiments (and therefore reduce the light exposure) and significantly decrease acquisition times. Combination of multi-laser and multi-color fluorescence spectroscopy may lead to new technical solutions.

Finally, we conclude that imaging below the diffraction barrier is a reality. The developed techniques are available already to a broad range of researchers. The new field of research already known as *'optical nanoscopy'* has emerged and it develops rapidly pointing to strong potential for new revolutionary discoveries.

13.3 Sensing and Imaging on a Single Molecule Level

Many molecular components in the living cells are present in a very small number of copies and their functioning occurs in very heterogeneous environments often in the conditions far from thermodynamic equilibrium. Therefore the description of such systems in terms of statistical ensemble of identical in all properties molecules may become inadequate and the results of experiments with isolated molecules in solutions misleading. Single molecular detection of fluorescent emitters allows instead of common ensemble-averaged description to observe and analyze the behavior of *individual molecules*, their interactions and chemical reactivity (Chen et al. 2014). They can reveal the commonly hidden dynamic properties depending on exact molecular interactions *in vivo*. For disclosing these properties there is a possibility of using all the arsenal of fluorescence detection methods (Orrit et al. 2014).

On initial steps of single-molecular studies, the fluorescent molecules were fixed by adsorption to the surface or in the volume of solid glass solvent in cryogenic conditions, and the microscopic technique the best fitting for these studies was the total internal reflection microscopy. With the development of confocal and two-photon microscopy they began to be more actively used, and more researchers started to study the diffusing and interacting single molecules in solutions. This opened the roads for extensive development of single-molecular sensing.

13.3.1 Observation of Single Molecules

Fluorescence probing of *individual sensor molecules* and events occurring on their target binding and/or their image formation needs an ultimate degree of sensitivity. This is not achievable in common spectroscopic or microscopic experiment, which operates with micromolar to nanomolar concentrations. Meantime, under ideal conditions and with the use of sophisticated techniques it is possible to detect the

fluorescence emission from a single molecule and even see it with properly dark-adapted naked eye!

Observation of single molecules became real because the scientists managed to fulfill three important conditions. First, the illuminated volume was dramatically reduced, to the level of *femtoliters* (1 fl = 10^{-15} l). Also, the density of incident light was significantly increased; it was required for collecting sufficient number of quanta from a single emitter. And importantly, the synthesis of organic dyes with high photostability and the design of photostable nanoparticles were provided. They allowed achieving a great number of excitation-emission cycles without decomposition (photobleaching).

The transition from *ensemble-averaged* detection to a *single-molecule* detection can be illustrated with the aid of a scheme presented in Fig. 13.16. With high concentration of emitters in a large detection volume we always detect ensemble-averaged response. Lowering concentration and squeezing down the observation volume (confocal volume, for example) gives rise to fluorescence fluctuations for in-and-out diffusion of molecules. Further lowering the concentration to ensure primarily one molecule diffusing through at a time gives rise to fluorescence bursts. Because of such fluctuations, many studies have been performed on isolated immobilized dyes by their attachment to supramolecular structures (Gai et al. 2007). Meantime, as we will see below, this technique can be extended to the studies in solutions, and even in the living cells.

Detection of individual molecules is not a matter of mere curiosity. The possibility appeared not only to detect and identify the freely diffusing or immobilized molecules but also to detect the dynamic changes occurring in them (Tinnefeld and Sauer 2005). We will keep our interest in intermolecular interactions that are important for sensing. Progress in single-molecular microscopy occurs side by side with

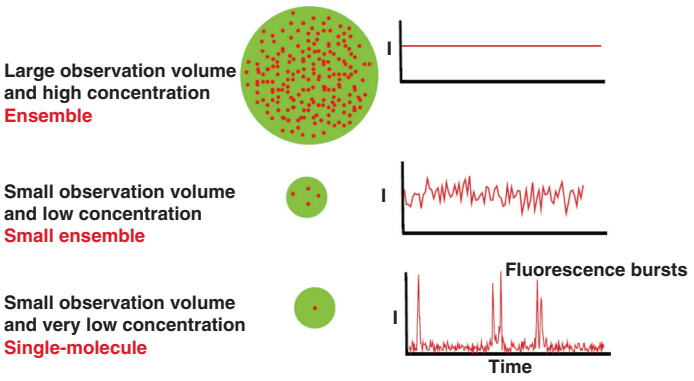

Fig. 13.16 Schematic illustrating the transition from ensemble fluorescence to single-molecule quantum bursts in a decreased detection volume (Mukhopadhyay and Deniz 2007). Lowering concentration and squeezing down the observation volume (confocal volume, for example) gives rise to fluorescence fluctuations for in-and-out diffusion of molecules. Further lowering the concentration to ensure primarily one molecule diffusing through at a time, gives rise to fluorescence bursts. These bursts contain information about the structure and dynamics of individual molecules

the progress in super-resolution imaging, so that individual emitters can be located with high spatial resolution.

13.3.2 Considerations on the Problem of Photobleaching

Our attempts to record emission from single molecule and to acquire its important characteristics, such as fluorescence spectra, anisotropies and emission decays will be successful if this molecule stays illuminated without degradation for relatively long time. The irreversible loss of emitters in time, *photobleaching,* occurs because of many chemical reactions proceeding much easier in the excited than in the ground state. They ruin the fluorophore making it non-fluorescent.

Usually the textbooks present an example of fluorescein. In an oxygenated saline solution, each fluorescein molecule can emit on the average only about 36,000 photons before being destroyed. When dissolved oxygen is removed from this solution, the rate of photobleaching diminishes about tenfold, so 360,000 photons can be emitted. Thus, the *quantum yield of photodestruction* (the ratio of the number of photobleaching events to the whole number of absorbed quanta) will be 2.8×10^{-4} to 2.8×10^{-5}. The photon fluxes used in confocal microscopy are of the order of 10,000–100,000 photons per second per molecule. The reader may calculate that in these conditions the dye will burn out in seconds. The dyes that are used for cellular imaging and sensing can be more photostable or less photostable than fluorescein. The reader must be aware of these problems.

A lot of promise appears from the side of quantum dots and other nanoparticles, since they are expected to display much higher photostability (Fu et al. 2007). This allows recording the response of single molecules longer than for several seconds and recording their individual spectra and fluorescence decay kinetics. From discussions in this Section we can derive that *photobleaching* and *phototoxicity* are two of the most severe limitations in fluorescence microscopy of living cells and tissues (Dittrich and Schwille 2001). Despite the fact that individual dyes and nanoparticles exhibit dramatic variations in these properties, they all contribute to this general problem.

13.3.3 Single Molecules Observed with Wide-Field Microscopic Techniques

The field of single molecular spectroscopy has grown over the past dozen years to the status of a powerful technique for exploring the individual nanoscale behavior of molecules in complex local environments (Moerner 2007; Hohlbein et al. 2010). In a wide-field microscopy, when a laser or arc lamp is used to illuminate an area of only several microns in diameter, the fluorescence of single molecule of interest can be recorded by a two-dimensional array detector, usually a CCD camera. However,

such fluorescence must be recognized in the presence of billions to trillions of solvent or host molecules and in the presence of noise from the measurement itself. In order to acquire sufficient amount of emitted quanta, it has to be recorded for an extended period, longer than the diffusion time through the laser focus. This requires an ultimate level of sensitivity.

The most valuable information is the intensity, polarization, decay rate of fluorescence of chosen individual molecules and of their chemical and photochemical reactivity in comparison to average molecules in ensemble of presumably identical species. Clearly, the standard ensemble measurements which yield the average value of a parameter for a large number of such molecules remain to be of great value. But by removing completely the ensemble averaging, the distribution of every measured parameter can be obtained and a frequency histogram of the actual distribution of values can be constructed. Such distribution contains more information than the average value alone (Hohlbein et al. 2010).

Introduction of new fluorophores into imaging and sensing technologies often addresses different questions that cannot be resolved on a population level but can be resolved on the level of single molecules. The spectral heterogeneity, such as the shifts of fluorescence spectra as a function of excitation wavelength, nonexponentiality of fluorescence decays, dependence of anisotropy and decay rates on excitation and emission wavelengths is commonly observed in an ensemble of chemically identical molecules (Demchenko 2002, 2008). Previously, we had only the possibility to select from the whole population of emitters the sub-population by wavelength selectivity and compare its spectroscopic properties and photochemical reactivity with that of the whole population (Demchenko and Sytnik 1991a, b). Now, the more informative histograms based on single molecular studies can be recorded.

The origin of such hidden heterogeneity can be different. Molecules can be in variable "environments" interacting with surrounding molecules. For biomolecules, such heterogeneity can appear when the various individual copies of a protein or oligonucleotide are in different folded states, different configurations, or different stages of an enzymatic cycle (Moerner 2007).

In ensemble measurements of any time-dependent process (e.g. chemical or photochemical reaction kinetics) there often is a need for synchronization of many single molecules participating in this process (Chen et al. 2014). Even if such synchronization is achievable, such as by starting photochemical reaction by short laser pulse, it can be rapidly lost in the course of process, because the coupled dynamical transitions of the individual molecules are stochastic and generally uncorrelated. The need for such synchronization is removed in single-molecular measurements. Here any one member of the ensemble is in only one state at a given time, and thus the specific sequence of states is available for study.

A final reason for the use of single-molecule techniques is the possibility of observing new effects in unexplored regimes. For example, several single-molecule systems have unexpectedly shown some form of stochastic behavior, such as "*blinking*" – reversible transitions between emissive and non-emissive states

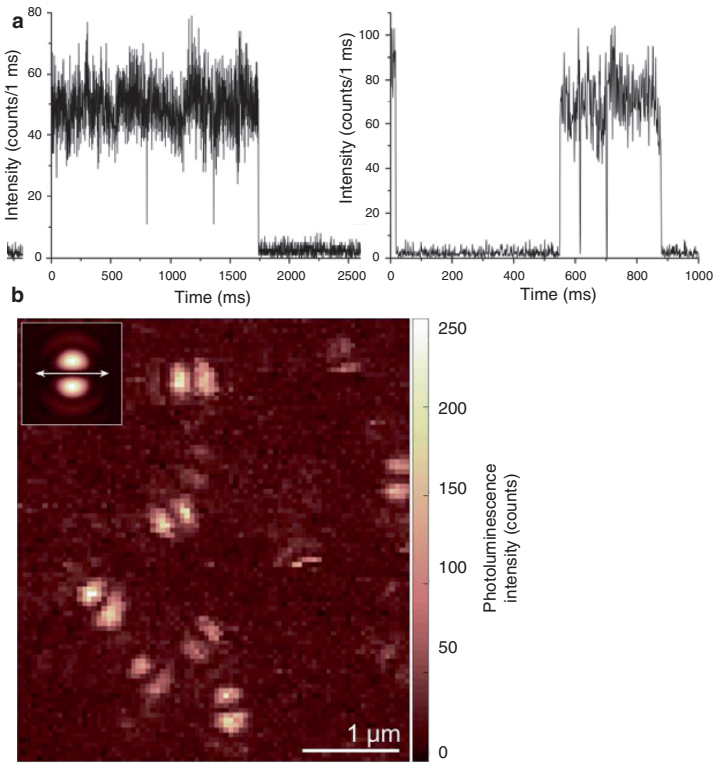

Fig. 13.17 The photoluminescence of individual carbon dots. (**a**) Time traces showing that the emission intermittency varies from short off-states near several milliseconds, to longer ones of the order of hundreds of milliseconds. (**b**) Single carbon dots excited with an azimuthally polarized laser beam. *Inset* shows a theoretically calculated excitation pattern for identical experimental conditions assuming a linear horizontal dipole. The orientation of the dipole is indicated by the *double arrow*

(Kozankiewicz and Orrit 2014; Ha and Tinnefeld 2012). Such fluctuations are important diagnostics of the single-molecule regime, needed in resolving the excited states of different fluorescent nanoparticles. Thus, it was shown that carbon dots are single fluorescence emitters since they demonstrate stochastically switchable two-state on-off blinking (Ghosh et al. 2014), see Fig. 13.17a.

Single organic dye molecule or fluorescent nanoparticle if it is a single emitting dipole displays characteristic emission pattern. The behavior of carbon dots as individual emitting dipoles was demonstrated on excitation with azimuthally polarized light (Fig. 13.17b). In this case the emission light forms a pattern consisting of two spots, relative intensity of which depending on dipole orientation.

Summarizing, the studies on single-molecular level even if they are performed on isolated molecules or particles provide unprecedented insight into behavior which is generally obscured by ensemble averaging.

13.3.4 Single-Molecular Studies in Solutions

The power of s*ingle molecule detection* technique to record rare events occurring with individual molecule is clearly seen in condensed phase. The details of intermolecular interactions that are very important for sensing and that cannot be seen on the level of molecular ensembles can be revealed. For instance, is the sensor-target binding a single-step process? If not, what are these individual steps? Success in the studies on a single-molecular level of interactions of such complex molecules as the molecular rotors kinesins (Xie et al. 2006) allow expecting a strong progress in the studies of other systems.

A typical setup for these studies is depicted in Fig. 13.18. A collimated laser beam is focused on a sample using a high numerical aperture objective. The fluorescence is collected through the same objective, and the emission light is separated from excitation light by an appropriate dichroic mirror. A 3D-gaussian observation volume (usually <1 fl) is achieved by using a pinhole (10–100 μm) on the detection path. After filtering, the emitted photons are detected using avalanche photodiodes (APDs), which are the point detectors with the fast time-resolution (down to the sub-nanosecond timescale). With such a detection geometry, when the dye concentration is sufficiently low (<200 pM), it is possible to detect fluorescence bursts arising from single diffusing molecules.

Microfluidic single-molecule detection setup allows decreasing sample volume below illuminated volume and thus reduce substantially the out-of-focus background emission (Foquet et al. 2004). Such experimental setup resembles a highly miniaturized flow cytometer. The cross-section of the microchannels can be made

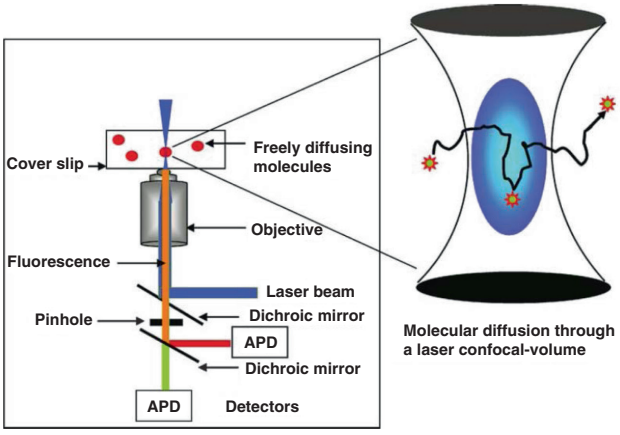

Fig. 13.18 The principle and experimental setup for single-molecule fluorescence measurements of diffusing molecules in solutions using confocal microscopic setup (Mukhopadhyay and Deniz 2007). For FRET measurements, photon bursts are separated from laser excitation light by a dichroic mirror and detected by using two avalanche photodiodes (APDs). Molecular diffusion through a laser illuminated confocal volume gives rise to fluorescence bursts

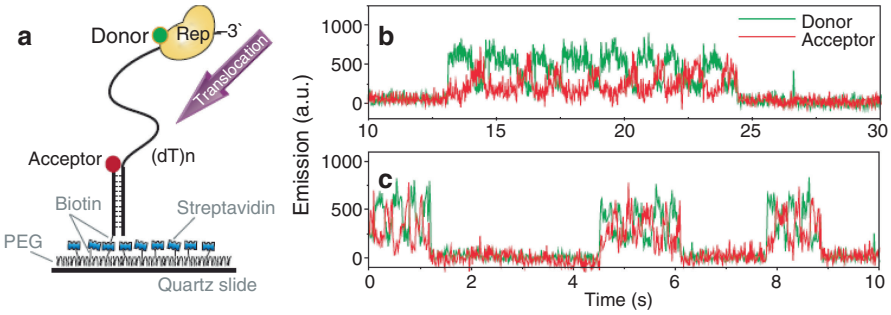

Fig. 13.19 The sliding behavior of Rep protein on a single-stranded DNA segment attached to the surface observed by single-molecule FRET (Myong et al. 2005). (**a**) Illustration of the basic setup. A single-stranded DNA segment is anchored to the surface, with an acceptor label (*red*) at the end. The *Escherichia coli* Rep enzyme with the donor label (*green*) binds to the distal end of the DNA with a low FRET signal and then slides along the DNA segment until it reaches the acceptor. (**b**) The time traces at 22 °C showing periodic changes of donor and acceptor signals arising because in each cycle the Rep enzyme quickly slides back to the end of the DNA, and the process repeats. (**c**) The same at 37 °C

so narrow that the examined molecules are allowed to diffuse in only one dimension and thus to be detected. Important is the fact that in such systems a very high dilution can be avoided and the single molecules can be detected even when their total concentration is in the micromolar range (Streets and Huang 2014).

In an example that already became classical (Myong et al. 2005) it was shown that a single-molecule fluorescence assay can visualize the binding and translocation of DNA processing enzyme *Escherichia coli* Rep helicase (Fig. 13.19). By placing both donor and acceptor fluorophores at precise locations on this molecule, information on the changes of distance (and angle) between the two fluorophores based on FRET mechanism was obtained. The motions of individual Rep monomers on single-stranded ssDNA were seen as the cyclic reciprocal changes in intensity of donor and acceptor emissions.

13.3.5 Single-Molecular Sensors

Sensing involves diffusion and association-dissociation kinetics of molecules is commonly provided in solution phase or in natural environments, such as biological fluids or living cells. However, diffusion typically limits the observation time to approximately 1 ms in many solution-phase single-molecule assays and therefore many authors prefer working with surface immobilized partners. Recently, combining the technical capabilities of high-sensitivity single-molecule fluorescence microscopy, real-time feedback control and electrokinetic flow in a

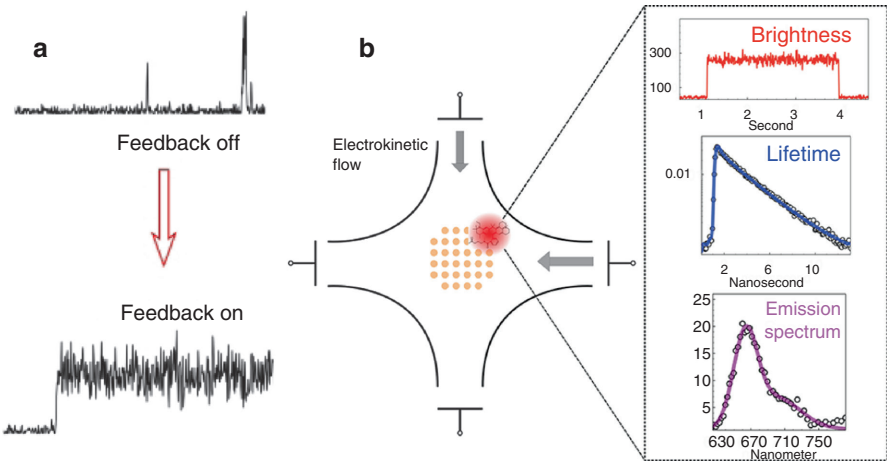

Fig. 13.20 The principle of operation of ABEL trap (Wang et al. 2012; Wang and Moerner 2012). (**a**) With the applied feedback on, the fluorescent object does not move out from illuminated laser spot demonstrating permanent level of intensity. (**b**) The fluorescent object is positioned within the laser spot by feedback forces that are applied to the microfluidic environment to cancel Brownian displacements. Using ABEL trap, simultaneous determination of fluorescence intensity, lifetime, and emission spectrum for single molecules in solution over time scales on the order of seconds has become possible

microfluidic chamber, a device called the *anti-Brownian electrokinetic trap* (ABEL trap) was developed (Wang et al. 2012) to significantly prolong the observation time of single biomolecules in solution. The principle of its operation is illustrated in Fig. 13.20.

The ABEL trap works by carefully measuring the tiny Brownian displacements of the object, and then using a feedback loop applies electric fields to the solution to exactly cancel these displacements using electrokinetic forces, which may arise from electrophoresis or electroosmosis. Eliminating the Brownian motion of a focused object in solution, it allows detailed examination of its properties on an extended time scale of seconds.

The power of fluorescence sensors to operate on single molecular level was demonstrated by many researchers. The *FRET technique* (Sect. 3.6) is commonly used, the advantage of which is the ability of ratiometric measurements of the internal distance in the molecular frame rather than in the laboratory frame. This information is largely insensitive to instrumental noise and drift, which allows simple measurement of even freely diffusing single molecules (Yang et al. 2014). The idea in these studies is simple: to detect the response in FRET between two labelled partners if they are in close contact. The change of fluorescence color change together with microscopic detection of the location of this pair in space (e.g. in a cell) on a

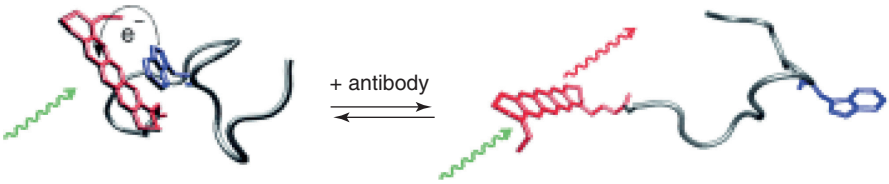

Fig. 13.21 The PET quenching on a single molecular level in detection of antibodies (Sauer 2003). Fluorescently labeled peptide epitopes derived from the immunodominant region of human p53 protein are used as PET biosensors to detect single p53 autoantibodies. Driven by hydrophobic effects the peptide adopts a conformation where the dye MR121 (*red*) undergoes PET quenching interactions with the tryptophan residue (*blue*). Upon specific binding to p53 autoantibody and subsequent conformational rearrangement the fluorescence intensity increases

high level of resolution can be observed. The use of two lasers for differential excitation of donor and acceptor producing the time-gated flashes allows making this approach more informative (Doose et al. 2007).

The choice of *fluorescent reporters* and the mechanisms of their response in sensing have to be the most carefully selected (Gust et al. 2014). The perylene 3,4,9,10-tetracarboxyl bisimide was suggested as a very prospective dye that can be excited by 488 nm line of argon ion laser and exhibits almost 100 % quantum yield. With this dye, both PET and FRET can be realized as the sensor transduction mechanisms (Sauer 2003), see Fig. 13.21.

Sensing on a single molecular level is commonly limited to very high dilutions of interacting partners, down to picomolar or low nanomolar concentration range (Gust et al. 2014). This limits the target detection to high-affinity binding, as it was explained in Chap. 2. This is a serious issue for biomolecular single-molecule sensing because biological binding constants are generally in the millimolar to nanomolar range. At low dilutions the fraction of molecules in the complexes is likely too small to be detected against a background of unbound molecules. The solution is coming from the field of nanophotonics suggesting the systems, in which the excitation light is confined to a nanometer scale (Acuna et al. 2014).

13.3.6 Fluorescence Correlation Spectroscopy and Microscopy

Fluorescence correlation spectroscopy (FCS) is the technique, in which the temporal fluctuations of fluorescence parameters are analyzed to obtain information about the processes that give rise to these fluctuations. Commonly, it uses Brownian motion to bring single molecules through a focused laser spot. By calculating the autocorrelation of the emitted bursts of light, time-dependent dynamics of moving in and out of this illuminated volume can be followed in detail. This information is provided by the *temporal autocorrelation function* of fluorescence fluctuations

(with one-channel recording) and *cross-correlation function* (recording with two or more channels).

The *autocorrelation function*, G(t), is a measure of the self-similarity of the signal after a lag time (t). It displays the conditional probability of finding a molecule in the focal volume at a later time, t, given it was there at t = 0. Decaying with time, this function measures the average duration of a *fluorescence fluctuation*. Its knowledge allows deriving a number of parameters characterizing the fluorescent molecules, their motions and interactions. The *cross-correlation function* can be used to study intermolecular interactions between two types of molecules labeled in different colors and providing the two-channel detection. The interaction is indicated by coincidence of signal fluctuations.

FCS is a rapidly developing field, and it is already recognized as an essential tool for *in vivo* characterization of absolute concentrations, molecular interactions, and kinetic processes, such as diffusion and chemical reactions (Haustein and Schwille 2007). In FCS the light emitted from a few (~1–10) molecules is recorded with microsecond–second time resolution, detecting the processes much longer than the fluorescence lifetime (~1 ns). On this time scale, which is typical of *molecular diffusion*, the fluorescence emission can be thought of as an instantaneous relaxation process (Krichevsky and Bonnet 2002). This technique allows not only sensing intermolecular interactions, but also determining the binding constants (Tetin and Hazlett 2000). Because of increased molecular mass the complexes of fluorescent sensor with the target diffuse slower than the sensor molecules alone. This can be easily detected using confocal fluorescence read-out techniques.

Fluorescence correlation microscopy (FCM) is an image analog of FCS. It is based on a spatial autocorrelation analysis of fluctuations in fluorescence intensity produced within a very small volume in a microscopic sample illuminated by a laser beam. In these conditions, FCS records information about the absolute concentrations of the fluorescent molecules, their state of aggregation and the dynamic properties of these molecules in a *cellular environment*. Based on that, information on molecular interactions, including the binding constants, can be obtained. Again, in a cell the diffusion of many molecules does not follow the law for a free diffusion, it can be the process with different and possibly interesting regularities. Researchers possess the means to study them, though the limitations exist here. The minimal illumination volume (~1 fl) is still comparable with the volumes of small bacterial cells.

The recent important development is the combination of FSC with STED. In STED technology the observation area is determined by illuminating light power and can be reduced to nanoscale dimension (Sect. 13.2), which allows diffusion in and out of this volume of individual labeled molecules. This method was applied for observing the diffusion of lipids in biological membranes and characterizing rafts (Owen et al. 2012).

As it was discussed above, photobleaching of reporter dyes used in sensing can create significant problems in obtaining good-quality images, especially with the application of FRET. However, there are at least two possibilities to get benefit from photobleaching effects. One is the rather old technique known as *fluorescence recovery after photobleaching* (FRAP) that allows determining the rates of translational diffusion in biomembranes of integral and membrane-bound compounds including lipids and proteins (Cheng and Aspinwall 2006; Hagen et al. 2005). When these labeled species are distributed in the membrane and an intensive laser light focused on its small spot bleaches all these species, this laser remaining focused on the same spot is switched to low-intensity fluorescence excitation. This allows monitoring the recovery of fluorescence emission due to diffusion of labeled species from outside the spot and thus determining their diffusion rates.

13.3.7 Single Molecules Inside the Living Cells

Living cell is a very special chemical reactor. Any biochemical reaction in a cell may have different thermodynamic and kinetic properties from the same reaction when studied in a test tube. This is because on a genomic level, a particular gene represented by DNA fragment exists in only one or a few number of copies. Many mRNA and enzyme molecules also exist in a small number of copies. Their reactions do not follow common thermodynamic and kinetic rules that are based on statistics of many molecules. These reactions often occur in *non-equilibrium* conditions being a part of complex multi-step processes with a constant supply of free energy and reactants and with a consumption of reaction products. They proceed in *localized compartments* inside the cell, so the diffusion of reaction partners may be very limited in space between different binding-release and catalytic events. Therefore, the sensing inside the cell at a single molecular level is a very challenging and very important task (Moerner 2007).

Recent developments in cellular research have demonstrated that in such complex systems a single molecular level can be reached. This can be done in different experiments, and they can provide the means for sensing different targets. Here are several examples.

1. The *single-channel recording of transmembrane ionic current*. Ionic current is observed when the ion channel formed by transmembrane protein is open. Opening and closing of ionic channels can be detected by single-channel recording of electrical current and also by the application of fluorescence reporter (Claydon and Fedida 2007). Since the operation of ionic channels is one of the

strongest modulators of cellular activity and the site of application of different drugs, the possibility of their studies on a single molecular level is extremely important.

2. Detection and tracking in a living cell of *single mRNA molecules* using multiple copies of a fluorescent mRNA-binding protein (Rafalska-Metcalf and Janicki 2007). With this approach it becomes possible to characterize the movement in real time of single mRNA-protein complexes in the cell nucleus (Shav-Tal et al. 2004). It is surprising, but it was found that in some cases these motions are diffusional and ATP-independent. In other cases the uneven distributions and directional motions of mRNAs are evident (Buxbaum et al. 2015).

Such achievements open new possibilities to study the gene expression on the very early steps.

3. Accurate quantitation of *microRNA (miRNA) gene expression* in human tissues. Such analysis shows the capability of quantitative detection of miRNA expression from as little as 50 ng of total RNA. Furthermore, by incorporating the locked nucleic acid (LNA)-DNA oligonucleotide probes, this method becomes highly specific and capable of discrimination between miRNA targets that differ by as little as a single nucleotide. Future extensions of single-molecular miRNA assays and their integration with the current microfluidic devices and nanotechnologies may prove important for understanding of the spatiotemporal regulation of miRNA expression across various tissue and cell types. This information is highly needed for clinical diagnostics (Puleo et al. 2006).
4. *Co-synthetic tracking of single proteins*. Using a fast-maturing and membrane-targeted visible fluorescent proteins as reporters, the expression of single protein molecules can be provided on a translational level (Yu et al. 2007). Immobilization by membrane attachment of protein reporter allows overcoming the problem of fast protein diffusion during fluorescence signal acquisition time that would spoil the image.
5. *Detection of single cytoplasmic proteins*. Particularly, this can be done if they are labeled with the fluorescent reporters. Microfluidic devices allow achieving such levels of confinement that the single molecules even present in a small number of copies in a single cell can be separated and individually counted (Huang et al. 2007).

The single molecules inside the cells can be ‘recognized’ both by wavelength and polarization of their emission. This information is especially useful when the co-localization of proteins (indicating their interaction) is studied. This can be shown by the presence of FRET between single pairs of fluorescent molecules bound to signaling receptors in the plasma membrane of live cells (Webb et al. 2006; Yang et al. 2014).

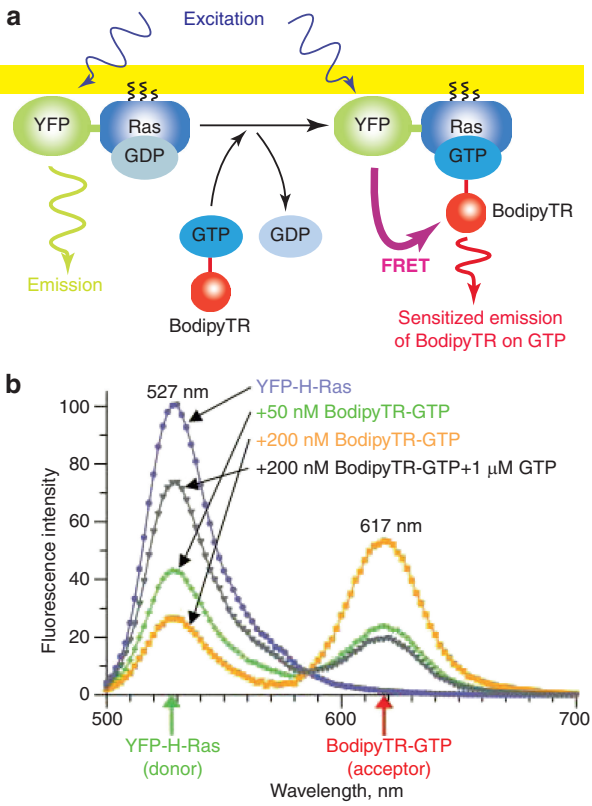

Fig. 13.22 Strategy for detecting the activation of individual single Ras molecules by GTP binding (Murakoshi et al. 2004). (**a**) Schematic drawing of the experimental design. (**b**) Fluorescence spectra showing FRET from purified YFP-H-Ras to BodipyTR-GTP

The possibility to observe biological processes directly at the single-molecule level in living cells has started to be explored by many researchers, where FRET between single molecules was efficiently used (Hohlbein et al. 2010; Yang et al. 2014). The activation of small G protein Ras was observed at a single-molecule level (Fig. 13.22). By binding fluorescent BODIPY-labeled GTP with yellow fluorescent protein (YFP) tagged Ras in human epidermoid mouth carcinoma cell, FRET results in easily recordable switching from donor to acceptor emissions (Murakoshi et al. 2004).

For recording the fluorescence from an individual molecule, one has to achieve the presence of this molecule as the *only emitter in the detection volume*. In liquid solvents, this can be done by multi-fold diluting the sample. In the studies inside the living cells, such possibility does not exist, and one has to manipulate with decrease of detection volume or by application of external emitters in very low quantities. In this way, single cellular receptors can be labeled with quantum dots (Vu et al. 2015).

13.3.8 Additional Comments

The single-molecule detection is an important achievement not only because it allows reaching an ultimate level of sensitivity in any sample analysis. It allows providing a conceptually important move from *ensemble analysis* to *individual event analysis*. Ensemble analysis is what is commonly measured and analyzed in chemistry and molecular science. It deals with ensemble-averaged properties. In contrast, the single-molecule detection allows catching the elementary events including those that are concealed from ensemble analysis. Fluctuations and statistical distributions that are sometimes seen on the level of molecular ensemble, on the level of single molecules are seen as distinct events (Deniz et al. 2008).

The other important achievement of single molecule spectroscopy is the ability to study small (in thermodynamic sense) systems. In common experiments in molecular physics or biology the researcher in reality operates with large molecular ensembles, so that only the ensemble-averaged properties are detected. They are used for system description and also for evaluating its behavior based on rules of thermodynamics. These rules do not necessarily operate in small systems.

The living cell represents a combination of a large and a small systems, in which some compounds are in high sub-molar quantities and diffuse freely throughout the cell, and the others are represented by only several copies and trapped in specific locations. Inside the cell, the biocatalytic transformations occur in cascades, so that the concentrations of many compounds are not at equilibrium. Therefore, it may be doubtful that all regularities derived in Chap. 2 for the conditions of equilibrium will be valid here. New physics of small systems has to be developed for the description of all these effects when applied to the living cells. The techniques that rely on nanometer level accuracy in the determination of molecular position, such as single-molecule super-resolution imaging, have proven immensely successful in their ability to access unprecedented levels of detail and resolution previously hidden by the optical diffraction. Combination of ensemble-averaged and single-molecular experiments with high spatial resolution is an important and probably the only way to shed light on these regularities.

13.4 Site-Specific Intracellular Labeling and Genetic Encoding

The field of cellular fluorescence develops so rapidly that many techniques suggested a decade or so ago and still actively used by histologists and cytologists may be considered as ‘pre-historic’. In some of these applications, fluorescent dyes are used as staining agents to identify the cells and to distinguish small organelles. In doing so, they succeed in achieving a very high contrast. Their staining specificities, however, often rely on poorly understood interactions. It is the understanding of

these interactions, active manipulation with them, and even more, inducing the cell to synthesize fluorescent interacting partners, characterize the frontier of modern research.

Success in exploring specific interactions in the sensing and imaging domains depends totally on the researcher's ability to provide specifically the fluorescence reporter to a desired site. Many possibilities exist for that. There can be a covalent attachment that requires chemical reaction with the correspondent groups of atoms and also a high-affinity noncovalent binding. In the latter case, the formed complex should be highly stable in a cellular milieu, with the dissociation constant lower than nanomolar. The interacting partners have to find and recognize each other among tens of thousands of different types of molecules constituting the cells.

13.4.1 Attachment of Fluorescent Reporter to Any Cellular Protein

The general solution of the problem of intracellular labeling was not found, and probably it does not exist at all. The researcher has to select between different possibilities:

(a) *Labeling in vitro* with subsequent incorporation into the cell. This is the simplest procedure that was frequently used in the past. The labeling occurs in controlled conditions of a chemical lab. The labeled protein, nucleic acid or nanoparticle can penetrate into the cell through a variety of *cell-loading techniques*, such as endocytosis, permeabilization or microinjection. Different methods have been developed to facilitate such incorporation. Thus, the attachment of oligoarginine peptides facilitates spontaneous entry into the cell of proteins and nanoparticles (Bullok et al. 2006). These membrane-permeant peptides are commonly based on the HIV-1 Tat basic domain sequence, GRKKRRQRRR.

The DNA molecules can be modified with the shell of cationic lipids or polymers, and many of these techniques have been developed for the request of targeted *gene delivery*.

(b) *Labeling 'in situ'*, inside the cell. Such labeling should be based on a strong and specific complex formation. In view of tens of thousands of different molecules existing inside the cell in a high total concentration, only the reagents of exceptional affinity can avoid nonspecific binding. The general protein labeling strategy in this case is to introduce into the protein sequence a specific recognition pattern (*affinity tag*) and to provide the labeling reagent with high affinity to this sequence.

Several technologies were developed for that. One is the attachment to the target protein of oligohistidine segment of six and more His residues, the *histidine tag*, that can be recognized by interacting partner (Guignet et al. 2004). This partner has

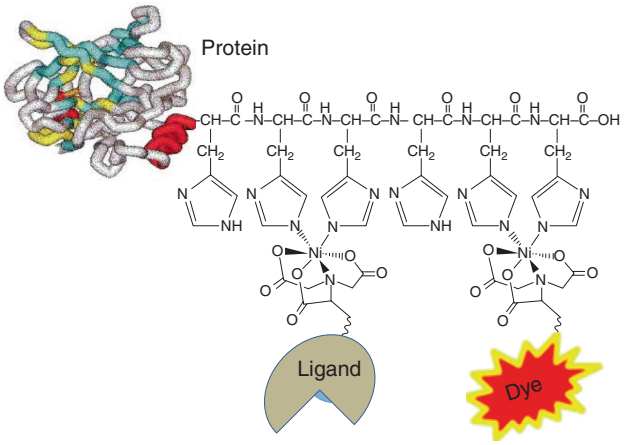

Fig. 13.23 Oligo-His sequence in a protein (hisitidine tag) that allows specific complexation with different ligands, including fluorescent dyes, via nickel chelating nitrilotriacetate moiety

to be a metal-ion-chelating nitrilotriacetate (NTA) moiety, which can be attached to a fluorescence reporter (Fig. 13.23). In addition to transition-metal complexes used earlier, the application of lanthanide complexes can also lead to successful result (Tsukube et al. 2007).

Another technology requires genetic incorporation into the protein of the unique hexapeptide sequence -Cys-Cys-X-X-Cys-Cys-, where X is any other amino acid (Adams et al. 2002). Inside the cell it can be specifically recognized by a membrane-permeant fluorescein derivative with two arsenical As(III) substituents. This method got the acronym 'FlAsH' (*fluorescein arsenical helix binder*). The derivative of fluorescein was so selected that it is fluorescent only after the arsenics bind to the cysteine thiols. Very low dissociation constant (~10^{-11} M) allows providing a highly specific binding. Meantime, the selection of fluorescein is not optimal in view of its relatively low photostability and pH dependence of the emission. Application of fluorinated fluorescein derivative improves significantly these properties (Spagnuolo et al. 2006). Many bi-arsenical dye analogues have been synthesized (such as ReAsH), including a resorufin derivative excitable at 590 nm and fluorescing in the red. Different biarsenicals enable localization of tetracysteine-tagged proteins together with their co-localization based on FRET (Martin et al. 2005).

Highly specific intramolecular labeling with fluorescent dye is needed in determining the mechanisms of pathological protein aggregation associated with Parkinson and Alzheimer diseases and other related pathologies. The key protein that exhibits pathogenic folding is α-synuclein, a single-chain 15 kDa protein. Labeling it with a 27 kDa fluorescent protein is not reasonable, since the large-size label can interfere into the aggregation process. Meantime, introduction of short tetracystein-containing insertion with intracellular binding a biarsenical dye derivative (FlAsH or ReAsH) allowed providing intracellular labeling without observable affecting the aggregation process (Roberti et al. 2007). Fluorescence microscopy

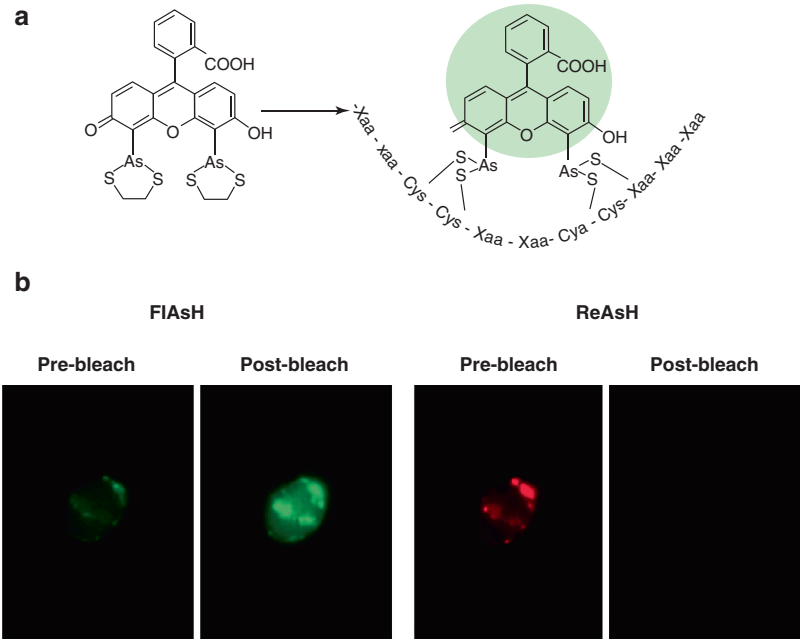

Fig. 13.24 Biarsenical fluorescein derivative binds specifically to tetracystein motive in living cell. (**a**) The binding results in de-quenching of fluorescence. (**b**) Observation of α-synuclein aggregates with site-specific labeling with two biarsenical dyes (Roberti et al. 2007). The dyes FlAsH and ReAsH were attached to terminal 12-mer peptide sequence of α-synuclein. In the formed aggregate, both FRET between FlAsH and ReAsH and the reduction of FRET by bleaching the acceptor (ReAsH) can be observed as the enhancement of donor (FlAsH) emission in a microscope image

established the intracellular distribution of labeled species in an aggregate. It was shown that the topology of the aggregate can be studied by FRET between two attached biarsenical dyes, so that one of them can be selectively photobleached (Fig. 13.24).

(c) *Enzyme-based transfer* of fluorescent dye to a specific protein. Several technologies for such labeling are known. One uses enzyme alkylguanine transferase (AGT), which reacts with benzylguanine derivatives to form a covalent linkage, allowing rapid and irreversible labeling of AGT-fusion proteins. This technique is known as SNAP tag (Gautier et al. 2008). The presence of an additional polypeptide, a so-called tag, allows binding of fluorescent dye in a highly specific manner. This peptide can be endowed with the sensor properties, and in combination with responsive dye an efficient sensor can be designed.

The small (~8 kDa) acyl carrier protein (ACP) can be also used as the tag. In this system, the modified coenzyme A-based probes are covalently linked to ACP-tagged targets by an engineered synthase enzyme (George et al. 2004). Such approach is restricted to cell-surface proteins. However, by using different synthase enzymes one can achieve multiple-color labeling.

The more detailed information on the developments of these techniques can be found in different publications (Keppler et al. 2003; Marks and Nolan 2006). The major requirement to the attached molecules is that they must be *bioorthogonal*, meaning that they may not interact with the biological system in any way, nor may they be toxic. Their desired property is that they possess switchable fluorescence and in this way applicable for super-resolution microscopic techniques (Lukinavičius and Johnsson 2011).

13.4.2 Genetically Engineered Protein Labels

The problem of generation of fluorescence emitters directly inside the cells by using their biosynthetic mechanisms can be resolved with the *visible fluorescent proteins* (Sect. 4.3). The genetically engineered green fluorescent protein (GFP) and other proteins of this family providing emissions in different colors can be *synthesized inside the cells*. Moreover, they can be fused to other proteins on a genetic level. This allows to establish the proximity relations between the structure-forming proteins, their interactions with soluble proteins and also the interactions between these proteins in cytoplasm and organelles (Giepmans et al. 2006). The ultimate goal in these studies is to establish the whole magnitude of intermolecular interactions in the cell (often called '*interactome*', Sect. 15.1).

The Förster resonance energy transfer (FRET) (see Sect. 3.6) can be a straightforward approach for establishing the target protein location and interactions. Labeling of the FRET partners (donor and acceptor) is usually made with organic dyes, but the pairs of fluorescent proteins of different colors or the combinations of dye and fluorescent protein have started to be actively used for this purpose (Shaner et al. 2004). The range of these applications is still narrow but it continues to grow with the discovery of many clever possibilities offered by protein fusions.

Remarkable in this respect was the construction of 'chameleons' that are able to sense Ca^{++} ions. Such fused protein sensors consist of linear fusions of two fluorescent proteins serving as FRET donor and acceptor, which flanked calmodulin and calmodulin-binding peptide (Miyawaki et al. 1997, 1999). Calmodulin is known as the protein that changes dramatically its conformation upon binding calcium ions. Upon Ca^{++} binding, calmodulin wraps around the peptide so that the distance between the flanking fluorescent proteins is reduced producing the proper spectroscopic response (see Fig. 8.17).

There were other attempts to develop protein sensors that could be fully synthesized and that can attain the binding and reporting functions inside the living cell. Interesting is the possibility to modify the maltose binding protein, which is the classical protein sensor scaffold, by fusion with two fluorescent proteins. One of them can be fused to its N-terminal and serve as the FRET donor and the other one fused to C-terminal and serving as the acceptor (Fehr et al. 2002). Maltose binding protein is known to undergo a dramatic conformation change (the hinge-bending motion) upon ligand binding (Sect. 8.5, see Fig. 8.16). This change in the sensing event brings the two fluorescent protein moieties together with the appearance of

FRET. Since the acceptor is fluorescent, the ratio of two emission intensities can be recorded. Moreover, an image can be obtained displaying this ratiometric signal as the maltose distribution inside the cell. The uptake of maltose into living yeast cells could be directly visualized with this sensor. Using this elegant methodology, the glucose and ribose fluorescent sensors have also been constructed with the glucose and ribose binding proteins, respectively. Though dynamic range of fluorescence response of proposed sensors is not great, it allows obtaining images of distribution of these metabolites and following their dynamics inside the cells.

Direct visualization of protein interactions in living cells can be achieved using the *bimolecular fluorescence complementation* (BiFC) technique (Kerppola 2008; Pinaud and Dahan 2011). Here, two proteins of interest are fused to two nonfluorescent fragments of fluorescent protein, so that interaction between these proteins drives the complementation of the fragments into an assembly of this protein with the appearance of bright emission.

Genetically encoded probes for the optical imaging of excitable cell activity have been constructed by fusing the fluorescent proteins to functional proteins. These proteins can be involved in physiological signaling systems, controlling membrane potential, free calcium, cyclic nucleotide concentrations and pH. Using specific promoters and the means for targeting, such probes can be introduced into an intact organism. They can be directed to specific tissue regions, the cell types, and subcellular compartments, thereby extracting specific signals more efficiently and in a more relevant physiological context because of the ability to follow the sensor location (Miyawaki 2003).

13.4.3 Co-synthetic Incorporation of Fluorescence Dyes

The methods of labeling the cellular proteins discussed above can be applied only to known proteins, the genetic manipulation with which is possible. A more global analysis of protein synthesis and transport requires a different approach that excludes genetic manipulation but allows *protein labeling coupled with synthesis*. Co-translational incorporation of noncanonical amino acids provides a solution to this problem (Fig. 13.25). In the simplest approach to metabolic labeling, an amino acid analog replaces one of the natural amino acids specified by the protein's gene (or genes) of interest. This approach is often termed *residue-specific incorporation* (Ngo and Tirrell 2011).

In procedures similar to isotopic labeling, non-canonical amino acids are incorporated into proteins during a "pulse" in which newly synthesized proteins are tagged. The set of tagged proteins can be distinguished from those made before the pulse by bioorthogonal ligating of their side chain to probes that permit detection, isolation, and visualization of the labeled proteins. Such amino acids with side chains containing azide, alkyne, or alkene groups can be incorporated into proteins in the form of methionine analogs that are substrates for the natural translational machinery. An example is a co-translational introduction of an alkynyl aminoacid

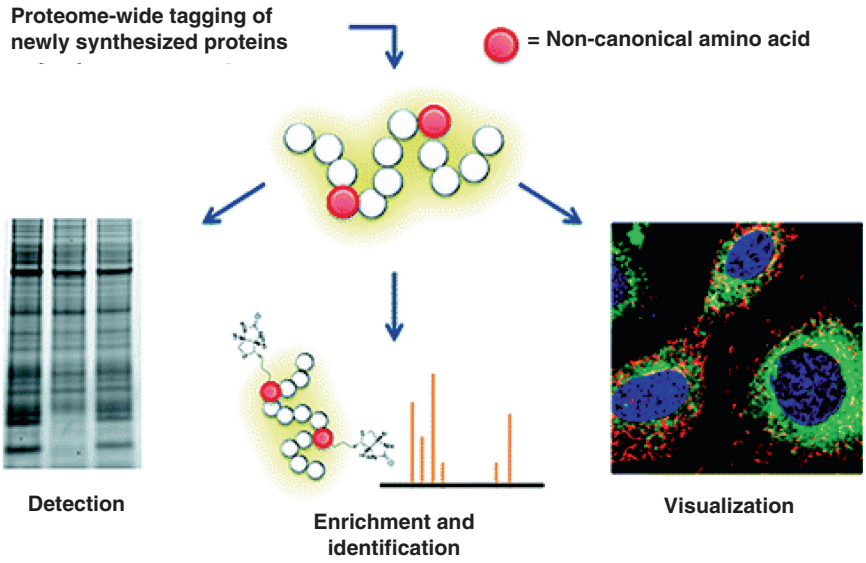

Fig. 13.25 Non-canonical amino acid probes used as protein tags for affinity enrichment and identification or to dyes for visualization by in-gel fluorescence scanning or fluorescence microscopy (Ngo and Tirrell 2011)

followed by selective Cu(I)-catalyzed ligation of the alkynyl side chain to the fluorescent dye 3-azido-7-hydroxycoumarin (Beatty et al. 2006). Protein tagging with homopropargylglycine (Hpg) in the absence of Met synthesis in mammalian cells and the promiscuity of the methionyl-tRNA synthetase make it straightforward to incorporate Hpg into mammalian proteins in competition with Met. After incorporation, Hpg is susceptible to labeling with the membrane-permeable dye for in situ imaging (Fig. 13.26).

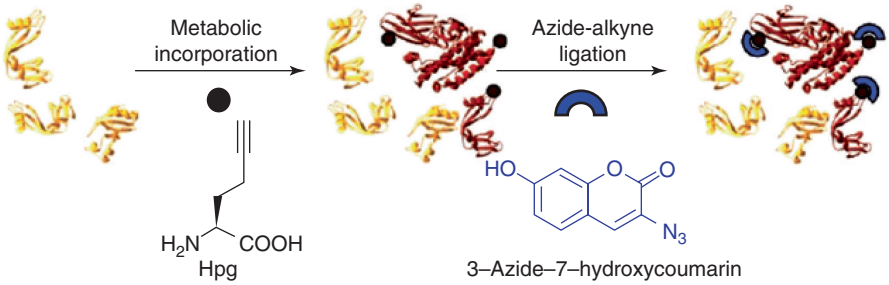

Fig. 13.26 Bioorthogonal labeling of newly synthesized proteins for fluorescence visualization in mammalian cells (Beatty et al. 2006). An alkynyl aminoacid is incorporated in a co-translational way and is followed by selective Cu(I)-catalyzed ligation of the alkynyl side chain to the fluorescent dye 3-azido-7-hydroxycoumarin

There are alternative possibilities for incorporation of noncanonical amino acids for labeling newly synthesized proteins in mammalian cells. The synthetic fluorescent amino acid dansylalanine was genetically encoded in *Saccharomyces cerevisiae* by using an amber nonsense codon and corresponding orthogonal tRNA – aminoacyl-tRNA synthetase pair (Summerer et al. 2006). This environmentally sensitive fluorophore was selectively introduced into human superoxide dismutase and used to monitor unfolding of this protein.

Already mentioned in Sect. 4.3, 2,7-azatryptophan is of value not only as noncanonical artificial fluorescent Trp analog but also as amino acid that can be incorporated into proteins instead of Trp by normal protein synthetic machinery (Shen et al. 2013). Moreover, in addition to emission spectrum at ~340 nm (which is common for indole derivatives) it exhibits additional band in the visible, at ~500 nm. This band originates due to excited-state proton transfer reaction mediated by water molecule. Because of that, the fluorescence spectrum is strongly sensitive to hydration of fluorophore environment, which allows analyzing the exposure of Trp residues in native protein using wavelength ratiometry (see Fig. 4.17).

It is believed that such strategy should be applicable to a number of different fluorophores that could be easily incorporated into the cells of both prokaryotic and eukaryotic organisms. This should facilitate both biochemical and cellular studies and sensing applications.

13.4.4 Concluding Remarks

The 'affinity labeling' inside the cells is a powerful strategy that needs a dramatic improvement with substantial contribution of synthetic chemistry. It is essential to devise chemistries that render the reagents fluorescent or change dramatically their emission (color, polarization or lifetime) only after the binding to the target site. This advancement should go side by side with improvements of specificity and affinity of the tags.

For successful application of visible fluorescent proteins, a different type of improvement is needed. Besides the complexity of genetic fusion technique, the GFP-like proteins are adding considerable bulk. In addition, their fusion is often limited by delayed maturation and increased risk of misfolding or aggregation. Therefore, the steps must be made towards dramatic miniaturization of these proteins, probably with the change in chemistry of spontaneously formed fluorophores. Alternative strategies for live-cell labeling deserve rapid development. Prospective in this respect are the genetically encoded fusion tags that are not themselves fluorescent but act as targets for labeling with chemical probes that incorporate fluorophores or other functional groups.

One of the most expected trends in cellular imaging is the incorporation of unnatural amino acids that can serve as fluorescent reporters themselves or that allowing highly specific modifications.

13.5 Advanced Nanosensors Inside the Cells

Chemical sensing inside the cells requires new tools. The properties that should be primarily improved for proceeding further into cellular studies are the brightness and photostability. A variety of new materials, such as dye-doped, carbon and semiconductor nanoparticles (Chap. 5) conform to these requests better than organic dyes and therefore they become increasingly popular in cellular research (Li et al. 2014). Much like with fluorescent organic dyes, there is no general solution of the problem of delivery of nanoparticles into the cells. Currently used methods include picoinjections, conjugation with cationic peptides, liposomal delivery, sequestration into macrophages and gene gun (Webster et al. 2007). Each of these methods can be tried but no one of them is perfect or generally applicable.

13.5.1 Fluorescent Dye-Doped Nanoparticles in Cell Imaging

The cell imaging and intracellular sensing are important fields in the application of fluorescence emitters in the form of nanosensors. *Nanosensors* are considered here as the nano-scale hybrid systems that integrate recognition and reporting functionalities and their support matrix for detection and quantitative analysis of target binding. The properties of basic nanomaterials are discussed in Chap. 5 and of their composites in Chap. 6. Their advantages over molecular sensors can be summarized as follows:

(a) An *increased number of analytes* can be measured with one type of sensors, because the nanosensors are not limited to using a single recognition or reporter unit and can utilize cooperative interactions between ionophores, enzymes, reporter dyes, etc.
(b) The nanosensors of composite design can be *prepared in vitro* by highly reproducible fabrication technologies. The calibration of nanosensors that can be easily made *in vitro* is commonly valid for *in vivo* measurements.
(c) The dyes immobilized with the matrix of nanoparticles can be *protected* from potential interferences in the cellular environment, e.g. from non-specific binding proteins and organelles.
(d) The particles can exhibit the *size-exclusion selectivity*. Porosity of such composite nanoparticles can be designed in a way that allows easy penetration into contact with the recognition and detection units of ions and small molecules, while large proteins are blocked from entering the nanoparticle matrix and from interacting with the dyes.
(e) Solubility, affinity and penetration properties can be modulated by designing the nanoparticle surface.
(f) In nanocomposites, different spectroscopic properties, i.e. wavelengths of excitation and emission, anisotropy, lifetime and ratiometric response can be varied in broad ranges.

(g) Nanocomposites can be made multifunctional. In addition of being light emissive they can attain magnetic, electron-dense, NMR-contrasting and other properties.

All these already realized advantages stimulate strongly their application for intracellular imaging and sensing.

13.5.2 The Quantum Dots Applications in Imaging

Semiconductor QDs have rapidly found a broad range of applications as optical imaging agents (Grecco et al. 2004; Lidke et al. 2007). They are characterized by high brightness, improved photostability, and multicolor size-dependent light emission (Sect. 5.5). A special feature of QDs that is very attractive for imaging is their fluorescence lifetime of 10–40 ns, which is at least one order of magnitude longer than that of typical organic dyes and also of intracellular pigments causing autofluorescence. Therefore, a combination of pulsed excitation with the time-gated detection can produce the images with greatly reduced levels of background interference.

An additional and very significant advantage of quantum dots is their significant two-photon absorbance that is two to three orders of magnitude greater than that of typical organic dyes (Larson et al. 2003). Therefore, it is natural to observe their increased level of application in two-photon microscopy with all the benefits that are offered by this method.

These remarkable properties suggest many opportunities for imaging. In the studies of living cells and in operation with *in vivo* animal models they bring unprecedented sensitivity and spatial resolution (Smith et al. 2006). Combined with biomolecular engineering strategies for tailoring the particle surfaces at the molecular level, the bio-conjugated quantum dot probes are well suited for imaging the single-molecule dynamics in living cells, for monitoring protein-protein interactions within specific intracellular locations, and for detecting diseased sites and tissues (Delehanty et al. 2012). The explosive increase in the use of QDs in biological imaging was triggered by an improved synthesis of water-stable QDs, the development of approaches to introduce them efficiently into the cells, and the improvements in conjugating QDs to specific biomolecules.

Although the success in using QDs for applications in cellular research is apparent, the routine use of these powerful tools meets with some unresolved problems related mainly with their conjugation (Jaiswal et al. 2004). For providing the binding specificity, the QDs must be conjugated to biomolecules that can label specific cellular proteins. Here their surface properties are important that are determined by their shells. Conjugation with functional molecules can be provided in one step by covalent attachment to shell-forming molecules or in two steps by attachment the self-assembly partners (such as avidin, oligohistidine or leucine zipper peptide) and following self-assembly of functional complex. The use of avidin permits a stable conjugation of the QDs to ligands, antibodies or other molecules that can be bioti-

nylated, whereas the use of proteins fused to a positively charged peptide or oligohistidine peptide obviates the need for biotinylating the target molecule (Rajh 2006).

Solution of the problems of QDs delivery into the cells and their functionalization should be made simultaneously. One of the possibilities could be the incorporation onto their surface of a bifunctional oligoarginine cell penetrating peptide (based on the HIV-1 Tat protein motif) bearing a terminal polyhistidine tract (Delehanty et al. 2006). The polyhistidine sequence allows the peptide to self-assemble onto the QD surface via metal-affinity interactions while the oligoarginine sequence allows specific QD delivery across the cellular membrane and intracellular labeling. By incorporating the differently colored QDs into a variety of live cells there is a possibility to generate a unique and spectrally resolvable code for each cell type (Mattheakis et al. 2004).

The coating of CdSe/ZnS QDs with neurotransmitter molecule dopamine (Clarke et al. 2006) allows obtaining in the living cells a redox-sensitive pattern. Dopamine may serve as photoinduced electron transfer quencher. Under reducing conditions, the fluorescence is only seen in the cell periphery and lysosomes. As the cell becomes more oxidizing, QD signal appears in the perinuclear region, including mitochondria. With the most-oxidizing cellular conditions, QD labeling throughout the cell is seen. This principle is extendable to any QD, conjugated to an electron donor.

Research of signaling pathways between and within the cells relies heavily on bright and sensitive fluorophores. QDs have begun to play a major role in this field. Thus, using serotonin-linked QDs it is possible to target the neurotransmitter receptor on the cell surface. The QD probes not only recognize and label the serotonin-specific neurotransmitters on cell membranes, but also inhibit the serotonin transportation in a dose-dependent manner (Tomlinson et al. 2007). Although one to two orders of magnitude less potent at inhibiting the receptor than free serotonin, the behavior of QD conjugates was similar to that of free serotonin, making QDs valuable probes for exploring the serotonin transportation mechanism.

Though the concern of toxicity of QDs remains, most experiments conducted to date have shown that QDs do not interfere with normal cell physiology and cell differentiation.

13.5.3 Self-Illuminating Quantum Dots

The QDs commonly require excitation from external light source. Meantime, they can be excited by the energy transfer from other molecules or particles that serve as the FRET donors (Sect. 6.3). This mechanism of transfer allows using the excited species obtained in bioluminescence reaction as the FRET donors (Sect. 10.2). Luciferase that is needed for this reaction can be covalently attached to QDs, and the substrate can be incorporated spontaneously into the cells and tissues. This construction allows the QDs to be ‘self-illuminated’ without any light source, by converting the chemical energy into the light emission of QDs as the FRET acceptors.

The QDs can emit light in the spectral region 600–800 nm, which are the wavelengths convenient for observation. Luciferase emission at 480 nm fits the QDs absorption band, which is very broad and increases dramatically in intensity on the transition to shorter wavelength.

This idea has been realized (So et al. 2006). It was shown that the self-illuminating QD conjugates possess a greatly enhanced sensitivity in imaging of not only the cells but also of small living animals. This allows avoiding many problems existing in common illumination of the surface by light, such as strong autofluorescence and light-scattering.

13.5.4 Detection of Intracellular Motions

High brightness and long-term stability of fluorescence response is needed for tracking the dynamics of nanoparticles in live cells. Ideal for this purpose are fluorescent nanodiamonds (see Sect. 5.4). They are inert nanoscale bodies and their phototoxicity, in contrast to quantum dots, was neither detected nor even questioned. Their extremely stable fluorescence emission originates from the negatively charged nitrogen-vacancy centers, $(N\text{-}V)^-$, which absorb light strongly at ~560 nm and emits fluorescence efficiently at ~700 nm. This emission is well separated from the spectral region where endogenous fluorescence occurs.

When incorporated into live cell, single nanodiamond particle produces a track that can be recorded on a rather extended time scale (Fig. 13.27).

Viruses can be stained with fluorescent dyes, and their motions can be traced. In this way, every step of penetration into the cell of virus particle can be visualized (Seisenberger et al. 2001).

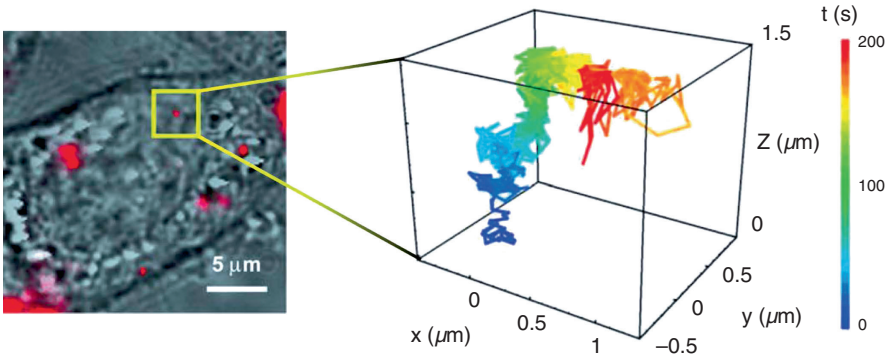

Fig. 13.27 3D tracking of a single fluorescent nanodiamond in a live cell (Chang et al. 2008). Overlay of bright-field and epifluorescence images (*left*) shows a single 35-nm fluorescent nanodiamond moving in the cytoplasm of a live HeLa cell. The fluorescence is sufficiently bright and stable to allow tracking of this particle in three dimensions over a time span of 200 s (*right*)

13.5.5 Extending the Range of Detection Methods

Summarizing the results discussed in this Section, we must indicate a growing interest from the side of researchers to novel functional brightly emitting nanoparticles. Despite their greater dimensions, they are superior to organic dyes in many aspects and allow overcoming some limitations in their use for cellular imaging. Fluorescent quantum dots have proved to be a useful alternative for the studies that require long-term and multicolor imaging of cellular and molecular interactions. Very positive results in this respect can be also achieved with nanoparticles composed of organic dyes and metal chelating complexes hosted by silica or organic polymeric matrices. These nanocomposites can explore the versatility of already developed molecular sensors that is highly needed in the studies of biosystems.

13.6 Sensing Within the Cell Membrane

In this Section, without attempt to go deeply into membrane biology, we will outline some remarkable applications of fluorescence sensing and probing techniques. Membrane surrounding the living cell has the important functions of maintaining the specific composition and properties of cell interior and also of communication with other cells and with surrounding media. The cell membrane contains a specific recognition pattern related to its function. Fluorescence probing is one of the most powerful and commonly used tools in the studies of biomembrane structure and dynamics that can be applied on different levels, from lipid monolayers and bilayers to living cells, tissues and whole bodies (Demchenko et al. 2009). Being smaller than the membrane width, functional organic dyes can characterize the microscopic analogs of viscosity, polarity, and hydration, as well as the molecular order, environment relaxation, and electrostatic potentials at the sites of their location (Demchenko et al. 2015).

13.6.1 Membrane Structure and Dynamics

In model phospholipid membranes, the environment-sensitive probes, such as Laurdan and Prodan (Sect. 4.3), can easily reveal the differences between the fluid and gel and also between Ld and Lo phases (Dietrich et al. 2001; Bagatolli 2006). In Lo phase, these probes demonstrate with a blue-shifted emission a less polar environment compared to Ld phase, that is close to that of a gel phase. High sensitivity in this respect demonstrate also the 3-HC probes, due to their switching between the emission bands in response to changes of membrane properties, such as polarity and hydration (Oncul et al. 2010). The most characterized F2N8 probe is of particular interest to study lipid domains in different model vesicles

mimicking different membrane phases. In Lo phase an exceptionally low hydration was observed, and this parameter increases in the following order: Lo << gel ≈ Ld (with cholesterol) < fluid (without cholesterol). Remarkably, the membrane fluidity shows a somewhat different trend, namely Lo ≈ gel < Ld < fluid. Thus, gel and Lo phases exhibit similar fluidity, while the Lo phase is significantly less hydrated than the gel phase. This means that cholesterol, due to its specific H-bonding interactions with lipids and its ability to fill the voids in lipid bilayers, efficiently expels water molecules from the highly ordered gel phase to form the Lo phase (Oncul et al. 2010).

The ability of 3-HC probes to provide strong spectroscopic response to Lo phase was applied to visualize lipid domains using the model of giant unilamellar vesicles, which due to their large size (5–100 μm) can be directly used in fluorescence microscopy. It was found that the F2N12S probe (Fig. 13.28) incorporates into both phases, probably due to the presence of the long dodecanoyl tail. Steady-state fluorescence studies showed that its dual emission is strongly modified depending of the lipid phase and can be correlated with the changes in hydration (Oncul et al. 2010). Using two-photon excitation microscopy on GUVs, F2N12S probe allows to individually visualize both Lo and Ld phases (Klymchenko et al. 2009). Moreover, by using a linearly polarized excitation laser light, a strong photoselection was observed for F2N12S in Lo phase, indicating that its chromophore is nearly parallel to the lipid chains of the bilayer.

13.6.2 Lipid Asymmetry and Apoptosis

Normal cells exhibit remarkable asymmetry of lipid distribution between inner and outer leaflets of cell membranes, which is lost during the early steps of *apoptosis* (programmable cell death) when the cell integrity is not yet disrupted. The most characteristic in this change is the exposure to cell surface of anionic phospholipids, such as phosphatidylethanolamine (PE) and phosphatidylserine (PS). This exposure is functionally important; it provides the signal for recognition and elimination of apoptotic cells by macrophages.

The methods based on molecular recognition of *surface-exposed* PS and PE allow to identify and characterize apoptotic cells (Demchenko 2013). The most popular of them are based on the property of the protein annexin V to interact with exposed PS in a Ca^{2+}-dependent manner. Because of this selectivity, the binding of labelled protein occurs specifically only to apoptotic cells. Different variants of this method were developed. For instance, annexin V labelled with fluorescein is used for flow cytometry, while its labeling with red and near-IR dyes is efficient for tissue imaging (Petrovsky et al. 2003; Ntziachristos et al. 2004). The recently reported conjugation of annexin V with quantum dots allowed achieving an increased sensitivity of detection (Koeppel et al. 2007).

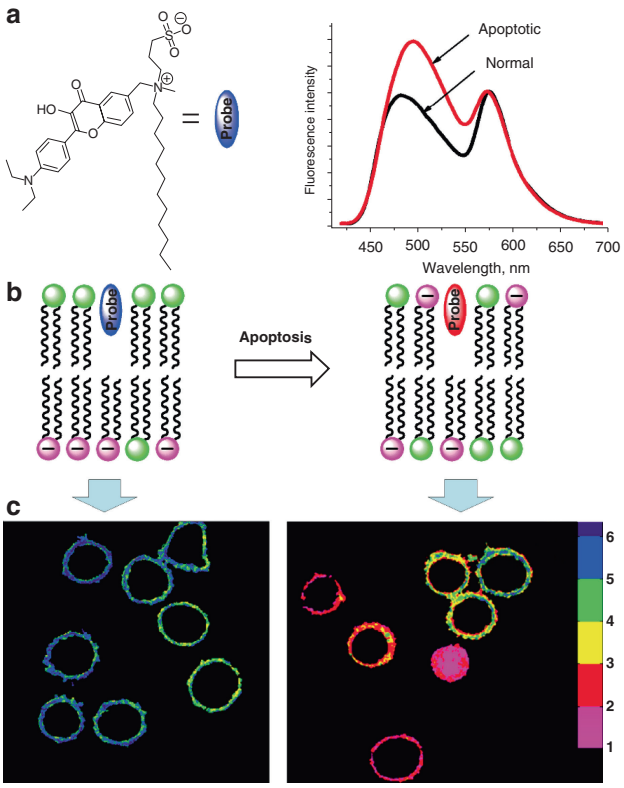

Fig. 13.28 Detection and characterization of apoptotic cells using membrane-incorporated dye (Shynkar et al. 2007). (**a**) Structure of 3-hydroxychromone wavelength-ratiometric dye **F2N12S** (probe) and its fluorescence spectra in normal and apoptotic cells. (**b**) Cartoon illustrating the mechanism of fluorescence response. Normal cells exhibit asymmetry in lipid composition between inner and outer leaflet of their membranes: anionic lipids are oriented inside the cell. In apoptotic cells they appear in the outer leaflet. The dye incorporates spontaneously into outer leaflet and reports on the appearance of anionic lipids. Its response is based on the ability to sense the change of surface potential and of hydration in this leaflet. (**c**) Confocal fluorescence ratiometric images of human lymphoid CEM T cells and the same cells with induced apoptosis by treatment with actinomycin D. The ratios of intensities of the T* band to those of the N* band are displayed in pseudocolor by using the color code on the right scale

There can be a different approach to the same problem. It can be based on detecting the *change of membrane order*, *surface potential* and *hydration* that must be the result of appearance of anionic lipids in the outer membrane leaflet. A very high sensitivity of 3-hydroxychromone probes to variation of these parameters allowed developing the molecular sensor for apoptosis that could incorporate spontaneously into the outer leaflet of the membrane and report on apoptotic cell transformation in a wavelength-ratiometric manner (see Fig. 13.28).

This approach can be applied in three formats – in fluorescence spectroscopy of cell suspensions, in confocal microscopy of individual cells and in flow cytometry (Shynkar et al. 2007). In the latter case, compared to annexin V labeling we observe much smaller dispersion of measured parameter within the sub-populations of living and apoptotic/dead cells, and a combination with cell-permeable dye (e.g. propidium iodide) allows obtaining quantitative measure of living, early apoptotic and dead cells.

It is essential to note that here the development of apoptosis is revealed by the change of emission color, in contrast to methods based on labeled proteins binding selectively to apoptotic cells and resulting in changes from dark to light. The reader may evaluate the advantages of wavelength-ratiometric imaging. The proposed methodology is not limited to apoptosis. Since the appearance of anionic lipids was detected on the surface of different cancer cells, it may probably find application for studying the development of cancer tissues and of the efficiency of applied anticancer drugs. Also the appearance on the cell surface of anionic lipids is a remarkable event during activation of platelets and may be useful for monitoring the blood-clotting events.

13.6.3 Sensing the Membrane Potential

Transmembrane potential (V_m) is the most dynamic component of electrostatic field in cell plasma membranes. It plays important role in a variety of cellular functions related to bioenergetics, ion transport, motility, and cell communication. It is highly important to monitor this potential, notably in neuronal cell assemblies, because its propagation can provide clues to understand the mechanisms of brain activity. Therefore, V_m has to be measured with high time resolution, in milliseconds. Being reactive on much shorter time scale of ESIPT, the 3HC dyes can provide such fast response. The high two-band ratiometric sensitivity of these dyes to electric filed (Klymchenko et al. 2003; Klymchenko and Demchenko 2002) is in the background of these applications. A new 3HC dye possessing deep vertical incorporation into the lipid bilayer was developed for this purpose (Klymchenko et al. 2006).

In order to achieve the highest sensitivity to the electric field associated with V_m, the fluorophore must be located in phospholipid environment of the membrane as deeply as possible in its hydrophobic area, where the dielectric constant is minimal, which means a smaller dielectric screening. This requirement cannot be easily satisfied with any hemicyanine or styryl pyridinium dyes that are also used in sensing the membrane potential (Gross et al. 1994) because in these dyes the positive charge is the part of fluorophore. In contrast, 3-hydroxychromones are uncharged molecules of relatively low polarity, which can be introduced at any position within the bilayer. Rigid skeleton of the probe and the presence of

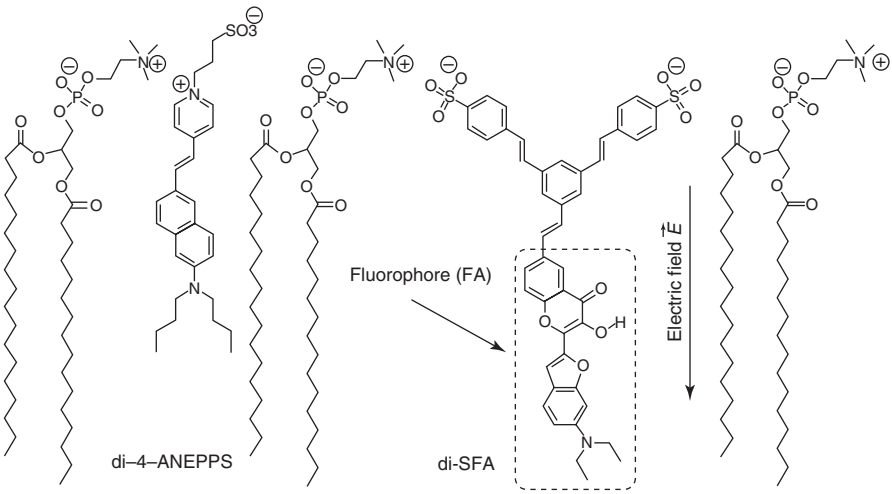

Fig. 13.29 Assumed location of di-4-ANEPPS (a styrylpyridinium dye) and di-SFA (a 3-hydroxychromone derivative) in lipid bilayers. The fluorophore part of the probe di-SFA is boxed. Only half of the bilayer is shown being represented by phosphatidylcholine structures

two segments bearing the negative charges allow fixing the position and orientation of fluorophore part FA (Fig. 13.29).

The new dye exhibits fast response to transmembrane potential by *variation of relative intensities of the two emission bands*. Its sensitivity is *ca* 15 % in the change of ratiometric signal per 100 mV, which is one of the best results obtained so far in a fast-response fluorescence probing. This dye is prospective for a variety of applications for monitoring the membrane potential in cell suspensions and its imaging in single cells, especially in neurons having fast electrical activity.

A broad field of studying the spatio-temporal pattern of neuronal activity in vivo is open for application of fast-responding voltage-sensitive dyes. It needs involvement of two-photon microscopy, and the first steps for evaluation of aminostyryl voltage-sensitive dyes at two-photon excitation have been made (Fisher et al. 2008)

It has been known that natural membranes generate a very strong electric field gradient known as *dipole potential* (V_d) (Gross et al. 1994). This potential arises due to oriented hydrated carbonyl groups of phospholipids and is well reproduced in phospholipid biomembrane models. Neutral dipolar molecules when incorporate into the bilayer can provide a strong modulation of (V_d). It was demonstrated that the compounds increasing or decreasing the dipole potential on their incorporation into the bilayers (Klymchenko et al. 2003) and cell membranes (Shynkar et al. 2005) induced opposite effects on the response of two-color ratiometric fluorescent probes. The effect on this incorporation of V_d modulator 6-ketocholestanol was

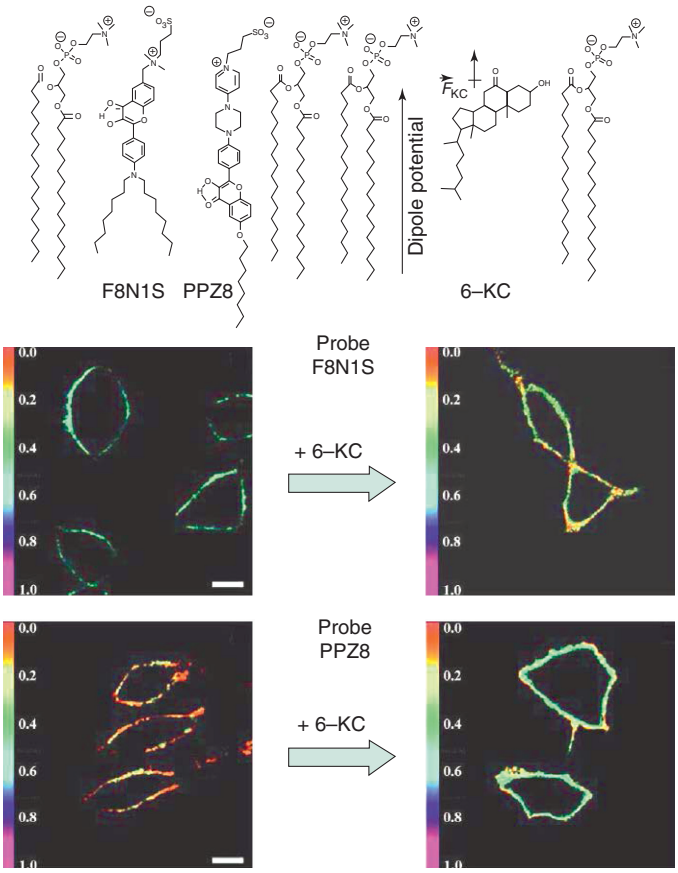

Fig. 13.30 Probing of dipole potential of cellular membrane using membrane-incorporated dyes (Shynkar et al. 2005). Schematic representation of lipid monolayer with four phospholipids (*above*) shows the location in opposite orientations of two wavelength-ratiometric 3-hydroxyflavone dyes **F8N1S** and **PPZ8**. Being electrochromic, they respond to the change of membrane electric field by spectroscopic changes in different directions. Also depicted is the 6-ketocholestanol (6-KC) molecule that being a strong dipole can incorporate spontaneously into the membrane and increase its dipole potential. In confocal microscopic images it is clearly seen that treatment of cells with 6-KC produces opposite effect in changing the color of fluorescence emission of two dyes

clearly seen in confocal microscope (Fig. 13.30).It was also observed that incorporation of the dye in opposite orientation produces reversal of spectroscopic effects, which allows distinguishing vectorial electric field effects from orientation-independent effects such as polarity and hydration.

Here we have to stress that with two-color wavelength-ratiometric probes the absolute intensity forming the image of cell membrane in confocal microscope is not very informative since it depends on the local probe concentration and its location with respect to fluorescence quenching groups. In contrast, the ratio of intensities of the two fluorescence bands is independent on these factors and reflects the true magnitude of electrostatic effects.

13.6.4 Membrane Receptors

Examination of signaling pathways that involve interaction of specific cellular receptors with their targets requires labeling of both the receptor and the target. A productive strategy could be a co-synthetic labeling of receptor with visible fluorescent protein of GFP family and of the target with brightly fluorescent nanoparticles. Such possibility was demonstrated (Lidke et al. 2007) for the epidermal growth factor receptor (EGFR) and correspondent epidermal growth factor (EGF), see Fig. 13.31.

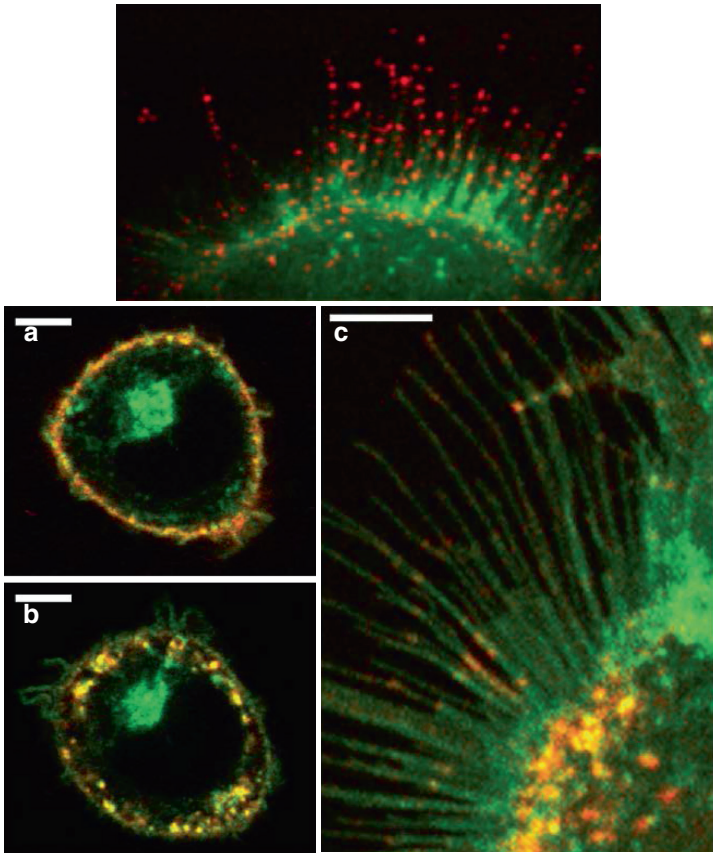

Fig. 13.31 Visualization of epidermal growth factor receptors on the surface of carcinoma cells (Lidke et al. 2004, 2007). *Top*: A Programmable Array Microscope (PAM) image showing a maximum intensity projection of 20 optical sections of a living human carcinoma cell expressing a GFP-fusion protein of epidermal growth factor receptor (*green*) binding quantum dot-epidermal growth factor (QD-EGF) ligand (seen as *red spots*). The binding of QD-EGF to individual EGF receptors on the filopodia and the cell membrane is observed. *Bottom*: Single confocal sections of living cells showing QD-EGF ligand binding to the surface expressed membrane receptor and subsequent activation. The cells express a green fluorescent protein-fused EGF receptor. (**a**) *Red* QD-EGF and *green* GFP-EGF receptor co-localize on the cell membrane 3 min after addition of ligand and **b** are rapidly internalized together into endosomes in the cytoplasm. (**c**) Individual receptors labeled with QD-EGF on long sensory filaments called filopodia can be visualized and seen to transport to clathrin coated pits for internalization at the cell body

It was shown that EGF conjugated to quantum dots is still capable of binding to and activating its receptor, which triggers internalization of both EGF-QD and its receptor via endocytosis. High photostability of QD allows the study of EGF-QD binding and internalization kinetics with great detail. The family of these receptors is implicated in the development and progression of cancer, and is expressed in many human epithelial malignancies. Such quantitative understanding of the transduction mechanism is essential for receptor-targeted therapeutics. Quantum dots become a valuable tool for this kind of investigation because of their much higher brightness and photostability than that of organic dyes.

The results of the studies on other types of receptors, e.g. glycine receptors in neuronal membranes (Dahan et al. 2003) are good illustrations of that. In these studies, tracking individual dots and analyzing their trajectories is possible with the evaluation of QD diffusion coefficients.

13.6.5 Future Directions

Cellular membrane is the means for a cell to communicate with the whole world, so it has enough room for communicating with our fluorescent labels and probes. The cell membrane is a very complex structure that demonstrates both site-specific and integrated properties. The *integrated properties* allow mediating the functional response via cooperative structural transitions of the lipid component forming the bilayer. The change of lipid mobility and lipid segregation (e.g. formation of 'rafts') are a part of this mechanism. The response of this system to external stimuli is great, and the study is relatively easy, since many amphiphilic dye derivatives can incorporate spontaneously into membrane structure from external medium. In these studies the dyes exhibiting multiparametric approach and that are able to characterize the membrane in terms of effects on its hydration, polarity and membrane potential are of great importance. We expect their rapid exploration not only in basic research but also in applications using the 'whole-cell biosensors' for detection and testing differently biologically active compounds.

The *specific properties* of membranes are provided by receptor proteins that provide either direct response (such as the opening-closing the ion channels) or transduce the signal into the cell interior that can be mediated by second messagers and their receptors. For membrane receptor proteins the most important methodology based on fluorescence involves their covalent dye labeling for establishing proximity relations in the receptor system and the labeling of ligands for finding the stimulus-response correlations.

13.7 Sensing Different Targets in Cell Interior

The living cell demonstrates a high level of organization among tens of thousands types of molecules that constitute it. Here we will demonstrate the applicability of microscopic imaging technique for sensing some of its important constituents. The

overview of analytical methods addressing determination of different targets was presented in Chap. 12. In present discussion we focus on determining the most important metabolites and regulatory factors.

Many fluorescent sensors used in intracellular sensing are small molecules, and it is highly preferable for them to be *trappable*. This means that they have to cross initially the cell membrane easily but do not have to recross it after initial uptake. A common strategy for modifying probes to be trapped in cells involves the incorporation of ester groups to the probe structure. Hydrolysis of the ester moieties by intracellular esterases releases a negatively charged membrane-impermeable form of the probe.

13.7.1 Ion Sensing

Calcium is the most common target for intracellular imaging and sensing because this divalent cation is probably the most ubiquitous and important second messenger in cells. It is involved in key cellular events controlling muscle contraction, nerve cell communication, hormone secretion and activation of immune cells.

Selective measurement of *free calcium concentration* in living cells requires the sensor molecules with selectivity for calcium by many orders of magnitude higher than to other cations. This is because in living cells the Ca^{+2} ion concentration is maintained on a level of 10^{-7} M in the resting state and upon transmission of cellular messages it rises to 10^{-6}–10^{-5} M. This is in strong contrast with its high extracellular concentration, which can be on the level of 10^{-3} M. The calcium sensing should be discriminative from other ions that may interfere into assay. Therefore, the intracellular concentrations of Ca^{+2} should be determined on the level of 10^{-7}–10^{-5} M in the presence of 10^{-3} M Mg^{+2}, 10^{-2} M Na^{+} and 10^{-1} M K^{+} ions. This is possible with calcium indicators that combine specific ion binding with strong light-emission response. Presently the researcher can select between calcium indicators built on the basis of several different principles.

1. *Fluorescent dyes* with attached ion chelator groups. In current use are the dyes Fura-2 (ratiometric in excitation) and Indo-1 (ratiometric in emission) (Grynkiewicz et al. 1985). Their major disadvantage is their near-UV excitation and emission that overlaps the emission of some cellular pigments. A detailed investigation of Indo-1 shows that its ratiometric signal can be influenced by the factors unrelated to analyte concentration. Those are the photobleaching with the production of fluorescent but Ca^{++}-insensitive forms (Scheenen et al. 1996) and temperature (Oliver et al. 2000), which is probably due to the difference in thermal quenching of ligand-bound and ligand-free forms of the sensor.

Many probes respond to calcium ions by the change in intensity of a single fluorescence band (Oheim et al. 2014). Their response to calcium depends not only in ion binding but also on their local concentration. Therefore popular approach is to use combination of two dyes that are excited at the same wavelength but demonstrate well separated emission bands. Thus, both Fluo-3 and Fura Red can be excited

at 488 nm by argon-ion laser, but on binding Ca^{++} ions Fluo-3 increases its emission at 520–530 nm and Fura Red exhibits decrease in intensity of its spectral band at 660–670 nm. Working with living cells, researchers must be cautious in interpreting these data, since being different chemical structures, these dyes may be distributed differently within the cell.

2. Molecular sensors based on conformation change of a *calcium binding protein calmodulin*. Calmodulin mutations can alter the binding affinities for calcium in a concentration-dependent manner, so that with a combination of sensors, Ca^{++} can be detected in the range 10^{-8}–10^{-2} M (Miyawaki et al. 1999). The sensor together with two fluorescent FRET donor and acceptor can be fully synthesized inside the cell (see Fig. 7.17).
3. *Luminescent calcium binding protein aequorin* that can be genetically expressed in the cells and synthesized in the form fused to different proteins (Rogers et al. 2005). To emit light, aequorin needs an imidazopyrazine cofactor (or its synthetic analog), which is membrane permeable and can be added to intact cells containing an engineered aequorin.
4. The sensors based on known *calcium-binding protein troponin C*, which can be fused to a variant of green fluorescent protein to provide the response based on FRET (Mank et al. 2006). Such chimeric structure can be synthesized inside the cell. It shows a maximum fractional fluorescence change of 400 % in its emission ratio and linear response properties over an expanded calcium regime.

Determinations of calcium ions on the level of single cells allows demonstrating inhomogeneous distribution of these ions inside the cells, rhythmic oscillations of their levels, the so-called *spikes* and *waves* and other interesting phenomena that are in the background of mechanisms of cell regulation. Therefore all the applied detection methods should allow submillisecond temporal resolution.

Zinc is the second after calcium important cation in biological systems. It is an essential structural element of a number of DNA binding proteins and enzymes (over 300, including carbonic anhydrase and alcohol dehydrogenase). It plays important role in neurotransmission, signal transduction and gene expression. Perturbation in its homeostasis is related to a number of disorders including Alzheimer's disease, diabetes, and cancer. The lack in understanding of molecular mechanisms of zinc physiology and pathology is partially due to the lack of tools for measuring the changes in its intracellular concentrations with high spatial and temporal fidelity.

The total concentration of zinc ions in human blood serum is ~12 μM. But in cells the major part of zinc ions is tightly bound to proteins and cell organelles, so that the amount of free or rapidly exchangeable zinc is very low, on a *picomolar level*. Measuring these concentrations with picomolar sensitivity in the presence of much higher and variable Mg^{+2} and Ca^{+2} levels requires a highly specific and sensitive fluorescent sensor.

Addressing this complex task, a number of solutions have been found (Pluth et al. 2011). The most attractive of them are the single-excitation-dual-emission ratiometric probes. One of them uses the mechanism of controllable Zn^{2+}-induced

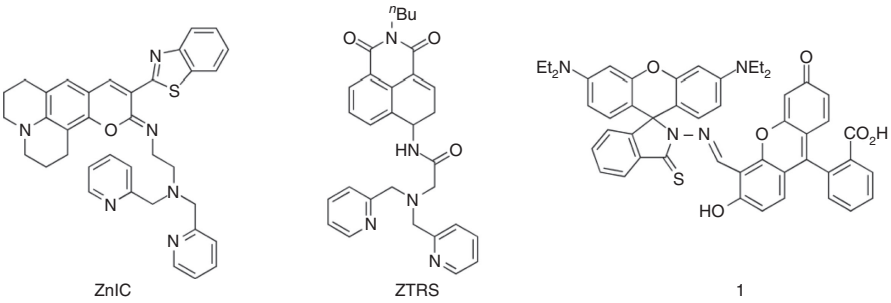

Fig. 13.32 Selected λ-ratiometric fluorescent probes for biological zinc (Pluth et al. 2011)

switching between the fluorescein- and naphthofluorescein-like tautomer forms of the dye (Chang et al. 2004). In other developments for λ-ratiometric zinc measurements, iminocoumarin as a fluorophore and (ethylamino)dipicolylamine (DPA) as a Zn^{2+} chelator were suggested (Fig. 13.32).

The DPA-bound Zn^{2+} interacts with an iminocoumarin moiety, thereby influencing the internal charge transfer process connected to the fluorescence emission (Komatsu et al. 2007).

In the amide-DPA sensor ZTRS, zinc coordination induces tautomerization of the amide moiety and causes a red shift of the emission profile of the naphthalimide fluorophore directly connected to the amide nitrogen atom. The construct denoted as **1** in Fig. 13.32 explores the zinc-induced modulation of FRET. In this fluorescein-rhodamine pair a zinc-induced ring opening of a rhodamine spirolactam restores emission of the rhodamine fluorophore that results in FRET between the xanthenone dyes. This modulation provides highly selective zinc detection over a large concentration range (from 2.0×10^{-7} M to 2.0×10^{-5} M) by measuring the ratio of the well-separated emission intensities of the two fluorophores (Han et al. 2010).

In addition to small molecules, a series of *peptide-based zinc sensors* have been developed. Their structures are borrowed from the so-called 'zinc-finger' sections of the DNA-binding proteins. The sensing is based on conformational change in peptide upon Zn^{2+} binding (Walkup and Imperiali 1997). The peptide wraps around the ion, which results in the change of environment of attached dye or brings two dyes attached to peptide terminals together with the observation of FRET (see Fig. 8.13).

Although a variety of synthetic fluorescent sensors for zinc have been developed and applied in recent years, their affinity does not fully match the required concentration range. Therefore, the attempts were made to build the sensor based on the scaffold of one of zinc binding proteins. The ratiometric fluorescent sensor based on enzyme carbonic anhydrase (Thompson et al. 2002) explores the binding of zinc in its active site and generation of wavelength-ratiometric response due to a zinc-dependent FRET between the two dyes. Exhibiting a picomolar sensitivity, this sensor is well adapted to zinc imaging in a physiologically important concentration range.

Sodium and *potassium* ions are also important for understanding the cellular life. The living cells actively pump-out sodium ions by substituting them into potassium

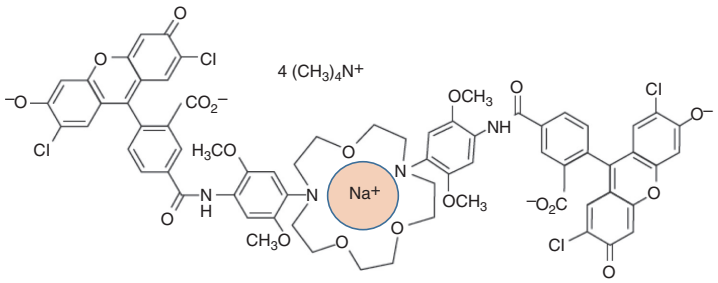

Fig. 13.33 The cellular indicator of sodium ions Sodium Green. It comprises two 2′,7′-dichlorofluorescein dyes that are linked to two nitrogen atoms of a crown ether that serves as ion recognition unit with K_d of 6.0 mM

ions. Reverse process, their exchange occurs in membrane ionic channels. Therefore, determining the sodium and potassium ion concentrations is important for cell physiology. The actively used at present and for observable future are the dyes incorporating crown ethers and responding to ion binding by PET or ICT mechanisms. A typical example is a commercial sodium indicator Sodium Green (Fig. 13.33) that can be used to signal the presence of sodium ions *in vivo* and quantify them on a millimolar scale of concentrations (Haugland 2005). This and similar dyes typically respond to ion binding by the change (increase) of fluorescence intensity without observable spectral shifts, so they share all disadvantages of intensity measurements that were discussed many times throughout this book.

13.7.2 Tracking Cellular Signaling

Determination of factors that provide *intercellular signaling* (first messengers) and *intracellular signaling* (second messengers) is very important for cell biology and pharmacology. The *first messengers* are neurotransmitters, cytokines and hormones functioning respectively in nerve, immune and endocrine systems. They bind either to ion-channel, kinase or G protein-coupled membrane receptor proteins of different cells transmitting the signals to them, and trigger the respective downstream intracellular signaling.

Small molecules that are known as *second messengers* play a central role in signal transduction modulating many physiological and pathological processes in living cells. Therefore many attempts have been made for their detection and tracking inside the cells. Calcium ions and cyclic nucleotides are the second messengers. One of them is also *nitric oxide* (NO).

Direct recognition of such small molecules on sub-nanomolar level of detection is problematic, since it is hard to develop a sensor of sufficiently high affinity. Therefore one of the most interesting suggestions was, instead of detecting NO, to determine the product of the NO-activated reaction producing cyclic guanosine

monophosphate (cGMP). Here the principle of catalytic amplification is used. Because a single NO molecule leads to production of many cGMP molecules, this test system possesses a required very high sensitivity. The cGMP sensor is based on the change in relative intensity of two visible fluorescent proteins that are coupled via FRET mechanism, which allows a wavelength-ratiometric response in microscopic images (Sato et al. 2005).

The attempts of direct NO sensing using functional fluorescent dyes have also been reported (Pluth et al. 2011). Thus, highly sensitive and pH-independent fluorescence probe for NO was suggested based on 4-methoxy-substituted BODIPY dye. This sensor explores the PET mechanism of intensity-based response (Gabe et al. 2006).

Since the use of FRET in sensor reporting usually requires the change in distance between two labels, this approach can also be applied to a sensor protein composed of two or several subunits if the sensing event involves changing the distance between them. This possibility was demonstrated for *detection of cAMP* in smooth muscle cells by labeling the catalytic and regulatory subunits of c-AMP-dependent protein kinase with two different dyes (Adams et al. 1991)

Hydrogen peroxide (H_2O_2) is produced endogenously in living systems as a destructive oxidant to ward off pathogens or as a finely tuned second messenger in dynamic cellular signaling pathways. A palette of fluorescent and luminescent probes that react chemoselectively with hydrogen peroxide utilizing a boronate oxidation trigger has been developed (Lin et al. 2012). These indicators can be used to examine hydrogen peroxide in a number of experimental setups, including in vitro fluorometry, confocal fluorescence microscopy, and flow cytometry. Using functional nanocomposites is a more advanced approach along this line. For detecting mitochondrial H_2O_2 the nanoprobe was prepared by covalent linking a mitochondria-targeting ligand (triphenylphosphonium, TPP) and a H_2O_2 recognizing element (PFl) onto carbon dots. For this nanoprobe, the carbon dot serves as both the carrier and the FRET donor. Staining the mitochondria, the PFl moieties in the presence of H_2O undergo structural and spectral conversion, affording a λ-ratiometric determination of H_2O_2 (Du et al. 2014).

13.7.3 Oxygen in Living Cells

Oxygen is one of the key metabolites in aerobic organisms providing a source of energy for different cellular processes. In cellular respiration, oxygen plays a major role as the terminal acceptor of the electron transport chain and oxidative phosphorylation. Oxygen deprivation (hypoxia) is connected with various diseases and occurs in tumors. Therefore it is important to quantify oxygen levels in biological cells and tissues to understand cellular physiology in norm and disease and to control the effect of drugs in cancer therapies.

The analytical methods of determining oxygen concentrations are discussed in Sect. 12.3. Dual emission from oxygen sensitive and oxygen insensitive probe can be explored for constructing the λ-ratiometric sensors. The most efficient is the combination of fluorescent and phosphorescent dyes incorporated into polymeric nanoparticle.

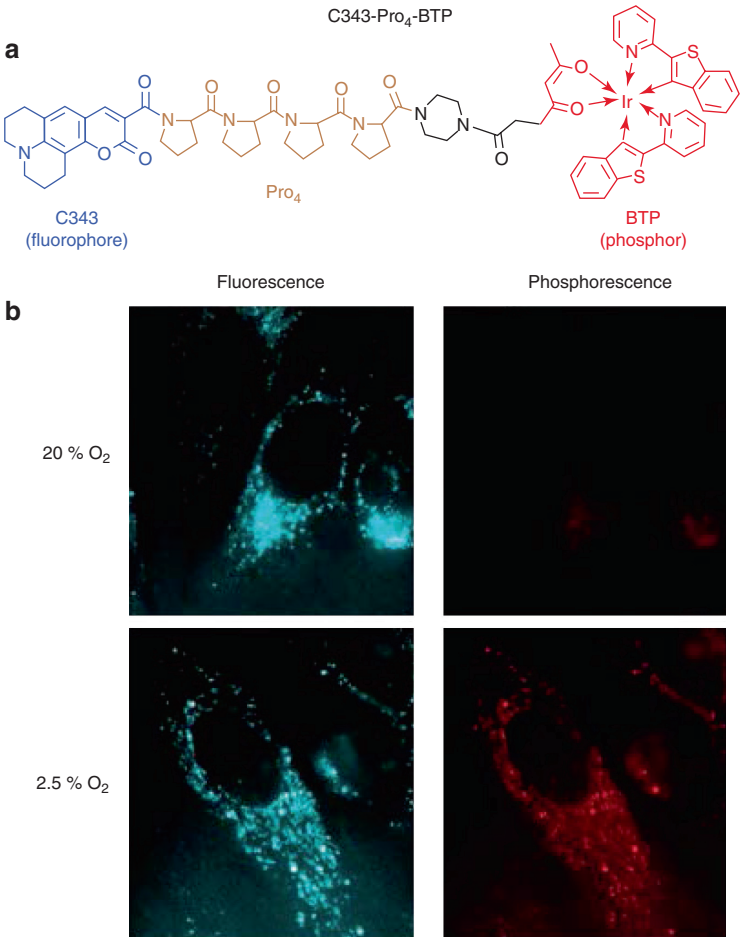

Fig. 13.34 Imaging of intracellular oxygen (Yoshihara et al. 2012). (**a**) Chemical structure of ratiometric probe C343-linker-BTP. (**b**) Luminescent images of HeLa cells incubated under aerobic and hypoxic conditions

The short-living fluorescence is insensitive to quenching by oxygen in physiological concentrations, and long-living phosphorescence may be strongly sensitive to it. The sensors should not be reactive to other variables, such as polarity or pH.

Such requirements can be satisfied also by designed composite of molecular emitters. One of such constructions and the result of its application for oxygen imaging in cell are presented in Fig. 13.34. Coumarin 343 (C343) was chosen as the fluorescent group and the iridium complex BTP as the phosphorescent group connected by a tetraproline linker (Yoshihara et al. 2012). When C343-linker-BTP is excited at 405 nm, the excitation photons are mainly absorbed by the C343 moiety, and the electronic energy is partially transferred from C343 to the BTP moiety by singlet-singlet energy

transfer, resulting in both blue fluorescence of C343 and red phosphorescence of BTP. Quenching phosphorescence in oxygenated conditions was manifested.

13.7.4 Location of Metabolites and Tracking Metabolic Events

Distribution of metabolites and their transport within and between the cells can be understood only if we know subcellular distribution of metabolites in living (not fixed) cells obtained in a nondestructive way. In addition, we need to observe their dynamics, especially under the influence of different stimuli. The novel techniques addressing this problem based on fluorescence imaging are emerging.

The attempts to suggest a flexible strategy for designing the intracellular sensors for a wide spectrum of solutes and their concentrations were made by different researchers. Platform based on bacterial periplasmic binding proteins (PBPs) uses the ability of these proteins to bind different ligands, the number of which can be expanded by genetic engineering. The response to binding such targets is based on the ability of these proteins to transform their hinge-bend movement (see Sect. 8.5) into increased fluorescence resonance energy transfer (FRET) between two coupled visible fluorescent proteins (Fehr et al. 2002). This allows obtaining wavelength-ratiometric response. By using the maltose-binding protein as a prototype, nanosensors were constructed allowing *in vitro* determination of FRET changes in a concentration-dependent fashion. For physiological applications, mutants with different binding affinities were generated, allowing dynamic *in vivo* imaging of the increase in *cytosolic maltose concentration* in single yeast cells. This approach is promising in the case of successful development of a myriad of PBPs recognizing a wide spectrum of different substrates.

13.7.5 In-situ Hybridization

Fluorescent in situ *hybridization* (FISH) is the method for gene mapping and the identification of chromosomal abnormalities that utilizes fluorescently labeled DNA probes. FISH provides the means to visualize and map the genetic material in cells, including specific genes or portions of genes. In malignant cells it allows quantifying gene copy numbers that have abnormal gene amplification (Tsuchiya 2011).

The *in situ* hybridization procedure requires application of probing DNA or its fragments that have to be conjugated with fluorescent labels. Different labels can be used on a condition that the labeling does not interfere with the recognition between complementary oligonucleotide sequences. Moreover, the dyes were developed for staining each of the human chromosomes in different colors (Geigl et al. 2006). Fluorescent nanobeads and quantum dots have shown their applicability in these assays, and, due to their higher brightness and photostability, they offer important advantages over organic fluorescent dyes.

13.7.6 Looking Forward

It is hard to imagine the modern cell biology without fluorescence methods, and the selected examples presented above are good illustrations for that. We observe that the more and more sophisticated fluorescence sensors are applied in cellular research. They become brighter, possess increased stability and required functionality, become amendable for application in novel high-resolution technologies.

In addition to molecules and particles that are applied to cell by diffusion, injection or endocytosis, an increasing number of visible fluorescent proteins was suggested. They can be synthesized inside the cell by using their biosynthetic machinery. The most attractive and possibly prospective for future development are the hybrid systems composed of incorporated segments of protein structure that contain recognition units for functional dyes and of these dyes with the ability of self-assembly with these segments inside the cells.

It is expected, that the structural aspect in cellular studies will soon give priority to the dynamic studies that will involve tracking and modulating the regulatory mechanisms of the cell. The key instruments in these studies will be luminophores forming the nanoparticles with extremely long emission (milliseconds) that could allow exploring the time-resolved capability coupled with elementary cell signaling events. Dealing with the dynamic nature of living systems and new important steps for understanding the cell signaling and regulation will be essential for further progress.

13.8 Sensing and Thinking: Intellectual and Technical Means for Addressing the Systems of Great Complexity

The improved resolution, sensitivity, and versatility of fluorescence microscopy and the development of fluorescent targeting and labelling of proteins and nucleic acids in live cells, probing the membranes and organelles have yielded a clearer understanding of the dynamics of intracellular networks, signal transduction, and cell-to-cell interactions. New demands of portraying whole proteome, metabolome and interactome require new tools that can be applicable to the studies on cellular level.

Reaching an ultimate single-molecular sensitivity is the major achievement in recent years. In order to get maximal benefit of it, one has to understand the background of these methods that contain hidden tricks. Common wisdom tells us that better result could be obtained with the increase of number of fluorescence reporters and of the intensity of excitation source. Sometimes, it is not the case. Excessive number of reporters spoils resolution in super-resolution image and excessive light intensity depopulates the ground state that may only decrease the response and enhance photochemical damage. Compromise should be found in all these cases.

Analysis of presently observed tendencies allows suggesting that future progress will be connected with the following steps forward in methodology.

1. Dramatic increase of spatial resolution in microscopy down to tens of nanometers. Recent studies demonstrate that this can be achieved by several independent approaches, both in near-field and in far-field microscopy.
2. Extensive use of single-molecule methods adapted to cellular research. The complex milieu encountered inside live cells requires substantial adaptations of common *in vitro* techniques. This adaptation will proceed step-by-step together with progress in high-resolution microscopy.
3. Dramatic increase of brightness and photostability of fluorescence reporters to satisfy the demands of high-resolution microscopy and single-molecule detection. In this sense, organic fluorophores alone have probably reached the limit of their perfection, but nanocomposites with their participation promise a great future.
4. Solving the problem of incorporation into the cell of any desirable (nano)probe and attachment of fluorescent label (or even, sensor) to any cellular protein.

What remains is to explore these fascinating possibilities.

Questions and Problems

1. Explain the basic principles that are applied for eliminating the out-of-focus emission and the constructions of devices that operate based on these principles.
2. Can we obtain a sharp image of the nucleus of a typical human blood cell of diameter 10–15 μM with total internal reflection microscope?
3. Can we observe a sharp image of cellular membrane in confocal microscope?
4. Will the microscope that combines the principles of two-photon and confocal microscope be efficient?
5. Explain the advantages of time-resolved imaging.
6. How to make the light source smaller than the wavelength of light?
7. In the near-field scanning microscopy, is there a possibility to substitute the optical probe with a nano-size electrode to generate localized emission by using electrogenerated chemiluminescence (Sect. 10.1)?
8. What is the diffraction limit and how to overcome it in the wide-field microscopy?
9. Why the dye photobleaching depends on the presence of oxygen? Can the photobleaching be guided by the researcher? Is there a useful application of this phenomenon?
10. What is the reasonably achieved minimal volume for allowing the single-molecular detection? How it is compared with the volumes of typical cells?
11. What are the auto-correlation and cross-correlation? How they can be used to study intermolecular interactions?
12. What requirements are needed to observe for specific labeling of molecules inside the living cells by an externally applied dye? What controls have to be applied for proving the correct labeling?
13. Compare the sensors based on organic dyes and on nanoparticles in their advantages and disadvantages for cellular applications.
14. Can the luminescent nanoparticles be used inside the cell without optical excitation?

15. What is the mechanism of response of the sensor based on a 3-hydroxychromone dye to the changes of cellular membranes on apoptosis?
16. Can the molecular sensors developed for use in detection of Ca^{+2} ions inside the cells be used for detecting them in blood? In drinking water?
17. How to obtain the image of maltose distribution inside the cell?
18. Oxygen sensing in living cells, why it is important and what means can be applied to visualize its distribution in cells?

References

Acuna G, Grohmann D, Tinnefeld P (2014) Enhancing single-molecule fluorescence with nanophotonics. FEBS Lett 588(19):3547–3552

Adams SR, Harootunian AT, Buechler YJ, Taylor SS, Tsien RY (1991) Fluorescence ratio imaging of cyclic AMP in single cells. Nature 349(6311):694–697

Adams SR, Campbell RE, Gross LA, Martin BR, Walkup GK, Yao Y, Llopis J, Tsien RY (2002) New biarsenical Ligands and tetracysteine motifs for protein labeling in vitro and in vivo: synthesis and biological applications. J Am Chem Soc 124(21):6063–6076

Bagatolli LA (2006) To see or not to see: lateral organization of biological membranes and fluorescence microscopy. Biochim Biophys Acta 1758(10):1541–1556. doi:10.1016/j.bbamem.2006.05.019

Beatty KE, Liu JC, Xie F, Dieterich DC, Schuman EM, Wang Q, Tirrell DA (2006) Fluorescence visualization of newly synthesized proteins in mammalian cells. Angew Chem Int Ed Engl 45(44):7364–7367

Berezin MY, Achilefu S (2010) Fluorescence lifetime measurements and biological imaging. Chem Rev 110(5):2641–2684

Bergermann F, Alber L, Sahl SJ, Engelhardt J, Hell SW (2015) 2000-fold parallelized dual-color STED fluorescence nanoscopy. Opt Express 23(1):211–223

Blom H, Widengren J (2014) STED microscopy—towards broadened use and scope of applications. Curr Opin Chem Biol 20:127–133

Bullok KE, Gammon ST, Violini S, Prantner AM, Villalobos VM, Sharma V, Piwnica-Worms D (2006) Permeation peptide conjugates for in vivo molecular imaging applications. Mol Imaging 5(1):1–15

Buxbaum AR, Haimovich G, Singer RH (2015) In the right place at the right time: visualizing and understanding mRNA localization. Nat Rev Mol Cell Biol 16:95–109

Chang CJ, Jaworski J, Nolan EM, Sheng M, Lippard SJ (2004) A tautomeric zinc sensor for ratiometric fluorescence imaging: application to nitric oxide-induced release of intracellular zinc. Proc Natl Acad Sci U S A 101(5):1129–1134

Chang Y-R, Lee H-Y, Chen K, Chang C-C, Tsai D-S, Fu C-C, Lim T-S, Tzeng Y-K, Fang C-Y, Han C-C (2008) Mass production and dynamic imaging of fluorescent nanodiamonds. Nat Nanotechnol 3(5):284–288

Chen P, Zhou X, Andoy NM, Han K-S, Choudhary E, Zou N, Chen G, Shen H (2014) Spatiotemporal catalytic dynamics within single nanocatalysts revealed by single-molecule microscopy. Chem Soc Rev 43(4):1107–1117

Cheng ZL, Aspinwall CA (2006) Nanometre-sized molecular oxygen sensors prepared from polymer stabilized phospholipid vesicles. Analyst 131(2):236–243

Clarke SJ, Hollmann CA, Zhang ZJ, Suffern D, Bradforth SE, Dimitrijevic NM, Minarik WG, Nadeau JL (2006) Photophysics of dopamine-modified quantumdots and effects on biological systems. Nat Mater 5(5):409–417

Claydon TW, Fedida D (2007) Voltage clamp fluorimetry studies of mammalian voltage-gated K(+) channel gating. Biochem Soc Trans 35(Pt 5):1080–1082

Dahan M, Lévi S, Luccardini C, Rostaing P, Riveau B, Triller A (2003) Diffusion dynamics of glycine receptors revealed by single-quantum dot tracking. Science 302(5644):442–445
De Serio M, Zenobi R, Deckert V (2003) Looking at the nanoscale: scanning near-field optical microscopy. TrAC Trends Anal Chem 22(2):70–77
de Vries AH, Cook NP, Kramer S, Arndt-Jovin DJ, Jovin TM (2015) Generation 3 programmable array microscope (PAM) for high speed, large format optical sectioning in flourescence. Proc SPIE 9376:93760C. doi: 10.1117/12.2076390
Delehanty JB, Medintz IL, Pons T, Brunel FM, Dawson PE, Mattoussi H (2006) Self-assembled quantum dot-peptide bioconjugates for selective intracellular delivery. Bioconjug Chem 17(4):920–927
Delehanty JB, Susumu K, Manthe RL, Algar WR, Medintz IL (2012) Active cellular sensing with quantum dots: transitioning from research tool to reality; a review. Anal Chim Acta 750:63–81
Demchenko AP (2002) The red-edge effects: 30 years of exploration. Luminescence 17(1):19–42
Demchenko AP (2008) Site-selective Red-Edge effects. Chapter 4. Methods Enzymol 450:59–78
Demchenko AP (2010) The concept of lambda-ratiometry in fluorescence sensing and imaging. J Fluoresc 20(5):1099–1128
Demchenko AP (2013) Beyond annexin V: fluorescence response of cellular membranes to apoptosis. Cytotechnology 65(2):157–172. doi:10.1007/s10616-012-9481-y
Demchenko AP, Sytnik AI (1991a) Site-selectivity in excited-state reactions in solutions. J Phys Chem 95:10518–10524
Demchenko AP, Sytnik AI (1991b) Solvent reorganizational red-edge effect in intramolecular electron transfer. Proc Natl Acad Sci U S A 88(20):9311–9314
Demchenko AP, Mely Y, Duportail G, Klymchenko AS (2009) Monitoring biophysical properties of lipid membranes by environment-sensitive fluorescent probes. Biophys J 96(9): 3461–3470
Demchenko AP, Duportail G, Oncul S, Klymchenko AS, Mély Y (2015) Introduction to fluorescence probing of biological membranes. In: Methods in membrane lipids. Springer, New York, pp 19–43
Deniz AA, Mukhopadhyay S, Lemke EA (2008) Single-molecule biophysics: at the interface of biology, physics and chemistry. J R Soc Interface 5(18):15–45
Dickenson NE, Mooren OL, Erickson ES, Dunn RC (2014) Near-field scanning optical microscopy: a new tool for exploring structure and function in biology. In: Surface analysis and techniques in biology. Switzerland: Springer, p 225–253
Dietrich C, Bagatolli LA, Volovyk ZN, Thompson NL, Levi M, Jacobson K, Gratton E (2001) Lipid rafts reconstituted in model membranes. Biophys J 80(3):1417–1428
Dittrich P, Schwille P (2001) Photobleaching and stabilization of. fluorophores used for single-molecule analysis. with one-and two-photon excitation. Appl Phys B 73(8):829–837
Donnert G, Keller J, Medda R, Andrei MA, Rizzoli SO, Lurmann R, Jahn R, Eggeling C, Hell SW (2006) Macromolecular-scale resolution in biological fluorescence microscopy. Proc Natl Acad Sci U S A 103(31):11440–11445
Doose S, Heilemann M, Michalet X, Weiss S, Kapanidis AN (2007) Periodic acceptor excitation spectroscopy of single molecules. Eur Biophys J Biophys Lett 36(6):669–674
Du F, Min Y, Zeng F, Yu C, Wu S (2014) A targeted and FRET-based ratiometric fluorescent nanoprobe for imaging mitochondrial hydrogen peroxide in living cells. Small 10(5): 964–972
Fehr M, Frommer WB, Lalonde S (2002) Visualization of maltose uptake in living yeast cells by fluorescent nanosensors. Proc Natl Acad Sci U S A 99(15):9846–9851
Fisher JA, Barchi JR, Welle CG, Kim GH, Kosterin P, Obaid AL, Yodh AG, Contreras D, Salzberg BM (2008) Two-photon excitation of potentiometric probes enables optical recording of action potentials from Mammalian nerve terminals in situ. J Neurophysiol 99(3):1545–1553
Foquet M, Korlach J, Zipfel WR, Webb WW, Craighead HG (2004) Focal volume confinement by submicrometer-sized fluidic channels. Anal Chem 76(6):1618–1626
Fu AH, Gu WW, Boussert B, Koski K, Gerion D, Manna L, Le Gros M, Larabell CA, Alivisatos AP (2007) Semiconductor quantum rods as single molecule fluorescent biological labels. Nano Lett 7(1):179–182

Fürstenberg A, Heilemann M (2013) Single-molecule localization microscopy–near-molecular spatial resolution in light microscopy with photoswitchable fluorophores. Phys Chem Chem Phys 15(36):14919–14930

Gabe Y, Ueno T, Urano Y, Kojima H, Nagano T (2006) Tunable design strategy for fluorescence probes based on 4-substituted BODIPY chromophore: improvement of highly sensitive fluorescence probe for nitric oxide. Anal Bioanal Chem 386(3):621–626

Gai HW, Griess GA, Demeler B, Weintraub ST, Serwer P (2007) Routine fluorescence microscopy of single untethered protein molecules confined to a planar zone. J Microsc 226(3): 256–262

Gautier A, Juillerat A, Heinis C, Correa IR Jr, Kindermann M, Beaufils F, Johnsson K (2008) An engineered protein tag for multiprotein labeling in living cells. Chem Biol 15(2):128–136

Geigl JB, Uhrig S, Speicher MR (2006) Multiplex-fluorescence in situ hybridization for chromosome karyotyping. Nat Protoc 1(3):1172–1184

George N, Pick H, Vogel H, Johnsson N, Johnsson K (2004) Specific labeling of cell surface proteins with chemically diverse compounds. J Am Chem Soc 126(29):8896–8897

Ghosh S, Chizhik AM, Karedla N, Dekaliuk MO, Gregor I, Schuhmann H, Seibt M, Bodensiek K, Schaap IA, Schulz O, Demchenko AP, Enderlein J, Chizhik AI (2014) The photoluminescence of carbon nanodots: dipole emission centers and electron-phonon coupling. Nano Lett 14(10):5656–5661

Giepmans BNG, Adams SR, Ellisman MH, Tsien RY (2006) Review – the fluorescent toolbox for assessing protein location and function. Science 312(5771):217–224

Grecco HE, Lidke KA, Heintzmann R, Lidke DS, Spagnuolo C, Martinez OE, Jares-Erijman EA, Jovin TM (2004) Ensemble and single particle photophysical properties (two-photon excitation, anisotropy, FRET, lifetime, spectral conversion) of commercial quantum dots in solution and in live cells. Microsc Res Tech 65(4–5):169–179

Grichine A, Haefele A, Pascal S, Duperray A, Michel R, Andraud C, Maury O (2014) Millisecond lifetime imaging with a europium complex using a commercial confocal microscope under one or two-photon excitation. Chem Sci 5(9):3475–3485

Gross E, Bedlack RS, Loew LM (1994) Dual-wavelength ratiometric fluorescence measurement of the membrane dipole potential. Biophys J 67(1):208–216

Grotjohann T, Testa I, Leutenegger M, Bock H, Urban NT, Lavoie-Cardinal F, Willig KI, Eggeling C, Jakobs S, Hell SW (2011) Diffraction-unlimited all-optical imaging and writing with a photochromic GFP. Nature 478(7368):204–208

Grynkiewicz G, Poenie M, Tsien RY (1985) A new generation of Ca2+ indicators with greatly improved fluorescence properties. J Biol Chem 260(6):3440–3450

Guignet EG, Hovius R, Vogel H (2004) Reversible site-selective labeling of membrane proteins in live cells. Nat Biotechnol 22(4):440–444

Gust A, Zander A, Gietl A, Holzmeister P, Schulz S, Lalkens B, Tinnefeld P, Grohmann D (2014) A starting point for fluorescence-based single-molecule measurements in biomolecular research. Molecules 19(10):15824–15865

Ha T, Tinnefeld P (2012) Photophysics of fluorescence probes for single molecule biophysics and super-resolution imaging. Annu Rev Phys Chem 63:595–617

Hagen GM, Roess DA, de Leon GC, Barisas BG (2005) High probe intensity photobleaching measurement of lateral diffusion in cell membranes. J Fluoresc 15(6):873–882

Han Z-X, Zhang X-B, Li Z, Gong Y-J, Wu X-Y, Jin Z, He C-M, Jian L-X, Zhang J, Shen G-L (2010) Efficient fluorescence resonance energy transfer-based ratiometric fluorescent cellular imaging probe for Zn2+ using a rhodamine spirolactam as a trigger. Anal Chem 82(8):3108–3113

Hanley QS, Arndt-Jovin DJ, Jovin TM (2002) Spectrally resolved fluorescence lifetime imaging spectroscopy. Appl Spectrosc 56:155–156

Haugland RP (2005) The handbook. A guide to fluorescent probes and labeling technologies, 10th edn. Invitrogen corp, Eugene

Haustein E, Schwille P (2007) Fluorescence correlation spectroscopy: novel variations of an established technique. Annu Rev Biophys Biomol Struct 36:151–169

Heilemann M, van de Linde S, Mukherjee A, Sauer M (2009) Super-resolution imaging with small organic fluorophores. Angew Chem Int Ed 48(37):6903–6908
Hell SW (2007) Far-field optical nanoscopy. Science 316(5828):1153–1158
Hensel M, Klingauf J, Piehler J (2013) Imaging the invisible: resolving cellular microcompartments by superresolution microscopy techniques. Biol Chem 394(9):1097–1113
Hohlbein J, Gryte K, Heilemann M, Kapanidis AN (2010) Surfing on a new wave of single-molecule fluorescence methods. Phys Biol 7(3):031001
Huang B, Wu HK, Bhaya D, Grossman A, Granier S, Kobilka BK, Zare RN (2007) Counting low-copy number proteins in a single cell. Science 315(5808):81–84
Jaiswal JK, Goldman ER, Mattoussi H, Simon SM (2004) Use of quantum dots for live cell imaging. Nat Methods 1(1):73–78
Jameson DM, Ross JA (2010) Fluorescence polarization/anisotropy in diagnostics and imaging. Chem Rev 110(5):2685–2708
Keppler A, Gendreizig S, Gronemeyer T, Pick H, Vogel H, Johnsson K (2003) A general method for the covalent labeling of fusion proteins with small molecules in vivo. Nat Biotechnol 21(1):86–89
Kerppola TK (2008) Bimolecular fluorescence complementation (BiFC) analysis as a probe of protein interactions in living cells. Annu Rev Biophys 37:465–487
Klymchenko AS, Demchenko AP (2002) Electrochromic modulation of excited-state intramolecular proton transfer: the new principle in design of fluorescence sensors. J Am Chem Soc 124(41):12372–12379
Klymchenko AS, Duportail G, Mely Y, Demchenko AP (2003) Ultrasensitive two-color fluorescence probes for dipole potential in phospholipid membranes. Proc Natl Acad Sci U S A 100(20):11219–11224
Klymchenko AS, Stoeckel H, Takeda K, Mely Y (2006) Fluorescent probe based on intramolecular proton transfer for fast ratiometric measurement of cellular transmembrane potential. J Phys Chem B 110(27):13624–13632
Klymchenko AS, Oncul S, Didier P, Schaub E, Bagatolli L, Duportail G, Mely Y (2009) Visualization of lipid domains in giant unilamellar vesicles using an environment-sensitive membrane probe based on 3-hydroxyflavone. Biochim Biophys Acta 1788(2):495–499
Koeppel F, Jaiswal JK, Simon SM (2007) Quantum dot-based sensor for improved detection of apoptotic cells. Nanomedicine 2(1):71–78
Komatsu K, Urano Y, Kojima H, Nagano T (2007) Development of an iminocoumarin-based zinc sensor suitable for ratiometric fluorescence imaging of neuronal zinc. J Am Chem Soc 129(44):13447–13454
Kozankiewicz B, Orrit M (2014) Single-molecule photophysics, from cryogenic to ambient conditions. Chem Soc Rev 43(4):1029–1043
Krichevsky O, Bonnet G (2002) Fluorescence correlation spectroscopy: the technique and its applications. Rep Prog Phys 65(2):251–297
Kumar AT (2011) Fluorescence lifetime-based optical molecular imaging. In: Molecular imaging. Springer, p 165–180
Lakowicz JR (2006) Principles of fluorescence spectroscopy. Methods in Molecular Biology. Berlin-Heidelberg: Springer; 680:165–180
Larson DR, Zipfel WR, Williams RM, Clark SW, Bruchez MP, Wise FW, Webb WW (2003) Water-soluble quantum dots for multiphoton fluorescence imaging in vivo. Science 300(5624):1434–1436
Lereu A, Passian A, Dumas P (2012) Near field optical microscopy: a brief review. Int J Nanotechnol 9(3):488–501
Li Q, Liu L, Liu J-W, Jiang J-H, Yu R-Q, Chu X (2014) Nanomaterial-based fluorescent probes for live-cell imaging. TrAC Trends Anal Chem 58:130–144
Lidke DS, Nagy P, Heintzmann R, Arndt-Jovin DJ, Post JN, Grecco HE, Jares-Erijman EA, Jovin TM (2004) Quantum dot ligands provide new insights into erbB/HER receptor–mediated signal transduction. Nat Biotechnol 22(2):198–203

Lidke DS, Nagy P, Jovin TM, Arndt-Jovin DJ (2007) Biotin-ligand complexes with streptavidin quantum dots for in vivo cell labeling of membrane receptors. Methods Mol Biol 374: 69–79

Lim CS (2013) Invited mini review: two-photon probes for biomedical applications. Biochem Mol Biol Rep 46(4):188–194

Lin VS, Dickinson BC, Chang CJ (2012) Boronate-based fluorescent probes: imaging hydrogen peroxide in living systems. Methods Enzymol 526:19–43

Lukinavičius G, Johnsson K (2011) Switchable fluorophores for protein labeling in living cells. Curr Opin Chem Biol 15(6):768–774

Lukinavičius G, Umezawa K, Olivier N, Honigmann A, Yang G, Plass T, Mueller V, Reymond L, Corrêa IR Jr, Luo Z-G (2013) A near-infrared fluorophore for live-cell super-resolution microscopy of cellular proteins. Nat Chem 5(2):132–139

Ma ZY, Gerton JM, Wade LA, Quake SR (2006) Fluorescence near-field microscopy of DNA at sub-10 nm resolution. Phys Rev Lett 97(26):260801

Mank M, Reiff DF, Heim N, Friedrich MW, Borst A, Griesbeck O (2006) A FRET-based calcium biosensor with fast signal kinetics and high fluorescence change. Biophys J 90(5): 1790–1796

Marks KM, Nolan GP (2006) Chemical labeling strategies for cell biology. Nat Methods 3(8):591–596

Marriott G, Clegg RM, Arndt-Jovin DJ, Jovin TM (1991) Time resolved imaging microscopy. Phosphorescence and delayed fluorescence imaging. Biophys J 60(6):1374–1387

Martin BR, Giepmans BN, Adams SR, Tsien RY (2005) Mammalian cell-based optimization of the biarsenical-binding tetracysteine motif for improved fluorescence and affinity. Nat Biotechnol 23(10):1308–1314

Mattheakis LC, Dias JM, Choi YJ, Gong J, Bruchez MP, Liu J, Wang E (2004) Optical coding of mammalian cells using semiconductor quantum dots. Anal Biochem 327(2):200–208

Mauser N, Hartschuh A (2014) Tip-enhanced near-field optical microscopy. Chem Soc Rev 43(4):1248–1262

Meier RJ, Fischer LH, Wolfbeis OS, Schäferling M (2013) Referenced luminescent sensing and imaging with digital color cameras: a comparative study. Sens Actuators B 177:500–506

Miyawaki A (2003) Fluorescence imaging of physiological activity in complex systems using GFP-based probes. Curr Opin Neurobiol 13(5):591–596

Miyawaki A, Llopis J, Heim R, McCaffery JM, Adams JA, Ikura M, Tsien RY (1997) Fluorescent indicators for Ca2+ based on green fluorescent proteins and calmodulin. Nature 388(6645):882–887

Miyawaki A, Griesbeck O, Heim R, Tsien RY (1999) Dynamic and quantitative Ca2+ measurements using improved cameleons. Proc Natl Acad Sci U S A 96(5):2135–2140

Moerner WE (2007) New directions in single-molecule imaging and analysis. Proc Natl Acad Sci U S A 104(31):12596–12602

Moerner W (2012) Microscopy beyond the diffraction limit using actively controlled single molecules. J Microsc 246(3):213–220

Morozova KS, Piatkevich KD, Gould TJ, Zhang J, Bewersdorf J, Verkhusha VV (2010) Far-red fluorescent protein excitable with red lasers for flow cytometry and superresolution STED nanoscopy. Biophys J 99(2):L13–L15

Mukhopadhyay S, Deniz AA (2007) Fluorescence from diffusing single molecules illuminates biomolecular structure and dynamics. J Fluoresc 17(6):775–783

Murakoshi H, Iino R, Kobayashi T, Fujiwara T, Ohshima C, Yoshimura A, Kusumi A (2004) Single-molecule imaging analysis of Ras activation in living cells. Proc Natl Acad Sci U S A 101(19):7317–7322

Myong S, Rasnik I, Joo C, Lohman TM, Ha T (2005) Repetitive shuttling of a motor protein on DNA. Nature 437(7063):1321–1325

Ngo JT, Tirrell DA (2011) Noncanonical amino acids in the interrogation of cellular protein synthesis. Acc Chem Res 44(9):677–685

Ntziachristos V, Schellenberger EA, Ripoll J, Yessayan D, Graves E, Bogdanov A Jr, Josephson L, Weissleder R (2004) Visualization of antitumor treatment by means of fluorescence molecular tomography with an annexin V-Cy5.5 conjugate. Proc Natl Acad Sci U S A 101(33):12294–12299

Oheim M, van't Hoff M, Feltz A, Zamaleeva A, Mallet J-M, Collot M (2014) New red-fluorescent calcium indicators for optogenetics, photoactivation and multi-color imaging. Biochim Biophys Acta Mol Cell Res 1843(10):2284–2306

Oliver AE, Baker GA, Fugate RD, Tablin F, Crowe JH (2000) Effects of temperature on calcium-sensitive fluorescent probes. Biophys J 78(4):2116–2126

Oncul S, Klymchenko AS, Kucherak OA, Demchenko AP, Martin S, Dontenwill M, Arntz Y, Didier P, Duportail G, Mely Y (2010) Liquid ordered phase in cell membranes evidenced by a hydration-sensitive probe: effects of cholesterol depletion and apoptosis. Biochim Biophys Acta 1798(7):1436–1443

Orrit M, Ha T, Sandoghdar V (2014) Single-molecule optical spectroscopy. Chem Soc Rev 43(4):973–976

Owen DM, Magenau A, Williamson D, Gaus K (2012) The lipid raft hypothesis revisited–new insights on raft composition and function from super-resolution fluorescence microscopy. Bioessays 34(9):739–747

Peng X, Yang Z, Wang J, Fan J, He Y, Song F, Wang B, Sun S, Qu J, Qi J (2011) Fluorescence ratiometry and fluorescence lifetime imaging: using a single molecular sensor for dual mode imaging of cellular viscosity. J Am Chem Soc 133(17):6626–6635

Petrovsky A, Schellenberger E, Josephson L, Weissleder R, Bogdanov A Jr (2003) Near-infrared fluorescent imaging of tumor apoptosis. Cancer Res 63(8):1936–1942

Pinaud F, Dahan M (2011) Targeting and imaging single biomolecules in living cells by complementation-activated light microscopy with split-fluorescent proteins. Proc Natl Acad Sci 108(24):E201–E210

Pluth MD, Tomat E, Lippard SJ (2011) Biochemistry of mobile zinc and nitric oxide revealed by fluorescent sensors. Annu Rev Biochem 80:333–355

Puleo CM, Liu K, Wang TH (2006) Pushing miRNA quantification to the limits: high-throughput miRNA gene expression analysis using single-molecule detection. Nanomedicine 1(1):123–127

Rafalska-Metcalf IU, Janicki SM (2007) Show and tell: visualizing gene expression in living cells. J Cell Sci 120(14):2301–2307

Rajh T (2006) Bio-functionalized quantum dots: tinkering with cell machinery. Nat Mater 5(5):347–348

Rasmussen A, Deckert V (2005) New dimension in nano-imaging: breaking through the diffraction limit with scanning near-field optical microscopy. Anal Bioanal Chem 381(1):165–172

Rego EH, Shao L, Macklin JJ, Winoto L, Johansson GA, Kamps-Hughes N, Davidson MW, Gustafsson MG (2012) Nonlinear structured-illumination microscopy with a photoswitchable protein reveals cellular structures at 50-nm resolution. Proc Natl Acad Sci 109(3):E135–E143

Roberti MJ, Bertoncini CW, Klement R, Jares-Erijman EA, Jovin TM (2007) Fluorescence imaging of amyloid formation in living cells by a functional, tetracysteine-tagged alpha-synuclein. Nat Methods 4(4):345–351

Rogers KL, Stinnakre J, Agulhon C, Jublot D, Shorte SL, Kremer EJ, Brulet P (2005) Visualization of local Ca2+ dynamics with genetically encoded bioluminescent reporters. Eur J Neurosci 21(3):597–610

Sato M, Hida N, Umezawa Y (2005) Imaging the nanomolar range of nitric oxide with an amplifier-coupled fluorescent indicator in living cells. Proc Natl Acad Sci U S A 102(41):14515–14520

Sauer M (2003) Single-molecule-sensitive fluorescent sensors based on photoinduced intramolecular charge transfer. Angew Chem Int Ed Engl 42(16):1790–1793

Schäferling M (2012) The art of fluorescence imaging with chemical sensors. Angew Chem Int Ed 51(15):3532–3554

Scheenen WJ, Makings LR, Gross LR, Pozzan T, Tsien RY (1996) Photodegradation of indo-1 and its effect on apparent Ca2+ concentrations. Chem Biol 3(9):765–774

Seisenberger G, Ried MU, Endress T, Buning H, Hallek M, Brauchle C (2001) Real-time single-molecule imaging of the infection pathway of an adeno-associated virus. Science 294(5548):1929–1932

Shaner NC, Campbell RE, Steinbach PA, Giepmans BNG, Palmer AE, Tsien RY (2004) Improved monomeric red, orange and yellow fluorescent proteins derived from Discosoma sp red fluorescent protein. Nat Biotechnol 22(12):1567–1572

Sharonov A, Hochstrasser RM (2006) Wide-field subdiffraction imaging by accumulated binding of diffusing probes. Proc Natl Acad Sci U S A 103(50):18911–18916

Shav-Tal Y, Darzacq X, Shenoy SM, Fusco D, Janicki SM, Spector DL, Singer RH (2004) Dynamics of single mRNPs in nuclei of living cells. Science 304(5678):1797–1800

Shen J-Y, Chao W-C, Liu C, Pan H-A, Yang H-C, Chen C-L, Lan Y-K, Lin L-J, Wang J-S, Lu J-F (2013) Probing water micro-solvation in proteins by water catalysed proton-transfer tautomerism. Nat Commun 4:2611

Shynkar V (2005) Fluorescent ratiometric probes based on the 3-hydroxyflavone derivatives: photophysical properties and applications in cell biology. University of Louis Pasteur, Illkirch

Shynkar VV, Klymchenko AS, Duportail G, Demchenko AP, Mely Y (2005) Two-color fluorescent probes for imaging the dipole potential of cell plasma membranes. Biochim Biophys Acta 1712(2):128–136

Shynkar VV, Klymchenko AS, Kunzelmann C, Duportail G, Muller CD, Demchenko AP, Freyssinet JM, Mely Y (2007) Fluorescent biomembrane probe for ratiometric detection of apoptosis. J Am Chem Soc 129(7):2187–2193

Smith AM, Ruan G, Rhyner MN, Nie SM (2006) Engineering luminescent quantum dots for In vivo molecular and cellular imaging. Ann Biomed Eng 34(1):3–14

So MK, Xu CJ, Loening AM, Gambhir SS, Rao JH (2006) Self-illuminating quantum dot conjugates for in vivo imaging. Nat Biotechnol 24(3):339–343

Spagnuolo CC, Vermeij RJ, Jares-Erijman EA (2006) Improved photostable FRET-competent biarsenical-tetracysteine probes based on fluorinated fluoresceins. J Am Chem Soc 128(37):12040–12041

Stich MI, Fischer LH, Wolfbeis OS (2010) Multiple fluorescent chemical sensing and imaging. Chem Soc Rev 39(8):3102–3114

Straub M, Lodemann P, Holroyd P, Jahn R, Hell SW (2000) Live cell imaging by multifocal multiphoton microscopy. Eur J Cell Biol 79(10):726–734

Streets AM, Huang Y (2014) Microfluidics for biological measurements with single-molecule resolution. Curr Opin Biotechnol 25:69–77

Summerer D, Chen S, Wu N, Deiters A, Chin JW, Schultz PG (2006) A genetically encoded fluorescent amino acid. Proc Natl Acad Sci U S A 103(26):9785–9789

Tetin SY, Hazlett TL (2000) Optical spectroscopy in studies of antibody-hapten interactions. Methods 20(3):341–361

Thompson RB, Cramer ML, Bozym R (2002) Excitation ratiometric fluorescent biosensor for zinc ion at picomolar levels. J Biomed Opt 7(4):555–560

Tinnefeld P, Sauer M (2005) Branching out of single-molecule fluorescence spectroscopy: challenges for chemistry and influence on biology. Angew Chem Int Ed 44(18):2642–2671

Tomlinson ID, Warnerment MR, Mason JN, Vergne MJ, Hercules DM, Blakely RD, Rosenthal SJ (2007) Synthesis and characterization of a pegylated derivative of 3-(1,2,3,6-tetrahydropyridin-4yl)-1H-indole (IDT199): a high affinity SERT ligand for conjugation to quantum dots. Bioorg Med Chem Lett 17(20):5656–5660

Tsuchiya KD (2011) Fluorescence in situ hybridization. Clin Lab Med 31(4):525–542

Tsukube H, Yano K, Ishida A, Shinoda S (2007) Lanthanide complex strategy for detection and separation of histidine-tagged proteins. Chem Lett 36(4):554–555

van de Linde S, Löschberger A, Klein T, Heidbreder M, Wolter S, Heilemann M, Sauer M (2011) Direct stochastic optical reconstruction microscopy with standard fluorescent probes. Nat Protoc 6(7):991–1009

Voronin YM, Didenko IA, Chentsov YV (2006) Methods of fabricating and testing optical nanoprobes for near-field scanning optical microscopes. J Opt Technol 73(2):101–110
Vu TQ, Lam WY, Hatch EW, Lidke DS (2015) Quantum dots for quantitative imaging: from single molecules to tissue. Cell Tissue Res 360(1):71–86
Walkup GK, Imperiali B (1997) Fluorescent chemosensors for divalent zinc based on zinc finger domains. Enhanced oxidative stability, metal binding affinity, and structural and functional characterization. J Am Chem Soc 119(15):3443–3450
Wang Q, Moerner W (2012) Lifetime and spectrally resolved characterization of the photodynamics of single fluorophores in solution using the anti-brownian electrokinetic trap. J Phys Chem B 117(16):4641–4648
Wang Q, Goldsmith RH, Jiang Y, Bockenhauer SD, Moerner W (2012) Probing single biomolecules in solution using the anti-Brownian electrokinetic (ABEL) trap. Acc Chem Res 45(11):1955–1964
Wang S, Moffitt JR, Dempsey GT, Xie XS, Zhuang X (2014) Characterization and development of photoactivatable fluorescent proteins for single-molecule–based superresolution imaging. Proc Natl Acad Sci 111(23):8452–8457
Webb SED, Needham SR, Roberts SK, Martin-Fernandez ML (2006) Multidimensional single-molecule imaging in live cells using total-internal-reflection fluorescence microscopy. Opt Lett 31(14):2157–2159
Webster A, Coupland P, Houghton FD, Leese HJ, Aylott JW (2007) The delivery of PEBBLE nanosensors to measure the intracellular environment. Biochem Soc Trans 35:538–543
Westphal V, Lauterbach MA, Di Nicola A, Hell SW (2007) Dynamic far-field fluorescence nanoscopy. New J Phys 9(12):435
Willig KI, Harke B, Medda R, Hell SW (2007) STED microscopy with continuous wave beams. Nat Methods 4(11):915–918
Wurm CA, Kolmakov K, Göttfert F, Ta H, Bossi M, Schill H, Berning S, Jakobs S, Donnert G, Belov VN (2012) Novel red fluorophores with superior performance in STED microscopy. Opt Nanosc 1(1):1–7
Xie XS, Yu J, Yang WY (2006) Perspective – living cells as test tubes. Science 312(5771):228–230
Yang K, Yang Y, Zhang C-y (2014) Single-molecule FRET for ultrasensitive detection of biomolecules. NanoBioImaging 1(1):13–24
Yoshihara T, Yamaguchi Y, Hosaka M, Takeuchi T, Tobita S (2012) Ratiometric molecular sensor for monitoring oxygen levels in living cells. Angew Chem 124(17):4224–4227
Yu BZ, Ju YM, West L, Moussy Y, Moussy F (2007) An investigation of long-term performance of minimally invasive glucose biosensors. Diabetes Technol Ther 9(3):265–275
Zhang X, Xiao Y, Qi J, Qu J, Kim B, Yue X, Belfield KD (2013) Long-wavelength, photostable, two-photon excitable BODIPY fluorophores readily modifiable for molecular probes. J Org Chem 78(18):9153–9160

Chapter 14
Sensing the Whole Body and Clinical Diagnostics

In recent years, clinical diagnostics has made dramatic steps from exploring empirical correlations between the appearance and severity of disease and its visual or tested characteristic features towards their understanding on the basis of cell physiology. Many clinical tests that actively explore fluorescence techniques were developed. The so-called '*ex vivo*' diagnostics involves the microscopic studies of histological slices and extracted cells and also, on molecular level, the changes in metabolic biomarkers, the appearance of disease-specific biomarkers and the detection of pathology originated from mutations on molecular level (Fig. 14.1). The '*in vivo*' methods are more limited and involve the whole body tissue imaging and contrasting of blood vessels. Attempts are being made to develop efficient fluorescence tomography and to control by fluorescent imaging the surgical operations.

Fluorescence is the only method with high versatility that in target detection can combine *ex vivo* and *in vivo* studies. It offers the testing that is simple in performance, low invasive and applicable to point-of-care conditions. The progress in

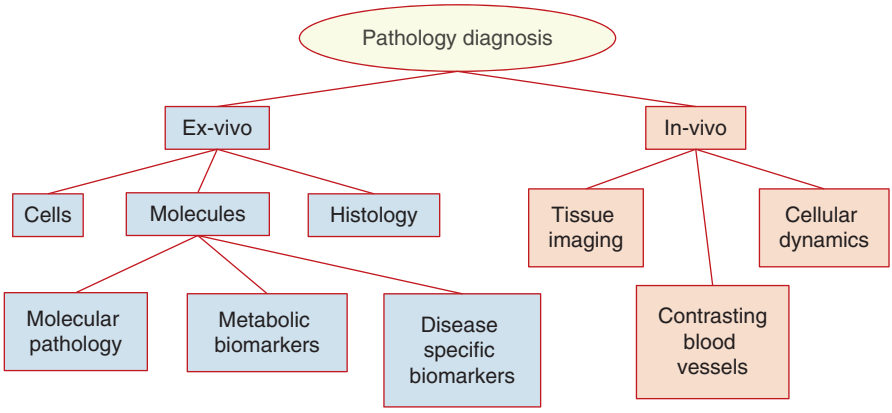

Fig. 14.1 Pathology diagnosis techniques, in which fluorescence is implied

A.P. Demchenko, *Introduction to Fluorescence Sensing*,
DOI 10.1007/978-3-319-20780-3_14

nanotechnology brings to biosensors the possibility for constructing the microarrays for high throughput parallel measurements of many analytes and for integration of biosensors with microfluidics into lab-on-a-chip devices. Moreover, a combination of disease diagnosis and treatment has become possible, which brought the appearance of a new field in research and development, the *theranostics*. Present Chapter focuses on these issues. It terminates with "Sensing and thinking" section on the strategy of controlling the diagnostics and treatment by light.

14.1 Ex-vivo Diagnostics

To make the diagnosis most precise, a number of *biomarkers* (the output parameters of diagnostic value) have to be analyzed in parallel, and therefore several channels of fluorescence response have to be activated on a cellular and tissue level. Novel biosensor technologies address cancer biomarkers, cardiac biomarkers as well as biomarkers for autoimmune disease, and also infectious diseases. Mutations are analyzed on the DNA level. These biomarkers can be produced either by the malignant tissues and cells themselves or by the body in response to the presence of disease. In disease the dramatic changes in concentration level of normal metabolites in blood (such as glucose in diabetes), the appearance of certain proteins in blood and urine (such as in inflammation or in kidney diseases), the DNA modifications and the changed levels of specific mRNAs can be observed. The most informative are the changes in cells, cell components and the appearance of specific proteins or change in their normal level that can be detected in patient's blood (Fig. 14.2). Of diagnostic value can be also saliva, tears and, of course, urine.

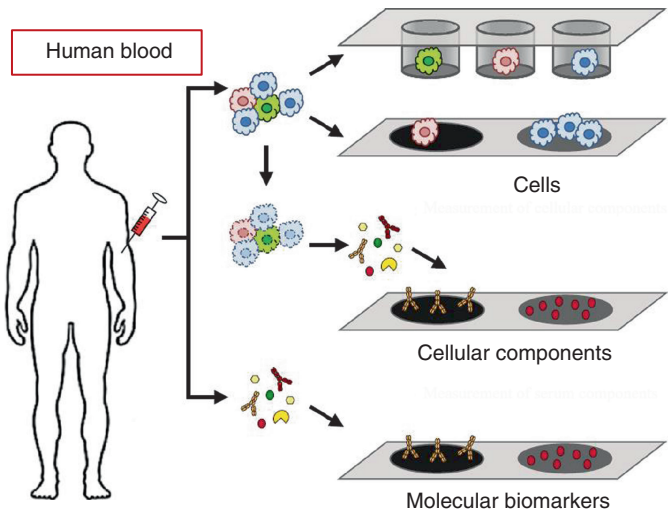

Fig. 14.2 Peripheral blood as the source of samples for clinical analysis (Herbáth et al. 2014). The white blood cells originate from the bone marrow, lymph nodes, spleen and other lymphoid tissues. The serum component of blood carries proteins from all over the body and some of them are of diagnostic value. The analysis includes screening of plasma membrane constituent of intact cells as well as measurement of cellular components after cell lysis or by using specific extraction methods

14.1.1 Diagnosis and Treatment of Diabetes

Dramatic increase and oscillation of *blood glucose* level in blood over its normal value of 3.3–5.5 mM is the characteristic feature of *diabetes*. Close monitoring of glucose is needed for diabetes patients, so that its increase requires immediate treatment. Many different methods were suggested for quantitative determining of glucose, and different glucose recognition units were suggested for that. They include small-molecular organic boronic acids, concanavalin A and bacterial periplasmic saccharide binding proteins, as well as glucose transforming enzymes (Steiner et al. 2011). Their choice dictates the application of reporting methods.

The majority of commercial self-test glucose measurement systems are now based on redox-couple-mediated enzymatic oxidation of glucose by either glucose oxidase or glucose dehydrogenase with electrochemical detection. Their application is not easy or reliable, since enzyme reactions depend on many uncontrolled factors and requires frequent calibration. It is hard to make an instrument with performance coupling continuously measured glucose level with desirable automatic administration of insulin when this level increases to critical values. The aim of producing such sensors is still not achieved despite the market that is estimated in tens of billions euros (Steiner et al. 2011; Vashist 2012). Such situation stimulates very tough competition between different technologies, one of which is the fluorescence.

Boronic acids readily form boronate complexes with sugars in water with increased affinity towards glucose that can be further increased in dimeric derivatives (see Fig. 14.3). The boronic acid group is an electron-deficient Lewis acid having an sp2-hybridized boron atom with a trigonal planar conformation. The anionic form of the boronic acid that is formed in the presence of glucose is characterized by a more electron-rich sp3-hybridized boron atom with a tetrahedral geometry (see also Sec. 7.2 and 12.3). The change in the electronic properties and the geometry at the boron atom induces the fluorescence spectral changes of the attached

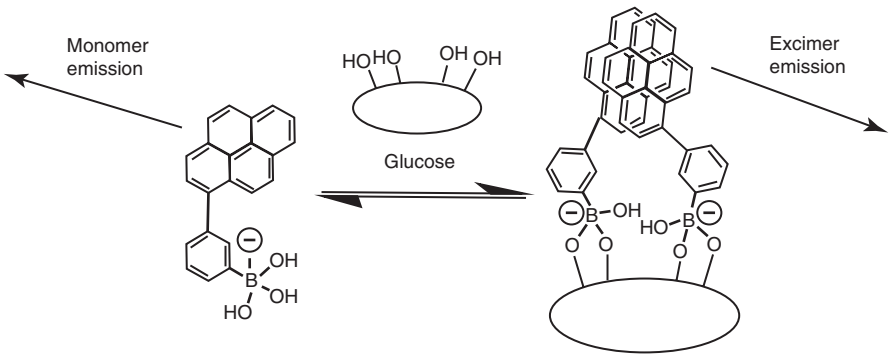

Fig. 14.3 Selective glucose sensing utilizing complexation with fluorescent boronic acid on polycation (Kanekiyo and Tao 2005). Excimer formation between attached pyrenes is used for reporting. Before addition of glucose: monomer emission. After addition of glucose: 1: 2 complex formation between glucose and fluorescent boronic acid in the presence of polycation poly(diallyl dimethylammonium) chloride results in excimer emission

aromatic groups. Upon addition of glucose the electron density on the boron atom is increased, facilitating the partial neutralization of the positively charged quaternary nitrogen of the quinolinium moiety.

But how can this property be used for measurements in human tissues? A very elegant solution was suggested on implanting glucose sensor protected by membrane from interference of blood cells and proteins. Since the increased glucose level can be also detected in tears, applying smart disposable and colorless *contact lenses* was suggested (Fig. 14.4). These contact lenses can be worn by diabetics patients who can see the changes in their contact lens color or other fluorescence-based properties, giving an indication of tear and blood glucose levels (Badugu et al. 2004).

The sensors using the *glucose binding proteins* can benefit from the property of these proteins to exhibit extended conformational changes on ligand binding (see Sect. 8.5). In this case the environment-sensitive fluorescence probes and the pairs of dyes with the modulation of FRET between them can be used for sensing (Pickup et al. 2013).

Urinary excretion of *human serum albumin* (HSA) can be used to diagnose not only incipient renal disease but also of type II diabetes, and its progression is one of the most studied clinical indices using biosensor devices. HSA is excreted in native form, in which it specifically binds a number of dyes, and simple and reliable methods of its identification and quantitative assay are based on this principle (Kessler et al. 1997; Harvey et al. 2001) avoiding the use of more expensive immunoassays.

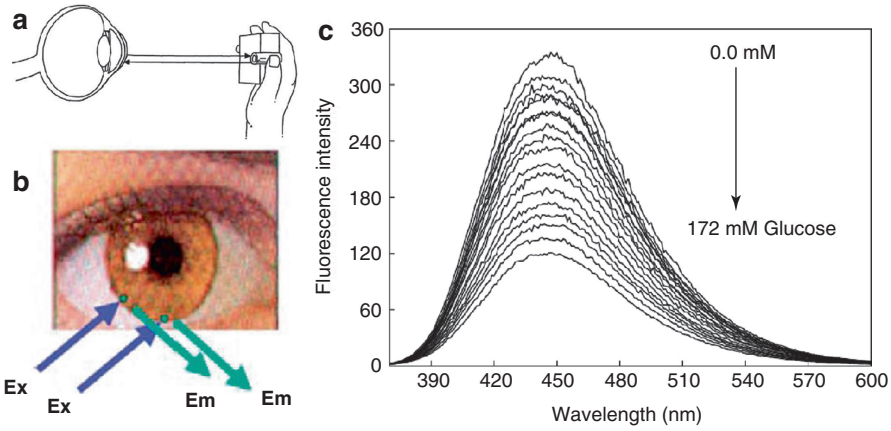

Fig. 14.4 The non-invasive tear-analyzing glucose sensor (Badugu et al. 2004). (**a**) Schematic of a device. The hand-held device works by flashing a light into the eye and measuring the emission intensity. (**b**) Contact lens doped with optical probe for glucose with sensor spots on the surface of the lens that allow providing the excitation (*Ex*) and monitoring the emission (*Em*). Other analytes, in addition to glucose, such as chloride or oxygen, can be measured, allowing for ratiometric, lifetime or polarization based fluorescent sensing. (**c**) Variation of fluorescence intensity as a function of glucose concentration

14.1.2 Diagnostics with Cardiac Biomarkers

Many current activities are directed towards the use of biosensors for achieving sensitive detection of cardiac biomarkers for early diagnosis of acute *myocardial infarction*. Identification of biomarkers provides a powerful approach for screening, diagnosis, prognosis and therapeutic monitoring especially in the emergency room, which is crucial to design an appropriate patient care strategy (Vasan 2006; Christenson et al. 2014). Addressing and improving the detection of early-stage disease permits early intervention with more efficient disease management and a significant reduction in premature mortality. This condition is associated with increase in the blood of several key protein-based biomarkers (Yang and Zhou 2006).

These markers indicate different features of *cardiac disease*. C-reactive protein reports on inflammation that is associated with cardiovascular damage, the D-dimer fragment of fibrinogen is the risk factor of thrombosis, troponin I and troponin T levels in blood indicate the damage of muscle cells. Therefore simultaneous measurement of several biomarkers not only reduces the errors but allows to characterize the disease in most detail (Wang et al. 2006). Of diagnostic value are lactate dehydrogenase1 (H4), aspartate aminotransferase and creatine phosphokinase (Batta et al. 2012).

It was noted however, that the use of current biomarkers that are determined in popular sandwich immunoassays improves standard assessment only moderately, even in a multiplexing approach. Therefore, there is an urgent need for technological advances that could allow not only to determine these *protein biomarkers* quantitatively above their background levels, but also to do this in a most rapid procedure to provide correct clinical decision timely. The progress must be associated with fluorophore-mediated multi-analyte sensing systems (Tang et al. 2006).

The problem is in extremely low concentration level of some of these biomarkers not only in norm but also in disease (in the pM ~ nM range) and the presence of other structurally similar proteins. The sandwich immunoassays are of sufficient sensitivity, but they are time-consuming, expensive and technically complicated. Therefore, they cannot satisfy practical medicine that needs rapid decisions. Direct and competitive assays (see Chap. 1) are still on initial steps of their development, but offer promise. The recently reported application of competitive anisotropy assay allowed achieving in the detection of human cardiac troponins I and T the limit of 15 pM concentration rapidly in homogeneous conditions (Qiao et al. 2011).

Myoglobin, while not cardiac specific, is one of the very early markers that increases its concentration in blood directly after an acute myocardial infarction and therefore it can be used as a suitable marker for rapid diagnosis using the new microwave-accelerated metal-enhanced fluorescence approach (Aslan and Geddes 2006). Presently it is developed for immunoassay and offers an ultra-rapid and sensitive platform.

Screening cholesterol, triglycerides, and other plasma lipids, indicating biomembrane damage, is also an important component in the management of cardiovascular disease. Stroke and diabetes are also linked to high cholesterol level, strengthening its importance as a diagnostic target. Meantime, express methods for its determination in blood are still lacking.

14.1.3 The Markers of Autoimmune Diseases

Autoimmune diseases are the disorders characterized by the presence of autoantibodies which bind the patient's own proteins, peptides or other structural compounds as target antigens. Serum autoantibodies accompany or even determine many diseases, such as cystemic sclerosis, they are biomarkers in early cancer detection (Tan et al. 2009). The understanding of their role in different pathologies, especially in the field of central nervous system disorders, has dramatically improved in recent years mainly due to novel methods of screening antigens with the aid of microarray techniques. Identification of antibodies directed against ion channels, receptors and other synaptic proteins helped in assigning their causative roles in different disorders.

Knowledge about immunological disorders is likely to be further expanded as more antibody targets are discovered. Therefore, protein microarrays may become an established tool for routine diagnostic procedures in the future. The identification of relevant target proteins requires the development of new strategies to handle and process the vast quantities of data so that these data can be evaluated and correlated with relevant clinical issues, such as disease progression, clinical manifestations and prognostic factors (Abel et al. 2014).

14.1.4 Diagnostics of Infectious Diseases

Infectious diseases are caused by *harmful microbes*, and their diagnosis follows three major trends: determining microbes themselves, determining the products of their harmful action to the bodies (*toxins*) and determining the specific antibodies raised in the body that struggle against the disease (Singh et al. 2014).

Most important in this analysis is the function of time. Traditional way of culturing microbes requires at least several hours but often more than a week, rendering it broadly inappropriate for getting response in urgent situations. In contrast, immunoassays and nucleic acid assays that still need sample manipulations and incubation times can be realized within an hour and the assays based on direct sensing can be realized in minutes. Rapid identification of the causative pathogen of a serious infection can save significant treatment cost, reduce

suffering, help stem the spread of disease, and save lives. Toxicity and infections caused by foodborne pathogens also represent an increasing public health problem.

Here the diagnostic tests in multiplex format are the only efficient solutions. In this situation, the front-line '*mix-and-read*' sensors that could allow determining multiple targets still did not occupy their proper position on the level of practical medicine (Clerc and Greub 2010).

The diagnostic devices suitable for pathogens involve specific *DNA and RNA detection*. However, most of them rely on PCR-based procedures that can only be used in hospitals and are still relatively complex and expensive. Integrating sample preparation with nucleic acid amplification and detection in a cost-effective, robust, and user-friendly format remains challenging. Recent technical advances in isothermal nucleic acid amplification methods might be able to overcome these limitations (Niemz et al. 2011).

Bioconjugated nanoparticle-based bioassays can detect a *single bacterium* within 20 min (Zhao et al. 2004). Identification of bacteria can be made with multicolored fluorescent silica nanoparticles conjugated with antibodies specific for pathogenic bacteria species (Wang et al. 2007). This approach eliminates completely the sample enrichment and amplification steps. The up-converting phosphor technology that uses rare-earth-doped ceramic (nano)particles (see Sect. 5.6), offers new step of improvement, providing more specific barcode pattern and minimizing background signal relative to conventional fluorescence labeling (Ouellette et al. 2009).

The strategy for the detection of *viruses* is somewhat different. Viruses are the sub-microscopic infectious agents that are able to reproduce themselves only inside a host cell. Their genetic material in the form of DNA or RNA or a protective coat made of proteins (called a capsid) can be used as targets for detecting viral infection. Meantime, the antibodies raised in the organism in response to this infection are often of most efficient diagnostic value. An example is the early detection of *human immunodeficiency virus* (HIV), which is an extremely important problem in all efforts to stop epidemic propagation of AIDS disease. Currently, the standard diagnostic tests for HIV infection are based on the *ELISA technique* for the detection of anti-viral antibodies. A great variety of synthetic and phage-displayed peptides have been presently collected as test antigens (Palacios-Rodriguez et al. 2007), so what remains is to develop simpler methods that could be equal or superior in precision.

Peptide beacons have started to be used for the detection of anti-HIV antibodies (Oh et al. 2007). These peptides contain the sequence recognized by the antibodies and adopt different conformations in the free and antibody-bound forms, which influences the effect of bound quencher on the fluorescence of dye bound in a different position in peptide sequence. The application of time-resolved detection of Eu^{3+}-doped luminescence nanoparticles was shown to improve dramatically the sensitivity of adenovirus detection (Valanne et al. 2005).

14.1.5 Diagnostics of Cancer

Early diagnosis of cancer is an urgently needed strategy to reduce the incidence of the disease and improve significantly the survival rate. Still now, the commonly used cancer diagnostic and prognostic indicators are the morphological and histological characteristics of tumors. Meantime, *biomarkers* have started to play their important role as molecular signatures of the disease. They can be of two types: *metabolic* and specific *protein-based*. Differential metabolic profile between cancerous cells and normal cells was observed in many types of cancer cells, resulting in discovery of metabolic biomarkers specific to cancerous cells and, most importantly, to different cancer types. As an example, the metabolic biomarkers indicating prostate cancer are citrate and spermine (Giskeødegård et al. 2013).

Single specific protein biomarkers, such as *prostate specific antigen* (PSA) have already found their use in practice. Meantime, since tumor development involves many biological changes, the signatures of this disease can be very complex and characteristic for particular type of tumor (McShane et al. 2005; Jain 2007). Therefore, multiple targets have to be determined simultaneously. Proteomics approaches based on comparative detection of increased levels of several among many thousands proteins have been used to generate differential protein expression maps of the normal cells. They can be compared to that of cancer cells with the detection of proteins, whose levels change significantly (Kuramitsu and Nakamura 2006). The microarrays with fluorescence readout (Zajac et al. 2007) and microfluidic devices (Kartalov et al. 2006) must be of efficient use for their detection.

14.1.6 Kidney and Liver Related Diseases

In *kidney-related diseases*, urine is a potential source for biomarkers to be analyzed. Recently, it has been shown that the identification of *urinary polypeptides* as biomarkers of kidney-related diseases allows to diagnose the severity of the disease several months before the manifestation of pathology (Devarajan 2007). Also, the rate of urinary excretion of human *serum albumin* (HSA) can be used to diagnose incipient renal disease, as well as type II diabetes (see above). In competition between HSA-specific immunoassays and sensing based on specific binding of fluorescence dyes the latter demonstrate many advantages.

In addition to specific peptide and protein biomarkers, *metabolic biomarkers*, such as creatinine, ammonia and urea are also of diagnostic value. Creatinine, a byproduct of kidney function, is produced at an almost constant rate in healthy individuals; its level is diagnostic for defective renal function through estimation of the glomerular filtration rate (Shephard et al. 2010). Renal dysfunction, liver disease, and asthma can often be detected through the measurement of urea and ammonia levels. Breath analysis becomes a new field of diagnostic medicine (Wang and Sahay 2009).

An optical array biosensor for simultaneous measurement of markers for *renal disease* (urea, creatinine, uric acid, glucose) was produced by immobilizing the appropriate enzymes and fluorescent dyes in a sol–gel matrix. For urea and creatinine, actions of the hydrolase enzymes urease and creatinine deiminase produced hydroxide ions, which were detected via an immobilized pH-sensitive fluorescent indicator. For glucose and uric acid, actions of the oxidase enzymes glucose oxidase and uricase produced hydrogen peroxide, which was consumed by co-immobilized horseradish peroxidase to give a fluorescent signal at 590 nm as a result of reduction of Amplex red to resorufin. Measurement of analytes in serum was in good agreement with traditional laboratory methods (Tsai and Doong 2004).

14.1.7 Prospects of Ex-vivo Clinical Diagnostics Technologies

One of the key aims for the future development is achieving the point-of-care settings in clinical analyses without laboratory support. In this case, the impact of biosensor technology will be the greatest. The diabetes patients, the patients in critical conditions in rural locations and the population under the risk of infectious diseases in developing countries have to get the greatest benefit from these developments. It is expected that quantitative performance metrics of these biosensor devices will soon become comparable to laboratory methods with the advantages of convenience, low cost and high speed.

Addressing this aim, we observe that the progress is unexpectedly slow. Essentially, the limiting factors are not in instrumentation, which is quite sufficient to support current developments. Major progress is expected from substituting the procedures requiring manipulation steps with the sample (reagent addition, washing, temperature cycling) by direct '*mix-and-read*' tests. Since these steps are unavoidable for amplification of output signal (generating the chromogenic or fluorescent product, as in ELISA, or increasing the copies of target molecules, as in PCR) we have to avoid such amplification by increasing dramatically the efficiency of fluorescence (luminescence) reporting. Possibilities for that exist, as can be seen in other chapters in this book. They are in using novel materials and forming their nanocomposites, in optimizing the photophysical mechanisms of their response.

The other direction of future progress is in making our tests non-invasive or low-invasive for the patient. The most common clinical diagnostic application will continue to be blood protein analysis. Blood in systemic circulation reflects the state of health or disease of most organs providing a sensitive assessment of health and disease. The use of urine as the traditional test material will continue. Meantime, dramatic decrease of sample volume and use of fluids that are easily collected, but in which the target concentrations can be very small (e.g. saliva or tears) should be a promising alternative if it will be accompanied by strong increase of sensitivity.

The third direction that determines the progress is the multiplicity of analyzed data attributed to particular person. Parallel sensing of many targets including spe-

cific and metabolite biomarkers should be analyzed with algorithms clearly understood to doctors making clinical decisions. Only on this condition, the attempts of establishing *personalized medicine* will make sense.

14.2 Sensing the Whole Body

In this Section we have to find answers to a number of important questions regarding the fluorescence imaging and sensing on the level of the whole body. Will this sensing have a prospect in application to humans addressing the needs of clinical diagnostics and treatment? What are the technological challenges here and the possibilities for their solution? Here we address the problems related to the technologies of introducing the imaging agents and sensors and to producing the informative reporter signal.

14.2.1 On the Optical Properties of Human Body

It should be primarily stated that the human body is highly protected to penetration of UV and visible light. This is because of the presence in our tissues of many pigments. The most important of them is the skin pigment melanin that absorbs light in the whole visible range down to about 800 nm and the porphyrins that are prosthetic groups of hemoglobin and myoglobin that possess strong absorption bands in the visible. The light scattering and autofluorescence also decreases with the increase of wavelength. On the other side, in the near-IR, starting from 1100 to 1200 nm, there appears a strong light absorption due to collective vibrations of water molecules, so this range also becomes opaque in living systems. Therefore, there only remains a *window of relative transparency* between ~700 and 900 nm, in which the energy of light quanta is already too high to excite vibrations but still insufficient for exciting the electronic transitions of intrinsic light absorbers (Fig. 14.5).

Why the transparency is ‘relative’? Because the cells and tissues possess many structures (e.g. cell nuclei and mitochondria), the sizes and refractive index gradients of which lead to efficient *light-scattering* (Ntziachristos 2006). These light-scattering effects are not as large as in the UV or visible region, but still they produce strong problems in sensing and imaging. Both incident and luminescent light can be scattered. The light scattering occurs at different angles, and with the necessary presence of multiple scattering, the photon direction may become randomized. Substantial improvement of tissue imaging can be achieved by injection under the skin of immersing liquid reducing the refractive index gradients, e.g. glycerol. But it is hard to apply this technique on a general scale to human patients.

Regarding strong absorbance of incident light, the only possibility to treat this problem beside the choice of proper wavelength is to insert into the studied system the ‘self-illuminating’ nanocomposites, as it is described in Sect. 10.3.

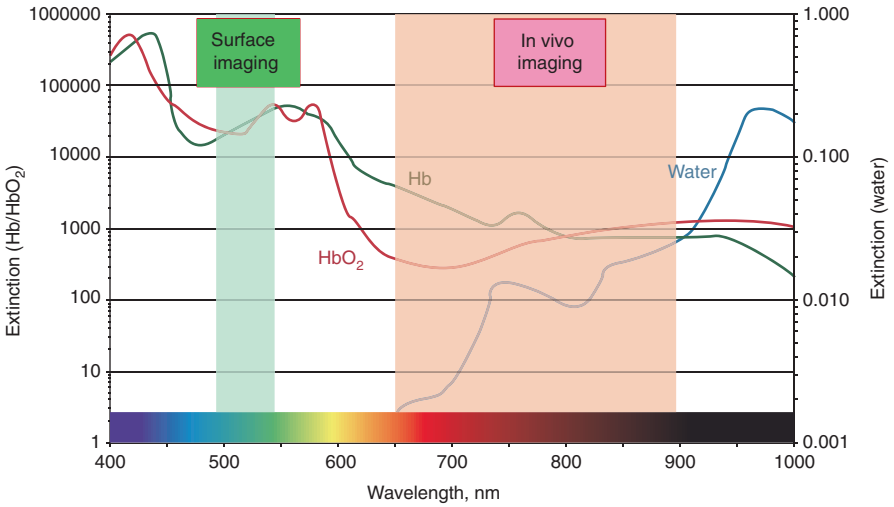

Fig. 14.5 Extinction coefficients (on logarithmic scale) of water, oxy- and deoxy-hemoglobin in the range from visible to near-IR wavelengths

14.2.2 Optimal Imaging Techniques

There are several modes of collecting the images (Fig. 14.6). *Planar near-IR imaging* methods that explore epi- and trans- illumination have the advantage that they require relatively inexpensive instrumentation, are easy to operate and facilitate high-throughput imaging of animals. However, they have some limitations. The detected fluorescence emission depends linearly on the fluorophore concentration

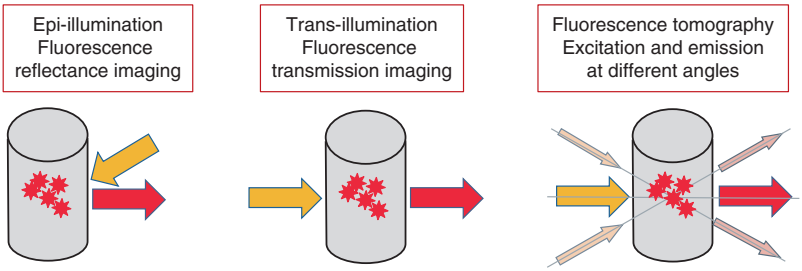

Fig. 14.6 Modes of data acquisition in near-IR fluorescence imaging. The excitation light is applied and the fluorescence emission is collected from the same side of the object (epi illumination). In trans illumination the excitation has to travel through the object before it gets collected by the detector on the opposite site of the object. In the tomography mode the object is sequentially illuminated at different locations. The fluorescence emission is collected by the detector and a three-dimensional image is reconstructed

and nonlinearly on the depth of the fluorescent object and the optical properties of the surrounding tissue. As a consequence, such images do not allow for absolute quantification of the detected fluorescence. Hence, in most studies the fluorescence emission is expressed in terms of a contrast, i.e., as a ratio of the fluorescence intensity measured over the disease-affected region to the intensity of measured over a nonaffected region, termed target-to-background ratio.

In fluorescence *reflectance imaging*, the excitation light propagates a few millimeters below the surface and the fluorescence is collected from the same side of the object and is detected using a CCD camera. In *trans-illumination* fluorescence imaging, the excitation light source and the detector are on opposite sides. The advantage is that the entire volume of the object is sampled upon the passage of the excitation light.

Photon propagation in tissue can be modeled by stochastic methods which consider the probability of photon scatter, scattering angle, and absorption for each incremental step of the photon path. Quantitative analysis of fluorescence emission can be achieved using fluorescence molecular tomography (Ntziachristos 2006). Here the excitation light is coupled sequentially to the object at different locations, while the position of the detector array is fixed (see Fig. 14.6).

Recording multiple projections yields a sufficient number of source–detector pair combinations for constructing a synthetic measurement and to apply to an inversion code for three-dimensional reconstruction of the fluorophore distribution (Hielscher 2005). The reconstruction leads also to an improved image resolution of the order of 1 mm in all three dimensions as compared to planar techniques, where image resolution is about 2–3 mm with no information on depth.

Fluorescence molecular tomography has found increasing applications in small animal imaging. It can be applied with time resolution that allows providing a superior dataset for accurate functional imaging and offers the potential to separate multiple reporters based on lifetime contrast (Kumar et al. 2008).

14.2.3 Fluorescence Contrast Agents and Reporters

Fluorescence studies on the level of whole living body are always aimed at obtaining information on particular cells or tissues. Therefore, dilution of fluorescence labels or sensors over the whole body that decrease dramatically the readout signal have to be diminished. There are two possibilities for that – to achieve addressable binding of sensors to the chosen sites or to label the cells *ex vivo* and then incorporate them into the body.

There is a choice of fluorophores for imaging and reporting absorbing and emitting light in the near-IR region. The *near-IR organic dye* molecules are composed

of several conjugated aromatic heterocycles or a long polymethine chain (Zaheer et al. 2002). These dyes can attain important functional properties. They can be used for targeted fluorescence imaging of bacterial infection in a living whole animal (Leevy et al. 2006). The near-IR probe was found that has a strong and selective affinity for the surfaces of bacteria, and after intravenous injection, it selectively accumulates at the sites of localized bacterial infections. Also, anticancer antibodies conjugated with near-IR dyes like Cy7 could be administrated *in vivo* and their accumulation in site of tumor growth could be visualized using the whole-body fluorescence imaging (Zou et al. 2009).

Organic dyes demonstrate two important advantages over other luminescence emitters that can be used on tissue and body levels. They can be responsive by parameters of their emission to their medium conditions and to the binding to particular targets and also they can be easily modified with moieties providing target recognition. In Fig. 14.7 the application of such of these dyes is illustrated for the imaging of tumor and its metastases. A pH-sensitive cyanine dye was coupled with cyclic Arg-Gly-Asp peptide targeting αvβ3 integrin (ABIR), a protein that is highly overexpressed in endothelial cells during tumor angiogenesis. The dye has negligible fluorescence above pH 6 but becomes highly fluorescent below pH 5, which is ideal for imaging acidic cell organelles such as tumor lysosomes or late endosomes. A fluorescence enhanced locus visualizing the tumor becomes evident within 4 h post injection (Lee et al. 2011).

Nanocomposites based on *dye-doped silica* nanoparticles are interesting in different aspects (Biffi et al. 2014). They can be doped with a multitude of dyes with broad selection of different colors and particle recognition possibilities.

Very efficient is the application of semiconductor *quantum dots* (see Sect. 5.5). Those of them that absorb light in the near-IR can be applied in the conditions of either single-photon or two-photon excitation. A variety of such nanoparticles exist, for instance, those composed of a cadmium-tellurium core with a cadmium-selenium shell. In both conditions of single-photon or two-photon excitation, the quantum dots have the brightness 100–1000 times higher than that of typical organic dyes, and the long-wavelength excitation conditions still further decrease the possibility of photobleaching and photodamage. Upon excitation with two photons in the near-IR they can serve not only as reporters but also as sensitizers providing photodynamic properties to excited-state energy acceptors (Dayal and Burda 2008). Whereas many results are reported on application of these quantum dots in the studies of animal models, their potential toxicity restricts administration to humans.

As luminescent probes for molecular imaging, lanthanide-doped *up-conversion* nanoparticles (see Sect. 5.6) exhibit superior performance compared to many other luminophores (Zhang et al. 2013). They demonstrate high tissue penetration depth together with minimized autofluorescence and photobleaching. The core-shell

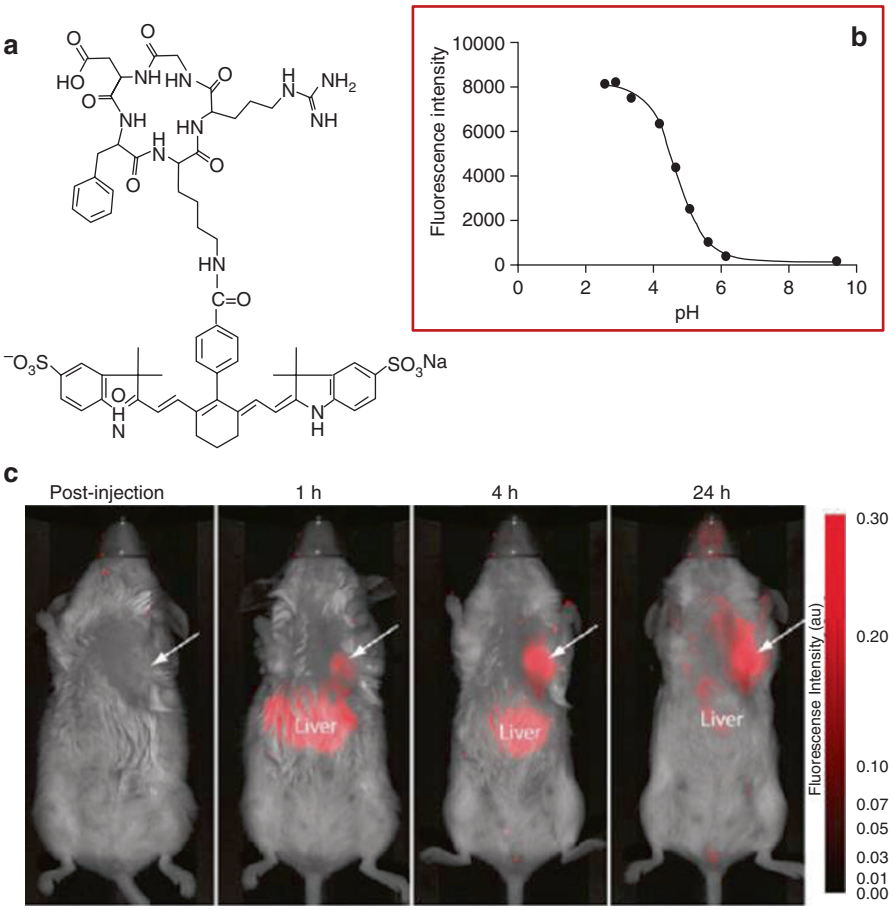

Fig. 14.7 Tumor imaging with conjugate of pH-sensitive cyanine dye coupled with tumor-recognizing cyclic peptide (Lee et al. 2011). (**a**) The conjugate structure. The reversible pH-sensitivity arises from the protonation-deprotonation of indolium nitrogen atom. (**b**) The pH dependence of fluorescence intensity at 795 nm. (**c**) Fluorescence images in orthotopic 4 T1/*luc* tumor-bearing mice at various time points. Fluorescence intensity in the tumor region (*arrow*) increased with time relative to non-tumor areas, reaching a plateau by 24 h

nanocomposites made with these particles make them particularly advantageous for imaging analysis. Lanthanide-based nanoprobes are unique combining rich optical, magnetic, radioactive, and X-ray attenuation properties. Combining them in the form of NaLuF4:Yb,Tm core and 153Sm3þ-doped NaGdF4 as the shell, the particles were developed for optimized multimodal imaging. The results of their application as the long-lifetime up-converting probes are seen in Fig. 14.8 (Sun et al. 2013).

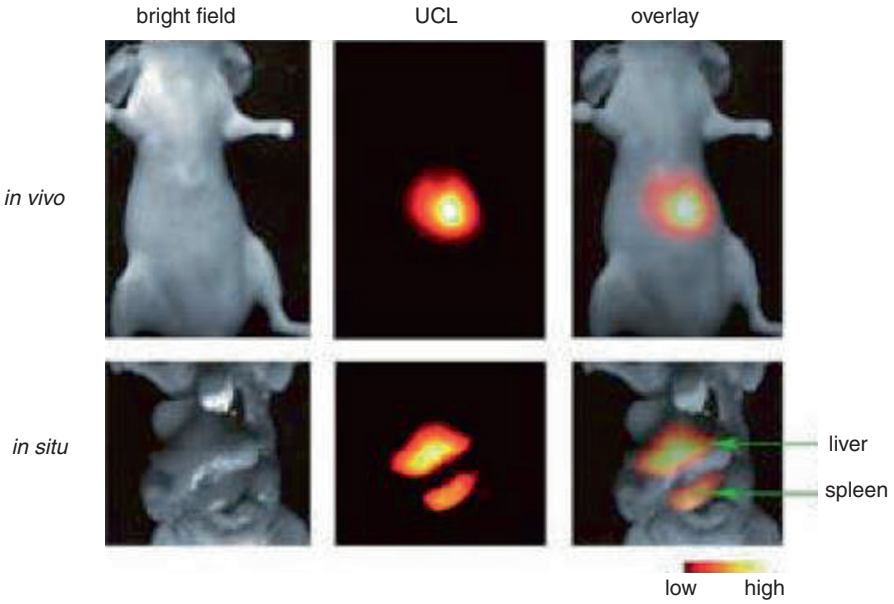

Fig. 14.8 The up-conversion images ($\lambda_{ex} = 980$ nm, $\lambda_{em} = 800$ nm) of the nude mice after intravenous injection of NaLuF4:Yb, Tm@NaGdF4(153Sm) core-shell nanocomposites displaying different imaging modalities (Sun et al. 2013)

14.2.4 Imaging Cancer Tissues

The most important field of application of fluorescence tracers are in the detection, imaging and control on treatment of cancer tissues (Sharrna et al. 2006; Gao and Dave 2007). The ability of *quantum dots* to target tumor vasculature was impressively demonstrated in experiments on mice (Akerman et al. 2002). Being conjugated to several peptides that differentially recognized blood vessels located in the lung, tumor blood vessels and tumor lymphatic vessels, these nanoparticles were injected into mice. Guided by these peptides, the nanoparticles were delivered to the appropriate sites *in vivo* allowing to visualize and to characterize the tumor.

Targeting and imaging the cancer tissue *in vivo* can be also provided using quantum dots in conjugation with antibodies (Gao et al. 2004) as it was shown with antibody specific for the prostate cancer cell marker. After injection into mice that contained transplanted prostate cancer, the nanoparticle-tagged antibodies recognized the tumor site that allowed observing clearly its image *in vivo*.

The progression of cancer often involves the development of metastasis. It was shown (Voura et al. 2004) that metastatic cells can be identified *in vivo* by using the two-photon response of functional QDs. No toxicity of QDs have been detected, and spectral imaging allowed the simultaneous identification of five different populations of cells.

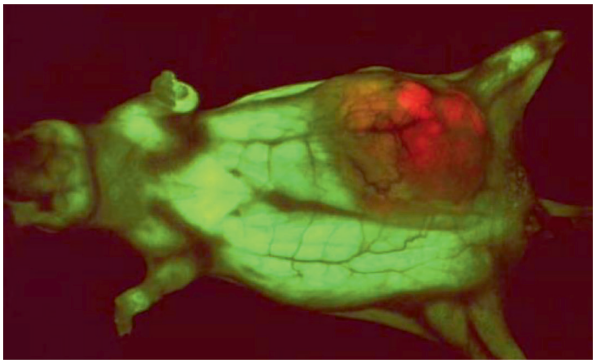

Fig. 14.9 Whole-body image of orthotopically growing HCT 116-RFP human colon cancer in GFP nude mouse (Yang et al. 2003). Image was acquired in a fluorescence light box with a CCD camera 10 weeks after orthotopic implantation of HCT116-RFP cells. The host and the tumor were labeled with fluorescent proteins producing different color of fluorescence emission, which enables the interaction between the cancer cells and the host cells to be visualized in real time

The advantage of QDs is obviously evidenced in comparison with *fluorescent proteins*, the often insufficient brightness of which makes difficult obtaining the image recognizable from the background. However, proper manipulation with GFP and its analogs allows obtaining images after genetic incorporation of these proteins labeling both the tumor and the whole body, in different colors. In an example presented in Fig. 14.9 the cells of the host body were genetically labeled with GFP and the tumor tissue with another fluorescent protein producing red color (Yang et al. 2003). On such models it is easy to follow the development of disease, formation of metastases, interaction of tumor with normal cells and blood vessels and also the efficiency of different anti-cancer treatments.

Fluorescent proteins, as well as organic fluorophores possess a different advantage: they can report not only on tumor size and location, but also on biochemical processes occurring inside the tumor and thus extending the deeper understanding of its formation. The data on change in pH, hypoxia, free radicals, enzyme activities and other important parameters of cell life can be obtained *in vivo* (Wu et al. 2013).

The *decrease of pH* in intercellular medium of cancer tissue that becomes slightly acidic (pH 6.2–6.9), in contrast to that in normal tissues (pH 7.4), can be traced with fluorescent dyes. Much stronger changes occur inside the cells, and that allows very good contrast in imaging (see Fig. 14.7). In addition to small molecular probes, the nanocomposites that fluoresce in the acidic tumor microenvironment but not in normal tissues were developed (Wang and Li 2011).

14.2.5 Monitoring the Response to Therapy

Accurate monitoring of the *response to therapy* is essential to progress novel therapeutics to the clinic. In many diseases these responses are extremely complex and diverse. Fluorescence imaging facilitates their monitoring suggesting the techniques

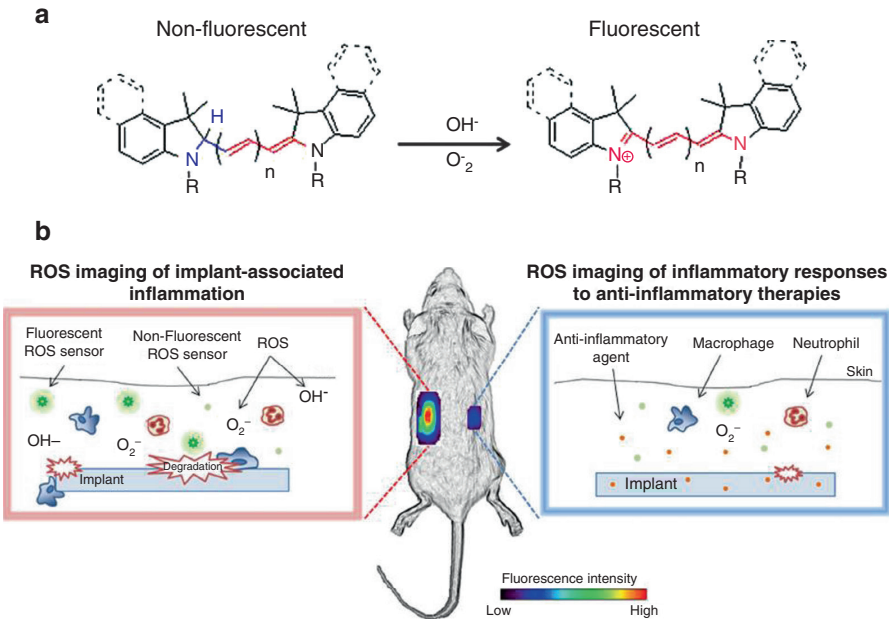

Fig. 14.10 Near-IR fluorescence imaging of reactive oxygen species (ROS) as a surrogate measure for monitoring implant-associated inflammation (Selvam et al. 2011). (**a**) Superoxide or hydroxyl radicals oxidize the hydrocyanines into fluorescent cyanine dyes, which can be detected *in vivo* by fluorescent imaging. (**b**) ROS released by inflammatory cells in response to implanted biomaterials can be detected and monitored using these dyes delivered either locally or intravenously in living mice (*left panel*). Attenuation of inflammatory development in response to controlled release of anti-inflammatory agents can also be detected using this sensitive imaging approach (*right panel*)

that allow multichannel imaging in different colors. Such possibilities are not limited to cancer treatment. Different implants can produce *inflammation* that can be studied via fluorescence imaging using near-IR dyes delivered either locally or intravenously in the body. Important parameter in this case is the level of reactive oxygen species released by inflammatory cells (Fig. 14.10).

The evaluation of efficacy of therapeutic approaches to reduce the host inflammatory responses to implanted medical devices can be performed using proper imaging technique. In the same way the body response to tissue transplantation can be monitored.

14.2.6 Contrasting the Blood Vessels and Lymph Nodes

Safe and non-invasive fluorescence tracers are needed to contrast the blood and lymph systems. *Indocyanine Green* is a very special dye addressing this need (Fig. 14.11). The absorption and fluorescence spectra of this tricarbocyanine dye fit the near-IR window of high relative transparency (see Fig. 14.5). Its fluorescence emission with a

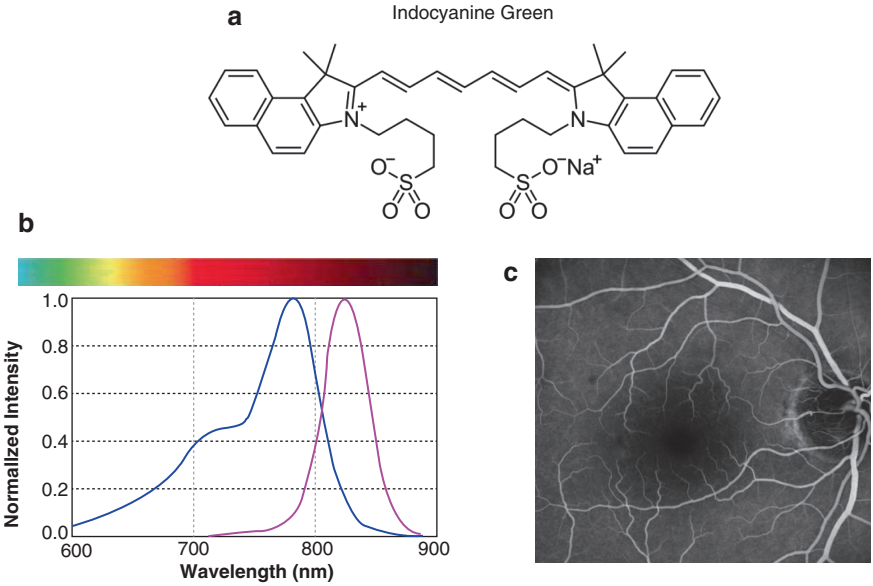

Fig. 14.11 Indocyanine Green (**a**) and its absorption and emission spectra (**b**). Typical image of contrasted eye blood vessels (**c**)

maximum at 830 nm allows minimizing the re-absorption and light-scattering effects in tissues. Being injected into blood vessel it is well tolerated by human body and demonstrates very rapid clearance, on a scale of several minutes. It is considered to be one of the least toxic agents ever administered to humans. Being amphiphilic with one positive and two negative charges and extended hydrophobic part, it binds with serum proteins and in this form distributes throughout the body.

Indocyanine Green is serving in clinics for visualizing the *blood vessels* already for more than 50 years (Frangioni 2003). Many researchers report on improvement of dye performance on its modification and incorporation into nanoparticles, especially if its prolonged circulation is needed (Rajagopalan et al. 2000). The dyes of this type are presently used to image heart vasculature and the myocardial perfusion. The near-IR fluorescence imaging (*fluorescent angiography*) is used in the common practice of ophthalmology clinics. With the aid of confocal microscope this allows not only to study blood microcirculation in detail but also to predict the appearance of small melanomas (Mueller et al. 2002).

In an attempt of improving the optical properties a variety of dyes were suggested including those with high two-photon absorption cross-section (Helmchen and Denk 2005). Coupling of cyanine dyes with molecules providing target recognition allows resolving different pathological states, including *thrombus formation* and *angiogenesis* (Klohs and Rudin 2011).

Despite many experimental studies, introduction of fluorescent nanoparticles into whole-body clinical diagnostics is slow (Choi and Frangioni 2010). This is because many fundamental questions remain unresolved. It is not clearly known,

how these particles enter the body, how they are taken up by the cell, how they are distributed and eliminated in the body, and how they influence human health. In the Section on theranostics we will discuss these issues in more detail.

14.2.7 Fluorescence Image Guided Surgery

The main goal of cancer surgery is the complete excision of tumors with adequate tumor-free margins while minimizing surgical morbidity. In the present common practice an intraoperative assessment of tumor margins relies on palpation and visual inspection. Near-IR fluorescence imaging is a promising technique for intraoperative tumor identification by its visualization (Gioux et al. 2010; van Dam et al. 2011; Vahrmeijer et al. 2013). Contrasting the tumor with fluorescent dyes could help the surgeon in determining and controlling resection margins. Such possibility is especially attractive for skin, breast and other forms of cancer, where the light does not need to penetrate deeply. The most expected application is in breast cancer sentinel lymph node mapping.

For serving a guide for surgeon, the image should appear in real time (seconds) with a sufficiently high spatial resolution. Efficient illumination and collection of fluorescent image with on-line computer analysis is technically achievable, and the limiting factor are fluorescence emitters. In order fluorescent dyes or nanoparticles to be applicable they must satisfy a number of conditions. Although imaging with visible light is possible in some cases (van Dam et al. 2011), the near-IR dyes that allow deeper light penetration into tissues are preferable. They should possess sufficiently high brightness and photostability together with high biocompatibility and rapid clearance from the body. The necessary condition should be also their ability to be modified by covalent attachment of ligands recognizing the cancer cells. It is hard to satisfy all these conditions simultaneously. Indocyanine Green (Fig. 14.11) presently remains in most active use in these applications (Polom et al. 2011). It is non-toxic, still its quantum yield is rather small. Among new developments are the zwitterionic heptamethine dyes that possess advanced spectroscopic properties, demonstrate high solubility and rapid renal clearance (Njiojob et al. 2015). Their covalent modification is possible via appended amino or carboxylic groups. However, their Stokes shift is small (Fig. 14.12), which leads to intensity losses in separating excitation and emission channels.

Many problems could be resolved with the application of properly designed fluorescent nanoparticles and nanocomposites (see Chaps. 5 and 6). Meantime, it was reported that the clearance of nanoparticles depends on their size, and their passage through kidney membranes may be difficult if their dimensions are larger than 5.5 nm (Choi et al. 2007). Their structure and surface composition are important, and additional studies are needed to optimize them. These particles should possess high affinity towards cancer cells and strong discriminative power against healthy cells. The rapid progress in identification of cancer cell surface markers (Jain 2007) offers good prospects for inducing such affinity to fluorescence contrast agents.

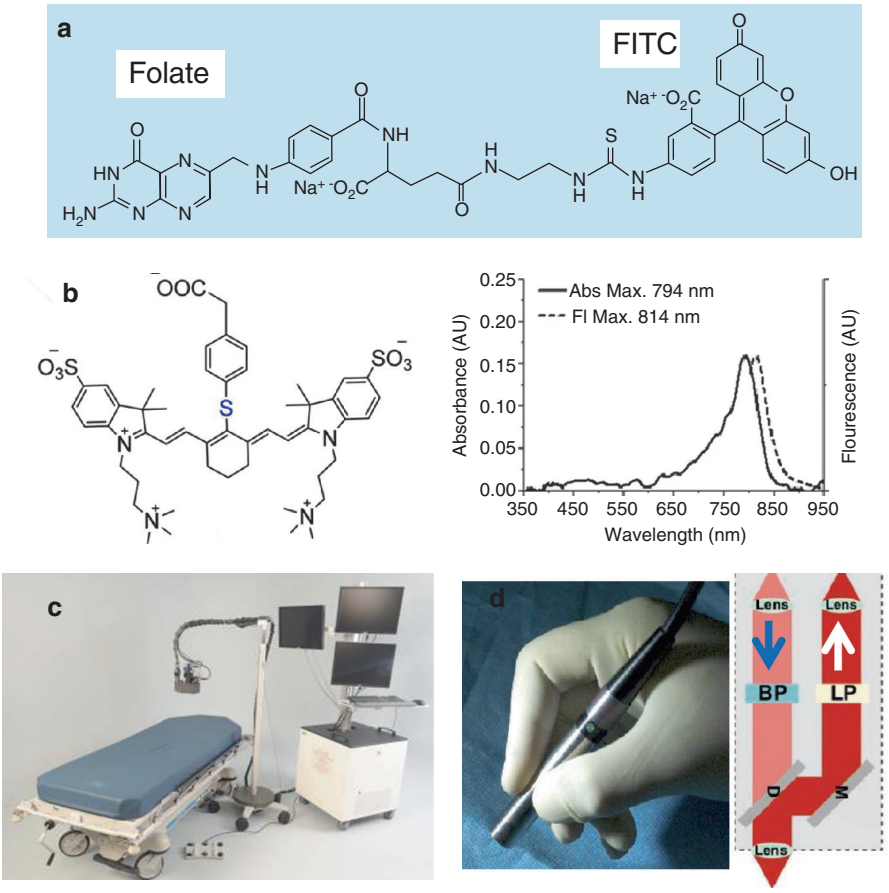

Fig. 14.12 The fluorescence reporters and instruments applied in image-guided surgery. (**a**) The conjugate of FITS (fluorophore) and folate (ligand for specific cancer cell labeling) used in the first image-guided operation on humans (van Dam et al. 2011). (**b**) One of novel zwitterionic heptamethine near-IR fluorophores with improved brightness, biocompatibility and ability for covalent conjugation (Njiojob et al. 2015) (**c**) The imaging system for surgical operation that allows obtaining near-IR image and its projection on computer screen (Gioux et al. 2010). (**d**) Hand-held spectroscopic device for intraoperative tumor detection *in vivo* (Mohs et al. 2010). This pen-shaped device utilizes a near-IR diode laser (emitting at 785 nm) coupled to a compact head unit for light excitation and collection. It allows sensitive analysis of both fluorescent and surface-enhanced Raman scattering contrast signals

During surgery under control of near-IR image, neither scattered incident light nor fluorescence light is visible to human eye, so the agent should be visualized using an imaging system above the surgical field for open surgery or encased within a fiberscope for minimally-invasive and robotic surgery. An optimal imaging system should be coupled with visible (white light) illumination of the surgical field. The surgeon's display can be one of several form factors, including a standard computer monitor, goggles or a wall projector. Current imaging systems operate at a sufficient

working distance that enables the surgeon to operate illuminating a sizable surgical field (Gioux et al. 2010; Vahrmeijer et al. 2013), Prototypes of adequate, manageable, intra-operative camera systems already exist and they are on trial in different clinics (Vahrmeijer et al. 2013). Such systems allow manifold enlargement for inspecting very small features, on a millimeter scale. The most appealing advantage of such technologies is the potential possibility of multi-targeted imaging that can be realized in real-time multi-color pictures.

Figure 14.12 illustrates two technical developments in this line. One is the surgery workplace unit that is equipped with visible and near-IR imaging devices. The other is miniaturized probe requiring scanning the operation field but allowing response not only in fluorescence but also in Raman scattering signal. Development of 'smart glasses' with near-IR vision is a promising alternative to the screen-based imaging systems and scanning devices. Still, this idea was not realized by the time of writing this book.

14.2.8 Conclusions

In summary, fluorescence imaging has full chances to be developed into an important tool of non-invasive investigation in clinics. It could allow monitoring the treatment and even visualize and control the surgical operations. Perpetual improvements in optical contrast agents with the expected more active involvement of nanoparticles emitters paralleled with innovations in imaging technologies pave the way for the widespread utilization of this technology. Many present and foreseen achievements can be focused on its development. The key issues are functionalization and targeting of fluorescence (luminescence) emitters together with increase of their brightness with respect to endogenous background signals. Together with further development of fluorescence detection technique, new algorithms are needed for supporting high-level tomography together with resolution from the background and between multiple emitters. Special efforts are needed for achieving quantitative data, since the energy of excitation light penetrates poorly and decays strongly as a function of penetration depth and its significant part is scattered.

14.3 Monitoring the Cells Inside the Living Body

Now we address a different but related problem. We can incorporate into the body a living cell and then follow in dynamics its behavior. It could be a stem cell for substitution therapy or the cell carrying vector for gene transfer. Of special interest are hematopoietic and cancer cells that have to be searched on the whole body level (Kalchenko et al. 2011). The changes in tissue organization and organ growth, the cells rejection during transplantation, the hemodynamics, vascular permeability, muscle contraction, cardiac function, cognitive brain activity and other physiology-related processes and their pathological disorders have to be studied. Molecular

imaging allows for *in vivo* detection of gene or cell surface marker expression, monitoring and analysis of enzymatic activity. Cellular imaging methods allow for tracking of cell migration, differentiation, proliferation, and survival within the living organism. Tight monitoring of cell fate is critical during fetal growth, pathological processes and therapeutic treatments, such as tissue repair.

14.3.1 The Labeling Procedure

In the cases addressing the problems denoted above, a strategy different from that incorporating the sensor fluorophores *in vivo* can be applied. Cells can be labeled with fluorescent agent *ex vivo*, using endogenously expressed reporter genes that allow synthesis of fluorescent proteins and then applied *exogenously* (Hong et al. 2010) Also, the cell labeling can be made by synthetic dyes and nanoparticles selecting them from innumerable libraries. In this case many cell types can be labeled and at different sites, but rapid cell proliferation may lead to dye dilution and loss of signal. This may not happen with the cells possessing the active genes synthesizing fluorescent proteins or the components of bioluminescence system. Therefore the researcher has to make selection between different strategies, and an optimization of fluorescence signal is one of the key issues.

This procedure of *ex-vivo labeling* can be followed with Fig. 14.13. The cells are extracted from the body and/or are *cultivated in vitro*. To ensure effective labeling and diminish the label leakage, the fluorescent molecule must cross the cell membrane or be strongly coupled with it. This requires the choice of dyes and nanoparticles based on their ability to enter the cell, either spontaneously or with the aid of membrane permeabilizing treatments (such as the use transfection agents),

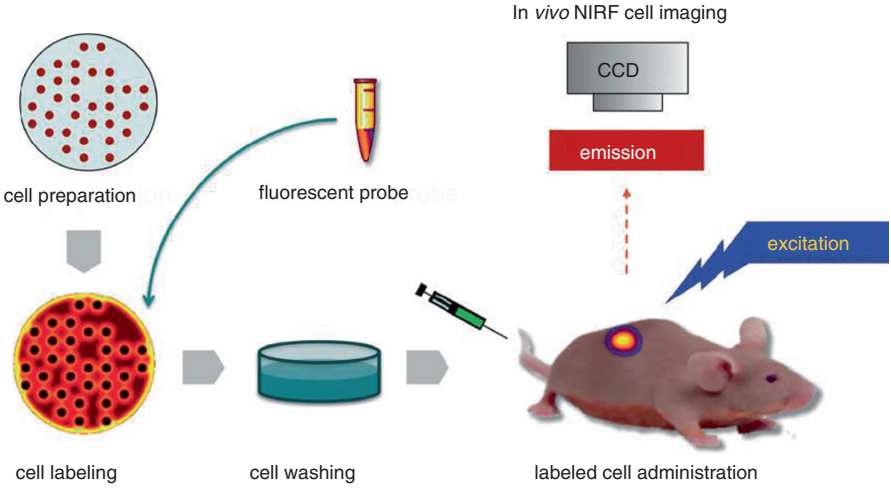

Fig. 14.13 A schematic representation of the whole-body near-infrared imaging of *ex vivo* fluorescently labeled hematopoietic or cancer cells (Kalchenko et al. 2011)

and remain within the cell for an extended period. After cell labeling and incubation period the cells are administered to the body.

The cell membrane with its lipid bilayer provides an important target for labeling cells using lipophilic fluorescent probes. Lipophilic carbocyanine dyes with long hydrocarbon chains and lipophilic styryl fluorescent dyes, each with its unique chemical and optical specifications, are often used for *ex vivo* imaging – *in vivo* administration technologies. The cells remain labeled for extended periods, providing a powerful tool for routine cell labeling and the whole-body optical imaging. The results obtained with one of these dyes, DiIC18, are illustrated in Fig. 14.14. Labeling the cell membranes with nontoxic organic dye occurring spontaneously in mild conditions may be the least damaging to the cell. Meantime, the label transfer to other cells *in vivo* may be noticed in some cases (Kalchenko et al. 2011).

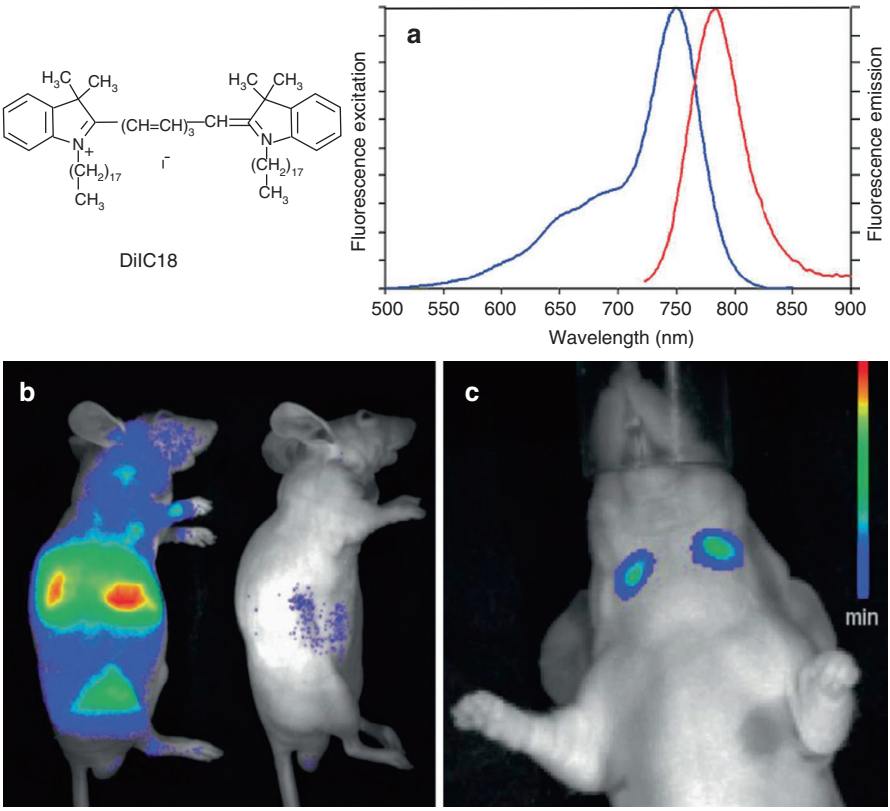

Fig. 14.14 Application of fluorescent cell membrane labeling dye DiIC18 in whole animal studies (Kalchenko et al. 2011). (**a**) Fluorescence excitation and emission spectra of DiIC18 bound to phospholipid bilayer membranes. (**b**) Near-IR images of labeled and unlabeled human leukemic Pre-B ALL G2 cells homing in CD1 nude mice, 48 h after transplantation and following noninvasive imaging. (**c**) Color coded image of labeled mice splenocyte homing overlaid on a photographic image. The color bar defines fluorescence intensity (from *blue*/minimum to *red*/maximum)

14.3.2 Tracking Hematopoietic and Cancer Cells

The single-cell sensitivity of modern fluorescence techniques opens many new possibilities in the studies of selected cells within a living body. Some relevant examples for the use of lipophilic dyes in human cancer and murine hematopoietic cell models are presented elsewhere (Kalchenko et al. 2011). Imaging of transendothelial migration of macrophages in a cutaneous granuloma model by means of two-dimensional fluorescence imaging and by three-dimensional fluorescence-mediated tomography are versatile techniques to monitor and quantify cellular inflammatory response in vivo.

In a related study the near-IR imaging was applied to study the migration of monocytes and macrophages as the earliest events in response to *inflammation*. After inducing the local inflammation in mice, the fluorescence-labeled murine macrophages were injected intravenously, and their 3-dimensional distribution was assessed. In this way the inflammatory cells were tracked in a non-invasive way for several days *in vivo* allowing to monitor and quantify cellular inflammatory responses (Eisenblätter et al. 2009).

Different types of cell labels were applied for fluorescence reporting. In the studies of bone marrow transplantation the cells labeled with DiIC18 cyanine dye (see Fig. 14.14) and commercially supplied quantum dots were compared and it was stated that these nanoparticles inhibited cell proliferation, while organic dyes – not (Rutten et al. 2010). Probably, because of that reason different authors prefer providing 'indirect labeling' by inclusion into tested cells of genes coding fluorescent proteins or the components of luciferin-luciferase system.

Thus, the *whole-body imaging* of hematopoietic and cancer cells facilitates monitoring of complex biological processes, disease progression, and response to therapy. Observation of hematopoietic cell rolling, homing and interactions within vessels and tissues such as bone marrow, spleen, lymph-nodes and liver contributes to in-depth understanding of the cells in their natural environments in norm and disease. Similarly, the acquired possibility of visualization of cancer cell in living animals reveals tumor growth and metastasis, allowing researchers to monitor tumor burden and assess the efficacy of candidate antitumor and antimetastatic agents.

14.3.3 Trafficking the Stem Cell

Human *embryonic stem cells*, capable of self-renewal and differentiation into virtually all cell types with proper conditioning, hold many expectations for application in regenerative medicine (Solanki et al. 2008), combating cardiovascular diseases, neural disorders, bone/cartilage and other diseases. Their application in oncology is also very promising (Hong et al. 2010). The ability to non-invasively track the delivery of these and other therapeutic cells (e.g. T cells) to the tumor site, and/or subsequent differentiation/proliferation of these cells, would allow better understanding

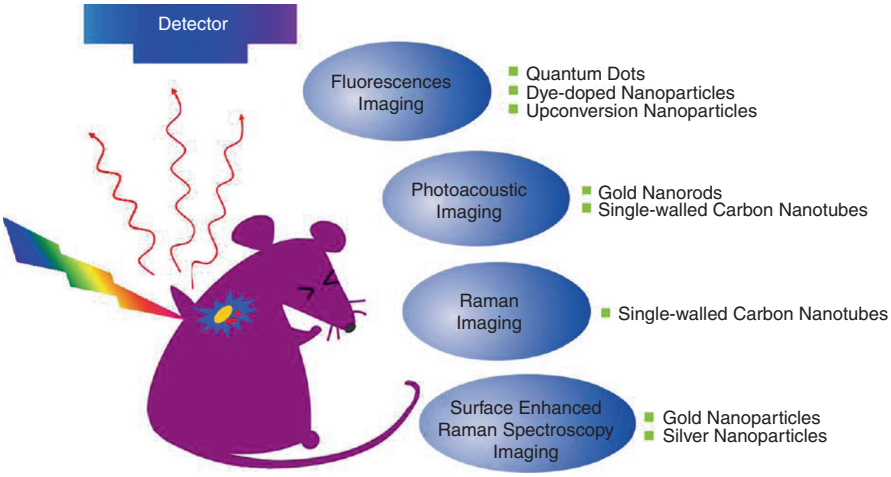

Fig. 14.15 Optical imaging strategies for stem cells tracking with optically active nanoparticles (Gao et al. 2013). Note that fluorescence imaging stands first due to its advantages of high sensitivity, resolution in space and time and also relative simplicity and low price of experiments

of the cancer development and intervention mechanisms. In all these cases, cell visualization *in vivo* is highly needed and it can be provided by labeling with different types of dyes and nanoparticles (Xu et al. 2011; Gao et al. 2013). The stem cells have to renew, proliferate and differentiate over long period of time and the problem is to probe their location and fate.

Criteria for application of different types of markers to trace the stem cells have been recently discussed and the prospects for application of fluorescent nanoparticles were demonstrated (Xu et al. 2011). In this respect, fluorescence competes very favorably with other types of tracking cells and their distribution within the body (Fig. 14.15). However, inorganic nanocrystals are not so favorable in this respect because of their potential cellular toxicity and problematic clearance on the whole body level. If these issues are properly addressed, the up-converting nanoparticles reveal their merit due to deep penetration of exciting near-IR light and the practical absence of luminescence/light scattering background (Wang et al. 2012; Min et al. 2014). Because of high biocompatibility, dye-doped silica nanoparticles (Accomasso et al. 2012) and carbon nanomaterials (Zhang et al. 2012) offer very favorable prospect.

14.3.4 Conclusions

In current research the ability to follow simultaneously the multiple cell lineages, to analyze their patterns of migration, to determine their sites and rates of proliferation have been realized. It became possible to monitor their differentiation and

functioning at the terminal site, which have significantly broadened scientific research capacities. Meantime, noninvasive *in vivo* monitoring of cell behavior presents a major challenge to researchers. It is important to verify that labeling remains stable once it is in the cell, it does not impair cell phenotype or influence engrafting behavior. Laboratory tests showed that the cells retained their usual surface markers and that they were still functional after the labeling process. These methods could soon enable researchers and physicians to track directly the cells used in medical treatments. Such tracking ability could prove useful for monitoring tumors and diagnosing as well as treating cardiovascular and some other medical problems.

It is clear that the *in vitro* labeling technology offers significant advantages over other cell-labeling technologies in the studies *in vivo*. What is gained is the selectivity. Only the labeled cells and the cells that derive from them will provide reporting signal in the body. The other unlabeled cells remain in the dark, and the lack of their interference enables measurement of very low amounts of the labeled cells and estimation of their number on the basis of the brightness of the image.

14.4 Theranostics: Combining Targeting, Imaging and Therapy

Theranostics (therapy and diagnostics) is emerging as a great multidisciplinary field of research and development, and it is not the task of the author to present it in full complexity. We will focus on the possibilities of combining the fluorescence sensing and imaging with the generation of therapeutic effect. Modern fluorescence technologies develop towards multifunctionality. Under *multifunctionality* we mean a combination of important properties that may include guiding to a particular target by physical means (e.g. by being magnetic), selective binding to a particular target (macromolecule, living cell or its organelle), physical (by heat) or photochemical (photodynamic) treatment and the transportation/release of drugs (Fig. 14.16).

Although some typical medical drugs are fluorescent (e.g. deoxorubicin) and typical dyes possess therapeutic effect (e.g. 3-hydroxyflavones), the most efficient combination of these functionalities can be realized on nanoscale level. According to Ref. (Jokerst and Gambhir 2011) the ideal *theranostic* nanoparticle should be: (1) selectively and rapidly accumulates in diseased tissue, (2) reports biochemical and morphological characteristics of the area, (3) delivers a non-invasive therapeutic, and (4) is safe and biodegrades with non-toxic byproducts. We will discuss the routes how to approach to this ideal behavior.

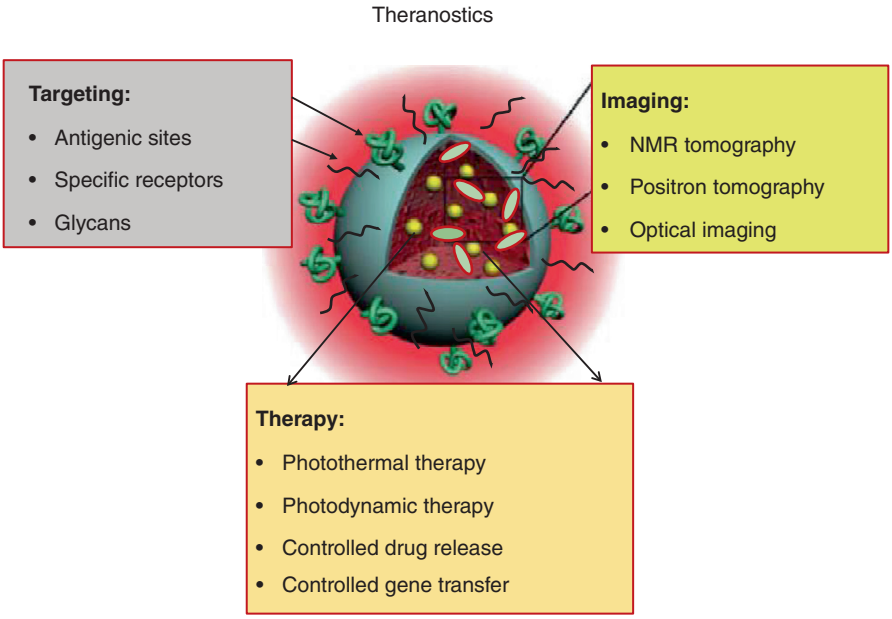

Fig. 14.16 Schematic presentation of the areas of research and development combined in theranostics

14.4.1 Combining Different Imaging Functionalities

Integration of near-IR fluorescence imaging with the imaging modalities based on other principles extends molecular information derived from fluorescent probing and interpretation of the data. The techniques currently operating with macroscopic imaging systems of the whole living bodies include *magnetic resonance imaging* (MRI), *positron emission tomography* (PET), and *computed X-ray tomography* (CT). Each of these imaging modalities has its own merits and disadvantages, and a single technique does not possess all the required capabilities for comprehensive imaging and observing distribution of required targets within the image area. Whereas for MRI and PET the sensitivity is on the level of hundreds of cells and spatial resolution of several millimeters, the resolution of fluorescence methods can be easily achieved on a single-cell level. Therefore, multimodal imaging methods are important tools for state-of-the-art clinical diagnostics and therapeutics.

Two basic fluorescence imaging technologies are the most promising in the development of such composites. One is based on *near-IR organic dyes* encapsulated into silica or organic polymer nanoparticles and the other – on *up-conversion*

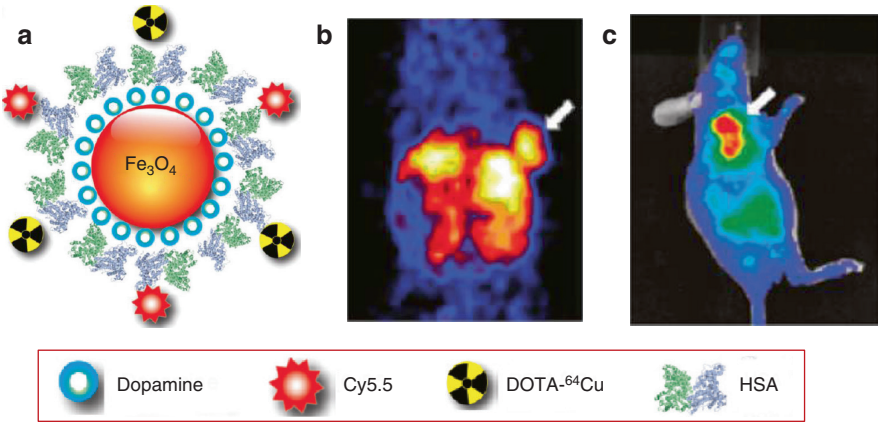

Fig. 14.17 Multifunctional theranostic nanocomposite based on iron oxide (Xie et al. 2010). (**a**) Schematic arrangement of components. (**b**) The PET image and (**c**) the near-IR fluorescence image of a mouse containing a subcutaneous glioblastoma tumor taken 18 h post injection of the particles at the site indicated by an *arrow*

nanocrystals that allow near-IR excitation with emission in the visible (Zheng et al. 2015). Both these techniques allow multicolor imaging, combination with other imaging modalities and carrying drugs.

There are many possibilities for constructing multimodal species. *Magnetic nanoparticles* can serve as core platforms for the addition of other functional moieties, including fluorescence. Coupling of fluorescence with magnetic properties can be achieved with Fe_3O_4/CdSe nanocomposites (Dong et al. 2012). Silica scaffolds can be also used efficiently (Chen et al. 2010). As additional functionality, they can be coated by poly(ethyleneglycol) chains as a cloaking agent to extend the blood circulation time. Many similar types of design can be found in the literature. They allow one to vary the contribution of each function in broad ranges and adding new functions. The Fe_3O_4 core can also be surrounded in a corona-like fashion by gold nanoparticles representing the plasmonic module. The iron oxide nanoparticles were also covered with dopamine to make them moderately hydrophilic and allowing coverage with human serum albumin (HSA) molecules (Fig. 14.17). Then for fluorescence imaging the particles were surface functionalized with cyanine Cy5.5 dye and with [^{64}Cu] for PET imaging. The animal models were prepared by subcutaneously injecting glioblastoma cells into the front flank of each mouse. They demonstrate excellent contrasting of the tumor (Xie et al. 2010). Such modules can carry different drugs and their release can be coupled with photothermal treatment (see below).

14.4.2 Combining Imaging and Targeting

Specificity in targeting of nanoparticles carrying drugs or producing damaging action can be achieved by different means. First, the nanoparticles of 20–300 nm in size can preferentially accumulate in tumor tissues. This happens because the newly

formed tumor blood vessels possess less disorganized, leaky vasculature. In addition, the nanoparticles can be decorated with recognition units targeting the structures that in cancer cells can be distinguished from that in normal cells.

G*lycans* located on the cell surface are particularly attractive due to their key role in cellular activity and disease occurrence and development. They are recognized by *lectins*, the proteins that can provide their multivalent binding. The selective labeling of highly metastatic hepatocellular carcinoma cells *in vitro* and successful *in vivo* imaging can be achieved by targeting glycans (Rouhanifard et al. 2013). In a similar way glycans on the surface of pathogenic bacteria can be recognized (Tra and Dube 2014).

Folate receptors are present at the surfaces of cancer cell in much greater amount than in normal cells. Therefore, *folic acid* has become very popular in modification of nanoparticles with different functionalities for targeting the cancer cells (Maity et al. 2013). The methods were developed to control the number of folate molecules per nanoparticle to optimally tune the interaction with cells.

Peptides. Different tumor cells overexpress some transmembrane receptors on their surface. For example, cyclic peptide Arg-Gly-Asp (cRGD) has a high binding affinity to the $\alpha v\beta 3$ integrin receptor that is critical in tumor angiogenesis. Therefore, nanoparticles decorated with these peptides demonstrate affinity towards tumor cells (Xiong et al. 2009).

Finally the specific antigenic determinants on cell surfaces can be recognized by *antibodies* and the latter remain to be important tools in targeting cancer cells (van Scheltinga et al. 2011). Endothelial growth factor is one of such cell surface antigens.

14.4.3 Photothermal Therapy

Photothermal therapy is probably the least invasive method to treat cancer. It produces action only in illuminated areas and only where the therapeutic particles are located and does not leave a toxic effect of reactive molecules throughout the body. It is based on an ability of near-IR light, penetrating into the tissues, to produce heat effect that kills the cancer cells. Such effect can be generated with different molecular and nanoscale light absorbers, but it is the greatest for those possessing the highest absorbance at the wavelength of illumination. The excess heat dissipates in the medium and, due to higher thermal sensitivity of cancer cells it produces selective therapeutic effect of killing them. Inexpensive continuous-wave 980 nm diode lasers can be used in most cases, and special materials absorbing light in this range that can generate this nonspecific effect have to be applied.

The *nanocomposites* that are able not only to target and visualize cancer cells but can also kill them efficiently in a photothermal way were synthesized. The examples are the particles made for *up-conversion* imaging (Dong et al. 2011). The quantum yield of their emission is commonly low, and the non-emissive decay to the ground state results in local heating. Regarding *magnetic* nanocomposites, like those depicted in Fig. 14.17, their local heating can be achieved by high-frequency magnetic field.

14.4.4 Photodynamic Therapy

Photodynamic therapy of cancer is based on the property of different fluorescent molecules and nanoparticles to produce damage to targeted cells and tissues by generating the *active oxygen* species in the electronic excited states. These species appear in photochemical reactions of different dyes that are called *photosensitizers*. The primary event is the generation of singlet oxygen according to the mechanism discovered and studied by Michael Kasha and his students (Fig. 14.18). In detail, this mechanism is described in different textbooks and reviews, see (Ogilby 2010). Possessing excessive energy and being highly reactive, the active oxygen species destroy molecular structures leading to cell death.

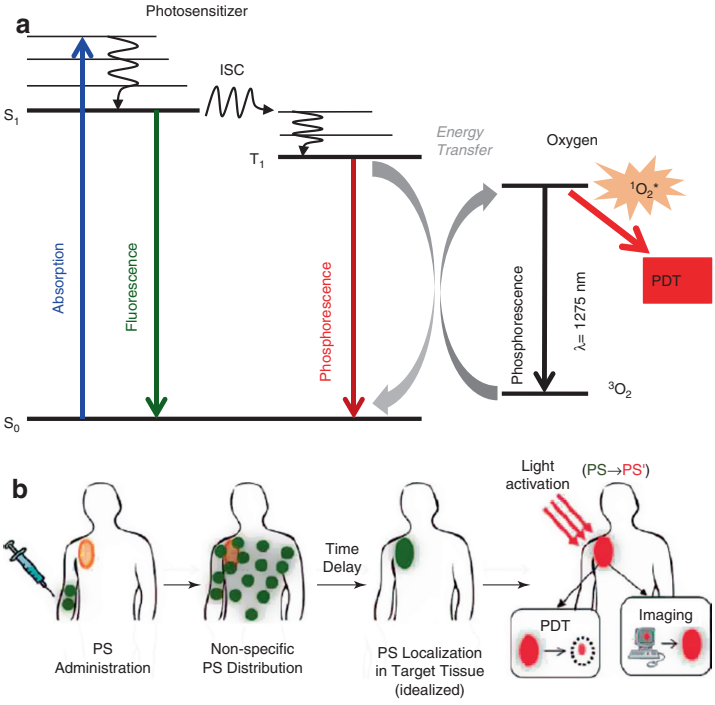

Fig. 14.18 Generation of singlet oxygen $^1O_2$* in a photochemical reaction (Demchenko et al. 2014) (**a**) and the sequence of administration, localization, and light activation of photosensitizers for fluorescence imaging or photodynamic therapy (**b**) (Celli et al. 2010). The photosensitizer dye is excited to S_1 energy state and exhibits intersystem crossing (ISC) to T_1 state that can generate either phosphorescence or excitation energy transfer to the ground-state triplet oxygen $^3O_2$ resulting in transition to the excited $^1O_2$* state. The latter can emit phosphorescence in the near-IR region or generate different photochemical processes

Photodynamic therapy has a high potential as a noninvasive procedure for dealing with tumors, the dyes acting as both imaging agents and therapeutic agents (Celli et al. 2010). Similarly to photothermal therapy, there are two possibilities to provide spatial control of cytotoxic action: (a) by concentrating the photodynamically active molecules or particles in the desired location and (b) by selective illumination of this location. The photosensitizer must be present in sufficient concentrations in the sites of interest and possess high quantum yield of singlet oxygen generation. Attachment of targeting groups can help to reduce an important limitation associated with photodynamic therapy – an increased patient photosensitivity due to prolonged accumulation of the drug within the skin. The treatment can be combined with identification and imaging of the target cells (Stefflova et al. 2007).

The energy of near-IR quanta is insufficient for generating the singlet oxygen in photochemical reactions. Therefore for generating this effect *in vivo*, the dyes with high two-photon cross-section (Kim et al. 2007) and up-conversion nanoparticles (Wang et al. 2011b) are commonly used as primary absorbers. This allows the photosensitizers located within the same nanocomposites to be excited via FRET by quanta of sufficient energy for producing the photodynamic effect (Fig. 14.19). Compared to the traditional treatment using visible excitation light, the treatment efficacy for tumors is significantly improved by achieving higher tissue penetration depth of incident light. Among novel fluorescent nanomaterials that exhibit both photodynamic and photothermal effects upon irradiation by near-IR light are graphene dots (Nurunnabi et al. 2014).

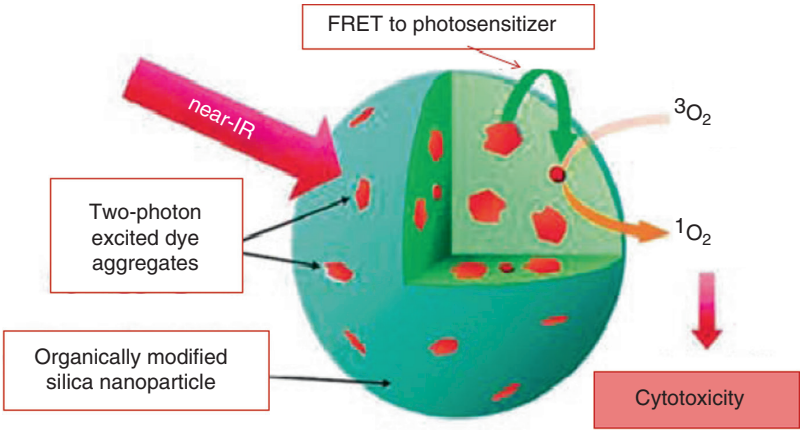

Fig. 14.19 Generation of cytotoxic singlet oxygen ($^1O_2$) in designed nanocomposites by near-IR light (Kim et al. 2007). The incorporated dye excited by two photons transfers its energy to photosensitizer

14.4.5 Controlled Drug Release

In clinical practice it is highly preferable for the drug release profile to be activated at required locus, in required time and monitored in a quantitative manner in real time, to avoid insufficient or excess drug doses (Weinstain et al. 2010). For achieving that, three possibilities may be considered: (1) the drug is caged in a nanocomposite, and its de-caging is coupled with the modulation of fluorescence response; (2) the structural changes in nanocomposite are activated by light and they trigger the coupled reactions of drug release and fluorescence response; (3) the drug quenches the emission by interacting with fluorophore directly via excited-state electron or energy transfer and its release results in de-quenching effect.

Thus, a number of drug delivery systems was developed for fluorescence monitoring of anticancer drug release by a coupled *photocaged compound* that on de-caging produces the fluorescence reporting signal (Jana et al. 2012). The problem is that the energy of near-IR quanta is usually not sufficient for generation of de-caging reaction.

The porous nanomaterial may contain the groups of atoms that are "*molecular valves*" blocking the drug release and, simultaneously, the FRET pair (Lai et al. 2013). Dissociation in cellular environment of the blocking fragment allows the drug leakage and simultaneously disrupts the FRET pair. This approach is not limited to particular type of drug. Unfortunately such suggestions could be presently realized only with UV-visible but not with near-IR excitation.

The third possibility is to explore the property of some drugs (such as doxorubicin, a commonly used anti-cancer drug) to be the *FRET acceptors*, so that their release can be seen as an enhancement of the donor emission. Its realization was reported for several theranostic composites. The most attractive is the use of carbon dots that demonstrate very high two-photon absorbance as both scaffolds and FRET donors (Tang et al. 2013). The up-conversion nanoparticles can be also used for this purpose. In one of reported studies (Wang et al. 2011a) they were functionalized with a polyethylene glycol (PEG) grafted amphiphilic polymer and then loaded with doxorubicin by simple physical adsorption (Fig. 14.20). The loading and releasing of the drug are controlled by varying pH, with its increased dissociation rate in acidic environment of the cancer cell. By conjugating nanoparticles with folic acid, which targets folate receptors over-expressed on various types of cancer cells, the targeted drug delivery was demonstrated and the up-conversion luminescence imaging controlled in time the intracellular delivery.

Since many drugs do not display light absorbance in the required spectral range, this approach cannot be considered universal. The nanocomposites containing shells composed of temperature and pH responsive polymers can release in a programmed way the incorporated pharmaceutical drugs (Culver et al. 2014), but it is really difficult to couple directly the drug release and the optical signal reporting on this

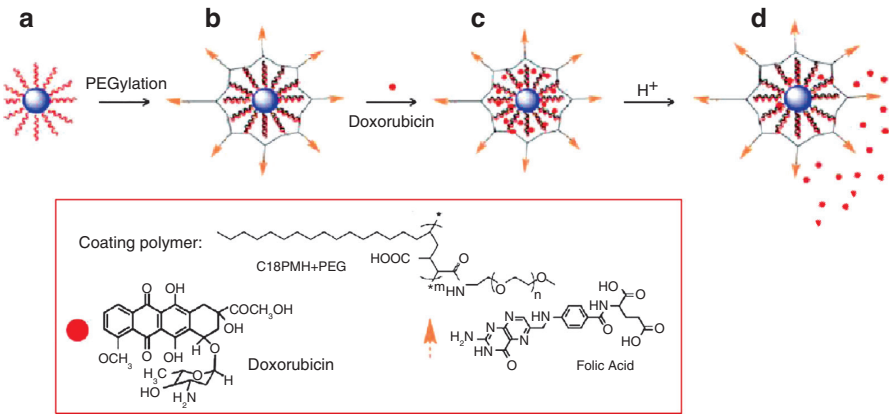

Fig. 14.20 Schematic illustration of the drug delivery system based on up-converting nanoparticles (Wang et al. 2011a). (**a**) As-synthesized oleic acid capped particles. (**b**) C18PMH-PEG-folic acid functionalized particles. (**c**) Doxorubicin loading on particles. The drug molecules are physically adsorbed into the oleic acid layer on the particle surface by hydrophobic interactions; (**d**) Release of doxorubicin from the particles triggered by decreasing pH

event. The simple solution is to provide simultaneously with drug release the fluorophore release, whose emission can be enhanced. But this idea cannot be realized universally.

14.4.6 Gene Targeting and Release

Gene therapy holds promise in the treatment of both acquired and inherited diseases (Ibraheem et al. 2014). Being introduced externally, a defective gene copy must be replaced with a functional (therapeutic) one. The success of this treatment relies on efficient delivery of nucleic acid species to the site of disease. Because of their negative charge, these large molecules cannot be easily internalized by cells, and also, they are highly susceptible to enzymatic degradation. Therefore, specific "vectors" are being developed for their delivery. The archetype of a highly efficient nanoscale delivery agent is a virus, as its life cycle requires the intracellular release of the viral genome through specific mechanisms for cell targeting, endocytosis, and hijacking of the cellular machinery. Viruses can be inactivated by the removal of their own genetic information replacing it with targeted one. In addition, the self-assembled "*virus-like*" structures have been designed that are often called "nanocages". Success in gene delivery is usually tested by the expression of green fluorescent protein gene that is delivered simultaneously and by the observation of fluorescence image (Chudakov et al. 2005).

Different new materials were suggested that combine gene binding, transport and release with fluorescence imaging, particularly the carbon dots (Liu et al. 2012). Photothermal enhancement of gene delivery can be realized in these systems (Feng et al. 2013).

14.4.7 Conclusions and Prospects

The prototypes of versatile multifunctional platforms for imaging, drug delivery, and theranostics have been designed and the progress in their improvement is very fast. They are excellent tool for fundamental research and a great promise for extensive translation to clinical practice improving early diagnosis and also the safe and efficient therapy. In the application of smart multifunctional nanostructures, cancer diagnosis and treatment has been the area that has attracted the strongest research effort. Their use, however, is not at all limited to this field but spans the diagnosis and imaging of many other diseases, and particularly those that have bacteria and viruses as etiologic agents (White et al. 2012).

Fluorescence, and luminescence in general, is the valuable tool in these technologies being the simplest technically and the most informative (within the accessible range) among all available *in vivo* imaging technologies. The non-emissive action of excited fluorophores is also valuable contributing greatly to destruction of targeted cells by producing photothermal and photodynamic effects in a well-controlled manner.

Owing to modern chemistry, the production of nanocomposites of great complexity becomes a matter not so complex. The problem is in biocompatibility of these novel nanostructures in the conditions of their long-term presence in living body. Their circulation, degradation and release should be always predicted and fully controlled.

14.5 Sensing and Thinking: The Strategy of Controlling by Light Diagnostics and Treatment

Clinical diagnostics is a very competitive industry, where many companies and university research groups are continuously developing new products and techniques. The results need to meet or exceed several criteria already achieved by the current diagnostic tests: sensitivity, specificity, reproducibility and relatively low cost. In addition, the rapidity of the diagnostic tests is important in emergent situations. It becomes an essential issue in the event of an outbreak of an infectious disease or a biological terror attack that has immediate impact on human health. New challenges and possibilities appear with the attempts to combine diagnostics and imaging with surgical operation and pharmaceutical treatment. Several important steps already have been made in this direction.

The reader has to recognize novel trends and think, how these developments can result in new diagnostic and treatment tools. In ex-vivo sensing the recognition of disease biomarkers and its coupling with fluorescence output is not conceptually new, as we see in other chapters of this book, but search for new targets and for their recognition partners remains as important task. Essentially new is considering the light not only as the instrument for optical probing but also as the tool for providing the treatment and realizing its control. The insufficient energy of tissue-penetrating near-IR quanta can be doubled by absorption of two photons, and clever solutions have been suggested for utilizing this electronic excitation energy in triggering and control of theranostic events.

Coupling of different functionalities can be most efficiently realized on the level of nanocomposites. This extends the limits of current molecular diagnostics and enables integration of diagnostics with therapeutics, development of point-of-care diagnostics and personalized medicine. The devices based on nanotechnology, which can make thousands of measurements very rapidly and very inexpensively, are expected to become available in near future. The surgical treatment and drug release in the desired time and desired site under control of fluorescence image have been realized and expects further development.

Questions and Problems

1. What is a conceptual difference between *ex-vivo* and *in-vivo* diagnostics? On what levels of organization of living matter they are directed?
2. What are the metabolic and specific protein-based biomarkers? Present examples.
3. List the methods of glucose determining and explain their basic recognition and reporting mechanisms.
4. What is special in diagnostics of viral diseases?
5. Explain what intrinsic light absorbing and scattering species complicate the imaging of human tissues. Indicate the wavelength range of their relative transparency.
6. How can the fluorescence tomography of small animal tissues be realized? What types of emitters should be selected?
7. What property of cancer cells allows their contrasting with fluorescent dyes?
8. Explain the structure-properties correlation of Indocyanine Green and similar dyes. How are they applied and what information do they allow to gain?
9. How can fluorescent imaging during operative treatment be realized? What instrumentation is needed for that?
10. Explain different methods of labeling the cells in living body and of their advantages and disadvantages. How are they used in cell tracking?
11. What is theranostics? Why functional nanocomposites are being developed for this application? What can be the combination of their functionalities? What requirements they should satisfy for applications *in vivo*?
12. What are the advantages and disadvantages of fluorescence imaging compared to magnetic resonance imaging and positron emission tomography? What could be a rational combination of these functions in one nanoscale unit?

13. How to provide targeting of nanocomposites to particular cells and tissues? List the most applicable recognition elements and explain how molecular recognition can be realized.
14. What is the mechanism of photodynamic action? Explain how it is realized for cancer treatment. What are the criteria for choosing photosensitizers? How to provide sufficient energy for photodynamic therapy with near-IR excitation?
15. How to activate and control by light the drug release at the desired sites of living body?

References

Abel L, Kutschki S, Turewicz M, Eisenacher M, Stoutjesdijk J, Meyer HE, Woitalla D, May C (2014) Autoimmune profiling with protein microarrays in clinical applications. Biochimica et Biophysica Acta (BBA)-Proteins and Proteomics 1844(5):977–987

Accomasso L, Rocchietti EC, Raimondo S, Catalano F, Alberto G, Giannitti A, Minieri V, Turinetto V, Orlando L, Saviozzi S (2012) Fluorescent silica nanoparticles improve optical imaging of stem cells allowing direct discrimination between live and early-stage apoptotic cells. Small 8(20):3192–3200

Akerman ME, Chan WC, Laakkonen P, Bhatia SN, Ruoslahti E (2002) Nanocrystal targeting in vivo. Proc Natl Acad Sci U S A 99(20):12617–12621

Aslan K, Geddes CD (2006) Microwave-accelerated and metal-enhanced fluorescence myoglobin detection on silvered surfaces: potential application to myocardial infarction diagnosis. Plasmonics 1(1):53–59

Badugu R, Lakowicz JR, Geddes CD (2004) Noninvasive continuous monitoring of physiological glucose using a monosaccharide-sensing contact lens. Anal Chem 76(3):610–618

Batta A, Panag K, Singh J (2012) Cardiac markers–role in diagnosis of myocardial infarction. Int J Cur Bio Med Sci 2(2):262–267

Biffi S, Petrizza L, Rampazzo E, Voltan R, Sgarzi M, Garrovo C, Prodi L, Andolfi L, Agnoletto C, Zauli G (2014) Multiple dye-doped NIR-emitting silica nanoparticles for both flow cytometry and in vivo imaging. RSC Advances 4(35):18278–18285

Celli JP, Spring BQ, Rizvi I, Evans CL, Samkoe KS, Verma S, Pogue BW, Hasan T (2010) Imaging and photodynamic therapy: mechanisms, monitoring, and optimization. Chem Rev 110(5):2795–2838

Chen W, Xu N, Xu L, Wang L, Li Z, Ma W, Zhu Y, Xu C, Kotov NA (2010) Multifunctional magnetoplasmonic nanoparticle assemblies for cancer therapy and diagnostics (theranostics). Macromol Rapid Commun 31(2):228–236

Choi HS, Frangioni JV (2010) Nanoparticles for biomedical imaging: fundamentals of clinical translation. Mol Imaging 9(6):291

Choi HS, Liu W, Misra P, Tanaka E, Zimmer JP, Itty Ipe B, Bawendi MG, Frangioni JV (2007) Renal clearance of quantum dots. Nat Biotechnol 25(10):1165–1170

Christenson ES, Collinson PO, deFilippi CR, Christenson RH (2014) Heart failure biomarkers at point-of-care: current utilization and future potential. Expert Rev Mol Diagn 14(2):185–197

Chudakov DM, Lukyanov S, Lukyanov KA (2005) Fluorescent proteins as a toolkit forin vivoimaging. Trends Biotechnol 23(12):605–613

Clerc O, Greub G (2010) Routine use of point-of-care tests: usefulness and application in clinical microbiology. Clin Microbiol Infect 16(8):1054–1061

Culver HR, Daily AM, Khademhosseini A, Peppas NA (2014) Intelligent recognitive systems in nanomedicine. Curr Opin Chem Eng 4:105–113

Dayal S, Burda C (2008) Semiconductor quantum dots as two-photon sensitizers. J Am Chem Soc 130(10):2890–2891

Demchenko AP, Heldt J, Waluk J, Chou PT, Sengupta PK, Brizhik L, del Valle JC (2014) Michael Kasha: from photochemistry and flowers to spectroscopy and music. Angew Chem Int Ed 53(52):14316–14324
Devarajan P (2007) Emerging biomarkers of acute kidney injury. In: Acute kidney injury. Contrib Nephrol 156:203–212
Dong B, Xu S, Sun J, Bi S, Li D, Bai X, Wang Y, Wang L, Song H (2011) Multifunctional NaYF4: Yb 3+, Er 3 + @ Ag core/shell nanocomposites: integration of upconversion imaging and photothermal therapy. J Mater Chem 21(17):6193–6200
Dong Y, Wang R, Li H, Shao J, Chi Y, Lin X, Chen G (2012) Polyamine-functionalized carbon quantum dots for chemical sensing. Carbon 50(8):2810–2815. doi:10.1016/j.carbon.2012.02.046
Eisenblätter M, Ehrchen J, Varga G, Sunderkötter C, Heindel W, Roth J, Bremer C, Wall A (2009) In vivo optical imaging of cellular inflammatory response in granuloma formation using fluorescence-labeled macrophages. J Nucl Med 50(10):1676–1682
Feng L, Yang X, Shi X, Tan X, Peng R, Wang J, Liu Z (2013) Polyethylene glycol and polyethylenimine dual-functionalized nano-graphene oxide for photothermally enhanced gene delivery. Small 9(11):1989–1997
Frangioni JV (2003) In vivo near-infrared fluorescence imaging. Curr Opin Chem Biol 7(5):626–634
Gao X, Dave SR (2007) Quantum dots for cancer molecular imaging. Adv Exp Med Biol 620:57–73
Gao X, Cui Y, Levenson RM, Chung LW, Nie S (2004) In vivo cancer targeting and imaging with semiconductor quantum dots. Nat Biotechnol 22(8):969–976
Gao Y, Cui Y, Chan JK, Xu C (2013) Stem cell tracking with optically active nanoparticles. Am J Nucl Med Mol Imaging 3(3):232
Gioux S, Choi HS, Frangioni JV (2010) Image-guided surgery using invisible near-infrared light: fundamentals of clinical translation. Mol Imaging 9(5):237
Giskeødegård GF, Bertilsson H, Selnæs KM, Wright AJ, Bathen TF, Viset T, Halgunset J, Angelsen A, Gribbestad IS, Tessem M-B (2013) Spermine and citrate as metabolic biomarkers for assessing prostate cancer aggressiveness. PLoS One 8(4), e62375
Harvey MD, Bablekis V, Banks PR, Skinner CD (2001) Utilization of the non-covalent fluorescent dye, NanoOrange, as a potential clinical diagnostic tool – Nanomolar human serum albumin quantitation. J Chromatogr B 754(2):345–356
Helmchen F, Denk W (2005) Deep tissue two-photon microscopy. Nat Methods 2(12):932–940
Herbáth M, Papp K, Balogh A, Matkó J, Prechl J (2014) Exploiting fluorescence for multiplex immunoassays on protein microarrays. Methods Appl Fluoresc 2(3):032001
Hielscher AH (2005) Optical tomographic imaging of small animals. Curr Opin Biotechnol 16(1):79–88
Hong H, Yang Y, Zhang Y, Cai W (2010) Non-invasive cell tracking in cancer and cancer therapy. Curr Top Med Chem 10(12):1237
Ibraheem D, Elaissari A, Fessi H (2014) Gene therapy and DNA delivery systems. Int J Pharm 459(1):70–83
Jain KK (2007) Cancer biomarkers: current issues and future directions. Curr Opin Mol Ther 9(6):563–571
Jana A, Devi KSP, Maiti TK, Singh NP (2012) Perylene-3-ylmethanol: fluorescent organic nanoparticles as a single-component photoresponsive nanocarrier with real-time monitoring of anticancer drug release. J Am Chem Soc 134(18):7656–7659
Jokerst JV, Gambhir SS (2011) Molecular imaging with theranostic nanoparticles. Acc Chem Res 44(10):1050–1060
Kalchenko V, Neeman M, Harmelin A (2011) Whole-body imaging of hematopoietic and cancer cells using near-infrared probes. In: Advanced fluorescence reporters in chemistry and biology III. Springer Berlin Heidelberg, Springer Ser Fluoresc 10:329–346 doi:10.1007/978-3-642-18035-4
Kanekiyo Y, Tao H (2005) Selective glucose sensing utilizing complexation with fluorescent boronic acid on polycation. Chem Lett 34(2):196–197
Kartalov EP, Zhong JF, Scherer A, Quake SR, Taylor CR, Anderson WF (2006) High-throughput multi-antigen microfluidic fluorescence immunoassays. Biotechniques 40(1):85

Kessler MA, Meinitzer A, Petek W, Wolfbeis OS (1997) Microalbuminuria and borderline-increase albumin excretion determined with a centrifugal analyzer and the Albumin Blue 580 fluorescence assay. Clin Chem 43(6):996–1002

Kim S, Ohulchanskyy TY, Pudavar HE, Pandey RK, Prasad PN (2007) Organically modified silica nanoparticles co-encapsulating photosensitizing drug and aggregation-enhanced two-photon absorbing fluorescent dye aggregates for two-photon photodynamic therapy. J Am Chem Soc 129(9):2669–2675

Klohs J, Rudin M (2011) In vivo imaging of vascular targets using near-infrared fluorescent probes. In: Advanced fluorescence reporters in chemistry and biology III. Springer Berlin Heidelberg, Springer Ser Fluoresc 10:313-328 doi:10.1007/978-3-642-18035-4

Kumar AT, Raymond SB, Bacskai BJ, Boas DA, Georgescu R, Khismatullin D, Holt RG, Castagner JL, A'amar O, Bigio IJ (2008) Comparison of frequency-domain and time-domain fluorescence lifetime tomography. Opt Lett 33(5):470–472

Kuramitsu Y, Nakamura K (2006) Proteomic analysis of cancer tissues: shedding light on carcinogenesis and possible biomarkers. Proteomics 6(20):5650–5661

Lai J, Shah BP, Garfunkel E, Lee K-B (2013) Versatile fluorescence resonance energy transfer-based mesoporous silica nanoparticles for real-time monitoring of drug release. ACS Nano 7(3):2741–2750

Lee H, Akers W, Bhushan K, Bloch S, Sudlow G, Tang R, Achilefu S (2011) Near-infrared pH-activatable fluorescent probes for imaging primary and metastatic breast tumors. Bioconjug Chem 22(4):777–784

Leevy WM, Gammon ST, Jiang H, Johnson JR, Maxwell DJ, Jackson EN, Marquez M, Piwnica-Worms D, Smith BD (2006) Optical imaging of bacterial infection in living mice using a fluorescent near-infrared molecular probe. J Am Chem Soc 128(51):16476–16477

Liu C, Zhang P, Zhai X, Tian F, Li W, Yang J, Liu Y, Wang H, Wang W, Liu W (2012) Nano-carrier for gene delivery and bioimaging based on carbon dots with PEI-passivation enhanced fluorescence. Biomaterials 33(13):3604–3613

Maity AR, Saha A, Roy A, Jana NR (2013) Folic acid functionalized nanoprobes for fluorescence-, dark-field-, and dual-imaging-based selective detection of cancer cells and tissue. Chem Plus Chem 78(3):259–267

McShane LM, Altman DG, Sauerbrei W, Taube SE, Gion M, Clark GM (2005) Reporting recommendations for tumor marker prognostic studies. J Clin Oncol 23(36):9067–9072

Min Y, Li J, Liu F, Padmanabhan P, Yeow EK, Xing B (2014) Recent advance of biological molecular imaging based on lanthanide-doped upconversion-luminescent nanomaterials. Nanomaterials 4(1):129–154

Mohs AM, Mancini MC, Singhal S, Provenzale JM, Leyland-Jones B, Wang MD, Nie S (2010) Hand-held spectroscopic device for in vivo and intraoperative tumor detection: contrast enhancement, detection sensitivity, and tissue penetration. Anal Chem 82(21):9058–9065

Mueller AJ, Freeman WR, Schaller UC, Kampik A, Folberg R (2002) Complex microcirculation patterns detected by confocal indocyanine green angiography predict time to growth of small choroidal melanocytic tumors: MuSIC Report II. Ophthalmology 109(12): 2207–2214

Niemz A, Ferguson TM, Boyle DS (2011) Point-of-care nucleic acid testing for infectious diseases. Trends Biotechnol 29(5):240–250

Njiojob CN, Owens EA, Narayana L, Hyun H, Choi HS, Henary M (2015) Tailored near-infrared contrast agents for image guided surgery. J Med Chem 58(6):2845–2854

Ntziachristos V (2006) Fluorescence molecular imaging. Annu Rev Biomed Eng 8:1–33

Nurunnabi M, Khatun Z, Reeck GR, Lee DY, Y-k L (2014) Photoluminescent graphene nanoparticles for cancer photo-therapy and imaging. ACS Appl Mater Interfaces 6(15):12413–12421

Ogilby PR (2010) Singlet oxygen: there is indeed something new under the sun. Chem Soc Rev 39(8):3181–3209

Oh KJ, Cash KJ, Hugenberg V, Plaxco KW (2007) Peptide beacons: a new design for polypeptide-based optical biosensors. Bioconjug Chem 18(3):607–609

Ouellette AL, Li JJ, Cooper DE, Ricco AJ, Kovacs GT (2009) Evolving point-of-care diagnostics using up-converting phosphor bioanalytical systems. Anal Chem 81(9):3216–3221

Palacios-Rodriguez Y, Gazarian T, Rowley M, Majluf-Cruz A, Gazarian K (2007) Collection of phage-peptide probes for HIV-1 immunodominant loop-epitope. J Microbiol Methods 68(2):225–235

Pickup JC, Khan F, Zhi Z-L, Coulter J, Birch DJ (2013) Fluorescence intensity-and lifetime-based glucose sensing using glucose/galactose-binding protein. J Diabetes Sci Technol 7(1):62–71

Polom K, Murawa D, Ys R, Nowaczyk P, Hünerbein M, Murawa P (2011) Current trends and emerging future of indocyanine green usage in surgery and oncology. Cancer 117(21): 4812–4822

Qiao Y, Tang H, Munske GR, Dutta P, Ivory CF, Dong W-J (2011) Enhanced fluorescence anisotropy assay for human cardiac troponin I and T detection. J Fluoresc 21(6):2101–2110

Rajagopalan R, Uetrecht P, Bugaj JE, Achilefu SA, Dorshow RB (2000) Stabilization of the optical tracer agent indocyanine green using noncovalent interactions. Photochem Photobiol 71(3):347–350

Rouhanifard SH, Nordstrøm LU, Zheng T, Wu P (2013) Chemical probing of glycans in cells and organisms. Chem Soc Rev 42(10):4284–4296

Rutten M, Janes MA, Laraway B, Gregory C, Gregory K (2010) Comparison of quantum dots and CM-DiI for labeling porcine autologous bone marrow mononuclear progenitor cells. Open Stem Cell J 2:25–36

Selvam S, Kundu K, Templeman KL, Murthy N, García AJ (2011) Minimally invasive, longitudinal monitoring of biomaterial-associated inflammation by fluorescence imaging. Biomaterials 32(31):7785–7792

Sharrna P, Brown S, Walter G, Santra S, Moudgil B (2006) Nanoparticles for bioimaging. Adv Colloid Interface Sci 123:471–485

Shephard M, Peake M, Corso O, Shephard A, Mazzachi B, Spaeth B, Barbara J, Mathew T (2010) Assessment of the Nova StatSensor whole blood point-of-care creatinine analyzer for the measurement of kidney function in screening for chronic kidney disease. Clin Chem Lab Med 48(8):1113–1119

Singh R, Mukherjee MD, Sumana G, Gupta RK, Sood S, Malhotra B (2014) Biosensors for pathogen detection: a smart approach towards clinical diagnosis. Sens Actuators B 197: 385–404

Solanki A, Kim JD, Lee K-B (2008) Nanotechnology for regenerative medicine: nanomaterials for stem cell imaging. Nanomedicine (Lond) 3(4):567–578

Stefflova K, Chen J, Zheng G (2007) Killer beacons for combined cancer imaging and therapy. Curr Med Chem 14(20):2110–2125

Steiner M-S, Duerkop A, Wolfbeis OS (2011) Optical methods for sensing glucose. Chem Soc Rev 40(9):4805–4839

Sun Y, Zhu X, Peng J, Li F (2013) Core–shell lanthanide upconversion nanophosphors as four-modal probes for tumor angiogenesis imaging. ACS Nano 7(12):11290–11300

Tan HT, Low J, Lim SG, Chung M (2009) Serum autoantibodies as biomarkers for early cancer detection. FEBS J 276(23):6880–6904

Tang L, Ren Y, Hong B, Kang KA (2006) Fluorophore-mediated, fiber-optic, multi-analyte, immunosensing system for rapid diagnosis and prognosis of cardiovascular diseases. J Biomed Opt 11(2):021011-021011-10

Tang J, Kong B, Wu H, Xu M, Wang Y, Wang Y, Zhao D, Zheng G (2013) Carbon nanodots featuring efficient FRET for real-time monitoring of drug delivery and two-photon imaging. Adv Mater 25(45):6569–6574

Tra VN, Dube DH (2014) Glycans in pathogenic bacteria–potential for targeted covalent therapeutics and imaging agents. Chem Commun 50(36):4659–4673

Tsai H-c, Doong R-a (2004) Simultaneous determination of renal clinical analytes in serum using hydrolase-and oxidase-encapsulated optical array biosensors. Anal Biochem 334(1):183–192

Vahrmeijer AL, Hutteman M, van der Vorst JR, van de Velde CJ, Frangioni JV (2013) Image-guided cancer surgery using near-infrared fluorescence. Nat Rev Clin Oncol 10(9):507–518

Valanne A, Huopalahti S, Soukka T, Vainionpaa R, Lovgren T, Harma H (2005) A sensitive adenovirus immunoassay as a model for using nanoparticle label technology in virus diagnostics. J Clin Virol 33(3):217–223

van Dam GM, Themelis G, Crane LM, Harlaar NJ, Pleijhuis RG, Kelder W, Sarantopoulos A, de Jong JS, Arts HJ, van der Zee AG (2011) Intraoperative tumor-specific fluorescence imaging in ovarian cancer by folate receptor-[alpha] targeting: first in-human results. Nat Med 17(10):1315–1319

van Scheltinga AGT, van Dam GM, Nagengast WB, Ntziachristos V, Hollema H, Herek JL, Schröder CP, Kosterink JG, Lub-de Hoog MN, de Vries EG (2011) Intraoperative near-infrared fluorescence tumor imaging with vascular endothelial growth factor and human epidermal growth factor receptor 2 targeting antibodies. J Nucl Med 52(11):1778–1785

Vasan RS (2006) Biomarkers of cardiovascular disease molecular basis and practical considerations. Circulation 113(19):2335–2362

Vashist SK (2012) Non-invasive glucose monitoring technology in diabetes management: a review. Anal Chim Acta 750:16–27

Voura EB, Jaiswal JK, Mattoussi H, Simon SM (2004) Tracking metastatic tumor cell extravasation with quantum dot nanocrystals and fluorescence emission-scanning microscopy. Nat Med 10(9):993–998

Wang L, Li C (2011) pH responsive fluorescence nanoprobe imaging of tumors by sensing the acidic microenvironment. J Mater Chem 21(40):15862–15871

Wang C, Sahay P (2009) Breath analysis using laser spectroscopic techniques: breath biomarkers, spectral fingerprints, and detection limits. Sensors 9(10):8230–8262

Wang TJ, Gona P, Larson MG, Tofler GH, Levy D, Newton-Cheh C, Jacques PF, Rifai N, Selhub J, Robins SJ (2006) Multiple biomarkers for the prediction of first major cardiovascular events and death. N Engl J Med 355(25):2631–2639

Wang L, Zhao WJ, O'Donoghue MB, Tan WH (2007) Fluorescent nanoparticles for multiplexed bacteria monitoring. Bioconjug Chem 18(2):297–301

Wang C, Cheng L, Liu Z (2011a) Drug delivery with upconversion nanoparticles for multi-functional targeted cancer cell imaging and therapy. Biomaterials 32(4):1110–1120

Wang C, Tao H, Cheng L, Liu Z (2011b) Near-infrared light induced in vivo photodynamic therapy of cancer based on upconversion nanoparticles. Biomaterials 32(26):6145–6154

Wang C, Cheng L, Xu H, Liu Z (2012) Towards whole-body imaging at the single cell level using ultra-sensitive stem cell labeling with oligo-arginine modified upconversion nanoparticles. Biomaterials 33(19):4872–4881

Weinstain R, Segal E, Satchi-Fainaro R, Shabat D (2010) Real-time monitoring of drug release. Chem Commun 46(4):553–555

White AG, Gray BD, Pak KY, Smith BD (2012) Deep-red fluorescent imaging probe for bacteria. Bioorg Med Chem Lett 22(8):2833–2836

Wu Y, Zhang W, Li J, Zhang Y (2013) Optical imaging of tumor microenvironment. Am J Nucl Med Mol Imaging 3(1):1

Xie J, Chen K, Huang J, Lee S, Wang J, Gao J, Li X, Chen X (2010) PET/NIRF/MRI triple functional iron oxide nanoparticles. Biomaterials 31(11):3016–3022

Xiong L, Chen Z, Tian Q, Cao T, Xu C, Li F (2009) High contrast upconversion luminescence targeted imaging in vivo using peptide-labeled nanophosphors. Anal Chem 81(21):8687–8694

Xu C, Mu L, Roes I, Miranda-Nieves D, Nahrendorf M, Ankrum JA, Zhao W, Karp JM (2011) Nanoparticle-based monitoring of cell therapy. Nanotechnology 22(49):494001

Yang Z, Zhou DM (2006) Cardiac markers and their point-of-care testing for diagnosis of acute myocardial infarction. Clin Biochem 39(8):771–780

Yang M, Li L, Jiang P, Moossa A, Penman S, Hoffman RM (2003) Dual-color fluorescence imaging distinguishes tumor cells from induced host angiogenic vessels and stromal cells. Proc Natl Acad Sci 100(24):14259–14262

Zaheer A, Wheat TE, Frangioni JV (2002) IRDye78 conjugates for near-infrared fluorescence imaging. Mol Imaging 1(4):354–364

Zajac A, Song D, Qian W, Zhukov T (2007) Protein microarrays and quantum dot probes for early cancer detection. Colloids Surf B Biointerfaces 58(2):309–314

Zhang M, Bai L, Shang W, Xie W, Ma H, Fu Y, Fang D, Sun H, Fan L, Han M (2012) Facile synthesis of water-soluble, highly fluorescent graphene quantum dots as a robust biological label for stem cells. J Mater Chem 22(15):7461–7467

Zhang W, Peng B, Tian F, Qin W, Qian X (2013) Facile preparation of well-defined hydrophilic core–shell upconversion nanoparticles for selective cell membrane glycan labeling and cancer cell imaging. Anal Chem 86(1):482–489

Zhao X, Hilliard LR, Mechery SJ, Wang Y, Bagwe RP, Jin S, Tan W (2004) A rapid bioassay for single bacterial cell quantitation using bioconjugated nanoparticles. Proc Natl Acad Sci U S A 101(42):15027–15032

Zheng W, Huang P, Tu D, Ma E, Zhu H, Chen X (2015) Lanthanide-doped upconversion nanobioprobes: electronic structures, optical properties, and biodetection. Chem Soc Rev 44(6):1379–1415

Zou P, Xu S, Povoski SP, Wang A, Johnson MA, Martin EW Jr, Subramaniam V, Xu R, Sun D (2009) Near-infrared fluorescence labeled anti-TAG-72 monoclonal antibodies for tumor imaging in colorectal cancer xenograft mice. Mol Pharm 6(2):428–440

Chapter 15
Opening New Horizons

In this Chapter we try to evaluate the most rapidly progressing application areas of fluorescence sensing technologies and to make prognosis for future developments. The problem of lifting limitations on the detection of any required target will be reviewed. This will allow putting forward an ambitious task of simultaneous detection of not only the whole genome (which is tens of thousands of genes presented by DNA sequences) but also of proteome comprising all the results of their expression as the synthesized proteins. Their spatial location and their interactions are becoming in the mainstream of the present research. The sensors of emerging generation responding to strong demands from medicine and pharmacology will be discussed. With the appearance of this new level of personal diagnostics it is not only an *improvement of health care* is expected, but also the *influence on everyday life*, in a profound way. Monitoring all kinds of industrial processes and all aspects of human environment – all this will provide a deep influence on human society, which will become a 'sensorized' society.

It is expected that in twenty-first century the sensor science and technology will address two major problems presenting a great challenge. One is related to biological world and, particularly, to analysis of genomic and proteomic information. Possessing this information is an important step for starting active operation with it. This will open new presently even unpredictable possibilities in many areas: victory over human diseases, safety of the environment, superior agricultural products. The other problem refers to chemical world and is related to new synthetic products and new materials. Millions of new compounds are synthesized by chemical industry and many of them find industrial application and finally improve our life. However, their reactivity, safety in production and use, their degradation as waste products are largely unknown. Therefore, evaluation of their properties and their quantitative assay should go together to provide optimal use and optimal protection.

A.P. Demchenko, *Introduction to Fluorescence Sensing*,
DOI 10.1007/978-3-319-20780-3_15

15.1 Genomics, Proteomics and Other 'Omics'

Understanding complex functional mechanisms requires the global and parallel analysis of different cellular processes on several structural levels schematically presented in Fig. 15.1.

Recent completion of human *genome* mapping, which contains about 30,000 genes, was achieved with the aid of fluorescence-based techniques. Now this research continues in assessment of genomes of individuals, finding mutations and markers of diseases. Fully or in part, genomes of many microbes, plants and animals become available. Genomics has become a broad field of studying the organism's entire genome and identification of its variations, including those that may lead to inherited diseases.

The first step of expression of this information is the *transcriptome*, which is the set of all messenger RNA (mRNA) molecules, or "transcripts", produced in one or a population of cells. By using high-throughput techniques based on DNA microarray technology, the study of mRNAs expression level (transcriptomics) can be provided. The transcriptome can vary with functional state of the cell and under the action of external stimuli.

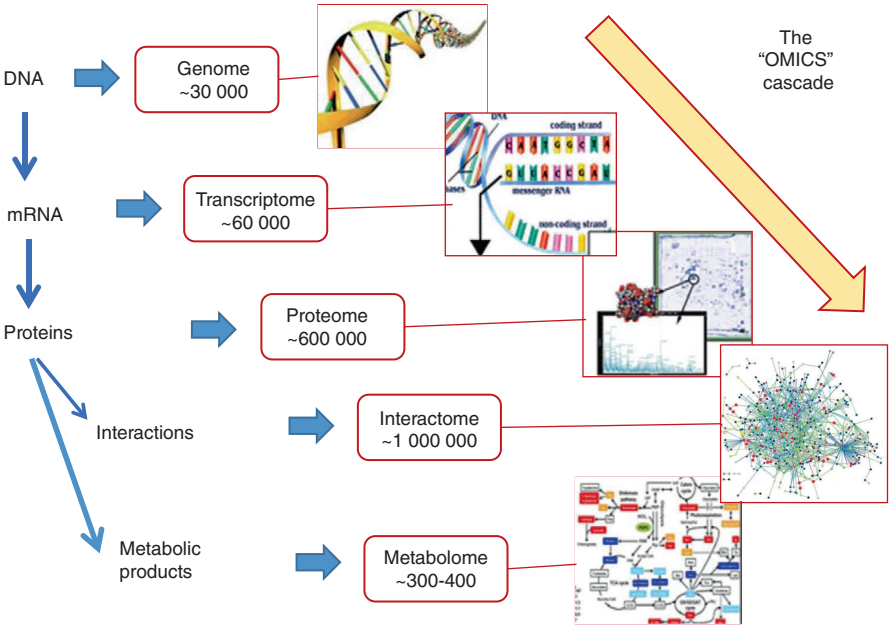

Fig. 15.1 Schematics of information flow from the genes to functional constituents of the living cell and the relations between genome, proteome, interactome and metabolome

Genomic information is not sufficient for understanding functioning of living cells. We have to understand the role of all proteins and their mutual interactions in a given organism. Therefore, completing its *proteome* is a new formidable task that will require new approaches and tools. Proteomics is the large-scale study of proteins, particularly of their structures and functions. The number of synthesized proteins in a human body is much larger than of the genes; it is estimated to be on the level of one million. Such protein diversity is due to their alternative gene splicing and post-translational modifications. The amount of particular protein types does not correlate directly with the amount of coding mRNA, so the expression level of every protein should be determined in the analysis of proteome. Proteomics is much more complicated than genomics also because, in contrast with genome constancy, a proteome differs from cell to cell and exhibits substantial changes on perturbations on cellular level.

The terms metabolome and interactome become increasingly popular. *Metabolome* represents metabolic profiling, the collection of all metabolites in a biological organism, which are the end products of its gene expression (Theodoridis et al. 2012). It includes also the consumed substances and those produced by symbiotic microorganisms. *Interactome* is the whole set of molecular interactions in cells (Vidal et al. 2011). It includes protein-protein interaction network and interaction networks with DNA, RNA, different metabolites. The study of metabolome and interactome produces further dramatic increase of a massive amount of information to be collected.

A new epoch is approaching, in which this information will be the most actively used in medicine, agriculture, environment protection and other areas. Fluorescence sensing becomes one of the major tools for exploring in full these new possibilities.

15.1.1 Gene Expression Analysis

After the sequencing of human genome was achieved, the DNA microarrays have become the major tools in *gene-expression studies*. The level of synthesized specific mRNA sequences on DNA templates is not only the reflection of genome but also the reflection of the functional state of the cell and the whole organism. This information is called the *gene expression profile* – the pattern of gene expression produced by the studied sample. Genes exhibit different expression levels on different steps of growth, cell cycle, differentiation, response to stimulation, etc. Therefore, quantitative determination of specific RNA molecules from biological samples is important for the study of regulated gene expression, which may indicate the change in many metabolic processes and in synthesis of many proteins using

mRNAs as synthetic templates. The expression profiles may help to understand, how these processes occur and how the disease may start on the background of normal process. They have started to be used as prognosis factors in practical medicine (Subramanian and Simon 2010; Kim and Paik 2010).

DNA and RNA quantification and sequencing offer an efficient strategy for rapid identification of unknown biological agents of bacterial and viral origin. It is expected to develop into sufficiently fast, accurate and cheap methodology to be used in routine clinical microbiology practice, where it could replace many complex current techniques with a single, more efficient workflow (Didelot et al. 2012).

The standard microarray technology known also as DNA chips allows obtaining the pattern of mRNA molecules synthesized in the cell, which can be referred as *transcriptome profiling*. It involves the production of amplified number of DNA copies of mRNAs, their labeling with fluorescent dye and deposition on DNA array formed by single-chain oligonucleotides (Sect. 11.3). Commonly, this allows only the identification of difference in composition between two samples that can be labeled with two dyes of different colors and hybridized together. Such *differential expression pattern* is obtained on the basis of two-color response from every array spots representing competitive binding of two samples of labeled sensing DNA. Polychromatic microarrays based on larger number of colors offered by quantum dots were also suggested (Shepard 2006). Meantime, the reported simultaneous hybridization of eight samples is probably the limit that can be reached with the basic pool-labeling technology.

The *sandwich hybridization* platform has larger potential for development, since it is not limited to comparative studies. This potential is harder to achieve reaching a comparative level of scalability with the double size of recognizing sequences. Meantime, there is a strong demand towards dramatic increase of the sensor scale in microarray technology. This requires assembling of a great number of sensor sites responsive to different analytes. If we take as a reference the human genome content of 30,000 genes, some applications may require much smaller capacity, but for some – the increased capacity is needed to include also the genes of harmful microbes, viruses, etc. This justifies the search for new analytical methods.

Thus, for many applications the problem of determining the *expression levels* of all the genes coded by the genome can be reduced to determining a smaller number of *characteristic genes*. When these special genes are screened-out from the human genome, the analytical procedure with them becomes more efficient. They become particular targets in gene expression analysis, and corresponding sensor sequences have to be spotted on a microarray. For reliable identification of these genes, the microarrays monitoring the expression of 10^3–10^4 genes simultaneously in one hybridization experiment can probably be sufficient. By comparing the series of such experiments one can construct the profiles of differentially expressed genes.

Regarding the total transcriptome analysis, new solutions have to be found. It is expected that they will involve further dramatic reduction of spot sizes, down to 100 nm and less, to produce *nanoarrays*. Their operation can be based on different

technologies. Attractive in this respect is a fiber optic platform with the highest presently achieved packing density of any array format (Lafratta and Walt 2008).

15.1.2 The Analysis of Proteome

Proteome profiling is the identification of all proteins expressed in a sample (Didelot et al. 2012). The proteome cannot be represented in full by the transcriptome, since the correlation between the extent of determined mRNA and that of synthesized (and active) proteins in a cell is not linear and the protein lifetimes in a cell vary over a broad range of values. Moreover, the proteins need to pass many post-translational modifications such as phosphorylation, glycosylation or oxidation that finally determine their functional activity. Therefore, in the protein world not only the expressed proteins but also their post-translationally modified forms may need to be determined.

Presently the leading positions in the studies of proteome are occupied by the methods of 2D electrophoresis, chromatography and mass spectrometry (Theodoridis et al. 2012). Meantime, the protein diversity estimated as ten billion species on earth (Frishman 2007) needs the new methods. They have to allow extremely high throughput and comparative analysis capability, and it is expected that fluorescent protein arrays will be developed to an extent satisfying the needs of researchers. It is desirable that the new methods should allow obtaining in a parallel way a very high capacity of information, which requires a high density of locating the sensor units. Such methods still do not exist, and the attempts to transfer the technology developed in hybridization of DNA by now are not very successful. The major difficulties are the following:

(a) Each protein has a unique chemistry and biochemistry. Unlike nucleic acids, there is no simple possibility for molecular recognition based on complementarity of target and sensor receptor sequences.
(b) There are no possibilities to achieve homogeneous labeling of proteins with a standard protocol. Broad variations in the extent of labeling are observed when the labeling reagent is introduced into protein pool.
(c) In a cell, in blood or in any other biosystem, the divergence of concentrations between individual proteins is tremendous, covering six orders of magnitude and more.
(d) Even larger divergence exists in protein affinities towards their natural substrates and ligands. These affinities do not correlate with the protein size or the number of groups available for intermolecular interactions.

Still, there are many attempts to develop the '*protein chips*'. One of operational concepts on this trend is borrowed from DNA hybridization assays. It is the comparison of proteomic maps of healthy and diseased cells (Borrebaeck and

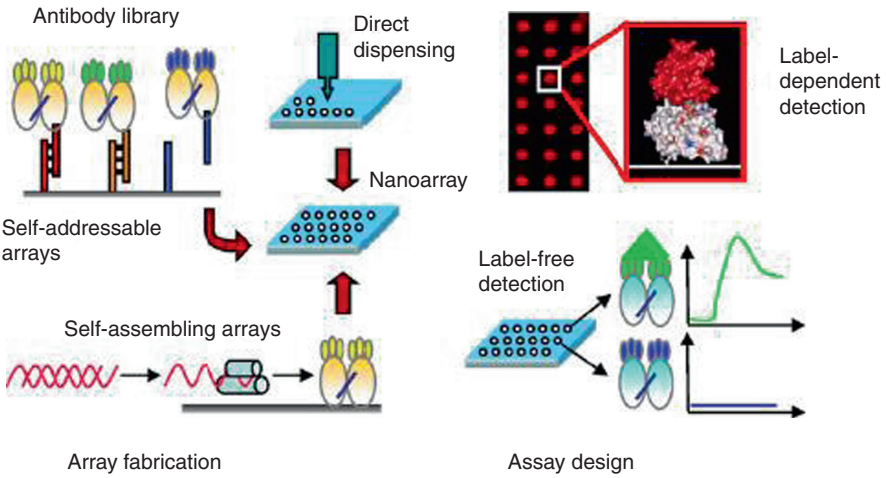

Fig. 15.2 The scheme illustrating one of the strategies for comparative global analysis of the proteome based on high-density antibody arrays (Borrebaeck and Wingren 2009). High-density nanoarrays with about 106 spots per mm^2 must be fabricated by direct dispensing, formation of self-addressable or, preferably, of self-assembling nanoarraying (*left*). Array readout must be provided either by label-dependent detection (fluorescence) or by using the label-free methods, such as advanced SPR or mass-spectrometry (*right*)

Wingren 2009). It uses the broad-scale detection based on antibodies as the recognition units (Fig. 15.2).

The first generation of *antibody microarrays* has demonstrated its potential for generating detailed protein expression profiles, or protein atlases, of human body fluids in health and disease, paving the way for new discoveries within the field of disease proteomics.

Presently such antibody arrays are applied for specific tasks, for instance, for identification of disease biomarkers. The proteomes derived from normal and tested (e.g., malignant) tissues are separated. These proteomes are used to select the antibodies, subsequently spotted on the chips. The selection is based on the availability of a highly functional phage display antibody library. The samples to be analyzed are then allowed to react with the functionalized microarray with subsequent read-out and analysis.

The process of designing highly miniaturized, high-density and high-performing antibody microarray set-ups have, however, proven to be challenging. Huge antibody libraries have to be created and the arrays of ~10 000 spots (*nanoarrays*) are needed. The process of fabricating such antibody arrays will be a key step in going from today's focused and semi-dense array layouts to truly high-density array designs. High demands will clearly be placed on the sensing technology. Ultrasensitive detection capabilities of fluorescence-based read-outs will probably remain the main choice of detection technology. To date, a variety of methodologies

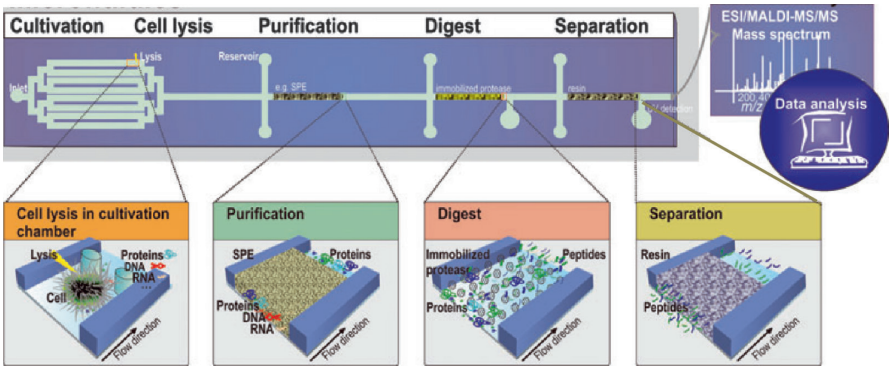

Fig. 15.3 Microfluidics-enabled proteomics workflows (Chao and Hansmeier 2013). Integration of several operations within a nanolitre-volume microfluidic platform enables providing sequential sample handling steps automatically, in a parallel way, without loss of efficiency and being coupled with very low sample consumption

that have been evaluated for label-free sensing in the array format, such as SPR and mass-spectrometry, cannot compete in resolution.

Microfluidic devices show high potential to overcome current limitations of proteomic analyses, especially in the biomedical field (Fig. 15.3). They allow avoiding numerous manual handling steps and sample transfers that increase the risk of introducing variability and contaminations that severely affect data analysis. In an idealized case, all sample handling steps would be integrated into a single platform, eliminating the need of sample transfer steps, and minimizing manual input, thus reducing variability that can be introduced by the experimenter (Chao and Hansmeier 2013). The major constraints here remain on the side of detection system.

The combination of separation and analytical techniques is a general approach for elucidation of whole proteome. Meantime the practical use of this information does not necessarily need determination of hundreds thousands components. Detection of specific proteins or some number of them is the most frequently requested. Then a specific binder to a specific protein can be developed and incorporated into an array. This long and difficult way needs a lot of effort. In the long run, it will allow scientists to understand the cell signaling and metabolic networks, which will further stimulate the rapid development of future therapeutics.

On this pathway, the selection of specific binders (receptors) for recognition of every protein on proteomic scale is extremely important. This issue is actively discussed in the literature (Taussig et al. 2007). In evaluating the technologies for production of the binders that could satisfy the demand, it is argued that it will be not the antibodies but a number of different binders that allow *in-vitro* evolution (Fig. 15.4).

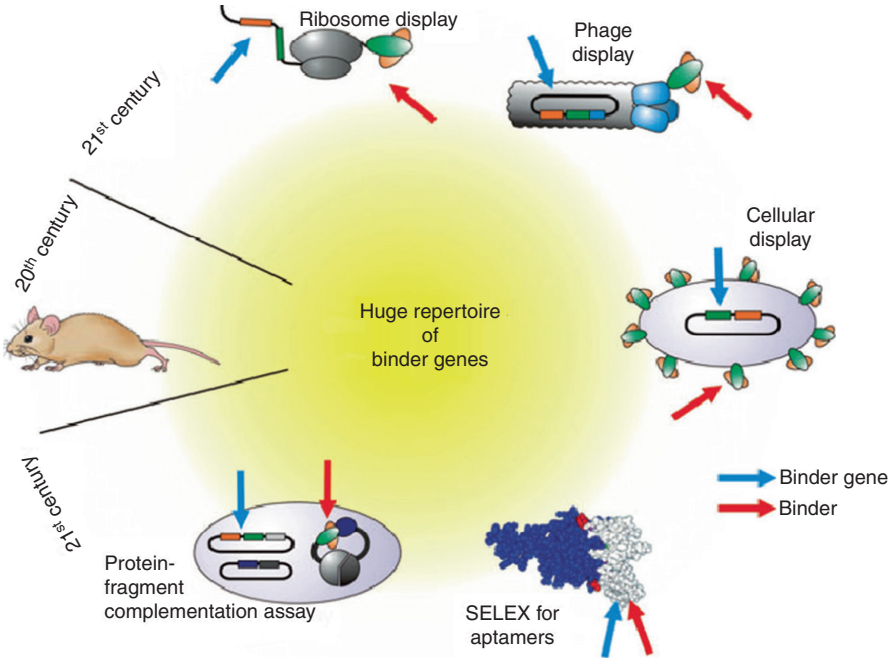

Fig. 15.4 The methods of generating the proteomic-scale binders prospective for technologies of twenty-first century (Taussig et al. 2007)

The systems based on the principle of *recombinant selection in vitro* link genotype and phenotype of the binding molecule. In contrast to antibodies they possess important features, such as:

(a) The absence of any limit on the scope of targets, which for antibodies is limited by the response of the immune system.
(b) The ability to achieve by multiple mutagenesis-selection rounds the binders that can be matured to the often necessary picomolar affinity.
(c) The ability to make the binders polyvalent and polyfunctional. Functional domains and tags can be fused to allow combining the binding abilities to different targets and also for binding targets together with the assembly to supramolecular structure or immobilization on a support.

It is believed that this will allow establishing a comprehensive, characterized and standardized collection of specific binders directed against all individual human proteins, including different variant forms and modifications. Establishing a binder collection will allow developing a new generation of high-throughput assay systems and protein-detection technologies.

To be able to address efficiently the protein function, expression, and localization on a proteome-wide scale, a lot of effort has been and will be directed toward the development of miniaturized and parallel assays (Uttamchandani et al. 2006). This approach will not be limited to antibodies but also involve synthetic peptides and

oligonucleotide aptamers selected from very large libraries (see Chapter 7) that will offer the solution of the problem of sensing on a scale of a ~100 000 species. Once developed, high density microarrays and nanoarrays will play a key role within proteomics in norm and disease for years to come.

15.1.3 Addressing Interactome

Intermolecular interactions between receptors and their ligands, nucleic acids and proteins, as well as between various proteins are tightly regulated within living cells (Petrey and Honig 2014). They compose innumerable molecular-level mechanisms that perform all biochemical processes and provide their regulation. Therefore an identification of particular molecular interactions is always a crucial step in cellular research. When improperly established, these interactions lead to pathology; they are the points of application of various drugs. In this respect, classical biochemical *in vitro* studies are not sufficient. The cellular environment cannot be adequately modeled *in vitro*, and localization of different functions in the cell is extremely important.

There were the times, when the major part of biochemical experiments started from preparation of cell homogenates, and then the fractions containing individual molecules were extracted from this mixture. In this way the information about intermolecular interactions (except those forming cell organelles) was lost. Presently all the efforts are made to localize the molecules inside the cells, to estimate their intracellular amount and to find their interaction partners. Meantime, a general approach for addressing this problem is absent (Vidal et al. 2011).

To date, cellular networks are mostly available for the "super-model" organisms, such as yeast, worm, fly, and plant (Fig. 15.5). The high-throughput interactome mapping relies upon genome-scale resources. Several types of interactome networks depictions seem very dense, but they represent only small portions of available interactome network maps, which themselves constitute only a few percent of

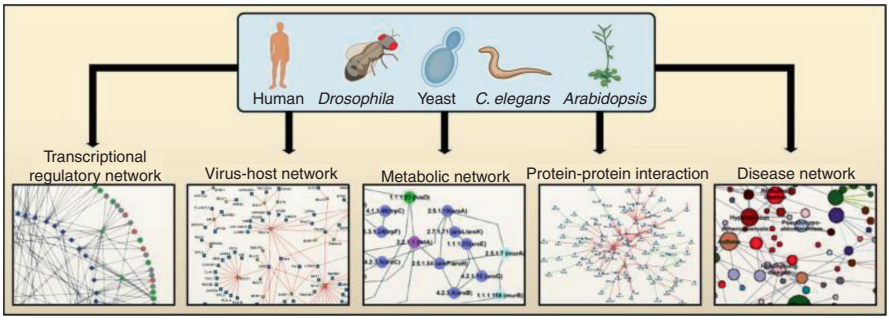

Fig. 15.5 Networks in cellular systems (Vidal et al. 2011). The field of interactome mapping has been helped by developments in several model organisms, primarily the yeast *Saccharomyces cerevisiae*, the fly *Drosophila melanogaster*, and the worm *Caenorhabditis elegans*

the complete interactomes within cells (Vidal et al. 2011). As it is shown in Fig. 15.5, they can be formally separated into several nodes.

The straightforward technique to track these interactions is to label two molecules of interest with spectrally distinct fluorescent markers and to study the cell images using either confocal, two-photon or total internal reflectance fluorescence microscopy with spectrally separated image acquisition in two detection channels. Then the interactions are revealed by observing signal co-localization between the two images (Comeau et al. 2006). This information can be considered as a strong predictor of interactions but still not the proof of their existence.

What is presently done efficiently is the *double labeling* of potential interaction partners. Then their interaction can be manifested from their co-localization in microscopy or from FRET observation. The labeling of both partners can be made in different ways. Presently, two strategies are popular:

(a) Fusion of the partner proteins with genetically incorporated emitters (visual fluorescent proteins and luciferase) (Pfleger and Eidne 2006).
(b) Affinity labeling with cell-permeating dyes targeted to genetically engineered sequences incorporated into partner proteins (Sects. 9.3 and 13.4).

The combination of these two approaches is often employed. Meantime, there are alternative possibilities that are less frequently used. They are based on genetic encoding into potentially interacting partners of complementary parts of a fluorescent or enzyme protein (*split proteins*). In this case the fluorescent moiety or the catalytic activity generating fluorescent product can be formed on their self-assembly (Piehler 2005), and their detection could witness molecular interactions inside the cell.

The networks of protein interactions mediate cellular responses to environmental stimuli and direct the execution of many different cellular functional pathways. Small molecules synthesized within the cells or incoming from the external environment mediate many protein interactions. The study of small molecule-mediated interactions of proteins is important to understand abnormal signal transduction pathways in cancer; they are essential for drug development and validation. Combining the FRET response with flow cytometric analysis is one of the pathways for achieving an efficient and versatile methodology (Chan and Holmes 2004).

Despite great progress, the structural information for the majority of proteins in the proteome is still unknown, which limits the application of assays based on genetic engineering. Therefore the study of interactions *in vitro* by presently established methods remains actual. Meantime, it is currently impossible to design a huge amount of molecules that could constitute the arrays for their detection and for characterization of their interactions. The *high throughput screening* (HTS) approach that will be discussed below in relation to drug discovery does not require prior information on protein structure and function and can be extensively used in interactome studies. The whole yeast proteome was deposited on microarray and many unexpected interactions were found on screening for their ability to interact with proteins and phospholipids (Zhu and Snyder 2003). These studies are expected to be extended to larger proteomes. The microarrays can also be used to screen protein-drug interactions and to detect posttranslational modifications.

15.1.4 Metabolomics

The cell's *metabolome* is its full complement of small-molecule metabolites. It is a direct indicator of phenotypic diversity of living cells and a nearly immediate readout of how cells react to environmental influences. Recent technological advances in accurate mass spectrometry and data analysis have revolutionized metabolomics experimentation. Activity-based and global metabolomic profiling methods allow simultaneous and rapid screening of hundreds of metabolites from a variety of chemical classes, making them useful tools for the discovery of novel enzymatic activities and metabolic pathways (Prosser et al. 2014).

Strong current interest exists in broad molecular profiling of single cells, since in view of cell diversity and the absence of their synchronization, the population-averaged parameters are low informative. However, the metabolome is very difficult to measure at the single-cell level because of rapid metabolic dynamics, the structural diversity of the molecules, and the inability to amplify or tag small-molecule metabolites (Zenobi 2013). Applied on a single-cell level, measurement techniques including mass spectrometry, capillary electrophoresis, and the application of fluorescence sensors have led to impressive advances in metabolomics. Even though none of these methodologies can currently measure the metabolome of a single cell completely, rapidly, and nondestructively, progress has been sufficient such that the field is witnessing a shift from feasibility studies to investigations that yield new biological insight. Rapid progress is expected in such fields of application as cancer biology, stem cell research, and monitoring of xenobiotics and drugs in tissue sections at the single-cell level.

15.1.5 Outlook

It is hard to imagine how challenging is the goal of complete characterization of transcriptome, proteome and interactome in view of the massive amount of information that has to be obtained and analyzed in parallel. But the process has started, the information is highly needed and the tools, may be still on the basic level, already exist (Lafratta and Walt 2008). Next generations of these tools may speed up the progress tremendously. Broader scaling and higher level of miniaturization will definitely be requested, up to transition from microarrays to nanoarrays and further to manipulations with single molecules and their complexes.

Immense data sets, with hundreds of thousands to millions of data points, necessitate a new level of computer processing (Berger et al. 2013). Drawing meaningful correlations among the data of this size is beyond human capability, therefore, new powerful and user-friendly algorithms have to be developed.

Comparative analysis will continue to be an efficient approach in these studies, at least in observable future. Therefore, introduction of 'standard' transcriptome, proteome and interactome will be needed for every type of human cells, and on their background a new step in research will get a new impulse.

15.2 The Sensors to Any Target and to Immense Number of Targets

In order to be ready to address new challenges and new goals, we need highly specific targeting of particular analytes together with collecting a great massive of information about related and unrelated analytes. This information should be collected in a systematic way and in reasonably short time to provide timely decisions and actions.

15.2.1 Combinatorial Approach on a New Level

The *trial-and-error* approach is still widely used for chemical sensor design, owing to our inability to predict structural requirements for a perfect sensor for each analyte and in view of a great number of potential analytes. Therefore, the implementation of *combinatorial concept* is the most prospective possibility for the discovery of both the binding partners and fluorescent building blocks. This concept is based on the production of large libraries of compounds or devices and providing their multi-step selections. Only on initial phase of establishing the library, the concepts of 'classical' *rational design* could be applied, but they do not lead directly to individual design and production (Lavigne and Anslyn 2001).

Many requirements have to be satisfied for successful application of combinatorial approach. First is the building of *proper library*, the size of which should be large enough to incorporate successful hits and the building blocks that are easy to construct and reproduce. Then, there should be efficient *search algorithm* and its practical realization in screening techniques, an optimal methodology of evaluating successful hits, a formation of sub-libraries of second generation, etc. Testing of successful candidates should be multiparametric, with the use of optimization algorithms. Despite all these difficulties, it should be realized that this is the only methodology foreseen to satisfy the task displayed in the title of this Section.

Combinatorial methodology has started to be successfully applied in various fields, such as drug discovery, catalysis, bimolecular interaction studies or discovery of sensor receptors (Rasheed and Farhat 2013). *Combinatorial chemistry* has revolutionized approaches to drug candidate synthesis and screening by the possibility of simultaneous testing of a great number of related compounds. These activities are stimulated by pharmaceutical industry, which is oriented to development of new drugs that are commonly the inhibitors of different metabolic pathways. Interestingly, the platforms originally exploited in the field of biosensors (such as microtiter plates, microarray technologies or fiber optic tips), have been applied for facilitating the high-throughput drug screening (Sect. 15.4).

The other actual field of research is the development of new fluorescent dyes (Chap. 3) with improved reporter properties. The only remark that has to be made here is that the combinatorial concept is applicable in search within quite different

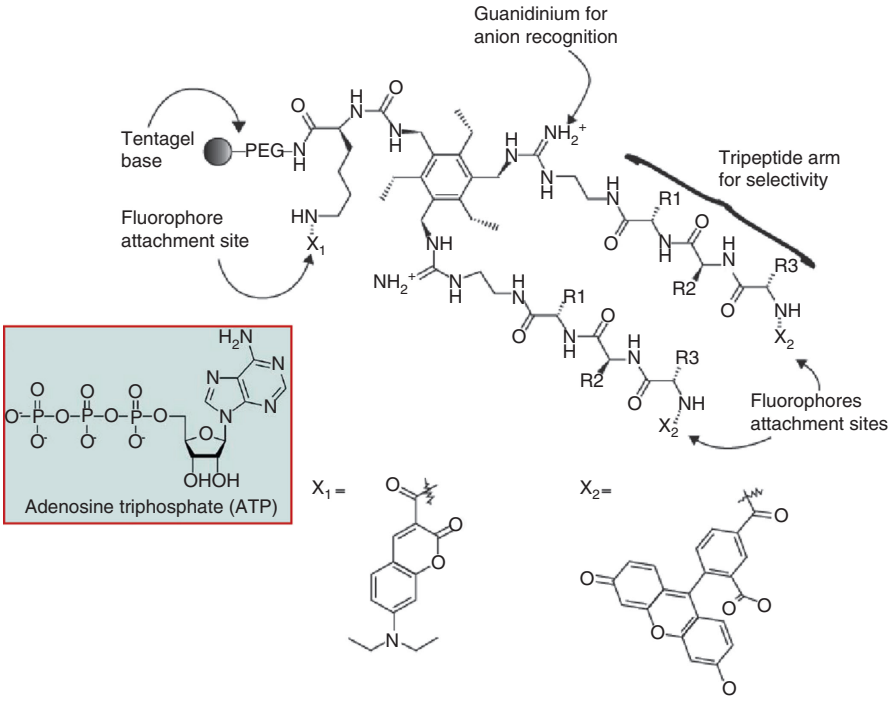

Fig. 15.6 Example of some probes for ATP sensing based on resin-bound tripeptides generated by combinatorial methods (Schneider et al. 2000)

types of reporters, such as various fluorescent dyes with ion-chelating function (Szurdoki et al. 2000). It is equally well applicable for the selection of support materials (Apostolidis et al. 2004). Novel nanoparticles and their composites (Chaps. 4 and 5) are still waiting for their improvement based on combinatorial design principles.

Solid-phase organic synthesis is a well-established tool for the production of combinatorial libraries. Being mainly used for drug discovery, now it finds application for the design of resin-bound chemosensors. Thus, for the discovery of ATP binding sensors, the split and pool method was used to generate a combinatorial library of more than 4000 different resin-bound tripeptides (Schneider et al. 2000). After selecting the ATP binding receptor, the fluorophores were appended to the ends of the peptide chain in order to produce a reporter signal (Fig. 15.6).

Antibodies can be considered as the products of directed evolution ‘in a body’ (Sect. 7.3). They develop guided by particular target, antigen, in several amplification-selection steps. Presently they are the most available molecules that can allow detection of huge variety of targets. The SELEX procedure used in generation of aptamers is based on the same selection-amplification principle but is performed with human hands (Sect. 7.6) and generation of random peptide libraries (Sect. 7.5) offers new possibilities. This principle can be further explored. New tools are

needed in the conditions, in which old tools such as antibodies have reached the limit of their perfection.

The use of the so-called *protein scaffolds* (Sect. 7.4) for the generation of novel binding proteins via combinatorial engineering has recently emerged as a powerful alternative to natural or recombinant antibodies. This concept requires an extraordinary stable protein architecture tolerating multiple substitutions or insertions at the primary structural level. With respect to broader applicability it should involve a type of polypeptide fold which is observed in differing natural contexts and with distinct biochemical functions, so that it is likely to be adaptable to novel molecular recognition purposes. It is expected that such artificial receptor proteins should be based on monomeric scaffolds and small polypeptides that are robust, easily engineered, and efficiently produced in inexpensive prokaryotic expression systems.

Today, the progress in *protein library* technology allows for the parallel development of both antibody-clone and scaffold-based affinity units. Both biomolecular tools have the potential to complement each other, thus expanding the possibility to find an affinity reagent suitable for a given application. The repertoire of protein scaffolds hitherto implied for combinatorial protein engineering purposes will probably be further expanded in the future, including both additional natural proteins and de novo designed proteins, contributing to the collection of libraries available at present (Taussig et al. 2007).

We also note that the combinatorial approaches have started to be used to increase the performance of *diagnostic devices* for both clinical and field uses with optimization on the level of performance (Moats and Sullivan 2004). This offers substantial improvement in detection of many analytes. The research efforts in this direction are motivated by a general need to detect as many different pathogens or hazardous materials as there may exist in the studied medium using the smallest, most inexpensive and fastest system possible. These devices would be powerful if the effective library schemes are invented. It is important that the mathematical frameworks be more and more actively used in the development of novel combinatorial biosensor systems for their optimization and performance prediction. In addition to providing linear response to particular targets, the novel sensors will be able to perform logical operations, as described in Sect. 8.7.

15.2.2 Toxic Agents and Pollutants Inconvenient for Detection

In Chap. 12, we already mentioned that the present researchers in sensor development favor addressing either one of the two types of targets, ‘convenient’ and ‘needed’. Convenient are those that demonstrate in the simplest way the advantages of newly developed technology. Needed are those, for which there is a range of potential applications and the market. We will not discuss the cases ‘convenient but not needed’ but better concentrate on those that are highly needed but very inconvenient. One of them is the sensor for *dioxin*, which is the potent industrial

pollutant, producing strong accumulating effect on human health. Until recently, this toxic agent was determined only by combination of mass spectrometry and gas chromatography, which is time-consuming and very costly. The problem is the extremely low solubility of this compound in common solvents and the absence of ability to form strong and specific noncovalent bonds that could be efficiently used in recognition. Solution of this problem was found by synthesizing a pentapeptide for its highly sensitive on-bead detection assay (Nakamura et al. 2005).

For finding this peptide, a full peptide library consisting of 2.5 million possible amino acid combinations was constructed by a solid-phase split synthesis approach using 19 natural amino acids. The beads with immobilized peptides were then subjected to a competitive binding assay using 2,3,7-trichlorodibenzo-p-dioxin and N-NBD-3-(3′,4′-dichlorophenoxy)-1-propylamine (NBD-DCPPA) as a competitor. Two almost identical pentapeptides, FLDQI and FLDQV that could bind dioxin were identified from combinatorial library. The peptides synthesized on resin beads in combination with NBD-DCPPA constitute an attractive assay to determine dioxin concentrations. The fluorescence intensity of the beads measured using fluorescence microscopy reports on dioxin-dependent binding of fluorescent competitor to the beads after making a calibration curve for the dioxin concentrations. On the next step, to optimize the peptide sequence, a one-amino acid-substituted library was prepared with the inclusion of nonnatural amino acids. It was found that the amino acids internal in sequence, LDQ, could not be substituted without loss of affinity, which indicates their essential role in recognition of dioxins. From this result one may derive an unexpectedly strong potential of short peptides as a practical sensor material targeting low molecular weight compounds, including such ‘inconvenient’ as dioxin.

This detection system was tested on real environmental samples (Inuyama et al. 2007). About 0.5 nM (150 pg ml^{-1}) of 2,3,7,8-tetrachlorodibenzo-p-dioxin (2,3,7,8-TeCDD) could be detected under the optimized conditions.

On a general scale, *endocrine disruptors* represent a large family of industrial pollutants that in extremely low concentrations may bring irreversible changes in human health and affect also domestic animals and wildlife. They have to be identified and determined in the environment and in human body at extremely low concentrations (Rodriguez-Mozaz et al. 2004). Presently, tens of thousands of chemicals are under consideration for screening as potential endocrine disruptors, so it is essential that rapid, sensitive, and reproducible high-throughput screening systems targeting them have to be developed. This is a difficult but feasible task.

15.2.3 The Problem of Coding and Two Strategies in Its Solution

Rapid, multiplexed, sensitive and specific simultaneous detection of immense number of analytes is in great demand for gene profiling, drug screening, clinical diagnostics and environmental analysis. In all systems that serve for this purpose,

individual result on particular analyte binding-reporting should be recognized from other results. Therefore it is necessary to supply each sensor element with a different 'barcode'. The construction of such barcodes based on combination of emitters providing specific patterns of fluorescence spectrum was described in other chapters of this book. Here we approach this issue from a more general perspective. There are two possibilities for such barcoding.

One is the *positional encoding*. It requires providing spatial resolution in location of sensor elements, so the coding is based on *spatial location of sensors* deposited on solid support. This possibility is used in *spotted microarray* technologies (Sect. 11.3). In this case, the sensor elements should be necessarily immobilized on the surface, and spatial resolution is needed in reading the response signal. This approach operates with all 'responsive' sensing methodologies.

If 'irresponsive' labeling is applied, there are two possibilities. First of them is an *additional washing* operation needed to remove the unbound reporter dye. Presently it is commonly used. The other, more progressive, offers excitation of only those reporters that are *located in a pre-surface layer* by exploring electrochemiluminescence (Sect. 10.1), evanescent wave excitation (Sect. 10.6) or plasmonic enhancement on interaction with metal surface (Sect. 10.7). In these cases the targets that are located not at interface do not interfere with the analysis. Meantime, this strategy is not applicable or convenient if the target size is larger than pre-electrode area or the layer excited by evanescent wave (such as the living cells) and if the response is limited to slow target diffusion to the surface. It is also not beneficial if the response units are the large particles themselves. This can make steric difficulties and does not allow exploring in full the particle surface.

The other possibility is to provide *sensing in solutions*, so that many sensor molecules or particles are dissolved together in an analyzed system. Reaction of target binding in solutions has its own advantages (such as faster diffusion rates), but without additional coding the resolution of fluorescent signal from different sensors in the system is commonly insufficient. In this case, every type of sensor units should contain a specific fluorescent 'barcode'. This is the strategy of *optical encoding*. Following this strategy, we have to be able to read a huge number of different barcodes. The barcode can be connected or not connected with specific response to target binding. The best for the purpose of their selective detection is flow cytometry and its microscopic versions (possibly realized in microflow devices), in which the sensor particles pass through detector in line, one by one, and during this passage, different types of reading signal can be obtained. With flow cytometry, the barcodes based on fluorescence intensity profile can be used efficiently (Rasheed and Farhat 2014). If the particles with two or three emissions on different intensity levels are used, this expands the possibility of barcode recognition to many millions (Wang et al. 2007). In some simple cases, other methods based on chromatographic separation can also be used.

In parallel with coding the sensor units, the problem of obtaining the reporter signal should be solved (see Sect. 11.4). For every sensor, the two signals identifying the sensor and identifying target binding to this sensor should not interfere.

15.2.4 Prospects

In this Section we outlined the areas, in which the rapid progress in the nearest future is expected in response to strongest demand for more efficient sensors. The reader must be convinced that already on the present step of research and technology development there is technical possibility to satisfy any demand for detecting any target and any (reasonable) number of targets. In almost all the areas where the sensor technologies are applied, our present ability to obtain the results is ahead of our ability to properly analyze them. The proper balance in this respect is expected to be achieved soon.

15.3 New Level of Clinical Diagnostics

Revolutionary changes are emerging in clinical diagnostics, in which the methods based on fluorescence detection have already become the most frequently used (see Chap. 14). Invasive techniques have to be substituted for *noninvasive* or *low invasive* ones. The traditional samples of blood and urine taken for analysis can be strongly reduced in size. Together with the possibility of dramatic miniaturization, the biological fluids available in small quantities, such as microscopic skin cuts, saliva, sweat and tears become applicable for diagnostics. Multiplexing techniques allow sensing many targets together and thus determine many clinically useful parameters. Their combined evaluation leads to more reliable diagnosis and clinical decisions.

The ideal diagnostic instrument would be a device that is simple to use, hand-held and inexpensive, combining high specificity with sensitivity in the presence of optically dense organic material, such as blood, and capable of detecting a number of required targets simultaneously. The technological progress described in this book allows predicting the appearance of such instruments in a broad-scale use already in the nearest future. In this respect, of special interest are the problems that, at present, seriously limit these applications. They are in speed of analysis and in sensing in the whole blood without separation of components. We will discuss different possibilities for their solutions.

15.3.1 The Need for Speed

An important factor is the duration of analytic procedure from sample application to obtaining the result. Direct sensing substituting traditional sandwich techniques as described in Chap. 1 can allow its dramatic reduction by eliminating the steps additional to that of target binding. Miniaturization of the system can further increase the speed by reducing the time for target diffusion preceding the binding

step. Meantime, even in these cases the analysis may take many minutes and hours. This is because most biological recognition events, such as the antigen–antibody interactions and DNA hybridization, are kinetically slow. The time is needed not only for the target diffusion in space, but mostly for structural adaptation of two interacting partners and their multi-point binding (molecular recognition).

In this regard, a new platform technology based on *microwave acceleration* of metal-enhanced fluorescence (described briefly in Sect. 10.7) deserves close attention (Aslan and Geddes 2005). It combines the benefits of metal-enhanced fluorescence with the use of low power microwaves to accelerate the sensor-target molecular recognition. The metal-enhancement significantly increases the fluorescence signals of fluorophores in close proximity (~10 nm) to metallic nanostructures. Its combination with the low-power microwave heating it leads to the development of assays that can become completed within few seconds. This new technology can be potentially applied to many other important assays, such as to the clinical assessment of myoglobin (see below), where both the speed and sensitivity is paramount for the assessment and treatment of acute myocardial infarction.

15.3.2 The Whole Blood Sensing

The fluorescence signal of interest is often corrupted by high *background luminescence*, and often it is the major factor affecting the sensitivity of fluorescence-based medical diagnostic tests. Several approaches have been suggested to minimize the background signal caused by the sample matrix (e.g., serum or whole blood in clinical diagnostics). The most efficient of them are based on the application of time-resolved or time-gated emission of luminophores with long lifetimes, and the use of up-converting nanoparticles or fluorophores with two-photon excitation (Baker et al. 2000). Because of high optical density, light-scattering and fluorescence background of the blood, clinical tests commonly start from serum or plasma, in which the blood cells have been removed. Alternatively, washing steps have to be applied after the application of sample (Von Lode et al. 2004). Therefore, there is a continuous and unequivocal need for the development of better reporter molecules and/or detection methods for the direct analysis of whole blood samples.

Several pathways can be outlined for that. Primarily it is the improvement of methods based on *two-photon detection* and also on using *up-converting luminophores* (Xu et al. 2013). This allows decreasing the light-scattering background and the absorption of pigments. The second important possibility is to raise the reporter signal over the background by using the emitters with brighter response and longer lifetimes, which is offered by designed nanocomposites.

Immunoassay being one of the most widely used biomedical diagnostic methods can be developed in microfluidic lab-on-a-chip format (Jiang et al. 2011). Such merging of two technologies allows achieving not only the sensitivity and specificity of assay but also exploring the advantages of portability, integration, and automation leading to a pathway for point-of-care diagnostics using the unprocessed samples such as the *whole blood*.

15.3.3 Testing the Non-invasive Biological Fluids

Non-invasive sample collection is a very interesting possibility for multiparametric monitoring of health status. *Human saliva* is an attractive body fluid for the disease diagnosis because its collection is simple, safe and noninvasive. The information content of saliva-based testing is significant and is not limited to oral infectious diseases. It is known that the clinically relevant analyte concentrations in saliva mirror the tissue fluid levels. Furthermore, recent studies have recognized the relevance of its protein composition to the development and progression of oral (Samaranayake 2007), as well as systemic diseases, including HIV infection (Martinez-Manez et al. 2005). Saliva can be used to reliably detect viral hepatitis A, B and C and genetic biomarkers related to certain types of cancer. However, whereas many point-of-care diagnostic methods already exist for blood-borne analytes, the development of similar saliva-based techniques is still in its infancy. The use of saliva has been hindered by inadequate sensitivity of previously applied methods to detect the lower salivary concentrations of many constituents compared to serum. Development of nanoscale and microscale biosensor technologies to detect salivary protein and genetic biomarkers for point-of-care applications has the prospect to resolve this problem.

It is expected that comprehensive analysis and identification of the proteomic content in human whole saliva will not only contribute to the understanding of oral health and disease pathogenesis, but also form a foundation for the discovery of saliva protein biomarkers for human disease detection (Hu et al. 2007). With the fast development of proteomic technologies, the saliva protein biomarkers will be developed for clinical diagnosis and prognosis of human diseases in the future.

One such biomarker, whose measurement in saliva could potentially contribute in a significant manner to the understanding and diagnosis of disease, is the C-*reactive protein*. This is an important inflammation marker and cardiovascular disease predictor that is derived from the liver and whose production is regulated by cytokines. It was found to be a stronger predictor of coronary heart disease. Microsystem-based diagnostics of this protein with the use of saliva is on the steps of active development (Christodoulides et al. 2005).

It should be noted that the diagnostically important concentrations of *glucose* can be measured not only in blood, but in different body fluids, such as tears, saliva and sweat (Mitsubayashi et al. 1995). This opens many possibilities for designing the simple and convenient sensors for continuous monitoring of this and other metabolites.

15.3.4 Gene-Based Diagnostics

Gene-based molecular diagnostics is changing the practice of medicine and will continue to do so for the foreseeable future (Finan and Zhao 2007). Two major fields that are actively explored now are the *detection of pathogens* and finding the *disease-related gene mutations*. The major underlying principle of these diagnostic tests is

the comparison of two nucleic acid sequences for their presence in tested sample. The sequence used for comparison is labeled and introduced into the system as it is described in Sect. 12.4. Microarray recordings of mRNA expression profiles allow not only detection but also classification of tumors based on a distinct set of signature genes that comprise differently expressed transcripts between the cancer types. The gene expression patterns and the factors that control them represent potential and potent targets for therapeutic intervention. Application of similar approach to diagnostics of other diseases is expected to have a great prospect.

Automation is the current trend for high-volume molecular testing of *infectious diseases*. Molecular profiling of various diseases using genomic or proteomic approaches opens up a molecule wonderland with promise and emergence of new molecular-based testing. It will likely impact the practice of medicine and allow introduction of highly needed personalized testing.

Once a complex *gene expression pattern* valuable for diagnostics can be reduced to a few genes, the biosensor-based detection becomes practical and advantageous for cancer clinical testing, since it is faster, more user-friendly, less expensive and less technically demanding than microarray or proteomic analyses. However, a significant technical development is still needed, particularly for protein-based biosensors.

15.3.5 Prospects

Biological fluids are the source of rich information about the health condition of human organism. They contain the proteins that can serve specific biomarkers of the disease. Increased attention is also directed to specific *DNAs circulating in blood* as disease biomarker (Schwarzenbach et al. 2011). A number of such molecular diagnostic tools have been identified already, but their much larger number wait for discovery. Traditional and most frequently used diagnostic fluids are blood and urine. Miniaturization of sensor devices causes not only dramatic reduction in the volume of collected test samples, but also increases the speed and precision of their analysis, which can be further improved by application of low-energy microwaves. Saliva, sweat and tears, which can be collected in a noninvasive way, were previously considered as the biological fluids of minor diagnostic value. The situation changes dramatically with miniaturization and increase of precision of diagnostic tools.

15.4 Advanced Sensors in Drug Discovery

Nowadays the field of drug discovery has passed the period of empirical search and relies strongly on the achievements of molecular and cellular biology. *In vitro* search for particular biological activities and in-cell testing becomes common in seeking for optimal drug candidates. Combinatorial libraries generated by chemical synthesis together with immense number of natural compounds that are mostly extracted

from the plants form the multi-million number of drug candidates. Therefore the major tool becomes the *high-throughput screening* (HTS), which is the process of testing a large number of diverse chemical structures against disease targets to identify 'hits'. This approach is based on the concept, which assumes that when sufficiently large library of compounds is tested, the chance for discovering a new active compound is increased. Traditional drug screening methods cannot compete with HTS in simplicity, rapidness, cost, and efficiency.

15.4.1 High Throughput Screening

Fluorescence-based techniques are among the most important detection approaches used for HTS due to their many advanced features, such as high sensitivity and amenability to automation, simplification, miniaturization, and speeding up assays (Bosch et al. 2007). As a general technology, HTS involves highly sensitive testing system based on several components. They are an automated operation platform, a specific screening model (*in vitro*), an abundant components library together with a data acquisition and processing system. This combination makes possible the screening of more than 100,000 samples per day. Therefore, the highly multiplexed optical-biosensor arrays become the most important tools in this technology. The capacity of such microarrays is growing, and presently the application of the plates with 1,536 wells is not uncommon.

High throughput screening should be *multiparametric* and involve many variables, such as:

(a) *Specific activity*, which is commonly the binding to particular target in the organism leading to inhibition of some enzyme system or antagonism to some receptor. The array composed of targets or target analogs is an appropriate strategy, at least on the first step of testing. In order to estimate the drug dissociation constant K_d, the series of targets with different affinities should be applied. In view of substantial dilution of drugs on administration into patient's body, of pharmacological interest are commonly only those of them, which have K_d in the concentration range of 10^{-7}-10^{-9} M or lower.
(b) *Toxicity* (or selectivity in toxicity between normal and malignant cells). The arrays of whole-cell biosensors may be a great help for that (Durick and Negulescu 2001). For instance, a disruption of cell integrity can be the most easily revealed with such fluorescence dyes as propidium iodide.
(c) *Pharmacokinetics*, which is the determination of fate of drug in the body. It allows and requires many preliminary *in vitro* tests. Fluorescence and long-lifetime luminescence-based techniques provide the proper response in acquiring this information (Gomez-Hens and Aguilar-Caballos 2007).

Pharmacokinetics itself includes many parameters, such as chemical (biochemical) stability in biological media, ability to cross biological membranes, affinity towards serum albumin and other carriers in blood, ability to be destroyed by microsome oxidation system, etc. To some extent, this information can be obtained in

simple fluorescence tests. For instance, the binding to serum albumin can be provided based on competitive substitution for drugs of fluorescent dyes (Ercelen et al. 2005). The liposome-based biosensors are useful by their ability to model the drug affinity towards biological membrane and its permeability through it (Przybylo et al. 2007).

Regarding fluorescence detection method it is the ultimate means in operation with high-capacity microarrays. Here the preference is presently given to polarization assays and to lifetime-based or lifetime-gated detection with long-lifetime luminophores. However, other detection methods, such as bioluminescence, offer good potential, primarily because of their ability to provide low background emission. Fluorescence microscopy-based methods that allow decreasing the sample volume to femtoliters have also found many applications in HTS (Eggeling et al. 2003) and the scope of these applications is expected to increase.

15.4.2 Screening the Anti-cancer Drugs

Screening for anti-cancer substances is one of the most important activities in drug discovery. Primarily the tests that are usually done are on the *cell toxicity* and on the difference in toxicity between the lines of normal and cancer cells using viability assays. An inherent problem with this approach is that all the compounds that are toxic and growth inhibitory, irrespective of mechanism of action, will score positive. Therefore, the search for anti-cancer drugs should involve the tests for specific binding to the cancer cells and for their ability to influence their life in culture by inducing *apoptosis* (the programmed cell death).

There are two major approaches to detect apoptosis on its early stages. One is targeted at detection of protease that is activated on apoptosis, called Caspase 3. An interesting assay method available for HTS was developed recently (Tian et al. 2007). It employs a stable HeLa cell line expressing a biosensor protein that can be split by Caspase 3 generating the FRET-based response. Activation of *Caspase 3* cleaves this sensor protein with the disruption of FRET donor-acceptor pair, which causes its fluorescence emission to shift from a wavelength of 535 nm (green) to 486 nm (blue). A decrease in the green/blue emission ratio thus gives a direct indication of apoptosis.

The other approach for detecting the apoptosis is focused on cell membrane and is based on its property to expose anionic lipids to the outer leaflet on apoptotic transformation (Demchenko 2013), as discussed in Sect. 13.6. Fluorescence techniques are extensively used for detection of these changes.

15.4.3 Future Directions

High-throughput screening, which includes automated preparation of a large number of samples and then screening of their properties in multi-well plates or multipoint arrays allows both molecular and cellular testing. It improves the efficiency

of research not only in drug discovery, but also in many other areas, from chemical synthesis to food processing and toxicology. There are two current limits that will gradually go away with the advancement of technology. One is the size (scale) of arrays that has all chances to be increased to 10^4 spots and higher. The other limit is imposed by this immense information in view of huge number of low-specific interactions and 'cross-talks'. Some solutions for these problems were prompted by sensory systems used by Nature. They will be discussed in the next Section.

15.5 Towards Sensors That Reproduce Human Senses

For many years, the scientists discuss the possibility of creating artificial intellect. Whether this goal is real or not, it is definitely sure that such intellect cannot operate without connections with outer world. These connections have to be provided by artificial senses. Since the dawn of time, ideal sensing systems were developed by Nature and imposed into living organisms. We observe them being developed into sensory nerve cells of our eyes, ears and nose to detect scents and those of the tong to taste meals and drinks. The sensual perception is formed from many simultaneous responses to the presence of different compounds forming a recognizable bunch of tastes and odors (Deisingh et al. 2004). Thus, the artificial sensors reproducing human senses should be multiparametric in collecting primary information and have to use sophisticated algorithms for its analysis. Seeing the smells and tastes in fluorescent colors is very insufficient for recognition of real odor of perfumes or real taste of vine.

15.5.1 Electronic Nose

The *olfactory system* recognizes the smell when the gas-phase molecules interact with the surface of specialized nerve cells that generate electrical signal. The natural receptors sense different odors as a complex signal composed of responses to many substances often existing simultaneously in very small concentrations. The primary responses are probably not very selective, but they form a pattern that allows high level of integration on the pathway to odor recognition. Understanding the operation of this system may provide a clue for the development of artificial olfactory sensing.

Hitherto developed optical *gas sensors* also exhibit low specificity in the ability to recognize different odors. These facts prompt us the strategy to simulate the odor perception. The sensors for different gases should be developed and combined as arrays. Employing chemical sensors in an array format with proper *pattern recognition* should provide a highly reliable identification of odors even if individual sensors are low specific. The systems based on this approach are termed '*electronic noses*' or *photonic noses*' (Bonifacio et al. 2011). In addition to simulating human perceptions, their design will lead to an extensive range of applications. These

applications will range from food industry and medicine to environmental monitoring and process control (James et al. 2005).

The field of *artificial olfaction* and gas identification is one of the fastest growing areas in sensing. This active field of development uses many sensor materials and technologies described in this book. These include conjugated polymers, metal oxide semiconductors, porous silica and other materials and are based on response in fluorescence. The sensing material is usually presented as a thin film or the film of high porosity to facilitate the analyte diffusion for its detection. Polymeric materials with incorporated organic dyes and composites employing different metalloporphyrins and phthalocyanins lead this application (Maggioni et al. 2007). The sensor designers may benefit from the fact that luminescence of different metalloporphyrins is quenched by different vapors in a different manner (Rakow and Suslick 2004). Many of suggested sensors are not sensitive to humidity and allow sensing in the air (Rakow and Suslick 2004).

An essential task is to make the sensors superior to that made by Nature so that they could sense the compounds to which the man had no contact in his historic development and which appeared in industrial era. Those are the poisonous organic compounds and explosive-like vapors. Thus, smelling with photonic generation of color is a simple and cost-effective method to tackle sensing problems of great practical relevance, including water-quality analysis and monitoring of high-value foods and drinks.

15.5.2 Electronic Tongue

In evolution, the *taste perception* was developed for selection and evaluation of food, including avoidance of potentially harmful substances, such as bitter tasting poisons. The physiology of this response is still not understood in full, but the morphology of location of specialized nerve cells (taste cells) on the surface of the tongue is well studied. Enzymes present in saliva modify the chemical senses somehow. Since cell surface receptors for particular taste stimuli have not yet been isolated, a traditional classification into four classes: sweet, salty, sour, and bitter, is commonly used. Meantime it is known that the cells can respond to more than one type of taste stimulus and this response can be more or less specific. Like in odor perception, a *pattern of response* is formed with efficient but still unknown mechanism of its operation. The output of the sensory system is already not the amount of taste substances present, but the taste in all its specific features.

An important concept can be borrowed for artificial sensor design (Wiskur et al. 2001). For identifying the taste produced by complex mixtures of chemical substances we need the sensor arrays based on a *combination of sensors* with narrow and broad specificities. The narrow specific sensors (Wiskur et al. 2001) should provide such fine resolution as the recognition between stereoisomeric forms of the same compounds. For example, most D-amino acids are sweet, while their L counterparts are bitter (Pu 2004).

The sensors with broader specificity are also needed. They should ‘cross-talk’ and thus participate in formation of *integrated response*. The latter do not need to be

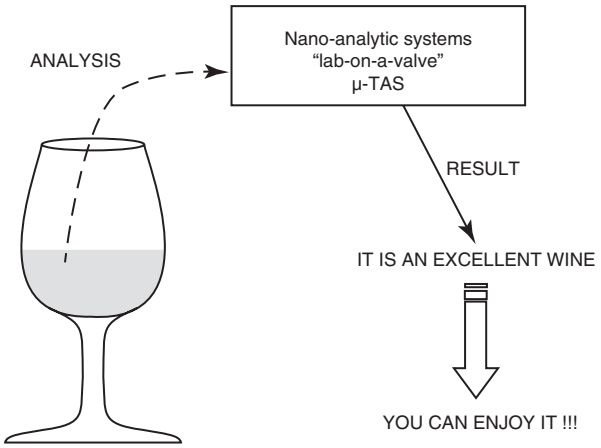

Fig. 15.7 An operation principle for a modern portable laboratory for wine characterization (Simonet and Valcarcel 2006)

completely rationally designed to target specific analytes. They simply need to be different (Lavigne and Anslyn 2001). This concept leads us to '*artificial tongue*' devices that should be able to perform sensory evaluation in complex mixtures of chemically unrelated compounds. Such artificial tongues have been developed for the analysis of liquids (Rakow and Suslick 2004).

The major field of application of these devices is, of course, the analysis of food (Deisingh et al. 2004) and of beverages such as vines ((Di Natale et al. 2004); (Gallagher et al. 2012)). In these cases, the problem of correlating sensorial descriptors and chemical parameters should be resolved (Fig. 15.7). In the case of red vine testing, the results demonstrate the capability of such systems to be trained according to the behavior of a practical panel of tasters.

In one of recent developments, the fluorescence-based array was established based on the principle of indicator displacement. Here peptide sensors were used with different flavonoids as fluorescence indicators. The recognition pattern of every type of vine was obtained even without knowing the structures of vine components (Umali et al. 2011).

15.5.3 Olfactory and Taste Cells on Chips and the Whole-Animal Sensing

In mammalian olfactory system the detection of a great number of odorants results from the association of the odorant molecules with olfactory receptors, carried by olfactory sensory neurons. Olfactory and taste sensors can be constructed based on the *whole-cell sensor technology* (see Sect. 11.6) using the corresponding cultured nerve cells. Such approach is very close to natural recognition of odours and taste. In addition, the methods of molecular biology allow transferring the genes coding these receptors to the cells that are convenient for manipulation, for instance, to yeast cells (Minic et al. 2005). Together with the receptor, a bioluminescent luciferin-luciferase complex (see Sect. 10.2) can be incorporated as a reporting element.

On this pathway, the sensors closely related to biological odor recognition can be constructed and suggested for different uses.

In this respect, it has to be recollected that the whole animals have been used as biosensors for the purpose of evaluating the quality of environment and for detecting the hazardous compounds for centuries. Fish survival was a common test for the quality of water, and caner birds were taken into the mines to indicate the presence of explosive methane gas, which is undetectable by human senses. Different animals can react by their behaviour to approaching earthquakes and tsunamis. At the beginning of eighties Dr. Boris Roytrub (Roitrub and Zlatin 1983) demonstrated an astonishing fact – detection of 10^{-20} M acetyl choline in a simple test using contraction of common medicinal leech, probably a record sensitivity in the days when about single-molecule detection nobody has heard of. This is an example to show that the senses of humans and animals are extremely sensitive. But they are divergent and still they are far from being ideal. The modern devices have to create a strong competition to them.

15.5.4 Lessons Obtained for Sensing

Electronic noses/tongues were suggested as technological attempts to mimic the functions of human chemical senses. Beside this scientifically challenging objective, they have shown potential to be developed into practical instruments for analysis and characterizing the systems of complex composition. However, it is not expected that electronic tongs and noses will make any strong competition to precise analytical tools, such as gas chromatograph/mass spectrometer couplings (Gopel 2000), since the latter are the established instruments of analytical chemistry and should demonstrate a superior performance responding to certain classes of molecules.

The systems based on *pattern recognition* principle should be different. They should allow characterizing the whole specimen by applying such array of receptors, that each of them can recognize not one, but several analytes with different affinities (*differential receptors*). The array of receptors thus produces a pattern of signals that is unique for each analyte, thereby enabling identification of a specific analyte by producing a "fingerprint" pattern. This principle can be applied for recognition of specific DNA sequences (Bengtson and Kolpashchikov 2014).

Thus, a significant cross-reactivity may exist, in line with performance of the mammalian olfactory system, in which a limited number of cross-reactive receptors of low selectivity are able to generate a *response pattern*. The sensor arrays can be created in such a way that the specificity is distributed across the array's entire reactivity pattern rather than being contained in a single recognition element. Such patterns can be then incorporated in an artificial neural network for recognition of mixtures of different analytes (Lavigne and Anslyn 2001). New methods for the selection of statistically relevant, multivariate information can enhance results and bring real applications closer to practice (Bonifacio et al. 2011).

It is expected that the arrays of cross-sensitive sensors can provide more accurate and reliable results as compared with sensors dedicated to a particular analyte. The

simple, fast and low-cost instrumentation detecting a relatively small number of analytes - this is probably the niche for allocation of electronic noses and tongues. Such sensors may become disposable. Though one-use nose or tong sounds uncomfortable, this may be the best technical solution.

15.6 Sensors Promising to Change the Society

What will be the future role of chemical sensors and biosensors? Will their application be limited to special usage like in clinics or they will become mass products available for everyday personal use? On the present step, we already observe that industrial needs, community needs and personal needs combine to provide a strong stimulus for the development of sensors for a broad range of applications. Due to development of inexpensive portal devices (Vashist et al. 2014; Boppart and Richards-Kortum 2014; Ozcan 2014), sensing will come to everyday life, but not alone. Merging of sensing and biosensing with digital communication systems and, particularly, with wireless telemetry, will affect the society in a very profound manner.

15.6.1 Industrial Challenges and Safe Workplaces

In any automatic systems supervising complex technological process, the sensors together with their signal-processing instrumentation has started to play a dominant role (Bakeev 2010). Fluorescence-based sensors successfully compete over the sensors based on other response principles in many areas, where their advantages are requested. The whole arsenal of industrial sensors may include multichannel optical waveguides for continuous process monitoring, arrays for multifunctional characterization of intermediates or products in complex reaction schemes and microfluidic devices for rapid one-use testing.

Sensors are beginning to be integrated into intelligent automatic systems of decision-making and supervision over technological process with a feedback for implementing corrections in this process. Thus, suggesting or deployment of appropriate actions in response to deviation from established process regalement will be made automatically, based on the readings of sensors that are integrated into powerful decision-support systems. Personnel will become excluded from this role and will have to intervene only in critical situations.

Many industrial areas have already started to use or are ready to use such systems, including the production and quality control of food and beverages and also the production of drugs and plant-protecting chemicals. All areas of chemical industry may benefit from these possibilities, especially if the workplaces are connected with potential danger to personnel.

Industrial control and measurement tools can be classified into three basic categories: off-line, on-line and in-line. *Off-line* systems require the removal of samples for subsequent analysis by wet-chemical methods or automated laboratory units.

Such techniques are time and labor consuming, they are not applicable for any kind of continuous monitoring and do not allow automatic feedback control. *On-line* systems are developed for continuous sampling of instrumentation with the aim of providing the readout of result with such a speed that can allow making rapid control decisions. *In-line* systems are those that use the sensors that are incorporated directly into the industrial process reactor and report continuously 'from inside', providing all the necessary information for automatic control on the process.

In many cases, not only the physical parameters are needed for monitoring, such as the temperature, pressure or density in reaction medium but also the concentrations of all necessary reactants and reaction products. In addition, it is often required to detect the trace amounts of impurities and in bioprocess industries also to provide control for microbial contamination. All that can be presently done with fluorescence sensors. Some systems still did not grow up in performance or did not go down in price for opening their broad-scale application, and this is expected in the nearest future.

The examples can be presented from polymer processing industry (Reyes et al. 1999). Here a very small amount of dye is added to polymerized sample for controlling the industrial process, which allows providing the information on the properties of a product on molecular level.

In different biotechnology processes, the multiparametric sensors have become valuable tools for bioprocess monitoring with a capacity of continuous improvement. This is important because the bioreactors are the closed systems, in which the microorganisms and different cell lines can be cultivated under defined and controllable conditions, and non-invasive control on this process is especially important. Spectroscopic technologies are commonly employed with the use of fiber optics attached to disposable sensing connectors. They can be adapted to latest reactor concepts (Beutel and Henkel 2011).

Since modern bioprocesses are extremely complex and differ from process to process (e.g., fungal antibiotic production versus mammalian cell cultivation), the appropriate analytical systems must be set up from different basic modules, designed to meet the special demands of each particular process (Ulber et al. 2003). The advantages of obtaining multiparametric information by non-invasive detection will allow putting all the bioprocess technologies under the full control.

15.6.2 Biosensor-Based Lifestyle Management

In view of current and prospective achievements of sensing technologies should we further tolerate the current situation with clinical diagnostics? It is presently still a common practice that even in critical situations the samples for analysis are taken, sent to specialized laboratory and the doctor with patient have to wait for the result. One or two more efforts and this situation will change dramatically, and not only in the speed of clinical decisions. An easily accessible self-control on health status will definitely induce self-control on human behavior.

Together with the increase of welfare and the lasting tendency for cultural globalization, more and more of the world population adopt the western-society

lifestyle with all its pleasures, many of which are the risk-factors of disease. Additional risk-factors are brought by industrial pollution. More and more people require medical treatment and even lifetime surveillance. Meantime, for centuries the practical medicine developed along the '*illness treatment*' *model*. This is because diagnosis and treatment of disease was based on experience acquired by doctors by learning or by personal practice that classified illnesses with reference to an 'average' patient. Despite the efforts of many generations of the best doctors, this system could not become personalized, in principle. The doctors prescribe the treatments that 'helped other people' and often do that by trial and error. This situation will change only in a sensor-rich environment (Vashist et al. 2014; Ozcan 2014).

Based on multiparametric genomic and proteomic personal data if properly treated and analyzed, the '*wellness support*' *model* will be constructed. It should become the basis of all clinical decisions realizing the principle of personalized medicine. Moreover, if transformed in a clearly understood way this information can be actively used by the patient himself. The common people will get the tools to monitor their own condition and to maintain it properly. The notice 'SMOKING KILLS' does not stop a heavy smoker because he thinks that smoking will probably kill someone else but not him. But if he observes deterioration of his own health-related personal indices approaching a critical limit, then the right decision to quit smoking becomes personally motivated.

Such redistribution of responsibility for health maintenance from doctors to individuals must have a great psychological effect. Moreover, such factors as the distance to hospital and availability of nursery personnel will begin to play a minor role. Adding the sensing, communication and data-processing capabilities at the point-of-care and commonly at patient's home will be one of the most significant contributions to radical changes that must happen in presently centralized health systems.

Post-genomic individual chemical diagnostics are based on already well established concept that not only inherited diseases but also common acquired diseases, such as cancer and heart failure are related to genetics of the individual. Therefore, their risk can be evaluated and minimized. It is expected that in the years to come the DNA screening and expression sensing will become a routine examination not only in diagnostic tests for genetic defects but also to identify the conditions related to metabolic or environment-induced stresses, to acquired AIDS, etc. (Swendeman et al. 2015). The great number of targets can serve as medical markers that can predict onset of malady and monitor its development. They will be established and used in common practice. As we observed from previous chapters of this book, the technological possibilities for that already exist, and the work in this direction proceeds.

As a result, a strong feedback can be established allowing the knowledge-based intervention into a disease process along the following scheme:

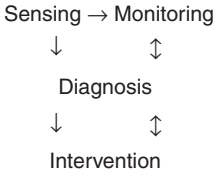

15.6.3 Wearable Sensors

All the future diagnostic devices have to become friendly and cost-effective. They are expected to provide minimum trouble to even the unskilled person who will be able to initiate the system and to obtain understandable results. There are many suggestions regarding the construction of these devices. For instance, they can be made as wrist-type watches or even *integrated into textile clothes*.

We observe the increase of activity for development in this direction, Thus, the method of detecting amines based on a smart dye painting textile and producing both absorption and fluorescence response have been reported (Staneva et al. 2007). Since polymeric coating with appended dyes can be provided on different surfaces, it was suggested to construct the junction sites of polymer chains containing different fluorophores as the sensor sites forming the arrays of high density for the detection of ions as described in Fig. 15.8. There are many expectations associated with wearable sensors.

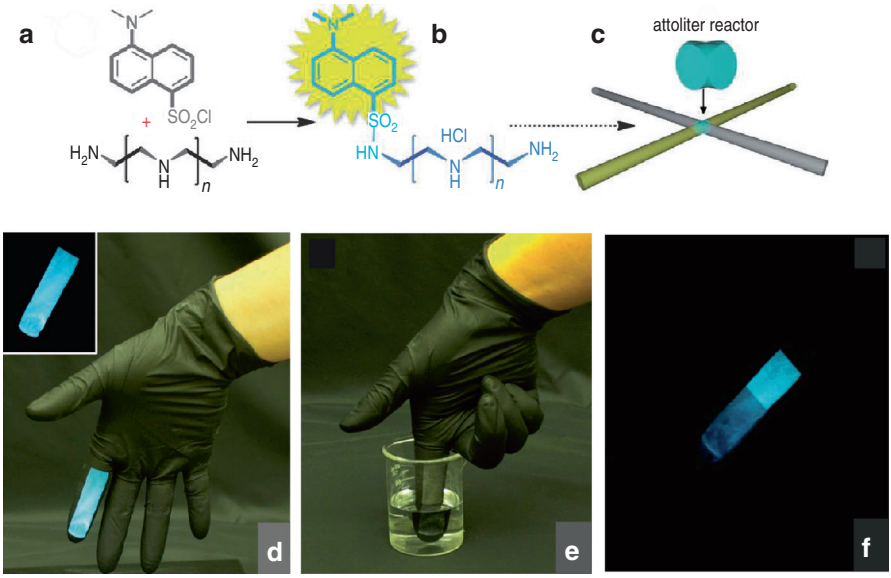

Fig. 15.8 Toward wearable sensors (Anzenbacher et al. 2012). Overlap of two types of polymer nanofibers (~300 nm diam.), each carrying a different reagent, for example, dansyl chloride and polyamine (**a**), to produce fluorescent products (**b**) in the fiber junctions, attoliter volume reactors comprising zeptomolar amounts of fluorescent products (**c**) in the form of a highly porous mat that can be deposited by a shadow mask on a variety of surfaces. When it is deposited on a glove (**d**), it emits fluorescence under near-UV light (365 nm) and after being exposed to a solution of CO_2^+ ions (**e**) results in fluorescence attenuation (**f**)

15.6.4 Living in a Safe Environment and Eating Safe Products

Pollution of the environment caused by industrialization, growth of human population and rise in consumption of industrial products is a serious problem that to a greater and greater extent threatens the existence of men and natural habitats. The *environment pollution* problem has many sides. The pollutant dosage effects are non-linear; they include both synergistic and antagonistic components as well as potential effects of unknown, modified or chemically undetected substances. Thus, monitoring the environment by detecting pollutants with chemical sensors is necessary but not sufficient; the role of biological tests including the application of whole-cell biosensors becomes increasingly important. Thus, bioelectronics, nanotechnology, miniaturization, and especially biotechnology seem to be the growing areas that will have a marked influence on the development of new biosensing strategies in the next future (Rodriguez-Mozaz et al. 2004).

Likewise the health system, the domains of environment monitoring and control technologies in *agriculture* currently use advanced and complex techniques that are still based on *in-vitro* test facilities. In most of these procedures, the use of rapid and powerful instrumental techniques for the final separation and detection of the analytes contrasts with the time-consuming and usually manual methods used for sample preparation, which slows down the analysis. Revolutionary changes are expected in these areas (Rasooly and Jacobson 2006). Miniaturization in sample treatment will speed up its preparation (Ramos et al. 2005) and multiplex sensing will substitute the more complicated chromatographic techniques.

Among the novel techniques, the sensors and sensor arrays based on bioluminescent bacteria are expected to gain popularity. They will be in common use to detect various pollutants. Meantime, with their aid, it is difficult to predict the effects of these pollutants on human physiology, and only the cultured mammalian cells can offer this possibility (Sect. 11.6).

Control for food and beverage contaminants also exhibits dramatic changes with the introduction of sensor arrays (Sapsford et al. 2006) and will continue to do so (Thakur and Ragavan 2013). Rapid detection is needed for *foodborne contaminants* that come in a variety of sizes ranging from simple chemical compounds to entire bacterial cells (Pérez-López and Merkoçi 2011), and the development and application of correspondent multi-analyte sensor systems are in close approach.

It is expected that in the near future the consumers instead of smelling the food products will start to use the sensors indicating their freshness and quality. The characteristic compounds that can be used for sensing the quality of meat are the amines putrescine and cadaverine (Pircher et al. 2007; Landete et al. 2007). Respective fish freshness analyte can be hypoxanthine (Venugopal 2002). Such '*freshness markers*' can be found for every consumer product. Moreover, simultaneous detection of a number of these markers will reduce the number of false decisions and will make any falsifications impossible.

15.6.5 Implantable and Digestible Miniature Sensors Are a Reality

Recent progress in technology allows predicting that very soon all or nearly all in-tube chemical and biochemical testing will be substituted by advanced multiparametric sensor systems. They will be miniaturized and, if necessary, one-use. On the next step, smart implantable or even digestible sensors will become rudimentary in clinical analysis and welfare monitoring. Let us summarize pre-requisites for that.

The *implantable sensors* are already in active development, they are mostly related with highly needed continuous monitoring of glucose level (Schiller et al. 2007; Yu et al. 2007). As the support media they use specially prepared hydrogels and as a response mechanism – the competition assay between glucose and competitor bearing either the fluorescent dye or the quencher. They compete for the sensor binding site formed by fluorescent boronic acid derivative. The same principle is in the background of smart contact lenses reacting to glucose level (see Sect. 14.1).

Another interesting possibility that emerges is the combination of sensing with the *sensing-guided drug delivery*. In Chap. 14 we discussed actuating the drug release from nanocomposites under the effect of local heating or near-IR radiation (Brambilla et al. 2014). This can also be done with the use of minimally invasive feedback-controlled delivery (Hsieh and Zahn 2007). Miniaturized medical diagnostic and treatment devices are on a way to monitor glucose level in diabetic patients and to microinject insulin automatically at the times of reduction of its level. Different multi-scale architectures were proposed for transporting a pharmaceutical compound in the human body (Zhou et al. 2014). Time will show, which of these interesting research and development products will be selected for practical use.

Coupling of monitoring the biomarker level with drug delivery can be provided. The first steps in this direction were made already, for minimally invasive feedback-controlled insulin delivery (Hsieh and Zahn 2007). Miniaturized medical diagnostic and treatment devices are on a way to monitor glucose level in diabetic patients and to microinject automatically insulin at the times of reduction of its level.

Miniaturization of electronics stimulated development of implantable sensors that use wireless communication to send bioanalytical data to mobile phones. The advantages of using such implanted approach include autonomous and continuous collection of data. Wirelessly controlled drug delivery can be realized in these systems (Chertok et al. 2013).

The time will show, which of these interesting research and development products will be selected for practical use.

The problem of transmission of the signal to recording system known as *real-time biotelemetry* is addressed and its interesting solutions have already been found. Based on such developed platforms, miniaturized *digestible sensors* can be devised.

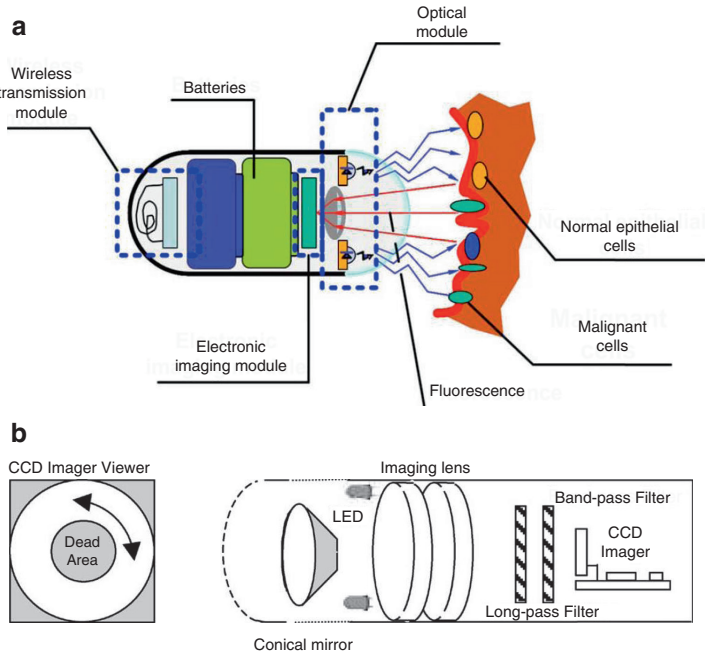

Fig. 15.9 The prototype of a miniature, 'lab-in-a-pill', wireless fluorescence imaging system for noninvasive clinical diagnosis of gastrointestinal tract (Kfouri et al. 2008). (**a**) Conceptual design. The 'pill' contains optical module for the excitation and collection of fluorescence emission and the wireless transmission module. (**b**) Schematic showing the optical imaging module (*right*) and field of view on the CCD imaging sensor (*left*). UV excitation is achieved via the 360 nm LEDs. Side view fluorescence images are projected to the CCD through the conical mirror and two imaging lenses. A long-wavelength-pass filter is used to block scattered excitation light, while spectral band selection is achieved using the narrow bandpass filter placed in front of the CCD camera

They have already got the name '*lab-in-a-pill*'. One of its first prototypes can measure the temperature and pH within gastrointestinal tract with a wireless communication (Johannessen et al. 2006). Further developments allowed substituting the catheter-bases video endoscopes for examining the tissue autofluorescence, which is different for normal and bleeding or malignant tissues. An attractive ingestible capsule-size camera, typically the size of a large vitamin pill, is able to provide visible illumination and to acquire the images in fluorescent light. Prototypes of such *fluorimeters-in-a-pill* have already been described (Kfouri et al. 2008, 2014; De Falco et al. 2014). Construction of one of them is presented in Fig. 15.9.

The spectrally resolved detection can be achieved in these systems. Diagnostics is based on the known facts that abnormal tissues display significant decrease in fluorescence intensity along with an increase in the ratio of red-to-green fluorescence. The detection of this difference can be improved by introduction into the patient's body of fluorescent contrast agent before the examination.

15.6.6 Robotic Operations Coupled with Fluorescence Imaging

In Sect. 14.2 we discussed different technical possibilities for on-line control of surgical operations by fluorescent imaging and observed rapid progress in such technologies, up to manufacturing and practical use of novel devices. We also observe that imaging coupled with *real-time biotelemetry* can be realized with the autonomous instruments of millimetre size. These small devices can attain the ability of controlled motion in space and of performing surgical operations.

The active capsule, namely the *capsule robot*, is a new prospective instrument expected to substitute for the traditional endoscope and the capsule endoscope. Such devices can go forward, backward, or stand under the control (Pan and Wang 2011). There are many practically realizable ideas how to incorporate into them the locomotive function. This kind of active medical robot can perform different tasks, such as imaging the local site, sensing temperature, pH and chemical agents, biopsy, drug delivery, microsurgery, and so on. The prototype presented in Fig. 15.10 is only 10 mm in diameter and 20 mm in length. It integrates the micro-optical images module, the physiological parameter sensors, the micromechanical arm and pump for biopsy, drug delivery and microsurgery, and locomotion. It has the ability of advancing forward and backward, orientating, stopping, and anchoring itself onto biological tissue wall under the control outside. It is equipped with a micromanipulator arm that is able to perform therapeutic procedures like taking biopsy, microsurgery, and injection.

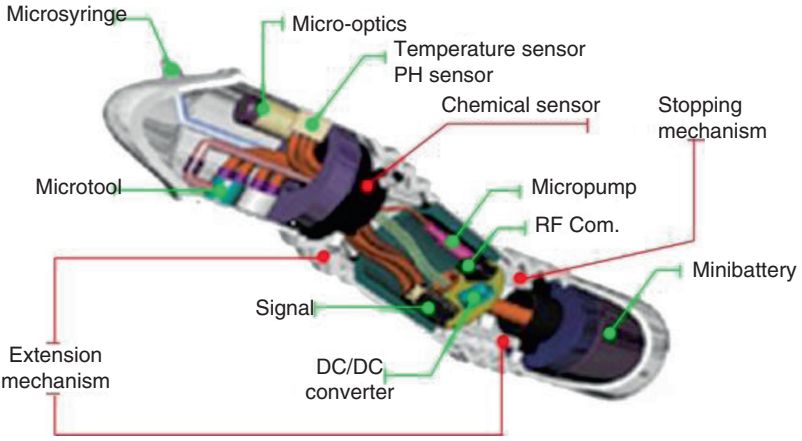

Fig. 15.10 The concept prototype of the active medical robot proposed by Korean IMC (Intelligent Microsystems Center) (Pan and Wang 2011)

15.6.7 Prospects

It is not a dream but a realistic prediction that the sensor-aided early diagnosis as well as a healthy and preventive lifestyle will help slowing the onset of many health problems and save many millions of lives. In order to achieve this goal, a long-term and if necessary a continuous monitoring of human vital signs are required. And ordinary person after getting access to the most detailed information on his/her health status will be able and will be willing to change the lifestyle accordingly. This is quite achievable in the near future with the mass production of inexpensive and user-friendly portable systems. Global benefits are expected from these developments (Fig. 15.11).

Implantable nanosensors may contribute to the broad concept of *personalized medicine* by providing continuous physiologic monitoring and characterizing an individual's personal homeostasis. Such a high-impact contribution would require major advancements from the current state of technology as well as large investments into research.

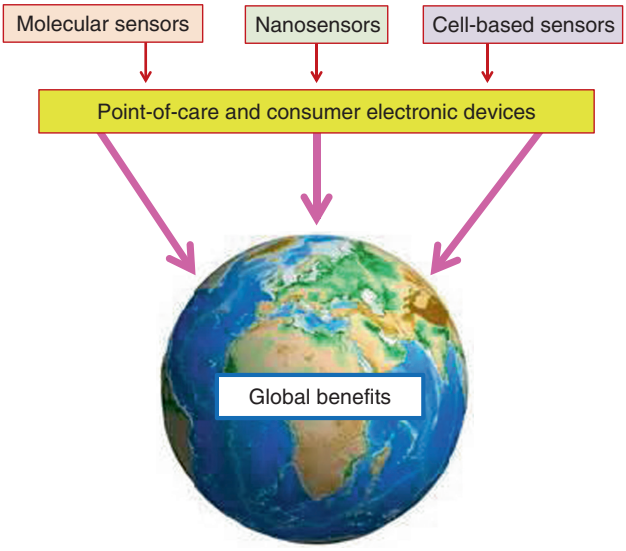

Fig. 15.11 Implication of sensor devices into global benefits (points of care, welfare monitoring, control over the environment, food and drinks quality assurance, etc.). On the basic level are molecular, nanoscale and whole cell sensors. They will be incorporated into different types of low-cost devices that are seen already as a part of consumer electronics such as digital cameras and smartphones. They will improve globally the efficiency and accessibility of health care and the quality of life

Monitoring the environment and providing control on its pollution is the necessary step for achieving its improvement. This problem is commonly addressed to the governments and community leaders. Correctness of their activities will heavily depend upon the information presented to them and to the society as a whole. The decisions that can involve many community members should be based on massive collection of primary information that has to be obtained from sensing.

Addressing all these application areas, it can be seen that in addition to the need for improvements in the electronic engineering aspects of future devices, there are very significant challenges for the chemical-sensor research community. The sensing platforms must be developed to be ideally appropriate for an integration into novel devices. A powerful set of algorithms must be developed that transform sophisticated sensing output data into parameters easily understood by common citizen to become the basis of their decisions.

Healthy workplace, healthy food, healthy environment and healthy lifestyle, this is an optimistic prognosis for the development of human society in twenty-first century. Will with this advancement the person become happier? This remains to be seen.

15.7 Sensing and Thinking: Where Do We Stand and Where Should We Go?

The last decade has seen dramatic transformations in chemical sensing and biosensing technologies. The general trends have been marked towards optimization of sensor receptor and reporter units and of their coupling. Novel materials and techniques of their fabrication and new techniques of optical detection contribute to this rapid progress. All that allows approaching the nanometer length and volume scale, applying novel means of signal transduction and fabricating novel devices. The processing of a huge amount of data can be acquired, so the new powerful computerized tools for their analysis are needed, and they develop rapidly.

In this respect, two important problems are standing ahead: how to generate a huge amount of data and how to analyze it. These problems will remain actual for a long time and many of their solutions are expected to come. Multiparametric input can be provided by multi-sensor microarrays formed of sensor elements selected from large libraries and by high-resolution images. Multiparametric outputs have to be dealt with by applying sophisticated algorithms that have to be developed. After achieving that, what remains? Presentation of results of this analysis in a conceivable and user-friendly way. This goal will be achieved under a pressure of strong demand by the users.

The reader's imagination and creativity has to be focused on these issues.

Questions and Problems

1. Compare the DNA and the protein array techniques. What factors do not allow developing them within the same scale of methodology? Suggest the most prospective arrays for proteomics specifying the receptors, reporters and transduction principles.

2. The suggestions to apply antibodies as receptors in proteome analysis are illustrated in Fig. 15.2. Is it possible to apply for this purpose the library-selected peptides or DNA aptamers?
3. Which one, in your opinion, would be the more prospective strategy for developing the arrays for proteomics – with positional or with optical encoding? Provide pro and contra arguments regarding each of these possibilities.
4. Describe the essence of combinatorial approach and outline the steps in its application. Select any polyphenolic compound or endocrine disruptor as a target and describe your proposed activities in developing a sensor for its detection.
5. What are the disease biomarkers and what are the criteria of their establishment? Explain the sequential steps for their discovery (refer also to Sect. 14.1).
6. What are the present and what will be the future trends in discovery of new drugs? Explain the essence of High Throughput Screening and evaluate the applicability of different fluorescence sensing technologies for that.
7. What is the need for simulating the human senses? What lessons for the development of fluorescence sensors of new generation do we have? Explain the concepts of pattern recognition and of integrated response.
8. Analyze different types of instrumentation for industrial control and measurement and, based on the knowledge obtained in Chap. 11, provide the choice between different types of fluorescence-based devices that can be used for this purpose.
9. Explain essential features that make 'illness treatment model' and 'wellness support model' very different on the personal and community levels.
10. Suggest the most convenient method of the wearable sensor application for the analysis of chemical composition of sweat. Propose one-time use and continuous monitoring versions.
11. Provide your vision on future development of 'smart sensor capsules' that combine in one miniaturized unit many functionalities, including fluorescence sensing and wireless transmission of reporter signal.
12. Imagine that we reach the goal of developing efficient and applicable on a large scale sensors for personalized medicine. Explain how these sensors of future are expected to change your personal life.

References

Anzenbacher P, Li F, Palacios MA (2012) Toward wearable sensors: fluorescent attoreactor mats as optically encoded cross-reactive sensor arrays. Angewandte Chemie 124(10): 2395–2398

Apostolidis A, Klimant I, Andrzejewski D, Wolfbeis OS (2004) A combinatorial approach for development of materials for optical sensing of gases. J Comb Chem 6(3):325–331

Aslan K, Geddes CD (2005) Microwave-accelerated metal-enhanced fluorescence: platform technology for ultrafast and ultrabright assays. Anal Chem 77(24):8057–8067

Bakeev KA (2010) Process analytical technology: spectroscopic tools and implementation strategies for the chemical and pharmaceutical industries. Wiley, Chichester, West Sussex, UK

Baker GA, Pandey S, Bright FV (2000) Extending the reach of immunoassays to optically dense specimens by using two-photon excited fluorescence polarization. Anal Chem 72(22): 5748–5752

Bengtson HN, Kolpashchikov DM (2014) A differential fluorescent receptor for nucleic acid analysis. Chembiochem 15(2):228–231. doi:10.1002/cbic.201300657
Berger B, Peng J, Singh M (2013) Computational solutions for omics data. Nat Rev Genet 14(5):333–346
Beutel S, Henkel S (2011) In situ sensor techniques in modern bioprocess monitoring. Appl Microbiol Biotechnol 91(6):1493–1505
Bonifacio LD, Ozin GA, Arsenault AC (2011) Photonic nose–sensor platform for water and food quality control. Small 7(22):3153–3157
Boppart SA, Richards-Kortum R (2014) Point-of-care and point-of-procedure optical imaging technologies for primary care and global health. Sci Translat Med 6(253):253rv252
Borrebaeck CA, Wingren C (2009) Design of high-density antibody microarrays for disease proteomics: key technological issues. J Proteomics 72(6):928–935
Bosch ME, Sanchez AJR, Rojas FS, Ojeda CB (2007) Optical chemical biosensors for high throughput screening of drugs. Comb Chem High Throughput Screen 10(6):413–432
Brambilla D, Luciani P, Leroux J-C (2014) Breakthrough discoveries in drug delivery technologies: the next 30 years. J Control Release 190:9–14
Chan FK, Holmes KL (2004) Flow cytometric analysis of fluorescence resonance energy transfer: a tool for high-throughput screening of molecular interactions in living cells. Methods Mol Biol 263:281–292
Chao TC, Hansmeier N (2013) Microfluidic devices for high-throughput proteome analyses. Proteomics 13(3–4):467–479
Chertok B, Webber MJ, Succi MD, Langer R (2013) Drug delivery interfaces in the 21st century: from science fiction ideas to viable technologies. Mol Pharm 10(10):3531–3543
Christodoulides N, Mohanty S, Miller CS, Langub MC, Floriano PN, Dharshan P, Ali MF, Bernard B, Romanovicz D, Anslyn E, Fox PC, McDevitt JT (2005) Application of microchip assay system for the measurement of C-reactive protein in human saliva. Lab Chip 5(3):261–269
Comeau JWD, Costantino S, Wiseman PW (2006) A guide to accurate fluorescence microscopy colocalization measurements. Biophys J 91(12):4611–4622
De Falco I, Tortora G, Dario P, Menciassi A (2014) An integrated system for wireless capsule endoscopy in a liquid-distended stomach. IEEE Trans Biomed Eng 61(3):794–804
Deisingh AK, Stone DC, Thompson M (2004) Applications of electronic noses and tongues in food analysis. Int J Food Sci Technol 39(6):587–604
Demchenko AP (2013) Beyond annexin V: fluorescence response of cellular membranes to apoptosis. Cytotechnology 65(2):157–172. doi:10.1007/s10616-012-9481-y
Di Natale C, Paolesse R, Burgio M, Martinelli E, Pennazza G, D'Amico A (2004) Application of metalloporphyrins-based gas and liquid sensor arrays to the analysis of red wine. Anal Chim Acta 513(1):49–56
Didelot X, Bowden R, Wilson DJ, Peto TE, Crook DW (2012) Transforming clinical microbiology with bacterial genome sequencing. Nat Rev Genet 13(9):601–612
Durick K, Negulescu P (2001) Cellular biosensors for drug discovery. Biosens Bioelectron 16(7–8): 587–592
Eggeling C, Brand L, Ullmann D, Jager S (2003) Highly sensitive fluorescence detection technology currently available for HTS. Drug Discov Today 8(14):632–641
Ercelen S, Klymchenko AS, Mely Y, Demchenko AP (2005) The binding of novel two-color fluorescence probe FA to serum albumins of different species. Int J Biol Macromol 35(5):231–242
Finan JE, Zhao RY (2007) From molecular diagnostics to personalized testing. Pharmacogenomics 8(1):85–99
Frishman D (2007) Protein annotation at genomic scale: the current status. Chem Rev 107(8): 3448–3466
Gallagher LT, Heo JS, Lopez MA, Ray BM, Xiao J, Umali AP, Zhang A, Dharmarajan S, Heymann H, Anslyn EV (2012) Pattern-based discrimination of organic acids and red wine varietals by arrays of synthetic receptors. Supramol Chem 24(2):143–148
Gomez-Hens A, Aguilar-Caballos MP (2007) Modern analytical approaches to high-throughput drug discovery. TRAC Trend Anal Chem 26(3):171–182

Gopel W (2000) From electronic to bioelectronic olfaction, or: from artificial “moses” to real noses. Sens Actuators B Chem 65(1–3):70–72
Hsieh YC, Zahn JD (2007) On-chip microdialysis system with flow-through sensing components. Biosens Bioelectron 22(11):2422–2428
Hu S, Loo JA, Wong DT (2007) Human saliva proteome analysis and disease biomarker discovery. Expert Rev Proteomics 4(4):531–538
Inuyama Y, Nakamura C, Oka T, Yoneda Y, Obataya I, Santo N, Miyake J (2007) Simple and high-sensitivity detection of dioxin using dioxin-binding pentapeptide. Biosens Bioelectron 22(9–10):2093–2099
James D, Scott SM, Ali Z, O'Hare WT (2005) Chemical sensors for electronic nose systems. Microchim Acta 149(1–2):1–17
Jiang H, Weng X, Li D (2011) Microfluidic whole-blood immunoassays. Microfluid Nanofluid 10(5):941–964
Johannessen EA, Wang L, Reid SWJ, Cumming DRS, Cooper JM (2006) Implementation of radiotelemetry in a lab-in-a-pill format. Lab Chip 6(1):39–45
Kfouri M, Marinov O, Quevedo P, Faramarzpour N, Shirani S, Liu LWC, Fang Q, Deen MJ (2008) Toward a miniaturized wireless fluorescence-based diagnostic imaging system. IEEE J Sel Top Quantum Electron 14(1):226–234
Kim C, Paik S (2010) Gene-expression-based prognostic assays for breast cancer. Nat Rev Clin Oncol 7(6):340–347
Kiourti A, Psathas KA, Nikita KS (2014) Implantable and ingestible medical devices with wireless telemetry functionalities: a review of current status and challenges. Bioelectromagnetics 35(1):1–15
Lafratta CN, Walt DR (2008) Very high density sensing arrays. Chem Rev 108(2):614–637
Landete JM, de las Rivas B, Marcobal A, Munoz R (2007) Molecular methods for the detection of biogenic amine-producing bacteria on foods. Int J Food Microbiol 117(3):258–269
Lavigne JJ, Anslyn EV (2001) Sensing a paradigm shift in the field of molecular recognition: from selective to differential receptors. Ange Chem Int Ed 40(17):3119–3130
Maggioni G, Manera MG, Spadavecchia J, Tonezzer M, Carturan S, Quaranta A, Fernandez CDJ, Rella R, Siciliano P, Della Mea G, Vasanelli L, Mazzoldi P (2007) Optical response of plasma-deposited zinc phthalocyanine films to volatile organic compounds. Sens Actuators B Chem 127(1):150–156
Martinez-Manez R, Soto J, Garcia-Breijo E, Gil L, Ibanez J, Llobet E (2005) An “electronic tongue” design for the qualitative analysis of natural waters. Sens Actuators B Chem 104(2):302–307
Minic J, Persuy MA, Godel E, Aioun J, Connerton I, Salesse R, Pajot-Augy E (2005) Functional expression of olfactory receptors in yeast and development of a bioassay for odorant screening. Febs J 272(2):524–537
Mitsubayashi K, Dicks JM, Yokoyama K, Takeuchi T, Tamiya E, Karube I (1995) A flexible biosensor for glucose. Electroanalysis 7(1):83–87
Moats RK, Sullivan BM (2004) Combinatorial augmentation for a multi-pathogen biosensor: signal analysis and design. Biosens Bioelectron 19(12):1673–1683
Nakamura C, Inuyama Y, Goto H, Obataya I, Kaneko N, Nakamura N, Santo N, Miyake J (2005) Dioxin-binding pentapeptide for use in a high-sensitivity on-bead detection assay. Anal Chem 77(23):7750–7757
Ozcan A (2014) Mobile phones democratize and cultivate next-generation imaging, diagnostics and measurement tools. Lab Chip 14(17):3187–3194
Pan G, Wang L (2011) Swallowable wireless capsule endoscopy: progress and technical challenges. Gastroenterol Res Pract 2012:841691
Pérez-López B, Merkoçi A (2011) Nanomaterials based biosensors for food analysis applications. Trends Food Sci Technol 22(11):625–639
Petrey D, Honig B (2014) Structural bioinformatics of the interactome. Ann Rev Biophys 43(1):193–210. doi:10.1146/annurev-biophys-051013-022726
Pfleger KDG, Eidne KA (2006) Illuminating insights into protein-protein interactions using bioluminescence resonance energy transfer (BRET). Nat Methods 3(3):165–174

Piehler J (2005) New methodologies for measuring protein interactions in vivo and in vitro. Curr Opin Struct Biol 15(1):4–14
Pircher A, Bauer F, Paulsen P (2007) Formation of cadaverine, histamine, putrescine and tyramine by bacteria isolated from meat, fermented sausages and cheeses. Eur Food Res Technol 226(1–2):225–231
Prosser GA, Larrouy-Maumus G, Carvalho LPS (2014) Metabolomic strategies for the identification of new enzyme functions and metabolic pathways. EMBO Rep 15(6):657–669
Przybylo M, Borowik T, Langner M (2007) Application of liposome based sensors in high-throughput screening systems. Comb Chem High Throughput Screen 10(6):441–450
Pu L (2004) Fluorescence of organic molecules in chiral recognition. Chem Rev 104(3):1687–1716
Rakow NA, Suslick KS (2004) Novel materials and applications of electronic noses and tongues (vol 406, pg 710, 2000). Mrs Bullet 29(12):913
Ramos L, Ramos JJ, Brinkman UAT (2005) Miniaturization in sample treatment for environmental analysis. Anal Bioanal Chem 381(1):119–140
Rasheed A, Farhat R (2013) Combinatorial chemistry: a review. J Pharm Sci Res 4(7):2502–2516
Rasooly A, Jacobson J (2006) Development of biosensors for cancer clinical testing. Biosens Bioelectron 21(10):1851–1858
Reyes FL, Jeys TH, Newbury NR, Primmerman CA, Rowe GS, Sanchez A (1999) Bio-aerosol fluorescence sensor. Field Anal Chem Technol 3(4–5):240–248
Rodriguez-Mozaz S, Marco MP, de Alda MJL, Barcelo D (2004) Biosensors for environmental applications: future development trends. Pure Appl Chem 76(4):723–752
Roitrub BA, Zlatin RS (1983) A method of increasing the sensitivity of the acetylcholine bioassay. Fiziol Zh 29(2):237–239
Samaranayake L (2007) Saliva as a diagnostic fluid. Int Dent J 57(5):295–299
Sapsford KE, Ngundi MM, Moore MH, Lassman ME, Shriver-Lake LC, Taitt CR, Ligler FS (2006) Rapid detection of foodborne contaminants using an array biosensor. Sens Actuators B Chem 113(2):599–607
Schiller A, Wessling RA, Singaram B (2007) A fluorescent sensor array for saccharides based on boronic acid appended bipyridinium salts. Angew Chem Int Ed 46(34):6457–6459
Schneider SE, O'Neil SN, Anslyn EV (2000) Coupling rational design with libraries leads to the production of an ATP selective chemosensor. J Am Chem Soc 122(3):542–543
Schwarzenbach H, Hoon DS, Pantel K (2011) Cell-free nucleic acids as biomarkers in cancer patients. Nat Rev Cancer 11(6):426–437
Shepard JRE (2006) Polychromatic microarrays: Simultaneous multicolor array hybridization of eight samples. Anal Chem 78(8):2478–2486
Simonet BM, Valcarcel M (2006) Analytical chemistry in modern society: what we can expect. Microchim Acta 153(1–2):1–5
Staneva D, Betcheva R, Chovelon J-M (2007) Optical sensor for aliphatic amines based on the simultaneous colorimetric and fluorescence responses of smart textile. J Appl Polym Sci 106:1950–1956
Subramanian J, Simon R (2010) Gene expression–based prognostic signatures in lung cancer: ready for clinical use? J Natl Cancer Inst 102(7):464–474
Swendeman D, Comulada WS, Ramanathan N, Lazar M, Estrin D (2015) Reliability and validity of daily self-monitoring by smartphone application for health-related quality-of-life, antiretroviral adherence, substance use, and sexual behaviors among people living with HIV. AIDS Behav 19(2):330–340
Szurdoki F, Ren DH, Walt DR (2000) A combinatorial approach to discover new chelators for optical metal ion sensing. Anal Chem 72(21):5250–5257
Taussig MJ, Stoevesandt O, Borrebaeck CAK, Bradbury AR, Cahill D, Cambillau C, de Daruvar A, Dubel S, Eichler J, Frank R, Gibson TJ, Gloriam D, Gold L, Herberg FW, Hermjakob H, Hoheisel JD, Joos TO, Kallioniemi O, Koegl M, Konthur Z, Korn B, Kremmer E, Krobitsch S, Landegren U, van der Maarel S, McCafferty J, Muyldermans S, Nygren PA, Palcy S, Pluckthun A, Polic B, Przybylski M, Saviranta P, Sawyer A, Sherman DJ, Skerra A, Templin M, Ueffing M, Uhlen M (2007) ProteomeBinders: planning a European resource of affinity reagents for analysis of the human proteome. Nat Methods 4:13–17

Thakur M, Ragavan K (2013) Biosensors in food processing. J Food Sci Technol 50(4): 625–641
Theodoridis GA, Gika HG, Want EJ, Wilson ID (2012) Liquid chromatography–mass spectrometry based global metabolite profiling: a review. Anal Chim Acta 711:7–16
Tian H, Ip L, Luo H, Chang DC, Luo KQ (2007) A high throughput drug screen based on fluorescence resonance energy transfer (FRET) for anticancer activity of compounds from herbal medicine. Br J Pharmacol 150(3):321–334
Ulber R, Frerichs JG, Beutel S (2003) Optical sensor systems for bioprocess monitoring. Anal Bioanal Chem 376(3):342–348
Umali AP, LeBoeuf SE, Newberry RW, Kim S, Tran L, Rome WA, Tian T, Taing D, Hong J, Kwan M (2011) Discrimination of flavonoids and red wine varietals by arrays of differential peptidic sensors. Chem Sci 2(3):439–445
Uttamchandani M, Wang J, Yao SQ (2006) Protein and small molecule microarrays: powerful tools for high-throughput proteomics. Mol Biosyst 2(1):58–68
Vashist SK, Schneider EM, Luong JH (2014) Commercial smartphone-based devices and smart applications for personalized healthcare monitoring and management. Diagnostics 4(3):104–128
Venugopal V (2002) Biosensors in fish production and quality control. Biosens Bioelectron 17(3):147–157
Vidal M, Cusick ME, Barabasi A-L (2011) Interactome networks and human disease. Cell 144(6):986–998
Von Lode P, Rainaho J, Pettersson K (2004) Quantitative, wide-range, 5-minute point-of-care immunoassay for total human chorionic gonadotropin in whole blood. Clin Chem 50(6):1026–1035
Wang L, Drysdale TD, Cumming DRS (2007) In situ characterization of two wireless transmission schemes for ingestible capsules. IEEE Transact Biomed Eng 54(11):2020–2027
Wiskur SL, Ait-Haddou H, Lavigne JJ, Anslyn EV (2001) Teaching old indicators new tricks. Acc Chem Res 34(12):963–972
Xu CT, Zhan Q, Liu H, Somesfalean G, Qian J, He S, Andersson-Engels S (2013) Upconverting nanoparticles for pre-clinical diffuse optical imaging, microscopy and sensing: current trends and future challenges. Laser Photonics Rev 7(5):663–697
Yu BZ, Ju YM, West L, Moussy Y, Moussy F (2007) An investigation of long-term performance of minimally invasive glucose biosensors. Diabetes Technol Ther 9(3):265–275
Zenobi R (2013) Single-cell metabolomics: analytical and biological perspectives. Science 342(6163):1243259
Zhou Y, Qian L, Wang C, Chen Y, Wang R, Zhang Q. System architecture and simulation methodology of a multi-scale drug delivery platform using transient microbots. In: Antennas and Propagation Society International Symposium (APSURSI), 2014 IEEE. 2014. Memphis, TN: IEEE, pp 514–515
Zhu H, Snyder M (2003) Protein chip technology. Curr Opin Chem Biol 7(1):55–63

Epilogue

The community of common citizens should prepare itself for a great revolution. This revolution should produce the changes in human lifestyles greater than mobile phones and internet. At the beginning of twenty-first century, the most developed countries have reached the level of a computerized society. In a decade ahead, we will enter into a *sensorized society*. This means that sensors will become a part of everyday life, and the results of their application will become strongly involved in human decisions both on personal and on community levels.

To say that fluorescence sensing technologies develop rapidly is to say nothing. In fact, the development is explosive. The reader may compare the present usage of analytical methods with that achieved in advanced laboratories. Until now, in many industrial laboratories the measurements are made by taking a sample and analyzing it for a single analyte. When multiple analytes have to be measured from a single sample, the sample conventionally is divided into appropriate aliquots and each aliquot is analyzed separately, often according to different protocol. This approach is exemplified by many of the clinical analyzers employed in today's hospital laboratories. The patient may need to wait hours and days for the results of analysis. And now, there come the novel sensor technologies that bring revolutionary changes. The analysis becomes possible for hundreds and thousands of analytes simultaneously, its results can be obtained in minutes and even seconds and they can be automatically communicated to a central unit for on-line analysis and making decisions. Very soon, monitoring the technological process will be made possible from mobile phone, and the patient that needs monitoring a complex of health-related parameters will go and buy a smart pocket-size instrument in a nearby supermarket.

Such a rapid technological development is heated up by the fact that in every aspect of sensor design and application there is a strong competition of different technologies based on different principles. This can be seen starting from the first pages of this book, introducing the reader to this exciting field. Will the direct sensing beat in performance the sandwich assays, and what will be the role of competitive assays? (Chap. 1). How the theoretically imposed limit on dynamic range of

A.P. Demchenko, *Introduction to Fluorescence Sensing*,
DOI 10.1007/978-3-319-20780-3

target detection has to be overcome? (Chap. 2). What is the best choice of fluorescence detection method among a number of powerful techniques offered by optical instrumentation? (Chap. 3). What are the best fluorescence reporters of organic (e.g. dyes) or biosynthetic (e.g. green fluorescent protein) origin? (Chap. 4). What are the advantages of inorganic nanoparticles, e.g. quantum dots (Chap. 5). Can we modulate at will fluorescence properties of nanocomposites and modify them for achieving many different functionalities? (Chap. 6). How to select optimal recognition units that originate from chemical and biological worlds? Should it be rational design or a process of selection involving huge libraries? (Chap. 7). How to combine the recognition and reporting units, providing proper signal transduction? This can be done by different physical mechanisms that may involve the effects of proximity and the conformational variables (Chap. 8). How to provide assembly of smart supramolecular sensors on different surfaces or their nano-scale self-assembly in solution? (Chap. 9). Exciting non-conventional methods exist for excitation and monitoring emission, how to employ them optimally? (Chap. 10). Using all this immense information, many possibilities exist for constructing the instrumentation. So which one is the best for particular needs? (Chap. 11). Are we presently able to respond to the challenges of detecting the most important targets of physical, chemical and biological worlds? (Chap. 12). Can we transfer these sensing technologies to observations inside the living cells? (Chap. 13). What new opportunities in clinical diagnostics and treatment will then open? (Chap. 14). And finally, what are the prospects of sensing technologies and what opportunities and limitations we will observe behind the horizon? (Chap. 15).

Throughout this book, we did not attempt to respond to all these questions because of immense number of existing possibilities, both realized and unrealized yet. Only one final remark should be made. In the present days, we often observe excellent technological solutions based on seemingly outdated concepts and, at the same time, the ideas offering revolutionary breakthrough but presented only on the level of ‘proof of concept’ and based on a rather primitive form of technology. This is indispensable in explosive development. The usable products based on frontier science combined with frontier technology – this is the challenge for future generations of researchers.

The author has to admit that this frontier of science and technology cannot be recognized easily because the sensor research is the crossing point of many disciplines. It is the field of mutual penetration of science and technology of inorganic and organic man-made materials with biotechnology that is derived from the studies of living matter. The new technical solutions are the result of combining the highly specific recognition ability of biomolecules with the unique structural character of inorganic nanomaterials such as nanocrystals, nanotubes and nanowires. Endowing these materials with reporting functions is the crossing points of these disciplines with photophysics and photochemistry, plus optics and photonics, microelectronics and many more. Various kinds of researchers are required to cooperate in order to achieve a valuable result stimulating the research and bringing the useful product.

Potentially existing multitude of solutions will be finally selected by the end users. To summarize, we can outline only the general tendencies that are becoming the criteria for this selection. They are *miniaturization*, *simplification* and *multifunctionality*. The sensors with such advanced properties are expected to be produced in mass and be as useful to everyone as the mobile phones.

This field of sensor development bringing together research and technology should be extremely attractive for fresh bright minds that will make a selection among these possibilities for exploration of their personal skills. New skills and, moreover, new ways of thinking is needed also from the side of users. The ways we make measurements, process the data from these measurements and use the information that can be extracted from these data – all that should change profoundly.

Every day brings in this hot field new information in the form of presentations, publications and patents. Navigating in this ocean of information becomes difficult without guidance. The author will be happy if this book will be useful to the reader serving as such a guide.

Appendix: Glossary of Terms Used in Fluorescence/Luminescence Sensing

Absorbance (Molar, expressed in M^{-1} cm^{-1}) is a measure of the probability for a fluorophore to absorb light. The broadly used term 'extinction' includes both absorbance and light scattering. Absorbance is a unique characteristic of a molecule under certain environmental conditions. In general, the bigger the fluorophore size, the greater is the probability that the photon will be absorbed. See: *Molar absorbance*.

Anisotropy Is the parameter used in the analysis of polarized fluorescence emission. It characterizes fluorescence probe rotation during the excited state lifetime. Polarized excitation selects the dye molecules with particular orientation in space and their emission will be also polarized in the case of absence of their rotation. Rotation during fluorescence lifetime will depolarize its emission, resulting in a mechanism with which to measure the rigidity (viscosity) of the environment containing the dye or the mass of rotating unit to which it is attached. Fluorescence anisotropy is defined as the ratio of the difference between the emission intensity parallel to the polarized electric vector of the exciting light and the intensity perpendicular to the vector, divided by the total intensity. Possible and useful are the measurements of anisotropy in time-resolved format.

Antibodies (Ab) Are the proteins synthesized by the immune system to recognize, bind and produce the functional response to molecules, particles, viruses and cells foreign to this organisms (antigens). Two types of antibodies are used as recognition elements in sensing: monoclonal, produced in cell cultures called hybridomas, and gene-recombinant antibodies. The latter can be of reduced size (Ab fragments).

Aptamers Are the single-strand DNA or RNA molecules that have been selected from random pools based on their ability to bind other molecules. Using repetitive binding-enrichment procedure, aptamers have been obtained that bind with high affinity the nucleic acids, proteins, small organic compounds, and even entire organisms. The basis of their target recognition is the tertiary structure formed by the single-stranded oligonucleotides that allows the target-induced conformational changes.

A.P. Demchenko, *Introduction to Fluorescence Sensing*,
DOI 10.1007/978-3-319-20780-3

Argon ion laser Is the laser that is the most commonly used in microscopy and flow cytometry. Its principal emission lines are at 488.0 and 514.5 nm.

Array technology Is any high-throughput methodology permitting analysis of many (hundreds, thousands) binding events of different specificity in parallel, usually using spotting of many sensors on the surface of the same unit (spotted arrays) or dispersing them (suspension arrays).

Avidin Is the protein that binds a small molecule biotin with high specificity and affinity. Avidin or its bacterial analog streptavidin are the most frequently used to form self-assembled macromolecular structures.

Barcode Is the identification system that is commonly used in supermarkets. It employs a series of machine-readable lines of varying widths of black and white and read with a laser scanner. In sensing technologies it is the system for identification of sensor particles in multiplex detection arrays.

Binder Is the sensor recognition unit that interacts with the target with good affinity and specificity. It has to be obtained in response to the requirement for the target structure that can be as small as an ion chelating group and as large as a macromolecule, such as protein or DNA or even an imprinted polymer structure.

Binder-reporter coupling Is the coupling between sensing elements (binders) with fluorescent elements (reporters) that provides transduction of signal on target binding into detectable signal.

Biochip Is a broad term for various types of highly parallel functioning miniaturized detection devices that are deposited on solid supports. They include various types of DNA and protein chips and microarrays.

Bioluminescence Is a biochemical oxidative process that results in the release of energy as emitted light. Firefly luminescence, which requires the enzyme luciferase to catalyze a reaction between the substrate luciferin and molecular oxygen (in the presence of adenosine triphosphate), is a commonly employed example of bioluminescence. This phenomenon occurs in a wide variety of marine organisms and insects. The luciferin-luciferase complex can be genetically engineered within the living cells allowing many possibilities for sensing.

Biosensor Is a device that allows the detection and quantification of biomolecules commonly by biospecific interaction between macromolecules (molecular recognition). Usually this occurs in a single step. Molecular recognition, which is the formation of a complex between the biomolecule of interest (target) and its recognition element (binder or receptor), generates a recordable signal.

Blue shift Also called the hypsochromic shift is the shift of spectra in the direction of higher energies (shorter wavelengths).

Brightness Is an important characteristic of fluorescence reporter, which determines the absolute sensitivity of detection. It is defined as the product of molar absorbance at the wavelength used for fluorescence excitation and the fluorescence quantum yield.

Calibration Is establishing an unequivocal quantitative relationship between the measured parameter and the analyte concentration. In fluorescence, sensing is the operation, as a result of which at every sensing element (molecule, nanopar-

ticle, etc.) or at every site of the image the fluorescence signal becomes independent of any other factor except the concentration of bound target.

Charge coupled device (CCD) Is a monolithic semiconductor device used for collecting the image. It is arranged as an array of elements such that the output from one element provides the stimulus for the next. A response in the form of image in artificial colors can be created in these devices.

Chemical sensor Is a designed molecule or miniaturized analytical device that delivers real-time and online information on the presence of specific compounds in complex samples. According to the definition recommended by IUPAC, 'chemical sensor is a device that transforms chemical information, ranging from the concentration of a specific sample component to total composition analysis, into an analytically useful signal'.

Combinatorial chemistry Is a branch of chemistry that is concerned with the mass synthesis (creating a 'library') of compounds and their systematic evaluation (screening) for desired property or function.

Confocal laser scanning microscopy Is the technique that allows achieving high resolution within focal plane by using a so-called pinhole that discriminates the out-of-plane emission. This enables a sharp image at different depths in the specimen. For obtaining the image, a focused laser beam is scanned laterally along the **x** and **y** axes of a specimen in a raster pattern to generate fluorescence emission. The latter is sensed by a photomultiplier tube and displayed in pixels on a computer monitor. The pixel display dimensions are determined by the sampling rate of the electronics and the dimensions of the raster. This technique enables the specimen to be optically sectioned along the **z** axis. Multiple images taken at different depths can be composed into a three-dimensional object representation.

Dextran Is a polysaccharide with a high molecular weight of 3000–70,000 that can be used in sensing technologies for different purposes. It can serve as support for supramolecular structures and as competitor in glucose sensing. It can be labeled with a fluorescent dye and constitute the shell of a nanoparticle.

Diffraction limit Is the limit of resolution that cannot be overcome in standard optical methods because of diffraction property of light. This limit is about 200–400 nm, a half wavelength of illumination source.

Diode laser Is the semiconductor light source that can be of small (less than 1 mm) dimension and emit coherent radiation.

Direct sensors Are the sensors in which the transduction of signal produced on complex formation with analyte does not need any additional steps or third interacting partners. Direct sensors demonstrate the highest speed of response that is limited only by the rate of target binding.

Dual fluorescence Is the emission showing two *fluorescence* bands. Several nontrivial molecular properties may be at the basis of a dual fluorescence, such as conformational equilibrium in the *ground state* and a mixture of *excited states*.

Dynamic range Is the range between the maximum to minimum measurable values of the parameter used for sensing response. In imaging, it is the difference in intensity between the lightest and darkest points of the image.

Electrochromism (Stark effect) Is the effect of change of energy of electronic transition and correspondent shift of absorption and emission spectrum under the influence of applied electric field. Electrochromic dyes are used for probing electrostatic potentials at interfaces of nanoparticles, biological membranes and their phospholipid models.

Electronic state Is the well specified overall configuration of electrons in an atom or molecule. Any given molecule can exist in one of several electronic states (ground or multiple excited), depending upon the total electron energy and on the symmetry of the electron spins in the orbitals. Under normal conditions, the majority of molecules exist in the electronic state with the least energy (the *ground state*). When the molecule absorbs a photon, electrons are excited to higher energy states (*excited states*).

Emission spectrum Is the wavelength or the energy (wavenumber) function of the intensity of light emitted by a fluorophore after it has been excited by absorbing a light quantum. Usually the emission spectrum is located at lower energies than the absorption spectrum (Stokes shift) and is independent on excitation wavelengths, even if the fluorophore is excited to different high-energy electronic states (Kasha rule).

Energy of Light Quanta Matter absorbs light in discrete quanta (photons). The energy of light quantum is proportional to position of corresponding band in the spectrum on a wavenumber scale and is inversely proportional to its position on wavelength scale. The relation is $E = h\nu = 10^7 hc/\lambda$, where ν is the wavenumber in cm^{-1} and λ is the wavelength in nm, h is the Planck's constant and c the velocity of light.

Enzyme linked immunosorbent assay (ELISA) Is the sensor technique based on sandwich methodology. It involves antibody or antigen sensing by complementary antigen or antibody immobilized on the surface. The binding is detected by additional antibody coupled with enzyme that produces colored enzyme reaction. The method requires the addition of auxiliary reagents and/or the separation between free and bound interacting partners.

Epi-fluorescence microscopy (EFM) Is the microscopic technique in which the illumination source (often termed a vertical illuminator) is placed on the same side of the specimen as the objective, which serves the dual role as both condenser and imaging lens system. The monochromatic excitation light is used to excite the fluorophores in the specimen via the microscope objective. The fluorescence light emitted from the specimen is again captured by the objective lens and filtered to the appropriate detection wavelength window by passage through a dichroic mirror in the microscope. This part of the emitted light is detected by an electronic camera or can be observed at the microscope oculars.

Excimers and exciplexes Are the dimers formed in the excited state. Their formation requires proximity and proper orientation of interacting partners. Often they are non-fluorescent. But in some cases (such as for pyrene exciplexes) a bright structureless and long-wavelength shifted fluorescence spectrum can be detected.

Excitation Is the process of absorption of light quanta which raises a molecule from its ground energy state to an excited state of higher energy.

Excitation spectrum Is the wavelength or the energy (wavenumber) function of the intensity of light excited by a fluorophore and detected at a fixed emission wavelength. Usually the excitation spectrum matches the absorption spectrum.

Excited state Is the higher electronic energy level (higher orbital) that is achieved on absorption of light quantum (photon). The excited states are relatively short-lived and tend to return to ground states by radiative (*fluorescence* or *phosphorescence*) or nonradiative transitions.

Excited state intramolecular proton transfer (ESIPT) Is the reaction occurring between two groups of atoms located closely within the same molecule, the donor and the acceptor. ESIPT results in reorganization of electronic system leading to dramatic transformations in fluorescence spectra.

Excitons Are the imaginary particles (quasi-particles) that allow describing the propagation of electronic excitation in the solid. Exciton is composed of negative and positive charges (electron + hole) and are electrostatically neutral. In sensor technologies they are used for describing the properties of semiconductor nanoparticles, aggregates of organic dyes and conjugated polymers.

Extinction Is a quantitative measure of weakening of light intensity passing through the sample. It involves two parameters – *absorbance* and light scattering.

Fiber optics Represents a flexible bundle of glass, plastic or quartz fibers, with a cladding of lower refractive index designed for transmission of light without losses at long distances. Light is transmitted along individual fibers by total internal reflection. Fiber optic elements are broadly used for illumination and imaging.

Filter (optical) Is a device that reduces the radiant power or spectral range of transmitted light. Bandpass filters isolate particular wavelength range, whereas the cut-off filters only permit the transmission of radiation longer or shorter than the specified wavelength.

Flow cytometry Is a technique allowing the cells or particles to be counted and analyzed during their flow through a very thin capillary at a rate of thousands per second. The analysis may involve several channels of fluorescence detection and therefore several markers can be used simultaneously and together with light-scattering detection. Flow cytometric analysis is usually displayed on a computer window as a two-dimensional image with dots representing counted objects (cells or particles) as a function of forward versus side-scatter, or forward scatter versus fluorescence intensity, or two fluorescence intensities at different wavelengths.

Fluorescence Is spontaneous emission (*luminescence*) of short duration occurring on optical excitation.

Fluorescent label Is the fluorescent reporter group that is bound covalently to a natural or synthetic macromolecule, to nanoparticle or at an interface. In proteins the easiest modification is achieved upon labeling at their –SH and $–NH_2$ groups.

Fluorescent latex particles Are mono-dispersed polymeric, commonly polystyrene, beads (microspheres) having a diameter between 0.01 and 15 μm with incorporated fluorescent dye. They allow achieving high brightness and are used for observing the transport in axons, research into phagocytosis and measurement

of blood flow, or as the standard for determining resolution and microscopy performance in fluorescence microscopy.

Fluorescence biosensors Are the biosensor devices for which the transduction mechanism transforming the act of biospecific recognition into response is based on fluorescence.

Fluorescence correlation spectroscopy Is the technique that uses measurement of fluorescence intensity fluctuations in a microscopic volume. This volume is formed by tightly focused laser beam. The response is sensitive to diffusion rate in and out this volume that allows detecting intermolecular interactions.

Fluorescence lifetime (Or, more generally, the excited-state lifetime) is the characteristic time during which a molecule remains in an excited state prior to returning to the ground state. Usually it is an averaged parameter that does not depend upon the dye concentration. In a homogeneous system without excited-state reactions it follows the law of exponential decay. In this case, the fluorescence lifetime can be defined as the time in which the initial fluorescence intensity of a fluorophore decays to 1/e (approximately 37 %) of the initial intensity. This quantity is the inverse of the rate constant of the fluorescence decay from the excited state to the ground state.

Fluorescence lifetime imaging microscopy (FLIM) Is a sophisticated technique that enables simultaneous recording of both the fluorescence lifetime and the spatial location of fluorophores throughout every site in the image. FLIM results are independent of localized fluorophore concentration, photobleaching artifacts and path length (specimen thickness), but are sensitive to excited state reactions such as resonance energy transfer or dynamic quenching. For long-lifetime luminophores it is sensitive to quenching by diffusing oxygen. The methodology provides a mechanism to investigate different intracellular processes in spatial and temporal dimensions and intracellular sensing of various parameters, such as pH, ion concentration, solvent polarity and oxygen tension.

Fluorescence recovery after photobleaching (FRAP) Is the technique developed for studying the translational mobility (lateral diffusion coefficients) of fluorescently labeled macromolecules, fluorescent nanoparticles and small fluorophores. In FRAP, a very small selected volume is subjected to intense laser illumination to produce complete photobleaching of fluorophores. After the photobleaching pulse, the rate and extent of fluorescence intensity recovery in the bleached region is monitored as a function of time to generate information about repopulation by fluorophores and the kinetics of recovery.

Förster resonance energy transfer (FRET) Is the physical process in which the primary excited fluorescent molecule (donor) instead of emission transfers its excitation energy to another molecule (acceptor), so that the latter can be either emissive or quenched. Efficiency of transfer depends on donor-acceptor distance, and in the case of weak electronic coupling between them the distance dependence is observed in the range 1–10 nm and is very steep. This makes the background for design of molecular sensors, in which this distance changes in the binding event. Efficiency of this transfer depends on the properties of donor and acceptor (overlap of fluorescence and absorption spectrum between them),

which allows efficient selection of donor-acceptor pairs. The acronym FRET is often presented as 'Fluorescence Resonance Energy Transfer', which is incorrect, since this mechanism does not necessarily involve light emission in the form of fluorescence.

Fluorophore Is the molecule or particle and also their structural domain or specific region that is capable of emitting fluorescence.

Fluorescence probe Is a fluorescent molecule designed to localize within a specific region of a structurally heterogeneous specimen and/or to respond to a specific stimulus by change of its parameters of fluorescence.

Fluorescence reporter Is the functional unit that provides the response to target binding by the change of one or several fluorescence parameters. In most cases, it is the organic dye that contains extended π-electronic system with excitation and emission in the convenient visible range of spectrum. Coordinated transition metal ions that produce luminescence emission with extended lifetimes can be also used. The systems that use green fluorescent protein (GFP) and its analogs are applied in cellular research. Some metal and metal oxide nanoparticles known as quantum dots can function as reporters.

FRET microscopy Is an adaptation of the resonance energy transfer phenomenon to fluorescence microscopy in order to obtain quantitative temporal and spatial information about the binding and interaction of proteins, lipids, enzymes and nucleic acids in living cells. FRET microscopy is performed using either steady state or time-resolved techniques, but time-resolved FRET imaging has the advantage of more accurately mapping the transfer efficiency and therefore the donor-acceptor distance.

Graphene Is a crystalline allotrope of carbon where the atoms arrange into 2-dimensional structure forming a network of carbon atoms in their *sp2* configuration, densely packed into a single-atom thickness. This makes it the thinnest but strongest material in the universe. The nano-sized pieces of graphene are strongly fluorescent in the visible range.

Green fluorescent protein (GFP) Is the protein that was originally isolated from jellyfish and emits green fluorescence under blue-light excitation. The emission originates from spontaneously formed fluorophore by the reaction of three amino acids in its sequence during protein folding inside the living cells. The GFP gene has been isolated and improved to obtain different color variants. By gene fusion and expression in living cells, different proteins and structures formed by them can be visualized, which allows to determine the location, concentration, interactions and dynamics. Visible fluorescent proteins of different colors can be isolated from different species or obtained by mutations.

Ground state Is the normal electronic state of unexcited molecule. In this state, molecule may still have excess vibrational and rotational energy.

Image analysis Is a methodology used to extract data from images rather than counting or measuring directly. The advantages are that the captured images are permanent, allowing more time for study, and they can be subjected to enhancement and automated analysis techniques to improve data quality. Image analysis begins with a digitized image, which means that the image is composed of a

rectangular array of individual points of color, called pixels. The pixel value represents a color that can be displayed on a computer monitor or some other display device. Using computers, the image pixels can be manipulated mathematically to change the appearance of the image or to determine some quality of the image.

Immunoassay Is a general term for any technique or device that relies on recognition between an analyte called antigen and specific protein, antibody (Ab). Various detection techniques use specific antigen-antibody complexation for analytical purposes. Radioimmunoassays, enzyme immunoassays and fluorescence immunoassays are well-established in clinical diagnostics.

Immunosensors Are important analytical tools for monitoring antibody-antigen reactions in real time. Recent developments in immunosensors have produced systems that allow rapid and continuous analysis of the binding event without the requirement for added reagents or separation/washing steps.

Intercalators Are small planar molecules that insert specifically between adjacent base pairs in double-stranded DNA.

Intramolecular charge transfer (ICT) Electronic transition in which a large fraction of an electronic charge is transferred from one region of a molecular entity, called the electron donor, to another, called the electron acceptor. Such overall charge distribution in a molecule is a frequently observed process in the excited states of organic dyes.

Lab-on-a-chip Is a highly miniaturized device that is able to carry out instant analysis often in combination with sample preparation and separation of its components.

Light emitting diode (LED) Is a small, efficient, low-voltage, low-power, cold light source that can be supplied at any visible wavelength and produced narrow-spectrum light emission.

Limit of detection (LOD) Is the lowest level of concentration or quantity of a substance at which the sensor still provides reliable results. It depends on two factors: the background response and the standard deviation (noise) of analytical signal.

Luminescence Is the emission of light from any substance (usually a molecule or atom) that occurs from an electronically excited state generated either by a physical (light absorption), mechanical or chemical mechanism. Luminescence is formally divided into *fluorescence* and *phosphorescence*. The generation of luminescence can occur through excitation by ultraviolet or visible light photons (photoluminescence), an electron beam (electrochemiluminescence), application of heat (thermoluminescence), chemical energy (chemiluminescence) or a biochemical enzyme-driven reaction (bioluminescence).

Membrane potential Is an important parameter characterizing electric fields in and across biological membranes. In a living cell, three types of membrane potential are distinguished with the use of fluorescence probes. It is the surface potential produced by charged proteins and lipids on membrane surface and partially screened by counter-ions. This potential becomes strongly negative on apoptosis due to externization of anionic lipids. The cell usually possess strong

(200–500 V/cm) dipole potential produced mostly by lipid carbonyl groups and also transmembrane potential. The latter is of about −70 mV (negative inside the cells). Mitochondria possess stronger transmembrane potential, of about −150 mV. A family of fluorescence membrane potential sensitive probes have been developed.

Microarrays Is the high-throughput version of array technology that allows spotting sensor molecules with a high density.

Molar absorbance Is a direct measure of the ability of a molecule to absorb light. It is also an important molecular parameter used for converting units of absorbance into units of molar concentration for a variety of chemical substances. It is determined by measuring the absorbance at a given wavelength characteristic of the absorbing molecule (usually, the band maximum) for a 1 molar (M) concentration (one mole per liter) of the target chemical in a cuvette having a 1 cm path length.

Molecular biosensors Are devices of molecular size that are designed for sensing different analytes on the basis of biospecific recognition. They should provide two coupled functions – the recognition (specific binding) of the target and the transduction of information about the recognition event into a measurable signal.

Molecular library Is a body of entities designed to handle a large numbers of molecules usually with similar properties at the same time.

Molecular recognition Is a strong and highly specific interaction between biological macromolecules based on multipoint noncovalent interaction. Often it requires steric complementarity in contact areas. The contact areas of interacting molecules may be flexible and local structuring occurs in the course of interaction in these cases. Also, the conformational change may occur in one of the components.

Monochromatic light Is the light beam that is composed of a single wavelength. In a sense, this is an idealization, since even the laser emission or the emission line of a mercury lamp has a measurable bandwidth.

Multiplex analysis Is simultaneous analysis of many targets usually in the same sample and using the same assay conditions.

Near-field microscopy Is the principle of increasing the resolution of optical image to sub-wavelength scale. In its realization in scanning near-field optical microscopy (SNOM) the sample is illuminated through a small aperture held less than 10 nm from sample surface.

Nanosensors Are nano-scale hybrid systems that integrate, together with recognition and reporting functionalities and their support matrix, other components allowing a synergistic approach in modulating the target binding and improving or enhancing the response.

Optical sensor Is an analytical device, the response of which is based on the measurement of either intrinsic optical properties of target molecules (supramolecular structures, cells), or of optical properties of indicator dyes, nanoparticles or labeled biomolecules in solutions or attached to solid supports.

Optodes Are integrated optical sensors, the sensing principle of which is based on a chemical transduction of the signal on analyte binding event on the surface of

polymeric membrane. The coupled fluorescence dye can respond to the produced change of pH. The polymeric membrane can be deposited onto the tip of optical fiber. Such optodes are actively used for detection of Na^+, K^+, Ca^{++} and Cl^- ions in clinical samples.

Phosphorescence Is the long-lifetime (measured in milliseconds to seconds) *luminescence* emission from the fluorophore triplet state. This state can be achieved from the initially excited singlet state in a process called *intersystem crossing*.

Photobleaching Is the irreversible loss of fluorescence intensity over a period of time due to chemical destruction leading to nonfluorescent products (color fading). High photostability is a very desirable property for various applications, especially for those in which intense illumination is needed (e.g. in microscopy). The rate of photobleaching can be dramatically reduced by lowering the excitation light flux or by limiting the oxygen concentration in the medium. Quantum dots exhibit much higher photostability over organic fluorophores. *Photostability* is a measure of fluorophore to resist photobleaching.

Photochemical reactions Are the reactions of chemical transformations that need photoexcitation and occur in the *excited states*. Many reactions of electron and proton transfer as well as isomerizations cannot occur in the ground state because of high energy barrier separating reactant and product states. This barrier may become negligible in the excited state and therefore many photochemical reactions are very fast. These reactions are actively used for providing fluorescent response in sensing. Meantime, some of them producing photobleaching are not desirable.

Photoinduced electron transfer (PET) Is the electron transfer occurring in the excited state. It is a short-distance reaction that can be both intramolecular and intermolecular (with the participation of other molecules and the solvent). PET commonly leads to *quenching* and is in the background of operation of many sensors responding by the change of fluorescence intensity.

Photomultiplier tube (PMT) Is an electrical device designed to collect and amplify photon signals. Incoming photons strike a target in the face of photomultiplier to liberate free electrons, which are accelerated onto a dynode that in turn liberates an amplified stream of electrons. Several dynodes are arranged in series to produce a tremendous degree of amplification from each original photon and then transmit the signal to a processing circuit. Unlike area-array detectors such as charge-coupled devices (CCDs), photomultipliers do not form an image.

Pinhole Is a device used in confocal microscopy for obtaining a sharp image in a focal plane. It allows to produce thin optical sections of focal planes in the specimen.

Polarization of fluorescence When fluorescence is excited by polarized light it is observed as partially depolarized and the extent of depolarization depends on rotation of fluorescent dye (together with rigidly attached molecules or their segments) during fluorescence lifetime. The measurements of polarization are used in fluorescence polarization assays. *Anisotropy* of fluorescence is the parameter similar to polarization.

Quantum dots Are the semiconductor nanoparticles that are characterized by broad excitation and very sharp emission spectrum, high brightness and extremely high photostability. The narrow symmetric emission spectrum is tunable by variation of particle size (within 1–10 nm), which makes them good tracers for cellular research and donors or acceptors for FRET.

Quantum yield of fluorescence Is the ratio of the number of photons emitted as fluorescence to the total number of absorbed photons. In other words, the quantum yield represents the probability that a given excited fluorophore will produce an emitted (fluorescence) photon. It is a measure of efficiency of fluorescence compared to other processes occurring during excited-state lifetime: static and collisional quenching, transition to triplet state, etc. Commonly the quantum yield is determined by integration over the whole fluorescence spectrum and comparison with well-characterized standard. In some dyes (e.g. rodamins) it may approach 100 %. In common cases when the excitation and the absorption spectrum match, the quantum yield does not depend on excitation wavelength.

Quenching Is the reduction or complete disappearance of fluorescence emission. Different intermolecular interactions either induce the quenching or protect from the quenching produced by other interactions. There are two types of quenching: static and dynamic, and they influence differently the parameters of emission. Fluorescence quenching is frequently used in different sensing technologies.

Quencher Is a molecule or a group of atoms that upon interaction with fluorophore induces transition from excited to ground state without emission. A substituent may provide this effect by electron transfer or by hydrogen bond formation. External molecule may provide *quenching* by forming a complex with fluorescent dye (static quenching) or by collisional approach to it (dynamic quenching). Dynamic quenching reduces *fluorescence lifetime*, whereas static quenching is not.

Ratiometric dyes Are the dyes that respond to different environment perturbations in such a way that allows convenient detection of these changes by evaluation of the ratio of 2 independently measured parameters, usually of intensities at selected wavelengths. Ratiometric effect can be produced either by spectral shift or by variation of relative intensities of two or more bands. In the case of spectral shifts the ratio of intensities at two wings of spectrum and in the case of two bands at two band maxima are recorded.

Recognition elements (Receptors or binders) are the functional sensor components that are responsible for strong and selective target binding. They can be chemical constructs such as ion chelators but can be also natural and designed biopolymers (proteins and nucleic acids).

Red shift Also called the bathochromic shift is the shift of spectra to lower energies (longer wavelengths).

Relaxation Is the process of attaining thermal equilibrium with the environment of an excited or otherwise perturbed system. Orientational relaxation of dipoles in the probe environment leading to long-wavelength shift of their spectra is the key mechanism of response to variation of polarity of many fluorescence probes.

Response function Is the dependence of recorded parameter of fluorescence on the target concentration in sensed medium. This function is determined in sensor calibration.

Rotational relaxation time Is the parameter describing the time dependence of the tumbling of a molecular entity in a medium of given viscosity. It can be obtained from the decay of the *fluorescence* or *phosphorescence anisotropy* and is related to the hydrodynamic molecular volume of the *fluorophore* or to supramolecular structure, into which it is incorporated. Its change is actively used in different sensor techniques.

Selectivity (or specificity) Is a capability of sensor to establish an especially strong interaction with the target analyte, thus recognizing it in the presence of other competing and less affine targets. Its quantitative estimate is usually made by comparison of binding constants for specific and nonspecific targets.

Signal-to-noise ratio (S/N) Is the standard ratio of the reporter optical signal from a specimen to the unwanted optical signals of the surrounding background. Noise is defined as the square root of the sum of the variances of contributing noise components. It is different from the background emission that can be produced by steady contribution from the impurities. In fluorescence sensing both the noise and the background emission can be suppressed by using brighter reporting emitters and increasing their concentration.

Single molecule detection Represents a family of techniques that detect intermolecular interactions on the level of single molecules. They allow obtaining response from single molecules in conditions of their high dilution and dramatic decrease of illumination/detection volume down to femtoliters. This technique is extremely useful in detecting rare events and in the studies of heterogeneous systems, where the interesting effects can be hidden within ensemble-averaged signal obtained in common conditions.

Singlet state Is the ground state in which the fluorophores usually reside without excitation or the excited state reached directly from this state by absorption of light quantum. It is characterized by electron pairs with opposite spins without single orbitals, so that their magnetic moments are compensated.

Steady-state fluorescence Encompasses all spectroscopic and imaging measurements performed with constant illumination and observation.

Solvatochromism Is the change in energy of electronic transition and corresponding shift in the wavelength of excitation and emission spectra in response to change in polarity of fluorophore environment. The dyes exhibiting strong solvatochromism are called solvatochromic or polarity-sensitive dyes.

Spectral overlap Is the overlap between donor and acceptor in *FRET*. Its variation may provide strong response in fluorescence sensing.

Stokes shift Is the shift in energy between absorbed and emitted quanta. It is measured as a difference in positions of absorption and emission band maxima on an energy (wavenumber) scale (in cm^{-1}). The Stokes shift reflects the loss of excitation energy in different relaxation processes before the emission and is commonly observed in the direction of low energies (long wavelengths). The dyes exhibiting stronger Stokes shift are preferable for fluorescence sensing and

imaging because this enables more efficient isolation of excitation and emission light by optical filters. For these dyes, the effects of light-scattering, re-absorption of emitted light and of *quenching* at high concentrations are smaller.

Stroboscopic techniques Are used in illumination and in detection of fluorescence in time domain. For excitation, they use the short-duration intense pulses (strobes) of light, often repeated at regular intervals. In time-resolved spectroscopy the strobes are synchronized with pulsed excitation repeated cycles of opening-closing the high voltage on photodetector.

Suspension arrays Are the arrays of sensor elements that are not fixed in position but float freely and are available for target binding in solution. The size of these elements can be ~5 μm or less. For their identification they should possess optical or other type of 'barcodes' and be analyzed one by one by flow cytometry or its specialized version.

Theranostics Is a term for the combination of diagnostics and therapeutics in application of multifunctional biomaterials. The combination enables the simultaneous treatment and feedback process to effectively monitor the efficacy of drug used.

Transducer Is a functional element that converts a change in properties such as molecular mass, refraction index or formation/disruption of noncovalent bonds upon complex formation into a recordable analytical signal. In fluorescence sensing the most important mechanisms of transduction are the influence of target binding on electronic polarization, conformation, freedom of rotation and ionization of fluorescence reporter. Intermolecular interactions resulting in *quenching*, formation of *excimers* and *exciplexes* and also the distance-dependent or *spectral overlap* dependent *FRET* can also be used. In contrast with classical bioassays, such as ELISA, the detection of an interaction between the recognition unit and the target with the aid of transducer is direct and rapid.

Triplet state Is the electronic state, in which a pair of nonbonding electrons exist in two separate orbitals with their parallel spins (angular momenta). Transitions between singlet and triplet states are called *intersystem crossings*. Such transitions are of low probability. Therefore, the *phosphorescence*, which is the emission from triplet state, has long lifetime.

Twisted intramolecular charge transfer (TICT) Is the excited-state charge transfer reaction coupled with reorientation of fragments in the dye molecule. The change from planar to twisted configuration leads to their electronic decoupling. The dyes exhibiting TICT are used as the local viscosity probes.

Two-photon excitation Is the electronic excitation by simultaneous absorption of two light quanta. The sum of their energies should fit the energy of common single-photon excitation. Since simultaneous absorption of two photons is a low-probable event, the two-photon excitation has to be achieved by properly focused pulsed lasers that provide extremely high instantaneous intensity. In this case, the rate of excitation is not a linear but a square function of light intensity. This allows achieving a very high contrast and sharpness of images. In two-photon fluorescence microscopy, the problems of photobleaching and autofluorescence are much less important than in confocal microscopy.

Up-conversion Is the process by which two photons with frequencies ν_2 and ν_3 combine in a nonlinear medium to produce a higher-energy photon with frequency ν_1 such that $\nu_1 = \nu_2 + \nu_3$. In the form of nanoparticles, the up-converting materials demonstrate great advantages in fluorescence imaging.

Visible light Is the part of the spectrum (400–760 nm) that can be detected by the naked eye. This part of light spectrum is used in most fluorescence sensor applications because it is less damaging and has better transmission and less scattering in many media compared to ultraviolet light. Inexpensive optical elements made of plastic and glass can be used with visible light.

Wavenumber (ν, measured in cm^{-1}) is the reciprocal to wavelength (λ, measured in nm) or the number of waves per length along the direction of light propagation. The correlation is $\nu = 10^7/\lambda$. Wavenumber is proportional to the energy of electronic transition.

Index

A
Acoustic sensing, 9
Acrydine dyes, 145
Acrylodan, 116–117, 157, 184, 325, 326
Acyl carrier protein (ACP), 642
Affibodies, 323, 327, 328
Affinity
  affinity coupling, 419–420, 423, 439, 444, 452, 524
  avidin-biotin, 241, 243, 282, 342, 419, 420, 452
  definition, 2, 444
  single-chain antibody fragments, 419
  streptavidin-biotin, 420
Aggregation-induced emission, 216–217, 265
Alexa dyes, 143–144, 282
Alkylsiloxane, 440
Allosteric enzymes, 26–28
Amino acid analogs
  color-switching, 168
  ESIPT reaction, 176
  nucleobases, 170
  SH groups, 167
  synthetic peptides, 167
  (2,7-aza)tryptophan, 169
  two-band wavelength switching, 169
Amino acids, 330
Amino groups modifications, 433
Amphiphilic molecules, 241
Amplification of reporting signal, 26
Amplified stimulated emission (ASE), 477–479
Amyloid fibrils, 431
Anionic lipids, 654, 740
Angle-resolved emission, 487
Anisotropy
Anisotropy measurements, 270
  competitive immunoassays, 90
  depolarization of emitted light, 84
  direct reagent-independent sensing, 88
  homogeneous immunoassay, 90
  molecular-weight dependent, 88–89
  nanosensors, application, 91
  polarization immunoassays, 90
  polarization microscopy, 276–277
  principle of sensing, 395
  ratiometric parameter, 86
  Red-Edge effect, 276–277
  rotational mobility, 87, 90
  rotation rate, 84–85
  sensing, 276
  Stokes–Einstein relation, 88
Antenna effect, 271–273
Antenna pigments, 271
Antibiotics, 96, 335, 576, 746
Antibodies
  antigen (Ag) binding sites, 317
  antigenic determinants, 318
  heavy-chain, 319
  immunoassays, 319–321
  monoclonal, 318, 336
  polyclonal, 318
  recombinant fragments, 317–321
  structure, 317
  technologies, 327
Anticalins, 326, 327
Antigenic determinants (epitops), 23, 318, 348, 419, 705
Antimicrobial peptides, 335, 590, 593
Anti-Stokes emission, 248
APD. *See* Avalanche photodiodes (APD)

A.P. Demchenko, *Introduction to Fluorescence Sensing*,
DOI 10.1007/978-3-319-20780-3

Apoptosis, 14, 167, 613, 652–654, 668, 740, 772
Aptamers
  microarrays, 342
  structure-switching, 340
ASE. *See* Amplified stimulated emission (ASE)
Association and aggregation phenomenon
  association-induced FRET and quenching, 400
  nanoparticles on binding polyvalent target, 399–400
ATP, 731
Autofluorescence, 84, 98, 135, 229, 235, 469, 570, 604, 648, 650, 686, 689–690, 751, 771
Autoimmune diseases, 334, 682
Avalanche photodiodes (APD), 513, 631
Azacrown ethers, 167, 306

B
Bacteria
  harmful, 589
  spores, 590–591
Bacterial periplasmic binding proteins (PBP), 116, 324–325, 665
Barcodes, for microsphere arrays, 533
Bilayers, lipid and polymer
  core-shell liposomes, 448
  features, 451
  liposomes, 445–447
  nanoparticles, 448
  phospholipids, 445
  planar surfaces, 449
  polymersomes, 449–450
  protein layer formation, 450–451
  self-assembly, 448–449
  stabilized phospholipid bilayers, 448–449
Binding
  constant, 44–45
  fractional saturation, 47
  Kb determination, titration, 46–49
  Klotz/Scatchard coordinates, 47–49
  linearized transformations, 48
  serial dilutions (Bobrovnik method), 50–51
  stoichiometry, 81
Biochips, 438, 523, 579, 766
Bioluminescence
  luciferase, 468–469
  luciferin-luciferase system, 468
  resonance energy transfer, 469–470
Biomarkers, cardiac biomarkers, |678, 681–682
Biomembrane, lipid asymmetry, 652–654
Biotelemetry, real-time, 750, 752
Biotin
  biotinylated hydrogel, 439
  streptavidin complex, 420
Bivalent and polyvalent target binding
  dimers, 52
  limitation, 53
  mass action law, 54
  polyvalent binding, 53
Blood sensing, 536, 736
Borondipyrromethane (BODIPY) dyes, 136, 142, 144, 150, 218, 274, 638, 663
Boronic acid, 116, 305–308, 570, 571, 679, 750
Bottom-up approach, 418, 421, 429, 453
B-phycoerythrin, 175
Brownian rotational diffusion, 88

C
Calcium-binding protein
  calmodulin, 660
  troponin C, 660
Calibration in fluorescence, 79
Calix[n]arenes, 311–314
  covalent conjugation, 313
  environment-sensitive dyes, 313
  structure, 311
Calmodulin, 387, 394–396, 643, 660
Calorimetry, 7, 8
Cancer
  associated proteins, 341
  cell marker, 243, 691
  diagnostics, 685–686
Carbon nanomaterials
  fullerenes, 231–232
  graphene nanoscale sheets (G-dots), 229–230, 425–426
  graphene oxide nanoparticles (GO-dots), 227–231, 283, 425–426
  nanodiamonds, 227–229
Carbon nanoparticles (C-dots)
  elements, structure, 231
  optical properties, 231
  photoluminescence, 630
  synthesis, 231
Carbon nanotubes
  as strong electron acceptors, 233
  structures, 227, 228
  supramolecular, 428
Carbonyl groups, 155–156, 231, 362, 446, 655, 773
Cardiac biomarkers, 678, 681–682
Cascade energy transfer, 273–275, 529
Caspase 3, 740
Catalytic biosensors

advantages and limitations, 28–29
allosteric enzyme sensors, 27
amplification, 27–28
Cathodic electroluminescence, 459
Cationic conjugated polymers, 344, 582–583
CCD. *See* Charge-coupled device (CCD)
Cell
arrays, 543
biosensors, 114, 176, 468, 470, 544, 658, 739, 749
calcium, 396
ion sensing, 659–662
labeling, 229, 532, 646, 696, 698, 699, 702
living and fixed, 540
in microfluidic devices, 540–542
Cell membrane
dipole potential, 655
epidermal growth factor receptors, 657
fluorescence probing, 651
lipid asymmetry and apoptosis, 652–654
signaling pathways, 657
structure and dynamics, 651–652
transmembrane potential, 654–656
Cells inside living body
in vitro labeling technology, 702
labeling procedure, 698–699
molecular imaging, 689
stem cell, 700–701
tracking hematopoietic and cancer cells, 699, 700
yeast, 570
Cellular signaling
first messengers, 662
hydrogen peroxide, 663
second messengers, 662
Charge-coupled device (CCD), 473, 514, 515, 531, 532, 606, 607, 614, 628, 688, 692, 698, 751, 767, 774
Chelate effect, 305
Chemical and photochemical cross-linking, 436–437
Chemiluminescence
chemical reaction, 460
horseradish peroxidase, 462
immunoassays, 462
luminol transformations, 461
nanoparticle-based platforms, 462–463
organic peroxides, 461
trace amounts, blood, 461–462
Cherenkov effect, 470–474
Cholera toxin, 449
Cholesterol, 308, 349, 446, 447, 572, 652, 682
Clinical diagnostics
biological fluids, 735
blood sensing, 736
gene-based molecular diagnostics, 737–738
metal-enhanced fluorescence, 736
non-invasive biological fluids, 737
two-photon detection, 736
CMOS. *See* Complementary metal-oxide-semiconductor (CMOS)
CMOS imagers, 514–515
Collective effects in sensing
light harvesting, 272
superquenching, 270
wavelength converters, 269
Collisional quencher of phosphorescence, 96
Combinatorial chemistry
discovery of fluorescent dyes, 152–153
library selection, 348
Competitor displacement assay
advantages and limitations, 21–22
binding sites, 20–21
intercalator dyes, 19
peptide indicator displacement assay, 17–18
principle, 16–17
RNA binding, 18
Complementary metal-oxide-semiconductor (CMOS), 514–515
Concentrational quenching
dimers formation, 210
fluoresceins and rhodamines, 210
homo-FRET mechanism, 210
Condensed matter
fluorescence probing, 565–566
ionic liquids, 562–563
liquid-liquid interfaces, 566
polarity probing, liquids and mixtures, 557–560
polymers, 564–565
solid-liquid interfaces, 566
solid-solid compositions, 566
supercritical fluids, 563–564
viscosity and molecular mobility sensing, 560–562
Confocal microscopy, 143, 604, 608–609, 611, 612, 615, 628, 654, 774, 777
Conformational changes
calmodulin, 394–396
in conjugated polymers, 386–388
electronic conjugation, 398
engineering, 396
excited-state isomerism, small molecules, 386
folding reactions, polypeptides and, 398
molecular beacons, 581
ologonucleotides, 398
in peptide sensors and aptamers, 388–390
periplasmin binding proteins, 324

Conjugated polymers
chain conformation, 222–223
chemical structures, 220–221
conformational changes, 388–390
dendritic conjugated polymers, 226
DNA-PNA hybrids bind cationic, 344
DNA sensing, 227, 345, 582–583
excitons, 268, 270
fluorescence quenching, 222
sensors, usage, 280
superenhancement, 224
superquenching effect, 222, 224, 275, 344, 443
water-soluble, 587
Conjugation, labeling and cross-linking
amino groups and SH-groups, 433
biomolecules, 432
chemical and photochemical cross-linking, 436–437
co-synthetic modifications, 435
covalent linkage, 433
nano-bio conjugation, 433
solid phase synthesis, 433
Contact quenching, 209, 283
Copper
ion detection, 399
nanoparticles, 65
Core-shell compositions, 452
Core-shell liposomes, 448
Coupled emitters
excimers, 364–365
FRET-based mechanism, 365
reporting with reference, 364
Critical micelles concentration, 453
Crown ethers, 305–306, 372, 662
Cryptands, 177, 305–306, 372
Cucurbiturils, 137, 314–317
Cuvette-type fluorescence detection, 509
Cyanine dyes, 142, 143, 145–147, 149, 267, 272, 313, 385, 392, 475, 559, 574–576, 579, 693, 694, 699
Cyclodextrins
α-CD, β-CD and γ-CD, 308–309
conjugation, fluorescence dyes, 310
polarity, dehydration and immobilization effects, 309
selectivity and affinity, 310
Cytokines, 14–15, 341, 662, 737

D

Delayed fluorescence, 150–152
Dendrimers
arrangement, 215
flexibility, 216
generations, 215
internal dynamic cavities, 216
intrinsically fluorescent, 216
luminescent metal chelates, 212
PAMAM, 215, 219, 433
single-molecular micelles, 215
spectroscopic properties, 212
ultrasensitive bioanalysis, 213
Dendrimers doping, technique, 209
Dendritic conjugated polymers, 226
Deoxyribozymes, 405
Depolarization of emitted light, 84
Detergent micelles, 183
Dexter energy transfer, 110
Diabetes
blood glucose, 679
contact lenses, 680
glucose binding proteins, 680
Dielectric relaxation, 162, 209, 265, 373, 561, 562, 566
Differential expression pattern, 722
Diffraction limit
near-field technique, 616
STED, 618
Diffusion-controlled chemical inputs, 534
Digestible sensors, 750
Dioxin, 732, 733
Diphtheria toxin, 243
Dipole moment, 14, 114, 157, 159–161, 163, 171, 190, 267, 363, 371, 372, 375, 378, 558, 559
Direct reagent-independent sensing
advantages and limitations, 32–33
remote sensing, 30–32
thermodynamic equilibrium, 30
Direct sensors, direct molecular immunosensor, 116
Disease-related gene mutations, 737–738
Disorder, static and dynamic, 562, 565
Dissociation constant, 16, 43, 45, 46, 81, 96, 304, 316, 331, 366, 374, 389, 420, 524, 640, 641, 739
Dissociation-enhanced lanthanide fluoroimmunoassay (DELFIA), 181
DNA chip technology
fabrication, 578
polymerase chain reaction (PCR); RT-PCR, 578, 579
target pool labeling, 580–581
transcriptome profiling, 579
DNA hybridization, fluorescence in situ hybridization (FISH), 576, 665
DNA recognition

conjugated polymer, 582–583
cyanine dyes, 574
double-helical oligonucleotides, 577
dye dimers, 574
groove binders, 576
intercalating dyes, 573
molecular beacons, 580–582
oligonucleotides, 579
peptide nucleic acids (PNA), 576
sandwich assays, 24, 580
synthetic molecules, 576
YOYO dye, 573
zinc fingers, 576
DNA single stranded (ssDNA), 233, 344, 574–576, 578, 579, 581, 632
DNA templates
application, 428
origamis, 428
Domain antibodies, 319
Drug discovery
high throughput screening (HTS), 739–740
screening, anti-cancer drugs, 740
Dye-doped nanoparticles
aggregation-induced emission, 216–217
applications, 218–220
brightness, 209
concentrational quenching, 209–210
dendrimers, 220
in ion sensing, 219
micro-emulsion polymerization, 211
optical microscopy imaging, 219
polystyrene latexes, 211
porous, 210–211
silica particles, 212
sol-gel matrices, 212–213
Dyes, fluorescent
amino acid analogs, 167, 324
chemical modifications, 171
computer design, 171
nucleic acid bases, 167–170
Dyes, responsive
electric field sensitive (electrochromic), 160–162
electronic polarizability, 166
environment-sensitive (solvatochromic), 156–159
fluorescence reporters, requirements, 154
hydrogen bond responsive dyes, 155–156
protic equilibrium. pH-reporting, 155
supersensitive multicolor ratiometric, 162–167
Dynamic association-dissociation equilibrium
dissociation constant, 45
intermolecular interactions, 45–46
mass action law, 45
molarity, 45

E
ECL. *See* Electrogenerated chemiluminescence (ECL)
Electrochromic (electric field sensitive) dyes
electric field sensing, 165–166
styryl and naphthyl styryl dyes, 161
styrylpyridinium dyes, 162
Electrochromic modulation, ESIPT, 165–166
Electrochromism (Stark effect), 160, 166, 363, 768
Electrogenerated chemiluminescence (ECL)
application, novel nanomaterials, 465
ECL reactions, 463–464
indirect generation, 464
$Ru(bpy)_3^{2+}$, structure, 463
single molecules, 464
Electronic noses/photonic noses, 741–742
Electronic tongue, 741–742
Electron transfer
electronic conjugation, 370
intramolecular charge transfer (ICT), 370–376
photoinduced electron transfer (PET), 367–370
Electrostatic forces in self-assembly
Langmuir–Blodgett films, 442
layer-by-layer technology, 421, 442–444
ELISA. *See* Enzyme-linked immunosorbent assay (ELISA)
Enantioselective sensing, 309, 313
Endocrine disruptors, 310, 733
Environment polution, 539
Enzyme-linked immunosorbent assay (ELISA), 24, 25, 27, 28, 32, 319, 341, 343, 462, 495, 586, 591, 592, 683, 685, 768, 777
Epi-fluorescence microscopy, 605–606
ESICT. *See* Excited-state intramolecular charge transfer (ESICT)
ESIPT. *See* Excited-state intramolecular proton transfer (ESIPT)
Ethidium bromide, 19, 52, 104, 145, 381, 405, 573
Evanescent field excitation, 484, 495
total internal reflection, 484
waveguide surface, 484–485
Evanescent-field waveguides
evanescent wave, 521
optical fiber-based techniques, 522
waveguides, planar geometry, 521

Evanescent-wave fluorescence sensors
applications, 484–485
heterogeneous assays, 484
hybridization-based detection, 485
immunoassays, 485
Excimers and exciplexes
aptamers, 100
dyes forming, 98–99
emission spectrum, 98
in fluorescence sensing, 98
Excited-state energy transfer-FRET
collective effects, 381–383
Dexter energy transfer, 110
efficiency, 75
sensing and imaging, 383
spectroscopic parameters, 379–381
variation of distance, flurophores, 378–379
Excited-state intramolecular charge transfer (ESICT), 162. *See also* Intramolecular Charge Transfer (ICT)
Excited-state intramolecular proton transfer (ESIPT)
electrochromic modulation, 363–364
equilibrium, 122
hydrogen bond donor and acceptor groups, 121
Excitons
conjugated polymers, 203, 221, 222, 234, 237, 266–269, 294, 385, 405, 443, 479, 769
cyanine and squaraine dyes, 266
H-aggregates, 266
J-aggregates, 266–267
migration and energy transfer, 266
plasmon interactions, 268
splitting, 148
Explosives, 8, 479, 556
Ex-vivo diagnostics
autoimmune diseases, 682
biomarkers, 678
cancer, 684
cardiac biomarkers, 681–682
diabetes, 679–680
infectious diseases, 682–683
kidney and liver related diseases, 684–685
peripheral blood, 678

F

Far-field optical nanoscopy, 605
Fatty acid, 116, 144, 242, 442, 444
FCS. *See* Fluorescence correlation spectroscopy (FCS)
Few-atom clusters of gold and silver
excitation and fluorescence emission spectra, 188–190
light absorption and emission mechanisms, 187–188
near-IR-emitting silver clusters, 190
organic dyes coupled with silver clusters, 190
structures and stability, 186–187
Fiber optics, 11, 83, 185, 484, 518, 519, 561, 569, 617, 723, 730, 746, 769
FID. *See* Fluorescent intercalator displacement (FID)
FISH. *See* Fluorescence in situ hybridization (FISH)
FLASH. *See* Fluorescein arsenical helix binder (FLASH)
FLIM. *See* Fluorescence lifetime imaging microscopy (FLIM)
Flow cytometry, 11, 16, 136, 137, 143, 175, 275, 286, 525, 529–533, 538–540, 652, 654, 663, 734, 766, 769, 777
Fluorescein, 63, 75, 79, 119, 135–137, 141–143, 148, 151, 152, 207–208, 210, 213, 323, 339, 345, 381, 406, 496, 628, 641, 642, 652, 660–662
Fluorescein arsenical helix binder (FLASH), 641, 642
Fluorescence correlation spectroscopy (FCS)
autocorrelation function, 634–635
cross-correlation function, 634–635
fluorescence fluctuation, 634–635
Fluorescence emission parameters
anisotropy, 276–277
intensity, 272, 273, 279, 280
lifetimes, 270, 275
modulation by light, 277–279
Fluorescence enhancement
dendrimers, 265
excitons, 266–269, 294
plasmons, 265–266
Fluorescence image guided surgery, 695–697
Fluorescence in situ hybridization (FISH), 576, 665
Fluorescence lifetime imaging microscopy (FLIM), 174, 612, 613, 770
Fluorescence microscopy
confocal microscopy, 604, 608–609, 615, 628, 654
diffraction limit, 603–605, 615, 616, 618, 622, 625, 667
epi-fluorescence, 605–607, 615, 768
total internal reflection, 484, 516, 518, 566, 604, 607–608, 615, 626

two-photon and three-photon, 611–612
wavelength-ratiometric imaging, 613–614, 654
Fluorescence parameters
lifetime, 74, 75, 77–78
molar absorbance, ε, 83, 103, 134
photostability, 83, 119, 136–139, 143, 145, 146, 150, 171, 174, 187, 192, 219, 225, 237–239, 273, 287, 648, 665, 667, 695
quantum yield, Φ, 62, 64, 73, 76, 134–135, 141, 144, 174, 180, 187, 238, 313, 492–494
Stokes shift, 70, 71, 76, 115, 135–136, 142, 150, 210, 269, 379, 695
Fluorescence polarization immunoassays, 90, 319–320
Fluorescence quantum yield, Φ, 73, 76, 135, 141, 148, 159, 170, 174, 187, 212, 222, 268, 313, 766
Fluorescence quenching
electron transfer, 106, 400
graphene oxide, 283
static quenching, 78, 97, 210, 270, 384, 775
Stern–Volmer relationship, 78, 93
temperature effects, 78
Fluorescence tomography, 677, 711
Fluorescent angiography, 694
Fluorescent dyes
bioorthogonal labeling, 645
near-IR, 688–689
non-canonical amino acid probes, 645
Fluorescent intercalator displacement (FID), 124, 573
Fluorimeters-in-a-pill, 751
Focal plane and volume, 603
Foodborne contaminants, 749
Förster resonance energy transfer (FRET), 19, 70, 136, 204, 264, 305, 364, 440, 462, 525, 553, 612, 680, 728
See also Excited-state energy transfer-FRET
cascade, 273–275, 277, 280, 287, 381, 385, 529
with competitor, 19, 20, 108, 126, 282, 320, 365, 395
conformational change, 108–109, 367, 386, 395
directed, 226
donor-acceptor distance, 102–104, 110, 379, 770–771
double-labeling, 106–107, 370
efficiency of energy transfer, 103
Förster radius, 103, 207
FRET-gating, 381
hetero-FRET, 104–105, 210, 269–270, 273, 277, 381, 382
homo-FRET, 75, 104–105, 136, 209–210, 269–271, 276, 277, 294, 313, 381, 382, 384, 385, 408
imaging, 96, 106, 192, 275, 383, 613, 771
immunoassays, 19, 96, 175, 320
modulation by light, 277–280
to non-fluorescent acceptor, 105, 392
photo-switching quenching, 106
quenching, 105, 225, 243, 283
spectral overlap, 108, 109, 365, 408, 776, 777
Frequency-modulation technique, 510
Freshness markers, 749
FRET. *See* Förster resonance energy transfer (FRET)
FRET applications
carbon nanoparticles, 232, 252, 283, 463
conjugated polymers, 104, 106, 225–226, 270–271, 277, 281, 294, 305, 381, 385
fluorescent proteins, 104, 106, 277, 282, 283, 395, 613, 660, 665
lanthanide chelates, 181, 281, 282, 294, 613
metal nanoparticles, 204, 207, 283–284, 384
nanoparticles, 19, 104, 185–186, 207, 208, 210, 707, 775
optimal donors and acceptors, 104, 174, 208, 210, 264, 269, 273, 280–284, 408–409
organic dyes, 104, 207, 210, 225–226, 275, 277, 281, 283, 287, 294, 383, 395, 408, 452, 584, 643
photochromic compounds, 106
semiconductor quantum dots, 192, 281, 282
up-conversion materials, 282–283

G

Gas sensors, 555, 556, 741
G-dots. *See* Graphene dots (G-dots)
Gene expression profile
nanoarrays, 722
sandwich hybridization, 722
transcriptome profiling, 722
Genetic encoding, 639–646, 728
GFP. *See* Green fluorescent protein (GFP)

Glucose sensing
binding proteins, 82, 116, 184, 526
bioanalytical recognition units, 570
biosensor competitive, 570
blood glucose, 570
boronic acid, 307, 570
competitive displacement assays, 570
excimers, 100
general, 10, 33, 570–571
nanoparticles of gold, 400
noninvasive monitoring, 570
Glutamine, 184
Glycan arrays, 591, 593
Glycolipids, 23, 444, 588–589
Glycoproteins, 317, 588–589
GO-dots. *See* Graphene oxides (GO-dots)
Gold
clusters, 186, 188, 189
nanoparticles, 207–208, 226, 267, 399, 400, 436, 437, 443, 448, 463, 494, 585, 586, 704
surface modifications, 440
Graphene dots (G-dots), 229–231, 234–235, 476, 571, 707
Graphene oxides (GO-dots)
reduced graphene oxide (rGO), 426
structure and properties, 227–228, 230–231, 283, 425–426
Graphite, 229, 230, 425, 426
Green fluorescent protein (GFP)
family, proteins, 172–174, 280, 364, 381, 539, 543, 568, 615, 643, 646, 657
fluorophores, 172, 176
jellyfish Aequorea Victoria, 171, 173
sensor, 396

H

H-aggregates, 147, 217, 266
3HCs. *See* 3-Hydroxychromones (3HCs)
Heart disease biomarkers, 737
Heavy metal ions, 400, 569, 570, 593
Hematopoietic cells, 697, 698, 700
Heterocyclic hydrocarbons, 315, 316
Hetero-FRET, 104–105, 210, 269–270, 273, 277, 381, 382
Heterogeneous formats, 6
High throughput screening (HTS), 90, 251, 288, 496, 533, 580, 728, 733, 739–740, 755
Hinge-bending motions, 324, 394, 643
Histidine tag, 640
HIV. *See* Human immunodeficiency virus (HIV)
H_2O_2. *See* Hydrogen peroxide (H_2O_2)
Homo-FRET, 75, 104–105, 136, 209–210, 269–271, 276, 277, 294, 313, 381, 382, 384, 385, 408
Homogeneous assays, 4, 5, 11, 17–19, 90, 219, 243, 288, 340, 369–370, 466, 469–470, 507
Horseradish peroxidase, 462, 685
Hot electrons injection, 465, 466
HSA. *See* Human serum albumin (HSA)
HTS. *See* High throughput screening (HTS)
Human genome mapping, 720
Human immunodeficiency virus (HIV), 168, 533, 540, 576, 577, 591, 640, 649, 683, 737
Human serum albumin (HSA), 116, 585, 680, 684, 704
Hybridization in-situ, 665
Hydrogel layers, 438, 453
Hydrogen bond, 2, 14, 29, 53, 77, 114, 117, 121, 122, 137, 154–156, 158, 159, 162, 163, 165, 166, 169, 193, 301, 303, 344, 362, 376, 391, 407, 418, 421, 422, 428, 430, 431, 446, 452, 556, 558, 566, 574, 576–578, 583, 585, 775
Hydrogen-bonding complementarity, 422
Hydrogen peroxide (H_2O_2), 461, 462, 571, 572, 663, 685
Hydrophobic interactions, 224, 303, 314, 349, 421, 431, 709
3-Hydroxychromones (3HCs), 113, 122, 153, 158, 159, 162, 163, 165, 166, 169, 170, 244, 285, 334, 364, 377, 397, 407, 446, 558, 563, 567, 572, 653–655, 668

I

Illness treatment model, 747, 755
Imaging, cancer tissues, 691–692
Immobilization, surface, 335, 438, 440, 444, 483, 632
Immunoglobulin E (IgE) detection, 91
Immunosensor techniques, 22
Implantable sensors, 750
Imprinted polymers, 345–350, 766
Inclusion complexes, 308, 309, 316
Indocyanine green, 149, 693–695, 711
Induced and assisted folding, 388, 389
Induced fitting, 332, 422

Industrial sensor applications, 745
Infectious diseases
bacteria, 710
diagnostic devices, 683
harmful microbes, 682
mix-and-read sensors, 683
peptide beacons, 683
viruses, 683
Inorganic colloidal scaffolds
decoration, 431
ligand exchange, 432
phase transfer, 432
Instrumentation, fluorescence spectroscopy
cellphone-based, 515
charge coupled device (CCD), 514
CMOS, 514
integrated systems, 516–517
light detectors, 512–515
light emitting diode (LED), 512
light sources, 510–512
microchannel plate photomultipliers, 513
monochromaticity, 511
photodetectors, 513
signal-to-noise (S/N) ratio, 512
silicon-based detectors, 514
single-photon counting mode, 513
solid-state semiconductor devices, 513
spectrofluorimeter, 509–510
time-resolved detection methods, 511
Intensiometric sensors, 84
Intensity-weighted format
anisotropy sensing, 62
lifetime sensing, 63
Interactions in a small volume, 57–58
Interactome
cellular networks, 727
double labeling, 728
Intercalator dyes, 19, 52, 124, 146, 574
Internal calibration, 79–83, 123–125, 363, 525
Intersystem crossing, 71, 569, 706, 774, 777
Intracellular imaging, 240, 648, 659
Intracellular labeling and genetic encoding
biarsenical dyes, 641, 642
cell-loading techniques, 640
fluorescent proteins, 644–646
FRET, 643–644
hexapeptide sequence, 641
oligo-His sequence, 640–641
Intramolecular charge transfer (ICT)
electronic conjugation, 370–371
electronic density, 376
environment sensitivity, 373
ICT-based sensor for zinc ions, 374
LE-ICT switching, 371–372
modulation of electronic conjugation, 373–374
wavelength-ratiometric ion sensor, 375
Intramolecular dynamics of protein, 394
Intramolecular electron transfer (IET), 76. *See also* Photoinduced Electron Transfer (PET)
Ionic liquids
dynamic disorder, 563
3-hydroxyflavone probing, 563
solvation dynamics, 563
Ion sensing
anions, 182, 361, 372
calcium, 659–662
mercury, 235, 386, 569
sodium and potassium, 661–662
zinc, 660
Irreversible binding, 39, 64
Isoemissive point, 62, 115
Isomerization, 59, 139, 386, 398, 405, 407, 408, 560, 561, 565, 774

J
Jablonski diagram, 112
J-aggregates, 147–148, 251, 266–268, 294, 385, 476

K
Kasha heavy atom effect, 96, 151–152
Kasha's rule, 2, 77, 96, 152, 231, 267, 768
Ketocyanine dyes, 53, 156, 408
Kinetics of target binding, 40, 58–60, 66, 533
Klotz plot, 47–49

L
Label-based techniques, 11–12
Labeled pool of potential targets, 13, 34
Label-free approach, 8–10
Lab-on-a-chip devices, 508, 534–537, 541, 545, 678, 736, 772
Langmuir–Blodgett films, 160, 442–443, 453
Lanthanides
europium, 177, 179
lanthanide-chelator complexes, 178
terbium, 177, 179

Lasers
lasing threshold, 478, 479
light sources, 472
pulsed, 476, 495, 511, 629
Layer-by-layer approach, 443–444
Lectins, 33, 303, 307, 388, 420, 526, 570, 588, 705
Leucine-rich repeat proteins, 328
Lifetime sensing
discrete form with different lifetimes, 93
long-lifetime luminescence, 95
modulation by dynamic quencher, 93
phase-modulation technique, 94
single-photon counting, 94
squaraine dyes, 96
time-resolved anisotropy, 95
Ligand binding isotherms
bivalent and polyvalent reversible target binding, 52–54
bound competitor and target ligands, 56
competitor and reversible binding, 54–57
Ligand-binding proteins
affibodies, 327
anticalins, 326–327
in vitro evolution, 322
immunoglobulins, 328
leucine-rich repeat proteins, 328
minimal protein scaffolds, 328
periplasmic binding proteins (PBPs), 324–325
Ligand-to-metal charge transfer (LMCT)
applications, 190
states, 190
Light-addressable potentiometric sensors (LAPS), 33, 480–481
Light emission phenomenon
absorption of light quanta, 71
characteristic features of luminescence, 73
elastic light scattering, 72
intersystem crossing, 71
phosphorescence emission, 71
Raman scattering, 72
Stokes shift, 71
Light emitting diodes (LEDs), 512, 537, 751, 772
Light-harvesting, 271–273, 275, 279, 408
Light-scattering sensitivity, 42, 69, 71–73, 76, 82–84, 92, 94, 95, 97, 113, 115, 126, 136, 150, 176, 178, 186, 187, 237, 251, 320, 469, 490, 494, 510, 530, 534, 650, 686, 694, 701, 736, 765, 769, 777
Limit of detection (LOD), 40–42, 241, 264, 772
Limit of quantitation (LOC), 42
Linearly polarized light, 84, 85, 87, 245, 652
Linear response format, 61–62
Lipid asymmetry and apoptosis, 652–654
Lipid vesicles (liposomes)
cholesterol detection, 447
hydration, 445
stabilized, 448–449
structural and dynamic properties, 446
Lipobeads, 448
Lipocalins, 326–327
Liquid-liquid interfaces, 566
Localized surface plasmon resonance (LSPR), 488, 490–491
Logical operations
excited-state reactions, 407
in fluorescence sensing, 401–402
information inputs and outputs, 400
logic gates, molecular, 401–407
signal transduction mechanisms, 403–405
Luciferin-luciferase system, 468, 499, 700
Luminescent metal complexes
anisotropy sensors, 184
DELFIA, 181
immunoassays, 184
ion-heterocyclic chelates, 184
labels and reference emitters, 180–181
lanthanide chelates, 180
metal-chelating porphyrins, 184–185
quantum yields, 180
reference emitters, 184
ruthenium ions, 183
terbium complexes, 179
transition metal complexes, 183–184
Luminol, 461–463

M

Magic-sized nanoclusters, 206, 244–245
Maltose binding protein (MBP), 52, 116, 310, 324, 325, 395, 643, 665
Mass action law, 33, 40, 44–46, 49, 52, 54, 55, 57, 65, 304
Membrane potential, 114, 119, 143, 147, 160, 161, 174, 539, 549, 644, 645, 648, 772–773
Mercury sensing, 235, 386, 569
Metabolites, 185, 322, 539, 551, 556, 562, 585, 644, 659, 663, 665, 678, 721, 729, 737
Metabolomics, 729
Microarrays
DNA sensors, 581
immunosensors, 15

spotted, 522–526
Microbes, harmful
bacterial spores, 590–591
detection and identification, 589–590
toxins detection, 591
viruses, sensors, 591–592
Microcantilever, 9, 33
Micro-emulsion polymerization, 211
Microfluidic optical chemosensor (mFOC), 535
Microplate readers, 510
Microsphere suspension arrays
barcodes, 530
flow cytometry, 530–531
imaging devices, 532
magnetic microbeads, 531
microscope imaging system, 530
Micrototal analysis systems (m-TAS), 534
Microviscosity, 557, 560, 562
Microwave acceleration, 481, 496–497, 736
Mini-emulsion polymerization, 211
Mix-and-read sensing, 29–30, 683
Molar absorbance, 62, 64, 83, 103, 134, 135, 144–146, 148, 173, 175, 177, 180, 184, 185, 187, 192, 193, 220, 228, 238, 271, 279, 283, 475, 765, 766, 773
Molecular barometry, 554–555
Molecular beacon technique, 485, 580–582
Molecular chaperones, 167, 388
Molecular computing, 406
Molecularly imprinted polymers, 345–348
Molecular recognition, 2, 11, 16, 24, 32, 44, 94, 100, 208, 209, 293, 301–303, 305, 306, 310, 323, 326, 330–332, 342, 346, 348, 359, 365, 389, 418, 421, 430, 432, 526, 551, 557, 652, 723, 732, 736, 766, 773
Molecular rotors, 154, 561, 562, 585, 631
Molecular thermometry, 552–554
Molecular wires, 221, 405
Multi-analyte spotted microarrays
multiple spotting technique, 522
nanoarrays, 528
proteome and interactome, 528
read-out and data analysis, 525–526
Multifunctional nanocomposites
drug release, 292, 708–709
luminescent plus magnetic, 289–290
multimodal imaging, 291–292
Multi-photon fluorescence
Goeppert–Mayer units, 476
molar absorbances, 475
Multiplexing and multicolor coding, 264, 284–289
Multivalency
chelate effect, 305
cooperativity, 303
entropy effects, 303, 305
macrocyclic effect, 305

N
Nano-bio conjugation, 433–435
Nanocages, 709
Nanocomposites
design, 265–266
fluorescence enhancement, 265–271
multicolor coding, 287
multifunctional, 289
multiplex assays, 286
suspension arrays, 286
wavelength referencing, 284–285
Nanodiamonds (NDs), 203, 227–229, 283, 650
Nanorods, 205, 245, 494, 496
Nanosensors inside cells, 647–651
Nanoviscosity, 557
Near-field scanning microscopy (NSOM/SNOM), 616–618, 667
Near-infrared (IR) dyes
BODIPY dyes, 150
cyanines and pyrrolopyrrole cyanines, 149
indocyanine green, 149, 693–695, 711
porphyrins and phthalocyanines, 150
squaraines, 150
for two-photon microscopy, 150
Nile Red, phenoxazone dye, 157–158
Nipkow disks, 609
Nucleic acid aptamer
cytokines, 341
Nucleic acid aptamers
cocaine, 339
combinatorial library, 336
double labeling, 340
microarrays, 342
selection-amplification techniques, 336
SELEX procedure, 337–338
thrombin, 340
Nucleic acid detection
DNA microarrays, 584
DNA sensing, conjugated polymer, 582–583
molecular beacon technique, 580–582
quadruplex DNA, 583
sandwich assays, 580
sequence-specific DNA recognition, 576–577
ssDNA, 576–577

O
Olfactory system, 585, 741, 743, 744
Optical fiber sensors, 508, 518–521
Optical waveguides, 83, 449, 483–485, 507, 508, 510, 516, 518–522, 537, 541, 542, 545, 617, 745
Optodes
  applications, 518
  evanescent-field waveguides, 521–522
  optical fiber sensors, 519–521
Organic dyes
  acrydine and ethidium dyes, 145
  Alexa dyes, 143–144
  cyanine dyes, 145–146
  fluoresceins, 143
  fluorescence sensing technologies, 140–141
  near-IR dyes, 149–150
  optimal FRET pairs, 148–149
  phosphorescent dyes, 150–152
  polymethine cyanines, 146–148
  resonant or mesomeric dyes, 141
  rhodamines, 143
Organic peroxides, 461
Origami, 428, 429
Overlap integral, 103, 104, 107, 108, 148, 210, 270, 273, 306
Oxygen sensing
  collisional quencher, 568
  fiber-optic probe, 569
  fluorescence and phosphorescence, 568
  λ-ratiometric imaging, 568

P
PBP. *See* Bacterial periplasmic binding proteins (PBP)
Peptide nucleic acid (PNA)
  and conjugated polymers, 526
  DNA and RNA recognition, 344
  structure and properties, 343–344
Peptides
  advantages in sensing, 178
  affinity selection, 332
  antimicrobial, 335
  beacons, 333
  in vitro selection, 336
  phage display, 331–333
  randomly synthesized, 329–330
  ribosome display, 331–332
  sensor arrays, 333–334
Peptide scaffolds, 310, 331, 332, 429–431
Periplasmic binding proteins (PBPs)
  computational methods, 324
  E. coli, maltose binding protein, 324–325
  environment-sensitive dyes, 325–326
Phage display, 318, 319, 321, 322, 331–333, 335, 591, 683, 724, 726
Pharmacokinetics, 739
Phosphate binding protein, 325, 395
Phosphatidylethanolamine (PE), 652
Phosphatidylserine (PS), 430, 447, 652, 655, 706
Phospholipid bilayers on planar surfaces, 7
Phospholipid monolayers, 440
Phosphorescence, 70, 71, 73, 96–97, 101, 150–152, 178, 183–185, 213, 216, 281, 347, 361–362, 390, 489, 495, 511, 552, 553, 568, 569, 663–665
Photo-acids, 376
  eosin and erythrosine, 96, 151
Photobleaching, 80, 83, 84, 86, 106, 115, 136, 186, 193, 212, 235, 246, 280, 380, 381, 427, 495, 609–611, 623, 624, 627, 628, 636, 642, 659, 667, 689, 770, 774, 777
Photocell sensors, 482
Photochromes, FRET, 107, 380, 381
Photodynamic therapy
  cytotoxic singlet oxygen, 707
  photosensitizers, 706
Photoinduced electron transfer (PET)
  association/dissociation, 369
  carbon nanomaterials, 701
  cation binding, 368
  concentrational quenching effects, 370
  conjugated polymers, 369
  intramolecular transfer, 407
  quenching, 83
Photomultiplier tubes (PMT), 509, 513, 767, 774
Photosensitizers, 33, 190, 191, 706, 707, 712
Photostability, 24, 83, 100, 119, 136–138, 140, 141, 143–146, 150, 159, 171, 174, 180, 187, 190, 192, 213, 218, 219, 225, 237–239, 273, 287, 317, 348, 380, 478, 487, 495, 529, 568, 615, 620, 627, 628, 641, 647, 648, 658, 665, 667, 695, 774, 775
Phototautomer (T^*), 122
Photothermal therapy, 705, 707
pH sensing
  incide cells, 276
  protonation-deprotonation equilibrium, 378

Phycobiliproteins, 175
Plasmonic enhancement
  angle-ratiometric fluorescence sensing, 494
  optimal distance, 494
  quantum yield, 493
  sensor, microwave acceleration, 496–497
  surface plasmon-field enhanced fluorescence, 486–487
Plastic scintillator, 70, 472, 512
Platelet-derived growth factor (PDGF), 312
Polarity probing
  empirical scaling, 557, 559
  polymethine chain, 559–560
  pyrene, 558
Polarity-sensitive dyes, 113, 442, 561, 776
Polarization assays, immunoassays, 90
Poly(amidoamine) (PAMAM)
  bioconjugation, 433
  immunoasssay, 218
  physical properties, 214
Polymerase chain reaction (PCR), 336, 337, 495, 536, 578, 579, 584, 589, 683, 685
Polymers
  glass transition, 565
  highly elastic state, 565
  polymethine dye, 565–566
  structure and dynamics, 564–565
Polymersomes, 278, 449–450
Polymethine cyanines
  Cy3 and Cy5 dyes, 146
  groove binding, 147
  intercalation, 146
  J-aggregates, 147–148
Polysaccharides, 144, 588–589, 767
Polystyrene latexes, 211, 288
Porous silicon, 205, 245–246, 516, 742
Porphyrins, zinc binding, 116, 315, 325, 661
Positional encoding, 734
Pressure sensors, 154, 555, 592
Prodan, 157–159, 558, 651
Programmable array microscope (PAM), 609–610, 615, 657
Prostate-specific antigen, 218
Proteins
  detecting microarrays, 526, 663
  disease biomarkers, 711, 724, 738, 755
  folding code, 329, 330, 388
  function arrays, 14
  labeling coupled with synthesis, 644
  protein layers, 450–451
  scaffolds, 732
  targets, 486
  total content, 33
Proteome
  antibody microarrays, 724
  global analysis, 724
  microfluidic devices, 725
  protein chips, 723
Proton transfer
  protonation-deprotonation of fluorescent dyes, 378
Push-pull structures, 113

Q

Quadruplex DNA, 583
Quantum confinement, 232, 246, 398
Quantum dots (QDs)
  applications, 648
  barcodes, 683
  blinking, 239
  brightness, 648
  composition, 241, 243
  conjugation, 240, 241
  emission, origin, 246
  FRET donors and acceptors, 264, 269
  imaging, 58
  immunoassays, 251
  magic-sized, 206, 244–245
  multiplexed assays, 241
  photochromic composites, 278
  porous silicon, 245–246
  quantum rods, 245
  radiation-excited, 473
  self-illuminating, 469
  spectra, 242, 244
  two-photon excitation, 239
Quantum efficiency (QE), 464, 512, 513
Quantum yield of fluorescence, Φ, 73, 142, 493, 775

R

Radiative and non-radiative decay, 121, 492
Radioluminescence, x-ray excitable probes, 471, 472
Raman scattering, 71, 72, 188, 486, 696, 697
λ-Ratiometry, 75, 101, 113, 122, 124, 159, 274–275, 528, 604, 613
Reagent-independent sensors, 5, 29–33, 88
Real-time biotelemetry, 750, 752

Recognition units
antibodies (Abs), 317–321
boronic acid derivatives, 306–308
calix[n]arenes, 311–314
crown ethers and cryptands, 305–306
cucurbit[n]urils, 314–315
cyclodextrins, 308–310
ligand-binding proteins, 321–329
molecularly imprinted polymers, 345–348
nucleic acid aptamers, 336
peptides, 335
porphyrins, 315–316
Red-Edge effect, 75, 104, 277, 561, 563
Remote sensing, 31
Reproduction of human senses
olfactory system, 741, 743, 744
pattern recognition principle, 744
taste perception, 742
Response function, non-linear, 27, 30, 51, 61, 62, 359, 401, 452, 776
Reversible saturable optical fluorescence transitions (RESOLFT), 621, 622, 625
Reversible target-receptor binding, 52–54
Rhodamines, 76, 79, 136, 137, 141–143, 148, 210, 213, 217, 476, 565, 566, 661
Ribosome display, 331, 332
RNA, 14–16, 18, 20, 43, 100, 146, 169, 170, 224, 241, 242, 282, 336, 338, 341–344, 391, 428, 485, 495, 497, 528, 572, 574–579, 581, 583, 586, 590–591, 637, 720–722, 765
Rotamers, 386
Rotational correlation time, 86, 88, 184, 560
Rotational diffusion, 39, 84, 87, 88, 560, 565
Ruthenium, 96, 152, 183–184, 214, 242, 281, 361, 395, 463, 520, 555, 569

S

Sandwich assays
antigens and antibodies, 22–23
DNA hybridization assays, 24
Scintillator, 512
Self-assembled monolayers (SAMs), 439–441, 444
Self-assembled supramolecular systems
affinity coupling, 419–420
electrostatic interactions, 418
hydrogen-bonding complementarity, 42
hydrophobic interactions, 421
multivalent interactions, 422
S-layer proteins, 422–423
template-assisted assembly, 423–424
Self-quenching
concentrational, 210
in dimers, 210
on homo-FRET, 210
Sensor response function, 51, 401
Sensors
biotechnology processes, 746
combinatorial methodology, 731
diagnostic devices, 732
environment pollution, 749
guided drug delivery, 750
implantable, 750–751
industrial control and measurement tools, 745
lifestyle management, 746–747
real-time biotelemetry, 750, 752
robotic operations, 752
wearable, 748
Sensor sensitivity and limit of detection, 41–42
Sensor technologies
optical encoding, 734
positional encoding, 734
Signaling aptamers, 338, 340
Signal transduction
association and aggregation, 398–400
conformational changes, 398
electron, charge and proton transfer, 366–378
release of information-containing signal, 360
smart sensing, logical operations, 400–407
superenhancement and superquenching, 83–385
Single molecules
inside cells, 636
sensors, 632
Single nucleotide polymorphism (SNP), 170, 219, 345, 579, 583
Single-photon counting mode, 94, 292, 475, 478, 479, 513, 514, 571, 613, 689
Single-stranded DNA (ssDNA)
detection, 580
RNA binding, 581
Site-specific intracellular labeling., 639–646
Solid-state semiconductor devices, 513
Solvatochromic (environment-sensitive) dyes, 156–160, 165, 170, 309, 776
Spectral shifts
in emission spectra, 71
in excitation spectra, 118, 119
Spectrofluorimeter
fluorescence detection, 509, 512

microplate readers, 510
miniaturization and simplification, 510
Spotted microarrays, 507, 522–528, 533, 544, 734
Stark effect, Electrochromism, 160
Stem cells, 700
Stern-Volmer relation, 78, 93
Stimulated emission depletion (STED) microscopy, 618–622
Stokes–Einstein relation, 88
Stokes shift, 70–72, 76, 79, 83, 92, 97, 104, 115, 135–136, 141–143, 145, 150, 175, 179, 180, 183–185, 187, 190, 192, 210, 223, 229, 238, 239, 244, 285, 371, 379, 473, 565, 574, 606, 695, 768, 776
Structured illumination microscopy (SIM), 625
Supercritical fluids, 563–564
Superenhancement and superquenching, 383–385
Super-resolution microscopy
diffraction limit, 616
near-field scanning microscopy, 616–618
stochastic photo-switching, 623
Supersensitive multicolor ratiometric dyes, 162–167
Supporting and transducing surfaces
gold and silver, 439
Langmuir–Blodgett films, 442–443
layer-by-layer approach, 443–444
Surface plasmon-field enhanced fluorescence, 486–487
Surface plasmon resonance (SPR), 7–9, 11, 438, 486–488, 490, 491, 725
Surgery image-guided, 695
Suspension arrays, 236, 264, 286–287, 495, 499, 529–533, 580, 766, 777

T

Taste perception, 742
Temperature sensors, 154, 251, 520, 553, 554
Template-assisted assembly, 423–424
Template-directed polymerization, 212, 346
Thiophlavine T, 191
Theranostics
drug release, 708–709
imaging functionalities, 703–704
photodynamic therapy, 706–707
photothermal therapy, 705
Thermal quenching, 117, 520, 552, 553, 659
Thermosensitive polymer, 100
Time-resolved
anisotropy, 95
decay, 466
immunoassays, 319–321
microscopy, 612
spectroscopy, 613
Tip-enhanced near-field optical microscopy (TENOM), 618
Topological saturation, 418
Total internal reflection microscopy (TIRF), 604, 607–608, 615, 626
Toxicity testing, 542
Transcriptome profiling, 579, 722
Transparency window, tissues, 149, 686
Trinitrotoluene (TNT), 20, 243, 348, 479, 556
Tryptophan, 12, 156, 157, 167–170, 634
Twisted intramolecular charge transfer (TICT), 121, 374, 378, 777
Two-band wavelength-ratiometry
detection and quantitative analysis, 124
direct sensing arrays, 124
excited-state reactions, 119–121
ground-state isoforms, 119
Two-photon microscopy, 150, 495, 511, 538, 611, 612, 618, 626, 648, 655

U

Up-converting nanocrystals
color barcoding, 250
electronic excited states, 247
energy transfer acceptors, 250
imaging, 246, 251
resonance energy transfer donors, 249

V

Vavilov's law, 74
Viruses, viral antigens, 592
Viscosity and molecular mobility
fluorescence probes, 562
molecular rotors, 561, 562
Red-edge effects, 561
translational/rotational diffusion, 560
wavelength-ratiometric response, 560
Visible fluorescent proteins. *See also* Green fluorescent protein (GFP)
algae phycobiliproteins, 175
B-phycoerythrin, 175
green fluorescent protein (GFP) fluorophore, 172, 173
labeling and sensing applications, 174–175
proteins of GFP family, 172–175

W
Water-in-oil micro-emulsion, 211
Waveguides, planar, 516, 521, 522, 537, 591
Wavelength conversion
  cascade energy transfer, 273–275
  excitons, 266–269
  light-harvesting, 271–273
Wavelength converters, 269, 273, 274, 279
Wavelength-ratiometric imaging
  confocal microscope, 614
  λ-ratiometry, 613
Wavelength referencing, 284–289
Wavelength-shift sensing
  direct molecular immunosensor, 116
  energy levels and transitions, 112
  environment-sensitive dyes, 116–117
  hydrogen bonding, 114
  molecular relaxations, 112
  physical background, 111–113
Wavenumber scale, 71, 111, 125, 135, 768, 776
Wearable sensors, 748, 755
Whole body sensing
  blood vessels and lymph nodes, 693–695
  contrast agents and reporters, 688–691
  fluorescence image guided surgery, 695–697
  imaging cancer tissues, 691–692
Whole living cell devices
  bacterial cells, 539, 543
  cell-based biosensors, 543
  cultured human cells, 543
  fixed cells, 540, 665
  flow cytometry, 538–540
  fluorescence microscopy, 538
  microarray technology, 543
  microfluidic devices, 538, 540–543
Wide-field microscopy, 616, 625, 628–630, 667

X
X-ray excited IR-luminescent (X-IR) nanocomposites, 471
X-ray luminescence optical tomography (XLOT), 472

Z
Zero dimension (0-D) nanostructures, 204
Zinc, detection, 661
Zinc-finger, 116, 168, 389, 390, 576, 661